Interagency Flood Risk Management (InFRM)

Watershed Hydrology Assessment for the Lower Colorado River Basin

January 2024

InFRM
INTERAGENCY FLOOD RISK MANAGEMENT

Table of Contents

Appendices

The InFRM Team

As flooding remains the leading cause of natural-disaster loss across the United States, the Interagency Flood Risk Management (InFRM) team brings together federal agencies with mission areas in water resources, hazard mitigation, and emergency management to leverage their unique skillsets, resources, and expertise to reduce long term flood risk throughout the region. The Federal Emergency Management Agency (FEMA) Region VI began sponsorship of the InFRM team in 2014 to better align Federal resources across the States of Texas, Oklahoma, New Mexico, Louisiana, and Arkansas. The InFRM team is comprised of FEMA, the U.S. Army Corps of Engineers (USACE), the US Geological Survey (USGS), and the National Weather Service (NWS), which serves under the National Oceanic and Atmospheric Administration (NOAA). One of the first initiatives undertaken by the InFRM team was performing Watershed Hydrology Assessments for large river basins in the region.

The Federal Emergency Management Agency (FEMA) funded the Watershed Hydrology Assessments to leverage the technical expertise, available data, and scientific methodologies for hydrologic assessment through the InFRM team. This partnership allows FEMA to draw from the local knowledge, historic data and field staff of its partner agencies and develop forward leaning hydrologic assessments at a river basin level. These studies provide outcomes based on all available hydrologic approaches and provide suggestions for areas where the current flood hazard information may require update. FEMA will leverage these outcomes to assess the current flood hazard inventory, communicate areas of change with community technical and decision makers, and identify/prioritize future updates for Flood Insurance Rate Maps (FIRMs).

The U.S. Army Corps of Engineers (USACE) has participated in the development of the Watershed Hydrology Assessments as a study manager and member of the InFRM team. USACE served in an advisory role in this study where USACE's expertise in the areas of hydraulics, hydrology, water management, and reservoir operations was required. USACE's primary scientific contributions to the study have been in rainfall runoff watershed modeling and reservoir analyses. The reservoir analyses in this study are based on USACE's firsthand reservoir operations experience and the latest scientific techniques from USACE's Dam Safety program.

The U.S. Geological Survey (USGS) Texas Water Science Center has participated in the development of this study as an adviser and member of the InFRM team. USGS served in an advisory role for this study where USGS' expertise in stream gaging, modeling, and statistics was requested. USGS's primary scientific contribution to the study has been statistical support for flood flow frequency analysis. This flood flow frequency analysis included USGS firsthand stream gaging expertise as well as advanced statistical science.

NOAA National Weather Service (NWS) has participated in the development of this study as an adviser and member of the InFRM team. NOAA NWS served in an advisory role of this study where expertise in NOAA NWS' area of practice in water, weather and climate was requested. NOAA's primary scientific contribution to the study has been the NOAA Atlas 14 precipitation frequency estimates study for Texas. This precipitation-frequency atlas was jointly developed by participants from the InFRM team and published by NOAA. NOAA Atlas 14 is intended as the U.S. Government source of precipitation frequency estimates and associated information for the United States and U.S. affiliated territories.

More information on the InFRM team and its current initiatives can be found on the InFRM website at www.InFRM.us.

EXECUTIVE SUMMARY

The Federal Emergency Management Agency (FEMA) administers the National Flood Insurance Program (NFIP), which was created in 1968 to guide new development (and construction) away from flood hazard areas and to help transfer the costs of flood damages to the property owners through the payment of flood insurance premiums. The standard that is generally used by FEMA in regulating development and in publishing flood insurance rate maps is the 1% annual chance (100-yr) flood. The 100-yr flood is defined as a flood which has a 1% chance of happening in any year. The factor that has the greatest influence on the depth and width of the 100-yr flood zone is the expected 1% annual chance (100-yr) flow value.

This report summarizes new analyses that were completed as part of a study to estimate the 1% annual chance (100-yr) flow, along with other frequency flows, for various stream reaches throughout the Lower Colorado River Basin in Texas. For the purposes of this study, the term "Lower Colorado River Basin" refers to the study area of this Watershed Hydrology Assessment (WHA) which included all portions of the Colorado River basin from E.V. Spence Reservoir near Robert Lee, Texas to the Gulf of Mexico. This study was conducted for FEMA Region VI by an Interagency Flood Risk Management (InFRM) team. The InFRM team is a partnership of federal agencies that includes subject matter experts (SME) from FEMA, the U.S. Army Corps of Engineers (USACE), the U.S. Geological Survey (USGS), and the National Weather Service (NWS). In addition to the federal partners of the InFRM team, regional stakeholders such as the Lower Colorado River Authority (LCRA), the City of Austin, and the Texas Water Development Board (TWDB) also participated in the progress updates and review processes for this study. This study represents a significant step forward towards increasing resiliency against flood hazards in the Lower Colorado River basin.

The InFRM team used several hydrologic methods, including statistical hydrology, rainfall-runoff modeling, period of record simulations, and reservoir analyses, to estimate the 1% annual chance (100-yr) flow and then compared those results to one another as well as to previously published values. The purpose of the study is to produce 100-yr flow values that are consistent and defendable across the basin.

The InFRM team used up-to-date statistical analysis along with state-of-the-art rainfall-runoff watershed modeling and reservoir analyses to estimate the 1% annual chance (100-yr) flow values throughout the Lower Colorado River Basin. In the statistical analysis, the gage records were updated through the year 2020 to include all recent major flood events. However, since statistical estimates inherently change with each additional year of data, their results were compared to the results of a detailed watershed model, which is less likely to change over time.

Rainfall-runoff watershed modeling is used to simulate the physical processes that occur during storm events including how water moves across the land surface and through the streams and rivers. An existing watershed model was updated for the Lower Colorado River Basin to current land use conditions with input parameters that represented the physical characteristics of the watershed. The InFRM team then calibrated the model to verify that it was accurately simulating the response of the watershed to a range of observed flood events, including large events similar to a 1% annual chance (100-yr) flood. A total of 38 recent storm events were used throughout different parts of the watershed to fine tune the model.

For the 38 storm events used to fine tune the model, the availability of National Weather Service (NWS) hourly rainfall radar data allowed for more comprehensive calibration of the watershed model than would have been possible during earlier modeling efforts. In total, over 400 individual calibrations were completed as part of this study. The final watershed model accurately simulated the response of the Lower Colorado watershed, as it reproduced the timing, shape, and magnitudes of the observed floods very well. An example plot of the modeled flow versus the recorded flow is shown below in Figure ES.1, but many more examples are available in Appendix B.

The model calibration and verification process undertaken during this study substantially exceeds the standard of a typical FEMA floodplain study. Because these rainfall-runoff models have been calibrated to observed watershed responses to storm events, there is more assurance that these models, when paired with best available rainfall frequency information, can provide a more accurate representation of flood risk.

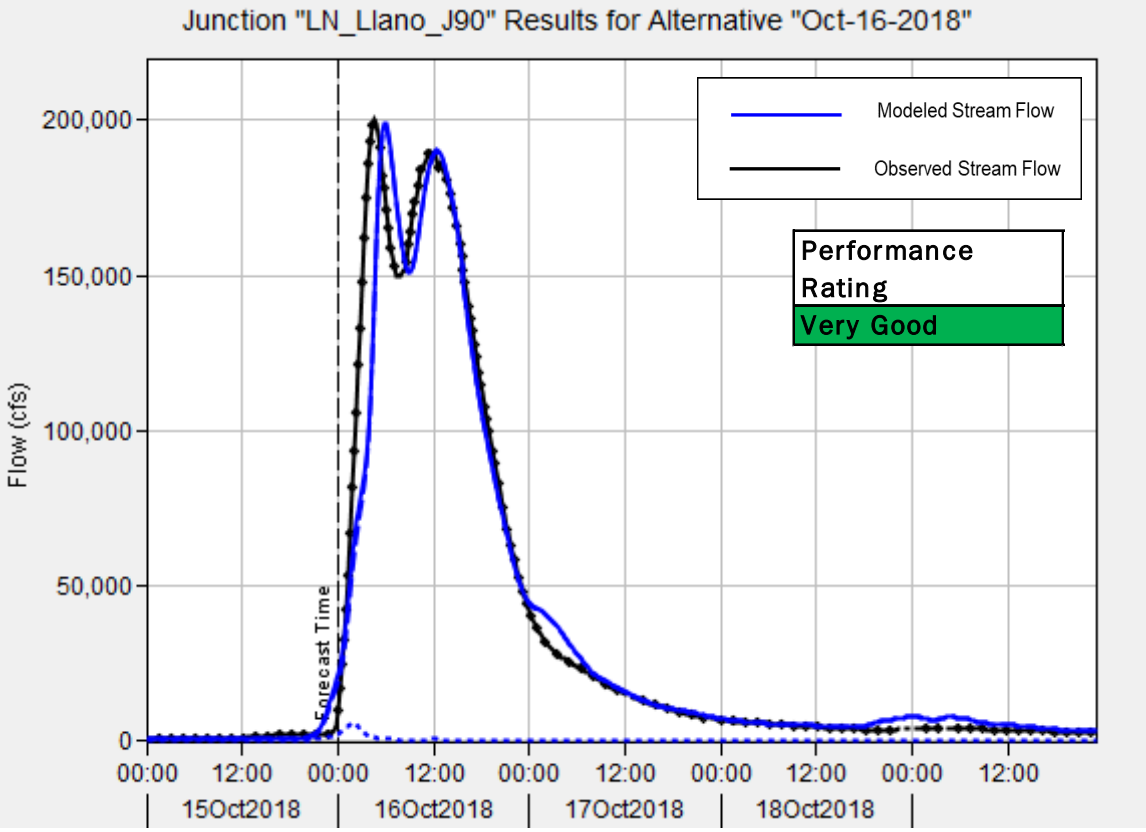

Figure ES.1: Example of Watershed Model Results versus Recorded Flow at the USGS Streamgage

The 1% annual chance (100-yr) flow values were then calculated by applying a 100-yr storm to the watershed model. Rainfall estimates for the 100-yr storm are considered more reliable than statistical estimates for the 100-year flow due to the larger number of rainfall stations and the longer periods of time during which rainfall measurements have been made. The accuracy of those rainfall frequency estimates was further advanced by the release of NOAA Atlas 14 for Texas in 2018 (NOAA, 2018). NOAA Atlas 14 is the U.S. Government source of precipitation frequency estimates and is the most accurate, up-to-date, and comprehensive study of rainfall depths in Texas. The regional approach used in NOAA Atlas 14 incorporated at least 1,000 cumulative years of daily data into each location's rainfall estimate, yielding better estimates of rare rainfall depths such as the 100-yr storm. These frequency rainfall depths from NOAA Atlas 14 were applied to the calibrated watershed model for the Lower Colorado River basin.

After completing the model runs, the watershed model results were compared to previous studies and to the results of other hydrologic methods. Where there were significant differences, investigations were made into the drivers of those differences. Extensive comparisons were made between the watershed model results, the statistical analyses of USGS streamflow gage records, historic storms, RiverWare modeling, storm shifting, and previously published flow values, as shown in Chapter 12 of this report. The expected impacts of reservoir operations for the major reservoirs in the basin were also analyzed in detail for this study, and frequency dam

releases and pool elevations were recommended for the reaches immediately upstream and downstream of the dams.

Significant downward trends in streamflow were observed in this study, particularly in the portion of the Colorado River basin that is upstream of the Colorado River near San Saba, TX. The data indicate that a pronounced and enduring shift in basin hydrology likely occurred sometime in the 1960s followed by a slower, more gradual decline in stream flows that persists to the present time. These downward trends in streamflow were also confirmed in another study by Harwell and others (2020), which analyzed precipitation, streamflow, and potential flood storage trends in the Colorado River basin in Texas. Additionally, the Harwell study (2020) found no significant trends in annual precipitation across the Colorado River basin. However, the gages that indicated a downward trend in annual peak streamflow also showed downward trends in the ratio of streamflow volume to precipitation volume on an annual time step, which indicates a change in the way the Colorado River basin responds to rainfall events over time. Figure ES.2 gives an example of these declining streamflow trends in the annual peak streamflow data for the Colorado River near Ballinger, Texas. More information on the declining flow trends can be found in Chapter 5.

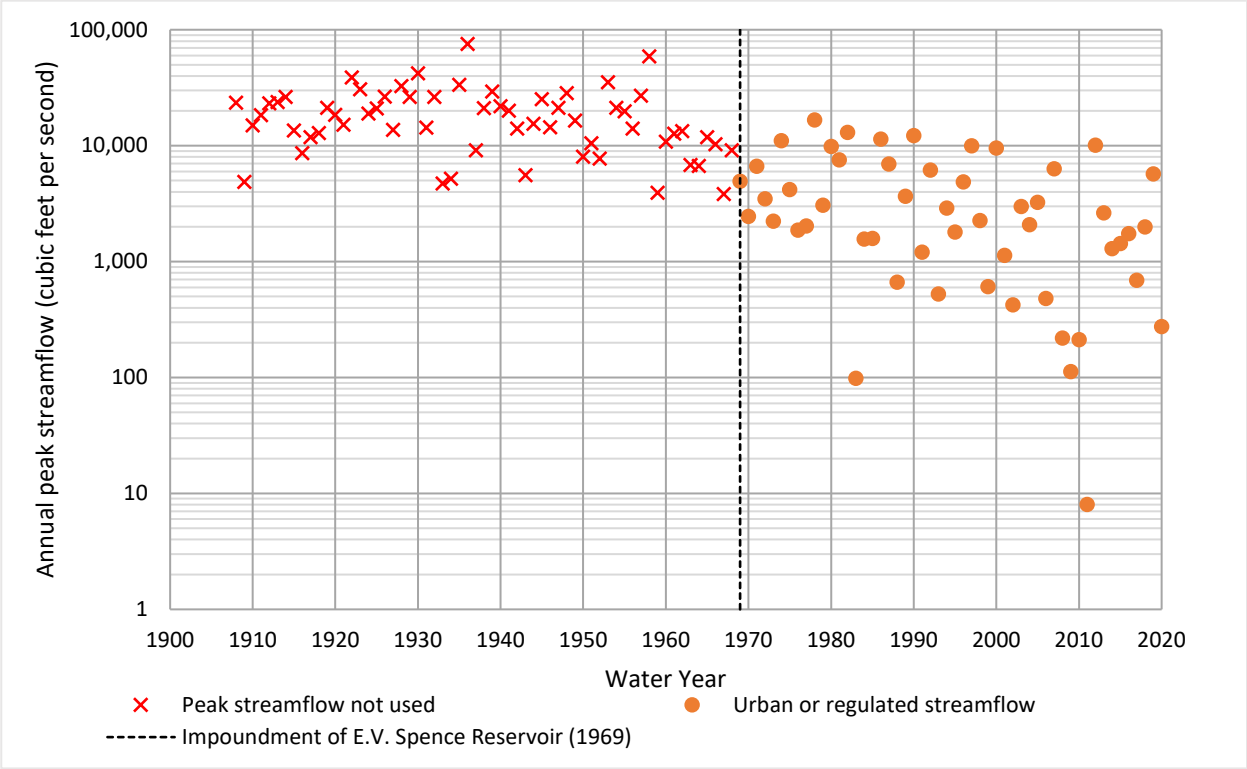

Figure ES.2: Example of Declining Streamflow Trends for the Colorado River near Ballinger, TX

One other unique aspect of the history of flooding in the Lower Colorado River basin led to an additional analysis for the InFRM Watershed Hydrology Assessment (WHA). For many locations in the Lower Colorado River basin, the largest floods of record occurred in the 1930s, and since then, no other observed floods have some close to the magnitudes of flooding observed in the 1930s. In many cases, the rainfall and peak discharges from these floods were on the order of a 1% AEP (100-yr) flood or larger, which means that they are of high interest for flood studies such as this one. However, there is a complication in that those floods occurred before most of the major reservoirs in the river basin were built.

For this study, additional analysis was performed in HEC-HMS to recreate two of those 1930s storm events with the goal of estimating what the peak flows on the rivers would have been with all of the current reservoir regulation in place. The regulated peak flows from those storm events were then added to the Bulletin 17C analysis of select stream gages as a sensitivity test of the statistical flood frequency estimates. The results of the historic 1930s storm analysis are documented in Chapter 10 and in Appendix F.

The final recommendations for the Lower Colorado Watershed Hydrology Assessment were formulated through a rigorous process which required technical feedback and collaboration between all of the InFRM subject matter experts. This process included the following steps: (1) comparing the results of the various hydrologic methods to one another, (2) performing an investigation into the reasons for the differences in results at each location in the watershed, (3) selecting of the draft recommended methods, (4) performing internal and external technical reviews of the hydrologic analyses and the draft recommendations, and finally, (5) finalizing the study recommendations. After completing this process, the flows that were recommended for adoption by the InFRM team came from a combination of the watershed model results using NOAA Atlas 14 uniform rain, elliptical storms, and reservoir analysis techniques. Other methods, such as the statistical and RiverWare results, were used as points of comparison to fine tune the model for the frequent storms, but they were not adopted directly due to their tendency to change after each significant flood event.

Figure ES.3 shows the trends in the recommended 1% AEP (100-year) peak flows versus drainage area for all the major rivers and tributaries in the Lower Colorado study area. This figure shows that the discharges for the analyzed locations followed generally expected patterns of increasing peak flow with drainage area, with exceptions for the effects of flood control reservoirs. The relative magnitudes of the 1% AEP (100-year) discharges of different tributaries in this graph generally make sense. For example, the Concho and Pecan Bayou watersheds in the upper, drier portion of the study area have the lowest peak discharges relative to their drainage areas, while steep, flashy rivers like the Llano and Pedernales, on the other hand, have the highest peak discharges relative to their drainage areas. This study also found that peak flows on the Colorado River are largely driven by its major tributaries. Upstream of the Concho River, Colorado River flows are similar to those in the Concho watershed. Between the Concho River and the San Saba River, Colorado River 1% AEP (100-year) flows generally stay between 100,000 and 150,000 cfs. Downstream of the San Saba River, the 100-year flows increase to about 200,000 cfs. Downstream of the Llano River, Colorado River peak flows jump up to about 400,000 cfs and then climb to over 500,000 cfs downstream of the Pedernales River. Below Lake Travis, Colorado River 1% AEP (100-year) flows are greatly reduced to between 90,000 and 150,000 cfs upstream of Onion Creek. Just below Onion Creek, the 1% AEP flows on the Colorado River peak jump to about 250,000 cfs and then begin to decrease in the downstream direction due to floodplain storage and a lack of major tributaries between Onion Creek and the Gulf. Between Bastrop and the Gulf, 1% AEP peak flows on the Colorado River generally stay between 150,000 and 100,000 cfs and decrease in the downstream direction.

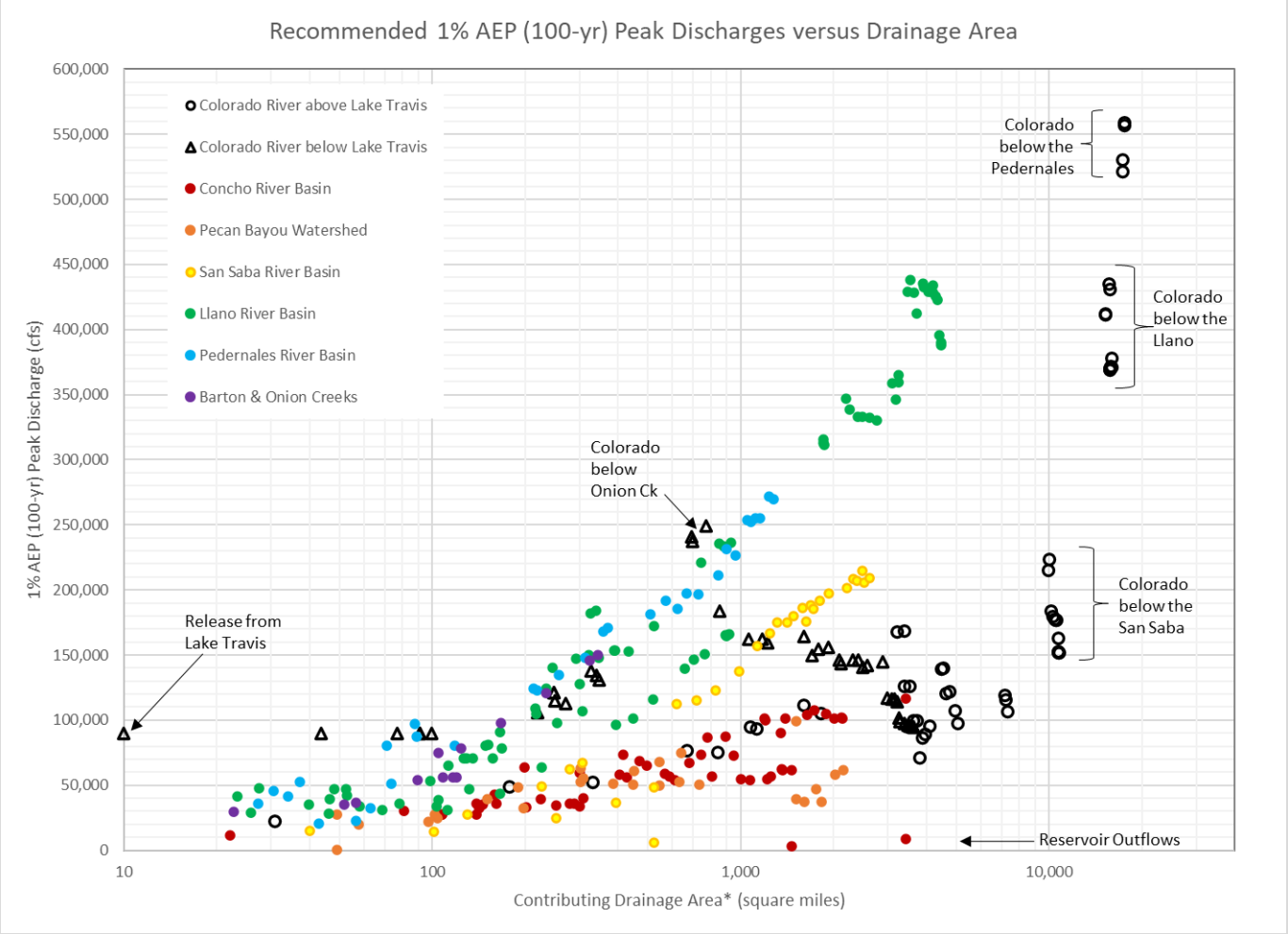

* NOTE: The Drainage Areas shown on this figure only include the contributing areas below significant flood control reservoirs.

Figure ES.3.: Recommended 1% AEP (100-year) Peak Flows versus Drainage Area

Previously published frequency discharges from effective FEMA Flood Insurance Studies (FIS) in the Colorado River Basin were available for approximately 27% of the locations that were analyzed in this study, and the results of the current study were compared to those previously published values. The recommended results from this study differed significantly from the effective FEMA Flood Insurance Studies (FIS) frequency flows in many locations. The new flow frequency results were higher than the previously published results in some areas, while they were lower in other areas. Figure ES.4 shows the percent difference between the recommended 1% AEP peak flows versus the previously published FEMA FIS 1% AEP peak flows.

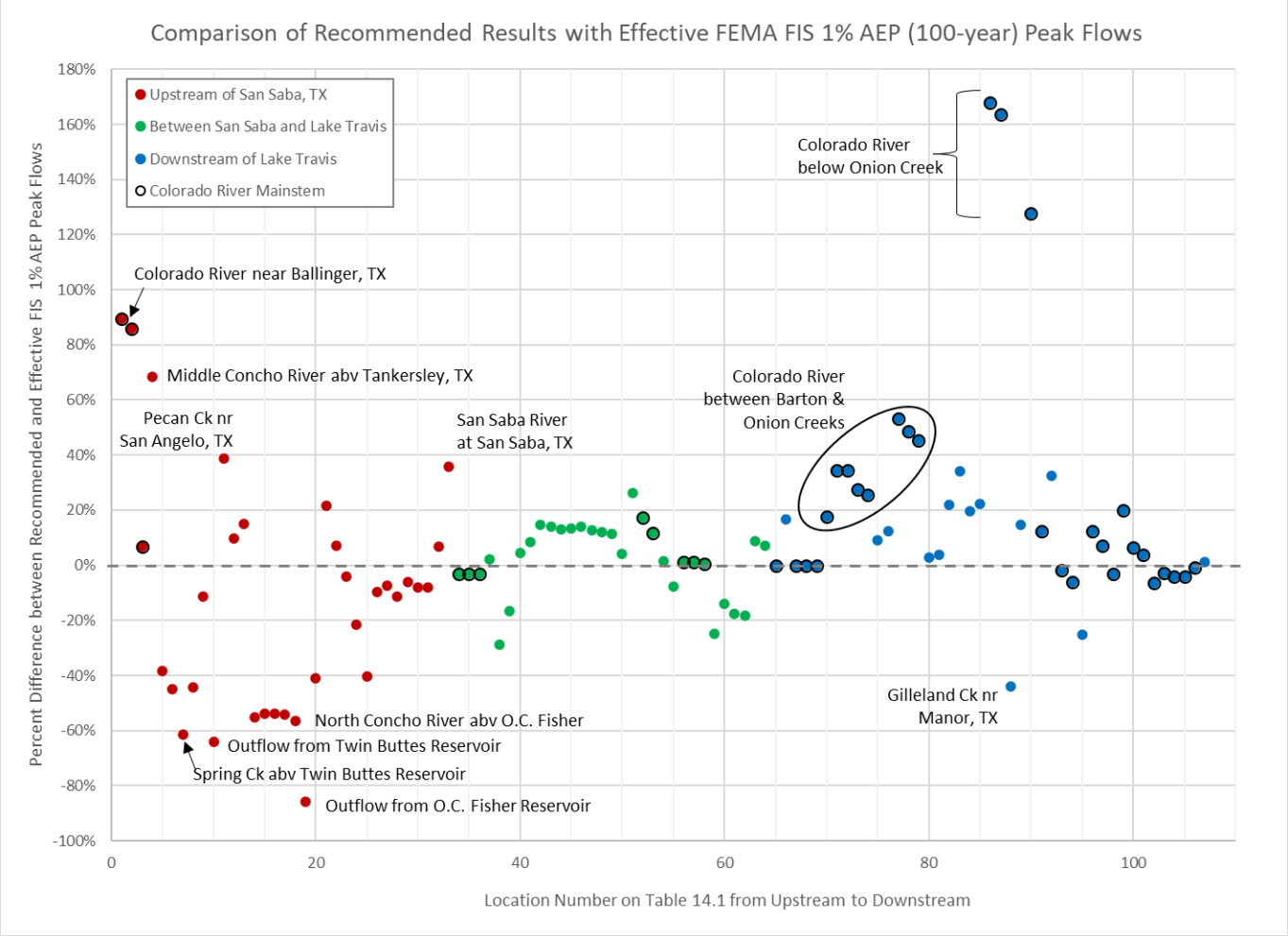

Figure ES.4: Percent Difference between the Recommended vs. Effective FEMA FIS 100-year Peak Flows

The largest percent differences were generally seen in the area upstream of San Saba (red dots), which is also the portion of the basin that is experiencing declining stream flow trends. Most of the locations upstream of San Saba showed a decrease in the recommended 1% AEP (100-yr) peak flows when compared to the effective FIS discharges. This result is consistent with the observed declining trends in streamflow. The differences in the 1% AEP (100-year) flow estimates upstream of San Saba were as high as +/- 80%. There were also some locations upstream of San Saba that showed a significant increase from the effective FIS 1% AEP (100-year) peak flow values. The locations that showed a significant increase upstream of San Saba were generally locations whose FIS hydrology had not been updated in more than 30 years, and those FIS flows were often based on outdated methods and/or statistics.

For the areas of the basin between San Saba and Lake Travis, which includes the Llano and Pedernales Rivers, the percent differences from the effective FIS discharges were generally smaller. Figure ES.4 shows that most of the differences in this area of the basin were less than 20%, and the average percent difference was +/- 10%. This portion of the basin did not show any significant trends in streamflow, and some of the FIS discharges in this area came from the 2002 Flood Damage Evaluation Project (FDEP), which used similar methods to the current study. Therefore, it makes sense that the changes in flood frequency estimates were smaller in this portion of the basin.

For the portion of the basin that is downstream of Lake Travis, the percent differences in peak flow were mostly positive, indicating an increase in the 1% AEP (100-year) flow estimates, as shown on Figure ES.4. In fact, the average difference in the 1% AEP peak flow for this portion of the basin was +20%. One reason for this increase are the increased frequency rainfall depths from NOAA Atlas 14. The 100-year rainfall in Austin, Texas increased by close to 30% when compared to previous rainfall estimates (NOAA, 2018). These increases in rainfall depths led to increases in peak flow on many of the tributaries around Austin such as Barton and Onion Creeks.

For the Colorado River mainstem downstream of Lake Travis, the other contributing factor to the increases in the 100-year peak flow estimates had to do with the assumption surrounding the dominant source of flooding. For the effective FIS, the 100-year peak flow on the Colorado River was assumed to originate from a large release from Lake Travis of 90,000 cfs. The current study also recommended 90,000 cfs as the 100-year peak release from Lake Travis. However, the current study's rainfall runoff modeling showed that runoff from the uncontrolled drainage area downstream of Lake Travis surpasses 90,000 cfs downstream of Barton Creek. Figure ES.4 shows that the difference in the 100-year flow estimate jumps from zero percent upstream of Barton Creek to between 20% and 50% between Barton and Onion Creeks. Downstream of Onion Creek, the increase in the 100-year peak flow jumps to more than 100% of the effective FIS flow. This is because the effective FIS assumed that the 100-year peak flow on the Colorado River downstream of Onion Creek would still be the 90,000 cfs release from Lake Travis. However, the current study showed that Onion Creek alone can produce a 100-year peak discharge of 150,000 cfs. When combined with the urbanized and uncontrolled drainage area between Lake Travis and Onion Creek, the recommended 1% AEP (100-year) discharges on the Colorado River below Onion Creek were found to be as much as 240,000 cfs, which represents a 167% increase over the effective FIS flow for that reach.

At the time of this publication (2023), FEMA's Base Level Engineering (BLE) data was not yet available for most of the study area. BLE data are an approximate source of flood hazard estimation, similar to FEMA's Zone A mapping. As such, the hydrology for most of the currently available BLE data is based on approximate methods. As of 2023), BLE data was only available for Llano County, the Pedernales River basin, and the Lower Colorado watershed between Austin and Columbus, Texas.

Overall, there are significant differences between the hydrology used in the BLE data and the results of the present study. FEMA and the TWDB have plans to regularly update the BLE data throughout Texas on a recurring cycle. Since the results of the InFRM Watershed Hydrology Assessments (WHAs) provide a more detailed and accurate estimate of frequency flows across a given watershed, it is recommended that the hydrology of the BLE data be updated to be consistent with the results of the InFRM WHAs whenever they are available. Updating the hydrology with the WHA results will greatly increase the accuracy of the flood risk estimates in the BLE data.

As a result of the level of investment, analyses, and collaboration that went into this Watershed Hydrology Assessment, the flood risk estimates contained in this report are recommended as the basis for future NFIP studies or other federal flood risk studies within the Lower Colorado River basin. These federally developed frequency flow results form a consistent understanding of hydrology across the Colorado watershed, which is a key requirement outlined in FEMA's General Hydrologic Considerations Guidance. Furthermore, the models and data used to produce these flood risk estimates are available upon request, at no charge, to communities, local stakeholders, and architecture engineering firms. Requests for the models should be sent to the InFRM team through the InFRM website at www.InFRM.us.

While the results from this study should be considered the best available estimates of flood risk for many areas of the Colorado River basin, significant uncertainty still remains, as it does in any hydrologic study. Because of this uncertainty and because of the potential impacts that these estimates can have on life and property, the InFRM team strongly recommends and supports local communities that implement higher floodplain standards, such as additional freeboard requirements, floodplain management practices based on standards greater than the 1%

annual chance flood, and/or "no valley storage loss" criteria. Higher freeboard requirements and standards greater than the 1% annual chance flood help mitigate for the uncertainty and variability in flood risk estimation, while the preservation of valley storage helps to stabilize flood elevations while allowing permitted development in the floodplain (NCTCOG, 2020).

One issue that has not been adequately addressed in the present study is the impact of future land use and future climate conditions on the hydrology of the Lower Colorado River basin. Future growth of the Austin metropolitan area is expected to increase urban land use in Travis County and the surrounding areas. While there are straightforward and standard techniques that can be used to estimate the impacts of future land use on the hydrology of the Lower Colorado River basin, estimating the effects of future climate conditions on flood frequency and severity is still an area of ongoing research.

NOAA's Hydrometeorological Design Study Center (HDSC) is currently working on a national publication called NOAA Atlas 15, which will include estimates of frequency rainfall depths under future climate conditions (NOAA, 2022b). The InFRM team is currently waiting on additional guidance from NOAA Atlas 15, which is scheduled to be completed in 2026, to quantify the effects of future climate change on the hydrology of Texas and the Lower Colorado River basin. A quantitative assessment of future climate and future land use conditions may then be added as an addendum to this report.

1 Study Background and Purpose

1.1 THE NATIONAL FLOOD INSURANCE PROGRAM

The National Flood Insurance Program (NFIP) was created in 1968 to guide new development (and construction) away from flood hazard areas and to help transfer the costs of flood damages to the property owners through the payment of flood insurance premiums. The NFIP program is administered by FEMA within the Department of Homeland Security. The NFIP is charged with determination of the 1% and 0.2% annual chance flood risk and with mapping that flood risk on the Flood Insurance Rate Maps (FIRMs). FEMA Region 6 has an inventory of hundreds of thousands of river miles across Texas, Louisiana, Arkansas, Oklahoma, and New Mexico that are in need of flood risk mapping updates or validation. The current flood hazard inventory is available for viewing on FEMA's National Flood Hazard Layer (NFHL) Viewer at https://msc.fema.gov/nfhl.

FEMA's inventory is focused on determining the extent and areas that are vulnerable to flooding during the 1% annual chance (1 in 100 chance of occurrence each calendar year) and 0.2% chance (1 in 500 chance of occurrence each calendar year). Flood hazards are assessed along natural drainage elements such as rivers, streams, and creeks. The program focuses on comprehensive and broad analysis to define, determine and communicate flooding potential.

The Flood Insurance Rate Maps (FIRMs) published by FEMA define the area where flood insurance purchase is mandatory. The mandatory purchase area includes insurable structures within the defined 1% annual chance floodplain with federally backed mortgages. However, the engineering modeling and the flood extents produced and released on FIRMs do not describe the full potential for flooding, as the FIRMs focus on natural streams, creeks and rivers that traverse the watershed and generally do not determine flood hazards related to highly urbanized flooding problems from man-made drainage systems such as sewers and pipe networks.

The standard that is generally used by FEMA in publishing Flood Insurance Rate Maps (FIRMs) for the NFIP is the 1% annual exceedance probability (AEP) flood, also known as the 100-year flood. The 1% AEP, or 100-year flood is defined as a 1 in 100 chance of occurrence each calendar year. The chance of a 100-year flood occurring during the life of a 30-year mortgage or over the life of a structure is much more probable than its name suggests, as shown in Figure 1.1. These statistics underline the need to minimize uncertainty in flood frequency estimates.

Engineering modeling prepared by Federal, State, local, academic and private industry utilize standard engineering practices to determine:

- **Hydrologic Conditions in a Study Area.** In a hydrologic analysis, ground slope, land use, soil types and climatic factors are analyzed to determine how much flood water is expected to collect on the landscape. This flood volume is entered into hydraulic engineering models.

- **Hydraulic Conditions.** Hydraulic engineering efforts generalize stream and channel geometries utilizing ground elevation information to define the areas available to convey flood volumes. These analyses describe stream cross-sections that are analyzed to determine how high the water will rise in the stream channel and/or if it will expand into the natural floodplain areas adjacent to these stream channels. The output of these analysis is a series of calculated water surface elevations.

- **Flood Extent.** The water surface elevations determined by the hydraulic analysis are then reviewed against ground elevation information to define the areas which are prone to flooding during the analyzed event.

Figure 1.1: Example Probabilities of the 100-yr Flood

1.2 THE CHALLENGE AND IMPORTANCE OF HYDROLOGY

In standard engineering practice, the factor that has the greatest influence on the depth and width of the 100-year floodplain is the 1% annual chance (100-yr) flow estimate. As a result, hydrology remains the single largest source of uncertainty in the estimation of flood risk. The challenge of hydrology is that there are many different commonly used and accepted methods for estimating the 1% annual chance flow, and every method will result in a different answer. In Texas, where the climate can cause dramatic shifts between drought and flood cycles, the variation in flood risk estimation can be quite extreme. The challenge of climactic and hydrologic variation points to the need for a more thorough approach to hydrology using multiple scientific methods.

In addition to the natural variation described above, urbanization and reservoir regulation provide additional challenges to hydrology and the estimation of flood risk. For basins which include major reservoirs, such as the Lower Colorado River basin, first-hand knowledge of reservoir operations and additional analysis is needed for accurate flood risk estimation. For basins experiencing major population growth and urban development, land use change must also be considered in the analysis.

1.3 PURPOSES OF THE WATERSHED HYDROLOGY ASSESSMENT

The InFRM Watershed Hydrology Assessment for the Lower Colorado River Basin summarizes new analyses that were completed as part of a study to estimate the 1% annual chance (100-yr) flow, along with other frequency flows, for various stream reaches across the river basin. This study also produces greatly refined meteorologic and hydrologic tools, analysis and data, including verification studies that ensure that the tools accurately reflect the basin's response to intense rainfall events. The tools, analyses and data produced in this study can be leveraged by local communities to manage their growth and development and to better estimate the risk of flooding associated with constructing infrastructure and urban development in the vicinity of significant streams and rivers.

This study was conducted for FEMA Region 6 by the InFRM team. The InFRM team includes subject matter experts (SME) from USACE, the USGS, and the NWS. The Watershed Hydrology Assessment employed a thorough approach to the hydrology of the Lower Colorado River basin. The multi-layered analysis used in this assessment applied a range of hydrologic methods, including rainfall runoff modeling, statistical hydrology, period-of-record simulations, and reservoir analyses, and then compared the results of those methods to one another. This type of multi-layered analysis helped to reduce the uncertainty in the 1% annual chance (100-yr) flow estimates by ensuring that all possible variables affecting flood risk in the basin have been examined. The analysis also accounts for the impacts of non-stationary factors, such as reservoir regulation and climate variation, which helps to tell the story of how the 1% annual chance flow estimate has changed over time.

The purpose of this study is to produce 1% annual chance and other frequency flows that are consistent and defendable across the Lower Colorado River basin based on multiple lines of evidence. The end product of this hydrology assessment will include a hydrology report for use as a reference to evaluate against existing studies and to support new local studies. The results of the watershed hydrology assessment will provide FEMA suggested 1% and 0.2% peak flow rates along the major rivers and tributaries and will inform future updates to Flood Insurance Rate Maps (FIRMs). These analyses will allow Federal, State and Local entities to leverage these basin wide results in a variety of ways.

FEMA will leverage the outcomes from this study to assess the current flood hazard inventory, communicate areas of change with community technical staff and decision makers, and identify/prioritize future updates for FIRMs. This watershed hydrology assessment also provides the recommended hydrologic methods and results needed for use on local studies, which may add the detail necessary to develop frequency flows at a smaller scale. The watershed assessment gives a consistent avenue of updating the hydrology for large, complex river systems, such as the Lower Colorado River basin, much of which is either mapped with approximate methods or has not had its hydrology updated in decades.

This report summarizes all of the hydrologic analyses that were completed to estimate frequency peak stream flows for significant stream reaches throughout the Lower Colorado River Basin. The results of all hydrologic analyses and the recommended frequency discharges are summarized herein. Additional technical detail is also available in the appendices to this report.

1.4 STUDY TEAM MEMBERS

The following table lists the primary InFRM team members who participated in the development of the InFRM Watershed Hydrology Assessment for the Lower Colorado River Basin. Helena Mosser, a hydraulic engineer from USACE Fort Worth District, served as the team lead for this study. In addition to those listed, the InFRM team would also like to acknowledge the many others who served supervisory and support roles during this effort.

Table 1.1: Study Team Members

	Name	Agency	Office
1	Simeon Benson	USACE	Fort Worth
2	Landon Erickson	USACE	Fort Worth
3	Heitem Ghanuni	USACE	Fort Worth
4	Tim Helms	USACE	Fort Worth
5	Kris Landers	NWS	WGRFC
6	Matt Lepinski	USACE	Fort Worth
7	Gina Martinez-Velez	USACE	Fort Worth
8	Edward Michaels	USACE	Fort Worth
9	Helena Mosser	USACE	Fort Worth
10	Alex Parola	USACE	Fort Worth
11	Jon Thomas	USGS	Fort Worth
12	Sam Wallace	USGS	Fort Worth
13	Kara Garvin	USGS	Fort Worth
14	Matt Whelan	USACE	Fort Worth

1.5 TECHNICAL REVIEW PROCESS

The InFRM Watershed Hydrology Assessments undergo a rigorous review process. Numerous peer reviews are performed by InFRM team members throughout the study. Each model, analysis, and technical product is peer reviewed as it is developed by an InFRM Subject Matter Expert (SME). Any technical issues that are discovered during the review process are thoroughly discussed and resolved, often with input from multiple team members. This same review process is also applied to the process of comparing the results from different methods. Any significant differences in the results are thoroughly investigated and discussed with multiple team members, which sometimes leads to changes in the assumptions of the analyses. After completing all the comparisons and investigations, the draft results are shared with the rest of the InFRM team, and input is solicited from multiple subject matter experts. The draft study recommendations are then documented in the draft report, which is sent out for peer review.

Representatives from the following entities were invited to participate as peer reviewers of the InFRM Watershed Hydrology Assessment of the Lower Colorado River basin: the Lower Colorado River Authority (LCRA), the City of Austin, Travis County, the Texas Water Development Board (TWDB), the Texas Department of Transportation (TxDOT), the General Land Office (GLO) of Texas, and the InFRM Academic Council. The InFRM Academic Council is comprised of a select group of professors from local universities with unique skillsets and regional expertise in water resources and hydrology. Their involvement provides an independent and unbiased review of the InFRM team's methods and results. Collaboration with the InFRM Academic Council also helps the InFRM team to stay abreast with the latest advances in hydrologic science and technology. The peer review comments that were received for this study and the responses from the InFRM team have been documented in Appendix H.

2 Lower Colorado River Basin

The Lower Colorado River basin was selected for study by FEMA based upon their NFIP mapping needs and the availability of existing models and LiDAR data. For the purposes of this study, the term "Lower Colorado River Basin" refers to the study area of this Watershed Hydrology Assessment (WHA) which included all portions of the Colorado River basin from E.V. Spence Reservoir near Robert Lee, Texas to the Gulf of Mexico. Sufficiently detailed modeling products for this analysis were available as a starting point for the Lower Colorado River Basin's WHA from USACE's Corps Water Management System (CWMS) Implementation program as well as from LCRA's River Operations Control Center and the 2002 Flood Damage Evaluation Project (FDEP) for the Colorado River. CWMS is the automated decision support tool developed by the Hydrologic Engineering Center (HEC) for USACE Water Managers. In 2013, USACE began a national implementation effort to have all watersheds containing USACE managed flood control systems (dams, levees, etc.) fully modeled within CWMS. The models that were developed for the national CWMS implementation included basin-wide models for surface water hydrology in HEC-HMS, reservoir operations in HEC-ResSim, and river hydraulics in HEC-RAS. For the Lower Colorado River basin, CWMS implementation modeling was completed in 2015, and representatives of FEMA Region 6 attended the CWMS handoff meeting at the USACE Fort Worth District office. In addition, FEMA had future floodplain mapping activities scheduled in the basin.

2.1 WATERSHED AND RIVER SYSTEM DESCRIPTION

The Colorado River originates on the High Plains near Lamesa, TX and flows southeast for over 860 miles before emptying into Matagorda Bay on the Gulf of Mexico. The river begins at an approximate elevation of 3,300 ft. While the perennial portion of the river is entirely located within Texas, its drainage basin of approximately 42,000 square miles does encompass a portion of eastern New Mexico. Of the 42,300 square miles, approximately 11,500 square miles are considered to be non-contributing drainage area. The contributing drainage area of the Colorado River watershed originates in Dawson County south of Lubbock and flows in a southeasterly direction for approximately 860 miles before emptying into the Gulf of Mexico at Matagorda Bay. The width of the basin is 70-160 miles in the upper and middle portions. The basin width shrinks drastically in the lower portions of the basin to anywhere from 15-30 miles downstream of Austin, TX (USACE, 2015).

The Colorado River has seven significant tributaries: the Concho River, Pecan Bayou, the San Saba River, the Llano River, Sandy Creek, Pedernales River, and Onion Creek. Other than Pecan Bayou, all of other major tributaries are spring-fed streams. These streams originate in the Edwards Plateau region. The aforementioned streams enter the Colorado River at the following river miles: Concho River, 628.9; Pecan Bayou, 513.1; San Saba River, 479.8; Llano River, 405.1; Sandy Creek, 398.5; Pedernales River, 358.9; and Onion Creek, 278.1 (USACE, 2015).

Three distinct topographic zones exist within the Colorado River. The upper portion of the basin lies in the Great Plains region of New Mexico and Texas. This area is a gently undulating plain with a regional slope to the southeast. The land elevation at the New Mexico/Texas state border is about 4,000 ft NAVD 88. The elevation falls to less than 2,700 ft NAVD 88 near Lake J.B. Thomas. The eastern and southern boundaries of the Great Plains region are represented by the Caprock Escarpment. The escarpment is more defined on the eastern boundary. It is generally accepted that most of the land area within the Great Plains region of the basin does not contribute to runoff due to sandy soils and playa lakes without surface outlets (USACE, 2015).

The middle basin is represented by the North Central Plains region. Within this zone, the basin is characterized by gently sloped to steep rolling hills and eroded areas. The Edwards Plateau lies within this zone. The plateau area is rugged, and it includes steep hills and many streams. Land elevation at the northwestern boundary is

approximately 2,600 ft NAVD 88. At the southwestern edge, known as Balcones Escarpment, elevation falls below 1,000 ft NAVD 88. Most of the reservoirs within the basin lie within this zone (USACE, 2015).

The last topographic zone, which extends from the Balcones Escarpment near Austin, TX to the Gulf of Mexico, is known as the Gulf Coastal Plains. This area is represented by rolling hills at the northwestern boundary to flat relief near the coast. Surface elevations, from northwest to southeast, range from 700 ft NAVD 88 to sea level.

This watershed assessment focuses on all portions of the Colorado River basin from E.V. Spence Reservoir near Robert Lee, Texas to the Gulf of Mexico, and that study area will be referred to as the Lower Colorado River basin throughout the remainder of this report. Figure 2.1 displays a general map of the Lower Colorado River Basin study area.

The unique shape and variable topography of the Colorado River basin drive a highly variable experience of flood risk throughout the basin. Peak flood flows on the Colorado River mainstem tend to be driven by its major tributaries. The steep hill country tributaries in the middle portion of the basin in particular (San Saba, Llano, Pedernales, etc.) have generated some of the highest observed peak stream flows observed within the Colorado basin. Downstream of Austin, the narrowing shape of the Colorado watershed and the widening floodplains of the coastal plains tend to reduce peak flows of the floods as they travel downstream.

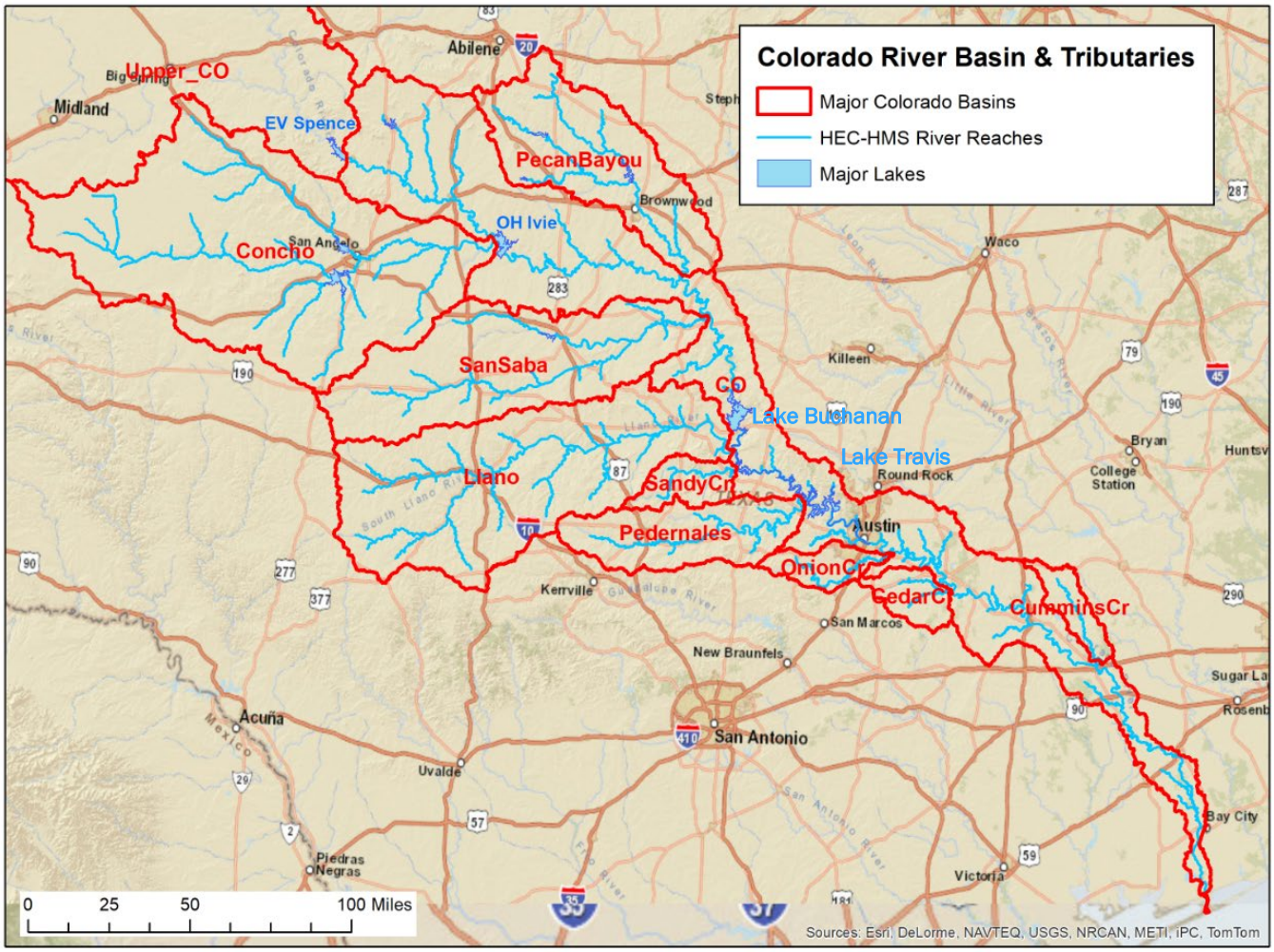

Figure 2.1: Lower Colorado River Basin Location

The Colorado River Basin includes four USACE reservoir projects, two of which are Section 7 dams. According to Section 7 of the Flood Control Act of 1944 (58 Stat. 890, 33 U.S.C. 709), USACE is responsible for prescribing flood control regulations and operational guidance for reservoirs constructed wholly or in part with Federal funds. In the Colorado basin, Twin Buttes Reservoir and Lake Travis are considered Section 7 projects, and USACE has coordinated with the agencies primarily responsible for their operations and maintenance in the development and implementation of their operational plans.

The primary purpose of the USACE reservoir projects is to prevent flood damages to the Austin and San Angelo urban areas but other purposes include hydropower generation, fish and wildlife, water quality, recreational use and water supply. Three USACE reservoirs are located in the Upper Colorado watershed: O.C. Fisher Reservoir (on North Concho River), Twin Buttes Reservoir, a Bureau of Reclamation owned Section 7 project (on South Concho River), and Hords Creek Lake (on Hords Creek, which is a tributary of Pecan Bayou). One reservoir is located in the Lower Colorado River near Austin, Texas: Lake Travis (Marshall Ford Dam), a Section 7 project (on the Colorado River). Lake Travis is part of a system of water supply reservoirs owned and operated by the Lower Colorado River Authority (LCRA). Lake Travis is the fifth downstream reservoir of the Highland Lakes system (USACE, 2013).

LCRA operates six dams on the Colorado River in Central Texas which form the six Highland Lakes: Lake Buchanan, Inks, LBJ, Marble Falls, Travis and Austin. Two of the Highland Lakes – Buchanan and Travis – are regional water supply reservoirs that serve more than 1 million people in the lower Colorado River basin. The reservoirs were also built to help manage floods and generate hydroelectric power.

2.2 CLIMATE

Like most of Texas, climate conditions within the Colorado River basin vary from west to east. Climate conditions over the watershed are generally mild and vary from subtropical along the Gulf Coast to semiarid in the upper headwater regions. The rainfall decreases rather uniformly from the Gulf toward the headwaters. Average annual precipitation ranges from 14-16 inches in the western portion of the basin to over 40 inches near the Gulf of Mexico. The Lower Colorado basin, particularly in the southeast, can experience extremely intense precipitation events capable of producing staggering rainfall totals. These systems range from intense thunderstorms to hurricanes.

The average annual temperatures over the Basin are generally moderate, with the highest at the Gulf and decreasing gradually with the increase in latitude and elevation. Winter months are generally mild, but occasional cold periods of short duration result from the rapid movement of cold high-pressure air masses from the northwest. Snowfall, while not frequent, does occur in the upper portions of the basin. Snowfall is not a major runoff generator partly due to its location within the basin and partly due to the small amount received. Evaporation varies within the basin, but generally the highest monthly evaporation totals occur during the April through September period. Lake Travis, near Austin, TX, has an average annual evaporation rate of 54.0 inches per year. Prevailing winds come from the south or southeast during the majority of the year. During the winter months, prevailing winds shift to the north due to high pressure systems from Canada and the Pacific Northwest. Summer temperatures are high throughout the Basin. The average temperatures over the watershed are moderate, ranging from 63^{o} F at Colorado City to 69^{o} F at Austin. The maximum summer temperatures vary from 109^{o} F to 117^{o} F and the minimum winter temperatures from -9^{o} F to -2^{o} F.

Storms within the basin follow three general types: thunderstorms, frontal storms, and tropical storms. Approximately 75% of the precipitation within the watershed is derived from thunderstorms/frontal storms. Tropical storms make up the remaining 25%. Thunderstorms can result in rainfall for periods of eight hours or longer, but normally do not impact an extensive area. Localized flash flooding can be caused by thunderstorms.

These floods often damage agricultural crops as they tend to occur during the growing season. Moisture rising from the Gulf of Mexico that meets tropical or polar air masses result in the frontal storms within the Colorado River Basin. These storms typically occur in late summer and can last for several days. Tropical storms occur when tropical air masses that are brought ashore by hurricanes converge with an onshore cold air mass. These storms can produce torrential rainfall and can impact large areas of land. The timing of these storms is typically June through November.

The middle section of the basin, which includes portions of the Hill Country and Central Texas, has a greater risk of flash flooding than most regions of the United States. This region of Texas has been called "Flash Flood Alley" due to the area's steep terrain, shallow soil and unusually high rainfall rates. The uplift of moist Gulf air at the Balcones Escarpment just west of Austin has produced some of the greatest rainfall intensities (and flash floods) that have been observed anywhere in the United States. Heavy rains can quickly transform into fast moving flood waters with great destructive potential along these sections of the basin.

2.3 MAJOR FLOODS IN THE LOWER COLORADO RIVER BASIN

The Lower Colorado River basin experiences periodic major flooding due to thunderstorms or tropical storm events. Table 2.1 summarizes the historical peak discharges for major floods at selected stream gages on the Colorado, Concho, Llano, and Pedernales Rivers.

Consistent observation of Colorado River streamflow began in 1898 when the USGS established a gage on the Colorado River at Austin. In 1903, NOAA established gages on the Colorado River at Columbus and Ballinger. However, records of major floods go back even further.

The historic flood of July 1869 is considered to be the worst flood on record on the lower Colorado River. The Colorado River crested at 51 feet at Austin with an estimated peak flow of 550,000 cfs. It also produced record crests of 60.3 feet at Bastrop, 56.7 feet at La Grange, 51.6 feet at Columbus, 51.9 feet at Wharton and 56.1 feet at Bay City. The cities of Bastrop and La Grange were completely inundated. Reports describe rainfall as incessant for 64 hours, and the Colorado River at Austin was reported to be more than 10 miles wide from bluff to bluff (USGS, 1963).

The 1930s was a very active storm period in the Lower Colorado River basin, and for many locations in the Lower Colorado River basin, the largest floods of record occurred in the 1930s. These include the major floods of June 1935, Sep 1936 and July 1938. During the June 1935 flood, the Llano River near Junction experienced a peak flow of 319,000 cfs, and further downstream, the Llano River near Castell had a peak discharge of 388,000 cfs. The flood from the Llano River then joined a smaller flood from the Pedernales River and caused the Colorado River at Austin gage to reach a peak discharge of 481,000 cfs on June 15, 1935 (Dalrymple, 1939).

The Sep 1936 storm event caused widespread flooding throughout the Concho River basin and on the Colorado River from Ballinger all the way to Austin. Over a four-day period, up to 30 inches of rain fell in portions of the Concho, San Saba and Llano River basins. The most destructive floods occurred in the Concho River Basin, and the city of San Angelo suffered great damage. The Concho River at San Angelo peaked at a flow rate of 230,000 cfs (Dalrymple, 1937). It has been estimated that structural damages start as early as 15,000 cfs on the Concho River in San Angelo (USACE, 2015).

In July 1938, heavy rains fell in the watersheds of the San Saba and South Concho Rivers, with 30 inches of rain reported from one place and 20 inches or more from about 70 places. The greatest 1-day rain reported was 13 inches. The resulting flood in the Colorado River was the greatest on record from the mouth of the San Saba

River to Buchanan Dam, and the peak discharge on the Colorado River at San Saba was 224,000 cfs (Breeding, 1944).

Table 2.1: Major Floods in the Lower Colorado River Basin

Date of Flood	Observed Peak Flow (cfs)				
	Concho River at San Angelo	Colorado River nr San Saba	Llano River at Llano	Pedernales River nr Johnson City	Colorado River at Austin
	USGS 08136000	USGS 08147000	USGS 08151500	USGS 08153500	USGS 08158000
	4,411 sqmi	19,819 sqmi	4,192 sqmi	901 sqmi	27,600 sqmi
July 1869					550,000
Jun 1899					113,000
1900		184,000			236,000
1906	246,000				78,500
1908					100,000
1922	92,000	130,000			120,000
Jun 1930	40,200				
Jun 1935		86,000	380,000		481,000
Sep 1936	230,000	179,000			234,000
July 1938	85,100	224,000			276,000
Apr 1941					47,100
Sep 1952	-	69,000	232,000	441,000	
May 1957	106,000	66,200		125,000	40,800
Oct 1959	122,000			142,000	
Oct 1969			154,000		
Oct 1973			154,000		
Aug 1978			139,000	127,000	
Sep 1980	11,500		210,000		
Jun 1997		56,400	260,000	94,900	31,000
Oct 1998					39,400
Oct-Nov 2000		58,300	151,000		
Jul 2002				108,000	
Jun 2004		52,100	85,200		
Nov 2004		33,100	79,600		38,000
Jun-Jul 2007			72,700		
Aug 2007	6,880			90,600	
Sep-Oct 2012	5,270				
Oct 2013					34,400
May 2015	8,730			40,100	34,700
Oct 2015					33,200
Oct-Nov 2018		49,100	278,000	27,800	27,900
May-Jun 2019	6,790			35,100	

The flood of September 1952 exceeded all known floods at many locations in the San Saba, Llano, and Pedernales Rivers. Before the flood, central Texas was suffering from a severe and prolonged drought with many creeks and streams at their lowest levels or having completely dried up. Heavy rains of up to 26 inches fell in the Texas Hill Country during a three-day period of September 9-11, 1952. The most extreme rainfall occurred on the Pedernales River, which caused the Pedernales River at Johnson City to reach a peak discharge of 441,000 cfs (Breeding, 1954). Inflows into Lake Travis on the Colorado River reached a peak of 803,000 cfs and caused the lake to rise 56 feet in less than 24 hours. Prior the flood, Lake Travis was more than 60 feet below normal pool. This extremely low lake level allowed Lake Travis to absorb the entire flood hydrograph without causing damages to the City of Austin downstream (USACE, 2013).

2.4 PREVIOUS STUDIES AND CURRENTLY EFFECTIVE FEMA FLOWS

The hydrology of the Colorado River and some of its tributaries has been analyzed many times over the years. Data and models from several existing hydrologic and hydraulic studies were available at the time of this study. Table 2.3 below summarizes some of the notable existing studies, models, and hydrologic information that were available in the Lower Colorado River basin.

A significant portion of the currently effective FEMA flows for the Colorado River came from the 2002 FDEP study, which used elliptical design storms on a rainfall-runoff model (Halff, 2002). For the tributaries, the currently effective FEMA flows came from various methods including statistical analyses of the gage records, rainfall-runoff modeling, and regression equations. From Table 2.3, one can see that many of the frequency flows in the currently effective FEMA Flood Insurance Studies (FIS) have not been updated in the last 20, 30, or even 50 years. The differences between the effective FEMA FIS flows and the results of the current study depend to a great degree on how and when those effective FEMA flows were calculated. More discussion on these differences can be seen in Chapter 12 of this report.

Table 2.2: Previous Hydrologic Studies in the Lower Colorado River Basin

Study Name	River Extents	Frequency Flows	Hydrologic Methods	Description
City of Mason Flood Insurance Study (FIS) 1979	Comanche Ck	Yes	Rainfall-runoff modeling	1970s SCS unit hydrograph method calculations
City of Coleman Flood Insurance Study (FIS), 1980	Hords Creek	Yes	Statistical analysis	Bulletin 17B analysis of the gage record through 1972.
City of Brady Flood Insurance Study (FIS) 1981	Brady Creek	Yes	Rainfall-runoff modeling	1970s SCS unit hydrograph method calculations
Menard County Flood Insurance Study (FIS), 1987	San Saba River	Yes	Statistical analysis	Bulletin 17B analysis of the gage record through 1986.
City of Ballinger, TX Flood Insurance Study (FIS), 1990	Colorado River and Elm Creek near Ballinger, TX	Yes	Rainfall-runoff modeling	1988 uncalibrated NUDALLAS rainfall-runoff model.
Blanco County Flood Insurance Study (FIS), 1991	Pedernales River in Blanco County	Yes	Unknown	1979 USACE study
San Saba County Flood Insurance Study (FIS), 1991	San Saba River	Yes	Rainfall-runoff modeling	1988 SCS unit hydrograph, uncalibrated rainfall-runoff model
Hays County Flood Insurance Study (FIS), 1994	Onion Creek	Yes	Regression equations & statistical analysis	1994 USGS regression equations with some Bulletin 17B analyses

Study Name	River Extents	Frequency Flows	Hydrologic Methods	Description
City of Junction, TX Flood Insurance Study (FIS), 1997	North Llano, South Llano and Llano Rivers near Junction	Yes	Statistical analysis	Bulletin 17B analysis of the gage record through 1978.
Gillespie County Flood Insurance Study (FIS), 2001	Pedernales River in Gillespie County	Yes	Statistical analysis	Bulletin 17B analysis of the gage record through 1997
Colorado River Flood Damage Evaluation Project (FDEP), 2002	Colorado River from San Saba to the Gulf	Yes	Elliptical Storms, Rainfall-runoff modeling, SUPER, and statistical analysis	Detailed analysis of the Colorado mainstem hydrology and hydraulics sponsored by LCRA & USACE.
Fayette County Flood Insurance Study (FIS), 2006	Colorado River and Buckners Creek in Fayette County	Yes	Rainfall-runoff modeling	2002 FDEP study elliptical storm on rainfall-runoff model for Colorado River.
Colorado County Flood Insurance Study (FIS), 2011	Colorado River in Colorado County	Yes	Rainfall-runoff modeling	2002 FDEP study elliptical storm on rainfall-runoff model.
City of Llano Pending Flood Insurance Study (FIS), 2012	Llano River, Hickory, San Fernando, and Johnson Creek	Yes	Rainfall-runoff modeling	2012 Rainfall runoff model
Tom Green County Flood Insurance Study (FIS), 2012	Middle Concho, South Concho, Concho River, Dove, Spring & Pecan Ck	Yes	Rainfall-runoff modeling and Statistical Hydrology	1990 uncalibrated SWFHYD rainfall runoff model and 1990 SUPER statistical analysis.
Colorado CWMS Implementation Forecast Models, 2015	Colorado River basin below EV Spence Reservoir	No	Rainfall-runoff modeling	USACE reservoir forecast models and calibrated rainfall runoff models developed for the Colorado River Basin.
Bastrop County Flood Insurance Study (FIS), 2016	Colorado River and Cedar Creek in Bastrop County	Yes	Regression equations & statistical analysis	Bulletin 17B analysis of the gage record through 1987 and 1977 USGS regression equations.
Wharton County Flood Insurance Study (FIS), 2017	Colorado River in Wharton County	Yes	Rainfall-runoff modeling	2002 FDEP study elliptical storm on rainfall-runoff model
Brown County Flood Insurance Study (FIS), 2018	Pecan Bayou	Yes	Rainfall-runoff modeling	HEC-1 Rainfall runoff model
Burnet County Flood Insurance Study (FIS), 2019	Colorado River in Burnet County	Yes	Statistical analysis	Bulletin 17B analysis of the gage record through 1990
Llano County Flood Insurance Study (FIS), 2019	Colorado River in Llano County	Yes	Rainfall-runoff modeling	2002 FDEP study elliptical storm on rainfall-runoff model
Travis County Flood Insurance Study (FIS), 2020	Pedernales and Colorado Rivers, Big Sandy Ck, Bull Ck, Walnut Ck, Onion Ck, Gilleland Ck	Yes	Statistical analysis, regression equations and rainfall-runoff modeling	Colorado River flows from the 2002 FDEP study. Tributary methods varied.
Matagorda County Pending Flood Insurance Study (FIS), 2021	Colorado River in Matagorda County	Yes	Rainfall-runoff modeling	2002 FDEP study elliptical storm on rainfall-runoff model

FEMA's Base Level Engineering (BLE) data was also available for some portions of the study area. The BLE data is an approximate source of flood hazard estimation, similar to FEMA's Zone A mapping. As such, the hydrology for most of the currently available BLE data is based on approximate methods such as USGS' regional regression equations. The regional regression equations provide a simple method to estimate frequency discharges based on physical parameters such as area and slope. However, it can be hit-or-miss as to whether those equations are a good fit for a particular watershed. More discussion on the BLE data can be seen in Chapter 12 of this report.

2.5 THE EFFECTS OF FUTURE CONDITIONS

Future conditions can impact the hydrology of a given watershed due to changes in both land use and climate. Since the Lower Colorado River Basin includes the Austin metropolitan area, future conditions can be expected to include increases in urban land use in Travis County and the surrounding areas. Increases in urban land use typically lead to increases in impervious area, runoff volume, and peak streamflow magnitudes. However, since flows on the Colorado River through Austin are primarily controlled by releases from Lake Travis, flows on the mainstem Colorado River may not see as much impact from future land use changes as could some of the currently undeveloped tributaries in the Austin area. For example, future urban development could significantly increase peak frequency flows on Bull Creek, Barton Creek, and Onion Creek if those watersheds were to become fully developed.

Future climate change, on the other hand, is expected to increase the intensity of heavy rainfall events in the Lower Colorado River basin and throughout Texas. Records from the National Centers for Environmental Information (NCEI) show that while temperatures in Texas have been slowly increasing since 1895, the increase has become more significant in recent decades. Since 1975, the increasing temperature trend in Texas has averaged about 0.61°F per decade, and this trend has been observed across all seasons and all regions of Texas (Nielsen-Gammon et al., 2021a).

Basic physics tells us that warmer air can hold more moisture than cooler air. This means that as global temperatures increase, the total amount of water vapor that the atmosphere is capable of holding also increases (USGCRP, 2017). Since heavy rainfall events occur when the air in the atmosphere is almost completely saturated, the expected increase in atmospheric water vapor due to a warming climate directly translates to a similar increase in rainfall intensity. In other words, when rainfall does occur, the amount of rain falling in a given storm event tends to be greater due to the increased water vapor that is available. This is the physical driver to why heavy rainfall is expected to increase in intensity and frequency both globally and across Texas through the end of the century (USGCRP, 2017).

Many studies have documented an increase in extreme rainfall in Texas and the surrounding areas for a variety of durations and thresholds (Nielsen-Gammon et al., 2021a). For example, a median increase of about 7% has been observed in Texas since 1960 in the 1% annual exceedance probability (AEP) rainfall intensity, but this relatively small increase in rainfall intensity corresponds to a 30% increase in the frequency of the historic 100-year or 1% AEP rainfall depths (Nielsen-Gammon et al., 2021a).

While the predicted impacts of climate change on future rainfall intensity are fairly straightforward, the impacts of climate change on future riverine flooding in Texas are more complex and uncertain. Changes to streamflow and riverine flooding depend on many factors in addition to rainfall, including changes in land use, urbanization, reservoir regulation, evaporation and soil moisture conditions. For highly urbanized portions of the Colorado River basin with high amounts of impervious cover, the expected increases in extreme rainfall depths should translate directly to increased runoff and flood risk. In larger, more rural portions of the watershed, however, the situation is

more complicated. Warmer temperatures directly lead to decreases in soil moisture content, which will lead to a greater threshold of rainfall being required to induce runoff over initially dry soils (Nielsen-Gammon & Jorgensen, 2021b). Based on limited modeling studies, the Texas State Climatologist concluded that the effects of increased rainfall intensity are likely to dominate over decreased soil moisture conditions for large flood events (Nielsen-Gammon et al., 2021a). This is because the increased soil moisture deficits are likely to have the greatest relative effect on small rainfall events, whereas for larger, more extreme rainfall events like the 100-yr storm, the initial soil moisture deficit becomes less significant relative to the total rainfall depth. This may mean that minor floods become less likely while major floods may become more likely in Texas under future climate conditions (Nielsen-Gammon & Jorgensen, 2021b).

Current research is rapidly improving estimates of future rainfall patterns. For example, in 2022, NOAA completed a pilot project testing new methods to incorporate a nonstationary climate into NOAA Atlas 14's frequency rainfall estimates (NOAA, 2022a). After the completion of that pilot project, NOAA's Hydrometeorological Design Study Center (HDSC) kicked off an effort to apply those recommended methods nationally and to estimate frequency rainfall depths under future climate conditions. The product of that effort will be called NOAA Atlas 15 (NOAA, 2022b). After its initial publication, Atlas 15 will continue to be updated on a 10-year cycle. NOAA Atlas 15 is one of the biggest research needs in flood hydrology as it will allow engineers to easily apply climate change informed future rainfall estimates to hydrologic rainfall-runoff models, just as they do now with existing conditions rainfall data. Once that future rainfall data becomes available, the other research need that quickly becomes apparent is how to alter the hydrologic model's loss parameters for future soil moisture conditions.

While there is strong scientific consensus that a warmer future climate will increase the intensity of future heavy rainfall events, additional research is needed to quantify the effects of these changes on flood frequency and severity. The InFRM team is currently waiting on additional guidance from NOAA Atlas 15 in order to quantify the effects of future climate change on the hydrology of Texas and the Lower Colorado River basin. A quantitative assessment of future climate conditions may be added as an addendum to this report when the appropriate data is available to support it.

3 Methodology

Assessing flood potential within complex river basins requires considerable expertise and experience. The methodology that was used for this watershed hydrology assessment was a multi-layered analysis that calculated frequency flows in the Lower Colorado River Basin through several different methods and then compared their results to one another before making final flow recommendations. The purpose of this analysis was to produce a set of frequency flows across the basin that are consistent and defendable based on multiple lines of evidence.

The current study builds upon the information that was available from previous hydrology studies by combining detailed data from different models, updating land use data, calibrating the models to multiple recent flood events, and updating statistical analyses to include the most recent flood events.

The multi-layered analysis for the current study of the basin consists of four main components: (1) statistical analysis of the stream gages, (2) rainfall-runoff watershed modeling in the Hydrologic Engineering Center's Hydrologic Modeling System (HEC-HMS), (3) extended period-of-record modeling in RiverWare, and (4) reservoir analyses. Details on the methodology of each analysis are included in their respective report chapters and appendices.

After completing all of these different types of analyses, the final recommendations for the InFRM Watershed Hydrology Assessment were then formulated through a rigorous process which required technical feedback and collaboration between all of the InFRM subject matter experts. This process included the following steps at a minimum: (1) comparing the results of the various hydrologic methods to one another, (2) performing an investigation into the reasons for the differences in results at each location in the watershed, (3) selecting the draft recommended methods, (4) performing internal and external technical reviews of the hydrologic analyses and the draft recommendations, and finally, (5) finalizing the study recommendations. The comparisons of results are included in Chapter 12, and additional details on the process of selecting draft recommendations and finalizing the results can be found in Chapter 13.

4 Data Sources

This chapter provides a general summary of the data that was collected, reviewed, or utilized in the InFRM Watershed Hydrology Assessment of the Lower Colorado River Basin, including geospatial data, climatic information, field observations and previous reports. A more complete list of the data sources used in each type of analysis is included in their respective appendices.

4.1 SPATIAL TOOLS AND REFERENCE

ArcGIS version 10.8.2 (developed by ESRI) was used to process and analyze the data necessary for hydrologic modeling. The geographic projection parameters used for this study are listed below:

- Horizontal Datum: North American Datum 1983 (NAD83)
- Projection: USA Contiguous Albers Equal Area Conic USGS version
- Vertical Datum: North American Vertical Datum, 1988 (NAVD 88)
- Linear Units: U.S. feet

The subbasin boundaries that were used in this study were taken from the existing Colorado CWMS Implementation HEC-HMS model. The CWMS model contained 357 subbasins with an average size of 75 square miles in the Lower Colorado River Basin. The upstream extents of the CWMS HEC-HMS model started just downstream of E.V. Spence Reservoir near Robert Lee, Texas, and the downstream extents ended at the Gulf of Mexico. The subbasins were delineated using the HEC-GeoHMS program and utilized 30-meter National Elevation Dataset (NED) terrain data (USACE, 2015). More information on the HEC-HMS model updates for this study are given in Chapter 6 of this report and in Appendix B.

4.2 TERRAIN DATA

As part of USACE's Corp Water Management System (CWMS) implementation for the Colorado River basin, 30-meter DEMs were collected from the seamless USGS National Elevation Dataset (NED, accessed January 2013) for the study watershed from the USGS National Map website (https://apps.nationalmap.gov/lidar-explorer/#/). The elevations of the NED are in meters. The vertical elevation units were converted from meters to feet, and the datasets were projected into the standard map projection used in this study. The watershed and subbasin delineations for the Lower Colorado HEC-HMS model were performed using the 30-meter NED data. While more detailed terrain data is available, the 30-meter data is sufficient for hydrologic modeling and is consistent with the previous modeling efforts in this basin.

4.3 VECTOR AND RASTER GEOSPATIAL DATA

The mapping team member utilized web mapping services and downloaded the USGS hydrologic unit boundaries, USGS stream gages, USGS medium resolution National Hydrography Dataset (NHD), National Inventory of Dams (NID) data, National Levee Database (NLD) levee centerlines as well as general base map layers. Additional vector data were obtained from the ESRI database and used in figures prepared for the final report. Raster Data includes the National Land Cover Database (NLCD) 2016 land cover and percent imperviousness layers from the https://seamless.usgs.gov website, accessed Oct 2019. The 2016 NLCD data was the newest available land use data at the time of this study's kickoff in 2019.

4.4 AERIAL IMAGERY

The Colorado CWMS implementation team utilized current high-resolution imagery from the National Aerial Imagery Program (NAIP) with a horizontal accuracy based upon National Map Accuracy Standards (NMAS), with 1"=200' scale (1-foot imagery) accuracy of +/- 5.0-feet and the 1"=100' scale (0.5-foot imagery) accuracy of +/-

2.5-feet. Digital photos were used to verify watershed boundaries as well as delineate centerlines and other geographic features. In addition, Google Earth and Google Maps were also used to locate important geographic features.

4.5 SOIL DATA

Gridded Soil Survey Geographic (gSSURGO) datasets were obtained from the NRCS soil survey website during the Colorado CWMS implementation (NRCS, 2014). These datasets were used to estimate loss rates for the frequency storm events in HEC-HMS.

4.6 PRECIPITATION DATA

4.6.1 Radar Data for Observed Storms

Historic precipitation data for observed storm events were collected from the NWS gridded precipitation data files. The NWS radar data for precipitation generally started in the mid-1990s, and NWS' radar products have continuously improved over the past 30 years. As a result, the early radar data from the 1990s is generally not as accurate as the radar data from most recent decade. NEXRAD Stage IV gridded datasets were used for the basin. The NEXRAD Stage IV gridded datasets are stored in a binary file format called XMRG. The historical XMRG data were processed into hourly precipitation grids in HEC-DSS format using HEC-METVUE. This data was acquired from the NWS West Gulf River Forecasting Center (WGRFC). The radar rainfall data has the spatial resolution of approximately a 4 km x 4 km grid, and the rainfall depths are calibrated by the NWS to on-the-ground observations at rainfall gages.

4.6.2 NOAA Atlas 14 Frequency Point Rainfall Depths

Frequency point rainfall depths of various durations and recurrence intervals were collected from NOAA Atlas 14. NOAA Atlas 14 contains precipitation frequency estimates for the United States along with their associated lower and upper 90% confidence bounds. The Atlas is divided into volumes based on geographic sections of the country. NOAA Atlas 14 is intended as the U.S. Government source of precipitation frequency estimates. NOAA Atlas 14 Volume 11, which covers the state of Texas, was published in September of 2018 (NOAA, 2018). The new rainfall depths that were published in NOAA Atlas 14 (NA14) were applied to the HEC-HMS model for this study, as they represented the most up-to-date precipitation frequency estimates in Texas. NOAA Atlas 14 point rainfall depths from the annual maximum series for various durations and recurrence intervals were collected from the NA14 Precipitation Frequency Data Server (PFDS) for the centroid of each HEC-HMS subbasin (NOAA, 2021).

4.7 STREAM FLOW AND STAGE DATA

The USGS stream flow and reservoir pool elevation gages located in the basin are listed in Table 4.1, while Table 4.2 lists the LCRA maintained stream flow and reservoir gage locations that were used in this study. Tables 4.1 and 4.2 also indicate whether the gage record was used in this study's statistical analysis or in the calibration of the HEC-HMS model. Statistical analyses were only performed for gages that had at least 20 years of record, and HEC-HMS calibrations were only performed for gages that were recording during one or more significant flood events during the past 30 years. The periods of record for these gages will be shown in the next chapter in Table 5.1. For these gage sites, annual peak flow data and 15-minute stream flow and stage data was collected from the USGS National Water Information System (NWIS) database (USGS, 2020). For the LCRA gages, daily and hourly data was obtained directly from the staff at LCRA's River Operations Center.

Table 4.1: USGS Stream Flow and Reservoir Pool Elevation Gages in the Lower Colorado River Basin

	USGS ID	Gage Name	HEC-HMS Drainage Area (sq mi)	Data Type	Used in HEC-HMS Model Calibration	Used for Statistical Analysis
1	08124000	Colorado River at Robert Lee, TX	30.9	Flow	Yes	Yes
2	08125500	Oak Ck Res nr Blackwell; TX	237.4	Elevation	Yes	
3	08126380	Colorado River near Ballinger, TX	1076.2	Flow	Yes	Yes
4	08127000	Elm Creek at Ballinger, TX	466.8	Flow	Yes	Yes
5	08128400	Middle Concho River abv Tankersley	2133.0	Flow	Yes	Yes
6	08129300	Spring Creek above Tankersley, TX	427.2	Flow	Yes	Yes
7	08130500	Dove Creek at Knickerbocker, TX	224.4	Flow	Yes	Yes
8	08130700	Spring Creek near San Angelo, TX	678.9	Flow	Yes	
9	08128000	South Concho River at Christoval, TX	415.4	Flow	Yes	Yes
10	08131200	Twin Buttes Reservoir nr San Angelo TX	3422.5	Elevation	Yes	Yes
11	08131400	Pecan Creek nr San Angelo, TX	81.0	Flow	Yes	Yes
12	08133500	North Concho River at Sterling City	586.0	Flow	Yes	Yes
13	08134000	North Concho River nr Carlsbad, TX	1220.7	Flow	Yes	Yes
14	08134250	North Concho River nr Grape Creek	1364.9	Flow	Yes	
15	08134500	O. C. Fisher Lk at San Angelo; TX	1462.8	Elevation	Yes	Yes
16	08136000	Concho River at San Angelo, TX	161.2	Flow	Yes	Yes
17	08136500	Concho River at Paint Rock, TX	1202.9	Flow	Yes	Yes
18	08136600	O. H. Ivie Res nr Voss; TX	3395.3	Elevation	Yes	Yes
19	08136700	Colorado River near Stacy, TX	3535.2	Flow	Yes	Yes
20	08140770	Lk Coleman nr Novice, TX	302.3	Elevation	Yes	
21	08140860	Jim Ned Creek nr Coleman, TX	447.0	Flow	Yes	
22	08141000	Hords Ck Lk nr Valera; TX	48.9	Elevation	Yes	Yes
23	08142000	Hords Creek near Coleman, TX	57.8	Flow	Yes	Yes
24	08140700	Pecan Bayou nr Cross Cut, TX	543.9	Flow	Yes	
25	08143000	Lk Brownwood nr Brownwood; TX	1513.0	Elevation	Yes	Yes
26	08143500	Pecan Bayou at Brownwood, TX	1603.8	Flow	Yes	Yes
27	08143600	Pecan Bayou nr Mullin, TX	2023.2	Flow	Yes	Yes
28	08144500	San Saba River at Menard, TX	1136.9	Flow	Yes	Yes
29	08144600	San Saba River nr Brady, TX	1636.4	Flow	Yes	Yes
30	08144900	Brady Ck Res nr Brady; TX	524.0	Elevation	Yes	
31	08145000	Brady Creek At Brady, TX	130.3	Flow	Yes	Yes
32	08146000	San Saba Rv at San Saba, TX	2523.4	Flow	Yes	Yes
33	08147000	Colorado River at San Saba, TX	10002.8	Flow	Yes	Yes
34	08148000	LCRA Lake Buchanan nr Burnet; TX	10694.7	Elevation	Yes	Yes
35	08149900	South Llano River at Flat Rock Ln at Junction, TX	878.9	Flow	Yes	
36	08148500	North Llano River nr Junction, TX	901.7	Flow	Yes	Yes
37	08150000	Llano River nr Junction, TX	1858.2	Flow	Yes	Yes
38	08150700	Llano Rv nr Mason, TX	3250.8	Flow	Yes	Yes

	USGS ID	Gage Name	HEC-HMS Drainage Area (sq mi)	Data Type	Used in HEC-HMS Model Calibration	Used for Statistical Analysis
39	08150800	Beaver Ck nr Mason, TX	215.3	Flow	Yes	Yes
40	08151500	Llano River at Llano, TX	4202.0	Flow	Yes	Yes
41	08152000	Sandy Ck nr Kingsland, TX	346.2	Flow	Yes	Yes
42	08152500	LCRA Lake LBJ nr Marble Falls; TX	15701.7	Elevation	Yes	Yes
43	08152900	Pedernales Rv nr Fredericksburg	369.6	Flow	Yes	Yes
44	08153500	Pedernales Rv nr Johnson City, TX	900.9	Flow	Yes	Yes
45	08154500	LCRA Lake Travis nr Austin; TX	17530.7	Elevation	Yes	Yes
46	08154700	Bull Ck at Loop 360 nr Austin, TX	22.7	Flow	Yes	Yes
47	08155200	Barton Ck at SH 71 nr Oak Hill, TX	89.6	Flow	Yes	Yes
48	08155240	Barton Ck at Lost Ck Blvd nr Austin	107.9	Flow	Yes	Yes
49	08155300	Barton Ck at Loop 360, Austin	116.9	Flow	Yes	Yes
50	08155400	Barton Ck abv Barton Spgs at Austin	120.0	Flow	Yes	Yes
51	08158000	Colorado River at Austin, TX	250.2	Flow	Yes	Yes
52	08158600	Walnut Ck at Webberville Rd, Austin	51.7	Flow	Yes	Yes
53	08158700	Onion Ck nr Driftwood, TX	123.7	Flow	Yes	Yes
54	08158827	Onion Ck at I-35 nr Twin Creeks Rd	234.0	Flow	Yes	
55	08159000	Onion Ck at US Hwy 183, Austin, TX	323.7	Flow	Yes	Yes
56	08159200	Colorado River at Bastrop, TX	1223.8	Flow	Yes	Yes
57	08159500	Colorado Rv at Smithville, TX	1705.8	Flow	Yes	Yes
58	08160400	Colorado Rv abv La Grange, TX	2117.3	Flow	Yes	Yes
59	08161000	Colorado River at Columbus, TX	2885.1	Flow	Yes	Yes
60	08162000	Colorado Rv at Wharton, TX	3248.3	Flow	Yes	Yes
61	08162500	Colorado River near Bay City, TX	3529.6	Flow	Yes	Yes
62	08162501	Colorado River near Wadsworth, TX	3595.2	Flow	Yes	

Table 4.2: LCRA Stream Flow and Reservoir Pool Elevation Gages in the Lower Colorado River Basin

	LCRA ID	Gage Name	HEC-HMS Drainage Area (sq mi)	Data Type	Used in HEC-HMS Model Calibration	Used for Statistical Analysis
1	1199	Colorado River at Winchell, TX	4535.4	Flow	Yes	Yes
2	1277	Colorado River near Goldthwaite, TX	7228.4	Flow	Yes	
3	1925	Colorado River at Bend, TX	10139.1	Flow	Yes	
4	1929	Cherokee Creek nr Bend, TX	158.8	Flow	Yes	Yes
5	2313	Johnson Fork near Junction, TX	292.8	Flow	Yes	Yes
6	2399	James River near Mason	326.3	Flow	Yes	Yes
7	2424	Comanche Creek near Mason	46.3	Flow	Yes	Yes
8	2443	Willow Creek near Mason	57.9	Flow	Yes	Yes
9	2498	Hickory Creek near Castell	168.0	Flow	Yes	Yes
10	2616	San Fernando Creek near Llano	128.9	Flow	Yes	Yes
11	2625	Johnson Creek near Llano	46.6	Flow	Yes	Yes
12	2669	Little Llano River near Llano	48.2	Flow	Yes	Yes
13	2694	Honey Creek near Kingsland	25.9	Flow	Yes	
14	2851	Sandy Creek near Willow City	151.6	Flow	Yes	Yes
15	2878	Sandy Creek near Click	300.0	Flow	Yes	Yes
16	2897	Walnut Creek near Kingsland	23.3	Flow	Yes	
17	2992	Backbone Creek at Marble Falls	30.1	Flow	Yes	Yes
18	3018	Hamilton Creek near Marble Falls	77.5	Flow	Yes	Yes
19	3328	South Grape Creek near Luckenbach	27.3	Flow	Yes	
20	3343	Pedernales River at LBJ Ranch near Stonewall	625.6	Flow	Yes	Yes
21	3369	North Grape Creek near Johnson City	89.0	Flow	Yes	Yes
22	3491	Miller Creek near Johnson City	87.5	Flow	Yes	
23	3529	Flat Creek nr Pedernales Falls State Park	30.7	Flow	Yes	
24	3558	Cypress Creek near Cypress Mill	71.2	Flow	Yes	Yes
25	3920	Cow Creek near Lago Vista	42.7	Flow	Yes	
26	3953	Big Sandy 2 Creek near Jonestown	34.1	Flow	Yes	
27	4595	Onion Creek at Buda	167.3	Flow	Yes	Yes
28	5417	Gilleland Creek near Manor	41.4	Flow	Yes	Yes
29	5423	Colorado River near Webberville	774.5	Flow	Yes	
30	5464	Wilbarger Creek near Elgin	163.7	Flow	Yes	Yes
31	5476	Colorado River at Sim Gideon River Plant	1171.4	Flow	Yes	
32	5521	Cedar Creek near Bastrop	130.4	Flow	Yes	
33	5523	Cedar Creek below Bastrop	345.4	Flow	Yes	
34	5525	Colorado River near Upton	1602.9	Flow	Yes	
35	5608	Buckners Creek near Muldoon	91.6	Flow	Yes	Yes
36	5696	Cummings Creek near Frelsburg	251.9	Flow	Yes	Yes
37	6377	Colorado River near Altair	2979.6	Flow	Yes	
38	6537	Colorado River near Lane City, TX	3277.9	Flow	Yes	

4.8 RESERVOIR PHYSICAL DATA

According to the National Inventory of Dams (NID), approximately 720 dams exist within the Lower Colorado River basin, most of which are NRCS structures or other small dams. Of these, 12 reservoirs were selected to be modeled in detail due to their sizable flood storage and their noticeable influence on the discharges of the major rivers downstream. Table 4.3 summarizes the reservoir data obtained for the 12 dams that were modeled in detail and their corresponding data sources. The twelve modeled reservoirs include two USACE reservoirs and three major LCRA operated reservoirs. The remaining 700+ smaller dams were scattered throughout the rural areas of the basin. These dams were not modeled in detail but were accounted for in the model through adjustments to the subbasins' initial losses and peaking coefficients. Data for these dams was obtained from the National Inventory of Dams (USACE, 2016).

Table 4.3: Reservoir Data and Sources for Dams Modeled in Detail

Reservoir Name	Drainage Area (sq mi)	Normal Storage (ac-ft)	Data Type	Sources
Oak Creek Reservoir	237	39,360	Elevation-Storage Curve, Spillway Rating Curve	City of Sweetwater, 1976 Phase 1 Dam Inspection Report
Ballinger Lakes, Upper and Lower	231	2700, 6000	Elevation-Storage Curve, Spillway Rating Curve	City of Ballinger, National Inventory of Dams, USACE calculations
Twin Buttes Reservoir	3423	186,468	Elevation-Storage Curve, Spillway Rating Curve, Observed Releases	Bureau of Reclamation, USACE Fort Worth District
O.C. Fisher Reservoir	1463	119,200	Elevation-Storage Curve, Spillway Rating Curve, Observed Releases	USACE Fort Worth District
O.H. Ivie Reservoir	3395	554,340	Elevation-Storage Curve, Observed Releases	Colorado River Municipal Water District, USACE Fort Worth District
Lake Coleman	302	38,076	Elevation-Storage Curve, Combined Elevation-Discharge Curve	Texas Water Development Board (TWDB), 1993 USACE Pecan Bayou report
Hords Creek Reservoir	49	8,640	Elevation-Storage Curve, Spillway Rating Curve, Observed Releases	USACE Fort Worth District
Lake Brownwood	1513	131,530	Elevation-Storage Curve, Combined Elevation-Discharge Curve	TWDB, 1993 USACE Pecan Bayou report
Brady Creek Reservoir	524	30,430	Elevation-Storage Curve, Combined Elevation-Discharge Curve	1980 Phase I Dam Inspection Report, USACE Fort Worth District
Lake Buchanan	10695	886,626	Elevation-Storage Curve, Existing and Proposed Water Management Plans, Observed Releases	LCRA
Lake LBJ	15702	133,090	Elevation-Storage Curve, Water Management Plan, Observed Releases	LCRA
Lake Travis	17531	1,134,956	Elevation-Storage Curve, Water Management Plan, Observed Releases	LCRA

4.9 SOFTWARE

The following table provides a summary of the significant computer software programs and versions that were used in in this study for the hydrologic analyses of the Lower Colorado River basin.

Table 4.4: Summary of Software Used in the Watershed Hydrology Assessment

Program	Version	Capability	Developer
ArcGIS	10.8.2	Geographical Information System	ESRI
HEC-DSSVue	3.2.3	Plot, tabulate, edit and manipulate data in HEC-DSS format	HEC
HEC-GeoHMS	10.2	Watershed delineation and generating HEC-HMS input	HEC
HEC-METVUE	3.1	Processing and viewing precipitation data	HEC
HEC-HMS	4.10	Rainfall-Runoff Simulation	HEC
HEC-RAS	6.2	1D and 2D Hydraulic Routing	HEC
HEC-SSP	2.3	Statistical Software Package	HEC
RiverWare	8.0.1	River and Reservoir Simulation	CADSWES
RMC-RFA	1.1.0	Reservoir Frequency Analysis	RMC
PeakFQ	7.2	Statistical Analysis of Gage Records for Flood Frequency	USGS

5 Statistical Hydrology

Statistical analysis of the observational record from U.S. Geological Survey (USGS) streamgaging stations and other historical information provides an informative means of estimating flood flow frequency. Flood flow frequency is defined by values or quantiles of discharge for selected annual exceedance probabilities (AEPs) (England and others, 2019). The annual peak discharge data as part of systematic operation of a streamgaging station provides the foundation for a detailed analysis of peak discharge, but additional historical information pertaining to peak discharges also can be used. An annual peak discharge is defined as the maximum instantaneous discharge for a streamgaging station for a given water year, and annual peak discharge data for USGS streamgaging stations can be acquired through the USGS National Water Information System (NWIS) database (USGS, 2022). The statistical analyses are based on water-year increments. A water year is the 12-month period from October 1 of a given year through September 30 of the following year designated by the calendar year in which it ends.

For the statistical hydrology portion of the multifaceted hydrologic analysis, InFRM team members from the USGS analyzed annual peak streamflow records for the 45 USGS streamgages (gages) and 21 Lower Colorado River Authority (LCRA) streamgages (gages) in the Lower Colorado River Basin. The locations of USGS gages are shown on Figure 5.1, and the locations of LCRA gages are shown in Figure 5.2. The USGS and LCRA gages are also listed in Tables 5.1 and 5.2, respectively. Any use of trade, firm, or product names is for descriptive purposes only and does not imply endorsement by the U.S. Government.

This chapter provides a general summary of the data, analyses and results of the statistical analyses of the stream gage records that were completed for the InFRM Watershed Hydrology Assessment of the Lower Colorado River Basin. The remainder of this chapter is organized as follows: Section 5.1 provides a brief review of statistical methods, Section 5.2 investigates downward trends observed in annual peak streamflow in the upper part of the study area, Section 5.3 provides a review of USGS gage data and settings for computations, Section 5.4 provides a review of LCRA streamgage (gage) data and settings for computations, and Section 5.5 contains an analysis of changes to flood frequency estimates over time. Additional details on the statistical analyses are available in Appendix A: Statistical Hydrology.

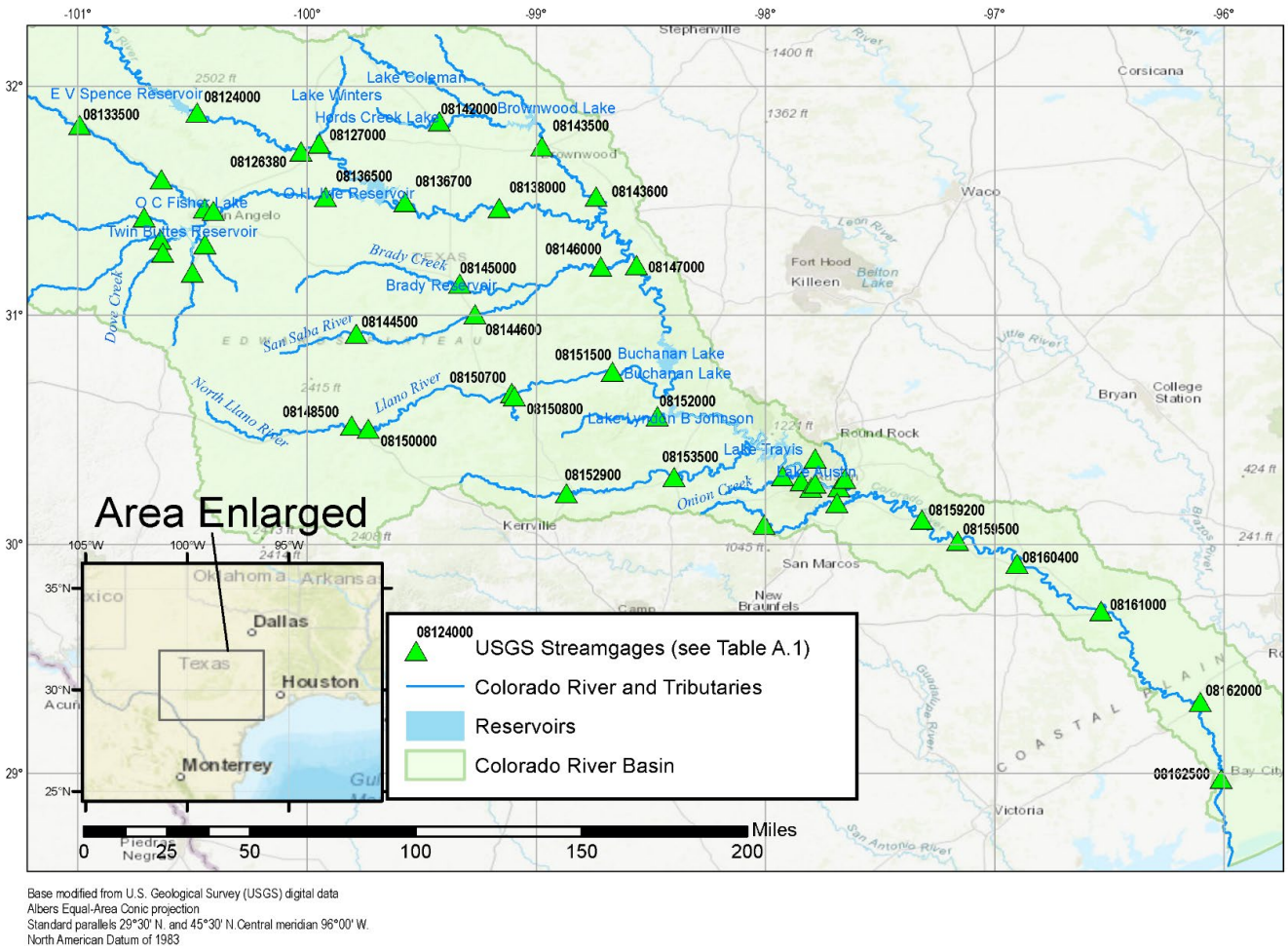

Figure 5.1: Map of U.S. Geological Survey (USGS) Streamgaging Stations included in the Statistical Analysis

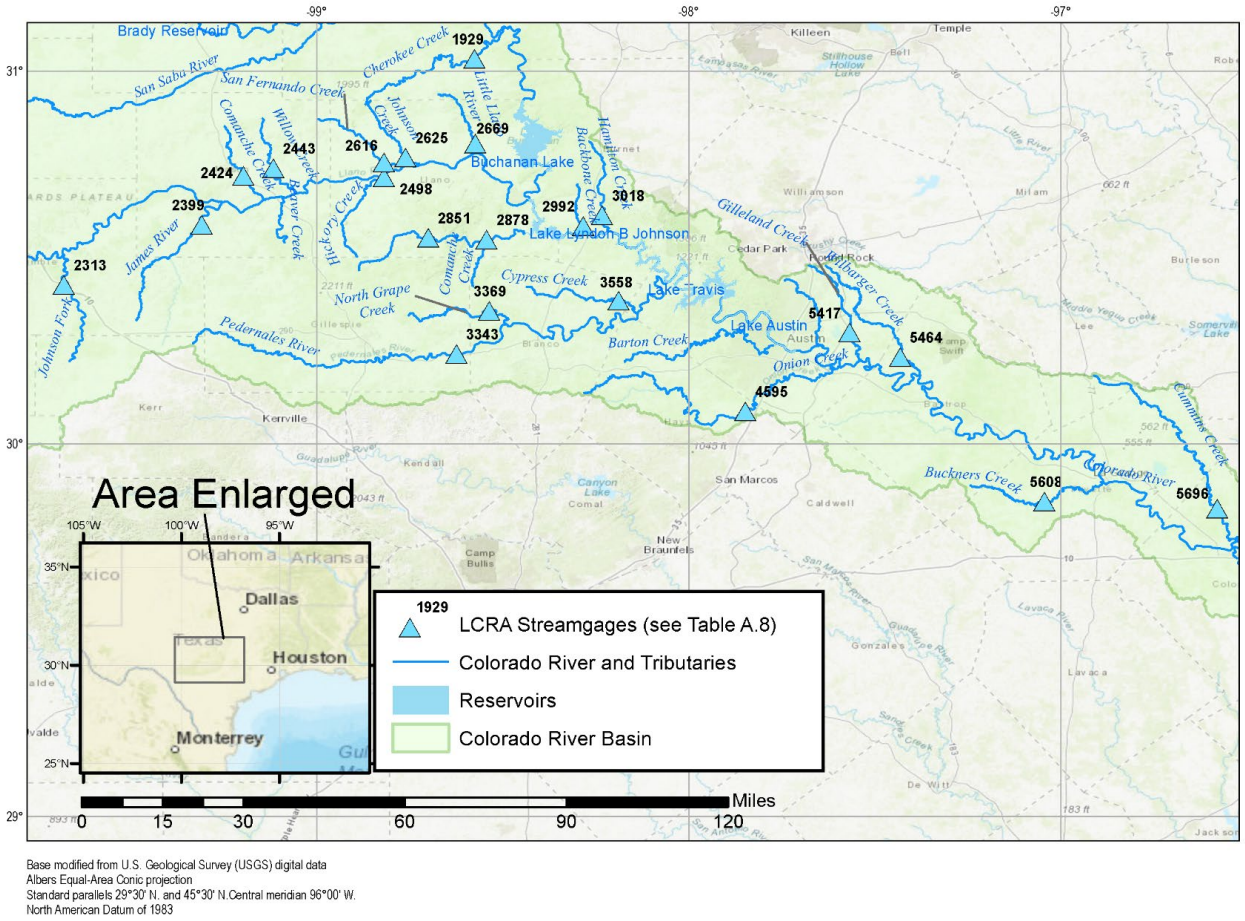

Base modified from U.S. Geological Survey (USGS) digital data
Albers Equal-Area Conic projection
Standard parallels 29°30' N. and 45°30' N.Central meridian 96°00' W.
North American Datum of 1983

Figure 5.2: Map of Lower Colorado River Authority (LCRA) Streamgages Included in the Statistical Analysis

Table 5.1: Summary of the U.S. Geological Survey Streamgaging Stations in the Lower Colorado River Basin Study Area, Texas with Ancillary Information

[(U), unregulated annual peak streamflow; (R), regulated annual peak streamflow (NWIS Peak Code 6); (U/R) a shift from unregulated to regulated peak streamflow during period of record; mi^2, square miles; --, dimensionless or not applicable; in., inches; PRISM, data product of the PRISM Climate Group Northwest Alliance for Computational Science and Engineering (PRISM Climate Group, 2018)]

Station number	Streamgage Name	Latitude	Longitude	Period of available annual peak streamflow	Period of analyzed annual peak streamflow	Contributing drainage area (mi^2)	Mean annual rainfall (PRISM 1981–2010) (in.)
08124000	Colorado River at Robert Lee, TX	31.8853	-100.4803	1924–2020	1969–2020(R)	5,047	22.7
08126380	Colorado River near Ballinger, TX	31.7153	-100.0261	1908–2020	1969–2020(R)	6,098	24.2
08127000	Elm Creek at Ballinger, TX	31.7492	-99.9475	1933–2020	1933–2020(U/R)	450	24.2
08133500	N. Concho River at Sterling City, TX	31.8300	-100.9933	1940–2020	1940–2020(U)	568	19.7
08134000	N. Concho River nr Carlsbad, TX	31.5925	-100.6367	1925–2020	1962–2020(U)	1,191	21.8
08135000	N. Concho River at San Angelo, TX	31.4658	-100.4475	1916–1990	1952–1990(R)	1,450	21.9
08128400	Middle Concho River abv Tankersley, TX	31.4272	-100.7108	1961–2020	1961–2020(U)	1,116	21.1
08129300	Spring Creek abv Tankersley, TX	31.3300	-100.6400	1960–2020	1960–2020(R)	425	21.8
08130500	Dove Creek at Knickerbocker, TX	31.2739	-100.6306	1961–2020	1961–2020(U)	218	22.0
08128000	S. Concho River at Christoval, TX	31.1869	-100.5017	1906–2020	1906–2020(U)	354	22.8
08131400	Pecan Creek nr San Angelo, TX	31.3089	-100.4456	1936–2020	1936–2020(U)	81	22.4
08136000	Concho River at San Angelo, TX	31.4544	-100.4103	1906–2020	1963–2020(R)	4,411	21.8
08136500	Concho River at Paint Rock, TX	31.5158	-99.9192	1882–2020	1963–2020(R)	5,443	25.1
08136700	Colorado River near Stacy, TX	31.4936	-99.5736	1936–2020	1990–2020(R)	12,802	26.8
08138000	Colorado River at Winchell, TX	31.4678	-99.1619	1924–2011	1963–2011(R)	13,788	28.1
08142000	Hords Creek near Coleman, TX	31.8467	-99.4247	1941–2020	1941–2020(U/R)	107	28.2
08143500	Pecan Bayou at Brownwood, TX	31.7364	-98.9755	1918–2020	1933–2020(R)	1,660	29.8
08143600	Pecan Bayou nr Mullin, TX	31.5172	-98.7403	1968–2020	1968–2020(R)	2,073	29.5
08144500	San Saba River at Menard, TX	30.9189	-99.7853	1916–2020	1916–2020(U/R)	1,128	24.4
08144600	San Saba River nr Brady, TX	31.0039	-99.2686	1980–2012	1980–2012(U)	1,626	26.2
08145000	Brady Creek at Brady, TX	31.1381	-99.3347	1931–2020	1963–2020(R)	588	27.0
08146000	San Saba River at San Saba, TX	31.2131	-98.7192	1916–2020	1916–2020(U/R)	3,039	28.6
08147000	Colorado River near San Saba, TX	31.2178	-98.5642	1900–2020	1963–2020(R)	19,819	29.3
08148500	N. Llano River nr Junction, TX	30.5172	-99.8058	1889–2020	1889–2020(U)	914	24.1
08150000	Llano River nr Junction, TX	30.5042	-99.7342	1916–2020	1916–2020(U/R)	1,849	24.1
08150700	Llano River nr Mason, TX	30.6606	-99.1089	1889–2020	1889–2020(U)	3,242	28.4
08150800	Beaver Creek nr Mason, TX	30.6433	-99.0956	1964–2020	1964–2020(U)	215	28.6
08151500	Llano River at Llano, TX	30.7511	-98.6694	1935–2020	1935–2020(U)	4,192	27.3

Station number	Streamgage Name	Latitude	Longitude	Period of available annual peak streamflow	Period of analyzed annual peak streamflow	Contributing drainage area (mi^2)	Mean annual rainfall (PRISM 1981–2010) (in.)
08152000	Sandy Creek nr Kingsland, TX	30.5575	-98.4719	1952–2020	1952–2020(U)	346	30.0
08152900	Pedernales River near Fredericksburg, TX	30.2203	-98.8694	1979–2020	1979-2020(U)	369	31.0
08153500	Pedernales River near Johnson City, TX	30.2917	-98.3992	1940–2020	1940–2020(R)	901	32.7
08154700	Bull Creek at Loop 360 near Austin, TX	30.3719	-97.7844	1979–2020	1979–2020(U)	22	33.3
08155200	Barton Creek at SH 71 nr Oak Hill, TX	30.2961	-97.9253	1976–2020	1976–2020(U)	90	33.3
08155240	Barton Creek at Lost Creek Blvd nr Austin, TX	30.2739	-97.8444	1929–2020	1929–2020(U)	107	33.4
08155300	Barton Creek at Loop 360, Austin, TX	30.2444	-97.8019	1929–2020	1929–2020(U)	116	33.6
08155400	Barton Creek abv Barton Springs at Austin, TX	30.2633	-97.7719	1999–2020	1999–2020(U)	125	33.6
08158000	Colorado River at Austin, TX	30.2461	-97.6801	1869–2020	1940–2020(R)	27,606	34.1
08158600	Walnut Creek at Webberville Rd, Austin, TX	30.2831	-97.6547	1966–2020	1966–2020(U)	51	34.1
08158700	Onion Creek near Driftwood, TX	30.0828	-98.0075	1941–2020	1941–2020(U)	124	35.6
08159000	Onion Creek at US Hwy 183, Austin, TX	30.1778	-97.6883	1921–2020	1921–2020(U/R)	321	34.4
08159200	Colorado River at Bastrop, TX	30.1044	-97.3192	1961–2020	1961–2020(R)	28,576	35.7
08159500	Colorado River at Smithville, TX	30.0125	-97.1617	1931–2020	1941–2020(R)	28,968	37.8
08160400	Colorado River above La Grange, TX	29.9122	-96.9036	1989–2020	1989–2020(R)	29,471	39.8
08161000	Colorado River at Columbus, TX	29.7061	-96.5367	1908–2020	1941–2020(R)	30,237	43.3
08162000	Colorado River at Wharton, TX	29.3089	-96.1036	1919–2020	1941–2020(R)	30,600	46.8
08162500	Colorado River near Bay City, TX	28.9739	-96.0122	1940–2020	1941–2020(R)	30,837	47.8

Table 5.2: Summary of the Lower Colorado River Authority (LCRA) Streamgaging Stations in the Lower Colorado River Basin Study Area, Texas with Ancillary Information

[mi^2, square miles; --, dimensionless or not applicable; in., inches; PRISM, data product of the PRISM Climate Group Northwest Alliance for Computational Science and Engineering (PRISM Climate Group, 2018)]

Streamgage Name	LCRA Site Number	Latitude	Longitude	Period of analyzed annual peak streamflow	Contributing drainage area (mi^2)	Mean annual rainfall (PRISM 1981–2010) (in.)
Cherokee Creek near Bend, TX	1929	31.0321	-98.5774	1999–2020	160	29.1
Johnson Fork near Junction, TX	2313	30.4265	-99.6801	2000–2020	293	26.0
James River near Mason, TX	2399	30.5876	-99.3094	1999–2000	326	28.0
Comanche Creek near Mason, TX	2424	30.7186	-99.1978	2000–2020	46	27.6
Willow Creek near Mason, TX	2443	30.7384	-99.1177	1999–2020	57	27.8
Hickory Creek near Castell, TX	2498	30.7148	-98.8205	2000–2020	168	28.2
San Fernando Creek near Llano, TX	2616	30.7550	-98.8197	1999–2020	128	28.1
Johnson Creek near Llano, TX	2625	30.7681	-98.7617	2003–2020	46	27.7
Little Llano River near Llano, TX	2669	30.8055	-98.5747	2000–2020	48	27.8
Sandy Creek near Willow City, TX	2851	30.5528	-98.7013	2003–2020	151	29.3
Sandy Creek near Click, TX	2878	30.5470	-98.5445	2002–2020	300	29.5
Backbone Creek at Marble Falls, TX	2992	30.5837	-98.2841	1998–2020	32	30.7
Hamilton Creek near Marble Falls, TX	3018	30.6122	-98.2339	2003–2020	77	30.7
Pedernales River at LBJ Ranch near Stonewall, TX	3343	30.2408	-98.6253	1925–2020	625	32.5
North Grape Creek near Johnson City, TX	3369	30.3558	-98.5373	2002–2020	89	31.8
Cypress Creek near Cypress Mill, TX	3558	30.3839	-98.1899	2001–2020	71	32.0
Onion Creek at Buda, TX	4595	30.0864	-97.8485	1929–2020	168	35.2
Gilleland Creek near Manor, TX	5417	30.2978	-97.5681	1995–2020	42	34.3
Wilbarger Creek near Elgin, TX	5464	30.2318	-97.4327	2003–2020	164	34.8
Buckners Creek near Muldoon, TX	5608	29.8452	-97.0447	1998–2020	92	38.3
Cummins Creek near Frelsburg, TX	5696	29.8258	-96.5807	1997–2020	252	41.8

5.1 STATISTICAL METHODS

The statistical methods applied in this analysis include the fitting of a log-Pearson type III probability distribution (LPIII) to the annual peak streamflow data for the Lower Colorado River Basin. The general purpose of fitting a probability distribution is to provide an objective mechanism to extrapolate to hazard levels (as represented by AEPs and equivalently expressed as annual recurrence interval or recurrence interval measured in years) beyond those represented by the sample size of annual peak streamflow data for a given gage. The LPIII distribution was fit to the logarithm (base-10) of the annual peak streamflow data. The USGS-PeakFQ software version 7.2 (Veilleux and others, 2013; USGS, 2014) provides the foundation for the results of the flood flow frequency estimates that are specified by average annual recurrence intervals computed and extracted from software output at 2, 5, 10, 25, 50, 100, 200, and 500 year recurrence intervals or respective AEPs of 0.500, 0.200, 0.100, 0.040, 0.020, 0.010, 0.005, and 0.002 along with the accompanying 95-percent confidence limits. The terms “flow,” “streamflow,” and “discharge” are synonymous and are used interchangeably in this report. All three terms refer to the volume of water that passes a given point within a given period of time; all are expressed in units of cubic feet per second (cfs).

A complementary statistical technique used for initial data analysis included the non-parametric rank based Pettitt test (Pettitt, 1979). The Pettitt test is a commonly used technique to test for an abrupt shift in a data series, such as annual peak streamflow data (Mallakpour and Villarini, 2016; Ryberg and others, 2019). For this analysis, the Pettitt test was used to aid in the determination of the point at which a new reservoir upstream from a gage began to have an effect on peak streamflow, referred to as the “change point.” The Pettitt test was used to identify the water year of the change point and measure of its statistical significance with a probability value (p-value). Taken together with a simple visual analysis of the plotted annual peak streamflow series, an analysis of the type and extent of the upstream reservoir (or reservoirs), and the intervening drainage area between the upstream reservoir and gage among other considerations, the Pettitt test is a powerful tool for determining whether the NWIS code ‘6’ designation (discharge affected by regulation or diversion) has a measurable or statistically significant effect on flows at the gaged location. A statistically significant change point was determined when the p-value for the Pettitt test at a given gage was less than 0.05. These values and the specific change point indicated by the Pettitt test are discussed further in the next section with the flood flow frequency results for each gage.

A second statistical technique used for data evaluation included the Kendall’s tau (correlation) test. The Kendall’s tau test (Hollander and Wolfe, 1973; Helsel and others, 2020) was used through the USGS-PeakFQ software to detect for the presence of monotonic upward or downward trends in the annual peak streamflow data. The test is only applied to the peak streamflow data used in the analysis. For example, if a portion of the annual peak streamflow record is removed because it represents a period of record prior to reservoir impoundment (that is, the completion of reservoir construction by deliberate impoundment of water), then the test will only be applied to the record that is kept after reservoir construction. The Kendall’s tau test is a popular statistic for quantifying the presence of monotonic changes in the central tendency of streamflow data in time. Many of the gages showed a trend in annual peak streamflow at a 0.1 significance level (probability value [p-value] of 0.10). Because the Kendall’s tau test is a two-tailed test, the p-value must be divided by two to determine whether the identified trend is a statistically significant upward or downward trend (Helsel and others, 2020). Therefore, a p-value of 0.05 was used as the threshold for determining whether annual peak streamflow is trending upward or downward in the Colorado River basin.

All of the gages except two that exhibited a statistically significant trend showed a statistically significant downward trend as indicated by the p-values less than 0.05 and negative Kendall's tau values. Similar results are shown in Harwell and others (2020), who found a strong downward trend in annual peak streamflow for most of the Colorado River basin upstream from the Colorado River near San Saba, Texas streamgage. A key difference in the Harwell and others (2020) study is that they analyzed the full record of annual peak streamflow at a gage, not accounting for the influence of regulation as was done in the present study. Therefore, it is even more notable that these downward trends in annual peak streamflow are observed after streamflow became regulated in Colorado River basin upstream from the Colorado River near San Saba, Texas streamgage. Downward trends in streamflow are discussed further in the next section.

Flood flow frequency analyses were done for each gage by using annual peak data from the USGS NWIS database (USGS, 2022) augmented with historical observations prior to gage installation and other types of data when necessary. The Interagency Advisory Committee on Water Data (IACWD, 1982) describes the Bulletin 17B method (B17B) to conduct the frequency analysis (USGS, 2014), but the statistical frequency analysis performed for the gages in the Lower Colorado River basin use the updated guidelines from the Bulletin 17C (England and others, 2019). In particular, the use of the expected moments algorithm (EMA) was used for this study (England and others, 2019; USGS, 2014).

EMA enables sophisticated interpretations of the historical record intended to enhance the estimates of peak streamflow, especially for the rare frequency events such as the 100-year streamflow (AEP of 0.010). When available, inclusion of historical record interpretations can have the net effect of lowering (decreasing) flood flow frequency estimates for the largest of streamflows because the largest documented events are assigned lower empirical probabilities. EMA also permits inclusion of nonstandard information such as data censoring. For example, an annual peak might be known to be lower than a specified streamflow threshold. EMA can also accommodate time varying streamflow thresholds based on assigning a streamflow threshold as a 'highest since' within discrete intervals of time. This nonstandard information collectively can be thought of as a framework fostering record extension. Not all gages have nonstandard information, but the use of EMA is preferred because confidence limits and associated standard errors of sampling for the flood quantiles are mathematically correct.

Asquith and Slade (p. 1, 1995) explain "the Interagency Advisory Committee on Water Data (IACWD) (1982) provides a standard procedure for peak-streamflow frequency calculation that involves a standard frequency distribution—the log-Pearson Type III (LPIII) distribution. The LPIII distribution uses systematic and historical peak-streamflow values to define its frequency distribution. The curvature in the distribution is defined by a skew coefficient used in the calculation procedure." Skew coefficients can be site-specific (station skew coefficients) or regional in nature (regional skew coefficients). The choice of skew is emphasized in IACWD (1982) to mitigate for the extreme variance in annual peak streamflows found in streamgage records of varying lengths. The regional skew coefficient is a built-in feature of the USGS PeakFQ software but can be overridden by the user. Asquith and others (2021) developed generalized (regional) skew coefficients for Texas, and these estimates may be considered contemporary, and therefore valid, for this study (2020). The period of record at several of the streamgages in the lower Colorado River basin did not characterize the range of peak streamflow well for various reasons. For example, there might have been few or no appreciable floods (for example, floods exceeding bank-full conditions) during the available period of record, the period of record might have been shortened as a result of substantial removal of "potentially influential low floods" (England and others, 2019), or the period of record might represent a unique flood distribution influenced by regulation or site-specific features such as the shape of the floodplain (Asquith and Slade, 1997). Citing the work of others, Ryberg

and others (p. 24, 2020) explain "small floods may be the result of a different hydrologic process than the larger floods with low annual exceedance probabilities (AEPs) and they can have a large effect on the distribution fitting procedure (Cohn and others, 2013; England and others, 2019), hence the name "potentially influential low floods." It was decided to weight the HEC-SSP computed skew of the selected streamgages in the Lower Colorado River basin with the regional skew values obtained from Asquith and others' (2021) plots of regional skew for Texas, Oklahoma, and eastern New Mexico. In order to use the regional skew values, the weighted-skew option in the PeakFQ software was required in conjunction with manual entry of skew information (USGS, 2014). The Asquith and others (2021) regional skew values used are listed in Appendix A.

A brief sensitivity analysis was performed at sites where the station skew deviated considerably from published regional skew values, or where the calculated flood frequency curve did not appear to fit the ordered peak floods well, or the calculated flood frequency curve produced estimates that were not consistent with flood-frequency estimates at upstream and downstream streamgages. Otherwise, preference was given to utilizing the station skew at each streamgage. Although a calculated station skew that differs greatly from the regional skew estimate is cause for further investigation, it is not necessarily justification for weighting by the regional skew value. This is because the gaged location may have hydrological characteristics that differ from the greater regionalized hydrology. If a choice other than station skew was selected for an analysis, the details of the skew selection are discussed in each gage's analysis listed in Section 5.3.

PeakFQ and HEC-SSP incorporate the Multiple Grubbs Beck Test (MGBT) to detect potentially influential low floods, also known as low outliers (Cohn and others, 2013). Low outliers within a time series of peak streamflow often need special consideration during a flood frequency analysis. These low outliers may include annual peak streamflows that either were not generated from storm runoff or may have been only generated from a highly localized storm. These low outliers are not representative of the overall flood risk of the watershed and are given special consideration in the form of a conditional probability adjustment. The MGBT was used to identify and partially exclude potentially influential low floods from the analysis (the potentially influential low floods are retained in the dataset, but partially excluded from analysis). Within PeakFQ, those peaks identified as potentially influential low floods are recoded as less than a threshold streamflow and treated as interval data in the expected moments algorithm because potentially influential low floods do not convey meaningful information about the magnitude of floods with very low AEPs, but if retained in the analysis they can influence the frequency estimates of very low AEP floods. See appendix 7 of Bulletin 17C (England and others, 2019) for more information on the treatment of potentially influential low floods in the expected moments algorithm. For streamgage-specific reasons, the analyst can manually specify a low-outlier threshold. Low-outlier threshold values for each streamgage are identified and discussed further in the individual writeups for each streamgage that follow in this section. Although the ultimate decision for specifying a low-outlier threshold to identify influential low floods is based on engineering judgment, Bulletin 17C provides some general guidelines for choosing an appropriate threshold (England and others, 2019). For each flood frequency analysis, the computed curve is evaluated for its fit to the data. If the data appear to have a clear inflection point or shift in the ordered peaks that the MGBT did not identify, then the low outlier may be adjusted (England and others, 2019).

Additionally, a brief sensitivity analysis is performed at all sites to determine the effects of the selected low-outlier threshold on the flood frequency curve. Can the low-outlier threshold be adjusted to improve the station skew? Can the low-outlier threshold be adjusted to bring the estimates more in line with flood-frequency curves from upstream and downstream streamgages? These factors and more are considered for the low-outlier threshold for each gaged location analyzed. Low-outlier threshold values for each gage are identified in Appendix A.

Confidence limits of flood flow frequency can be informative to decision makers. The lower and upper limits of 95-percent confidence intervals were computed for this study. Confidence intervals can be expected to encompass the true value 95 percent of the time (Good and Hardin, 2006, p. 101). The range in these numbers for the lower and upper 95-percent confidence limits increases with the more extreme events.

5.2 DOWNWARD TRENDS IN ANNUAL PEAK STREAMFLOW

Statistically significant downward trends in annual peak streamflow were observed in this study, particularly in the part of the Colorado River basin upstream from the Colorado River near San Saba, TX streamgage (this part of the Colorado River basin is hereinafter referred to as the "upper Colorado River basin"). Similar results are shown in Harwell and others (2020), who analyzed precipitation, streamflow, and potential flood storage trends in the Colorado River basin in Texas. Harwell and others (2020) found moderate to strong downward trends in both streamflow volume and annual peak streamflow in nearly half of the gages analyzed in their study, most in the upper sections of the basin. A key difference in the Harwell and others (2020) study is that they analyzed the full record of annual peak streamflow at a gage and did not account for the influence of regulation. The present study accounts for the influence of regulation and analyzes only the period of record representative of the basin's recent (2020) regulation following Bulletin 17C guidelines (England and others, 2017). The downward trends in annual peak streamflow observed in this study occurred even after the establishment of a regulated watershed. Additionally, the Harwell study (2020) found no significant trends in annual precipitation across the Colorado River basin. However, the gages that indicated a downward trend in annual peak streamflow also showed downward trends in the ratio of streamflow volume to precipitation volume on an annual time step, which indicates a change in the way the Colorado River basin responds to precipitation events over time. The report also analyzed groundwater-level trends in relation to precipitation and streamflow trends in the basin. Although downward trends in groundwater levels were observed in the Carrizo-Wilcox and Gulf Coast aquifers, downward trends in streamflow were not observed in the outcropping of either aquifer. However, downward groundwater-level trends in the Trinity aquifer outcrop do appear to correspond with streamflow declines upstream.

The Concho River basin, a major tributary to the Colorado, also experienced widespread downward trends. Harwell and others (2020) identified downward trends in annual peak streamflow on the North Concho River and mainstem Concho River downstream from Twin Buttes Reservoir, Lake Nasworthy, and O.C. Fisher Lake. Barbie and others (2012) analyzed streamflow trends in the Concho River Basin through 2009 and found similar declines in not only annual instantaneous peak streamflow, but also in annual maximum daily streamflow. Furthermore, declines were also observed in annual mean daily stream and annual 7-day minimum streamflow for USGS streamflow gaging station 08134000 North Concho River near Carlsbad, just upstream from O.C. Fisher Lake. Although the authors attributed declines in streamflow in the lower Concho River to the cumulative effects of the three major upstream reservoirs, declines in streamflow in the upper part of the basin indicate that the reservoirs are not the sole reason for the declines in streamflow the basin.

5.2.1 Climatic Trends

Though no significant trends in regional precipitation was found in the upper Colorado River basin, an analysis of the annual mean daily maximum temperature throughout the basin reveals a striking trend. Daily maximum temperature data for all counties overlapping the upper Colorado River basin were downloaded from the National Oceanic and Atmospheric Administration's (NOAA) National Climate Data

Center (NCDC) website (NOAA, 2020). Stations with less than 20 years of data or with data beginning after 1980 were excluded from the analysis. Annual mean daily maximum temperatures were calculated for each station with data coverage of at least 90 percent for a given year. Figure 5.3 plots these annual mean daily maximum temperatures for all sites meeting these criteria along with the mean of all stations and a 9-year moving average. After a relatively stable temperature regime in the first half of the century, a marked shift occurs in the late 1950s following the record drought of the same decade. Annual mean daily maximum temperatures decreased approximately 2 degrees Fahrenheit and remained relatively stable before they again began to increase in the 1990s. Although the approximately 100 years of record is informative, long-term (100+ year) climatic trends or cycles cannot be ascertained from the data. Instead, the record highlights an important warming trend of the past 30 years as well as a period of pronounced change in the middle of the century, coincident with the end of a drought and many change points identified in annual peak streamflow records analyzed in this report.

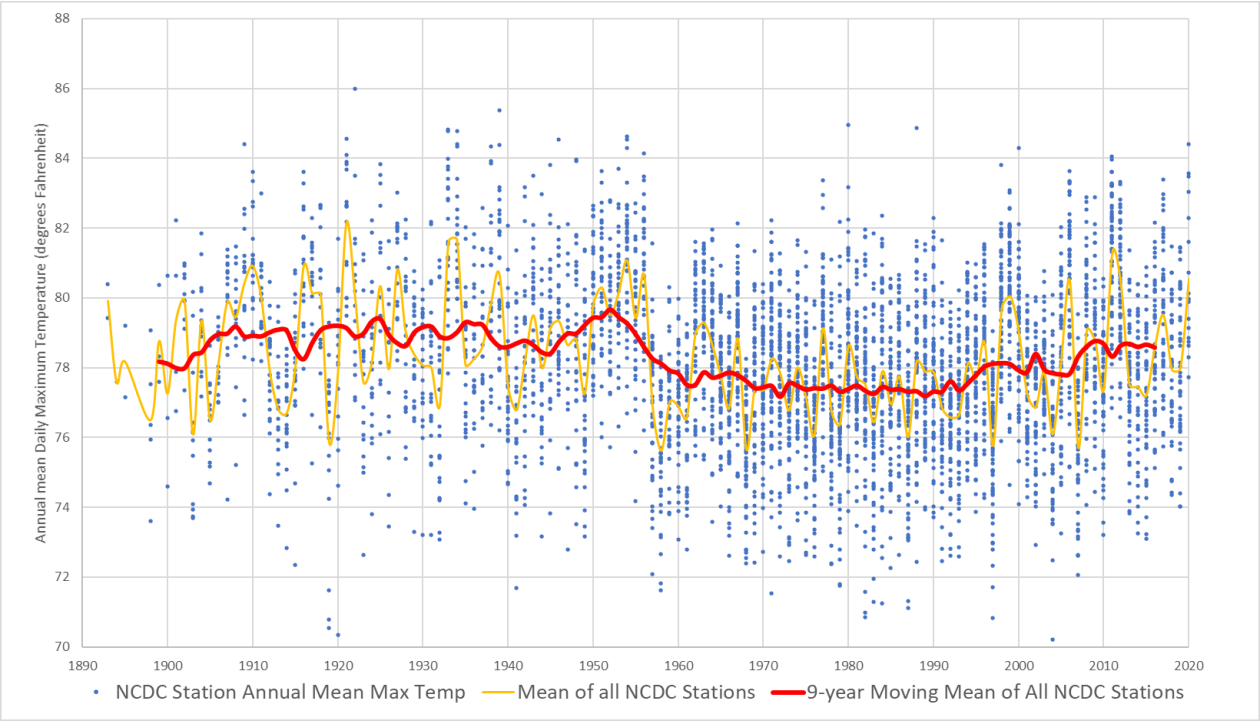

Figure 5.3: National Climatic Data Center (NCDC) Station Annual Mean Maximum (Max) Temperature (Temp) Plotted Alongside the Mean of all Stations and the 9-year Moving Mean.

Although many other factors are presented here that may affect annual peak streamflow, the relation between annual mean maximum daily temperature and annual peak streamflow is apparent, especially after the climatic shift circa 1960. Figure 5.4 plot the annual peak streamflow beside the regional temperature trends for the Colorado River near Ballinger, Texas. Visually there appears to be a correlation between temperature and streamflow, with a delayed decrease in streamflow in the 1960s associated with a decrease in temperatures and an inverse trend between streamflow and temperature observed thereafter.

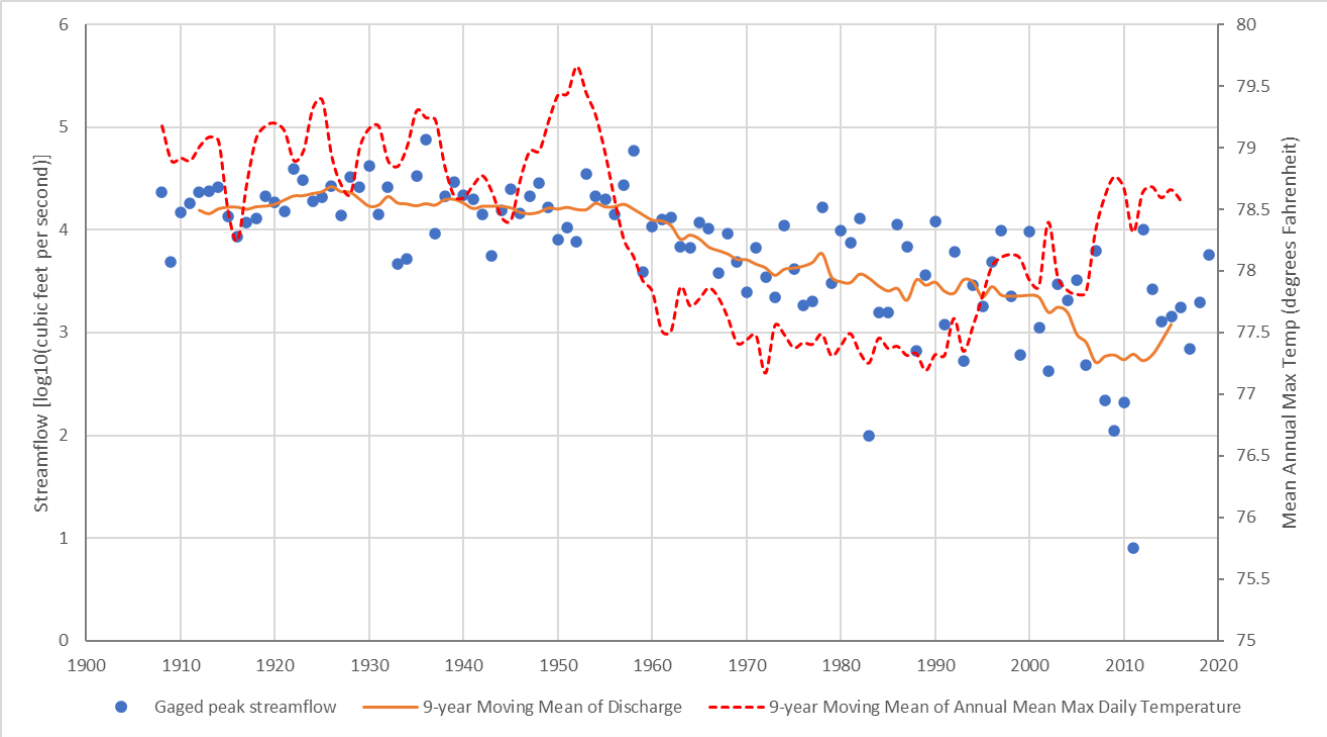

Figure 5.4: Gaged Peak Streamflow and the 9-year Moving Mean of Streamflow at USGS streamgage 08126380 Colorado River near Ballinger, TX Plotted Alongside the 9-year Moving Mean of Annual Mean Daily Maximum (Max) Temperature for all National Climatic Data Center Stations within the upper Colorado River basin.

The gradual increase in temperature beginning in the 1990s might be related to a larger region-wide trend of increasing temperatures across Texas and the southwestern part of the United States. A recent evaluation of climate models for Texas projects climatic responses that vary across the state, with regions that encompass the upper Colorado River basin experiencing upward trends in temperature with no identifiable trends in precipitation, leading to droughts of greater intensity and length (Venkataraman and others, 2016). Other studies of climate projections have suggested similar trends in increasing temperature for Texas and the southwestern part of the United States (Banner and others, 2010; Liu and others 2012; Jiang and Yang, 2012; Hoerling and others, 2013).

5.2.2 Reservoir Construction

Although the timing of the impoundment of O.C. Fisher Lake (1952) and Twin Buttes Reservoir (1963) coincided with a statistically significant shift in streamflows throughout the basin, as evidenced by downward trends in annual peak streamflows and statistically significant change points in the 1960s, the effects on streamflow downstream from the Concho River reservoirs are coincidental. Declines in peak streamflow are observed upstream from these reservoirs in both the North and South Concho Rivers. In fact, it may appear as though O.C. Fisher and Twin Buttes were designed for a system that generates greater streamflow volume than has been observed in the basin since their construction. Both reservoirs were constructed prior to the shift in peak streamflow, which means that the lower flows in the latter half of the century would not have been considered in their design. O.C. Fisher and Twin Buttes took approximately 5 and 11 years (1957 and 1974) to reach conservation pool elevation respectively, and neither has reached that level since Twin Buttes last reached conservation pool in 1977 (TWDB, 2020).

In the period between 1989 and 2019, O.C. Fisher and Twin Buttes have averaged 11 percent and 24 percent of normal pool respectively.

Minor reservoir construction has increased throughout the basin as well. The U.S. Army Corps of Engineers (USACE) National Inventory of Dams (NID) records an increase in storage for minor reservoirs (defined here as reservoirs with a smaller storage than Lake Nasworthy near San Angelo) in the upper Colorado River basin from just under 5,000 acre-ft in 1900 to nearly 900,000 acre-ft in as shown in Figure 5.5 (USACE, 2016). A greater proportion of 'larger' minor reservoirs (greater than 10,000 acre-ft max storage) were constructed in the 1950s and '60s.

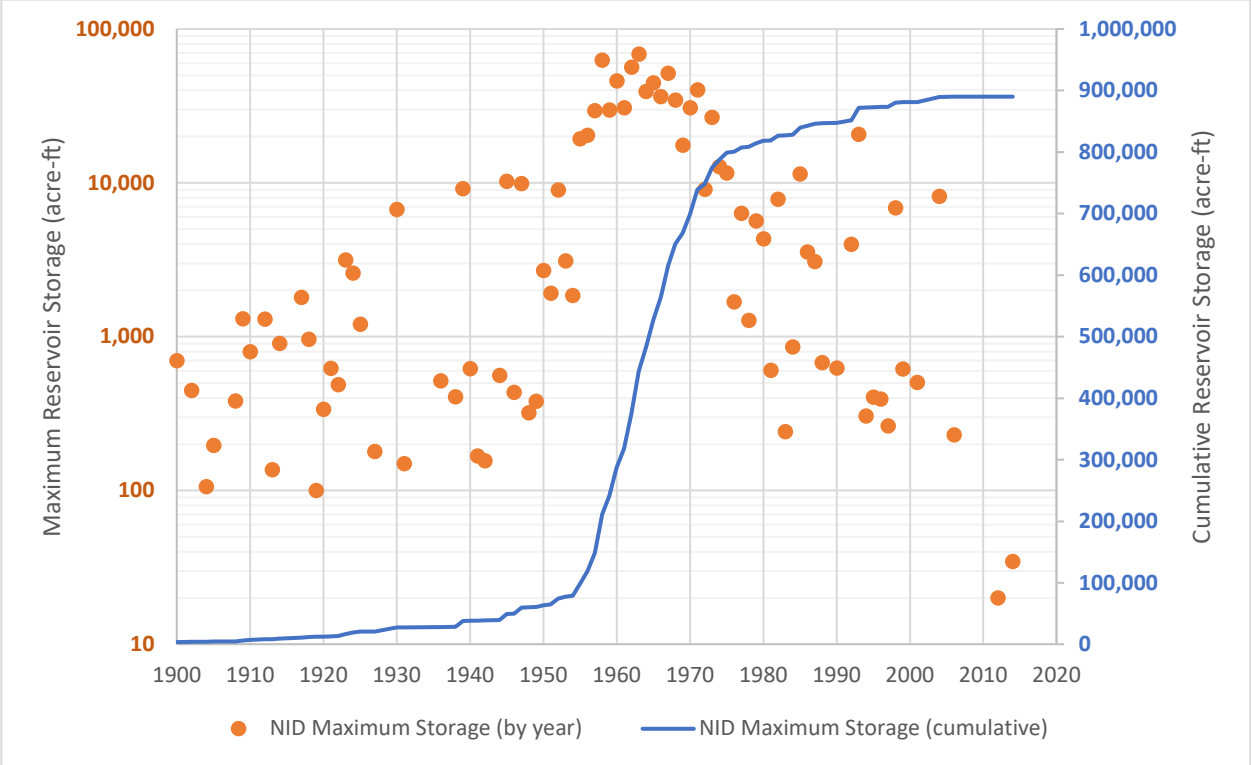

Figure 5.5: National Inventory of Dams (NID) Reservoir Maximum Storage (Left Axis) and Cumulative Reservoir Maximum Storage (Right Axis) in Acre-Feet for the upper Colorado River basin.

More details on the effects of irrigation, evapotranspiration, and vegetation on streamflow trends in the Lower Colorado River basin are included in Appendix A.

5.2.3 Summary of Declining Peak Trends

The Pettitt test identified many change points in the analyzed gages in the 1960s. The data indicate that a pronounced and enduring shift in basin hydrology likely occurred sometime in the 1960s followed by a slower, more gradual decline in streamflows that persists to the present time. Following the record historical drought of the 1950s, many Colorado River and tributary reservoirs were constructed during this time period (E.V. Spence Reservoir, 1969; Twin Buttes Reservoir, 1963; Coleman Lake, 1966; Brady Creek Reservoir, 1963).

However, it is unlikely that streamflow declines in the Colorado and Concho River basins upstream from the Highland Lakes can be attributed to a single factor. Rather, it is more likely the cumulative effect of

multiple changes within the basin that have resulted in a decades-long reduction in streamflow volumes and peak streamflow values. These multiple changes include, but are not limited to, increased evaporation due to reservoir and retention pond construction, increased reliance on irrigation use, and climactic changes. Therefore, the authors are confident that analyzing recent data (circa 1960 through WY 2020) in FFQ analysis is appropriate for those gages in the Colorado River Basin upstream from the Highland lakes exhibiting significant declines in annual peak streamflow. The distribution of flood events that occurred prior to 1960 would not be expected to occur with the same frequency in the future due to the fundamental land use, reservoir storage, irrigation, and climactic changes that the Colorado River basin has undergone.

Fifteen USGS gages exhibit downward trends in annual peak streamflow upstream from Austin, Texas when analyzing the full period of record available. If the record is shortened to 1963 to recent (2020), results from the Kendall's tau test indicate seven gages no longer exhibit statistically significant downward trends at a 0.05 significance level (p-value less than 0.05), as shown in Table 5.3. Of the remaining eight gages, 08142000 Hords Creek near Coleman, TX is missing 29 years of record (approximately 50 percent of record length). Furthermore, 08127000 Elm Creek at Ballinger, TX may be influenced by reservoir construction in the 1980s. The p-value of two gages, 08147000 Colorado River near San Saba, TX and 08150700 Llano River near Mason, TX, are greater than 0.05 but less than 0.1, meaning that a monotonic trend is identified but it cannot definitively be stated that those trends are significant downward trends. The remaining four gages are located on the main stem of the Colorado River, including the Colorado River gages near Ballinger, Stacy, Winchell, and San Saba. Although several gages still exhibit downward trends in annual peak streamflow, it is notable that many of the originally identified trends are no longer statistically significant following the period after 1963.

For the majority of gages where downward trends in annual peak streamflow were observed, removing data prior to the circa-1960s change point results in a peak streamflow record with no statistically significant downward trends. For the remaining gages, the multiple drivers of trends and their complexity prevents any simple treatment or de-trending of the nonstationary data. The issue of nonstationary data is not a new topic in flood frequency analyses. It is a common practice to test for trends in streamflow data and understand how those trends may affect the flood frequency analysis. The problem arises when these trends are not only long-term and persistent, but also a result of multiple, perhaps interconnected, factors. The science and methodology behind untangling these intertwined causes of peak flow declines are beyond the scope of the present study and are in fact still on the cutting edge of science (Cunderlik and Burn, 2003; Cohn and Lins, 2005; Khaliq and others, 2009; Hodgkins and others, 2019; Ryberg and others, 2020).

However, the conclusion that the Lower Colorado basin has undergone fundamental changes circa-1960 holds true for the gages which cannot be 'corrected' for continued declining streamflow through present. This means that while the projection of future streamflow trends is beyond the scope of this study, one can be confident in two things. First, as with the gages exhibiting no trends post-1963, we can be confident that the watershed would respond differently to storms of the first half of the century given the hydrologic changes observed in the watershed. Second, the analysis of these gages exhibiting persistent downward trends in annual peak streamflow will result in conservative annual exceedance probability estimates, which provide some factor of safety over results that may under-estimate flows in food frequency analyses.

Table 5.3: U.S. Geological Survey Streamflow Gaging Stations (Streamgages) in the Lower Colorado River Basin upstream from Austin, TX that Exhibit a Downward trend in Annual Peak Streamflow. Trends in Annual Peak Streamflow are Analyzed using the Kendall's tau test, and the Kendall's tau, p-value, and Trend Indicator are Listed for the Full Record and Record Beginning in 1963.

[p-value, probability value; --, unitless]

Station number	Streamgage Name	Period of available annual peak streamflow	Kendall's tau, Full Record	Kendall's tau *p*-value, Full Record	Kendall's tau Trend, Full Record (*p*-value < 0.05, downward -, upward +, monotonic[1])	Kendall's tau, 1963-present	Kendall's tau *p*-value, 1963-present	Kendall's tau Trend, 1963-present (*p*-value < 0.05, negative -, positive +, monotonic *[1])
			(--)	(--)	(--)	(--)	(--)	(--)
08124000	Colorado River at Robert Lee, TX	1924–2020	-0.582	>0.001	-	-0.310	0.001	-
08126380	Colorado River near Ballinger, TX	1908-2020	-0.540	>0.001	-	-0.326	>0.001	-
08127000	Elm Creek at Ballinger, TX	1933-2020	-0.255	>0.001	-	-0.193	0.034	-
08133500	N. Concho River at Sterling City, TX	1940-2020	-0.242	0.002	-	-0.132	0.160	
08134000	N. Concho River nr Carlsbad, TX	1925-2020	-0.351	>0.001	-	-0.130	0.151	
08128000	S. Concho River at Christoval, TX	1906-2020	-0.217	0.002	-	-0.033	0.712	
08136700	Colorado River near Stacy, TX	1936-2020	-0.539	>0.001	-	-0.521	>0.001	-
08138000	Colorado River at Winchell, TX	1924-2011	-0.477	>0.001	-	-0.288	0.002	-
08142000	Hords Creek near Coleman, TX	1941-2020	-0.300	0.002	-	-0.266	0.044	-
08143500	Pecan Bayou near Brownwood, TX	1918-2020	-0.192	0.017	-	-0.095	0.275	
08144500	San Saba River at Menard, TX	1916-2020	-0.204	0.002	-	-0.112	0.220	
08146000	San Saba River at San Saba, TX	1916-2020	-0.232	0.001	-	-0.152	0.102	
08147000	Colorado River near San Saba, TX	1900-2020	-0.282	>0.001	-	-0.153	0.091	*
08148500	N. Llano River nr Junction, TX	1889-2020	-0.206	0.006	-	-0.121	0.301	
08150700	Llano River nr Mason, TX	1889-2020	-0.254	0.007	-	-0.167	0.086	*

[1]Monotonic trends are determined at the 0.1 significance value for the Kendall's tau p-value. Because the p-value computed by this Kendall's tau analysis is the two-tailed test statistic, it must be divided by two to evaluate whether the identified trend is a significant downward or significant upward trend.

5.3 STREAM GAGE DATA AND STATISTICAL FLOW FREQUENCY RESULTS

This section provides a summary of available stream gage data and graphical flow frequency results for a handful of example stream gages in the Lower Colorado River basin along with a summary of results for all analyzed USGS gages in Tables 5.4 through 5.8. A full description of the stream gage data, assumptions and flow frequency results for all analyzed gages in the basin can be found in Appendix A.

08126380 Colorado River near Ballinger, TX

The period of record at USGS streamgage 08126380 Colorado River near Ballinger, TX (hereinafter referred to as the "Colorado River near Ballinger gage") was from 1908 through 2020 (USGS, 2022). Starting with the 1969 water year, the record is flagged as influenced by regulation in the USGS NWIS database (USGS peak code 6; USGS, 2022). The Pettitt test returns a *p*-value of less than 0.001 for the gaged record, indicating a significant change point in the data. Although the test identified water year 1963 as the change point, this may simply be a result of an anomaly in the unregulated dataset of several years of lower peak flows before the impoundment of E.V. Spence Reservoir on the Colorado River in 1969 (TWDB, 2022). To maintain a homogenous record of regulated streamflow conditions, peak streamflows recorded from 1924 through 1968 prior to the construction of E.V. Spence Reservoir were not included in the analysis. The Kendall's tau test identified a significant downward trend in annual peak streamflow, which is clearly visible in the data (Table 5.3; Figure 5.6).

The largest peak of record for the location is the 1978 peak streamflow of 16,600 cfs at a stage of 23.95 ft. The data as set up for statistical frequency analysis are shown in a log-normal plot of annual peak streamflow versus water year in Figure 5.6. The flood flow frequency for the Colorado River near Ballinger gage is shown in Figure 5.7. The figure is exported from PeakFQ (USGS, 2014) and plots annual peak streamflow versus AEP in percent. The low-outlier threshold was computed by the MGBT in PeakFQ at 1,130 cfs, and a total of 12 low outliers were identified.

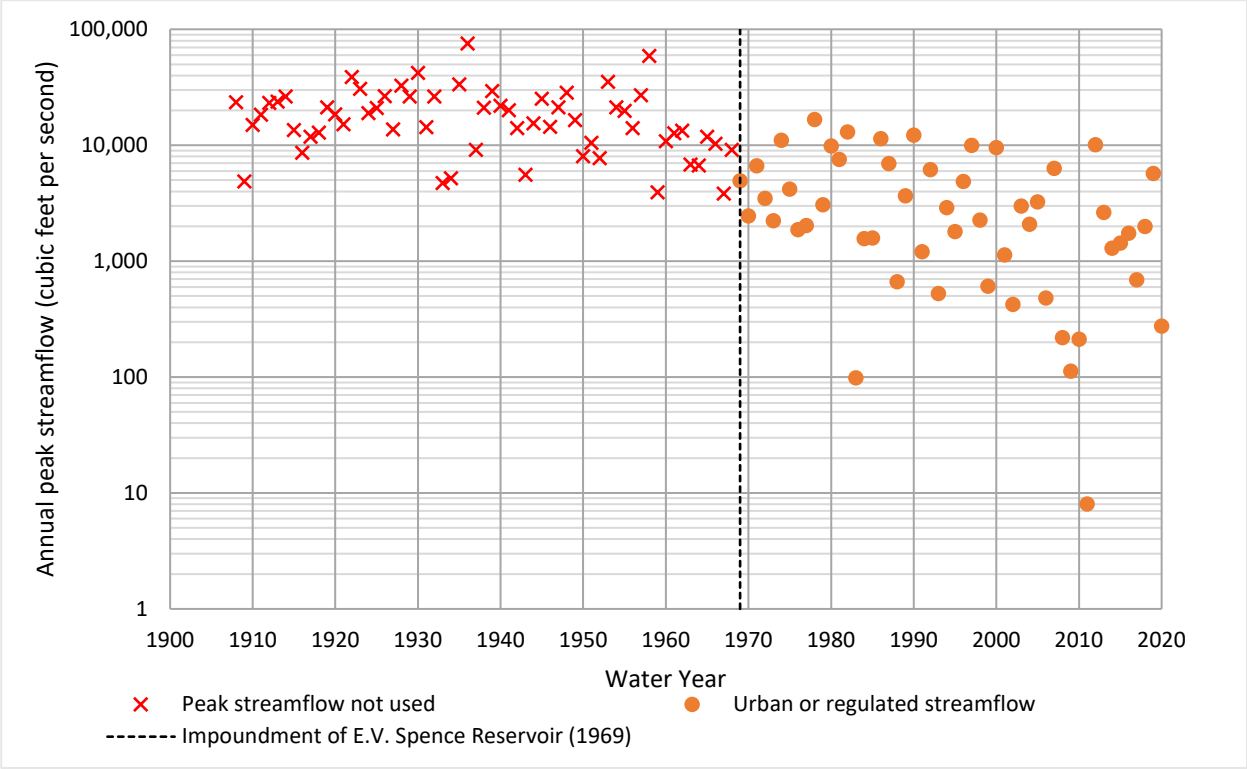

Figure 5.6: Annual Peak Streamflow Data for U.S. Geological Survey Streamgage 08126380 Colorado River near Ballinger, TX

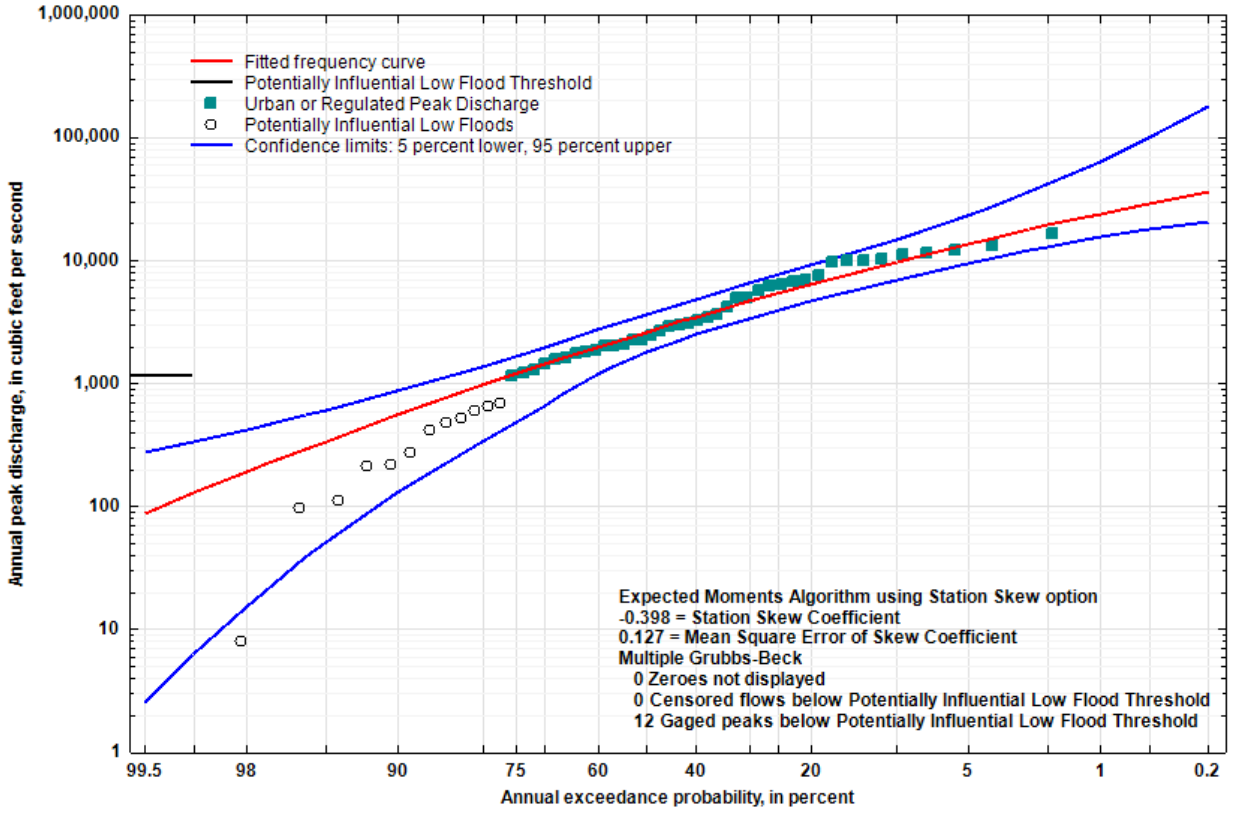

Figure 5.7: Flood Flow Frequency Curve for U.S. Geological Survey Streamgage 08126380 Colorado River near Ballinger, TX

08134000 North Concho River near Carlsbad, TX

The period of record at USGS streamgage 08134000 North Concho River near Carlsbad, TX (hereinafter referred to as the "North Concho River near Carlsbad gage") was from 1925 through 2020 (USGS, 2022). No peak streamflows were coded as being influenced by regulation, but the Pettitt test detects a change point occurring in water year 1962. Although no known regulation, diversion, or physical changes have been positively identified upstream from the North Concho River near Carlsbad gage, a change of some form has occurred or is occurring in the basin and are evident in the analyzed data. There is a notable decrease in the frequency of peak streamflows greater than 10,000 cfs and an increase in peaks less than 1,000 cfs beginning in the 1960s (Figure 5.8). Therefore, peak streamflow prior to water year 1962 were removed from the analysis. After removal of these data, the Kendall's tau test does not identify a statistically significant trend in annual peak streamflow.

The largest peak in the analyzed record for the location is the 1974 peak streamflow of 20,000 cfs at a stage of 22.00 ft. The peak streamflow data after being processed for statistical frequency analysis are shown in a log-normal plot of annual peak streamflow versus water year in Figure 5.8. The flood flow frequency for the North Concho River near Carlsbad gage is shown in Figure 5.9. The figure is exported from PeakFQ (USGS, 2014) and plots annual peak streamflow versus AEP in percent. The low-outlier threshold was computed by the MGBT in PeakFQ at 1,000 cfs, and a total 16 low outliers were identified. One zero-flow year was also identified.

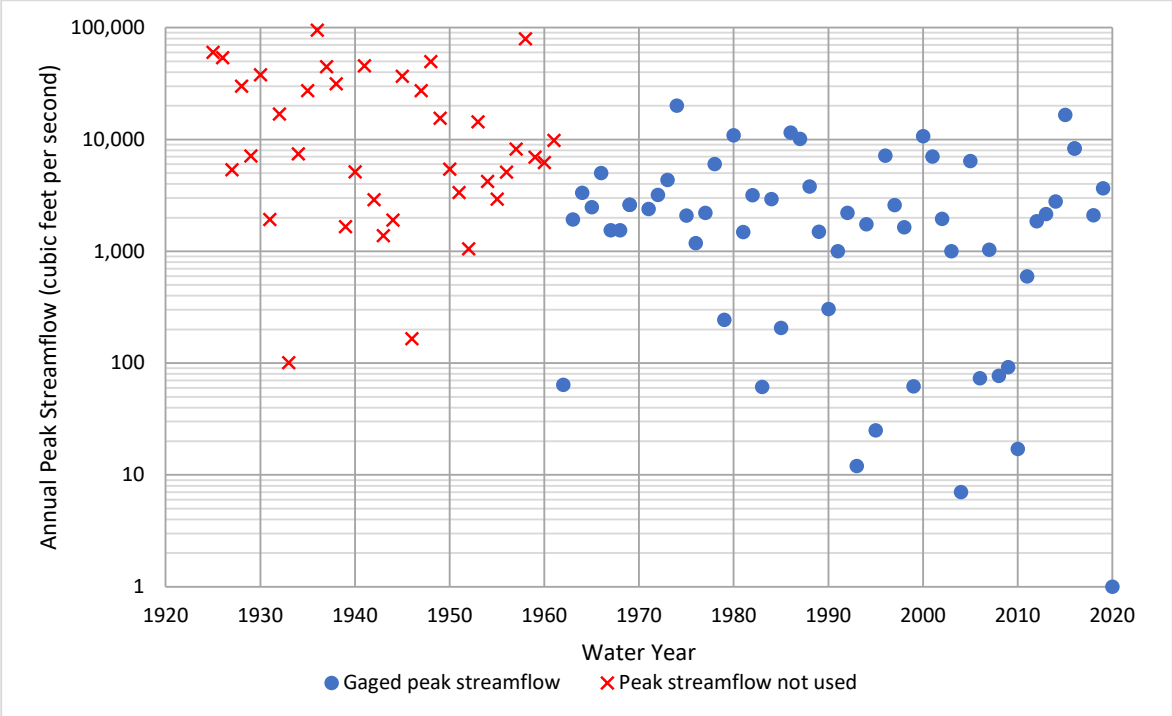

Figure 5.8: Annual Peak Streamflow Data for U.S. Geological Survey Streamgage 08134000 North Concho River near Carlsbad, TX

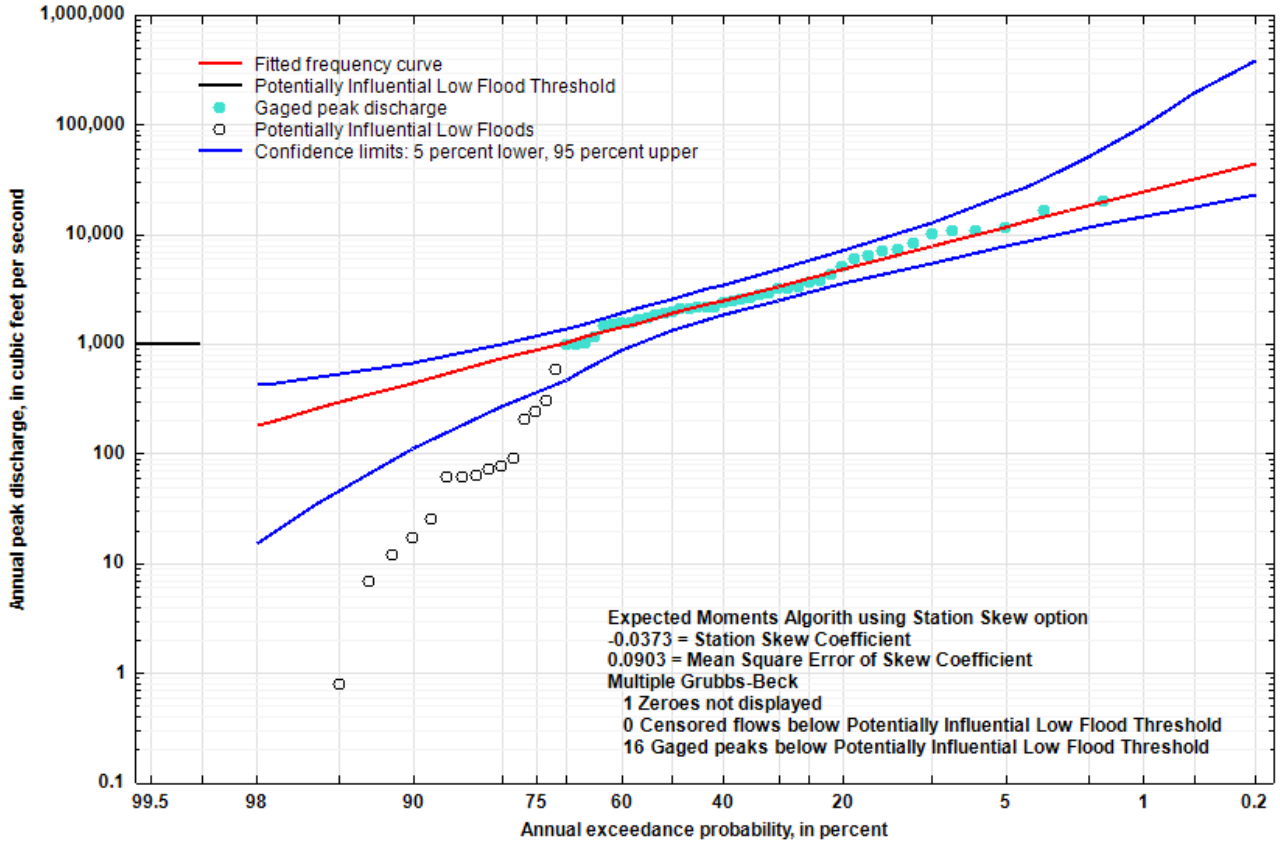

Figure 5.9: Flood Flow Frequency Curve for U.S. Geological Survey Streamgage 08134000 North Concho River near Carlsbad, TX

08134000 North Concho River near Carlsbad, TX (Alternate Analysis)

An alternate analysis is presented here for the North Concho River near Carlsbad gage to highlight the effects of including gage data prior to 1962. For the alternate analysis, the full period of record was analyzed. Because the calculated station skew coefficient was positive, the alternate analysis was weighted by a regional skew value to better match the behavior of flood frequency curves in the region and in the Concho River basin. A downward trend in annual peak streamflow is observed when analyzing the entire period of record.

With the entire period of record included, the largest peak increases from 20,000 cfs to 94,600 cfs at a stage of 29.10 ft in 1936. The alternate analysis of the flood flow frequency for the North Concho River near Carlsbad gage is shown in Figure 5.10. The figure is exported from PeakFQ (USGS, 2014) and plots annual peak discharge versus AEP in percent. The low-outlier threshold was computed by the MGBT in PeakFQ at 1,000 cfs, and a total of 17 low outliers were identified. One zero-flow year was also identified.

Including the full period of record results in a pronounced increase in return interval estimates. The 100-year flood increases from 24,500 cfs to 99,000 cfs, and the 10-year flood increases from 7,790 cfs to 23,200 cfs. These alternate results are only meant for comparison to the original results, which better reflect recent (2020) conditions at the gage. A comparison of the original and alternate flood frequency curves is shown in Figure 5.11.

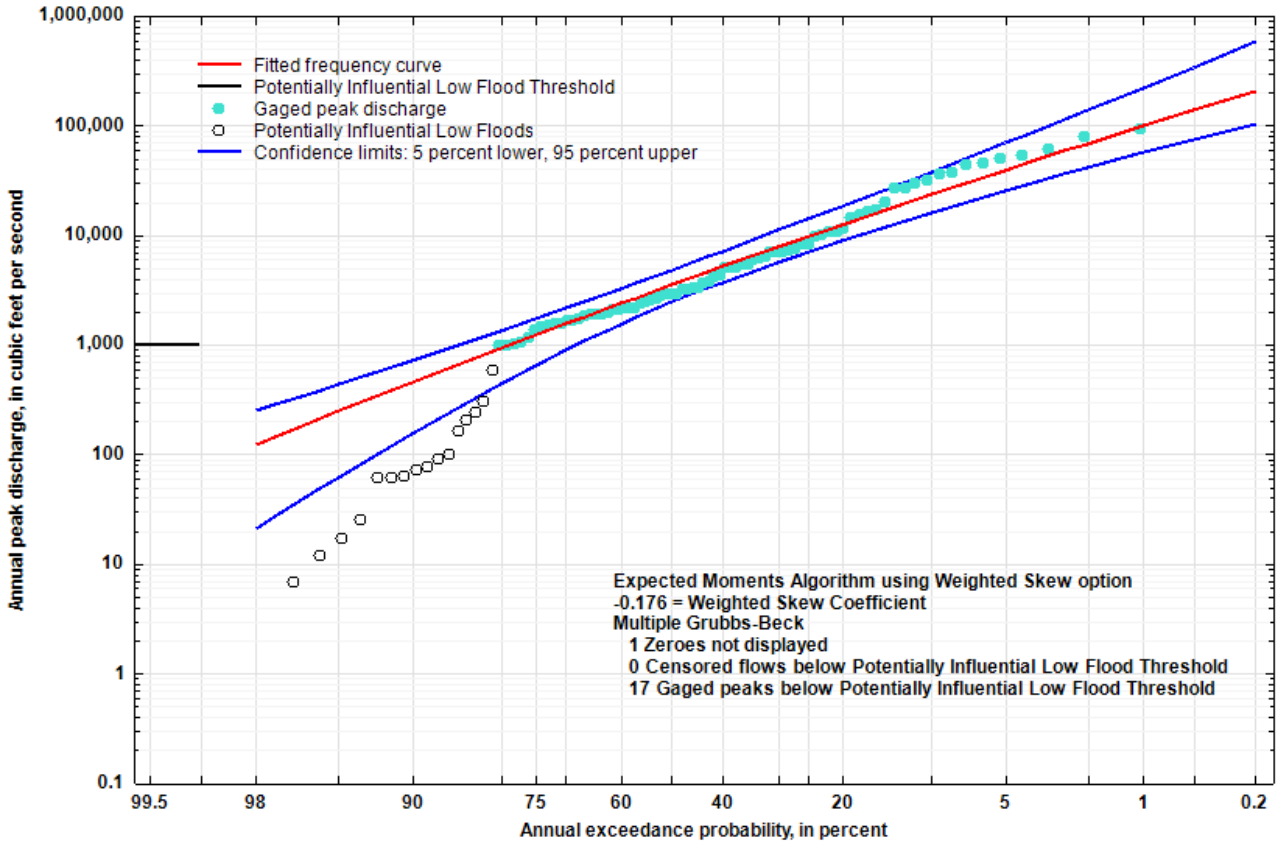

Figure 5.10: Flood Flow Frequency Curve (Alternate Analysis) for U.S. Geological Survey Streamgage 08134000 North Concho River near Carlsbad, TX

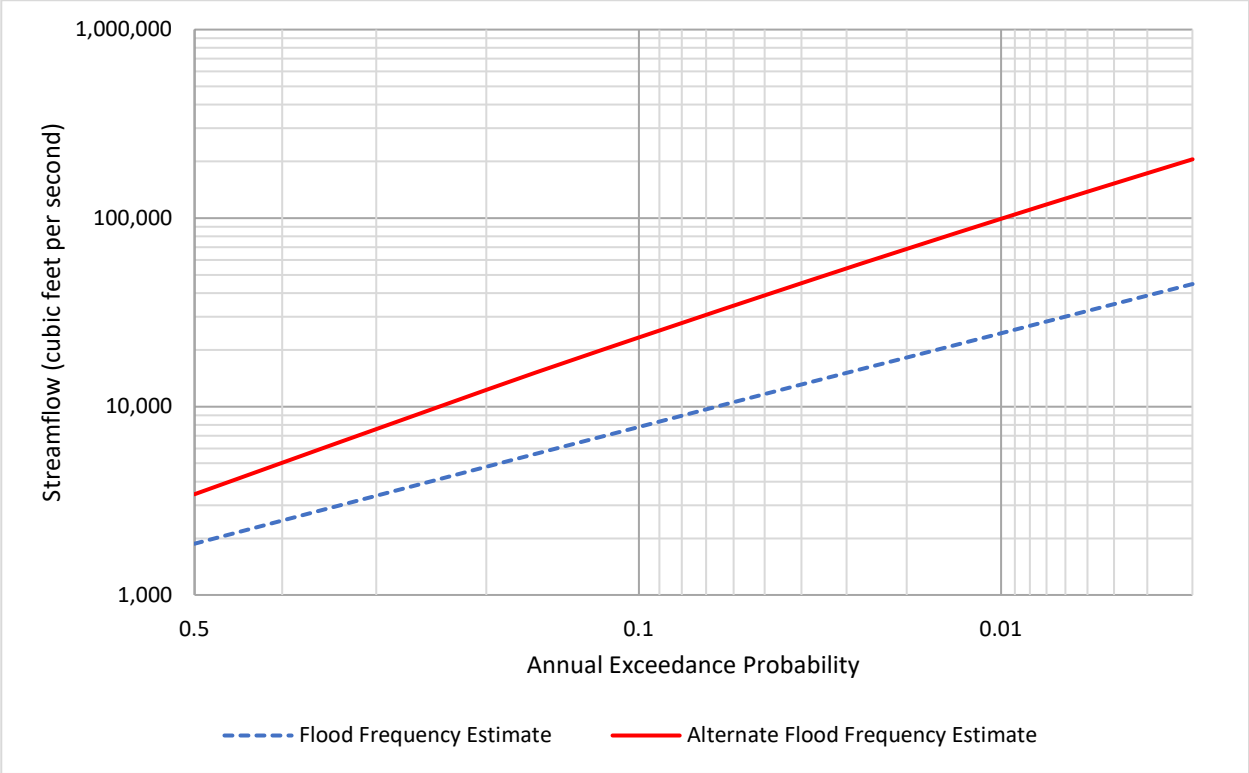

Figure 5.11: Comparison of Flood Flow Frequency Curves for the Original (1963-2020) and Alternate (1906-2020) Datasets for USGS Streamgage 08134000 North Concho River near Carlsbad, TX

08143500 Pecan Bayou at Brownwood, TX

The period of record at USGS streamgage 08143500 Pecan Bayou at Brownwood, TX (hereinafter referred to as the "Pecan Bayou at Brownwood gage") was from 1924 through 2020 (USGS, 2022). Data collected prior to 1933 were not used in the analysis because the impoundment of Lake Brownwood on Pecan Bayou, which went into service in 1933 (TWDB, 2022), had a noticeable effect on annual peak streamflow at the gage. A historical peak is available in 1918, but this peak as well as the gaged record prior to 1933 were removed from the record to maintain a homogenous record coinciding with the regulated basin associated with Lake Brownwood. In 1982, the original dam was raised approximately 20 feet (TWDB, 1997). As a consequence, the gage was decommissioned in 1984, and gaged record is missing through 2018. Reservoir data including pool elevation, is available beginning in 1999, and using a spillway rating curve for Lake Brownwood and applying a drainage area ratio, streamflow was estimated at the downstream gage for Pecan Bayou at Brownwood. A perception threshold of 5,000 cfs was also set for that time period to cover those years where reservoir outflow was zero. Pool elevations are known for three notable flooding events in 1990, 1991, and 2002, and using the spillway rating curve and a drainage area ratio, streamflow at the Pecan Bayou at Brownwood gage was estimated (USACE, 2003). However, only the peaks are available for these three years; no antecedent pool elevations or reservoir releases are known. Therefore, we have less confidence in translating this streamflow downstream to the gage at Brownwood. Instead of discrete values, interval peaks of 15,000-22,000 cfs, 12,000-31,000 cfs, and 23,000-27,000 cfs were set for the flooding events recorded at Lake Brownwood in 1990, 1991, and 2002 respectively. These intervals consider the streamflow at the reservoir, that reservoir streamflow translated downstream to the Brownwood gage with a drainage area ratio, and a drainage area ratio estimate at the Brownwood gage using the downstream gage at Mullin. With less known about the other pool elevations from 1984 through 1998, a perception threshold of 20,000 cfs was set for missing record during that time period.

The Pettitt test identified a change point in water year 1962, but it does not appear to correspond to any reservoir construction or physical changes in the watershed. Kendall's tau test identified a statistically significant downward trend in annual peak streamflow at the gaged location.

The largest peak of record for the Pecan Bayou at Brownwood gage is the 1956 peak streamflow of 26,500 cfs at a stage of 16.08 ft. The peak streamflow data after being processed for statistical frequency analysis are shown in a log-normal plot of annual peak streamflow versus water year in Figure 5.12. The flood flow frequency for Pecan Bayou at Brownwood gage is shown in Figure 5.13. The figure is exported from PeakFQ (USGS, 2014) and plots annual peak streamflow versus AEP in percent. The low-outlier threshold was computed by the MGBT in PeakFQ at 1,630 cfs, and a total of 11 low outliers were identified.

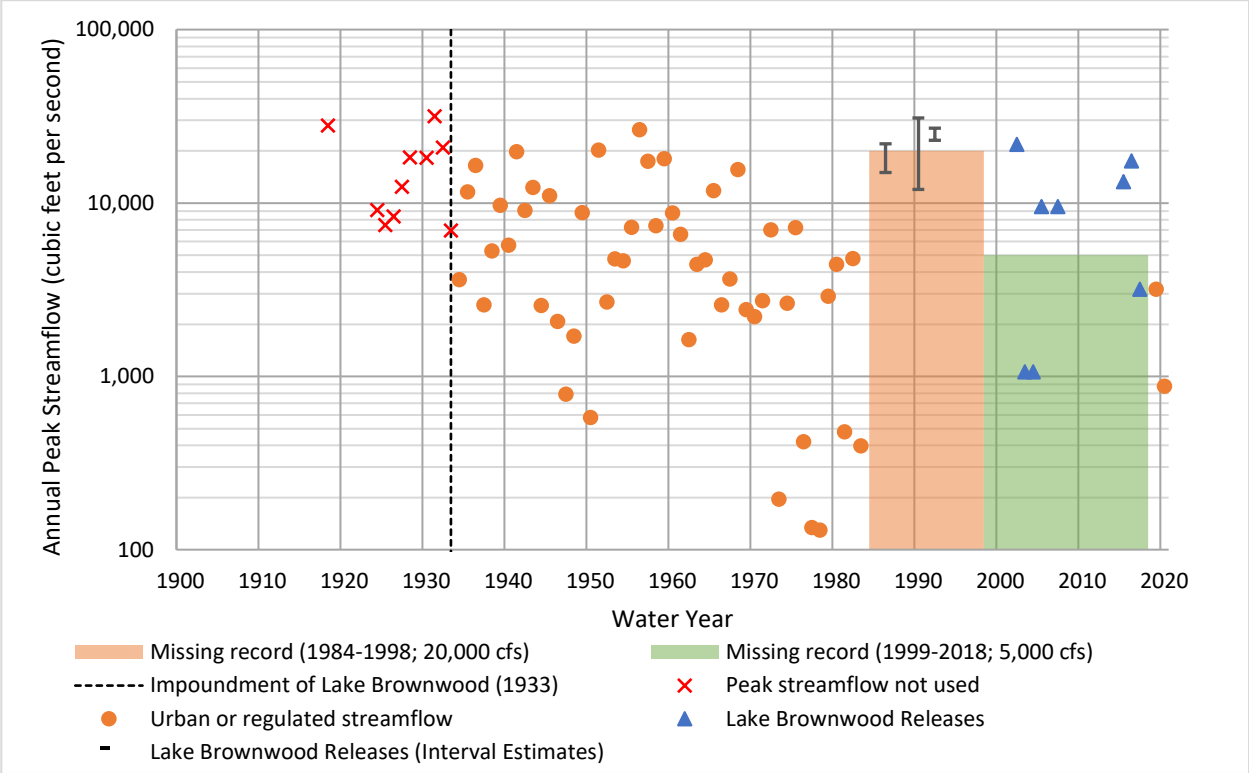

Figure 5.12: Annual Peak Streamflow Data for USGS Streamgage 08143500 Pecan Bayou at Brownwood

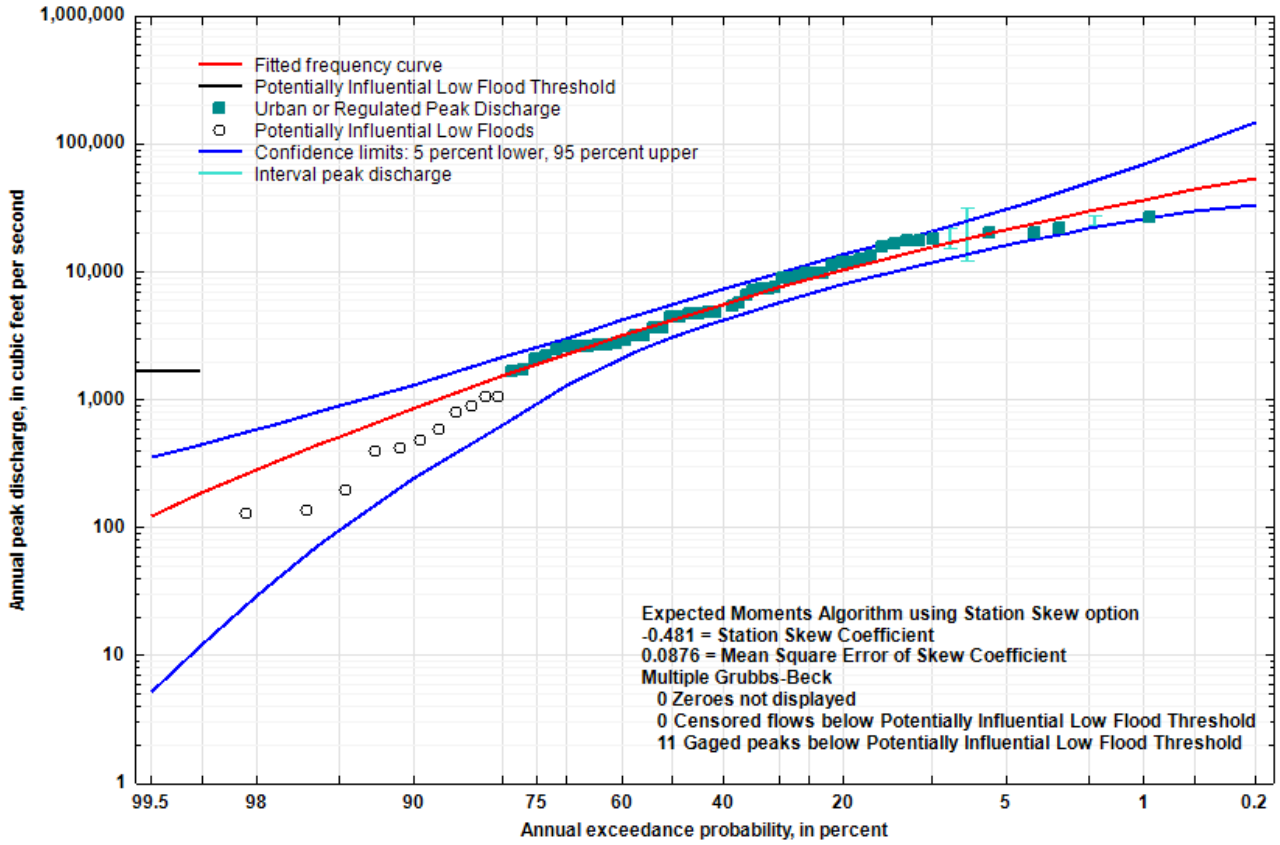

Figure 5.13: Flood Flow Frequency Curve for USGS Streamgage 08143500 Pecan Bayou at Brownwood

08146000 San Saba River at San Saba, TX

The period of record at USGS streamgage 08146000 San Saba River at San Saba, TX (hereinafter referred to as the "San Saba River at San Saba gage") was from 1916 through 2020 (USGS, 2022). Peak streamflow beginning in 1963 is coded as being influenced by regulation associated with the impoundment of Brady Creek Reservoir on Brady Creek, although little difference is observed in peak streamflows before and after 1963. The Pettitt test identified a change point in water year 1981, but this change is not associated with reservoir construction or any other known physical change to the watershed, so the entire period of record is used in the analysis. Ownership of the San Saba River at San Saba gage was transferred to the LCRA from 1995 through 1997. The LCRA provided hourly streamflow data for these time periods, and annual peak streamflows were extracted and included with the USGS annual peak series in the analysis. The Kendall's tau test identified a statistically significant downward trend in annual peak streamflow at the gaged location.

The largest peak of record for the San Saba River at San Saba gage is the 1938 peak streamflow of 203,000 cfs at a stage of 39.30 ft. The peak streamflow data after being processed for statistical frequency analysis are shown in a log-normal plot of annual peak streamflow versus water year in Figure 5.14. The flood flow frequency for San Saba River at San Saba gage is shown in Figure 5.15. The figure is exported from PeakFQ (USGS, 2014) and plots annual peak streamflow versus AEP in percent. The low-outlier threshold was manually set at 672 cfs, and a total of four low outliers were identified.

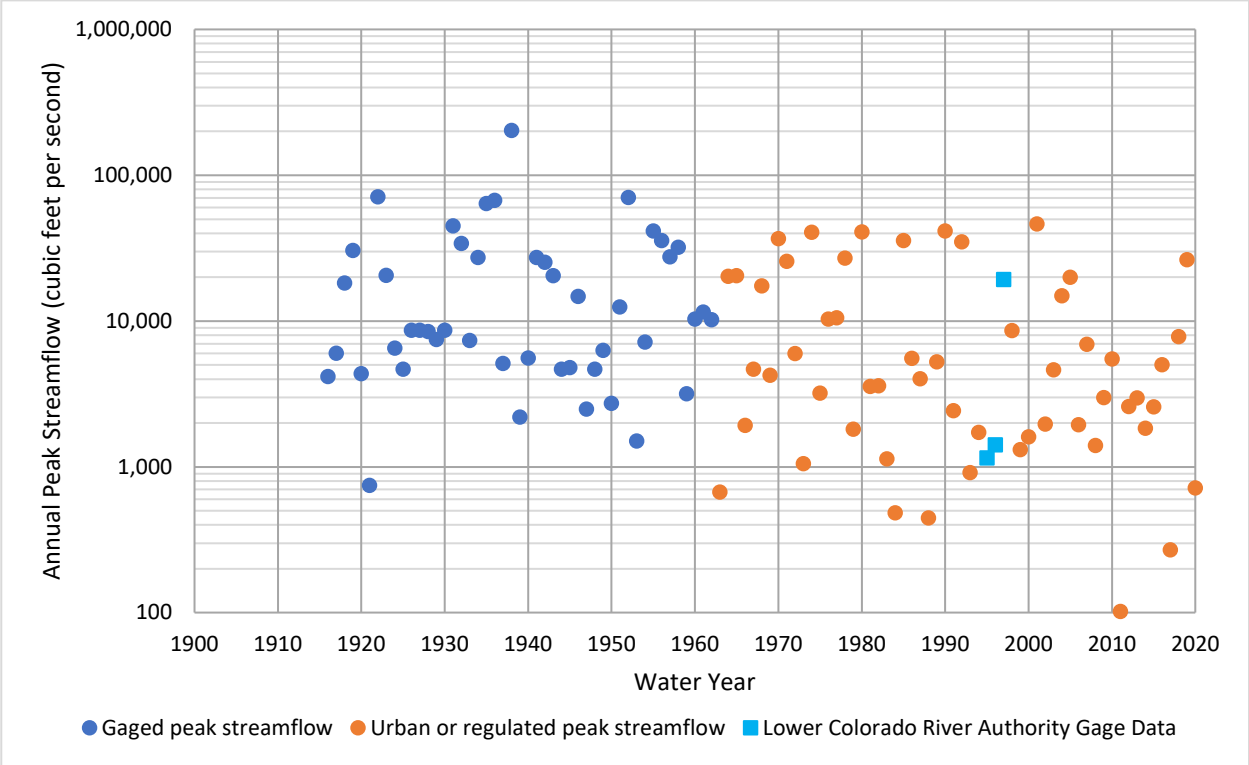

Figure 5.14: Annual Peak Streamflow Data for USGS 08146000 San Saba River at San Saba, TX

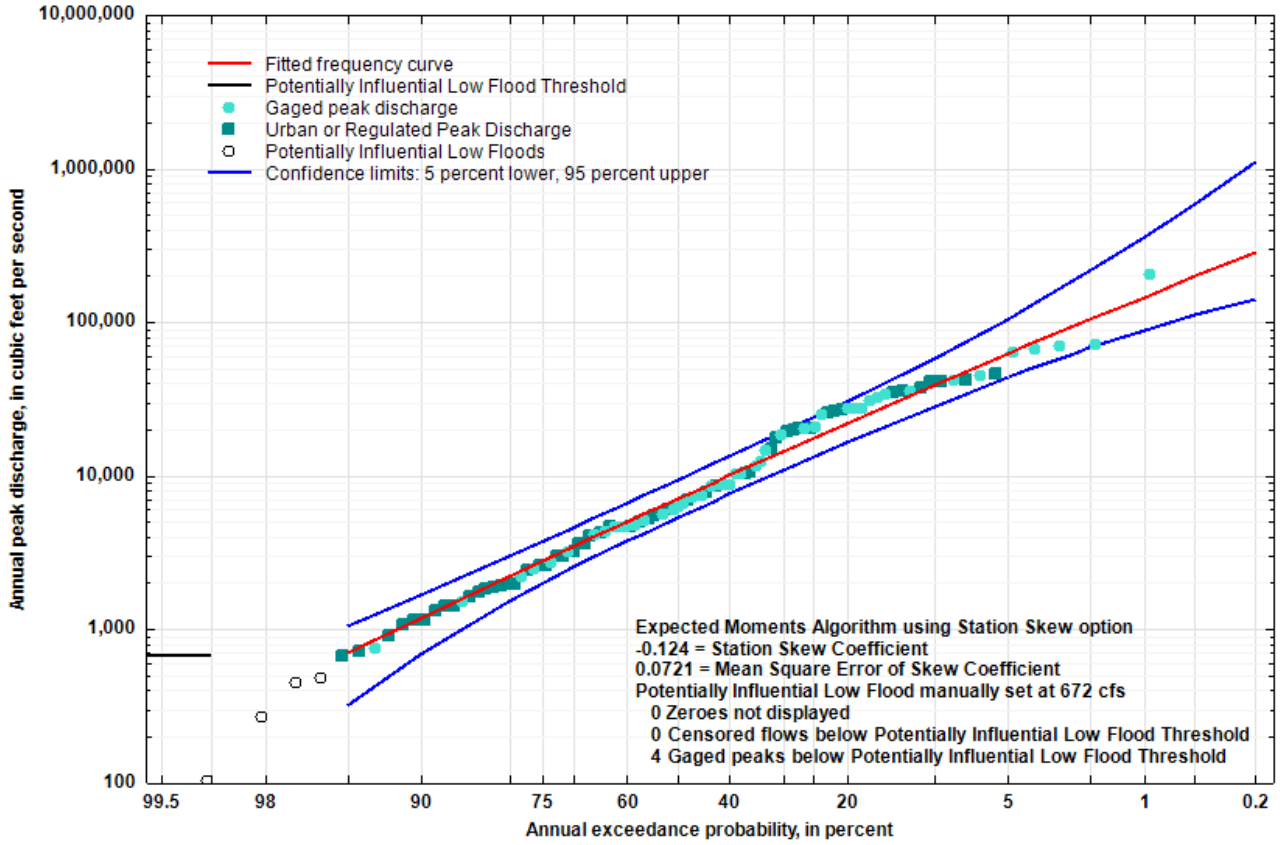

Figure 5.15: Flood Flow Frequency Curve for USGS Streamgage 08146000 San Saba River at San Saba

08146000 San Saba River at San Saba, TX (Alternate Analysis)

An alternate analysis is presented for the San Saba River at San Saba gage by considering the change point in 1981. Although no known physical change occurred in the San Saba River basin at this time, the change point exhibits strong statistical significance and changes similar to those observed in the Concho River and greater Colorado River basins in the 1960s could be occurring here as well, albeit on a different timestep. The peak of record during 1981–2020 (the shortened period of record) is the 2001 annual peak streamflow of 46,200 cfs. Before 1981, annual peaks greater than 46,200 cfs were recorded during 6 years at the San Saba River at San Saba gage. The Kendall's tau test identified a statistically significant downward trend in annual peak streamflow for the full period of record, but for shortened period of record used in the alternate analysis, no statistically significant trends in annual peak streamflow were detected, with a Kendall's tau value of -0.013 and a p-value of 0.916.

The flood flow frequency for the San Saba River at San Saba gage alternate analysis is shown in Figure 5.16. The figure is exported from PeakFQ (USGS, 2014) and plots annual peak streamflow versus AEP in percent. The MGBT did not detect any low outliers in the analyzed record. A comparison of the original and alternate flood frequency curves is shown in Figure 5.17. Both frequency curves exhibit nearly the same near-zero station skew and almost mirror one another with the alternate analysis plotting well below the original curve. The 1 percent AEP event flood decreases substantially from the original analysis from 145,000 cfs to 88,000 cfs for the alternate analysis, and the 10-year flood decreases from 38,700 cfs to 20,400 cfs respectively.

Although not as pronounced as what was observed with the shift in annual peak streamflows at the San Saba River at Menard gage after 1980, Figure 5.14 illustrates that the San Saba River at San Saba gage recorded 23 peaks less than 4,000 cfs during 1981–2020 (the 40-year period or record used in the alternate analysis). In the 65 years of record prior to 1981, an annual peak streamflow less than 4,000 cfs was only recorded during 11 years.

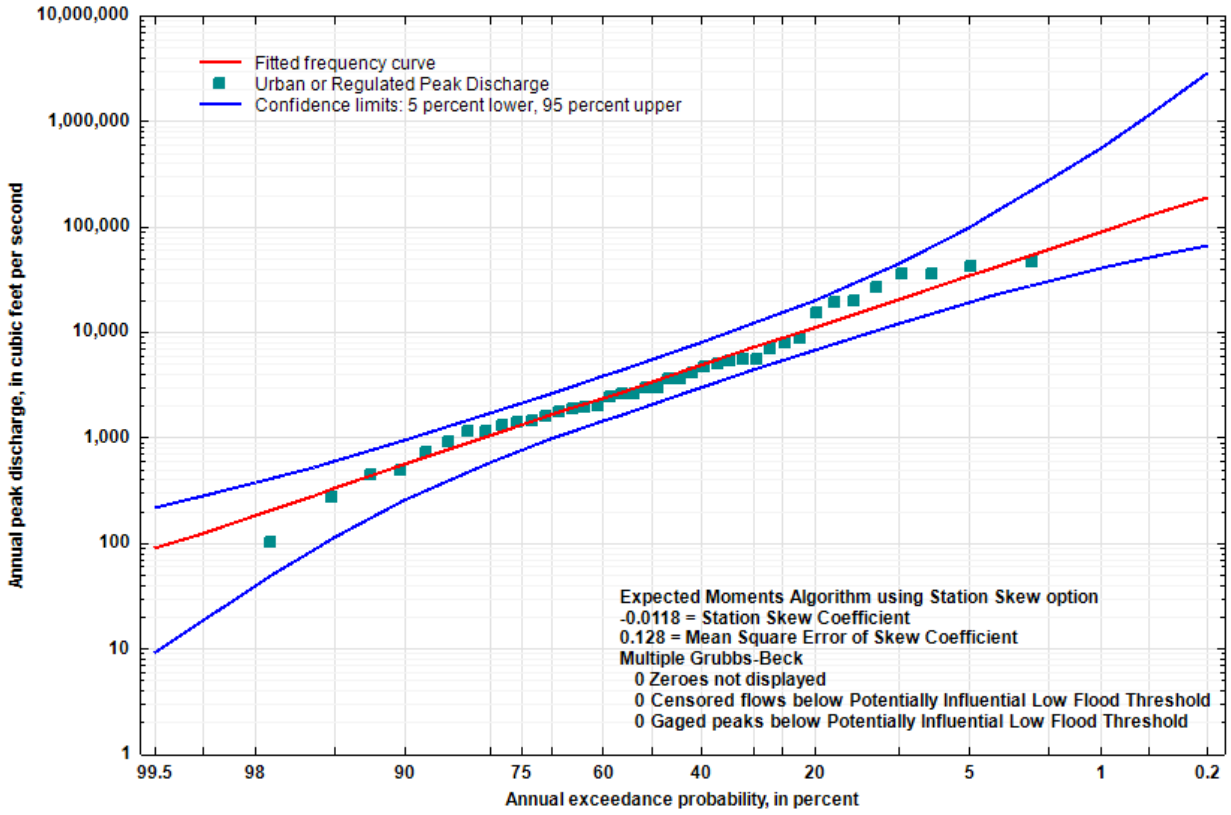

Figure 5.16: Flood Flow Frequency Curve for USGS Streamgage 08146000 San Saba River at San Saba, TX (Alternate Analysis)

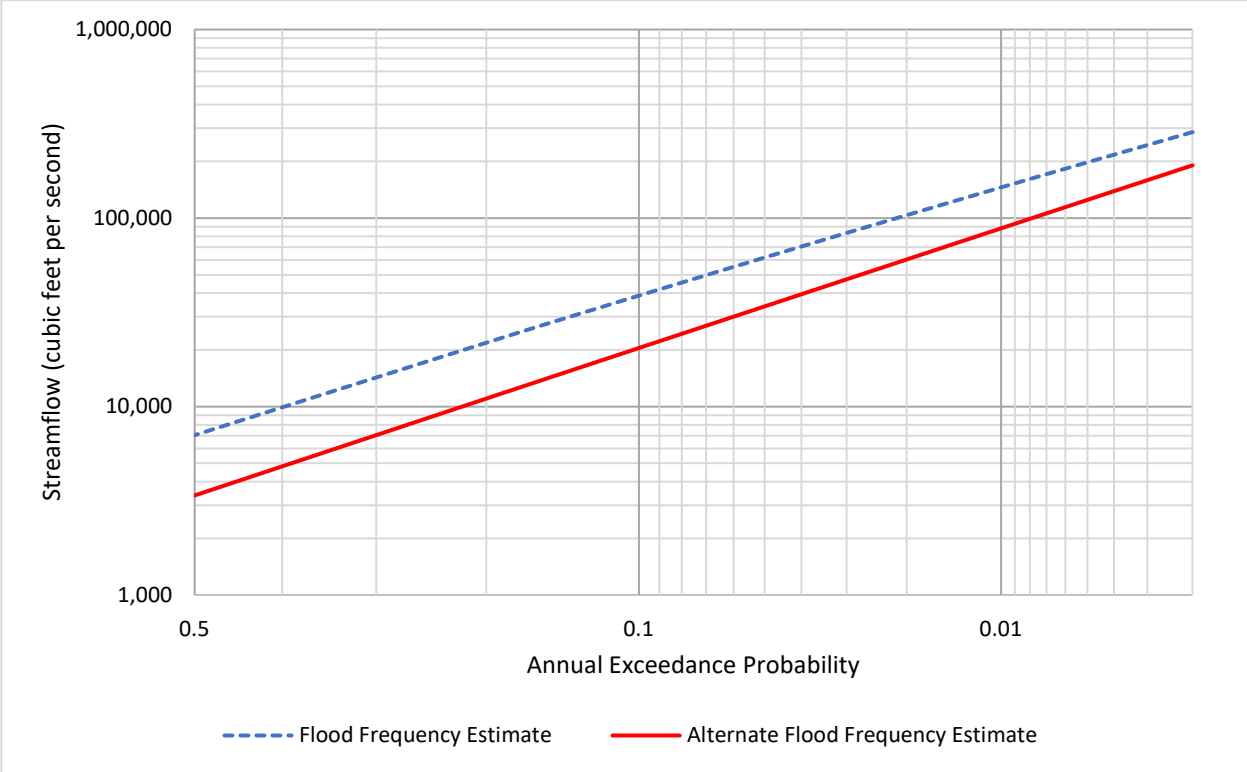

Figure 5.17: Comparison of Flood Flow Frequency Curves for the Original (1916-2020) and Alternate (1981-2020) Datasets for USGS Streamgage 08146000 San Saba River at San Saba, TX

08150000 Llano River near Junction, TX

The period of record at USGS streamgage 08150000 Llano River near Junction, TX (hereinafter referred to as the "Llano River near Junction gage") was from 1916 through 2020 (USGS, 2022). Peak streamflow beginning in 1964 is coded as being influenced by regulation, although no difference is observed in peak streamflows before and after 1964, so the entire period of record is used in the analysis. Ownership of the Llano River near Junction gage was transferred to the LCRA from 1994 through 1997. The LCRA provided hourly streamflow data for these time periods, and annual peak streamflows were extracted and included with the USGS annual peak series in the analysis. The Pettitt test does not identify a change point at this location, nor does the Kendall's tau test detect a statistically significant trend in annual peak streamflow.

The largest peak of record for the Llano River near Junction gage is the 1935 peak streamflow of 319,000 cfs at a stage of 43.30 ft. The peak streamflow data after being processed for statistical frequency analysis are shown in a log-normal plot of annual peak streamflow versus water year in Figure 5.18. The flood flow frequency for Llano River near Junction gage is shown in Figure 5.19. The figure is exported from PeakFQ (USGS, 2014) and plots annual peak streamflow versus AEP in percent. The low-outlier threshold was computed by the MGBT in PeakFQ at 7,250 cfs, and a total of 43 low outliers were identified.

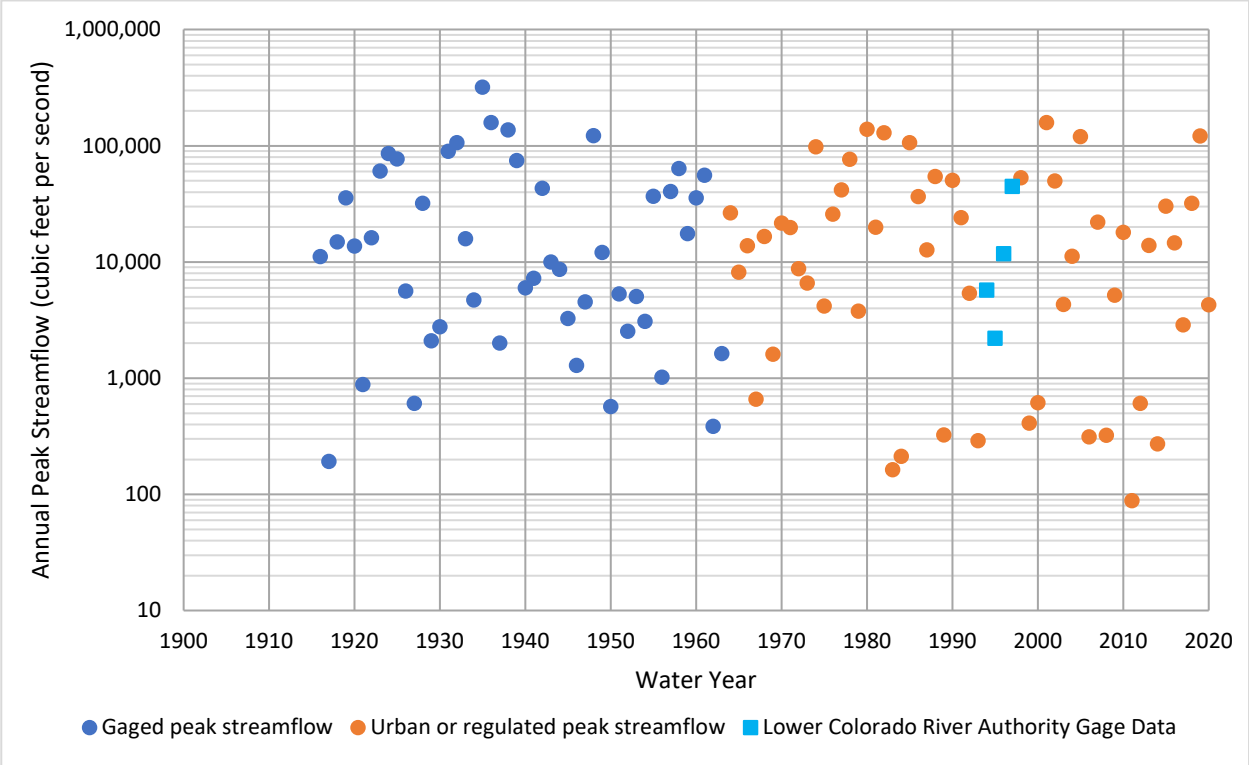

Figure 5.18: Annual Peak Streamflow Data for U.S. Geological Survey Streamgage 08150000 Llano River near Junction, TX

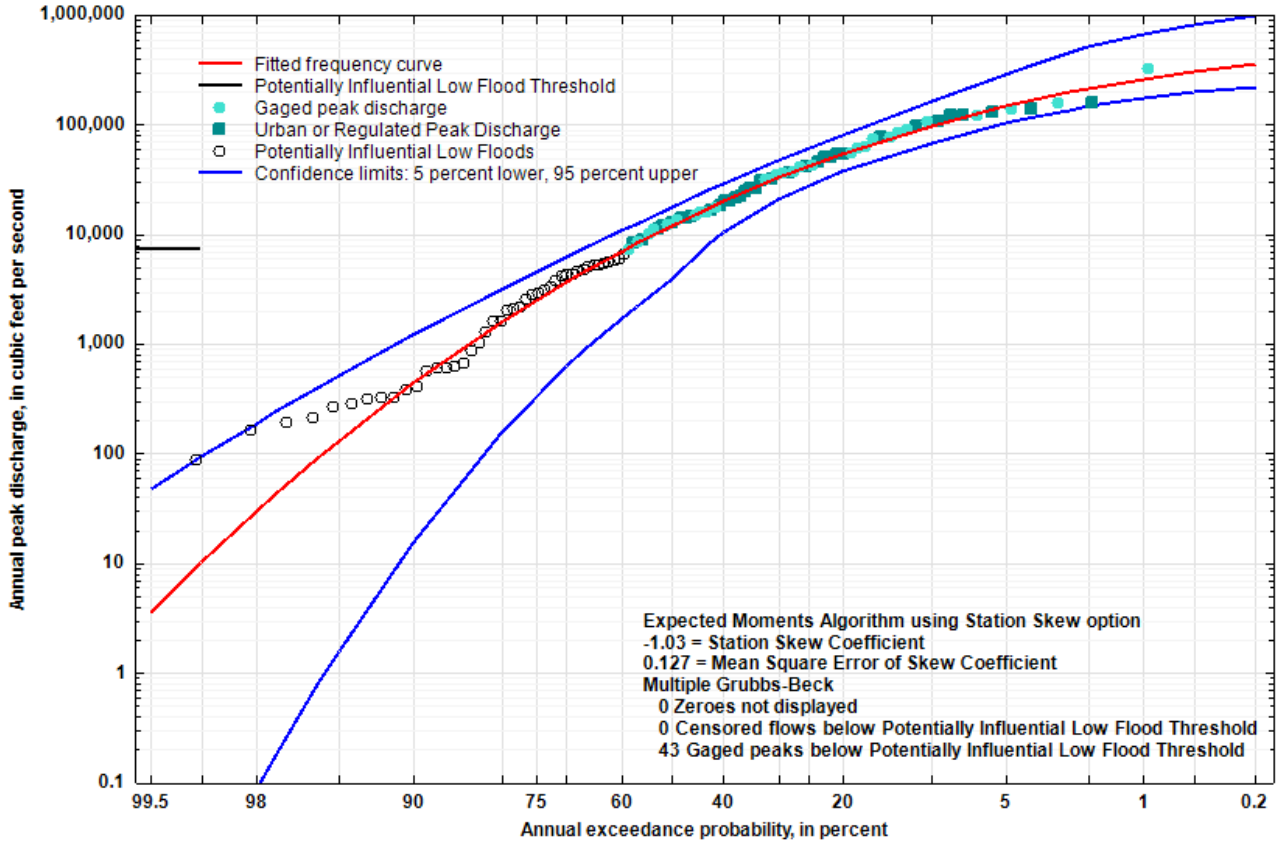

Figure 5.19: Flood Flow Frequency Curve for U.S. Geological Survey Streamgage 08150000 Llano River near Junction, TX

08153500 Pedernales River near Johnson City, TX

The period of record at USGS streamgage 08153500 Pedernales River near Johnson City, TX (hereinafter referred to as the "Pedernales River near Johnson City gage") was from 1939 through 2020 (USGS, 2022). The largest peak of record for the Pedernales River near Johnson City gage is the 1952 peak streamflow of 441,000 cfs at a stage of 42.50 ft. The Pettitt test does not detect a change point in the gaged record, nor does the Kendall's tau test find a statistically significant trend in the annual peak streamflow data.

The data as set up for statistical frequency analysis are shown in a log-normal plot of annual peak streamflow versus water year in Figure 5.20. The flood flow frequency for the Pedernales River near Johnson City gage is shown in Figure 5.21. The figure is exported from PeakFQ (USGS, 2014) and plots annual peak streamflow versus AEP in percent. The low-outlier threshold was computed by the MGBT in PeakFQ at 5,270 cfs, and a total of 12 low outliers were identified.

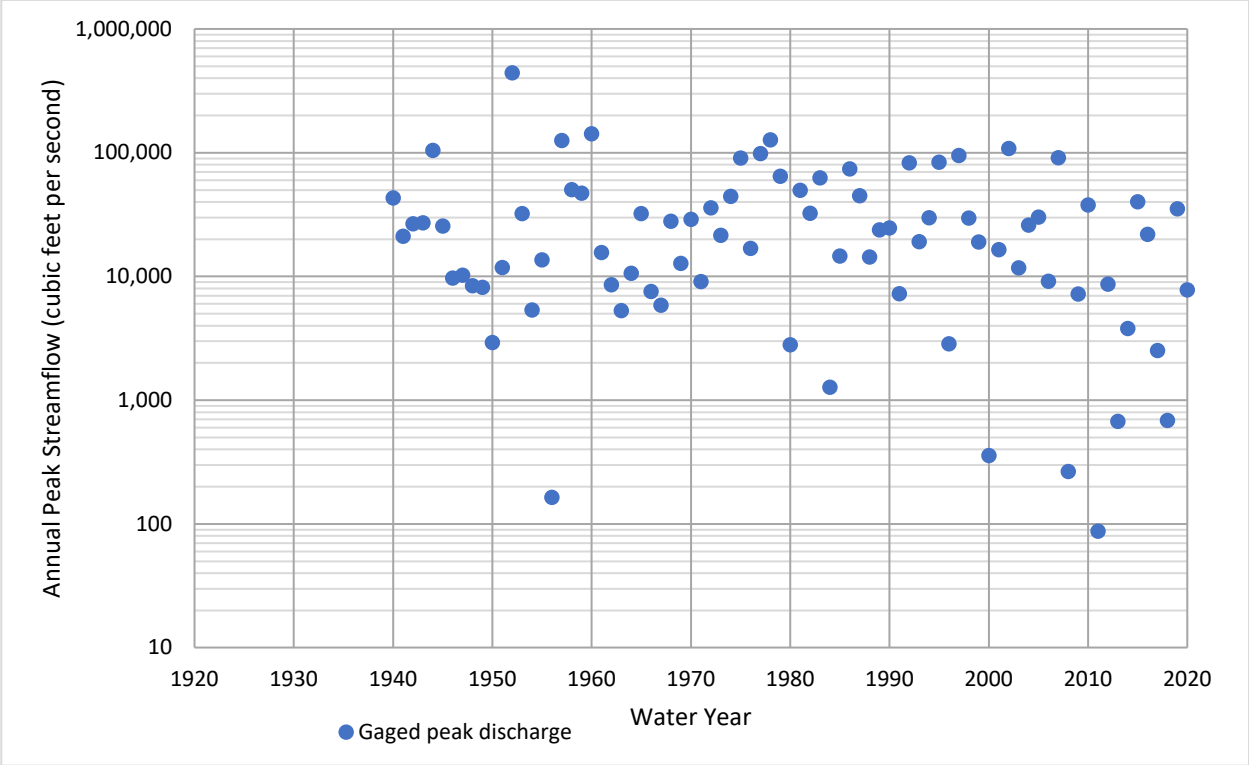

Figure 5.20: Annual Peak Streamflow Data for USGS Streamgage 08153500 Pedernales River near Johnson City, TX

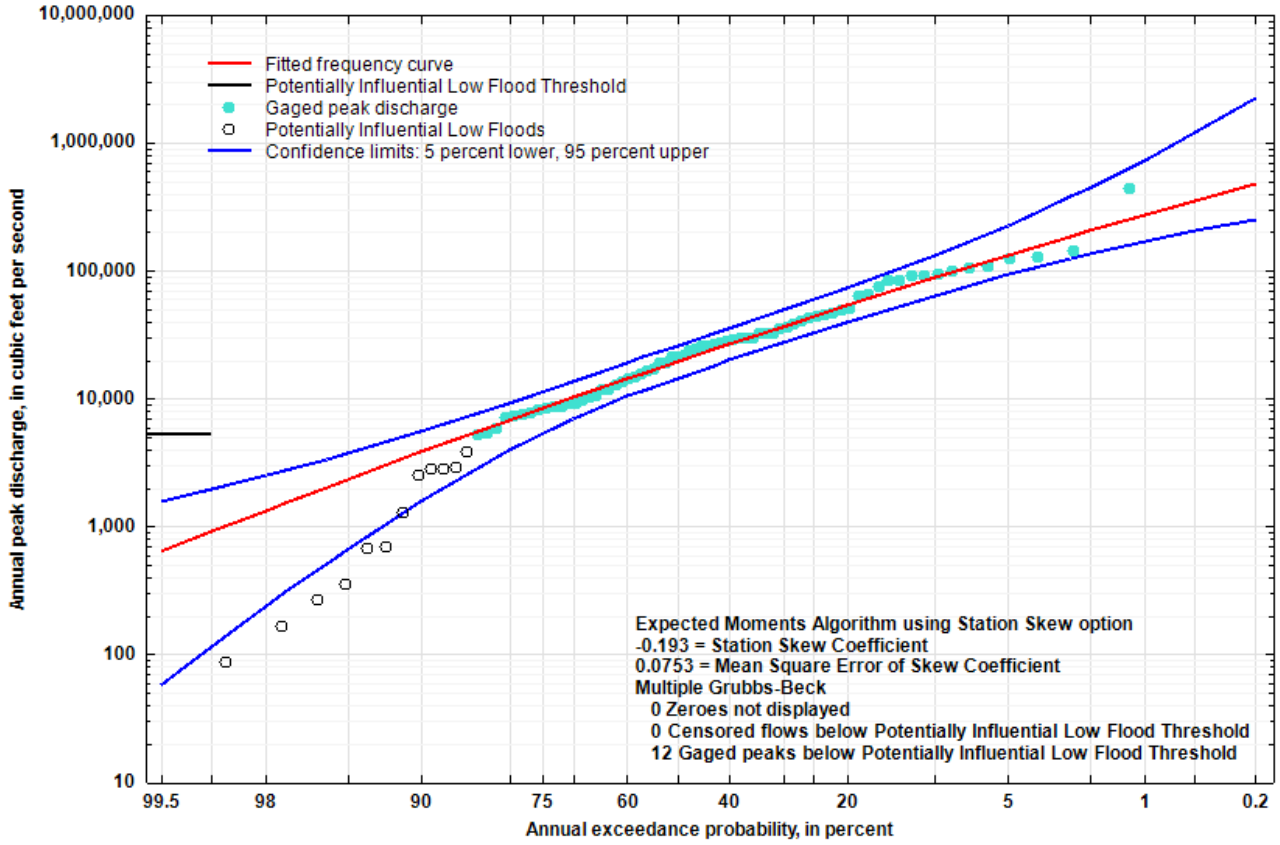

Figure 5.21: Flood Flow Frequency Curve for USGS Streamgage 08153500 Pedernales River near Johnson City, TX

08158000 Colorado River at Austin, TX

The period of record at USGS streamgage 08158000 Colorado River at Austin, TX (hereinafter referred to as the "Colorado River at Austin gage") was from 1898 through 2020 (USGS, 2022). The Pettitt test detects a change point in water year 1942, somewhat coincident with the impoundment of Lake Travis on the Colorado River, which went into service in September of 1940 (TWDB, 2022), which had a noticeable effect on annual peak streamflow at the gage. A historic peak is available in 1869, but this peak as well as the gaged record prior to 1941 were removed from the record to maintain a homogenous record coinciding with the regulated basin associated with Lake Travis. The Kendall's tau test detects a statistically significant upward trend in annual peak streamflow at the gaged location.

The largest peak in the analyzed record for the Colorado River at Austin gage is the 1941 peak streamflow of 47,600 cfs at a stage of 18.55 ft. The peak streamflow data after being processed for statistical frequency analysis are shown in a log-normal plot of annual peak streamflow versus water year in Figure 5.22. The flood flow frequency for the Colorado River at Austin gage is shown in Figure 5.23. The figure is exported from PeakFQ (USGS, 2014) and plots annual peak streamflow versus AEP in percent. The low-outlier threshold was manually set at 10,000 cfs, and a total of 35 low outliers were identified. Because of the regulation that occurs immediately upstream from the gage, the observed flows do not appear to follow a typical Log Pearson III distribution. Peak flows begin to plateau around 30,000 to 40,000 cfs. Releases from Lake Travis are typically regulated such that streamflow at the Colorado River at Austin gage does not exceed 30,000 cfs until the lake elevation exceeds a certain level (LCRA, 2022). Therefore, the computed flood flow frequency curve at the Colorado River at Austin gage may not be as reliable as a result of the stringent regulation from Lake Travis.

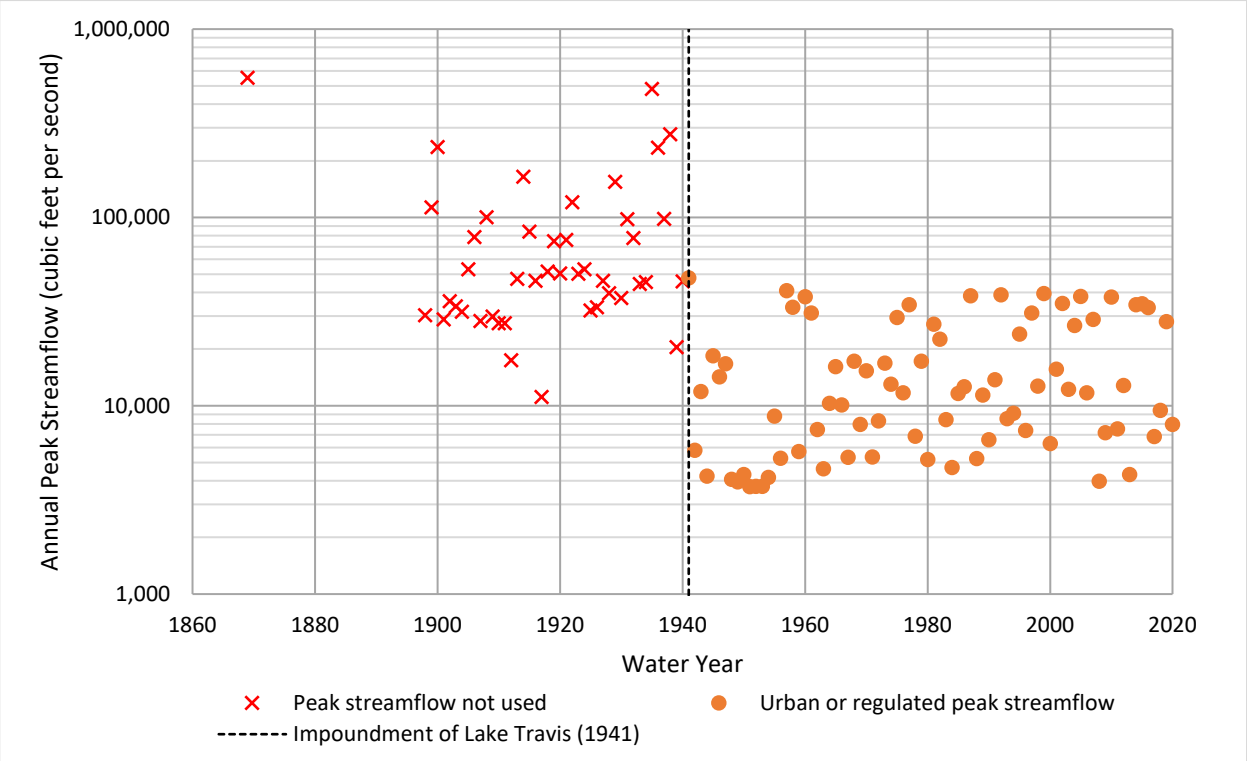

Figure 5.22: Annual Peak Streamflow Data for USGS Streamgage 08158000 Colorado River at Austin

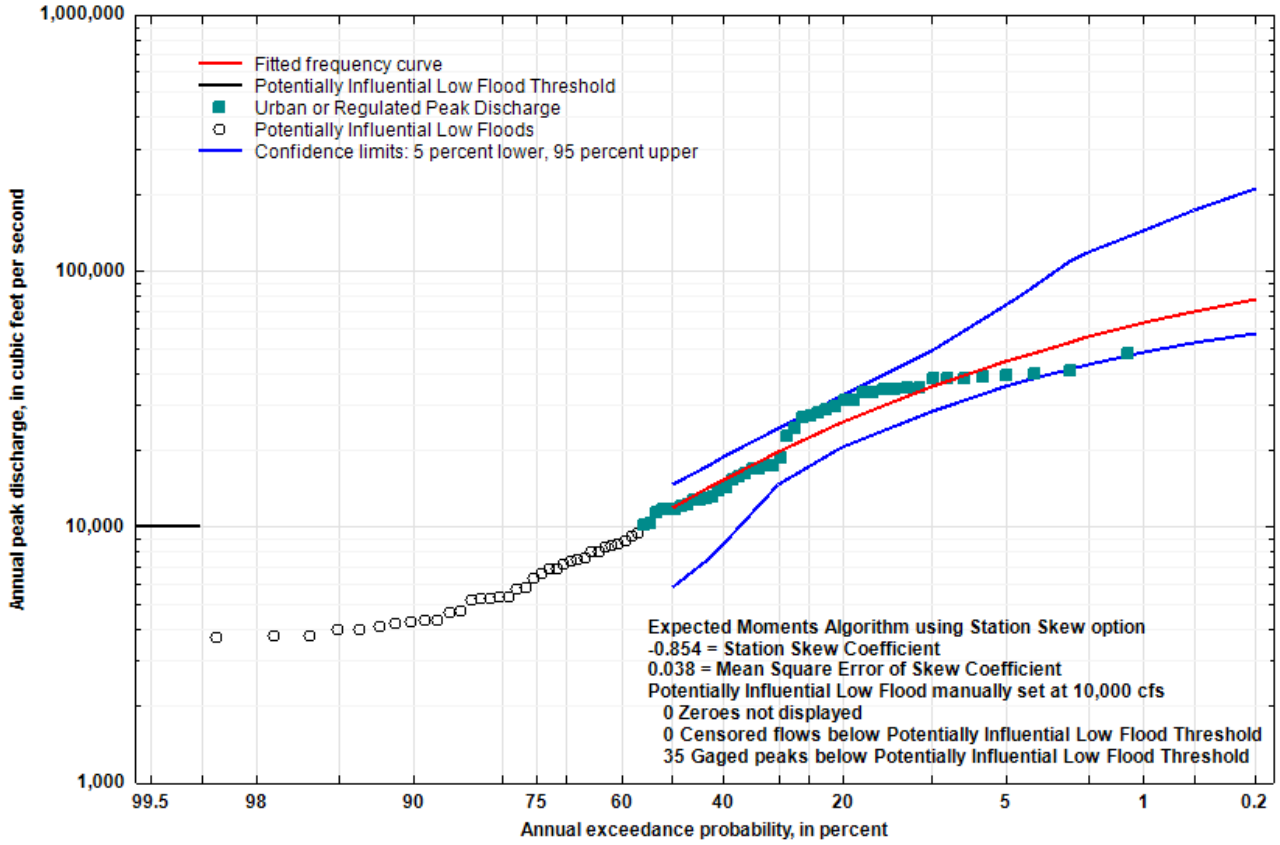

Figure 5.23: Flood Flow Frequency Curve for USGS Streamgage 08158000 Colorado River at Austin, TX

08159000 Onion Creek at US Hwy 183, Austin, TX

The period of record at USGS streamgage 08159000 Onion Creek at US Hwy 183, Austin, TX (hereinafter referred to as the "Onion Creek at Austin gage") was from 1924 through 2020 (USGS, 2022). A historical peak streamflow of 138,000 cfs is available for 1921, and a perception threshold of that value was set for the time period between that historical peak and the beginning of gaged record in 1924. A large gap in the gaged record exists from 1930 through 1975, with a historical peak streamflow of 100,000 cfs recorded in 1941. A perception threshold of 100,000 cfs was set for the time periods before and after the 1941 historical peak to fill the gap in the gaged record. When gaged record begins again in 1976, it is coded as 'C' in NWIS, which means that the streamflow is "affected by urbanization, mining, agricultural changes, channelization, or other" (USGS, 2022). Because little to no difference is observed between the gaged record with and without this code, the entire period of record is used in the analysis. The Pettitt test does not detect a change point in the gaged record, nor does the Kendall's tau test find a statistically significant trend in the annual peak streamflow data.

The largest peak of record for the Onion Creek at Austin gage is the 2013 peak streamflow of 135,000 cfs at a stage of 40.13 ft. The peak streamflow data after being processed for statistical frequency analysis are shown in a log-normal plot of annual peak streamflow versus water year in Figure 5.24. The flood flow frequency for the Onion Creek at Austin gage is shown in Figure 5.25. The figure is exported from PeakFQ (USGS, 2014) and plots annual peak streamflow versus AEP in percent. No low outliers were identified by the MGBT in the PeakFQ software.

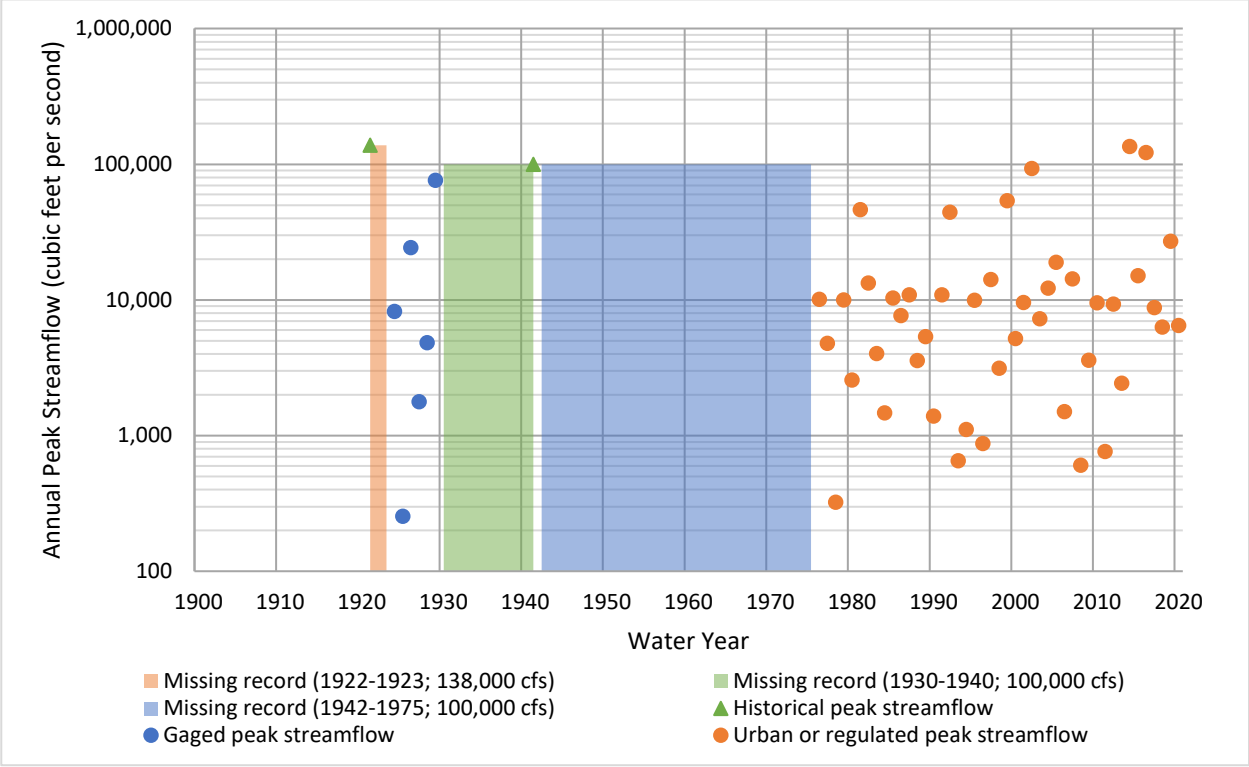

Figure 5.24: Annual Peak Streamflow Data for USGS Streamgage 08159000 Onion Creek at US Hwy 183, Austin, TX

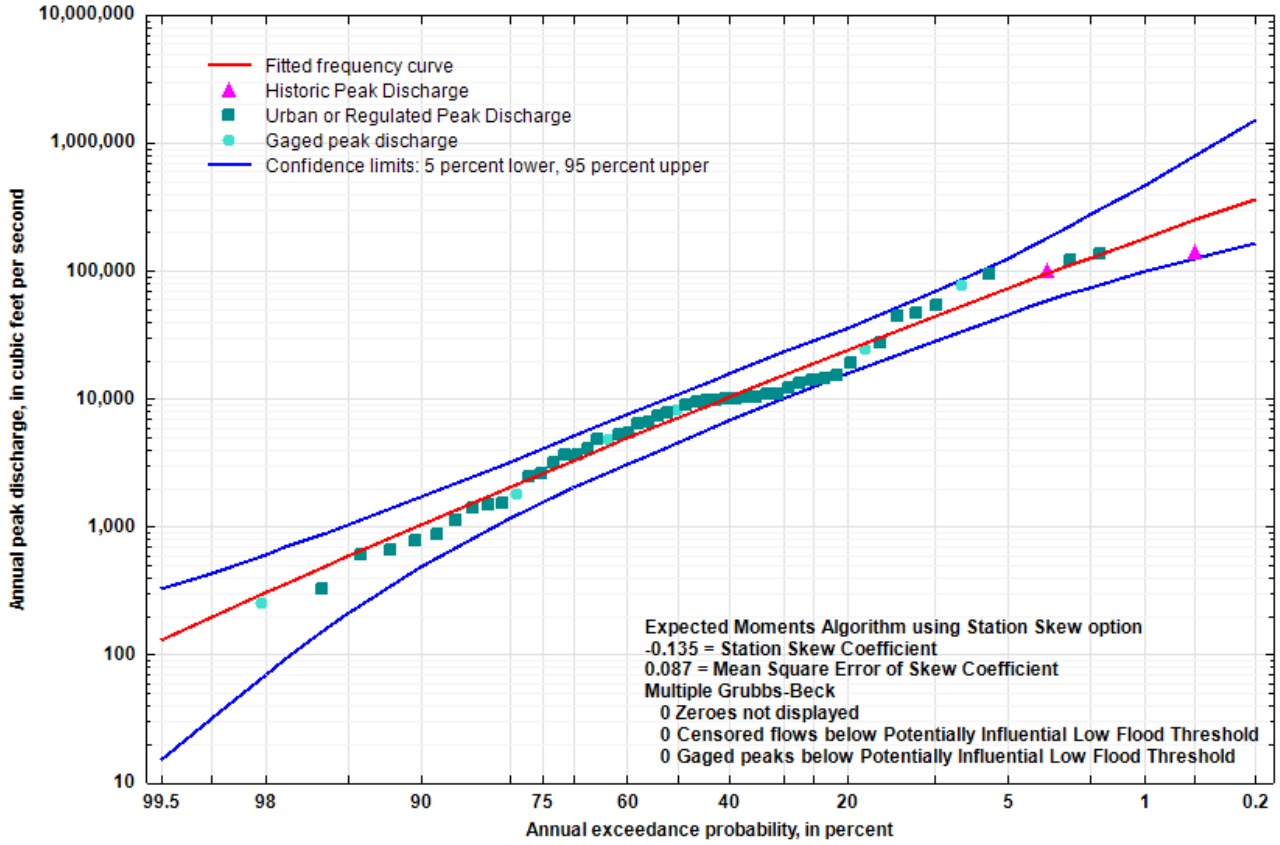

Figure 5.25: Flood Flow Frequency Curve USGS Streamgage 08159000 Onion Creek at US Hwy 183, Austin, TX

08161000 Colorado River at Columbus, TX

The period of record at USGS streamgage 08161000 Colorado River at Columbus, TX (hereinafter referred to as the "Colorado River at Columbus gage") was from 1908 through 2020 (USGS, 2022). Peak streamflow prior to the impoundment of Lake Travis (1941) on the Colorado River is excluded from the analysis. Contributing drainage area increases by only approximately 10 percent between the two Lake Travis and the Colorado River at Columbus gage (USGS, 2022). Furthermore, the Pettitt test detects a change point in water year 1943, corresponding to the impoundment of water in Lake Travis in 1941 (TWDB, 2022). Although there are several peak streamflows of greater than 100,000 cfs before and after reservoir impoundment, an analysis of the flooding events greater than 75,000 cfs at the Colorado River at Columbus gage indicate that most of those events originated upstream from Austin, TX The attenuation of runoff during flooding events by Lake Travis and possibly the other Highland Lakes reduced peak streamflows downstream from these reservoirs. After removal of all annual peaks prior to 1941, a significant trend in annual peak streamflow at the gaged location was not detected by using the Kendall's tau test.

The largest peak in the analyzed record for the Colorado River at Columbus gage is the 2017 peak streamflow of 165,000 cfs at a stage of 48.17 ft. The 2017 peak streamflow was a result of Hurricane Harvey. The peak streamflow data after being processed for statistical frequency analysis are shown in a log-normal plot of annual peak streamflow versus water year in Figure 5.26. The flood flow frequency for the Colorado River at Smithville gage is shown in Figure 5.27. The figure is exported from PeakFQ (USGS, 2014) and plots annual peak streamflow versus AEP in percent. The low-outlier threshold was manually set at 12,000 cfs, and a total of 13 low outliers were identified.

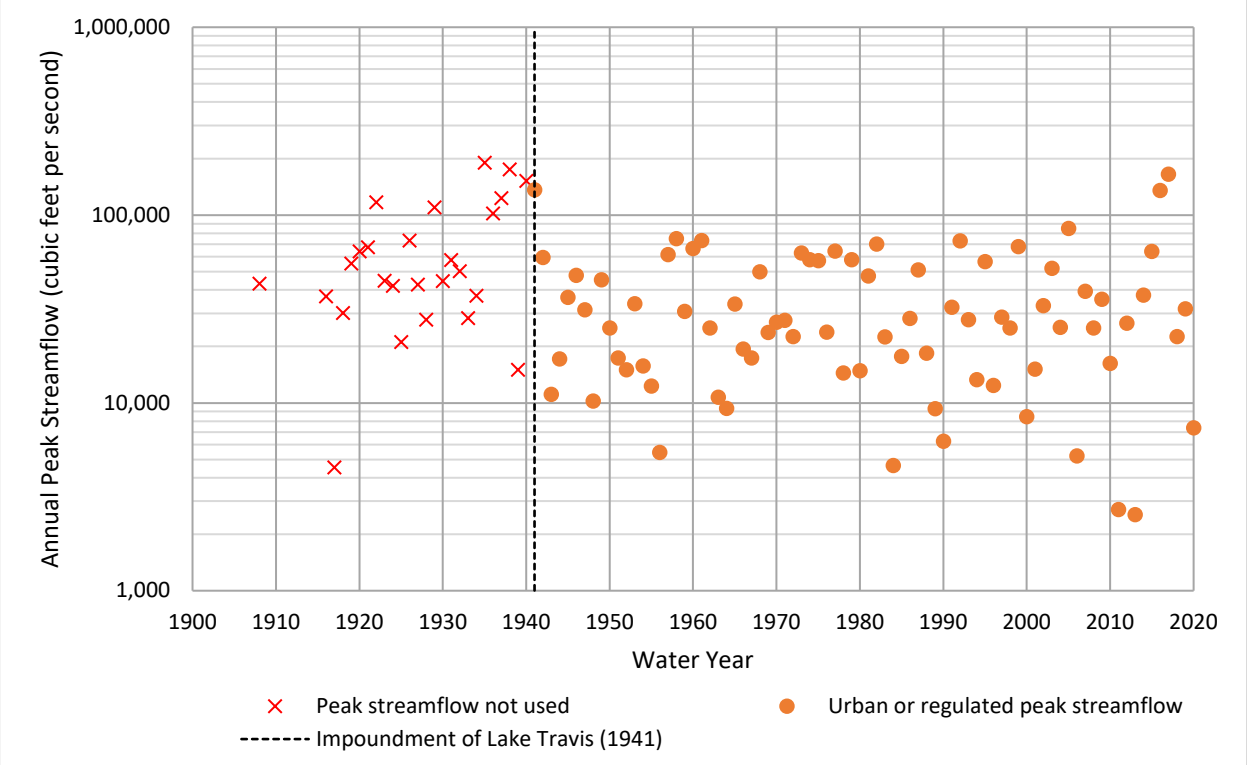

Figure 5.26: Annual Peak Streamflow Data for USGS Streamgage 08161000 Colorado River at Columbus

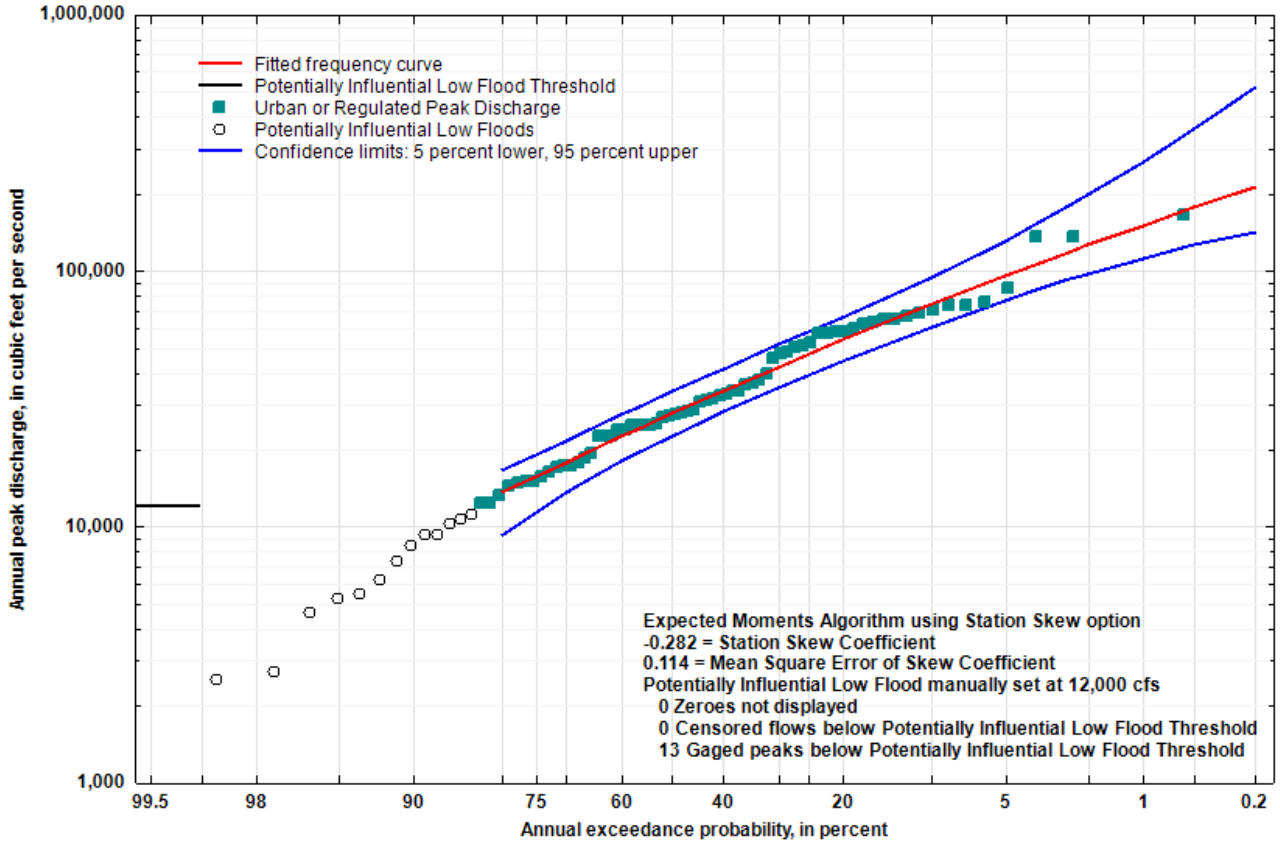

Figure 5.27: Flood Flow Frequency Curve for USGS Streamgage 08161000 Colorado River at Columbus

Table 5.4: Statistically Estimated Annual Flood Flow Frequency Results and Confidence Intervals for the Twelve U.S. Geological Survey Streamgages on the Mainstem of the Colorado River, Texas

[cfs, cubic feet per second; %, percent; CI, confidence interval; Note, table contents derived from EXP file (file extension name) of USGS-PeakFQ software output (USGS, 2014). The estimates are of primary interest and are accentuated using a bold typeface.]

Station number and name	Flood flow frequency by corresponding average return period (recurrence interval) in years							
	2 year (cfs)	5 year (cfs)	10 year (cfs)	25 year (cfs)	50 year (cfs)	100 year (cfs)	200 year (cfs)	500 year (cfs)
08124000 Colorado River at Robert Lee, TX								
Lower 95%-CI	180	795	1,610	3,270	5,020	7,260	10,000	14,600
Estimate	**304**	**1,340**	**2,840**	**6,260**	**10,300**	**16,100**	**24,200**	**39,200**
Upper 95%-CI	502	2,490	6,060	16,400	31,900	58,900	105,000	214,000
08126380 Colorado River near Ballinger, TX								
Lower 95%-CI	1,780	4,630	6,960	10,300	12,900	15,400	17,800	20,600
Estimate	**2,620**	**6,370**	**9,730**	**14,900**	**19,200**	**24,000**	**29,100**	**36,400**
Upper 95%-CI	3,630	9,090	14,900	26,800	41,400	64,000	99,100	178,000
08136700 Colorado River near Stacy, TX								
Lower 95%-CI	306	1,370	2,740	5,440	8,240	11,700	16,000	22,700
Estimate	**604**	**2,630**	**5,540**	**12,000**	**19,600**	**30,300**	**44,800**	**71,500**
Upper 95%-CI	1,160	5,940	15,000	42,100	84,300	160,000	291,000	612,000
08138000 Colorado River at Winchell, TX								
Lower 95%-CI	6,120	15,000	19,500	24,600	28,400	32,100	35,900	40,900
Estimate	**10,600**	**17,900**	**23,500**	**31,300**	**37,500**	**44,200**	**51,300**	**61,300**
Upper 95%-CI	12,200	22,400	31,800	50,200	71,000	99,200	136,000	201,000
08147000 Colorado River near San Saba, TX								
Lower 95%-CI	12,400	25,400	34,900	46,200	52,600	57,400	61,000	64,600
Estimate	**16,200**	**32,300**	**44,000**	**59,100**	**70,200**	**80,900**	**91,300**	**105,000**
Upper 95%-CI	21,000	40,800	58,100	87,500	114,000	145,000	183,000	246,000
08147000 Colorado River near San Saba, TX (alternate analysis)								
Lower 95%-CI	18,800	39,100	55,700	79,000	97,200	115,000	133,000	157,000
Estimate	**22,700**	**47,200**	**68,200**	**100,000**	**128,000**	**158,000**	**192,000**	**242,000**
Upper 95%-CI	27,400	57,500	85,600	136,000	188,000	254,000	338,000	483,000
08158000 Colorado River at Austin, TX								
Lower 95%-CI	5,740	20,500	28,300	37,300	43,100	48,100	52,300	56,800
Estimate	**11,800**	**25,400**	**35,100**	**47,000**	**55,100**	**62,600**	**69,400**	**77,500**
Upper 95%-CI	14,500	32,300	48,700	83,100	117,000	144,000	172,000	209,000
08159200 Colorado River at Bastrop, TX								
Lower 95%-CI	11,800	33,900	45,300	57,600	66,400	75,000	83,300	93,900
Estimate	**22,700**	**41,700**	**55,900**	**75,300**	**90,400**	**106,000**	**122,000**	**144,000**
Upper 95%-CI	27,000	53,500	80,500	137,000	201,000	292,000	392,000	544,000
08159500 Colorado River at Smithville, TX								
Lower 95%-CI	16,900	36,800	52,600	74,300	90,900	108,000	124,000	145,000
Estimate	**22,000**	**47,000**	**68,100**	**99,100**	**125,000**	**153,000**	**183,000**	**226,000**
Upper 95%-CI	27,900	60,500	91,200	143,000	191,000	250,000	320,000	433,000

Table 5.4 (continued): Statistically Estimated Annual Flood Flow Frequency Results and Confidence Intervals for the Twelve U.S. Geological Survey Streamgages on the Mainstem of the Colorado River, Texas

Station number and name	Flood flow frequency by corresponding average return period (recurrence interval) in years							
	2 year (cfs)	5 year (cfs)	10 year (cfs)	25 year (cfs)	50 year (cfs)	100 year (cfs)	200 year (cfs)	500 year (cfs)
08160400 Colorado River above La Grange, TX								
Lower 95%-CI	16,300	36,400	52,300	73,900	90,500	107,000	124,000	145,000
Estimate	**23,500**	**51,200**	**75,000**	**110,000**	**140,000**	**173,000**	**208,000**	**258,000**
Upper 95%-CI	33,000	77,000	122,000	203,000	284,000	384,000	509,000	719,000
08160400 Colorado River above La Grange, TX (alternate analysis)								
Lower 95%-CI	21,500	42,400	58,000	78,600	94,000	109,000	124,000	142,000
Estimate	**26,100**	**51,200**	**71,100**	**99,300**	**122,000**	**146,000**	**172,000**	**207,000**
Upper 95%-CI	31,500	63,100	91,200	136,000	176,000	224,000	278,000	363,000
08161000 Colorado River at Columbus, TX								
Lower 95%-CI	22,700	44,000	60,200	81,600	97,300	112,000	126,000	142,000
Estimate	**27,700**	**53,500**	**73,900**	**103,000**	**126,000**	**150,000**	**176,000**	**212,000**
Upper 95%-CI	33,600	65,800	94,100	145,000	198,000	268,000	358,000	520,000
08162000 Colorado River at Wharton, TX								
Lower 95%-CI	20,900	38,000	50,400	66,800	79,400	92,200	105,000	122,000
Estimate	**24,900**	**45,100**	**60,900**	**83,400**	**102,000**	**122,000**	**143,000**	**173,000**
Upper 95%-CI	29,300	54,700	76,800	111,000	142,000	178,000	220,000	286,000
08162500 Colorado River near Bay City, TX								
Lower 95%-CI	20,300	37,900	50,500	67,700	81,100	94,900	109,000	128,000
Estimate	**24,900**	**45,400**	**62,000**	**86,000**	**106,000**	**128,000**	**152,000**	**187,000**
Upper 95%-CI	29,400	56,500	81,400	122,000	160,000	206,000	260,000	347,000

Table 5.5: Statistically Estimated Annual Flood Flow Frequency Results and Confidence Intervals for the Eleven U.S. Geological Survey Streamgages in the Concho River Basin, Texas

[cfs, cubic feet per second; %, percent; CI, confidence interval; Note, table contents derived from EXP file (file extension name) of USGS-PeakFQ software output (USGS, 2014). The estimates are of primary interest and are accentuated using a bold typeface.]

Station number and name	Flood flow frequency by corresponding average return period (recurrence interval) in years							
	2 year (cfs)	5 year (cfs)	10 year (cfs)	25 year (cfs)	50 year (cfs)	100 year (cfs)	200 year (cfs)	500 year (cfs)
08127000 Elm Creek at Ballinger, TX								
Lower 95%-CI	3,170	8,540	13,500	20,900	26,600	32,000	37,100	43,200
Estimate	**4,220**	**11,300**	**18,000**	**28,800**	**38,300**	**48,900**	**60,600**	**77,800**
Upper 95%-CI	5,600	15,000	25,100	46,300	70,700	105,000	152,000	244,000
08127000 Elm Creek at Ballinger, TX (alternate analysis)								
Lower 95%-CI	1,280	3,960	6,580	10,700	13,900	17,100	20,100	23,800
Estimate	**2,130**	**6,280**	**10,500**	**17,700**	**24,200**	**31,800**	**40,300**	**53,200**
Upper 95%-CI	3,430	10,400	19,600	44,000	80,900	149,000	271,000	599,000
08128000 South Concho River at Christoval, TX								
Lower 95%-CI	774	7,060	14,900	29,700	43,700	59,200	75,400	96,700
Estimate	**1,980**	**11,200**	**24,100**	**49,400**	**74,600**	**105,000**	**139,000**	**191,000**
Upper 95%-CI	3,150	18,500	42,400	97,100	159,000	242,000	351,000	548,000
08128000 South Concho River at Christoval, TX (alternate analysis)								
Lower 95%-CI	88	3,220	7,640	15,300	21,100	26,000	29,800	33,500
Estimate	**793**	**6,470**	**14,500**	**28,100**	**39,300**	**50,400**	**60,800**	**72,800**
Upper 95%-CI	1,680	13,700	40,400	176,000	291,000	436,000	609,000	872,000
08128400 Middle Concho River above Tankersley, TX								
Lower 95%-CI	188	3,480	6,950	9,840	11,600	13,000	14,000	15,100
Estimate	**1,570**	**6,180**	**10,300**	**15,400**	**18,700**	**21,600**	**23,900**	**26,400**
Upper 95%-CI	2,490	9,990	25,100	80,900	142,000	220,000	313,000	456,000
08129300 Spring Creek above Tankersley, TX								
Lower 95%-CI	23	1,330	3,990	11,000	19,700	31,700	46,900	71,600
Estimate	**253**	**2,950**	**9,310**	**28,800**	**56,600**	**101,000**	**166,000**	**294,000**
Upper 95%-CI	525	7,520	30,500	160,000	488,000	1,300,000	3,110,000	8,680,000
08130500 Dove Creek at Knickerbocker, TX								
Lower 95%-CI	133	2,900	5,980	9,920	12,800	15,500	17,800	20,400
Estimate	**1,050**	**5,120**	**9,680**	**16,800**	**22,400**	**28,000**	**33,300**	**39,700**
Upper 95%-CI	1,720	9,230	25,100	105,000	204,000	351,000	557,000	918,000
08131400 Pecan Creek near San Angelo, TX								
Lower 95%-CI	45	955	2,290	5,270	8,680	13,200	18,700	27,200
Estimate	**278**	**1,980**	**4,950**	**12,200**	**21,000**	**33,200**	**49,600**	**78,300**
Upper 95%-CI	560	4,270	11,700	37,500	84,100	176,000	338,000	717,000
08133500 North Concho River at Sterling City, TX								
Lower 95%-CI	246	2,600	4,780	8,210	11,100	13,900	16,600	19,800
Estimate	**905**	**3,890**	**7,210**	**12,600**	**17,200**	**22,100**	**27,000**	**33,500**
Upper 95%-CI	1,360	5,910	12,100	28,500	53,100	89,300	122,000	173,000

Table 5.5 (continued): Statistically Estimated Annual Flood Flow Frequency Results and Confidence Intervals for the Eleven U.S. Geological Survey Streamgages in the Concho River Basin, Texas

Station number and name	Flood flow frequency by corresponding average return period (recurrence interval) in years							
	2 year (cfs)	5 year (cfs)	10 year (cfs)	25 year (cfs)	50 year (cfs)	100 year (cfs)	200 year (cfs)	500 year (cfs)
08134000 North Concho River near Carlsbad, TX								
Lower 95%-CI	1,320	3,490	5,480	8,680	11,500	14,600	17,800	22,500
Estimate	**1,870**	**4,790**	**7,790**	**13,100**	**18,200**	**24,500**	**32,200**	**44,700**
Upper 95%-CI	2,560	7,030	12,700	27,200	50,300	96,900	190,000	380,000
08134000 North Concho River near Carlsbad, TX (alternate analysis)								
Lower 95%-CI	2,370	8,760	16,000	29,000	41,700	56,900	74,600	102,000
Estimate	**3,420**	**12,200**	**23,200**	**45,100**	**68,500**	**99,000**	**138,000**	**205,000**
Upper 95%-CI	4,700	18,000	37,300	82,000	137,000	220,000	340,000	584,000
08135000 North Concho River at San Angelo, TX								
Lower 95%-CI	282	668	1,090	1,810	2,520	3,400	4,490	6,280
Estimate	**407**	**996**	**1,700**	**3,170**	**4,870**	**7,330**	**10,800**	**17,700**
Upper 95%-CI	585	1,730	3,880	13,600	36,900	85,500	199,000	606,000
08136000 Concho River at San Angelo, TX								
Lower 95%-CI	1,230	2,670	4,010	6,110	7,970	10,100	12,400	16,000
Estimate	**1,590**	**3,520**	**5,460**	**8,930**	**12,400**	**16,800**	**22,300**	**31,800**
Upper 95%-CI	2,060	4,960	8,830	19,100	34,700	63,300	116,000	253,000
08136500 Concho River at Paint Rock, TX								
Lower 95%-CI	2,130	5,790	9,400	15,100	19,800	24,600	29,400	35,800
Estimate	**3,000**	**8,140**	**13,500**	**23,000**	**32,100**	**43,300**	**56,700**	**78,400**
Upper 95%-CI	4,220	12,000	22,200	46,800	78,200	127,000	200,000	356,000

Table 5.6: Statistically Estimated Annual Flood Flow Frequency Results and Confidence Intervals for the Seven U.S. Geological Survey Streamgages in the Pecan Bayou and San Saba River Basins, Texas

[cfs, cubic feet per second; %, percent; CI, confidence interval; Note, table contents derived from EXP file (file extension name) of USGS-PeakFQ software output (USGS, 2014). The estimates are of primary interest and are accentuated using a bold typeface.]

Station number and name	Flood flow frequency by corresponding average return period (recurrence interval) in years							
	2 year (cfs)	5 year (cfs)	10 year (cfs)	25 year (cfs)	50 year (cfs)	100 year (cfs)	200 year (cfs)	500 year (cfs)
08142000 Hords Creek near Coleman, TX								
Lower 95%-CI	1,050	2,880	4,640	7,470	9,880	12,400	14,900	18,100
Estimate	**1,530**	**4,100**	**6,660**	**10,900**	**14,900**	**19,500**	**24,900**	**33,100**
Upper 95%-CI	2,170	5,770	9,740	18,600	30,700	50,700	83,000	158,000
08143500 Pecan Bayou at Brownwood, TX								
Lower 95%-CI	3,040	7,820	11,800	17,300	21,600	25,500	29,200	33,600
Estimate	**4,200**	**10,200**	**15,400**	**23,100**	**29,400**	**36,200**	**43,200**	**53,100**
Upper 95%-CI	5,490	13,300	20,800	34,300	48,900	68,800	95,700	146,000
08143600 Pecan Bayou near Mullin, TX								
Lower 95%-CI	3,940	8,330	12,200	18,000	22,800	27,900	33,400	41,100
Estimate	**5,110**	**11,000**	**16,500**	**25,800**	**34,600**	**45,200**	**57,900**	**78,500**
Upper 95%-CI	6,650	15,300	25,900	51,200	85,200	141,000	230,000	435,000
08144500 San Saba River at Menard, TX								
Lower 95%-CI	2,530	13,400	26,400	48,500	66,700	84,200	99,900	118,000
Estimate	**4,200**	**19,900**	**39,000**	**72,400**	**103,000**	**136,000**	**172,000**	**222,000**
Upper 95%-CI	6,370	29,700	59,400	122,000	196,000	305,000	461,000	774,000
08144500 San Saba River at Menard, TX (alternate analysis)								
Lower 95%-CI	47	3,380	9,800	20,600	31,000	43,500	57,100	75,600
Estimate	**1,130**	**8,850**	**22,000**	**51,600**	**84,200**	**126,000**	**176,000**	**255,000**
Upper 95%-CI	2,300	24,600	90,500	969,000	3,280,000	8,540,000	19,400,000	51,000,000
08144600 San Saba River near Brady, TX								
Lower 95%-CI	1,700	7,320	14,200	27,200	39,500	53,100	67,700	87,900
Estimate	**3,170**	**13,000**	**26,100**	**53,000**	**82,400**	**121,000**	**171,000**	**256,000**
Upper 95%-CI	5,700	25,100	58,900	178,000	423,000	1,030,000	2,510,000	6,810,000
08144600 San Saba River near Brady, TX (alternate analysis)								
Lower 95%-CI	4,360	15,400	27,400	47,800	66,200	86,600	109,000	140,000
Estimate	**6,030**	**20,900**	**38,300**	**70,300**	**102,000**	**141,000**	**188,000**	**262,000**
Upper 95%-CI	8,170	29,500	57,200	116,000	183,000	277,000	405,000	644,000
08145000 Brady Creek at Brady, TX								
Lower 95%-CI	227	1,000	2,090	4,350	6,760	9,750	13,300	18,800
Estimate	**407**	**1,810**	**3,920**	**8,900**	**15,100**	**24,200**	**37,300**	**62,800**
Upper 95%-CI	726	3,450	8,630	28,600	72,000	180,000	447,000	1,470,000

Table 5.6 (continued): Statistically Estimated Annual Flood Flow Frequency Results and Confidence Intervals for the Seven U.S. Geological Survey Streamgages in the Pecan Bayou and San Saba River Basins, Texas

Station number and name	Flood flow frequency by corresponding average return period (recurrence interval) in years							
	2 year (cfs)	5 year (cfs)	10 year (cfs)	25 year (cfs)	50 year (cfs)	100 year (cfs)	200 year (cfs)	500 year (cfs)
08146000 San Saba River at San Saba, TX								
Lower 95%-CI	5,290	16,300	28,300	48,800	67,300	87,800	110,000	141,000
Estimate	**7,050**	**21,800**	**38,700**	**70,600**	**103,000**	**145,000**	**197,000**	**285,000**
Upper 95%-CI	9,380	29,900	57,400	125,000	216,000	360,000	587,000	1,090,000
08146000 San Saba River at San Saba, TX (alternate analysis)								
Lower 95%-CI	2,080	6,760	12,100	21,500	30,200	39,900	50,500	65,600
Estimate	**3,370**	**11,000**	**20,400**	**39,400**	**60,100**	**88,000**	**125,000**	**190,000**
Upper 95%-CI	5,450	19,700	44,600	127,000	270,000	559,000	1,130,000	2,810,000

Table 5.7: Statistically Estimated Annual Flood Flow Frequency Results and Confidence Intervals for the Eight U.S. Geological Survey Streamgages in the Llano River, Sandy Creek, and Pedernales River Basins, Texas

[cfs, cubic feet per second; %, percent; CI, confidence interval; Note, table contents derived from EXP file (file extension name) of USGS-PeakFQ software output (USGS, 2014). The estimates are of primary interest and are accentuated using a bold typeface.]

Station number and name	Flood flow frequency by corresponding average return period (recurrence interval) in years							
	2 year (cfs)	5 year (cfs)	10 year (cfs)	25 year (cfs)	50 year (cfs)	100 year (cfs)	200 year (cfs)	500 year (cfs)
08148500 North Llano River near Junction, TX								
Lower 95%-CI	3,810	18,900	34,900	59,200	76,500	90,100	100,000	109,000
Estimate	**6,640**	**28,200**	**49,800**	**80,900**	**104,000**	**126,000**	**146,000**	**169,000**
Upper 95%-CI	10,500	40,400	68,800	114,000	157,000	208,000	269,000	373,000
08150000 Llano River near Junction, TX								
Lower 95%-CI	3,880	37,300	68,300	113,000	146,000	174,000	197,000	222,000
Estimate	**12,000**	**53,500**	**97,000**	**161,000**	**211,000**	**258,000**	**302,000**	**353,000**
Upper 95%-CI	17,600	79,500	160,000	336,000	508,000	674,000	818,000	990,000
08150700 Llano River near Mason, TX								
Lower 95%-CI	9,030	38,100	72,900	140,000	197,000	249,000	292,000	337,000
Estimate	**15,200**	**59,600**	**113,000**	**211,000**	**306,000**	**420,000**	**552,000**	**755,000**
Upper 95%-CI	26,000	90,500	164,000	344,000	572,000	901,000	1,370,000	2,290,000
08150800 Beaver Creek near Mason, TX								
Lower 95%-CI	2,930	9,690	16,500	25,500	30,800	34,600	37,300	39,900
Estimate	**4,620**	**14,500**	**24,000**	**38,600**	**50,600**	**63,200**	**76,200**	**93,500**
Upper 95%-CI	7,200	21,300	38,200	73,100	110,000	162,000	232,000	369,000
08151500 Llano River at Llano, TX								
Lower 95%-CI	17,500	56,000	96,000	159,000	207,000	252,000	294,000	344,000
Estimate	**24,800**	**77,800**	**134,000**	**231,000**	**321,000**	**425,000**	**545,000**	**725,000**
Upper 95%-CI	35,100	110,000	201,000	403,000	639,000	975,000	1,450,000	2,370,000
08152000 Sandy Creek near Kingsland, TX								
Lower 95%-CI	5,860	15,000	23,800	38,600	52,200	67,900	85,600	112,000
Estimate	**8,170**	**21,000**	**34,900**	**60,900**	**87,900**	**123,000**	**167,000**	**245,000**
Upper 95%-CI	11,400	31,600	58,000	129,000	250,000	514,000	1,130,000	2,730,000
08152900 Pedernales River near Fredericksburg, TX								
Lower 95%-CI	2,570	11,700	20,900	36,000	49,100	63,400	78,400	99,200
Estimate	**5,120**	**19,400**	**36,200**	**66,900**	**97,000**	**133,000**	**175,000**	**240,000**
Upper 95%-CI	8,400	36,200	80,300	189,000	327,000	532,000	825,000	1,390,000
08153500 Pedernales River near Johnson City, TX								
Lower 95%-CI	14,500	39,500	63,900	103,000	136,000	170,000	205,000	251,000
Estimate	**19,500**	**53,000**	**87,600**	**147,000**	**204,000**	**272,000**	**352,000**	**479,000**
Upper 95%-CI	26,100	73,300	130,000	264,000	444,000	734,000	1,200,000	2,240,000

Table 5.8: Statistically Estimated Annual Flood Flow Frequency Results and Confidence Intervals for the Six U.S. Geological Survey Streamgages in the Barton Creek, Walnut Creek, and Onion Creek Tributaries of the Colorado River, Texas

[cfs, cubic feet per second; %, percent; CI, confidence interval; Note, table contents derived from EXP file (file extension name) of USGS-PeakFQ software output (USGS, 2014). The estimates are of primary interest and are accentuated using a bold typeface.]

Station number and name	Flood flow frequency by corresponding average return period (recurrence interval) in years							
	2 year (cfs)	5 year (cfs)	10 year (cfs)	25 year (cfs)	50 year (cfs)	100 year (cfs)	200 year (cfs)	500 year (cfs)
08154700 Bull Creek at Loop 360 near Austin, TX								
Lower 95%-CI	1,990	4,600	6,720	9,780	12,200	14,500	16,900	19,800
Estimate	**2,840**	**6,350**	**9,490**	**14,400**	**18,700**	**23,500**	**28,800**	**36,800**
Upper 95%-CI	3,940	9,260	15,200	29,000	48,100	82,100	143,000	249,000
08155200 Barton Creek at SH 71 near Oak Hill, TX								
Lower 95%-CI	1,480	5,400	9,240	15,200	19,700	23,700	27,200	30,900
Estimate	**2,730**	**8,870**	**15,000**	**24,600**	**32,800**	**41,600**	**50,800**	**63,400**
Upper 95%-CI	4,580	14,300	25,600	51,400	84,200	135,000	214,000	395,000
08155240 Barton Creek at Lost Creek Boulevard near Austin, TX								
Lower 95%-CI	1,410	5,460	9,470	16,300	21,700	25,600	28,000	29,700
Estimate	**2,780**	**9,570**	**16,500**	**27,300**	**36,400**	**46,000**	**56,000**	**69,400**
Upper 95%-CI	6,470	16,900	25,200	42,700	63,800	92,800	132,000	205,000
08155300 Barton Creek at Loop 360, Austin, TX								
Lower 95%-CI	870	6,270	10,400	16,300	21,400	26,800	32,500	40,400
Estimate	**2,990**	**9,540**	**16,500**	**28,500**	**39,600**	**52,500**	**67,300**	**89,400**
Upper 95%-CI	4,310	15,100	30,100	70,400	127,000	221,000	368,000	681,000
08155400 Barton Creek above Barton Springs at Austin, TX								
Lower 95%-CI	1,240	4,260	7,270	12,000	16,000	20,200	24,700	30,800
Estimate	**2,460**	**7,820**	**13,700**	**23,900**	**33,600**	**45,200**	**58,700**	**79,600**
Upper 95%-CI	4,520	16,500	33,500	72,900	121,000	192,000	293,000	493,000
08158600 Walnut Creek at Webberville Road, Austin, TX								
Lower 95%-CI	4,350	7,320	9,250	11,500	12,800	13,800	14,700	15,500
Estimate	**5,300**	**8,760**	**11,000**	**13,800**	**15,800**	**17,700**	**19,400**	**21,700**
Upper 95%-CI	6,390	10,500	13,700	18,800	23,300	28,600	34,600	44,400
08158700 Onion Creek near Driftwood, TX								
Lower 95%-CI	1,320	6,260	9,300	13,100	16,000	18,800	21,600	25,200
Estimate	**3,600**	**8,810**	**13,400**	**20,400**	**26,200**	**32,500**	**39,200**	**48,600**
Upper 95%-CI	4,880	13,900	25,600	53,700	89,700	143,000	220,000	354,000
08159000 Onion Creek at US Hwy 183, Austin, TX								
Lower 95%-CI	4,560	15,500	28,200	51,400	73,600	98,600	126,000	163,000
Estimate	**7,070**	**23,700**	**43,700**	**83,000**	**125,000**	**179,000**	**247,000**	**365,000**
Upper 95%-CI	10,800	35,600	68,000	151,000	270,000	468,000	789,000	1,530,000

5.4 LOWER COLORADO RIVER AUTHORITY STREAMGAGE DATA AND FREQUENCY RESULTS

Additional statistical analyses were performed on 21 Lower Colorado River Authority (LCRA) streamflow gaging stations (Table 5.2; Figure 5.2). The same methodology was used to analyze the LCRA gages as was used on the USGS gage data, including the use of the Kendall's tau test for trends in the annual peak streamflow record. However, the Pettitt test was not conducted on the LCRA datasets because of the relatively short periods of record. The longest period of record available was only 26 years. Additionally, because of the short record lengths in the LCRA datasets, each analysis was weighted by a regional skew value from Asquith and others (2021).

PeakFQ input must conform to specific data formatting requirements (Flynn and others, 2006), which means that constructing a synthetic data input file can be problematic and potentially lead to errors. USGS peak streamflow data are available from the USGS NWIS database (USGS, 2022) in a format compatible with PeakFQ, but other data sources do not provide this formatting option. Therefore, flow frequency analyses performed on Lower Colorado River Authority (LCRA) gage datasets are done in the USACE HEC-SSP software, which has flexible data input requirements (USACE, 2016). While the program interface might be slightly different than PeakFQ, the basic setup and methodology are the same, and when given identical input both programs will provide the same results. The results of the simulated record flood flow frequency analyses in this section are listed in Table 5.9.

This section also provides a summary of available stream gage data and graphical flow frequency results for a few example LCRA stream gages in the Lower Colorado River basin. A full description of the stream gage data, assumptions and flow frequency results for all 21 analyzed LCRA gages in the basin can be found in Appendix A.

2399 James River near Mason, TX

The period of record at LCRA streamgage 2399 James River near Mason, TX (hereinafter referred to as the "James River near Mason gage") was from 1999 through 2020. The largest peak of record for the James River near Mason gage is the 2019 peak streamflow of 114,000 cfs. The Kendall's tau test does not identify a statistically significant trend in the annual peak streamflow data.

The data as set up for statistical frequency analysis are shown in a log-normal plot of annual peak streamflow versus water year in Figure 5.28. The flood flow frequency for the James River near Mason gage is shown in Figure 5.29. The figure is exported from HEC-SSP (USACE, 2016), and plots annual peak streamflow versus AEP in percent. Because the period of record is relatively short (22 years), the station skew computed by HEC-SSP was weighted by a regional value from Asquith and others (2021). The low-outlier threshold was manually set at 100 cfs, and a total of 2 low outliers were identified.

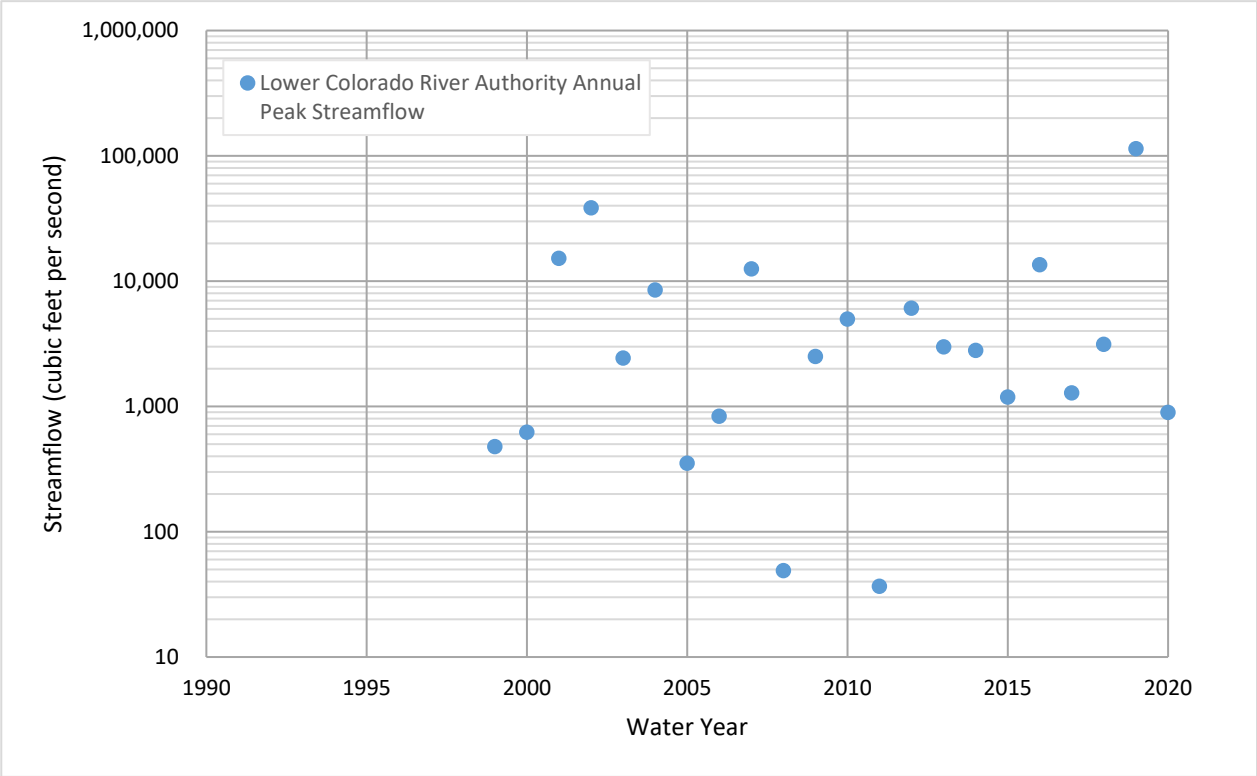

Figure 5.28: Annual Peak Streamflow Data for LCRA Streamgage James River near Mason, TX

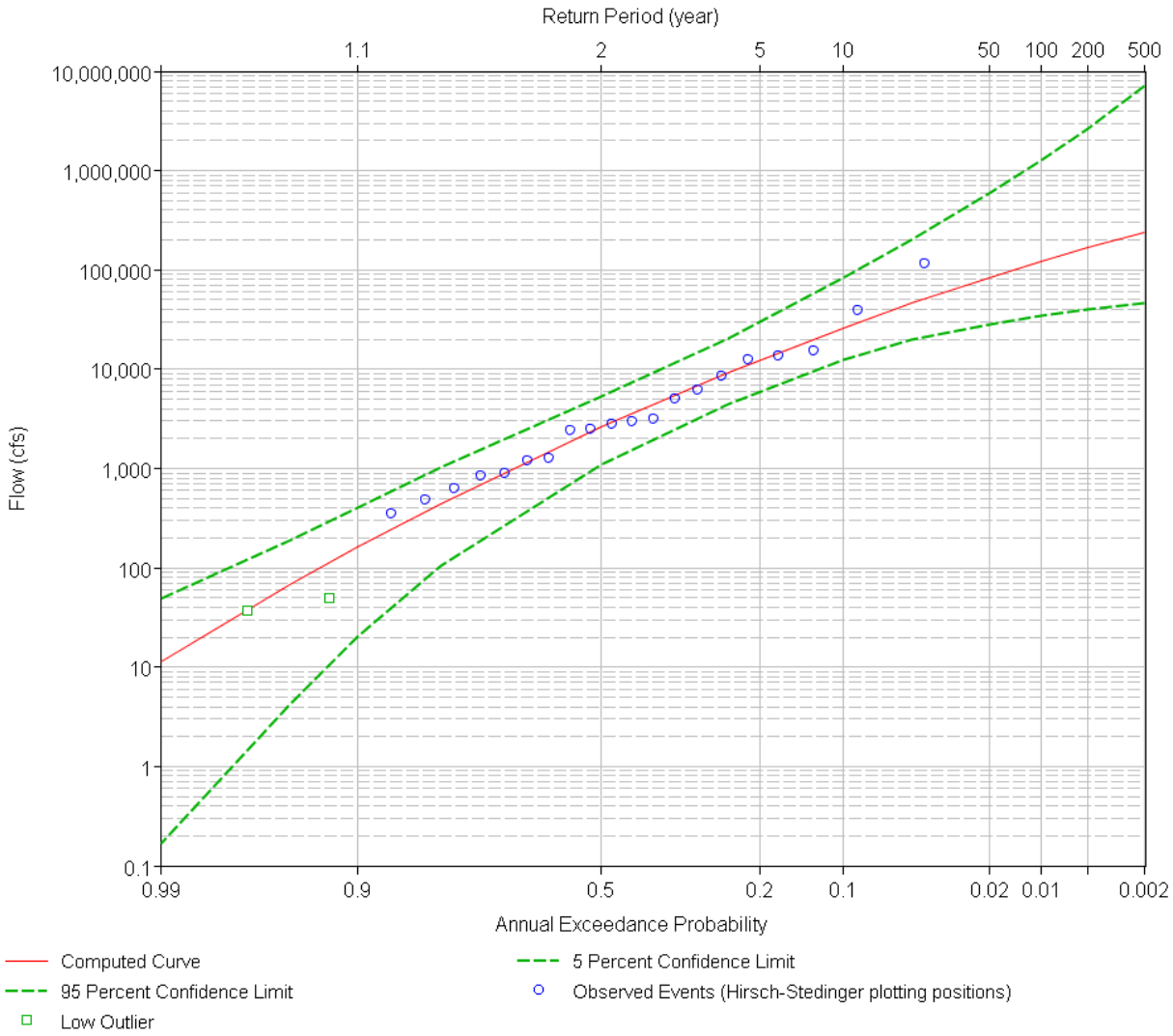

Figure 5.29: Flood Flow Frequency Curve for LCRA Streamgage James River near Mason, TX

2878 Sandy Creek near Click, TX

The period of record at LCRA streamgage 2878 Sandy Creek near Click, TX (hereinafter referred to as the "Sandy Creek near Click gage") was from 2002 through 2020. The largest peak of record for the Sandy Creek near Click gage is the 2019 peak streamflow of 38,100 cfs. The Kendall's tau test does not identify a statistically significant trend in the annual peak streamflow data.

The data as set up for statistical frequency analysis are shown in a log-normal plot of annual peak streamflow versus water year in Figure 5.30. The flood flow frequency for the Sandy Creek near Click gage is shown in Figure 5.31. The figure is exported from HEC-SSP (USACE, 2016), and plots annual peak streamflow versus AEP in percent. Because the period of record is relatively short (19 years), the station skew computed by HEC-SSP was weighted by a regional value from Asquith and others (2021). The low-outlier threshold was computed by the MGBT in HEC-SSP at 745.8 cfs, and a total of two low outliers were identified.

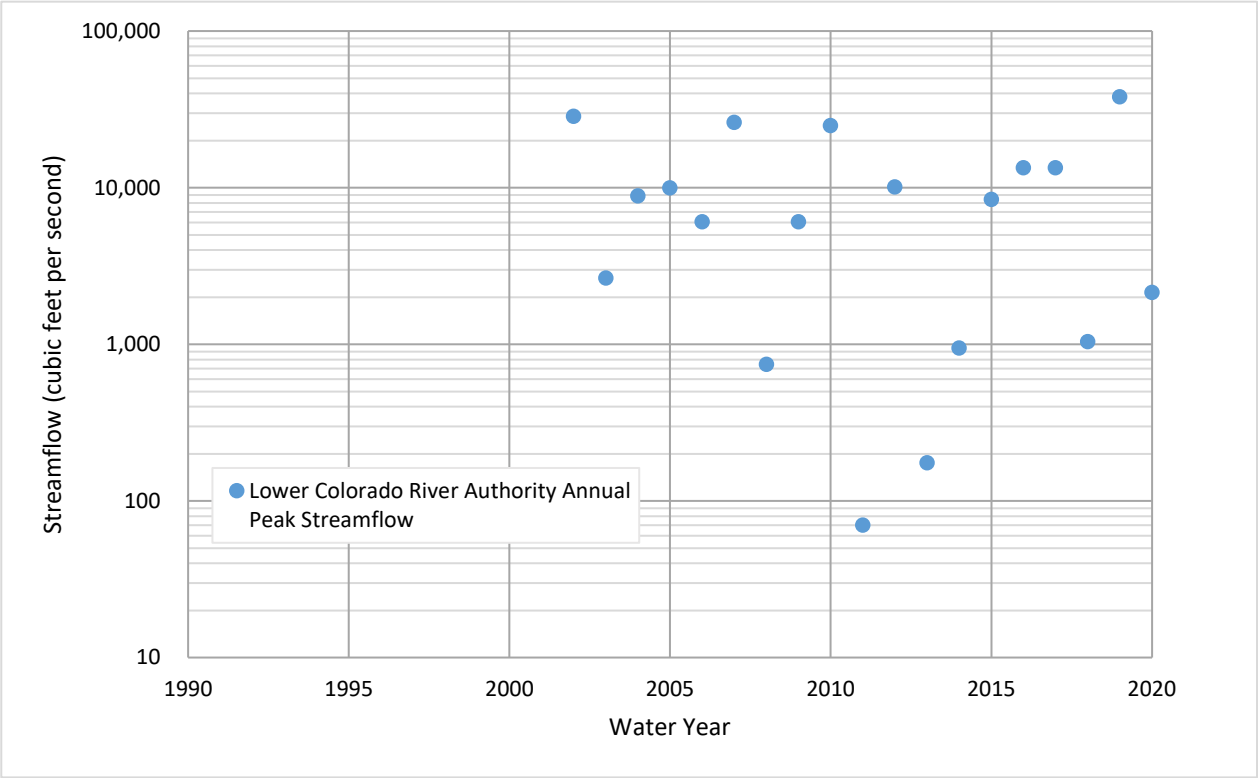

Figure 5.30: Annual Peak Streamflow Data for LCRA Streamgage Sandy Creek near Click, TX

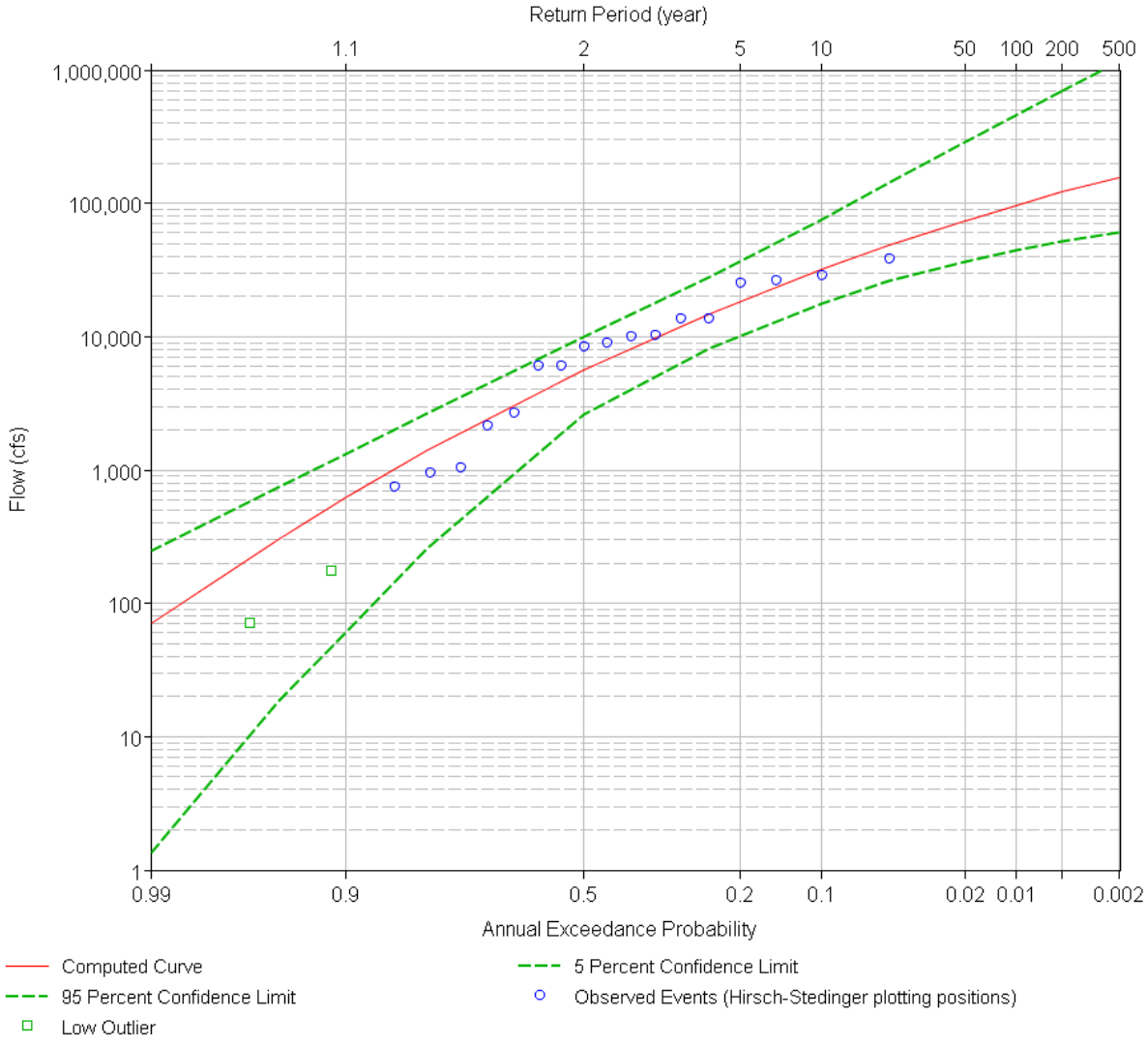

Figure 5.31: Flood Flow Frequency Curve for LCRA Streamgage Sandy Creek near Click, TX

5696 Cummins Creek near Frelsburg, TX

The period of record at LCRA streamgage 5696 Cummins Creek near Frelsburg, TX (hereinafter referred to as the "Cummins Creek near Frelsburg gage") was from 1997 through 2020. The largest peak of record for the Cummins Creek near Frelsburg gage is the 2016 peak streamflow of 97,300 cfs. The Kendall's tau test does not identify a statistically significant trend in the annual peak streamflow data.

The data as set up for statistical frequency analysis are shown in a log-normal plot of annual peak streamflow versus water year in Figure 5.32. The flood flow frequency for the Cummins Creek near Frelsburg gage is shown in Figure 5.33. The figure is exported from HEC-SSP (USACE, 2016), and plots annual peak streamflow versus AEP in percent. Because the period of record is relatively short (24 years), the station skew computed by HEC-SSP was weighted by a regional value from Asquith and others (2021; Table A.8). The low-outlier threshold was computed by the MGBT in HEC-SSP at 3,432.3 cfs, and a total of four low outliers were identified.

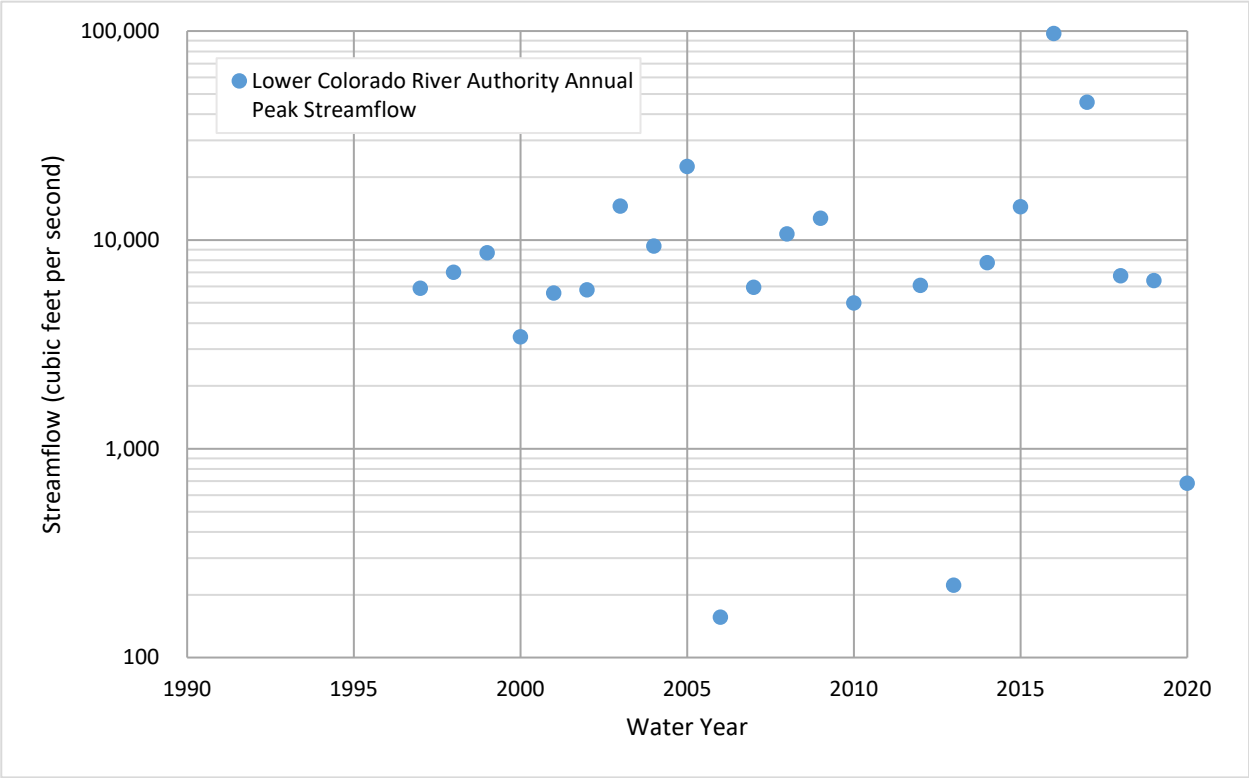

Figure 5.32: Annual Peak Streamflow Data for LCRA Streamgage Cummins Creek near Frelsburg, TX

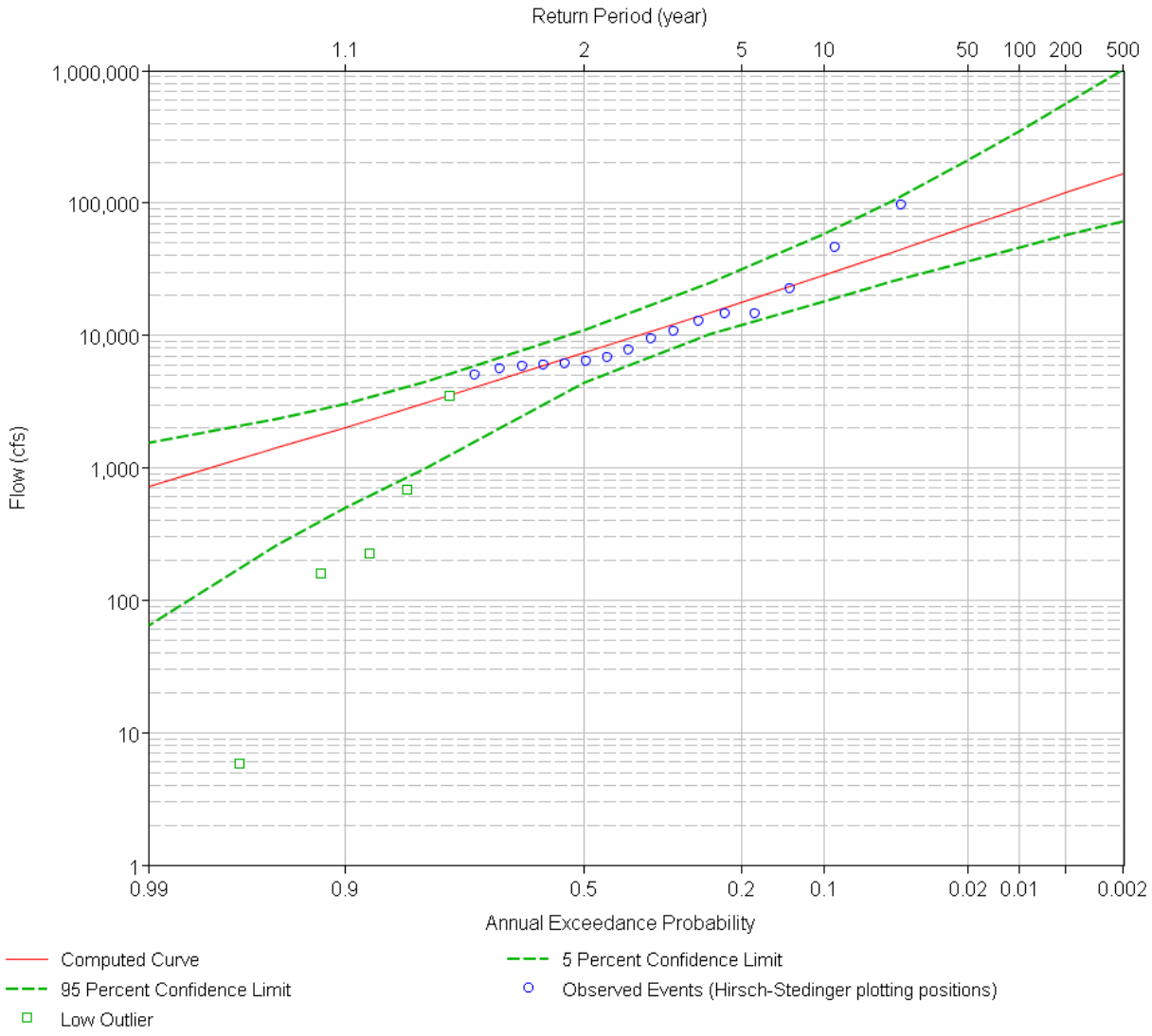

Figure 5.33: Flood Flow Frequency Curve for LCRA Streamgage Cummins Creek near Frelsburg, TX

Table 5.1: Peak-Streamflow Frequency Quantiles and 90-percent Prediction Limits for Lower Colorado River Authority Streamflow-Gaging Stations (Streamgages) in the lower Colorado River Basin, Texas.

[cfs, cubic feet per second; %, percent; CI, confidence interval; Note, table contents derived from HEC-SSP software output (USACE, 2016). The estimates are of primary interest and are accentuated using a bold typeface.]

Station name	Flood flow frequency by corresponding average return period (recurrence interval) in years							
	2 year (cfs)	5 year (cfs)	10 year (cfs)	25 year (cfs)	50 year (cfs)	100 year (cfs)	200 year (cfs)	500 year (cfs)
Cherokee Creek near Bend, TX								
Lower 95%-CI	684	3,490	6,760	12,200	16,800	21,500	26,200	32,100
Estimate	**1,570**	**6,720**	**13,200**	**25,600**	**37,900**	**53,000**	**70,600**	**98,100**
Upper 95%-CI	3,040	14,500	34,400	89,100	165,000	287,000	479,000	897,000
Johnson Fork near Junction, TX								
Lower 95%-CI	340	2,720	7,380	19,800	35,600	58,400	89,300	144,000
Estimate	**897**	**7,100**	**20,600**	**63,200**	**130,000**	**246,000**	**441,000**	**889,000**
Upper 95%-CI	2,320	23,300	91,400	457,000	1,390,000	3,970,000	10,800,000	38,300,000
James River near Mason, TX								
Lower 95%-CI	1,090	6,120	12,600	21,900	28,500	34,500	39,900	45,900
Estimate	**2,620**	**12,500**	**26,000**	**53,600**	**82,900**	**120,000**	**166,000**	**242,000**
Upper 95%-CI	5,310	29,600	82,600	264,000	588,000	1,260,000	2,670,000	7,080,000
Comanche Creek near Mason, TX								
Lower 95%-CI	155	969	1,960	3,530	4,720	5,810	6,770	7,820
Estimate	**419**	**2,040**	**4,010**	**7,420**	**10,500**	**13,800**	**17,200**	**21,900**
Upper 95%-CI	905	4,550	10,400	25,200	44,100	72,600	114,000	199,000
Willow Creek near Mason, TX								
Lower 95%-CI	25	814	1,980	4,320	6,800	9,920	13,700	19,500
Estimate	**285**	**1,900**	**4,730**	**11,800**	**20,800**	**33,700**	**51,800**	**85,300**
Upper 95%-CI	588	5,570	19,300	96,000	324,000	1,070,000	2,960,000	8,410,000
Hickory Creek near Castell, TX								
Lower 95%-CI	1,480	3,860	6,060	9,440	12,300	15,400	18,600	23,000
Estimate	**2,330**	**5,970**	**9,660**	**16,000**	**22,100**	**29,500**	**38,200**	**52,300**
Upper 95%-CI	3,590	10,300	19,100	39,300	64,700	104,000	163,000	289,000
San Fernando Creek near Llano, TX								
Lower 95%-CI	553	3,660	7,990	16,100	23,500	31,500	39,700	50,500
Estimate	**1,430**	**7,920**	**17,600**	**38,300**	**61,100**	**90,600**	**127,000**	**188,000**
Upper 95%-CI	3,120	19,500	53,500	162,000	335,000	642,000	1,170,000	2,470,000
Johnson Creek near Llano, TX								
Lower 95%-CI	59	622	1,740	4,550	7,800	12,000	17,100	25,100
Estimate	**206**	**1,860**	**5,400**	**15,800**	**30,600**	**54,300**	**90,000**	**163,000**
Upper 95%-CI	620	7,010	28,200	136,000	392,000	1,040,000	2,580,000	8,100,000
Little Llano River near Llano, TX								
Lower 95%-CI	47	1,030	2,750	6,170	9,210	12,300	15,100	18,300
Estimate	**313**	**2,980**	**7,590**	**17,400**	**27,300**	**39,000**	**51,800**	**69,700**
Upper 95%-CI	932	9,520	31,700	121,000	281,000	575,000	1,070,000	2,200,000

Table A.9 (continued): Peak-Streamflow Frequency Quantiles and 90-percent Prediction Limits for LCRA Streamgages in the lower Colorado River Basin, Texas.

Station name	Flood flow frequency by corresponding average return period (recurrence interval) in years							
	2 year (cfs)	5 year (cfs)	10 year (cfs)	25 year (cfs)	50 year (cfs)	100 year (cfs)	200 year (cfs)	500 year (cfs)
Sandy Creek near Willow City, TX								
Lower 95%-CI	1,060	3,960	6,680	10,700	13,800	16,900	19,800	23,500
Estimate	**2,230**	**6,980**	**11,900**	**20,200**	**27,800**	**36,400**	**46,100**	**60,300**
Upper 95%-CI	3,940	13,800	28,300	63,300	107,000	173,000	269,000	461,000
Sandy Creek near Click, TX								
Lower 95%-CI	2,590	10,400	17,800	28,600	36,900	44,700	52,000	60,700
Estimate	**5,600**	**18,500**	**31,900**	**54,300**	**74,300**	**96,800**	**121,000**	**157,000**
Upper 95%-CI	10,000	36,600	75,800	170,000	286,000	456,000	699,000	1,180,000
Backbone Creek at Marble Falls, TX								
Lower 95%-CI	159	2,660	5,380	9,560	13,100	16,900	20,700	25,800
Estimate	**1,140**	**5,210**	**10,500**	**21,000**	**31,700**	**44,900**	**60,700**	**85,500**
Upper 95%-CI	2,060	12,000	32,000	112,000	280,000	672,000	1,520,000	3,360,000
Hamilton Creek near Marble Falls, TX								
Lower 95%-CI	1,580	5,360	9,170	15,400	20,900	26,900	33,300	42,300
Estimate	**3,020**	**9,430**	**16,700**	**30,200**	**43,900**	**61,100**	**82,300**	**117,000**
Upper 95%-CI	5,310	19,300	41,400	99,800	182,000	318,000	537,000	1,040,000
Pedernales River at LBJ Ranch near Stonewall, TX								
Lower 95%-CI	3,670	15,500	27,500	47,000	64,000	82,200	101,000	126,000
Estimate	**7,250**	**26,600**	**48,200**	**85,500**	**120,000**	**159,000**	**203,000**	**268,000**
Upper 95%-CI	12,600	46,500	87,000	165,000	249,000	358,000	498,000	746,000
North Grape Creek near Johnson City, TX								
Lower 95%-CI	774	5,630	9,280	14,200	18,000	21,700	25,200	29,600
Estimate	**3,180**	**9,500**	**15,800**	**26,100**	**35,300**	**45,600**	**56,900**	**73,300**
Upper 95%-CI	5,200	18,400	38,100	93,100	175,000	315,000	544,000	1,060,000
Cypress Creek near Cypress Mill, TX								
Lower 95%-CI	1,230	8,220	14,300	23,200	30,300	37,400	44,300	53,000
Estimate	**4,280**	**14,500**	**25,800**	**45,200**	**63,300**	**84,300**	**108,000**	**144,000**
Upper 95%-CI	7,370	29,700	66,200	173,000	333,000	607,000	1,050,000	2,040,000
Onion Creek at Buda, TX								
Lower 95%-CI	1,340	7,150	12,200	20,400	28,000	36,500	45,700	58,600
Estimate	**3,600**	**11,600**	**20,300**	**35,500**	**50,000**	**67,100**	**86,900**	**117,000**
Upper 95%-CI	5,650	18,200	33,200	68,100	114,000	185,000	291,000	504,000
Gilleland Creek near Manor, TX								
Lower 95%-CI	1,540	3,010	4,000	5,120	5,800	6,350	6,800	7,270
Estimate	**2,090**	**3,900**	**5,180**	**6,800**	**7,980**	**9,120**	**10,200**	**11,600**
Upper 95%-CI	2,730	5,170	7,270	10,600	13,400	16,700	20,400	26,200

Table A.9 (continued): Peak-Streamflow Frequency Quantiles and 90-percent Prediction Limits for Lower Colorado River Authority Streamgages in the lower Colorado River Basin, Texas.

Station name	Flood flow frequency by corresponding average return period (recurrence interval) in years							
	2 year (cfs)	5 year (cfs)	10 year (cfs)	25 year (cfs)	50 year (cfs)	100 year (cfs)	200 year (cfs)	500 year (cfs)
Wilbarger Creek near Elgin, TX								
Lower 95%-CI	2,650	9,880	15,100	22,000	27,100	32,000	36,600	42,300
Estimate	**6,170**	**15,500**	**24,100**	**37,200**	**48,400**	**60,700**	**73,900**	**92,800**
Upper 95%-CI	9,570	27,600	51,100	106,000	175,000	275,000	418,000	694,000
Buckners Creek near Muldoon, TX								
Lower 95%-CI	1,650	5,440	9,340	15,600	20,900	26,500	32,200	39,900
Estimate	**2,870**	**9,050**	**15,900**	**28,300**	**40,400**	**55,100**	**72,800**	**101,000**
Upper 95%-CI	4,770	16,500	33,200	73,300	125,000	206,000	329,000	595,000
Cummins Creek near Frelsburg, TX								
Lower 95%-CI	4,400	12,000	18,200	28,000	36,600	46,200	56,800	72,400
Estimate	**7,380**	**17,800**	**28,600**	**47,500**	**66,300**	**89,700**	**119,000**	**167,000**
Upper 95%-CI	10,900	30,900	58,200	124,000	210,000	347,000	561,000	1,030,000

5.5 CHANGES TO FLOOD FLOW FREQUENCY ESTIMATES OVER TIME

Statistically based flood flow frequency estimates are dependent on observational data and historical flow observations prior to gage installation. Examples of changes to flood flow frequency estimates over time are provided for 15 gages in the Lower Colorado River basin. Collectively, these are shown in the figures of section 1.5 in Appendix A, but the plots for a few gages are included in this section as examples. The annual recurrence intervals of interest here are 2, 10, 100, and 500 years, which correspond to AEPs of 0.500, 0.100, 0.010, and 0.002, respectively.

Each of these examples is intended to illustrate that there is a progression in statistical flood frequency estimates over time. Peak streamflows outside the analyzed period of record are not shown. Because the data used to plot the values of the 2, 10, 100, and 500-year streamflow estimates in a given year are dependent on all data before that year, it is anticipated to see more variation in the line for a given recurrence interval than the line shown in the extreme right of the plot. This occurs because the total sample size as a measure of information content of flood flows increases at a proportionally smaller rate. For example, one more year of data for a sample of 10 years represents a 10-percent increase in information, whereas one more year of data for a sample of 50 years is only a 2-percent increase in information. In other words, as the record length increases given other factors remaining relatively constant (land use for example), the curves should vary year to year to a lesser degree for the simple reason that proportionally less information is included with each successive year.

The USGS-PeakFQ software when set up for data processing by EMA does not readily facilitate computations such as those required for similar graphics. The computations involved were based on fitting the LPIII to the L-moments (Asquith, 2011a, 2011b) of the data points shown from a given year backwards in time. The computations included a minimum of 10 years. As a result, the actual starting year varies amongst the figures. The results of USGS-PeakFQ as listed in Table 5.3 through Table 5.7 provide the ordinates for 2020 (right-most side of the figures), and logarithmic-derived offsets between the L-moment-based LPIII fit in 2020 were used to adjust the curves in prior years for each of the four return intervals. Streamflow data in this section are plotted in both log-10 and arithmetic (linear) scale.

08134000 North Concho River near Carlsbad, TX

The relative effects of record length and magnitudes of substantial floods for the North Concho River near Carlsbad gage are shown in Figure 5.34. The magnitude of the flood events associated with several return intervals (specifically the 10-, 100-, and 500-year return period flood estimates) are smaller in the initial years when the length of record was small but increase appreciably with addition of the 1974 peak of 20,000 cfs to the period of record. Streamflow estimates then gradually stabilize over time until the second greatest peak of record of 16,500 cfs occurs in 2015, resulting in an approximately 20 percent increase in the 100-year streamflow estimate as compared to the year before. Although the Kendall's tau test does not identify a statistically significant downward trend in streamflow, there appears to be a gradual decrease in the 100- and 500-year streamflow estimates over time that also appears to continue after the incorporation of the 2015 peak. The 100-year streamflow estimate decreased from 28,200 cfs in 1990 to 24,500 cfs in 2020, and the 500-year streamflow estimate decreased from 54,500 cfs to 44,700 cfs. Likewise, during 1990–2020 the 10-year streamflow estimate decreased from 8,520 cfs to 7,790 cfs. Downward trends in annual peak streamflow are much more pronounced in the Concho River tributaries upstream from the basin's reservoirs compared to the downward trends on the mainstem Colorado River.

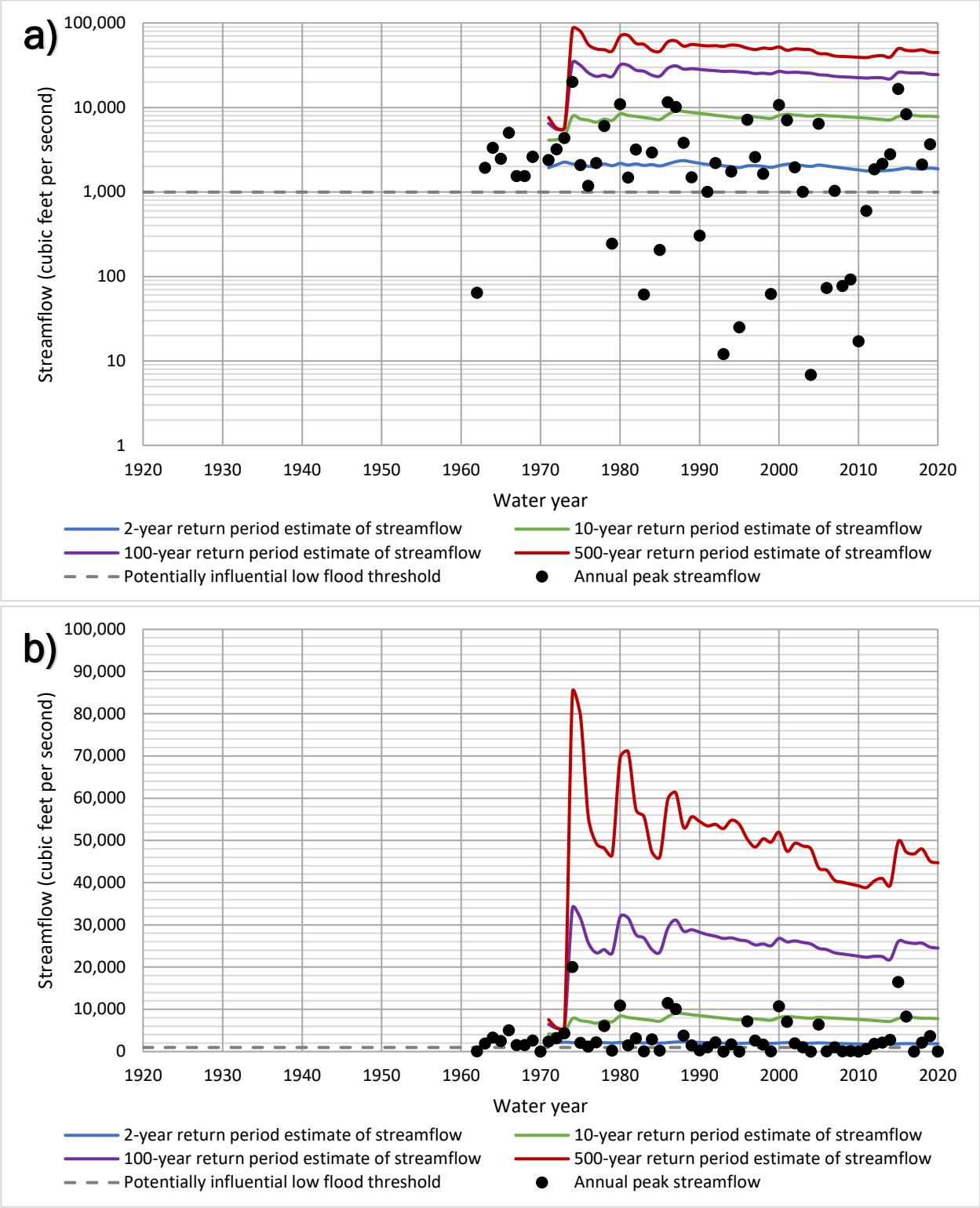

Figure 5.34: Statistical Frequency Flow Estimates versus Time in (a) log y-axis and (b) linear y-axis for U.S. Geological Survey Streamgage 08134000 North Concho River near Carlsbad, TX

08134000 North Concho River near Carlsbad, TX (Alternate Analysis)

An alternate analysis for the North Concho River near Carlsbad gage was run following the statistical analyses presented in the previous section. The relative effects of record length and magnitudes of substantial floods for the North Concho River near Carlsbad are shown in Figure 5.35. The inclusion of the entire period of record in the alternate analysis means that initial estimates are much higher when compared to Figure 5.34. Furthermore, all return interval estimates gradually decrease with time with no major interruptions to the data. It is unlikely a stable streamflow estimate has been reached for any return period at this location because of the persistence at which the streamflow estimates continue to decrease. The 10-year streamflow estimate decreases from 27,800 cfs in 2000 to 23,200 cfs in 2020, and the 100-year streamflow estimate decreases from 113,000 cfs to 99,000 cfs in the same time period. As stated in the statistical analysis in the previous section, there is evidence for a hydrologic shift in the basin circa 1960, and the peak streamflow prior to that date does not represent current conditions in the basin.

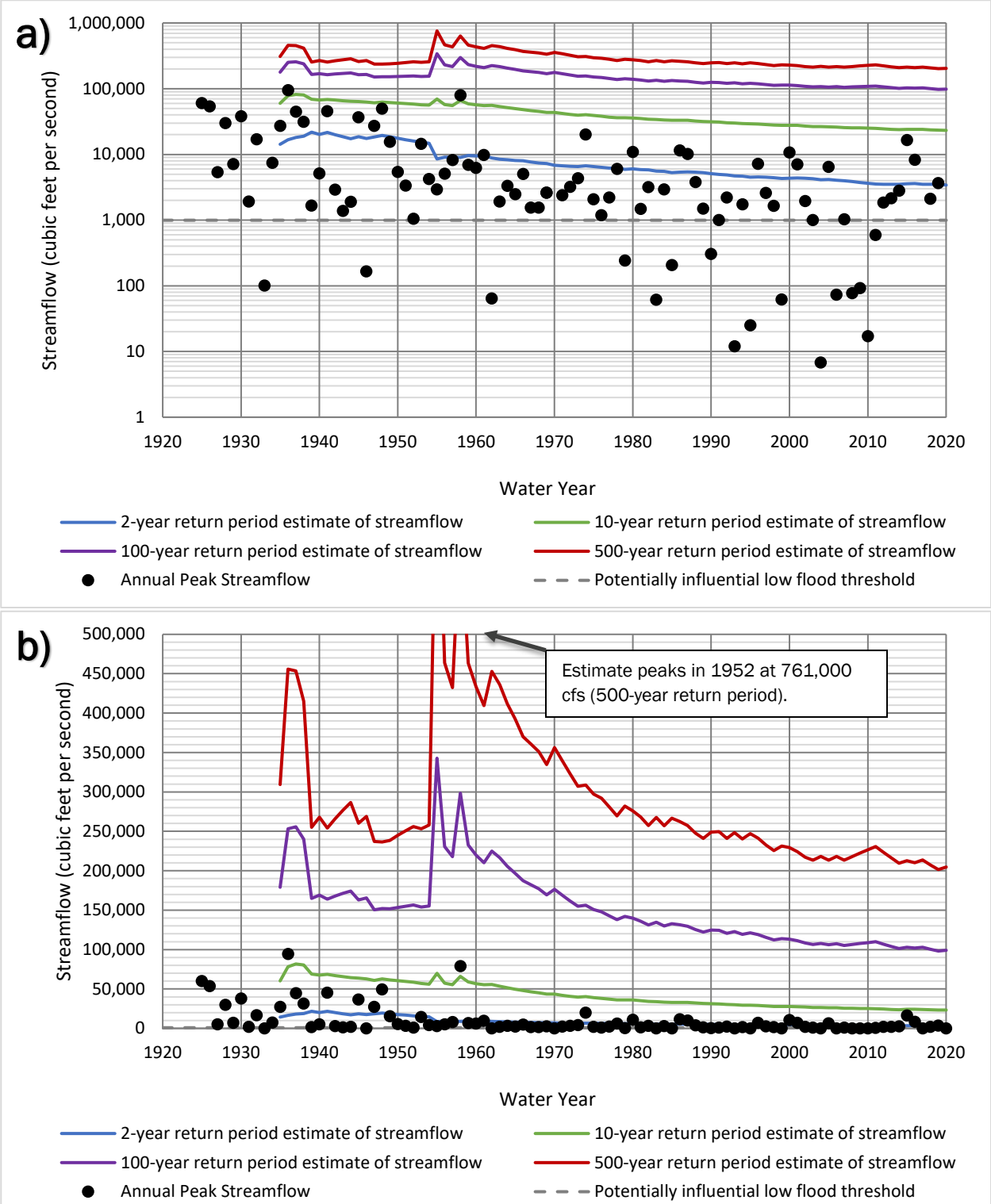

Figure 5.35: Statistical Frequency Flow Estimates versus Time in (a) log y-axis and (b) linear y-axis for U.S. Geological Survey Streamgage 08134000 North Concho River near Carlsbad, TX (Alternate Analysis)

08150000 Llano River near Junction, TX

The relative effects of record length and magnitudes of substantial flood effects for the Llano River near Junction gage are shown in Figure 5.36. After an initial spike corresponding to the 1935 flood of 319,000 cfs, the largest return-period estimates begin to decrease until all streamflow estimates appear to reach stable values by approximately water year 1990. The gradual decrease in streamflow estimates observed at other gages is not evident at this location, and the Kendall's tau test for the Llano River near Junction gage does not identify any statistically significant trends in annual peak streamflow. The 10-year streamflow estimate decreases from 104,000 cfs in 1990 to 97,000 cfs in 2020, and the 100-year streamflow estimate decreases only slightly from 259,000 cfs to 258,000 cfs during the same 1990 to 2020 time period.

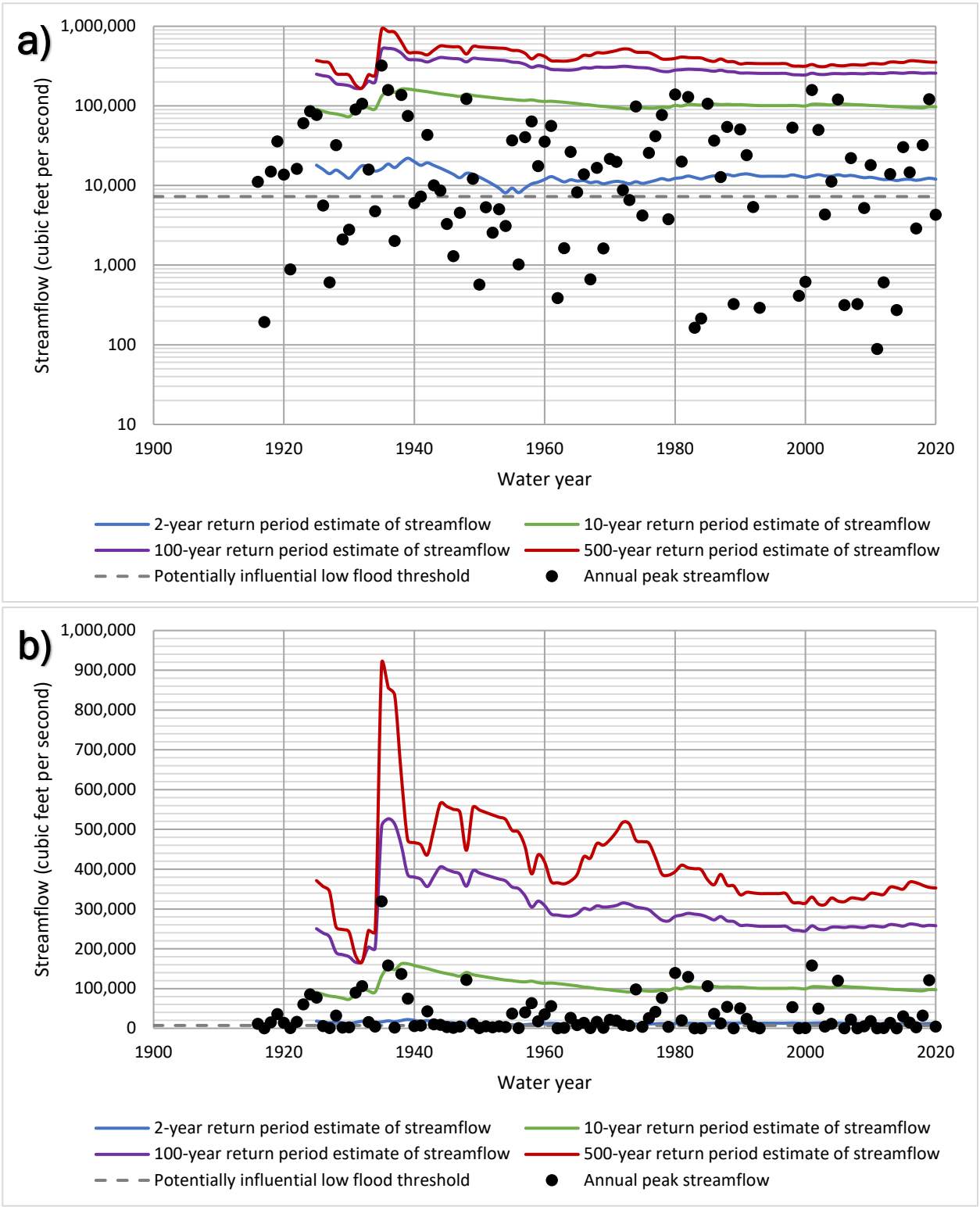

Figure 5.36: Statistical Frequency Flow Estimates versus Time in (a) log y-axis and (b) linear y-axis for U.S. Geological Survey Streamgage 08150000 Llano River near Junction, TX

08161000 Colorado River at Columbus, TX

The relative effects of record length and magnitudes of substantial flood effects for the Colorado River at Columbus gage are shown in Figure 5.37. As observed in other gages in the basin, a large event early in the period of record leads to a sharp increase in the 100 and 500-year streamflow estimates that quickly stabilizes over time. The Kendall's tau test identified a statistically significant downward trend in annual peak streamflow at the location, and all streamflow estimates appear to be remarkably throughout the period of record. However, two large events greater than 100,000 cfs in 2016 and 2017 stopped the gradual decrease in streamflow estimates for the 10, 100, and 500-year return periods with a sharp increase. The 2017 peak streamflow was attributable to Hurricane Harvey. From 1990 to 2015, the 100-year streamflow estimate decreases only slightly from 125,000 cfs to 116,000 cfs and the 500-year streamflow estimate decreases from 163,000 cfs to 147,000 cfs. Both streamflow estimates then increase to 150,000 cfs and 212,000 cfs respectively in 2020. During the same 1990 to 2015 time period, the 10-year streamflow estimate decreases only slightly from 69,000 cfs to 67,000 cfs, then increases to 73,900 cfs in 2020.

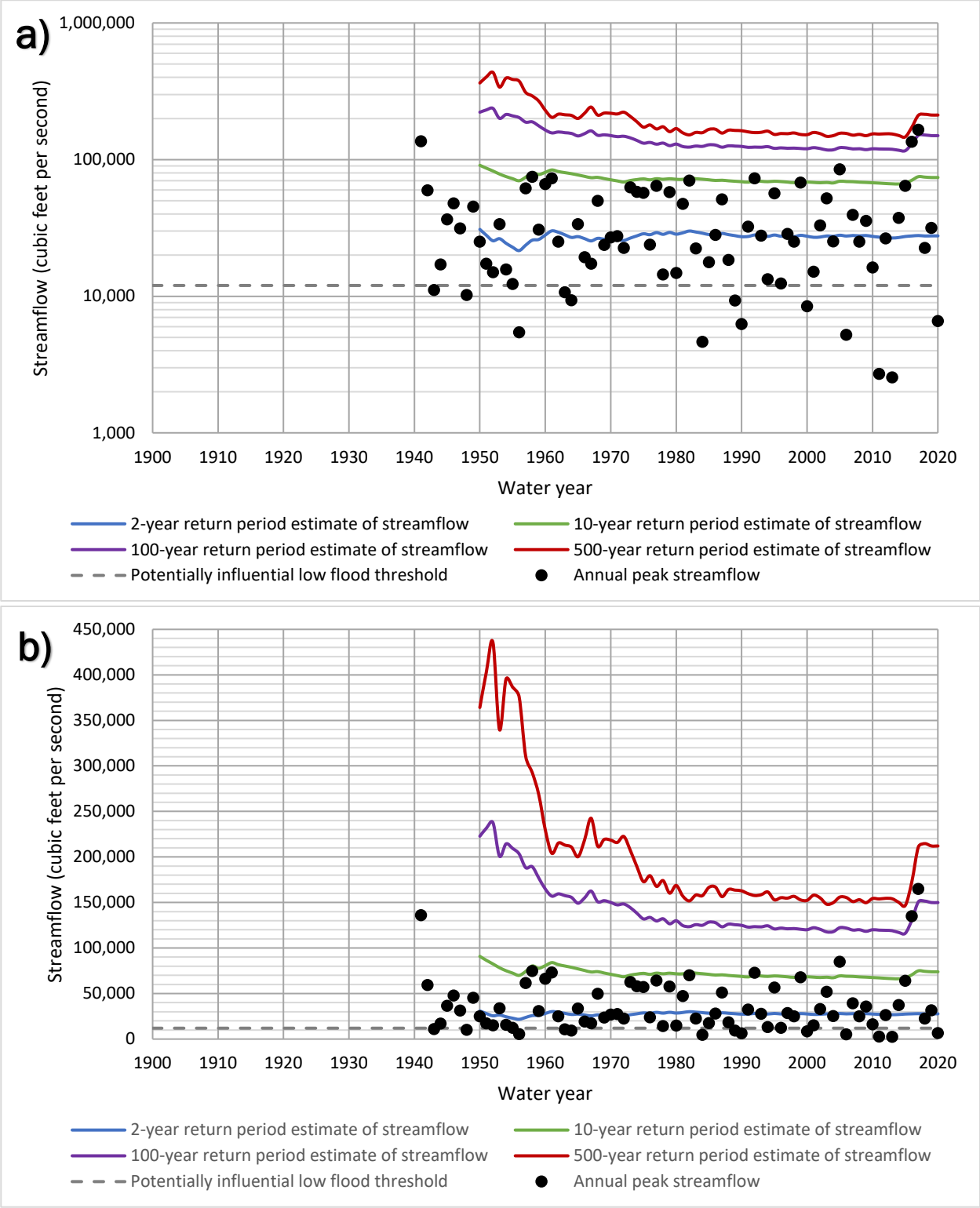

Figure 5.37: Statistical Frequency Flow Estimates versus Time in (a) log y-axis and (b) linear y-axis for U.S. Geological Survey Streamgage 08161000 Colorado River at Columbus, TX

6 Rainfall-Runoff Modeling in HEC-HMS

Rainfall-runoff watershed modeling is used to simulate the physical processes that occur during storm events that move water across the land surface and through the streams and rivers. While the statistical analyses of the gage records from Chapter 5 are a valuable means of estimating the magnitude of flood frequency flows at the gages, watershed rainfall-runoff modeling is often used to estimate the rare frequency events whose return periods exceed the gaged period of record as well as to account for non-stationary watershed conditions such as urban development, reservoir storage and regulation, and climate variability. Rainfall-runoff modeling also provides a valuable means of estimating flood frequency flows at other locations throughout the watershed that do not coincide with a stream gage.

In this phase of the multi-layered hydrologic analysis, a rainfall-runoff model was developed for the Lower Colorado River Basin with input parameters that represented the physical characteristics of the watershed. The rainfall-runoff model for the basin was completed using two existing basin-wide Hydrologic Engineering Center – Hydrologic Modeling System (HEC-HMS) models as a starting point. The first HEC-HMS model was developed for USACE's 2015 Colorado Basin Corps Water Management System (CWMS) Implementation (USACE, 2015), and the second was a basin-wide HEC-HMS model developed by the Lower Colorado River Authority (LCRA) for reservoir forecasting. These models were combined and then further refined by adding additional detailed data, updating the land use, and calibrating the model to multiple recent flood events. Through calibration, the updated HEC-HMS model was verified to accurately reproduce the response of the watershed to multiple recent observed storm events, including those similar in magnitude to a 1% annual chance (100-yr) storm. Finally, frequency storms were built using the depth area analysis in HEC-HMS and the latest published frequency rainfall depths from National Oceanic and Atmospheric Administration (NOAA) Atlas 14 (NOAA, 2018). These frequency storms were run through the calibrated model, yielding consistent estimates of the 1% annual chance (100-yr) and other frequency peak flows at various locations throughout the basin.

This chapter provides a general summary of the model development, calibration and results of the HEC-HMS rainfall runoff modeling that was completed for the InFRM Watershed Hydrology Assessment of the Lower Colorado River Basin, but additional details on the development and application of the HEC-HMS model are available in Appendix B: HEC-HMS Model Development and Uniform Rainfall Frequency Results. In addition to the uniform rainfall frequency storm results presented in this chapter, the InFRM team also developed elliptical frequency storms for stream reaches with drainage areas greater than 400 square miles in the Lower Colorado River Basin. The results from the elliptical frequency storms in HEC-HMS are presented in Chapter 7 of this report and in Appendix C: Elliptical Frequency Storms in HEC-HMS.

6.1 EXISTING HEC-HMS MODELS

Two existing HEC-HMS models were used as the starting point for the current study model: the Colorado CWMS Implementation HEC-HMS model and LCRA's forecasting HEC-HMS model.

The CWMS model contained 357 subbasins with an average size of 75 square miles in the Lower Colorado River Basin that totaled approximately 26,622 square miles. The upstream extents of the CWMS HEC-HMS model started just downstream of E.V. Spence Reservoir near Robert Lee, Texas, and the downstream extents ended at the Gulf of Mexico. The model read in observed outflows from E.V. Spence Reservoir at the upstream boundary of the model. The subbasins were delineated using the HEC-GeoHMS program and utilized 30-meter National Elevation Dataset (NED) terrain data (USACE, 2015).

The Colorado CWMS HEC-HMS model used the following methods:

- Losses – Deficit and Constant
- Transform – Snyder's
- Baseflow – Recession
- Routing – Modified Puls & Muskingum
- Computation Interval – 60 minutes

A map of the Colorado CWMS subbasins is shown in Figure 6.1. More information on the CWMS model development is given in the final CWMS implementation report for the Colorado River Basin (USACE, 2015).

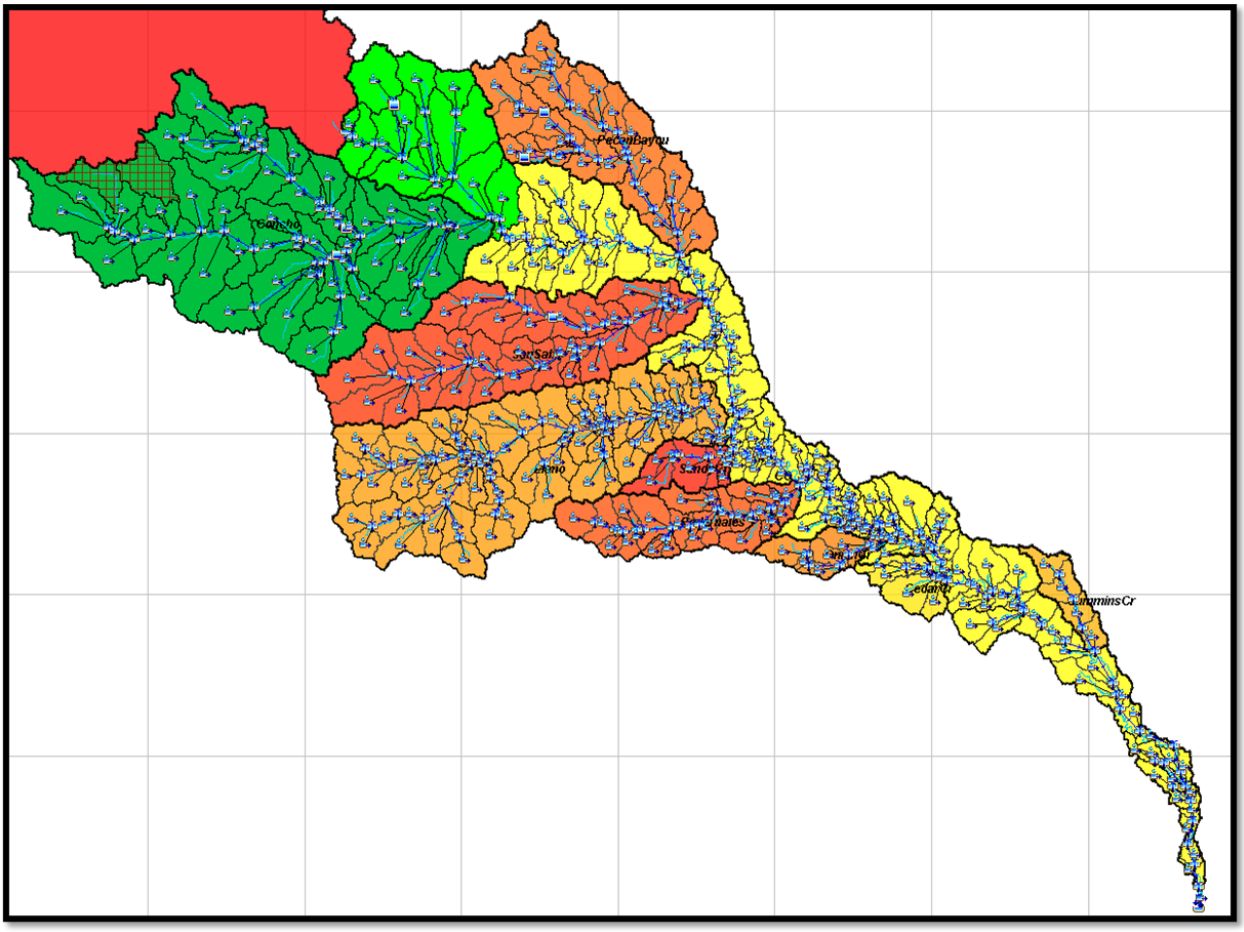

Figure 6.1: Existing CWMS HEC-HMS Subbasins for the Lower Colorado River Basin

The LCRA Forecast HEC-HMS model was originally developed as part of the 2002 Lower Colorado Flood Damage Evaluation Project (FDEP) as part of a joint project between USACE and LCRA (Halff, 2002). The model was later updated in 2006 for Phase II of the FDEP project (Halff, 2011). Since that time, LCRA staff performed additional updates to the HEC-HMS model as part of their normal reservoir forecasting duties. USACE obtained the latest copy of the HEC-HMS model from LCRA in 2022 at the kickoff for this study. The LCRA HEC-HMS model consisted of 295 subbasins with an average size of 62 square miles in the Lower Colorado River basin totaling 18,340 square miles. The upstream extents of the LCRA HEC-HMS model started just downstream of O.H. Ivie Reservoir near Stacy, Texas, and the downstream extents ended at the Gulf of Mexico. The model read in observed outflows from O.H. Ivie Reservoir at the

upstream boundary of the model. The subbasins were delineated using the HEC-GeoHMS program and utilized 30-meter National Elevation Dataset (NED) terrain data (Halff, 2002). The LCRA Forecast HEC-HMS model used the following methods:

- Losses – Deficit and Constant
- Transform – Snyder's Unit Hydrograph
- Baseflow – Recession
- Routing – Modified Puls
- Computation Interval – 60 minutes

A map of the LCRA HEC-HMS subbasins is shown in Figure 6.2. More information on the LCRA HEC-HMS model development is given in the FDEP reports for the Lower Colorado River (Halff, 2002; Halff, 2011).

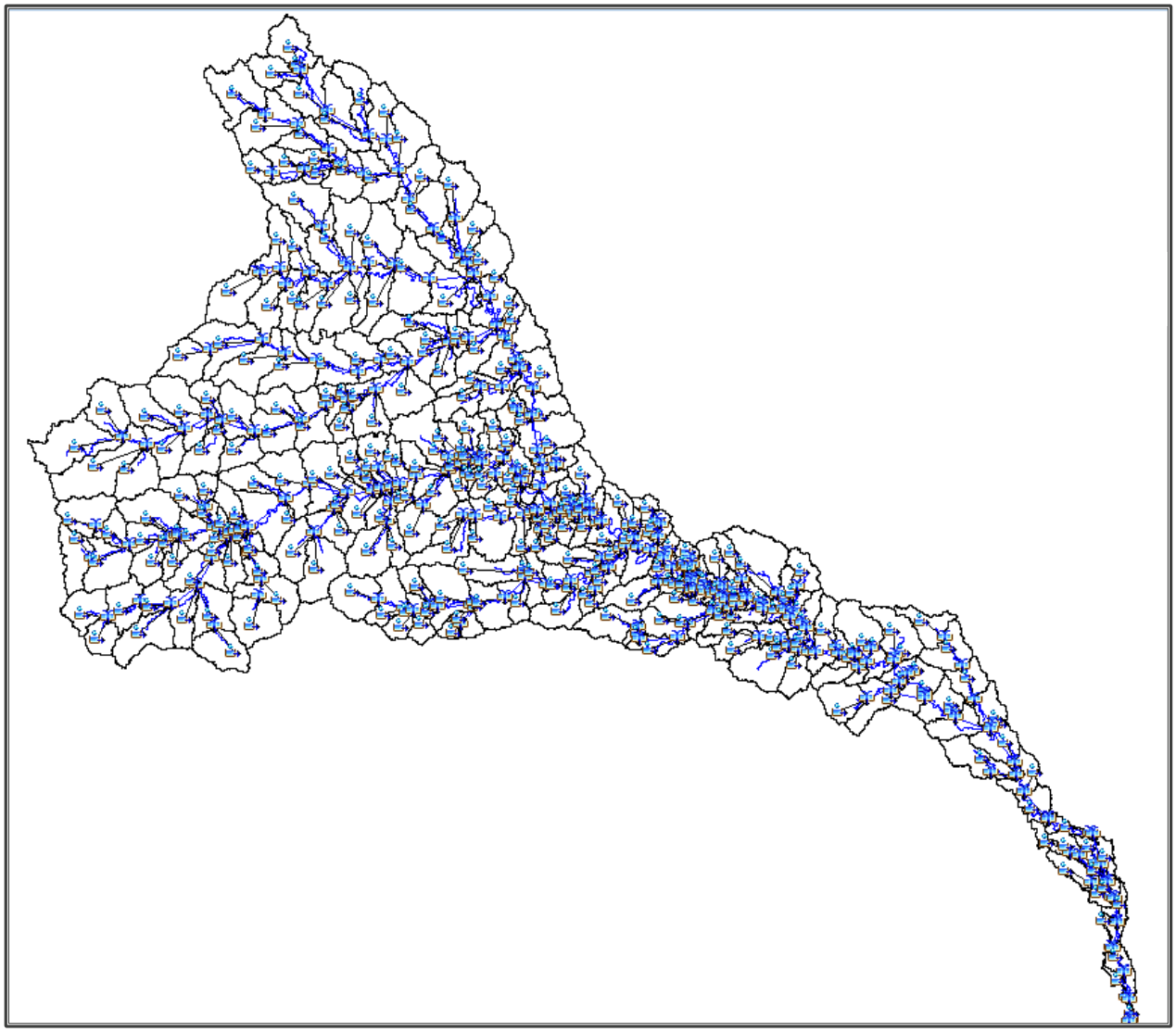

Figure 6.2: Existing LCRA Forecasting HEC-HMS Subbasins for the Lower Colorado River Basin

6.2 UPDATES TO THE HEC-HMS MODEL

To better define the hydrology of the Lower Colorado River Basin, the best available data was combined from both the CWMS and the LCRA HEC-HMS models. The CWMS HEC-HMS basin model was chosen as the base basin model because it covered an additional 8,300 square miles upstream of O.H. Ivie Reservoir that was not included in the LCRA forecast model (this area is shown in green on Figure 6.1). Downstream of O.H. Ivie, the subbasin delineations were compared and were found to be the same for the large majority of the watershed. Differences were primarily where the CWMS model had additional subbasin breaks at new USGS gage locations that were not broken out in the LCRA model. Therefore, the CWMS subbasin delineation was found to be the more detailed and was adopted for this study, as shown in Figure 6.3. After finalizing the subbasin delineation, additional updates were made to the HEC-HMS model's impervious area, transform parameters, routing reaches, reservoirs, junctions, computation points, and computation interval. These changes are summarized below with additional information in the next section.

First, the impervious area was updated to be consistent with the newest available land use data at the time of the kickoff of this study, which was the 2016 National Land Cover Database (NLCD) percent developed impervious dataset. Percent impervious values by subbasin were calculated from the 2016 NLCD data and were then compared to the existing percent impervious values in the LCRA model. For the model areas upstream of O.H. Ivie, the 2016 NLCD values were adopted for all subbasins. For the areas downstream of O.H. Ivie, only those subbasins that showed in increase in imperviousness from the LCRA values were updated with the 2016 NLCD values. The largest increases in percent imperviousness were observed in and around the area of Austin, Texas. In the overall model, the average percent impervious increased from 1.2% to 1.7%.

Next, the Snyder's Transform parameters were updated to use a combination of the CWMS and LCRA model parameters. For the area upstream of O.H. Ivie, the subbasins used the CWMS initial Snyder's parameters, as that model was the only one that included that area. For the subbasins downstream of O.H. Ivie, the Snyder's parameters from LCRA model except in areas where the subbasin delineation was different (i.e. the CWMS model delineation included breaks for new gages). In those cases, the CWMS model Snyder's parameters were adopted. This exception applied to just 24 out of 357 subbasins.

Next the routing reaches were updated to use the best available routing data. For the reaches downstream of O.H. Ivie, the Modified Puls data from the LCRA HEC-HMS model was adopted. For the 24 subbasins where the delineations had changed, the original routing HEC-RAS models from the 2002 FDEP study were used to update the storage-discharge curves for the new reach extents. Subreach values were also adjusted in proportion to the new delineation. For the reaches upstream of O.H. Ivie, the Muskingum routing data from the CWMS HEC-HMS model was adopted, except where better data was available. One of those areas was the North Concho and Concho Rivers between O.C. Fisher and O.H. Ivie. For those reaches, new Modified Puls data was developed from the final USACE CWMS HEC-RAS model and replaced the existing Muskingum data. Another area was the North Concho River upstream of O.C. Fisher Reservoir. For those reaches, better calibrated Muskingum routing data was available from the recent 2019 USACE Periodic Assessment of the reservoir, and that data was used to replace the existing CWMS Muskingum data.

For the reservoirs, new reservoir elements were added for OH Ivie, Twin Buttes, Nasworthy, OC Fisher, Coleman, Brownwood, Brady Creek, Buchanan, Inks, LBJ, Marble Falls, Marshall Ford, Lake Austin, and Lady Bird Lake, and best available reservoir data was added to the model as appropriate. In total, 17 significant reservoirs were modeled as reservoir elements in HEC-HMS, and outflows from E.V. Spence reservoir were modeled as a source element at the upstream end of the model. These reservoirs are

Lake Ballinger (upper and lower), OC Fisher lake, Twin Buttes, Nasworthy lake, O.H. Ivie Lake, Hords Creek Lake, Lake Coleman, Lake Brownwood, Brady Creek Reservoir, Lake Buchanan, Inks Lake, Lake LBJ, Lake Marble Falls, Lake Travis, Lake Austin, and Lady Bird Lake. Of these, the following reservoirs were modeled as inflow equals outflow due to their limited storage capacity in relation to their inflows: Lake Nasworthy, Inks Lake, Lake Marble Falls, Lake Austin, and Lady Bird Lake. The other 12 lakes were modeled in detail within HEC-HMS. Adjustments were also made to the storage-discharge curves in the routing reaches upstream of these reservoirs to ensure that that storage volumes within the lakes were not being double counted. While the National Inventory of Dams (NID) shows that approximately 720 dams exist within Lower Colorado River basin, these 12 reservoirs were selected to be modeled in detail due to their sizable flood storage and their noticeable influence on discharges on the major rivers downstream. Additional details on the reservoir data are included in Appendix B.

For E.V. Spence reservoir, which is at the upstream boundary of the HEC-HMS model, observed outflows from the reservoir were read in at the upstream boundary of the model for the calibration events. For the frequency storms, a low flow release from E.V. Spence of 10 cfs was assumed at the upstream boundary of the model. This is not an unreasonable assumption for two reasons: (1) E.V. Spence has only released more than 10 cfs once in the 50 plus years since the reservoir was built, and (2) the large flood storage capacity of E.V. Spence reservoir means that a large flood release from the reservoir would likely not occur until 1-2 days after the downstream runoff from a storm event has receded back into the channel. Therefore, E.V. Spence reservoir and the downstream watershed were treated as two independent sources of flooding, and the flood risk potential of releases from E.V. Spence reservoir was independently analyzed in Chapter 9.

After adding all of this detailed data, additional junctions were added to the model above major confluences, and the subbasins were resorted in hydrologic order. Additional computation points were also added at all observed data locations. Finally, the computation interval of the model was decreased from 60 to 15 minutes to show more refinement of the hydrographs on the smaller tributaries. The initial InFRM Lower Colorado HEC-HMS model was updated to HEC-HMS version 4.10 and used the following methods:

- Losses – Deficit and Constant
- Transform – Snyder's
- Baseflow – Recession
- Routing – Modified Puls & Muskingum
- Computation Interval – 15 minutes

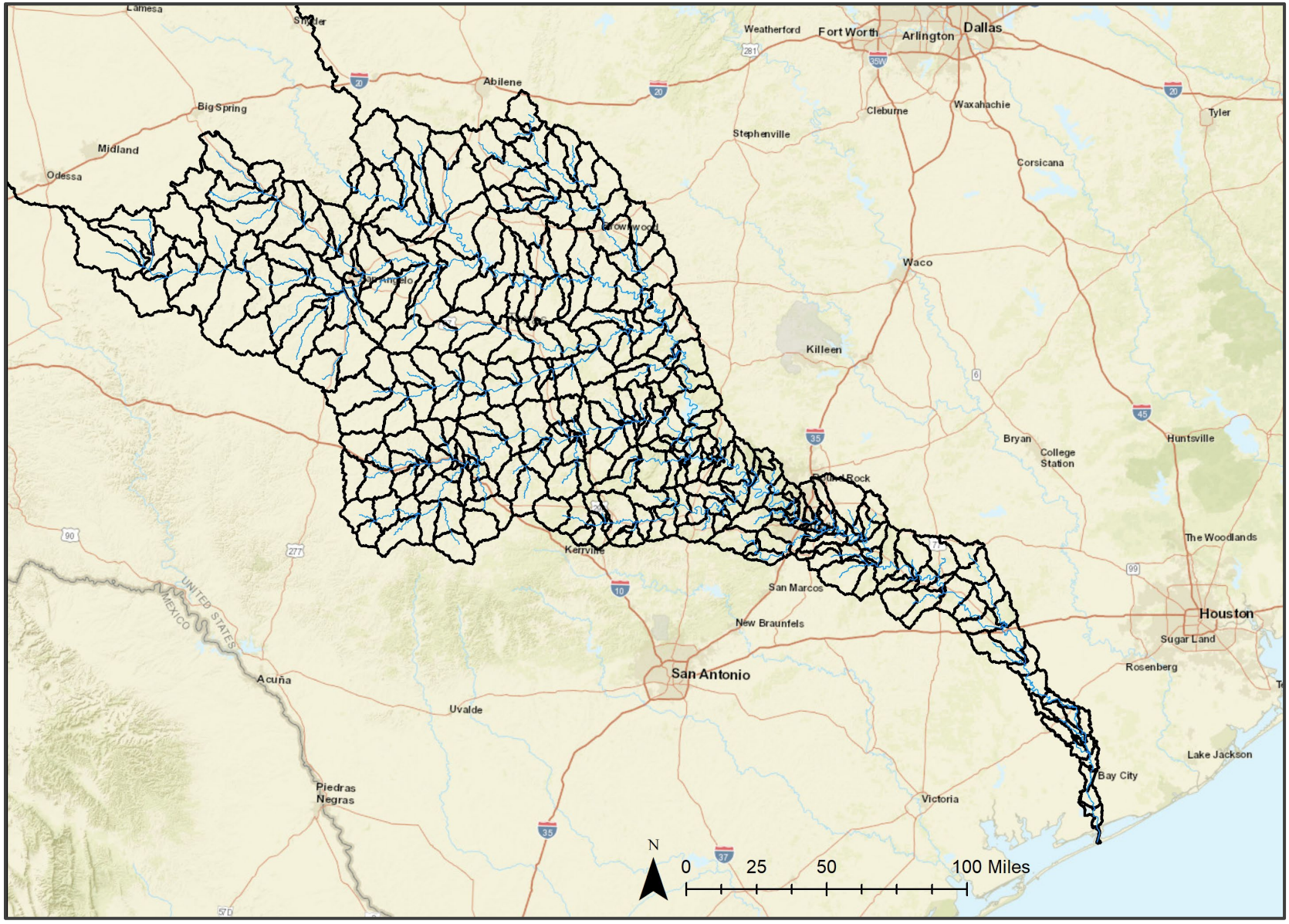

Figure 6.3: Final InFRM HEC-HMS Subbasins for the Colorado River Basin

6.3 HEC-HMS MODEL INITIAL PARAMETERS

6.3.1 Subbasin and Routing Initial Parameters

The Colorado River HEC-HMS model contains 357 subbasins totaling about 26,622 square miles. The subbasins were delineated using the HEC-GeoHMS program and utilized 30-meter NED terrain data. The Colorado River HEC-HMS model used deficit constant losses, Snyder's transform parameters, recession baseflows, and Modified Puls and Muskingum routing. The sources of the initial estimates for these parameters are described below.

- **Initial Loss and Constant Loss Rate** – For calibration, the initial and constant losses were taken from CWMS model and LCRA Forecast model. During calibration, the losses were increased or decreased according to the antecedent conditions of each individual storm event. The calibrated initial and constant losses varied for each calibration event based on the soil moisture condition. For the frequency storms, the initial and constant loss rates were first calculated based on the gSSURGO soil type, according to the Fort Worth District Loss Rate equations, which vary the loss rates by frequency (Rodman, 1977). The calculated frequency loss rates were then compared to the range of calibrated loss rates and adjusted regionally to represent typical average to wet conditions in the watershed. See section 6.5.2 for more information on the loss rates.

- **Percent Impervious** – The percent impervious values were developed based on the 2016 National Land Cover Database (NLCD) percent developed impervious dataset, which was the newest dataset that was available at be beginning of this study and was adjusted to account for open water surface in the river basin. Percent impervious values by subbasin were calculated from the 2016 NLCD data and were then compared to the existing percent impervious values in the LCRA forecast model. Only those subbasins that showed in increase in imperviousness from the LCRA values were updated with the 2016 NLCD values. In total, 90 out of the 295 LCRA subbasins were updated, and the largest increases in percent imperviousness were observed in and around the area of Austin, Texas.

- **Snyder's Transform Parameters** – Transform parameters were adopted according to the final values from the USACE CWMS and LCRA Forecast HEC-HMS models. These values were initially developed from regional equations for the Snyder's unit hydrograph method based on watershed characteristics such as length of slope that were extracted from HEC-GeoHMS. From this data, a regional equation was used to develop initial estimates of lag time for the Snyder unit hydrographs.

The regional equation that was used the develop initial estimates of lag time for the Snyder unit hydrograph was from the U.S. Army Corps of Engineers (USACE) Fort Worth District urban studies (Nelson, 1979) (Rodman, 1977) (USACE, 1989). This equation estimates subbasin lag time based on the length and slope of the watershed, the percent urban values taken from land cover data, and the percent sand values estimated from the NRCS soil data. These lag times were then further calibrated during previous efforts (Halff, 2002) (USACE, 2015) as well as the current study.

The following regional equation was used to calculate subbasin lag times in the Colorado watershed.

$$log\ (Tp) = .383log\ (L*Lca/(Sst\ ^\ .5))+(Sand*(log1.81-log.92)+log.92)-(BW*Urban./100)$$

where: Tp = Snyder's lag time (hours)

L = longest flow path within the subbasin (miles)

Lca = distance along the stream from the subbasin centroid to outlet (miles)

Sst = stream slope over reach between 10% and 85% of L (feet per mile)

Sand = percentage of sand factor as related to the permeability of the soils

(0% Sand = low permeability, 100% Sand = high permeability)

BW = log(tp) bandwidth between 0% and 100% urbanization = 0.266 (log hours)

Urban. = percentage urbanization factor

The Snyder's peaking coefficients varied from 0.4 to 0.8 based on the watershed type of different portions of the Colorado River basin. Steeper, hilly parts of the watershed were assigned a value closer to 0.8, while flatter, slower parts of the watershed were assigned a value closer to 0.4.

- **Baseflow Parameters** – Initial baseflow parameters were taken from the existing USACE Colorado CWMS HEC-HMS model. For the entire watershed, the recession baseflows were set at 0.0 cfs/square mile of initial baseflow, 0.9 for the recession constant, and 0.01 for the ratio to peak. These values were later adjusted during calibration.

- **Routing Parameters (Modified Puls)** – Wherever existing HEC-RAS models were available, Modified Puls routing data was developed by extracting storage-discharge functions from the hydraulic models. For most of the Colorado watershed, the Modified Puls data from the LCRA forecast HEC-HMS model was adopted. For the 24 subbasins where the subbasin delineations had changed, the original routing HEC-RAS models from the 2002 FDEP study were used to update the storage-discharge curves for the new reach extents (Halff, 2002). Subreach values were also adjusted in proportion to the new delineation. For the North Concho and Concho Rivers between O.C. Fisher and O.H. Ivie reservoirs, new Modified Puls data was developed from the final USACE CWMS HEC-RAS model (USACE, 2015).

- **Routing Parameters (Muskingum)** – For most of the area above O.H. Ivie reservoir, no HEC-RAS models were available. Therefore, Muskingum routing method was used for those reaches. For the area above O.H. Ivie, Muskingum parameters were adopted from the USACE CWMS HEC-HMS model (USACE, 2015), and the 2019 USACE Periodic Assessment HEC-HMS model for O.C. Fisher Reservoir.

The initial subbasin and routing parameters that were entered into the HEC-HMS model can be seen in Tables B.1 through B.4 of Appendix B. Some of these parameters were adjusted during calibration (see section 6.4.2 for additional information).

6.3.2 Initial Reservoir Data

According to the National Inventory of Dams (NID), approximately 720 dams exist within the Lower Colorado River basin, most of which are NRCS structures or other small dams. Of these, reservoir elements were used in the HEC-HMS rainfall-runoff model to represent seventeen reservoirs in the Colorado basin, and 12 of those reservoirs were selected to be modeled in detail due to their sizable flood storage and their noticeable influence on the discharges of the major rivers downstream. Another five reservoirs were modeled as inflow equals outflow due to their limited storage capacity in relation to their inflows, including Lake Nasworthy, Inks Lake, Lake Marble Falls, Lake Austin, and Lady Bird Lake. In addition, outflows from E.V. Spence reservoir were modeled as a source element at the upstream end of

the model. Table 6.1 summarizes the reservoir data obtained for the 12 dams that were modeled in detail and their corresponding data sources, and Figure 6.4 illustrates their locations within the basin.

Lake Ballinger has two lakes in tandem which are operated by the City of Ballinger. The upper dam was built in 1947. The lower dam was built in 1985. Both dams are operated by the City of Ballinger. Outlet structures are modeled as broad crested spillway way and spillway rating curve. These lakes were modeled using outlet structures with a broad crested spillway and a spillway rating curve.

OC Fisher Lake is a flood control reservoir that is operated by USACE. Its outlets consist of two 18-foot diameter conduits with 6 gated inlets at an invert elevation of 1840 ft (NGVD), and 6-7.5ft by 14.5-ft slide gates. Low flow Outlets consist of two 2.5-foot steel pipe, paralleling flood control conduits with an invert elevation of 1878.5 ft (NGVD). The ogee spillway crest is at elevation 1938.5 ft. and is 1,150 ft. long. O.C. Fisher was modeled using outlet structures with a spillway rating curve and additional gated releases.

Twin Buttes Reservoir is operated by the Bureau of Reclamation and is formed by a rolled earth fill dam 8.1 mi long, including a 200-foot-wide uncontrolled off-channel concrete gravity spillway with ogee weir section. The outlet works consist of three 15.5-foot concrete conduits, each controlled by a 12.0- by 15.0-foot fixed-wheel gate and a 12.0- by 15.0-foot radial gate, located in the Middle Concho-Spring Creek pool. Low-flow releases are made through 2.0- by 2.0-foot gates located in the center of three fixed-wheel gates. The South Concho and Middle Concho-Spring Creek pools are connected by a 3.22-mile equalizing channel. At a South Concho pool elevation of 1,926.5 ft (NGVD), the two pools join to form one lake. For lake level elevations below 1,926.5 ft, the gaged pool elevations represent the Middle Concho-Spring Creek pool only. Twin Buttes was modeled using outlet structures with a spillway rating curve and additional gated releases.

Lake Nasworthy is operated by the City of San Angelo's Parks Department. Its service spillway is a concrete ogee structure, with a 450 feet long crest at elevation 1855.3 feet. Fifteen tainter gates, each 25 feet wide by 18 feet high, with a crest elevation of 1873.2 (NGVD) control the opening. One 25 feet long automatic collapsible gate, with a crest elevation of 1869.2 feet, is located at the most northern end of the service spillway. The primary emergency spillway is 300 feet wide, at elevation 1879.1 feet. The secondary emergency spillway is 1,300 feet wide, at elevation 1880.1 feet. The low-flow outlet system consists of two 36-inch sluice gates located near the center of the service spillway structure, at an invert elevation of 1836 feet. In addition, two 24-inch diameter pipes, at an invert of 1860 feet, are located near each end of the structure. This lake was modeled as inflow equals outflow due to its limited storage capacity relative to Twin Buttes, which is directly upstream.

O.H. Ivie Lake is water supply lake that is operated by the Colorado River Municipal Water District. It is formed by a concrete dam and spillway with six 50- by 40-foot tainter gates, and a 6,000 ft overflow spillway with a 2,000 ft tapered fuse plug release feature. Total length of the dam is 12,000 ft. O.H Ivie was modeled using outlet structures with a spillway rating curve and additional gated releases.

Hords Creek Lake is a flood control reservoir that is operated by USACE. Its outlet works consists of 1 gate 8 ft controlled conduit at invert elevation 1,856 ft. and two 4 ft by 6 ft. slide gates at invert elevation 1876.5 ft (NGVD). It has a broad crested uncontrolled spillway at elevation 1920 ft (NGVD). Hords Creek was modeled using outlet structures with a simple broad crested spillway and additional gated releases.

Lake Coleman is operated by the City of Coleman. It has an uncontrolled emergency spillway that is 1,500 ft long across natural earth. The uncontrolled morning glory service spillway is 28 ft wide at the crest. A service outlet is provided for small releases through a 24-inch conduit. Lake Coleman was

modeled using outlet structures with an elevation-discharge rating curve representing the total flow from the dam.

Lake Brownwood is operated by the Brown County Water Improvement District. It was constructed in 1933 and is one of the oldest dams in the basin. Its uncontrolled emergency spillway is a broad-crested weir 479 ft long located 800 ft to left of dam. The controlled service spillway consists of two 48-inch horseshoe-shaped concrete conduits. Lake Brownwood was modeled using outlet structures with an elevation-discharge rating curve representing the total flow from the dam.

Brady Creek Reservoir is operated by the City of Brady. Its spillway is a cut channel through natural ground 1,000 ft wide located at right end of dam. The service spillway is an uncontrolled concrete drop-inlet structure that discharges through a 7.0- by 7.0-foot concrete box conduit and is designed to discharge 4,000 ft^3/s at a 19.4-ft head. The gated outlet is a 36-inch pipe that extends through the embankment and is equipped with three sluice gates for controlled releases downstream. The dam is an earth fill embankment of 8,400 feet long and 104 feet high with an elevation at the top of 1,783 feet above mean sea level, with an uncontrolled emergence spillway at the right end of the dam and its crest elevation is 1,762.4 feet above mean sea level. Brady Creek Reservoir was modeled using outlet structures with an elevation-discharge rating curve representing the total flow from the dam.

Lake Buchanan is the upstream dam in the Highland Lakes chain of lakes that is operated by the Lower Colorado River Authority (LCRA). Its operational spillway facilities include thirty 33' by 15.5' gates at a crest elevation of 1005.37 ft msl, seven 40' by 25.5' gates at a crest elevation of 995.37 ft msl, and an uncontrolled spillway on the northeast portion of the dam at a crest elevation of 1020.37 ft msl. Buchanan was modeled using outlet structures and gated releases.

Inks Lake is the next downstream dam in the Highland Lakes chain of lakes that is operated by LCRA. The dam has no gates, but it has an uncontrolled spillway with a crest elevation of 888 ft msl and one hydropower unit with an outlet capacity of 4,500 cfs. This lake was modeled as inflow equals outflow due to its limited storage capacity relative to Lake Buchanan directly upstream.

Lake LBJ is the next downstream dam in the Highland Lakes chain of lakes that is operated by LCRA. The dam has ten tainter gates 50' by 30' at a spillway elevation of 796 ft msl. Two units of hydropower have a maximum capacity of 9,200 cfs. Lake LBJ was modeled using outlet structures and gated releases.

Lake Marble Falls is the next downstream dam in the Highland Lakes chain of lakes that is operated by LCRA. It has ten 60' by 30' gates at a spillway crest elevation of 725.54-ft msl. Two units of hydropower can release about 9,400 cfs. This lake was modeled as inflow equals outflow due to its limited storage capacity relative to Lake LBJ directly upstream.

Lake Travis is the next downstream dam in the Highland Lakes chain of lakes that is operated by LCRA. It is a flood control reservoir that is operated in joint cooperation with USACE during flood events. The lake's controlled outlet consists of 24- 8.5' diameter conduits at an invert elevation of 535.75 ft msl. Each of three hydropower units has a capacity of 4,700 cfs. A 700 ft long ogee crest type uncontrolled spillway is at elevation 714.1 ft msl with 5 - 140' ft overflow bays. The dam was modeled using outlet structures with an uncontrolled spillway and additional gated releases.

Lake Austin is the last downstream dam in the Highland Lakes chain of lakes that is operated by LCRA. Its controlled releases are made through tainter gates consisting of four 51' by 18' gates at crest elevation of 475 ft msl and six 51' by 12' at crest elevation of 480 ft msl. A 458 ft long uncontrolled

spillway crest is at elevation at 492.8 ft. This lake was modeled as inflow equals outflow due to its limited storage capacity relative to Lake Travis directly upstream.

Lady Bird Lake is operated by the City of Austin. It has 506 ft long concrete type spillway with seven 50' by 13' lift gates at crest elevation 416 ft msl, and two 50' by 8' bascule gates at crest elevation 420 ft. This lake was modeled as inflow equals outflow due to its limited storage capacity relative to Lake Travis and the drainage area upstream.

Over 700 smaller dams were scattered throughout the rural areas of the basin. These dams were not modeled in detail but were accounted for in the model through adjustments to the subbasins' initial losses and peaking coefficients. Data for these dams was obtained from the National Inventory of Dams (USACE, 2016).

Table 6.1: Reservoir Data Sources for Dams Modeled in Detail in HEC-HMS

Reservoir Name	Data Type	Sources
Oak Creek Reservoir	Elevation-Storage Curve, Spillway Rating Curve	City of Sweetwater, 1976 Phase 1 Dam Inspection Report
Ballinger Lakes, Upper and Lower	Elevation-Storage Curve, Spillway Rating Curve	City of Ballinger, National Inventory of Dams, USACE calculations
Twin Buttes Reservoir	Elevation-Storage Curve, Spillway Rating Curve, Observed Releases	Bureau of Reclamation, USACE Fort Worth District
O.C. Fisher Reservoir	Elevation-Storage Curve, Spillway Rating Curve, Observed Releases	USACE Fort Worth District
O.H. Ivie Reservoir	Elevation-Storage Curve, Observed Releases	Colorado River Municipal Water District, USACE Fort Worth District
Lake Coleman	Elevation-Storage Curve, Combined Elevation-Discharge Curve	Texas Water Development Board (TWDB), 1993 USACE Pecan Bayou report
Hords Creek Reservoir	Elevation-Storage Curve, Spillway Rating Curve, Observed Releases	USACE Fort Worth District
Lake Brownwood	Elevation-Storage Curve, Combined Elevation-Discharge Curve	TWDB, 1993 USACE Pecan Bayou report
Brady Creek Reservoir	Elevation-Storage Curve, Combined Elevation-Discharge Curve	1980 Phase I Dam Inspection Report, USACE Fort Worth District
Lake Buchanan	Elevation-Storage Curve, Existing and Proposed Water Management Plans, Observed Releases	LCRA
Lake LBJ	Elevation-Storage Curve, Water Management Plan, Observed Releases	LCRA
Lake Travis	Elevation-Storage Curve, Water Management Plan, Observed Releases	LCRA

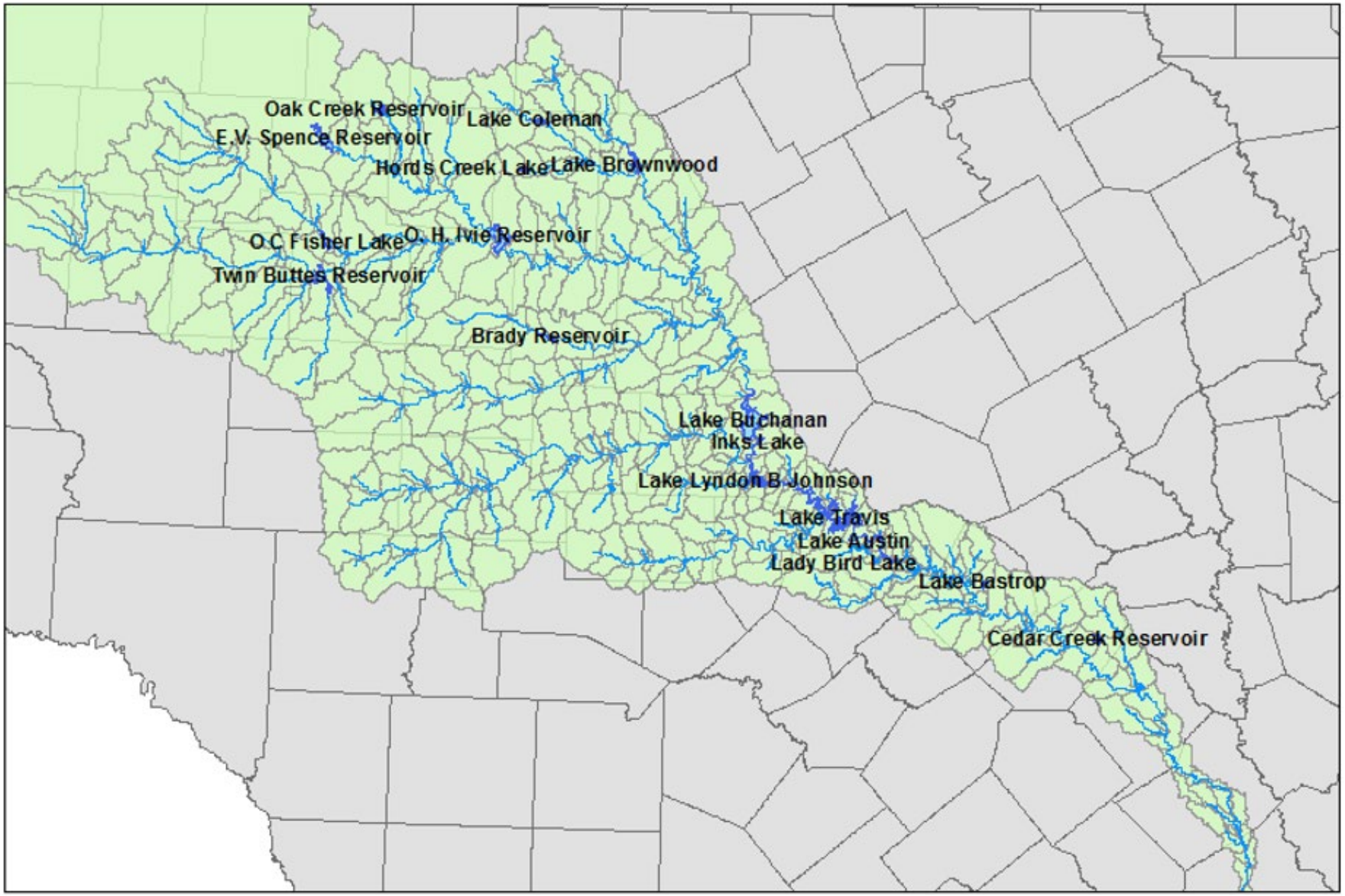

Figure 6.4: Locations of Reservoirs Modeled in HEC-HMS

6.4 HEC-HMS MODEL CALIBRATION

After updating the detailed HEC-HMS model with its initial parameters, the model was calibrated to ensure that it would accurately simulate the response of the watershed to a range of observed flood events, including large events similar to a 1% annual chance (100-yr) flood. The goal of calibration is to simulate the response of the watershed to a given storm by reproducing the timing, shape, and magnitudes of the observed flows at the stream gages and the observed pool elevation at the reservoir gages. A total of 38 recent storm events (from 1997 to 2019) were used throughout different parts of the watershed to calibrate the model. For these storms, the National Weather Service (NWS) hourly rainfall radar data allowed the team to fine tune the rainfall runoff model through detailed calibration. This radar rainfall data is a gridded product with a spatial resolution of approximately 4 km x 4 km cell sizes, and the rainfall depths are calibrated by the NWS to on-the-ground observations at rainfall gages. Prior to the late 1990s, the NWS radar data was not available for use during earlier modeling efforts. The model calibration and verification process undertaken during this study exceeds the standards of a typical FEMA floodplain study.

6.4.1 Calibration Storms

Table 6.2 lists the storms that were used to calibrate each portion of the watershed, and Figures B.4 through B.41 in Appendix B illustrate the total depth of rain for each calibration storm and how that rain was distributed spatially throughout the Lower Colorado River watershed. These storms were selected as the largest available storms of the past 30 years, during which time NWS radar data was also available.

Of the 32 calibration storms listed in Table 6.2, 22 storms had rainfall depths exceeding 10 inches at one or more locations, and 5 storms had rainfall depths exceeding 20 inches at one or more locations. See the calibration storm maps in section 1.4.1 of Appendix B for more information.

Since the rain fell on different parts of the basin from one historic storm event to another, the calibration of each storm was focused on those areas of the basin that received the greatest and most intense rainfall. Calibration was also only performed when the stream gages were recording and experienced a significant peak flow for that event.

Table 6.2 Storm Events Used for HEC-HMS Model Calibration

Historic Storm Events	Portion of the Basin that was Calibrated			
	EV Spence to OH Ivie	OH Ivie to the Colorado River at San Saba	Colorado River at San Saba to Lake Travis	Lake Travis to the Gulf
June 1997	Yes	Yes	Yes	
Oct 1998			Yes	Yes
Mar 2000	Yes			
Jun 2000 (2)	Yes	Yes		
Oct-Nov 2000	Yes	Yes	Yes	
Aug 2001	Yes			
Nov 2001			Yes	
Jul 2002	Yes	Yes	Yes	Yes
Jun 2004		Yes	Yes	
Nov 2004	Yes	Yes	Yes	Yes
Aug 2006	Yes			
Jun-Jul 2007	Yes	Yes	Yes	
Aug 2007	Yes		Yes	
Sep 2010			Yes	
Sep-Oct 2012	Yes			
May 2013			Yes	
Oct 2013 (2)	Yes		Yes	Yes
May 2014	Yes		Yes	
May-Jun-Jul 2015	Yes		Yes	
Oct 2015	Yes			
Oct-Nov 2015				Yes
Apr 2016				Yes
May 2016				Yes
May-Jun 2016		Yes	Yes	Yes
Sep 2016			Yes	
Early Aug 2017			Yes	
Aug-Sep 2017			Yes	Yes
Sep 2018	Yes			
Oct 2018 (2)	Yes		Yes	
Oct-Nov 2018				Yes
May 2019 (3)	Yes	Yes	Yes	Yes
May-Jun 2019		Yes		Yes

6.4.2 Calibration Methodology

Following the initial parameter estimates, calibration simulations were made using observed hourly Next-Generation Radar (NEXRAD) Stage IV gridded precipitation data obtained from the West Gulf River Forecast Center (WGRFC). For each storm event, the model's calculated flow hydrographs were compared to the observed streamflow data at the USGS and LCRA gages. The model's parameters were then adjusted to improve the match between the simulated and observed hydrographs for the observed events. Calibration was performed for the 38 storm events previously listed in Table 6.2. Subbasin parameters that were adjusted during calibration included the subbasins' initial and constant loss rates, Snyder's lag time and peaking coefficients, and baseflow parameters. For the routing reaches, the Modified Puls number of subreaches and Muskingum routing parameters were adjusted as needed.

Calibration was generally performed from upstream to downstream, with all subbasins upstream of a specific gage receiving uniform adjustments, unless specific rainfall or observed flow patterns necessitated adjusting subbasin parameters on an individual basis. Generally, subbasin parameters were adjusted in a consistent order: first baseflow parameters, then subbasin loss rates, and then Snyder's lag time and peaking coefficients. Modified Puls Routing subreaches and Muskingum routing parameters were the last to be adjusted. The methods of adjustment for each parameter are summarized in Table 6.3.

To the extent possible, effort was made to calibrate the model's results to the volume, timing, peak magnitude, and shape of the observed flow hydrograph. However, imperfections in the observed rainfall data and streamflow data did not always allow for a perfect match. For example, the gridded NEXRAD rainfall data from the National Weather Service was only available on an hourly basis. This meant that intense bursts of rain that occurred in 15-min or 30-min timespans might not be adequately represented in the hourly rainfall data. It also meant that even though the model was being run on a 15-min time step, the timing of the hydrographs could only be calibrated to the nearest hour. Likewise, the observed flow values at the gages are calculated indirectly from the observed stage and a limited number of flow measurements. While abundant flow measurements were usually available in the low flow range, the number and quality of USGS flow measurements were often very limited in the high flow range, leading to uncertainty in some of the observed flow hydrographs. In cases where all aspects of the observed flow hydrograph could not be matched simultaneously, priority was given to matching the peak flow magnitude first, followed by the peak timing, which are the aspects of model calibration that are most relevant to the final frequency flow estimation.

Table 6.3: HEC-HMS Calibration Approach

Parameter	Calibration Approach
Baseflow Parameters	First, the baseflow parameters were adjusted to match the observed flow rates at the start and end of each model simulation period. The initial discharges for the subbasins upstream of a certain gage were adjusted uniformly up or down to match the initial observed discharge at that gage. Similarly, the recession constant was adjusted to match the slope of the recession limb of the observed hydrograph, and the ratio to peak was adjusted to match the observed discharge at the end of the calibration event. All baseflow parameters were adjusted uniformly for all subbasins upstream of a given gage.
Initial Deficit (in)	After adjusting the baseflow parameters, the initial deficit and constant losses were adjusted to calibrate the total volume of the flood hydrograph. The initial soil moisture deficit was adjusted according to the antecedent conditions at the beginning of each observed storm event. The initial deficit was increased or decreased until the timing and volume of the initial runoff generally matched the observed arrival of the flow hydrograph at the nearest downstream gage. All subbasins that were upstream of each gage were generally adjusted uniformly, unless specific rainfall or observed flow patterns necessitated adjusting the subbasin initial deficits on an individual basis.
Constant Loss Rate (in/hr)	After adjusting the baseflow and initial deficit parameters, the constant losses were adjusted to calibrate the total volume of the flood hydrograph. The subbasins' constant loss rates were increased or decreased until the volume and magnitude of the simulated hydrographs generally matched the observed volume of the flow hydrograph at the nearest downstream gage. The combination of the adjusted baseflow and loss rate parameters led to the total calibrated volume of runoff at the gage.
Snyder Lag (hours)	After adjusting the loss rates, the Snyder Lags (T_p) were the next parameters to be adjusted upstream of an individual gage. The Snyder Lags were adjusted to match the timing of the observed peak flow at the gage. Normally, all of the subbasin T_p's upstream of an individual gage were adjusted uniformly and proportionally to their initial values, unless the magnitude or shape of the observed hydrograph necessitated making individual adjustments. Efforts were also made to ensure that the adjusted T_p's still fell within a reasonable range, using the equivalent Snyder's lag times from the Fort Worth District regional lag time equations as a guide.
Snyder Peaking Coefficient	Snyder Peaking Coefficients (Cp) were adjusted to match the general shape of the observed flow hydrograph as higher peaking coefficients produce steeper, narrower flood hydrographs, and lower peaking coefficients produce flatter, wider flood hydrographs. An attempt was made to use the same peaking coefficient for all subbasins with similar watershed characteristics. For example, steep, hilly subbasins were given a higher peaking coefficient, whereas flatter subbasins, such as those near the coast, were given lower peaking coefficients. Efforts were also made to ensure that the adjusted peaking coefficients fell within the typical range of 0.4 to 0.8. In most cases, peaking coefficients were adjusted once and left alone between subsequent events.
Modified Puls Routing Subreaches	The number of subreaches in the Modified Puls routing reaches were the final parameters to be adjusted when necessary. Calibration of routing parameters focused on storms that fell near the upstream end of the watershed and were routed downstream with little intervening subbasin flow. Adjustments to the number of subreaches in a given routing reach were made in order to match the amount of attenuation in the peak flow that occurred from the upstream end of a reach to the downstream gage.

Parameter	Calibration Approach
Muskingum Routing Parameters	For areas of the model that included Muskingum routing, the Muskingum k, X and subreach values were adjusted as needed. Calibration of the routing parameters focused on storms that fell near the upstream end of the watershed and were routed downstream with little intervening local flow. The Muskingum k values were adjusted to match the timing of the observed peak flow at the gage, while the Muskingum X values were adjusted to match the relative flatness or steepness of the hydrograph. Finally, adjustments to the number of subreaches were made in order to match the amount of attenuation in the peak flow that occurred from the upstream end of a reach to the downstream gage.

For the Lower Colorado River from Columbus, TX to the Gulf, some additional non-typical calibration methods were employed to aid in the calibration of the routing reaches on the Lower Colorado River. First, new storage-discharge relationships were calculated for the Colorado River modified puls reaches between Columbus and the Gulf using the final HEC-RAS model from the 2002 FDEP study. It was discovered during calibration that the original storage-discharge relationships for the modified puls routing did not provide enough definition to the curve between 50,000 and 100,000 cfs, which is the range of flows where the river transitions from in-channel to overbank flow. The original curves assumed a straight-line interpolation of the storage volumes between the discharge values of 50,000 and 100,000 cfs. For this study, the storage-discharge relationships for those reaches were updated by calculating additional storage values for 60,000, 70,000, 80,000 and 90,000 cfs using the FDEP HEC-RAS model. This better defined the shape of the routing relationships when the river transitions to out-of-bank flow. After updating the storage-discharge relationships, the model was better able to match the timing of the observed routing for the large flow events.

Second, two new diversions were added to the HEC-HMS model along the Colorado River between Columbus and Wharton, TX. These diversions were necessary because the USGS streamflow data recorded a decrease in flow volume between Columbus and Wharton for several large flood events, including Nov 2004, April 2016, May 2016, and Hurricane Harvey (Aug 2017). For these large flood events, it has been documented by the National Weather Service that an interbasin transfer occurs, where flow from the Colorado River flows over the eastern watershed boundaries and enters the San Bernard River's watershed. Figure 6.5 illustrates two examples of this phenomenon from Hurricane Harvey and April 2016.

To account for this loss of water due to interbasin transfer, two lateral weir diversions were added along the Colorado River between the Columbus and Wharton USGS gages. These diversions allow water to escape the system once the discharge on the Colorado River at Columbus exceeds approximately 70,000 cfs. The USGS rating curves for Columbus and Wharton were used to estimate the head on these lateral weirs, and their weir coefficients were adjusted through calibration. After calibrating these new diversions, the HEC-HMS model was able to match the observed peak flow and volume at Wharton much more closely for the four largest calibration events.

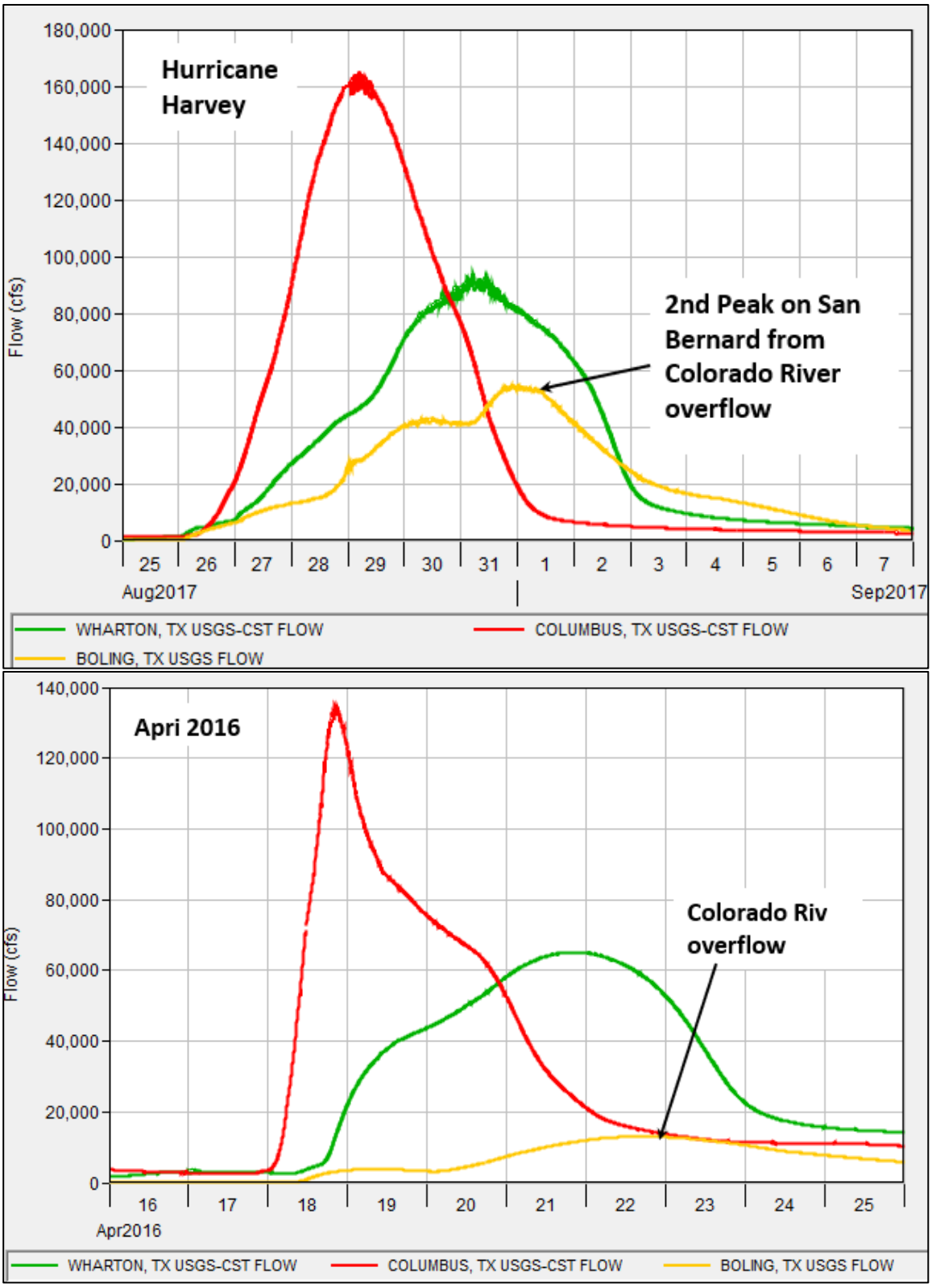

Figure 6.5: Examples of Interbasin Transfer from the Colorado River to the San Bernard River

6.4.3 Calibrated Parameters

The resulting calibrated subbasin and routing reach parameters that were adjusted for each storm event are shown in Tables B.8 through B.40 of Appendix B. Calibration was carried out by dividing the Lower Colorado River basin into five separate calibration regions: (1) EV Spence to OH Ivie, (2) OH Ivie to San Saba, TX, (3) San Saba to Lake Travis, (4) the Llano River and (5) Lake Travis to the Gulf. As such, the calibrated parameter tables are also broken out separately by these regions.

6.4.4 Calibration Results

The final calibration results showed that the HEC-HMS model was able to accurately simulate the response of the watershed, as it reproduced the volume, timing, shape, and peak magnitudes of most observed floods very well. Some examples of the resulting hydrograph comparisons can be seen in the following figures of this section. The figures show the HEC-HMS computed versus the USGS observed flow hydrographs at each stream gage location. For each reservoir, the figures show the HEC-HMS computed pool elevation versus the USGS observed pool elevation. Calibration figures are only shown for the locations where the USGS stream gages were recording for that event and where the magnitude of the flow was significant enough to warrant calibration.

In addition to graphical comparisons of simulated to observed flow hydrographs, statistical tests were also employed in evaluating model performance. The statistical metrics used to evaluate the HEC-HMS model performance included the Nash-Sutcliffe Efficiency (NSE), the Root Mean Square Error – Observed Standard Deviation Ratio (RSR), and the Percent Bias (PBIAS). For the purposes of this study, the performance metrics were evaluated using the performance ratings shown in Table 6.6. These performance ratings are consistent with standard practices in watershed modeling (Moriasi, 2007) (Moriasi, 2012). In cases where each metric had a different performance rating, the overall performance rating for that calibration was assigned as the lowest of the three ratings, which is the strictest method of assigning performance ratings.

Table 6.6: HEC-HMS Model Calibration Evaluation Metrics

Performance Rating	NSE	RSR	PBIAS
Very Good	$0.80 \leq NSE < 1.00$	$0 \leq RSR \leq 0.50$	$0 \leq PBIAS \leq \pm 5$
Good	$0.70 \leq NSE < 0.80$	$0.50 < RSR \leq 0.60$	$\pm 5 < PBIAS < \pm 10$
Satisfactory	$0.50 \leq NSE < 0.70$	$0.60 < RSR \leq 0.70$	$\pm 10 \leq PBIAS \leq \pm 25$
Unsatisfactory	$NSE < 0.50$	$RSR > 0.70$	$PBIAS > \pm 25$

6.4.4.1 Example Calibration Results

For the sake of brevity, only a handful of calibration plots have been included as examples in this section of the report. The resulting hydrograph comparisons for all 400+ calibrations performed for this study have been included in Appendix B.

There are two types of figures which are shown in this section of the report: streamflow gages and reservoirs. In the streamflow gage figures, the solid blue line represents the total modeled streamflow at the gage, while the black line represents the observed streamflow that was recorded by the gage. The other dotted blue lines on these figures represent the runoff from individual model components (i.e., a single subbasin or routing reach), and they should be ignored as they are not relevant to the gage comparison. In the reservoir figures, the observed pool elevation at the reservoir gage is compared to the modeled pool elevation in the top half of the figure. The other lines on this plot shows reservoir storage, inflow, and outflow, but they are not relevant to the comparison with the observed pool elevations and can be ignored.

The USGS stream gage on the Colorado River near Ballinger, TX has a 16,358 square mile drainage area of which only 1,076 square miles is downstream of E.V. Spence Reservoir. Flow is affected by Oak Creek Reservoir and at times by discharge from the floodwater-retarding structures in the Kickapoo and Valley Creeks drainage basins. The calibration area above this gage was modeled with multiple subbasin elements and routing reaches. The modeled flow versus the observed flow at the gage had “Good” and “Very Good” performance ratings in all five calibrations. The largest calibration event at this location was in September 2012 with a peak flow of 10,100 cfs.

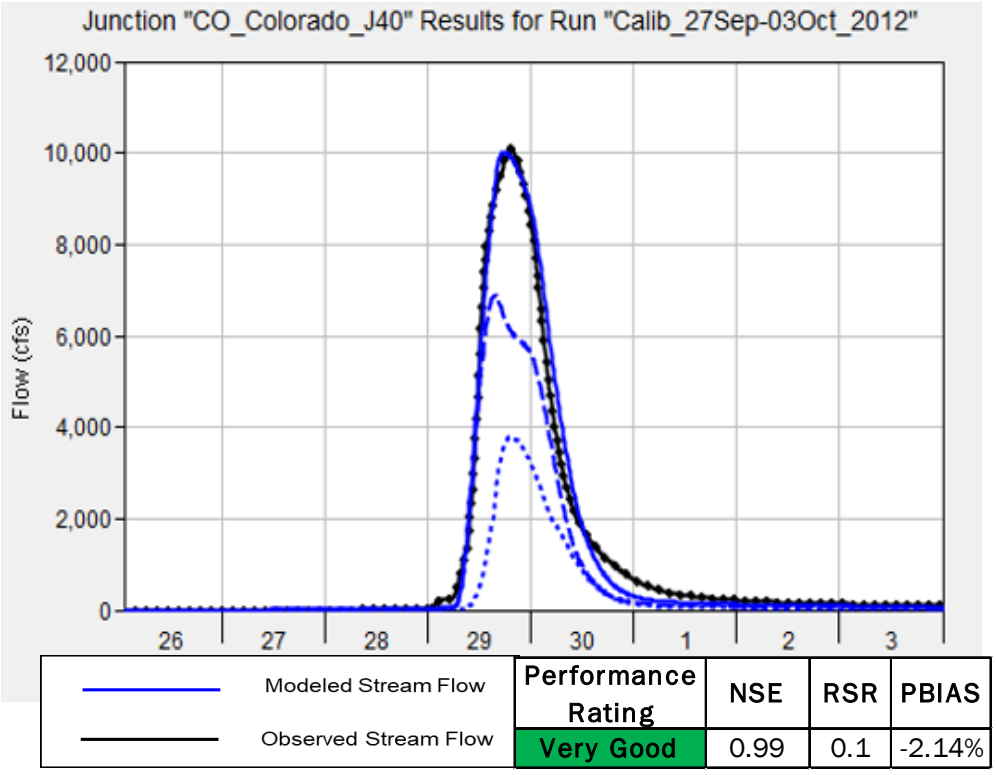

Performance Rating	NSE	RSR	PBIAS
Very Good	0.99	0.1	-2.14%

Figure 6.6: 26 Sep-03 Oct 2012 Calibration Results for the Colorado River near Ballinger, TX USGS Gage

USGS stream gage on the Concho River at Paint Rock, TX has a 6,574 square mile drainage area of which 1,131 square miles are probably noncontributing. Over 80% of the contributing drainage area is regulated by upstream reservoirs. Flow is also affected at times by discharge from two smaller floodwater-retarding structures in the Willow Creek drainage basin. The drainage area was modeled with multiple subbasin and routing reach elements representing the drainage area between the USGS gage for the Concho River at San Angelo, TX and the USGS gage for the Concho River at Paint Rock, TX. The modeled flow versus the observed flow at the gage had a "Very Good" performance rating for 4 out of 4 calibrations. The largest calibration event at this location was in September 2012 with an estimated peak flow of 29,600 cfs, as shown in Figure 6.7.

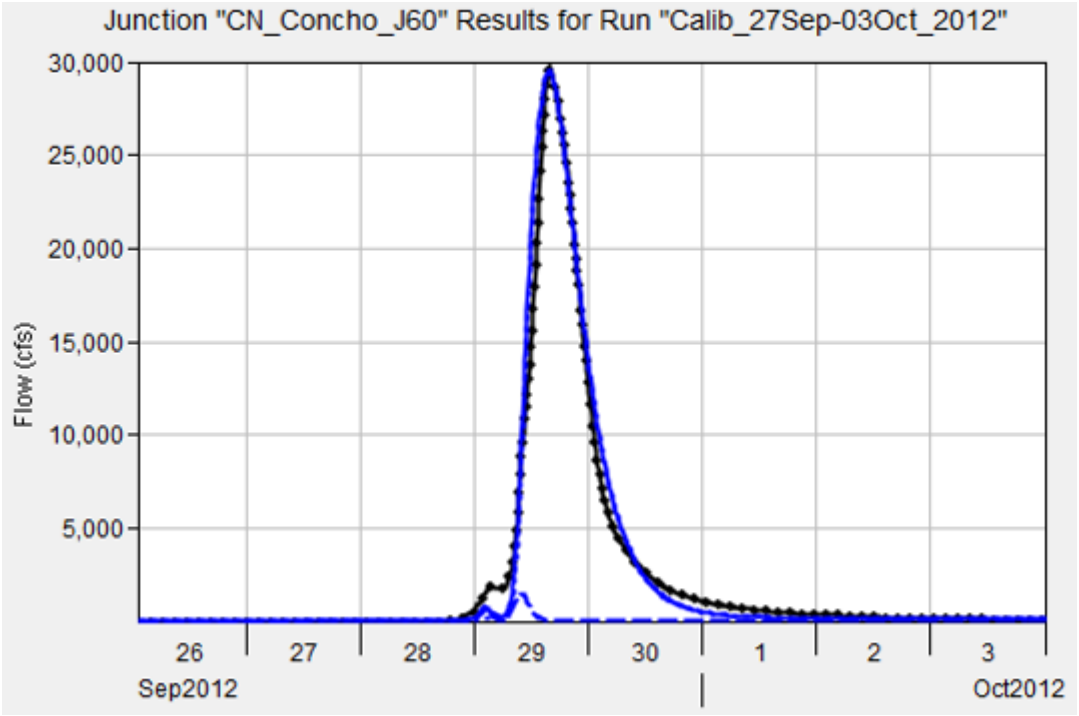

Performance Rating	NSE	RSR	PBIAS
Very Good	0.979	0.1	1.66%

Figure 6.7: 26 Sep-03 Oct 2012 Calibration Results for the Concho River at Paint Rock, TX USGS Gage

USGS Lake gage for Lake Brownwood near Brownwood, TX has a 1,565 square mile drainage area. Lake Brownwood is on Pecan Bayou, a tributary of the Colorado River. The Lake is operated by Brown County Water Improvement District #1 for water supply and recreation. Lake Brownwood has a gated service outlet (lowest invert at elevation 1,329.5 feet) and an uncontrolled spillway (crest elevation 1,424.6 feet). The drainage area above the dam was modeled with multiple subbasins and routing reach element representing the area between the upstream gages and reservoirs and Lake Brownwood. The modeled pool elevation versus the observed pool elevation had a "Very Good" performance ratings in 4 out of 4 final calibrations. The largest calibration event was July 2002 with a peak elevation of 1432.0 feet (NAVD88).

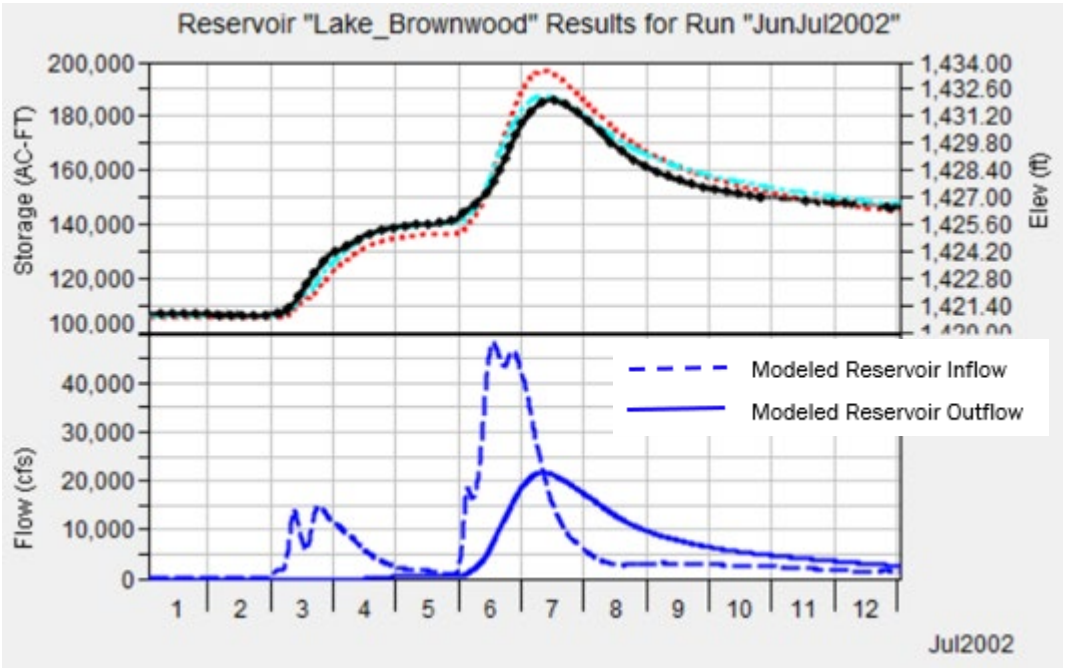

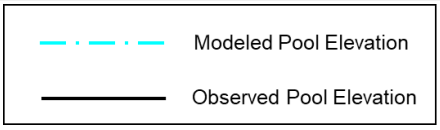

Performance Rating	NSE	RSR	PBIAS
Very Good	0.985	0.12	0.01%

Figure 6.8: 01-12 Jul 2002 Calibration Results for the Lake Brownwood near Brownwood, TX USGS Gage

The USGS stream gage on the Colorado River near San Saba, TX has a 31,217 square mile drainage area of which 11,398 square miles are probably noncontributing. A portion of the contributing drainage area is regulated by various upstream dams. Flow is also affected at times by discharge from 187 floodwater-retarding structures which control runoff from a 944 mi² area above this station. The drainage area above the gage was modeled with observed flows from the upstream USGS stream gages and multiple subbasin and routing reach elements. The modeled flow versus the observed flow at the gage had a "Good" or "Very Good" performance rating for 8 out of 9 calibrations. The largest calibration event at this location was in June 1997 with an estimated peak flow of 58,300 cfs, as shown in Figure 6.9.

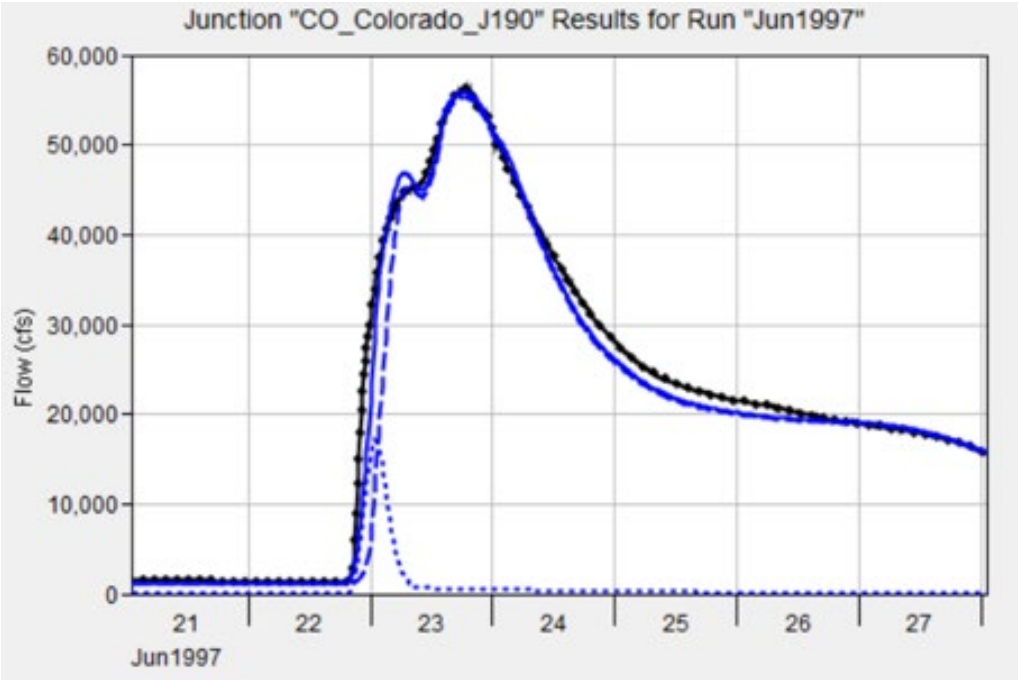

Performance Rating	NSE	RSR	PBIAS
Very Good	0.988	0.1	-3.26%

Figure 6.9: 21-27 Jun 1997 Calibration Results for the Colorado River near San Saba, TX USGS Gage

Lake Buchanan near Burnet, TX is operated by LCRA and has a drainage area of approximately 31,900 square miles. The drainage area above this gage was represented by multiple subbasins and routing reaches between this gage and the upstream gage locations. The modeled pool elevation versus the observed pool elevation at the reservoir had "Good" to "Very Good" performance rating for 4 out of 6 calibrations. The largest calibration event in terms of outflow at this location was October 2018 with an estimated peak release of approximately 55,000 cfs, as shown in Figure 6.10.

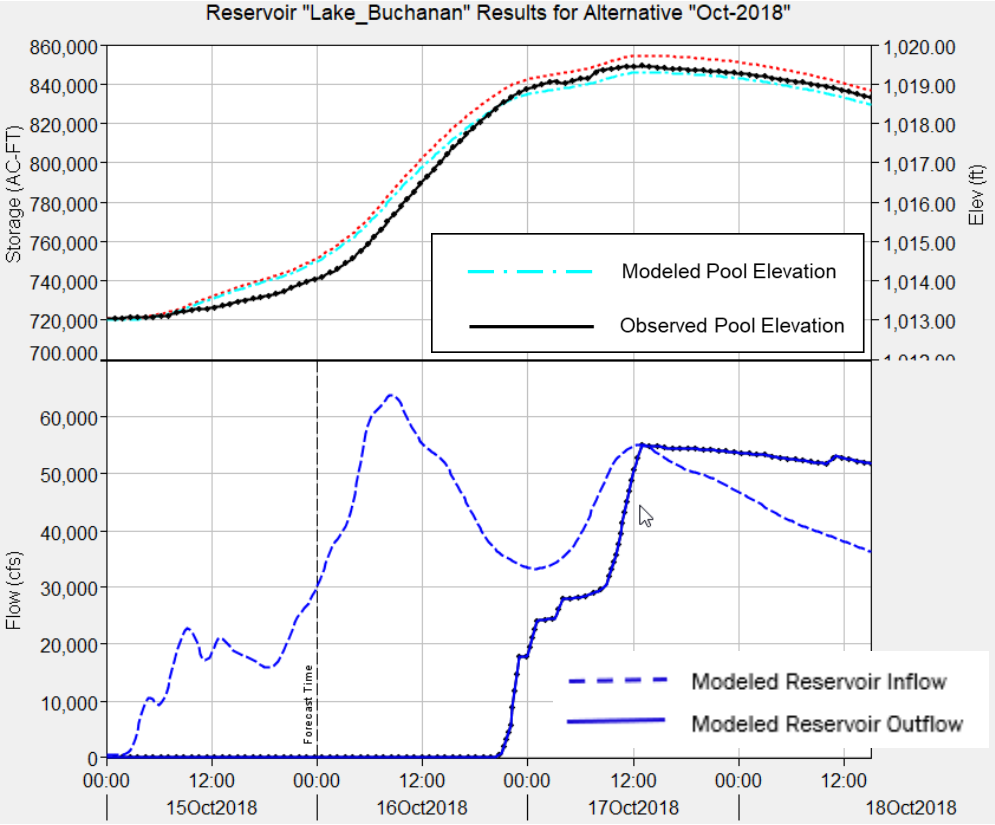

Performance Rating	NSE	RSR	PBIAS
Very Good	0.99	0.1	0.01%

Figure 6.10: October 2018 Calibration Results for LCRA Lake Buchanan nr Burnet; TX

The USGS stream gage on the Llano River near Mason, TX has a drainage area of approximately 3,250 square miles and is represented by multiple subbasins and routing reaches between this gage and the upstream gage locations. The modeled flow versus the observed flow at the gage had a “Good” to “Very Good” performance rating for 6 out of 7 calibrations. The largest calibration event at this location was 15 to 18 October 2018 with an estimated peak flow of 200,000 cfs, as shown in Figure 6.11.

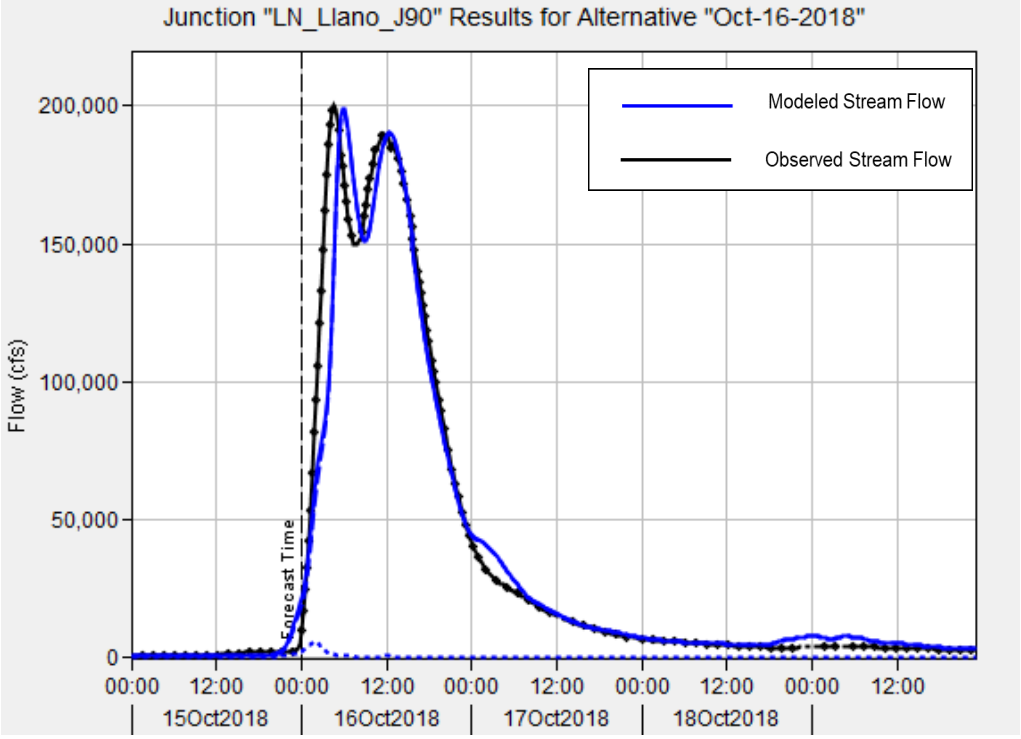

Performance Rating	NSE	RSR	PBIAS
Very Good	0.958	0.2	-1.64%

Figure 6.11: 15 – 18 October 2018 Calibration Results for Llano River near Mason, TX USGS Gage

Lake Travis near Austin, TX is a flood control reservoir that is operated by LCRA. The lake is on the Colorado River and has a drainage area of approximately 38,700 square miles. The area above the reservoir is represented by multiple subbasins and routing reaches between the dam and the next upstream gages. The modeled flow versus the observed flow at the gage had a "Good" to "Very Good" performance rating for 10 out of 10 calibrations. The largest calibration events at this location were in June 1997 and Oct 2018 with estimated peak elevations of 706 ft and 705 ft, respectively. Figure 6.12 shows the calibration results for the Oct 2018 inflow event.

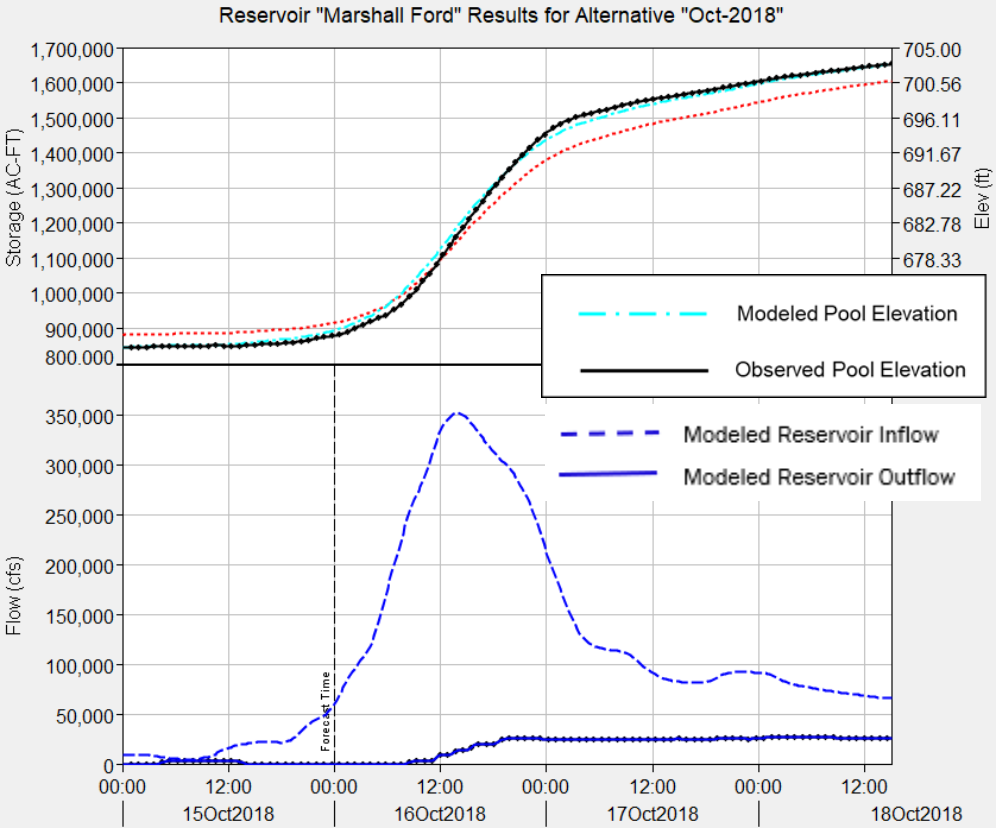

Performance Rating	NSE	RSR	PBIAS
Very Good	0.99	0.1	0.01%

Figure 6.12: October 2018 Calibration Results for LCRA Lake Travis near Austin, TX

The USGS stream gage on the Colorado River at Austin, TX has a 39,009 square miles drainage area of which all but 250 square miles is controlled by Lake Travis. The uncontrolled area is represented by multiple subbasins and routing reaches above the gage location. The modeled flow versus the observed flow at the gage had a "Good" to "Very Good" performance rating for 3 out of 4 calibrations. The largest calibration event at this location was in October 2013 with an estimated peak flow of 34,000 cfs, as shown in Figure 6.13.

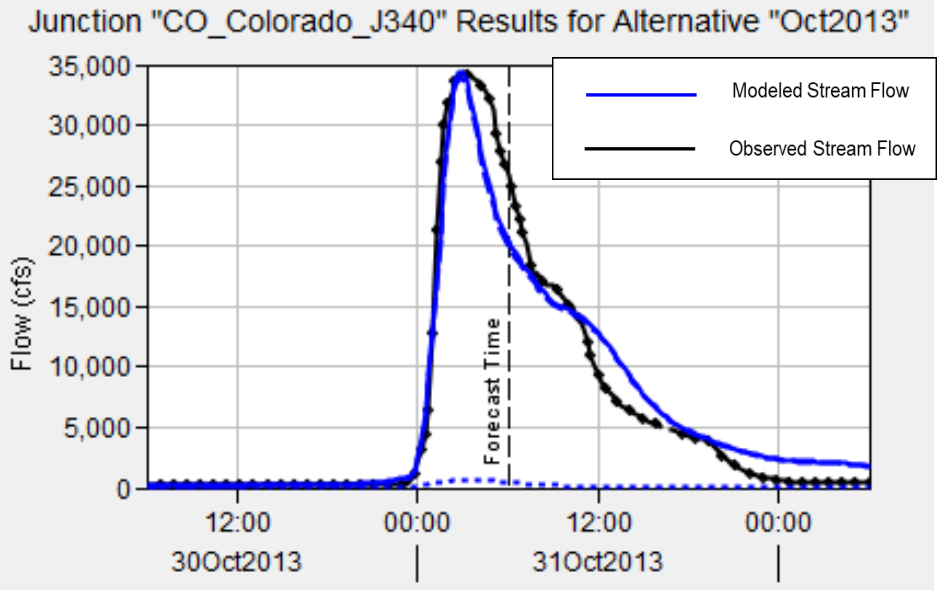

Performance Rating	NSE	RSR	PBIAS
Very Good	0.959	0.2	2.88%

Figure 6.13: October 2013 Calibration Results for Colorado Rv at Austin, TX USGS Gage

The USGS stream gage on Onion Creek at US Hwy 183, Austin, TX has a 321 square mile drainage area and is represented by multiple subbasins and routing reaches above the gage location. The modeled flow versus the observed flow at the gage had a “Good” to “Very Good” performance rating for 5 out of 5 calibrations, as shown in the figures below. The largest calibration event at this location was in October 2015 with an estimated peak flow of 120,000 cfs, as shown in Figure 6.14.

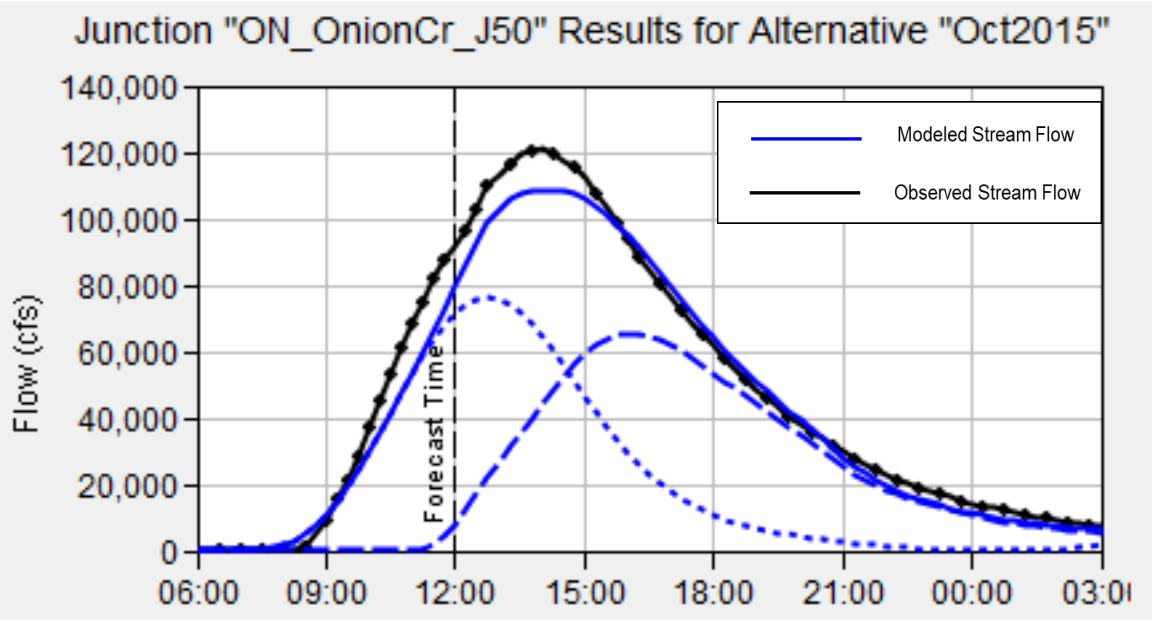

Performance Rating	NSE	RSR	PBIAS
Good	0.976	0.2	-6.82%

Figure 6.14: October 2015 Calibration Results for Onion Creek at US Hwy 183, Austin, TX USGS Gage

The USGS stream gage on Colorado River at Columbus, TX has a 41,640 square miles drainage area of which about 2,885 square miles is uncontrolled drainage area below Lake Travis. This area is represented by multiple subbasins and routing reaches between this gage and the upstream gage locations. The modeled flow versus the observed flow at the gage had a "Good" to "Very Good" performance rating for 4 out of 5 calibrations, as shown in the figures below. The largest calibration event at this location was Hurricane Harvey in August 2017 with an estimated peak flow of 165,000 cfs, as shown in Figure 6.15.

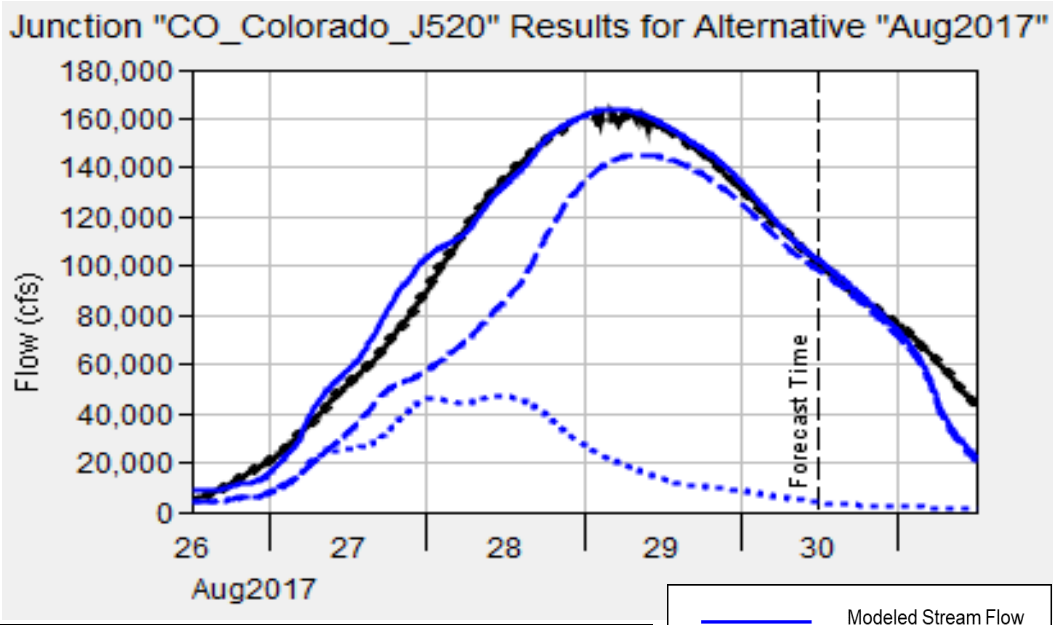

Performance Rating	NSE	RSR	PBIAS
Very Good	0.979	0.1	0.61%

Figure 6.15: August 2017 Calibration Results for Colorado River at Columbus, TX USGS Gage

6.4.4.2 Calibration Performance Ratings

Tables 6.7 to 6.14 contain a summary of the model performance ratings for all the HEC-HMS calibrations performed for this study. The statistical metrics used to assign these performance ratings are shown on the figures for each individual calibration in Appendix B. Overall, 76% of the 414 total calibrations performed achieved a rating of "Good" or Very Good." Most of the remaining calibrations that received a lower rating were affected by data issues such as missing gage data, inaccuracies in the rainfall data, or inconsistencies in the observed stream gage data or reservoir releases.

Table 6.7: Summary of HEC-HMS Model Calibration Performance Ratings from the Earlier Storm Events for EV Spence to OH Ivie

Observed Gage Location	21Jun-24Jun 1997	22Mar-26Mar 2000	01Jun-06Jun 2000	22Oct-25Oct 2000	27Aug-29Aug 2001	02Jul-09Jul 2002	13Nov-21Nov 2004	23Jun-29Jun 2007	16Aug-20Aug 2007
Colorado River at Robert Lee, TX USGS Gage				Unsatisfactory					
Oak Ck Res nr Blackwell; TX				Very Good					Very Good
Colorado Rv nr Ballinger, TX USGS Gage	Very Good		Very Good						
Elm Ck at Ballinger, TX USGS Gage	Very Good		Good			Good		Very Good	
Middle Concho Rv abv Tankersley, TX USGS Gage				Very Good			Very Good		
Spring Ck abv Tankersley, TX USGS Gage					Satisfactory				
Dove Ck at Knickerbocker, TX							Unsatisfactory		
Spring Ck abv Twin Buttes Res nr San Angelo, TX									
S Concho Rv at Christoval, TX					Satisfactory		Good		Very Good
Twin Buttes Reservoir nr San Angelo TX USGS Gage							Very Good		
Pecan Ck nr San Angelo, TX					Unsatisfactory				
N Concho Rv abv Sterling City, TX									
N Concho Rv at Sterling City, TX		Very Good					Very Good		
N Concho Rv nr Carlsbad, TX		Satisfactory		Good			Satisfactory		
N Concho Rv nr Grape Creek, TX		Unsatisfactory		Good			Very Good		Unsatisfactory
O. C. Fisher Lk at San Angelo; TX USGS Gage		Unsatisfactory		Good					Very Good
Concho Rv at San Angelo, TX USGS Gage									Unsatisfactory
Concho Rv at Paint Rock, TX USGS Gage									
O. H. Ivie Res nr Voss; TX USGS Gage							Very Good	Very Good	

Table 6.8: Summary of HEC-HMS Model Calibration Performance Ratings from the Later Storm Events for EV Spence to OH Ivie

Observed Gage Location	27Sep-03Oct 2012	13Oct-18Oct 2013	22May-29May 2014	18May-23May 2015	21Oct-27Oct 2015	14Oct-24Oct 2018	07May-10May 2019	17May-21May 2019	31May-05Jun 2019
Colorado River at Robert Lee, TX USGS Gage									
Oak Ck Res nr Blackwell; TX						Very Good			
Colorado Rv nr Ballinger, TX USGS Gage	Very Good					Very Good		Very Good	
Elm Ck at Ballinger, TX USGS Gage	Satisfactory								
Middle Concho Rv abv Tankersley, TX USGS Gage				Unsatisfactory		Very Good			
Spring Ck abv Tankersley, TX USGS Gage						Satisfactory	Unsatisfactory		
Dove Ck at Knickerbocker, TX			Good			Good			
Spring Ck abv Twin Buttes Res nr San Angelo, TX									
S Concho Rv at Christoval, TX			Good			Very Good			
Twin Buttes Reservoir nr San Angelo TX USGS Gage			Very Good	Very Good		Very Good			
Pecan Ck nr San Angelo, TX			Unsatisfactory			Very Good			
N Concho Rv abv Sterling City, TX					Unsatisfactory	Unsatisfactory			
N Concho Rv at Sterling City, TX					Very Good	Very Good			
N Concho Rv nr Carlsbad, TX				Very Good	Satisfactory				
N Concho Rv nr Grape Creek, TX		Good			Satisfactory				
O. C. Fisher Lk at San Angelo; TX USGS Gage				Very Good	Very Good				
Concho Rv at San Angelo, TX USGS Gage	Satisfactory		Unsatisfactory	Satisfactory					Very Good
Concho Rv at Paint Rock, TX USGS Gage	Very Good		Very Good			Very Good			Very Good
O. H. Ivie Res nr Voss; TX USGS Gage	Very Good					Very Good			

Table 6.9: Summary of HEC-HMS Model Calibration Performance Ratings for the OH Ivie to San Saba Calibration Region

Location Description	Jun 1997^	Jun 2000	Oct-Nov 2000^	Jul 2002	Jun 2004	Nov 2004*	Jun-Jul 2007	May-Jun 2016	Oct-Nov 2018	May-Jun 2019
Colorado Rv nr Stacy, TX USGS Gage		Very Good							Good	
Colorado River at Winchell, TX LCRA Gage		Very Good	Very Good	Very Good		Very Good	Very Good			
Lake Coleman				Very Good		Good		Very Good		Very Good
Jim Ned Creek at CR 140 nr Coleman, TX USGS Gage									Satisfactory	Very Good
Hords Ck Lk nr Valera; TX USGS Gage	Very Good					Very Good	Very Good	Very Good	Very Good	
Hords Creek near Coleman, TX USGS Gage								Satisfactory	Good	Very Good
Pecan Bayou nr Cross Cut, TX USGS Gage								Very Good	Very Good	
Lk Brownwood nr Brownwood; TX USGS Gage				Very Good			Very Good	Very Good	Very Good	
Pecan Bayou at Brownwood, TX USGS Gage									Good	
Pecan Bayou nr Mullin, TX USGS Gage						Satisfactory	Very Good	Very Good	Very Good	Very Good
Colorado River near Goldthwaite, TX LCRA Gage					Very Good	Very Good	Very Good	Very Good		Very Good
San Saba Rv at FM 864 nr Fort McKavett, TX USGS Gage										
San Saba Rv at Menard, TX USGS Gage			Very Good			Very Good			Satisfactory	Satisfactory
San Saba River near Brady LCRA Gage			Very Good			Satisfactory				
Brady Ck Res nr Brady; TX USGS Gage			Unsatisfactory			Unsatisfactory			Unsatisfactory	Satisfactory
Brady Ck at Brady, TX USGS Gage									Good	Very Good
San Saba Rv at San Saba, TX USGS Gage	Very Good		Very Good			Unsatisfactory			Good	
Colorado River at San Saba, TX USGS Gage	Very Good		Very Good	Very Good	Satisfactory	Very Good	Very Good	Very Good	Good	Very Good

Table 6.10: Summary of HEC-HMS Model Calibration Performance Ratings from Earlier Events for the San Saba to Lake Travis Calibration Region

Location Description	Jun 1997	Oct 1998	Oct-Nov 2000	Nov 2001	Jul 2002	Jun 2004	Nov 2004	Jun-Jul 2007	Aug 2007
Colorado River at Bend, TX LCRA Gage						Very Good			
Cherokee Creek near Bend, TX LCRA Gage				Very Good		Very Good			
LCRA Lake Buchanan nr Burnet; TX			Very Good				Very Good	Satisfactory	
Little Llano River near Llano, TX LCRA Gage					Very Good		Good		
Honey Creek near Kingsland, TX LCRA Gage							Unsatisfactory		
Sandy Creek near Willow City, TX LCRA Gage	Good	Very Good		Good					Very Good
Sandy Creek near Click, TX LCRA Gage					Satisfactory		Very Good	Very Good	
Sandy Ck nr Kingsland, TX USGS Gage	Good	Very Good	Good	Good			Good	Very Good	Very Good
Walnut Creek near Kingsland LCRA Gage	Very Good			Very Good		Good		Very Good	
LCRA Lake LBJ nr Marble Falls; TX	Unsatisfactory					Very Good	Good	Unsatisfactory	
Backbone Creek at Marble Falls LCRA Gage	Satisfactory			Satisfactory			Unsatisfactory	Satisfactory	
Hamilton Creek near Marble Falls LCRA Gage							Good	Good	
Pedernales Rv nr Fredericksburg, TX USGS Gage		Satisfactory	Very Good		Satisfactory	Very Good	Good		Very Good
South Grape Creek near Luckenbach, TX LCRA Gage					Very Good		Good		
Pedernales River at LBJ Ranch near Stonewall, TX LCRA Gage									
North Grape Creek near Johnson City, TX LCRA Gage				Satisfactory	Unsatisfactory			Satisfactory	
Pedernales Rv nr Johnson City, TX USGS Gage			Good	Good	Good	Satisfactory	Very Good	Satisfactory	Satisfactory
Miller Creek near Johnson City, TX LCRA Gage		Satisfactory		Very Good	Satisfactory				Good
Flat Creek near Pedernales Falls State Park LCRA Gage					Satisfactory				
Cypress Creek near Cypress Mill, TX LCRA Gage				Satisfactory	Satisfactory				
LCRA Lake Travis nr Austin; TX	Very Good	Very Good	Very Good	Very Good	Very Good	Very Good	Very Good	Very Good	Very Good

Table 6.11: Summary of HEC-HMS Model Calibration Performance Ratings from Later Events for the San Saba to Lake Travis Calibration Region

Location Description	Sep 2010	Sep-Oct-Nov 2013	May-Jun-Jul 2015 Early	May-Jun-Jul 2015 #	May-Jun 2016	Sep-Oct 2018	May-Jun 2019
Colorado River at Bend, TX LCRA Gage							
Cherokee Creek near Bend, TX LCRA Gage				Good	Unsatisfactory		
LCRA Lake Buchanan nr Burnet; TX		Very Good		Very Good		Very Good	
Little Llano River near Llano, TX LCRA Gage					Satisfactory		
Honey Creek near Kingsland, TX LCRA Gage							
Sandy Creek near Willow City, TX LCRA Gage							
Sandy Creek near Click, TX LCRA Gage					Unsatisfactory		
Sandy Ck nr Kingsland, TX USGS Gage						Good	
Walnut Creek near Kingsland LCRA Gage							
LCRA Lake LBJ nr Marble Falls; TX							
Backbone Creek at Marble Falls LCRA Gage							
Hamilton Creek near Marble Falls LCRA Gage							
Pedernales Rv nr Fredericksburg, TX USGS Gage		Very Good		Good		Very Good	
South Grape Creek near Luckenbach, TX							Unsatisfactory
Pedernales River at LBJ Ranch nr Stonewall, TX				Very Good	Very Good		
North Grape Creek near Johnson City, TX					Good		Satisfactory
Pedernales Rv nr Johnson City, TX USGS Gage	Very Good	Very Good		Very Good		Good	Very Good
Miller Creek near Johnson City, TX LCRA Gage			Very Good				Good
Flat Creek near Pedernales Falls State Park			Very Good				Satisfactory
Cypress Creek near Cypress Mill, TX LCRA Gage			Unsatisfactory	Satisfactory			
LCRA Lake Travis nr Austin; TX				Very Good	Very Good	Very Good	

Table 6.12: Summary of HEC-HMS Model Calibration Performance Ratings for the Earlier Storm Events for the Llano River

Location Description	Jun 1997	Oct-Nov 2000	Nov 2001	Jul 2002	Jun 2004	Nov 2004	Jun-Jul 2007	Aug 2007	May 2013
S Llano Rv at Flat Rock Ln at Junction, TX USGS Gage									
N Llano Rv nr Junction, TX USGS Gage						Good			Very Good
Llano Rv nr Junction, TX USGS Gage		Very Good	Very Good			Good			Satisfactory
Johnson Fork at I-10 nr Junction, TX LCRA Gage		Satisfactory	Unsatisfactory	Very Good					
James River near Mason, TX LCRA			Unsatisfactory	Satisfactory				Satisfactory	
Comanche Creek near Mason LCRA							Satisfactory		
Llano Rv nr Mason, TX USGS Gage		Good	Good	Good		Unsatisfactory		Very Good	
Beaver Ck nr Mason, TX USGS Gage			Unsatisfactory	Good	Very Good			Very Good	
Willow Creek near Mason LCRA Gage									
Hickory Creek near Castell LCRA Gage							Unsatisfactory		
San Fernando Creek near Llano LCRA					Very Good				
Johnson Creek near Llano LCRA Gage									
Llano Rv at Llano, TX USGS Gage	Very Good	Good	Good	Good	Good	Very Good	Very Good		

Table 6.13: Summary of HEC-HMS Model Calibration Performance Ratings for the Later Storm Events for the Llano River

Location Description	Oct-Nov 2013	May 2014	May-Jun-Jul 2015	May-Jun 2016	Sep 2016	Aug-Sep 2017	Sep-2018	Oct 08 2018	Oct 16 2018
S Llano Rv at Flat Rock Ln at Junction, TX USGS Gage			Very Good		Satisfactory			Very Good	Very Good
N Llano Rv nr Junction, TX USGS Gage			Good				Good		
Llano Rv nr Junction, TX USGS Gage			Very Good					Satisfactory	Satisfactory
Johnson Fork at I-10 nr Junction, TX LCRA Gage									
James River near Mason, TX LCRA Gage									
Comanche Creek near Mason LCRA									
Llano Rv nr Mason, TX USGS Gage			Very Good					Good	Very Good
Beaver Ck nr Mason, TX USGS Gage	Very Good	Satisfactory				Very Good		Good	Very Good
Willow Creek near Mason LCRA Gage									
Hickory Creek near Castell LCRA Gage			Very Good						Very Good
San Fernando Creek near Llano LCRA									Good
Johnson Creek near Llano LCRA Gage									
Llano Rv at Llano, TX USGS Gage	Very Good	Good	Very Good	Very Good				Very Good	Very Good

Table 6.14: Summary of HEC-HMS Model Calibration Performance Ratings for the Earlier Storm Events from Lake Travis to the Gulf

Gage Name	Oct 1998	Jul 2002	Nov 2004	Oct 2013	Oct-Nov 2015	Apr 2016	May-Jun 2016	Aug-Sep 2017	May-Jun 2019
Bull Ck at Loop 360 nr Austin, TX			Very Good	Very Good					Satisfactory
LCRA Lake Austin nr Austin, TX			Very Good	Satisfactory	Unsatisfactory				Good
Barton Ck at SH 71 nr Oak Hill, TX			Very Good	Very Good	Very Good				Good
Barton Ck at Lost Ck Blvd nr Austin, TX			Good	Very Good	Very Good				Very Good
Barton Ck at Loop 360, Austin, TX			Very Good	Very Good	Good				Very Good
Barton Ck abv Barton Spgs at Austin, TX		Good		Unsatisfactory	Very Good				Good
Colorado Rv at Austin, TX USGS Gage			Very Good	Very Good	Good				Unsatisfactory
Walnut Ck at Webberville Rd, Austin, TX			Very Good	Good	Very Good				Very Good
Colorado River at Del Valle, TX LCRA Gage									
Onion Ck nr Driftwood, TX USGS Gage			Good		Very Good		Very Good		Very Good
Onion Creek at Buda, TX LCRA Gage			Satisfactory				Very Good	Very Good	Unsatisfactory
Onion Ck at Twin Creeks Rd nr Manchaca, TX			Satisfactory		Satisfactory		Very Good	Good	Satisfactory
Onion Ck at US Hwy 183, Austin, TX			Good		Good		Good	Very Good	Very Good
Gilleland Creek near Manor LCRA Gage			Satisfactory				Good	Good	Satisfactory
Colorado Rv nr Webberville, TX						Satisfactory	Very Good	Good	
Wilbarger Creek near Elgin LCRA Gage			Satisfactory				Very Good	Very Good	Very Good
Big Sandy Creek near Elgin, TX LCRA Gage			Satisfactory				Good	Very Good	
Colorado Rv at Bastrop, TX USGS Gage	Unsatisfactory		Very Good		Very Good		Very Good	Very Good	Good
Cedar Creek near Bastrop, TX LCRA Gage							Very Good	Very Good	Very Good
Cedar Creek below Bastrop, TX LCRA Gage			Good				Very Good	Very Good	
Colorado River near Upton, TX LCRA Gage						Very Good	Very Good	Very Good	
Colorado Rv at Smithville, TX	Satisfactory		Good		Satisfactory		Very Good	Very Good	Very Good
Colorado Rv abv La Grange, TX	Very Good		Very Good		Satisfactory		Very Good	Good	Very Good
Buckners Creek near Muldoon, TX			Very Good			Very Good	Good	Very Good	Very Good
Cummings Creek near Frelsburg, TX						Good	Very Good	Very Good	Very Good
Colorado Rv at Columbus, TX USGS Gage	Satisfactory		Good			Good	Very Good	Very Good	
Colorado River near Altair, TX						Good	Good	Good	
Colorado Rv at Wharton, TX USGS Gage	Very Good		Very Good			Very Good	Very Good	Very Good	
Colorado River near Lane City, TX						Very Good	Very Good	Very Good	
Colorado Rv nr Bay City, TX USGS Gage	Good		Very Good			Very Good	Very Good	Very Good	
Colorado Rv nr Wadsworth, TX								Very Good	Good

6.5 FINAL MODEL PARAMETERS

6.5.1 Final Subbasin and Routing Parameters

After the initial parameter estimates were made and the calibration process was completed, the final model parameters were established. The final Snyder's lag times and peaking coefficients were developed by taking a weighted average of those parameters from the calibration events. The peak discharge from the subbasin for that event was used to weight the calibrated lag times. This method has the effect of granting a higher weight to the lag times and peaking coefficients that were calibrated from larger, more intense storms, and it ignores the storms that generated no runoff from a particular subbasin. The final Snyder's lag times and peaking coefficients are shown in Table B.50 of Appendix B.

The final baseflow parameters were selected based on the results of the calibration runs. Specifically, the initial flows per square miles were selected based on typical flow rates observed on each reach of the river prior to a large storm event, and the recession constant and ratio to peak were selected based on the slope and shape of the receding limb of the hydrograph at the downstream gages. The final baseflow parameters are also shown in Table B.50 of Appendix B.

The Modified Puls storage discharge relationships were calculated from the best available HEC-RAS models, and the final number of subreaches were selected based on calibration to the observed attenuation of the flood hydrograph in between stream gages. Once again, the final subreach values were calculated from a weighted average based on the peak magnitude of the flow through the reach for a given storm event. The final routing subreach values are shown in Table B.51 of Appendix B. A few routing reaches in the portion of the watershed above O.H. Ivie used Muskingum routing parameters. Similar to the Modified Puls routing, the final Muskingum K, X and subreach values were calculated from a weighted average based on the peak magnitude of the flow through the reach for a given storm event. The final Muskingum routing parameters are shown in Table B.52 of Appendix B.

6.5.2 Adopted Loss Rates for the Frequency Storms

In observed storm events, the initial and constant losses vary from storm to storm according to the antecedent moisture conditions of the soil. Therefore, the final set of loss rates was not directly calculated from the calibration results. Instead, the losses for the frequency storms were initially developed using the regional USACE Fort Worth District Method for determining losses based on soil type (percent sand) (Rodman, 1977). After calculating the default frequency loss rates based on soil type, three additional adjustments were made to the loss rate parameters. First, an adjustment was made to the initial deficits to account for the presence of NRCS flood control structures in the watershed that have not been modeled in detail. Second, a climate adjustment was made to both the initial deficits and constant losses to better align them with the observed "average" to "wet" loss rates from recent storm events for different regions of the basin. Third and finally, a Bulletin 17C adjustment was made to the loss rates of the frequent storm events (50% to 4% AEP) to better align the HEC-HMS results with the statistical results at the gages.

The USACE Fort Worth District Method for determining losses method produces a default set of loss rates for each frequency event, based on the soil type in each subbasin (Rodman, 1977). The method assumes that the antecedent moisture conditions become wetter and the losses decrease as the rarity of the flood event increases, which is consistent with other research (McEnroe, 2003). In general, the 50% AEP loss rates are intended to correspond to an "average" or "normal" antecedent soil moisture condition, and the 0.2% AEP loss rates should correspond to a "wet" soil moisture condition. Table 6.15 summarizes the range of default loss rates of the Fort Worth District method by frequency and soil type. A geospatial grid of percent sand for the State of Texas developed by the USACE Fort Worth District was used to spatially calculate the percent

sand for each subbasin. That percent sand value was then used to interpolate between the 0% and 100% sand loss rate values in Table 6.15 to assign the default initial and constant loss rates to each subbasin.

Table 6.15: Default Frequency Loss Rates by Soil Type for the USACE Fort Worth District Method

Annual Exceedance Probability (AEP) %	Initial Deficit (inches) for Soil with 0% Sand	Infiltration Rate (inches per hour) for Soil with 0% Sand	Initial Deficit (inches) for Soil with 100% Sand	Infiltration Rate (inches per hour) for Soil with 100% Sand
50%	1.50	0.20	2.10	0.26
20%	1.30	0.16	1.80	0.21
10%	1.12	0.14	1.50	0.18
4%	0.95	0.12	1.30	0.15
2%	0.84	0.10	1.10	0.13
1%	0.75	0.07	0.90	0.10
0.4%	0.61	0.06	0.73	0.09
0.2%	0.50	0.05	0.60	0.08

After calculating the default frequency loss rates based on soil type, three additional adjustments were made to the loss rate parameters. First, the default initial deficits were increased to account for the presence of NRCS type flood control structures in the watershed that have not been modeled in detail. This adjustment for the NRCS flood control structures was made based on data from the National Inventory of Dams (NID) (USACE, 2016). In this case, the percent of each subbasin area that was controlled by NRCS type structures was multiplied by the inches of runoff that can typically be stored between the riser and spillway of the NRCS structures in that basin (typically up to 4 inches of runoff). For the frequent storm events (50% to 4% AEP), the initial loss due to the NRCS structures was decreased in proportion to the total depth of rain for that event.

Second, a climate adjustment was made to both the initial deficits and constant losses to better align them with the observed "average" to "wet" loss rates from recent storm events for different regions of the basin. The climate adjustment allowed the modeling team to differentiate between west Texas soils, which tend to have drier antecedent conditions, versus central and coastal Texas soils, which tend to have wetter antecedent conditions. This adjustment was made by adding a factor to the previously calculated loss rates in order to ensure that the range of frequency loss rates (from 50% to 0.2% AEP) lined up well with the observed loss rates from the calibration storms for "average" to "wet" antecedent conditions. However, the InFRM team recognized that the calibration events represent a relatively small sample of observed storm events and may not always include enough data to accurately represent the true range of possible loss rates from "dry" to "wet." Therefore, this adjustment was applied on a regional basis rather than by individual subbasin in order to reduce the possible sample bias.

Third and finally, a Bulletin 17C adjustment was made to the loss rates to better align the HEC-HMS results with the statistical results for the frequent storm events (50% to 4% AEP) at the gages. A comparison was made between the preliminary HEC-HMS results with the calculated frequency loss rates and the statistical flow frequency curves from the USGS gage records. A final adjustment was then made to the initial deficits

and constant losses for the 50% through 10% AEP storms in order to have a better correlation with the statistical frequency curves estimated from the USGS gage records. This step was performed because of the increased confidence level in the gage records' statistical frequency curves for the 50% through 10% AEP range. The 4% AEP losses were also adjusted when needed to create a smoother transition between the 2% and 10% AEP flow values. Loss rates for events with an AEP at or below 2% were not adjusted based on the statistical frequency curves because stream gage records in Texas are not long enough and there is too much variability in the rare AEP statistical flow estimates over time (see the change over time plots in Appendix A) to justify adjusting the rare AEP loss rates. Generally, a stream gage record that is 3 to 4 times the length of the return period being estimated is needed before the statistical results can be considered reliable enough for this type of adjustment. For the 1% AEP event, this would require a stream gage record of 300 to 400 years in length, which is not available anywhere in Texas.

The final loss rates after all of these adjustments that were used for the uniform rainfall frequency storm events are documented in Tables B.54 and B.55 of Appendix B. These final loss rates line up well with the band of observed losses from the calibration storms, as shown in Figures 6.16 and 6.17. Based on the range of observed initial deficits and constant losses from the calibration storms, the adopted losses for the frequency storms could be characterized to represent "average" to "wet" conditions (the "average" moisture conditions being applied to the 50% AEP storm, and "wet" moisture conditions being applied to the 0.2% AEP storm), which are appropriate assumptions for modeling hypothetical flood events. However, none of the adopted frequency losses are at the extreme wet or extreme dry ends of the range of calibrated losses.

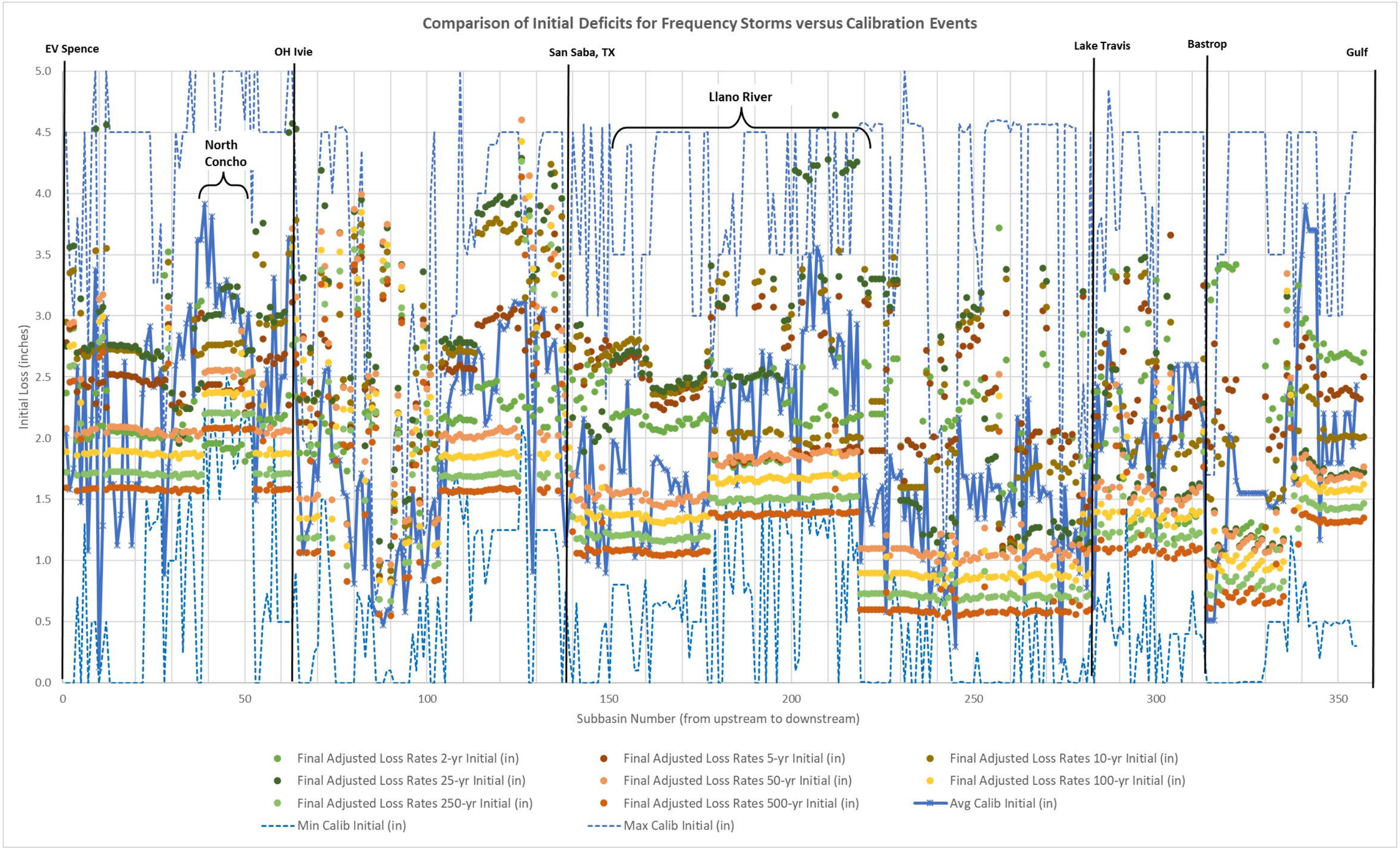

Figure 6.16: Comparison of the Adopted versus Calibrated Initial Deficits (inches)

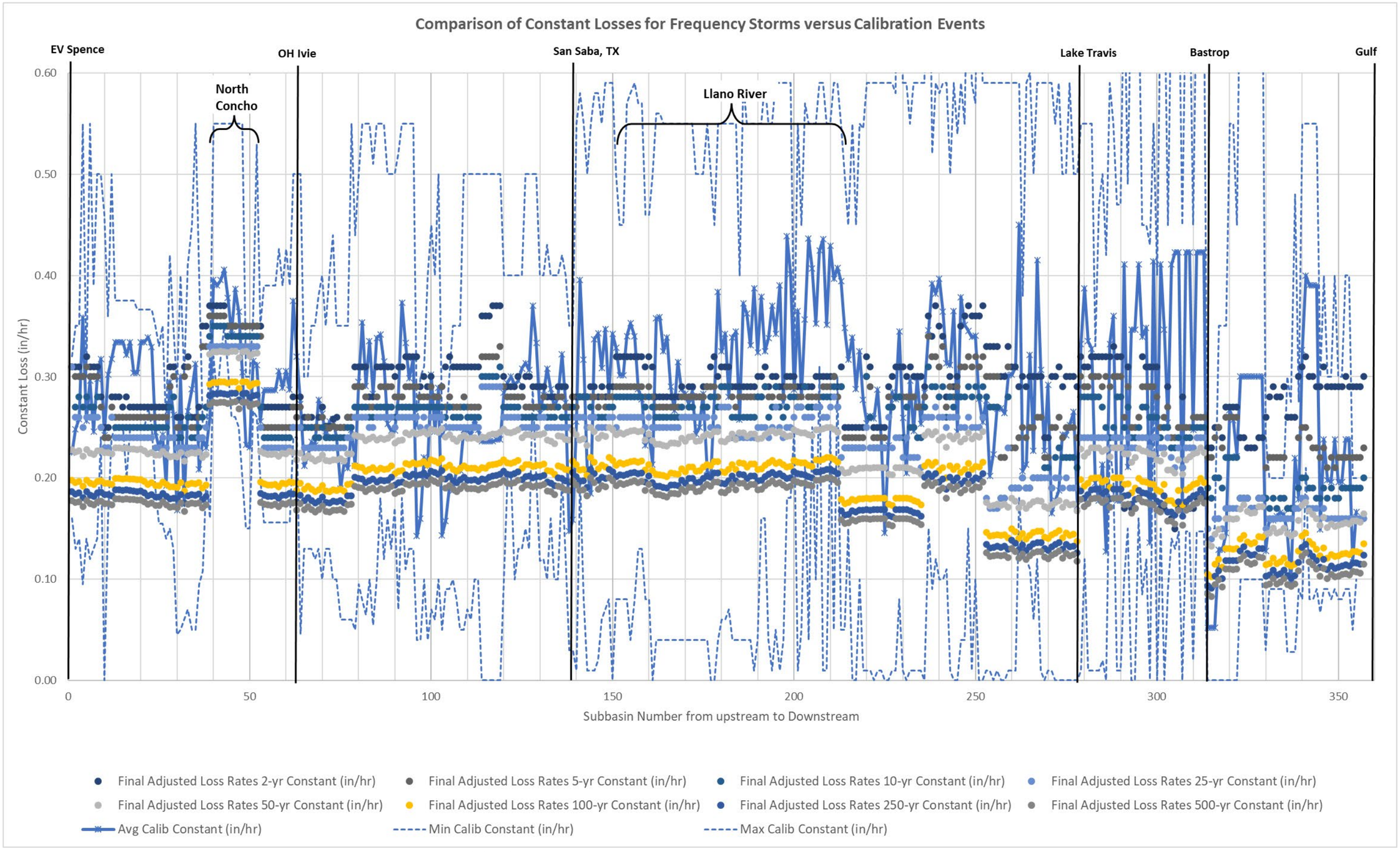

Figure 6.17: Comparison of the Adopted versus Calibrated Constant Losses (inches per hour)

6.5.3 Reservoir Assumptions for the Frequency Storms

For the reservoirs that were modeled in HEC-HMS, assumptions had to be made regarding the initial pool elevations and reservoir releases when running the hypothetical frequency storms. Table 6.16 summarizes the assumptions that were made, and the paragraphs following the table provide additional explanation.

For most reservoirs in the basin, it was assumed that the reservoir's pool elevation would be at top of conservation (also known as normal pool) at the beginning of the frequency storm simulation. However, there are a few notable exceptions. First, for some of the reservoirs in west Texas, top of conservation pool would be an overly conservative assumption. Due to the drier climate of west Texas, some of the reservoirs in that region have not reached the top of their conservation pool in several decades. O.C. Fisher reservoir is one good example. USACE records show that O.C. Fisher has not reached the top of its conservation pool since 1957 and that for the past three decades, the actual pool elevation has been 20 to 60 feet below its intended "normal pool". Therefore, for each reservoir in the basin that tends to have lower than "normal pool" elevations, the 10% exceedance pool was adopted, which is the pool elevation that has been exceeded 10% of the time during the last 30 years. This assumption accounts for the fact that the starting pool elevation may be higher than the average due to a preceding antecedent rain event, but it is still well within the elevations that have actually been experienced under current climate conditions. Therefore, for each reservoir in the model, the initial pool elevation was set to the lower of these two values: (1) top of conservation pool, or (2) the 10% exceedance pool.

The other notable exception was for Lake Buchanan. Lake Buchanan is a major water supply reservoir. Its pool elevation varies widely with water supply conditions. Special consideration was given to the appropriate initial pool elevation for Lake Buchanan due to a change in its operational plan which is being implemented in 2023. The prior operational plan called for limiting the conservation pool to not more than 1,020 feet msl from November through April and not more than 1,018 feet msl from May through October. Under the new operational plan, the conservation pool will be managed to a maximum elevation of not more than 1,020 feet msl all year round, but the operators will make releases that draw down the pool in advance of a forecasted inflow event. Inflows originating from above the confluence of the San Saba and Colorado rivers conservatively allow for an 18-houor forecast lead time to draw down the pool of Lake Buchanan. Therefore, for Lake Buchanan, it was assumed that the initial pool would be drawn down 1-foot for the smaller frequency events (50% to 25% AEP) and 2-feet for the larger frequency events (4% to 0.2% AEP). This is a simplifying assumption as the pool may be drawn down even further than that during an actual event.

Assumptions also had to be made regarding reservoir releases during the frequency storms. For most of the reservoirs in the basin that do not have complex gated operations, the same assumptions that were used for the initial parameters and the calibration events were also used for the frequency storms. For the reservoirs that do have gated operations, time series data of the observed releases were used for the calibration events, so different assumptions had to be made for the frequency storms. These assumptions varied from reservoir to reservoir based on their operational plans.

The USACE reservoirs of Hords Creek and O.C. Fisher were designed as flood control reservoirs. According to their operational plans, the gates of the reservoirs would remain closed until the downstream floodwaters had receded back into the channel. Therefore, for the frequency storms, it was assumed that no releases would be made during the storm event until the reservoirs' pool elevation reached the spillway crest. Above that elevation, releases would be governed by the rating curve of the uncontrolled spillway.

Table 6.16: Assumed Initial Pool Elevations and Reservoir Releases for the Frequency Storms

Reservoir Name	Initial Pool Elev (feet NAVD88)	Initial Pool Data Source	Reservoir Release Method	Reservoir Release Data Source
Oak Creek	2000.6	Top of Conservation	Uncontrolled Spillway	Same as initial parameters
Ballinger Lake, Upper	1695.4	Top of Conservation	Uncontrolled Spillways	Same as initial parameters
Ballinger Lake, Lower	1668.38	Top of Conservation	Uncontrolled Spillways	Same as initial parameters
Twin Buttes Reservoir	1932.8	10% Exceedance Pool	Elevation-Discharge Curve	Total release curve (gated + spillway) based on typical release data from the Reservoir Analysis (Appendix E)
O.C. Fisher Reservoir	1884.0	10% Exceedance Pool	Uncontrolled Spillway	Assumed gates closed until the spillway crest, then use the uncontrolled spillway rating curve.
O.H. Ivie Reservoir	1547.8	10% Exceedance Pool	Elevation-Discharge Curve	Total release curve (gated + spillways) based on typical release data from the Reservoir Analysis (Appendix E)
Lake Coleman	1717.95	Top of Conservation	Uncontrolled Outlet & Spillway	Same as initial parameters
Hords Creek Reservoir	1899.0	10% Exceedance Pool	Uncontrolled Spillway	Assumed gates closed until the spillway crest, then use the uncontrolled spillway rating curve.
Lake Brownwood	1425.0	Top of Conservation	Uncontrolled Spillway	Same as initial parameters
Brady Creek Reservoir	1743.2	Top of Conservation	Uncontrolled Outlet & Spillway	Same as initial parameters
Lake Buchanan	1018.26 - 1019.26	LCRA's New 2023 Operational Plan	Elevation-Discharge Curve	Initial Pool and Reservoir Releases are based on LCRA's new 2023 operational plan for Lake Buchanan. Assumed an initial drawdown from top of conservation where the larger frequency events have a larger initial drawdown. Total release curve is based on new rules from LCRA and data from the Buchanan sensitivity analysis in Appendix E.
Lake LBJ	825.0	Top of Conservation	Elevation-Discharge Curve	Total release curve based on allowable releases from the reservoir's water control plan.
Lake Travis	681.0	Top of Conservation	Elevation-Discharge Curve	Total release curve based on allowable releases from the reservoir's water control plan.

For Twin Buttes and O.H. Ivie, which do make gated releases during storm events, an elevation-discharge curve was added to the model to govern releases for the frequency events. The elevation-discharge curves were created to represent the total release from the reservoir (gated plus spillway) for the full range of possible pool elevations. These curves were calibrated to observed releases and pool elevations during their respective reservoir analyses, which are described in Appendix E.

For the three largest reservoirs that are operated by LCRA, Lake Buchanan, Lake LBJ and Lake Travis, an elevation discharge curve was used to represent the total release from the dam. Once again, this is a

simplifying assumption compared to the actual complex gated operations of these dams. However, even a simplified curve can produce reasonable results in terms of peak pool elevation and peak discharge when calibrated to observed pool elevations and releases. This was the approach that was taken for these three lakes, as was also shown their respective reservoir analyses in Appendix E. In addition, Lake Travis' operational rules regarding maximum allowable releases at specific pool thresholds were incorporated into the release curve. For Lake Buchanan, the release curve was modified to be consistent with its new 2023 operational plan, which specifies the maximum allowable releases at the current FEMA 1% and 0.2% AEP pool elevations. For more information on the 2023 operational plan, please see the Lake Buchanan sensitivity analysis in Appendix E.

6.6 UNIFORM RAINFALL FREQUENCY STORMS

After finalizing the model's parameters based on the calibration events, the frequency flow values were then calculated in HEC-HMS by applying frequency rainfall depths to the final watershed basin models through a series of depth-area analyses. This rainfall pattern is referred to as the uniform rainfall method because the assigned point rainfall depths for each subbasin are reduced uniformly over the entire watershed based on the published depth-area reduction factors from Figure 15 of the National Weather Service TP-40 publication (Herschfield, 1961). A depth area analysis was set up for every junction and node of interest within the HEC-HMS model in order to apply the appropriate depth-area reduction for each drainage area of interest.

In order to select the appropriate storm duration and temporal distribution for the frequency storms, sensitivity tests were run in HEC-HMS for a series of storm durations ranging from 12-hours to 10-days and for intensity positions ranging from 25% to 75% of the total storm duration, as shown in Tables 6.17 and 6.18. Please note that the peak flow results shown in these tables represent preliminary sensitivity tests that were performed in the model prior to completing calibration; therefore, they do not match the final flow frequency results shown later in this appendix.

From Table 6.17, one can see that increasing the storm duration tends to increase the peak discharge for the tested locations. This makes sense as increasing the storm duration increases to total volume of rainfall. However, these increases in peak discharge level off to 1% or less for most of the tested junctions for storm durations longer than 48 hours.

Similarly, from Table 6.18, one can see that moving the intensity position later in the storm tends to increase peak discharge. This means that a back-loaded storm tends to produce higher flow rates than a front-loaded storm. This makes sense because the initial soil moisture deficit will have a greater effect on the intense portion of the rainfall for a front-loaded storm. However, once again these changes level off to 1% or less for most of the tested junctions for intensity positions later than 50%.

After completing the sensitivity analyses, a 48-hour storm duration with a 50% intensity position and a 15-minute intensity duration was adopted for all the frequency storms in the HEC-HMS model.

Table 6.17: Sensitivity Test Results for Various Storm Durations

Peak Discharges for Tested Storm Durations						
Frequency	100yr	100yr	100yr	100yr	100yr	100yr
Duration	**12hr**	**24hr**	**48hr**	**96hr**	**7 day**	**10 day**
Model Location	(cfs)	(cfs)	(cfs)	(cfs)	(cfs)	(cfs)
PB_Pecan Bayou_J80	74550	85936	94804	100284	104886	107049
CN_Concho_J60	157738	175654	182410	183393	183433	183446
CO_Colorado_J130	193339	219889	239733	252334	259241	262204
SS_SanSaba_J150	427899	486368	510165	513533	514410	514689
LN_Llano_J170	732586	777557	791245	791663	791738	791788
PD_Pedernales_J100	249443	281856	285539	285617	285603	285588
ON_OnionCr_J50	152345	160067	162037	162287	162285	162270
CO_Coloradao_J560	102357	113065	117873	118737	118744	118550
% Difference in Results						
Model Location		**12 to 24hr**	**24 to 48hr**	**48 to 96hr**	**4 to 7 days**	**7 to 10 days**
PB_Pecan Bayou_J80	-	15%	10%	6%	5%	2%
CN_Concho_J60	-	11%	4%	1%	0%	0%
CO_Colorado_J130	-	14%	9%	5%	3%	1%
SS_SanSaba_J150	-	14%	5%	1%	0%	0%
LN_Llano_J170	-	6%	2%	0%	0%	0%
PD_Pedernales_J100	-	13%	1%	0%	0%	0%
ON_OnionCr_J50	-	5%	1%	0%	0%	0%
CO_Coloradao_J560	-	10%	4%	1%	0%	0%

Table 6.18: Sensitivity Test Results for Various Storm Intensity Positions

Peak Discharges for Tested Temporal Distributions					
Frequency	100yr	100yr	100yr	100yr	100yr
Intensity Position	**25%**	**33%**	**50%**	**67%**	**75%**
Model Location	(cfs)	(cfs)	(cfs)	(cfs)	(cfs)
PB_Pecan Bayou_J80	85936	89419	94804	99368	101850
CN_Concho_J60	175654	179113	182410	183317	183396
CO_Colorado_J130	219889	228336	239733	248402	253204
SS_SanSaba_J150	486370	498929	510165	512799	513684
LN_Llano_J170	777557	783867	791245	791624	792003
PD_Pedernales_J100	281856	284213	285539	285632	285817
ON_OnionCr_J50	160067	161218	162037	162250	162289
CO_Coloradao_J560	115689	116535	117873	118066	117768
% Difference in Results					
Model Location		25% - 33%	50% - 33%	67% - 50%	75% - 67%
PB_Pecan Bayou_J80	-	4%	6%	5%	2%
CN_Concho_J60	-	2%	2%	0%	0%
CO_Colorado_J130	-	4%	5%	4%	2%
SS_SanSaba_J150	-	3%	2%	1%	0%
LN_Llano_J170	-	1%	1%	0%	0%
PD_Pedernales_J100	-	1%	0%	0%	0%
ON_OnionCr_J50	-	1%	1%	0%	0%
CO_Coloradao_J560	-	1%	1%	0%	0%

6.6.1 Point Rainfall Depths for the Uniform Frequency Storms

NOAA Atlas 14 contains precipitation frequency estimates for the United States along with their associated lower and upper 90% confidence bounds. The Atlas is divided into volumes based on geographic sections of the country. NOAA Atlas 14 is intended as the U.S. Government source of precipitation frequency estimates. NOAA Atlas 14 Volume 11, which covers the state of Texas, was published in 2018 (NOAA, 2018). The point rainfall depths that were published in NOAA Atlas 14 (NA14) were applied to the HEC-HMS model for this study, as they are the most up-to-date precipitation frequency estimates in Texas.

NOAA Atlas 14 point rainfall depths from the annual maximum series for various durations and recurrence intervals were collected from the NA14 Precipitation Frequency Data Server (PFDS) for the centroid of each subbasin (NOAA, 2020). This method resulted in 357 separate point rainfall tables being applied in the Lower Colorado River basin, one for each subbasin. The appropriate point rainfall depth table was assigned to each subbasin within the HEC-HMS frequency storm editor. It should be noted that precipitation frequency estimates from NOAA Atlas 14 are point estimates and are not directly applicable to larger areas. The conversion from a point to an areal estimate was accomplished for the uniform rainfall method by using the depth area analyses in HEC-HMS with the default TP-40 area reduction curves.

Figure 6.18 illustrates how the NA14 1% Annual Exceedance Probability (AEP) point rainfall depths for the 48-hour durations vary spatially across the Lower Colorado River basin. As one can see from this figure, the 1% AEP 48-hr depth varies from less than 9 inches upstream of San Angelo, Texas to over 13 inches near Austin, Texas to almost 18 inches near the Gulf of Mexico. Geographically, it makes sense that the

downstream end of the basin would receive the most rainfall because of its proximity to the large source of moisture at the Gulf of Mexico.

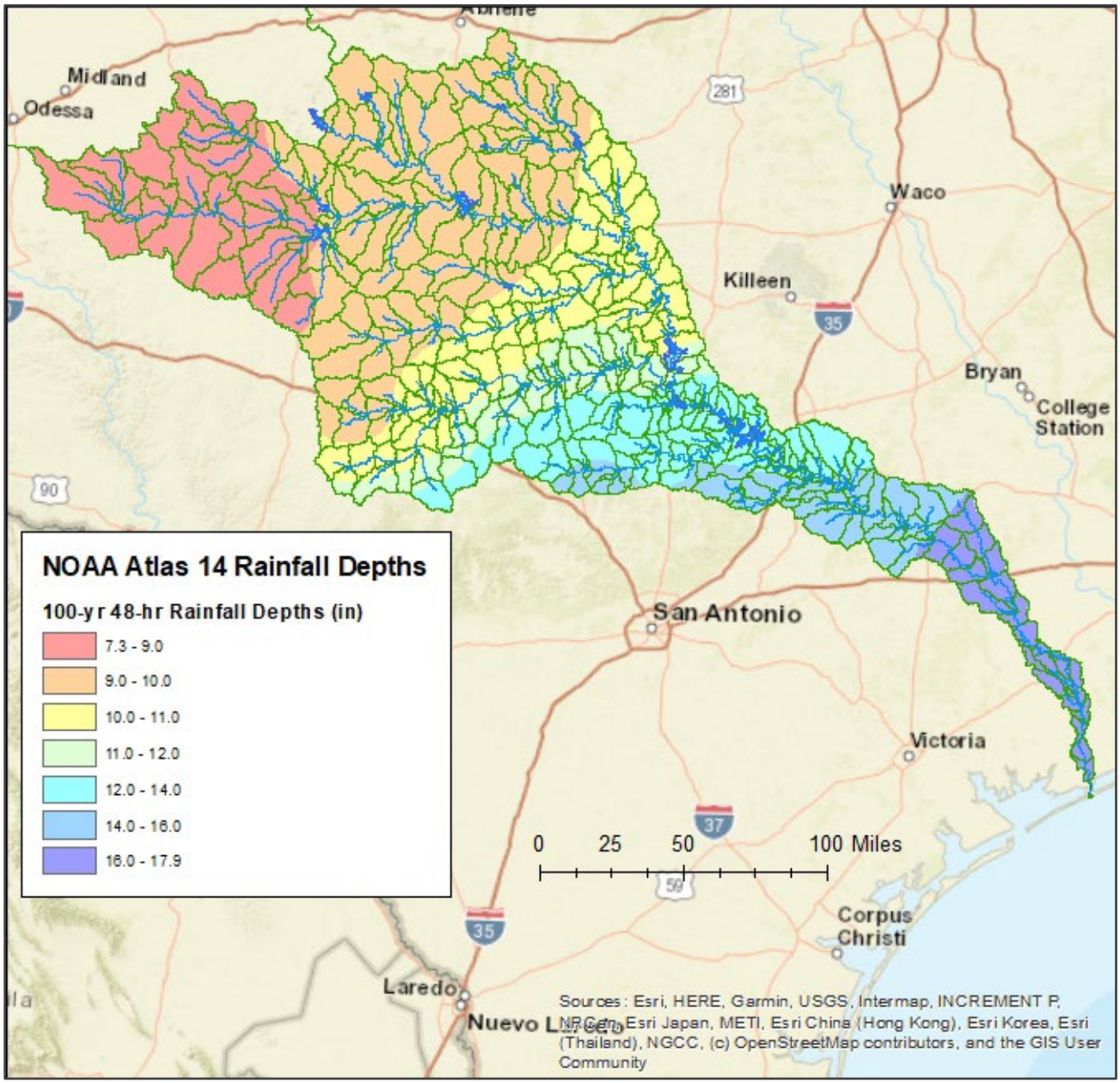

Figure 6.18: 1% AEP, 48-hour Rainfall Depths for the Lower Colorado River Basin from NOAA Atlas 14

6.6.2 Frequency Storm Results – Uniform Rainfall Method

The final frequency results for the uniform rainfall method were then computed in HEC-HMS by applying the NOAA Atlas 14 frequency rainfall depths to the final watershed model through a series of depth-area analyses of the applied frequency storms. This rainfall pattern is referred to as the uniform rainfall method because the assigned point rainfall depths for each subbasin are reduced uniformly over the entire watershed.

The final uniform rain HEC-HMS frequency flow results for all studied locations throughout the watershed model can be seen in Table 6.19. In this table, the highlighted rows indicate calibrated gage locations. The final uniform rain HEC-HMS frequency pool elevation results are summarized in Table 6.20. These results will then be compared to the elliptical shaped storm results from HEC-HMS along with other methods from this study, as shown in Chapter 12.

In some cases, one may observe in Table 6.19 that the simulated peak discharge decreases in the downstream direction. It is not an uncommon phenomenon to see decreasing frequency peak discharges for some river reaches as flood waters spread out into the floodplain and the hydrograph becomes dampened as it moves downstream. This can be due to a combination of peak attenuation due to river routing as well as the difference in timing between the peak of the main stem river versus the runoff from the local tributaries and subbasins.

Table 6.19: Summary of Peak Discharges (cfs) from the HEC-HMS Uniform Rainfall Frequency Storms

Location Description	HMS Element Name	HMS Drainage Area (sq mi)	50% AEP 2-yr	20% AEP 5-yr	10% AEP 10-yr	4% AEP 25-yr	2% AEP 50-yr	1% AEP 100-yr	0.5% AEP 200-yr	0.2% AEP 500-yr
Colorado River downstream of E.V. Spence Reservoir	SOURCE_SPENCE	0.01	10	10	10	10	10	10	10	10
Colorado River at Robert Lee, TX (USGS Gage 08124000)	CO_Colorado_J10	30.9	306	1,363	3,214	7,464	12580	15,708	18,544	22,402
Colorado River below Turkey Creek	CO_Colorado_J20	177.5	87	1,503	4,396	14,513	34133	49,015	63,166	79,308
Colorado River above Oak Creek	CO_Colorado_J29	330.8	135	1,466	4,129	15,151	36215	52,037	66,787	86,883
Inflow to Oak Creek Reservoir	OAK_CR_INFLOW	237.4	3,450	8,014	14,506	29,059	49643	64,988	79,306	99,175
Outflow from Oak Creek Reservoir	OAK_CR_RES	237.4	778	1,773	3,977	10,033	24365	39,246	53,501	76,064
Oak Creek above the Colorado River	CO_OakCr_J20	337.4	740	1,743	4,100	10,175	21307	32,573	44,499	62,184
Colorado River below Oak Creek	CO_Colorado_J30	668.2	781	3,031	7,940	24,466	54327	76,861	98,292	127,129
Colorado River above Valley Creek	CO_Colorado_J39	844.9	2,173	4,982	9,747	24,192	52312	74,932	98,123	130,139
Valley Creek below subbasin CO_ValleyCr_S10	CO_ValleyCr_J10	141.1	2,869	5,753	10,199	19,403	32998	42,831	52,102	64,765
Valley Creek above upper & lower Ballinger City Lakes	CO_ValleyCr_J20	231.2	2,364	4,941	9,029	17,551	30404	40,193	49,841	63,469
Valley Creek below the lower Ballinger City Lake	Ballinger_Lower	231.2	1,920	4,452	8,457	16,663	29007	38,440	48,321	61,282
Colorado River near Ballinger, TX (USGS Gage 08126380)	CO_Colorado_J40	1076.2	2,702	7,694	16,696	40,554	81006	113,061	146,049	190,896
Colorado River above Elm Creek	CO_Colorado_J49	1130.3	2,681	7,599	16,394	39,775	79601	111,159	143,583	188,123
Bluff Creek below Mill Creek (below subbasin CO_ElmCr_S10)	CO_ElmCr_J10	107.4	2,571	6,048	9,502	15,550	21802	31,433	40,714	52,500
Elm Creek at Ballinger, TX (USGS Gage 08127000)	CO_ElmCr_J20	466.8	3,953	10,478	17,181	29,088	41908	62,761	84,139	113,770
Colorado River below Elm Creek	CO_Colorado_J50	1597.2	6,614	17,173	29,647	58,785	106488	151,501	198,636	263,418
Colorado River above the Concho River	CO_Colorado_J59	1826.2	6,132	17,646	28,144	57,008	103861	147,912	194,159	259,115
High Lonesome Draw below subbasin CN_Mconcho_S20	CN_MConcho_J10	404.4	159	258	4,524	19,916	45699	62,772	76,721	96,690
High Lonesome Draw below subbasin CN_Mconcho_S30	CN_MConcho_J20	496.5	179	588	5,688	23,638	53496	73,577	90,468	114,753

Location Description	HMS Element Name	HMS Drainage Area (sq mi)	50% AEP 2-yr	20% AEP 5-yr	10% AEP 10-yr	4% AEP 25-yr	2% AEP 50-yr	1% AEP 100-yr	0.5% AEP 200-yr	0.2% AEP 500-yr
Centralia Draw below High Lonesome Draw	CN_MConcho_J30	745.2	261	1,417	8,272	30,197	66161	91,029	113,158	145,660
Centralia Draw below North Creek	CN_MConcho_J40	946.0	372	1,760	8,812	31,100	67305	92,480	115,134	148,654
Middle Concho River below the Centrailia Draw	CN_MConcho_J50	1349.1	843	4,031	13,799	39,513	78122	106,338	132,044	169,892
Middle Concho River above Kiowa Creek	CN_MConcho_J59	1642.5	1,335	5,807	18,105	50,259	97727	133,367	166,967	216,358
Middle Concho River below Kiowa Creek	CN_MConcho_J60	1731.3	1,486	6,275	19,062	52,615	101980	139,185	174,722	226,337
Middle Concho River below Big Hollow Draw	CN_MConcho_J70	1887.2	1,509	6,272	18,903	51,939	100430	137,051	172,231	223,442
Middle Concho River above West Rocky Creek	CN_MConcho_J79	2007.5	1,500	6,190	18,571	50,982	98519	134,459	169,082	219,560
Middle Concho River below West Rocky Creek	CN_MConcho_J80	2121.6	1,534	6,226	18,637	51,131	98758	134,773	169,470	220,038
Middle Concho River abv Tankersley (USGS Gage 08128400)	CN_MConcho_J90	2133.0	1,529	6,222	18,622	51,076	98657	134,623	169,298	219,870
Spring Creek below O-Nine Draw (below subbasin CN_SConcho_S30)	CN_SConcho_J30	198.5	209	4,134	13,145	31,652	49437	63,449	76,254	94,084
Spring Creek above Tankersley, TX (USGS Gage 08129300)	CN_SConcho_J35	427.2	331	2,805	9,044	22,976	36699	55,981	74,672	97,442
Dove Creek at Knickerbocker, TX (USGS Gage 08130500)	CN_SConcho_J40	224.4	1,082	5,126	10,577	19,792	30014	39,452	48,668	62,057
Dove Creek above Spring Creek	CN_SConcho_J49	251.7	929	4,473	9,266	17,359	26359	34,783	43,214	55,579
Spring Creek near San Angelo, TX (USGS Gage 08130700)	CN_SConcho_J50	678.9	1,071	6,736	16,990	37,399	58546	77,701	96,782	124,493
South Concho River below subbasin CN_Sconcho_S10	CN_SConcho_J10	159.3	915	5,248	13,888	26,080	33401	42,931	51,766	64,282
South Concho River at Christoval, TX (USGS Gage 08128000)	CN_SConcho_J20	415.4	1,076	8,801	25,596	49,470	64075	83,923	103,230	130,851
Inflow to Twin Buttes Reservoir	TWIN_BUTTES_INFLOW	3422.5	2,892	15,057	39,726	87,243	135769	182,850	232,406	305,102
South Concho River below Twin Buttes Reservoir	TWIN_BUTTES_OUTFLOW	3422.5	0	0	3,000	7,172	9000	9,000	16,480	42,143
Pecan Creek nr San Angelo, TX (USGS Gage 08131400)	CN_SConcho_J60	81.0	281	1,980	4,922	13,148	23732	29,987	36,179	43,475
Inflow to Lake Nasworthy	NASWORTHY_INFLOW	107.2	436	1,600	4,226	11,626	21222	27,405	33,907	41,819
South Concho River below Lake Nasworthy	NASWORTHY_OUTFLOW	107.2	436	1,600	4,226	11,626	21222	27,405	33,907	41,819

Location Description	HMS Element Name	HMS Drainage Area (sq mi)	50% AEP 2-yr	20% AEP 5-yr	10% AEP 10-yr	4% AEP 25-yr	2% AEP 50-yr	1% AEP 100-yr	0.5% AEP 200-yr	0.2% AEP 500-yr
South Concho River above the North Concho River	CN_SConcho_J70	139.2	1,743	2,209	4,933	12,057	21383	27,810	34,587	43,147
North Concho River abv Sterling City (USGS Gage 08133250)	CN_NConcho_J10	201.0	609	2,268	5,167	12,084	23497	33,061	41,321	52,570
North Concho River above Lacy Creek	CN_NConcho_J19	288.6	587	2,349	5,416	12,938	25356	35,800	45,055	57,678
Lacy Creek below Apple Creek	CN_NConcho_J20	146.1	428	2,077	4,674	12,175	24867	35,104	43,247	54,009
Lacy Creek above the North Concho River	CN_NConcho_J29	278.5	409	1,883	4,424	12,038	24978	35,579	44,697	56,500
North Concho River below Lacy Creek	CN_NConcho_J30	567.1	929	4,010	9,382	23,959	48402	68,819	86,545	110,190
North Concho River at Sterling City (USGS Gage 08133500)	CN_NConcho_J40	586.0	908	3,901	9,117	23,251	46962	66,826	84,132	107,287
North Concho River above Sterling Creek	CN_NConcho_J49	609.8	891	3,814	8,904	22,682	45784	65,167	82,178	104,903
North Concho River below Sterling Creek	CN_NConcho_J50	808.4	964	4,051	9,336	23,557	48101	68,464	86,490	110,566
North Concho River above Walnut Creek	CN_NConcho_J59	1004.0	1,133	3,973	9,119	22,918	46875	66,762	84,477	108,136
North Concho River below Walnut Creek	CN_NConcho_J60	1070.3	1,816	5,032	9,147	22,969	46985	66,915	84,667	108,377
North Concho River nr Carlsbad, TX (USGS Gage 08134000)	CN_NConcho_J70	1220.7	1,998	5,510	9,961	22,599	46295	65,948	83,539	107,011
North Concho River above Grape Creek	CN_NConcho_J79	1250.2	1,973	5,435	9,832	22,439	45982	65,499	83,015	106,379
North Concho River below Grape Creek	CN_NConcho_J80	1360.1	2,927	6,883	12,246	23,169	51497	72,801	92,744	120,477
North Concho River nr Grape Creek (USGS Gage 08134250)	CN_NConcho_J90	1364.9	2,874	6,835	12,187	23,030	51045	72,206	92,036	119,663
Inflow to OC Fisher Reservoir	OC_FISHER_INFLOW	1462.8	3,141	7,445	13,234	24,712	52074	73,626	93,916	122,459
North Concho River below OC Fisher Reservoir	OC_Fisher_OUTFLOW	1462.8	0	0	0	0	0	-	-	3,458
North Concho River at San Angelo (former USGS 08135000)	CN_NConcho_J100	22.1	1,462	1,861	2,705	4,776	9733	11,751	13,725	16,207
Concho River at San Angelo, TX (USGS Gage 08136000)	CN_Concho_J10	161.2	2,988	3,795	6,861	15,210	27372	36,237	45,283	56,152
Concho River above Crows Nest Creek	CN_Concho_J20	300.8	2,579	4,750	9,459	23,617	44721	59,703	74,830	94,753
Concho River above Lipan Creek	CN_Concho_S29	470.3	1,935	4,518	9,482	26,267	58599	77,045	94,527	114,339

Location Description	HMS Element Name	HMS Drainage Area (sq mi)	50% AEP 2-yr	20% AEP 5-yr	10% AEP 10-yr	4% AEP 25-yr	2% AEP 50-yr	1% AEP 100-yr	0.5% AEP 200-yr	0.2% AEP 500-yr
Dry Lipan Creek below Ninemile Creek	CN_Concho_J30	142.1	740	2,377	5,068	12,733	24832	32,667	39,915	50,110
Lipan Creek above Concho River	CN_Concho_S39	308.3	836	2,688	5,823	15,048	29994	40,411	50,725	65,745
Concho River below Lipan Creek	CN_Concho_J40	778.6	2,740	7,058	14,807	39,161	83760	111,412	139,868	175,791
Concho River above Kickapoo Creek	CN_Concho_J49	895.4	2,612	7,089	15,085	39,758	85673	115,025	143,969	181,928
Kickapoo Creek below Welch Creek	CN_KickapooCr_J10	138.7	1,159	3,159	6,506	14,910	27882	36,215	43,826	54,489
Kickapoo Creek above the Concho River	CN_KickapooCr_J20	300.0	1,124	2,952	5,861	13,503	25345	33,559	41,148	51,919
Concho River below Kickapoo Creek	CN_Concho_J50	1195.4	3,021	8,170	17,452	46,174	100150	135,469	168,664	216,367
Concho River at Paint Rock, TX (USGS Gage 08136500)	CN_Concho_J60	1202.9	2,994	8,125	17,407	46,036	99645	134,799	168,062	215,790
Concho River above the Colorado River	CN_Concho_J70	1393.8	2,968	10,724	17,606	46,255	102351	138,527	175,894	231,195
Colorado River below the Concho River	CO_Colorado_J60	3220.0	8,498	26,092	45,410	97,053	192991	267,593	341,754	447,400
Inflow to OH Ivie Reservoir	OH_IVIE_INFLOW	3395.3	8,505	26,184	45,593	97,311	195206	270,931	346,519	451,106
Colorado River below OH Ivie Reservoir	OH_IVIE_OUTFLOW	3395.3	15	2,999	16,838	79,903	152590	190,009	237,973	367,204
Colorado River near Stacy, TX (USGS Gage 08136700)	CO_Colorado_J70	3535.2	531	4,422	16,686	79,405	152640	190,031	237,502	365,703
Colorado River below Panther Creek	CO_Colorado_J80	3637.6	3,906	8,067	11,775	53,566	143246	181,957	228762	347628
Colorado River below Salt Creek	CO_Colorado_J90	3743.1	4,710	9,143	14,266	53,779	143566	182,620	229416	348272
Colorado River above Bull Creek	CO_Colorado_J99	3819.8	4,367	9,624	15,646	53,408	142469	182,180	227701	343404
Colorado River below Bull Creek	CO_Colorado_J100	3884.4	5,715	11,798	19,705	53,685	142909	182,750	228403	344289
Colorado River below Elm Creek	CO_Colorado_J110	3965.4	5,219	12,220	20,915	53,916	143028	183,229	228661	343525
Colorado River above Home Creek	CO_Colorado_J119	4104.2	**5,267**	13,471	**24,020**	54,370	143,607	184,213	229,831	344594
Home Creek at US-283 Hwy	CO_HomeCr_J10	148.2	3,349	4,493	6,731	9,403	25,450	39,423	53,020	71185
Home Creek above Mukewater Creek	CO_HomeCr_J20	250.3	2,438	3,193	5,249	8,650	26,169	42,483	58,656	81980

Location Description	HMS Element Name	HMS Drainage Area (sq mi)	50% AEP 2-yr	20% AEP 5-yr	10% AEP 10-yr	4% AEP 25-yr	2% AEP 50-yr	1% AEP 100-yr	0.5% AEP 200-yr	0.2% AEP 500-yr
Home Creek above the Colorado River	CO_HomeCr_J30	382.8	5,870	7,398	10,763	24,731	50,822	75,122	99,853	134386
Colorado River below Home Creek	CO_Colorado_J120	4487.0	10,808	20,843	33,678	69,232	145,642	187,102	235,583	349673
Colorado River at Winchell, TX (USGS Gage 08138000)	CO_Colorado_J130	4535.4	10,215	20,688	33,893	70,875	145888	187540	241110	350150
Colorado River above Clear Creek	CO_Colorado_J139	4635.4	10,743	21,449	34,398	65,296	144,523	186,777	236,860	349701
Colorado River below Clear Creek	CO_Colorado_J140	4758.9	11,885	22,134	36,097	66,229	144,681	187,021	248,189	352059
Colorado River below Buffalo Creek	CO_Colorado_J150	4940.0	11,954	21,547	36,564	64,550	143,860	186,705	234,004	349159
Colorado River above Pecan Bayou	CO_Colorado_J159	5045.9	11,740	21,054	35,793	61,316	142,515	186,109	233,704	348248
Jim Ned Creek above South Fork Jim Ned Creek	PB_JimNedCr_J10	150.7	2,540	9,778	14,351	21,897	30,238	39,650	48,731	60,952
Inflow to Lake Coleman	COLEMAN_INFLOW	302.3	1,689	7,173	12,524	25,703	42,108	63,292	84,177	111,723
Jim Ned Creek below Lake Coleman	COLEMAN_OUTFLOW	302.3	390	1,773	1,826	13,636	30,003	52,933	75,920	105,561
Jim Ned Creek above Indian Creek	PB_JimNedCr_J20	386.2	358	1,794	4,501	11,871	28,134	51,117	78,236	114,038
Jim Ned Creek nr Coleman, TX (USGS Gage 08140860)	PB_JimNedCr_J29	447.0	349	1,795	4,223	12,059	27,221	50,606	78,007	117,247
Inflow to Hords Creek Reservoir	HORDS_CR_INFLOW	48.9	2,281	6,194	10,593	18,612	22,850	27,676	32,396	39,131
Hords Creek below Hords Creek Reservoir	HORDS_CR_RES	48.9	0	0	0	0	-	-	244	1,092
Hords Creek near Coleman, TX (USGS Gage 08142000)	PB_HordsCr_J10	57.8	1,522	4,015	7,153	10,922	15,138	19,645	24,026	29,897
Hords Creek above Jim Ned Creek	PB_HordsCr_J20	97.1	1,657	4,984	7,071	10,723	15,980	21,981	28,212	37,874
Jim Ned Creek below Hords Creek	PB_JimNedCr_J30	544.0	1,470	4,668	9,720	20,448	33,449	57,472	90,130	137,338
Jim Ned Creek at FM-585	PB_JimNedCr_J40	632.9	1,702	7,703	11,675	20,855	35,413	56,304	82,248	131,952
Jim Ned Creek above Lake Brownwood	PB_JimNedCr_J50	732.6	11,022	16,263	21,327	28,754	35,680	57,497	81,466	126,617
North Prong Pecan Bayou at SH-36	PB_PecanBayou_J10	101.8	387	1,113	4,112	10,833	18,141	27,394	36,383	47,621
Pecan Bayou below South Prong Pecan Bayou	PB_PecanBayou_J20	189.6	2,322	3,310	5,933	17,672	30,829	48,379	65,181	86,183

Location Description	HMS Element Name	HMS Drainage Area (sq mi)	50% AEP 2-yr	20% AEP 5-yr	10% AEP 10-yr	4% AEP 25-yr	2% AEP 50-yr	1% AEP 100-yr	0.5% AEP 200-yr	0.2% AEP 500-yr
Pecan Bayou above Burnt Branch	PB_PecanBayou_J30	309.4	7,203	12,624	16,609	22,690	35,133	55,289	76,688	108,516
Pecan Bayou above Turkey Creek	PB_PecanBayou_J39	451.4	5,123	11,416	16,509	25,677	40,197	60,962	86,945	122,655
Pecan Bayou nr Cross Cut, TX (USGS Gage 08140700)	PB_PecanBayou_J40	543.9	5,218	12,029	18,701	30,678	45,029	67,890	97,708	138,697
Pecan Bayou below Red River	PB_PecanBayou_J50	642.7	9,884	15,073	21,990	37,441	53,066	75,063	101,281	145,958
Inflow to Lake Brownwood	BROWNWOOD_INFLOW	1513.0	22,036	33,059	43,611	59,124	88,384	134,935	186,786	265,934
Pecan Bayou below Lake Brownwood	BROWNWOOD_OUTFLOW	1513.0	4,156	9,184	15,039	26,740	42,821	66,654	94,437	132,937
Pecan Bayou at Brownwood, TX (USGS Gage 08143500)	PB_PecanBayou_J60	1603.8	4,231	9,302	15,001	25,776	41,307	62,883	88,986	125,806
Pecan Bayou below Devils River	PB_PecanBayou_J70	1753.0	4,282	9,816	15,175	25,872	39,418	57,844	81,531	116,018
Pecan Bayou above Blanket Creek	PB_PecanBayou_J79	1826.2	4,364	9,534	15,187	25,757	38,875	55,892	77,863	110,331
Blanket Creek at US-183 Hwy	PB_BlanketCr_J10	104.1	154	2,089	5,482	10,333	17,989	24,641	30,763	38,764
Blanket Creek above Pecan Bayou	PB_BlanketCr_J20	197.0	1,094	3,840	6,292	10,247	16,862	32,438	46,178	62,869
Pecan Bayou nr Mullin, TX (USGS Gage 08143600)	PB_PecanBayou_J80	2023.2	5,135	11,010	18,107	29,904	46,163	67,656	87,475	112,860
Pecan Bayou above Colorado River	PB_PecanBayou_J90	2155.4	5,813	12,769	22,566	39,390	57,722	79,970	107,659	146,462
Colorado River below Pecan Bayou	CO_Colorado_J160	7201.3	15,893	30,741	50,509	86,334	181,290	240,805	313125	461819
Colorado River near Goldthwaite, TX (LCRA Gage 1277)	CO_Colorado_J170	7228.4	14,723	28,524	48,578	84,771	175666	239358	305771	449288
Colorado River above the San Saba River	CO_Colorado_J179	7339.7	14,257	27,806	47,244	80,651	166,432	234,514	293867	425882
North Valley Prong below Poor Hollow	SS_SanSaba_J10	306.9	749	5,029	14,634	29,364	51,756	66,684	81,094	101,484
San Saba Rv at FM 864 nr Fort McKavett, TX (USGS Gage)	SS_SanSaba_J20	622.8	2,545	11,395	30,133	61,025	105,303	138,148	168,269	210,741
San Saba River above Rocky Creek	SS_SanSaba_J29	721.4	2,231	11,327	30,569	62,466	108,561	142,635	175,860	223,408
San Saba River below Rocky Creek	SS_SanSaba_J30	831.2	2,556	12,197	33,279	68,765	120,140	158,927	197,523	252,554
San Saba River above Las Moras Creek	SS_SanSaba_J40	989.0	2,800	12,943	35,813	75,271	134,808	179,675	225,001	292,226

Location Description	HMS Element Name	HMS Drainage Area (sq mi)	50% AEP 2-yr	20% AEP 5-yr	10% AEP 10-yr	4% AEP 25-yr	2% AEP 50-yr	1% AEP 100-yr	0.5% AEP 200-yr	0.2% AEP 500-yr
San Saba River at Menard, TX (USGS Gage 081445000)	SS_SanSaba_J50	1136.9	4,138	17,032	42,231	85,116	145,921	198,658	250,803	328,666
San Saba River above Elm Creek	SS_SanSaba_J59	1244.6	3,819	16,284	39,411	85,091	155,583	208,879	267,849	351,320
San Saba River below Elm Creek	SS_SanSaba_J60	1318.2	3,830	16,491	39,677	87,028	162,908	216,455	280,046	369,315
San Saba River above Calf Creek	SS_SanSaba_J69	1422.3	3,420	15,475	37,972	85,560	167,636	224,721	289,989	384,386
San Saba River below Calf Creek	SS_SanSaba_J70	1490.6	3,423	15,563	38,063	86,530	172,422	231,003	298,379	396,523
San Saba River below Rumsey Creek	SS_SanSaba_J80	1594.0	3,325	15,500	38,056	87,640	179,165	240,583	311,062	415,180
San Saba River nr Brady, TX (USGS Gage 08144600)	SS_SanSaba_J90	1636.4	3,204	15,325	37,901	87,548	180,674	243,153	314,667	420,600
Katemcy Creek below subbasin SS_KatemcyCr_S10	SS_KatemcyCr_J10	40.2	629	892	1,184	4,107	11,618	14,657	17,700	22,150
San Saba River below Katemcy Creek	SS_SanSaba_J100	1688.6	3,225	15,420	38,049	88,405	184,527	248,766	322,369	434,818
San Saba River above Tiger Creek	SS_SanSaba_J109	1721.9	3,094	15,169	37,974	88,434	185,956	250,868	324,973	438,172
San Saba River below Tiger Creek	SS_SanSaba_J110	1804.6	3,136	15,341	38,253	90,256	193,585	261,542	338,819	457,394
San Saba River above Brady Creek	SS_SanSaba_J119	1941.6	3,169	15,525	38,893	93,457	205,869	279,427	362,327	489,221
Brady Creek at US-83 Hwy near Eden, TX	SS_BradyCr_J10	101.6	424	857	1,417	3,419	6,667	13,975	21,374	30,949
Brady Creek near Melvin, TX	SS_BradyCr_J20	252.6	774	2,464	4,100	7,684	12,757	24,423	37,308	55,038
Brady Creek below South Brady Creek	SS_BradyCr_J30	396.5	819	3,094	5,559	11,186	18,849	36,446	55,600	79,787
Inflow to Brady Creek Reservoir	BRADY_INFLOW	524.0	1,219	4,085	7,548	15,538	25,741	48,263	73,403	104,943
Brady Creek below Brady Creek Reservoir	BRADY_OUTFLOW	524.0	139	388	606	1,028	1,480	5,794	23,768	49,699
Brady Creek At Brady, TX (USGS Gage 08145000)	SS_BradyCr_J40	130.3	390	1,831	3,949	10,618	18,906	26,946	35,015	54,653
Brady Creek below Little Brady Creek	SS_BradyCr_J50	226.2	724	1,005	3,297	14,313	34,318	48,578	61,875	79,136
Brady Creek above the San Saba River	SS_BradyCr_J60	279.3	1,017	1,168	2,904	14,321	45,115	61,666	78,033	100,382
San Saba River below Brady Creek	SS_SanSaba_J120	2220.9	3,362	16,045	41,678	102,991	229,375	313,334	406,478	549,539

Location Description	HMS Element Name	HMS Drainage Area (sq mi)	50% AEP 2-yr	20% AEP 5-yr	10% AEP 10-yr	4% AEP 25-yr	2% AEP 50-yr	1% AEP 100-yr	0.5% AEP 200-yr	0.2% AEP 500-yr
San Saba River above Wallace Creek	SS_SanSaba_J129	2324.2	3,092	15,394	40,965	102,433	234,667	322,075	419,738	568,251
San Saba River below Wallace Creek	SS_SanSaba_J130	2381.1	3,369	15,400	40,974	103,229	237,549	327,300	427,753	580,027
San Saba River below Richland Springs Creek	SS_SanSaba_J140	2486.6	3,584	15,380	40,920	103,965	242,867	336,709	441,848	600,620
San Saba Rv at San Saba, TX (USGS Gage 08146000)	SS_SanSaba_J150	2523.4	3,330	14,735	39,461	102,073	242,280	336,536	441,996	602,822
San Saba River above Colorado River	SS_SanSaba_J160	2626.2	2,542	13,327	33,901	100,545	247,182	344,456	453,128	619,306
Colorado River below San Saba River	CO_Colorado_J180	9965.8	16,533	40,223	75,332	152,733	294,570	405,296	528,079	710,476
Colorado River at San Saba, TX (USGS Gage 08147000)	CO_Colorado_J190	10002.8	16,487	40,087	75,349	152,734	294,550	405,160	528,064	710,909
Colorado River at Bend, TX (LCRA Gage 1925)	CO_Colorado_J200	10139.1	15,930	38,617	73,320	143,015	261,965	356,088	457,608	597,236
Cherokee Creek above Buffalo Creek	CO_CherokeeCr_J10	69.7	2,245	7,519	12,713	23,475	36,676	45,206	54,098	67,090
Cherokee Creek nr Bend, TX (LCRA Gage 1929)	CO_CherokeeCr_J20	158.8	1,569	6,756	14,280	33,707	61,971	80,222	97,816	124,597
Cherokee Creek above the Colorado River	CO_CherokeeCr_J30	175.9	991	5,291	11,833	28,638	55,778	74,763	93,819	123,218
Colorado River below Cherokee Creek	CO_Colorado_J210	10321.4	16,013	38,778	73,390	142,138	260,327	353,588	454,168	595,100
Colorado River below Yancey Creek	CO_Colorado_J220	10425.2	15,979	38,720	73,284	141,766	260,101	353,163	453,602	594,922
Colorado River above Fall Creek	CO_Colorado_J229	10494.2	15,884	38,552	73,237	141,662	260,179	353,212	453,598	595,216
Colorado River below Fall Creek	CO_Colorado_J230	10548.1	15,887	38,591	73,337	141,870	260,449	353,546	453,998	595,716
Inflow to Lake Buchanan	BUCHANAN_INFLOW	10694.7	15,954	38,717	73,561	142,275	260,991	354,223	454,860	596,949
Colorado River below Lake Buchanan	BUCHANAN_OUTFLOW	10694.7	15,241	35,756	73,355	141,607	252,595	346,454	452,471	564,443
Inflow to Inks Lake	INKS_INFLOW	10734.3	15,248	35,802	73,474	141,822	252,875	346,749	452,838	564,959
Colorado River below Inks Lake	INKS_OUTFLOW	10734.3	15,248	35,802	73,474	141,822	252,875	346,749	452,838	564,959
Colorado River above the Llano River	CO_Colorado_J239	10769.8	15,246	35,821	73,540	141,931	252,927	346,471	452,920	565,205
South Llano River below subbasin LN_SLlano_S20	LN_SLlano_J10	156.6	3,554	9,996	20,029	38,770	56,952	70,501	83,866	102,840

Location Description	HMS Element Name	HMS Drainage Area (sq mi)	50% AEP 2-yr	20% AEP 5-yr	10% AEP 10-yr	4% AEP 25-yr	2% AEP 50-yr	1% AEP 100-yr	0.5% AEP 200-yr	0.2% AEP 500-yr
South Llano River at CR-900	LN_SLlano_J20	253.2	2,164	9,248	22,033	48,708	76,900	97,544	117,222	145,218
South Llano River above Deer Creek	LN_SLlano_J29	305.9	2,029	8,658	22,040	50,923	82,948	106,949	130,074	162,374
South Llano River below Deer Creek	LN_SLlano_J30	433.8	4,119	13,723	30,224	71,603	118,039	153,354	187,750	233,494
South Llano River above Paint Creek	LN_SLlano_J39	524.1	3,636	13,590	33,386	78,653	130,968	172,303	213,001	267,833
Paint Creek below Hunger Creek	LN_PaintCr_J10	113.1	5,890	12,675	22,576	39,743	53,390	65,406	77,903	93,701
Paint Creek above the South Llano River	LN_PaintCr_J20	217.7	4,673	14,411	30,662	59,952	84,069	104,685	125,169	152,428
South Llano River at Telegraph (LCRA gage)	LN_SLlano_J40	741.8	8,007	27,468	62,759	130,182	202,416	263,940	325,488	406,325
South Llano River below Chalk Creek	LN_SLlano_J50	849.8	6,888	26,560	65,323	143,454	222,875	292,265	362,133	453,344
South Llano River at Flat Rock Ln at Junction, TX (USGS Gage 08149900)	LN_SLlano_J60	878.9	6,531	25,874	64,426	143,576	224,494	294,673	365,901	459,740
South Llano River above the Llano River	LN_SLlano_J70	932.6	6,480	25,991	65,116	146,698	229,972	302,837	376,936	475,230
North Llano River Headwaters	LN_NLlano_J20	103.0	2,319	6,744	11,442	18,741	27,164	33,986	40,609	49,934
Dry Llano River above the North Llano River	LN_NLlano_J29	226.5	3,117	11,651	20,278	33,990	50,087	63,363	76,279	94,447
North Llano River below Buffalo Draw	LN_NLlano_J10	111.6	1,940	5,954	10,120	16,927	24,807	31,184	37,488	46,338
North Llano River above Dry Llano River	LN_NLlano_J19	166.1	1,922	7,164	13,018	22,864	34,272	43,380	52,745	65,695
North Llano River below Dry Llano River	LN_NLlano_J30	392.6	4,612	18,054	32,468	55,764	83,013	105,307	127,424	158,280
North Llano River above Maynard Creek	LN_NLlano_J39	447.7	4,484	18,737	34,483	60,303	90,467	115,819	140,690	175,245
North Llano River below Maynard Creek	LN_NLlano_J40	520.6	4,808	20,751	38,666	68,610	103,630	133,107	162,326	202,383
North Llano River below Copperas Creek	LN_NLlano_J50	656.9	5,298	24,304	46,035	83,726	127,856	164,712	201,995	252,509
North Llano River near Roosevelt; below Bois D'Arc Creek (LCRA Gage)	LN_NLlano_J60	703.0	5,711	25,434	48,609	88,890	135,938	175,348	215,543	269,097
North Llano River above Bear Creek	LN_NLlano_J69	763.9	5,558	26,087	50,423	92,214	141,446	183,391	226,541	284,483
Bear Creek below West Bear Creek	LN_BearCr_J10	104.8	2,644	7,493	13,229	21,487	30,865	38,366	45,768	56,250

Location Description	HMS Element Name	HMS Drainage Area (sq mi)	50% AEP 2-yr	20% AEP 5-yr	10% AEP 10-yr	4% AEP 25-yr	2% AEP 50-yr	1% AEP 100-yr	0.5% AEP 200-yr	0.2% AEP 500-yr
Bear Creek above the North Llano River	LN_BearCr_J20	131.7	2,760	8,551	15,741	26,040	37,635	47,056	56,336	69,488
North Llano River below Bear Creek	LN_NLlano_J70	895.6	6,638	28,217	55,451	101,613	155,972	203,751	253,078	320,592
North Llano River nr Junction, TX (USGS Gage 08148500)	LN_NLlano_J80	901.7	6,560	28,205	55,416	101,460	155,819	203,524	252,844	320,331
North Llano River above the South Llano River	LN_NLlano_J90	919.1	6,510	28,270	55,594	101,824	156,666	204,654	254,547	323,216
Llano River below the North and South Llano Rivers	LN_Llano_J10	1851.7	11,997	53,482	116,641	231,754	366,458	478,993	596,236	761,598
Llano River nr Junction, TX (USGS Gage 08150000)	LN_Llano_J20	1858.2	11,957	53,378	116,369	231,114	365,942	478,393	595,785	761,286
Llano River above Johnson Fork	LN_Llano_J29	1869.2	11,785	52,758	114,213	229,109	363,619	475,911	592,040	756,211
Johnson Fork above Allen Creek	LN_JohnsonFork_J10	126.3	2,509	6,602	15,836	37,009	57,605	70,738	84,473	102,071
Johnson Fort below Mudge Draw	LN_JohnsonFork_J20	234.0	1,540	8,708	25,923	63,710	100,293	123,942	148,646	179,934
Johnson Fork near Junction, TX (LCRA Gage 2313)	LN_JohnsonFork_J30	292.8	885	7,187	26,017	70,995	116,122	146,507	175,976	214,012
Johnson Fork above the Llano River	LN_JohnsonFork_J40	322.1	2,131	6,222	24,339	70,748	118,165	150,203	181,635	223,060
Llano River below Johnson Fork	LN_Llano_J30	2191.3	12,339	57,011	124,036	256,928	412,734	547,374	684,297	873,590
Llano River below Gentry Creek	LN_Llano_J40	2247.6	12,380	56,967	123,555	254,665	411,040	546,174	683,491	874,211
Llano River above Big Saline Creek	LN_Llano_J49	2392.9	12,191	56,204	121,915	246,530	399,022	532,686	671,065	861,733
Llano River below Big Saline Creek	LN_Llano_J50	2478.2	18,293	56,354	122,127	246,821	399,408	533,157	671,620	862,548
Llano River below Leon Creek	LN_Llano_J60	2609.2	21,964	59,252	122,171	246,745	399,004	532,749	671,361	862,628
Llano River above the James River	LN_Llano_J69	2760.3	20,714	63,706	121,672	245,426	397,181	530,175	669,178	861,076
James River below Little Devils River	LN_JamesR_J10	244.5	2,957	11,730	30,413	87,998	114,105	140,017	165,492	201,942
James River near Mason (LCRA Gage 2399)	LN_JamesR_J20	326.3	2,613	12,584	35,568	111,847	147,581	181,583	215,088	262,950
James River above Llano River	LN_JamesR_J30	339.6	2,179	12,254	35,732	112,798	148,794	183,854	218,337	267,389
Llano River below the James River	LN_Llano_J70	3100.0	20,869	67,200	130,936	257,741	401,579	537,857	680,363	881,770

Location Description	HMS Element Name	HMS Drainage Area (sq mi)	50% AEP 2-yr	20% AEP 5-yr	10% AEP 10-yr	4% AEP 25-yr	2% AEP 50-yr	1% AEP 100-yr	0.5% AEP 200-yr	0.2% AEP 500-yr
Llano River above Comanche Creek	LN_Llano_J79	3175.6	18,946	65,073	125,017	251,540	399,247	533,544	676,862	878,821
Comanche Creek near Mason (LCRA Gage 2424)	LN_ComancheCr_J10	46.3	438	2,037	5,840	12,926	23,305	28,533	33,916	41,596
Comanche Creek above the Llano River	LN_ComancheCr_J20	68.7	4,674	9,615	12,861	16,904	24,452	31,291	38,344	48,193
Llano River below Comanche Creek	LN_Llano_J80	3244.3	19,076	66,018	128,569	261,223	399,697	534,202	677,806	880,352
Llano Rv nr Mason, TX (USGS Gage 08150700)	LN_Llano_J90	3250.8	19,016	65,707	127,795	259,406	399,340	533,476	677,106	879,760
Beaver Creek below Squaw Creek	LN_BeaverCr_J10	166.3	5,027	13,300	27,040	50,253	72,882	90,688	108,881	135,486
Beaver Ck nr Mason, TX (USGS Gage 08150800)	LN_BeaverCr_J20	215.3	4,695	14,461	30,695	58,678	87,130	109,167	131,711	164,513
Llano River below Beaver Creek	LN_Llano_J100	3470.0	21,634	76,025	151,404	308,576	445,506	564,416	685,484	895,462
Willow Creek near Mason (LCRA Gage 2443)	LN_WillowCr_J10	57.9	291	1,944	5,561	15,513	27,758	34,136	40,748	50,377
Willow Creek above the Llano River	LN_WillowCr_J20	78.2	2,095	7,531	10,406	13,829	27,827	35,822	43,949	55,835
Llano River below Willow Creek	LN_Llano_J110	3556.9	21,497	75,947	153,420	316,908	464,023	589,654	717,300	905,784
Llano River at RM-2768 at Castell, TX	LN_Llano_J120	3639.4	21,015	74,629	149,953	311,412	455,601	587,700	719,145	921,399
Llano River above Hickory Creek	LN_Llano_J129	3723.8	20,514	73,633	147,054	295,805	439,945	573,111	707,668	913,560
Hickory Creek below Marshall Creek	LN_HickoryCr_J10	98.4	3,522	6,781	12,475	25,727	42,337	53,273	64,775	81,849
Hickory Creek near Castell (LCRA Gage)	LN_HickoryCr_J20	168.0	2,286	5,973	13,405	33,302	60,346	77,983	96,558	123,468
Llano River below Hickory Creek	LN_Llano_J130	3891.8	21,724	77,648	155,918	313,854	471,256	616,478	764,350	994,235
Llano River above San Fernando Creek	LN_Llano_J139	3924.8	21,541	77,322	155,077	312,225	469,876	615,209	763,320	993,144
San Fernando Creek near Llano (LCRA Gage 2616)	LN_SanFernandoCr_J10	128.9	1,429	7,921	19,318	38,328	56,538	70,704	85,391	106,789
San Fernando Creek above the Llano River	LN_SanFernandoCr_J20	135.5	970	7,368	18,563	37,347	56,039	70,503	85,627	107,389
Llano River below San Fernando Creek	LN_Llano_J140	4060.3	21,689	78,468	158,439	318,192	480,419	631,606	785,572	1,028,915
Johnson Creek near Llano (LCRA Gage)	LN_JohnsonCr_J10	46.6	215	2,369	5,855	19,088	32,557	39,536	46,703	57,156

Location Description	HMS Element Name	HMS Drainage Area (sq mi)	50% AEP 2-yr	20% AEP 5-yr	10% AEP 10-yr	4% AEP 25-yr	2% AEP 50-yr	1% AEP 100-yr	0.5% AEP 200-yr	0.2% AEP 500-yr
Johnson Creek above the Llano River	LN_JohnsonCr_J20	52.8	558	2,428	6,087	18,280	34,410	42,366	50,333	62,049
Llano River below Johnson Creek	LN_Llano_J150	4118.4	21,623	78,317	158,315	318,651	480,887	633,169	789,365	1,035,430
Llano River below Pecan Creek	LN_Llano_J160	4187.0	21,549	78,496	158,728	318,363	482,549	636,402	794,464	1,045,051
Llano River at Llano, TX (USGS Gage 08151500)	LN_Llano_J170	4202.0	21,461	78,266	158,157	317,861	482,113	635,079	792,812	1,042,940
Llano River above the Little Llano River	LN_Llano_J179	4279.1	19,596	74,549	151,961	308,218	470,049	622,230	779,832	1,027,143
Little Llano River near Llano (LCRA gage 2669)	LN_LittleLlanoR_J10	48.2	313	2,935	8,120	22,549	39,071	46,999	55,334	67,545
Little Llano River above the Llano River	LN_LittleLlanoR_J20	52.6	137	2,360	7,245	21,396	38,423	46,753	55,462	68,089
Llano River below the Little Llano River	LN_Llano_J180	4331.6	19,597	74,600	152,095	308,545	470,608	623,036	781,187	1,030,114
Llano River above Honey Creek	LN_Llano_J189	4410.8	16,034	66,198	137,429	281,939	443,922	590,440	745,717	982,554
Honey Creek near Kingsland (LCRA Gage 2694)	LN_HoneyCr_J10	25.9	3,249	10,092	12,860	14,989	23,982	28,865	34,101	41,820
Honey Creek above the Llano River	LN_HoneyCr_J20	39.7	2,834	9,818	13,366	16,455	27,972	34,855	41,973	52,854
Llano River below Honey Creek	LN_Llano_J190	4450.5	16,068	66,365	137,681	282,250	444,462	591,170	746,844	984,627
Llano River above the Colorado River	LN_Llano_J200	4465.4	15,658	65,325	135,630	278,008	439,832	586,103	741,658	979,704
Colorado River below the Llano River	CO_Colorado_J240	15235.2	21,119	76,862	163,467	350,843	555,392	738,808	936,842	1,247,129
Colorado River above Sandy Creek	CO_Colorado_J249	15262.7	21,136	76,950	163,597	351,018	555,614	739,101	937,271	1,248,291
Sandy Creek below Crabapple Creek	SD_SandyCr_J10	148.4	2,289	7,052	16,448	39,570	63,914	80,418	97,875	123,726
Sandy Creek near Willow City (LCRA Gage 2851)	SD_SandyCr_J20	151.6	2,268	7,024	16,431	39,582	64,069	80,779	98,358	124,423
Sandy Creek near Click (LCRA Gage 2878)	SD_SandyCr_J30	300.0	5,655	19,405	37,857	69,673	100,140	128,381	157,925	201,455
Sandy Ck nr Kingsland, TX (USGS Gage 08152000)	SD_SandyCr_J40	346.2	8,174	21,056	42,421	79,283	115,687	148,409	182,705	233,586
Walnut Creek near Kingsland (LCRA Gage 2897)	SD_Walnut2Cr_J10	23.3	8,977	17,227	23,314	30,126	35,453	41,635	48,353	58,253
Walnut Creek above Sandy Creek	SD_Walnut2Cr_J20	27.4	9,829	19,459	26,759	34,673	40,695	47,775	55,572	67,262

Location Description	HMS Element Name	HMS Drainage Area (sq mi)	50% AEP 2-yr	20% AEP 5-yr	10% AEP 10-yr	4% AEP 25-yr	2% AEP 50-yr	1% AEP 100-yr	0.5% AEP 200-yr	0.2% AEP 500-yr
Sandy Creek below Walnut Creek	SD_SandyCr_J50	388.0	11,835	25,677	42,697	79,902	118,149	153,313	189,757	244,451
Sandy Creek above the Colorado River	SD_SandyCr_J60	391.2	10,805	25,596	42,635	79,892	118,181	153,478	190,097	245,049
Colorado River below Sandy Creek	CO_Colorado_J250	15653.9	21,462	83,400	178,282	376,854	597,556	795,996	1,014,510	1,360,558
Inflow to Lake LBJ	LBJ_INFLOW	15701.7	24,685	83,590	178,556	377,227	598,039	796,641	1,015,345	1,362,431
Colorado River below Lake LBJ	LBJ_OUTFLOW	15701.7	21,516	79,736	177,101	354,031	482,150	748,872	975,017	1,331,410
Backbone Creek at Marble Falls (LCRA Gage 2992)	CO_BackboneCr_J10	30.1	1,124	5,231	11,131	19,401	23,743	29,136	35,257	44,034
Backbone Creek above the Colorado River	CO_BackboneCr_J20	40.3	1,995	6,141	10,724	19,875	24,793	31,143	38,394	49,184
Colorado River below Backbone Creek	CO_Colorado_J255	15757.8	21,553	79,734	176,784	354,212	481,716	745,516	971,630	1,328,029
Inflow to Lake Marble Falls	MARBLE_FALLS_INFLOW	15783.9	21,591	79,781	176,837	354,382	481,826	745,586	971,797	1,328,171
Colorado River below Lake Marble Falls	MARBLE_FALLS OUTFLOW	15783.9	21,591	79,781	176,837	354,382	481,826	745,586	971,797	1,328,171
Hamilton Creek near Marble Falls (LCRA Gage 3018)	CO_HamiltonCr_J10	77.5	3,074	9,451	17,350	30,205	44,025	54,761	66,348	83,509
Hamilton Creek above the Colorado River	CO_HamiltonCr_J20	84.3	3,261	10,077	18,344	31,997	46,721	58,349	70,820	89,374
Colorado River below Hamilton Creek	CO_Colorado_J260	15874.3	21,619	79,535	175,966	354,622	481,159	743,407	970,461	1,328,559
Colorado River below Double Horn Creek	CO_Colorado_J270	15929.1	21,657	78,822	173,785	353,828	479,503	735,472	962,315	1,319,828
Colorado River above the Pedernales River	CO_Colorado_J279	16007.6	21,833	79,014	174,067	354,227	480,000	736,091	963,175	1,321,721
Pedernales River below North Creek	PD_Pedernales_J10	118.2	6,364	14,735	26,254	47,488	65,340	80,084	95,805	116,615
Pedernales River below Spring Creek	PD_Pedernales_J20	212.4	5,196	16,978	34,481	67,754	98,136	123,591	149,732	185,389
Pedernales River above Wolf Creek	PD_Pedernales_J29	218.1	4,920	16,550	34,047	67,132	97,350	122,822	149,140	185,085
Pedernales River below Wolf Creek	PD_Pedernales_J30	257.0	4,835	16,681	35,054	71,012	104,886	134,621	164,677	206,053
Pedernales River above Live Oak Creek	PD_Pedernales_J39	313.0	4,491	16,329	35,499	73,902	113,159	147,815	183,351	232,653
Pedernales River below Live Oak Creek	PD_Pedernales_J40	359.3	5,223	19,275	44,143	87,247	128,655	167,747	209,641	267,194

Location Description	HMS Element Name	HMS Drainage Area (sq mi)	50% AEP 2-yr	20% AEP 5-yr	10% AEP 10-yr	4% AEP 25-yr	2% AEP 50-yr	1% AEP 100-yr	0.5% AEP 200-yr	0.2% AEP 500-yr
Pedernales Rv nr Fredericksburg (USGS Gage 08152900)	PD_Pedernales_J50	369.6	5,148	19,341	44,825	89,010	131,408	171,346	214,860	273,650
Pedernales River above South Grape Creek	PD_Pedernales_J59	507.6	4,405	26,475	46,266	91,663	146,847	198,788	254,563	344,693
South Grape Creek near Luckenbach (LCRA Gage 3328)	PD_SGrapeCr_J10	27.3	4,029	10,854	17,669	25,408	30,030	35,676	41,723	50,623
South Grape Creek above the Pedernales River	PD_SGrapeCr_J20	63.0	2,706	8,114	14,014	21,833	26,335	32,059	38,166	46,962
Pedernales River below South Grape Creek	PD_Pedernales_J60	570.6	5,674	28,404	52,746	95,396	154,620	214,780	279,674	384,189
Pedernales River at LBJ Ranch near Stonewall (LCRA Gage)	PD_Pedernales_J70	625.6	7,185	28,997	56,567	101,932	156,085	221,587	290,552	400,763
Pedernales River below Williams Creek	PD_Pedernales_J80	668.2	7,132	33,338	65,929	114,541	160,244	229,733	303,216	419,937
Pedernales River above North Grape Creek	PD_Pedernales_J89	730.0	10,443	34,398	68,690	119,612	159,849	230,336	307,585	427,942
North Grape Creek near Johnson City (LCRA Gage 3369)	PD_NGrapeCr_J10	89.0	3,158	12,750	24,515	47,213	72,537	87,708	103,741	127,613
Pedernales River below North Grape Creek	PD_Pedernales_J90	845.3	15,723	39,081	73,752	130,265	177,007	235,992	319,205	448,548
Pedernales Rv nr Johnson City, TX (USGS Gage 08153500)	PD_Pedernales_J100	900.9	19,532	50,474	83,144	136,697	187,844	244,787	322,163	455,062
Pedernales River above Miller Creek	PD_Pedernales_J109	959.5	15,383	43,676	76,016	132,930	186,073	251,343	319,783	451,543
Miller Creek near Johnson City (LCRA Gage 3491)	PD_MillerCr_J10	87.5	14,072	30,220	47,155	64,492	79,317	96,785	116,177	143,250
Pedernales River below Miller Creek	PD_Pedernales_J110	1048.0	21,996	49,051	83,712	142,566	206,661	279,810	359,601	476,894
Pedernales River above Flat Creek	PD_Pedernales_J119	1080.1	16,422	46,180	83,451	143,283	209,975	284,904	366,940	487,515
Flat Creek nr Pedernales Falls State Park (LCRA Gage 3529)	PD_FlatCr_J10	30.7	8,066	16,383	23,790	31,331	37,966	45,706	54,459	67,189
Flat Creek above Pedernales River	PD_FlatCr_J20	37.1	8,711	18,276	27,149	35,939	43,679	52,731	63,103	78,112
Pedernales River below Flat Creek	PD_Pedernales_J120	1117.2	17,280	47,282	85,900	145,203	214,705	292,039	377,296	502,526
Pedernales River above Cypress Creek	PD_Pedernales_J129	1150.6	16,517	46,409	85,820	144,973	215,890	295,052	381,827	509,964
Cypress Creek near Cypress Mill (LCRA Gage 3558)	PD_CypressCr_J10	71.2	4,319	14,486	26,436	45,131	65,862	80,250	93,953	115,924
Pedernales River below Cypress Creek	PD_Pedernales_J130	1232.3	16,757	48,334	94,347	152,793	228,770	316,411	407,007	544,981

Location Description	HMS Element Name	HMS Drainage Area (sq mi)	50% AEP 2-yr	20% AEP 5-yr	10% AEP 10-yr	4% AEP 25-yr	2% AEP 50-yr	1% AEP 100-yr	0.5% AEP 200-yr	0.2% AEP 500-yr
Pedernales River above the Colorado River	PD_Perdenales_J140	1280.9	14,892	46,354	87,545	149,353	225,511	313,685	405,119	544,627
Colorado River below the Pedernales River	CO_Colorado_J280	17288.5	28,968	119,923	251,934	486,802	658,550	982,200	1,296,245	1,789,796
Cow Creek near Lago Vista (LCRA Gage 3920)	CO_CowCr_J10	42.7	2,394	5,197	8,425	12,571	16,099	20,920	25,331	32,062
Cow Creek above the Colorado River	CO_CowCr_J20	56.5	2,197	5,085	8,536	13,048	17,033	22,873	28,025	35,935
Colorado River below Cow Creek	CO_Colorado_J290	17353.4	30,608	121,038	254,433	490,997	663,202	989,089	1,305,698	1,803,679
Big Sandy 2 Creek near Jonestown (LCRA Gage 3953)	CO_BigSandy2Cr_J10	34.1	6,407	13,406	20,028	27,501	33,678	41,339	48,840	59,932
Big Sandy 2 Creek above the Colorado River	CO_BigSandy2Cr_J20	73.5	8,901	17,523	25,299	34,501	42,114	51,429	66,565	89,589
Colorado River below Big Sandy Creek 2	CO_Colorado_J300	17505.5	45,896	122,497	256,986	494,460	666,530	994,196	1,312,793	1,815,640
Inflow to Lake Travis / Marshall Ford	MARSHALL_FORD INFLOW	17530.7	52,019	122,621	257,161	494,681	666,788	994,511	1,313,165	1,816,394
Colorado River below Marshall Ford Dam	MARSHALL_FORD OUTFLOW	17530.7	15,480	30,000	35,593	106,854	276,842	488,592	717,722	1,190,590
Colorado River above Bull Creek	CO_Colorado_J310	43.7	9,990	18,569	24,566	34,034	41,726	51,196	61,653	77,473
Bull Ck at Loop 360 nr Austin, TX (USGS Gage 08154700)	CO_BullCr_J10	22.7	2,832	6,400	10,882	17,473	24,676	29,871	35,556	44,019
Colorado River below Bull Creek	CO_Colorado_J320	77.0	11,894	22,759	31,265	45,364	60,274	75,447	91,903	117,303
Inflow to Lake Austin	AUSTIN_INFLOW	91.1	11,442	23,666	33,997	49,951	67,260	84,527	103,356	132,803
Colorado River below Lake Austin	AUSTIN_OUTFLOW	91.1	11,442	23,666	33,997	49,951	67,260	84,527	103,356	132,803
Colorado River above Barton Creek	CO_Colorado_J329	99.7	10,254	23,526	34,629	51,964	69,385	88,020	108,082	141,362
Barton Ck at SH 71 nr Oak Hill, TX (USGS Gage 08155200)	CO_BartonCr_J10	89.6	2,763	10,246	16,971	28,073	41,280	53,733	67,481	86,982
Barton Ck at Lost Ck Blvd nr Austin (USGS Gage 08155240)	CO_BartonCr_J20	107.9	2,576	9,688	16,675	28,124	42,102	56,112	70,984	92,880
Barton Ck at Loop 360, Austin (USGS Gage 08155300)	CO_BartonCr_J30	116.9	3,035	9,567	16,573	27,997	41,937	56,081	71,198	93,631
Barton Ck abv Barton Spgs at Austin (USGS Gage 08155400)	CO_BartonCr_J40	120.0	3,058	9,514	16,520	27,953	41,877	56,042	71,205	93,792
Colorado River below Barton Creek	CO_Colorado_J330	219.7	11,963	25,748	39,364	61,132	83,124	106,406	131,389	170,633

Location Description	HMS Element Name	HMS Drainage Area (sq mi)	50% AEP 2-yr	20% AEP 5-yr	10% AEP 10-yr	4% AEP 25-yr	2% AEP 50-yr	1% AEP 100-yr	0.5% AEP 200-yr	0.2% AEP 500-yr
Inflow to Lady Bird Lake	LADYBIRD_INFLOW	248.3	12,224	26,694	42,599	69,123	93,681	120,650	150,716	195,546
Colorado River below Lady Bird Lake	LADYBIRD_OUTFLOW	248.3	12,224	26,694	42,599	69,123	93,681	120,650	150,716	195,546
Colorado River at Austin, TX (USGS Gage 08158000)	CO_Colorado_J340	250.2	11,608	25,415	41,100	65,713	88,907	114,624	143,191	187,086
Colorado River above Walnut Creek	CO_Colorado_J349	270.7	11,312	23,300	37,960	62,669	85,346	112,690	146,098	195,550
Walnut Ck at Webberville Rd, Austin (USGS Gage 08158600)	CO_Walnut1Cr_J10	51.7	5,339	8,796	13,363	20,444	28,602	35,418	42,781	53,647
Walnut 1 Creek above the Colorado River	CO_Walnut1Cr_J20	56.5	5,553	8,977	13,727	20,975	29,452	36,541	44,487	56,699
Colorado River below Walnut 1 Creek	CO_Colorado_J350	327.2	13,794	28,192	45,891	75,377	103,948	137,879	179,611	237,864
Colorado River at Del Valle, TX (LCRA Gage)	CO_Colorado_J360	341.2	14,044	28,031	45,478	73,906	102,114	133,995	173,984	226,520
Colorado River above Onion Creek	CO_Colorado_J369	347.8	13,369	25,630	42,005	71,015	98,629	130,868	169,385	225,672
Onion Creek at RR-1826	ON_OnionCr_J10	104.6	4,777	10,403	19,798	36,928	58,711	75,072	92,611	119,105
Onion Ck nr Driftwood, TX (USGS Gage 08158700)	ON_OnionCr_J20	123.7	3,679	8,876	18,271	35,798	59,833	78,344	98,102	127,501
Onion Creek at Buda (LCRA Gage)	ON_OnionCr_J30	167.3	3,669	11,604	26,138	50,266	74,215	97,786	122,920	156,091
Onion Ck at I-35 nr Twin Creeks Rd (USGS Gage 08158827)	ON_OnionCr_J40	234.0	5,047	17,068	34,161	65,762	99,927	121,276	152,839	193,973
Onion Ck at US Hwy 183, Austin, TX (USGS Gage 08159000)	ON_OnionCr_J50	323.7	6,949	23,631	41,805	78,032	115,962	146,380	179,526	227,758
Onion Creek above the Colorado River	ON_OnionCr_J60	345.0	7,678	24,452	42,458	78,357	117,818	150,123	184,508	234,211
Colorado River below Onion Creek	CO_Colorado_J370	692.9	18,869	44,724	78,753	146,138	209,586	274,297	348,724	455,923
Colorado River above Gilleland Creek	CO_Colorado_J379	699.2	18,685	43,490	75,606	141,124	205,957	271,968	345,590	453,502
Gilleland Creek near Manor (LCRA Gage 5417)	CO_GillelandCr_J10	41.4	2,053	3,888	6,391	10,119	14,935	18,757	22,685	28,789
Gilleland Creek above the Colorado River	CO_GillelandCr_J20	75.3	3,160	4,425	9,236	15,623	22,921	29,483	36,397	47,349
Colorado River near Webberville and below Gilleland Creek (LCRA Gage)	CO_Colorado_J380	774.5	19,875	45,463	79,340	148,195	217,141	287,165	364,732	478,784
Colorado River below Dry Creek	CO_Colorado_J390	855.1	20,016	43,435	68,991	114,123	162,558	221,998	296,756	408,402

Location Description	HMS Element Name	HMS Drainage Area (sq mi)	50% AEP 2-yr	20% AEP 5-yr	10% AEP 10-yr	4% AEP 25-yr	2% AEP 50-yr	1% AEP 100-yr	0.5% AEP 200-yr	0.2% AEP 500-yr
Wilbarger Creek near Elgin (LCRA Gage)	CO_WilbargerCr_J10	163.7	6,377	14,801	21,078	29,246	37,299	48,177	59,786	76,927
Wilbarger Creek above the Colorado River	CO_WillbargerCr_J20	181.1	6,580	14,573	20,906	29,256	37,343	48,442	60,597	78,559
Colorado River below Wilbarger Creek	CO_Colorado_J400	1058.9	20,518	40,974	64,705	105,037	145,588	192,618	247,885	339,988
Big Sandy 1 Creek near Elgin (LCRA Gage 5473)	CO_BigSandy1Cr_J10	62.6	5,561	5,655	9,470	13,984	17,536	22,431	27,608	35,527
Big Sandy 1 Creek above the Colorado River	CO_BigSandy1Cr_J20	109.6	6,459	6,573	12,201	18,767	24,085	31,631	40,284	53,062
Colorado River at Sim Gideon River Plant (LCRA Gage)	CO_Colorado_J410	1171.4	21,492	41,845	65,661	105,783	146,212	193,507	247,204	338,409
Colorado River at Bastrop, TX (USGS Gage 08159200)	CO_Colorado_J420	1223.8	21,320	41,197	64,985	104,297	143,691	190,192	238,834	323,887
Cedar Creek below Maha Creek	CD_CedarCr_J10	95.5	636	9,848	15,577	23,337	29,394	37,528	46,273	58,277
Cedar Creek near Bastrop (LCRA Gage 5521)	CD_CedarCr_J20	130.4	493	9,115	16,799	27,598	36,536	47,401	58,646	75,919
Cedar Creek above Walnut Creek	CD_CedarCr_J29	142.5	477	7,492	14,583	24,587	33,271	45,642	58,448	76,080
Cedar Creek below Walnut Creek	CD_CedarCr_J30	280.1	840	12,735	25,219	43,142	57,915	78,965	100,055	129,634
Cedar Creek below Bastrop (LCRA Gage)	CD_CedarCr_J40	345.4	1,036	13,840	27,870	48,803	65,990	91,277	116,618	152,729
Cedar Creek above the Colorado River	CD_CedarCr_J50	350.5	1,052	13,804	27,707	48,640	65,668	90,972	116,363	152,580
Colorado River near Upton (LCRA Gage)	CO_Colorado_J430	1602.9	22,053	46,460	71,819	112,080	151,316	200,051	245,239	329,764
Colorado Rv at Smithville, TX (USGS Gage 08159500)	CO_Colorado_J440	1705.8	22,181	46,624	72,066	112,973	152,115	201,022	247,447	331,507
Colorado River below Bartons Creek	CO_Colorado_J450	1789.8	22,346	46,551	71,647	110,686	148,579	195,810	244,700	324,414
Colorado River below Pin Oak Creek	CO_Colorado_J460	1925.4	23,197	47,775	72,935	111,875	149,690	197,082	247,594	327,558
Colorado River below Rabbs Creek	CO_Colorado_J470	2089.1	23,910	48,574	73,177	111,464	147,407	193,561	245,937	323,651
Colorado Rv abv La Grange, TX (USGS Gage 08160400)	CO_Colorado_J480	2117.3	23,994	48,579	73,063	110,435	145,389	190,701	241,788	316,896
Buckners Creek near Muldoon (LCRA Gage 5608)	CO_BucknersCr_J10	91.6	3,007	9,207	15,943	23,053	28,932	36,880	44,945	57,009
Buckners Creek above the Colorado River	CO_BucknersCr_J20	185.7	4,846	10,571	16,148	22,546	28,610	38,184	49,439	65,115

Location Description	HMS Element Name	HMS Drainage Area (sq mi)	50% AEP 2-yr	20% AEP 5-yr	10% AEP 10-yr	4% AEP 25-yr	2% AEP 50-yr	1% AEP 100-yr	0.5% AEP 200-yr	0.2% AEP 500-yr
Colorado River below Buckners Creek	CO_Colorado_J490	2305.9	24,994	50,781	76,234	114,635	150,502	197,229	249,806	330,304
Colorado River below Williams Creek	CO_Colorado_J500	2409.2	25,313	51,591	77,537	116,149	152,157	199,264	252,413	333,446
Colorado River below Bruch Creek	CO_Colorado_J510	2491.3	25,163	51,049	76,719	115,880	151,352	198,427	251,959	330,300
Colorado River above Cummins Creek	CO_Colorado River_J519	2569.8	25,225	51,139	76,736	116,198	151,713	199,177	253,255	331,320
Cummings Creek at SH-237	CU_CumminsCr_J10	80.8	3,261	9,844	14,615	20,521	26,601	34,640	42,614	53,868
Cummings Creek at SH-159	CU_CumminsCr_J20	176.7	6,939	13,100	19,391	29,442	41,225	57,027	73,458	96,776
.Cummings Creek near Frelsburg (LCRA Gage 5696)	CU_CumminsCr_J30	251.9	8,162	18,883	27,815	41,988	56,673	78,307	100,823	132,107
Cummins Creek above the Colorado River	CU_CumminsCr_J40	315.3	5,991	18,960	31,546	49,564	67,661	92,714	119,296	155,250
Colorado River at Columbus, TX (USGS Gage 08161000)	CO_Colorado_J520	2885.1	28,388	54,282	81,189	122,485	159,717	209,496	265,841	348,523
Colorado River near Altair (LCRA Gage 6377)	CO_Colorado_J525	2979.6	28,331	52,154	76,823	102,971	125,084	158,687	194,621	257,115
Colorado River near Garwood (LCRA Gage)	CO_Colorado_J530	3090.4	28,884	52,673	77,546	103,465	126,601	157,944	197,096	260,880
Colorado River below Marys Branch	CO_Colorado_J540	3153.1	29,359	52,669	77,945	104,059	127,258	158,776	198,274	262,779
Colorado River below Robb Slough	CO_Colorado_J550	3216.2	28,903	52,117	76,420	103,899	126,829	158,301	196,933	264,229
Colorado Rv at Wharton, TX (USGS Gage 08162000)	CO_Colorado_J560	3248.3	28,537	51,877	71,306	91,917	113,812	142,268	178,066	242,958
Colorado River near Lane City, TX (LCRA Gage 6537)	CO_Colorado_J570	3277.9	28,639	52,067	71,307	90,462	112,540	141,831	177,629	242,517
Jones Creek at US-59 Hwy at Pierce, TX	CO_JonesCr_J10	29.3	1,159	2,818	4,387	6,227	7,711	9,696	11,677	14,470
Jones Creek below East Fork Jones Creek	CO_JonesCr_J20	62.6	1,732	4,512	7,366	11,484	15,066	19,445	23,610	29,442
Jones Creek above the Colorado River	CO_JonesCr_J30	83.1	2,592	5,851	9,096	14,324	19,174	25,151	30,697	38,427
Colorado River below Jones Creek	CO_Colorado_J580	3396.5	29,301	52,948	72,214	90,586	112,145	143,677	179,835	245,636
Blue Creek below East Fork Blue Creek	CO_BlueCr_J10	50.6	2,745	6,528	9,793	13,677	16,756	20,784	24,825	30,724
Blue Creek above the Colorado River	CO_BlueCr_J20	80.4	4,373	10,318	15,494	22,152	27,170	33,773	40,382	50,055

Location Description	HMS Element Name	HMS Drainage Area (sq mi)	50% AEP 2-yr	20% AEP 5-yr	10% AEP 10-yr	4% AEP 25-yr	2% AEP 50-yr	1% AEP 100-yr	0.5% AEP 200-yr	0.2% AEP 500-yr
Colorado River below Blue Creek	CO_Colorado_J590	3498.6	29,737	53,876	73,303	91,272	112,360	145,024	181,553	247,797
Colorado River near Bay City, TX (USGS Gage 08162500)	CO_Colorado_J600	3529.6	29,809	54,156	73,614	90,865	110,471	143,314	180,716	246,240
Colorado River near Buckeye, TX	CO_Colorado_J610	3556.8	30,023	54,607	74,179	91,543	111,108	143,811	181,700	247,456
Colorado River near Wadsworth, TX (USGS Gage 08162501)	CO_Colorado_J620	3595.2	30,276	55,099	74,756	91,991	111,614	144,636	182,852	248,979
Colorado River nr Matagorda, TX (LCRA Gage)	CO_Colorado_J630	3629.9	30,673	55,492	75,014	92,484	112,015	145,701	183,977	250,277
Colorado River at the Gulf of Mexico	Outlet	3632.5	30,551	55,534	75,043	92,499	112,112	145,827	184,123	250,462

Table 6.20: Peak Reservoir Pool Elevations (feet NAVD88) from the HEC-HMS Uniform Rainfall Frequency Storms

Reservoir Name	HMS Drainage Area	50%	20%	10%	4%	2%	1%	0.50%	0.20%
	sq mi	2-YR	5-YR	10-YR	25-YR	50-YR	100-YR	200-YR	500-YR
Oak Creek	237.4	2,001.4	2,002.4	2,003.6	2,005.8	2,008.2	2,009.5	2,010.6	2,011.8
Ballinger Lake, Lower	231.2	1,669.3	1,670.0	1,670.8	1,672.4	1,674.1	1,675.3	1,676.4	1,677.8
Twin Buttes Reservoir	3422.5	1,934.3	1,938.8	1,944.0	1,955.1	1,965.1	1,972.2	1,978.0	1,984.5
O.C. Fisher Reservoir	1462.8	1,887.3	1,892.6	1,899.0	1,909.5	1,922.9	1,930.9	1,937.3	1,940.1
O.H. Ivie Reservoir	3395.3	1,549.4	1,551.4	1,552.0	1,553.3	1,556.4	1,560.1	1,564.0	1,567.4
Lake Coleman	302.3	1,719.5	1,722.7	1,726.2	1,728.9	1,730.4	1,731.8	1,733.0	1,734.5
Hords Creek Reservoir	48.9	1,901.5	1,905.1	1,908.6	1,914.2	1,917.0	1,920.0	1,920.7	1,921.3
Lake Brownwood	1513.0	1,427.3	1,429.0	1,430.6	1,433.2	1,436.1	1,439.6	1,442.9	1,447.1
Brady Creek Reservoir	524.0	1,744.4	1,746.7	1,748.6	1,752.3	1,756.6	1,763.2	1,765.7	1,768.5
Lake Buchanan	10694.7	1,019.5	1,020.0	1,020.3	1,020.6	1,022.0	1,022.9	1,023.3	1,025.1
Lake LBJ	15701.7	825.8	826.8	827.7	829.2	837.5	842.2	844.8	848.3
Lake Travis*	17530.7	686.2	695.4	711.1	724.3	736.24	742.6	748.8	755.9

*NOTE: Elevations for Lake Travis are in "msl", which is LCRA's Hydromet Datum. The datum conversion from msl to NAVD88 is +0.6 ft for Lake Travis.

6.6.3 Uniform Rainfall Frequency Results versus Drainage Area

As a quality check, the peak flow results from the 1% AEP uniform rainfall frequency storms were plotted versus drainage area and outliers were examined, as shown in Figure B.19. This figure shows that the analyzed junctions followed generally expected patterns of increasing peak flow with drainage area, with exceptions for the effects of large lakes and reservoirs. For example, the three outlier dots along the bottom of the graph represent reservoir outflows from Brady Creek Reservoir, OC Fisher and Twin Buttes.

The relative trends in this graph generally make sense. For example, the peak discharges for the Concho and Pecan Bayou watersheds in the upper, drier portion of the study area tend to be lower relative to their drainage areas. Steep, flashy rivers like the Llano and Pedernales, on the other hand, have higher peak discharges relative to their drainage areas.

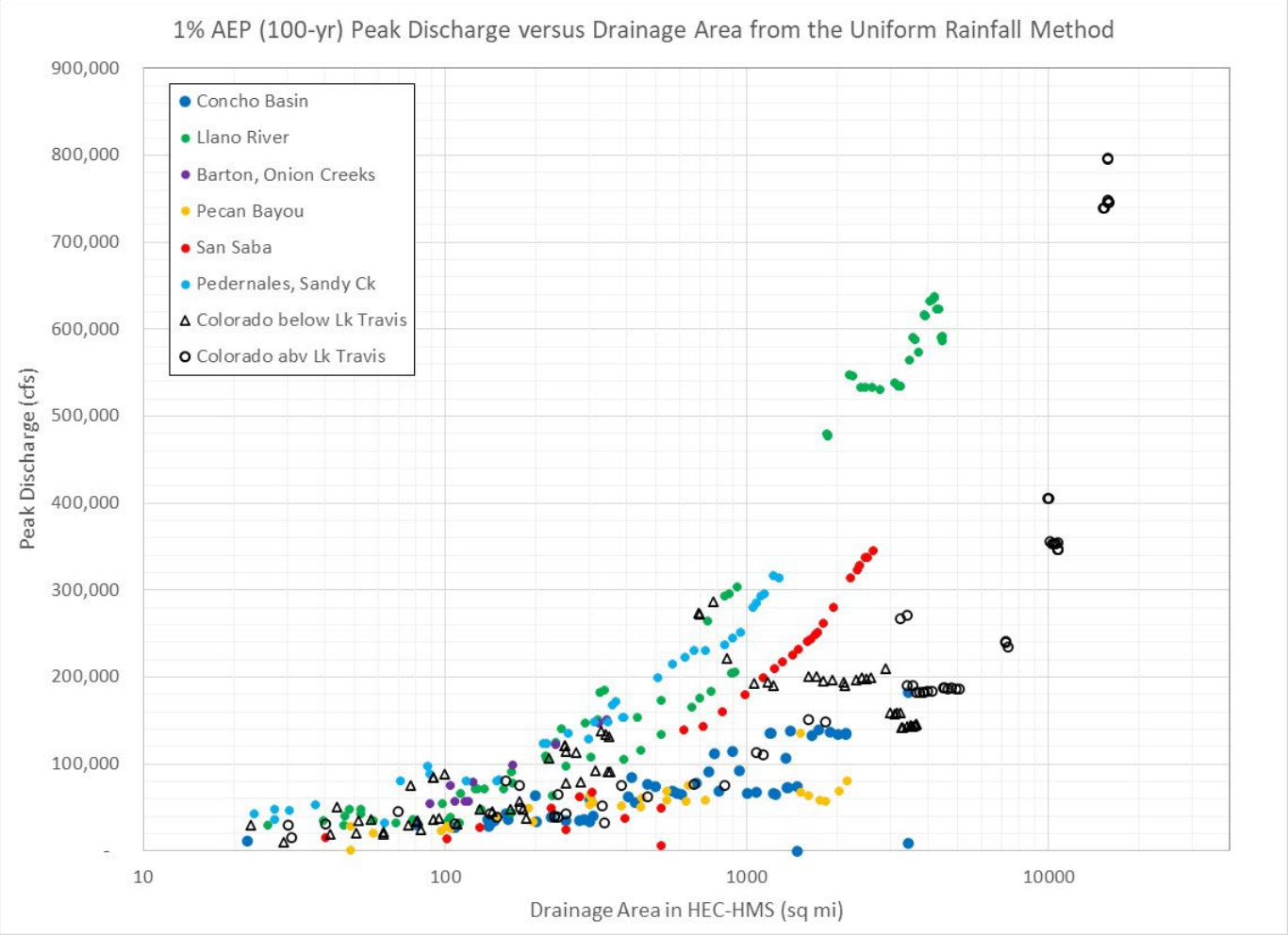

Figure 6.19: 1% AEP (100-yr) Peak Discharge versus Drainage Area for the Uniform Rainfall Results

6.7 HEC-HMS MODEL VERIFICATION

After the adoption of the final HEC-HMS parameters and the frequency storm results, two historic storm events were run in the HEC-HMS model as additional verification events. These historic storms occurred in the 1930s and were two of the largest storm events ever recorded in the Colorado River basin. The analysis and results for those historic 1930s events is documented in Chapter 10 and in Appendix F: Historic 1930s Storms Analysis.

7 Elliptical Frequency Storms in HEC-HMS

7.1 INTRODUCTION TO ELLIPTICAL STORMS

Observations of actual storm events show that average precipitation intensity decreases as the area of a storm increases. The uniform rainfall method results (documented in a separate appendix) use the depth-area analysis in HEC-HMS to produce frequency peak flow estimates (Version 4.10; USACE, 2022). The depth-area analysis in HEC-HMS applies the appropriate depth-area reduction factor to the given point rainfall depths based on the drainage area at a given evaluation point, which are derived from the published depth-area reduction factors from Figure 15 of the National Weather Service TP-40 publication (Hershfield, 1961), as shown in the figure below.

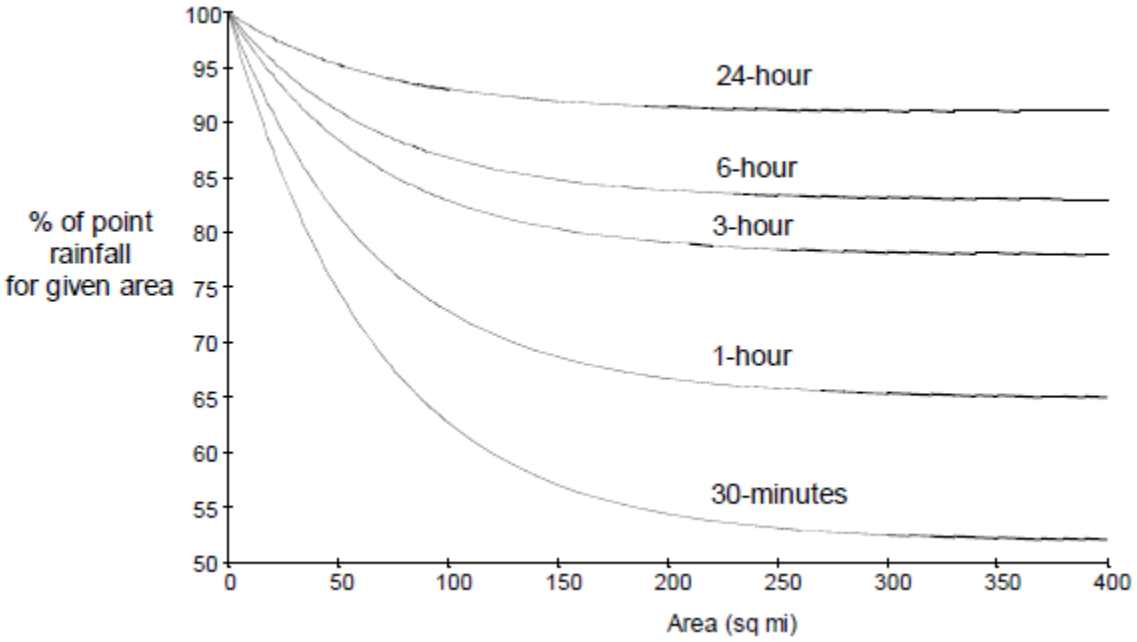

Figure 7.1: Published Depth-Area Reduction Curves from TP-40

When evaluating a stream location with a drainage area greater than 400 square miles, the HEC-HMS software issues a warning that the NWS depth-area reduction factors do not support storms beyond 400 square miles, as seen in the figure above. The program will still calculate the peak discharge, but the warning implies that the calculated volume of the storm may be overestimated for larger drainage areas.

Since the Colorado hydrology study involves calculating frequency discharges for points with up to nearly 10,000 square miles of drainage area, the InFRM team developed elliptical frequency storms for gage points and junctions with drainage areas greater than 400 square miles. In these elliptical frequency storms, the same point rainfall depths and durations were applied as in the uniform rainfall method, but the spatial distribution of the rainfall varied in an elliptical shaped pattern with higher rainfall amounts in the center of the ellipse and lesser amounts towards the outer fringes.

Elliptical shaped storms have been used in a variety of hypothetical design applications, including the Probable Maximum Precipitation (PMP) storms from Hydrometeorological Report No 52 (HMR 52) (Hansen, 1982). The elliptical frequency storms constructed for this study are similar to those of HMR 52 in that concentric ellipses are used to construct the storm's spatial pattern, and the storm's location is optimized over the watershed by identifying the storm center location and the angle of its major axis that led to a maximum peak flow at a

downstream junction of interest. Figure 7.2 shows an example of an elliptical 1% annual exceedance probability (100-yr) storm that was optimized over the watershed above the Colorado River at Columbus, TX USGS gage. This particular junction has a contributing drainage area of almost 2,900 square miles below Lake Travis.

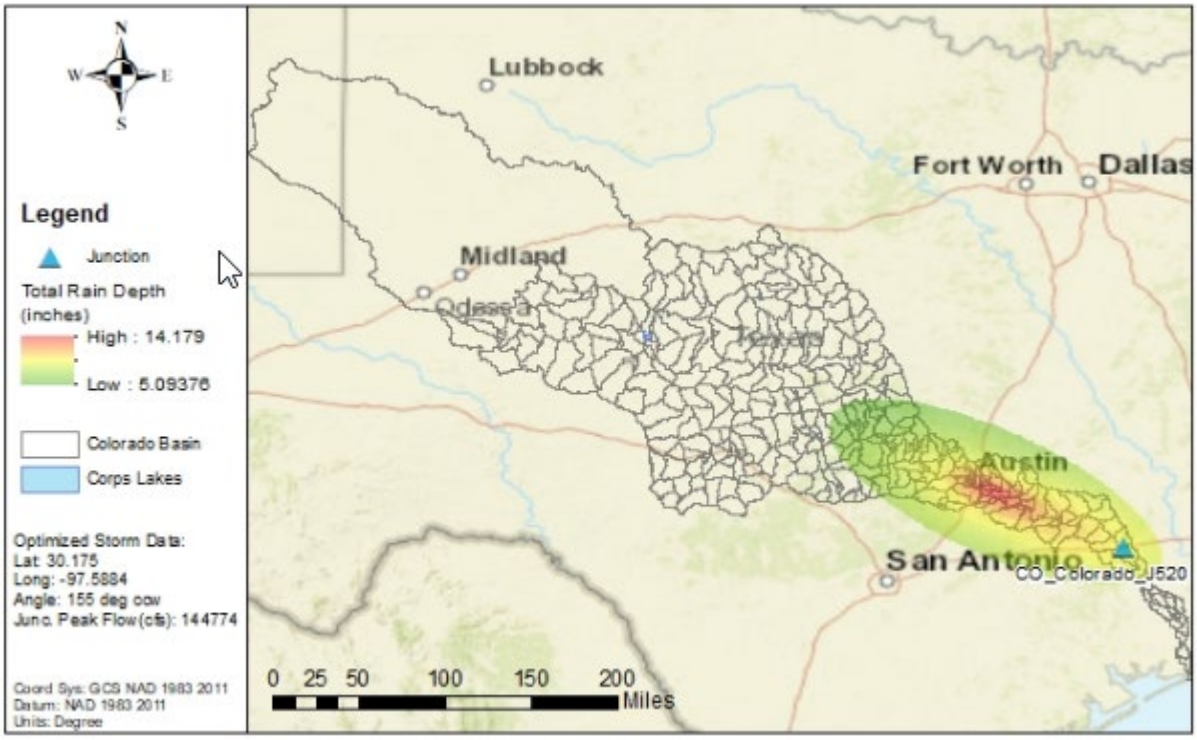

Figure 7.2: Example 1% AEP (100-yr) Elliptical Frequency Storm

7.2 ELLIPTICAL STORM PARAMETERS

The elliptical storm parameters covered below in sections 7.2.1 through 7.2.5 are applicable to the entire Lower Colorado study area. Unique, optimized elliptical storm configurations were developed for 230 different junction elements within the Colorado HMS model, 39 of which were USGS stream gage locations.

The meteorology of the Colorado Basin is noticeably different across different portions of the watershed, as shown below in Figure 7.3. This figure illustrates how the NOAA Atlas 14 rainfall depths for vary spatially across the Lower Colorado River basin. As one can see from this figure, the 1% AEP 48-hr depth varies from less than 9 inches upstream of San Angelo, Texas to over 13 inches near Austin, Texas to almost 18 inches near the Gulf of Mexico. Geographically, it makes sense that the downstream end of the basin would receive the most rainfall because of its proximity to the large source of moisture at the Gulf of Mexico.

The meteorological distinctions across the Lower Colorado River basin were addressed in the sampling of the point precipitation depths and in the development of the depth-area-reduction curves (covered in depth in sections 7.2.3 and 7.2.4 respectively).

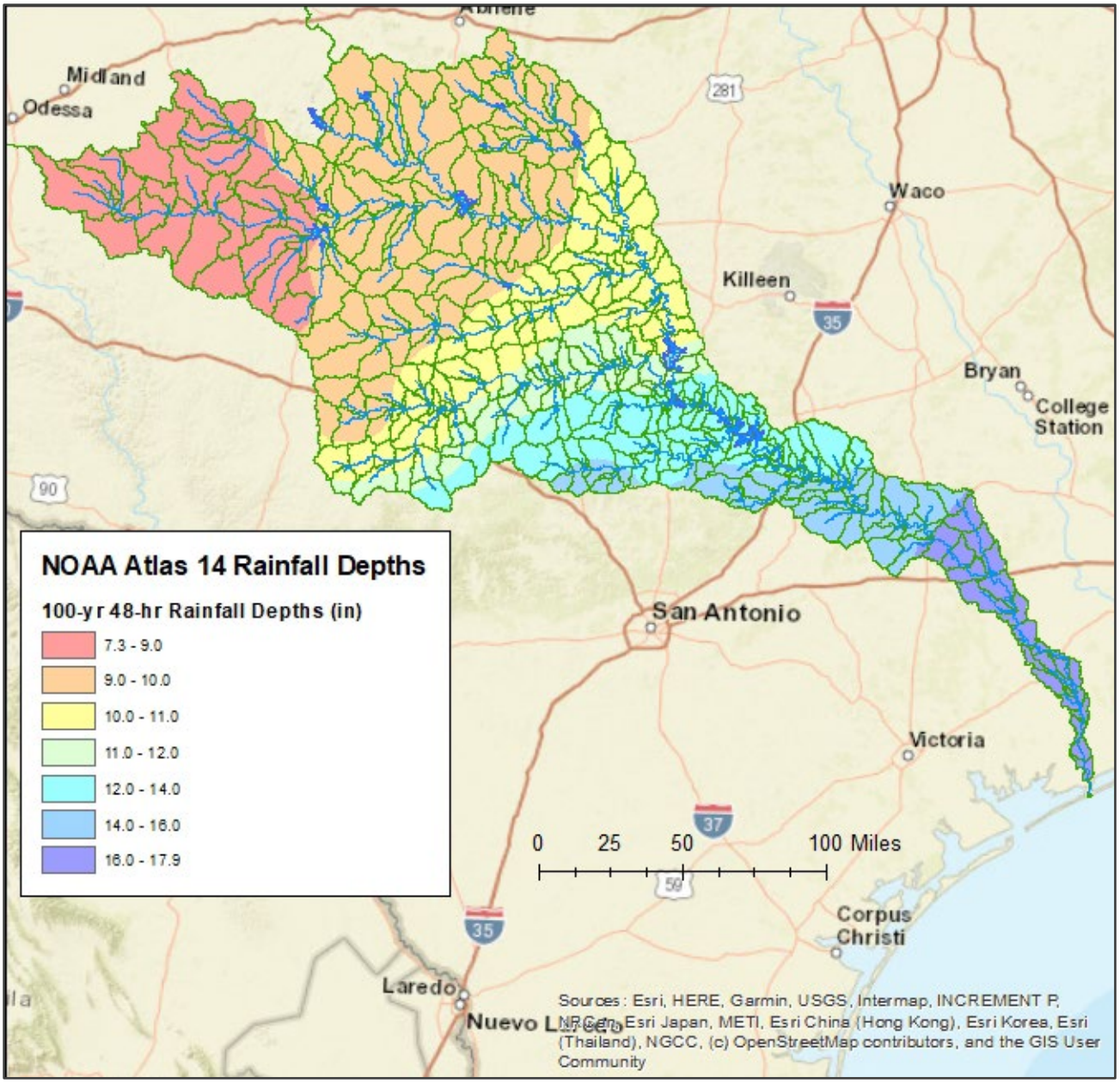

Figure 7.3: NOAA Atlas 14 100-yr 48-hr Precipitation Gradient for the Lower Colorado Basin

7.2.1 Elliptical Storm Area

This study uses a storm extent of 10,000 square miles. This is due, in part, to historical rainfall studies rarely including data beyond 10,000 square miles (USACE, 1945). However, many of the more recent, historic storm events analyzed in Texas for this study did extend to 10,000 square miles and beyond in coverage. While this storm extent is somewhat arbitrary, testing was done in previous InFRM studies to limit the storm extent to 3,000 square miles or increase it to 20,000 square miles and the resulting peak discharges were only slightly altered. Comparisons were also made between the InFRM results with a 10,000 square mile storm area and the 2002 FDEP study results, which used a 50,000 square mile storm area. Even with such a large difference in storm area, the resulting peak discharges were within 5% of one another at many locations. This is likely because the most intense portion of the storm, which drives the peak discharges on the rivers, occurs within the central 1,000 square miles of the storm. Therefore, even though the drainage area of the Lower Colorado River study area is

over 26,600 square miles, a 10,000 square mile storm area was adopted as it produced reasonable and realistic results compared to observed storms.

7.2.2 Storm Ellipse Ratio

The HMR-52 study presents the option to design a storm with a major: minor ellipse axis ratio ranging from 2:1 to 3:1. For the final results in the Lower Colorado River basin, a 2.5:1 ellipse was used, as it matched well with the general shape of the Colorado basin. Ellipse ratios of 3:1 and 2:1 were tested in previous InFRM studies, and they showed only nominal differences in regards to optimized storm centerings, storm orientations, and resulting peak flows when compared to the results obtained from using a 2.5:1 ellipse.

7.2.3 Elliptical Storm Rainfall Depths

Elliptical storms were designed for each of the following annual exceedance probabilities (AEP): 1 in 2 years, 1 in 5 years, 1 in 10 years, 1 in 25 years, 1 in 50 years, 1 in 100 years, 1 in 200 years and 1 in 500 years. Point rainfall depths and durations were applied directly from NOAA Atlas 14 Volume 11 which contains depth duration frequency estimates of precipitation for the state of Texas (NOAA, 2018). The point precipitation values that were applied to each elliptical storm were based on the storm's optimized location, not the location of the outlet of interest. It is important to note that out of all the design storm parameters that are discussed here, peak flows were most sensitive to adjustments in the NOAA Atlas 14 point frequency depths.

Since the precipitation gradient varies rapidly in some portions of the Colorado River basin, all of the precipitation depths that fell under the 10,000 sq mi elliptical storm positioning were queried instead of just the one depth at the storm center. Then all of the queried precipitation depths were reduced based on which of the concentric, DAR ellipses they overlapped with (demonstrated in Figure 7.7 of section 1.2.6). In regions where the precipitation depths vary greatly over a short distance, this method performs better since the precipitation gradient is reflected in the makeup of the elliptical storm.

7.2.4 Storm Depth Area Reduction (DAR) Factors

A depth-area-duration (DAD) table can be used to track the volume of a historic storm event, both spatially and temporally. For this design storm analysis, HEC-MetVUE software was utilized to compute a depth-area-duration table for each observed storm event (Version 3.1; USACE, 2019). A depth-area-reduction (DAR) factor table can be derived from a DAD table; applying DAR factors to a storm results in a storm that has been spatially normalized to a unit depth at the storm center. Thus, the remainder of the storm proceeding outward from the storm center is a fraction of the center depth. Examples of DAD tables, DAR factor tables, and DAR curves are available in Appendix C.

A storm catalog consisting of approximately 73 large, rainfall events that occurred within or in close proximity to the Colorado basin were used in the DAD and DAR analyses for this study. A set of DAR curves (1 hour to 48 hour) was developed for each event. Given the meteorological differences between the upper and lower Colorado, the rainfall event data were initially bifurcated into two groups for separate analysis; the separation was based on which half of the Colorado the storms fell closest to. Storms that fell in the upper half of the Colorado were classified as 100-year events if the maximum observed storm depths fell within the lower and upper 90% confidence bounds for the NOAA Atlas 14 100-year precipitation frequency estimates in the upper Colorado. Likewise, storms in the lower Colorado were similarly classified based on the confidence bounds for the 100-year precipitation frequency estimates in the lower Colorado. An individual storm was allowed to be classified as a

100-year event for one duration and not another. For example, the 48-hour precipitation depth for Hurricane Harvey was much greater than the 100-year 48-hour precipitation upper confidence limits for the lower Colorado basin. Therefore, Harvey was not classified as an eligible 100-year 48-hour event. However, the 1-hour precipitation depth for Harvey did fall within the 100-year 1 hour confidence bounds and was thus classified as a 100-year 1 hour event.

The 1, 24, and 48-hour DAR curves for the classified 100-year upper Colorado storms were averaged and compared to the 1, 24, and 48-hour DAR curves for the 100-year lower Colorado storms. Only nominal differences were observed when comparing the two averaged datasets for the 24 and 48-hour. When comparing the 1-hour average curves, the lower Colorado curve was more reducing than the upper Colorado curve. However, the 1 hour 100-year storm subset was also the smallest sample size due to hourly historic rainfall data having a shorter period of record than the longer durations. Therefore, a confident conclusion regarding the data could not be made, and the upper and lower Colorado curves were ultimately combined to create a singular set of DAR curves that were applied to the entire basin. After several sensitivity runs, the 50th percentile DAR curve for each duration was adopted. To ensure that the DAR curves for each duration nested nicely without any overlap, the 1hr, 6hr, 24hr, and 48hr curves were used and the intermediate durations were interpolated. The final set of 50th percentile nested DAR factors used in this study can be observed in Table 7.1 and Figure 7.4.

For this study, the adopted DAR table values were combined with the adopted storm extent of 10,000 square miles (section 7.2.1) and the adopted ellipse ratio of 2.5 to 1 (section 7.2.2) to create rasterized DAR ellipses for each duration. The rasterized DAR ellipse for the 48hr duration can be seen in Figure 7.5. The ellipses serve as a blueprint for creating the design storms; they are rotated, shifted and multiplied by the corresponding NOAA Atlas 14 precipitation rasters to create spatially reduced rainfall for each storm duration.

It is important to note that the same set of DAR rasters were applied for each elliptical frequency storm analysis (2 year through 500 year). Recent research has been done that compares the spatiotemporal characteristics of “fixed-area” DAR factors and “storm-centered” DAR factors (Kang et al., 2019). The "fixed-area" method is what was used in TP29 and later referenced in TP40 (shown previously in Figure C.1). It results from an unsynchronized frequency analysis between point and areal rainfall. A second method called the "storm-centered" method typically uses radar data to develop the DAR factors. It is a synchronized method in that the point and areal rainfall data are gathered during the same event. The research by Kang et al. concluded that while DAR curves developed via the “fixed-area” method are insensitive to different frequencies, DAR curves developed via the “storm-centered” approach may very well be sensitive to different frequencies. They found that DAR curves may be more reducing for rare frequencies (i.e. the 100yr event) and less reducing for more common frequencies (i.e. the 5yr event). The InFRM Colorado analysis discussed in this chapter used a “storm-centered” approach to develop the DAR curves but did not collect enough storm data to build different sets of DAR curves for different frequencies. The adopted set of DAR curves were built off of 100-year type events but were applied to all frequencies, rare and common.

Table 7.1: Adopted Depth-Area-Reduction Values for the Colorado InFRM Study

Area (sqmi)	1-hr DAR	2-hr DAR	3-hr DAR	6-hr DAR	12-hr DAR	24-hr DAR	48-hr DAR
10	1.000	1.000	1.000	1.000	1.000	1.000	1.000
20	0.970	0.972	0.974	0.976	0.978	0.980	0.980
30	0.940	0.953	0.964	0.966	0.968	0.970	0.970
40	0.910	0.930	0.950	0.954	0.957	0.960	0.961
50	0.880	0.907	0.933	0.945	0.948	0.951	0.953
60	0.854	0.882	0.917	0.935	0.938	0.942	0.946
70	0.831	0.861	0.900	0.925	0.929	0.934	0.938
80	0.812	0.843	0.883	0.914	0.921	0.926	0.932
90	0.795	0.827	0.867	0.902	0.914	0.920	0.926
100	0.780	0.813	0.850	0.890	0.908	0.915	0.922
200	0.680	0.719	0.758	0.797	0.822	0.846	0.865
300	0.635	0.676	0.716	0.761	0.787	0.813	0.834
400	0.603	0.645	0.687	0.735	0.763	0.790	0.811
500	0.579	0.621	0.664	0.715	0.744	0.772	0.793
600	0.559	0.602	0.645	0.694	0.725	0.755	0.777
700	0.542	0.585	0.629	0.677	0.709	0.740	0.763
800	0.527	0.571	0.615	0.662	0.695	0.727	0.750
900	0.514	0.558	0.603	0.649	0.682	0.716	0.740
1000	0.502	0.547	0.592	0.637	0.671	0.706	0.730
2000	0.435	0.474	0.512	0.553	0.593	0.633	0.658
3000	0.396	0.430	0.465	0.504	0.547	0.590	0.616
4000	0.368	0.400	0.431	0.469	0.514	0.559	0.587
5000	0.347	0.376	0.406	0.442	0.489	0.536	0.563
6000	0.329	0.357	0.384	0.417	0.465	0.513	0.541
7000	0.314	0.340	0.367	0.396	0.445	0.494	0.522
8000	0.301	0.326	0.351	0.378	0.428	0.477	0.506
9000	0.290	0.314	0.337	0.362	0.412	0.463	0.492
10000	0.280	0.303	0.325	0.348	0.399	0.449	0.479

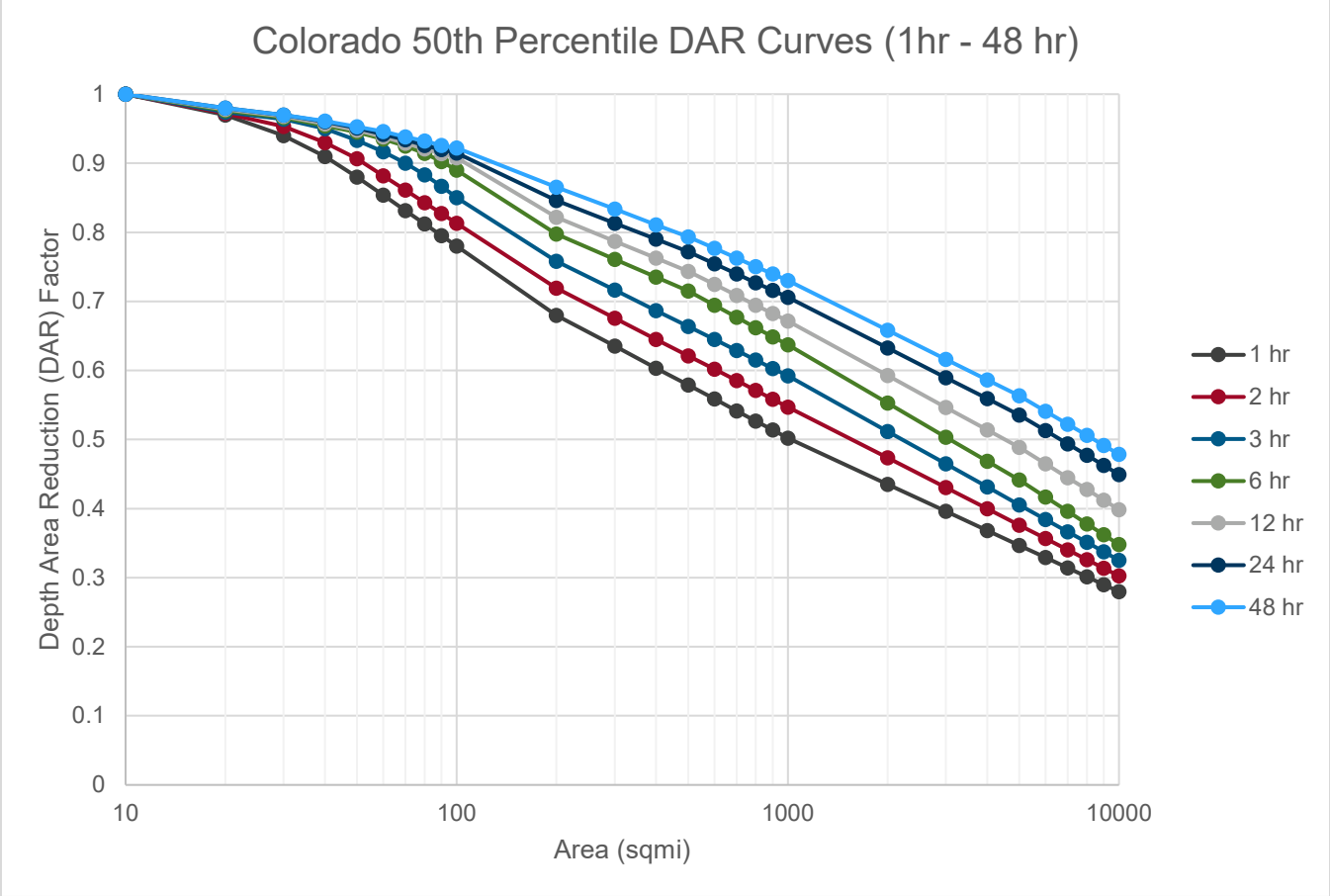

Figure 7.4: Adopted Depth-Area-Reduction Curves for the Colorado InFRM Study (Plotted from Table 7.1)

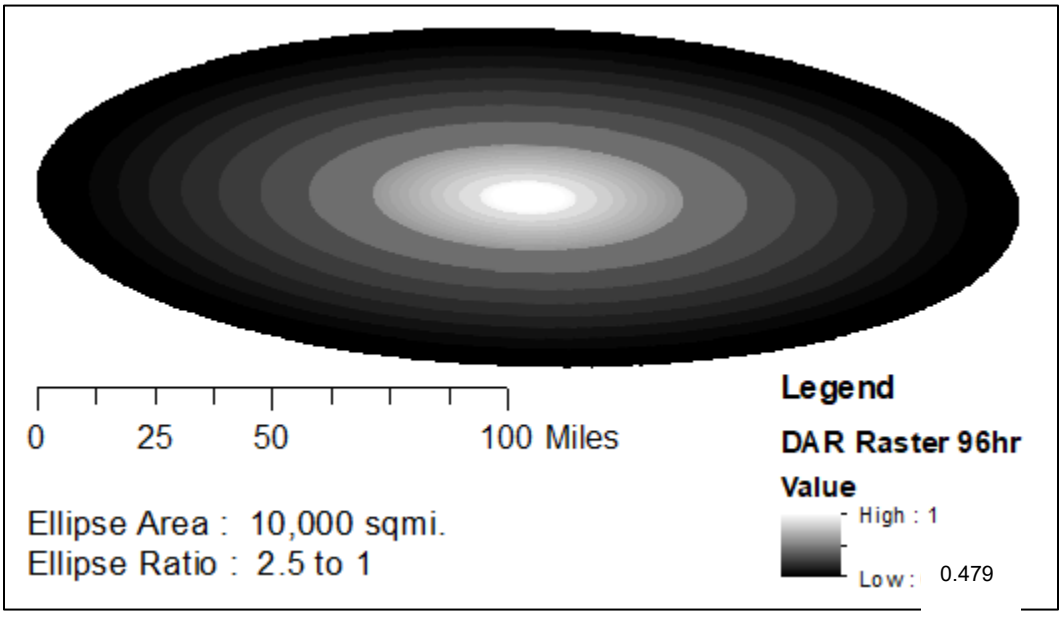

Figure 7.5: Adopted Depth-Area-Reduction Rasterized Ellipse for the 48-hr Duration

7.2.5 Storm Temporal Pattern / Hyetograph

Historically, storms have varied intensities and temporal distributions and many studies have been done to document storm patterns. The six storm temporal distributions that were tested for a previous InFRM study are shown in Figure 7.6. The Soil Conservation Service (1986) documented different distributions for the United States. Type II is the distribution applicable to Texas; it was included in the testing. Other distributions were also previously tested, including the alternating block Frequency Rainfall temporal distributions from HEC-HMS with the storm centroid occurring at the 25%, 33%, 50%, 67%, and 75% of the total distribution. The HEC-HMS Frequency Rainfall alternating block temporal distributions maintain the appropriate storm intensity for all durations throughout the storm. In other words, the 100-year, 1 hour rainfall depth is maintained within the 100-year, 2 hour rainfall depth and so on all the way through the 100 year, 48 hour rainfall depth. For this Colorado design storm study, temporal distributions with maximum intensities occurring at 33%, 50%, and 67% of the total distribution were tested with a negligible effect on downstream peak flows. Centrally distributed (50%) alternating block temporal distributions were adopted for the final runs.

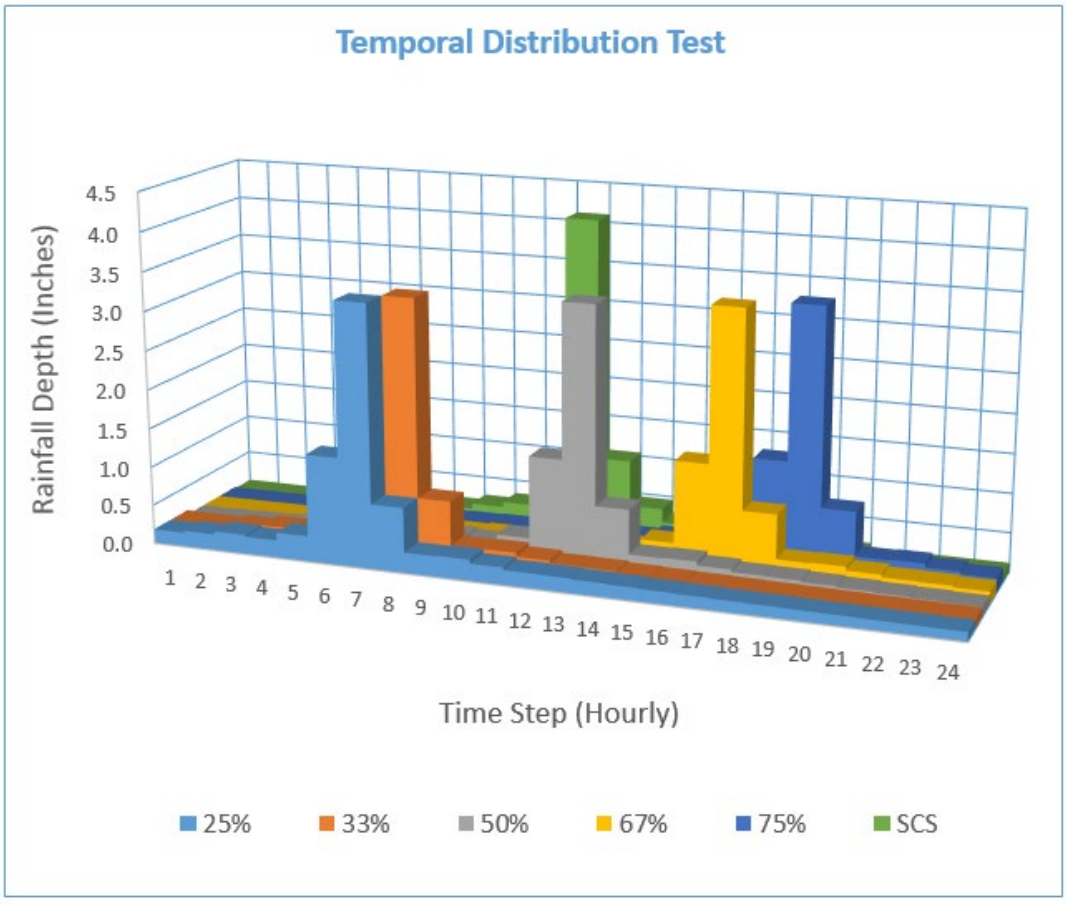

Figure 7.6: Previously Tested Storm Temporal Distributions

During the uniform rainfall analysis covered in Appendix B, storm durations ranging from 12 to 240 hours were tested on the Colorado basin. A duration of 48 hours was ultimately adopted for the uniform rainfall modeling. The 48-hour results yielded slightly higher peak flows when compared to the 24-hour results, and the difference in peak flows began to taper off for durations greater than 48 hours. Furthermore, the 48-hour duration also

coincides well with the duration of several observed, historic rainfall events. In order to be consistent with the uniform rainfall assumptions, the 48-hour duration was also adopted for the elliptical storm modeling.

7.2.6 Geospatial Process for Building the Elliptical Storms

For this Colorado InFRM study, a geospatial method was utilized for creating the rainfall hyetographs that were used as input into the design storm HMS model. This method is built on three principal sources of geospatial data: 1) NOAA Atlas 14 precipitation frequency raster data in asci format for the 1, 2, 3, 6, 12, 24, and 48-hour durations, 2) rasterized DAR ellipses that are built off of the adopted DAR curves for each of these durations, and 3) a HEC-HMS subbasin shapefile. For each unique storm location and orientation within the Colorado basin, the underlying precipitation data is queried and multiplied by the appropriate rasterized DAR ellipse to get the educed precipitation for each duration (Figure 7.7). Then zonal statistics are calculated to determine the average reduced precipitation for each subbasin. Using the subbasin-averaged reduced precipitation for the 1, 2, 3, 6, 12, 24, and 48-hour durations, the alternating block method is used to build rainfall hyetographs for each of the subbasins within the design storm HMS model. The geospatial algorithm employed builds the storm from the central, maximum intensity duration outwards so that the appropriate storm intensity is maintained throughout the entire storm. For example, the 100-year 1 hour rainfall is maintained within the 100 year 2-hour rainfall and so forth all the way out to the 48-hour duration.

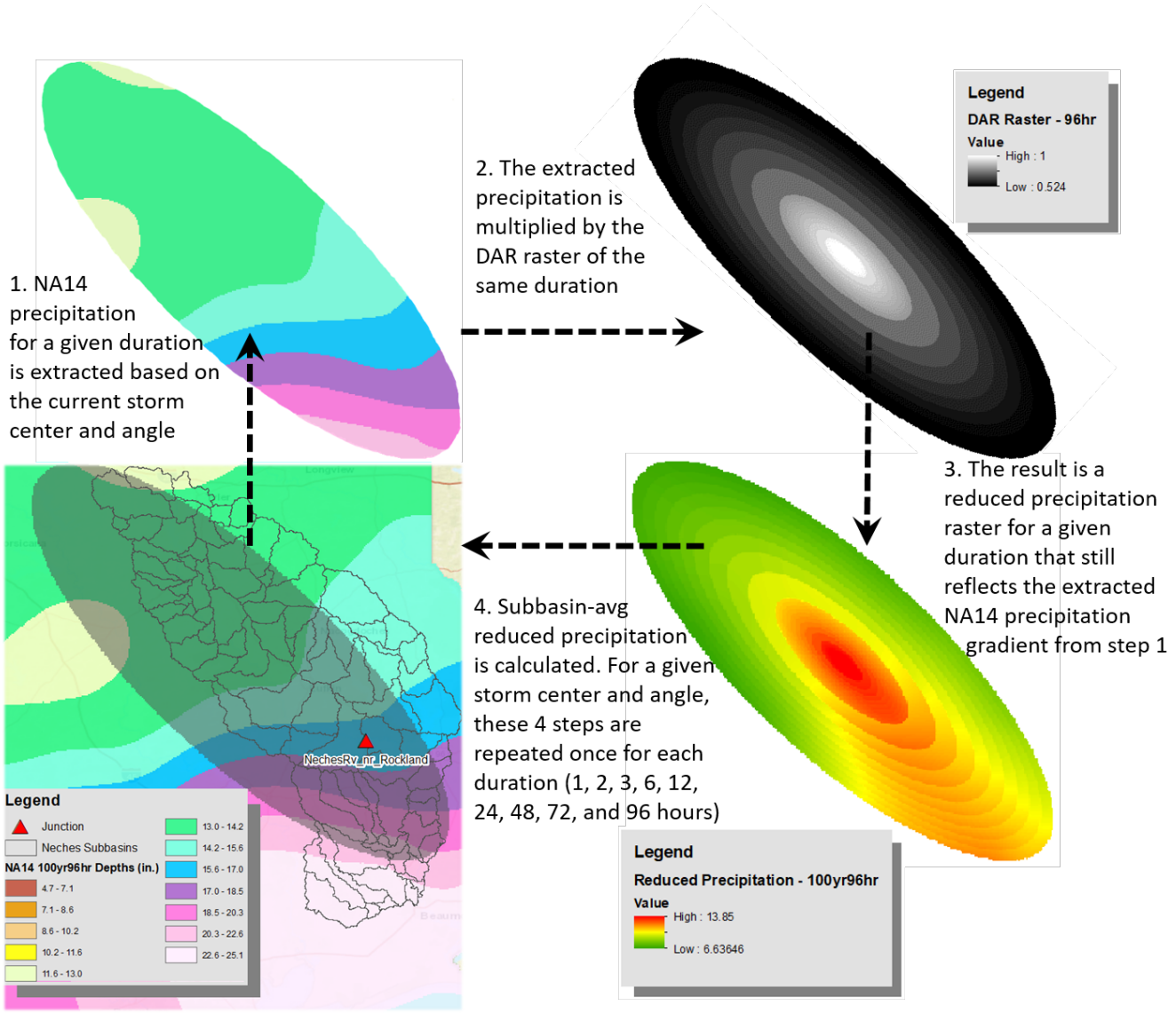

Figure 7.7: Geospatial Process for Building Elliptical Design Storms

7.3 OPTIMIZATION OF THE STORM CENTER LOCATION

For the InFRM Watershed Hydrology Assessments, a script was developed by the University of Texas at Arlington that automatically locates optimal centering locations (x and y) and rotations (ɵ) of spatially varied elliptical frequency storms for a list of receiving junctions in an HMS basin model. The script was expected to obtain the combination of the three parameters (x, y, and ɵ) that maximized either peak flow at desired junctions or reservoir pool elevations while achieving the following objectives:

- To complete the task efficiently.
- To allow users to customize the scripts easily based on their needs.
- To generate reasonable results that can be validated manually.
- To outperform the manual grid search method in terms of precision, accuracy and efficiency.
- To function normally on any machine at USACE with the available software and hardware.

The ArcPy Python library, part of Esri's ArcGIS software package, was leveraged for all geospatial operations. The "Optimization Loop" section of Figure 7.8 below illustrates the schematic flow of the storm optimization script. The loop consists of two major components: 1) parameter update/optimization and 2) automatic simulation of the HEC-HMS hydrologic model. In each iteration of the optimization process, the rasterized DAR ellipses for each duration are rotated and shifted to align with the updated parameters (x, y, and ɵ) and then are applied to the corresponding NOAA Atlas 14 precipitation rasters to create spatially reduced rainfall for each storm duration. The spatially reduced depths are then allocated into each subbasin as mean areal precipitation (MAP). The subbasin MAP values for each duration are then manipulated using the alternating block method to create a complete time series (covered in section 1.2.5). The time series MAP values, i.e. the hyetographs, are stored in DSS format and transmitted to the HMS model for simulations. After each simulation, the corresponding peak flow value at a desired junction is extracted from the output DSS file. Based on the extracted peak flow value, an optimization algorithm will update the parameters (x, y and ɵ) and then optimization proceeds into the next iteration. After all optimization iterations for a junction are complete, an optimized storm center (x and y) and orientation (ɵ) that leads to a peak flow at a given junction is determined. The optimization process can then be repeated for the next junction of interest.

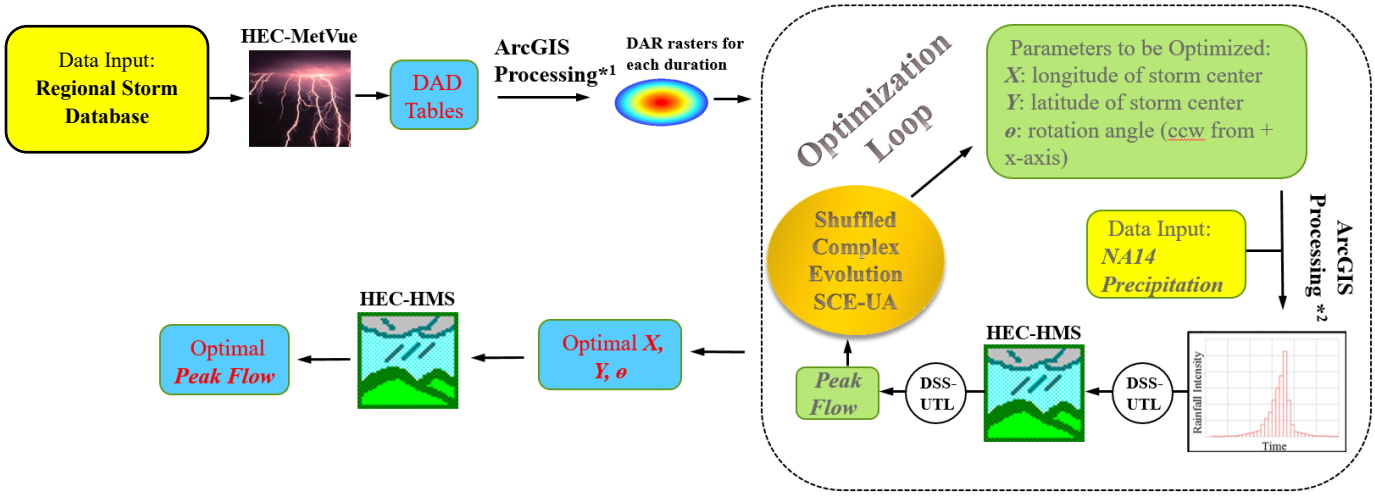

*1. involves creating rasterized ellipses for each NA14 duration with DAR values of 1 in the center, and decreasing values towards the outer rings.
*2. involves rotating and shifting each DAR raster, reducing the NA14 precipitation rasters, and calculating zonal statistics for each subbasin.

Figure 7.8: Schematic Flowchart for the Storm Optimization Script

Originally, the scripts were designed to automate a grid search, where all possible combinations of parameters (i.e. the 'grids') are exhaustively tested and the optimal combination of the three parameters (x, y, and ϴ) can then be obtained. Although the approach of grid search seems straightforward, it does suffer from high computational cost because the computational run time depends on the number of grids, which is further constrained by the range and the interval of each parameter. Given the need of maintaining a certain level of precision or keeping constant intervals of the parameters, the UTA team found that the grid search approach might not be appropriate for this project since the computational run time was excessively lengthy – it increases exponentially with greater drainage area (more possible x and y values).

In order to overcome this issue, the UTA team selected a global optimization (GO) algorithm entitled shuffled complex evolution (SCE) (Duan et al., 1993) - a random sampling approach. Instead of exhausting all possible grids, the random sampling approach tests the objective function around some sampled grids in an iteration while learning about the structure of the objective function for improving the sampling of grids in the next iteration. More details about GO and SCE are included in Appendix C.

7.4 ELLIPTICAL STORM LOCATIONS

The final optimized storm center locations (x, y) and rotations (ϴ) for every node of interest in the Lower Colorado watershed are listed in Appendix C. Rotation angles are measured counterclockwise from the positive x-axis. These location and rotation parameters were determined from 100yr frequency optimizations and are assumed to be the same for other frequency events in most cases (2yr – 500yr). Sensitivity testing showed that, in general, optimized locations and orientations did not significantly change between frequency events. Once the optimum storm center location and rotation were determined for each location of interest, the elliptical frequency storms for the standard eight frequency events were constructed using the appropriate NOAA Atlas 14 point rainfall depths. See Appendix C for additional information.

7.5 ELLIPTICAL FREQUENCY STORM LOSS RATES

The elliptical frequency storms were then applied to the final HEC-HMS basin model with the same frequency loss rates that were used for the uniform rainfall method which is discussed in Appendix B. In some cases, the 2-yr through 10-yr losses were re-adjusted in order to maintain consistency with the frequent end of the statistical frequency curves at the USGS gages. This final adjustment was performed because of the increased level of confidence in the statistical frequency curve for the 2-yr through 10-yr recurrence intervals. The final 2-yr through 25-yr loss rates used for the elliptical frequency storm events are given in Appendix C. The final 50-yr through 500-yr loss rates are the same as those used for the uniform rainfall method and are shown in Appendix C.

7.6 ELLIPTICAL FREQUENCY STORM RESULTS – PEAK FLOW

The frequency peak flow values were then calculated in HEC-HMS by applying the appropriate, optimized elliptical frequency storms for each junction of interest in the final HEC-HMS basin model. These results will later be compared to the uniform rain results from HEC-HMS along with other methods from this study.

In some cases, one may observe that the simulated peak discharge decreases in the downstream direction. It is not an uncommon phenomenon to see decreasing frequency peak discharges for some river reaches as flood waters spread out into the floodplain and the hydrograph becomes dampened as it moves downstream. This can

be due to a combination of peak attenuation due to river routing as well as the difference in timing between the peak of the main stem river versus the runoff from the local tributaries and subbasins.

7.6.1 Tabular Results

The final HEC-HMS peak frequency flow results for the locations of interest throughout the watershed model using the NOAA Atlas 14 rainfall depths can be seen below in Table 7.2. The peak flow results in Table 7.2 used storm locations that were optimized to maximize the peak flow at the junction of interest. For the reservoirs, the final HEC-HMS frequency pool elevation and peak outflow results are summarized in Tables 7.3 and 7.4, and the locations of the elliptical storms for these reservoirs were optimized to maximize the reservoir's pool elevation. Since the reservoirs were optimized for two different variables (peak inflow and elevation), the peak flow results in Tables 7.2 and 7.4 may differ, and the higher of the two values should be adopted as the final result of this method.

Table 7.2: Summary of Discharges (cfs) from the HEC-HMS Elliptical Frequency Storm Method

Location Description	HEC-HMS Element Name	HEC-HMS Drainage Area (sq mi)	50% AEP	20% AEP	10% AEP	4% AEP	2% AEP	1% AEP	0.5% AEP	0.2% AEP
			2-yr	5-yr	10-yr	25-yr	50-yr	100-yr	200-yr	500-yr
Colorado River below Oak Creek	CO_Colorado_J30	668.2	450	6,010	11,800	30,100	53,100	74,900	95,600	123,400
Colorado River above Valley Creek	CO_Colorado_J39	844.9	400	4,910	9,600	25,400	46,700	66,900	87,500	116,400
Colorado River near Ballinger, TX (USGS Gage 08126380)	CO_Colorado_J40	1076.2	2,590	7,500	13,700	34,300	67,400	95,000	123,200	163,100
Colorado River above Elm Creek	CO_Colorado_J49	1130.3	2,370	7,460	13,500	33,700	65,900	93,100	120,900	160,300
Elm Creek at Ballinger, TX (USGS Gage 08127000)	CO_ElmCr_J20	466.8	3,920	9,520	14,900	25,200	33,900	52,800	72,000	98,400
Colorado River below Elm Creek	CO_Colorado_J50	1597.2	2,310	7,580	14,500	39,300	74,100	111,300	148,400	202,200
Colorado River above the Concho River	CO_Colorado_J59	1826.2	2,220	6,920	13,400	36,800	69,400	105,300	141,000	193,300
High Lonesome Draw below subbasin CN_Mconcho_S20	CN_MConcho_J10	404.4	140	3,080	8,800	24,700	41,600	58,200	70,900	88,500
High Lonesome Draw below subbasin CN_Mconcho_S30	CN_MConcho_J20	496.5	170	2,810	9,100	27,000	46,200	65,300	80,300	100,900
Centralia Draw below High Lonesome Draw	CN_MConcho_J30	745.2	200	2,140	8,400	28,800	51,200	73,700	91,600	117,200
Centralia Draw below North Creek	CN_MConcho_J40	946.0	300	1,590	7,700	27,900	50,200	72,700	90,800	116,700
Middle Concho River below the Centrailia Draw	CN_MConcho_J50	1349.1	1,540	6,580	15,800	39,500	64,200	90,000	112,000	143,100
Middle Concho River above Kiowa Creek	CN_MConcho_J59	1642.5	1,770	6,680	16,500	43,900	73,200	104,100	130,600	169,700
Middle Concho River below Kiowa Creek	CN_MConcho_J60	1731.3	1,870	6,900	16,700	45,000	75,400	107,400	135,100	175,500
Middle Concho River below Big Hollow Draw	CN_MConcho_J70	1887.2	1,440	6,680	16,200	43,500	73,200	104,500	131,900	171,500
Middle Concho River above West Rocky Creek	CN_MConcho_J79	2007.5	1,520	6,290	15,300	42,000	70,900	101,600	128,300	167,000
Middle Concho River below West Rocky Creek	CN_MConcho_J80	2121.6	1,400	6,410	15,600	42,100	71,000	101,700	128,600	167,300
Middle Concho River abv Tankersley (USGS Gage 08128400)	CN_MConcho_J90	2133.0	1,520	6,250	15,300	41,800	70,700	101,300	128,000	166,700
Spring Creek above Tankersley, TX (USGS Gage 08129300)	CN_SConcho_J35	427.2	300	2,900	8,300	22,900	34,300	53,900	72,400	95,200
Spring Creek abv Twin Buttes Res (USGS Gage 08130700)	CN_SConcho_J50	678.9	260	8,850	20,000	35,100	50,000	67,400	84,100	108,500
South Concho River at Christoval, TX (USGS Gage 08128000)	CN_SConcho_J20	415.4	800	6,460	21,200	42,300	55,700	73,300	90,300	115,300
Inflow to Twin Buttes Reservoir	TWIN_BUTTES_INFLOW	3422.5	1,240	4,300	18,200	51,300	80,500	116,900	151,000	202,800
South Concho River below Twin Buttes Reservoir	TWIN_BUTTES_OUTFLOW	3422.5	0	0	0	3,000	5,000	9,000	9,000	9,000
Inflow to Lake Nasworthy	NASWORTHY_INFLOW	3529.7	350	5,180	9,600	16,700	23,600	29,700	36,300	44,500
South Concho River below Lake Nasworthy	NASWORTHY_OUTFLOW	3529.7	350	5,210	9,700	16,700	23,700	29,800	36,500	44,600
South Concho River above the North Concho River	CN_SConcho_J70	3561.7	1,710	2,300	5,000	14,600	23,100	30,300	37,400	46,600

Location Description	HEC-HMS Element Name	HEC-HMS Drainage Area (sq mi)	50% AEP	20% AEP	10% AEP	4% AEP	2% AEP	1% AEP	0.5% AEP	0.2% AEP
			2-yr	5-yr	10-yr	25-yr	50-yr	100-yr	200-yr	500-yr
North Concho River below Lacy Creek	CN_NConcho_J30	567.1	710	4,970	10,000	24,500	40,300	58,900	76,100	97,500
North Concho River at Sterling City (USGS Gage 08133500)	CN_NConcho_J40	586.0	870	4,740	9,700	23,600	38,900	56,900	73,700	94,500
North Concho River above Sterling Creek	CN_NConcho_J49	609.8	340	3,970	8,600	22,000	36,700	54,200	70,700	90,900
North Concho River below Sterling Creek	CN_NConcho_J50	808.4	570	4,520	9,300	22,900	38,300	56,600	73,800	95,000
North Concho River above Walnut Creek	CN_NConcho_J59	1004.0	620	4,190	8,800	21,800	36,700	54,500	71,200	92,000
North Concho River below Walnut Creek	CN_NConcho_J60	1070.3	550	4,220	8,700	21,600	36,200	53,900	70,500	91,000
North Concho River nr Carlsbad, TX (USGS Gage 08134000)	CN_NConcho_J70	1220.7	1,800	4,770	8,300	21,100	37,900	54,900	71,300	91,800
North Concho River above Grape Creek	CN_NConcho_J79	1250.2	2,840	6,120	9,800	22,900	39,700	57,000	73,400	93,700
North Concho River below Grape Creek	CN_NConcho_J80	1360.1	2,620	5,830	9,600	24,000	42,900	62,100	80,400	103,100
North Concho River near Grape Creek (USGS Gage 08134250)	CN_NConcho_J90	1364.9	2,170	5,610	9,300	23,600	42,400	61,400	79,500	102,200
Inflow to OC Fisher Reservoir	OC_FISHER_INFLOW	1462.8	2,080	5,460	9,100	23,300	42,200	61,500	79,800	102,900
North Concho River below OC Fisher Reservoir	OC_Fisher_OUTFLOW	1462.8	0	0	0	0	0	0	0	0
North Concho River at San Angelo, TX (USGS Gage 08135000)	CN_NConcho_J100	1484.9	1,350	1,830	2,400	5,000	9,800	11,900	13,900	16,400
Concho River at San Angelo, TX (USGS Gage 08136000)	CN_Concho_J10	5046.6	3,000	4,060	7,500	18,400	31,300	40,500	49,400	60,800
Concho River above Crows Nest Creek	CN_Concho_J20	5186.1	3,900	7,140	11,900	27,500	43,900	57,600	72,000	91,500
Concho River above Lipan Creek	CN_Concho_S29	5355.7	3,280	6,510	11,200	30,400	51,500	68,600	83,300	103,000
Concho River below Lipan Creek	CN_Concho_J40	5664.0	5,220	9,770	14,900	37,100	62,900	86,500	110,100	143,300
Concho River above Kickapoo Creek	CN_Concho_J49	5780.8	4,880	9,450	14,600	37,300	62,700	87,100	111,300	145,400
Concho River below Kickapoo Creek	CN_Concho_J50	6080.7	3,730	8,920	15,400	42,400	72,100	101,000	129,500	167,500
Concho River at Paint Rock, TX (USGS Gage 08136500)	CN_Concho_J60	6088.3	2,790	8,170	14,800	42,200	71,000	99,700	129,500	168,800
Concho River above the Colorado River	CN_Concho_J70	6279.2	3,830	8,760	15,300	43,700	72,700	101,600	130,200	171,500
Colorado River below the Concho River	CO_Colorado_J60	13123.4	4,290	12,000	21,600	63,500	112,000	168,000	223,600	305,400
Inflow to OH Ivie Reservoir	OH_IVIE_INFLOW	13298.7	4,220	12,000	22,100	64,100	112,200	168,100	224,200	306,000
Colorado River below OH Ivie Reservoir	OH_IVIE_OUTFLOW	13298.7	20	20	20	28,500	80,300	125,900	154,700	188,300
Colorado River near Stacy, TX (USGS Gage 08136700)	CO_Colorado_J70	13438.5	530	2,590	6,700	29,000	80,100	125,800	154,600	188,400
Colorado River below Panther Creek	CO_Colorado_J80	13541.0	420	740	2,400	20,100	55,500	99,800	139,000	178,400
Colorado River below Salt Creek	CO_Colorado_J90	13646.5	370	700	2,300	20,500	55,600	99,800	139,100	178,500

Location Description	HEC-HMS Element Name	HEC-HMS Drainage Area (sq mi)	50% AEP 2-yr	20% AEP 5-yr	10% AEP 10-yr	4% AEP 25-yr	2% AEP 50-yr	1% AEP 100-yr	0.5% AEP 200-yr	0.2% AEP 500-yr
Colorado River above Bull Creek	CO_Colorado_J99	13723.1	6,920	14,200	20,900	38,800	54,500	71,200	88,000	112,100
Colorado River below Bull Creek	CO_Colorado_J100	13787.8	7,840	16,200	24,100	45,600	65,900	86,300	106,600	135,800
Colorado River below Elm Creek	CO_Colorado_J110	13868.7	7,550	16,300	23,600	45,200	67,400	89,200	110,500	141,700
Colorado River above Home Creek	CO_Colorado_J119	14007.5	7,850	17,500	24,500	45,600	70,600	95,600	120,200	157,100
Colorado River below Home Creek	CO_Colorado_J120	14390.3	10,570	19,500	28,700	57,400	98,400	139,200	182,200	245,400
Colorado River at Winchell, TX (USGS Gage 08138000)	CO_Colorado_J130	14438.8	9,410	18,600	27,300	56,600	98,100	140,000	183,200	249,600
Colorado River above Clear Creek	CO_Colorado_J139	14538.7	8,770	17,500	25,100	48,700	78,700	120,600	166,400	234,700
Colorado River below Clear Creek	CO_Colorado_J140	14662.3	12,400	20,800	26,400	50,500	79,000	122,000	169,400	242,900
Colorado River below Buffalo Creek	CO_Colorado_J150	14843.3	15,380	22,400	24,800	48,700	74,600	107,400	156,300	218,500
Colorado River above Pecan Bayou	CO_Colorado_J159	14949.3	14,560	22,500	25,700	47,100	68,100	97,700	138,500	198,200
Jim Ned Creek nr Coleman, TX (USGS Gage 08140860)	PB_JimNedCr_J29	447.0	4,120	8,990	15,200	20,800	23,000	44,500	67,300	103,200
Jim Ned Creek below Hords Creek	PB_JimNedCr_J30	592.9	5,530	11,800	17,300	22,600	25,300	49,700	76,800	118,300
Jim Ned Creek at FM-585	PB_JimNedCr_J40	681.8	8,030	16,700	24,400	30,900	33,100	52,500	73,200	102,200
Jim Ned Creek above Lake Brownwood	PB_JimNedCr_J50	781.5	6,600	14,800	22,100	28,800	31,100	50,600	71,600	101,700
Pecan Bayou nr Cross Cut, TX (USGS Gage 08140700)	PB_PecanBayou_J40	543.9	6,690	15,400	23,900	31,600	37,900	58,200	82,900	119,900
Pecan Bayou below Red River	PB_PecanBayou_J50	642.7	10,400	21,500	31,100	41,500	49,300	69,500	89,600	116,400
Inflow to Lake Brownwood	BROWNWOOD _INFLOW	1561.9	10,340	25,200	37,100	53,800	66,500	99,300	133,400	189,500
Pecan Bayou below Lake Brownwood	BROWNWOOD_OUTFLOW	1561.9	4,240	9,870	14,900	20,500	25,000	39,100	54,300	82,500
Pecan Bayou at Brownwood, TX (USGS Gage 08143500)	PB_PecanBayou_J60	1652.7	4,060	9,270	13,900	18,900	22,800	37,100	53,300	80,400
Pecan Bayou below Devils River	PB_PecanBayou_J70	1801.9	7,200	12,400	17,900	26,500	35,200	46,700	58,100	72,800
Pecan Bayou above Blanket Creek	PB_PecanBayou_J79	1875.1	5,490	10,500	15,200	22,100	28,800	37,000	44,900	55,400
Pecan Bayou nr Mullin, TX (USGS Gage 0813600)	PB_PecanBayou_J80	2072.1	4,830	10,900	17,000	27,200	38,000	58,100	76,100	99,900
Pecan Bayou above Colorado River	PB_PecanBayou_J90	2204.3	5,200	11,400	16,900	27,800	39,200	61,900	84,000	115,700
Colorado River below Pecan Bayou	CO_Colorado_J160	12135.6	13,540	22,900	28,400	55,100	80,900	119,000	163,700	233,100
Colorado River near Goldthwaite, TX (LCRA Gage 1277)	CO_Colorado_J170	12162.7	10,750	21,100	25,100	51,500	78,000	115,700	147,500	216,800
Colorado River above the San Saba River	CO_Colorado_J179	12273.9	11,130	21,500	24,900	48,400	71,200	106,300	135,000	191,500
San Saba Rv at FM 864 nr Fort McKavett, TX (USGS Gage)	SS_SanSaba_J20	622.8	50	1,480	29,300	40,300	84,300	111,900	136,500	173,300

Location Description	HEC-HMS Element Name	HEC-HMS Drainage Area (sq mi)	50% AEP 2-yr	20% AEP 5-yr	10% AEP 10-yr	4% AEP 25-yr	2% AEP 50-yr	1% AEP 100-yr	0.5% AEP 200-yr	0.2% AEP 500-yr
San Saba River above Rocky Creek	SS_SanSaba_J29	721.4	990	5,920	29,300	41,100	86,900	114,800	141,600	183,600
San Saba River below Rocky Creek	SS_SanSaba_J30	831.2	1,530	6,820	29,300	43,000	91,600	122,600	151,400	197,600
San Saba River above Las Moras Creek	SS_SanSaba_J40	989.0	1,410	12,800	30,300	50,600	100,400	137,200	171,700	226,000
San Saba River at Menard, TX (USGS Gage 081445000)	SS_SanSaba_J50	1136.9	4,140	20,000	38,900	72,300	118,600	156,900	197,600	260,600
San Saba River above Elm Creek	SS_SanSaba_J59	1244.6	3,570	19,200	39,900	77,600	126,600	166,000	203,800	272,200
San Saba River below Elm Creek	SS_SanSaba_J60	1318.2	4,000	19,800	41,900	82,200	132,800	174,500	213,400	283,700
San Saba River above Calf Creek	SS_SanSaba_J69	1422.3	2,860	16,500	38,100	76,500	129,500	174,800	218,600	296,800
San Saba River below Calf Creek	SS_SanSaba_J70	1490.6	2,810	16,500	38,900	78,800	132,800	179,400	224,000	304,300
San Saba River below Rumsey Creek	SS_SanSaba_J80	1594.0	2,430	15,900	40,100	82,000	137,200	185,800	232,000	313,500
San Saba River nr Brady, TX (USGS Gage 08144600)	SS_SanSaba_J90	1636.4	3,630	17,700	38,300	78,700	129,000	175,600	218,200	290,500
San Saba River below Katemcy Creek	SS_SanSaba_J100	1688.6	2,370	15,900	39,800	81,700	137,800	188,200	236,300	321,200
San Saba River above Tiger Creek	SS_SanSaba_J109	1721.9	2,400	15,100	38,300	78,600	135,000	185,100	233,200	317,800
San Saba River below Tiger Creek	SS_SanSaba_J110	1804.6	2,170	15,700	39,500	80,800	139,100	191,200	240,800	328,400
San Saba River above Brady Creek	SS_SanSaba_J119	1941.6	2,030	15,300	39,700	80,800	142,100	197,200	249,900	342,400
Inflow to Brady Creek Reservoir	BRADY_INFLOW	524.0	1,670	4,760	8,000	12,600	20,300	39,300	60,400	90,800
Brady Creek below Brady Creek Reservoir	BRADY_OUTFLOW	524.0	170	430	600	800	1,200	1,900	13,200	37,200
Brady Creek At Brady, TX (USGS Gage 08145000)	SS_BradyCr_J40	654.2	430	1,770	4,000	10,000	20,000	28,100	36,000	46,900
Brady Creek below Little Brady Creek	SS_BradyCr_J50	750.2	5,020	9,380	10,700	13,600	33,200	47,300	59,900	77,800
Brady Creek above the San Saba River	SS_BradyCr_J60	803.2	4,340	9,730	11,000	18,200	46,100	61,100	74,000	96,100
San Saba River below Brady Creek	SS_SanSaba_J120	2744.9	5,170	19,000	55,800	91,400	137,900	201,100	255,900	340,000
San Saba River above Wallace Creek	SS_SanSaba_J129	2848.2	6,410	21,800	54,400	94,100	142,000	207,900	268,800	361,900
San Saba River below Wallace Creek	SS_SanSaba_J130	2905.1	5,510	20,700	53,700	94,000	139,600	206,900	269,400	363,000
San Saba River below Richland Springs Creek	SS_SanSaba_J140	3010.6	6,520	23,400	54,400	97,300	143,400	214,200	281,600	383,800
San Saba Rv at San Saba, TX (USGS Gage 08146000)	SS_SanSaba_J150	3047.4	8,760	26,400	50,000	93,300	137,800	205,400	272,200	374,200
San Saba River above Colorado River	SS_SanSaba_J160	3150.1	3,190	13,600	37,200	78,800	137,100	208,700	279,200	390,700
Colorado River below San Saba River	CO_Colorado_J180	20442.1	11,730	23,400	40,700	79,100	139,800	214,900	286,500	398,500
Colorado River at San Saba, TX (USGS Gage 08147000)	CO_Colorado_J190	20479.1	11,980	25,600	43,400	87,000	144,200	223,600	299,100	413,400
Colorado River at Bend, TX (LCRA Gage 1925)	CO_Colorado_J200	20615.4	5,070	14,700	33,900	62,700	115,500	183,600	239,100	329,600

Location Description	HEC-HMS Element Name	HEC-HMS Drainage Area (sq mi)	50% AEP 2-yr	20% AEP 5-yr	10% AEP 10-yr	4% AEP 25-yr	2% AEP 50-yr	1% AEP 100-yr	0.5% AEP 200-yr	0.2% AEP 500-yr
Colorado River below Cherokee Creek	CO_Colorado_J210	20797.7	7,990	18,700	36,500	63,500	112,900	179,600	236,000	326,700
Colorado River below Yancey Creek	CO_Colorado_J220	20901.5	9,250	20,700	36,600	63,100	111,900	177,200	234,700	325,700
Colorado River above Fall Creek	CO_Colorado_J229	20970.5	6,350	16,600	34,000	61,300	112,100	176,800	234,400	323,600
Colorado River below Fall Creek	CO_Colorado_J230	21024.4	5,090	14,800	33,100	60,700	112,400	176,500	234,200	323,000
Inflow to Lake Buchanan	BUCHANAN_INFLOW	21170.9	11,700	26,200	37,600	62,800	110,000	163,200	221,800	307,400
Colorado River below Lake Buchanan	BUCHANAN_OUTFLOW	21170.9	8,880	19,500	31,100	59,200	108,700	152,000	217,600	307,000
Inflow to Inks Lake	INKS_INFLOW	21210.6	8,820	19,200	30,500	59,200	109,500	152,300	219,700	308,100
Colorado River below Inks Lake	INKS_OUTFLOW	21210.6	8,820	19,200	30,500	59,200	109,300	152,300	219,300	308,100
Colorado River above the Llano River	CO_Colorado_J239	21246.0	8,350	18,700	30,700	58,200	108,200	152,000	218,100	307,300
South Llano River below Deer Creek	LN_SLlano_J30	433.8	10,620	30,200	50,100	82,000	110,100	140,700	172,800	215,700
South Llano River above Paint Creek	LN_SLlano_J39	524.1	9,980	31,900	52,800	86,900	118,100	153,400	191,100	241,500
South Llano River at Telegraph (LCRA gage)	LN_SLlano_J40	741.8	15,260	53,800	84,300	130,100	171,000	221,200	275,700	348,800
South Llano River below Chalk Creek	LN_SLlano_J50	849.8	13,920	51,200	84,400	136,100	179,900	235,400	293,300	373,900
South Llano River at Junction, TX (USGS Gage 08149900)	LN_SLlano_J60	878.9	12,990	49,300	82,300	134,400	178,800	233,800	292,600	374,000
South Llano River above the Llano River	LN_SLlano_J70	932.6	13,270	49,700	81,700	135,900	180,000	236,000	295,100	379,800
North Llano River below Dry Llano River	LN_NLlano_J30	392.6	7,050	22,000	35,300	58,600	77,100	96,300	116,100	144,700
North Llano River above Maynard Creek	LN_NLlano_J39	447.7	5,800	20,500	34,600	60,200	80,100	101,400	123,400	154,700
North Llano River below Maynard Creek	LN_NLlano_J40	520.6	5,620	22,200	38,800	68,300	90,900	116,100	141,500	177,900
North Llano River below Copperas Creek	LN_NLlano_J50	656.9	6,350	24,300	43,300	79,400	108,300	139,400	169,700	215,300
North Llano River near Roosevelt (LCRA Gage)	LN_NLlano_J60	703.0	6,300	25,000	45,000	83,100	113,600	146,500	178,500	226,600
North Llano River above Bear Creek	LN_NLlano_J69	763.9	6,190	25,800	45,700	84,300	116,100	150,600	184,000	236,600
North Llano River below Bear Creek	LN_NLlano_J70	895.6	6,190	27,600	50,200	92,200	127,300	165,300	203,200	263,100
North Llano River nr Junction, TX (USGS Gage 08148500)	LN_NLlano_J80	901.7	6,340	27,700	50,000	91,800	126,800	164,400	201,800	261,400
North Llano River above the South Llano River	LN_NLlano_J90	919.1	6,320	27,700	50,500	92,100	127,600	165,900	204,100	264,800
Llano River below the North and South Llano Rivers	LN_Llano_J10	1851.7	11,470	52,500	96,200	174,100	236,800	315,500	391,000	512,500
Llano River nr Junction, TX (USGS Gage 08150000)	LN_Llano_J20	1858.2	10,640	51,000	94,500	172,300	235,700	313,100	389,700	511,700
Llano River above Johnson Fork	LN_Llano_J29	1869.2	10,610	50,300	93,300	168,300	233,100	311,200	387,500	509,300
Llano River below Johnson Fork	LN_Llano_J30	2191.3	10,920	52,600	100,400	180,700	262,000	346,600	440,300	584,200

Location Description	HEC-HMS Element Name	HEC-HMS Drainage Area (sq mi)	50% AEP	20% AEP	10% AEP	4% AEP	2% AEP	1% AEP	0.5% AEP	0.2% AEP
			2-yr	5-yr	10-yr	25-yr	50-yr	100-yr	200-yr	500-yr
Llano River below Gentry Creek	LN_Llano_J40	2247.6	12,690	50,100	91,300	169,800	248,600	338,800	432,400	578,400
Llano River above Big Saline Creek	LN_Llano_J49	2392.9	8,790	51,200	97,100	175,700	247,300	332,700	423,100	565,200
Llano River below Big Saline Creek	LN_Llano_J50	2478.2	9,050	51,000	97,000	175,400	248,300	333,000	423,900	566,600
Llano River below Leon Creek	LN_Llano_J60	2609.2	8,460	50,900	97,000	175,500	246,900	332,200	422,400	564,400
Llano River above the James River	LN_Llano_J69	2760.3	8,010	49,300	97,000	175,100	244,600	330,100	418,800	559,500
Llano River below the James River	LN_Llano_J70	3100.0	19,570	70,600	126,600	222,600	283,100	359,000	430,400	534,500
Llano River above Comanche Creek	LN_Llano_J79	3175.6	13,140	58,400	111,800	207,800	267,400	345,900	420,000	529,100
Llano River below Comanche Creek	LN_Llano_J80	3244.3	17,130	66,400	122,100	217,600	283,600	364,900	441,100	554,400
Llano Rv nr Mason, TX (USGS Gage 08150700)	LN_Llano_J90	3250.8	17,760	62,700	114,800	209,800	277,200	359,200	435,500	547,500
Llano River below Beaver Creek	LN_Llano_J100	3470.0	17,500	73,000	133,800	246,700	327,400	428,800	524,800	663,500
Llano River below Willow Creek	LN_Llano_J110	3556.9	17,540	77,000	139,200	250,700	333,500	437,900	536,000	680,300
Llano River at RM-2768 at Castell, TX	LN_Llano_J120	3639.4	16,240	72,700	132,400	242,900	326,000	428,500	529,400	678,000
Llano River above Hickory Creek	LN_Llano_J129	3723.8	15,950	72,400	131,100	232,600	311,500	412,400	512,500	664,400
Llano River below Hickory Creek	LN_Llano_J130	3891.8	17,520	78,200	139,100	243,800	327,300	435,600	542,500	705,700
Llano River above San Fernando Creek	LN_Llano_J139	3924.8	18,270	77,100	137,300	242,200	325,300	432,800	540,300	703,100
Llano River below San Fernando Creek	LN_Llano_J140	4060.3	18,820	71,600	129,800	235,700	319,300	429,300	540,700	712,800
Llano River below Johnson Creek	LN_Llano_J150	4118.4	18,720	72,700	130,700	236,400	320,600	430,200	542,200	714,000
Llano River below Pecan Creek	LN_Llano_J160	4187.0	22,250	75,500	132,200	238,300	323,000	433,800	545,600	716,200
Llano River at Llano, TX (USGS Gage 08151500)	LN_Llano_J170	4202.0	20,110	71,700	127,100	233,300	317,200	428,100	541,400	716,900
Llano River above the Little Llano River	LN_Llano_J179	4279.1	17,240	73,100	130,100	235,000	317,400	425,400	534,900	705,100
Llano River below the Little Llano River	LN_Llano_J180	4331.6	15,910	72,500	129,700	233,900	316,000	423,000	532,500	702,100
Llano River above Honey Creek	LN_Llano_J189	4410.8	14,250	62,900	110,800	203,500	290,000	395,300	503,200	670,200
Llano River below Honey Creek	LN_Llano_J190	4450.5	13,010	60,400	107,500	199,600	286,400	390,000	495,600	655,900
Llano River above the Colorado River	LN_Llano_J200	4465.4	13,650	61,100	106,700	197,400	284,400	388,000	495,200	662,200
Colorado River below the Llano River	CO_Colorado_J240	25711.5	20,370	69,400	115,600	212,100	284,800	411,500	544,900	765,900
Colorado River above Sandy Creek	CO_Colorado_J249	25738.9	20,070	68,600	115,300	211,500	284,200	412,000	553,800	770,800
Sandy Ck nr Kingsland, TX (USGS Gage 08152000)	SD_SandyCr_J40	346.2	8,200	21,100	34,900	73,500	109,200	140,500	172,900	221,600
Colorado River below Sandy Creek	CO_Colorado_J250	26130.1	20,440	71,300	119,400	221,900	301,200	435,200	572,600	812,400
Inflow to Lake LBJ	LBJ_INFLOW	26178.0	19,510	70,200	117,700	218,900	298,400	431,000	566,100	804,000

Location Description	HEC-HMS Element Name	HEC-HMS Drainage Area (sq mi)	50% AEP	20% AEP	10% AEP	4% AEP	2% AEP	1% AEP	0.5% AEP	0.2% AEP
			2-yr	5-yr	10-yr	25-yr	50-yr	100-yr	200-yr	500-yr
Colorado River below Lake LBJ	LBJ_OUTFLOW	26178.0	18,270	63,400	106,600	205,300	299,300	368,800	436,100	649,700
Colorado River below Backbone Creek	CO_Colorado_J255	26234.1	19,970	69,300	114,500	214,700	295,900	370,500	473,300	736,800
Inflow to Lake Marble Falls	MARBLE_FALLS_INFLOW	26260.2	22,470	70,700	110,100	205,800	299,900	369,400	468,600	725,500
Colorado River below Lake Marble Falls	MARBLE_FALLS _OUTFLOW	26260.2	22,470	70,700	110,100	205,900	289,400	369,400	468,600	725,500
Colorado River below Hamilton Creek	CO_Colorado_J260	26350.6	22,070	71,100	113,400	212,500	296,100	371,600	484,700	747,900
Colorado River below Double Horn Creek	CO_Colorado_J270	26405.3	22,540	69,700	109,100	206,300	289,800	370,900	480,200	738,000
Colorado River above the Pedernales River	CO_Colorado_J279	26483.8	15,530	47,000	73,400	169,700	265,600	377,800	460,600	615,300
Pedernales Rv nr Fredericksburg, TX (USGS Gage 08152900)	PD_Pedernales_J50	369.6	5,130	19,300	36,300	73,500	116,500	154,300	194,000	249,300
Pedernales River above South Grape Creek	PD_Pedernales_J59	507.6	7,230	29,500	48,600	79,400	133,200	181,300	231,500	316,600
Pedernales River below South Grape Creek	PD_Pedernales_J60	570.6	8,720	30,900	52,600	82,700	138,000	191,700	249,800	346,600
Pedernales River at LBJ Ranch near Stonewall, TX (LCRA Gage)	PD_Pedernales_J70	625.6	7,250	26,700	47,300	79,700	132,400	185,300	245,700	340,300
Pedernales River below Williams Creek	PD_Pedernales_J80	668.2	11,490	34,100	57,300	93,600	140,400	197,600	265,200	369,400
Pedernales River above North Grape Creek	PD_Pedernales_J89	730.0	11,100	33,600	58,100	95,000	139,800	196,600	265,500	371,700
Pedernales River below North Grape Creek	PD_Pedernales_J90	845.3	17,280	44,400	76,000	121,800	160,800	211,500	264,700	349,300
Pedernales Rv nr Johnson City, TX (USGS Gage 08153500)	PD_Pedernales_J100	900.9	19,480	52,900	87,500	140,000	180,200	231,700	288,800	374,300
Pedernales River above Miller Creek	PD_Pedernales_J109	959.5	15,530	41,900	75,000	127,000	168,800	226,200	288,800	379,300
Pedernales River below Miller Creek	PD_Pedernales_J110	1048.0	15,910	44,800	81,500	140,800	188,900	253,900	327,900	431,000
Pedernales River above Flat Creek	PD_Pedernales_J119	1080.1	14,490	41,800	77,600	136,800	185,500	252,300	326,900	432,700
Pedernales River below Flat Creek	PD_Pedernales_J120	1117.2	15,190	51,300	81,300	133,500	185,800	254,800	327,100	433,200
Pedernales River above Cypress Creek	PD_Pedernales_J129	1150.6	13,420	48,400	79,800	132,900	185,100	255,400	330,100	437,000
Pedernales River below Cypress Creek	PD_Pedernales_J130	1232.3	13,810	53,700	90,500	145,800	198,400	271,700	353,400	471,900
Pedernales River above the Colorado River	PD_Perdenales_J140	1280.9	9,550	42,300	76,900	137,000	192,700	269,900	351,700	471,000
Colorado River below the Pedernales River	CO_Colorado_J280	27764.7	13,950	54,100	106,600	217,100	356,100	521,300	678,900	850,000
Colorado River below Cow Creek	CO_Colorado_J290	27829.7	13,880	54,400	108,800	220,900	361,300	530,200	685,200	862,700
Colorado River below Big Sandy Creek 2	CO_Colorado_J300	27981.8	14,000	54,900	108,200	228,900	375,200	556,500	729,700	908,500
Inflow to Lake Travis / Marshall Ford	MARSHALL_FORD _INFLOW	28007.0	14,160	55,500	107,700	230,000	376,500	558,900	735,100	914,100
Colorado River below Marshall Ford Dam	MARSHALL_FORD _OUTFLOW	28007.0	4,710	13,700	23,000	30,000	30,000	60,500	98,400	181,600
Colorado River at Austin, TX (USGS Gage 08158000)	CO_Colorado_J340	250.2	13,600	29,500	45,600	71,200	93,200	120,200	149,900	193,800

Location Description	HEC-HMS Element Name	HEC-HMS Drainage Area (sq mi)	50% AEP	20% AEP	10% AEP	4% AEP	2% AEP	1% AEP	0.5% AEP	0.2% AEP
			2-yr	5-yr	10-yr	25-yr	50-yr	100-yr	200-yr	500-yr
Colorado River above Walnut Creek	CO_Colorado_J349	270.7	12,960	27,200	41,600	66,800	87,900	115,800	148,900	195,400
Colorado River below Walnut 1 Creek	CO_Colorado_J350	327.2	16,080	33,600	49,900	78,500	102,700	135,900	177,600	233,000
Colorado River at Del Valle, TX (LCRA Gage)	CO_Colorado_J360	341.2	17,090	34,500	51,000	78,400	102,000	133,000	171,300	220,400
Colorado River above Onion Creek	CO_Colorado_J369	347.8	16,070	32,000	47,000	75,000	97,900	128,900	165,600	220,000
Onion Ck at US Hwy 183, Austin, TX (USGS Gage 08159000)	ON_OnionCr_J50	323.7	6,900	28,500	52,200	86,500	109,000	137,800	170,400	215,300
Onion Creek above the Colorado River	ON_OnionCr_J60	345.0	7,930	28,200	52,100	86,800	113,800	147,100	180,200	228,300
Colorado River below Onion Creek	CO_Colorado_J370	692.9	17,600	46,700	79,100	137,600	182,000	241,100	305,800	406,200
Colorado River above Gilleland Creek	CO_Colorado_J379	699.2	17,180	45,200	75,700	131,800	175,900	237,200	301,700	398,900
Colorado River near Webberville (LCRA Gage)	CO_Colorado_J380	774.5	19,670	48,500	79,900	137,900	183,200	249,300	316,400	417,600
Colorado River below Dry Creek	CO_Colorado_J390	855.1	17,950	45,600	69,400	107,100	137,000	183,400	245,100	341,700
Colorado River below Wilbarger Creek	CO_Colorado_J400	1058.9	19,400	42,600	64,400	97,600	122,900	162,300	206,700	280,100
Colorado River at Sim Gideon River Plant (LCRA Gage)	CO_Colorado_J410	1171.4	19,530	42,900	64,600	97,800	122,800	162,300	206,100	278,200
Colorado River at Bastrop, TX (USGS Gage 08159200)	CO_Colorado_J420	1223.8	19,790	42,700	64,200	96,900	121,000	159,600	202,400	267,200
Colorado River near Upton (LCRA Gage)	CO_Colorado_J430	1602.9	23,350	46,800	68,600	100,400	124,600	164,100	209,000	268,300
Colorado Rv at Smithville, TX (USGS Gage 08159500)	CO_Colorado_J440	1705.8	21,720	41,800	62,000	90,400	114,400	149,500	190,900	245,500
Colorado River below Bartons Creek	CO_Colorado_J450	1789.8	22,060	43,900	64,300	93,500	117,400	154,600	197,200	257,600
Colorado River below Pin Oak Creek	CO_Colorado_J460	1925.4	24,270	46,600	66,300	94,900	118,500	156,000	199,000	261,600
Colorado River below Rabbs Creek	CO_Colorado_J470	2089.1	24,550	45,200	62,600	87,500	110,700	146,400	186,700	250,100
Colorado Rv abv La Grange, TX (USGS Gage 08160400)	CO_Colorado_J480	2117.3	25,340	46,000	62,800	87,000	108,500	143,200	182,600	244,000
Colorado River below Buckners Creek	CO_Colorado_J490	2305.9	25,480	47,000	64,000	88,600	110,500	146,200	186,300	248,800
Colorado River below Williams Creek	CO_Colorado_J500	2409.2	27,290	48,900	65,600	89,400	111,000	146,300	186,100	248,500
Colorado River below Bruch Creek	CO_Colorado_J510	2491.3	26,350	47,600	62,500	84,200	105,800	140,400	179,000	241,300
Colorado River above Cummins Creek	CO_Colorado_River_J519	2569.8	26,920	48,700	63,400	84,400	106,600	141,800	180,300	242,900
Colorado River at Columbus, TX (USGS Gage 08161000)	CO_Colorado_J520	2885.1	28,700	51,000	65,700	86,400	108,400	144,800	183,800	246,200
Colorado River near Altair (LCRA Gage 6377)	CO_Colorado_J525	2979.6	28,840	49,300	61,500	78,300	93,100	116,900	139,100	181,100
Colorado River near Garwood (LCRA Gage)	CO_Colorado_J530	3090.4	29,040	49,900	62,100	79,000	93,700	116,200	140,300	181,400
Colorado River below Marys Branch	CO_Colorado_J540	3153.1	29,400	49,700	61,500	78,600	93,400	116,100	140,300	181,600
Colorado River below Robb Slough	CO_Colorado_J550	3216.2	28,690	48,700	59,100	75,800	91,400	114,500	138,900	177,100

Location Description	HEC-HMS Element Name	HEC-HMS Drainage Area (sq mi)	50% AEP 2-yr	20% AEP 5-yr	10% AEP 10-yr	4% AEP 25-yr	2% AEP 50-yr	1% AEP 100-yr	0.5% AEP 200-yr	0.2% AEP 500-yr
Colorado Rv at Wharton, TX (USGS Gage 08162000)	CO_Colorado_J560	3248.3	27,530	48,700	58,600	71,100	81,000	101,600	124,800	160,000
Colorado River near Lane City, TX (LCRA Gage 6537)	CO_Colorado_J570	3277.9	27,670	49,000	58,800	70,900	80,200	98,900	124,400	157,700
Colorado River below Jones Creek	CO_Colorado_J580	3396.5	27,900	49,400	59,200	71,000	79,800	97,300	121,500	157,300
Colorado River below Blue Creek	CO_Colorado_J590	3498.6	27,860	49,700	59,400	71,100	79,400	95,800	119,000	155,300
Colorado River near Bay City, TX (USGS Gage 08162500)	CO_Colorado_J600	3529.6	25,930	49,100	59,400	71,700	79,800	95,600	117,900	154,400
Colorado River near Buckeye, TX	CO_Colorado_J610	3556.8	27,290	49,900	59,800	71,400	79,700	95,200	116,700	153,200
Colorado River near Wadsworth, TX (USGS Gage 08162501)	CO_Colorado_J620	3595.2	27,130	50,000	59,900	71,400	79,700	94,800	116,300	152,700
Colorado River nr Matagorda, TX (LCRA Gage)	CO_Colorado_J630	3629.9	27,380	49,900	59,500	71,100	79,200	94,600	115,800	152,700
Colorado River at the Gulf of Mexico	Outlet	3632.5	27,610	49,800	59,300	70,900	79,000	94,500	115,700	152,800

Table 7.3: Peak Reservoir Pool Elevations (feet NAVD88) from the HEC-HMS Elliptical Frequency Storms

					Reservoir Elevations (ft NAVD 88)							
					50% AEP	20% AEP	10% AEP	4% AEP	2% AEP	1% AEP	0.5% AEP	0.2% AEP
Reservoir Name	HEC-HMS Drainage Area (sq mi)	Lon	Lat	Theta	2-yr	5-yr	10-yr	25-yr	50-yr	100-yr	200-yr	500-yr
O.C. Fisher Reservoir	1462.8	-100.85217	31.73665	7.40	1885.3	1887.5	1889.8	1899.1	1910.0	1919.2	1925.9	1932.6
Twin Buttes Reservoir	3422.5	-101.10568	31.30149	161.48	1933.5	1934.4	1937.5	1944.8	1952.2	1959.3	1964.7	1971.5
O.H. Ivie Reservoir	13298.7	-100.10964	31.74297	62.35	1548.3	1549.1	1550.1	1552.2	1553.8	1554.8	1557.1	1560.9
Lake Brownwood	1513.0	-99.27687	32.03359	138.90	1426.9	1428.8	1430.3	1431.6	1433.3	1435.4	1437.9	1441.7
Brady Creek Reservoir	524.0	-99.71700	31.17441	42.97	1744.1	1745.3	1746.4	1748.0	1752.4	1757.6	1763.1	1765.9
Lake Buchanan	21170.9	-99.29966	31.00310	15.06	1019.4	1019.7	1019.9	1020.3	1020.5	1021.0	1021.7	1022.5
Lake LBJ	26178.0	-99.16505	30.64069	17.06	825.6	826.5	827.1	827.9	828.7	831.0	837.2	842.2
Lake Travis	28007.0	-99.16812	30.60061	177.74	683.0	685.7	688.6	695.7	709.3	714.8	721.7	732.0

*NOTE: Elevations for Lake Travis are in "msl", which is LCRA's Hydromet Datum. The datum conversion from msl to NAVD88 is +0.6 ft for Lake Travis.

Table 7.4: Reservoir Peak Outflow (cfs) from the HEC-HMS Elliptical Frequency Storms

					Reservoir Peak Outflows (cfs)							
					50% AEP	20% AEP	10% AEP	4% AEP	2% AEP	1% AEP	0.5% AEP	0.2% AEP
Reservoir Name	HEC-HMS Drainage Area (sq mi)	Lon	Lat	Theta	2-yr	5-yr	10-yr	25-yr	50-yr	100-yr	200-yr	500-yr
O.C. Fisher Reservoir	1462.8	-100.85217	31.73665	7.40	0	0	0	0	0	0	0	0
Twin Buttes Reservoir	3422.5	-101.10568	31.30149	161.48	0	0	0	3,307	5,192	9,000	9,000	9,000
O.H. Ivie Reservoir	13298.7	-100.10964	31.74297	62.35	15	15	15	28,985	96,915	125,944	154,921	188,484
Lake Brownwood	1513.0	-99.27687	32.03359	138.90	4,242	9,844	14,872	20,415	28,056	38,980	54,013	81,639
Brady Creek Reservoir	524.0	-99.71700	31.17441	42.97	91	213	423	576	1,018	1,535	5,230	25,297
Lake Buchanan	21170.9	-99.29966	31.00310	15.06	9,716	21,340	32,006	60,401	122,219	152,000	217,643	306,986
Lake LBJ	26178.0	-99.16505	30.64069	17.06	22,885	71,173	112,056	210,862	323,651	370,169	487,438	752,336
Lake Travis	28007.0	-99.16812	30.60061	177.74	4,712	12,962	22,461	30,000	30,281	64,511	104,164	197,983

7.6.2 Map Results

The following ‘a’ figures represent the 100yr 48hr heatmap results for the optimization of each junction of interest in the Elliptical Frequency Storm HEC-HMS model. For each junction of interest, the optimization script ran 300 times or more recording the junction flow rate for various storm centerings and orientations. Each of the recorded storm centerings (x,y) and resulting flow rates (z) at the junction of interest were recorded and used to create a rasterized heat map. The red shading represents storm center locations that led to relatively high flow rates at the junction whereas the green shading represents storm center locations that led to relatively low flow rates.

The following ‘b’ figures show the final, total storm depths and optimized storm configurations for each junction. Note that the peak flow values recorded in the ‘a’ figures may differ slightly from the final peak flow values recorded in the ‘b’ figures and in Table 7.2 above. These differences are due to some small adjustments to the elliptical storm and HEC-HMS model parameters that occurred during the review process. The ‘b’ figures include the final peak flow values after peer review.

This section includes the figures for only a small sample of example locations from the Lower Colorado River basin. The elliptical storm maps for all of the locations that were analyzed can be found in Appendix C.

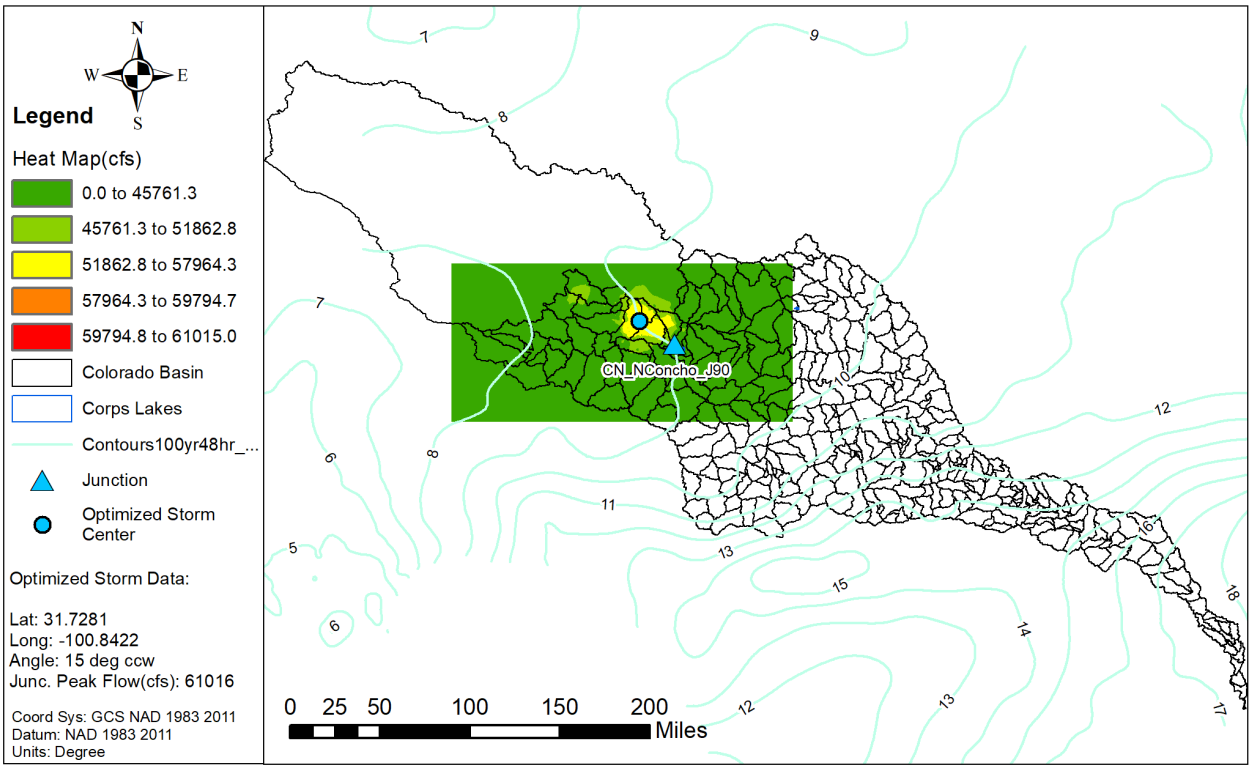

Figure 7.9a: Elliptical Storm Optimization Heat Map for North Concho River nr Grape Creek (CN_NConcho_J90)

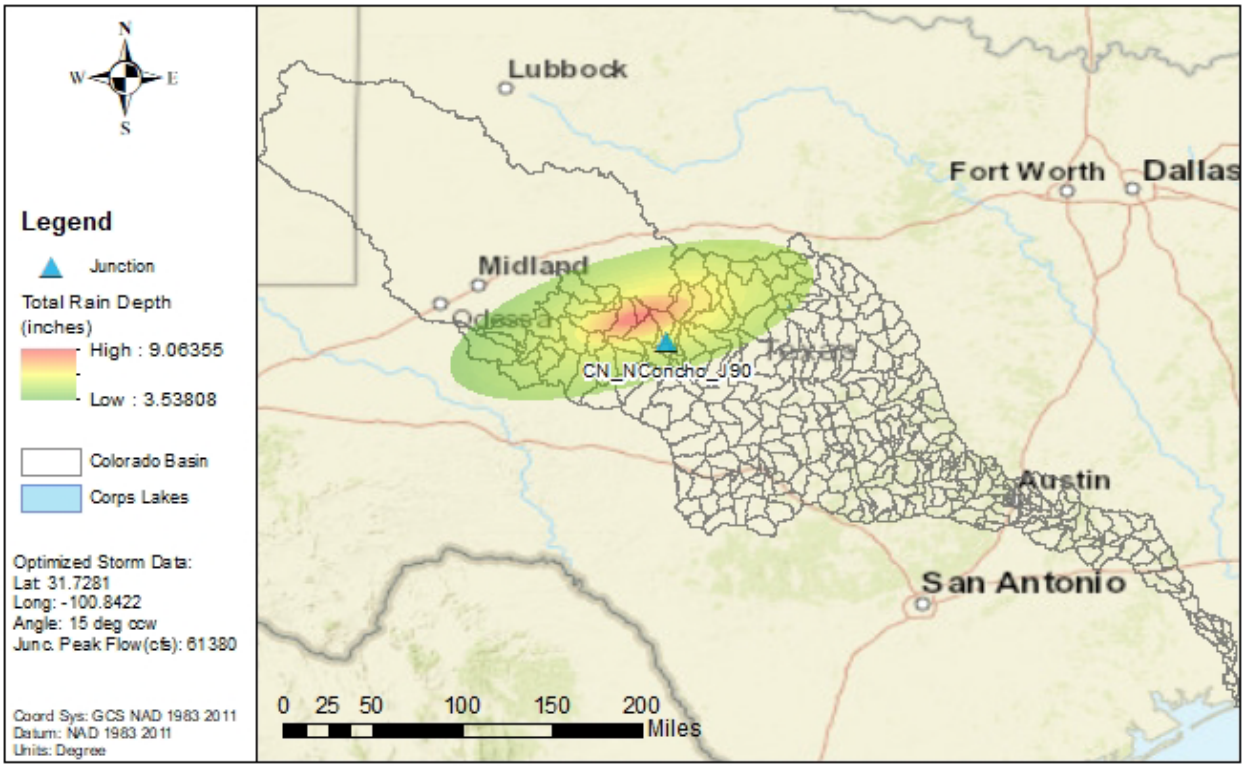

Figure 7.9b: NA14 1% AEP Elliptical Storm for North Concho River nr Grape Creek (CN_NConcho_J90)

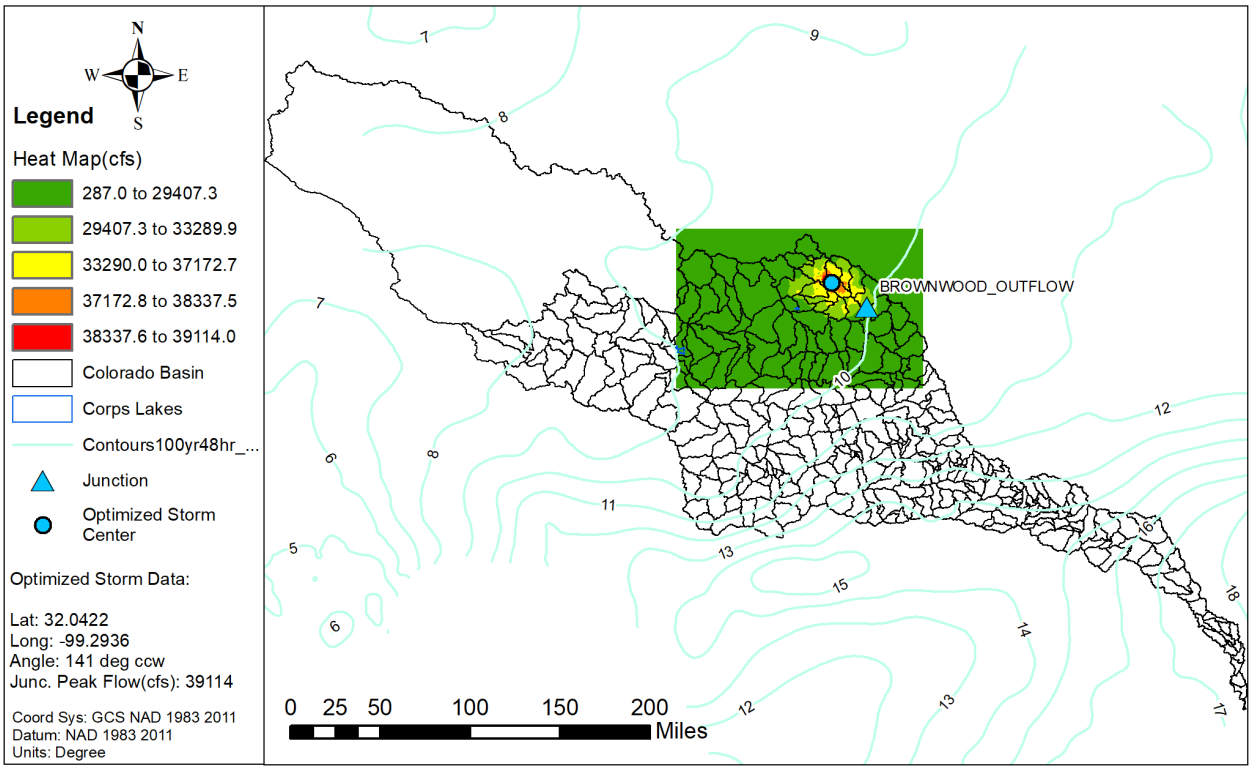

Figure 7.10a: Elliptical Storm Optimization Heat Map for Lake Brownwood

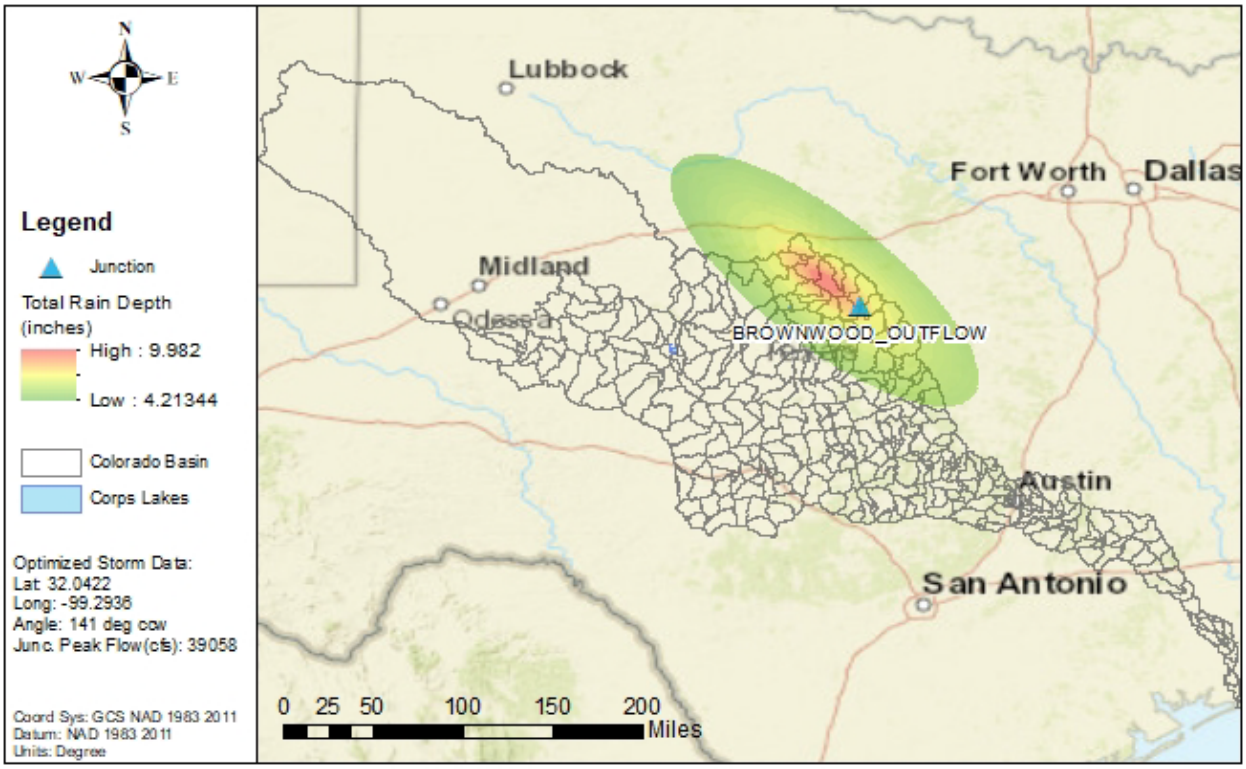

Figure 7.10b: NA14 1% AEP Elliptical Storm for Lake Brownwood

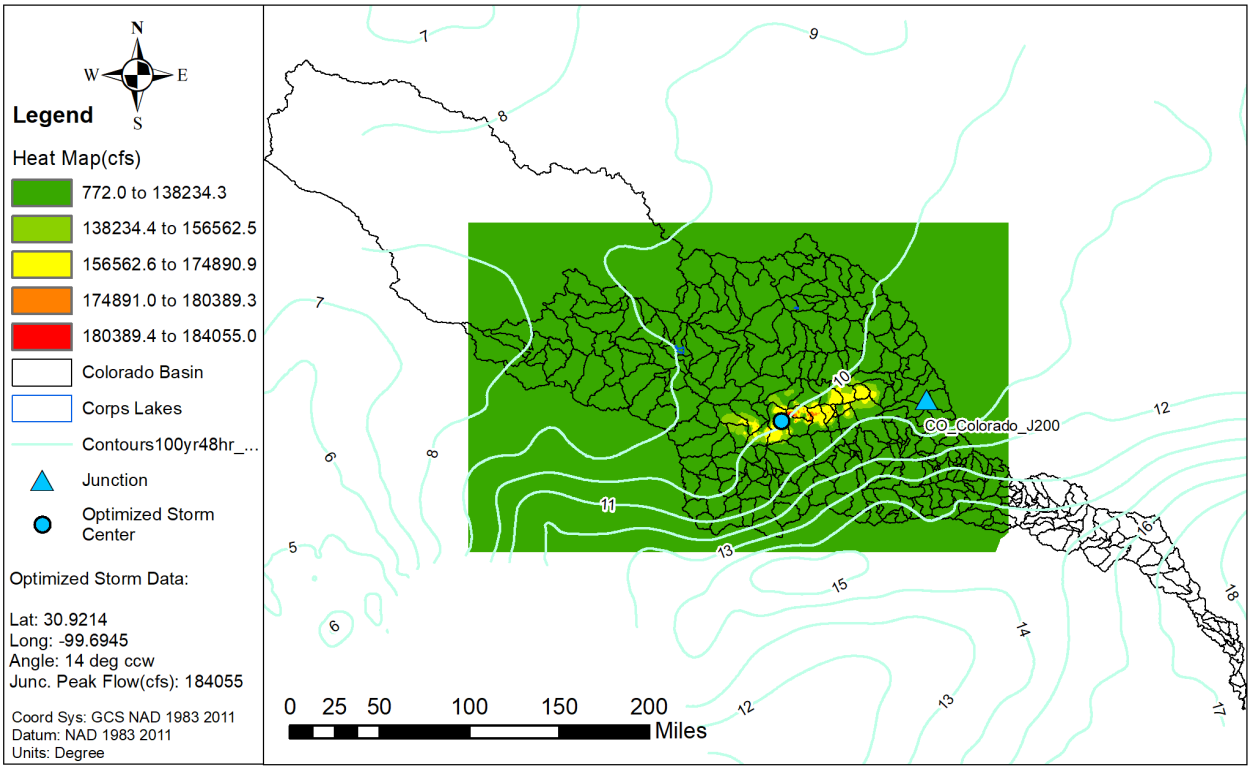

Figure 7.11a: Elliptical Storm Optimization Heat Map for the Colorado River at Bend, TX (CO_Colorado_J200)

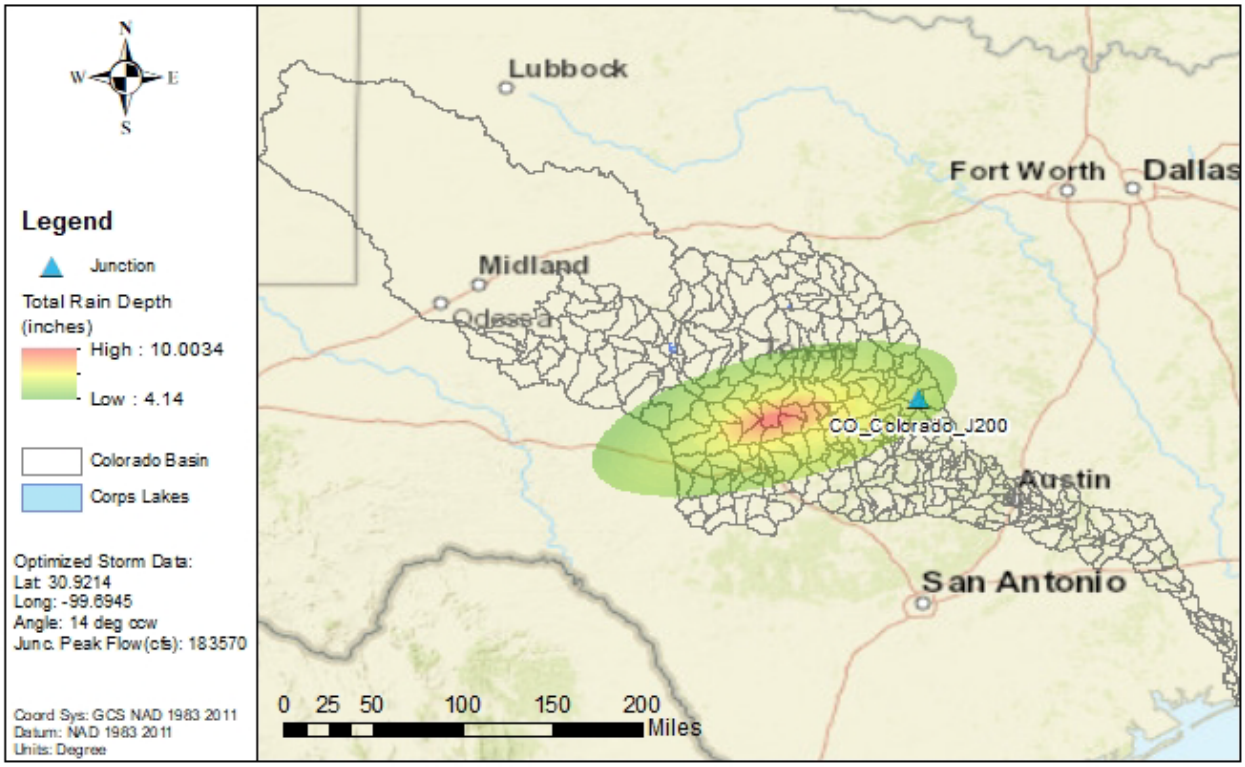

Figure 7.11b: NA14 1% AEP Elliptical Storm for the Colorado River at Bend, TX (CO_Colorado_J200)

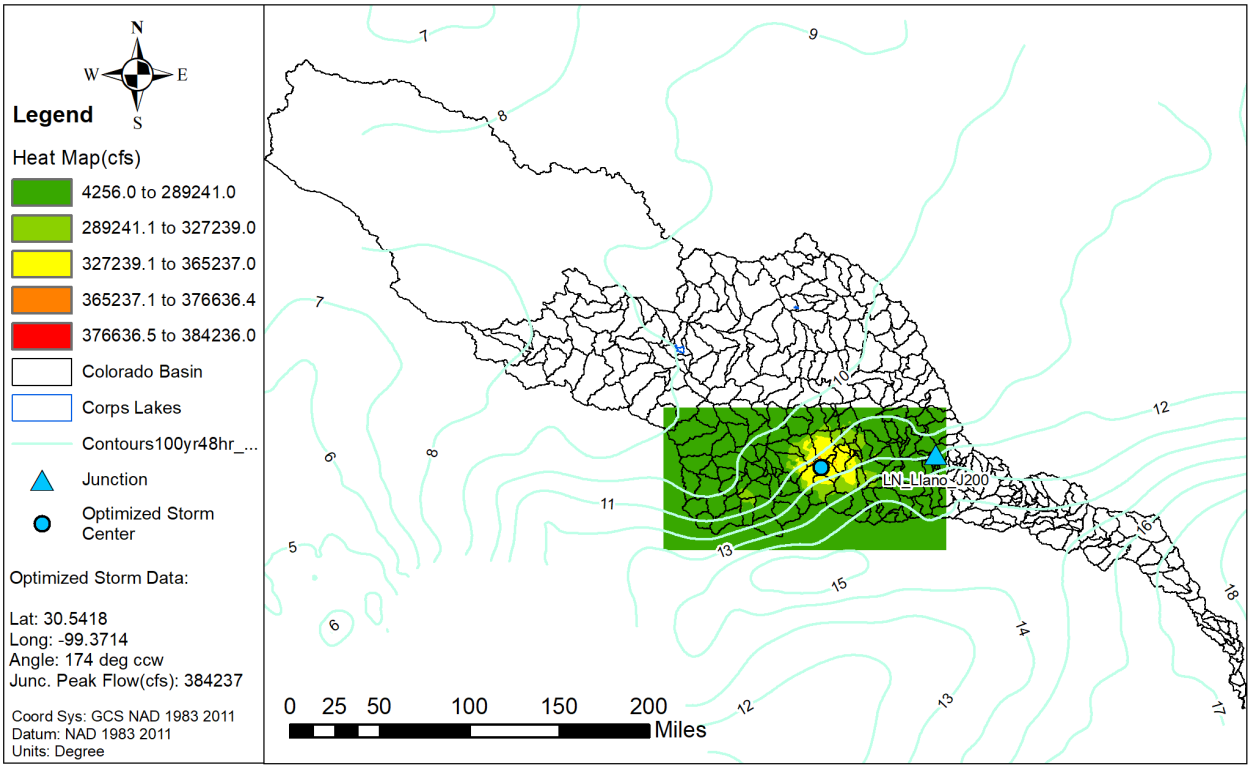

Figure 7.12a: Elliptical Storm Optimization Heat Map for the Llano River above the Colorado River (LN_Llano_J200)

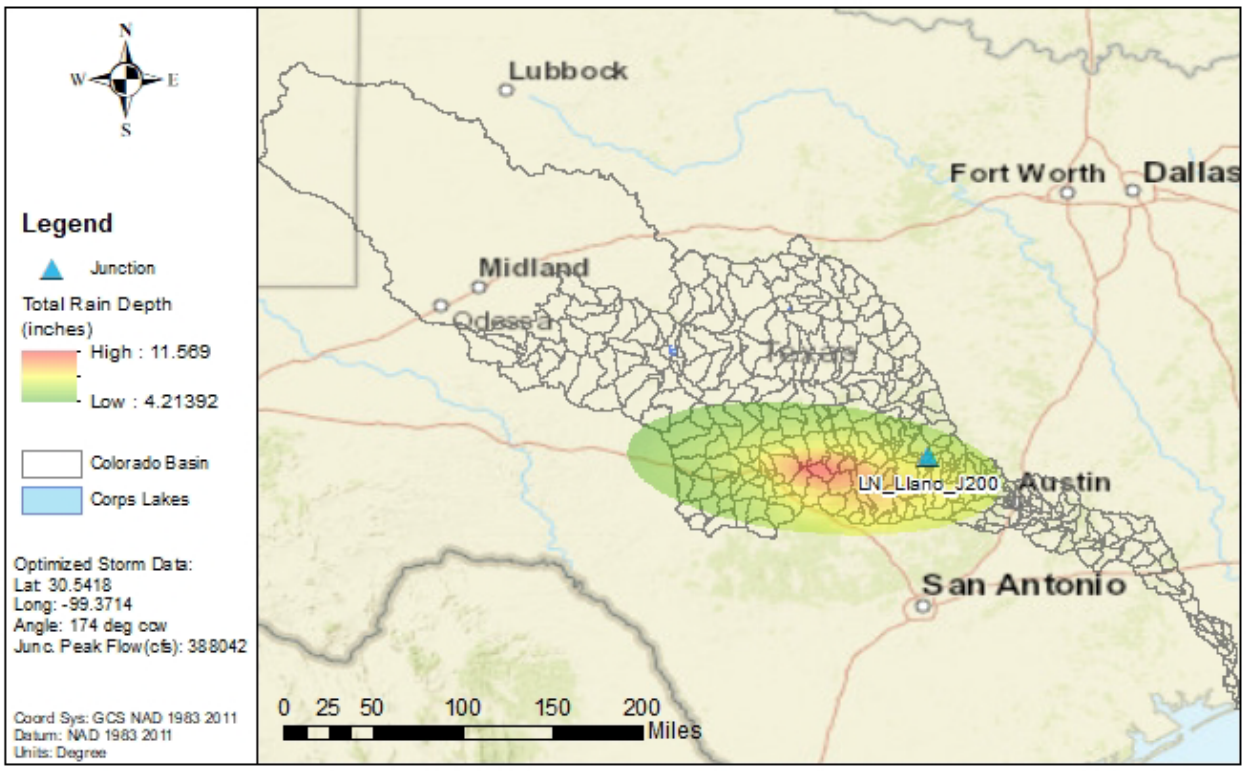

Figure 7.12b: NA14 1% AEP Elliptical Storm for the Llano River above the Colorado River (LN_Llano_J200)

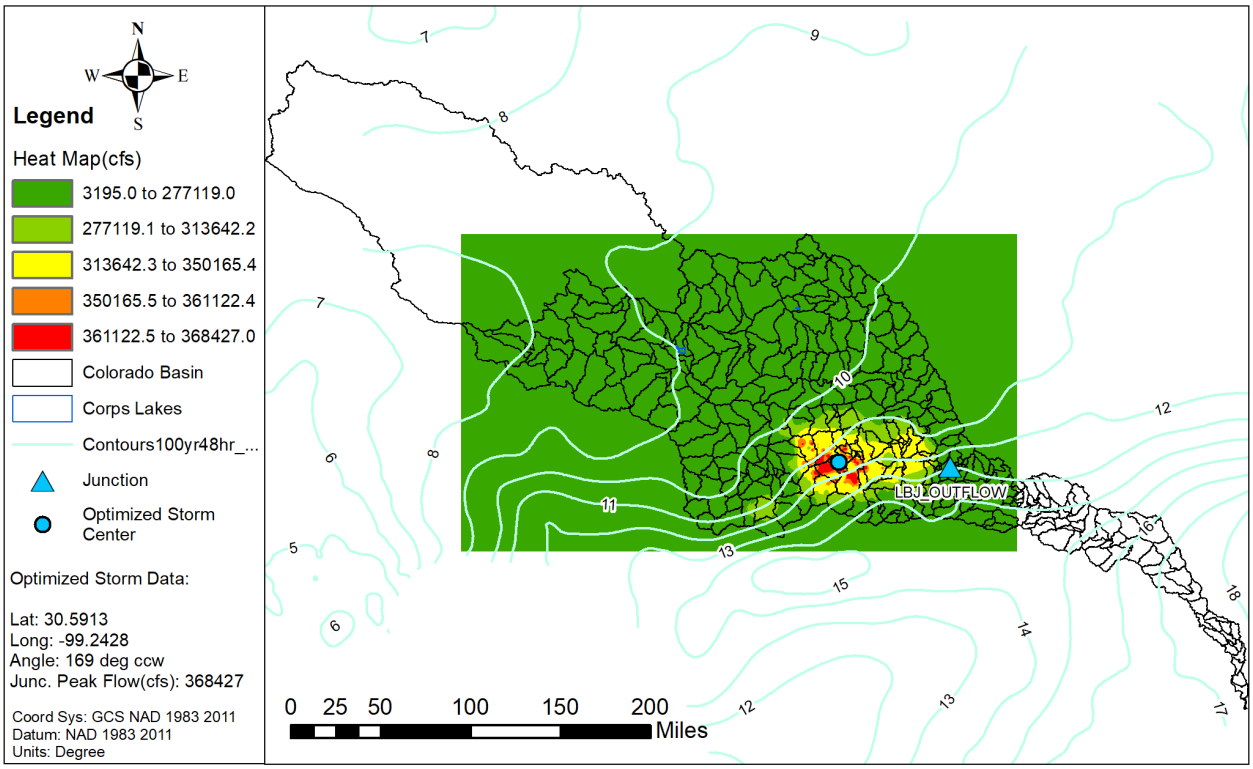

Figure 7.13a: Elliptical Storm Optimization Heat Map for Lake LBJ

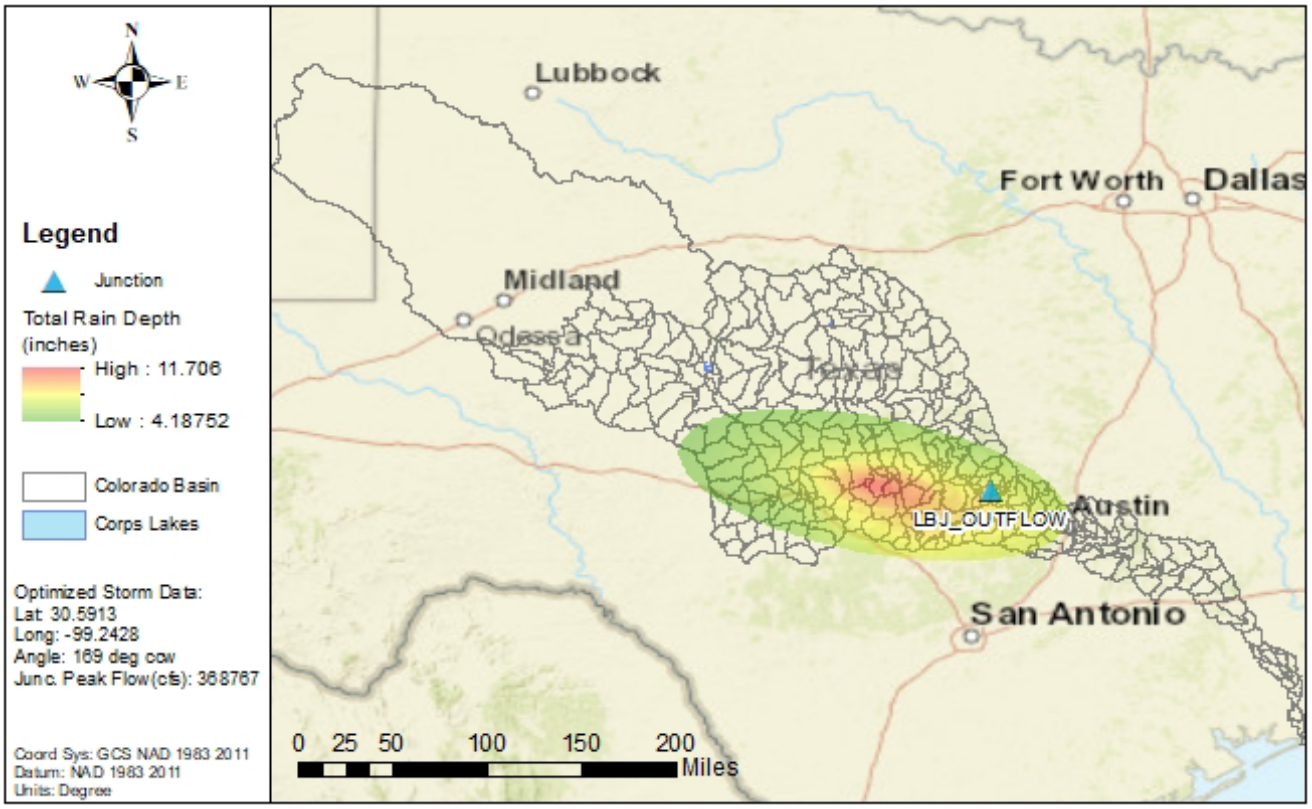

Figure 7.13b: NA14 1% AEP Elliptical Storm for Lake LBJ

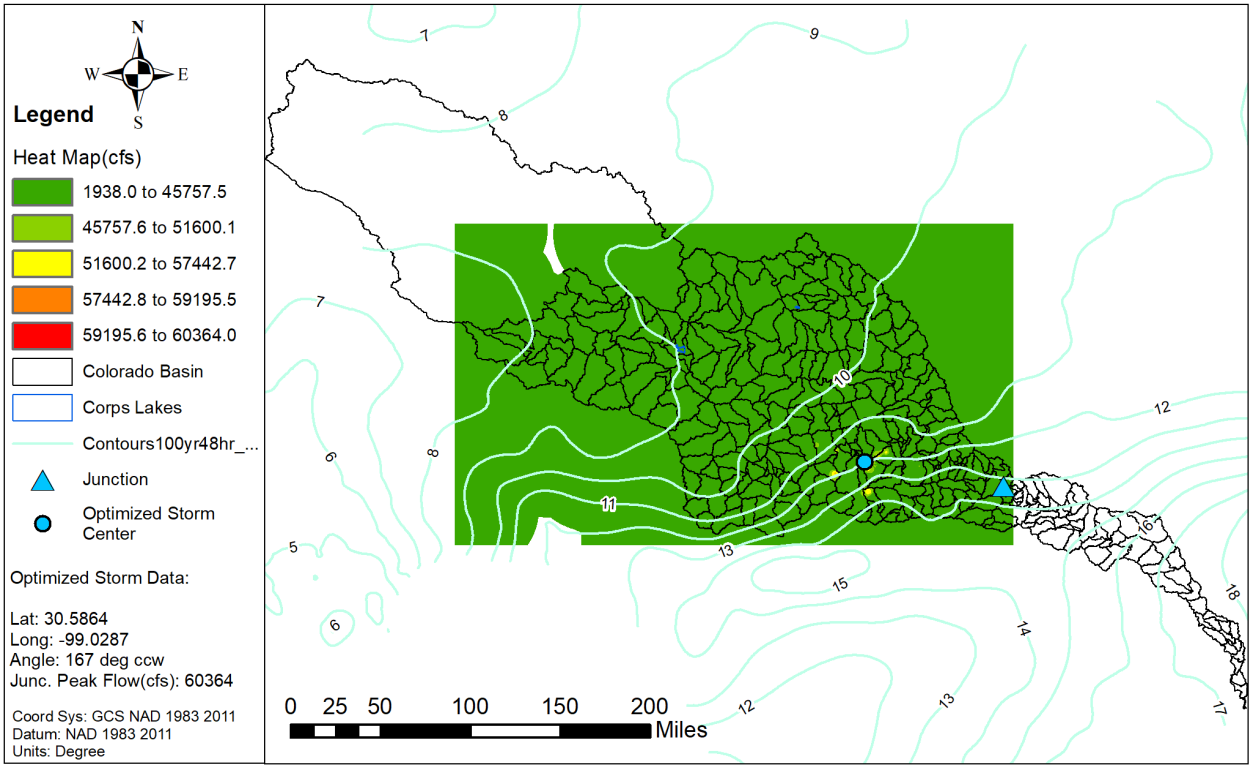

Figure 7.14a: Elliptical Storm Optimization Heat Map for Lake Travis (Marshall Ford)

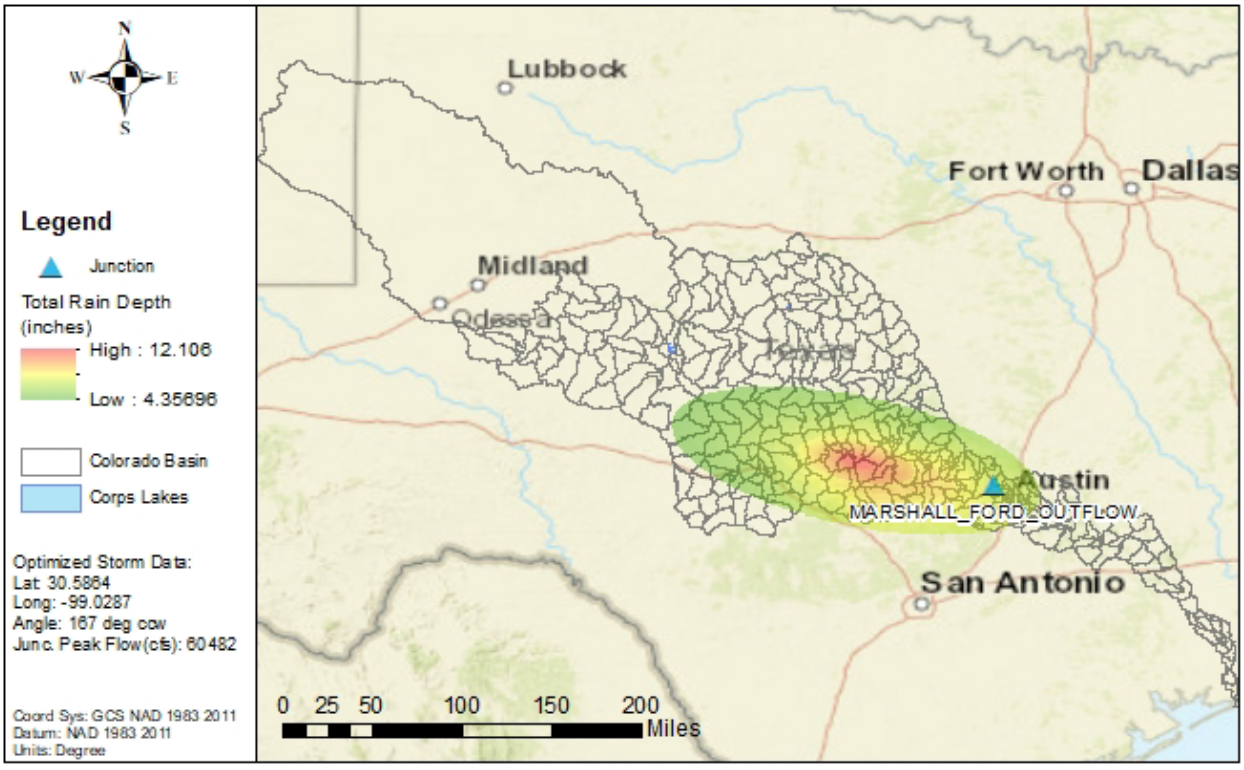

Figure 7.14b: NA14 1% AEP Elliptical Storm for Lake Travis (Marshall Ford)

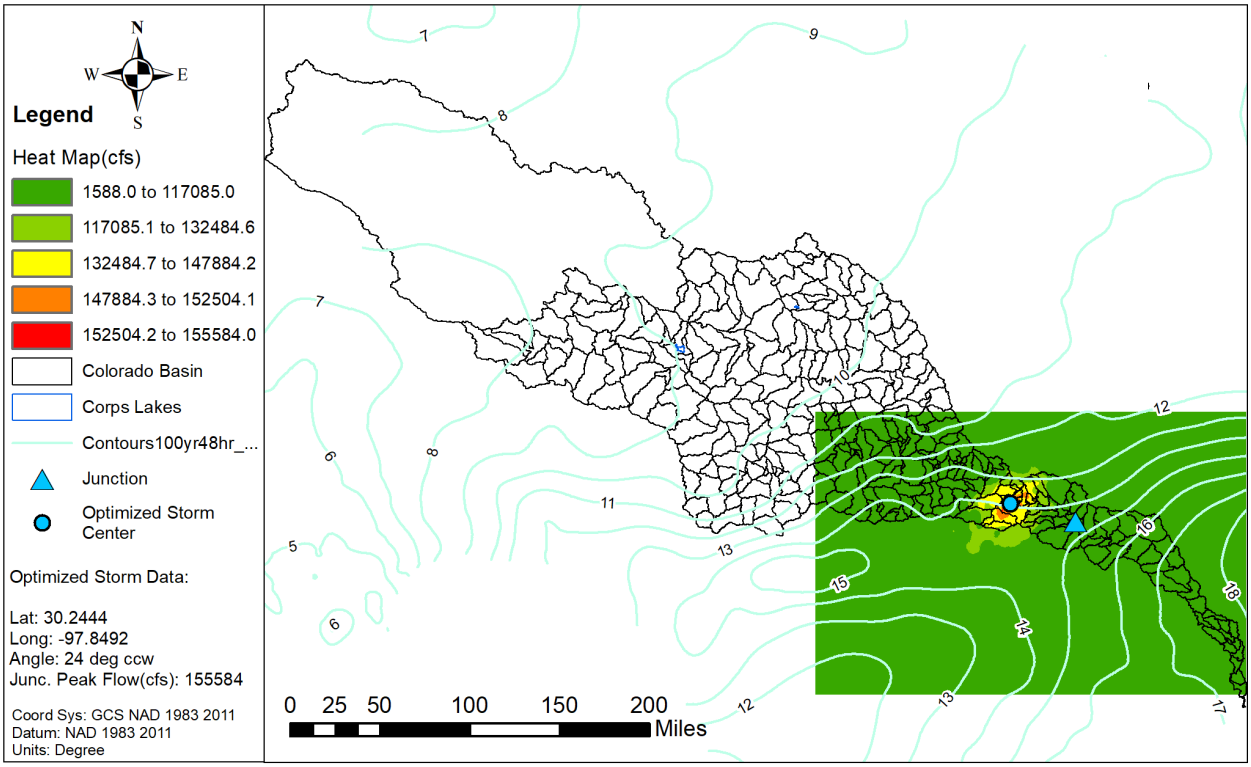

Figure 7.15a: Elliptical Storm Optimization Heat Map for the Colorado River at Bastrop (CO_Colorado_J420)

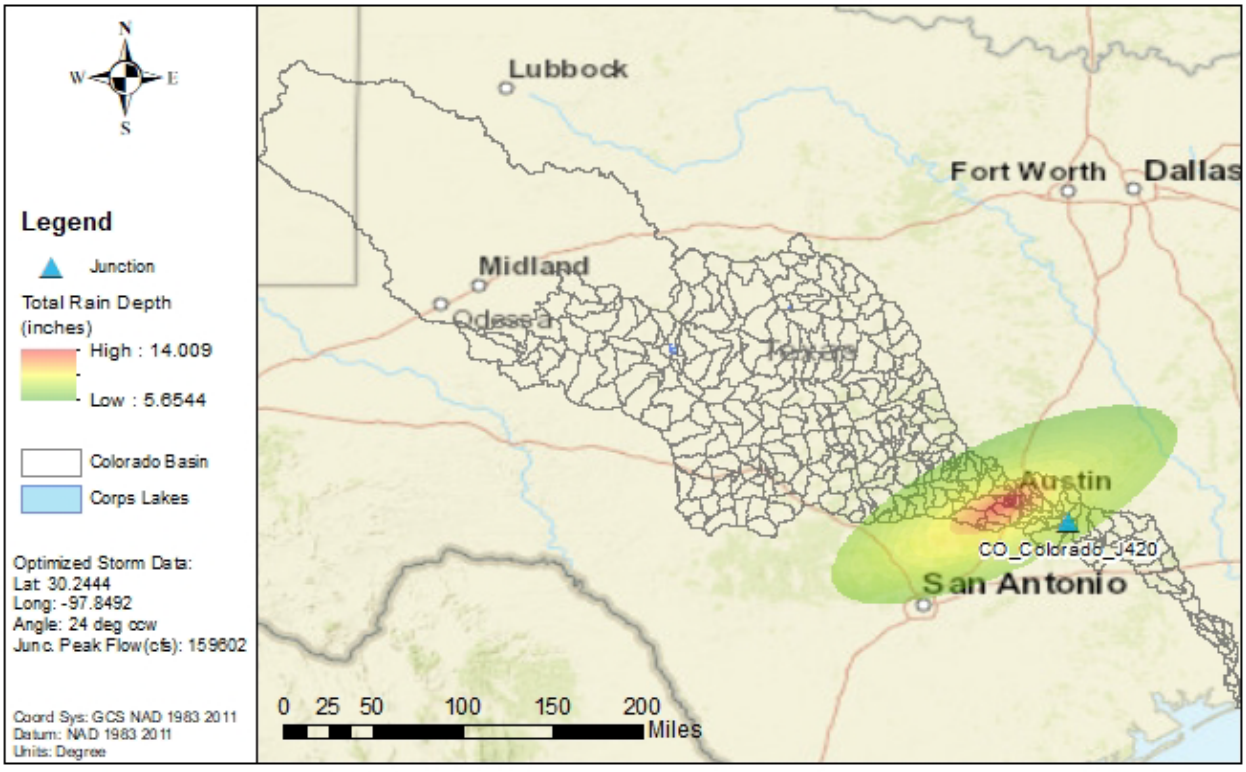

Figure 7.15b: NA14 1% AEP Elliptical Storm for the Colorado River at Bastrop (CO_Colorado_J420)

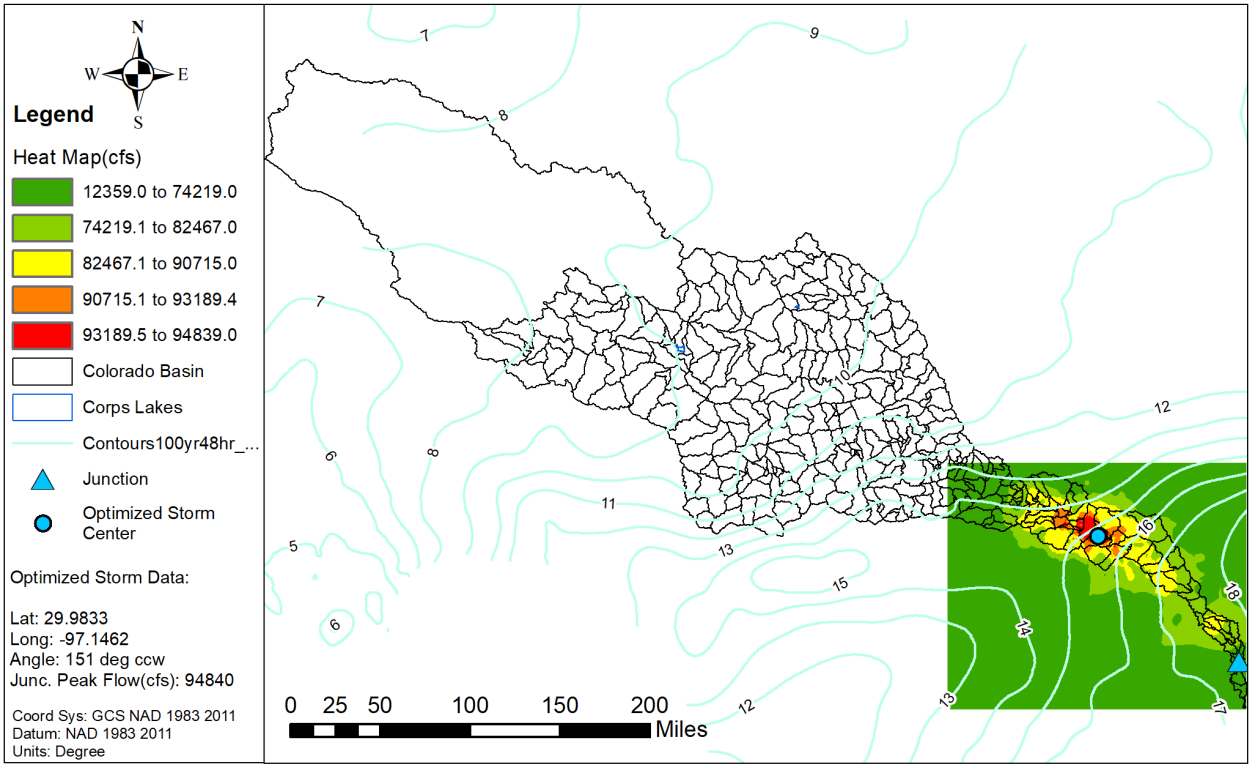

Figure 7.16a: Elliptical Storm Optimization Heat Map for the Colorado River near Bay City (CO_Colorado_J600)

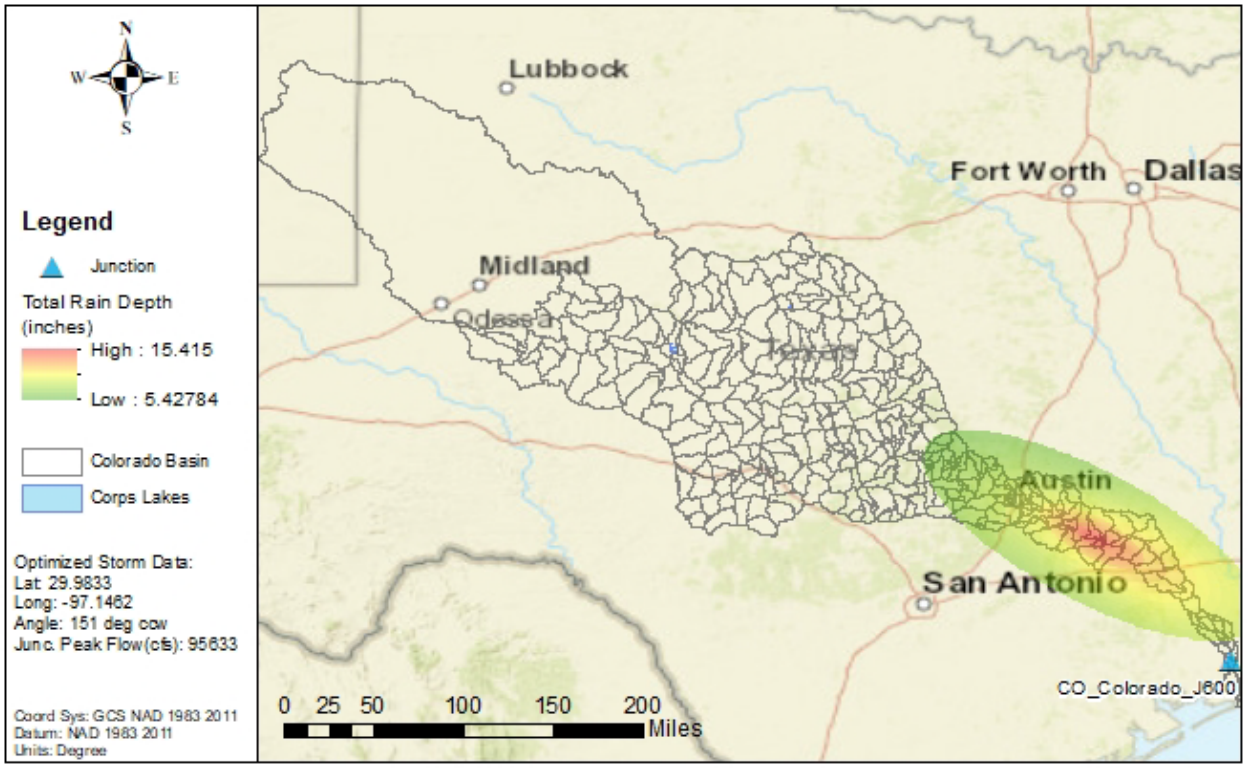

Figure 7.16b: NA14 1% AEP Elliptical Storm for the Colorado River near Bay City (CO_Colorado_J600)

7.7 ELLIPTICAL FREQUENCY STORM RESULTS VS. DRAINAGE AREA

As a quality check, the peak flow results from the 1% AEP elliptical frequency storms were plotted versus drainage area and outliers were examined, as shown in Figure 7.17. This figure shows that the analyzed junctions followed generally expected patterns of increasing peak flow with drainage area, with exceptions for the effects of large reservoirs. The relative trends in this graph generally make sense. For example, the Concho and Pecan Bayou watersheds in the upper, drier portion of the study area have lower peak discharges relative to their drainage areas. Steep, flashy rivers like the Llano and Pedernales, on the other hand, have higher peak discharges relative to their drainage areas.

Similarly, peak discharges on the Colorado River main stem are largely driven by its major tributaries. Upstream of the Concho River, Colorado River flows are similar to the Concho watershed. Between the Concho River and the San Saba River, Colorado River 1% AEP flows generally stay below 100,000 and 150,000 cfs. Downstream of the San Saba River, 1% AEP flows increase to about 200,000 cfs. Downstream of the Llano River, Colorado River peak flows jump up to about 400,000 cfs and then climb to over 500,000 cfs downstream of the Pedernales River. Below Lake Travis, Colorado River 1% AEP flows are greatly reduced to between 100,000 and 150,000 cfs upstream of Onion Creek. Below Onion Creek, the flows on the Lower Colorado River peak at over 200,000 cfs and then begin to decrease in the downstream direction due to a lack of major tributaries between Onion Creek and the Gulf.

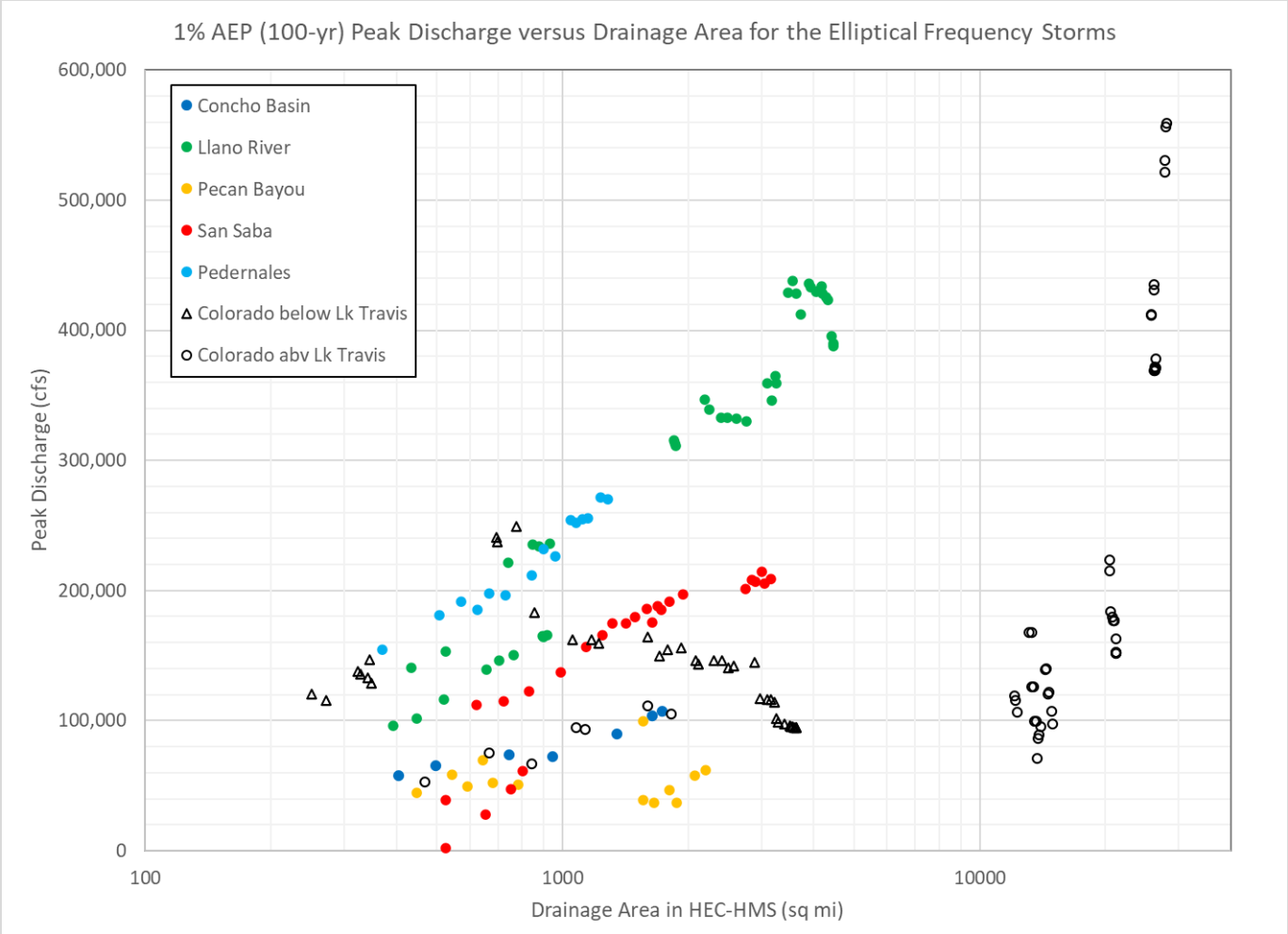

Figure 7.17: NA14 1% AEP Elliptical Storm Frequency Results versus Drainage Area

7.8 ELLIPTICAL STORM VS. UNIFORM RAIN FREQUENCY RESULTS

As mentioned at the beginning of this appendix, because the published depth-area reduction curves from TP-40 do not extend beyond 400 square miles, the uniform rainfall method may not always be appropriate for larger drainage areas. Therefore, elliptical frequency storms were computed in HEC-HMS as an alternate method to compare to the uniform rain frequency results for larger drainage areas.

Figure 7.18 below gives a comparison of the percent difference in the 1% annual chance (100-yr) peak flow estimate from the elliptical storms versus the uniform rainfall method. This percent difference is then plotted versus the drainage area of the point of interest. On this plot, a positive value indicates that the elliptical peak flow was higher than the uniform rain peak flow, and conversely, a negative value indicates that the elliptical peak flow was lower than the uniform rain peak flow.

From this figure, one may observe that the percent difference between the two methods generally increases as drainage area increases, which is as expected. For larger drainage areas encompassing several thousand square miles, the total volume of rainfall being applied to the HEC-HMS model is much less for an elliptical storm than for the uniform rainfall method. For drainage areas less than approximately 500 square miles, the results of the two methods generally stay within 10% of one another.

Large reservoirs also have varying effects on the difference in peak flow in the Colorado River basin and tend to cause some outliers. A few locations showed higher results from the elliptical method than with the uniform rainfall method. These were generally located just downstream of major reservoirs where the effective uncontrolled drainage area was less than 300 square miles. Reservoirs such also caused some low outliers. For example, Marshall Ford (Lake Travis) caused an 87% difference between the elliptical and uniform rainfall results for the outflows from the dam. This is because the large available flood storage in Marshall Ford was able to effectively capture the inflow from the elliptical storm, while inflows from the uniform rainfall method overwhelmed the reservoir by applying an unrealistically large rainfall volume to its 26,000 square mile drainage area. This example illustrates why the elliptical storm method produces more reliable estimates of frequency flows for very large drainage areas.

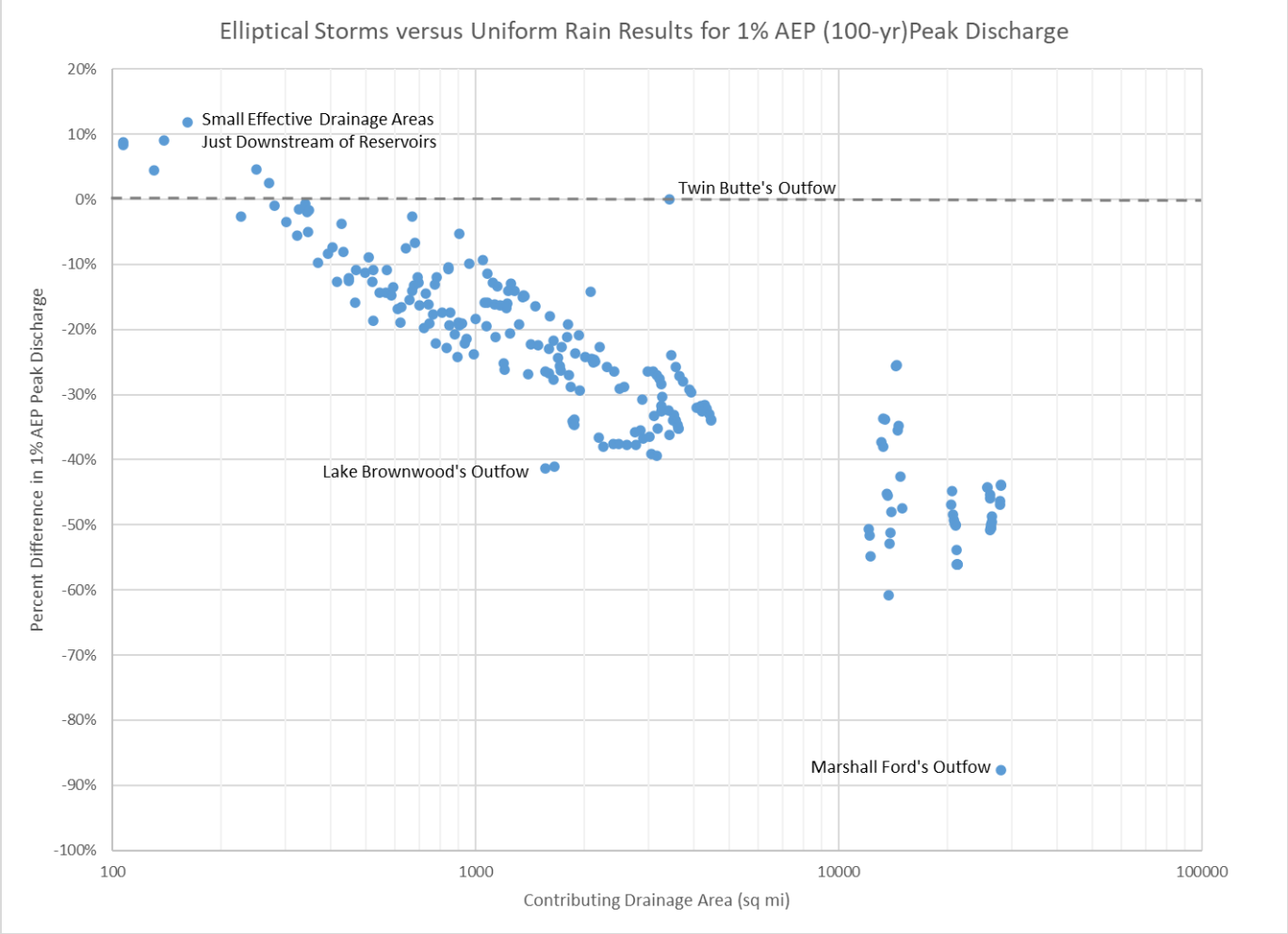

Figure 7.18: Percent Difference between Elliptical and Uniform Rain Estimates for the 1% ACE (100-yr) Peak Flow

8 RiverWare Analysis

For the RiverWare portion of the analysis, an existing US Army Corps of Engineers (USACE) Period of Record (POR) model in RiverWare (CADSWES, 2019) was updated for the Colorado River Basin. The POR data was extended to include the most current year's data, and improvements were added to the model as needed. RiverWare was then used to generate a regulated POR by simulating the basin as if the reservoirs and their current rule sets had been present in the basin for the entire time period. This analysis was used to extend flow records at various stream gaging stations within the basin from their observed records to an extended simulated record of 1930 to 2019. Statistical flow frequency analyses according to Bulletin 17C were then performed on the extended record. The statistical results from the RiverWare model were later compared with the results of other methods from this study.

8.1 INTRODUCTION TO RIVERWARE MODELING

RiverWare is a river system modeling tool developed by CADSWES (Center of Advanced Decision Support for Water and Environmental Systems) that allows the user to simulate complex reservoir operations and perform period-of-record analyses for different scenarios. For the InFRM hydrology studies, RiverWare is used to generate a homogeneous regulated POR by simulating the basin as if the reservoirs and their current rule sets had been present in the basin for the entire time period. Statistical analyses can then be performed on the extended records at the gages. This report summarizes the RiverWare portion of the hydrologic analysis being completed for the InFRM Hydrology study of the Colorado River Basin.

The RiverWare model described in this chapter presents development of the Colorado River Basin hydrology, which mimics current operational conditions. The use of the RiverWare program allows for data extension to periods prior to dam construction. The utilization of longer gage record improves discharge frequency results and increases the confidence of the analysis being performed. The modeling evaluation criteria are: (1) evaluate output based on validating policies and functions, and (2) prioritize operation based on surcharge and flood control. A detailed explanation of the Colorado River Basin POR hydrology will be in a later section.

Calibration results will also be shown that illustrate the overall model performance for the POR. The time window simulation run is for January 01, 1930 – September 30, 2019. This time window captures all big events occurred over the Colorado River basin. Each simulated water year was inspected individually to better validate the results.

Historical pool elevations along with observed inflows and outflows were compared against the model simulated results.

8.1.1 Existing USACE Models

One existing RiverWare model was available for the Colorado River basin at the onset of this study. The USACE Fort Worth District (SWF) Colorado RiverWare model, which was based off of hydrology from the USACE Southwestern Division (SWD) legacy FORTRAN SUPER program. Additionally, a new Colorado hydrology RiverWare model was built with an intent to extend POR through water year (WY) 2019. The model was developed with a functionality to replicate algorithms and consolidate object methods, defined functions, and other utilities from the SUPER program to the RiverWare program, the hydrology was then generated and fed into the RiverWare improved model. The latter was used to validate operations and mimic observed data throughout the Colorado River Basin. The concept of using two separate models was to generate local flows from the hydrology model that can be processed in the study model. The algorithmic based functions embedded in the hydrology model, enable the user to apply the right mass balance functions, and route flows throughout the network. The routing procedures capture lag time and peak attenuation. The parameters applied in the hydrology model are normally copied from the legacy SUPER program files. The hydrology model would also provide an accountability of

producing incremental and cumulative local flows for further processing. The model network was not included in this section due to its large size, but its layout reflects the river basin shown in Figure 8.1.

8.1.2 Updates to the RiverWare Model

Flow data was updated through WY 2019. The newly built hydrology model has flow data from 2000 through 2019. Data from 2000 to 2007 overlaps with flow years developed in SUPER. The RiverWare model is used to generate and pick up flows from when SUPER's simulation time window ended (i.e. 2007). The overlapping period was run to validate SUPER's model hydrology results. The operational (study) models begin on January 1st, 1930. Rule sets were written for the operational model to mimic current releases as conservation releases have changed throughout the years due to differing demands. The ruleset attempted to recreate recent demands to evaluate the last 12 years of record, from 2007-2019.

8.1.3 Model Description

The Colorado River Basin model was developed in RiverWare for Corps and non-Corps lakes operation. Many lakes (*i.e.* Marble falls and Lake Austin) in the river basin were excluded from this study, and therefore were not modeled using RiverWare. Lakes described under this section were among a list of priority lakes that were agreed upon for inclusion during the kickoff meeting held at the Lower Colorado River Authority (LCRA) office beforehand. In addition, these lakes were already part of the legacy Fortran SUPER program that was used as a replica model. Lakes owned and operated by USACE are O.C. Fisher and Hords Creek. Lake Travis, Lake LBJ, and Lake Buchanan are owned and operated by the LCRA, but the flood control portion of Lake Travis is operated by the Corps under Section 7 of the 1944 Flood Control Act, which requires USACE to develop flood control regulations for dams constructed wholly or in part with Federal funds. Twin Buttes Lake is also a Section 7 dam, which is owned by the Bureau of Reclamation (BOR) but operated by the Corps for flood control. Brown County Water Improvement District (BCWID) owns and operates Brownwood Lake. The Colorado River Municipal Water District (CRMWD) owns and operates the following lakes: JB Thomas, EV Spence, and OH Ivie, The upstream modeling boundaries are JB Thomas Dam located on the Colorado River (upstream of Colorado City), OC Fisher Dam located on the North Concho River, Twin Buttes Dam located on the South Concho River, Hords Creek Dam located on Hords Creek, Pecan Bayou Dam Site located on Pecan Bayou stream about 90 miles above junction with the Colorado River, immediately upstream of Brownwood Lake (Final Interim Feasibility Report, 2003), and Mason Dam Site (Llano River near Mason, TX, USGS streamgaging station 08150700). These boundary sites are represented as RiverWare Control Point objects with imported Deterministic Incremental Local Inflow slot values. The downstream modeling boundary is the Colorado River near Bay City, TX, USGS streamgaging station 08162500, located near Gulf of Mexico. There are additional local inflow points located throughout the model mainstem and tributaries.

Rules in the model adapted the RiverWare USACE-SWD regulation policies for the Colorado River Basin. The USACE-SWD rules solve the basin as a system and use SUPER model algorithms for flood control releases, conservation pool operations, and hydropower releases. The USACE-SWD rules also disaggregate local inflows and forecast cumulative inflows, in which the forecasted flows are used in the network algorithms. Table D.1 of Appendix D includes a complete list of model element names and types.

8.2 DATA SOURCES USED IN THE RIVERWARE MODEL

The modeling efforts in the study area heavily rely upon sound hydrology. Accurate hydrologic analyses reflect more realistic runoff conditions in the watershed, which can change overtime due to urbanization, population growth, agricultural demands, and climate change (*i.e*. drought or increased flooding due to changes in precipitation conditions). The developed hydrology was based on using the USGS streamgaging stations data at locations of interest. Streamgaging stations with the longest POR were used as the basis for developing gages

with missing flow records around the basin. Moreover, data consist of observed USGS discharges, which are measured by the USGS, and pool elevation, adjusted inflow, gated and turbine flows, and evaporation rates, which are maintained by the USACE – Fort Worth (SWF) Water Management Section, and the LCRA. Table D.2 of Appendix D lists all gaged and un-gaged data used in the RiverWare models. The locations of the USGS gages in the Colorado River Basin are shown in Figure 8.1.

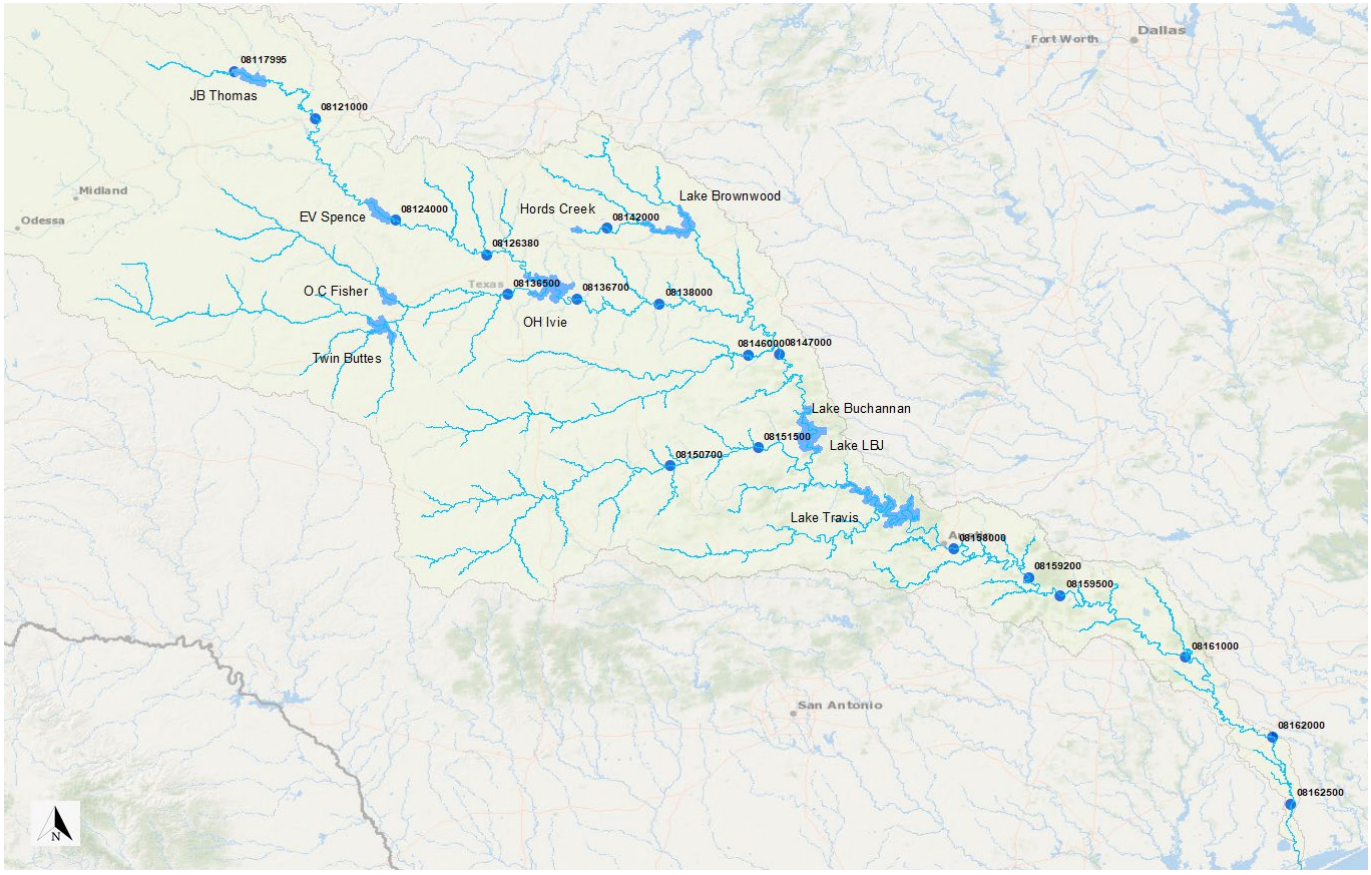

Figure 8.1: USGS Gage Locations in the Colorado River Basin

8.3 PERIOD OF RECORD HYDROLOGY DEVELOPMENT

8.3.1 Methodology Used to Develop Period of Record Hydrology

The important methods used to develop the POR hydrology for the Colorado River Basin in this chapter are the drainage-area-ratio method, reservoir inflow calculation, and reservoir inflow smoothing algorithm. This section describes the methodology used in developing the POR.

Rarely is there a POR watershed study where sufficient and consistent gage datasets exist. Incomplete streamgage datasets for streamgaging stations and reservoirs gages can be attributed to budget limitations and anthropogenic changes (*i.e.* installation of reservoirs). Once filling techniques were established for each gage, a few years with missing flows were observed. To reconcile the inconsistent dataset, the final missing discharges were generated using particular USGS streamgaging stations with continuous records. Examples of flow extension for the simulated period of 2007 through 2019 follow:

Flows at Winchell = Winchell flows + [(San Saba at San Saba routed) – (Fox Crossing Dam site routed)] X Drainage area ratio [(Colorado nr San Saba - Winchell / Colorado nr San Saba)] of 0.55.

Flows at Pecan Bayou Dam site = Inflows at Brownwood X Drainage area ratio [(Brownwood - Pecan Bayou)/ (Brownwood – Hords Creek)] of 0.22.

Flows at Cross Cut = Inflows at Brownwood X Drainage area ratio [(Cross Cut-Pecan Bayou)/ (Brownwood – Hords Creek)] of 0.128.

Flows at Coleman = Flows at Coleman X Increase in drainage area ratio [(Coleman - Hords Creek)/ (Hords Creek] of 1.23.

Flows at Bay City = Flows at Bay City routed + flows at Wharton X Increase in drainage area ratio [(Bay City-Wharton)/ (Wharton)] of 1.007 merged with flows at Wadsworth X Decrease in drainage area ratio [(Wadsworth - Bay City)/Wadsworth] of 0.98.

The drainage-area-ratio method provides a numerical approximation of the missing gage data, using gage datasets upstream or downstream on the same river (Equation 1).

$$Q_y = \frac{Q_x}{A_x} A_y$$

Equation 1: Drainage-Area-Ratio Method

$Q_y = Flow\ at\ gaged\ site\ Y\ of\ drainage\ area\ A_y\ [L^3/T]$

$Q_x = Flow\ at\ gaged\ site\ X\ of\ drainage\ area\ A_x\ [L^3/T]$

$A_y = Drainage\ area\ of\ ungaged\ site\ [L^2]$

$A_x = Drainage\ area\ of\ available\ gaged\ site\ X\ \ [L^2]$

The numerous arrays of reservoir inflow calculations tolerate for thoroughness, as well as discontinuity. All reservoir inflow calculations share the a priori mass balance approach. The method selection for the calculation of reservoir inflow is subjective and ultimately should be selected on a case-by-case basis. There is one method used to calculate reservoir inflows in this study. It is the “evaporation reservoir inflow method” (method applied to USACE datasets).

$$I = \Delta S + E + R + Q_{total}$$

Equation 2: Evaporation Reservoir Inflow Method

$I = Inflow\ into\ the\ reservoir\ [L^3/T]$

$\Delta S = Change\ in\ reservoir\ storage\ [L^3/T]$

$E = Evaporation\ from\ the\ reservoir\ [L^3/T]$

$Q_{total} = Total\ pumpage\ out\ of\ the\ reservoir\ [L^3/T]$

The calculated reservoir inflow is subject to measurement error and numerical error. The evaporation parameter is arguably the most difficult parameter to estimate when calculating reservoir inflow. The uncertainty in measurement often leads to negative reservoir inflow values, which violates the conservation of mass theory.

Reservoir release rates can also be inaccurate due to the imperfect nature of setting the gate height at the project. To resolve these inconsistencies the reservoir inflow values are numerically smoothed by scaling positive inflows and rectifying negative inflows. The smoothed inflow algorithm is applied over a monthly time period with a daily time step and preserves the volume of the monthly total (Equation 3, Equation 4, Equation 5, and Equation 6). There are additional inflow smoothing methods available, but this method is sufficient to resolve negative reservoir inflows in this case.

$$Montly\ Total\ Inflow = \sum_{i}^{i_f} I_i$$

Equation 3: Monthly Total Inflow Method

$$\text{Nonnegative Inflow} = \begin{Bmatrix} if\ I_i < 0 \\ 0 \\ else \\ I_i \end{Bmatrix}$$

Equation 4: Nonnegative Inflow Method

$$Montly\ Total\ Nonnegative\ Inflow = \sum_{i}^{i_f} Nonnegative\ Local$$

Equation 5: Monthly Total Nonnegative Inflow Method

$$Smoothed\ Inflow = \begin{Bmatrix} if\ Monthly\ Total\ Inflow < 0\ OR\ Montly\ Total\ Nonnegative\ Inflow = 0 \\ Nonnegative\ Inflow * 0 \\ else \\ Nonnegative\ Inflow * \dfrac{Monthly\ Total\ Inflow}{Montly\ Total\ Nonnegative\ Inflow} \end{Bmatrix}$$

Equation 6: Smoothed Inflow Method

$I = Inflow\ into\ the\ reservoir\ on\ the\ i^{th}\ day\ [L^3/T]$

$i = i^{th}\ day\ of\ the\ month$

$i_f = last\ day\ of\ the\ month$

$Montly\ Total\ Nonnegative\ Inflow = Summation\ of\ the\ monthly\ nonnegative\ inflows\ [L^3/T]$

$Montly\ Total\ Inflow = Summation\ of\ the\ monthly\ reservoir\ inflows\ [L^3/T]$

$Nonnegative\ Inflow = A\ nonnegative\ dataset\ of\ the\ reservoir\ inflows\ [[L^3/T]: [L^3/T]]$

$Smoothed\ Inflow = A\ smoothed\ dataset\ of\ the\ reservoir\ inflows\ [[L^3/T]: [L^3/T]]$

The methods presented above along with the RiverWare modeling software have permitted for the development of POR hydrology for the Colorado River Basin. The following Application section will describe how these methods were implemented within the framework of the RiverWare modeling software and the precursor to the RiverWare modeling software.

8.3.2 Period of Record Hydrology

The POR hydrology needed to evaluate the Colorado River Basin requires the use of numerical models. RiverWare version 8.0.1 was used to analyze the hydrology and hydraulic processes of the 10 aforementioned lakes in section 1.1.3, and the river reaches within the Colorado River Basin. The hydrologic analysis includes the use of a multiple-run and simulation-run RiverWare model. The multiple-run RiverWare model produced the POR hydrology from October 01, 2000 to September 30, 2019 for all streams and reservoirs gage sites. The RiverWare hydrology model output is compiled with the SUPER model to produce results from January 01, 1930 through September 30, 2019. The POR hydrology is the naturalized local flows, where major anthropogenic impacts have been removed, including effects of reservoir regulation. The simulation-run RiverWare model used the POR hydrology datasets to simulate the entire Colorado River basin reservoirs pool elevations with reservoir regulation policies incorporated for the entire POR, which will be used in the statistical frequency analysis portion of the study.

The process for developing POR hydrology, for the reservoirs and control points or stream gaging stations of interest, is to assimilate historical reservoir inflow and stream flow datasets, then implement drainage-area-ratio methods and reservoir inflow smoothing algorithms in a multiple-run RiverWare model to numerically solve for the POR hydrology. Analyzing pool elevations and operational release over the POR requires the POR hydrology and reservoir operational policies and rule sets to be incorporated into a simulation-run RiverWare model. The reservoir operational policies and rule sets applied to reservoirs can then be compared to historical pool elevations, releases, and local inflows to verify consistency with historical datasets. Ultimately the policies and rule sets can be applied to the POR hydrology to establish synthetic pool elevation and reservoir operation before the reservoirs existed.

8.4 WATER CONTROL PLANS FOR THE COLORADO BASIN RESERVOIRS

Tables 8.1, 8.2, 8.3, and 8.4 list some main operational procedures, flood control key points, and objectives of each Corps and non-Corps operation modeled reservoir in RiverWare. This information can be found in chapter 7 of the respective USACE reservoir's Water Control Manual (WCM) (USACE-SWF, 2019) (USACE-SWF, 1955), Chapter 4 of the Bureau of Reclamation Standard Operating procedures (SOP) (2001), and (USACE-SWF 2020). Non-Corps dams may have different operating procedures that may be less significant to flooding due to the reservoir's primary purpose *(i.e.* water supply).

Table 8.1: Highlights from the WCMs and SOPs for Hords Creek, O.C. Fisher, Twin Buttes, & Lake Travis

	Hords Creek	O.C. Fisher	Twin Buttes	Lake Travis
Dam Type	Storage	Storage	Storage	Storage
Purpose	Flood control, and water supply	Flood control, general recreation, and water supply	Flood control, general recreation, and water supply	Flood control, water supply, and hydroelectric power
Control Point **Located downstream of each project**	10,000cfs near Coleman (USGS) 08140770	20,000cfs on the Concho River between San Angelo and Paint Rock	Flows when combined with O.C Fisher, shall not exceed 25,000cfs at the Concho River gage near Paint Rock	30,000cfs on the Colorado River at Austin (USGS) 08158000
Pool zone	Elevation (NGVD-ft)	Elevation (NGVD-ft)	Elevation (NGVD-ft)	Elevation (NGVD-ft)
Top of conservation	1900.0	1908.0	1940.2	681.0
Top of flood	1920.0	1938.5	1969.1	714.0
Surcharge	Above 1920.0	Above1938.5	Above 1969.1	Above 714.0
Top of Spillway Crest	1920.0	1938.5	1969.1	714.0
Top of Dam	1939.0	1964.0	1991.0	750.0
Initial Impoundment Date	June 01, 1948	February 01, 1952	December 01, 1962	September 01. 1940

Table 8.2: Highlights from the LCRA Management Plans for Buchanan Lake and Lake L.B.J

Purpose/Downstream Control points/Pool zones	Lake Buchanan	Lake LBJ
Dam Type	Storage	Storage
Purpose	Water supply and hydroelectric power	Flood control, water supply, and hydroelectric power
Control Point Located upstream/downstream of each project	When USGS 08147000 (Upstream) inflows > 22,000cfs, Outflow < 22,000cfs. When inflows <22,000cfs, outflow = 85% inflow	When USGS (Upstream) 08151500 reach flood stage, maintain lake between 824.4 and 825.0. Lake should not exceed elevation 828.0 feet.
Pool zone Top of conservation Top of flood Surcharge Top of Spillway Crest Top of Dam	Elevation (NGVD-ft) 1018.0 Above 1018.0 Above 1020.0 1020.0 1025.0	Elevation (NGVD-ft) 824.7 825.0 Above 835.0 835.0 838.0
Initial Impoundment Date	May 20, 1937	1951

Table 8.3: Highlights from the Water Control Plans for J.B. Thomas, EV Spence, O.H. Ivie and Lake Brownwood

Purpose/Downstream Control points/Pool zones	Lake J.B Thomas	EV Spence	O.H. Ivie	Brownwood
Dam Type	Storage	Storage	Storage	Storage
Purpose	Water supply	Water supply	Water supply	Water supply
Control Point Located upstream/downstream of each project	5,000cfs at USGS (Downstream) 08121000 (Colorado River near Colorado, TX)	None	None	None
Pool zone	Elevation (NGVD-ft)	Elevation (NGVD-ft)	Elevation (NGVD-ft)	Elevation (NGVD-ft)
Top of conservation	2258.0	1898.0	1551.5	1425.0
Top of flood	2267.0	1908.0	1562.0	1425.0
Surcharge	Above 2267.0	Above 1908.0	Above 1562.0	1425.0
Top of Spillway Crest	2267.0	1908.0	1562.0	1425.0
Top of Dam	2280.0	1928.0	1584.0	1470.0
Initial Impoundment Date	1952	June 01, 1969	March 15, 1990	July 01, 1933

In RiverWare, policies and functions were written to reflect the current reservoir regulation schedule for each lake. Release procedures in these tables were also included in the RiverWare model for simulation. More information on how the reservoir release schedules are modeled in RiverWare is included in Appendix D.

8.5 RIVERWARE OPERATIONAL MODEL APPLICATION

The RiverWare simulation model executes all flood control releases, so as to maximize flood release within the period of perfect knowledge. This period is defined as: the number of time steps for which the forecast will equal the Deterministic Incremental Local Inflow, *i.e.,* the forecast is known with complete certainty. In real time historical operations, there are numerous and event-specific reasons as to why the reservoir was operated the way it was. Meteorological forecasts from the National Weather Service, as well as river stage forecasts issued by the West Gulf River Forecast Center could both potentially influence the rate of release from the project.

The Colorado River Basin RiverWare model includes policies implemented as rules. Rule number 1 is the highest priority rule and executes last (*i.e.* hydropower release rule) while the rule with the highest number is the lowest priority rule and executes first (*i.e.* Surcharge rule). Figure 8.2 below shows the priority list of policies

implemented in the model. As seen, the flood control policies execute first and this is mainly to control flooding at damage center locations located downstream.

The built in rules in USACE-SWD conservation pool operations apply to Corps and non-Corps dams regardless of operation. The written rules in RiverWare utilize specific elevations found in the operating level tables to trigger operations. These generic operating level tables reflect dams' conditions with or without flood storage. The other rules (*i.e.* Regulation discharge, flood control, reservoir diversion, and hydropower release rules) kick in based on priority.

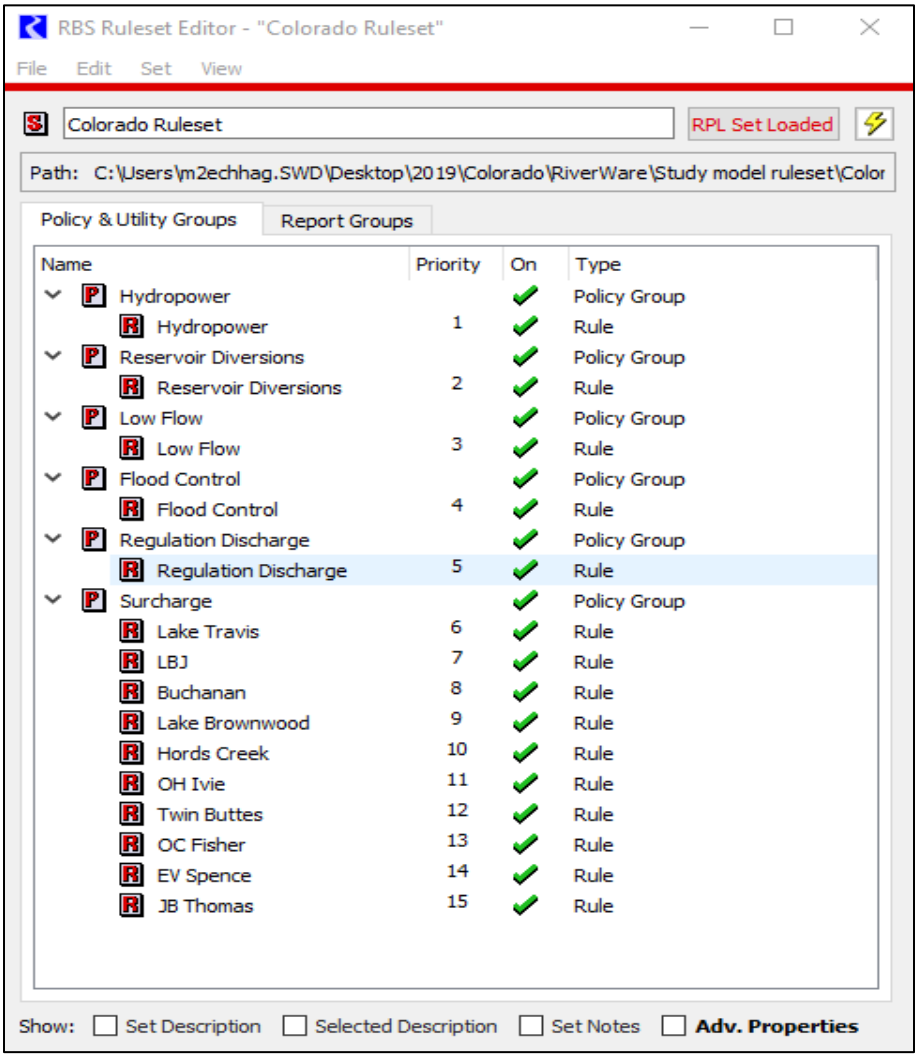

Figure 8.2: Colorado River Basin Rule-Based Simulation Groups

8.6 MODEL CALIBRATION RESULTS AND DISCUSSION

Overall, the model displays satisfactory results between simulated and observed considering operation limitations. The rules used for simulation do not always produce matching results of the historical (observed) flows, because real-time operation is normally based on real-time forecasting, which causes release deviations from the WCM schedule. The model uses the deterministic flow with a simple forecasting technique and a set of policies. The surcharge, regulating discharge, and flood control rules execute first, while also accounting for low flows at Lake Travis.

Due to the large size of the basin, discussion of results for the Colorado River Basin is arranged by groups. Lakes and key control points located on the same major tributaries are discussed together. The following color codes were assigned to each data set displayed in the figures: Blue for observed data, and green and orange for simulated results.

8.6.1 Results for the Concho River Reservoirs

For O.C. Fisher, observed (blue) and simulated (green) releases and pool elevations were compared for the period of 2008-2019, as shown in Figure 8.3. The basin was relatively dry during this period and releases were kept to minimum. The lake experiences significant evaporation during hot seasons. The simulated releases were zero while observed releases were very small (*i.e.* less than 40cfs). The simulated pool synchronized well with the observed pool. The lowest draw down elevation was set at 1840.0 feet. The lowest observed pool was 1850.0 feet. The highest lake inflow peak was observed in 2015 (about 7,400 cfs), which raised the lake elevation by more than 30 feet. Despite zero simulated releases from the lake, more simulated pool drawdown can be seen when compared to observed pool, and this is maybe related to the estimated evaporation rates used in the RiverWare model to account for storage losses from the lake. Additional information on O.C. Fisher's operations is included in Appendix D.

Twin Buttes Lake is located adjacent to O.C. Fisher Lake. The basin is dry and the observed pool never reached conservation (1940.2 feet) during the period of comparison. Releases are very minimum. The model showed very good match to the observed pool (Figure 8.4). Simulated pool for the period between 2015 and 2018 was lower than the observed. Simulated drawdown maybe impacted by the estimated evaporation rates used in the RiverWare model to account for storage losses from the lake. Dry basins can also be impacted by inaccurate measurements of pumpage. The model responded to excessive runoff in 2018. No adjustments were made to the modeled operations for Twin Buttes.

Figure 8.5 shows the flow comparison between RiverWare and observed for the Concho River at Paint Rock for moderate and big runoff events. The model shows very good match with actual flows at Paint Rock USGS gage. Overall, timing of peaking was accurate. Great match was seen during the 2018 event, and slight differences were encountered during the 2017 and 2019 events. Differences can be related to Twin Buttes and O.C Fisher's operations (*i.e.* null releases). Zero releases were maintained from O.C Fisher and Twin Buttes. No further changes were made to the routing parameters for these reaches.

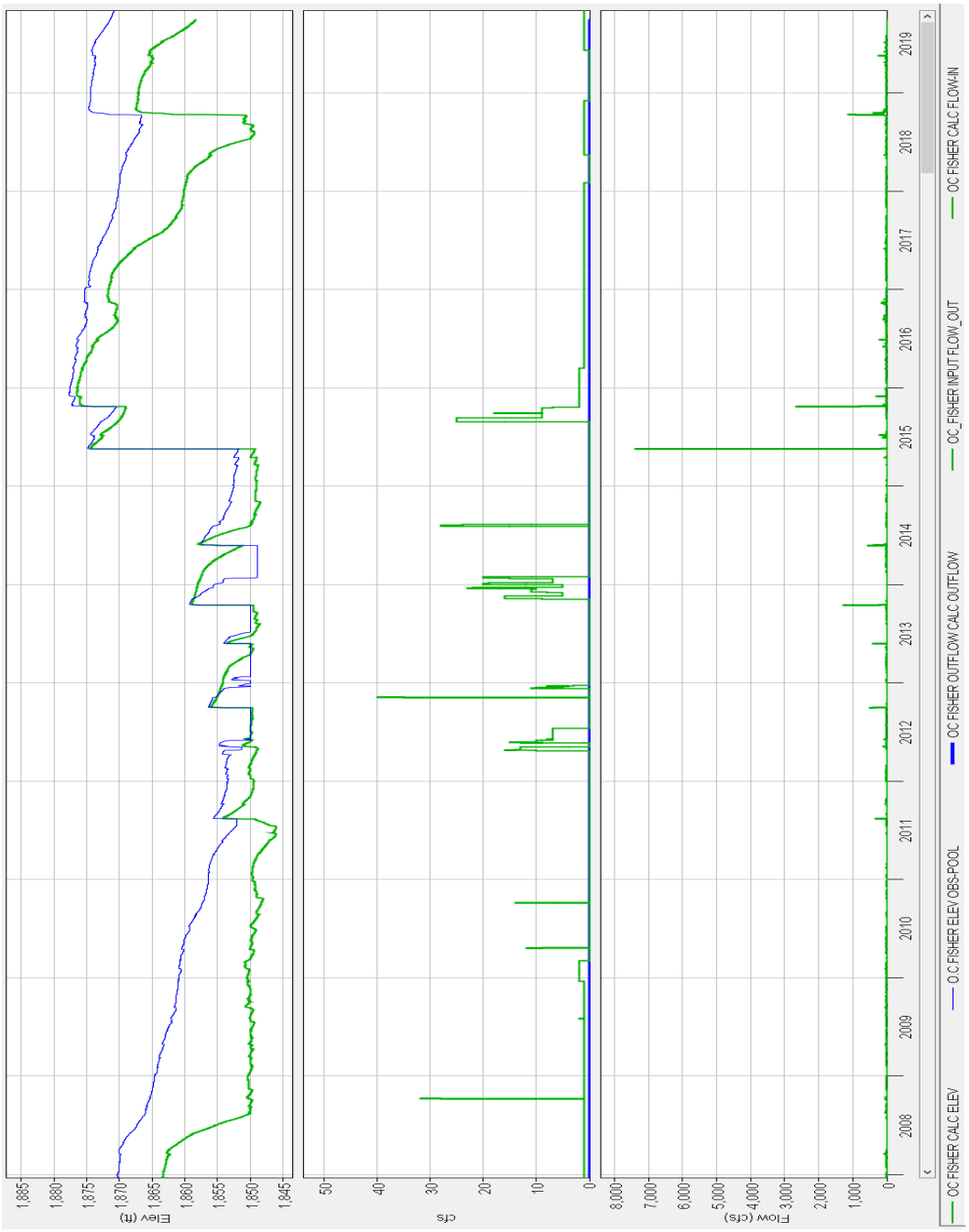

Figure 8.3: O.C. Fisher Lake Pool Comparison for POR 2007-2019

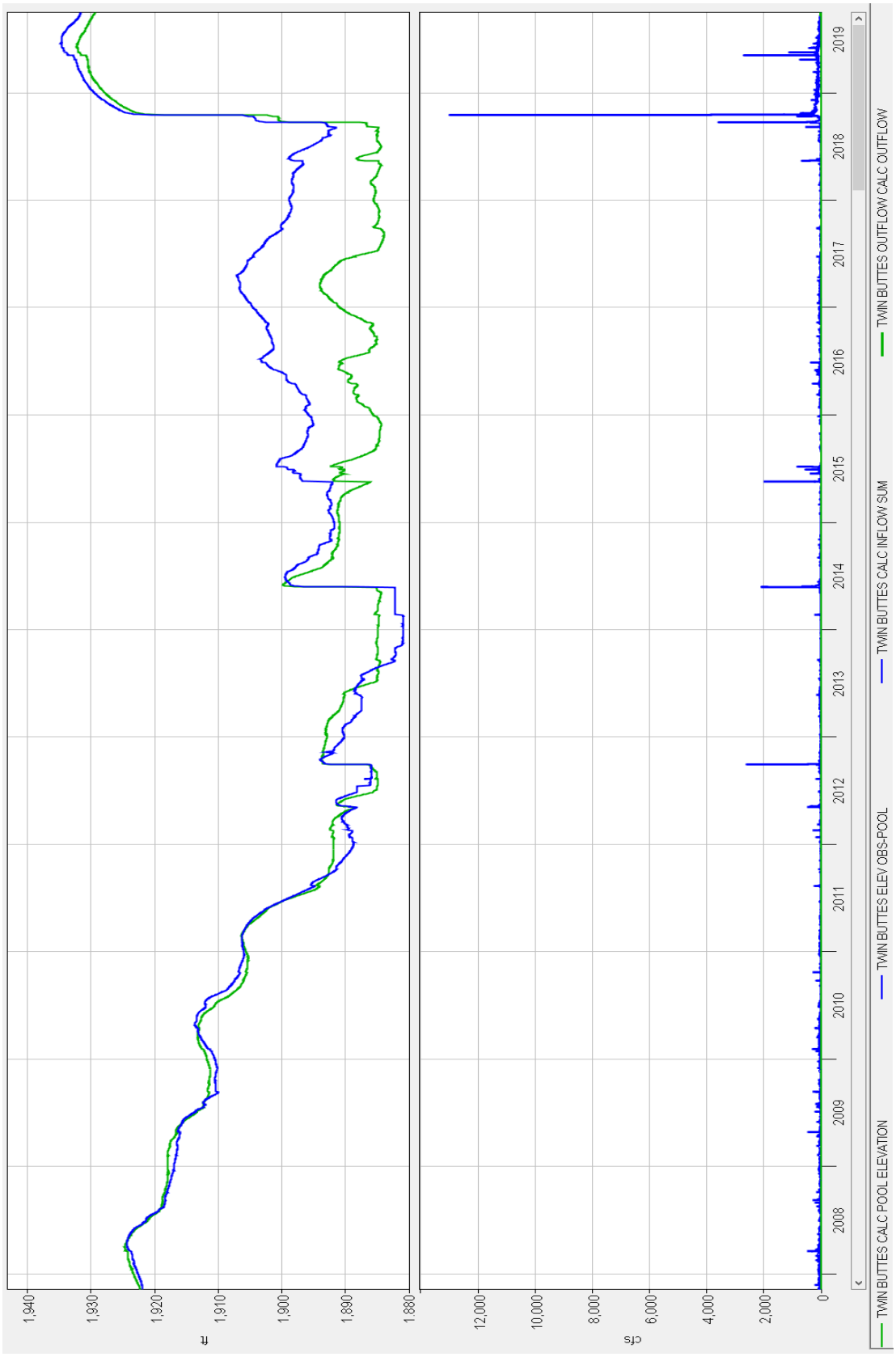

Figure 8.4: Twin Buttes Lake Model Performance

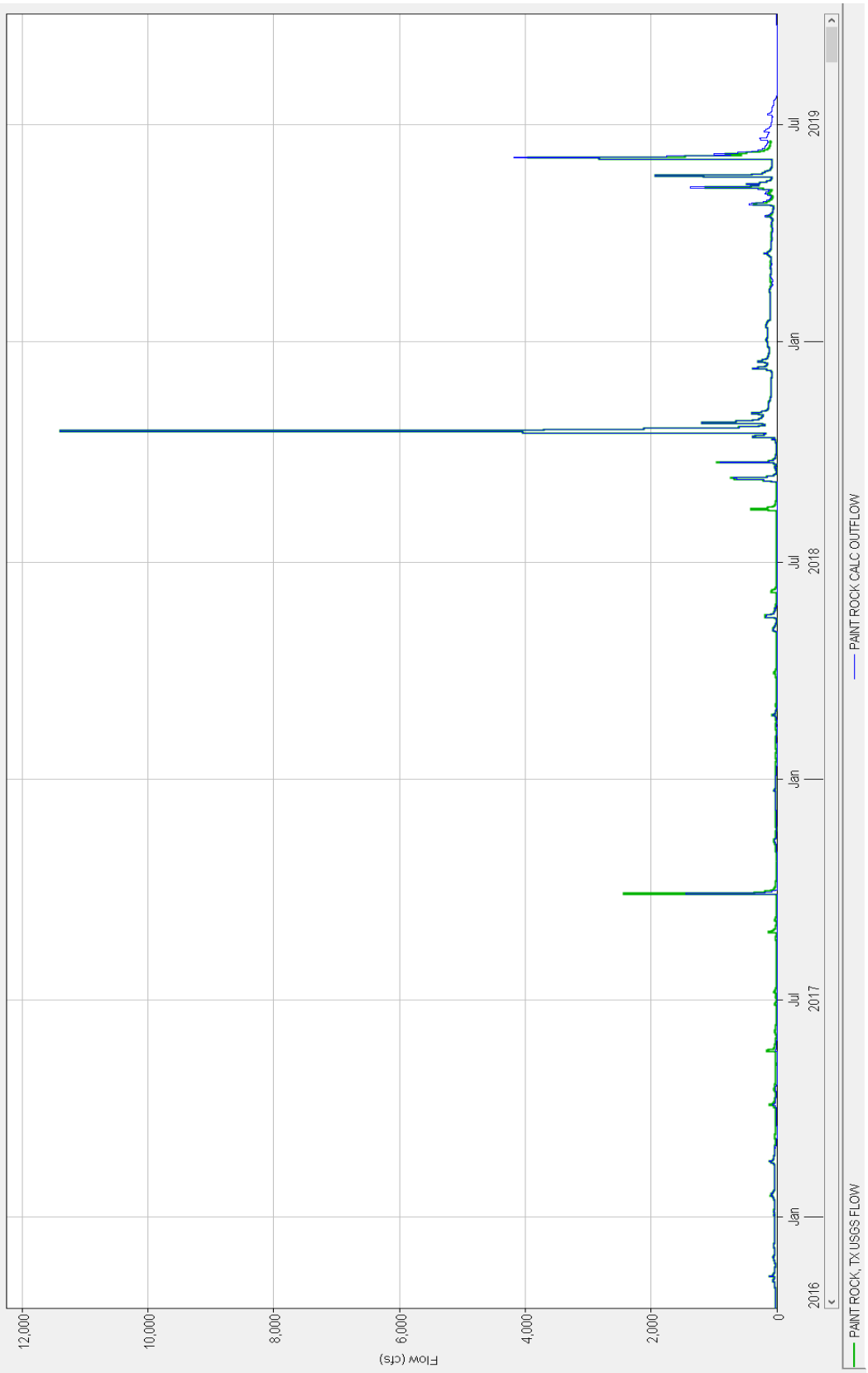

Figure 8.5: RiverWare Simulated and Observed Flow Comparison at Paint Rock

8.6.2 Results for the Upper Colorado River

E.V. Spence reservoir's pool simulation is shown in Figure 8.6. Overall, the model synchronizes well. Better matchups were seen during low flow years (2008 through 2011). More deviations were seen during moderate to big events (2012 to 2019). Some adjustments were made to zones 2 and 3 in the operating level table in the model to offset some of the deviations seen during 2011 and 2012. Pool elevations were bumped from 1790 feet to 1810 feet to hold drawdown from dipping too low and mimic observed pool level.

RiverWare flows at the Ballinger control point matched up with the USGS gage of Colorado River near Ballinger (USGS 08126380). The RiverWare model results are shown in Figure 8.7.

8.6.3 Results for the Pecan Bayou Reservoirs

Pool simulation for Hords Creek reservoir is captured in Figure 8.8. The model shows good pool simulation results. Deviations from the observed pool were more pronounced during drought years due to discrepancies in the estimates of evaporation rates and other unaccounted for losses (*i.e.* ungagged amounts for irrigation). Hords Creek is located in a dry basin. The pool has only reached conservation a handful times. Overall, the model performance was good and no further adjustments were made to improve results.

Figure 8.9 captured Lake Brownwood's pool simulation between 2007 and 2019. The simulated pool showed similar results to Hords Creek pool, where deviations from observed occurred during drought years (2008-2014). Lake Brownwood is a multipurpose dam and stores a large volume of water. The lake releases flow over the uncontrolled spillway crest (1425.0 feet). Over the years the project has spilled several times. Model results mimicked observed pool very well. It should be noted that there is no observed inflow gage to the lake to compare results to. The calculated lake inflow was based on utilizing data extracted from monthly canal inflow reports. These reports were obtained from Texas Commission of Environmental Quality (TCEQ). Monthly reports also included evaporation rates and pumping rates out of the lake. Future improvements can be made if actual gages are installed.

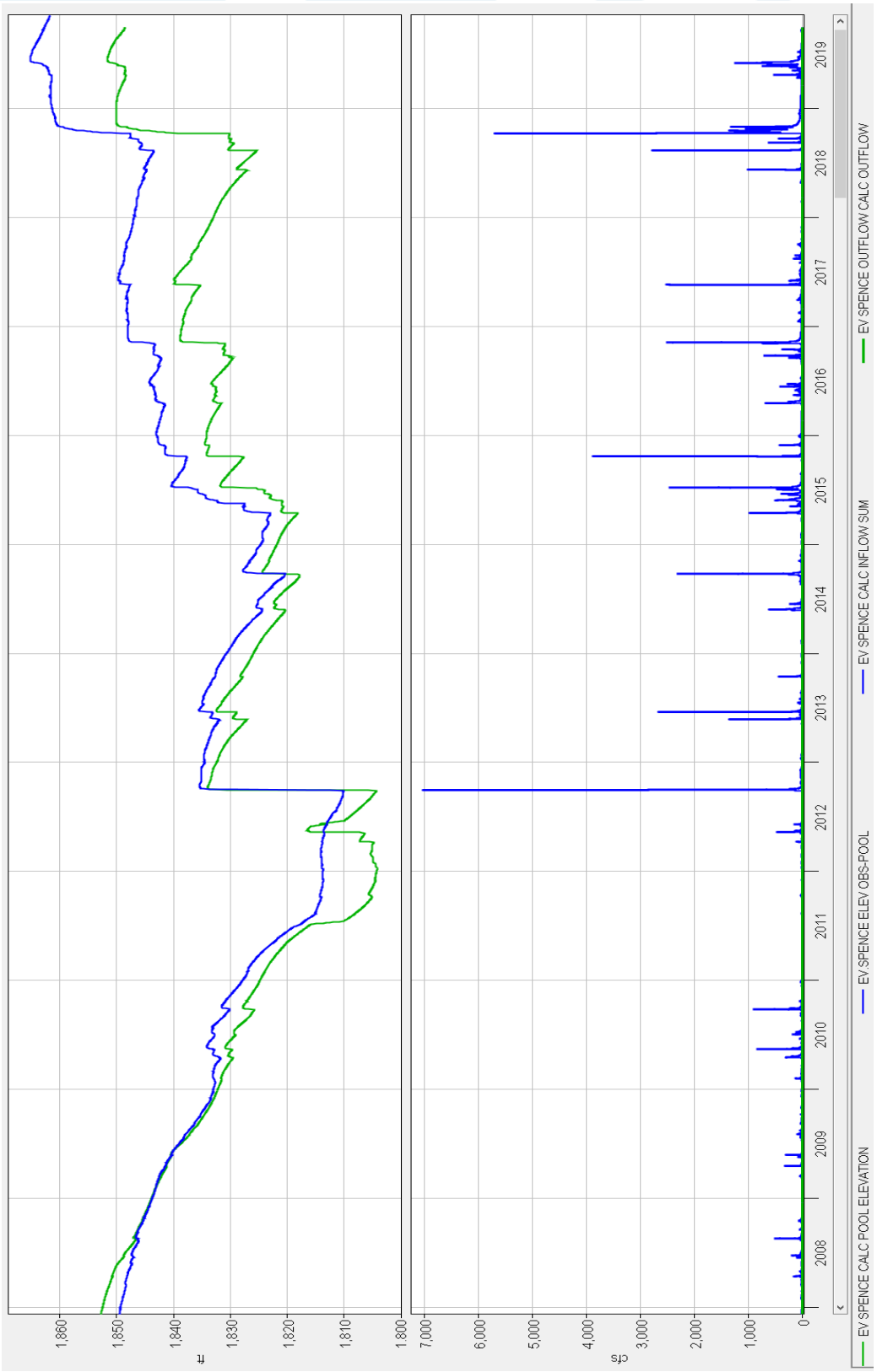

Figure 8.6: E.V. Spence Pool RiverWare Simulation Comparison

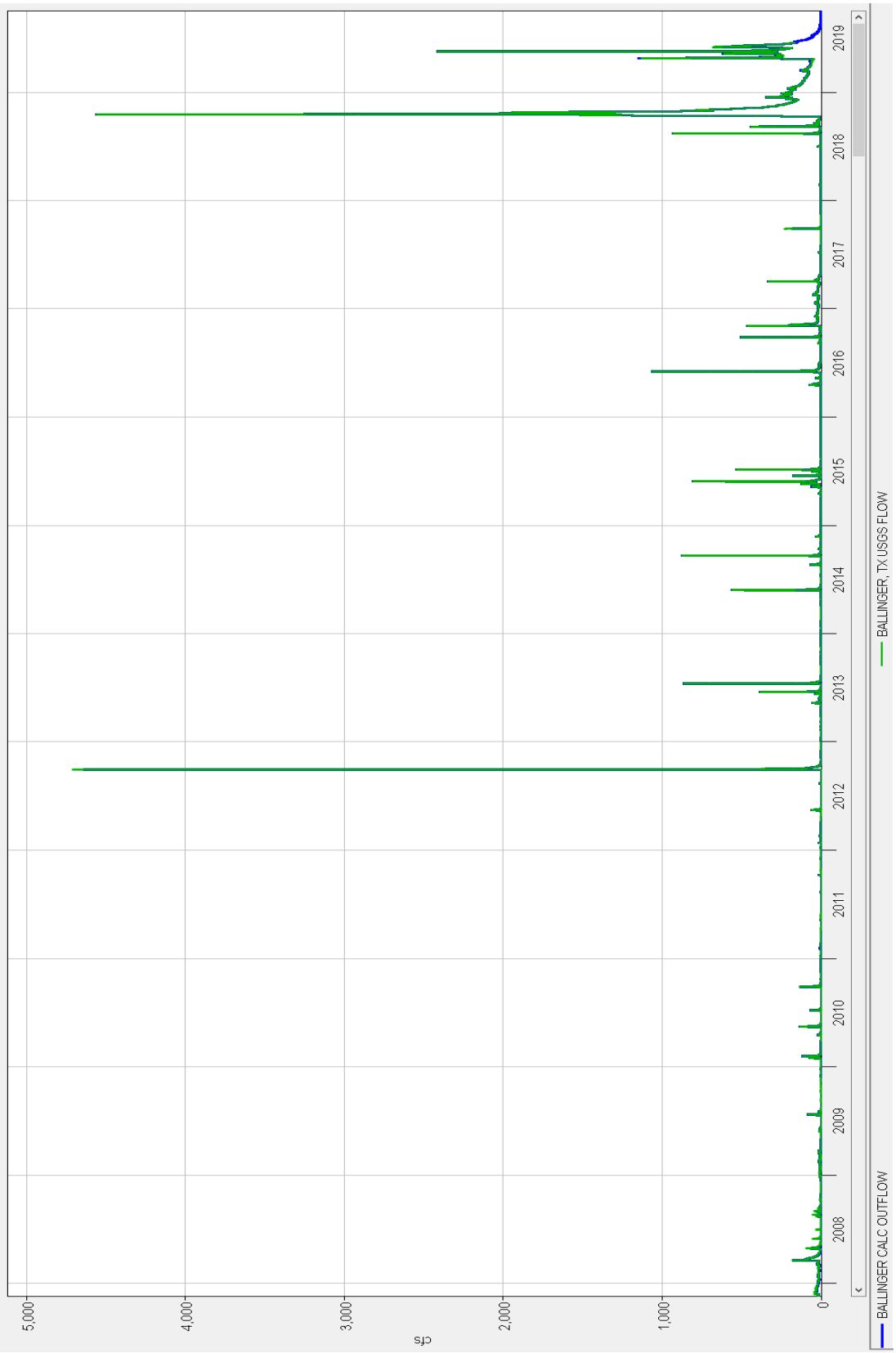

Figure 8.7: Comparison of Simulated and Observed Flows at the Colorado River near Ballinger

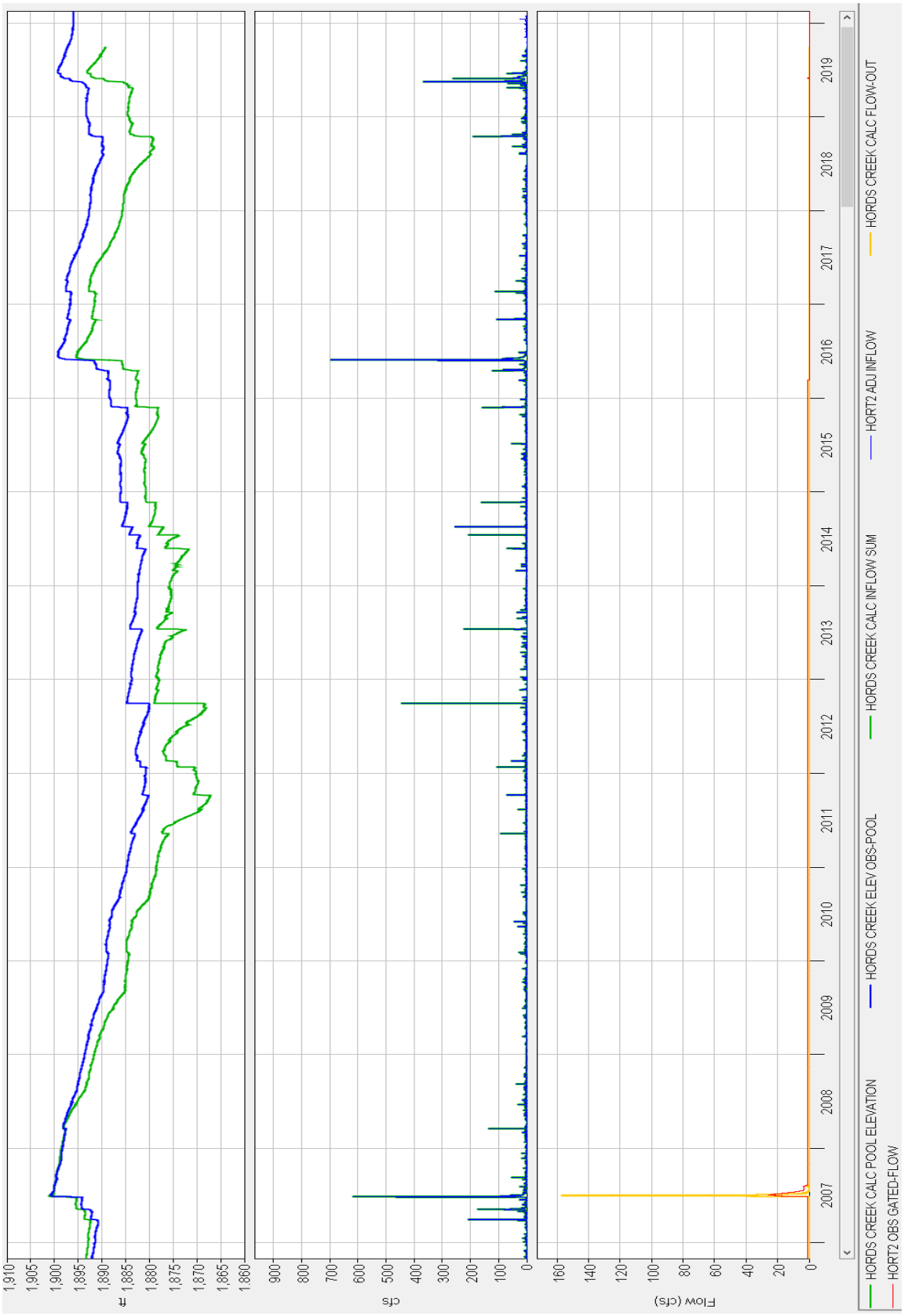

Figure 8.8: Hords Creek Pool RiverWare Simulation Comparison

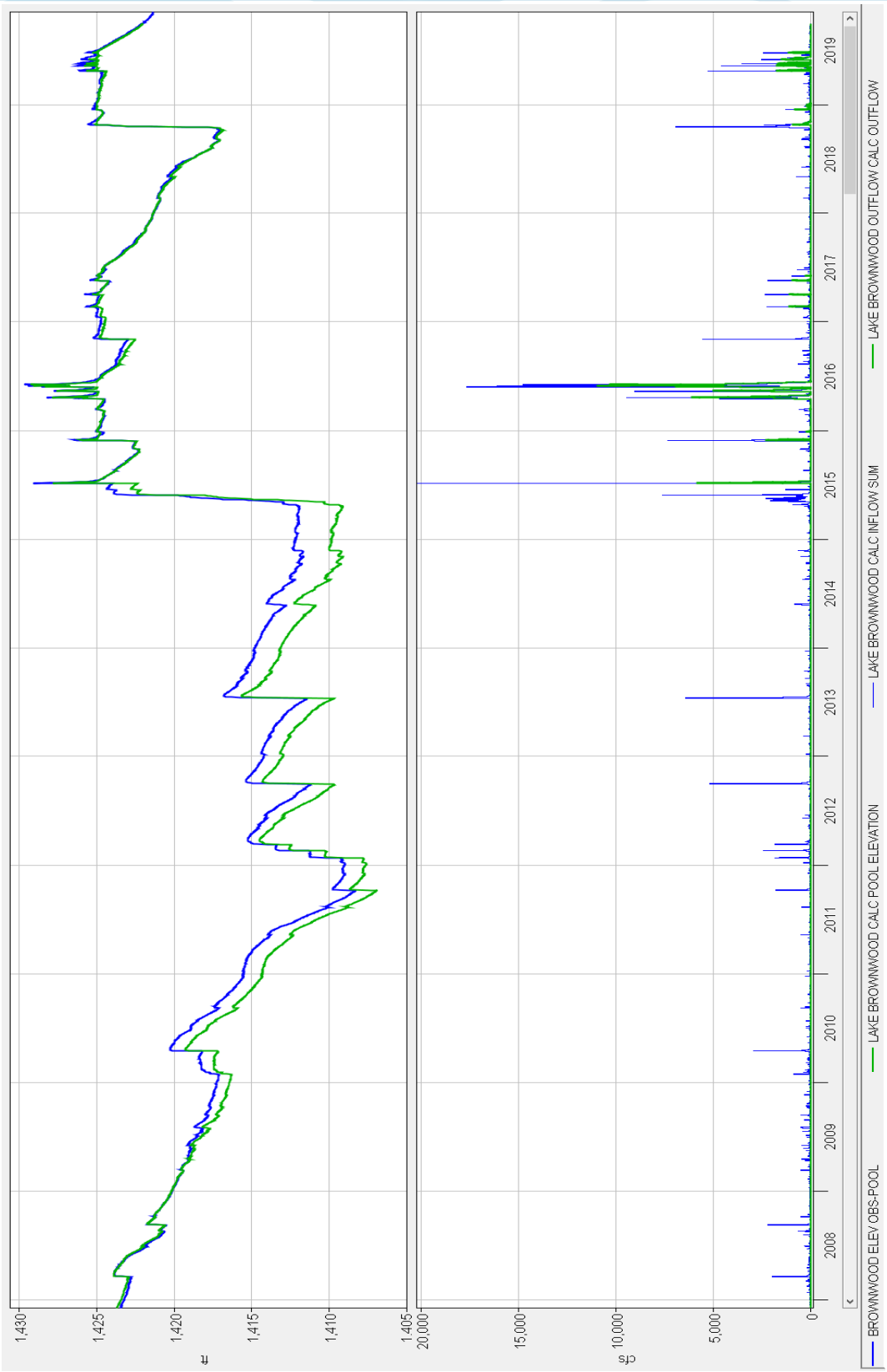

Figure 8.9: Lake Brownwood Pool RiverWare Simulation Comparison

8.6.4 Results from O.H. Ivie to Winchell, TX

This segment is bounded between the Concho River - O.H. Ivie confluence and Winchell - Pecan Bayou confluence. As seen in Figure 8.10, Lake O.H. Ivie releases were set to zero for the period between 2007 and 2019. The computed inflows were a result of back calculation of project release and change in storage. Evaporation and pumping rates were added in after being supplied by the Water Municipal Control District (WMCD). Observed data downstream of O.H. Ivie were used to compare to (Colorado River near Stacy, USGS 08136700). Pool deviations from observed were to be because of data supplement in monthly formats. However, the simulated pool performs well. During the period when the project released no flows, the pool tended to rise above observed. The operational values in the elevation pool table for the project were acceptable.

Figure 8.11 was made to show model results comparison to observed flows at the Colorado River at Winchell (USGS 08138000). The Winchell USGS gage was discontinued in July of 2011. For the period between 2007 and part of 2011, the simulated flows compared very well to the observed.

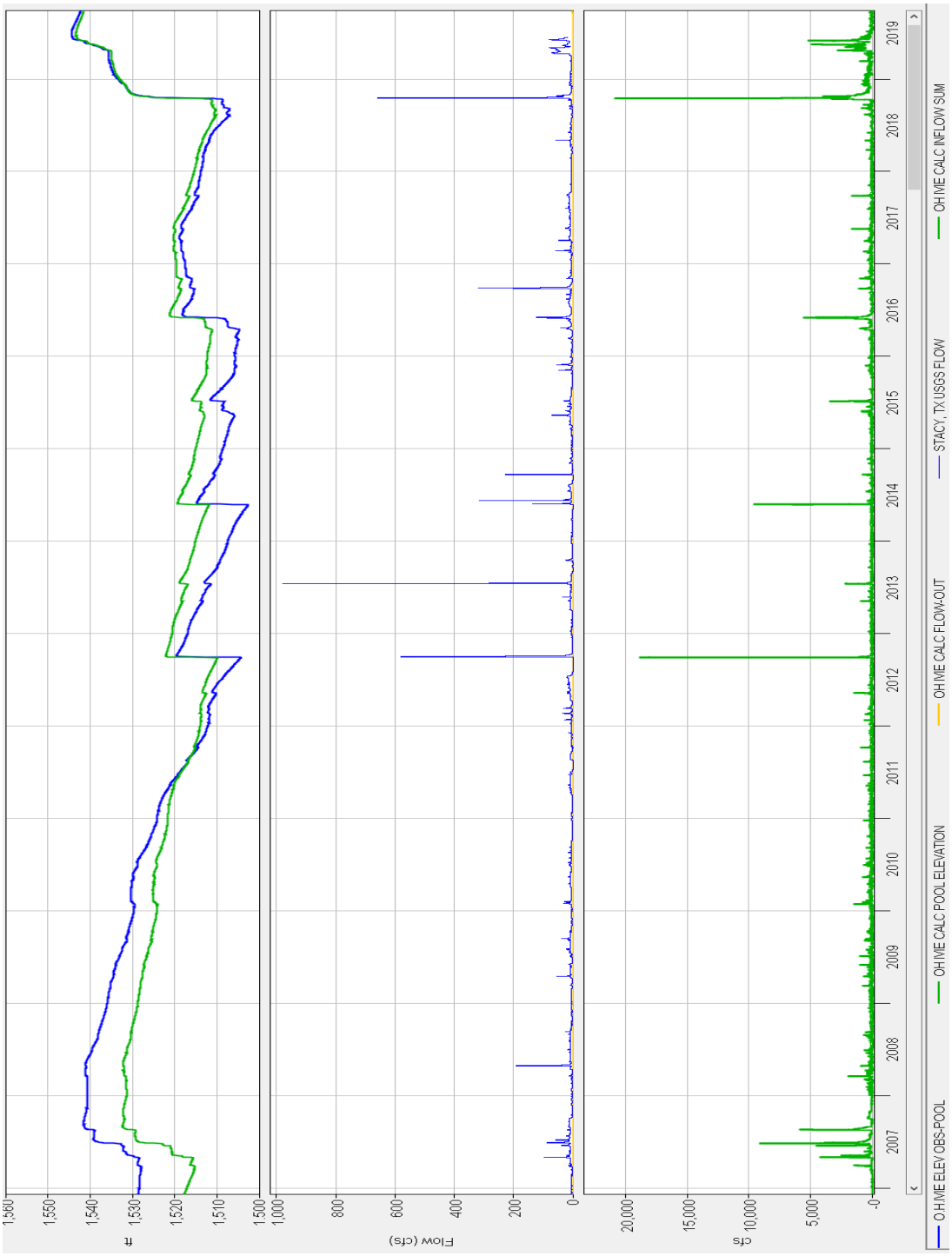

Figure 8.10: Lake O.H. Ivie Pool RiverWare Simulation Comparison

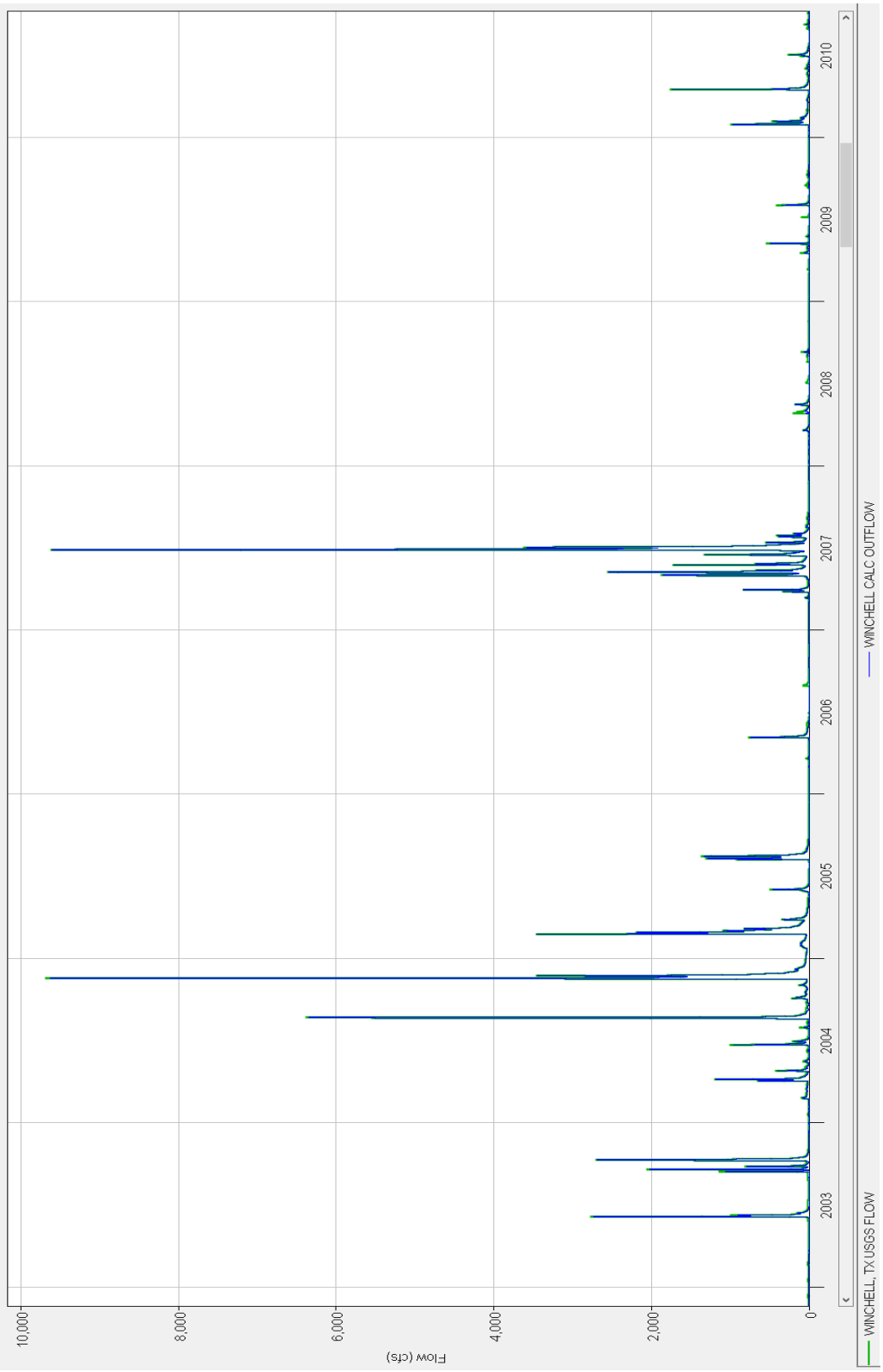

Figure 8.11: Comparison of Winchell Simulated and Observed Flows at USGS 08138000

8.6.5 Results from Lake Buchanan to the Gulf

Lake Buchanan observed pool fluctuated by more than 25 feet over the years. For power generation purposes, the lake was modeled as run of river dam. During drought years, releases were set to minimum, which limited the lake drawdown level (Figure 8.12). Pool simulation and operations looked to be valid, and the observed drawdown was due to drought. Sensitivity analysis was performed to adjust conservation pool level from 1020.5 feet to 1018.0 feet. The adjustment was established by setting up model's operation level table values in zones 5 through 13 to 1018.0 feet. The lake is impacted by power drawdown operations. Future model improvements can be made as more power operation data becomes available. It should be noted that downstream reservoirs such as Lake LBJ and Lake Travis were not impacted by the pool mismatch seen in Figure 8.12. There were less discrepancies in the flood control side of the operational modeling than were seen during periods of drought. More details on Lake Buchanan's modeled operations are included in Appendix D.

Figure 8.13 compares the Lake LBJ simulated pool. Results shown in the figure indicated good model performance. The simulated pool matched up with observed; pools in both datasets were flat. Observed pool oscillation comes from the data source provided by LCRA. Fluctuations at Buchanan Lake had little to no impact on LBJ's pool. The Llano River Basin, some 4,190 square miles of uncontrolled contributing drainage area adds enough flow to Lake LBJ to offset any operation changes coming from Buchanan Lake. The 2008 and 2017 observed pool drawdowns were temporary lake lowering per requests from stakeholders (*i.e.* maintenance). The model rules were not designed to follow such unusual operations.

Lake Travis (Marshall Ford) RiverWare simulation (Figure 8.14) showed decent results in comparison with the observed pool. The model maintained the pool at conservation when possible (681.0 feet). Model rules also controlled the pool from rising above spillway crest of 714.0 feet during high inflow events by triggering releases. The simulated pool filled during years with big flow events and drops during drought years. The model mimicked the observed pool drawdown between 2011 and 2015 (drought years). It also peaked for wet years such as 2007, 2015, 2016, and 2018.

The Colorado River at Austin gage in the RiverWare model was used as a control point downstream of Lake Travis. For flood control purposes, a threshold peak flow of 30,000 cfs was set and was not to be exceeded below surcharge pool. Austin's control point uses USGS gage 08158000, Colorado River at Austin, for comparison. Flows routed from Lake Travis to Austin are shown in Figure 8.15. Model results showed that 30,000 cfs was not violated during flood control operations. Flows at Austin were routed all the way down to the Gulf of Mexico through Bay City USGS gage 08162500.

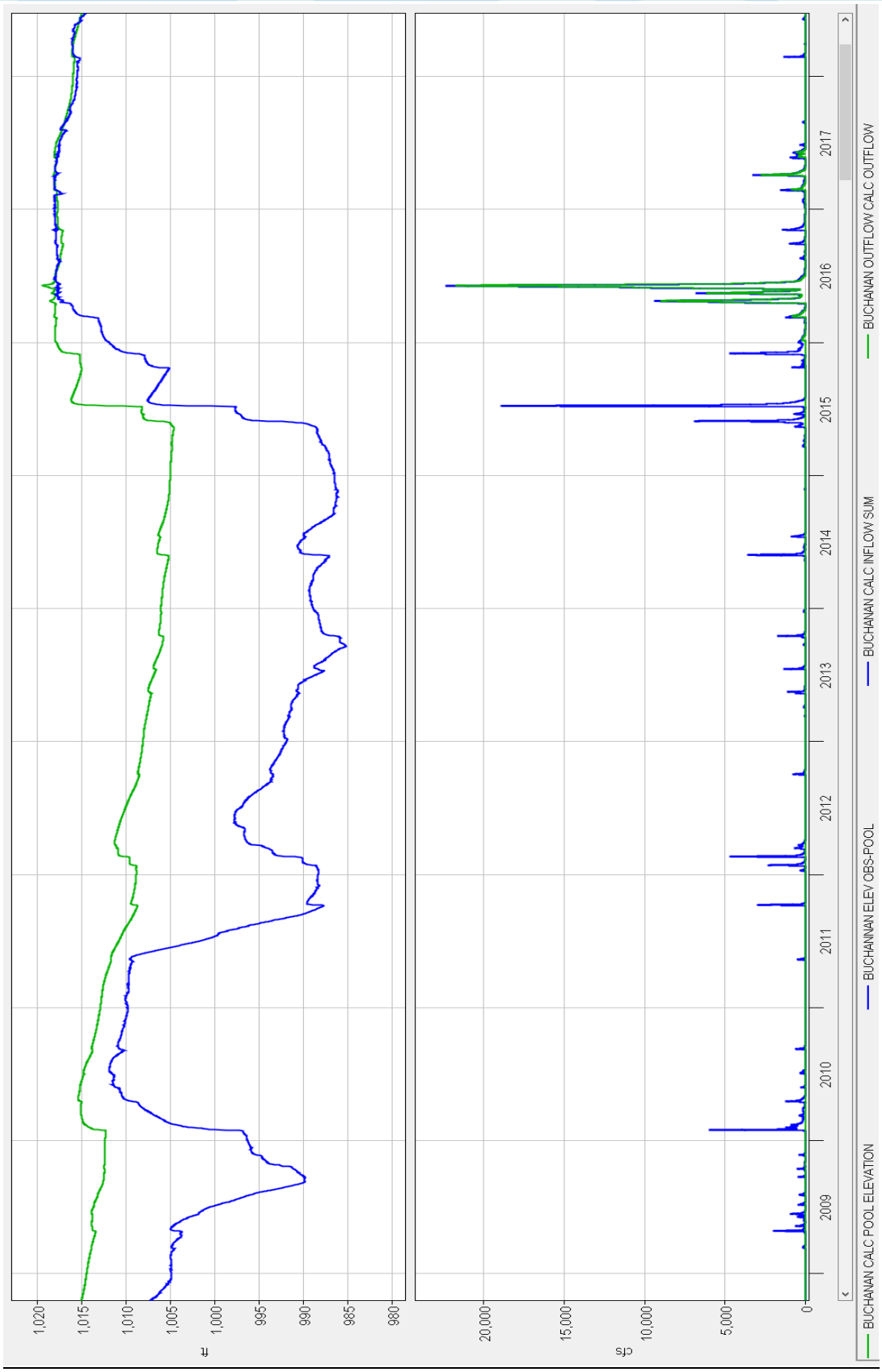

Figure 8.12: Lake Buchannan RiverWare Simulation Comparison

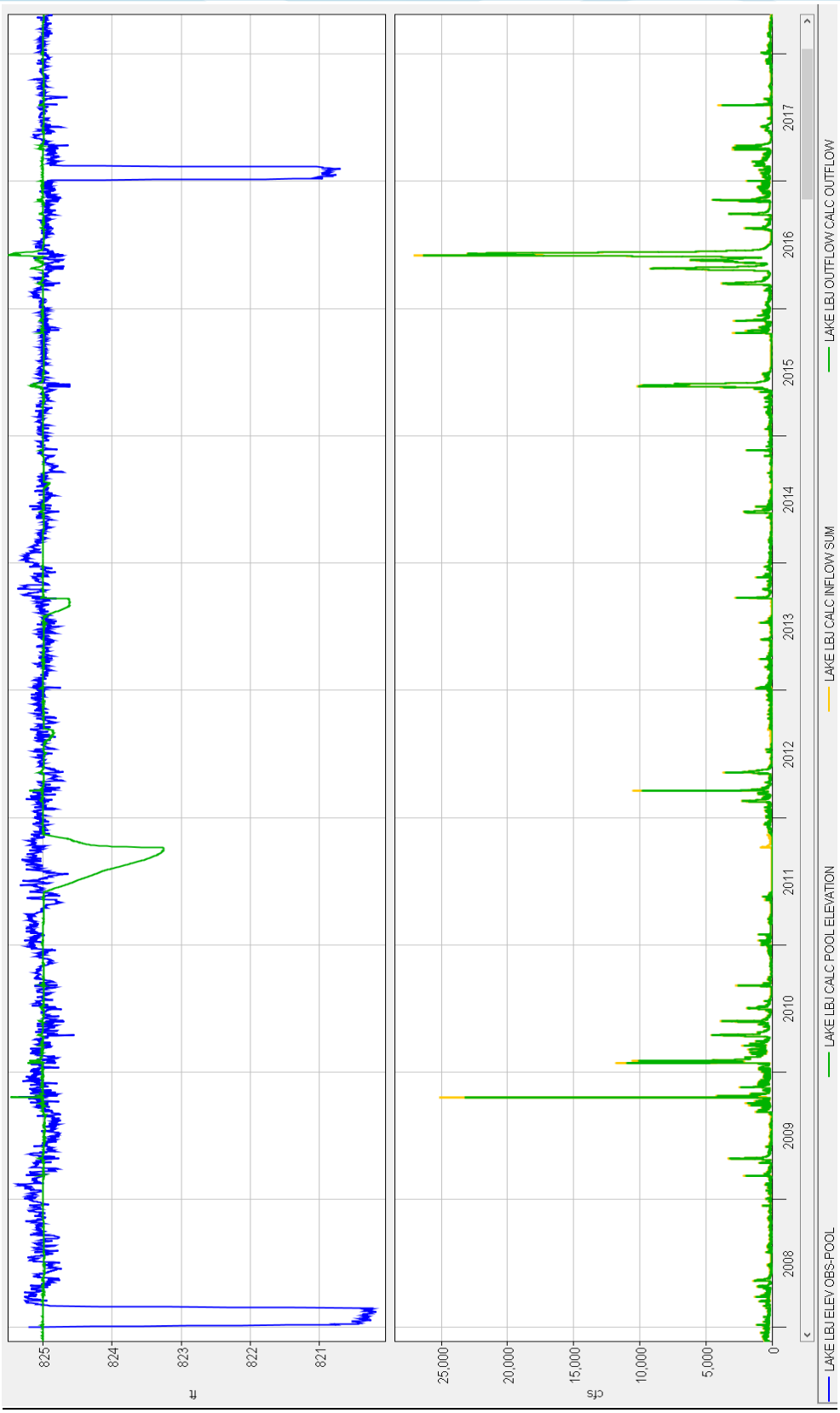

Figure 8.13: Lake LBJ RiverWare Simulation Comparison

Figure 8.14: Lake Travis (Marshall Ford) Pool RiverWare Simulation Comparison

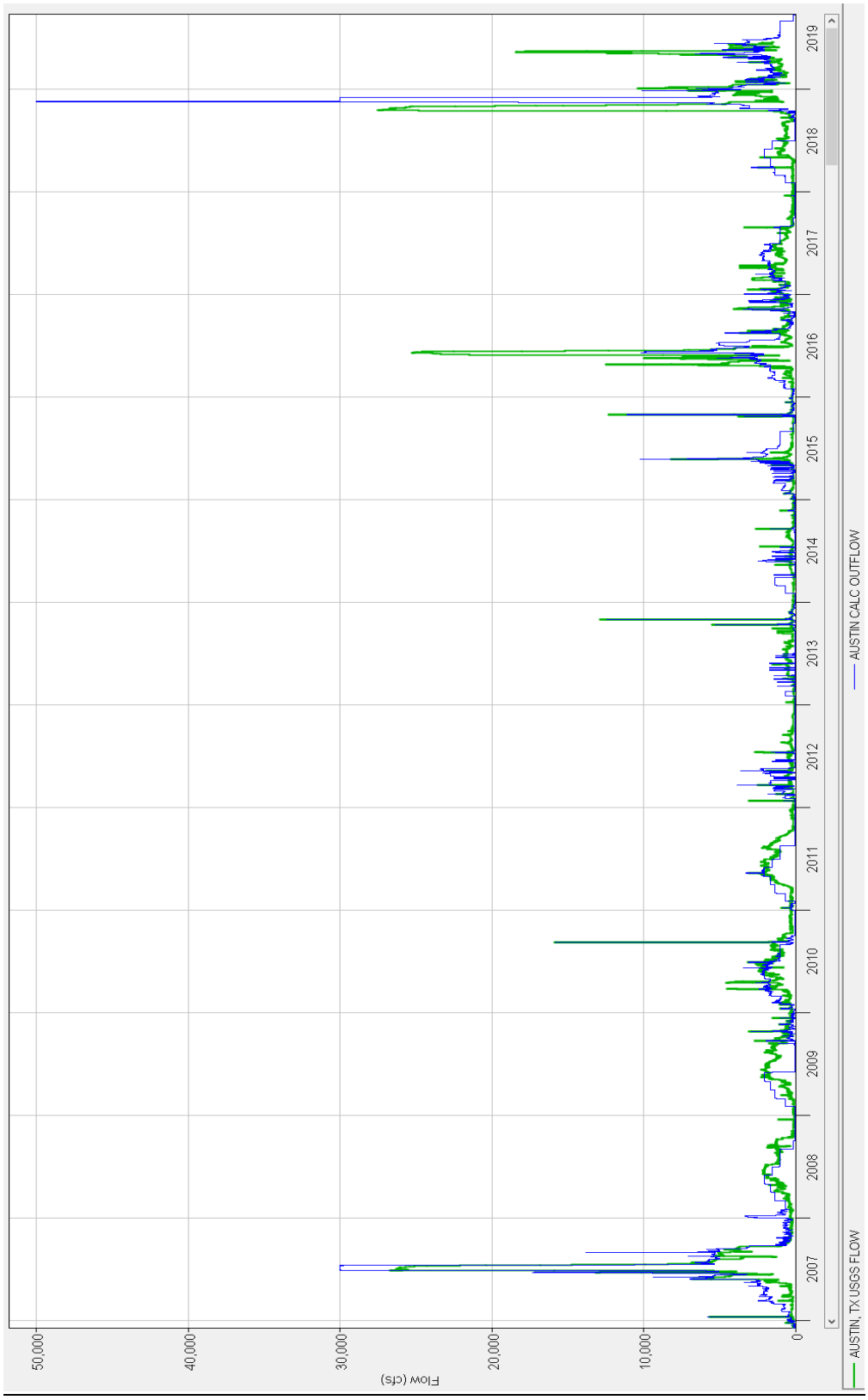

Figure 8.15: Comparison of Simulated and Observed Flows at the Colorado River at Austin

8.7 FINAL RIVERWARE MODEL PERIOD OF RECORD RESULTS

The final RiverWare simulation run results for the POR (*i.e.* January 1, 1930 – September 30, 2019) are shown in Figures D.23 to D.39 of Appendix D. These results reflect what the flows on the rivers would have been if all the current reservoirs in the basin had been in place for the entire period of record. The plots reflect good operational results and similarities with stream gaged (observed) data for the most part. Figure 8.16 below is an example POR plot for the Colorado River at Austin. The data in each plot was used in a tabular format as input to the flow frequency analyses described in the next sections.

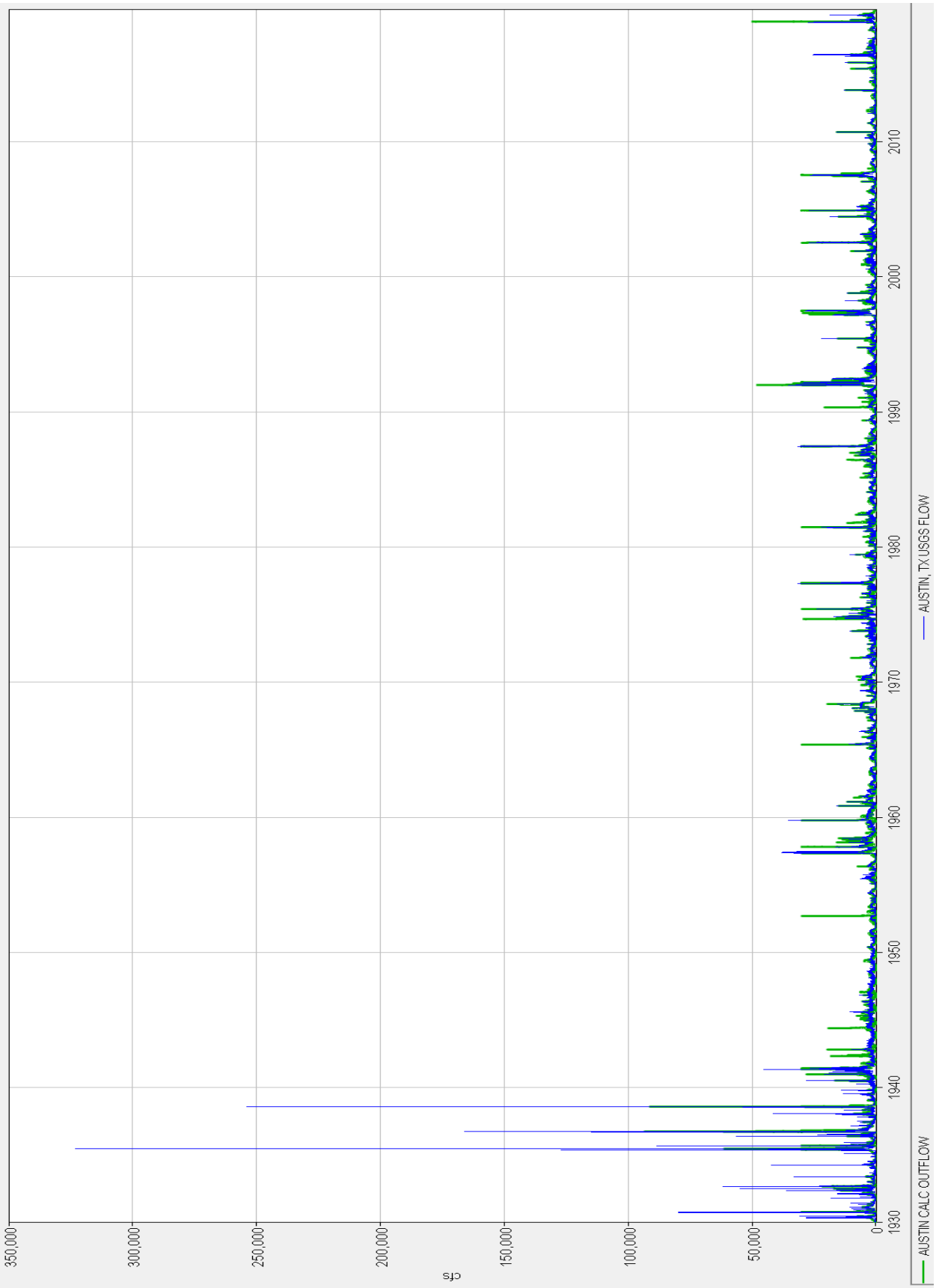

Figure 8.16: RiverWare Regulated Results Comparison for USGS 08158000 Colorado River at Austin, TX

8.8 CONVERSION OF DAILY DISCHARGES TO PEAK INSTANTANEOUS DISCHARGES

While the RiverWare model runs on a daily time step, instantaneous discharge peaks are needed for flow frequency analysis. Therefore, a comparison of USGS observed instantaneous peaks and the corresponding USGS daily average discharges were made in order to convert the RiverWare daily discharges to an equivalent instantaneous discharge peak for each streamgage of interest. A plot of instantaneous discharges versus USGS daily average peak discharges were made, and a regression equation was fit to each dataset. The regression equations were then applied to the daily peak flows from RiverWare to transform them into instantaneous peaks. Figures D.40 through D.54 of Appendix D illustrate the corresponding relationship between datasets used to generate peaking factors to transform peaks. Figure 8.17 below shows an example of one of these plots for the Colorado River at Winchell. Most of the reservoir projects' releases are not measured using USGS streamgages but are computed and stored in the operator's database (*i.e.* SWD and LCRA).

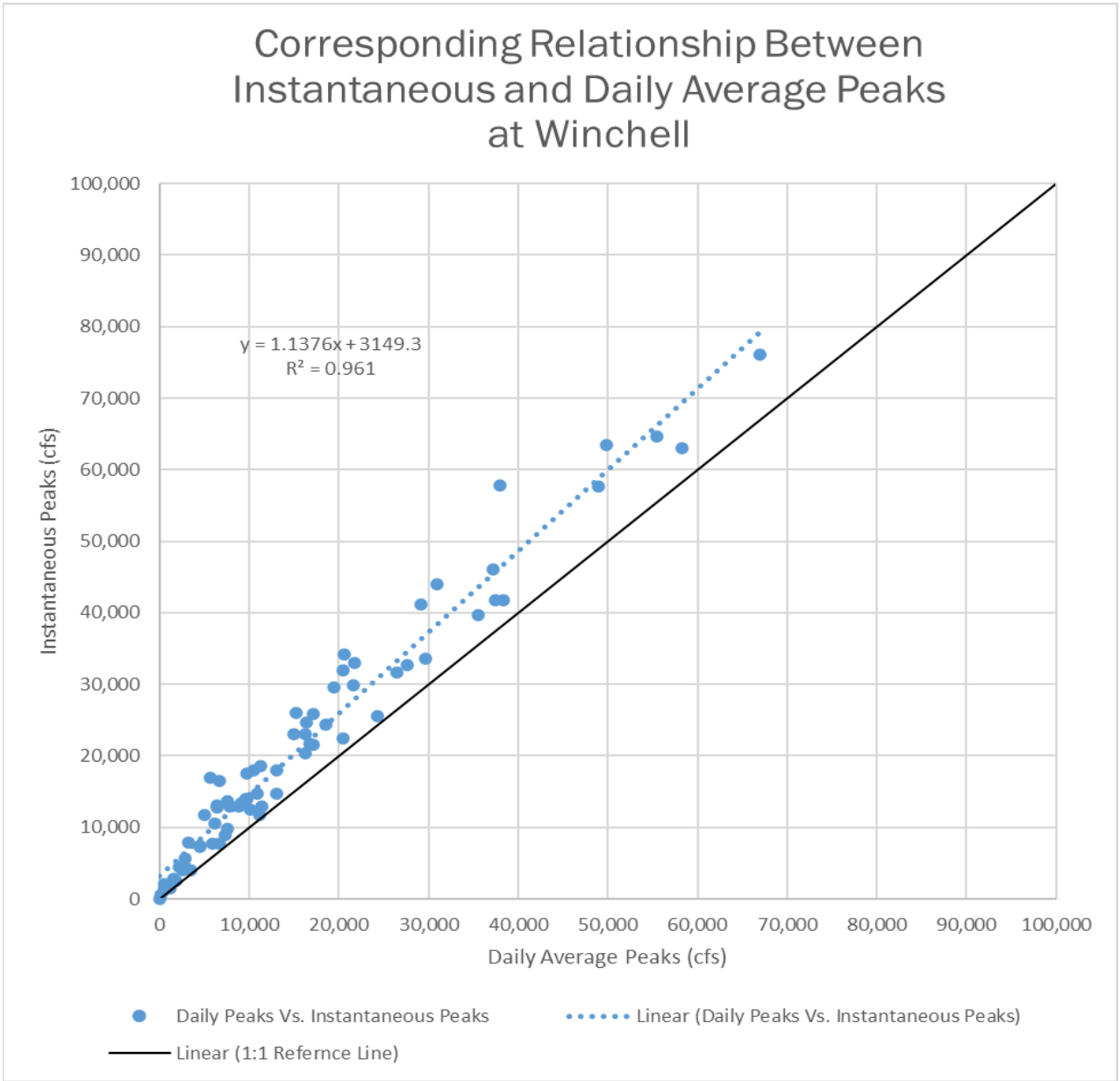

Figure 8.17: Instantaneous vs. Daily Average Peak Discharges for USGS 08138000 Colorado River at Winchell

The finalized discharge peaks, which will be used to develop the discharge frequency peaks, were a compilation of the USGS instantaneous observed peaks, downloaded from the USGS National Water Information System (NWIS) database (USGS, 2019), filled with the simulated RiverWare peaks when USGS peaks were missing and for years prior to when the reservoirs came online. The simulated peaks are the instantaneous annual maximum flow for each water year.

8.9 STREAMGAGE DATA AND STATISTICAL FLOOD FLOW FREQUENCY RESULTS

For the statistical analysis of the RiverWare modeling results, the simulated instantaneous peak streamflow was analyzed for 17 USGS streamgages and five reservoir outflows in the RiverWare model, as shown in Table 8.4. The U.S. Geological Survey contributed to the InFRM team's efforts by performing the statistical analysis of the simulated record and authored this section of the analysis to the Lower Colorado Watershed Hydrology Assessment. A peaking factor, described in detail in section 8.8 was applied to the RiverWare daily time-step data to convert daily peak streamflow to instantaneous peak streamflow. In this way, the annual peak streamflow was determined for each water year in the period of record (POR) for a given streamgage. The terms "flow," "streamflow," and "discharge" are synonymous and are used interchangeably in this report. All three terms refer to the volume of water that passes a given point within a given period of time; all are expressed in units of cubic feet per second. Any use of trade, firm, or product names is for descriptive purposes only and does not imply endorsement by the U.S. Government.

For regulated streamflow conditions in the POR, USGS observed peak streamflow data are considered to be the most reliable source of data because these data recorded actual events and are not simulated streamflow. However, the streamflow in many streams in Texas is currently (2022) regulated by impoundments (dams). Regulation of a watershed, especially the impoundment of a stream, typically leads to an attenuation in streamflow. This means that in general a regulated stream would be expected to have lower annual peak streamflow than the same stream without regulation. Because the attenuating effects of dams on peak streamflow are accounted for in the simulated streamflow data, RiverWare simulated annual peak streamflow computed by the U.S. Army Corps of Engineers (USACE) were substituted for USGS annual peak values obtained prior to when a dam was built on a given river. Hereinafter, "observed record (or dataset)" refers only to a record consisting solely of USGS observed peak streamflow values, whereas "simulated record (or dataset)" refers to the combined RiverWare and USGS peak streamflow record. The site-specific details of the POR for each streamgage are described in the individual writeups for each streamgage that follow in this section.

Flood flow frequency analyses were done following the same methodology as is used in the analysis of the observed POR defined in Chapter 5. Bulletin 17C guidelines (England and others, 2019) were followed, although with some caveats. For example, the expected moments algorithm and the sophisticated interpretation of historical peak streamflow, thresholds, and so forth described in Bulletin 17C were either of limited usefulness or not needed because the combination of observed USGS (or USACE-provided reservoir outflow) peak data and RiverWare peak data results in a relatively homogeneous dataset. The PeakFQ program is designed to analyze peak streamflow datasets obtained from USGS measurements; input files for PeakFQ must conform to specific data formatting requirements (Flynn and others, 2006), which means that constructing a synthetic data-input file can be problematic and potentially lead to errors. USGS peak streamflow data are available from the USGS National Water Information System (NWIS) database (USGS, 2022) in a format compatible with PeakFQ, but the RiverWare model does not provide this formatting option. Therefore, flow frequency analyses performed on RiverWare datasets are done in the USACE HEC-SSP software, which has flexible data input requirements (USACE, 2016). Although the software interface of HEC-SSP software might be slightly different than that of the PeakFQ program, the basic setup and methodology are the same, and when given identical input, both programs will yield the same results. Additional information on the methods and assumptions that were applied in the Bulletin 17C analyses is described in Appendix D.

Table 8.4: Summary of the 22 USGS, USACE and LCRA Streamgages used in the RiverWare model of the Lower Colorado River Basin Study Area, Texas with Ancillary Information Concerning Statistical Analyses.

USGS station number	Streamgage name	RiverWare model element[1]	Simulated period of record used in analysis (WY)[2]	Observed period of record used in analysis (WY)[2]	Station Skew (unitless)	Regional skew (Asquith and others, 2021)
08124000	Colorado River at Robert Lee, TX	E.V. Spence Outflow	1931–1969	1970–2020	-0.66	-0.25
08126380	Colorado River near Ballinger, TX	Ballinger	1931–1969	1970–2020	-0.86	-0.25
N/A[3]	Outflows from O.C. Fisher Reservoir	O.C. Fisher Outflow	1931–1952	1953–2020	0.03	-0.29
N/A[3]	Outflows from Twin Buttes Reservoir	Twin Buttes Outflow	1931–1962	1963–2020	0.18	-0.31
08136000	Concho River at San Angelo, TX	San Angelo_Confl	1931–1962	1963–2020	-0.13	-0.30
08136500	Concho River at Paint Rock, TX	Paint Rock	1931–1962	1963–2020	-0.34	-0.28
08136700	Colorado River near Stacy, TX	O.H. Ivie Outflow	1931–1990	1991–2020	-0.87	-0.28
08138000	Colorado River at Winchell, TX	Winchell	1931–1990	1991–2020	0.17	-0.29
08142000	Hords Creek near Coleman, TX	Coleman	1931–1947	1948–2020	-0.28	-0.21
08143500	Pecan Bayou at Brownwood, TX	Lake Brownwood Outflow	1931–1933, 1984–2018	1934–1983, 2019–2020	-0.74	-0.23
08147000	Colorado River near San Saba, TX	San Saba	1931–1990	1991–2020	0.05	-0.33
N/A[3]	Outflows from Lake Buchanan	Buchanan Outflow	1931–1990	1991–2020	-0.03	-0.41
08150700	Llano River near Mason, TX	Mason Dam Site	1931–1967	1968–2020	-0.77	-0.44
08151500	Llano River at Llano, TX	Llano Dam Site	1931–1935	1935–2020	-0.40	-0.42
N/A[4]	Outflows from Lake Lyndon B. Johnson	Lake LBJ Outflow	1931–1951	1952–2020	-0.44	-0.43
N/A[4]	Outflows from Lake Travis	Lake Travis Outflow	1931–1940	1941–2020	0.84	-0.41
08158000	Colorado River at Austin, TX	Austin	1931–1940	1941–2020	0.00	-0.38
08159200	Colorado River at Bastrop, TX	Bastrop	1931–1960	1961–2020	-0.86	-0.33
08159500	Colorado River at Smithville, TX	Smithville	1931–1940	1941–2020	-0.71	-0.29
08161000	Colorado River at Columbus, TX	Columbus	1931–1940	1941–2020	-0.53	-0.15
08162000	Colorado River at Wharton, TX	Wharton	1931–1940	1941–2020	-0.64	-0.03
08162500	Colorado River near Bay City, TX	Bay City	1931–1947	1948–2020	-0.34	0.02

[1]The name of the model element in RiverWare from which the streamflow data is derived as denoted in Section 1.2, Figure D.1 and Table D.2

[2]The years listed in the period of record refer to water years. A water year is a 12-month period from October 1 of the first year to September 30 of the following year and is designated by the calendar year in which it ends.

3Simulated peak streamflow at the site listed in the RiverWare model element column, plus observed values obtained from the USACE Fort Worth District

4Simulated peak streamflow at the site listed in the RiverWare model element column, plus observed values obtained from the Lower Colorado River Authority

The following pages contain figures of the data and results for a few example locations from the RiverWare statistical analyses. The full data and results for all 22 analyzed locations are included in Appendix D. These results are also summarized in Table 8.5 at the end of this chapter.

O.C. Fisher Lake Outflow (North Concho River)

The POR used for the flood flow frequency analysis for O.C. Fisher Lake Outflows on the North Concho River upstream from San Angelo, TX (hereinafter referred to as the "O.C. Fisher outflows") was from 1931 through 2019. Observed outflows (streamflow) were obtained from the USACE Fort Worth District (SWF) water management database. RiverWare simulated annual peak streamflow was substituted for USGS annual peak streamflow prior to the impoundment of the reservoir in 1952. In the resulting simulated dataset for the O.C. Fisher outflows, the 1937 peak streamflow of 23,000 cfs is the largest peak of record. The peak streamflow data after being processed for statistical frequency analysis are shown in Figure 8.18. The flood flow frequency results for the O.C. Fisher outflows simulated dataset is shown in Figure 8.19. The low-outlier threshold for peak streamflow was computed by the MGBT in HEC-SSP at 6 cfs, and 38 low outliers were identified. There were many zero-flow years in the simulated record that were also identified in the analysis. The station skew computed in HEC-SSP was used as the skew. Because there is not a USGS streamgage at this location, a comparison of the simulated flood flow frequency analysis from this section and observed flood flow frequency curve from Appendix A is unavailable.

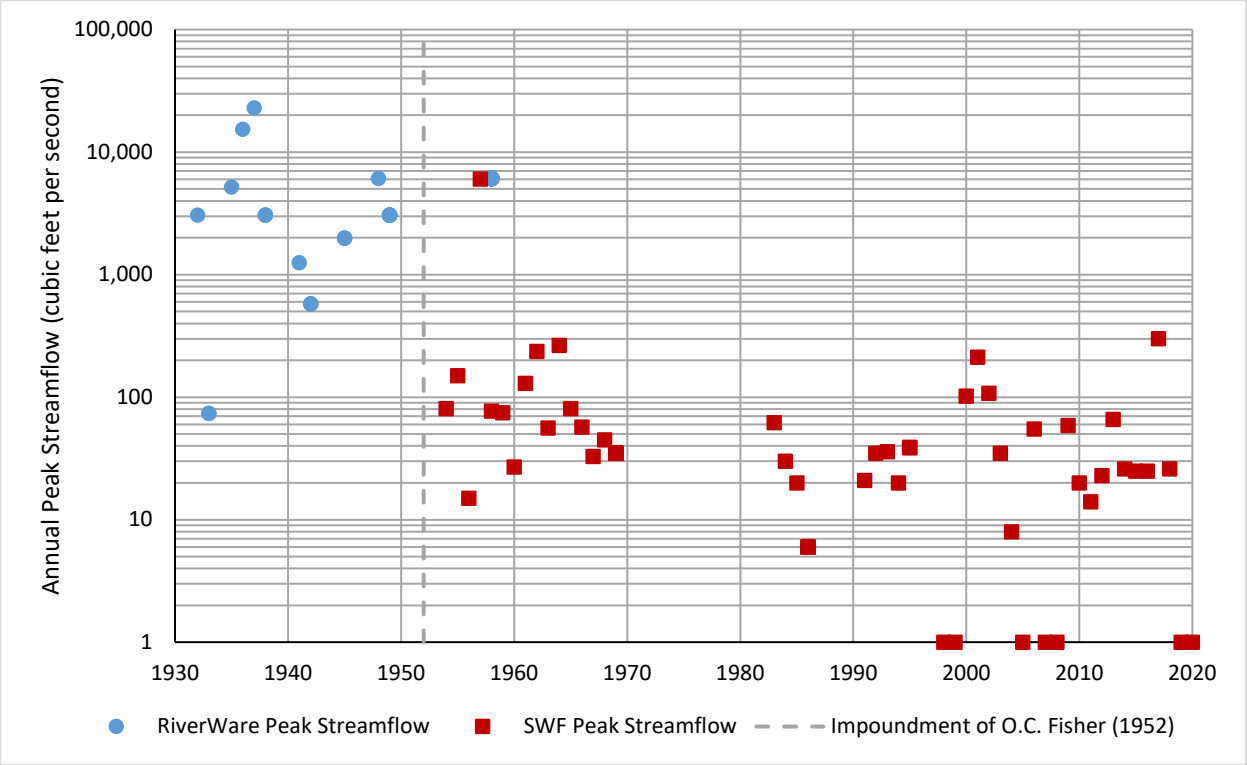

Figure 8.18: Simulated RiverWare and Observed U.S. Army Corps of Engineers Fort Worth District (SWF) Annual Peak Streamflow for O.C. Fisher Lake Outflow, TX

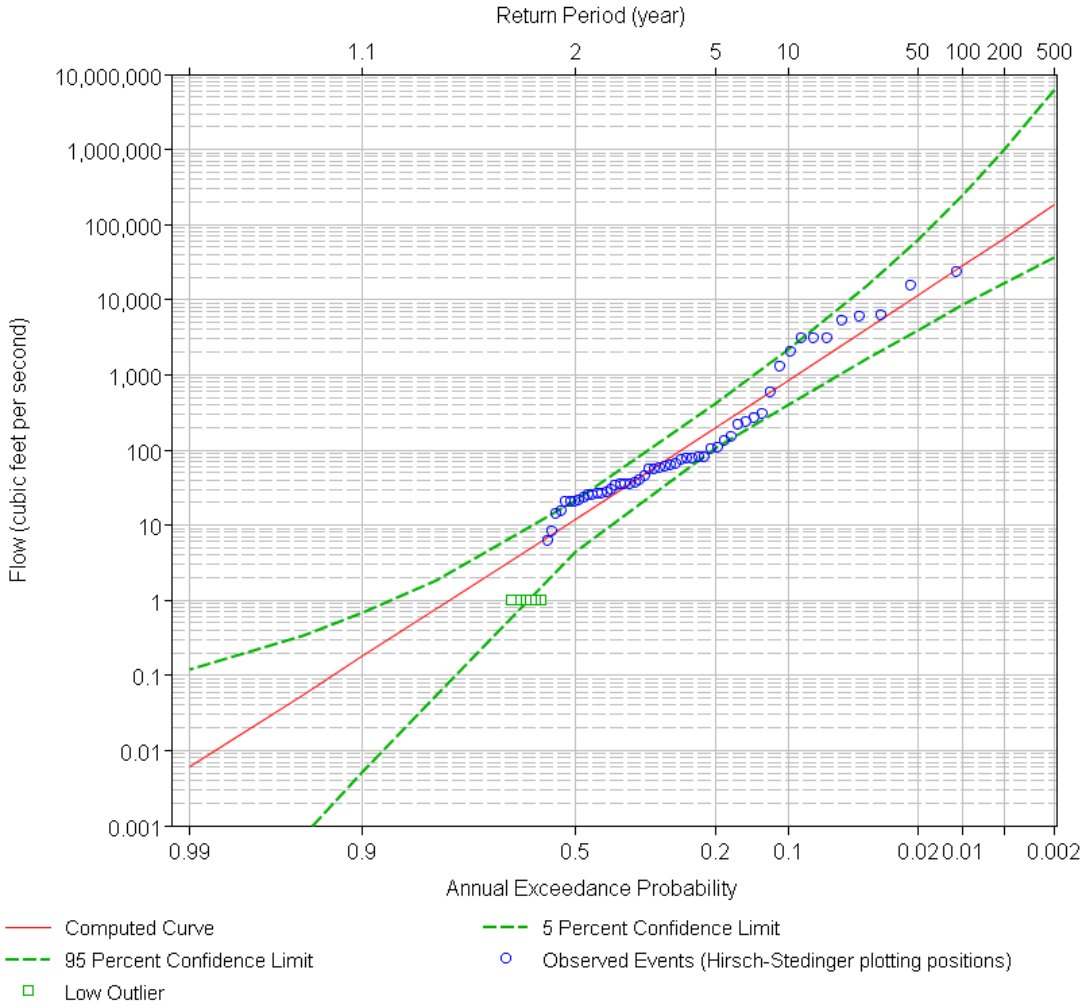

Figure 8.19: Simulated Flood Flow Frequency using log-Pearson Type III Distribution for O.C. Fisher Lake Outflows

08136700 Colorado River near Stacy, TX

The POR used for the flood flow frequency analysis at USGS streamgage 08136700 Colorado River near Stacy, TX (hereinafter referred to as the "Colorado River near Stacy gage") was from 1931 through 2020 (USGS, 2022). RiverWare simulated annual peak streamflow was substituted for USGS annual peak values prior to the impoundment of O.H. Ivie Reservoir on the Colorado River in 1990. In the resulting simulated dataset for the Colorado River near Stacy gage, the 1938 peak streamflow of 59,300 cfs is the largest peak of record. The peak streamflow data after being processed for statistical frequency analysis are shown in Figure 8.20. The flood flow frequency for the simulated dataset at Colorado River near Stacy gage is shown in Figure 8.21. The low-outlier threshold for peak streamflow was computed by the MGBT in HEC-SSP at 2,610 cfs, and 45 low-outliers were identified. There were many zero-flow years in the simulated record that were also filtered in the analysis. The station skew computed in HEC-SSP was used as the skew.

A comparison of the simulated flood flow frequency analysis from this section and observed flood flow frequency curve from Appendix A is shown in Figure 8.22. The difference between the simulated and observed flood flow frequency curves is substantial. The simulated dataset extends the period of record for the gage by another 60 years and includes events many times greater than those observed since 1990. As noted with the Colorado River at Ballinger gage, the pattern of declining streamflow and shift in peaks in the 1960s is causing the simulated RiverWare flood frequency curve to plot higher than the observed flood frequency curve, which only has data beginning in 1990, especially at the 0.5 AEP (2-year return) estimate (Figure 8.22).

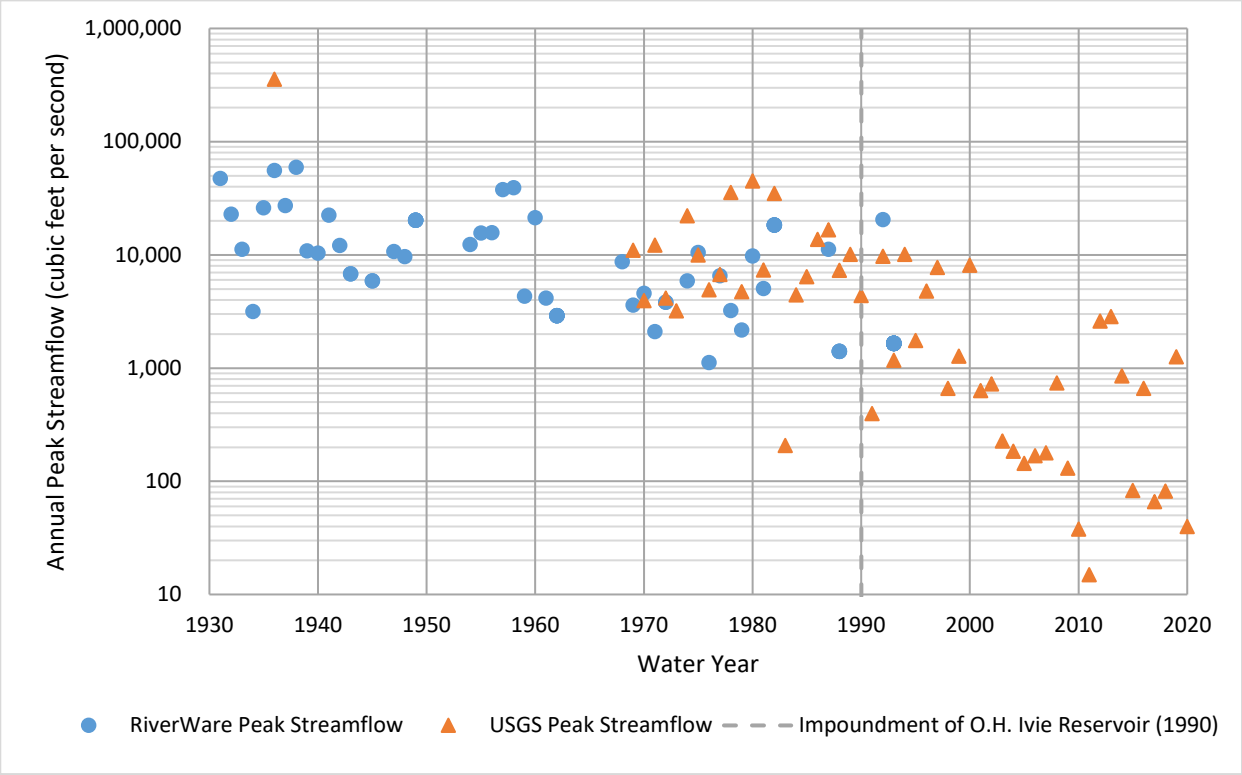

Figure 8.20: Simulated RiverWare and Observed USGS Annual Peak Streamflow for USGS 08136700 Colorado River near Stacy, TX

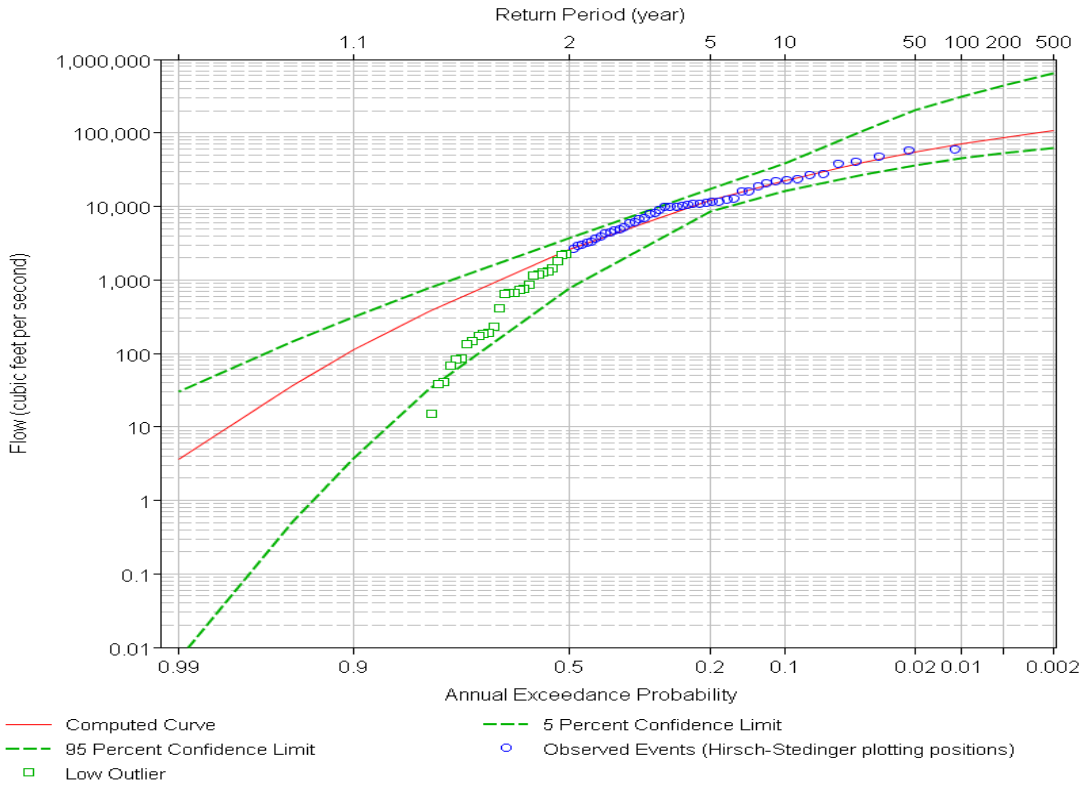

Figure 8.21: Simulated Flood Flow Frequency using log-Pearson Type III Distribution for USGS 08136700 Colorado River near Stacy, TX

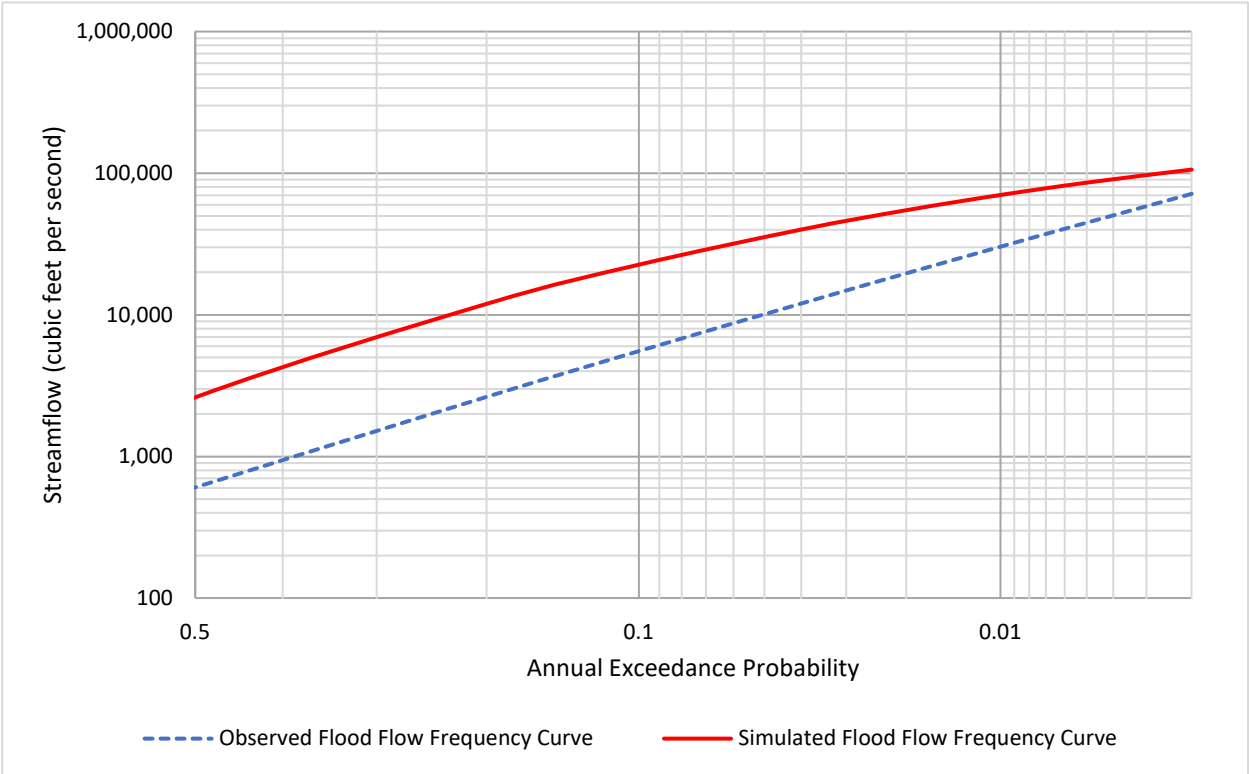

Figure 8.22: Comparison of Flood Flow Frequency Curves for the Observed (1990-2020) and Simulated (1931-2020) Datasets for USGS Streamgage 08136700 Colorado River near Stacy, TX

08158000 Colorado River at Austin, TX

The POR used for the flood flow frequency analysis at USGS streamgage 08158000 Colorado River at Austin, TX (hereinafter referred to as the "Colorado River at Austin gage") was from 1931 through 2020 (USGS, 2022). RiverWare simulated annual peak streamflow was substituted for USGS annual peak values prior to the impoundment of Lake Travis on the Colorado River in 1940. In the resulting simulated dataset for the Colorado River at Austin gage, the 1936 peak streamflow of 93,500 cfs is the largest peak of record. The peak streamflow data after being processed for statistical frequency analysis are shown in Figure 8.23. The flood flow frequency for the simulated dataset at the Colorado River at Austin gage is shown in Figure 8.24. The low-outlier threshold was manually set at 5,000 cfs, and a total of 12 low-outliers were identified. The station skew computed in HEC-SSP was weighted by the regional skew value listed in Table 8.4.

A comparison of the simulated flood flow frequency analysis from this section and observed flood flow frequency curve from Appendix A is shown in Figure 8.25. The two curves deviate noticeably in the upper AEP range, where the simulated curve has much greater frequency estimates. This could be a result of the inclusion of simulated RiverWare streamflows of greater than 100,000 cfs prior to the impoundment of Lake Travis in the 1930s.

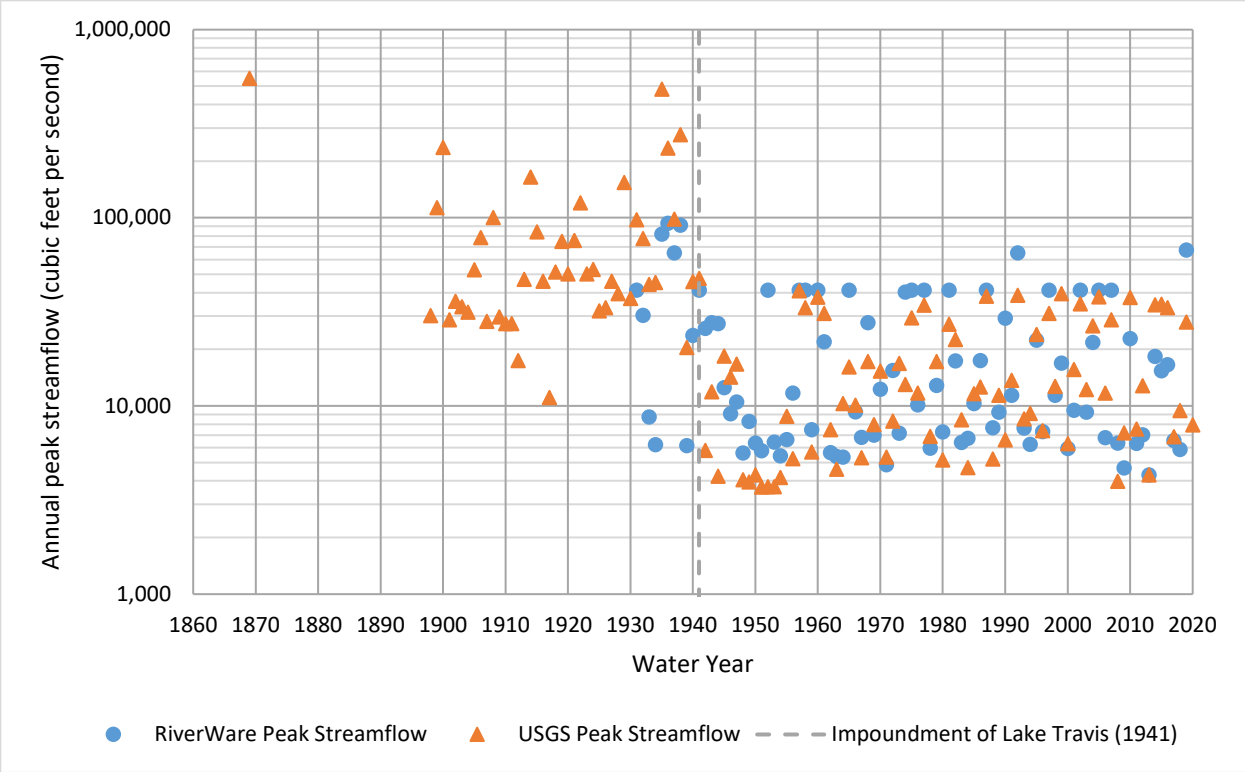

Figure 8.23: Simulated RiverWare and Observed USGS Annual Peak Streamflow for USGS Streamgage 08158000 Colorado River at Austin, TX

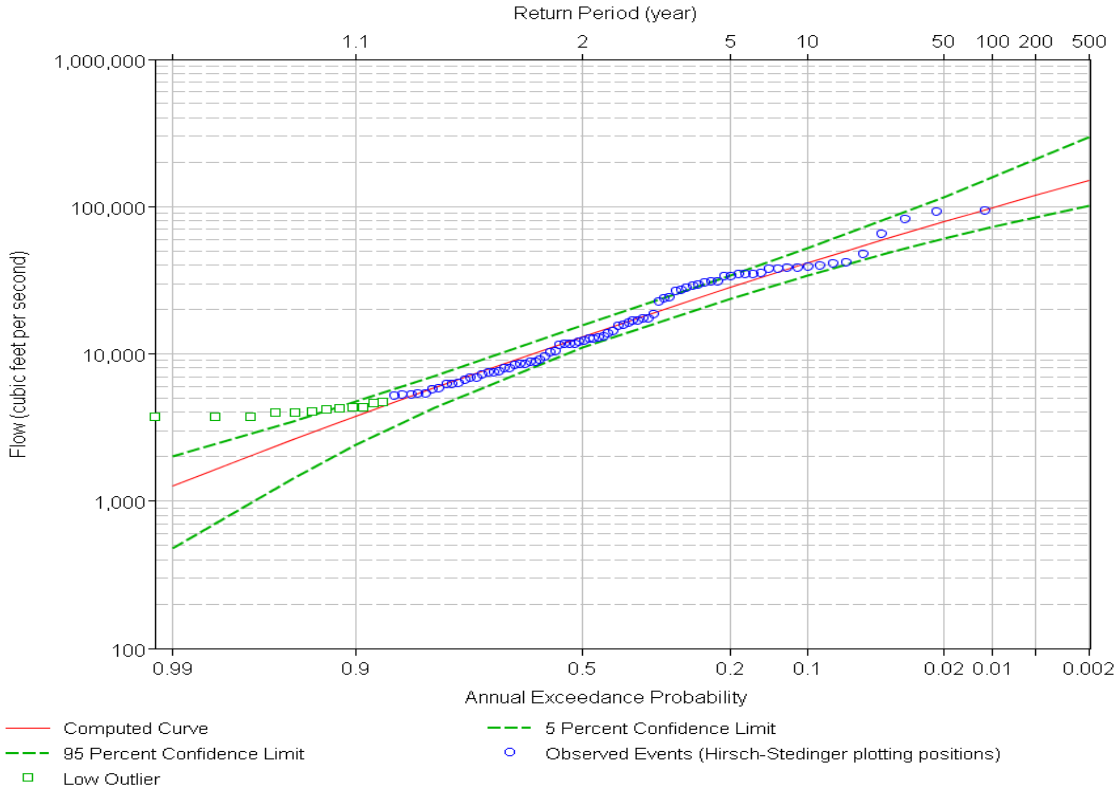

Figure 8.24: Simulated Flood Flow Frequency using log-Pearson Type III Distribution for USGS Streamgage 08158000 Colorado River at Austin, TX

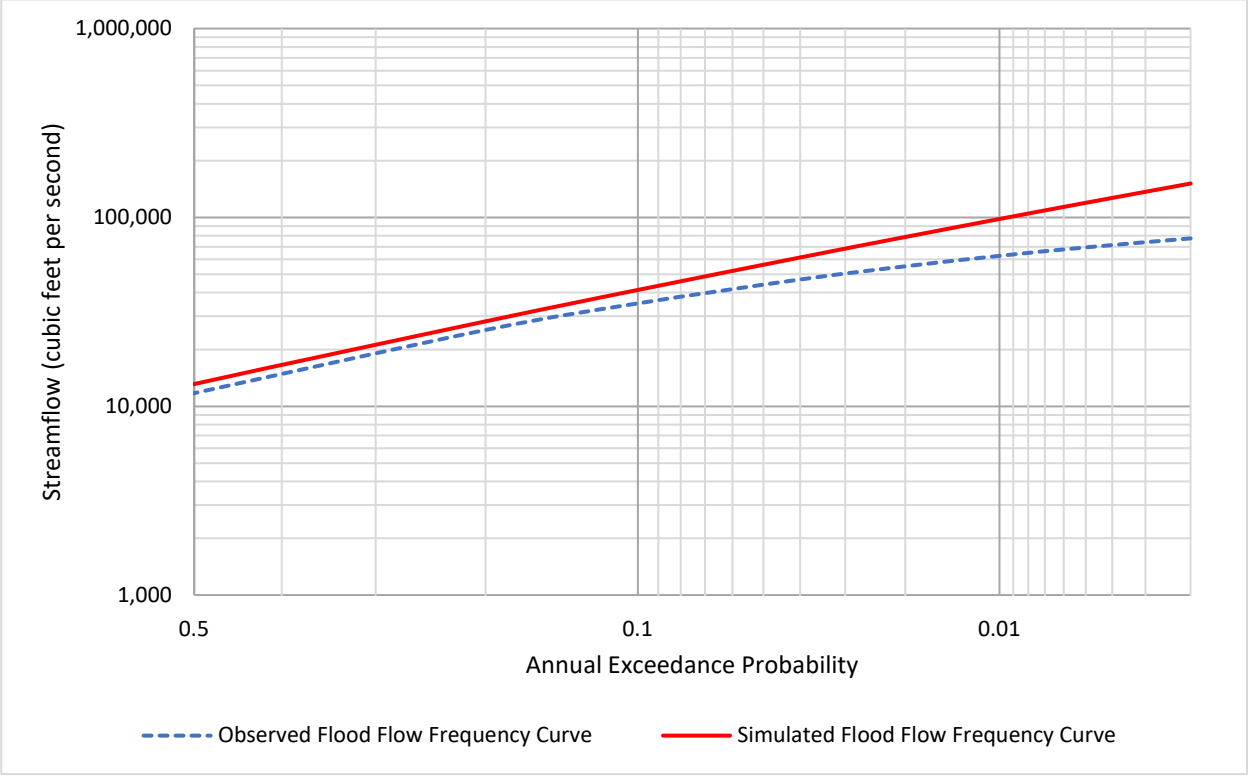

Figure 8.25: Comparison of Flood Flow Frequency Curves for the Observed (1941-2020) and Simulated (1931-2020) Datasets for USGS Streamgage 08158000 Colorado River at Austin, TX

Table 8.5: Statistically Estimated Annual Flood Frequency Results and Confidence Intervals Simulated for 22 U.S. Geological Survey Streamgages in the Lower Colorado River Basin, Texas, determined by Hydrologic Engineering Center-Statistical Software Package Software

[cfs, cubic feet per second; %, percent; CI, confidence interval; Note, table contents derived from HEC-SSP software output (USACE, 2016). The estimates are of primary interest and are accentuated using a bold typeface.]

Station name	Flood flow frequency by corresponding average return period (recurrence interval) in years							
	2 year (cfs)	5 year (cfs)	10 year (cfs)	25 year (cfs)	50 year (cfs)	100 year (cfs)	200 year (cfs)	500 year (cfs)
08124000 Colorado River at Robert Lee, TX								
Lower 95%-CI	66	1,320	3,920	10,600	18,400	28,400	40,100	57,100
Estimate	**190**	**2,320**	**7,070**	**20,100**	**36,800**	**60,500**	**91,800**	**146,000**
Upper 95%-CI	337	4,290	14,300	47,900	101,000	192,000	344,000	699,000
08126380 Colorado River near Ballinger, TX								
Lower 95%-CI	4,560	13,200	20,600	30,500	36,900	42,300	46,600	51,000
Estimate	**6,030**	**16,800**	**25,900**	**38,500**	**47,900**	**57,200**	**66,000**	**77,000**
Upper 95%-CI	7,820	21,100	32,900	52,300	70,400	91,800	117,000	158,000
O.C. Fisher Lake Outflows								
Lower 95%-CI	4	105	403	1,640	3,970	8,550	16,900	37,300
Estimate	**12**	**196**	**849**	**4,090**	**11,300**	**28,400**	**66,100**	**184,000**
Upper 95%-CI	21	420	2,190	15,200	61,400	245,000	985,000	6,280,000
Twin Buttes Reservoir Outflows								
Lower 95%-CI	64	420	1,050	2,750	5,080	8,710	14,100	24,800
Estimate	**103**	**641**	**1,730**	**5,110**	**10,400**	**20,100**	**36,900**	**77,900**
Upper 95%-CI	152	1,070	3,300	13,400	39,000	117,000	360,000	1,620,000
08136000 Concho River at San Angelo, TX								
Lower 95%-CI	1,260	4,630	8,220	13,900	18,400	22,800	26,700	31,400
Estimate	**1,740**	**6,220**	**11,100**	**19,200**	**26,400**	**34,500**	**43,300**	**55,700**
Upper 95%-CI	2,380	8,400	15,300	29,400	45,400	67,400	97,200	153,000
08136500 Concho River at Paint Rock, TX								
Lower 95%-CI	3,310	8,210	12,200	16,200	18,600	20,800	22,800	25,000
Estimate	**4,270**	**10,100**	**15,400**	**23,600**	**30,800**	**38,800**	**47,800**	**60,900**
Upper 95%-CI	5,340	12,600	20,800	37,800	57,900	87,400	131,000	221,000
08136700 Colorado River near Stacy, TX								
Lower 95%-CI	806	8,650	16,300	27,400	36,300	45,000	53,200	63,100
Estimate	**2,690**	**12,100**	**22,800**	**40,200**	**54,900**	**70,200**	**85,800**	**106,000**
Upper 95%-CI	3,840	17,400	38,100	104,000	197,000	298,000	420,000	615,000
08138000 Colorado River near Winchell, TX								
Lower 95%-CI	8,180	15,600	22,000	31,300	39,000	47,300	56,200	68,800
Estimate	**9,470**	**18,400**	**26,300**	**39,100**	**50,900**	**64,700**	**80,900**	**106,000**
Upper 95%-CI	11,000	22,000	33,300	56,200	82,900	121,000	176,000	286,000
08142000 Hords Creek near Coleman, TX								
Lower 95%-CI	1,140	3,050	4,730	6,570	7,760	8,830	9,820	11,000
Estimate	**1,500**	**3,820**	**6,090**	**9,840**	**13,300**	**17,400**	**22,000**	**29,200**
Upper 95%-CI	1,910	4,870	8,500	16,400	26,400	41,700	65,400	117,000

Table 8.5 (continued): Statistically Estimated Annual Flood Frequency Results and Confidence Intervals Simulated for 22 U.S. Geological Survey Streamgages in the Lower Colorado River Basin, Texas, determined by Hydrologic Engineering Center-Statistical Software Package Software

Station name	Flood flow frequency by corresponding average return period (recurrence interval) in years							
	2 year (cfs)	5 year (cfs)	10 year (cfs)	25 year (cfs)	50 year (cfs)	100 year (cfs)	200 year (cfs)	500 year (cfs)
08143500 Pecan Bayou near Brownwood, TX								
Lower 95%-CI	2,900	8,390	13,000	19,300	23,900	28,000	31,600	35,600
Estimate	**3,890**	**10,600**	**16,400**	**24,600**	**31,000**	**37,500**	**44,000**	**52,300**
Upper 95%-CI	4,950	13,400	21,000	33,400	45,100	59,300	76,500	105,000
08147000 Colorado River near San Saba, TX								
Lower 95%-CI	13,100	28,700	43,000	65,200	84,300	105,000	129,000	162,000
Estimate	**15,700**	**34,700**	**53,200**	**84,700**	**115,000**	**152,000**	**196,000**	**268,000**
Upper 95%-CI	18,700	42,900	70,000	127,000	195,000	294,000	437,000	724,000
Lake Buchanan Outflows								
Lower 95%-CI	9,460	23,000	35,300	54,700	71,600	90,100	110,000	139,000
Estimate	**11,800**	**28,300**	**44,600**	**72,300**	**98,600**	**130,000**	**168,000**	**229,000**
Upper 95%-CI	14,300	35,700	59,200	108,000	169,000	263,000	409,000	734,000
08150700 Llano River near Mason, TX								
Lower 95%-CI	10,900	53,200	101,000	180,000	244,000	307,000	365,000	434,000
Estimate	**17,100**	**74,600**	**142,000**	**256,000**	**358,000**	**469,000**	**588,000**	**750,000**
Upper 95%-CI	24,400	106,000	205,000	399,000	612,000	901,000	1,290,000	2,000,000
08151500 Llano River at Llano, TX								
Lower 95%-CI	20,500	64,200	109,000	177,000	230,000	281,000	329,000	388,000
Estimate	**27,000**	**83,300**	**142,000**	**240,000**	**331,000**	**434,000**	**551,000**	**725,000**
Upper 95%-CI	35,500	109,000	194,000	368,000	558,000	816,000	1,160,000	1,780,000
Lake Lyndon B. Johnson Outflows								
Lower 95%-CI	27,300	73,000	115,000	176,000	223,000	269,000	312,000	365,000
Estimate	**34,700**	**91,500**	**145,000**	**227,000**	**299,000**	**377,000**	**462,000**	**584,000**
Upper 95%-CI	43,800	116,000	189,000	326,000	472,000	665,000	919,000	1,370,000
Lake Travis Outflows								
Lower 95%-CI	5,000	11,900	18,600	29,800	40,100	51,900	65,500	86,200
Estimate	**6,060**	**14,700**	**23,700**	**40,000**	**56,500**	**77,500**	**104,000**	**149,000**
Upper 95%-CI	7,350	18,600	32,000	61,200	96,800	151,000	231,000	398,000
08158000 Colorado River at Austin, TX								
Lower 95%-CI	11,000	23,800	34,300	49,200	60,900	72,800	84,700	100,000
Estimate	**13,200**	**28,500**	**41,700**	**61,800**	**79,200**	**98,400**	**120,000**	**151,000**
Upper 95%-CI	15,700	34,600	52,700	84,500	116,000	157,000	208,000	296,000
08159200 Colorado River at Bastrop, TX								
Lower 95%-CI	14,600	38,300	51,500	67,700	79,300	90,500	101,000	114,000
Estimate	**22,800**	**44,300**	**60,700**	**82,800**	**99,900**	**117,000**	**135,000**	**159,000**
Upper 95%-CI	26,400	52,700	76,700	117,000	153,000	193,000	236,000	299,000

Table 8.5 (continued): Statistically Estimated Annual Flood Frequency Results and Confidence Intervals Simulated for 22 U.S. Geological Survey Streamgages in the Lower Colorado River Basin, Texas, determined by Hydrologic Engineering Center-Statistical Software Package Software

Station name	Flood flow frequency by corresponding average return period (recurrence interval) in years							
	2 year (cfs)	5 year (cfs)	10 year (cfs)	25 year (cfs)	50 year (cfs)	100 year (cfs)	200 year (cfs)	500 year (cfs)
08159500 Colorado River at Smithville, TX								
Lower 95%-CI	19,500	43,000	58,800	79,200	94,100	108,000	122,000	139,000
Estimate	**25,200**	**50,300**	**69,900**	**96,900**	**118,000**	**140,000**	**163,000**	**193,000**
Upper 95%-CI	29,300	60,200	87,200	129,000	165,000	205,000	250,000	318,000
08161000 Colorado River at Columbus, TX								
Lower 95%-CI	25,000	50,800	70,500	96,400	115,000	133,000	149,000	170,000
Estimate	**29,600**	**59,700**	**83,600**	**117,000**	**144,000**	**172,000**	**201,000**	**242,000**
Upper 95%-CI	34,800	70,800	102,000	152,000	199,000	253,000	317,000	417,000
08162000 Colorado River at Wharton, TX								
Lower 95%-CI	23,200	43,500	58,300	77,500	91,400	105,000	117,000	133,000
Estimate	**26,900**	**50,300**	**68,100**	**92,600**	**112,000**	**132,000**	**152,000**	**181,000**
Upper 95%-CI	31,100	58,800	81,700	117,000	149,000	187,000	231,000	300,000
08162500 Colorado River near Bay City, TX								
Lower 95%-CI	22,800	43,000	58,100	77,800	92,200	106,000	119,000	136,000
Estimate	**26,500**	**49,800**	**67,900**	**93,300**	**114,000**	**135,000**	**158,000**	**189,000**
Upper 95%-CI	30,600	58,200	81,800	120,000	154,000	195,000	242,000	317,000

9 Reservoir Analyses

9.1 INTRODUCTION

This section of the report describes the methods used to develop and update pool-frequency curves for reservoir projects within the Lower Colorado River Basin. Reservoir projects analyzed include Lake Travis, Lake Buchanan, Lake Lyndon B. Johnson (in this report will be referred to as Lake LBJ), E.V. Spence Reservoir, O.H. Ivie Reservoir, Lake Brownwood, O.C. Fisher Lake, Hords Creek Lake, Twin Buttes Reservoir, and Lake J.B. Thomas. Details of the reservoir owners and operators are listed in the previous chapter. The pool-frequency curves were developed to represent the current reservoir control plan and watershed conditions (as of 2019).

An event-based frequency analysis is a statistical method of prediction that consists of studying past events that are characteristic of a particular process to determine the probabilities of occurrence of these events in the future. A pool-frequency curve estimates the annual chance exceedance (ACE) of reservoir pool elevations. For example, if a reservoir pool elevation has an ACE of 2% (50 year), then that pool elevation has a 2% chance of being equaled or exceeded in any given year. The pool-frequency curve can be determined using empirical pool-frequency relationships based on observed data; however, the reservoir pool elevations associated with 1% ACE (100-year) or 0.2% ACE (500-year) are typically larger than what the observed reservoir pool elevation period of record (POR) can predict. Models serve the purpose of extrapolating reservoir pool-frequencies beyond the observed record. The pool-frequency curves in this study predict pool elevations resulting from the 50% ACE (2-year) to 0.2% ACE (500-year) events.

There is a lack of existing pool-frequency studies preceding this study for the purpose of comparison. However, some previous pool-frequency estimates (Table 9.1) were made by the Water Management section staff of Fort Worth District during periodic assessments (PA) as part of the USACE Dam Safety Program. In addition to the 2009 USACE estimates, there are also previous estimates from the Federal Emergency Management Agency (FEMA) Flood Insurance Studies (FIS) and the 2002 FDEP study. In this chapter, an emphasis is placed on estimating the 1% ACE (100-year) through 0.2% (500-year) events by utilizing the RMC-RFA program with data extending through WY 2019 for each reservoir project.

The Colorado River Basin encompasses a drainage area of 42,240 square miles above Bay City, of which 11,403 square miles are considered to be noncontributing in the hydrologic sense. The total contributing drainage area to each studied lake follows: Lake Travis is approximately 27,350 square miles, Lake Buchanan (20,500 square miles), Lake LBJ (24,390 square miles), EV Spence Reservoir (4,650 square miles), OH Ivie Reservoir (12,802 square miles), Lake Brownwood (1,565 square miles), OC Fisher (1,383 square miles), Hords Creek (48 square miles), Twin Buttes (2,813 square miles), and Lake JB Thomas is approximately 498 square miles.

Figure 9.1 shows the locations of the reservoir projects and the United State Geological Survey (USGS) gages used to develop the Colorado River Basin discharges. In many instances, project inflow reads recording gage data from the nearest USGS gage upstream of the dam, especially if the project drainage area does not vary significantly from the nearest USGS gage. The nearest USGS gage rating curve can also be used to estimate the historical peak discharges for the projects. Detailed analyses for hydrology development using RiverWare can be found in the RiverWare chapter of this report. The POR for Colorado River Basin reservoir projects' inflows were obtained from RiverWare.

=

Table 9.1: COLORADO RIVER BASIN PROJECTS PREVIOUS ESTIMATES OF POOL ELEVATION FREQUENCIES

Project	USACE 2009 Pool Annual Chance of Exceedance (ACE%) /Return Interval (N-Year)						
	50% (2-yr)	20% (5-yr)	10% (10-yr)	4% (25-yr)	2% (50-yr)	1% (100-yr)	0.2% (500-yr)
	Elevation (Feet) NGVD						
Hords Creek Lake	-	-	-	-	1,912.0	1,915.0	-
O.C.Fisher Lake	-	-	-	-	1,927.0	1,935.0	-
Twin Buttes Reservoir	-	-	-	-	1,955.0	1,958.0	-
Lake Travis	-	-	-	-	712.0	722.0	-
Project	FDEP 2002 Pool Annual Chance of Exceedance (ACE%) /Return Interval (N-Year)						
	50% (2-yr)	20% (5-yr)	10% (10-yr)	4% (25-yr)	2% (50-yr)	1% (100-yr)	0.2% (500-yr)
	Elevation (Feet) NGVD						
Lake Buchannan	1019.8	1019.8	1020.3	1020.3	1020.3	1020.8	1022.5
Lake LBJ	824.8	824.8	824.8	824.8	825.2	827.9	829.2
Lake Travis	685.0	690.9	696.8	713.5	716.5	721.8	736.4
Project	Effective FIS Pool Annual Chance of Exceedance (ACE%) /Return Interval (N-Year)						
	50% (2-yr)	20% (5-yr)	10% (10-yr)	4% (25-yr)	2% (50-yr)	1% (100-yr)	0.2% (500-yr)
	Elevation (Feet) NGVD						
O.C.Fisher Lake (2012)	-	-	1917.5	-	1929.5	1936.5	1947.5
Twin Buttes Reservoir (2012)	-	-	1946.4	-	1955.4	1959.4	1969.4
Lake LBJ (2012)	-	-	-	-	-	827.4	838.7
Lake Buchannan (2012)	-	-	1020.2	-	1020.2	1020.7	1022.4
Lake Travis (2020)	-	-	696.8	-	716.5	721.8	732.5

Figure 9.1: Reservoirs and USGS Gage Locations in the Colorado River Basin

9.2 METHODS OF ANALYSIS

The general workflow of the analysis for each reservoir project includes the following steps:

1) Inflow hydrograph and pool stage data gathering: Gather available reservoir inflow volumes and observed pool elevation from database systems, in the case where the reservoir project calculated inflow and observed pool elevation is limited for statistical analysis, apply RiverWare or other model to extend the available period of record representing current conditions.

2) Determine critical inflow duration: Examine the most extreme rainfall runoff inflow events and assign an appropriate threshold discharge peak to select the most appropriate hydrographs, which are analyzed to estimate the best critical inflow duration.

3) Historical discharge peak estimates: evaluate historic flood information to be translated into inflow volumes, establish a discharge peak correlation from regression equations with the nearest USGS gage, when available, to estimate the unrecorded historical discharge peaks at the lakes.

4) Volume/Flow frequency statistical analysis: incorporate both systematic and historic annual maximum inflow volumes into statistical software, Hydrologic Engineering Center-Statistical Software Package (HEC-SSP), to apply Bulletin 17C methods for establishing inflow volume-frequency relationships.

(5) Empirical frequency curve analysis: Gather reservoir annual maximum series (AMS) of pool peaks from the systematic period of record (RiverWare pool peaks output for the period of pre-dam construction and observed pool peaks for the period of post-dam construction) to develop an empirical pool-frequency curve.

6) RMC-RFA Analysis: Develop a reservoir pool-frequency model, Risk Management Center- Reservoir Frequency Analysis (RMC-RFA), to extrapolate the pool-frequency curve beyond the limits of empirical-pool-frequency curve and compute the best estimate pool frequency curves for the reservoir.

7) Pool frequency curve validation: Compare empirical pool-frequency curve and RMC-RFA modeled pool-frequency curve to validate RMC-RFA model simulation results. A closer fit between empirical and model simulated pool-frequency curves typically provides confidence in a model's ability to predict rarer frequencies.

Additional details on each step of the reservoir analyses are provided in the following sections and in Appendix E.

9.2.1 Empirical Stage-Frequency

An empirical pool-frequency curve is used to estimate the annual chance of exceedance (ACE) of a given pool elevation and can be used to evaluate the predictive capability of the simulated reservoir pool-frequency curve. An empirical pool-frequency curve is constructed by ranking the observed/simulated annual peak reservoir pools, assigning the data a plotting position, and then plotting the data on probability paper using a plotting position formula. Many plotting position formulas can be used for the orientation of an empirical pool-frequency curve, but a plotting position formula that is flexible and makes the fewest assumptions is preferred6. The Weibull plotting position formula was selected. This formula is an unbiased estimator of expected (mean) exceedance probability for all distributions and is used to plot the series of peak annual reservoir pools. The formula for Weibull is:

$$P_i = i / (n + 1)$$

Where, i is the rank of the event, n is the sample size in years, and Pi is the exceedance probability for an event with rank i pool-frequency.

9.2.2 Volume-Sampling Approach

A common method for estimating a pool-frequency curve for a dam is by volume-based sampling (USACE, 2017). In this method, a large number of flood events is generated using random sampling of flood volumes, the associated flood hydrographs are routed through the reservoir, and the peak reservoir elevation for each event is recorded.

The general workflow for a volume-based pool-frequency analysis is as follows:

1. Choose a pool for the reservoir to begin the flood event
2. Choose an inflow flood hydrograph to scale
3. Sample a flood volume from the reservoir inflow frequency curve
4. Scale the selected flood hydrograph to match the sampled flood volume
5. Route the scaled flood hydrograph through the reservoir using an operations model
6. Record the peak pool that occurred during the event

For the stochastic model, RMC-RFA, choices made in steps 1-3 are made using random selection from a probability distribution. The choice is random in the sense that it occurs without pattern, but the relative frequency of the outcomes in the long term is defined by a probability distribution. Reservoir pools for starting the simulation come from a pool duration curve, which is a probability distribution for the elevation of the reservoir

pool. They may be seasonally based, in which case first the season of the flood event occurrence is selected at random, and then a starting pool is selected at random from the pool duration curve for that particular season. Sampled flood volumes come from the familiar flow-frequency curve produced by fitting an analytical probability distribution to an AMS of river discharges. In the volume-based approach, instead of analyzing instantaneous peak discharge (as is typically the case in a Bulletin 17B/C-type analysis) (England, 2019), the analysis is performed on a longer-duration volume (i.e., 2-, 3-, 5-, 6-, 8-, 11-, and 14-day average discharge.)

When steps 1-6 are performed a large number of times (for example, 10,000 samples), the resulting peak pools are ranked and plotted, producing a pool-frequency curve for the reservoir. However, substantial uncertainty exists in several of the inputs to the model, especially the inflow volume-frequency curve. To account for these uncertainties, steps 1-6 are performed a large number of times with different parameters for the inputs. The input parameters are varied across realizations, and for each realization, steps 1-6 are repeated over a large number of samples. Thus, the full simulation with uncertainty will contain a number of events equal to the number of realizations times the number of samples.

By varying parameters across realizations, the uncertainty in the probability of an event, for example reaching spillway crest elevation, can be better assessed. Each realization will produce an estimate of the probability of reaching this elevation based on the parameters used to drive the realization. Percentiles (for example the 5th and 95th percentiles) of these probabilities produce a confidence interval for the probability of reaching the spillway. If the mean probability of exceeding any pool is taken, then the result is the expected frequency curve, which is the single best estimate for the probability of exceeding a particular pool.

9.2.3 Risk Management Center - Reservoir Frequency Analysis (RMC-RFA)

RMC-RFA software was developed by the USACE Risk Management Center for use in dam safety risk assessments (USACE, 2018). It can produce a pool-frequency curve with confidence bounds using a stochastic model with the volume-sampling approach. The model functions best in situations where dam operations are relatively simple, especially when the spillway is not regulated using gates. A simplification of the operational rules is assumed using an elevation-discharge table which is based on a combination of dam discharge structures and calibration to historical releases. Development of model inputs is aided by tools within the program that allow the user to estimate inputs, such as flood seasonality or pool duration curves, in a consistent and automated manner. Other inputs, such as the volume-frequency curve or reservoir operations, are developed by the user independently.

9.3 DATA ANALYSIS AND MODEL INPUT

9.3.1 Inflow Hydrograph and Pool Stage

Estimates of daily average discharges and pool elevations for the Colorado River Basin projects were retrieved from the USACE water management database system for water year (WY) 1930 through WY 2019. Records prior to project construction were simulated using RiverWare. The Colorado River Basin projects impoundment dates are shown in Table 9.3. RiverWare software mimics a watershed by modeling its features as linked objects, including storage or power reservoir objects, stream reach objects, groundwater storage objects, or diversion objects. In a simple model, these objects simulate basic hydrologic processes through mass balance calculations and can be linked to one another through inflow-outflow calculations. More advanced modeling is achieved by selecting object-specific methods that further define the hydrologic processes associated with each object. Additionally, RiverWare may operate under a rule-based simulation, which creates logic-based interdependency of objects through user-defined rules. These rules may look forwards and backwards in time and given priorities in one rule may supersede others depending on the importance defined by the user. These detailed yet simple modeling techniques allow RiverWare to simulate reservoir pool elevations and inflow efficiently.

Table 9.2: Deliberate Impoundment Dates for Colorado River Basin Dams

Project	Deliberate Impoundment Date	Project	Deliberate Impoundment Date
Lake Travis	September 01, 1940	Hords Creek Lake	June 01, 1948
Lake JBJ	1951	O.C Fisher	February 01, 1952
O.H Ivie	March 15, 1990	Twin Buttes	December 01, 1962
EV Spence Reservoir	June 01, 1969	Brownwood Lake	July 01, 1933
Lake Buchanan	May 20, 1937	Lake JB Thomas	1952

The Water Management Section inspected the dataset for quality before being used in the analyses. The instantaneous (hourly) lake inflows were gathered. Due to data limited availability, each dataset was supplied in groups. Figure 9.2 is an example of Lake Travis hourly inflows. Negative flows were removed from the dataset due to errors associated with data processing (*i.e.,* the n-day moving average was applied to smooth bad quality data). The hourly records may contain gaps. The gaps are for times when real time recording was missing. Data with missing records were not used in the analyses.

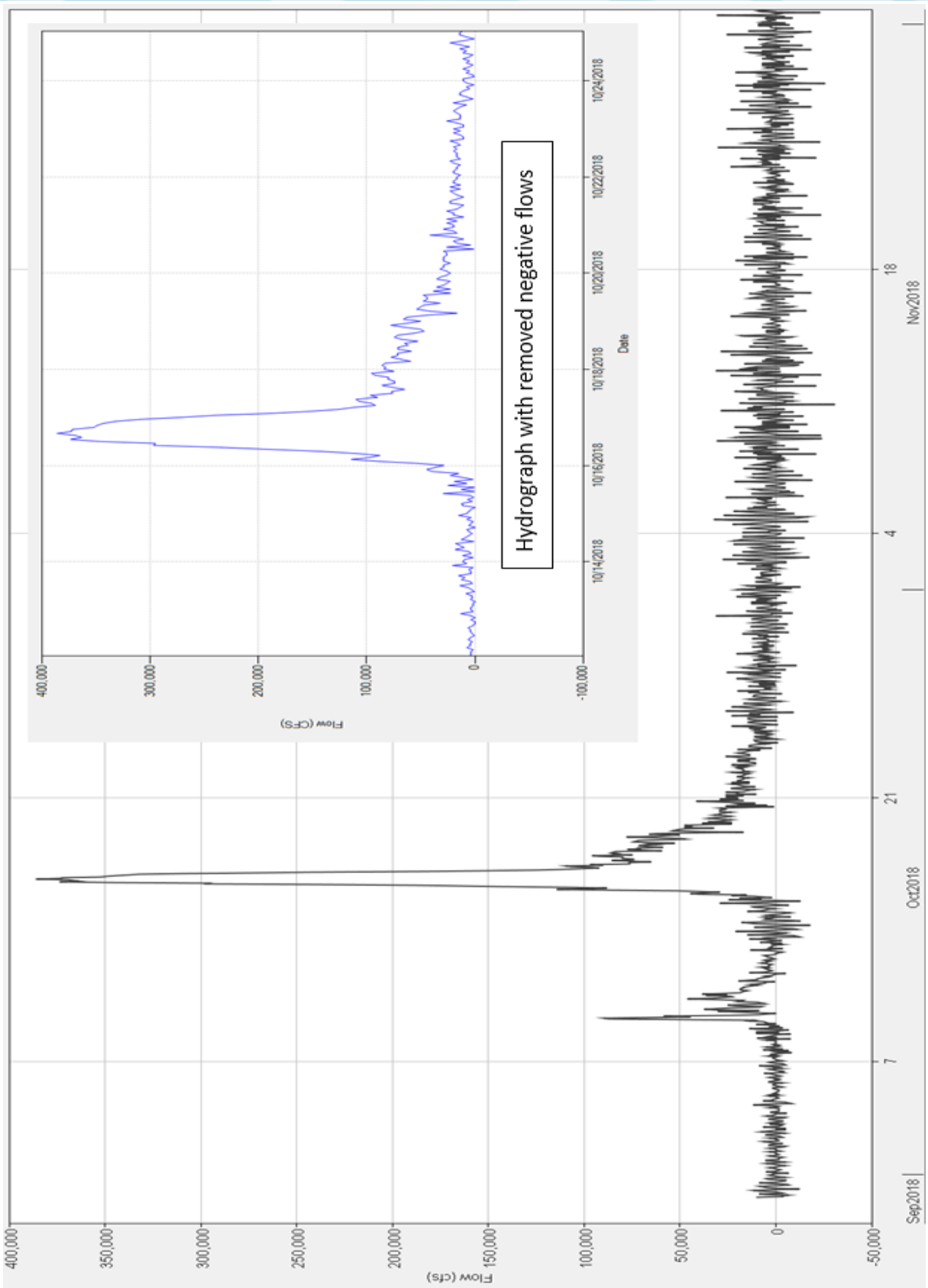

Figure 9.2: Example of Lake Travis Hourly Inflows for October 2018

9.3.2 Instantaneous Peak Estimates

The systematic inflow record contains a combined dataset of observed (recorded) post-dam construction discharges and pre-dam construction synthetic discharge generated using RiverWare. The unrecorded historical n-day peaks at the lakes were developed by establishing a discharge peak correlation with the nearest USGS gage when available. The USGS gages used for correlation are listed in Table 9.3. The criteria of selection were based on a gage's proximity to a corresponding lake, and a gage's drainage area in relation to the reservoir contributing drainage area. In addition, the observed hydrographs entering the reservoir must mimic similar patterns of those observed at the gage location to be considered. Lakes that are not listed in Table 9.3 don't have historical discharge peaks. Historical peaks at the selected USGS gages or lake inflows were generated by establishing a relationship between discharge peaks. Once a strong trendline correlation was maintained with high R^2 value, the corresponding trendline equation was used to estimate the missing peak. Examples of the peak-to-peak discharge relationships are included in Appendix E.

Table 9.3: Estimated Historical Peaks of Lake Inflows Based on Historic Data from USGS Gages

Location	USGS Gage ID	Contributing Drainage Area (mi^2)	Historical year	Instantaneous Historical Peak (CFS)	1-Day Historical Peak (CFS)
Colorado Rv at Austin	08158000	27,606	1869	550,000	524,508*
Lake Travis	N/A	27,352			519,683*
Colorado Rv nr San Saba	08147000	19,819	1900	184,000	173,660**
Lake Buchanan	N/A	20,500			179,627*
Lake Buchanan	Lake Buchanan	20,500	1900		179,627*
Lake LBJ	N/A	24,390			197,430**
Concho Rv at Paint Rock	08136500	5,443	1881	201,000	62,237**
			1905	176,000	54,380**
O.H Ivie Reservoir	N/A	12,802	1881		146,382*
			1905		127,903*
N Concho Rv nr San Angelo	08135000	1,191	1900		
O.C. Fisher	N/A	1,383		30,055****	10,916***
Hords Creek Lake	N/A	48	1900	19,320****	5,893**
Concho Rv at San Angelo	08136000	2,813	1862	228,000	79,199**
			1906	246,000	85,667**
Twin Buttes	N/A	4,411	1862		51,586*
			1906		56,196*

*Best estimate based on drainage area ratio
**Best estimate based on correlation
*** Best estimate based on correlation with Concho River near Carlsbad (USGS 08136500) peak
**** Recorded in the Water Control Manual and Design Memorandums (USACE-SWF)

9.3.3 Daily Average Annual Peak (AMS) Estimates

An extract of the 1-day average maximum annual peak for each project was made available for the analysis. The lakes systematic inflow records were generated using RiverWare, and the lakes historical 1-day and critical duration n-day inflow peaks were generated from the historical instantaneous discharge peaks. The critical duration best estimate in days is shown in the next section. Several attempts were made to better justify the best predictable n-day peaks. The n-day AMS historical peaks can be estimated using best engineering judgment once basin hydrology is well understood.

For the Colorado River Basin Lakes, the best corresponding relationship (formula) with the strongest R^2 value among all fitting curves was utilized, and the predicted peaks followed a logarithmic line trend for O.H Ivie, Lake

Travis, and the 1-, 2-, 3-, 4-day AMS for Twin Buttes Reservoir. On the other hand, the predicted peaks for Lakes Buchanan and LBJ, O.C Fisher Lake, Hords Creek Lake, and Twin Buttes Reservoir 5-, 6-, 7-day AMS followed a general linear trend. Those trends were used to estimate the 1-Day historical AMS peaks.

The critical duration annual peaks were estimated by establishing a correlation with the 1-Day AMS peaks. Trend lines with high R^2 values were maintained. Additional details on the best fitting trend line relationships are included in Appendix E. The critical duration AMS peaks are listed in Table 9.4.

Table 9.4: Colorado River Basin N-Day AMS Estimated Historical Discharge Peaks

Project	N-Day Duration AMS Peak (CFS) (Historical)						
	Year	1-Day	2-Day	3-Day	8-Day	11-Day	14-Day
Lake Travis	1869	519,682	N/A	N/A	N/A	70,020	N/A
Lake Buchanan	1900	179,627	N/A	N/A	N/A	N/A	68,712
Lake LBJ	1900	197,430	N/A	N/A	N/A	77,400	N/A
O.H Ivie Reservoir	1881	146,382	N/A	N/A	25,460	N/A	N/A
	1905	127,903	N/A	N/A	24,899	N/A	N/A
Hords Creek Lake	1900	5,893	N/A	2,381	N/A	N/A	N/A
O.C Fisher Lake	1900	10,916	7,318	N/A	N/A	N/A	N/A
Twin Buttes Reservoir	1862	51,586	N/A	16,171	N/A	N/A	N/A
	1906	56,196	N/A	16,737	N/A	N/A	N/A

9.4 CRITICAL INFLOW DURATION ANALYSIS

The critical inflow duration can be defined as the inflow duration that tends to produce most consistently the highest water surface elevation for the reservoir. Headwater projects on the Colorado River Basin are located on the upper portion of the basin, where weather patterns and climate are similar. Projects located on tributaries feeding to the Colorado main river (i.e., Hords Creek Lake, O.C Fisher Lake, and Twin Buttes Reservoir) have short critical durations. Lake JB Thomas is the most upstream reservoir of the Colorado River and its critical duration is the shortest among those located on the Colorado River mainstem. Rivers flowing to lakes located downstream have flatter slopes and wider floodplains, which allow for longer critical durations. The storm durations can also impact critical durations; longer storms result in longer critical durations.

In order to determine the critical inflow duration of the observed rainfall-runoff events, extreme rainfall runoff (inflow) events are examined. All large inflow events are considered independent, meaning that different year hydrographs can be presented in one figure to determine the proper critical duration. The duration peak inflow was used to determine a reasonable value for critical inflow duration. Although this method was found to accurately produce good estimates, the critical duration can be adjusted later during the analysis to reflect the most appropriate frequency curve. Best engineering judgment remains necessary in the final selection of the most appropriate value.

For each project, a set of historical inflow events (hydrographs) with daily peak inflows greater than a certain threshold were extracted from the RiverWare simulated daily average inflow period of record (i.e., examine the top

20% largest independent inflow events for each project inflow). The best-estimate inflow duration for the reservoir is estimated by taking the average hydrograph of the major events specified. Lake Travis was selected to demonstrate the lake inflow critical duration best estimate (Figure 9.3). Best estimates of the n-day critical durations for all projects are listed in Table 9.5. These results were finalized after making several sensitivity analyses while running the RMC-RFA program. The best critical duration estimate produced the most conservative elevation frequency in the lake. The purpose of this analysis is to have a better understanding of the runoff response from large single rain events to help establish what volume discharge frequency curves need to be examined.

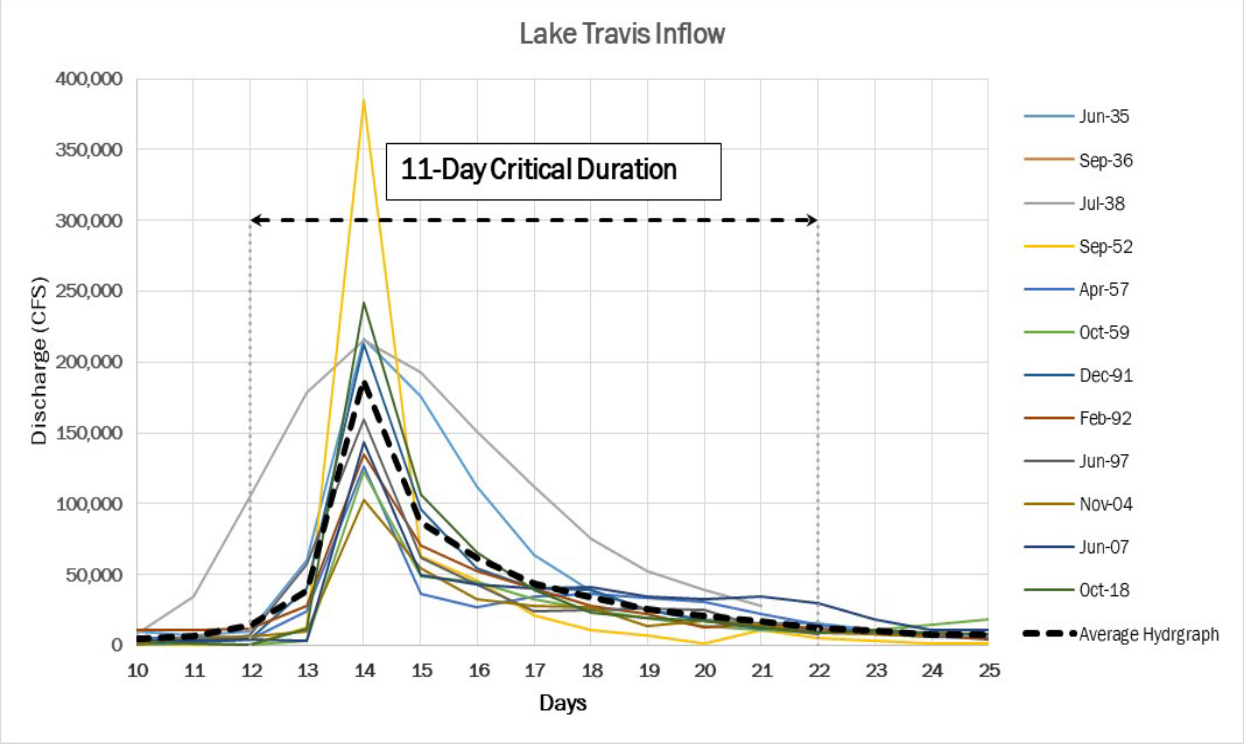

Figure 9.3: Example of Critical Duration Inflow Analysis for Lake Travis

Table 9.5 Colorado River Basin Critical Inflow Durations

Project	Minimum Threshold Peak (CFS)	Number of Analyzed Inflow Events	Critical Duration (Days)
Lake Travis	10,000	12	11
Lake Buchanan	15,000	12	14
Lake LBJ	15,000	13	11
O.H Ivie Reservoir	3,000	10	8
Lake Brownwood	4,000	9	5
EV Spence Reservoir	5,000	12	5
Hords Creek Lake	100	13	3
O.C Fisher Lake	3,000	11	2
Twin Buttes Reservoir	1,000	10	3
Lake JB Thomas	3,000	9	6

9.4.1 Volume/Flow Frequency Statistical Analysis

The volume/flow frequency analyses for the Colorado River Basin Lakes were estimated by following Bulletin 17C guidelines and procedures (statistical techniques) to determine annual exceedance probabilities associated with specific flow rates utilizing HEC-SSP 2.2. The observed and developed daily average annual maximum peaks were used to establish a relationship between flow magnitude and frequency. In this chapter, the term volume/flow frequency refers to the frequency with which a flow over a given duration, such as 1-, 2-, 3-, 5-, 6-, 8-, 11-, and 14-Day expected to be equaled or exceeded. The duration range selection was based on inspecting the shape of the hydrographs such as those shown in Figure 9.3, and the critical durations listed in Table 9.5.

To adequately assess the risk associated with the Colorado River Basin Dams' structures in question, the 2-Day critical duration was used to construct hypothetical inflow frequency events for O.C Fisher Lake; 3-Day critical duration was used for Hords Creek Lake and Twin Buttes Reservoir; 5-Day critical duration was used for Brownwood Lake and E.V Spence Reservoir; 6-Day critical duration was used for Lake JB Thomas; 8-Day critical duration was used for O.H Ivie Reservoir; 11-Day critical duration was used for Lake Travis and Lake LBJ; and 14-Day critical duration was used to construct hypothetical inflow frequency events for Lake Buchanan. The events were routed through the projects to estimate reservoirs' stage-frequency curves.

9.4.2 Bulletin 17C Application

The use of bulletin 17C guidance allows for computations of the annual exceedance probability of the instantaneous and daily average discharge peaks, using the Expected Moments Algorithm (EMA). It estimates distribution parameters based on sample moment in a more integrated manner that incorporates non-standard, censored, or historical data at once, rather than as a series of adjustment procedures (Cohn, 1997).

For the Bulletin 17C analysis, each project was assigned the associated historical peaks shown in Table 9.4. Values of perception thresholds from the historical peak events were set for the historical peak values for each project. The set of threshold peaks define the range of stream flow for which a flood event could have been observed; consequently, years for which an event was not observed and recorded, must have had a peak flow rate outside of the perception threshold. The use of bulletin 17C procedures provide confidence intervals for the resulting frequency curve that incorporate diverse information appropriately, as historical data and censored values impact the uncertainty in the estimated frequency curve (Cohn, 2001). Within the Bulletin 17C EMA methodology, every annual peak flow in the analysis period, whether observed or not, is represented by a flow range that might simply be limited to the gaged value when one exists. However, it could also reflect an uncertain flow estimate as is the case for the Colorado River Basin projects.

9.4.3 HEC-SSP Computations

A series of n-day volume frequency curves was developed for each of the Colorado River Basin projects. The volume duration frequency results from this analysis were developed using HEC-SSP. The Multiple Grubbs-Beck algorithm was used for the low outlier test. Plotting positions of the censored data was adopted from the Hirsch-Stedinger plotting position algorithm. The station skew option was used for the analysis for the projects using the systematic records. For consistency, each developed frequency curve went through the same analysis techniques before adoption. Table 9.6 contains skews and record lengths for each project analyzed using HEC-SSP. The Colorado River Basin Lakes computed critical duration frequency flows from HEC-SSP are listed in Table 9.7.

Table 9.6: Summary of HEC-SSP Input Parameters

Project	Systematic Record (years)	Historic Record (years)	Station Skew (Critical Duration)
Lake Travis	89	151	-0.472
Lake Buchanan	89	120	-0.326
Lake LBJ	89	120	-0.337
O.H Ivie Reservoir	89	138	-0.563
Lake Brownwood	89	89	-0.881
EV Spence Reservoir	89	89	-0.391
Hords Creek Lake	89	120	0.045
O.C Fisher Lake	89	120	0.025
Twin Buttes Reservoir	89	158	-0.183
Lake JB Thomas	89	89	-0.977

Note: The actual systematic record length is less than the systematic record length shown in the Table. The actual systematic record length was extended utilizing RiverWare.

Table 9.7: Colorado River Basin Lakes Bulletin 17C Computed Critical Duration Median Inflows

N	ACE	Bulletin 17C EMA Computed Average (Median) Peaks (CFS)									
Years	%	Lake Travis	Lake Buchanan	Lake LBJ	O.H Ivie	Lake Brown-wood	EV Spence Reservoir	Hords Creek Lake	O.C Fisher Lake	Twin Buttes Reservoir	Lake JB Thomas
		11-Day	14-Day	11-Day	8-Day	5-Day	5-Day	3-Day	2-Day	3-Day	6-Day
500	0.2	149,715	103,810	155,070	35,101	24,229	22,998	2,458	96,272	54,505	10,623
200	0.5	120,540	79,240	118,910	28,927	20,643	18,311	1,812	54,937	37,598	9,468
100	1	99,740	62,890	94,715	24,364	17,872	15,041	1,410	34,771	27,515	8,461
50	2	80,185	48,440	73,215	19,938	15,071	12,021	1,073	21,214	19,445	7,335
20	5	56,510	32,190	48,900	14,379	11,366	8,433	714	10,222	11,417	5,672
10	10	40,450	21,995	33,550	10,464	8,602	6,040	499	5,403	7,028	4,304
5	20	26,170	13,560	20,770	6,869	5,916	3,934	323	2,531	3,846	2,884
2	50	10,330	5,010	7,720	2,737	2,566	1,604	142	619	1,157	1,073

9.5 RMC-RFA DATA INPUT

9.5.1 Inflow Hydrographs

Several hourly inflow hydrographs were selected as representative hydrograph shapes to route through RMC-RFA. The selected hydrographs' characteristics represent different hydrograph shapes (from peaky to large volume events) seen at the Colorado River Basin Lakes. However, the selection of particular hourly hydrographs was determined by using the hydrographs that influence the best pool-frequency curve estimate through RMC-RFA. Hourly hydrographs can be replaced by 15-minute or daily hydrographs if found not suitable for the analyses performed on the reservoirs. Examples of the selected hourly inflow hydrographs for Lake Travis are shown in Figure 9.4.

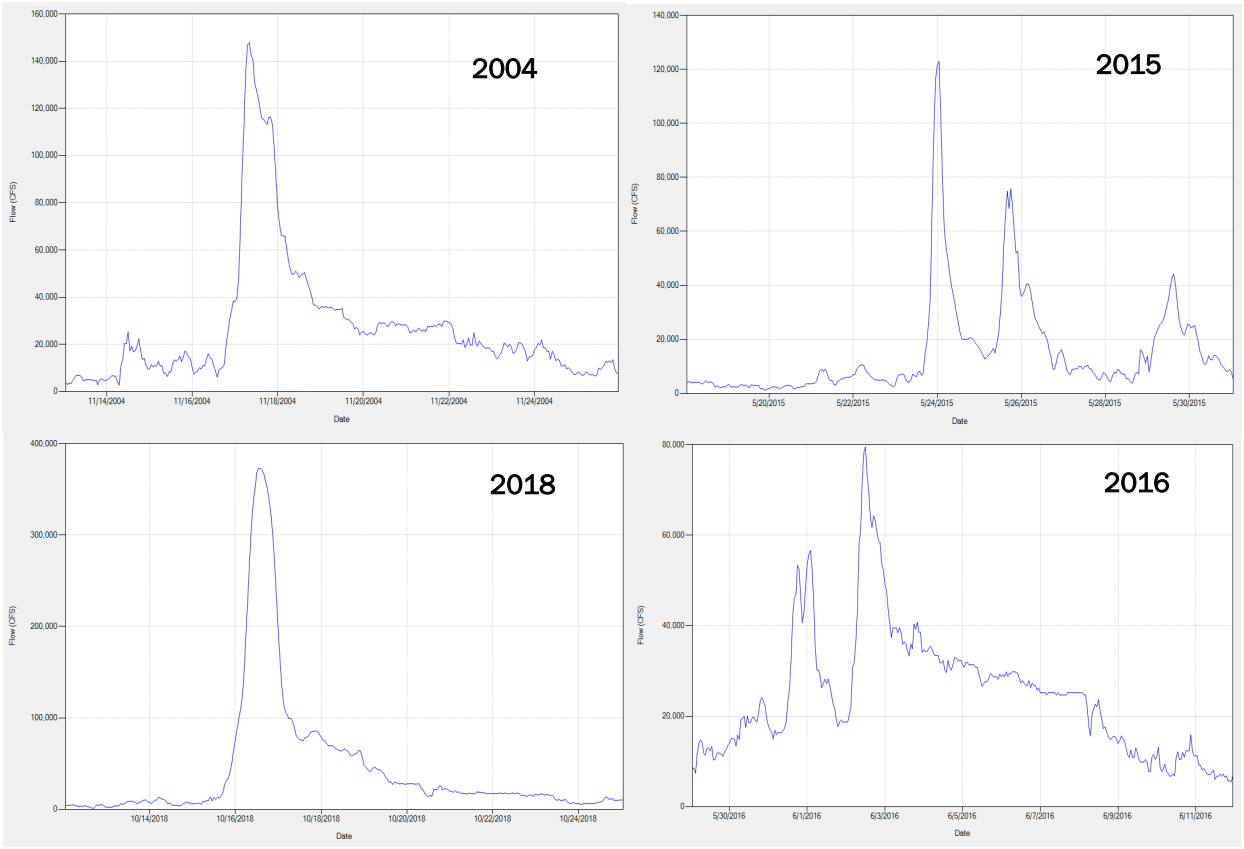

Figure 9.4: Examples of Hourly Inflow Hydrograph Shapes for Lake Travis

9.5.2 Volume Frequency Curve Computation

The computed volume frequency statistical parameters from the Bulletin 17C analysis were fed into the RMC-RFA program to produce the n-day duration inflows for all projects. As stated in the HEC-SSP computations section, Bulletin 17C procedures and guidelines were followed to produce the volume discharge frequencies. Plots of the critical duration 2-, 3-, 5-, 6-, 8-, 11-, and 14-Day discharge volume frequency curves for the Colorado River Basin Lakes are shown in Appendix E. Figure 9.5 shows an example of the computed 11-day volume frequency curve for Lake Travis.

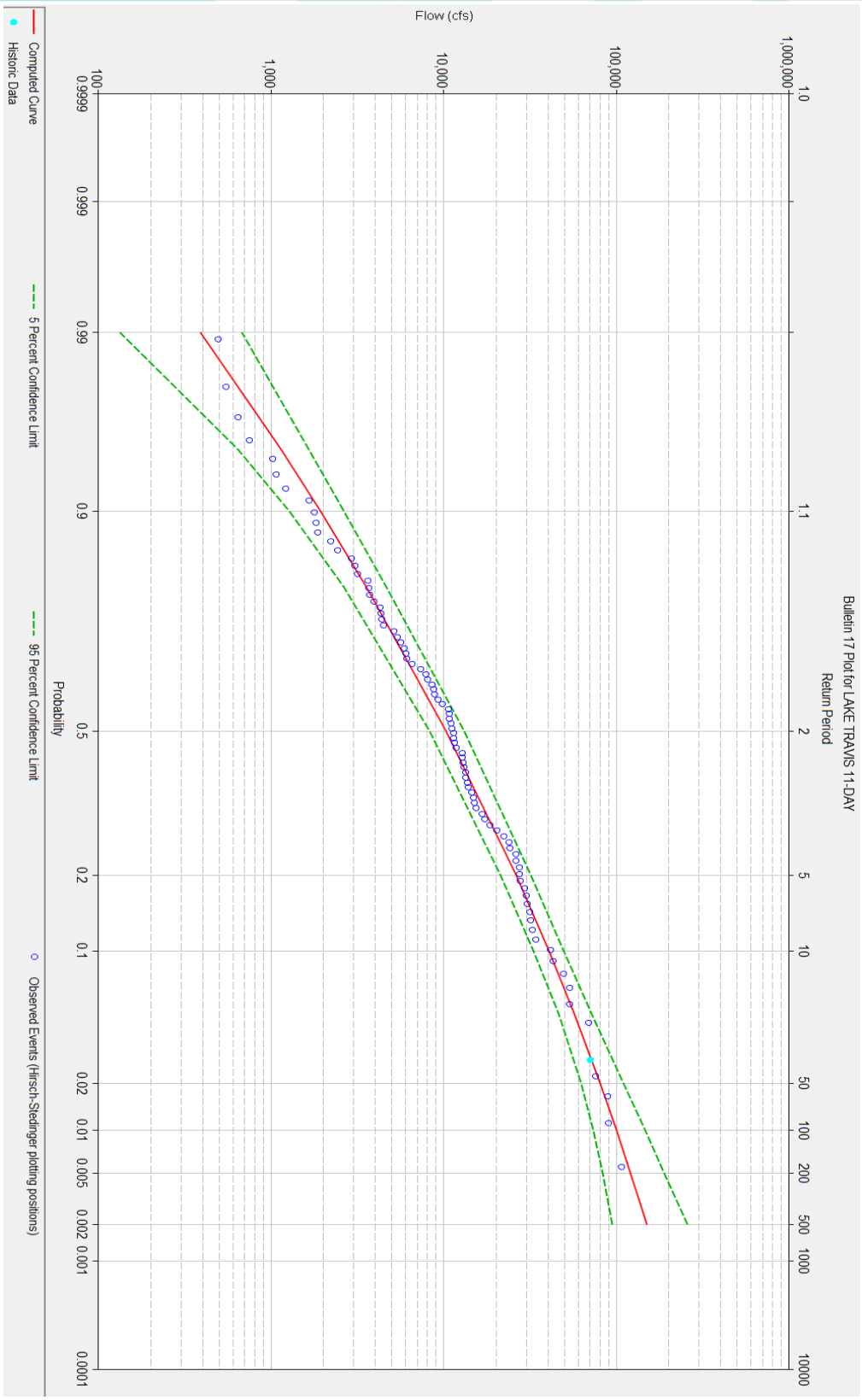

Figure 9.5: Lake Travis Computed 11-Day Volume Frequency Curve

9.6 RMC-RFA ANALYSIS

9.6.1 Flood Seasonality

Many reservoirs have operations (pool level) that vary by season in response to the cyclical changes in meteorology and hydrology throughout the year. The inflow patterns at the Colorado River Basin Lakes include three general types of flood-producing rainfall: thunderstorms, frontal rainfall, and tropical cyclones. Generally, the highest 24-hour and monthly precipitation periods have occurred during tropical cyclones. However, there are some instances of heavy precipitation resulting from local thunderstorms. It should be noted that thunderstorms can occur at any time of the year and tropical storms can happen between June and November. Due to meteorological and hydrologic conditions, most significant floods occur during the late spring, summer, and fall months.

The term flood seasonality is intended to describe the frequency of occurrence of rare floods on a seasonal basis, where a rare flood is defined as any event where the flow exceeds some user specified threshold for a specified flow duration. In the RMC-RFA model operation, a month of flood occurrence is first selected at random according to the relative frequency. Once the month of flood occurrence is specified, a starting pool elevation for the event can be determined from the reservoir stage-duration curve for that particular month. This approach ensures that seasonal variation in reservoir operations is a part of the peak-stage simulation.

The flood seasonality analysis is performed two (2) ways: 1) Assign critical n-day flood seasonality, threshold flow, maximum events per year, and minimum days between events. With these criteria, a total number of events can be calculated. It should be noted that the critical duration used could be different from the volume frequency curve adopted critical duration. 2) Screen out annual maximum peak inflows for the period of record. Peak inflows reflect peak reservoir pool elevations and variation of reservoir pool operations. A sensitivity analysis can be done to determine which method applies best when running the RMC-RFA; this is done to obtain the best starting pool answer corresponding to the most frequent events for each month. More details on the applied methods and results of the flood seasonality analysis for each reservoir are contained in Appendix E. Figure 9.6 illustrates the relative seasonal flood frequency results for Lake Travis.

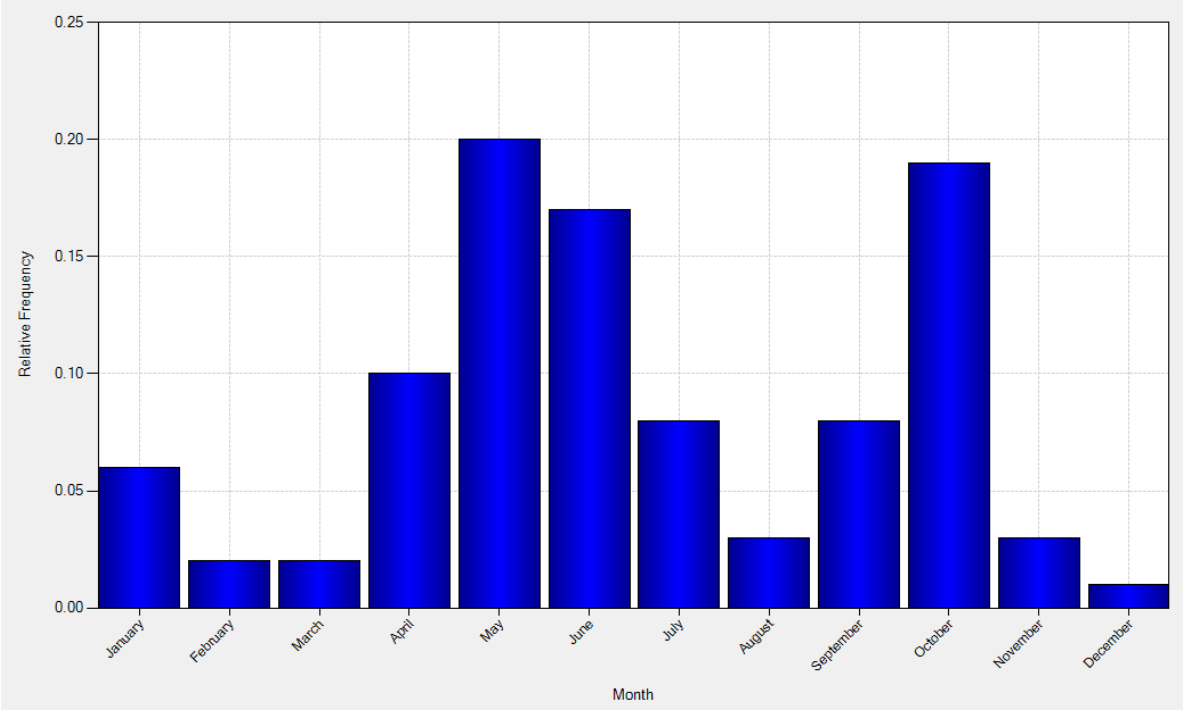

Figure 9.6: Lake Travis Histogram of RMC-RFA Relative Frequency Output

9.6.2 Reservoir Starting Stage

Reservoir starting pool duration curves represent the percent of time during which particular reservoir pools are exceeded. Reservoirs starting stage were estimated by analyzing pool elevations by first filtering observed daily average pools, so that they only represent typical starting pools based on a pool change threshold. Then, the filtered data set is stored by month or season. Because RMC-RFA chooses a starting pool elevation for its simulations based on historic data, the historic data must be filtered so that it is not influenced by flooding events. Starting pool elevations should form the basis for flooding events, not be the result of said events. Therefore, historic pool elevations were filtered with pool change thresholds and typical high (flood) pool durations that are reservoir dependent. This filtered stage data formed the basis for the randomly selected starting pool elevations for the RMC-RFA reservoir simulation. An example of the monthly starting pool elevation curves for Lake Travis is illustrated in Figure 9.10.

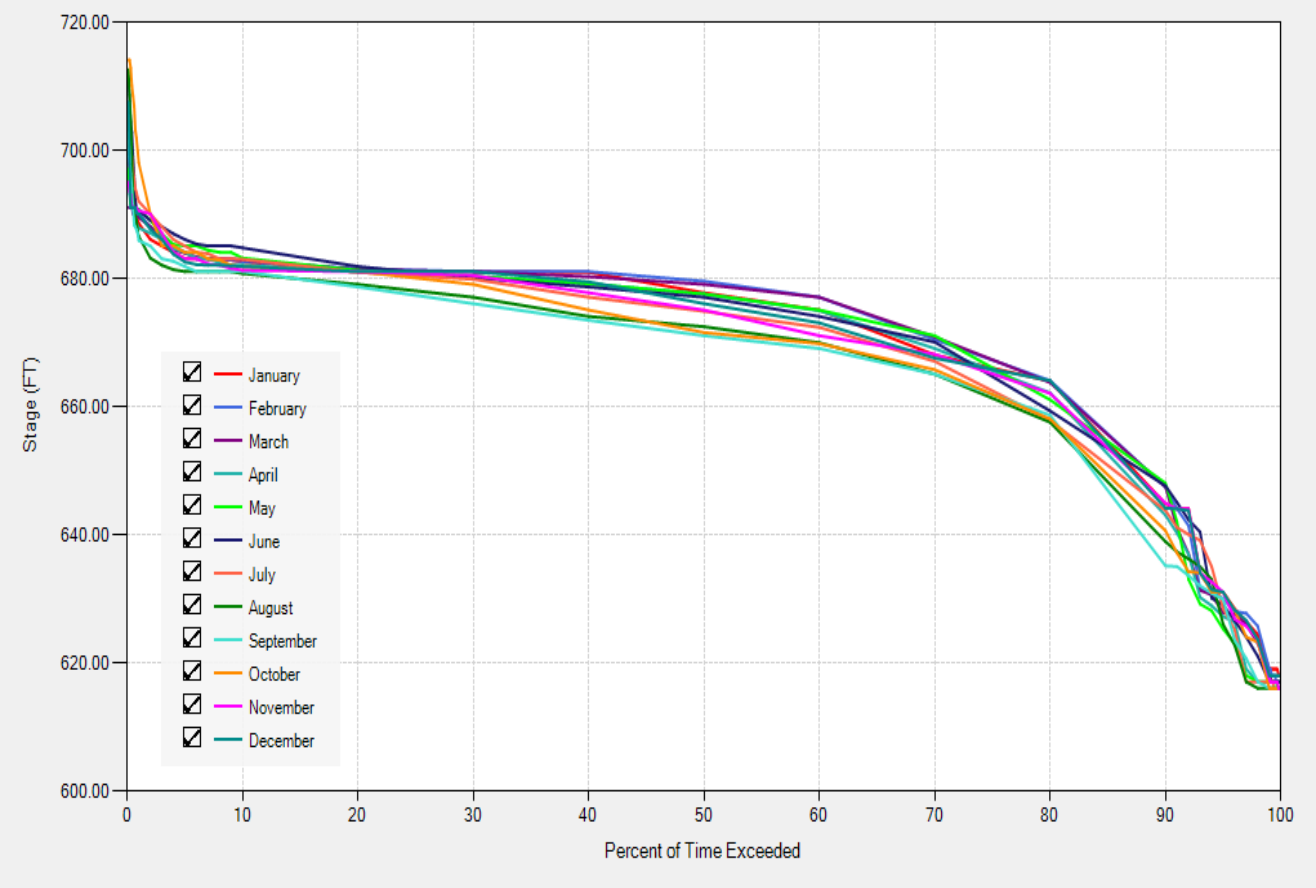

Figure 9.10: Lake Travis Starting Stage Exceedance Curves by Month

9.6.3 Empirical Frequency Curve

For the evaluation of hydrologic hazards of each project, an extreme-value series of annual maximum stage was generated from the n-year systematic (RiverWare + Observed) period of record. The RiverWare simulated pool elevation peaks were used prior to dam impoundment dates when the observed pool elevation peaks were not available, for an intent of extending pool record. Each POR annual maximum series was extracted, the AMS was ranked, and it was plotted on log probability paper using the Weibull plotting position formula shown in a previous section. Figure 9.11 shows the Lake Travis empirical pool-frequency relationship, when applying the Weibull plotting positions. The systematic frequency peaks for all the projects were plotted against the RMC-RFA expected

pool-frequency data points, which are shown in the figures of Section 9.7. The plotting position of the highest and lowest points are the most uncertain due to having insufficient record lengths necessary to inform accurate plotting positions at the extremes, as shown in Figure 9.11. For each project, a duration frequency plot comparison between annual maximum pool elevations for: Observed, simulated (RiverWare), and combined (RiverWare + Observed), were made using the Weibull plotting position formula. In general, reservoirs with longer observed pool records tend to show good distribution and match well when plotted against the extended pool records. However, reservoirs with shorter observed pool record increases the uncertainty in the Weibull plotting positions, and more differences are seen between the observed and extended data, especially at the extreme ends of the data. Another factor impacting the probability and elevation distribution is the use of simulated pools only. RiverWare simulations were simplified to mimic general rules of flood control operations and not abnormal withdraws of the pool, or situations of similar nature. The combined (simulated + observed) data was assumed to be the best available period of record data for the analyses.

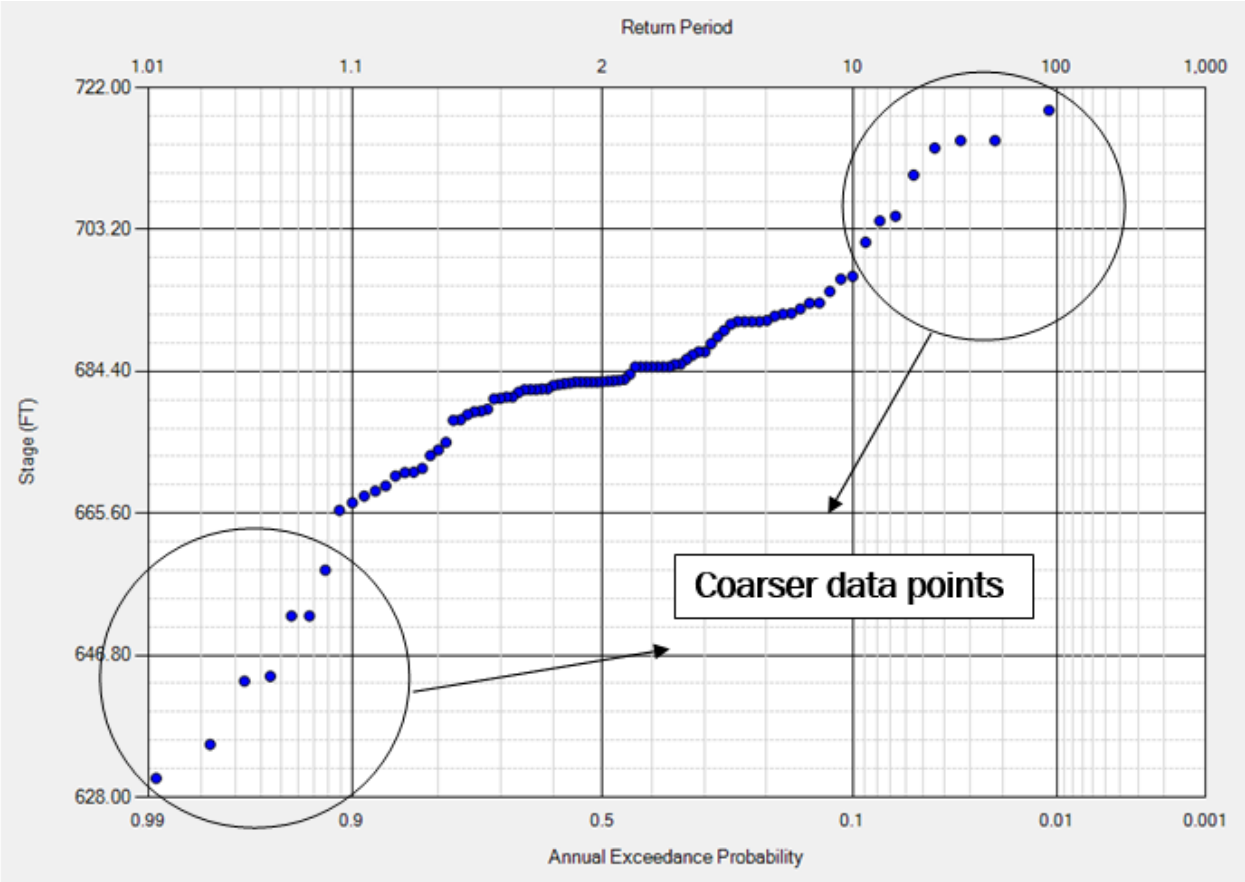

Figure 9.11: Empirical Stage Duration Frequency for Lake Travis

9.6.4 Reservoir Model

The reservoir parameters such as the Stage-Storage-Discharge function and top of dam and spillway elevations were obtained from the Fort Worth District USACE electronic library archived files. The latest volumetric surveys of reservoirs were obtained to update the reservoirs' storage information. This was done using current GPS, acoustical depth sounder, and GIS technology. Data was then gathered and processed to generate the stage-storage curves for the reservoirs. The information is needed in order for the simulation to run. The volumetric and sedimentation survey (mostly up to conservation) of the lakes were completed in the following years: Lake Travis (2008), Lake Buchanan (2006), Lake LBJ (2007), O.H Ivie Reservoir (1977), EV Spence Reservoir (1999), Lake

Brownwood (1997), Hords Creek Lake (1974), O.C Fisher Lake (1962), Twin Buttes (1970), and Lake JB Thomas (1999). The Texas Water Development Board (TWBD) website has most lakes up to date surveyed information as well as the Lower Colorado River Authority and Municipal Water District. Data for portions of the surveyed lakes above conservation are obtained from the original design documents. The Colorado River Basin projects' releases are assumed to be stage dependent in RMC-RFA. Therefore, a stage-storage-discharge function was estimated for each project. The Discharge-Elevation and Storage-Elevation curves for each project are shown in Appendix E. Other details about reservoir features, data sources, and survey dates are listed in Table 9.8.

Table 9.8: Colorado River Basin Reservoir Features

Project	Lake Travis	Lake Buchanan	Lake LBJ	O.H Ivie Reservoir	EV Spence Reservoir	Lake Brownwood	Hords Creek Lake	O.C Fisher	Twin Buttes	Lake JB Thomas
Pertinent Feature	Elevation (NGVD-Feet)									
Top of Dam	750.0	1025.87	838.0	1584.0	1928.0	1470.0	1939.0	1964.0	1991.0	2280.0
Top of Flood (Control Pool)	714.0	>1018.0	825.0	1562.0	1908.0	1425.0	1920.0	1938.5	1969.1	2267.0
Spillway Crest	714.0	1020.0	835.5	1562.0	1908.0	1425.0	1920.0	1938.5	1969.1	2267.0
Top of Conservation Pool	681.0	1018.0	824.7	1551.5	1898.0	1425.0	1900.0	1908.0	1940.2	2258.0
	Elevation-Storage Curves									
Data Source	TWDB	TWDB	TWDB	CRMWD	TWDB	TWDB	USACE	USACE	USGS	USGS
Survey Year	2008	2006	2007	1977	1999	2013	1968	1962	1970	1953

Notes: TWDB refers to Texas Water Development Board
CRMWD refers to the Colorado River Municipal water District

The importance of using accurate Storage-Discharge-Elevation (Stage) curves is that it results in more accurate estimates of the high extreme peak frequency values associated with a higher degree of uncertainty (*i.e.* 1% ACE and beyond). Such high peaks are normally observed near or above the spillway crest.

Validations of the adopted discharge-elevation curves used in RMC-RFA for the Colorado River Basin Lakes was performed by plotting the adopted curve against the observed releases and pool elevations. These plots are included in Appendix E along with additional information on the release assumptions for reach reservoir. The plots showed that the adopted curves were within the range of observed operations. The adopted elevation-release points for O.C Fisher, Twin Buttes, J.B Thomas, and Brownwood were maintained to null up to the spillway crest, and releases were only through surcharge (above spillway crest). This assumption helped maintain good best-estimate fitting curves through the empirical stage frequency curve points. See section 9.8 for results validation results.

9.7 RMC-RFA RESULTS

The RMC-RFA program was used to simulate rainfall-runoff floods using the inflow-frequency curve and the adopted flood seasonality. While RMC-RFA is easiest to apply for projects with uncontrolled spillways, USACE has been successful in using it for many projects with gated spillways. The key in this situation is to use the observed data to help guide the final results. The observed 15-minute, hourly, and daily inflow hydrographs and those found in the RMC-RFA's program, are weighted equally to account for each unique shape (i.e., volume and peak) and to have the same probability. Appropriate routing time windows were specified to calculate the full size of floods routed through the reservoir on an hourly basis. The RMC-RFA model was simulated using the expected pool-frequency curve only model option. This runs 10,000 realizations with 1,000,000 events per realization. This means RMC-RFA simulates a total of 10 billion events (10,000 x 1,000,000) to produce its best estimate of the expected curve.

The following sections list detailed results about each project's new simulated expected stage-frequency curve. Each federally owned project has a flowage easement elevation. The flowage easement land is privately owned land on which the Federal government (i.e. USACE) has acquired certain perpetual rights. These include the right to flood it in connection with the operation of the reservoir, the right to prohibit construction of any structure for human habitation, the right to approve all other structures constructed on flowage easement land, except fencing. Having imposed properties located above the easement elevation keeps from what would become damageable property out of the flood pool, so that the reservoir can be operated with a full focus upon downstream conditions and the concern for dam safety. To put things in perspective about the flowage easement, when known, figures in the following sections illustrate easement elevation references in relation to the reservoir pool frequencies, spillway crest elevation, and top of dam.

To assess regulation, the total release for each project corresponding to each pool-frequency was developed by analyzing each project's observed and simulated releases, where annual maximum peaks were plotted using the Weibull position distribution and applying a graphical curve, which would approximately fit through the data points. Sets of the Weibull plotting position distribution figures for the projects are shown in Section 1.10 of Appendix E. The regulated (simulated/observed) releases were used to best estimate release frequencies below spillway crest. High flood events that may exceed spillway crest elevation, would follow the discharge-elevation curve.

Several iterations were made using the RMC-RFA program to obtain the best simulated pool-frequency curves. The best fit is defined as the curve that fits well through the empirical stage points for the more frequent events (i.e. 10% ACE (10-year) through 2% ACE (50-year)). The best estimate curve is a result of applying release schedules that would not violate the most upper and lower bounds of discharge peaks. For lakes located in basins with unique climate conditions, reasonable justifications can be made to explain release deviations from actual schedules. As a result, and with degrees of uncertainty, the curves are believed to have captured good estimates of pool elevations beyond the 1% ACE (100-year) events. Figures of the adopted pool-frequency curves along with comparisons with the existing reported pool frequencies, when available, are shown in the sections below and in Appendix E.

9.7.1 Results for Lake Travis

The following tables summarize the final RMC-RFA results for Lake Travis. Additional comparison plots of the results are included in Appendix E.

Table 9.9: 2019 Lake Travis Computed Pool-Frequency Comparison with Previous Estimates

Lake Travis		RMC-RFA Best Estimate	Effective FIS	Change in Pool	2002 FDEP	Change in Pool	Easement Pool	Easement 1% ACE (100-year) Freeboard
N-Years	ACE %	Feet-NGVD	Feet-NGVD	Feet	Feet-NGVD	Feet	Feet-NGVD	Feet
2	50	683.16			685.00	-1.84		
5	20	690.76			690.90	-0.14		
10	10	698.48	696.80	+1.68	696.80	+1.68		
25	4	713.28			713.50	-0.22		
50	2	716.06	716.50	-0.44	716.50	-0.44		
100	1	721.69	721.80	-0.11	721.80	-0.11	715.00	-6.69
250	0.4	730.11						
500	0.2	735.23	732.50	+2.73	736.40	-1.17		

Table 9.10: 2019 Lake Travis Computed Frequency Discharge Release

Lake Travis		RMC-RFA Best Estimate			
N-Years	ACE %	Elevation-NGVD	Spillway Release (CFS)	Gate Release (CFS)	Total Release (CFS)
2	50	683.16	0	5,000	5,000
5	20	690.76	0	30,000	30,000
10	10	698.48	0	30,000	30,000
25	4	713.28	0	30,000	30,000
50	2	716.06	70,000	7,620	72,620
100	1	721.69	84,175	5,825	90,000
250	0.4	730.11	161,970	0	161,970
500	0.2	735.23	261,100	0	261,100

Note: Release is according to release schedule (Table 7-2) WCM.

9.7.2 Results for Lake Buchanan

The following tables summarize the final RMC-RFA results for Lake Buchanan using the 1990 operational plan. Additional comparison plots of the results are included in Appendix E. Additional RMC-RFA results of the new (2023) operational plan for Lake Buchanan are available in section 9.9.

Table 9.11: 2019 Lake Buchanan Computed Pool-Frequency Comparison with Previous Estimates

Lake Travis		RMC-RFA Best Estimate	Effective FIS	Change in Pool	2002 FDEP	Change in Pool	Easement Pool	Easement 1% ACE (100-year) Freeboard
N-Years	ACE %	Feet-NGVD	Feet-NGVD	Feet	Feet-NGVD	Feet	Feet-NGVD	Feet
2	50	1019.49			1019.80	-0.31		
5	20	1020.64			1019.80	+0.84		
10	10	1021.00	1020.24	+0.76	1020.30	+0.70		
25	4	1021.24			1020.30	+0.94		
50	2	1021.42	1020.24	+1.18	1020.30	+1.12		
100	1	1021.60	1020.74	+0.86	1020.80	+0.80	1,020.00	-1.6
250	0.4	1021.79						
500	0.2	1022.06	1022.44	-0.38	1022.50	-0.44		

Table 9.12 2019 Lake Buchanan Computed Frequency Discharge Release

Lake Buchanan		RMC-RFA Best Estimate			
N-Years	ACE %	Elevation-NGVD	Spillway Release (CFS)	Gate Release (CFS)	Total Release (CFS)
2	50	1019.49	0	12,000	12,000
5	20	1020.64	10	29,240	29,250
10	10	1021.00	45,400	4,600	50,000
25	4	1021.24	100,800	0	100,800
50	2	1021.42	155,235	0	155,235
100	1	1021.60	219,670	0	219,670
250	0.4	1021.79	302,000	0	302,000
500	0.2	1022.06	412,980	0	412,980

Note: Spillway release is from free spillway design curve. The gated releases were adjusted to be consistent with the Weibull plotting positions figure of the simulated releases.

9.7.3 Results for Lake LBJ

The following tables summarize the final RMC-RFA results for Lake LBJ. Additional comparison plots of the results are included in Appendix E.

Table 9.13: 2019 Lake L.B.J Computed Pool-Frequency Comparison with Previous Estimates

Lake L.B.J		RMC-RFA Best Estimate	2002 FDEP	Change in Pool	Easement Pool	Easement 1% ACE (100-year) Freeboard
N-Years	ACE %	Feet-NGVD		Feet	Feet-NGVD	Feet
2	50	825.44	824.84	+0.60		
5	20	825.79	824.84	+0.95		
10	10	826.58	824.84	+1.74		
25	4	828.05	824.84	+3.21		
50	2	828.63	825.24	+3.39		
100	1	829.30	827.94	+1.36	825.00	-4.30
250	0.4	830.03				
500	0.2	831.01	829.24	+1.77		

Table 9.14: 2019 Lake L.B.J Computed Frequency Discharge Release

Lake L.B.J		RMC-RFA Best Estimate				
N-Years	ACE %	Elevation-NGVD	Spillway Release (CFS)	Gate Release (CFS)	Total Release-Daily (CFS)	Total Release-Instantaneous (CFS)
2	50	825.44	19,800	0	19,800	32,000
5	20	825.79	47,520	0	47,520	80,000
10	10	826.58	71,300	0	71,300	122,500
25	4	828.05	105,000	0	105,000	183,700
50	2	828.63	133,975	0	133,975	237,000
100	1	829.30	163,480	0	163,480	292,000
250	0.4	830.03	194,120	0	194,120	350,000
500	0.2	831.01	236,000	0	236,000	429,000

Note: Since overflow spillway crest elevation is at 835.5 ft, all release is through gated spillways.

9.7.4 Results for Lake E.V. Spence

The following tables summarize the final RMC-RFA results for Lake E.V. Spence. Additional comparison plots of the results are included in Appendix E.

Table 9.15: 2019 Lake E.V Spence Computed Pool-Frequency Estimates

Lake E.V Spence		RMC-RFA Best Estimate
N-Years	ACE %	Feet-NGVD
2	50	1889.82
5	20	1896.93
10	10	1898.18
25	4	1899.09
50	2	1899.71
100	1	1900.33
250	0.4	1901.48
500	0.2	1902.60

Note: There was no previous estimates to compare current estimates to

Table 9.16: 2019 Lake E.V Spence Computed Frequency Discharge Release

Lake E.V Spence		RMC-RFA Best Estimate			
N-Years	ACE %	Elevation-NGVD	Spillway Release (CFS)	Gate Release (CFS)	Total Release (CFS)
2	50	1889.82	0	2,000	2,000
5	20	1896.93	0	2,000	2,000
10	10	1898.18	0	7,500	7,500
25	4	1899.09	0	11,000	11,000
50	2	1899.71	0	20,000	20,000
100	1	1900.33	0	22,000	22,000
250	0.4	1901.48	0	23,000	23,000
500	0.2	1902.60	0	25,000	25,000

Note: E.V Spence Lake inflow is unregulated. See section 1.11 for more details.

Since there is no written standard operating procedures manual for normal or flood conditions, the 2- and 5-year frequency releases are based on observed elevation-release data found in Figure E.57 of this report. Frequencies greater than 5-year events follow simulated releases found in Figure E.58.

9.7.5 Results for O.H. Ivie Reservoir

The following tables summarize the final RMC-RFA results for O.H. Ivie Reservoir. Additional comparison plots of the results are included in Appendix E.

Table 9.17: 2019 O.H Ivie Reservoir Computed Pool-Frequency Estimates

O.H Ivie Reservoir		RMC-RFA Best Estimate
N-Years	ACE %	Feet (NGVD)
2	50	1550.66
5	20	1551.66
10	10	1551.95
25	4	1552.12
50	2	1552.49
100	1	1552.74
250	0.4	1552.91
500	0.2	1553.38

Note: There was no previous estimates to compare current estimates to

Table 9.18: 2019 O.H Ivie Reservoir Computed Frequency Discharge Release

O.H Ivie Reservoir		RMC-RFA Best Estimate			
N-Years	ACE %	Elevation-NGVD	Spillway Release (CFS)	Gate Release (CFS)	Total Release (CFS)
2	50	1550.66	0	1,500	1,500
5	20	1551.66	0	1,500	1,500
10	10	1551.95	0	1,500	1,500
25	4	1552.12	0	32,700	32,700
50	2	1552.49	0	52,500	52,500
100	1	1552.74	0	67,350	67,350
250	0.4	1552.91	0	81,525	81,525
500	0.2	1553.38	0	94,945	94,945

Note: Gate release up to 2-year events is according to observed elevation-release data found in Appendix E. Releases greater than 2-year events are according to Simulated releases found in Appendix E and the release schedule found in RMC-RFA.

9.7.6 Results for Lake Brownwood

The following tables summarize the final RMC-RFA results for Lake Brownwood. Additional comparison plots of the results are included in Appendix E.

Table 9.19: 2019 Lake Brownwood Computed Pool-Frequency Estimates

Lake Brownwood		RMC-RFA Best Estimate
N-Years	ACE %	Feet-NGVD
2	50	1426.07
5	20	1427.88
10	10	1429.17
25	4	1430.77
50	2	1431.95
100	1	1433.19
250	0.4	1434.73
500	0.2	1436.18

Note: There was no previous estimates to compare current estimates to

Table 9.20: 2019 Lake Brownwood Computed Frequency Discharge Release

Lake Brownwood		RMC-RFA Best Estimate			
N-Years	ACE %	Elevation-NGVD	Spillway Release (CFS)	Gate Release (CFS)	Total Release (CFS)
2	50	1426.07	1,625	0	1,625
5	20	1427.88	7,860	0	7,860
10	10	1429.17	12,900	0	12,900
25	4	1430.77	16,100	0	16,100
50	2	1431.95	26,160	0	26,160
100	1	1433.19	33,585	0	33,585
250	0.4	1434.73	44,700	0	44,700
500	0.2	1436.18	56,760	0	56,760

Note: Release is based on discharge-elevation curve used in RMC-RFA.

9.7.7 Results for Hords Creek Lake

The following tables summarize the final RMC-RFA results for Hords Creek. Additional comparison plots of the results are included in Appendix E.

Table 9.21: 2019 Hords Creek Lake Computed Pool-Frequency Comparison with Previous USACE Estimate

Hords Creek Lake		RMC-RFA Best Estimate	2009 USACE	Change in Pool	Easement Pool	Easement 1% ACE (100-year) Freeboard
N-Years	ACE %	Feet-NGVD		Feet		
2	50	1896.72				
5	20	1900.81				
10	10	1902.44				
25	4	1904.96				
50	2	1907.02	1912.00	-4.98		
100	1	1909.82	1915.00	-5.18	1,925	+15.18
250	0.4	1914.47				
500	0.2	1917.98				

Note: The adopted 1% ACE (100-year) is higher than the maximum pool peak and is believed to be rare as less than 12% of the POR exceeded the 10% ACE (10-year) event.

Table 9.22: 2019 Hords Creek Lake Computed Frequency Discharge Release

Hords Creek Lake		RMC-RFA Best Estimate			
N-Years	ACE %	Elevation-NGVD	Spillway Release (CFS)	Gate Release (CFS)	Total Release (CFS)
2	50	1896.72	0	170	170
5	20	1900.81	0	180	180
10	10	1902.44	0	185	185
25	4	1904.96	0	195	195
50	2	1907.02	0	200	200
100	1	1909.82	0	205	205
250	0.4	1914.47	0	215	215
500	0.2	1917.98	0	500	500

Note: Release is according to rating curves of two gates + uncontrolled outlet (Plate 6) WCM.

9.7.8 Results for O.C. Fisher Reservoir

The following tables summarize the final RMC-RFA results for O.C. Fisher Reservoir. Additional comparison plots of the results are included in Appendix E.

Table 9.23: 2019 O.C Fisher Lake Computed Pool-Frequency Comparison with Previous USACE Estimate

Lake O.C Fisher Lake		RMC-RFA Best Estimate	Effective FIS	Change in Pool	Easement Pool	Easement 1% ACE (100-year) Freeboard
N-Years	ACE %	Feet-NGVD		Feet		
2	50	1886.36				
5	20	1904.08				
10	10	1907.94	1917.50	-9.56		
25	4	1911.11				
50	2	1915.34	1929.50	-14.16		
100	1	1923.42	1936.50	-13.08	1952.00	+28.58
250	0.4	1935.33				
500	0.2	1942.10	1947.50	-5.40		

Table 9.24: 2019 O.C Fisher Lake Computed Frequency Discharge Release

Lake O.C Fisher		RMC-RFA Best Estimate			
N-Years	ACE %	Elevation-NGVD	Spillway Release (CFS)	Gate Release (CFS)	Total Release (CFS)
2	50	1886.36	0	1,900	1,900
5	20	1904.08	0	2,400	2,400
10	10	1907.94	0	2,550	2,550
25	4	1911.11	0	2,600	2,600
50	2	1915.34	0	2,700	2,700
100	1	1923.42	0	2,850	2,850
250	0.4	1935.33	0	3,100	3,100
500	0.2	1942.10	0	3,250	3,250

Note: Release is according to release from two conduits with all gates open (Plate 4) WCM.

9.7.9 Results for Twin Buttes Reservoir

The following tables summarize the final RMC-RFA results for Twin Buttes Reservoir. Additional comparison plots of the results are included in Appendix E.

Table 9.25: 2019 Twin Buttes Reservoir Computed Pool-Frequency Comparison with Previous USACE Estimate

Twin Buttes Reservoir		RMC-RFA Best Estimate	Effective FIS	Change in Pool	Easement Pool	Easement 1% ACE (100-year) Freeboard
N-Years	ACE %	Feet-NGVD		Feet		
2	50	1934.00				
5	20	1940.35				
10	10	1942.54	1946.4	-3.86		
25	4	1946.95				
50	2	1951.55	1955.40	-3.85		
100	1	1957.06	1959.40	-2.34	1985.00	+27.94
250	0.4	1967.67				
500	0.2	1974.91	1969.40	+5.51		

Table 9.26: 2019 Twin Buttes Reservoir Computed Frequency Discharge Release

Twin Buttes Reservoir		RMC-RFA Best Estimate			
N-Years	ACE %	Elevation-NGVD	Spillway Release (CFS)	Gate Release (CFS)	Total Release (CFS)
2	50	1934.00	0	3,000	3,000
5	20	1940.35	0	3,000	3,000
10	10	1942.54	0	5,000	5,000
25	4	1946.95	0	5,000	5,000
50	2	1951.55	0	5,000	5,000
100	1	1957.06	0	9,000	9,000
250	0.4	1967.67	0	9,000	9,000
500	0.2	1974.91	9,100	0	9,100

Note: Release is according to simulated release (Figure E.51 of this report)

9.7.10 Results for Lake J.B. Thomas

The following tables summarize the final RMC-RFA results for Lake J.B. Thomas. Additional comparison plots of the results are included in Appendix E.

Table 9.27: 2019 Lake J.B Thomas Computed Pool-Frequency Estimates

Lake J.B Thomas		RMC-RFA Best Estimate
N-Years	ACE %	Feet-NGVD
2	50	2242.74
5	20	2256.81
10	10	2259.19
25	4	2261.09
50	2	2262.26
100	1	2263.63
250	0.4	2265.34
500	0.2	2266.64

Note: There was no previous estimates to compare current estimates to

Table 9.28: 2019 Lake J.B Thomas Computed Frequency Discharge Release

Lake J.B Thomas		RMC-RFA Best Estimate			
N-Years	ACE %	Elevation-NGVD	Spillway Release (CFS)	Gate Release (CFS)	Total Release (CFS)
2	50	2242.74	0	50	50
5	20	2256.81	0	100	100
10	10	2259.19	0	150	150
25	4	2261.09	0	2,800	2,800
50	2	2262.26	0	3,800	3,800
100	1	2263.63	0	6,400	6,400
250	0.4	2265.34	0	10,700	10,700
500	0.2	2266.64	0	15,000	15,000

Note: 2-Year to 50-Year Releases are according to RiverWare POR simulated release versus pool level
100-year to 500-year releases are according to rating curve schedule used in RMC-RFA

9.8 RESULTS VALIDATION

The pool-frequency results displayed in section 9.7 went through rigorous analyses before being finalized. Certain projects needed more sensitivity analysis than others to ensure accuracy. Further analyses were deemed necessary to close gaps associated with poor quality and limited data. See the validation section of Appendix E for details on the additional validation analyses that were made in order to validate the best estimate pool-frequency results for E.V. Spence, O.H. Ivie, Lake Brownwood, O.C. Fisher, Twin Buttes and Lake Travis.

9.9 LAKE BUCHANAN'S NEW OPERATIONAL PLAN

Some sensitivity analyses were performed in RMC-RFA for Lake Buchanan to assess the impacts of a new (2023) operational plan on current and future FEMA releases and pool elevations for the 1% and 0.2% ACE. This sensitivity analysis compares effects of the current 1990 operational plan (FEMA-LCRA agreement) to the new operations (2023) on the reservoir pool frequencies.

9.9.1 The 1990 Plan Operations

For the past 30+ years, the LCRA has been operating based on the 1990 FEMA-LCRA operations agreement. The 1990 agreement called for maintaining the pool at 1,020 feet msl from November through April and at 1,018 feet msl from May through October. Releases under the 1990 plan are specified to be 85 percent of the discharge observed in the upstream USGS gage for the Colorado River near San Saba. The prescriptive rules under this plan were fine-tuned to a hypothetical FEMA 100-year flood originating upstream of the confluence of the San Saba and Colorado rivers and may not be well-suited for other floods.

9.9.2 New 2023 Operations

The new operational plan for Lake Buchanan that has been proposed for adoption in 2023 will be referred to as the 2023 Operational Plan. This plan was developed to give more flexibility to reservoir operators to manage a wider range of flood scenarios. The new plan allows reservoir operators to take advantage of improved hydrological observations, flood forecasts and reservoir routing tools that have been developed during the past 30 years. Under the 2023 Operational Plan, releases are made based on real-time hydrological observations, forecasts and reservoir modeling with an assumed forecast lead time of 18 hours, which is the travel time from the upstream USGS gage for the Colorado River near San Saba, Texas. The 18-hour lead time allows operators to make releases that draw the pool down below elevation 1020 feet msl, which increases the available storage capacity in advance of significant inflow events. The major features of this plan are as follows:

(a) Lake Buchanan's pool shall be maintained at 1,020 feet msl all year round.

(b) Flood release decisions shall be made by experienced operators based on improved hydrological observations and forecasting tools.

(c) Peak discharge from Buchanan Dam shall not exceed the current FEMA 1% ACE (100-year) discharge (152,000 cfs) unless Lake Buchanan is forecasted or observed to rise above the FEMA 1% ACE (100-year) floodplain (1,020.74 feet msl, or spillway + 0.39 feet).

(d) Peak discharge from Buchanan Dam shall not exceed the current FEMA 0.2% ACE (500-year) discharge (308,000 cfs) unless Lake Buchanan is forecasted or observed to rise above the FEMA 0.2% ACE (500-year) floodplain (1,022.44 feet msl, or spillway + 2.09 feet).

(e) Peak discharge from Buchanan Dam shall not exceed the peak inflow to the reservoir.

9.9.3 RMC-RFA Sensitivity Test

The RMC-RFA software that was used in this sensitivity test was developed by the USACE Risk Management Center for use in dam safety risk assessments. This tool is useful in producing a pool-frequency curve with confidence bounds using a stochastic model with an inflow volume-sampling approach. RMC-RFA is best suited for situations where the dam operations are relatively simple and where the spillway is not regulated using gates. For Lake Buchanan, a simplification of the complex operational rules had to be assumed for both the 1990 Operational Plan and the new 2023 Operational Plan. For each operational plan, the more complex operational rules for gated releases were simplified to use an elevation-discharge table, which is meant to represent the total or maximum release from the dam at that elevation. For the 1990 plan, the elevation-discharge table was calibrated to match the maximum releases and peak pool elevations that have been observed over the life of the project. Above those observed pool elevations, the 1990 elevation-discharge table assumes a gates wide open operation. For the new 2023 operational plan, the elevation-discharge table was calibrated to meet the overall goals of the new plan, which included maintaining the current FEMA pool elevations and releases for the 1% and 0.2% ACE events. The assumed elevation-discharge tables that were used in RMC-RFA for both of these operational scenarios are shown in Table 9.29. RMC-RFA Results are displayed in Table 9.30 and Figure 9.12.

Table 9.29: Lake Buchanan Alternative Release Plan Comparison

The 1990 Plan: LCRA Current Operation Plan		New Operations: The 2023 Operation Plan	
Pool (ft)	Release (cfs)	Pool (ft)	Release (cfs)
1020.00	5,000	1020.00	5,000
1020.60	20,000	1020.60	152,000
		1020.74	152,000
1021.10	50,000	1021.10	308,000
1022.15	430,882	1022.15	308,000
		1022.44	308,000
1023.15	476,990	1023.15	476,500

Table 9.30: Lake Buchanan Sensitivity Analysis for FEMA Requirements with 18-hour Forecast

Lake Buchanan		FEMA Requirements		The 1990 Plan: LCRA Current Operation Plan		New Operations: The 2023 Operation Plan	
N-Years	ACE %	Pool Elevation (ft-msl)	Maximum Release (cfs)	Pool Elevation (ft-msl)	Assumed Peak Release (cfs)	Pool Elevation (ft-msl)	Assumed Peak Release (cfs)
100	1	1020.74	152,000	1021.60	219,670	1020.79	152,000
500	0.2	1022.44	308,000	1022.06	412,980	1021.17	308,000

The empirical data in Figure 9.12 shows that under the current 1990 operational plan, Lake Buchanan's pool elevation was allowed to approach elevation 1021 feet msl multiple times over its period of record (according to the RiverWare model). In contrast, the new 2023 operational plan makes forecast-informed releases that would keep peak pool elevations closer to elevation 1020-feet msl for most smaller flood events while also keeping the 1% and 0.2% ACE pool elevations and releases at or near the current FEMA pool-release targets.

While RMC-RFA is a useful tool producing an elevation-frequency relationship based on a stochastic sampling of a variety of inflow volumes, hydrograph shapes, seasonality and initial pool elevations, the software also has limitations in that it is not well suited for representing complex gated reservoir operations. Therefore, the results of this analysis should be used with caution, especially with regard to the assumed reservoir releases. The intent of this analysis is simply to assess the impact of the new 2023 operational plan on the dam's pool elevation frequency curve based on a variety of different inflow scenarios that have been sampled stochastically. A more detailed analysis of reservoir releases based on forecast-informed operations would require a different type of reservoir operations model, which is beyond the scope of this analysis.

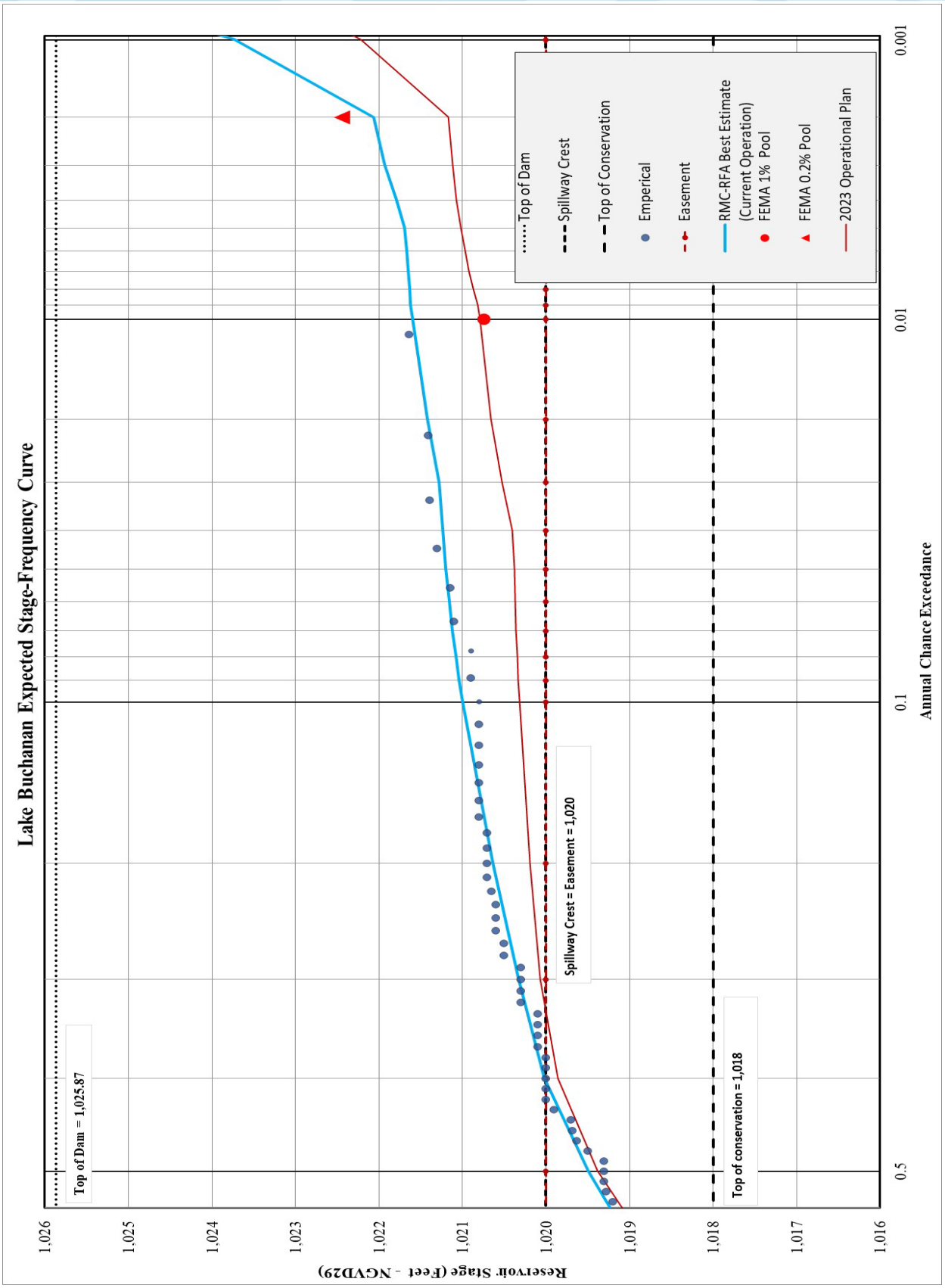

Figure 9.30: Lake Buchanan Pool Frequency Comparisons from RMC-RFA

10 Historic 1930s Storms Analyses

10.1 INTRODUCTION AND PURPOSE

For many locations in the Lower Colorado River basin, the largest floods of record occurred in the 1930s, and since then, no other observed floods have some close to the magnitudes of flooding observed in the 1930s. Figure 10.1 below illustrates the locations these floods of record from the 1930s. In many cases, the rainfall and peak discharges from these floods were on the order of a 1% AEP (100-yr) flood or larger, which means that they are of high interest for flood studies such as this one. However, there is a complication in that those floods occurred before most of the major reservoirs in the river basin were built.

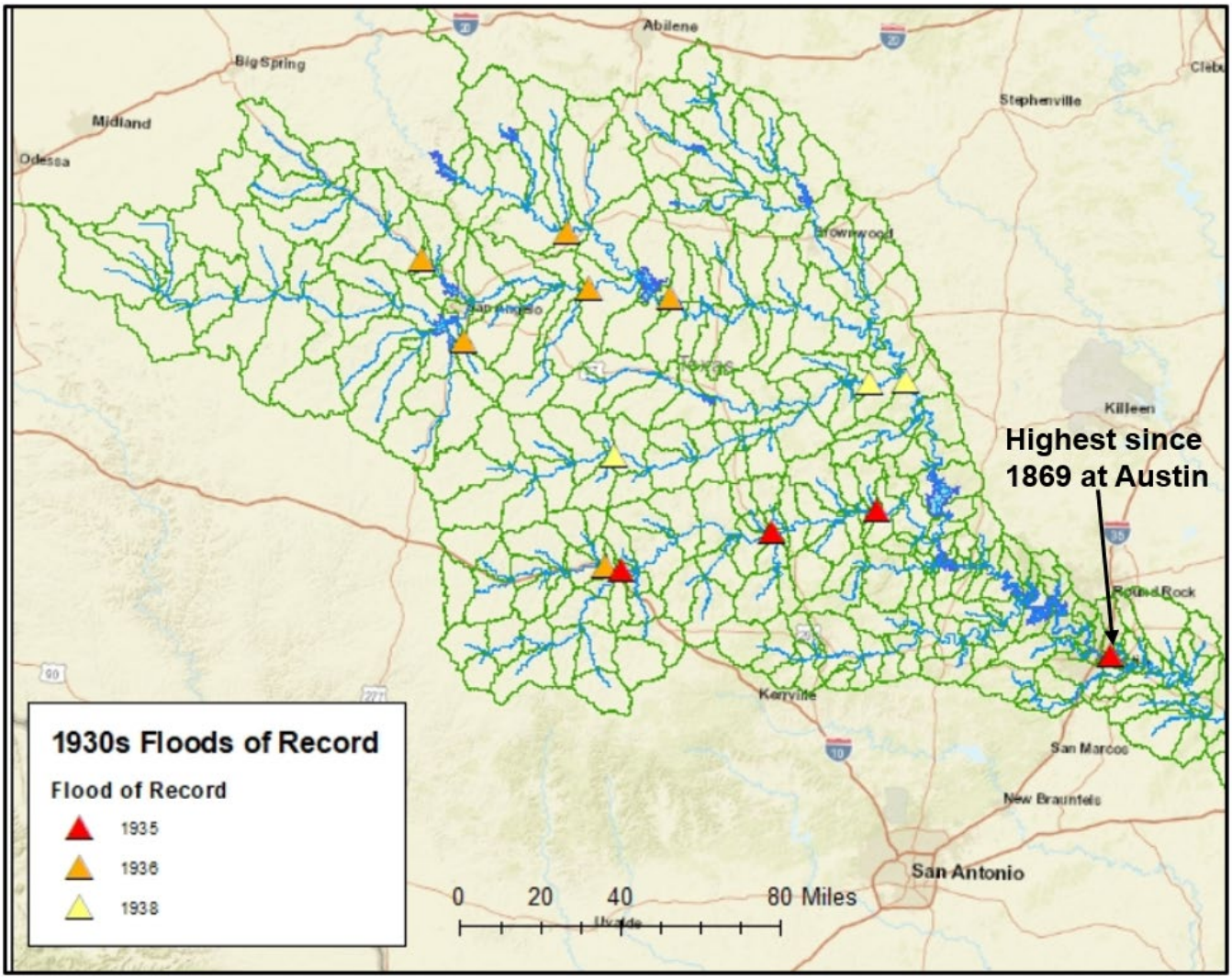

Figure 10.1: Map of the Highest Floods of Record in the Lower Colorado River Basin

The analysis that is documented in this chapter and in Appendix F used HEC-HMS to recreate two of those 1930s storm events with the goal of estimating what the peak flows on the rivers would have been with all of the current reservoir regulation in place. The regulated peak flows from those storm events were then added to the Bulletin 17C analysis of select stream gages as a sensitivity test of the statistical results.

10.2 ANALYZED STORMS

As shown in Figure 10.1, three of the major floods of record in the Lower Colorado River basin occurred in 1935, 1936 and 1938. Of those, the June 1935 and Sep 1936 events were selected for analysis in HEC-HMS. The July 1938 storm event was not selected for analysis as it primarily impacted the San Saba River, which is still largely unregulated, and Buchanan Lake, which was impounded in 1937. As a result, most of the significant regulated peak flows for the 1938 storm event would be expected to be the same as what was actually observed in the 1930s. Therefore, additional analysis in HEC-HMS was not warranted for that event.

10.2.1 June 1935 Storm Event

The June 1935 storm event was selected as it produced extremely high peak flows along the Llano River and downstream on the Colorado River through Austin. The 1935 event was selected for analysis in order to estimate what the regulated peak flows in Austin would have been with the current reservoir regulation of Lake LBJ and Lake Austin in place. Heavy rains of up 19 inches in 7 days fell over parts of the Colorado drainage basin during the period of June 9-15, as shown in Figure 10.2, causing floods greater than ever had been recorded along parts of the Llano and Colorado Rivers.

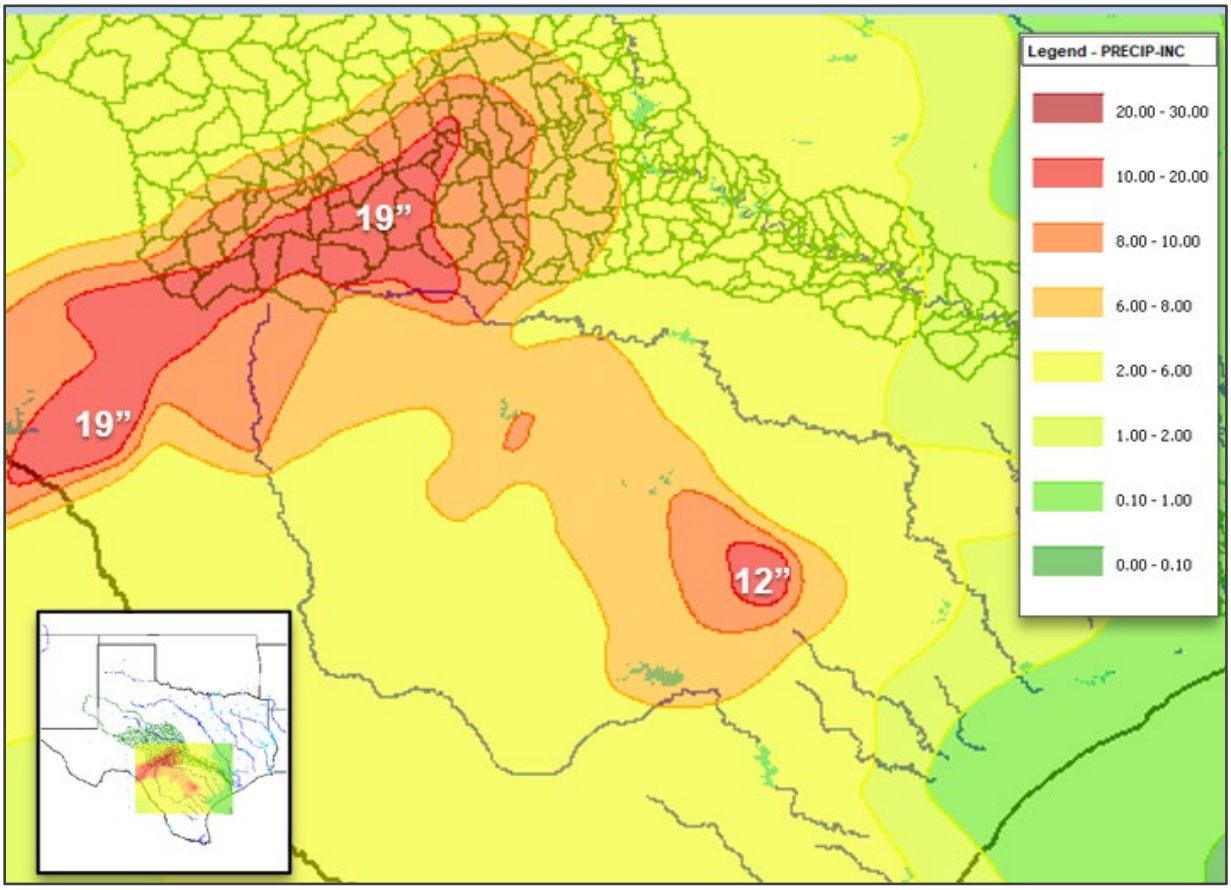

Figure 10.2: Total Rainfall Depths for the June 9-15, 1935 Storm Event

There had been general rains in the region for a period 6 weeks before the flood, and all stream gages were already above normal stage when the major 1935 storm began (Dalrymple, 1939). The Llano River near Junction experienced a peak flow of 319,000 cfs, and further downstream, the Llano River near Castell had a peak discharge of 388,000 cfs. The flood from the Llano River then joined a smaller flood from the Pedernales River and caused the Colorado River at Austin gage to reach a peak discharge of 481,000 cfs on June 15, 1935. Figure

10.3 is a photograph of the Congress Avenue bridge in Austin during the peak of the flood (Dalrymple, 1939). Below Austin there was little rainfall, and the flood peak decreased considerably.

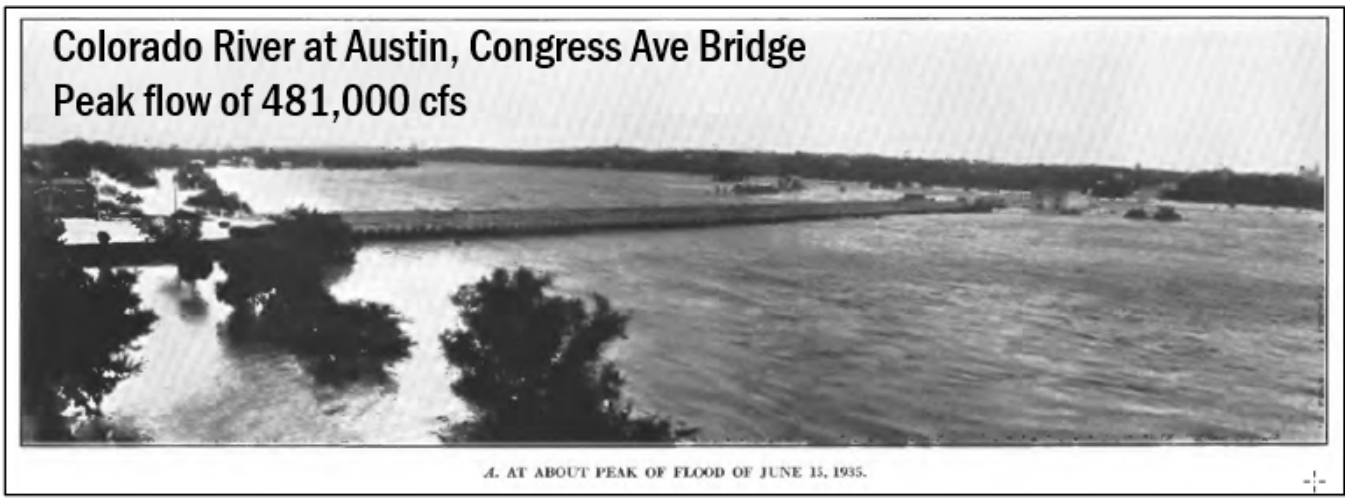

Figure 10.3: The Colorado River at Austin during the Peak of the June 1935 Flood (Dalrymple, 1939)

10.2.2 September 1936 Storm Event

The September 1936 storm event caused widespread flooding throughout the Concho River basin and on the Colorado River from Ballinger all the way to Austin. Over a four-day period, up to 30 inches of rain fell in portions of the Concho, San Saba and Llano River basins, as shown in Figure 10.4. The most destructive floods occurred in the Concho River Basin, and the city of San Angelo suffered great damage, as shown in Figure 10.5 (Dalrymple, 1937). The location on the North Concho River shown in Figure 10.5 experienced a peak flow of 184,000 cfs in September 1936, and a short distance downstream, the Concho River at San Angelo peaked at a flow rate of 230,000 cfs. Figure 10.6 shows the railroad bridge and USGS stream gage that were destroyed on the Concho River near Paint Rock, where the peak of the flood reached 301,000 cfs (Dalrymple, 1937). No other floods since 1936 have come close to those magnitudes in the Concho River basin. The September 1936 storm was selected for analysis in order to estimate what the regulated peak flows would have been with the current reservoir regulation in place from O.C. Fisher, Twin Buttes, and O.H. Ivie Reservoirs, along with LCRA's chain of Highland Lakes downstream.

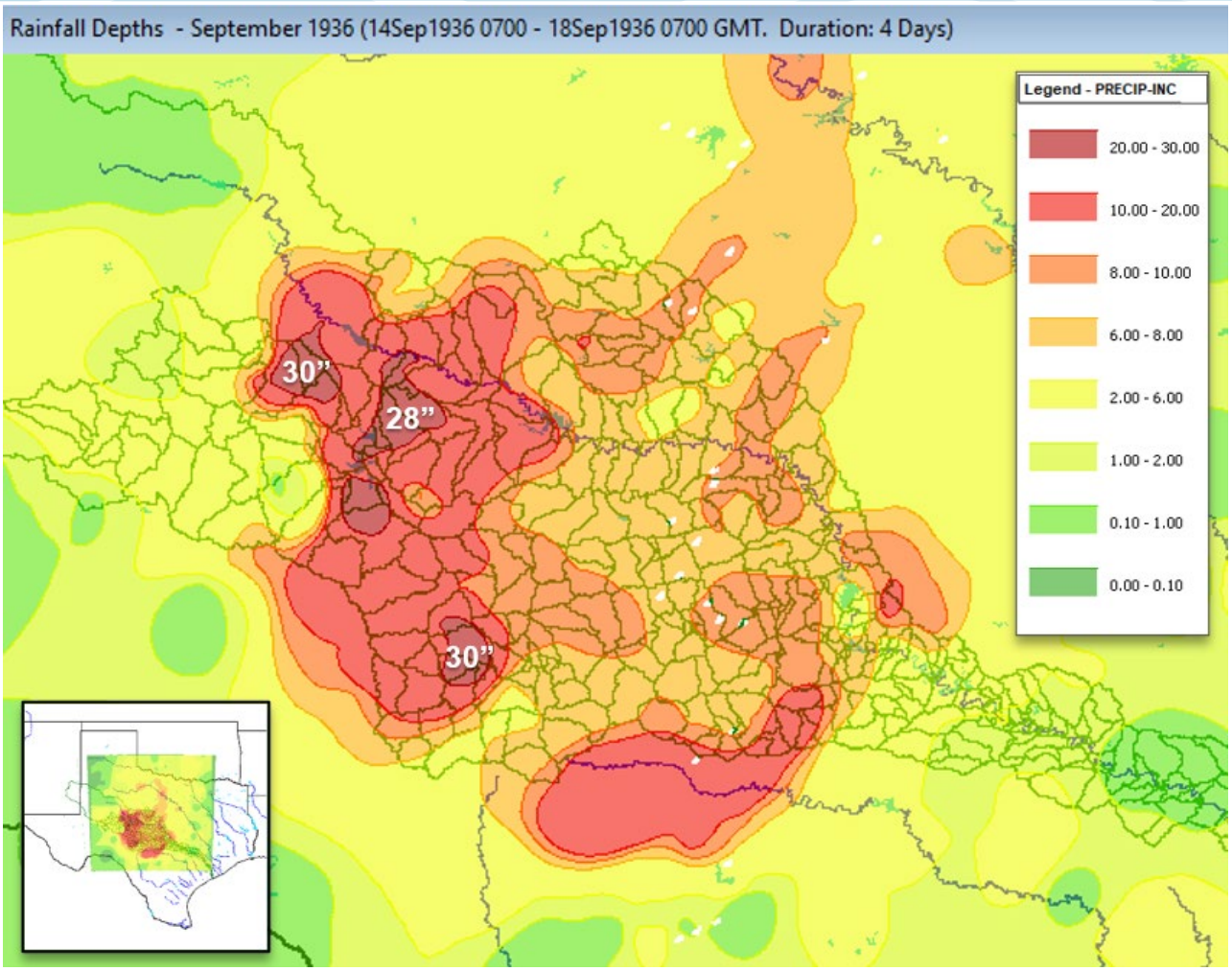

Figure 10.4: Total Rainfall Depths for the September 14-18, 1936 Storm Event

Figure 10.5: Flooded Buildings in San Angelo, Texas during the Sep 1936 Flood (Dalrymple, 1937)

A. CONCHO RIVER NEAR PAINT ROCK.

Figure 10.6: Destroyed Railroad Bridge on the Concho River after the Sep 1936 flood (Dalrymple, 1937)

10.3 METHODS AND ASSUMPTIONS

The HEC-HMS analysis of the 1935 and 1936 storm events involved several steps. First, gridded hourly rainfall data was created for each event in HEC-MetVue using historic rainfall data from the original 1930s storm reports and available precipitation gage data from that time period. Second, a 1930s conditions HEC-HMS basin model was created for each event, and the model's results for each event were verified using available stream gage data from the 1930s. Third, the same storm events were simulated in a current conditions HEC-HMS basin model, and the simulated peak flows on the rivers were recorded with all of the current reservoir regulation in place. Finally, the regulated peak flows from the 1930s storm events were added to the Bulletin 17C analysis of select stream gages as a sensitivity test of the statistical results at those locations. The methods and assumptions for each of these steps are documented in the following subsections.

10.3.1 Creating Gridded Rainfall Data

In order to simulate these two 1930s events in HEC-HMS, gridded hourly precipitation data had to be prepared for use in the Lower Colorado HEC-HMS model. For the June 1935 storm event, storm information came from a collaborative paper written by the United States Geological Survey and the United States Department of the interior called "Water-Supply Paper 796-G – Major Texas Floods of 1935" (Dalrymple, 1939). Precipitation data from that report were digitized using ArcGIS and HEC-MetVue. First, ArcGIS was used to develop an ASCII raster file that represented the total storm volumes. The contours of the precipitation volumes from the 1935 flood report were digitized in ArcMap along with the point values representing cumulative rainfall for the duration of the storm event. The final ASCII raster file utilized both point rainfall and the contour lines to estimate the storm totals. The final raster used the "USA Contiguous Albers Equal Area Conic USGS version" coordinate system with linear units in feet and a 2000-sqft cell size. Next, HEC-MetVue was used to disaggregate the ASCII raster storm totals into hourly gridded datasets. To ensure the disaggregated hourly raster files accurately represented the temporal pattern of the storm event, georeferenced hyetographs were used, as shown in Figure 10.7. The final storm event spanned 7 days, June 9-16, 1935 starting at 00:00 GMT. The largest measured precipitation point value was almost 19 inches.

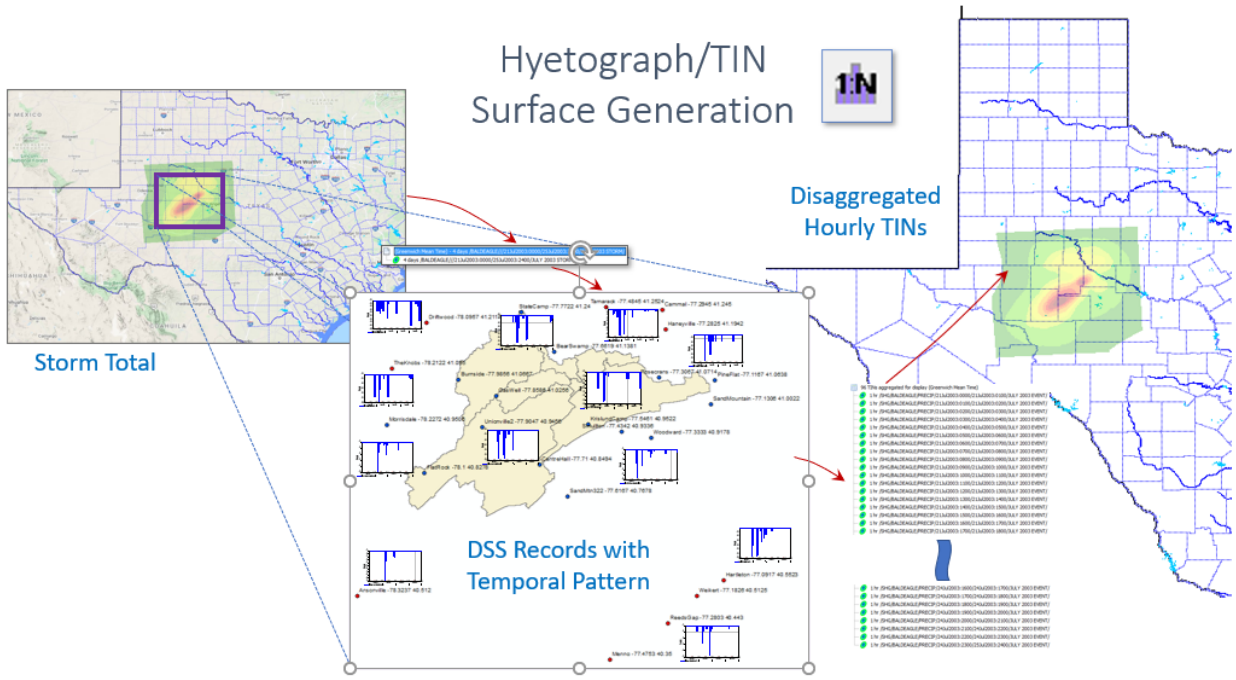

Figure 10.7: Process in HEC-MetVue for Creating Hourly Gridded Rainfall Data

For the September 1936 storm event, storm information primarily came from a collaborative paper written by the United States Geological Survey and the United States Department of the interior called "Water-Supply Paper 816 – Major Texas Floods of 1936" (Dalrymple, 1937). For this event, USACE had gridded hourly precipitation data that had been previously prepared by a meteorological contractor using similar methods to what was described above for the 1935 storm event (MetStat, 2017). The final storm event spanned 4 days, September 14-18, 1936 starting at 06:00 GMT. The largest measured precipitation point value was approximately 30 inches. Additional information on the methodologies used to create the 1936 gridded precipitation data is available in the 2017 MetStat report.

10.3.2 HEC-HMS Assumptions for 1930s Conditions

For the HEC-HMS analysis, first a new basin model was created to represent 1930s basin conditions. This 1930s basin model allowed the modeler to verify the HEC-HMS results by comparing the simulated results to the available observed streamflow data at the gages. To create this 1930s basin model, the final basin model from the uniform rain frequency storm analysis was used as the starting point. See Appendix B for more information about the development of that basin model. Next, all of the reservoirs that did not exist in 1935 and 1936 were removed from the HEC-HMS 1930s basin model. This meant that all of the current reservoirs were removed from the model except for Lake Nasworthy and Lake Brownwood, which were completed in 1930 and 1933, respectively. For all of the other reservoirs in the basin, the reservoir elements were deleted, and the upstream and downstream junctions were re-connected. The Modified Puls routing reaches upstream of the dams were also updated to reflect the storage volume in the natural river floodplain rather than the lake.

Once the 1930s basin model was set up, the gridded rainfall data and observed stream gage data was added to the HEC-HMS model, and forecast runs were set up for the June 1935 and Sep 1936 storm events. The observed stream gage data was used to adjust the loss rates and baseflows to match the antecedent conditions (i.e. the relative wetness or dryness) of the watershed at the time of those two storms. Specifically, the loss rates and baseflows were calibrated to better match the volumes of the observed flow hydrographs at the downstream streamgages. Since these storms were being run as a verification event, no other model parameters were adjusted for the 1930s simulations.

10.3.3 HEC-HMS Assumptions for Current Conditions

After recreating the two storms under the 1930s conditions, all of the current reservoirs were added back into the basin model, and those same two storms were simulated under current regulated conditions. The current conditions analysis would show what the flows would have been on the downstream rivers from those historic storms if all the current reservoir regulation had been in place at that time. To create the current conditions basin model, the final basin model from the uniform rain frequency storm analysis was used once again as the starting point, but this time, no modification was made to the reservoirs or routing reaches. Instead, the adjusted loss rates and baseflows from the 1930s conditions analysis were added to the current conditions basin model. That way the model would still reflect the antecedent conditions (i.e. the relative wetness or dryness) of the watershed at the time of the 1935 and 1936 storms.

Assumptions also had to be made regarding the reservoirs' initial pool elevations and releases during the 1935 and 1936 storms for the reservoirs that did not exist at that time. For the initial pool elevations, it was assumed that the reservoirs' pool elevations would be at top of conservation (also known as normal pool) at the beginning of the frequency storm simulation for all reservoirs in the Lower Colorado River basin. For the reservoir outflows, the releases were assumed to be the same as would be required under the current regulation plan for each reservoir. More specifically, this analysis used the same reservoir release assumptions as were used for the frequency storms, as described in Appendix B.

10.3.4 Bulletin 17C Sensitivity Analysis

Upon completion of the HEC-HMS analysis, an alternate statistical flood frequency analysis was performed for six streamgages in the basin that utilizes the HEC-HMS modeling to estimate the magnitude of the historical 1935 and 1936 floods as if the current (2022) reservoirs and land-use conditions were in place then. The alternate analysis consists of combining the regulated period of record analyzed in Appendix A with the 1935 and 1936 flood magnitude estimates from the HEC-HMS modeling added as historical events to the Bulletin 17C analysis (England and others, 2019). The results of this analysis were used as a sensitivity test against the Bulletin 17C statistical results of the observed regulated record that were presented in Appendix A.

The six streamgages that were analyzed were selected because they were significantly impacted by one or both of the 1935 and 1936 storm events and because they also would have been significantly impacted by upstream reservoir regulation if all the current reservoirs had been in place at that time. The analyzed streamgages include (1) USGS gage 08126380 Colorado River near Ballinger, (2) USGS gage 08136000 Concho River at San Angelo, (3) USGS gage 08136500 Concho River at Paint Rock, (4) USGS gage 08136700 Colorado River near Stacy, (5) USGS gage 08138000 Colorado River at Winchell, and (6) USGS gage 08158000 Colorado River at Austin, Texas.

10.4 HEC-HMS RESULTS

The following sections present the results of the June 1935 and September 1936 HEC-HMS simulations under both 1930s basin conditions and current basin conditions.

10.4.1 June 1935 Storm Event

10.4.1.1 1930s Conditions Verification Results

For the June 1935 storm event, observed streamflow data was available at 8 stream gages throughout the Lower Colorado River basin. Table 10.1 lists the gages with available streamflow data and the recorded peak flow from the June 1935 storm event. The flow hydrographs at these locations were used to adjust the upstream loss rates and baseflow to better match the observed data and the relative wetness or dryness of the watershed at the beginning of the June 1935 storm event.

Table 10.1: Available Streamflow Data Locations for the June 1935 Flood Event

USGS Gage Name	Observed Peak Flow (cfs)
Colorado River nr San Saba	71,000
North Llano River nr Junction	79,500
Llano River nr Junction	319,000
Llano River nr Castel, TX	388,000
Pedernales River nr Spicewood, TX	105,000
Colorado River at Austin	481,000
Colorado River at Smithville	305,000
Colorado River nr Eagle Lake, TX	177,000

Figures 10.8 and 10.9 show examples of the verification results from the 1930s basin model for the June 1935 storm event. A more complete set of verification results is included in Appendix F.

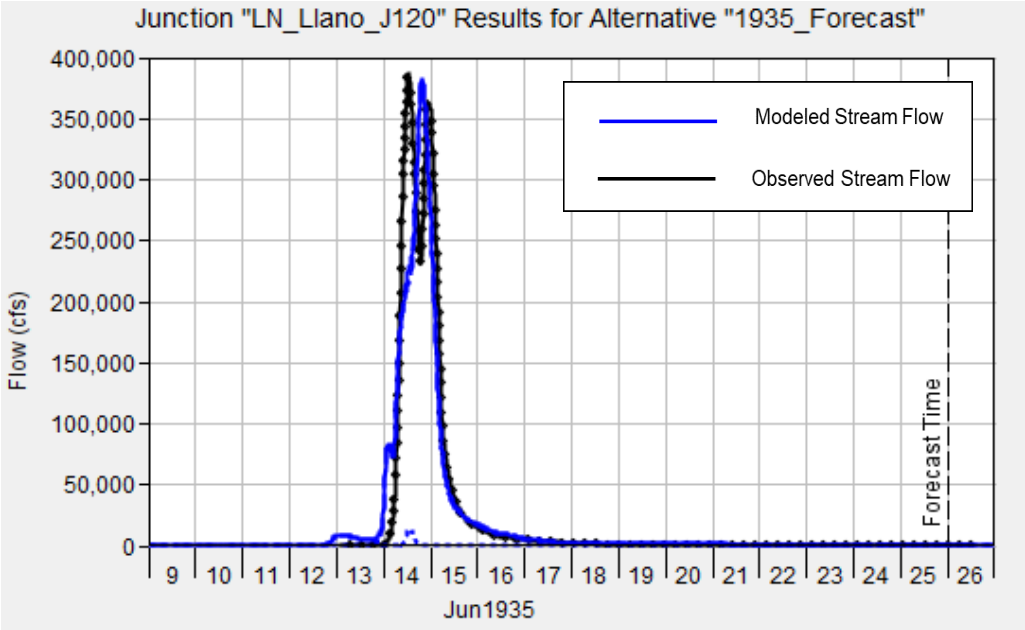

Performance Rating	NSE	RSR	PBIAS
Very Good	0.873	0.4	-3.89%

Figure 10.8: June 1935 Verification Results for the Llano River at Castel, TX

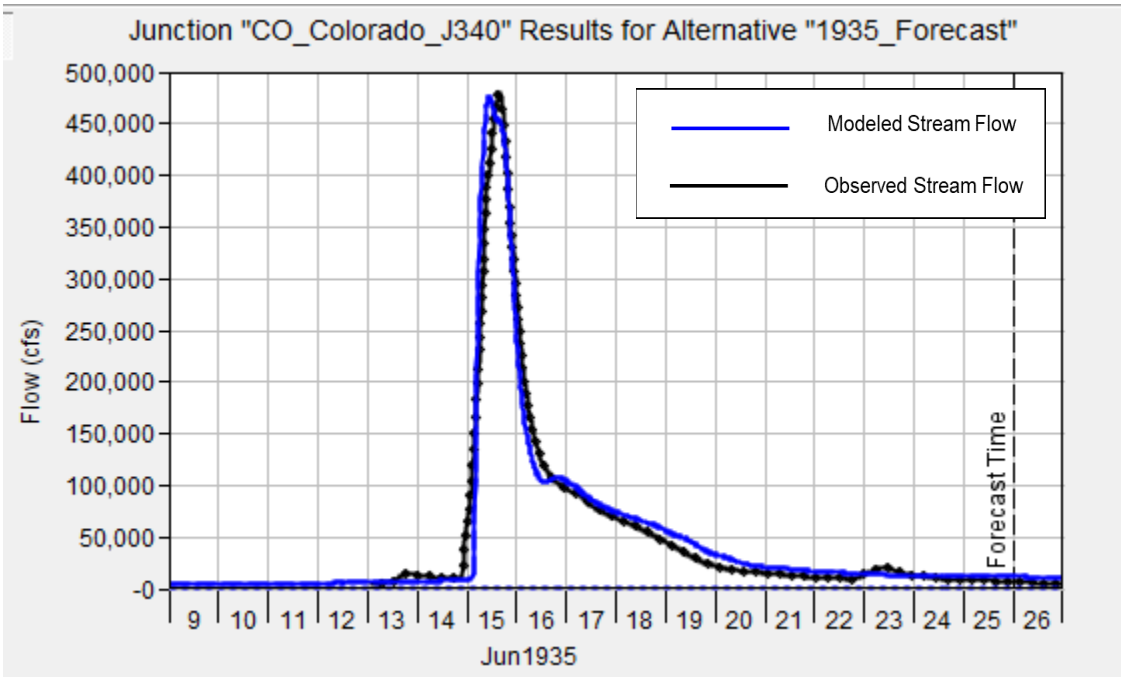

Performance Rating	NSE	RSR	PBIAS
Very Good	0.956	0.2	4.75%

Figure 10.9: June 1935 Verification Results for the Colorado River at Austin, TX

For the Llano River at Castel, the simulated results matched the volume of the observed flow hydrograph within 4%, and the timing and peak magnitude of the simulated hydrograph also matched the observed data well, as shown in Figure 10.8. The June 1935 adjusted loss rates for the Llano River at Castel had moderate loss rates with 3.5 inches of initial loss and a constant loss of 0.21 in/hr.

For the Colorado River at Austin, the simulated results matched the volume, timing, shape and peak magnitude of the observed flow hydrograph very well, as shown in Figure 10.9. The June 1935 adjusted loss rates for the Colorado River at Austin had a higher initial loss of 4 inches and a low constant loss of 0.1 in/hr.

10.4.1.2 Current Conditions Results

After adjusting the loss rates for the June 1935 antecedent conditions, the storm event was re-run in the current conditions basin model with all of the current reservoirs in place, and the streamflow results were compared downstream of the relevant reservoirs. For the Colorado River near San Saba, streamflows in the current conditions basin model are impacted by several upstream reservoirs, including O.C. Fisher, Twin Buttes, and O.H. Ivie reservoirs. These reservoirs had the effect of reducing the simulated peak flow by 20% and the streamflow volume by 35%. For the Llano and Pedernales Rivers, those watersheds remain unregulated to this day. Therefore, the current conditions results on the Llano and Pedernales Rivers are the same as the 1930s conditions results as presented in the previous section and in Appendix F.

For the Colorado River at Austin, streamflows in the current conditions basin model were primarily impacted by the regulation of Lake Travis. Figure 10.10 shows the simulated results for Lake Travis during the June 1935 storm event. Since the inflow hydrograph for the June 1935 event was fairly short in duration (only 2 days), the flood storage of Lake Travis was able to greatly reduce the peak flows downstream. The peak inflow to Lake Travis was 479,000 cfs, but the peak outflow was only 68,300 cfs. The lake reached a peak elevation of 715.8 ft NAVD88. This reservoir regulation reduced the peak flow for the Colorado River at Austin by 85%, as shown in Figure 10.11.

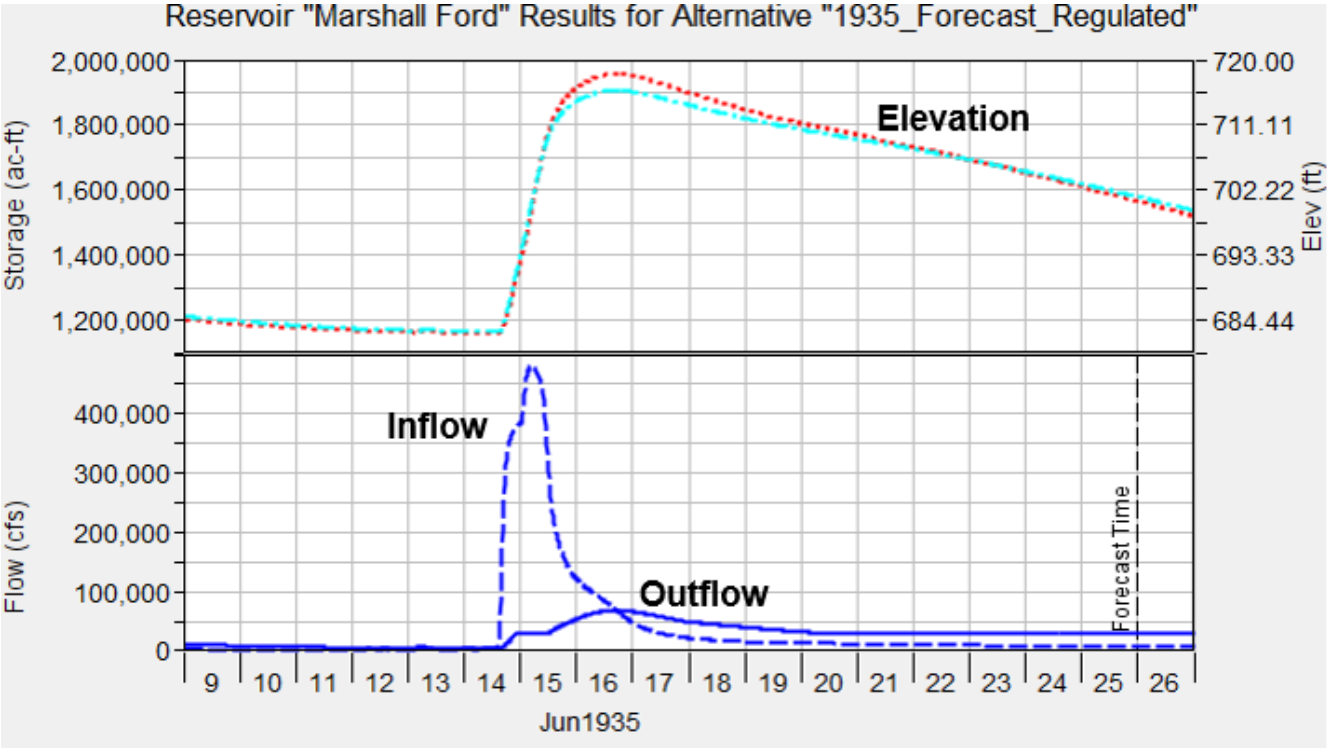

Figure 10.10: June 1935 Current Conditions Results for Lake Travis near Austin, TX

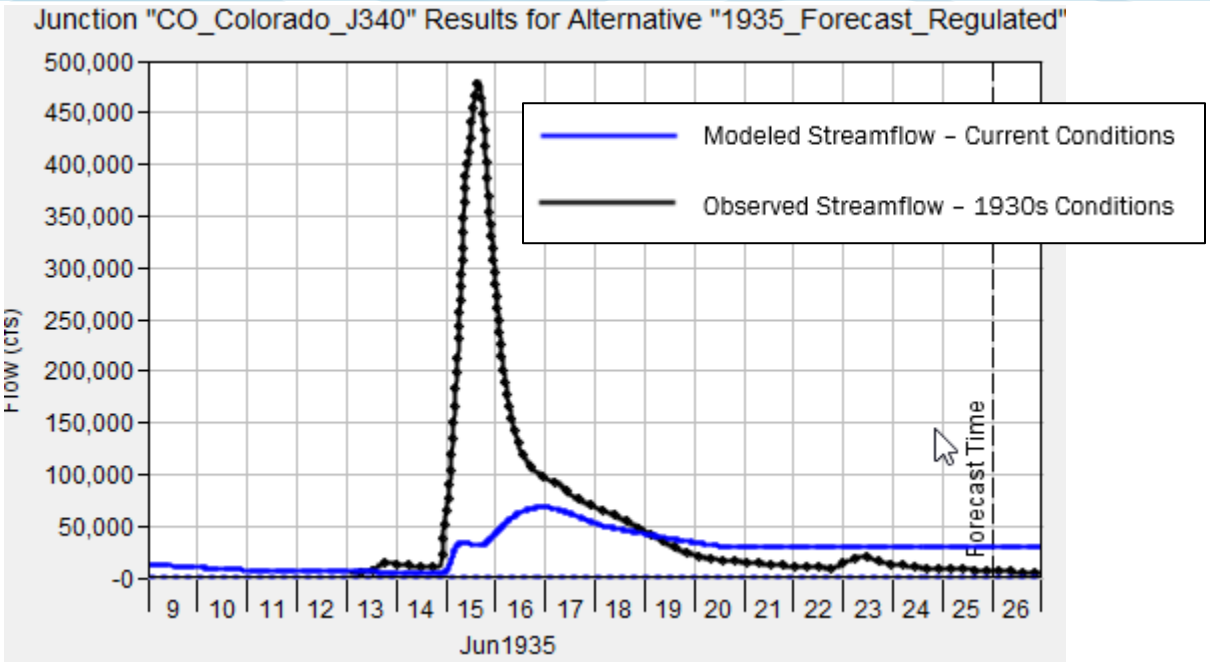

Figure 10.11: June 1935 Current Conditions Results for the Colorado River at Austin, TX

10.4.2 September 1936 Storm Event

10.4.2.1 1930s Conditions Verification Results

For the September 1936 storm event, observed streamflow data was available at 18 stream gages throughout the Lower Colorado River basin. Table 10.2 lists the gages with available streamflow data and the recorded peak flow from the September 1936 storm event. The flow hydrographs at these locations were used to adjust the upstream loss rates and baseflow to better match the observed data and the relative wetness or dryness of the different portions of the watershed at the beginning of the September 1936 storm event.

The following figures show a few examples of the verification results of the 1930s basin model for the September 1936 storm event. A more complete set of results is presented in Appendix F. The verification results for this event showed larger differences between the observed data and the model results. While the model was generally able to match the volume of the streamflow hydrographs, the timing and shape were often different. This is especially true for some of the gages in the Concho and San Saba watersheds. The reason for these differences in the upper watershed is likely due to rainfall inaccuracies as there were not many rain gages in this portion of the watershed in 1936 that could give an accurate indication of the timing and intensity of the rainfall. Forecast blending was used to replace the model result with the observed data at these gages to keep those errors from propagating further downstream.

Table 10.2: Available Streamflow Data Locations for the 14-18 September 1936 Flood Event

USGS Gage Name	Observed Peak Flow (cfs)
Colorado River at Ballinger	75,400
Middle Concho River nr Tankersly	35,000
Spring Creek nr Tankersly	23,900
South Concho River at Christoval	80,100
South Concho River at San Angelo	111,000
North Concho River nr Carlsbad	94,600
Concho River nr San Angelo	230,000
Concho River nr Paint Rock	301,000
Pecan Bayou at Brownwood	12,300
San Saba River at Menard	68,600
San Saba River at San Saba	45,500
Colorado River nr San Saba	219,000
Llano River nr Junction	158,000
Llano River nr Castel, TX	153,000
Pedernales River nr Spicewood, TX	50,700
Colorado River at Austin	137,000
Colorado River at Smithville	117,000
Colorado River nr Eagle Lake, TX	102,000

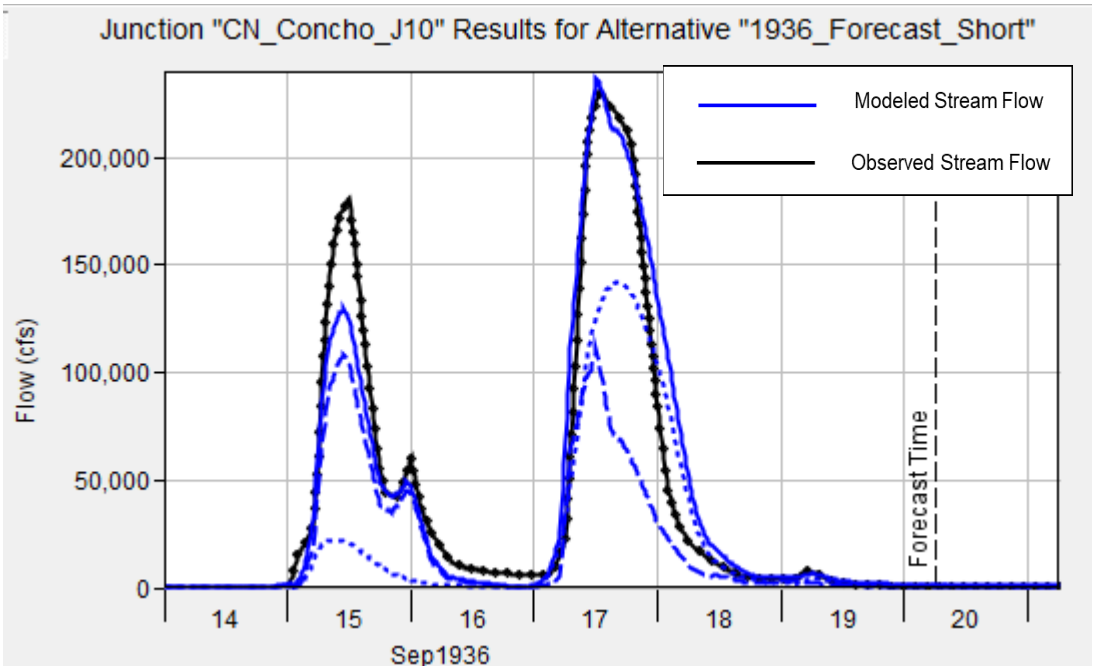

Performance Rating	NSE	RSR	PBIAS
Very Good	0.929	0.3	1.89%

Figure 10.12: September 1936 Verification Results for the Concho River at San Angelo, TX

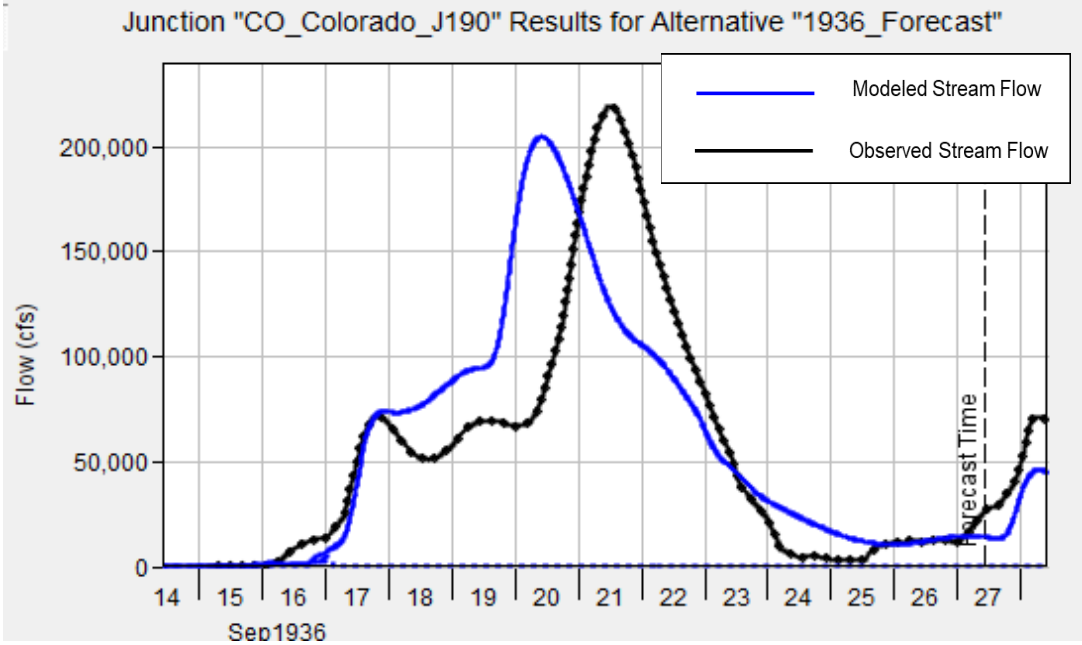

Performance Rating	NSE	RSR	PBIAS
Satisfactory	0.516	0.7	4.83%

Figure 10.13: September 1936 Verification Results for the Colorado River nr San Saba, TX

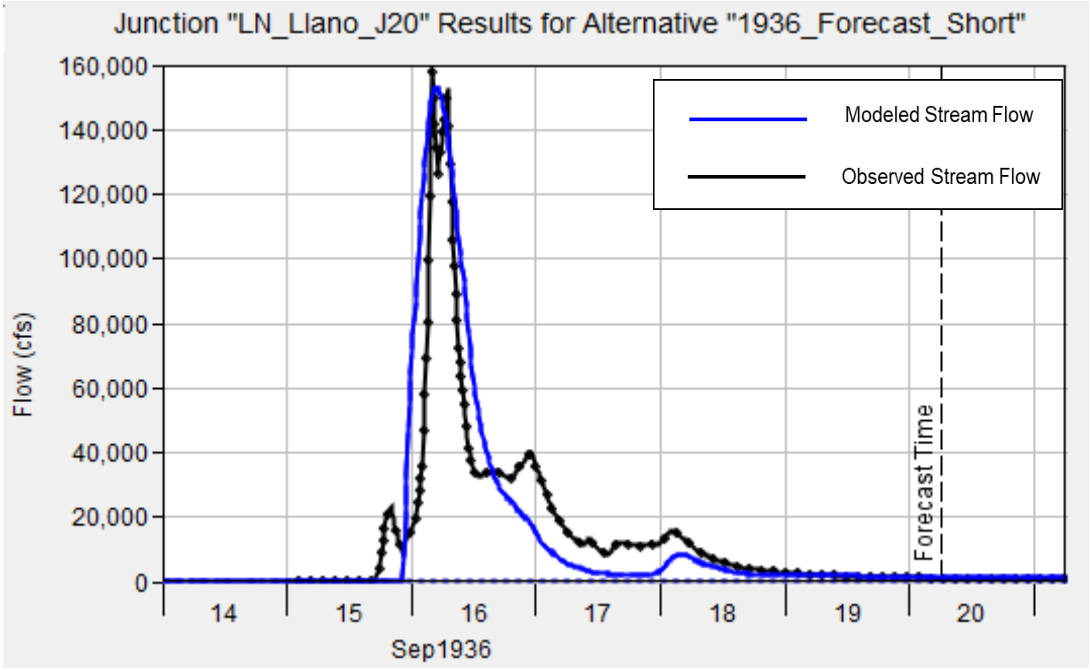

Performance Rating	NSE	RSR	PBIAS
Good	0.718	0.5	0.83%

Figure 10.14: September 1936 Verification Results for the Llano River nr Junction, TX

The range of adjusted loss rates above each gage is included in Appendix F. Overall, the initial and constant loss rates tended to be high which indicates that the watershed was relatively dry at the beginning of the September 1936 flood event.

10.4.2.2 Current Conditions Results

After adjusting the loss rates for the September 1936 soil moisture conditions, the storm event was re-run in the current conditions basin model with all of the current reservoirs in place, and the streamflow results were compared downstream of the relevant reservoirs. Forecast blending was used at any streamgages that were located upstream of modeled reservoirs in order to keep any rainfall or model error from propagating further downstream to the reservoirs and rivers. This included many of the gages on the Concho and San Saba watersheds that had errors in the 1930s simulations.

For the Concho River at San Angelo, streamflows in the current conditions basin model are impacted by reservoir regulation from O.C. Fisher and Twin Buttes. The model's showed that O.C. Fisher Reservoir would have been able to store the entire flood hydrograph from the North Concho River without making any releases. At Twin Buttes Reservoir, a peak inflow of 132,000 cfs was reduced to a peak outflow of less than 7,000 cfs. These two reservoirs had the effect of reducing the peak flow of the Concho River at San Angelo from 230,000 cfs under 1930s conditions to 49,700 cfs under current conditions, as shown in Figure 10.15. However, that regulated peak flow of 49,700 cfs is still 300% larger than any other peak that has been observed since the upstream reservoirs were built.

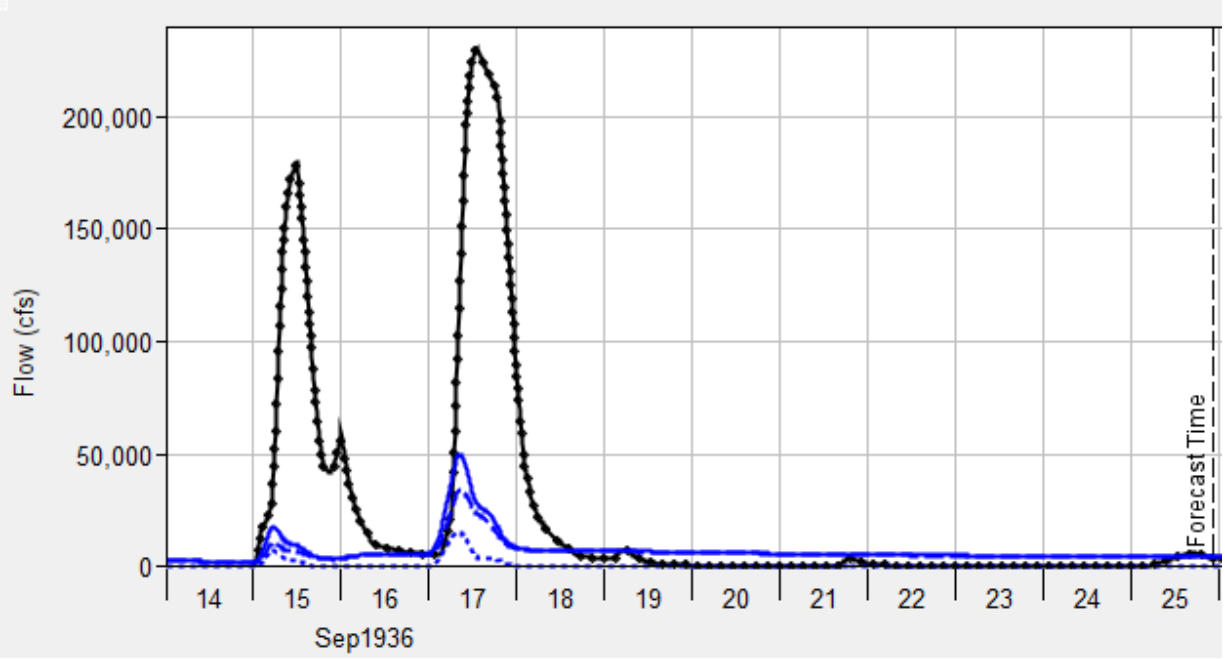

Figure 10.15: September 1936 Current Conditions Results for the Concho River at San Angelo, TX

Further downstream on the Concho River near Paint Rock, the observed 1936 peak of 301,000 cfs was reduced by almost half to 160,000 cfs by the two reservoirs upstream of San Angelo. However, this regulated 1936 peak is still 300% larger than any other peak that has been observed since the upstream reservoirs were built.

At the Colorado River near Stacy, streamflows in the current conditions basin model are impacted by reservoir regulation from O.H. Ivie as well as inflows from both the Concho and Colorado Rivers. The current conditions analysis for the 1936 storm event showed that O.H. Ivie reservoir would have reduced the peak flow downstream of the dam by about 30%, as shown in Figure 10.16. This resulted in a current conditions peak flow of 177,000 cfs at the downstream gage of the Colorado River near Stacy for the 1936 storm event. Further downstream at the Colorado River near Winchell, the current conditions analysis estimated a regulated peak flow of about 161,000 cfs for the 1936 storm event. No observed flow data was available for that location.

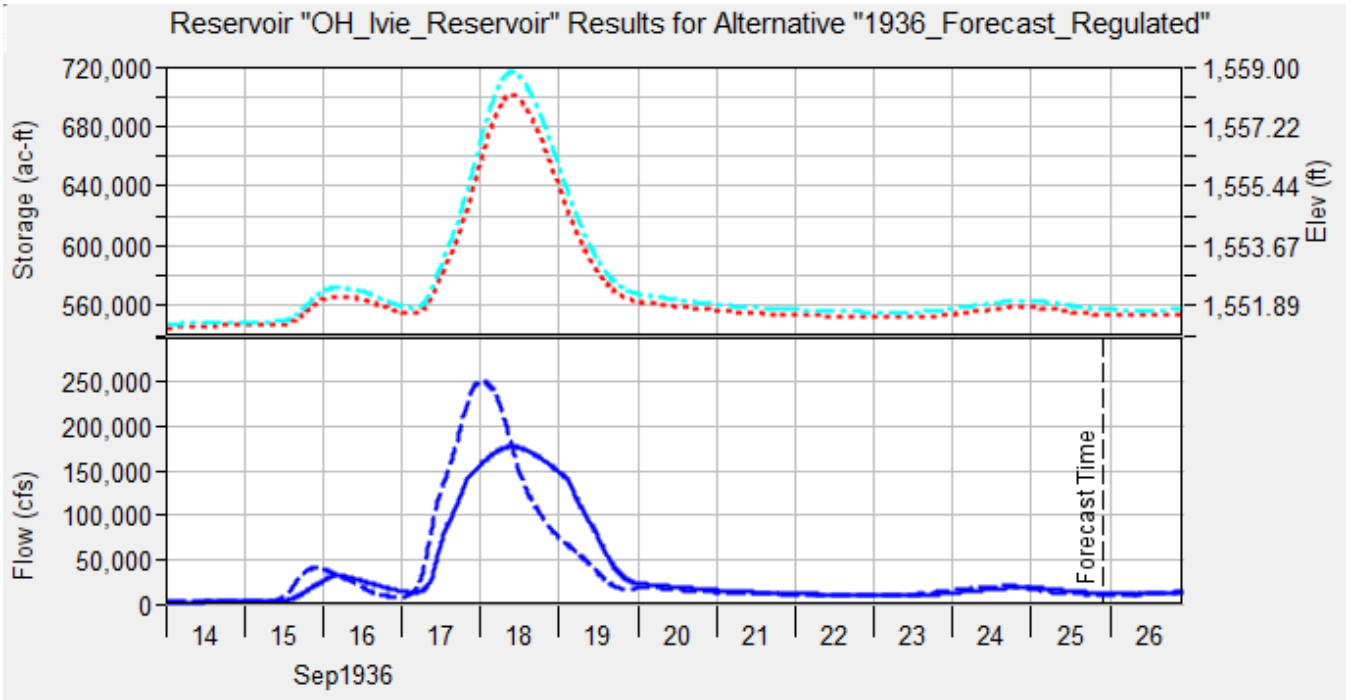

Figure 10.16: September 1936 Current Conditions Results for O.H. Ivie Reservoir

For the San Saba, Llano and Pedernales Rivers, whose watersheds remain largely unregulated to this day, forecast blending was used, and it was assumed that the current conditions peak flows would be the same as the observed 1930s peak flows.

For the Colorado River at Austin, streamflows in the current conditions basin model are primarily impacted by the regulation of Lake Travis and by inflows from the upstream watersheds. Figure 10.17 shows the simulated results for Lake Travis during the September 1936 storm event. From this plot, one can see the long duration of inflows that would have occurred from mid-September all the way through the first week of October. In this simulation, flows downstream of the dam were reduced by more than half to 77,900 cfs. The lake reached a peak elevation of 716.8 ft NAVD88. The current reservoir regulation also reduced the peak flow for the Colorado River at Austin by 67% from 234,000 cfs to 77,900 cfs.

However, this simulation is likely an underestimation of the total inflow to Lake Travis because it only includes rainfall from the 4-day period of 14-18 September. The 1936 storm report, however, indicates that additional significant rainfall (up to 6-10 inches in some areas) fell upstream of Lake Travis on 25-26 September, 1936 (Dalrymple, 1937). While not included in this analysis, the additional inflow from the rainfall during the last week of September could have easily pushed Lake Travis up to the 90,000 cfs release threshold, which would have similarly impacted the peak flow at the Colorado River at Austin.

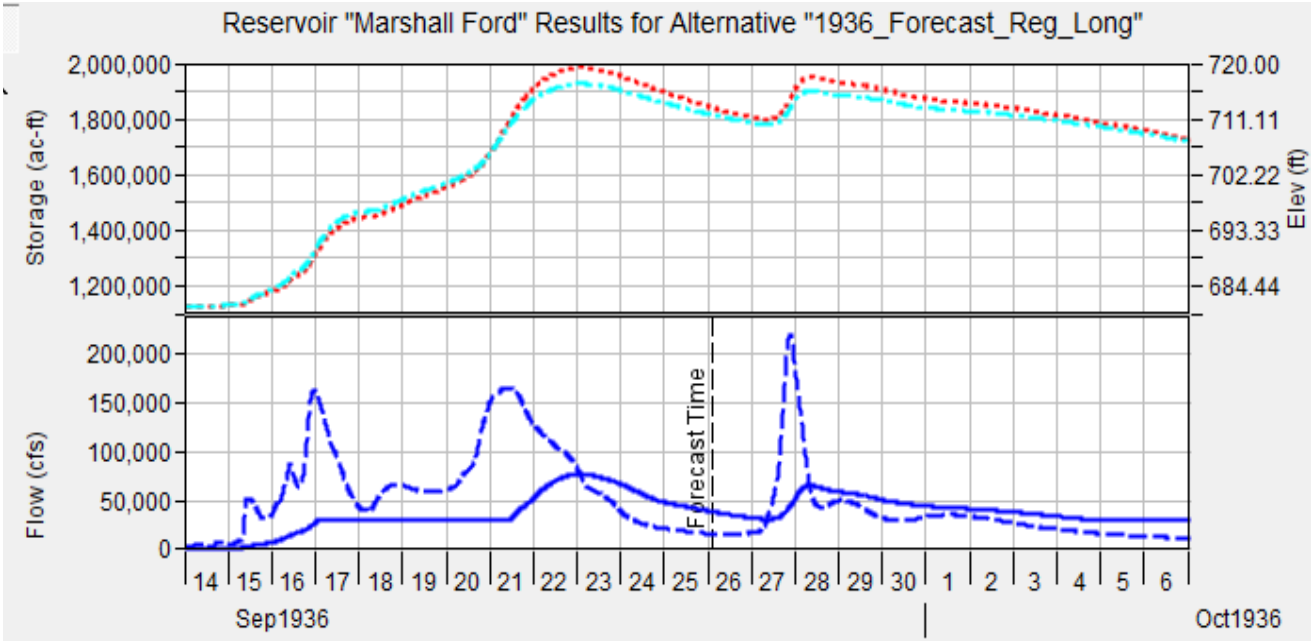

Figure 10.17: September 1936 Current Conditions Results for Lake Travis

10.5 STATISTICAL RESULTS

Upon completion of the HEC-HMS current conditions analysis of the 1935 and 1936 storms, an alternate statistical flood frequency analysis was performed for six streamgages in the basin. The six streamgages that were analyzed were selected because they were significantly impacted by one or both of the 1935 and 1936 storm events and because they also would have been significantly impacted by upstream reservoir regulation if all the current reservoirs had been in place at that time. The analyzed streamgages include (1) USGS gage 08126380 Colorado River near Ballinger, (2) USGS gage 08136000 Concho River at San Angelo, (3) USGS gage 08136500 Concho River at Paint Rock, (4) USGS gage 08136700 Colorado River near Stacy, (5) USGS gage 08138000 Colorado River at Winchell, and (6) USGS gage 08158000 Colorado River at Austin, Texas. The results of this analysis were used as a sensitivity test against the Bulletin 17C statistical results of the observed regulated record that were presented in chapter 5 and in Appendix A.

10.5.1 USGS 08126380 Colorado River near Ballinger, Texas

The period of record analyzed at USGS streamgage 08126380 Colorado River near Ballinger, TX. for the alternate analysis was from 1969 through 2020 (USGS, 2022). The modeled 1936 annual peak streamflow for current conditions was 75,400 cfs, which is equal to the observed event. Because this was the largest known event since 1908, a perception threshold of 75,400 cfs was set for the 1908 through 1968 time period. The low-outlier threshold was computed by the MGBT in HEC-SSP at 1,130 cfs, and a total of 12 low outliers were identified. The flood flow frequency curve plot from HEC-SSP for the Colorado River near Ballinger gage alternate analysis is shown in Appendix F.

A comparison of the above analysis with the statistical flood flow frequency results from Appendix A and the RiverWare flood flow frequency results from Appendix D is shown in Figure 10.18. The analysis incorporating the 1936 peak event appears to split the difference between the RiverWare results and statistical results of Appendix A. Flood frequency estimates from the alternate analysis track well with the statistical results through approximately the 0.1 Annual Exceedance Probability (AEP) but track closer to the RiverWare estimates for the 0.01 AEP and above.

The relative effects of record length and magnitudes of substantial floods for the Colorado River near Ballinger gage are shown in the change over time plots in Appendix F.

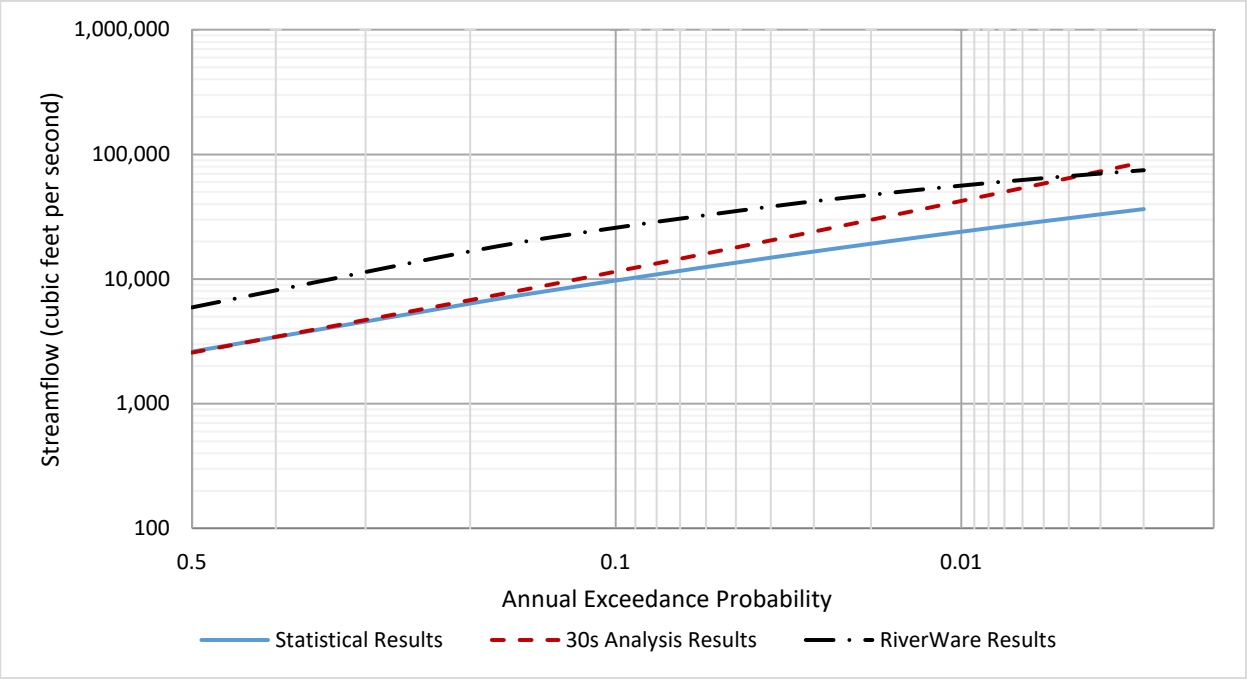

Figure 10.18: Comparison of Flood Flow Frequency Curves for the Statistical Results (1969-2020), 30s Analysis Results (1936, 1969-2020), and RiverWare Results (1931-2020) for USGS Streamgage 08126380 Colorado River near Ballinger, TX

10.5.2 USGS 08136000 Concho River at San Angelo, Texas

The period of record analyzed at USGS streamgage 08136000 Concho River at San Angelo, TX for the alternate analysis was from 1963 through 2020 (USGS, 2022). The modeled 1936 annual peak streamflow for current conditions of 49,700 cfs was added to the analysis as a historical event. Because this was the largest known event since 1906, a perception threshold of 49,700 cfs was set for the 1906 through 1962 time period. The flood flow frequency curve plot from HEC-SSP for the Concho River at San Angelo gage alternate analysis is shown in Appendix F. No low outliers were identified by the MGBT in HEC-SSP.

A comparison of the above analysis with the statistical flood flow frequency results from Appendix A and the RiverWare flood flow frequency results from Appendix D is shown in Figure 10.19. As seen with the Colorado River near Ballinger gage, the analysis incorporating the 1936 peak event appears to split the difference between the RiverWare results and statistical results of Appendix A. Flood frequency estimates from the alternate analysis track well with the statistical results through approximately the 0.1 Annual Exceedance Probability (AEP) but track closer to the RiverWare estimates for the 0.005 AEP. The relative effects of record length and magnitudes of substantial floods for the Concho River at San Angelo gage are shown in the change over time plot of Appendix F.

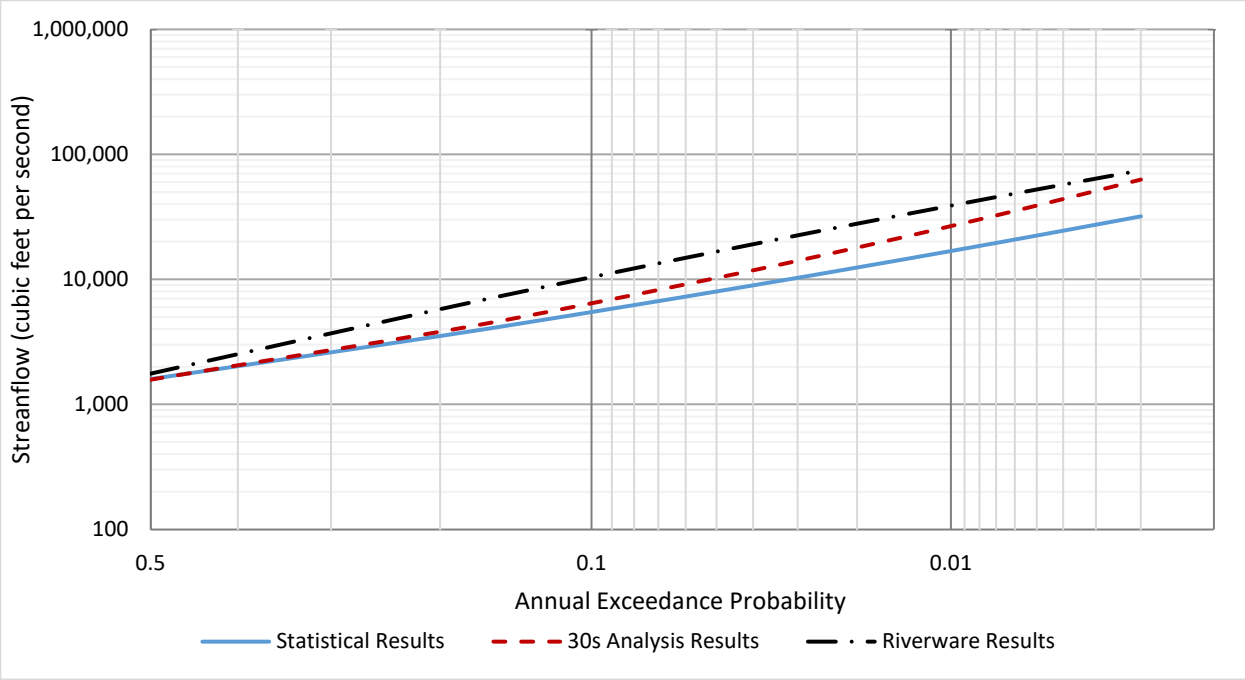

Figure 10.19: Comparison of Flood Flow Frequency Curves for the Statistical Results (1963-2020), 30s Analysis Results (1936, 1963-2020), and RiverWare Results (1931-2020) for USGS Streamgage 08136000 Concho River at San Angelo, TX

10.5.3 USGS 08136500 Concho River at Paint Rock, TX

The period of record analyzed at USGS streamgage 08136500 Concho River at Paint Rock, TX for the alternate analysis was from 1963 through 2020 (USGS, 2022). The modeled 1936 annual peak streamflow of 160,000 cfs was added to the analysis as a historical event. Because this was the largest known event since 1882, a perception threshold of 160,000 cfs was set for the 1882 through 1962 time period. The flood flow frequency curve plot from HEC-SSP for the Concho River at Paint Rock gage alternate analysis is shown in Appendix F. No low outliers were identified by the MGBT in HEC-SSP.

A comparison of the above analysis with the statistical flood flow frequency results from Appendix A and the RiverWare flood flow frequency results from Appendix D is shown in Figure 10.20. The alternate analysis including the 1936 peak streamflow has a near-identical 0.5 AEP value with the statistical results presented in Appendix A. However, above the 10-year return period, the alternate results are much higher than both the statistical and RiverWare results. The relative effects of record length and magnitudes of substantial floods for the Concho River at Paint Rock gage are shown in the change over time plots of Appendix F.

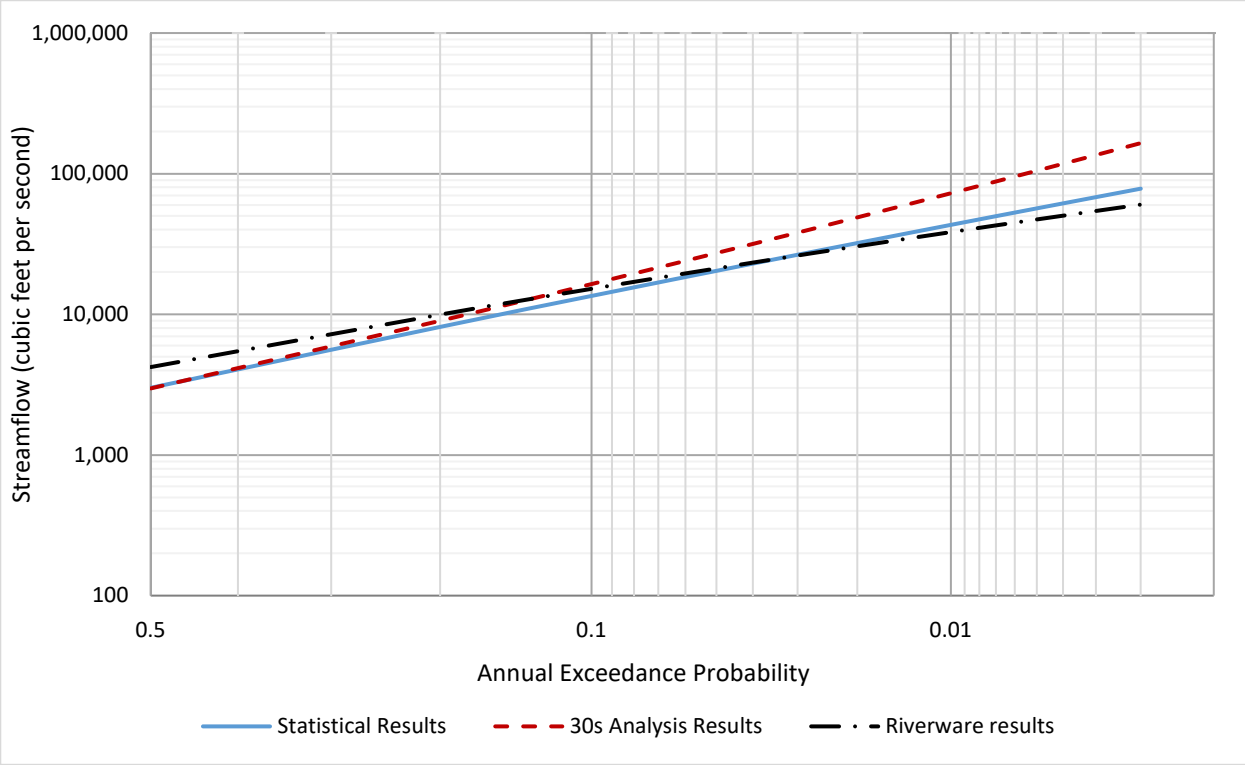

Figure 10.20: Comparison of Flood Flow Frequency Curves for the Statistical Results (1963-2020), 30s Analysis Results (1936, 1963-2020), and RiverWare Results (1931-2020) for USGS Streamgage 08136500 Concho River at Paint Rock, TX

10.5.4 USGS 08136700 Colorado River near Stacy, TX

The period of record analyzed at USGS streamgage 08136700 Colorado River near Stacy, TX for the alternate analysis was from 1990 through 2020 (USGS, 2022). The modeled 1936 annual peak streamflow of 177,000 cfs was added to the analysis as a historical event. Because this was the largest known event since 1936, a perception threshold of 160,000 cfs was set for the 1936 through 1989 time period. The flood flow frequency curve from HEC-SSP for the Colorado River near Stacy gage alternate analysis is shown in Appendix F. No low outliers were identified by the MGBT in HEC-SSP.

A comparison of the above analysis with the statistical flood flow frequency results from Appendix A and the RiverWare flood flow frequency results from Appendix D is shown in Figure 10.21. As seen with the Colorado River near Ballinger gage, the analysis incorporating the 1936 peak event appears to mostly split the difference between the RiverWare results and statistical results of Appendix A. Flood frequency estimates from the alternate analysis track well with the statistical results near the 0.5 Annual Exceedance Probability (AEP) but track closer to the RiverWare estimates near the 0.01 AEP and exceeds those estimates thereafter.

The relative effects of record length and magnitudes of substantial floods for the Colorado River near Stacy gage are shown in the change over time plot in Appendix F. The period of record for the Colorado River near Stacy gage is relatively short, and as expected, the change over time analysis does not appear to reach a stable estimate for any return period estimate.

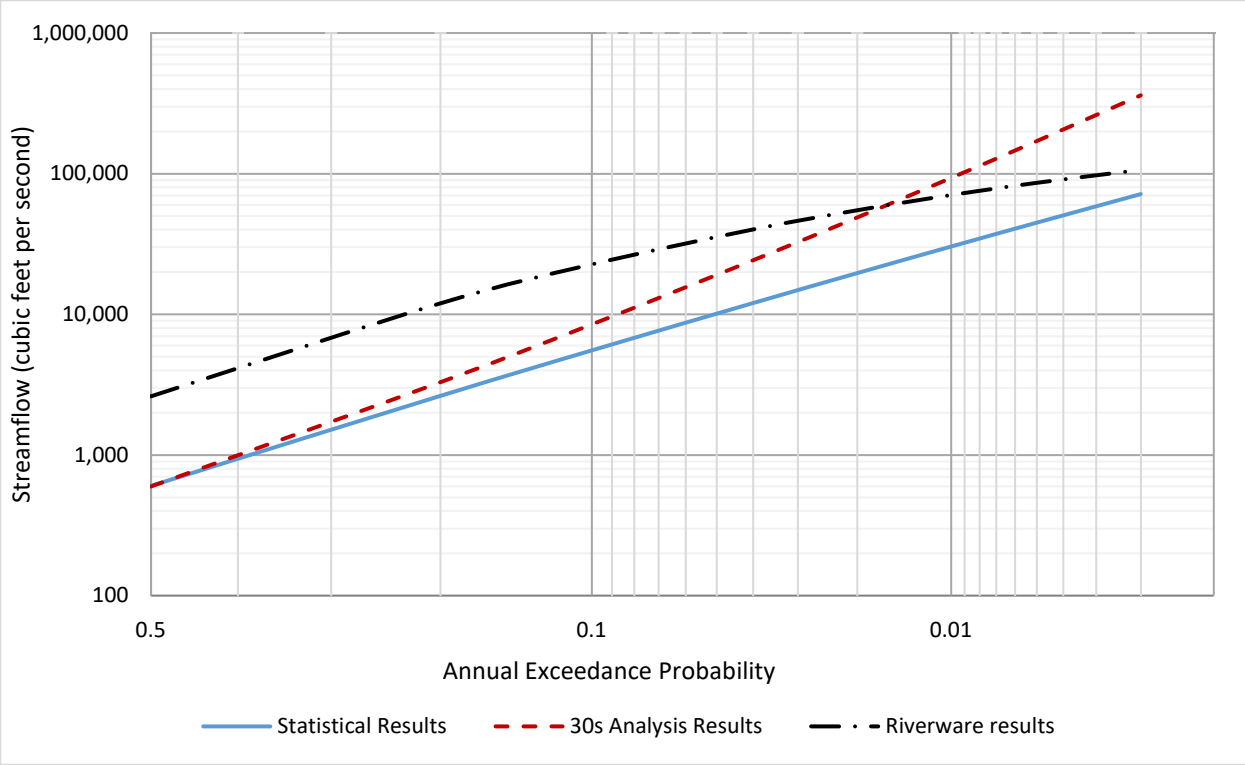

Figure 10.21: Comparison of Flood Flow Frequency Curves for the Statistical Results (1990-2020), 30s Analysis Results (1936, 1990-2020), and RiverWare Results (1931-2020) for U.S. Geological Survey Streamgage 08136700 Colorado River near Stacy, TX

10.5.5 USGS 08138000 Colorado River at Winchell, TX

The period of record analyzed at USGS streamgage 08138000 Colorado River at Winchell, TX for the alternate analysis was from 1963 through 2020 (USGS, 2022). The modeled 1936 annual peak streamflow of 161,000 cfs was added to the analysis as a historical event. Because this was the largest known event since 1924, a perception threshold of 161,000 cfs was set for the 1924 through 1962 time period. The flood flow frequency curve plot from HEC-SSP for the Colorado River at Winchell gage alternate analysis is shown in Appendix F. The low-outlier threshold was computed by the MGBT in HEC-SSP at 9,710 cfs, and a total of 28 low outliers were identified.

A comparison of the above analysis with the statistical flood flow frequency results from Appendix A and the RiverWare flood flow frequency results from Appendix D is shown in Figure 10.22. All three analyses track well with one another through approximately the 0.1 AEP where the RiverWare and alternate estimates then track higher than the statistical estimates. The alternate estimates are even higher than the RiverWare estimates in lower AEPs owing to the large positive skew resulting from the 1936 event plotting as a high outlier.

The relative effects of record length and magnitudes of substantial floods for the Colorado River at Winchell gage are shown in the change over time plots of Appendix F. Although there is nearly 60 years of record in the analysis, it appears as though a stable estimate hasn't been reached except for the 2-year return interval.

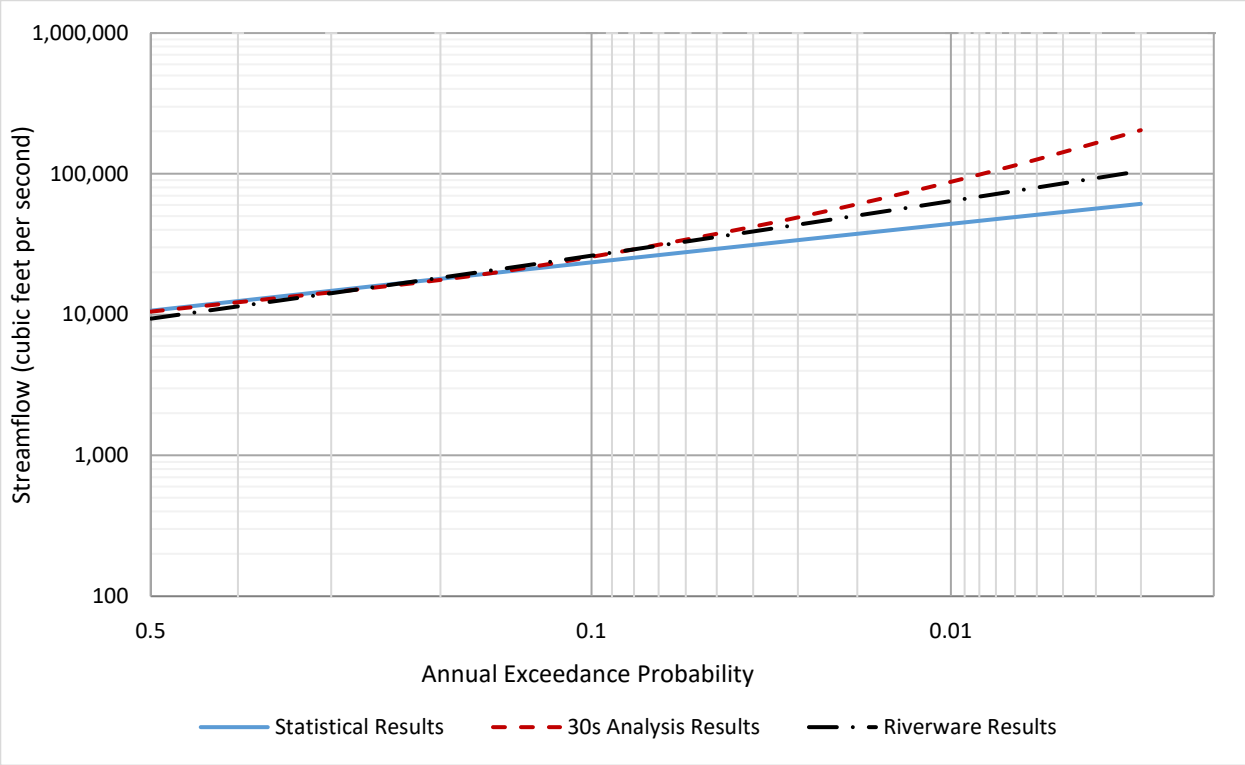

Figure 10.22: Comparison of Flood Flow Frequency Curves for the Statistical Results (1963-2020), 30s Analysis Results (1936, 1963-2020), and RiverWare Results (1931-2020) for U.S. Geological Survey Streamgage 08138000 Colorado River at Winchell, TX

10.5.6 USGS 08158000 Colorado River at Austin, TX

The period of record analyzed at USGS streamgage 08158000 Colorado River at Austin, TX for the alternate analysis was from 1941 through 2020 (USGS, 2022). The modeled 1936 annual peak streamflow for the Colorado River at Austin was 77,800 cfs. However, rainfall data was only available for the period of the 14th through the 18th of September, but we know that significant rainfall continued through the end of September 1936. Had Lake Travis been in place (as they are modeled in the present HEC-HMS analysis), the additional rainfall likely could have filled Lake Travis and required it to release at the maximum allowable discharge of 90,000 cfs, which is consequently what occurred in the RiverWare model in Appendix D. Therefore, rather than entering the 1936 modeled peak as a single historical value, it was entered as an interval threshold from 77,800 cfs to 90,000 cfs.

Additionally, the June of 1935 flood was modeled for this streamgage in HEC-HMS, and an annual peak flow of 68,500 cfs was added to the analysis as a historical event. The 1938 annual peak streamflow was not modeled in HEC-HMS as part of this analysis, but because it was similar in magnitude to the 1936 event, it was added to the analysis as an interval peak event with lower and upper bounds of 60,000 cfs and 90,000 cfs respectively. Because these were the largest known events since 1869, a perception threshold of 68,500 cfs was set for the 1869 through 1940 time period. The flood flow frequency curve plot from HEC-SSP for the Colorado River at Austin gage alternate analysis is shown in Appendix F. No low outliers were identified by the MGBT in HEC-SSP.

A comparison of the above analysis with the statistical flood flow frequency results from Appendix A and the RiverWare flood flow frequency results from Appendix D is shown in Figure 10.23. As seen in the analysis for the Colorado at Winchell gage, all three analyses track well with one another through approximately the 0.1 AEP

where the RiverWare and alternate estimates then track higher than the statistical estimates. The alternate estimates are slightly higher than the RiverWare estimates lower than about the 0.05 AEP.

The relative effects of record length and magnitudes of substantial floods for the Colorado River at Austin gage are shown in Appendix F. After initially high estimates, all four return intervals appear to stabilize relatively quickly at the highly regulated Colorado River at Austin streamgage. Beginning in approximately water year 2000, all four estimates change little for the remainder of the analysis through water year 2020 due to a lack of large floods during that time period.

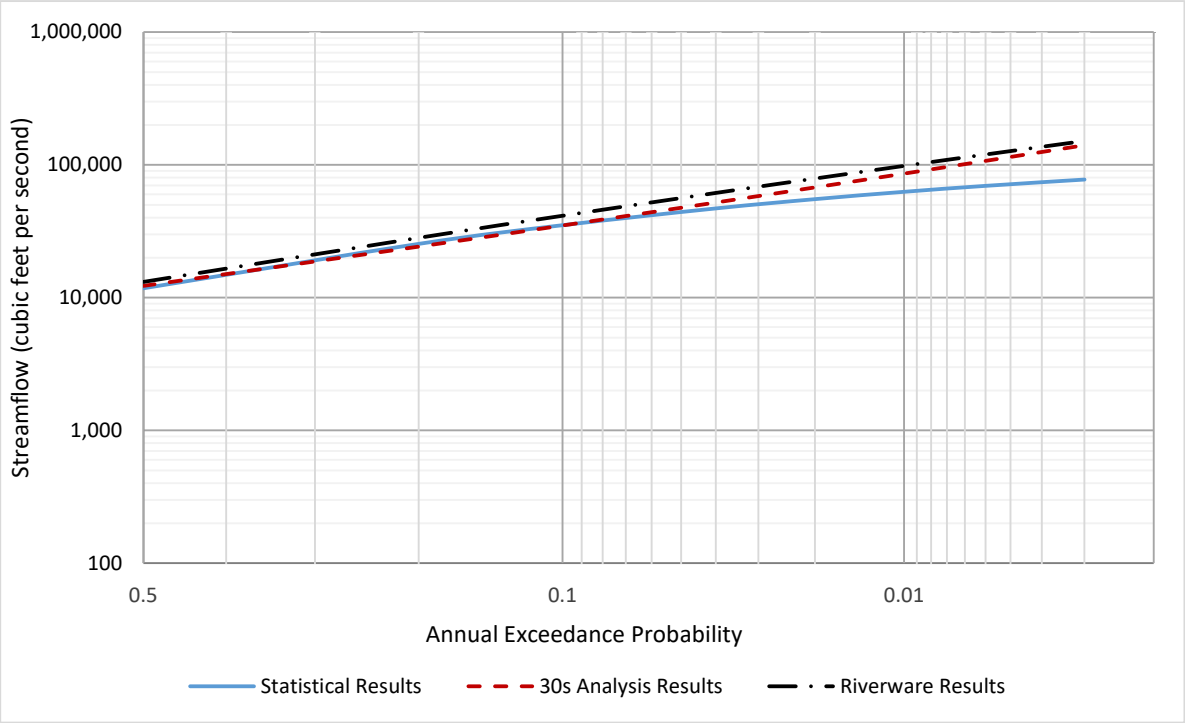

Figure 10.23: Comparison of Flood Flow Frequency Curves for the Statistical Results (1941-2020), 30s Analysis Results (1935, 1936, 1938, 1941-2020), and RiverWare Results (1931-2020) for U.S. Geological Survey Streamgage 08158000 Colorado River at Austin, TX

10.6 CONCLUSIONS

This 1930s historic storms analysis used HEC-HMS to recreate the June 1935 and September 1936 storm events with the goal of estimating what peak flows on the rivers would have been under current conditions with all of the current reservoirs in place. The estimated current conditions peak flows for those storm events were then added to the Bulletin 17C analyses of select stream gages as a sensitivity test of the statistical results.

For all six of the analyzed gage locations, no other flood in the past 80 years has come close to the magnitudes of flooding that were observed in the 1930s. The current conditions HEC-HMS analysis showed that while the upstream reservoirs would have reduced those peak flows by more than half in many cases, the resulting regulated 1935 and 1936 peak flows would still have been double or triple the highest floods that have been observed since the reservoirs have been in place at several locations.

The HEC-HMS analysis also revealed that the antecedent moisture conditions of these two events ranged from very wet for the 1935 storm to very dry in 1936, but the adjusted loss rates from these two storms were still within the range of those seen during calibration in the recent storm events. Therefore, there is nothing in this analysis to suggest that the response of the watershed to these types of large storm events is fundamentally

different today than it was in the 1930s, and since these 1930s events were the largest in the period of record, they should not be ignored in a flood frequency analysis.

Adding the 1935 and 1936 current conditions peak flows to the Bulletin 17C statistical analysis did not have much impact on the 2-yr through 10-yr flood frequency estimates, but it did significantly increase the statistical estimates for the 100-yr through 500-yr frequencies at several of the analyzed locations. It also completely changed the trajectories of the statistical frequency flow estimates versus time plots, as shown in Appendix F. This analysis provides one more valuable piece of information which is compared against the other hydrologic analyses in this report.

11 Storm Shifting Analysis

11.1 INTRODUCTION AND PURPOSE OF STORM SHIFTING

Transposing or shifting a storm event is a scientific and engineering concept that has been well documented since the 1950s (HMR35) (Myers, 1959). The concept is based on the idea that an observed storm could potentially occur over nearby watersheds when the meteorological forces and environment would be the same as the observed storm location. The period of record statistics at a specific discharge gage location may have a skewed or biased sample of data as compared to the surrounding watersheds, depending on what storms have hit that particular location. This hazard is especially true for short periods of observation. Since precipitation and discharge are correlated, though not perfectly, frequency statistical methods such as Bulletin 17C (B17C) are subject to misrepresenting the true flood risk at that gage location if the precipitation sample is not truly representative of the long-term precipitation patterns (England, 2018). In his landmark paper on storm transposition, Vance Myers of the U.S. Weather Bureau put it this way, "storm experience over a single basin alone is not a dependable indicator of what might occur over that basin in the future… Flood records are broken all the time, by wide margins" (Myers, 1966).

By shifting a storm from one watershed to a nearby watershed, a space for time substitution is made. Using more flood events from nearby watersheds allows for the extension of the effective record length (ERL) by assuming nearby storms could have occurred over the watershed of study (Hirsh, 1982). This application has been used in stochastic methods to estimate the flood risk at a specific location. That method is commonly referred to as stochastic storm transposition (SST). For this study, stochastic methods were not applied, only deterministic simulations were made. However, enough deterministic simulations were made to measure the variance or sensitivity of flood risk using a shifted storm. A fully stochastic analysis to measure the full uncertainty would be beneficial but was not within the scope of this study. More details on this storm shifting analysis are included in Appendix G: Storm Shifting Analyses.

11.2 SELECTED LOCATION OF INTEREST

The USGS Gage for the Colorado River at Austin was selected for this analysis. The Austin gage began recording in 1898 but was significantly impacted when Lake Travis was constructed and deliberate impoundment began in September of 1940. Lake Travis has a large flood storage capacity and effectively controls the releases from the 27,350 square miles of contributing drainage area upstream of the dam. Only 250 square miles of uncontrolled drainage area remain downstream of the dam and upstream of the gage at Austin. The highest estimated flow at this location was 550,000 cfs and occurred in 1869. Several other large floods occurred prior to the completion of the dam in 1935, 1936 and 1938. These floods resulted in peak flows at Austin of 481,000, 234,000 and 276,000 cfs, respectively. Since construction of the dam, the flood of record is only 47,600 cfs. This situation begs the question as to whether the 80 years of regulated gage record at Austin is subject to sample bias, which can skew the B17C results by having an annual maximum series that is too wet or too dry compared to the surrounding region.

In addition, the statistical results at this location are impacted by regulation. Releases from Lake Travis are typically regulated such that streamflow at the Colorado River at Austin gage does not exceed 30,000 cfs until the lake elevation exceeds a certain level (LCRA, 2022). Therefore, the computed flood flow frequency curve at the Colorado River at Austin gage may not be as reliable because of the stringent regulation from Lake Travis. This highlights the importance of utilizing all available evidence when estimating the 1% annual chance (100-yr) flood.

This chapter documents an analysis that transposed large observed storms and compute peak discharge at the Austin gage with the HEC-HMS model. This method would provide a verification of the 1% annual chance (100-yr) peak discharge estimate and a sensitivity test of the Bulletin 17C statistical analysis. Other methods used to compare against the flow frequency statistics included RiverWare period or record analysis and the HEC-HMS Frequency Storms. These analyses are detailed in other appendices of this report.

11.3 SELECTED STORMS

Observed storms with return periods between 50-yr to 500-yr are helpful in understanding how a watershed may respond to rainfall events that are larger than what has been experienced at that location, in this case since the impoundment of Lake Travis. Two nearby observed storms were selected for storm shifting as shown in Table 11.1. The return periods of these storms are estimated to be approximately 50-yr and 200-yr for the 2013 and 2015 events respectively, when compared to the NOAA Atlas 14 (NA14) rainfall depths. These events were two of the storms used to calibrate the HEC-HMS model; however, the majority of the precipitation fell outside of the drainage area between Lake Travis and the Austin Gage. Figures 11.1 and 11.2 illustrate the observed rainfall depths for these storms and their original location relative to the watershed between Lake Travis and the Colorado River at Austin gage. These figures show that each of these events narrowly missed the uncontrolled watershed above the Austin gage. In fact, these two storms resulted in the highest peak flows since 1921 on the nearby Onion Creek watershed in Austin, Texas.

Table 11.2: Selected Storms

Storm Event Date	Observed Maximum Rainfall Depth (inches)	Approximate Return Period of Storm
30 October – 01 November 2013	12.1	50-yr
30 October 2015	14.4	200-yr

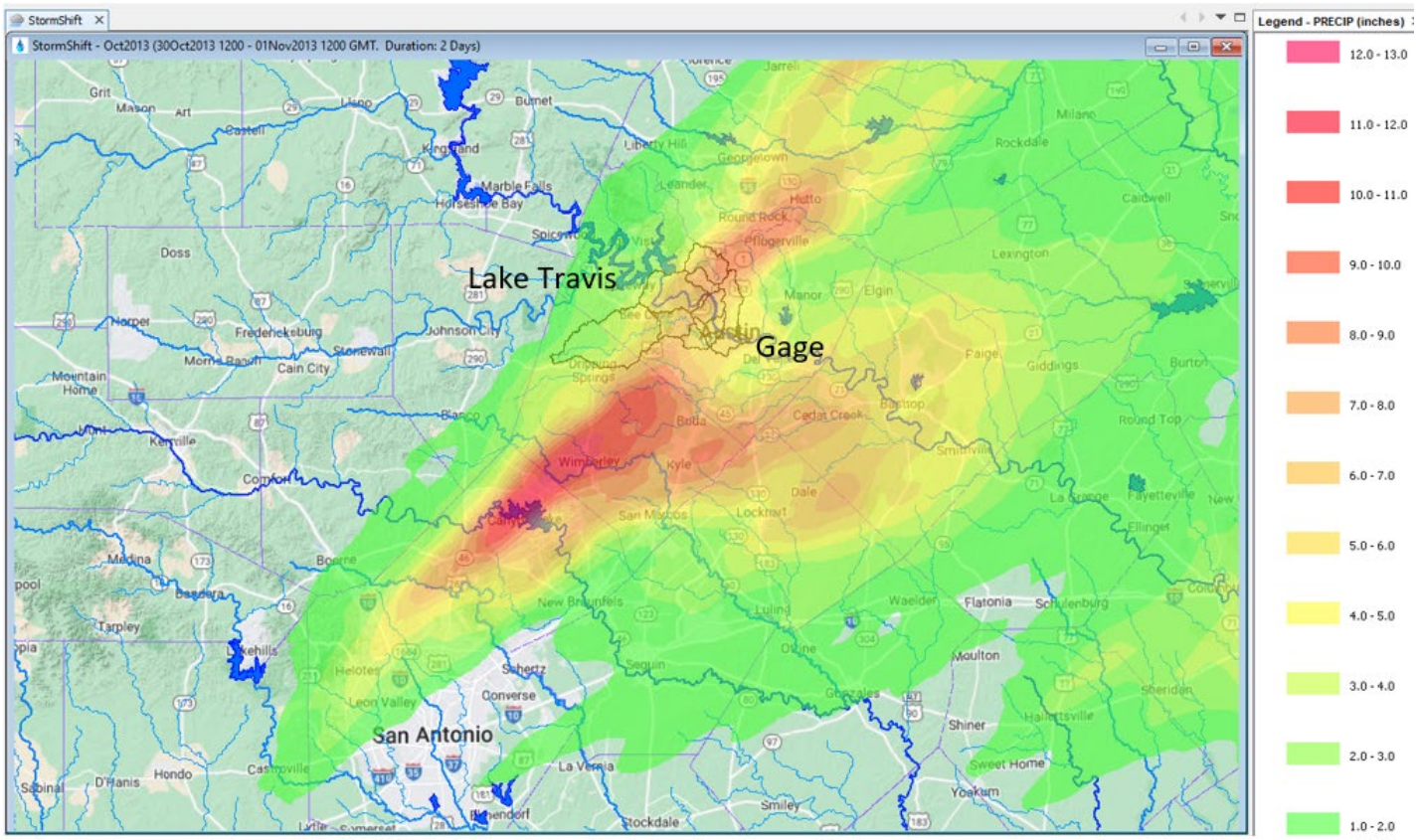

Figure 11.1: Observed Rainfall Depths for the October 2013 Storm Event

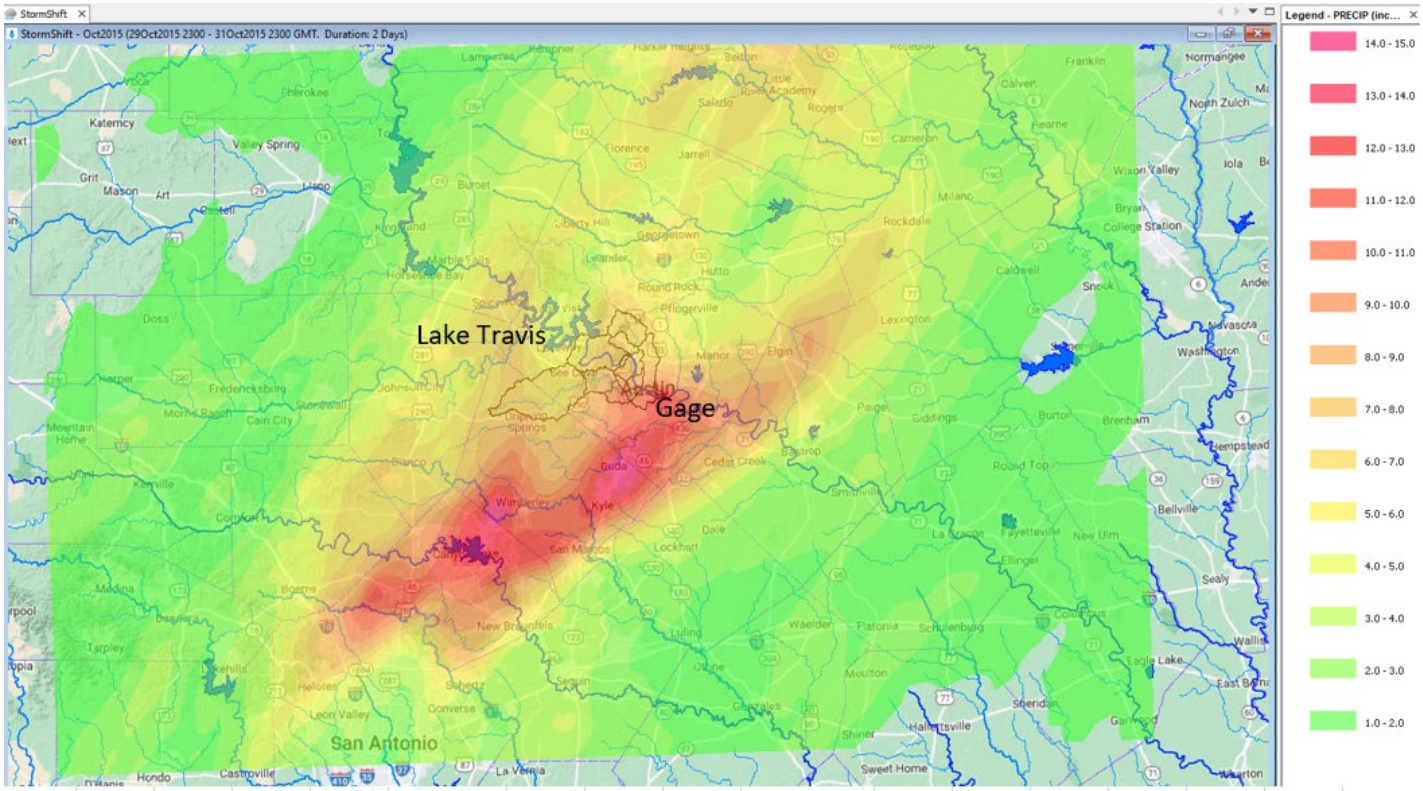

Figure 11.2: Observed Rainfall Depths for the October 2015 Storm Event

11.4 METHODS AND PROCEDURES

The locations of these two storms were optimized to produce the maximum peak discharge at the Colorado River at Austin gage using the final calibrated HEC-HMS model parameters from Appendix B. The observed storm grid locations were shifted using the optimization routine within HEC-HMS 4.11. The differential evolution method in HEC-HMS was used for the optimization. This method takes longer than the default simplex method but does a better job identifying the precipitation location producing the highest peak discharge. More details regarding the HEC-HMS optimization routines can be found in the HEC-HMS documentation on HEC's website (www.hec.usace.army.mil). More information on the storm shifting methods used in this analysis are also included in Appendix G: Storm Shifting Analyses.

Figures 11.3 and 11.4 illustrate the resulting transposed (shifted) storms. The green marker represents the original location of the observed storm, and the red marker represents the optimized location of the shifted storm. No rotation was performed on the observed storms in order to preserve their original meteorological orientation. The October 2013 storm was shifted 20 miles to the northeast, and the October 2015 storm was shifted 18 miles to the north to maximize the peak discharge at the Austin gage.

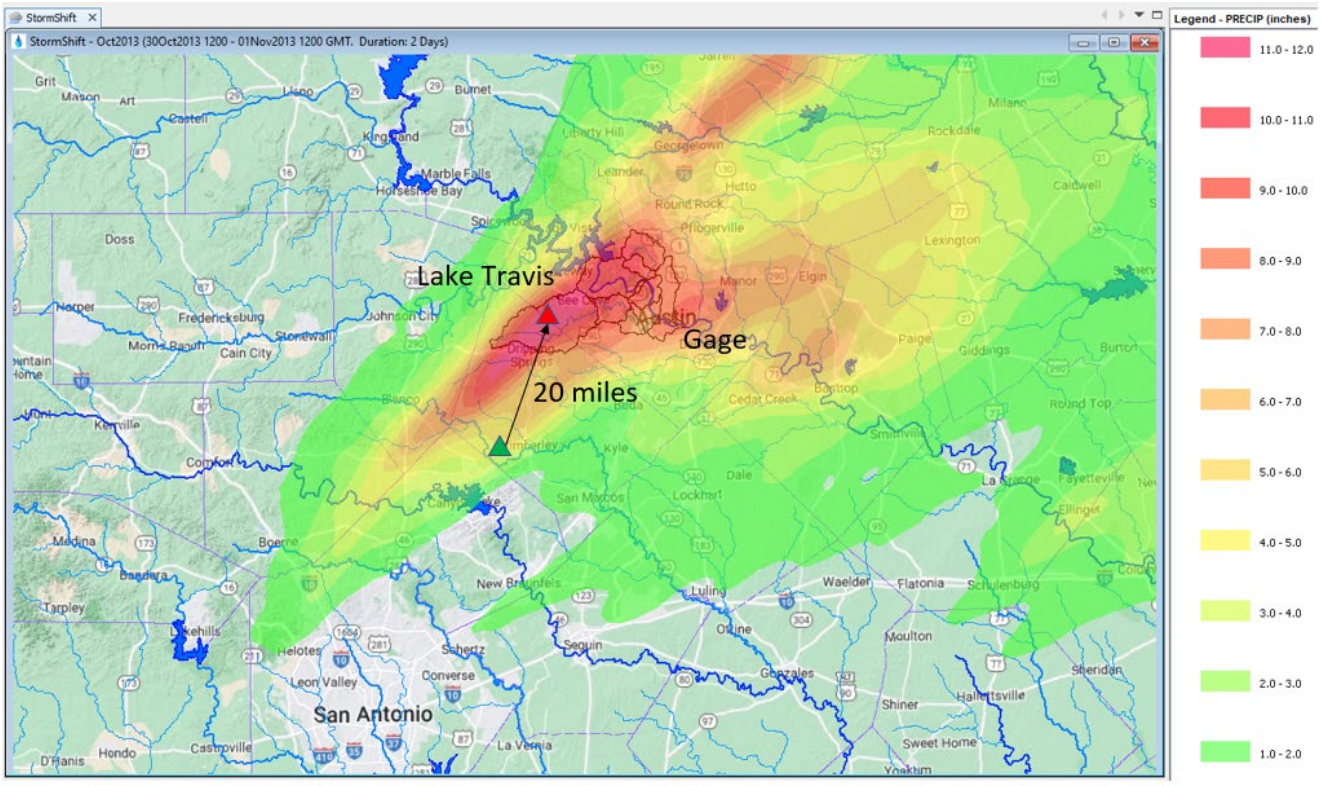

Figure 11.3: Shifted Location of the October 2013 Storm

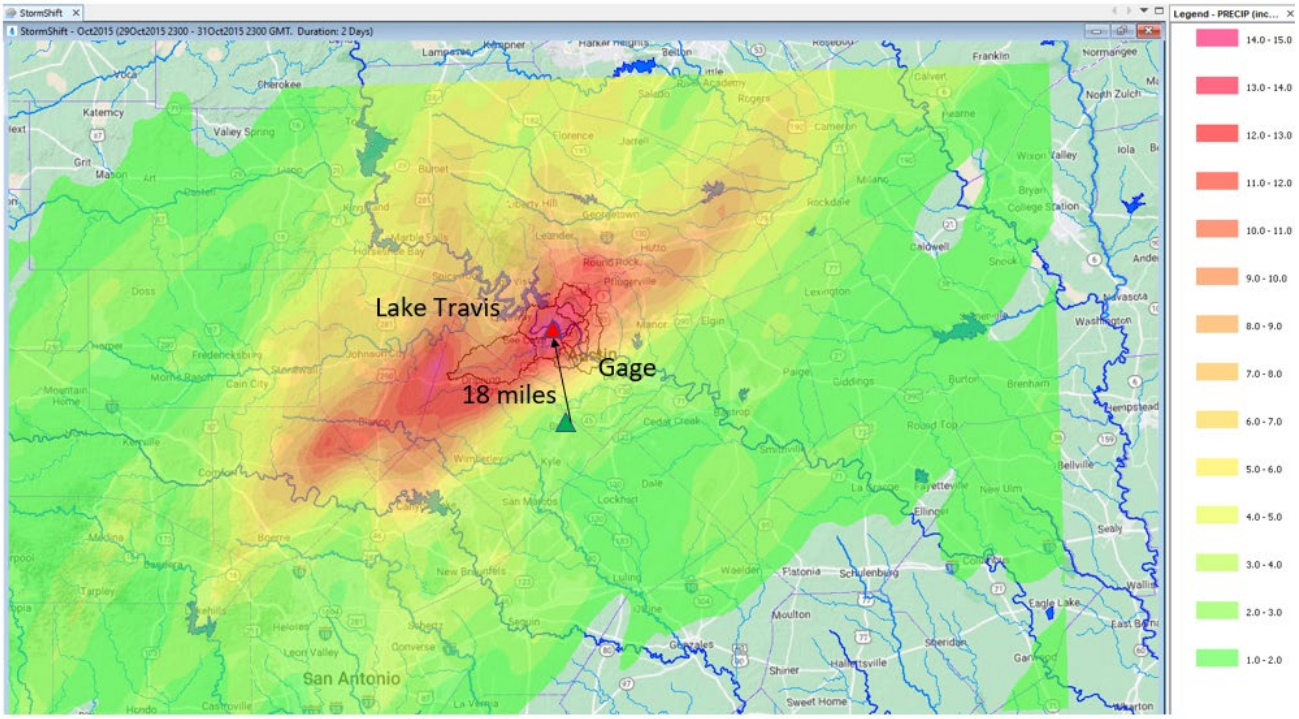

Figure 11.4: Shifted Location of the October 2015 Storm

One way to test the reasonableness of a storm shifting scenario is to compare the NA14 rainfall depths at the original storm location to the NA14 depths at the shifted storm location. This comparison showed that the NA14 100-yr, 24-hour rainfall depth changed very little from the observed 2013 storm location (13.1 inches) to the shifted 2013 storm location (12.8 inches). There is approximately a 2% reduction in precipitation volume estimates between the two locations supporting the assumption of homogeneity or similar probability of occurrence between the observed and shifted storm.

Similarly, for the October 2015 shifted storm, the 100-yr 24-hour volume changed very little from the observed 2015 storm location (13.1 inches) to the shifted 2015 storm location (12.7 inches). There is approximately a 3% reduction in precipitation volume estimates between the two locations supporting the assumption of homogeneity or similar probability of occurrence between the observed and shifted storm.

Tables 11.2 and 11.3 show precipitation characteristics of the shifted storm across different durations averaged over the 250 square mile drainage area above the Austin gage. Assigning a specific return period to the shifted storm is difficult since the storm characteristics differ by duration. After giving consideration to all durations, approximate return periods of 50-yr and 200-yr were estimated for the 2013 and 2015 events respectively.

Table 11.2: 2013 Shifted Storm Comparison of Area Averaged (250 sq mi) Precipitation Values

Rainfall Duration (hours)	Shifted Storm Totals (inches)	25-yr Totals (inches), NA14	50-yr Totals (inches), NA14	100-yr Totals (inches), NA14	200-yr Totals (inches), NA14	500-yr Totals (inches), NA14	Nearest Return Period
3	4.6	4.3	5.2	6.2	7.3	9.0	25-yr
12	9.7	6.7	8.2	9.8	11.8	14.8	100-yr
24	9.8	7.9	9.5	11.4	13.6	16.9	50-yr

Table 11.3: 2015 Shifted Storm Comparison of Area Averaged (250 sq mi) Precipitation Values

Rainfall Duration (hours)	Shifted Storm Totals (inches)	25-yr Totals (inches), NA14	50-yr Totals (inches), NA14	100-yr Totals (inches), NA14	200-yr Totals (inches), NA14	500-yr Totals (inches), NA14	Nearest Return Period
3	8.4	4.3	5.2	6.2	7.3	9.0	500-yr
12	10.4	6.7	8.2	9.8	11.8	14.8	100-yr
24	10.8	7.9	9.5	11.4	13.6	16.9	100-yr

The six hydrologic scenarios that were simulated in HEC-HMS are detailed in Table 11.4. The observed infiltration rates are the losses that result from the antecedent soil conditions before the storm occurred. The observed infiltration rates were developed by calibrating the HEC-HMS model using observed streamflow data and original (unshifted) precipitation. The losses were adjusted until the timing of initial runoff and total volume of the simulated hydrograph volume from the HEC-HMS model generally matched the initial runoff and total volume of the observed hydrograph at the USGS gage at Austin. More information on model calibration and specific loss rates can be found in the Appendix B. According to the US Drought Monitor, Travis County was experiencing abnormally dry conditions prior to the 2013 and 2015 storm events (NDMC, 2019), which resulted in less runoff than would have occurred under more normal conditions. Since antecedent conditions can vary significantly between storm events, the 2-yr and 100-yr infiltration rates were used in the HEC-HMS model to show a range of the effects of soil moisture conditions on the peak discharge. The 2-yr infiltration rates are higher than that of the 100-yr infiltration rates, and therefore the 2-yr infiltration rates would generate less runoff than the 100-yr infiltration rates.

Table 11.3: Hydrologic Simulation Key

Simulation Number	Storm	Infiltration Rates Used
1	2013	2-yr
2	2013	100-yr
3	2013	Observed
4	2015	2-yr
5	2015	100-yr
6	2015	Observed

11.5 RESULTS AND COMPARISONS

The resulting peak discharges from the hydrologic simulations using the shifted storms are listed in Table 11.5.

Table 11.4: Storm Shifting Results

Simulation Number	Storm	Approximate Rainfall Return Period	Infiltration Rates Used	Optimized Peak Discharge (cfs) at the Austin Gage
1	2013	50-yr	2-yr	88,000
2	2013	50-yr	100-yr	104,000
3	2013	50-yr	Observed	92,000
4	2015	200-yr	2-yr	135,000
5	2015	200-yr	100-yr	152,000
6	2015	200-yr	Observed	133,000

The 2-yr infiltration rates resulted in lower peak discharges than the 100-yr infiltration rates as expected. The two sets of optimized peak discharges were plotted with the other frequency analyses in Figure 11.5. The October 2013 simulations were used as an approximation to the 2% annual chance (50-yr) flood. October 2015 simulations were used as an approximation to the 0.5% annual chance (200-yr) flood. Each storm pairing had a low and high estimate using the 2-yr and 100-yr infiltration rates. One can see from this figure that the HEC-HMS Uniform Rainfall frequency storm at the Austin Gage produced results that are very similar to those that would result from shifting of the observed nearby storms of 2013 and 2015.

Figure 11.5 also shows that the HEC-HMS uniform rainfall and storm shifting results are higher than the statistical results. The HEC-HMS unform rain frequency storm method used NOAA Atlas 14 (NA14) rainfall depths to estimate the potential for flooding at the Austin gage. NA14 used over 2,000 rainfall gages, some having over 100 years of record individually. For each region, 15-25 gaging stations were included which provided anywhere from 700 to 1,800 data years. This indicates that NA14 is a more robust statistical analysis than the B17C analysis for the Austin gage on the Colorado River. Therefore, methods measuring flood risk based on NA14 are more stable and informative than B17C results in this unique case.

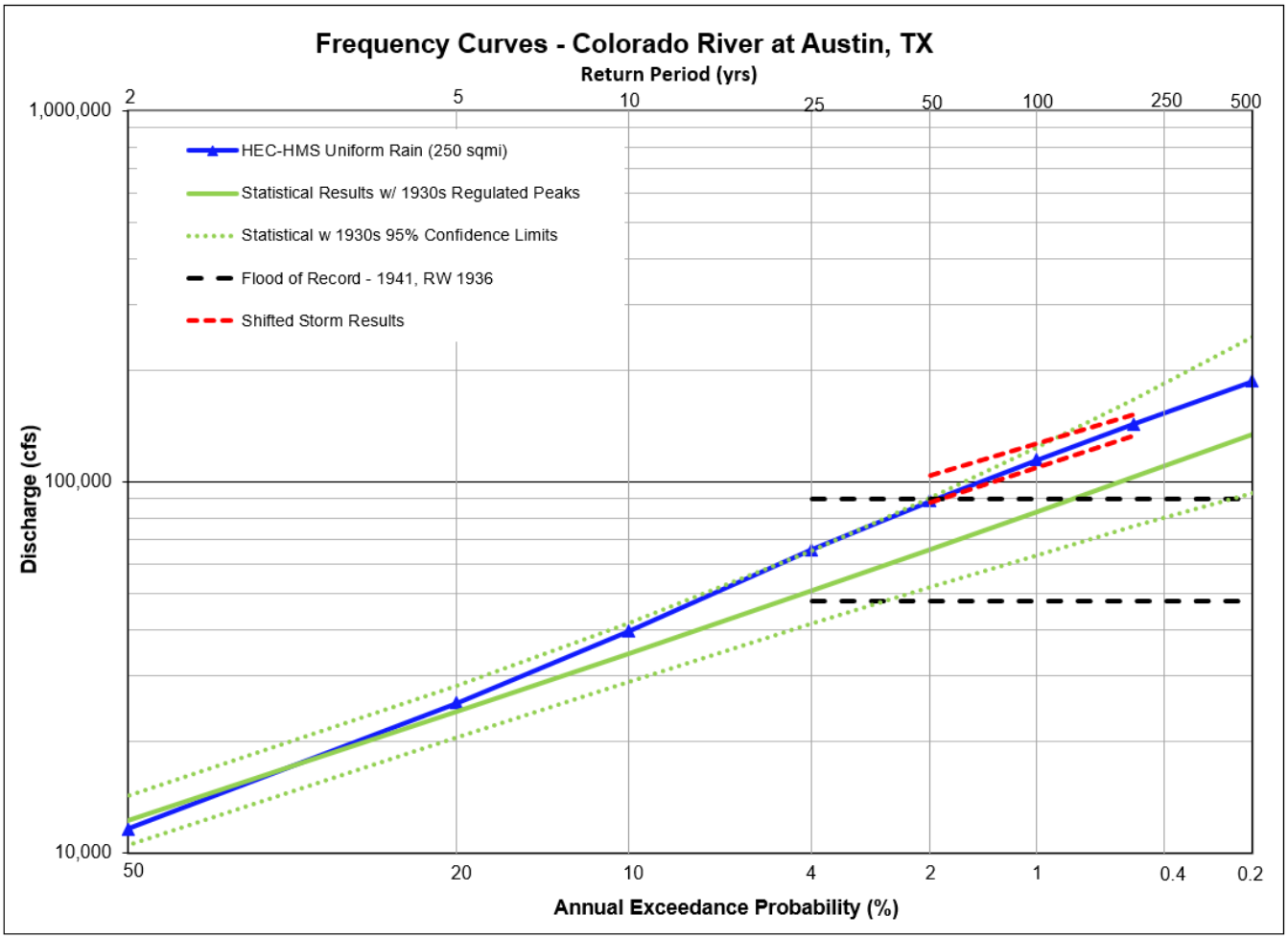

Figure 11.5: Storm Shifting Results at Colorado River at Austin Gage

The Variable Time Window tool in HEC-SSP 2.3 was also used to investigate how flood frequency estimates change over time and what the impact on the gage statistics would be if large nearby storms fell over the uncontrolled area above the Austin gage. At first glance, the B17C 1% annual chance (100-yr) flow estimate of the observed gage data in Figure 11.6 appears to be very stable since about 1980 with values slightly decreasing over time. To test the sensitivity of these results to large events, the water year (WY) 2014 and 2016 peak flow values were replaced with the results from the shifted October 2013 and October 2015 storms. Those results are shown in Figure 11.7. Although the period of record at the Austin gage is nearly 80 years, the two shifted storms caused the 1% annual chance (100-yr) flow estimate to increase by 65% and the 0.2% annual chance (500-yr) flow estimate to increase by over 100%. This highlights the sensitivity of the B17C results to storm positioning and available period of record, particularly for storm events rarer than the 2% annual chance (50-yr) flow. While B17C results may appear stable over time, Figure 11.7 illustrates how the inclusion of a large flood event can significantly increase the B17C results beyond previous estimates even with relatively long record lengths when compared with other gaged sites.

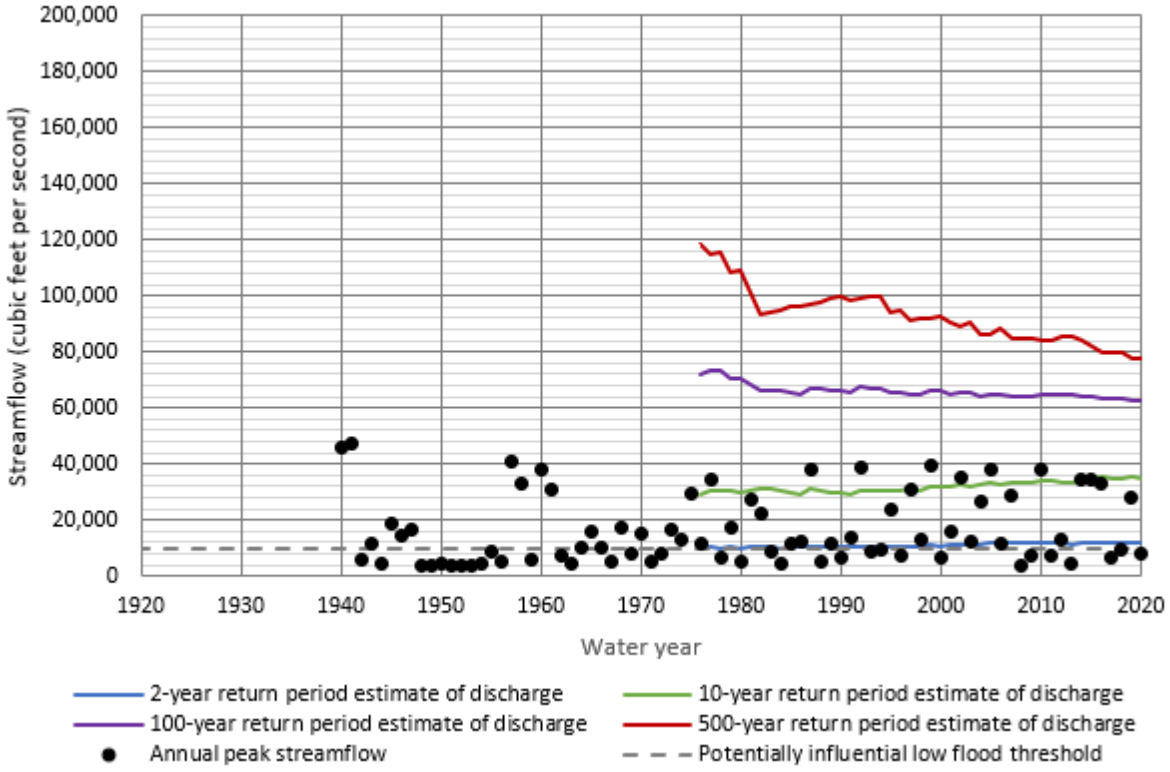

Figure 11.6: B17C Results Over Time without Shifted Storms

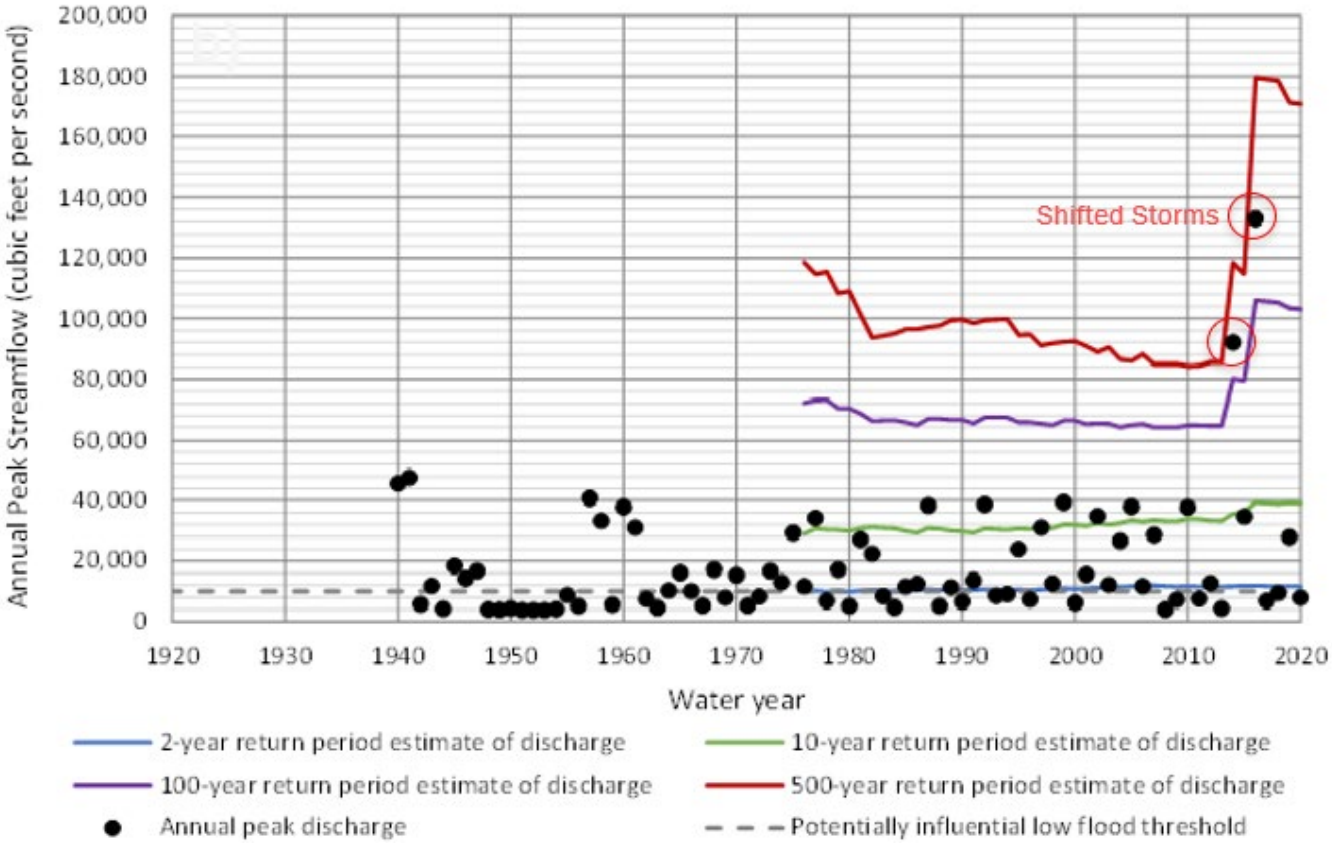

Figure 11.7: B17C Results Over Time with Shifted Storms

11.6 CONCLUSIONS

Overall, the storm shifting verified that the 250 square mile watershed below Lake Travis and above the Austin gage has flooding potential that is much higher than what has been observed since the impoundment of Lake Travis in 1940. Nearby storms that narrowly missed the watershed could have produced drastically different flood levels than those currently being estimated using the observed record alone. The HEC-HMS Uniform Rainfall results at the Austin Gage produce 1% annual chance (100-yr) results that are very similar to those that would result from shifting of the observed nearby storms of 2013 and 2015. The B17C results are lower than the HEC-HMS uniform rainfall results, however, the reliability and stability of the B17C 1% annual chance (100-yr) estimate is impacted by the short record length of the gage in addition to the strict regulation from Lake Travis. Generally, at least 300-400 years of record are needed before the 1% annual chance (100-yr) flow frequency estimates will stop significantly changing over time with additional years of record, unless additional information such as rainfall-runoff modeling estimates are utilized in the statistical analysis.

12 Comparison of Frequency Flow Estimates

As each of the hydrologic analyses was completed, their results were compared to one another in terms of frequency peak discharge estimates at the USGS stream gage locations. These comparisons of frequency flow estimates were made in table format as well as graphs of peak discharge versus probability and frequency discharge estimates versus time. The estimated frequency curves from each method were plotted along with their associated confidence limits and the previous published discharges from the effective FEMA Flood Insurance Studies (FIS), the Base Level Engineering (BLE) data, and the 2002 FDEP study for the Lower Colorado River basin.

Wherever there were significant differences in the resulting flood magnitudes, the InFRM team made an effort to investigate and understand the reasons for those differences to the extent practicable. The investigation process often uncovered one or more adjustments that should be made to the assumptions in a particular method that improved the results. These adjustments may or may not have led to better agreement in the results, but at the very least, the strengths and weaknesses of each method at a particular location were more fully understood through the process of investigation. The additional investigations also included the historic 1930s storms analyses described in chapter 10 and the storm shifting analyses described in chapter 11.

The results of all of these analyses are compared in the following sections, and the relative strengths and weaknesses of the various methods for each location are discussed in the text. The first section compares results in terms of peak frequency flows on the rivers, and the second section compares results at the reservoirs in terms of peak pool elevations.

12.1 FREQUENCY FLOW COMPARISONS

The final comparisons of the frequency flow estimates are given in the tables in this section of the report. Blank cells indicate data was not available at that specific location. The figures in this section of the report include plots of the estimated frequency curves at each gage along with their associated confidence limits and the previous published discharges from the BLE data the effective FEMA Flood Insurance Studies (FIS), and the 2002 FDEP study. Where available, statistical change over time comparison plots are also included in the figures of this section. Additional discussion of the results is included with the figures for each location.

Confidence Limits are shown on the flood frequency curve comparison plots for both the statistical analyses and the HEC-HMS model results. These confidence limits help illustrate the possible range of uncertainty associated with the computed frequency flow estimates as there is a 90% chance that the actual flood frequency discharge value is located somewhere in between those limits. The confidence limits for the statistical analyses were calculated in HEC-SSP or PeakFQ based on Bulletin 17C procedures. The confidence limits for the HEC-HMS frequency storms were calculated based on the lower and upper bounds of the 90% confidence interval for the NOAA Atlas 14 rainfall depths.

However, there are inherent assumptions within the statistical analyses that when violated can cause the confidence limits to underestimate the uncertainty. For example, a Bulletin 17C analysis assumes that the annual peak streamflow data contains a representative sample that is homogeneous and stationary. However, Section 5.2 of this report detected declining flow trends in the upper portions of the study area, which is a form of non-stationarity. In some cases, these declining flow trends may cause the entire range of the 90% confidence limits to shift over time (as will be shown in some of the figures of this section). Climate change is another possible source of non-stationarity which could cause the confidence limits to be underestimated.

12.1.1 Colorado River Gage Locations

Table 12.1: Frequency Flow (cfs) Results Comparison for the Colorado River at Robert Lee, TX

Annual Exceedance Probability (AEP)	Return Period (years)	Currently Effective FEMA FIS	Approximate BLE Data from FEMA	Statistical Analysis of the Gage Record (Ch 5) (52 years)	HEC-HMS Uniform Rain Frequency Storm (Ch 6) (31 sq mi)	Statistical Analysis of the Extended RiverWare Record (Ch 8) (89 years)	Reservoir Analysis of EV Spence Reservoir (Ch 9)
0.002	500			39,200	22,400	146,000	25,000
0.005	200			24,200	18,500	91,800	23,000
0.01	100			16,100	15,700	60,500	22,000
0.02	50			10,300	12,600	36,800	20,000
0.04	25			6,260	7,460	20,100	11,000
0.1	10			2,840	3,210	7,070	7,500
0.2	5			1,340	1,360	2,320	2,000
0.5	2			304	310	190	2,000

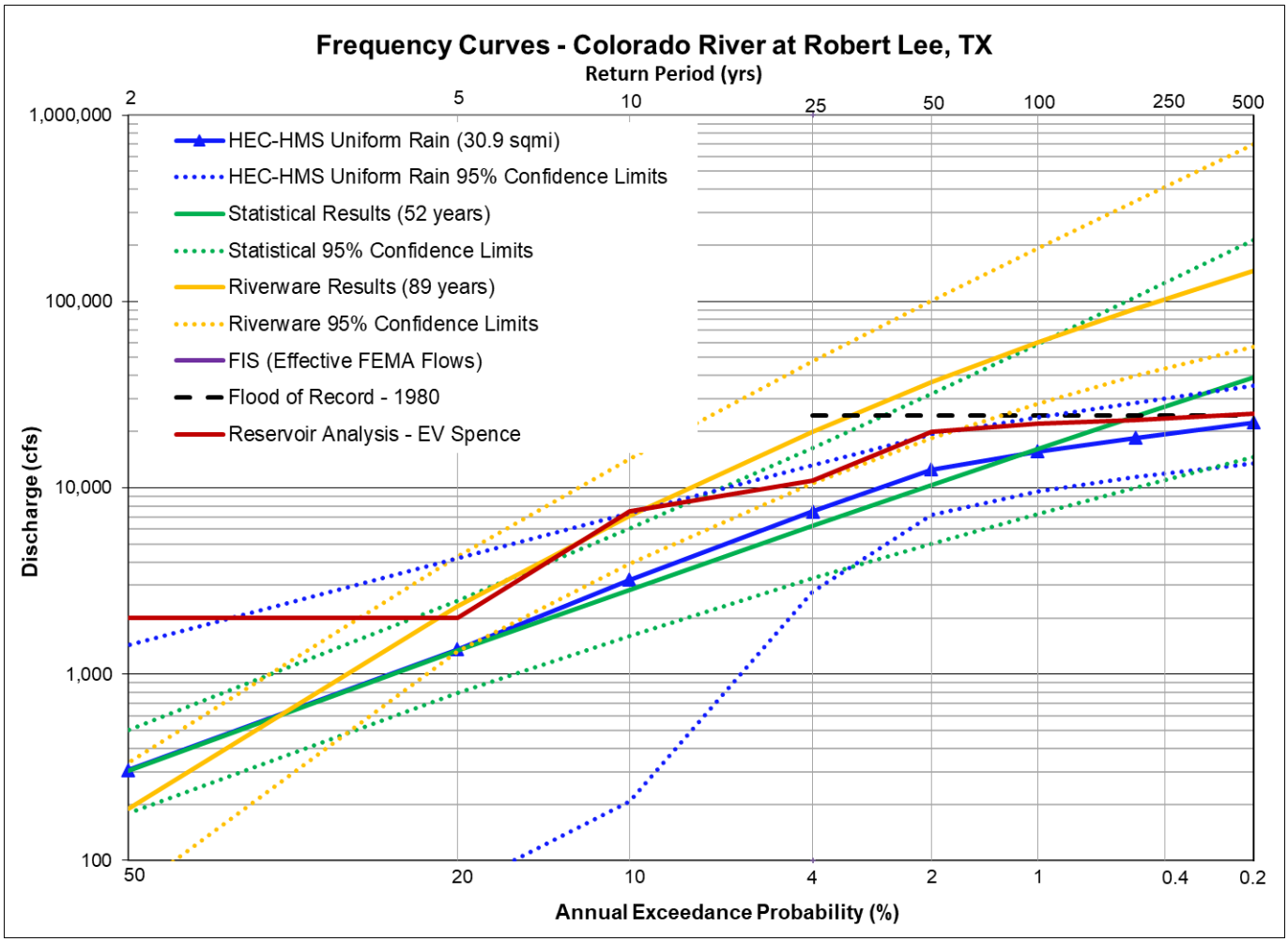

Figure 12.1: Flow Frequency Curve Comparison for the Colorado River at Robert Lee, TX

The most upstream point of comparison on the Colorado River is the USGS gage for the Colorado River at Robert Lee, Texas, as shown in Table 12.1 and Figure 12.1 above. This gage is located a short distance downstream from E.V. Spence Reservoir near the upstream limits of our study area. It has a total contributing drainage area of over 5,000 square miles, but only 31 square miles of that is below E.V. Spence Reservoir.

There are no published frequency flows from FEMA for this location. One can see in the figure that the HEC-HMS rainfall runoff 1% AEP (100yr) results from the 31 square miles of uncontrolled drainage area downstream of the reservoir were very close to the current Bulletin 17C statistical results from 52 years of gage record. However, the RiverWare results, which included a simulated period of record back to 1930, were significantly higher. Results from the reservoir analysis of EV Spence reservoir using the stochastic methods in RMC-RFA were also higher than the HEC-HMS results. This means that releases from the reservoir may have a higher potential to cause flooding than the downstream drainage area, at least at this nearby location.

Table 12.2: Frequency Flow (cfs) Results Comparison for the Colorado River near Ballinger, TX

Annual Exceedance Probability (AEP)	Return Period (years)	Currently Effective FEMA FIS	Approximate BLE Data from FEMA	Statistical Analysis of the Gage Record (Ch 5) (52 years)	HEC-HMS Uniform Rain Frequency Storm (Ch 6) (1080 sq mi)	HEC-HMS Elliptical Frequency Storm (Ch 7) (1080 sq mi)	Statistical Analysis of the Extended RiverWare Record (Ch 8) (89 years)	Statistical Analysis with Historic 1930s Storms (Ch 10)
0.002	500			36,400	190,900	163,100	77,000	87,100
0.005	200			29,100	146,100	123,200	66,000	58,600
0.01	100	50,120		24,000	113,100	95,000	57,200	42,400
0.02	50			19,200	81,000	67,400	47,900	29,900
0.04	25			14,900	40,600	34,300	38,500	20,400
0.1	10			9,730	16,700	13,700	25,900	11,500
0.2	5			6,370	7,690	7,500	16,800	6,780
0.5	2			2,620	2,700	2,590	6,030	2,570

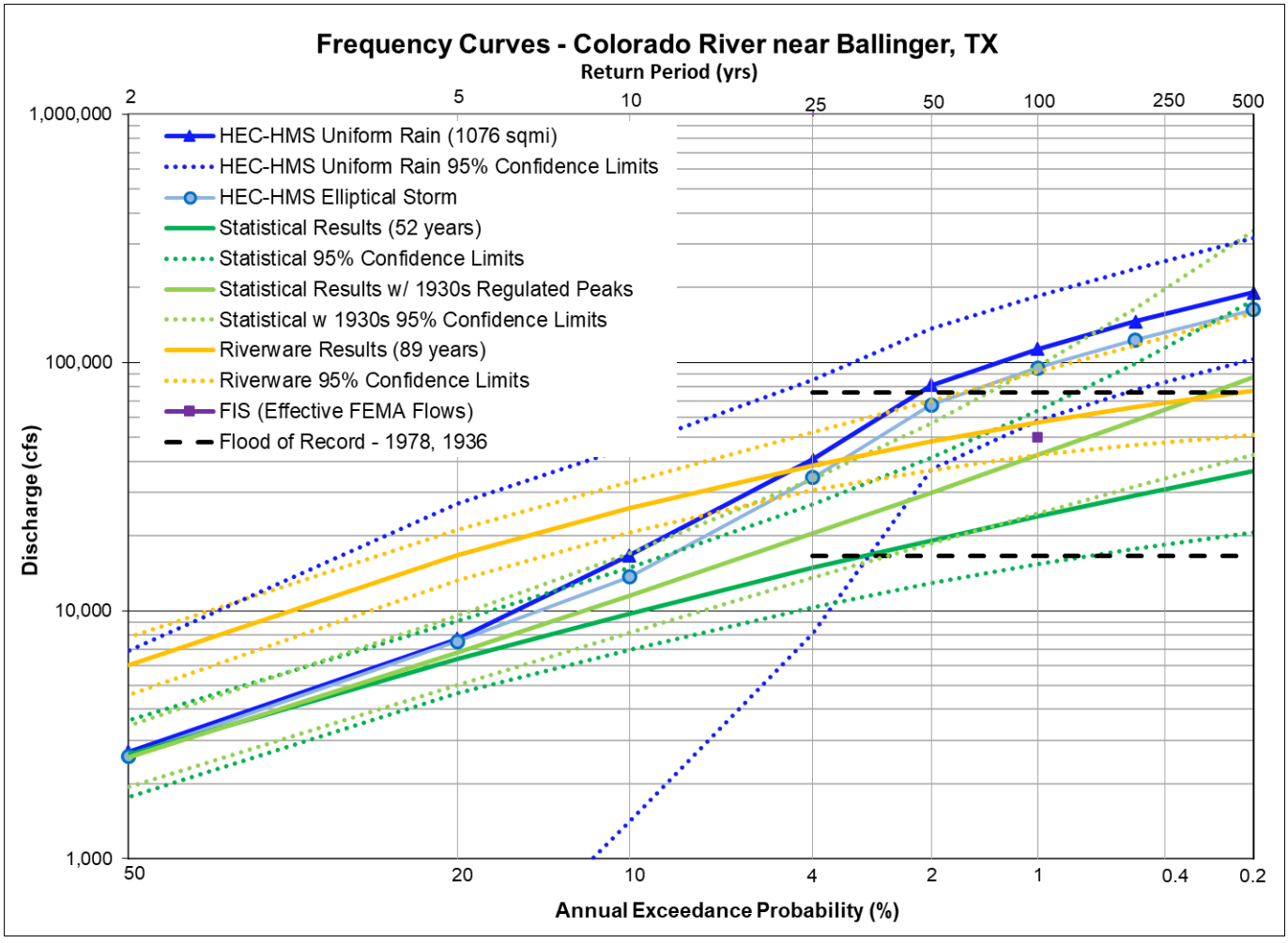

Figure 12.2a: Flow Frequency Curve Comparison for the Colorado River near Ballinger, TX

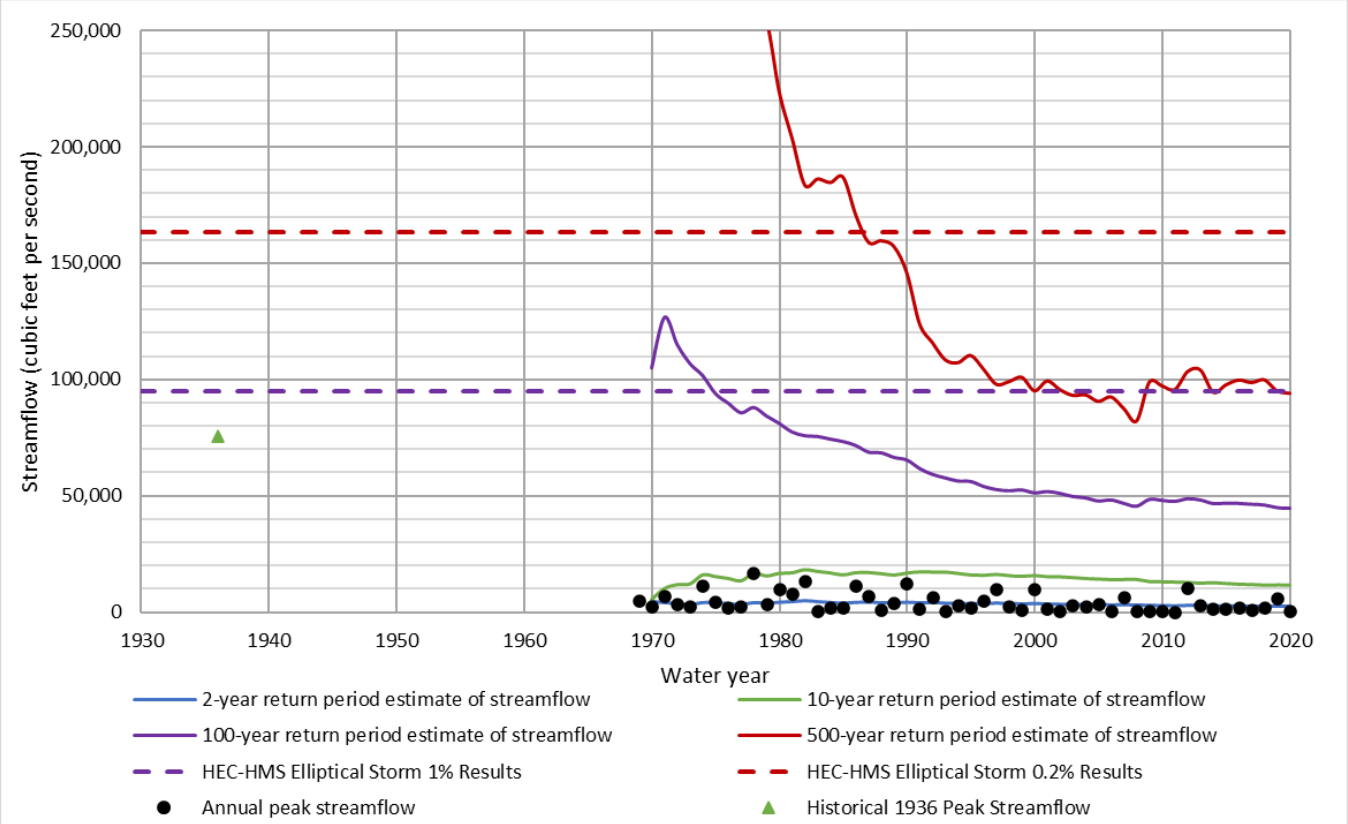

Figure 12.2b: Statistical Change Over Time Comparison for the Colorado River near Ballinger, TX

The next point of comparison on the Colorado River is the Colorado River near Ballinger, TX, as shown in the preceding table and figures. This gage has a total contributing drainage area of over 6,000 square miles, but only 1,000 square miles of that is below E.V. Spence Reservoir.

The effective FEMA 1% AEP (100-year) flow at this location is just over 50,000 cfs from the 1990 Flood Insurance Study (FIS) for the City of Ballinger. This flow was calculated using an uncalibrated 1988 rainfall runoff model. Figure 12.2a shows that the HEC-HMS 1% AEP (100-year) results from the one thousand square miles of uncontrolled drainage area were almost four times higher than the statistical results of the past 52 years of gage record. This is because there have been no large floods of over 17,000 cfs in the last 50 years, which is approximately a 10-year flood event according to Figure 12.2b. Since no large floods have been recorded at this location in the past 50 years, the current statistical results are likely underestimating the 1% AEP (100-year) flood potential.

Table 12.3: Frequency Flow (cfs) Results Comparison for the Colorado River near Stacy, TX

Annual Exceedance Probability (AEP)	Return Period (years)	Currently Effective FEMA FIS	Approx BLE Data from FEMA	Statistical Analysis of the Gage Record (Ch 5) (31 years)	HEC-HMS Uniform Rain Frequency Storm (Ch 6) (8420 sq mi)	HEC-HMS Elliptical Frequency Storm (Ch 7) (8420 sq mi)	Statistical Analysis of the Extended RiverWare Record (Ch 8) (89 years)	Reservoir Analysis of OH Ivie Lake (Ch 9)	Statistical Analysis with Historic 1930s Storms (Ch 10)
0.002	500			71,500	365,700	188,400	106,000	94,945	360,200
0.005	200			44,800	237,500	154,600	85,800	81,525	170,400
0.01	100			30,300	190,000	125,800	70,200	67,350	93,100
0.02	50			19,600	152,600	80,100	54,900	52,500	48,800
0.04	25			12,000	78,900	29,000	40,200	32,700	24,200
0.1	10			5,540	16,700	6,700	22,800	1,500	8,480
0.2	5			2,630	4,420	2,590	12,100	1,500	3,300
0.5	2			604	530	530	2,690	1,500	600

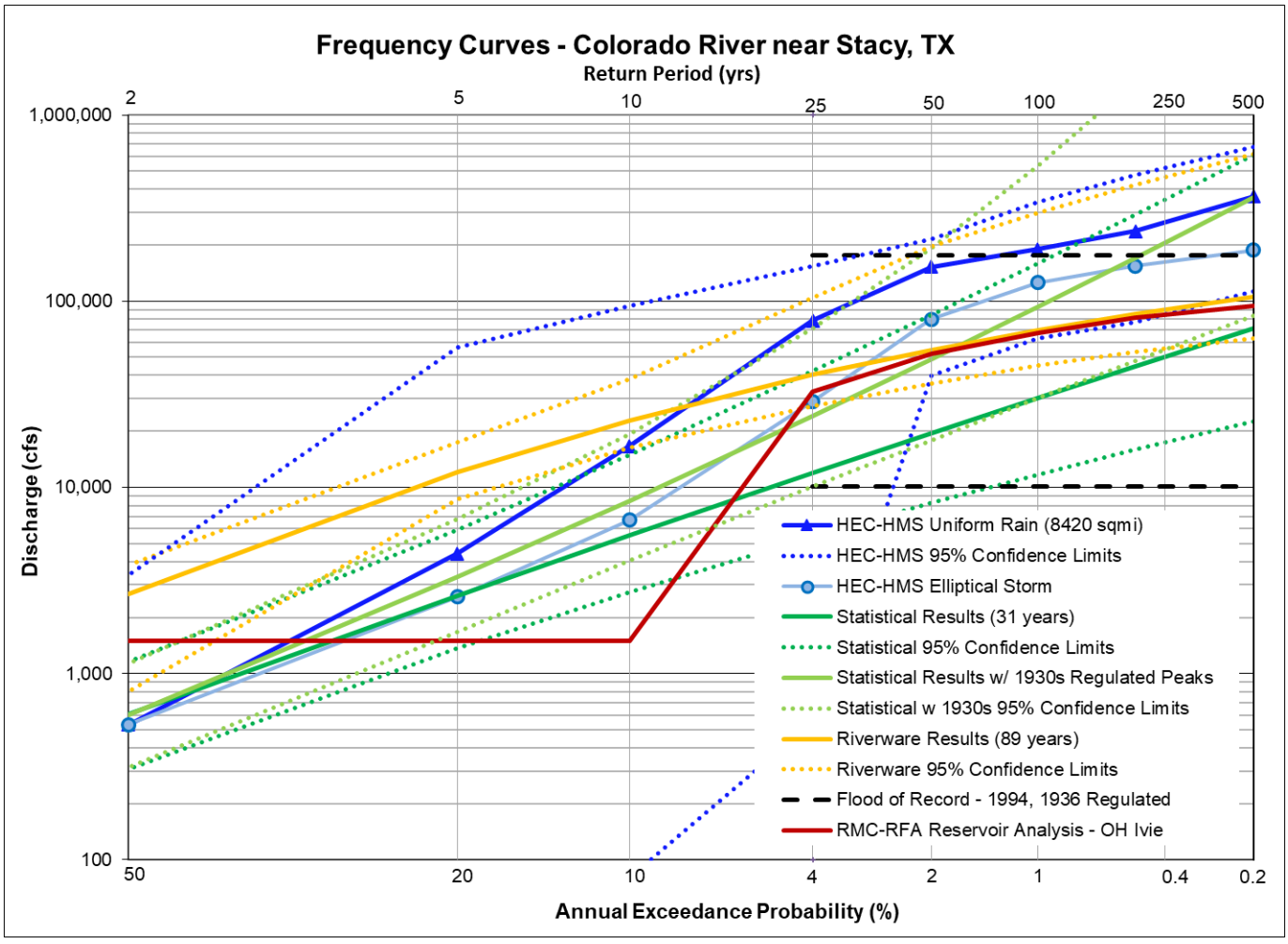

Figure 12.3a: Flow Frequency Curve Comparison for the Colorado River near Stacy, TX

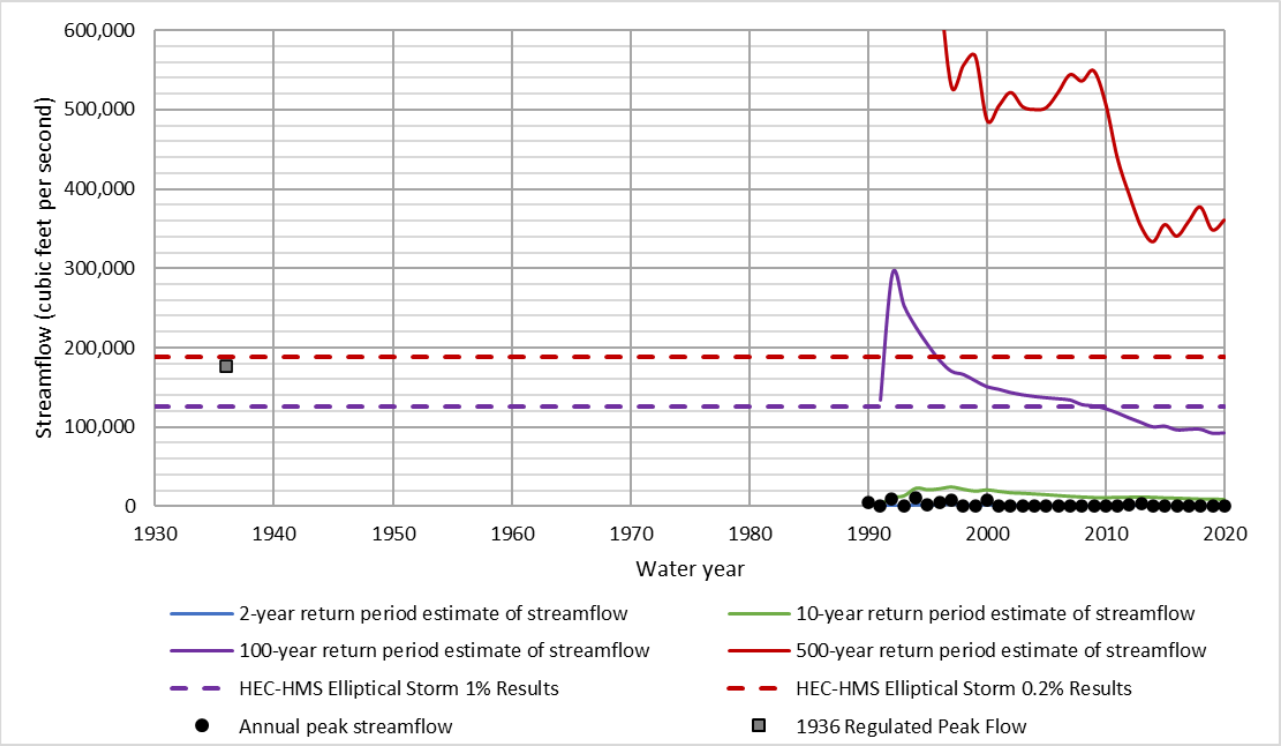

Figure 12.3b: Statistical Change Over Time Comparison for the Colorado River near Stacy, TX

The next point of comparison is the Colorado River near Stacy, TX, as shown in the preceding table and figures. This gage has a total contributing drainage area of over 12,800 square miles that includes the entire Concho River basin. However, flows at this location are regulated to a large degree by O.H. Ivie Reservoir, and only 140 square miles of uncontrolled drainage area exist between the reservoir and the gage.

There are no published FEMA flows for this location. Figure 12.3a shows that the HEC-HMS 1% AEP (100-year) elliptical storm results were almost four times higher than the statistical results of the past 31 years of gage record. This is because there have been no large floods larger than a 10-year event in the last 31 years, as shown by the green line in Figure 12.3b. However, the HEC-HMS elliptical storm 1% AEP (100-year) results are only slightly higher than the statistical results when the 1930s regulated peak flows are added to the record. The inclusion of that one regulated peak in the 1930s increased the Bulletin 17C 1% AEP (100-year) statistical estimate by more than 200%, as shown in Figure 12.3a. However, due to the relatively short record at this location, there is still a great deal of uncertainty in the statistical results.

Table 12.4: Frequency Flow (cfs) Results Comparison for the Colorado River at Winchell, TX

Annual Exceedance Probability (AEP)	Return Period (years)	Currently Effective FEMA FIS	Approx BLE Data from FEMA	Statistical Analysis of the Gage Record (Ch 5) (58 years)	HEC-HMS Uniform Rain Frequency Storm (Ch 6) (9420 sq mi)	HEC-HMS Elliptical Frequency Storm (Ch 7) (9420 sq mi)	Statistical Analysis of the Extended RiverWare Record (Ch 8) (89 years)	Statistical Analysis with Historic 1930s Storms (Ch 10)
0.002	500			61,300	350,200	249,600	106,000	204,030
0.005	200			51,300	241,100	183,200	80,900	126,334
0.01	100			44,200	187,500	140,000	64,700	87,777
0.02	50			37,500	145,900	98,100	50,900	60,882
0.04	25			31,300	70,900	56,600	39,100	42,132
0.1	10			23,500	33,900	27,300	26,300	25,764
0.2	5			17,900	20,700	18,600	18,400	17,648
0.5	2			10,600	10,200	9,400	9,470	10,513

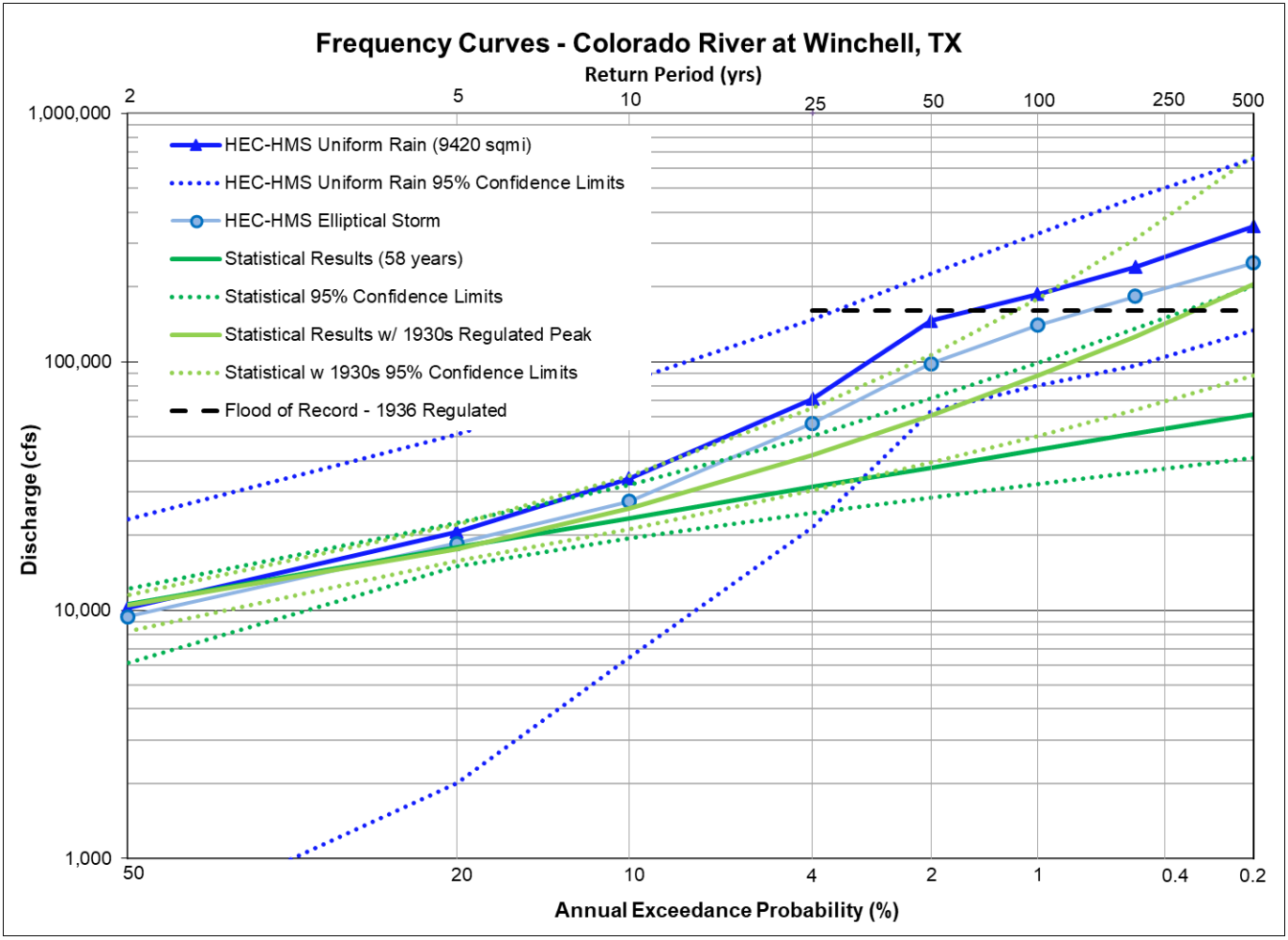

Figure 12.4a: Flow Frequency Curve Comparison for the Colorado River at Winchell, TX

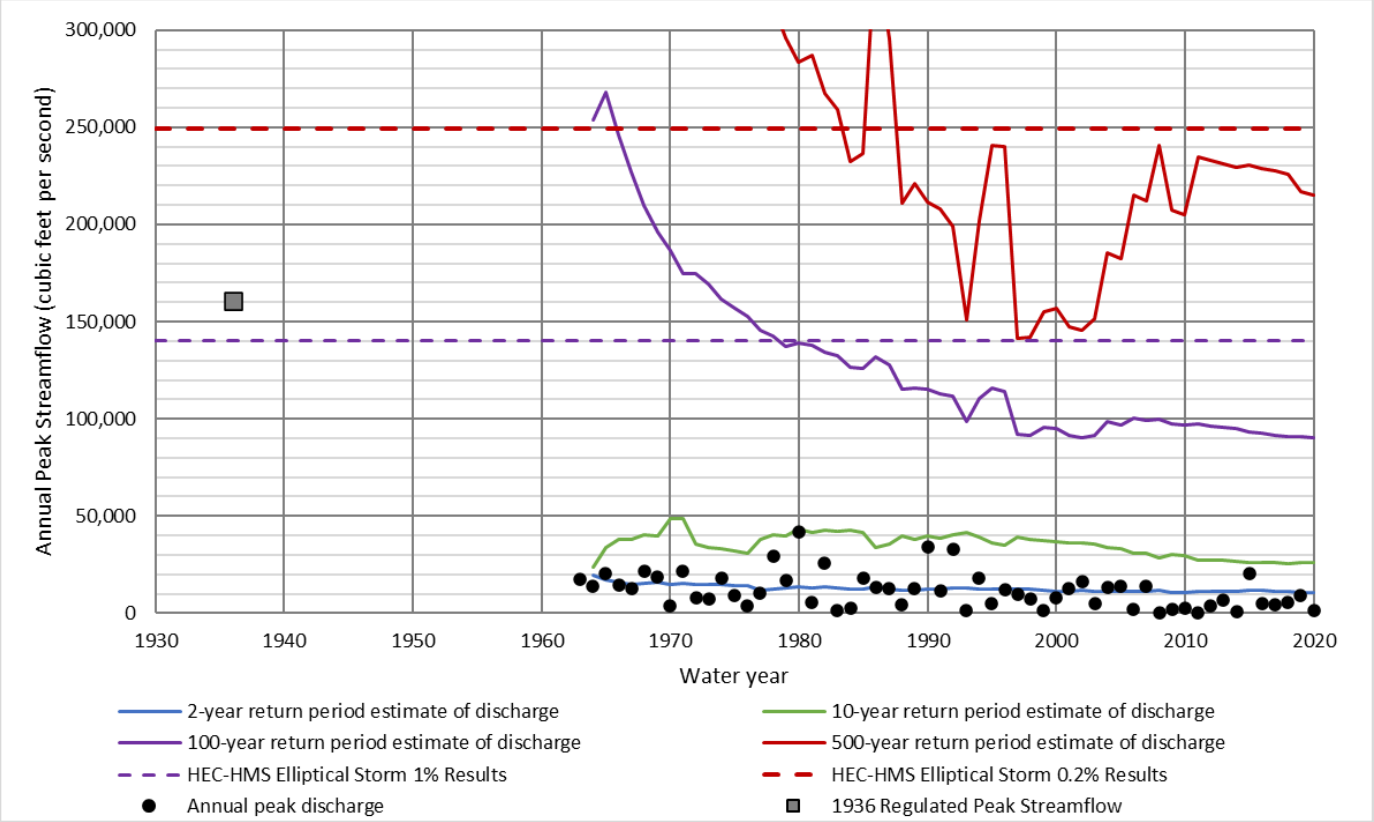

Figure 12.4b: Statistical Change Over Time Comparison for the Colorado River at Winchell, TX

The next point of comparison is the Colorado River at Winchell, TX, as shown in the preceding table and figures. This gage has a total contributing drainage area of over 13,700 square miles, but only 1,100 square miles of uncontrolled drainage area exist between O.H Ivie reservoir and the gage.

There are no published FEMA flows for this location. Figure 12.4a shows that the statistical estimate of the 1% AEP (100-year) peak flow doubled once the 1936 regulated peak was added to the record. Figure 12.4b shows that no large floods greater than a 10-year event have occurred in the past 50+ years (reference the green line in the plot above versus the annual peak discharges). This means that the current statistical results, with or without the 1936 peak, may be underestimating the 1% AEP (100-year) flood potential at this location. The HEC-HMS 1% AEP (100-year) elliptical storm results are significantly higher than the current statistical estimates, but Figure 12.4b shows that they are within the range of the variation in the statistical estimates that have occurred over the past 50 years.

Table 12.5: Frequency Flow (cfs) Results Comparison for the Colorado River near San Saba, TX

Annual Exceedance Probability (AEP)	Return Period (years)	Currently Effective FEMA FIS	2002 FDEP Study Elliptical Storm	Statistical Analysis of the Gage Record (Ch 5) (58 years)	Alternate Statistical Analysis of the Gage Record (Ch 5) (104 yrs)	HEC-HMS Uniform Rain Frequency Storm (Ch 6) (15,460 sq mi)	HEC-HMS Elliptical Frequency Storm (Ch 7) (15,460 sq mi)	Statistical Analysis of the Extended RiverWare Record (Ch 8) (89 years)
0.002	500		530,000	105,000	242,000	710,900	413,400	268,000
0.005	200		-	91,300	192,000	528,100	299,100	196,000
0.01	100		237,100	80,900	158,000	405,200	223,600	152,000
0.02	50		170,000	70,200	128,000	294,600	144,200	115,000
0.04	25		123,000	59,100	100,000	152,800	87,000	84,700
0.1	10		66,000	44,000	68,200	75,300	43,400	53,200
0.2	5		37,600	32,300	47,200	40,100	25,600	34,700
0.5	2		20,100	16,200	22,700	16,500	12,000	15,700

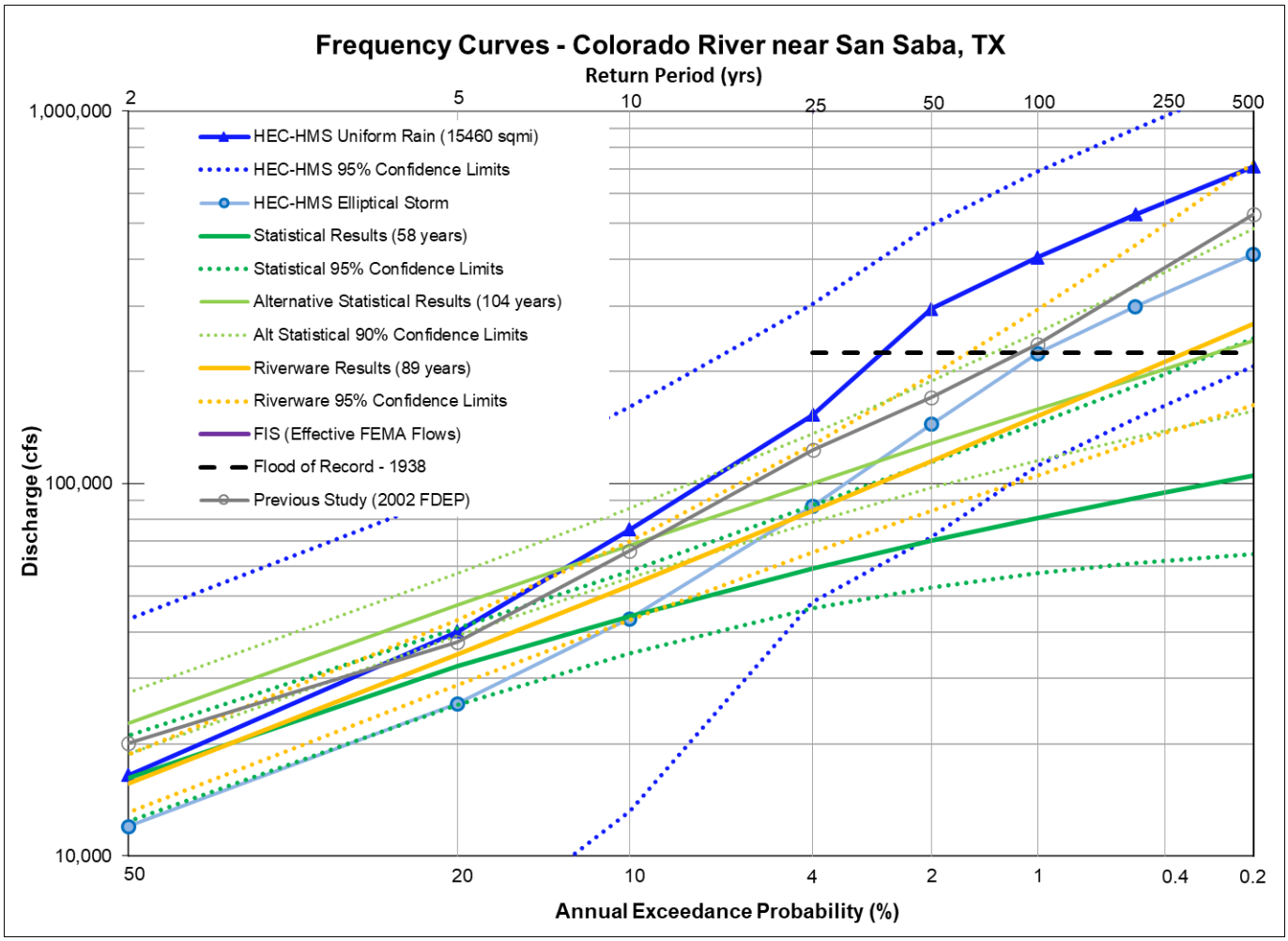

Figure 12.5a: Flow Frequency Curve Comparison for the Colorado River near San Saba, TX

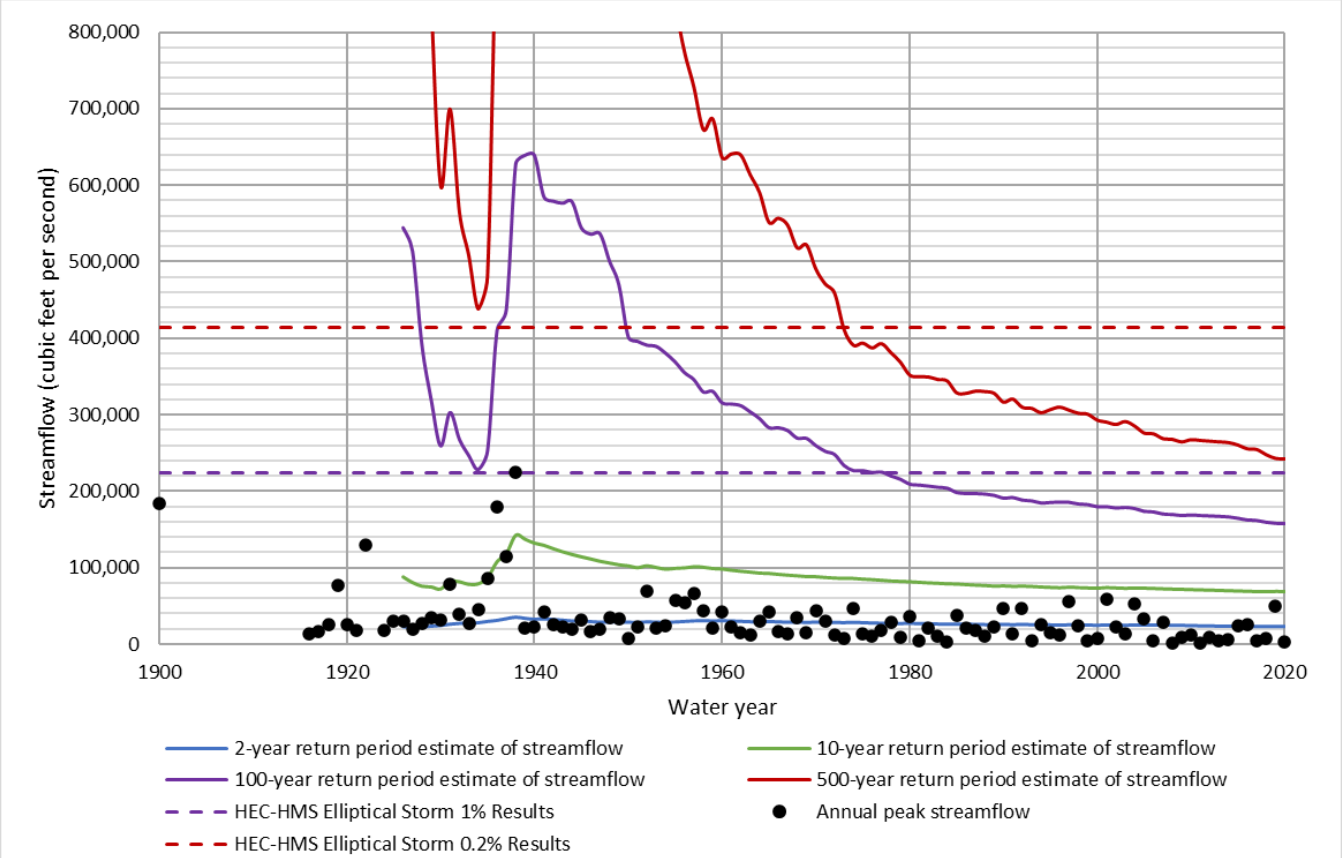

Figure 12.5b: Statistical Change Over Time Comparison for the Colorado River near San Saba, TX

The next point of comparison is the Colorado River near San Saba, TX, as shown in the preceding table and figures. This gage has a total contributing drainage area of almost 20,000 square miles that includes the entire watersheds for Pecan Bayou and the San Saba River. There are no published FEMA flows for this location, but there are published frequency flows from the 2002 Flood Damage Evaluation Project (FDEP) of the Lower Colorado Basin. The HEC-HMS 1% AEP (100-year) elliptical storm results are within 2% of the results from the previous 2002 FDEP study, which is encouraging since of these studies used elliptical design storms to estimate the frequency flows on the Colorado River.

Figure 12.5a shows that the HEC-HMS 1% AEP (100-year) elliptical storm results are significantly higher than the current statistical and RiverWare estimates. However, Figure 12.5b shows that no large floods greater than a 10-year event have occurred in the past 80 years at this location. This means that the current statistical results may be underestimating the 1% AEP (100-year) flood potential at this location. Figure 12.5b shows that the HEC-HMS results are well within the range of the variation in the statistical estimates that have occurred over the past 100 years, and the HEC-HMS 1% AEP results are almost identical to the 1938 observed flood of record.

Two different Bulletin 17C statistical analyses are included on Figure 12.5a. One includes the entire 100+ years of record (light green line), and the other includes just the most recent 58 years of record (dark green line). Not only have the magnitudes of most flood frequency estimates been cut in half between these two different periods of record, but the entire range of the 90% confidence limits have shifted downwards to such a degree that the "old" 1% AEP (100-year) estimate is no longer within the confidence bounds of the "newer" flood frequency estimate. The declining streamflow trends in this portion of the basin are a primary cause of these downward shifts in results, but this is also a good illustration of how sensitive the Bulletin 17C flood frequency estimates and their confidence bounds can be to the sample of floods that have occurred within the gage record.

Table 12.6: Frequency Flow (cfs) Results Comparison for the Colorado River below Lake Buchanan

Annual Exceedance Probability (AEP)	Return Period (years)	Currently Effective FEMA FIS	2002 FDEP Study Elliptical Storm	Statistical Analysis of the Gage Record (Ch 5) (N/A)	HEC-HMS Uniform Rain Frequency Storm (Ch 6) (16,150 sq mi)	HEC-HMS Elliptical Frequency Storm (Ch 7) (16,150 sq mi)	Statistical Analysis of the Extended RiverWare Record (Ch 8) (89 years)	Reservoir Analysis of Lake Buchanan - 1990 Operations (Ch 9)	Reservoir Analysis of Lake Buchanan - New 2023 Operations (Ch 9)
0.002	500	308,000	308,000		564,400	308,000	229,000	412,980	308,000
0.005	200				452,500	218,700	168,000	302,000	269,000
0.01	100	157,000	157,000		346,500	152,000	130,000	219,670	152,000
0.02	50	128,000	128,000		252,600	108,700	98,600	155,235	152,000
0.04	25	56,500	56,500		141,700	59,200	72,300	115,860	63,800
0.1	10				73,400	31,100	44,600	45,400	52,040
0.2	5				35,800	19,500	28,300	29,250	32,930
0.5	2				15,200	8,900	11,800	3,000	3,140

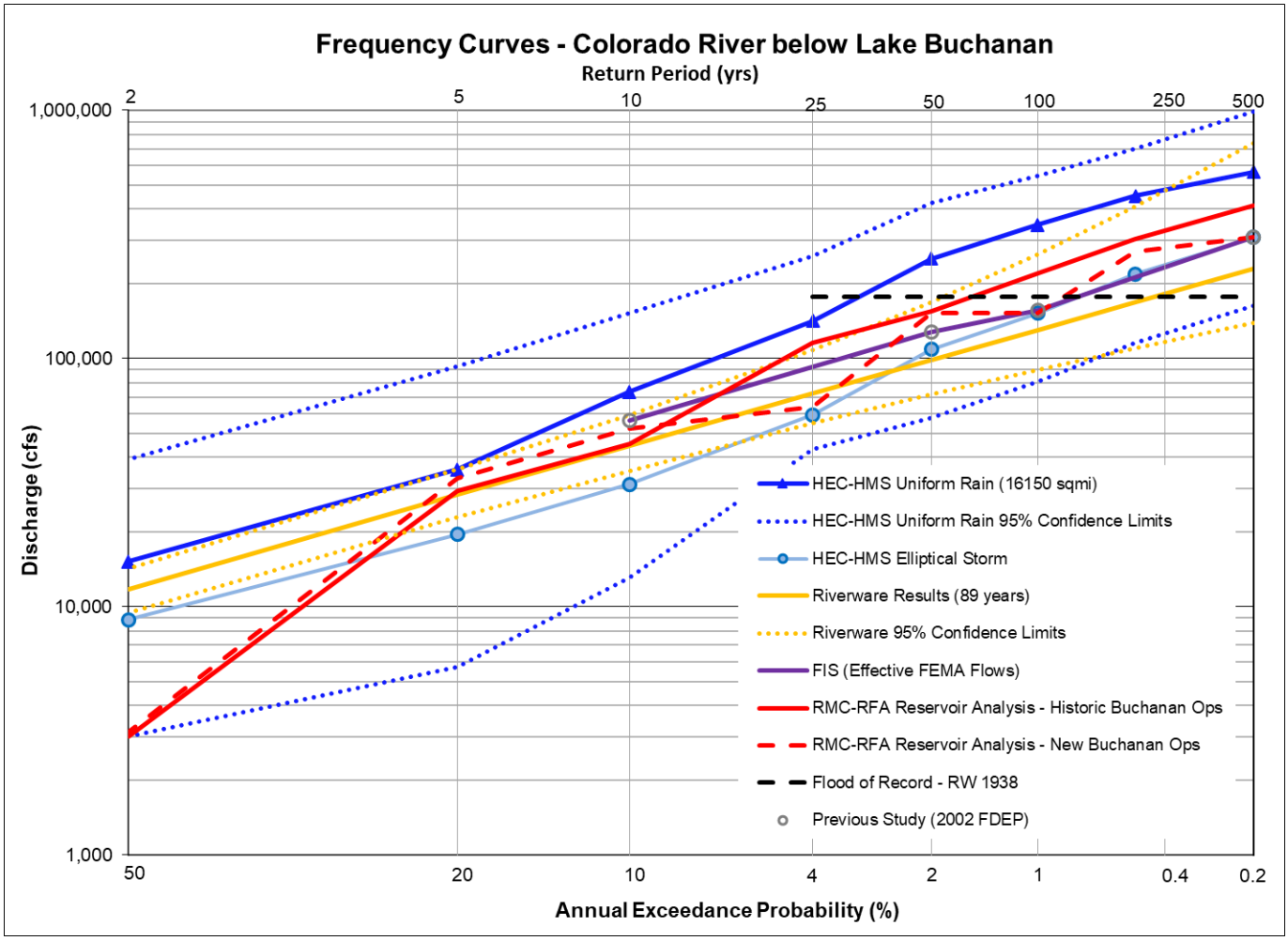

Figure 12.6: Flow Frequency Curve Comparison for the Colorado River below Lake Buchanan

The next point of comparison is the Colorado River below Lake Buchanan, as shown in the preceding table and figure. This lake has a total contributing drainage area of about 20,500 square miles and is just a short distance downstream from the Colorado River at San Saba USGS gage.

The published FEMA flows for this location came from the results of the 2002 FDEP study of the Lower Colorado Basin. Figure 12.6 shows that the HEC-HMS 1% AEP (100-year) elliptical storm results are within 2% of the results from the previous 2002 FDEP study, which is encouraging since both of these studies used elliptical design storms to estimate the frequency flows on the Colorado River. Figure 12.6 also shows that the HEC-HMS results are very close to the RMC-RFA reservoir analysis results with the new plan of operations for Lake Buchanan. Lake Buchanan recently (in 2023) underwent a change to its operational plan (see details in section 9.9 of Chapter 9); therefore, the New Buchanan Operations curve is a more appropriate estimate of existing conditions moving forward. Both the RMC-RFA results for the new operational plan and the HEC-HMS elliptical storm results show that the currently effective FEMA flows are still valid for the 1% and 0.2% AEP events.

Table 12.7: Frequency Flow (cfs) Results Comparison for the Colorado River below Lake LBJ

Annual Exceedance Probability (AEP)	Return Period (years)	Currently Effective FEMA FIS - Burnet County	Currently Effective FEMA FIS - Llano County	2002 FDEP Study Elliptical Storm	Statistical Analysis of the Gage Record (Ch 5) (N/A)	HEC-HMS Uniform Rain Frequency Storm (Ch 6) (21,200 sq mi)	HEC-HMS Elliptical Frequency Storm (Ch 7) (21,200 sq mi)	Statistical Analysis of the Extended RiverWare Record (Ch 8) (89 years)	Reservoir Analysis of Lake LBJ (Ch 9)
0.002	500	481,505	528,400	528,400		1,331,400	752,300	584,000	429,000
0.005	200					975,000	487,400	462,000	350,000
0.01	100	330,269	365,700	365,700		748,900	370,200	377,000	292,000
0.02	50		332,500	332,500		482,100	323,700	299,000	237,000
0.04	25					354,300	210,900	227,000	183,700
0.1	10	117,938	159,000	159,000		177,100	112,100	145,000	122,500
0.2	5					79,700	71,200	91,500	80,000
0.5	2					21,500	22,900	34,700	32,000

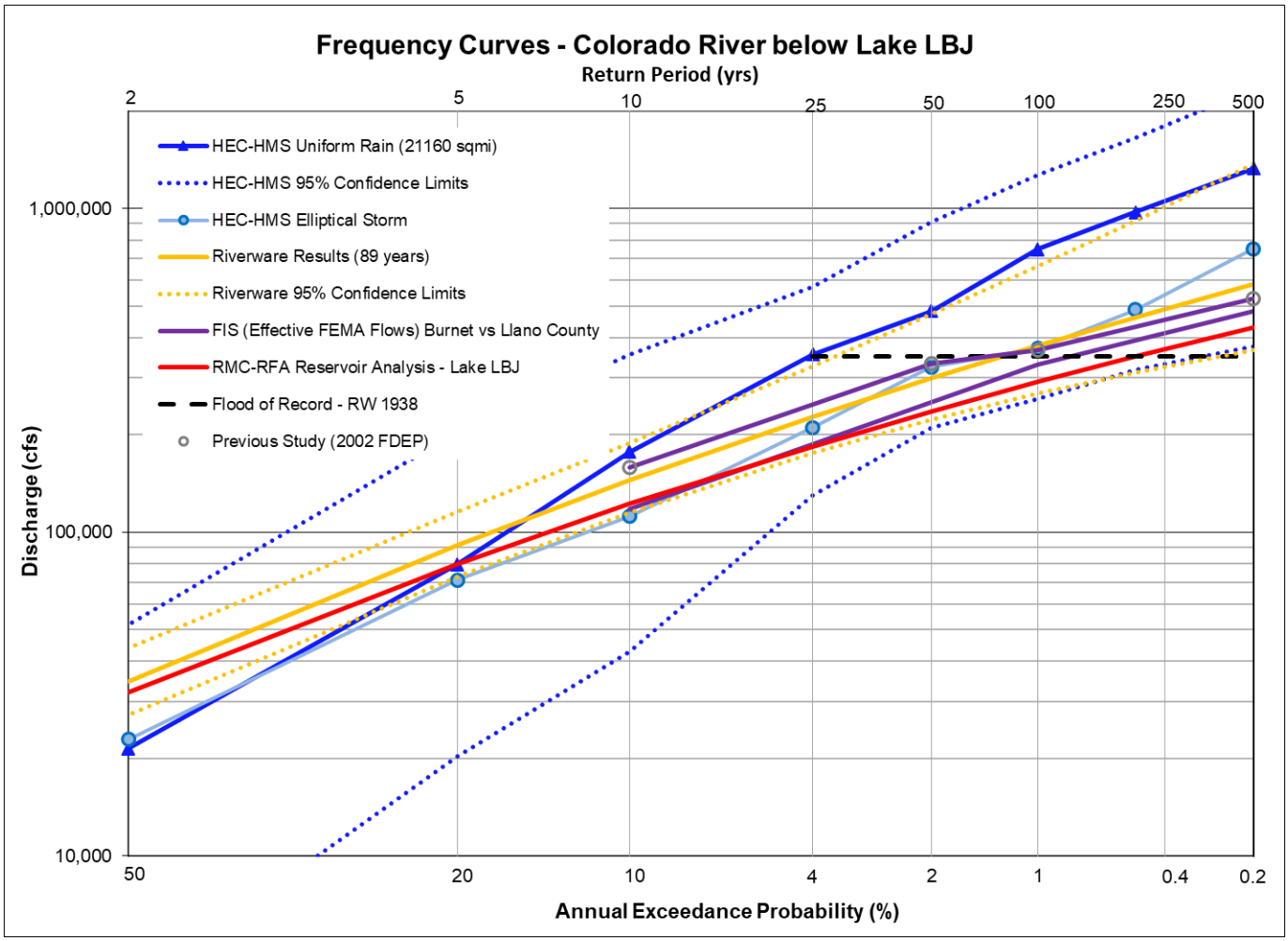

Figure 12.7: Flow Frequency Curve Comparison for the Colorado River below Lake LBJ

The next point of comparison is the Colorado River below Lake LBJ as shown in the preceding table and figure. This lake has a total contributing drainage area of over 25,000 square miles and includes the entire watershed for the Llano River. There are two different sets of effective FEMA flows for this location, depending on which bank of the river (and which side of the county line) one is located on. The published FEMA flows for Llano County came from the results of the 2002 FDEP study of the Lower Colorado Basin, while the FEMA flows for Burnet County came from a statistical analysis of the gage record in 1990 using Bulletin 17B methods.

Figure 12.7 shows that the HEC-HMS 1% AEP (100-year) elliptical storm results are within 2% of the results from the previous 2002 FDEP study, which is encouraging since both of these studies used elliptical design storms to estimate the frequency flows on the Colorado River. Figure 12.7 also shows that the HEC-HMS elliptical storm results are very close to the RiverWare results, especially at the 1% AEP. The RiverWare and HEC-HMS are significantly higher than the RMC-RFA results, but there is some uncertainty in outflows for that analysis due to the large differences between daily and hourly observed releases at this dam. The RiverWare and elliptical HEC-HMS 1% AEP results are also slightly higher that the highest observed release of 349,000 cfs from the October 2018 flood event that originated on the Llano River.

The next point of comparison is the Colorado River below Lake Travis (Marshall Ford) as shown in the following table and figure. Lake Travis has a total contributing drainage area of approximately 27.000 square miles which includes the Pedernales River watershed. The effective FEMA Flood Insurance Study (FIS) flows at Lake Travis were based on the results of the 2002 FDEP study of the Lower Colorado Basin. The 1% AEP (100-yr) effective FEMA flow of 90,000 cfs is identical to the 1% AEP results from the current study's RMC-RFA reservoir analysis. At this Lake the reservoir outflows from the HEC-HMS elliptical storms were lower than the effective FEMA and the RMC-RFA results for the 1% and 0.2% AEP frequencies, as shown in Figure 12.8. This is an indication that it would take more than a single 48-hour storm event to fill the large amount of flood storage in Lake Travis. In this case, the RMC-RFA stochastic analysis does a more robust evaluation of accounting for the effects of varying inflow durations and initial pool elevations on Lake Travis' pool elevation frequencies and reservoir outflows for rare frequencies.

Table 12.8: Frequency Flow (cfs) Results Comparison for the Colorado River below Lake Travis

Annual Exceedance Probability (AEP)	Return Period (years)	Currently Effective FEMA FIS	2002 FDEP Study Elliptical Storm	Statistical Analysis of the Gage Record (Ch 5) (N/A)	HEC-HMS Uniform Rain Frequency Storm (Ch 6) (23,000 sq mi)	HEC-HMS Elliptical Frequency Storm (Ch 7) (23,000 sq mi)	Statistical Analysis of the Extended RiverWare Record (Ch 8) (89 years)	Reservoir Analysis of Lake Travis (Ch 9)
0.002	500	366,900	366,900		1,191,000	198,000	149,000	261,100
0.005	200				717,700	104,200	105,000	161,970
0.01	100	90,100	90,100		488,600	64,500	77,500	90,000
0.02	50	90,000	90,000		276,800	30,300	56,500	72,620
0.04	25				107,500	30,000	40,000	30,000
0.1	10	29,900	29,900		35,600	22,500	23,700	30,000
0.2	5				30,000	13,000	14,700	30,000
0.5	2				15,500	4,700	6,060	5,000

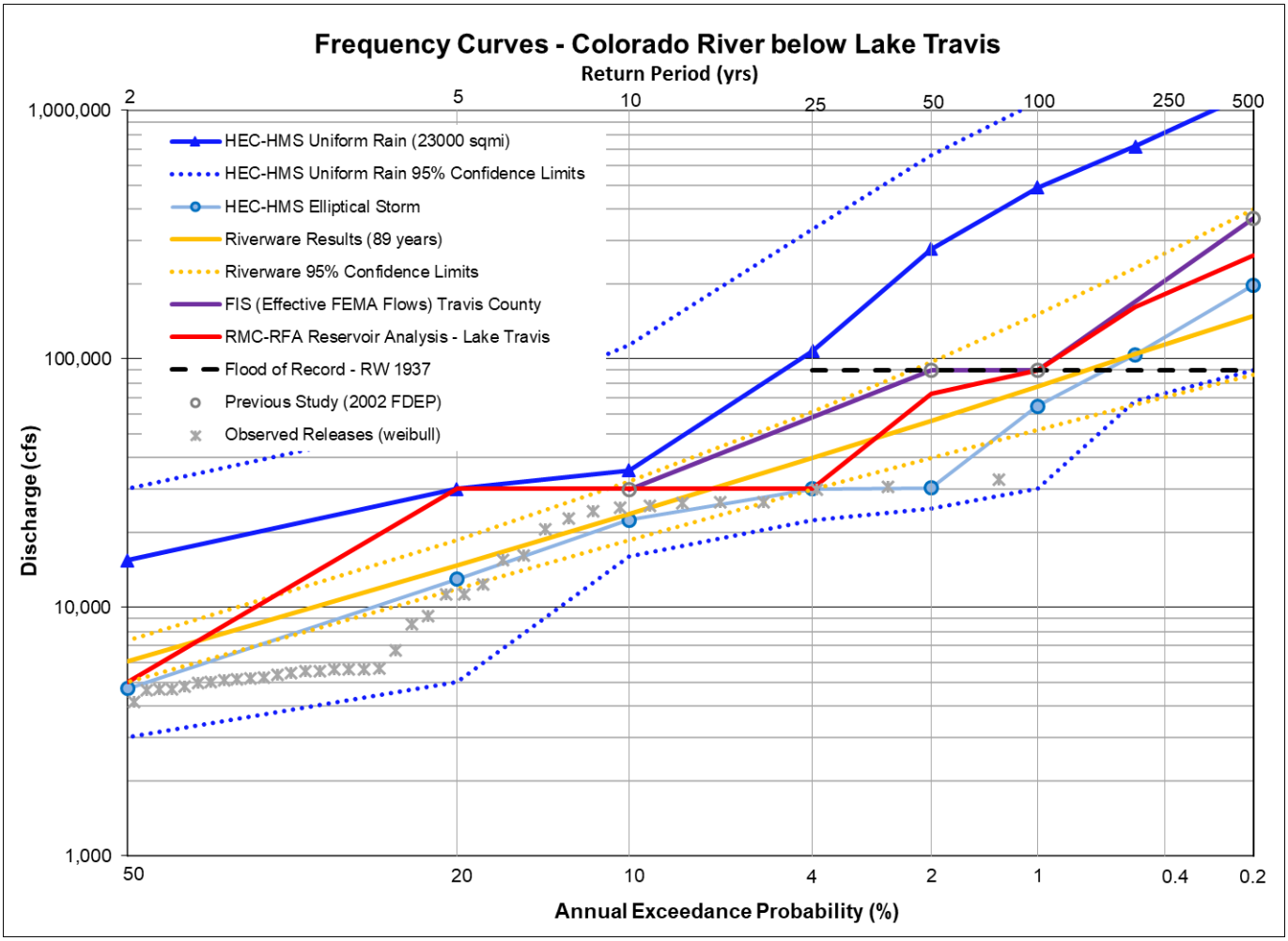

Figure 12.8: Flow Frequency Curve Comparison for the Colorado River below Lake Travis

Table 12.9: Frequency Flow (cfs) Results Comparison for the Colorado River at Austin, TX

AEP	Return Period (years)	Currently Effective FEMA FIS	Approx BLE Data from FEMA	2002 FDEP Study Elliptical Storm	Statistical Analysis of the Gage Record (Ch 5) (80 years)	HEC-HMS Uniform Rain Frequency Storm (Ch 6) (250 sq mi)	HEC-HMS Elliptical Frequency Storm (Ch 7) (250 sq mi)	Statistical Analysis of Extended RiverWare Record (Ch 8) (89 years)	Reservoir Analysis of Lake Travis (Ch 9)	Statistical Analysis with Historic 1930s Storms (Ch 10)
0.002	500	366,900	114,000		77,500	187,100	193,800	151,000	261,100	140,700
0.005	200				69,400	143,200	149,900	120,000	161,970	107,200
0.01	100	90,100	72,970	90,300	62,600	114,600	120,200	98,400	90,000	85,900
0.02	50	90,000	58,640		55,100	88,900	93,200	79,200	72,620	67,700
0.04	25		46,050		47,000	65,700	71,200	61,800	30,000	52,000
0.1	10	29,900	31,770		35,100	41,100	45,600	41,700	30,000	34,900
0.2	5				25,400	25,400	29,500	28,500	30,000	24,200
0.5	2				11,800	11,600	13,600	13,200	5,000	12,200

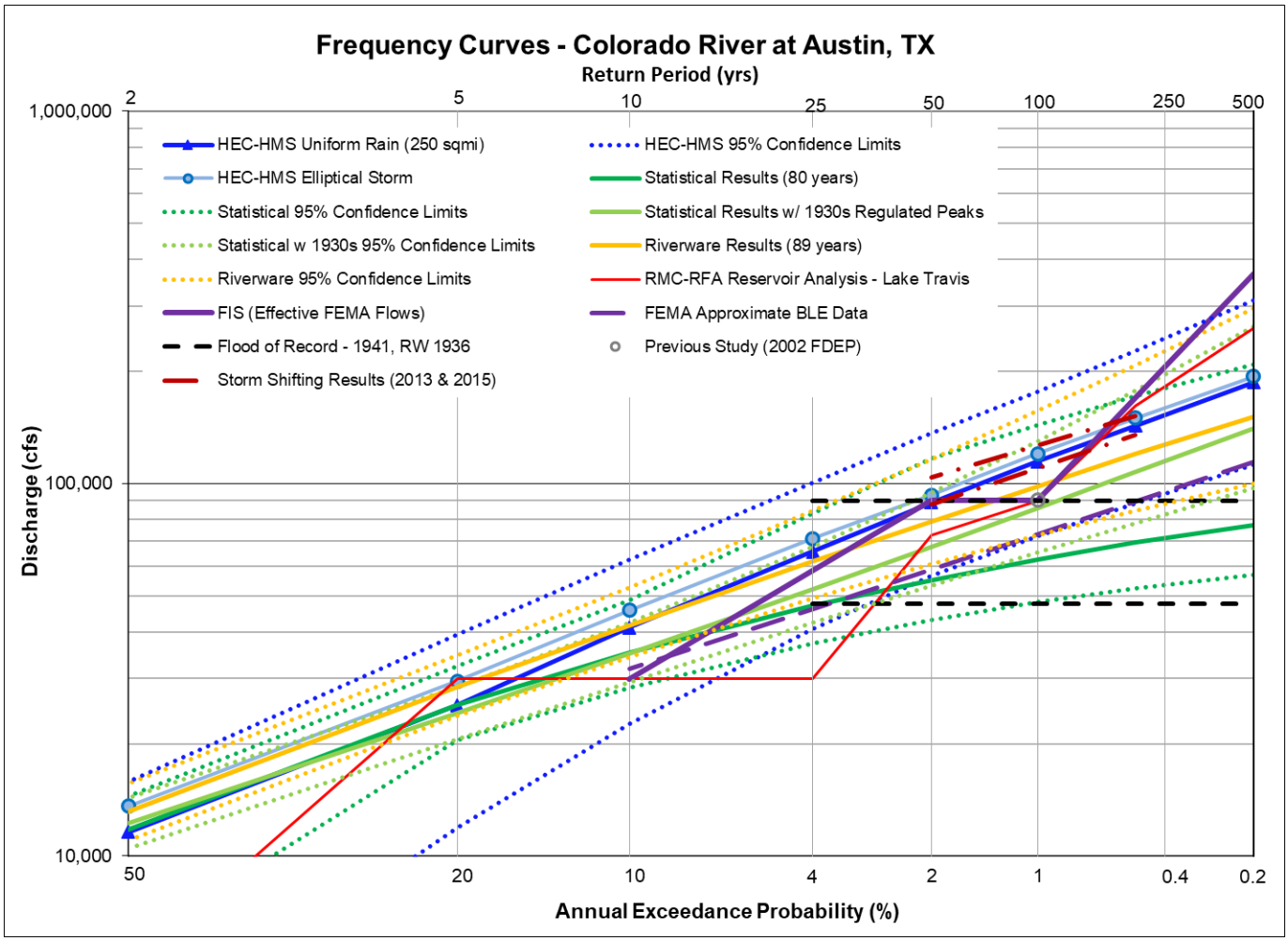

Figure 12.9a: Flow Frequency Curve Comparison for the Colorado River at Austin, TX

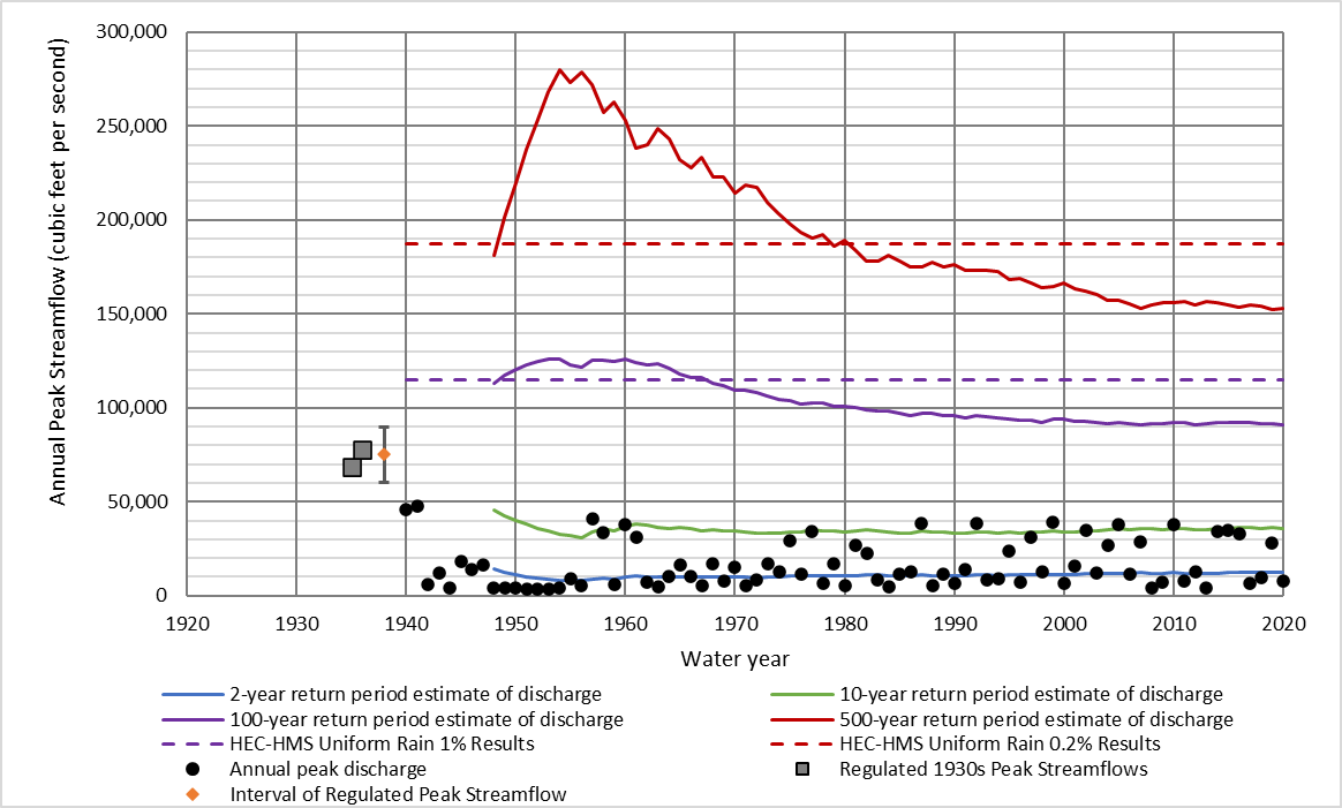

Figure 12.9b: Statistical Change Over Time Comparison for the Colorado River at Austin, TX

The next point of comparison is the Colorado River at Austin, Texas as shown in the preceding table and figures. This gage has a total contributing drainage area of over 27,000 square miles, but only 250 square miles of that area is downstream of Lake Travis. The effective FEMA Flood Insurance Study (FIS) flows at this location were based on the results of the 2002 FDEP study of the Lower Colorado Basin. The 1% AEP (100-yr) effective FEMA flow of 90,100 cfs is essentially identical to the 1% AEP results from the current study's RMC-RFA reservoir analysis of Lake Travis.

The largest observed flow at this location since Lake Travis was built in 1941 is 47,600 cfs. As a result, the statistical results for the past 80 years of record are quite low, as shown in Figure 12.9a. However, when the regulated 1930s peak flows from Chapter 10 were added to the record, the statistical estimate of the 1% AEP (100-yr) flood event increased to almost 86,000 cfs. However, Figure 12.9b shows that the Bulletin 17C statistical estimates are at a relative low point after experiencing several decades with no large flood events.

The HEC-HMS uniform rain results for this location showed a significantly higher discharge for the 1% AEP event of 115,000 cfs. That analysis only considered rainfall on the 250 square miles of uncontrolled drainage area in Austin that is downstream of Lake Travis, and it assumed that the dam's gates were shut. This is an indication that the uncontrolled area downstream of Lake Travis may have a higher flood potential than the releases from the dam at this location. To confirm the HEC-HMS results, a storm shifting analysis was completed, as documented in Chapter 11. That analysis shifted the October 2013 and October 2015 storm events by a distance of approximately 20 miles from Onion Creek to the uncontrolled watershed above the Austin gage. The results of that analysis are shown in the red lines on Figure 12.9a, and they verified the HEC-HMS uniform rain results. The HEC-HMS results are also well within the range of variation in the statistical estimates shown in Figure 12.9b. This confirms that a local rainfall event has a higher flood potential than a large release from Lake Travis, at least up to the 1% AEP frequency.

Table 12.10: Frequency Flow (cfs) Results Comparison for the Colorado River at Bastrop, TX

Annual Exceedance Probability (AEP)	Return Period (years)	Currently Effective FEMA FIS	Approximate BLE Data from FEMA	2002 FDEP Study Elliptical Storm	Statistical Analysis of the Gage Record (Ch 5) (59 years)	HEC-HMS Uniform Rain Frequency Storm (Ch 6) (1220 sq mi)	HEC-HMS Elliptical Frequency Storm (Ch 7) (1220 sq mi)	Statistical Analysis of the Extended RiverWare Record (Ch 8) (89 years)
0.002	500	319,352	179,300	319,000	144,000	323,900	267,200	159,000
0.005	200				122,000	238,800	202,400	135,000
0.01	100	142,020	125,100	142,000	106,000	190,200	159,600	117,000
0.02	50	120,920	103,600	121,000	90,400	143,700	121,000	99,900
0.04	25		83,280	103,400	75,300	105,400	96,900	82,800
0.1	10	71,975	58,370	72,000	55,900	65,000	64,200	60,700
0.2	5			49,100	41,700	41,200	42,700	44,300
0.5	2			26,800	22,700	21,300	19,800	22,800

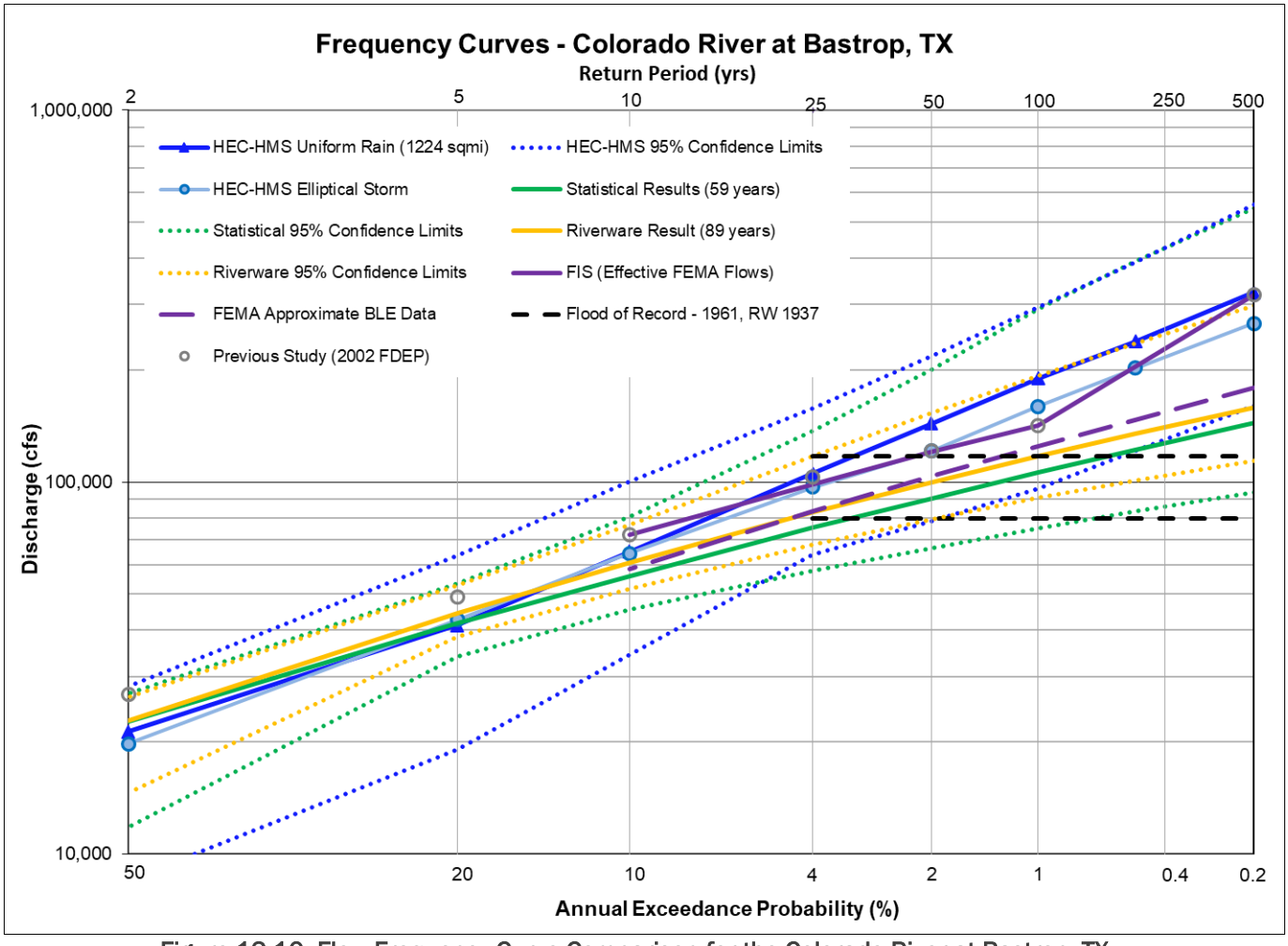

Figure 12.10: Flow Frequency Curve Comparison for the Colorado River at Bastrop, TX

The next point of comparison is the Colorado River at Bastrop, Texas as shown in the preceding table and figure. This gage has a total contributing drainage area of over 28,000 square miles, but only 1,200 square miles of that area is downstream of Lake Travis. The effective FEMA Flood Insurance Study (FIS) flows at this location were based on the results of the 2002 FDEP study of the Lower Colorado Basin.

The HEC-HMS elliptical storm results for this location are slightly higher than the effective FEMA flow for the 1% AEP, but they are slightly lower for the 0.2% AEP event. Both the HEC-HMS and FEMA flows are higher than the RiverWare and statistical results based on 59 years of gage record, as shown in Figure 12.10. This is likely because the largest flood of record occurred in 1961, and statistical estimates tend to trend downward if there are several decades without a large flood. However, as Figure 12.10 shows, the HEC-HMS results are still well within the confidence limits of the statistical analysis.

The next point of comparison is the Colorado River at Smithville, Texas as shown in the following table and figure. This gage has a total contributing drainage area of almost 29,000 square miles, of which 1,700 square miles is downstream of Lake Travis. The effective FEMA Flood Insurance Study (FIS) flows at this location were based on elliptical storm results from the 2002 FDEP study, which had a 1% AEP flow estimate of 152,000 cfs. The new HEC-HMS elliptical storm results for this location are within 2% of the 2002 FDEP elliptical storm results for the 1% AEP (100-yr) frequency. There is also close agreement between the HEC-HMS, RiverWare and statistical analysis results at Smithville, as shown in Figure 12.11.

Table 12.11: Frequency Flow (cfs) Results Comparison for the Colorado River at Smithville, TX

Annual Exceedance Probability (AEP)	Return Period (years)	Currently Effective FEMA FIS	Approximate BLE Data from FEMA	2002 FDEP Study Elliptical Storm	Statistical Analysis of the Gage Record (Ch 5) (59 years)	HEC-HMS Uniform Rain Frequency Storm (Ch 6) (1700 sq mi)	HEC-HMS Elliptical Frequency Storm (Ch 7) (1700 sq mi)	Statistical Analysis of the Extended RiverWare Record (Ch 8) (89 years)
0.002	500	308,043	221,200	308,043	226,000	331,500	245,500	193,000
0.005	200				183,000	247,400	190,900	163,000
0.01	100	152,200	152,900	152,200	153,000	201,000	149,500	140,000
0.02	50	130,000	125,900	130,000	125,000	152,100	114,400	118,000
0.04	25	78,300	100,500	111,000	99,100	115,600	90,400	96,900
0.1	10		69,520	78,300	68,100	72,100	62,000	69,900
0.2	5			50,500	47,000	46,600	41,800	50,300
0.5	2			28,200	22,000	22,200	21,700	25,200

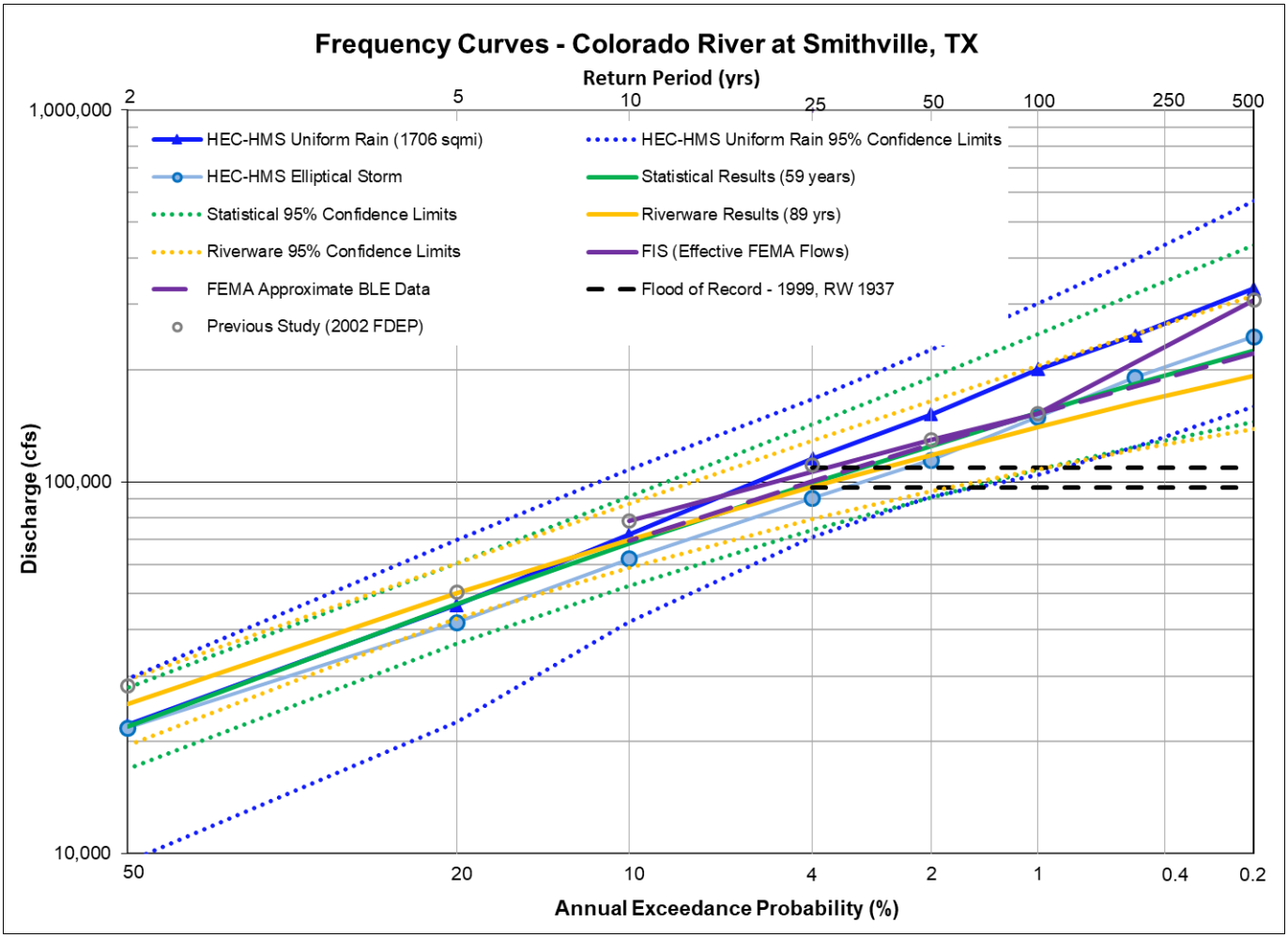

Figure 12.11: Flow Frequency Curve Comparison for the Colorado River at Smithville, TX

Table 12.12: Frequency Flow (cfs) Results Comparison for the Colorado River at La Grange, TX

Annual Exceedance Probability (AEP)	Return Period (years)	Currently Effective FEMA FIS	Approximate BLE Data from FEMA	2002 FDEP Study Elliptical Storm	Statistical Analysis of the Gage Record (Ch 5) (32 years)	Alternate Statistical Analysis of the Gage Record (Ch 5) (80 years)	HEC-HMS Uniform Rain Frequency Storm (Ch 6) (2120 sq mi)	HEC-HMS Elliptical Frequency Storm (Ch 7) 2120 sq mi)
0.002	500	308,043	274,600		258,000	207,000	316,900	244,000
0.005	200				208,000	172,000	241,800	182,600
0.01	100	152,200	183,500		173,000	146,000	190,700	143,200
0.02	50	130,000	148,700		140,000	122,000	145,400	108,500
0.04	25	78,300	116,800		110,000	99,300	112,600	87,000
0.1	10		78,860		75,000	71,100	73,100	62,800
0.2	5				51,200	51,200	48,600	46,000
0.5	2				23,500	26,100	24,000	25,300

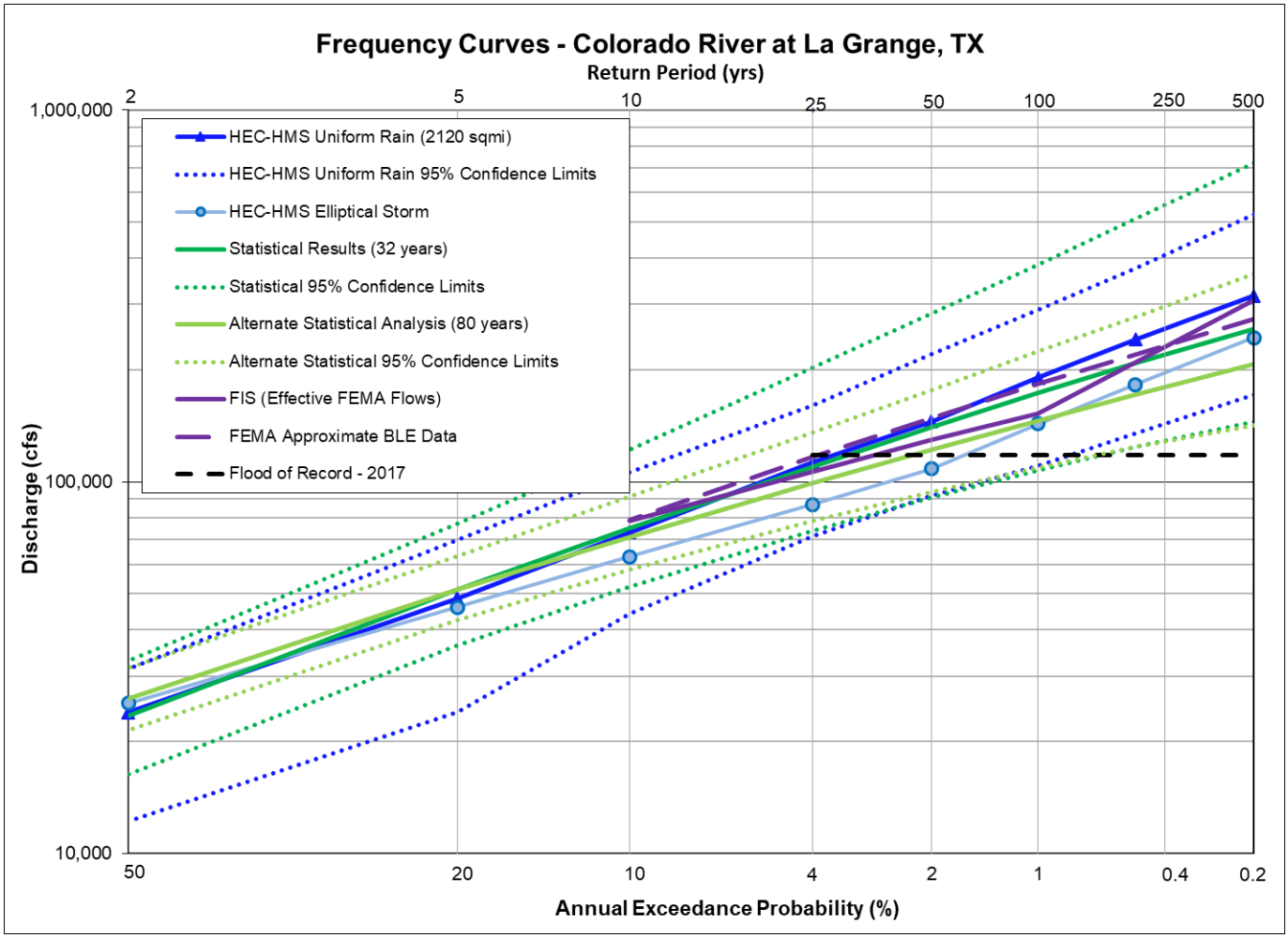

Figure 12.12: Flow Frequency Curve Comparison for the Colorado River at La Grange, TX

The next point of comparison is the Colorado River at La Grange, Texas as shown in the preceding table and figure. This gage has a total contributing drainage area of almost 29,500 square miles, of which 2,100 square miles are downstream of Lake Travis. The effective FEMA Flood Insurance Study (FIS) flows at this location were based on elliptical storm results from the 2002 FDEP study. The new HEC-HMS elliptical storm results for this location are slightly lower than the effective FEMA discharges, with a 1% AEP flow estimate of 143,200 cfs. There is close agreement between the HEC-HMS elliptical results and the alternate statistical analysis with 80 years of record, as shown in Figure 12.12.

The next point of comparison is the Colorado River at Columbus, Texas as shown in the following table and figures. This gage has a total contributing drainage area of over 30,000 square miles, of which almost 2,900 square miles are downstream of Lake Travis. The effective FEMA Flood Insurance Study (FIS) flows at this location were based on elliptical storm results from the 2002 FDEP study, which had a 1% AEP (100-yr) flow estimate of 135,000 cfs. The new HEC-HMS elliptical storm results for this location are slightly higher than the effective FEMA discharges, with a 1% AEP flow estimate of 144,800 cfs, but there is close agreement between the HEC-HMS elliptical results and the statistical analysis with 80 years of record, as shown in Figure 12.13a. In addition, the change over time plot in Figure 12.13b shows that the HEC-HMS 1% and 0.2% AEP elliptical storm results are well within the variation of the statistical estimates over time. Figure 12.13b also shows that the HEC-HMS 1% AEP flow estimate is lower than the observed peak for Hurricane Harvey but higher than the second and third highest observed peaks, which is right where one would expect the 1% AEP flood event to be.

Table 12.13: Frequency Flow (cfs) Results Comparison for the Colorado River at Columbus, TX

Annual Exceedance Probability (AEP)	Return Period (years)	Currently Effective FEMA FIS	Approximate BLE Data from FEMA	2002 FDEP Study Elliptical Storm	Statistical Analysis of the Gage Record (Ch 5) (80 years)	HEC-HMS Uniform Rain Frequency Storm (Ch 6) (2890 sq mi)	HEC-HMS Elliptical Frequency Storm (Ch 7) (2,890 sq mi)	Statistical Analysis of the Extended RiverWare Record (Ch 8) (89 years)
0.002	500	271,800	186,900	271,800	212,000	348,500	246,200	242,000
0.005	200				176,000	265,800	183,800	201,000
0.01	100	135,000	139,500	135,200	150,000	209,500	144,800	172,000
0.02	50	114,000	119,300	114,400	126,000	159,700	108,400	144,000
0.04	25		99,270	96,300	103,000	123,400	86,400	117,000
0.1	10	67,100	73,150	67,100	73,900	81,200	65,700	83,600
0.2	5			48,400	53,500	54,300	51,000	59,700
0.5	2			27,400	27,700	28,400	28,700	29,600

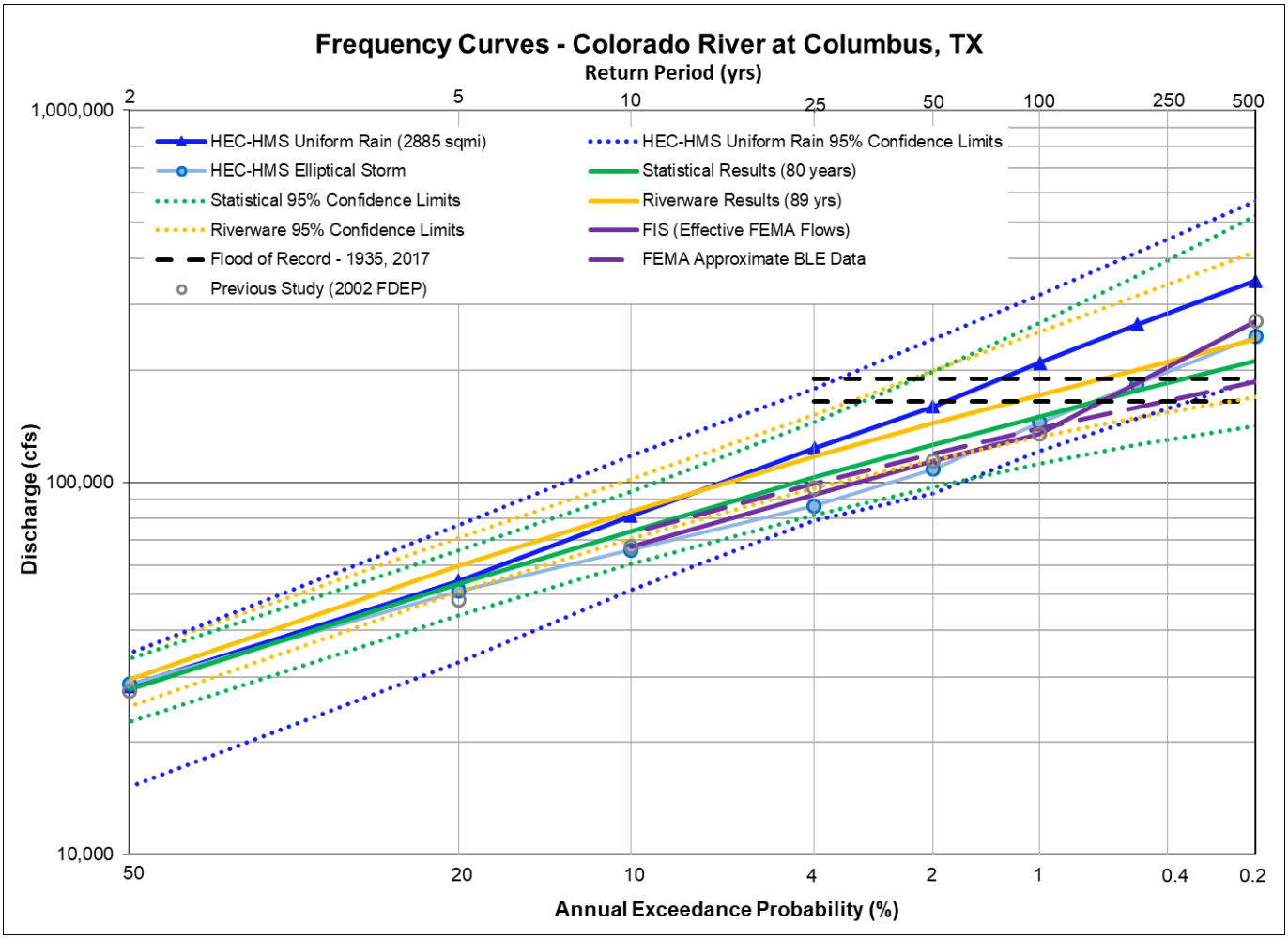

Figure 12.13a: Flow Frequency Curve Comparison for the Colorado River at Columbus, TX

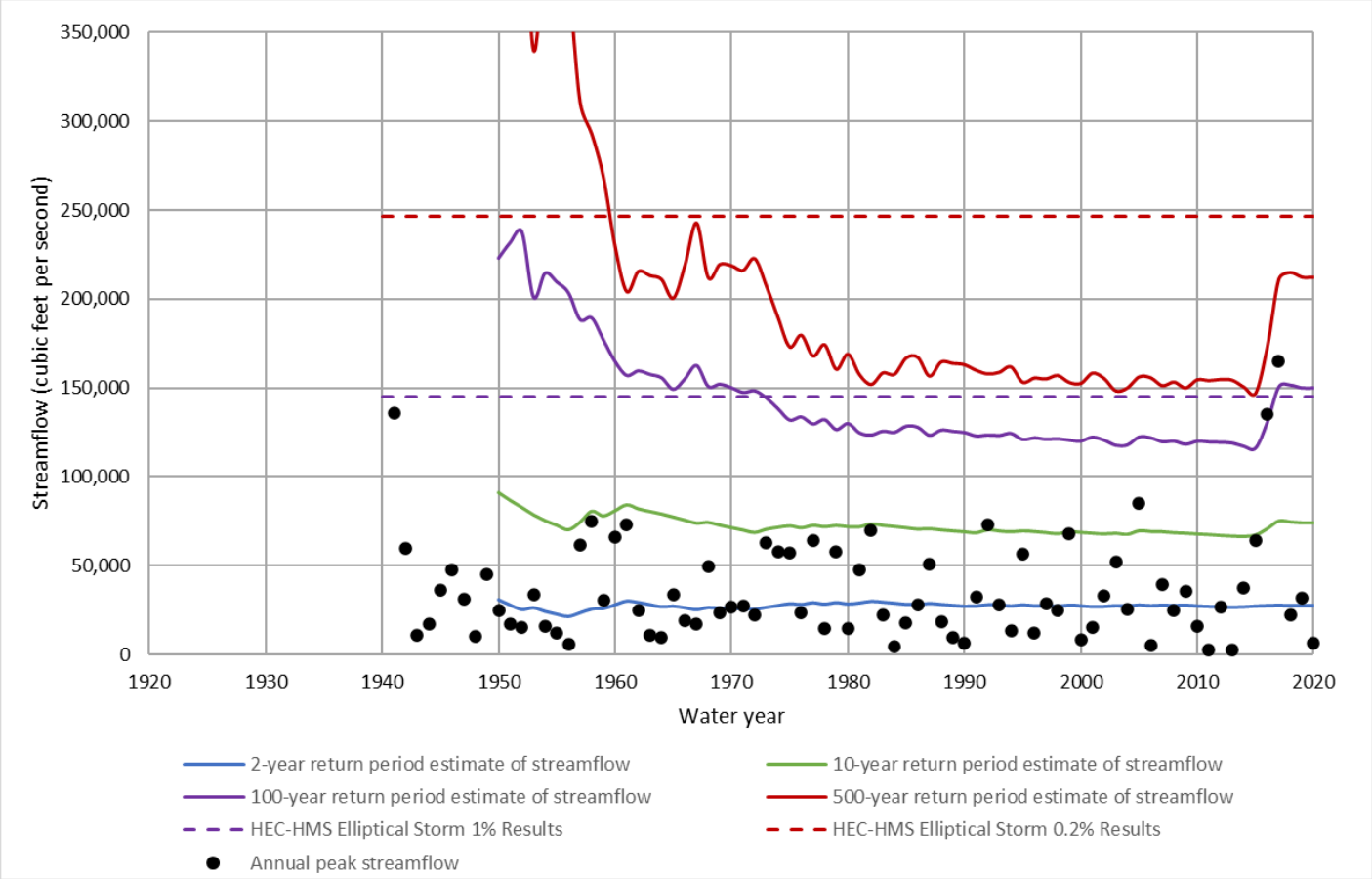

Figure 12.13b: Statistical Change Over Time Comparison for the Colorado River at Columbus, TX

Table 12.14: Frequency Flow (cfs) Results Comparison for the Colorado River at Wharton, TX

Annual Exceedance Probability (AEP)	Return Period (years)	Currently Effective FEMA FIS	Approx BLE Data from FEMA	2002 FDEP Study Elliptical Storm	Statistical Analysis of the Gage Record (Ch 5) (80 years)	HEC-HMS Uniform Rain Frequency Storm (Ch 6) (3,250 sq mi)	HEC-HMS Elliptical Frequency Storm (Ch 7) (3,250 sq mi)	Statistical Analysis of the Extended RiverWare Record (Ch 8) (89 years)
0.002	500	106,300			173,000	243,000	160,000	181,000
0.005	200				143,000	178,100	124,800	152,000
0.01	100	95,415		114,100	122,000	142,300	101,600	132,000
0.02	50	86,615		94,000	102,000	113,800	81,000	112,000
0.04	25	56,205		77,300	83,400	91,600	71,100	92,600
0.1	10			60,400	60,900	71,300	58,600	68,100
0.2	5			45,700	45,100	51,900	48,700	50,300
0.5	2			25,800	24,900	28,500	27,500	26,900

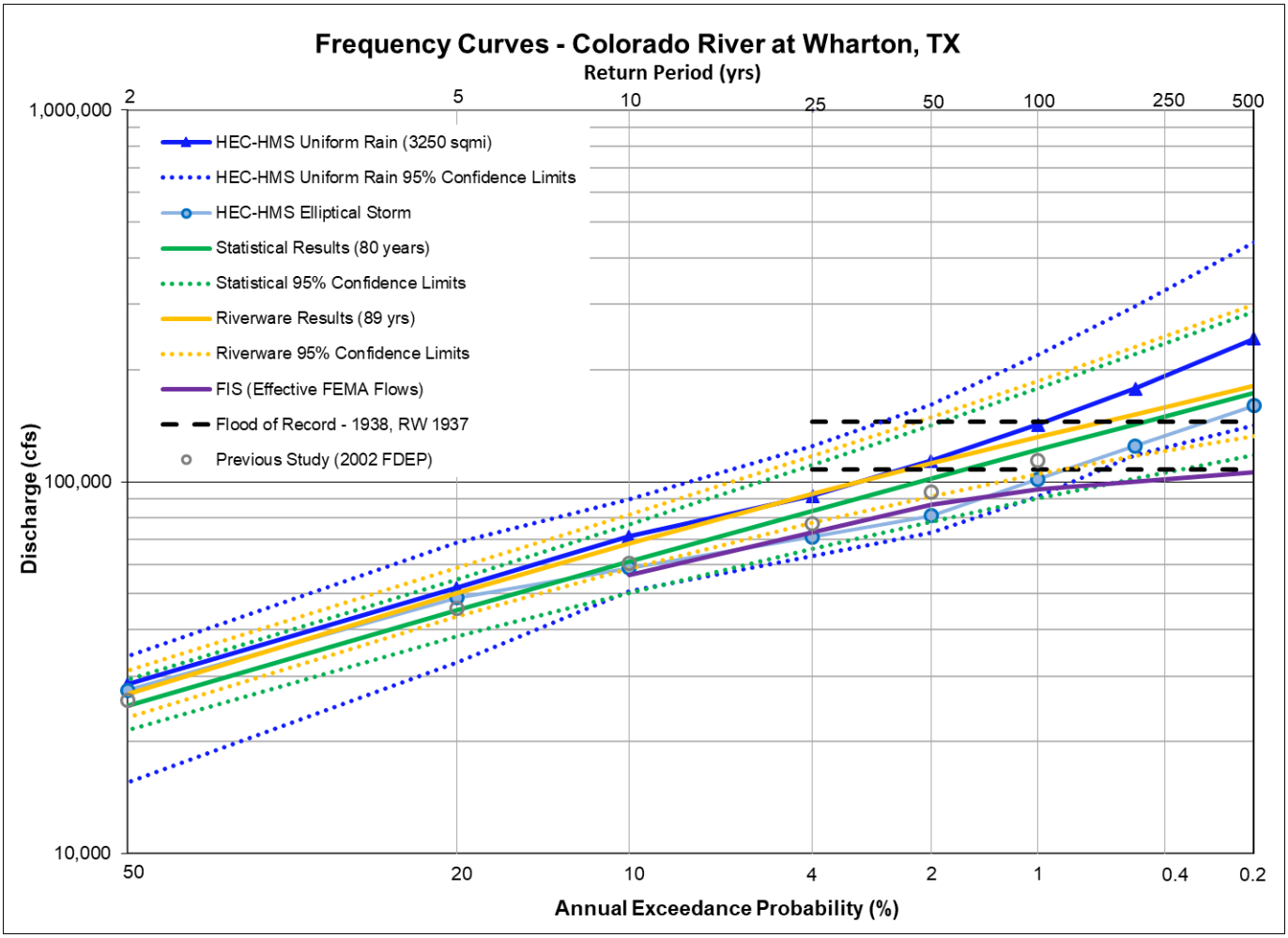

Figure 12.14a: Flow Frequency Curve Comparison for the Colorado River at Wharton, TX

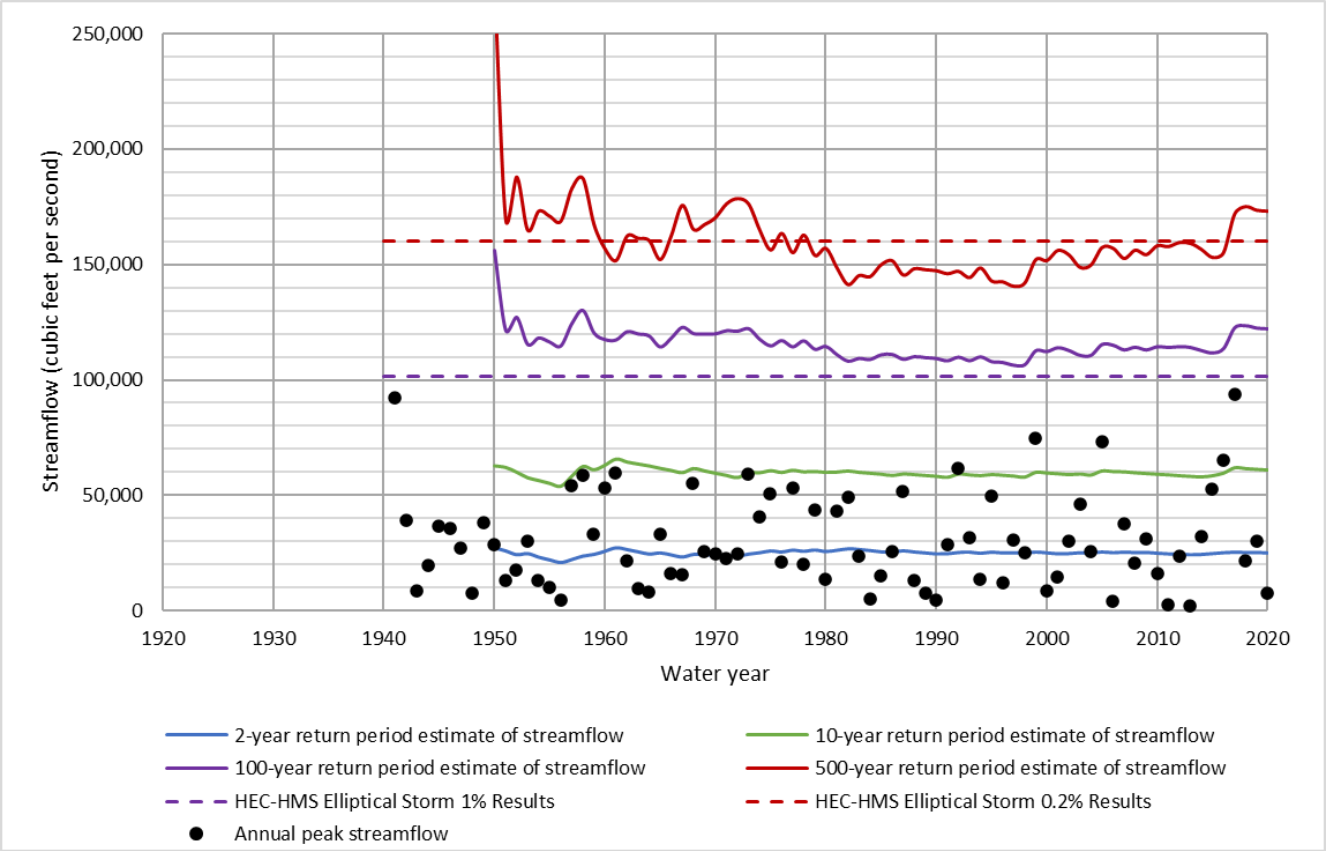

Figure 12.14b: Statistical Change Over Time Comparison for the Colorado River at Wharton, TX

The next point of comparison is the Colorado River at Wharton, Texas as shown in the preceding table and figures. This gage has a total contributing drainage area of over 30,600 square miles, of which almost 3,250 square miles are downstream of Lake Travis. This gage is also downstream of the areas of observed inter-basin transfer where water is diverted from the Colorado River to the San Bernard watershed during high flow events (see the Calibration Methodology section of Chapter 6 for more information). Diversions were added to the HEC-HMS model and calibrated to observed events in order to account for the inter-basin transfer.

The effective FEMA Flood Insurance Study (FIS) flows at this location came from the 2017 FIS for Wharton County, which had a 1% AEP (100-yr) flow value of 95,400 cfs. The elliptical storm results from the 2002 FDEP study were a bit higher with a 1% AEP (100-yr) flow estimate of 114,000 cfs. The new HEC-HMS elliptical storm results for this location fell right in between the FIS and the FDEP estimates, with a 1% AEP flow estimate of 101,600 cfs.

The HEC-HMS elliptical results are slightly lower that the current statistical analysis with 80 years of record, as shown in Figure 12.14a. However, the current statistical results may be slightly overestimating the 1% AEP discharge due to the effects of Hurricane Harvey. In addition, the change over time plot in Figure 12.14b shows that the HEC-HMS 1% AEP elliptical storm results are just above the two highest observed peaks, which is what one would expect to see after 80 years of record.

Table 12.15: Frequency Flow (cfs) Results Comparison for the Colorado River near Bay City, TX

Annual Exceedance Probability (AEP)	Return Period (years)	Currently Effective FEMA FIS	Approx BLE Data from FEMA	2002 FDEP Study Elliptical Storm	Statistical Analysis of the Gage Record (Ch 5) (72 years)	HEC-HMS Uniform Rain Frequency Storm (Ch 6) (3,600 sq mi)	HEC-HMS Elliptical Frequency Storm (Ch 7) (3,600 sq mi)	Statistical Analysis of the Extended RiverWare Record (Ch 8) (89 years)
0.002	500	177,200		177,200	187,000	246,200	154,400	189,000
0.005	200				152,000	180,700	117,900	158,000
0.01	100	99,700		99,700	128,000	143,300	95,600	135,000
0.02	50	80,700		80,700	106,000	110,500	79,800	114,000
0.04	25	58,500		58,500	86,000	90,500	71,700	93,300
0.1	10				62,000	73,600	59,400	67,900
0.2	5				45,400	54,200	49,100	49,800
0.5	2				24,900	29,800	25,900	26,500

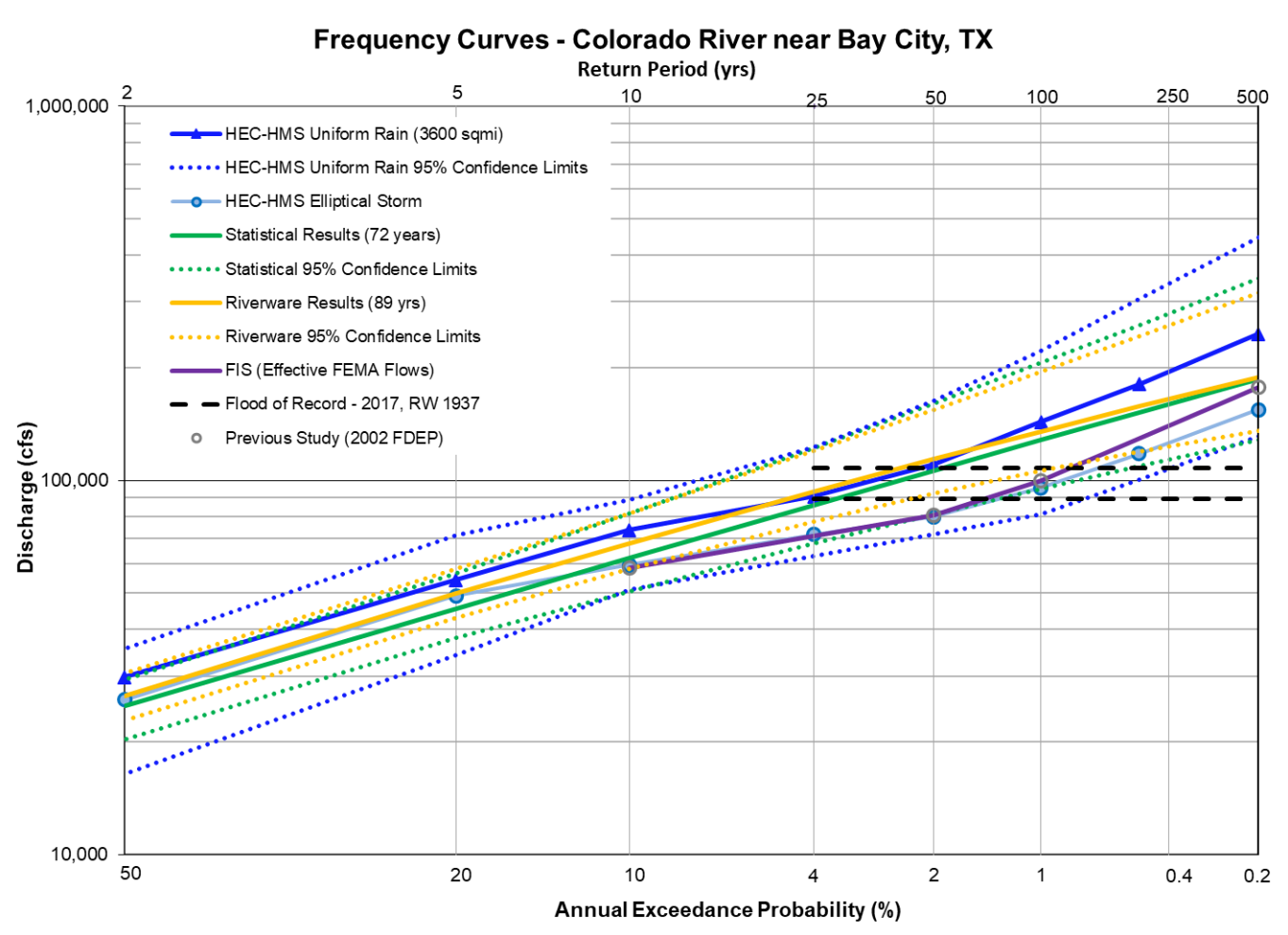

Figure 12.15: Flow Frequency Curve Comparison for the Colorado River near Bay City, TX

The final downstream point of comparison on the Colorado River is the Colorado River near Bay City, Texas as shown in the preceding table and figure. This gage has a total contributing drainage area of over 30,800 square miles, of which over 3,500 square miles are downstream of Lake Travis. This gage is in the narrow portion of the watershed approaching the Gulf of Mexico. Since there are no large tributaries joining the Colorado River in this area, flows tend to decrease in the downstream direction due to floodplain storage and attenuation.

The effective FEMA Flood Insurance Study (FIS) flows at this location came from the elliptical storm results from the 2002 FDEP study, which had a 1% AEP (100-yr) flow estimate of 99,700 cfs. The new HEC-HMS elliptical storm results for this location are slightly lower than the effective FIS, with a 1% AEP flow estimate of 95,600 cfs. The HEC-HMS elliptical results are also lower that the current statistical analysis with 80 years of record, as shown in Figure 12.15. However, the current statistical results may be slightly overestimating the 1% AEP discharge due to the effects of Hurricane Harvey.

12.1.2 Concho River Basin Gage Locations

The next point of comparison is Elm Creek at Ballinger, Texas as shown in the following table and figure. This gage is located near the upstream extents of the study area on a tributary to the Colorado River and has a drainage area of 450 square miles.

There are no published FEMA flows for this location. The HEC-HMS elliptical and uniform rain results showed a strong agreement with the current statistical analysis of the gage record based on 88 years of record, as shown in Figure 12.16. Since this gage is located in the portion of the basin that demonstrates declining flow trends, an alternate statistical analysis was also performed using only the most recent 38 years of record. The results of that analysis are substantially lower than all of the other results. However, since that smaller data sample did not include any large floods, it could easily underestimate the 1% AEP (100-yr) flood event if a large storm event were to occur in that vicinity.

Table 12.16: Frequency Flow (cfs) Results Comparison for the Elm Creek at Ballinger, TX

Annual Exceedance Probability (AEP)	Return Period (years)	Currently Effective FEMA FIS	Statistical Analysis of the Gage Record (Ch 5) (88 years)	Alternate Statistical Analysis of the Gage Record (Ch 5) (38 yrs)	HEC-HMS Uniform Rain Frequency Storm (Ch 6) (467 sq mi)	HEC-HMS Elliptical Frequency Storm (Ch 7) (467 sq mi)
0.002	500		77,800	53,200	113,800	98,400
0.005	200		60,600	40,300	84,100	72,000
0.01	100		48,900	31,800	62,800	52,800
0.02	50		38,300	24,200	41,900	33,900
0.04	25		28,800	17,700	31,300	25,200
0.1	10		18,000	10,500	17,200	14,900
0.2	5		11,300	6,280	10,500	9,520
0.5	2		4,220	2,130	3,950	3,920

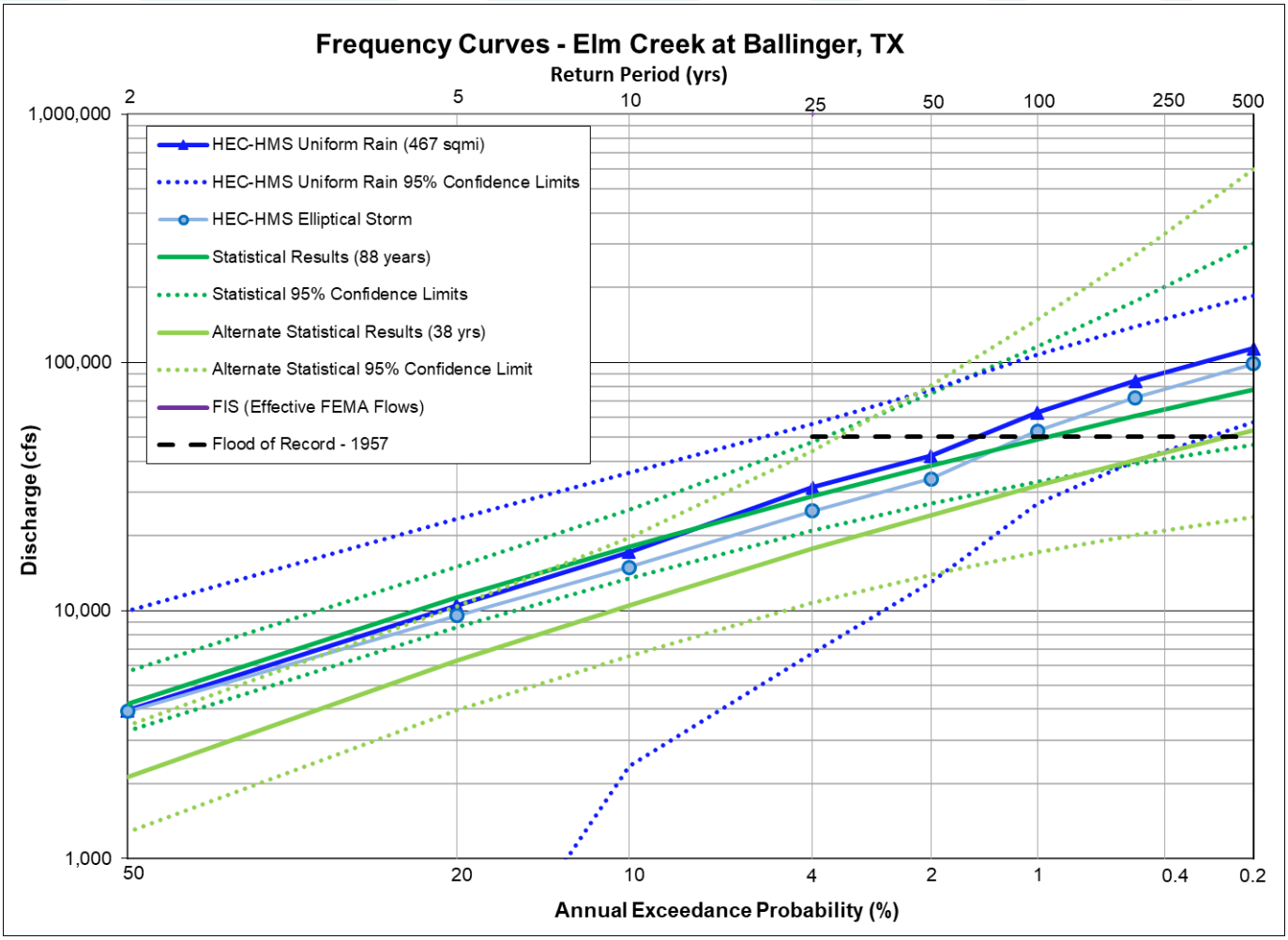

Figure 12.16: Flow Frequency Curve Comparison for the Elm Creek at Ballinger, TX

The next point of comparison is the South Concho River at Christoval, Texas as shown in the following table and figure. This gage is located upstream of Twin Buttes Reservoir in the Concho River basin and has a drainage area of 415 square miles. This gage is also located in the portion of the study area that is experiencing declining flow trends.

The effective FEMA flows for this location came from a 1990 uncalibrated rainfall runoff model for the Tom Green County's FIS. As shown in Figure 12.17 the effective FEMA flows are higher than both the current statistical results and the HEC-HMS results. Two statistical analyses were performed on the gage record for this location. One included the entire 90 years of record, and the alternate analysis included only the most recent 58 years due to the declining flow trends in the basin. The HEC-HMS elliptical and uniform rain results fell right in between the results for these two statistical analyses, as shown in Figure 12.17.

Table 12.17: Frequency Flow (cfs) Results Comparison for the South Concho River at Christoval, TX

Annual Exceedance Probability (AEP)	Return Period (years)	Currently Effective FEMA FIS	Statistical Analysis of the Gage Record (Ch 5) (90 years)	Alternate Statistical Analysis of the Gage Record (Ch 5) (58 yrs)	HEC-HMS Uniform Rain Frequency Storm (Ch 6) (415 sq mi)	HEC-HMS Elliptical Frequency Storm (Ch 7) (415 sq mi)
0.002	500	216,700	191,000	72,800	130,900	115,300
0.005	200		139,000	60,800	103,200	90,300
0.01	100	131,750	105,000	50,400	83,900	73,300
0.02	50	85,610	74,600	39,300	64,100	55,700
0.04	25		49,400	28,100	49,500	42,300
0.1	10	24,960	24,100	14,500	25,600	21,200
0.2	5		11,200	6,470	8,800	6,460
0.5	2		1,980	793	1,080	800

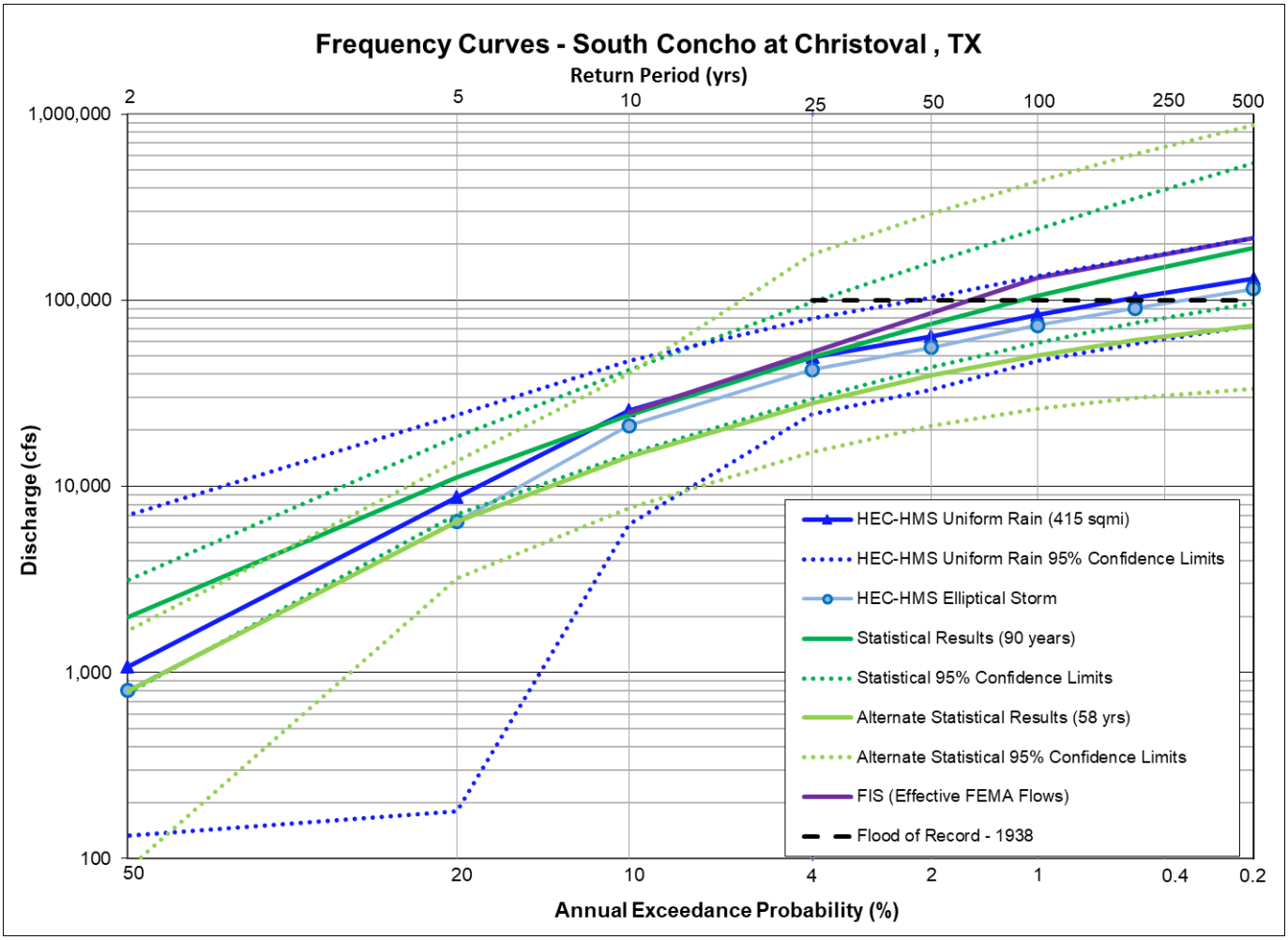

Figure 12.17: Flow Frequency Curve Comparison for the South Concho River at Christoval, TX

Table 12.18: Frequency Flow (cfs) Results Comparison for the Middle Concho above Tankersley, TX

Annual Exceedance Probability (AEP)	Return Period (years)	Currently Effective FEMA FIS	Statistical Analysis of the Gage Record (Ch 5) (60 yrs)	HEC-HMS Uniform Rain Frequency Storm (Ch 6) (2130 sq mi)	HEC-HMS Elliptical Frequency Storm (Ch 7) (2130 sq mi)
0.002	500	97,950	26,400	219,900	166,700
0.005	200		23,900	169,300	128,000
0.01	100	60,150	21,600	134,600	101,300
0.02	50	47,990	18,700	98,700	70,700
0.04	25		15,400	51,100	41,800
0.1	10	24,161	10,300	18,600	15,300
0.2	5		6,180	6,220	6,250
0.5	2		1,570	1,530	1,520

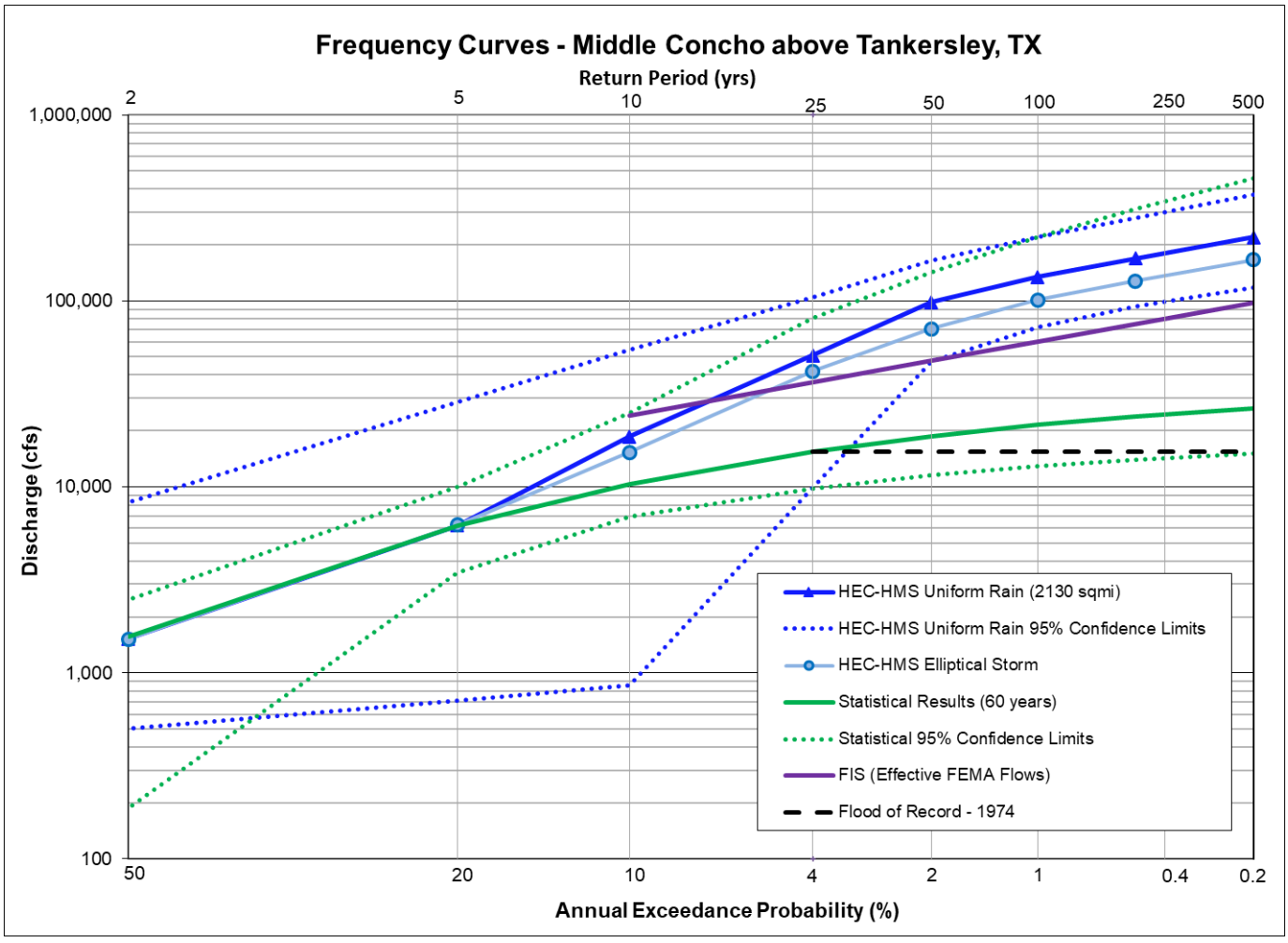

Figure 12.18: Flow Frequency Curve Comparison for the Middle Concho above Tankersley, TX

The next point of comparison is the Middle Concho River above Tankersley, Texas as shown in the preceding table and figure. This gage is upstream of Twin Buttes Reservoir in the Concho River basin and has a drainage area of 2,100 square miles. This gage is also located in the portion of the study area that is experiencing declining flow trends.

The effective FEMA flows for this location came from a 1990 uncalibrated rainfall runoff model for the Tom Green County's FIS. As shown in Figure 12.18, the effective FEMA flows are near the lower confidence limit of the calibrated HEC-HMS results. The statistical analysis of the gage record produced very low estimates of the frequency floods based on 60 years of gage record. This is because the largest flood in the record was the 1974 peak of 15,500 cfs, which is a very low flood for a drainage area of over 1,000 square miles. Therefore, the available data sample at this gage may not be representative of its true flooding potential from a large storm event.

The HEC-HMS elliptical storm results were substantially higher than both the statistical results and the effective FEMA flows. Those results are based on the expected regional rainfall depths from NOAA Atlas 14 as well as the calibrated loss rates and other model parameters. The HEC-HMS results are also well within the confidence limits of the statistical analysis based on 69 years of data.

The next point of comparison is the Spring Creek above Tankersley, Texas as shown in the following table and figure. This gage is located upstream of Twin Buttes Reservoir in the Concho River basin and has a drainage area of just over 400 square miles. This gage is also located in the portion of the study area that is experiencing declining flow trends.

There are no published FEMA flows for this location. Figure 12.19 shows that the HEC-HMS results from the elliptical and uniform rain methods are almost identical. This is due to its relatively small drainage area of about 400 square miles. Figure 12.19 also shows that the HEC-HMS results are substantially lower than the current statistical analysis of the gage record based on 61 years of record. However, the HEC-HMS results are still well within the confidence bounds of the statistical results.

The flood of record at this location was the 1959 flood peak of 82,100 cfs. That flood is over twice the magnitude of any other flood in the record, and one may note that it is over five times as large as the flood of record on the previous gage for the Middle Concho River, even though this gage has only one fifth of its drainage area. The contrast of these two gages clearly illustrates how statistical flood frequency results are substantially influenced by how "lucky" or "unlucky" a watershed has been according to the data sample of floods that have been recorded at a particular location. The HEC-HMS results, on the other hand, are based on the regional rainfall statistics of NOAA Atlas 14, which help to make the frequency flood estimates more consistent throughout a watershed.

Table 12.19: Frequency Flow (cfs) Results Comparison for the Spring Creek above Tankersley, TX

Annual Exceedance Probability (AEP)	Return Period (years)	Currently Effective FEMA FIS	Statistical Analysis of the Gage Record (Ch 5) (61 years)	HEC-HMS Uniform Rain Frequency Storm (Ch 6) (427 sq mi)	HEC-HMS Elliptical Frequency Storm (Ch 7) (427 sq mi)
0.002	500		294,000	97,400	95,200
0.005	200		166,000	74,700	72,400
0.01	100		101,000	56,000	53,900
0.02	50		56,600	36,700	34,300
0.04	25		28,800	24,100	22,900
0.1	10		9,310	9,040	8,320
0.2	5		2,950	2,800	2,900
0.5	2		253	330	300

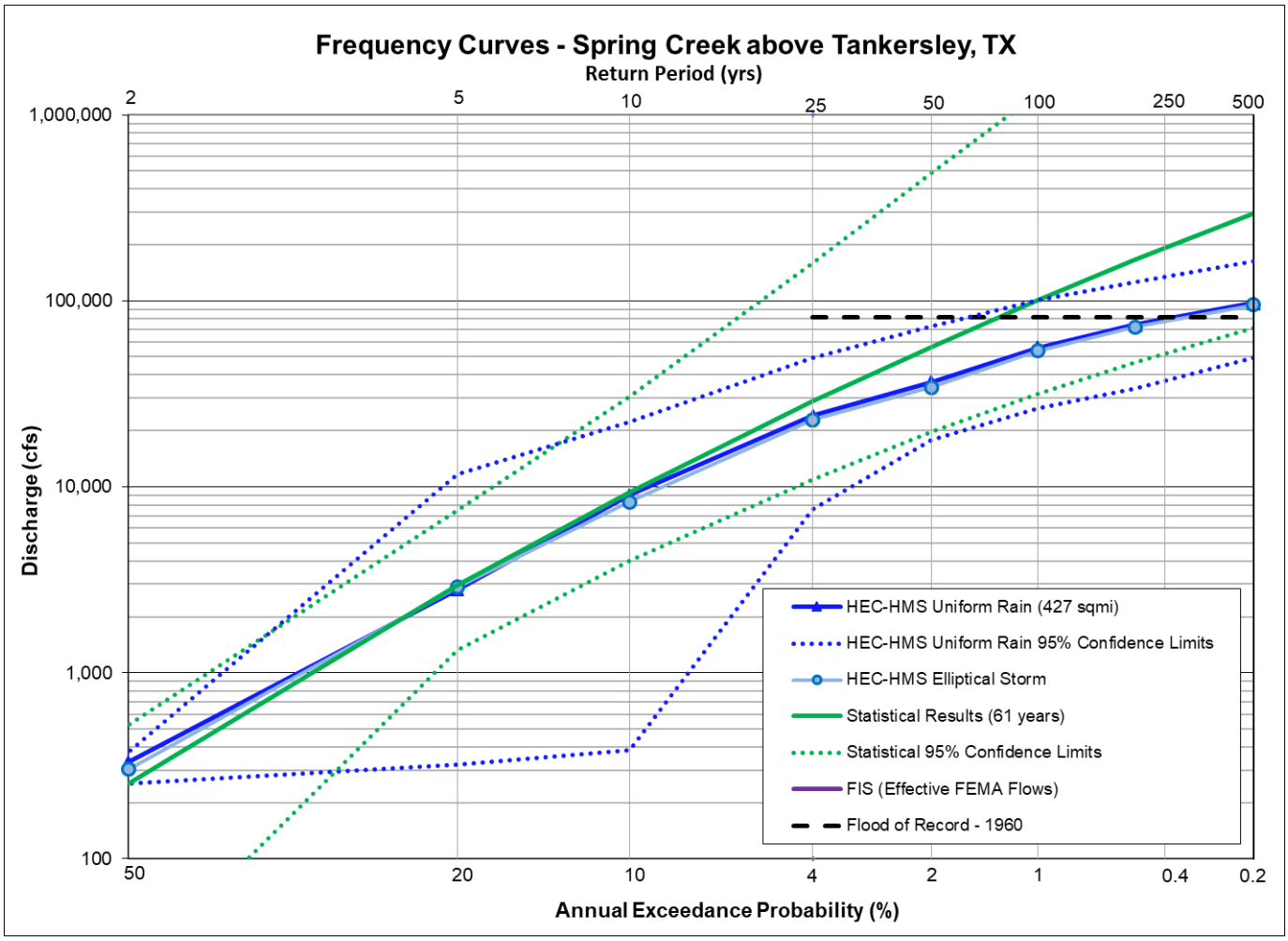

Figure 12.19: Flow Frequency Curve Comparison for the Spring Creek above Tankersley, TX

Table 12.20: Frequency Flow (cfs) Results Comparison for the Dove Creek at Knickerbocker, TX

Annual Exceedance Probability (AEP)	Return Period (years)	Currently Effective FEMA FIS	Statistical Analysis of the Gage Record (Ch 5) (60 years)	HEC-HMS Uniform Rain Frequency Storm (Ch 6) (224 sq mi)
0.002	500	120,310	39,700	62,100
0.005	200		33,300	48,700
0.01	100	64,240	28,000	39,500
0.02	50	45,120	22,400	30,000
0.04	25		16,800	19,800
0.1	10	16,420	9,680	10,600
0.2	5		5,120	5,130
0.5	2		1,050	1,080

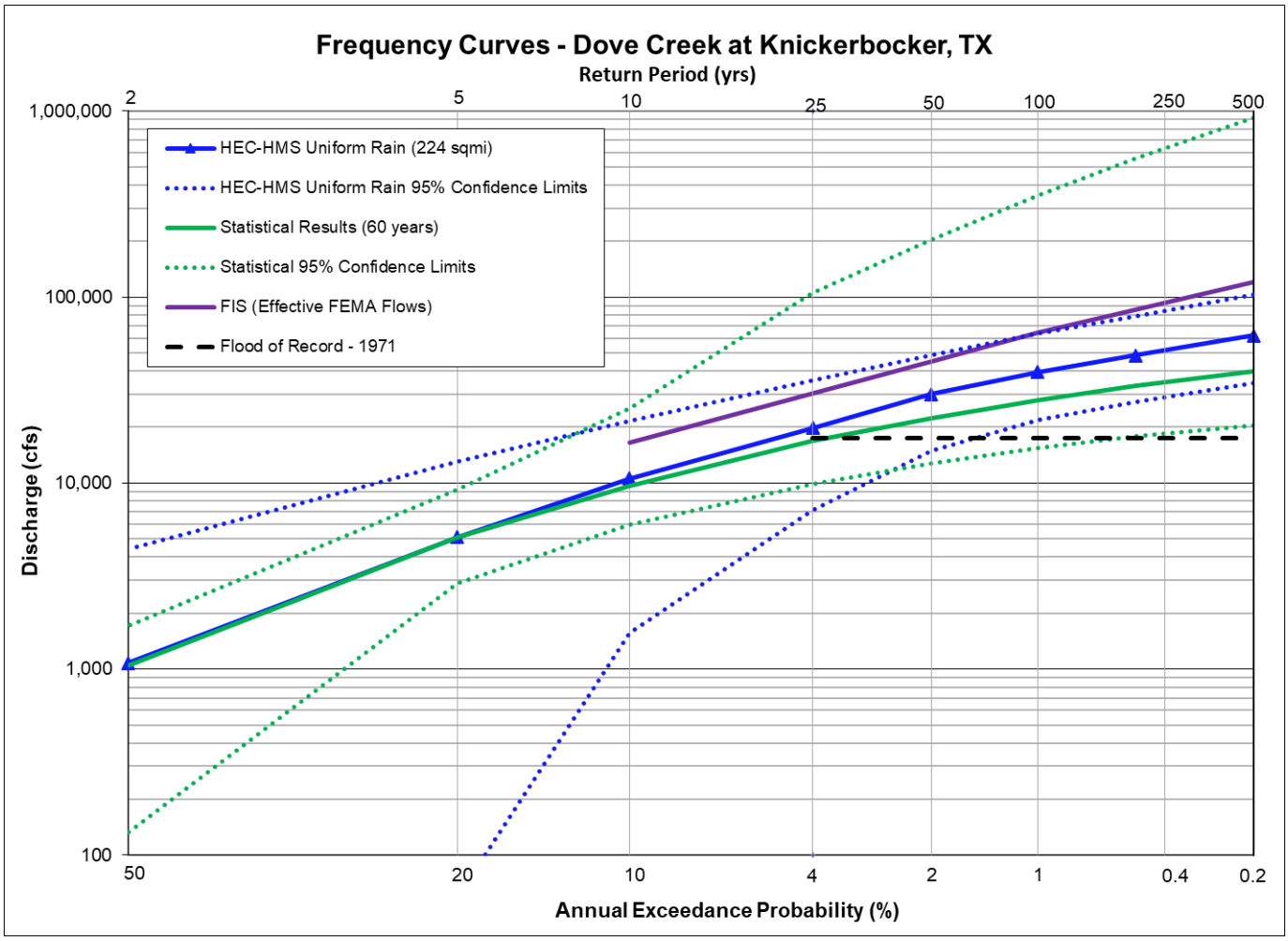

Figure 12.20: Flow Frequency Curve Comparison for the Dove Creek at Knickerbocker, TX

The next point of comparison is Dover Creek at Knickerbocker, Texas as shown in the preceding table and figure. This gage is upstream of Twin Buttes Reservoir in the Concho River basin and has a drainage area of about 220 square miles. This gage is also located in the portion of the study area that is experiencing declining flow trends.

The effective FEMA flows for this location came from a 1990 uncalibrated rainfall runoff model for the Tom Green County's FIS. As shown in Figure 12.20, the effective FEMA flows are near the upper confidence limits of the HEC-HMS results and are substantially higher than the statistical results.

The statistical analysis of the gage record produced lower estimates of the frequency floods based on 60 years of gage record. This is because the largest flood in the record at this location was the 1971 peak of 17,500 cfs, which is a relatively small flood. Since the available data sample at this gage may not be representative of its true flooding potential from a large storm event, the statistical results may be underestimating the 1% AEP (100-yr) flood event.

The HEC-HMS results were significantly higher than the statistical results but still well within their confidence bounds, as shown in Figure 12.20. The HEC-HMS results have the advantage of being based on regional rainfall depths from NOAA Atlas 14 combined with calibrated model parameters, which represents a more robust dataset than the sample of flood events that is available at a particular gage.

The next point of comparison is Pecan Creek near San Angelo, Texas as shown in the following table and figure. This gage is upstream of Lake Nasworthy in the Concho River basin and has a drainage area of about 81 square miles. This gage is also located in the portion of the study area that is experiencing declining flow trends.

The effective FEMA flows for this location came from a 1990 uncalibrated rainfall runoff model for the Tom Green County's FIS. As shown in Figure 12.21, the effective FEMA flows are lower than both the statistical analysis and the HEC-HMS results at the 1% AEP (100-yr) frequency.

Figure 12.21 shows that the HEC-HMS results are similar to the current statistical analysis of the gage record based on 60 years of record at the 1% AEP (100-yr) frequency, but the HEC-HMS results are significantly lower than the statistical results at the 0.2% AEP (500-yr) frequency. However, the 0.2% AEP statistical estimate is quite sensitive to the gage's data sample and any changes in the station skew, and this estimate is usually still very unstable after 60 years of record. The HEC-HMS results, on the other hand, are based on the regional rainfall statistics of NOAA Atlas 14, which tend to make their frequency flood estimates more consistent and less subject to change.

Table 12.21: Frequency Flow (cfs) Results Comparison for Pecan Creek near San Angelo, TX

Annual Exceedance Probability (AEP)	Return Period (years)	Currently Effective FEMA FIS	Statistical Analysis of the Gage Record (Ch 5) (60 years)	HEC-HMS Uniform Rain Frequency Storm (Ch 6) (81 sq mi)
0.002	500	40,340	78,300	43,500
0.005	200		49,600	36,200
0.01	100	21,620	33,200	30,000
0.02	50	17,100	21,000	23,700
0.04	25		12,200	13,100
0.1	10	8,620	4,950	4,920
0.2	5		1,980	1,980
0.5	2		278	280

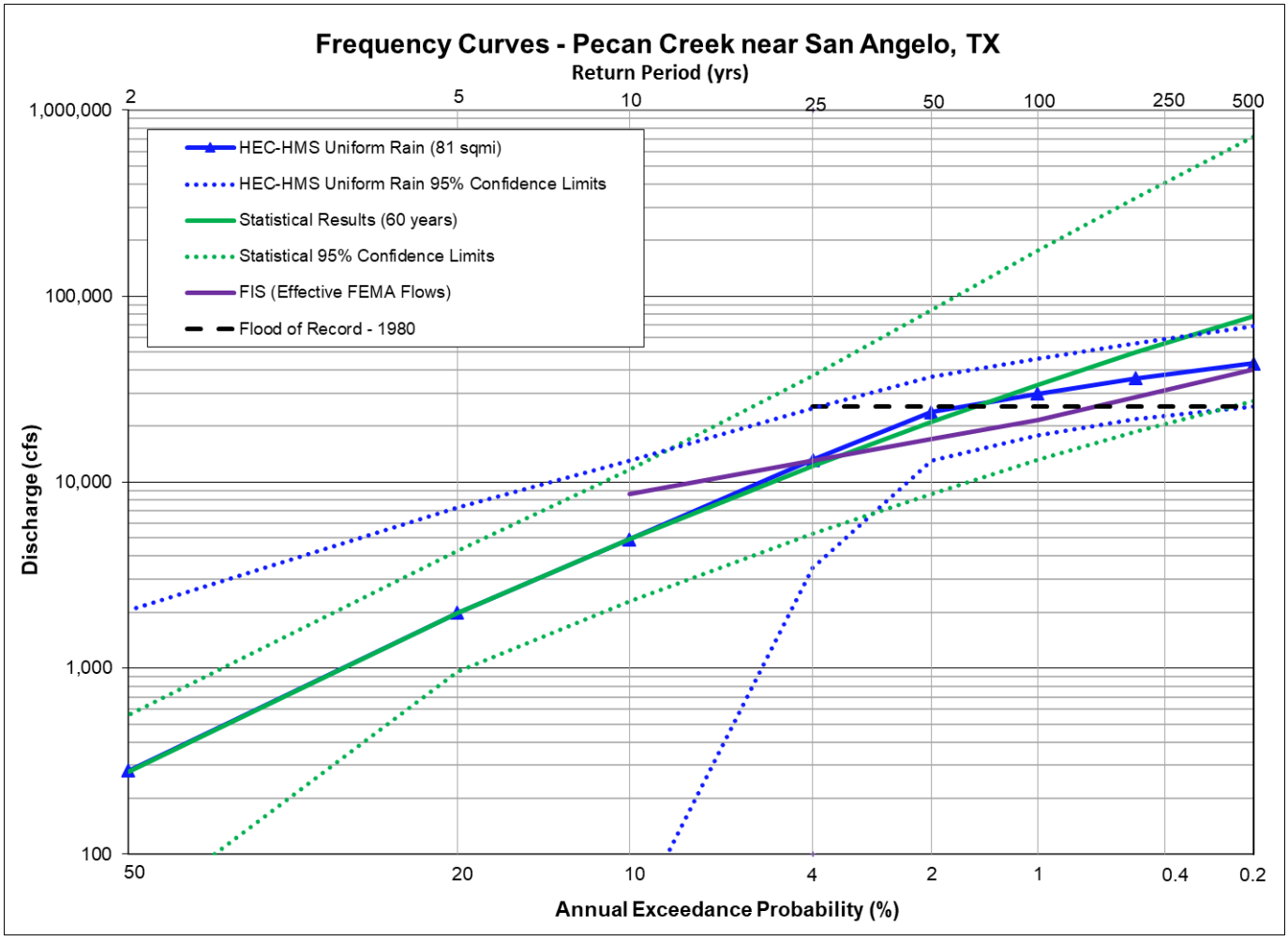

Figure 12.21: Flow Frequency Curve Comparison for Pecan Creek near San Angelo, TX

Table 12.22: Frequency Flow (cfs) Results Comparison for the North Concho River at Sterling City, TX

Annual Exceedance Probability (AEP)	Return Period (years)	Currently Effective FEMA FIS	Statistical Analysis of the Gage Record (Ch 5) (81 years)	HEC-HMS Uniform Rain Frequency Storm (Ch 6) (586 sq mi)	HEC-HMS Elliptical Frequency Storm (Ch 7) (586 sq mi)
0.002	500		33,500	107,300	94,500
0.005	200		27,000	84,100	73,700
0.01	100		22,100	66,800	56,900
0.02	50		17,200	47,000	38,900
0.04	25		12,600	23,300	23,600
0.1	10		7,210	9,120	9,690
0.2	5		3,890	3,900	4,740
0.5	2		905	910	870

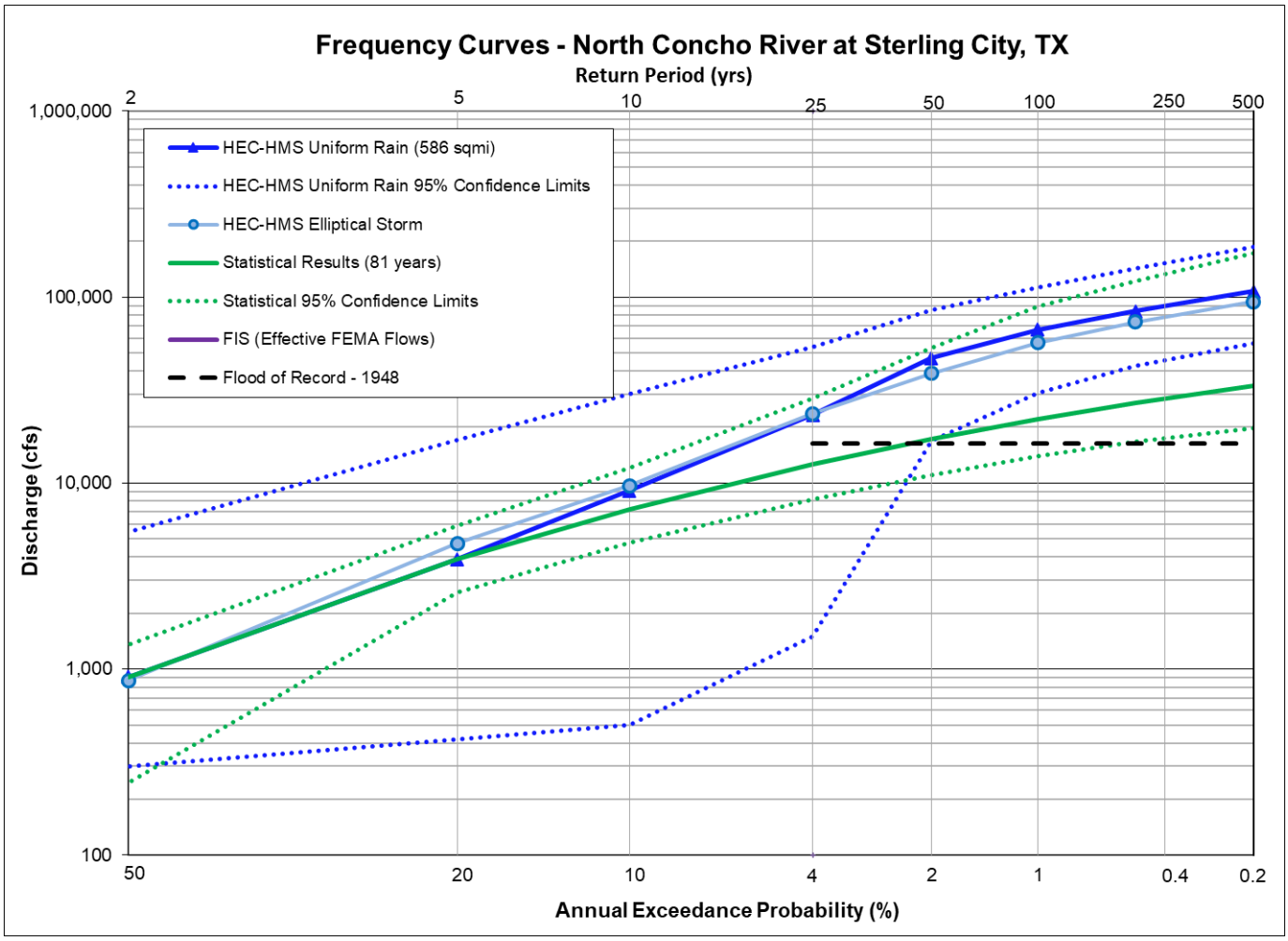

Figure 12.22: Flow Frequency Curve Comparison for the North Concho River at Sterling City, TX

The next point of comparison is the North Concho River at Sterling City, Texas as shown in the preceding table and figure. This gage is upstream of O.C. Fisher Reservoir in the Concho River basin and has a drainage area of over 500 square miles. This gage is also located in the portion of the study area that is experiencing declining flow trends.

There are no published FEMA flows for this location. As shown in Figure 12.22, the statistical analysis of the gage record produced relatively low estimates of the frequency floods based on 80+ years of gage record. This is because the largest flood in the record was the 1948 peak of 16,600 cfs, which is a relatively small flood peak for a watershed of several hundred square miles. Therefore, the available data sample at this gage may not be representative of the true flooding potential of the watershed with a large storm event. The HEC-HMS results were substantially higher than the statistical results. Those results are based on the expected regional rainfall depths from NOAA Atlas 14 as well as the calibrated loss rates and other model parameters. However, the HEC-HMS results are still well within the confidence limits of the statistical analysis.

The next point of comparison is the North Concho River near Carlsbad, Texas as shown in the following table and figure. This gage is upstream of O.C. Fisher Reservoir in the Concho River basin and has a drainage area of about 1,200 square miles. This gage is also located in the portion of the study area that is experiencing declining flow trends, and the data shows a dramatic change point in the 1960s, as shown in Figure 12.23c below. There are no reservoirs upstream of this gage nor is there any obvious change in the watershed which would explain the change in the streamflow shown in this figure. See the discussion declining flow trends in Chapter 5 for more information.

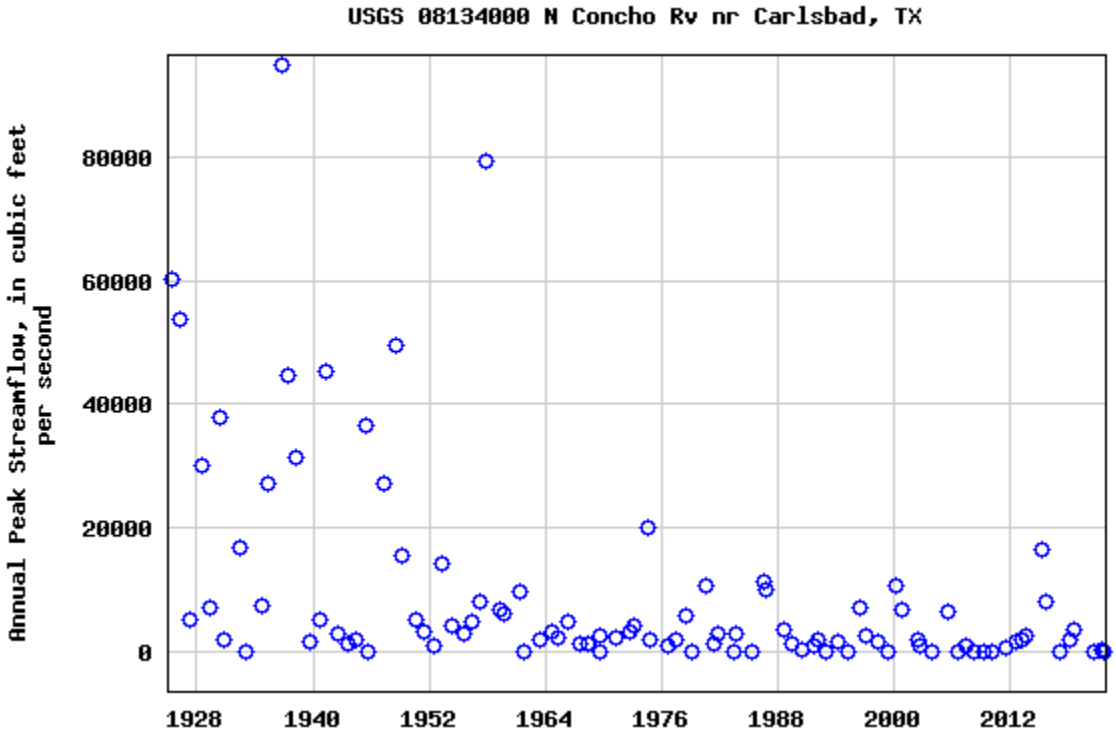

Figure 12:23c: Observed USGS Annual Peak Discharges for the North Concho River near Carlsbad

The effective FEMA flows for this location came from a 1990 uncalibrated rainfall runoff model for the Tom Green County's FIS. As shown in Figure 12.23a, the effective FEMA flows are significantly higher than both the statistical

analysis and the HEC-HMS results. In fact, the effective FEMA flows are above the upper confidence bounds for NOAA Atlas 14 in the HEC-HMS rainfall runoff modeling.

Table 12.23: Frequency Flow (cfs) Results Comparison for the North Concho River near Carlsbad, TX

Annual Exceedance Probability (AEP)	Return Period (years)	Currently Effective FEMA FIS	Statistical Analysis of the Gage Record (Ch 5) (59 years)	Alternate Statistical Analysis of the Gage Record (Ch 5) (96 yrs)	HEC-HMS Uniform Rain Frequency Storm (Ch 6) (1221 sq mi)	HEC-HMS Elliptical Frequency Storm (Ch 7) (1221 sq mi)
0.002	500	225,650	44,700	205,000	107,000	91,800
0.005	200		32,200	138,000	83,500	71,300
0.01	100	122,900	24,500	99,000	65,900	54,900
0.02	50	92,050	18,200	68,500	46,300	37,900
0.04	25		13,100	45,100	22,600	21,100
0.1	10	35,950	7,790	23,200	10,000	8,260
0.2	5		4,790	12,200	5,510	4,770
0.5	2		1,870	3,420	2,000	1,800

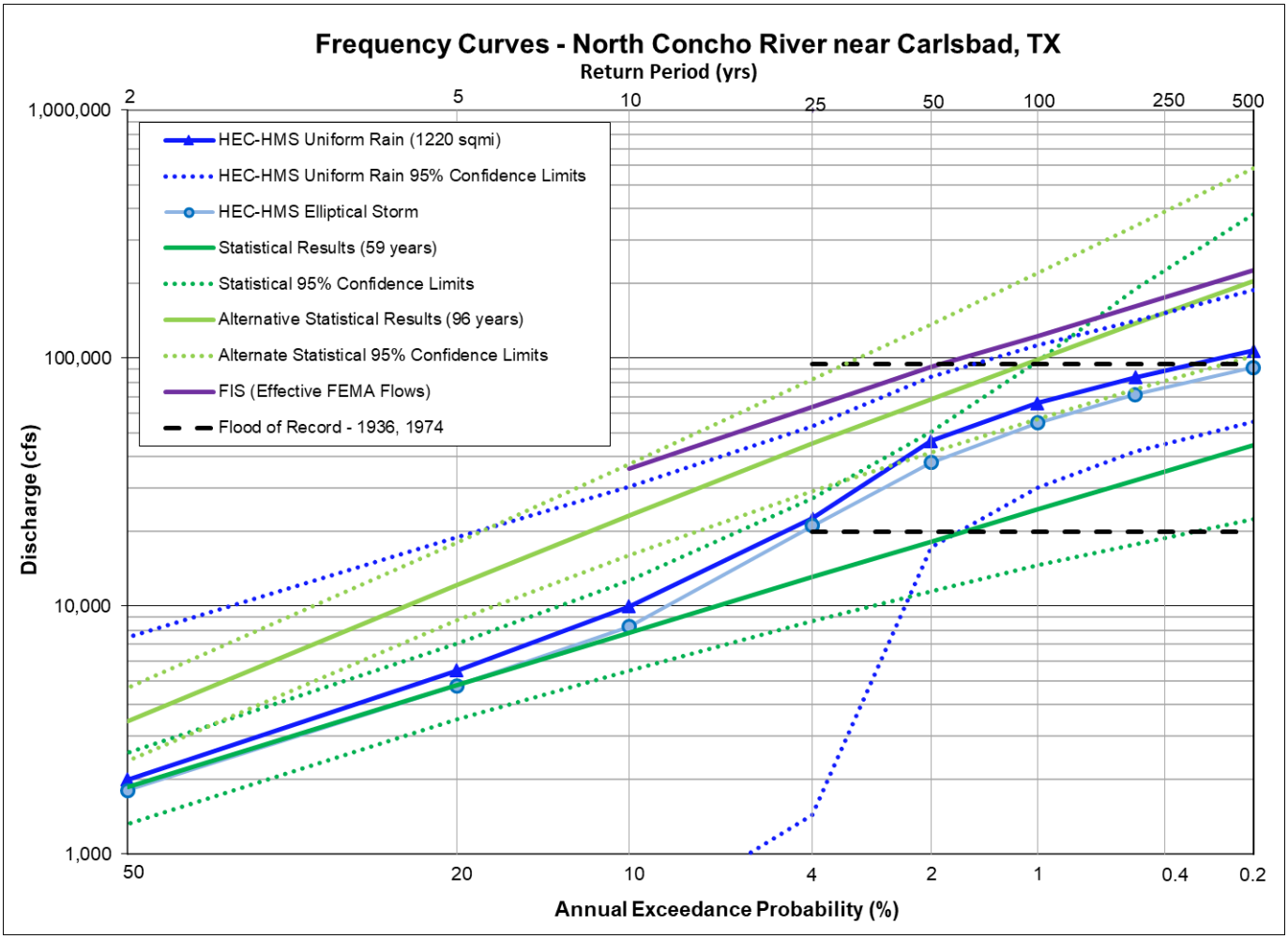

Figure 12.23a: Flow Frequency Curve Comparison for the North Concho River near Carlsbad, TX

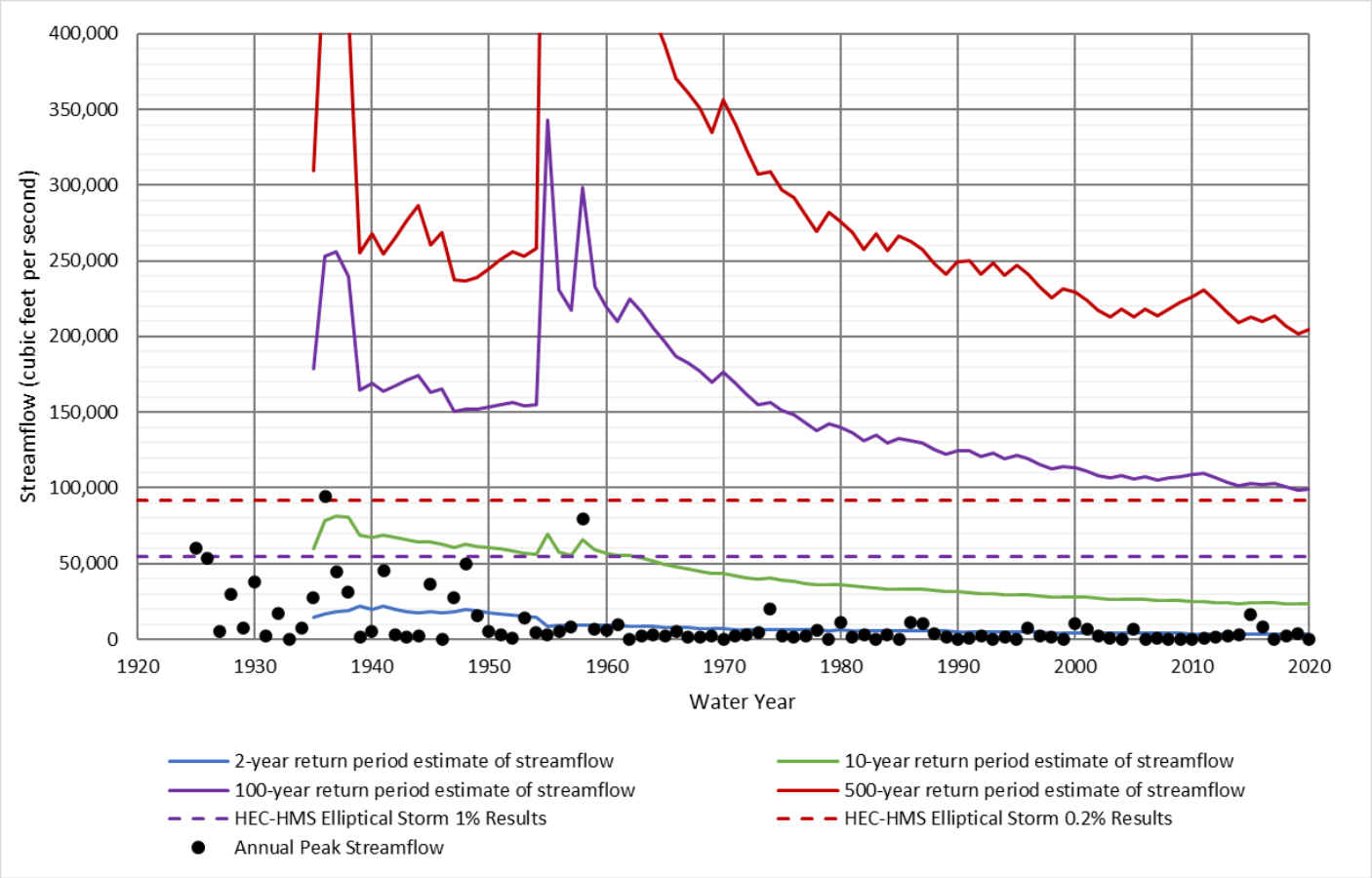

Figure 12.23b: Statistical Change Over Time Comparison for the North Concho River near Carlsbad, TX

Due to the declining flow trends at this location, two different statistical analyses of the gage record were performed, as shown in Figure 12.23a. The first was based on only the most recent 59 years of data (after that change point in the 1960s shown in Figure 12.23c), and the other was based on the entire 96 years of gage record. The results of these two statistical analyses are so dramatically different that even their confidence bounds do not overlap one another for a large portion of the frequency curve. For example, the flood of record for the whole period of record was 94,600 cfs in 1936, while the largest flood in the past 59 years is only 20,000 cfs. These differential results are obvious evidence of non-stationarity in the watershed, which Bulletin 17C statistical analyses are not equipped to address. The HEC-HMS results shown in Figure 12.23a happed fall in between the two statistical analyses with the 1% and 0.2% AEP estimates trending upward, while the common 50% and 20% AEP estimates fall close to the recent gage record statistical results.

Figure 12.23b is a plot of the changes in the flood frequency estimates over time when considering the entire period of record. In this plot, one can see several large floods in the 1930s through 1950s, but since 1960s, all observed stream flows have been below the 10-year statistical estimate. In a stationary watershed, one would expect the 10-year statistical estimate to stabilize within 30 to 40 years, but in this case, one can see that the 10-year estimate continued to decline after more than 90 years of data. This is another result of the declining flow trends in the basin. From this figure, one may also observe that the HEC-HMS 1% AEP estimate is equal to the 10-year estimate in 1960. The HEC-HMS elliptical result shown in this figure are based on the NOAA Atlas 14 regional rainfall statistics coupled with the calibrated model parameters.

The next point of comparison is the North Concho River at San Angelo, Texas as shown in the following table and figure. This is a discontinued USGS gage that was located a short distance downstream of O.C. Fisher Reservoir in the City of San Angelo in the Concho River basin. The gage had a drainage area of about 1,500 square miles; however, all but 22 square miles were controlled by O.C. Fisher Reservoir. This gage is located in the portion of the basin that is experiencing declining flow trends, which had caused the observed pool elevations of O.C. Fisher Reservoir to be well below their intended design levels for the past several decades.

The effective FEMA flows for this location came from a 1990 SUPER statistical analysis for the Tom Green County FIS. SUPER was a USACE software that was an early predecessor of RiverWare. More information on SUPER is available in Chapter 8. Figure 12.24 shows that the effective FEMA flows are significantly higher than all of the other results except for RiverWare. One reason for this is likely because the FEMA flows were based on an early period of record (1930 – 1989) that included several large flood events but did not include the recent declining flow period.

Figure 12.24 also shows that the HEC-HMS results were significantly higher than the statistical results even for the 1% AEP (100-yr) event and even for the common events such as the 50% AEP (2-year) flood. The reason for this difference at the 50% AEP (2-year) frequency stems from the assumed percent impervious in the City of San Angelo. The available gage record for the statistical analysis was from 1952-1990, and the watershed during that time did not have as much urban development as it does today. The gage statistics would reflect the percent impervious that existing in the 1950s through 1980s, whereas the HEC-HMS model results reflect the percent impervious as it existed in 2016. US Census data shows that the population of San Angelo increase by over 60% between 1970 and 2020; therefore, the newer HEC-HMS results would be expected to produce higher discharges based on the higher percent imperviousness. The HEC-HMS results are also higher than the statistical results for the rare events like the 1% AEP (100-year) flood due to a lack of large observed floods during the relatively short gage record period of 38 years.

Finally, Figure 12.24 also shows that the HEC-HMS results are higher than the RMC-RFA results for O.C. Fisher Reservoir. The difference here is that the HEC-HMS assumed that the gates of O.C. Fisher reservoir were closed, so the HEC-HMS peak flows were produced only from the 22 square miles of urban runoff downstream of the dam. The RMC-RFA reservoir analysis, on the other hand, considers only the inflows and outflows from the dam, and does not include any downstream runoff. Therefore, Figure 12.24 illustrates that local runoff becomes the dominant flood risk over releases from the dam for this particular location.

Table 12.24: Frequency Flow (cfs) Results Comparison for the North Concho River at San Angelo, TX

Annual Exceedance Probability (AEP)	Return Period (years)	Currently Effective FEMA FIS	Statistical Analysis of the Gage Record (Ch 5) (38 years)	HEC-HMS Uniform Rain Frequency Storm (Ch 6) (22 sq mi)	Statistical Analysis of Extended RiverWare Record (Ch 8) (90 years)	Reservoir Analysis of OC Fisher (Ch 9)
0.002	500	20,000	17,700	16,207	184,000	3,250
0.005	200		10,800	13,725	66,100	3,100
0.01	100	20,000	7,330	11,751	28,400	2,850
0.02	50	17,000	4,870	9,733	11,300	2,700
0.04	25		3,170	4,776	4,090	2,600
0.1	10	10,000	1,700	2,704	849	2,550
0.2	5		996	1,861	196	2,400
0.5	2		407	1,462	12	1,900

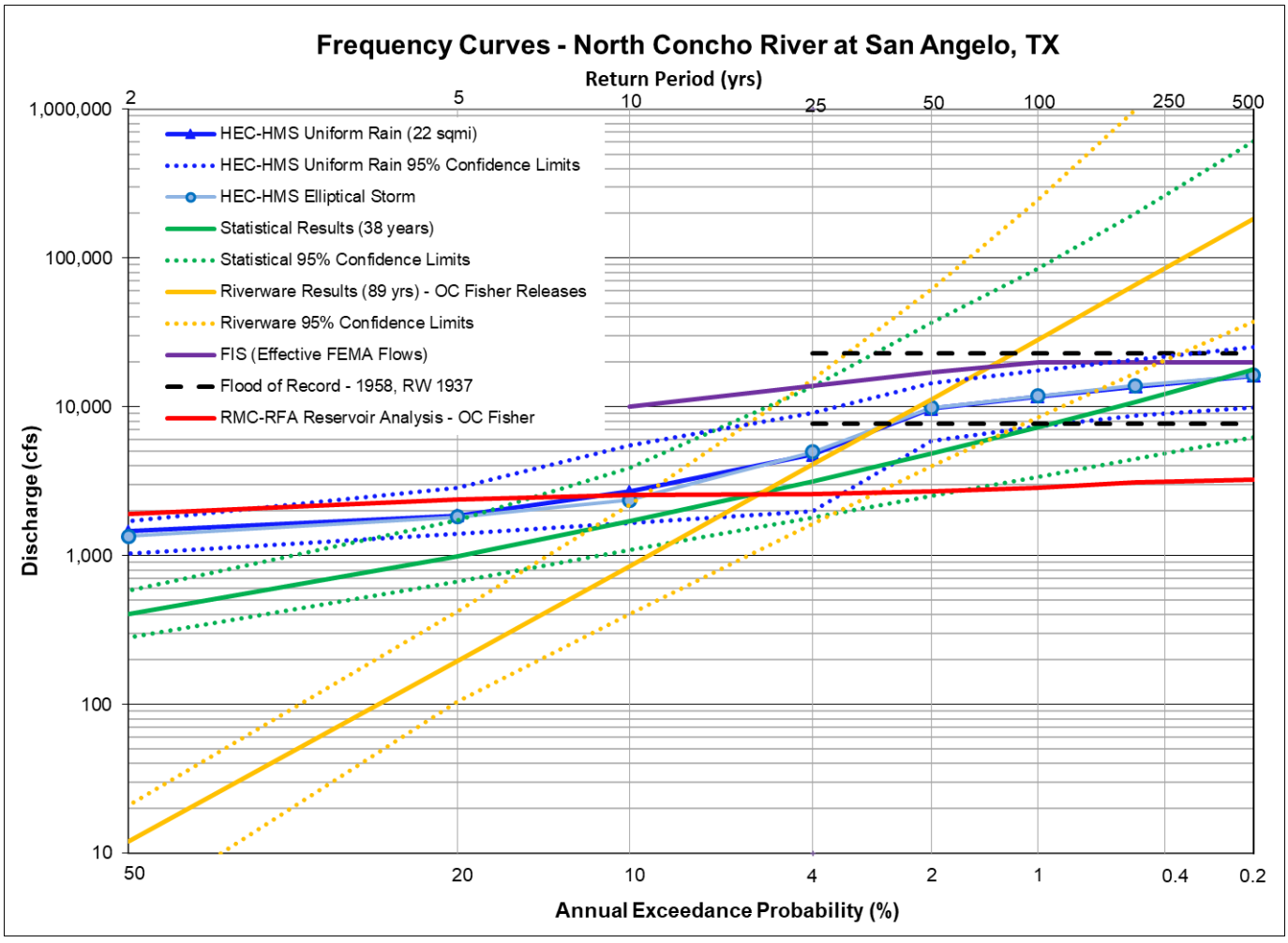

Figure 12.24: Flow Frequency Curve Comparison for the North Concho River at San Angelo, TX

Table 12.25: Frequency Flow (cfs) Results Comparison for the South Concho River below Twin Buttes Reservoir

Annual Exceedance Probability (AEP)	Return Period (years)	Currently Effective FEMA FIS	Statistical Analysis of the Gage Record (Ch 5)	HEC-HMS Uniform Rain Frequency Storm (Ch 6) (3420 sq mi)	HEC-HMS Elliptical Frequency Storm (Ch 7) (3420 sq mi)	Statistical Analysis of Extended RiverWare Record (Ch 8) (90 years)	Reservoir Analysis of Twin Buttes Reservoir (Ch 9)
0.002	500	25,000		42,100	9,000	77,900	9,100
0.005	200			16,500	9,000	36,900	9,000
0.01	100	25,000		9,000	9,000	20,100	9,000
0.02	50	21,000		9,000	5,000	10,400	5,000
0.04	25			7,200	3,000	5,110	5,000
0.1	10	12,500		3,000	3,000	1,730	5,000
0.2	5			-	700	641	3,000
0.5	2			-	100	103	3,000

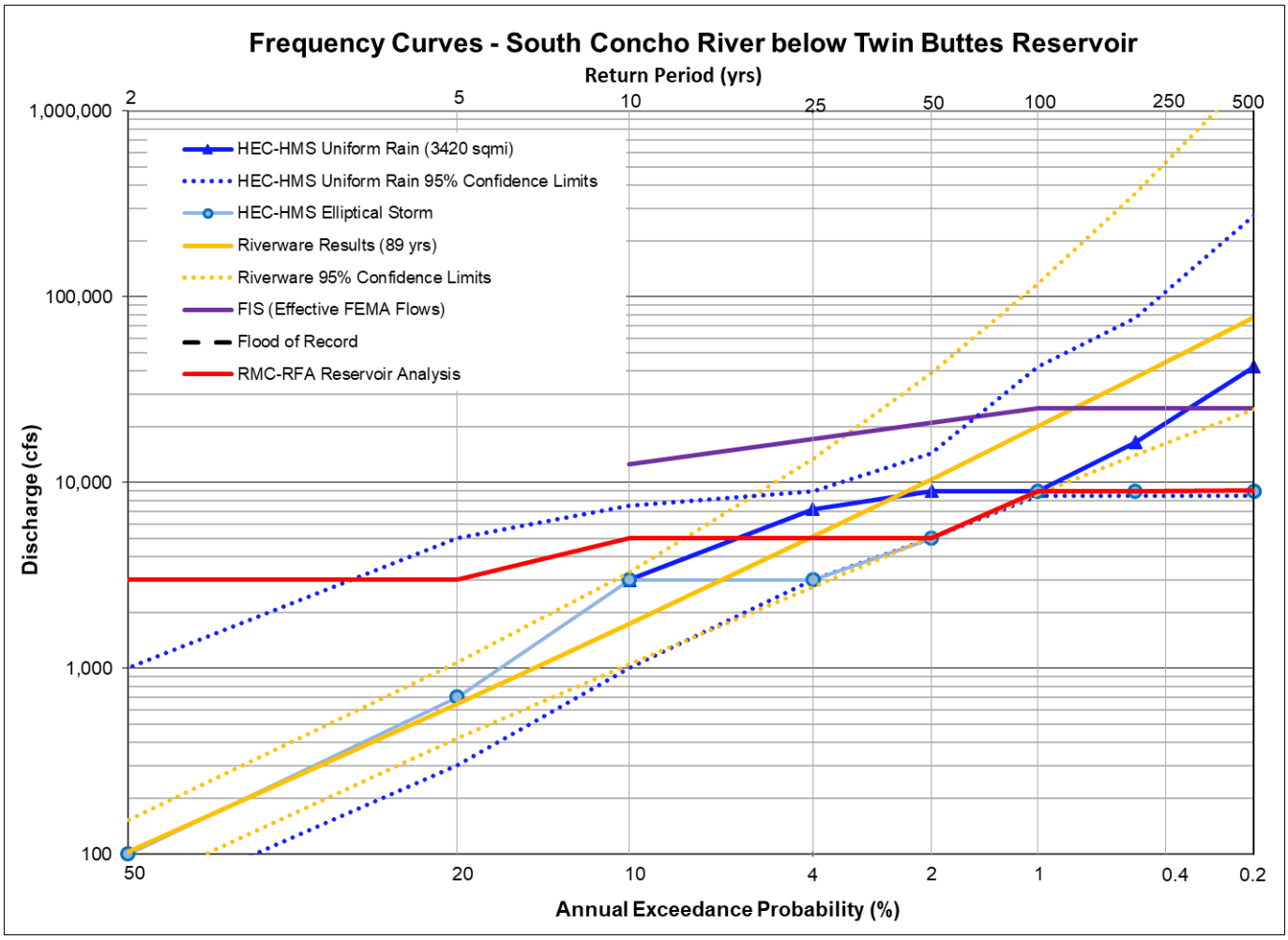

Figure 12.25: Flow Frequency Curve Comparison for the South Concho River below Twin Buttes Reservoir

The next point of comparison is the South Concho River below Twin Buttes Reservoir as shown in the preceding table and figure. Twin Buttes Reservoir is a flood control reservoir that is operated by the Bureau of Reclamation. It has a drainage area of about 3,400 square miles. Because it is located in the portion of the basin that is experiencing declining flow trends, the observed pool elevations in Twin Buttes are often significantly below the designed conservation pool level.

The effective FEMA flows for this location came from a 1990 SUPER statistical analysis for the Tom Green County FIS. SUPER was a USACE software that was an early predecessor of RiverWare. More information on SUPER is available in Chapter 8. Figure 12.25 shows that the effective FEMA flows are significantly higher than all of the other results at the 1% AEP (100-year) frequency (except perhaps for RiverWare). One reason for this is likely because the FEMA flows were based on an earlier period of record (1930 – 1989) that included several large flood events but did not include the recent declining flow period.

The HEC-HMS elliptical storms and the RMC-RFA results were identical to one another for the 2% through 0.2% AEP (50-year through 500-year) frequency events. Both of these analyses take into account the recent low observed pool elevations which would be expected to lower the expected magnitudes of the frequencies pool elevations and releases from the dam. For the more frequent events, (50% to 4% AEP) (2-year to 25-year), the HEC-HMS results are similar to the statistical results of the RiverWare simulated record, whereas the RMC-RFA releases reflect the maximum releases that are allowable from the dam at their corresponding frequency elevations.

The next point of comparison is the Concho River at San Angelo, Texas as shown in the following table and figures. This gage is located below the confluence of the North and South Concho Rivers in the City of San Angelo. It has a total drainage area of over 5,000 square miles, but only 161 square miles of that is not controlled by O.C. Fisher or Twin Buttes Reservoir.

The effective FEMA flows for this location came from a 1990 uncalibrated rainfall runoff model for the Tom Green County's FIS. As shown in Figure 12.26a, the effective FEMA flows are similar to the results from several of the analyses in this study including the statistical results with the 1930s regulated peaks, the RiverWare results, and the HEC-HMS uniform rainfall results. The outlier on Figure 12.26a is the statistical results from the most recent 58 years of record because that period did not experience any large floods, as shown in Figure 12.26b. The change over time plot of Figure 12.26b, which includes the regulated peak of 1936, also shows that the HEC-HMS uniform rainfall results fall near the mid-point of the range of variation in the 1% AEP (100-year) statistical estimates that have been observed over the past 50 years.

Table 12.26: Frequency Flow (cfs) Results Comparison for the Concho River at San Angelo, Texas

Annual Exceedance Probability (AEP)	Return Period (years)	Currently Effective FEMA FIS	Statistical Analysis of the Gage Record (Ch 5) (58 years)	HEC-HMS Uniform Rain Frequency Storm (Ch 6) (161 sq mi)	HEC-HMS Elliptical Frequency Storm (Ch 7) (5047 sq mi)	Statistical Analysis of Extended RiverWare Record (Ch 8) (90 years)	Statistical Analysis with Historic 1930s Storms (Ch 10)
0.002	500	54,950	31,800	56,200	60,800	55,700	62,800
0.005	200		22,300	45,300	49,400	43,300	38,900
0.01	100	29,800	16,800	36,200	40,500	34,500	26,700
0.02	50	29,350	12,400	27,400	31,300	26,400	17,900
0.04	25		8,930	15,200	18,400	19,200	11,800
0.1	10	13,550	5,460	6,860	7,470	11,100	6,430
0.2	5		3,520	3,800	4,060	6,220	3,810
0.5	2		1,590	2,990	3,000	1,740	1,570

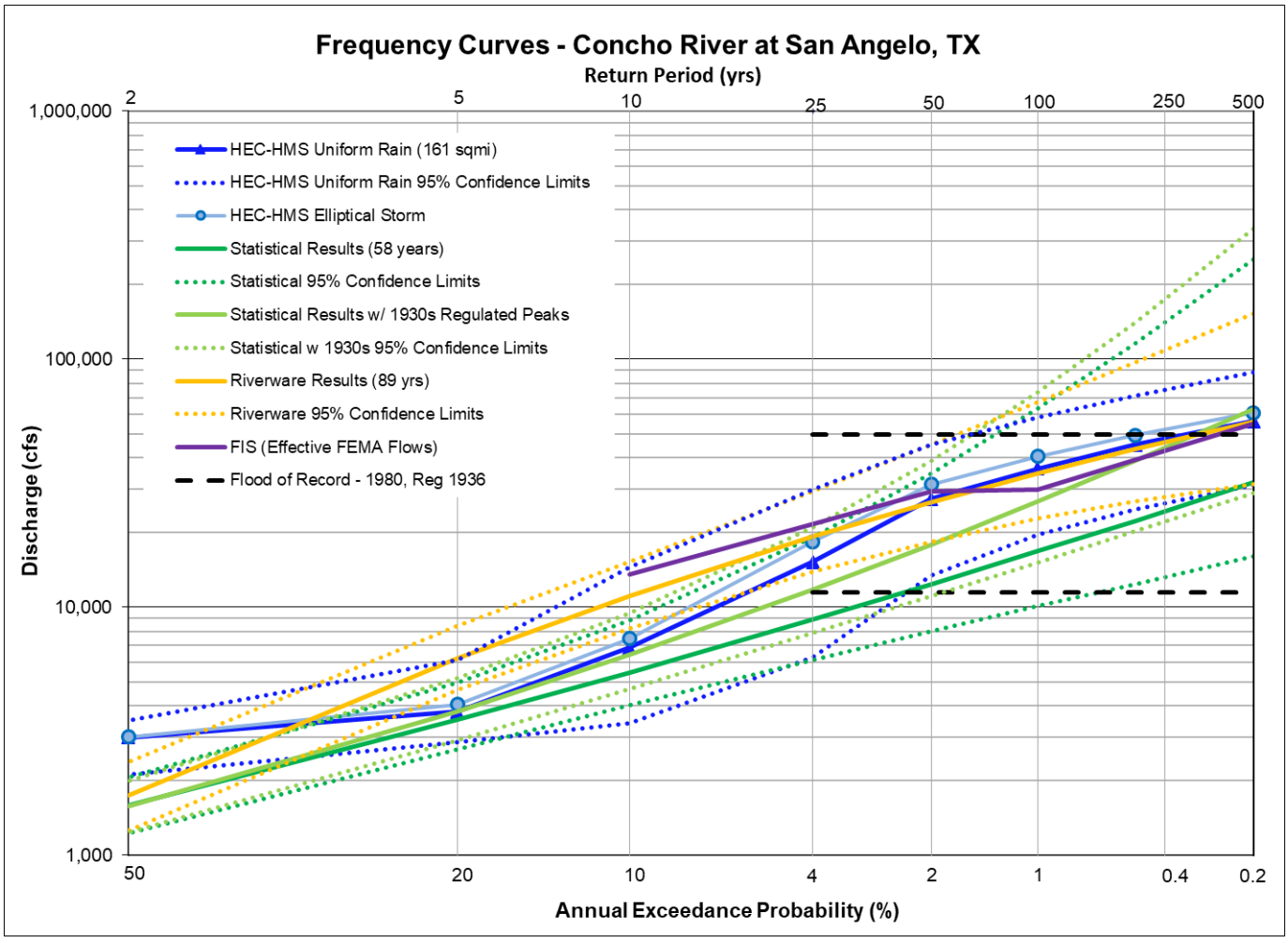

Figure 12.26a: Flow Frequency Curve Comparison for the Concho River at San Angelo, Texas

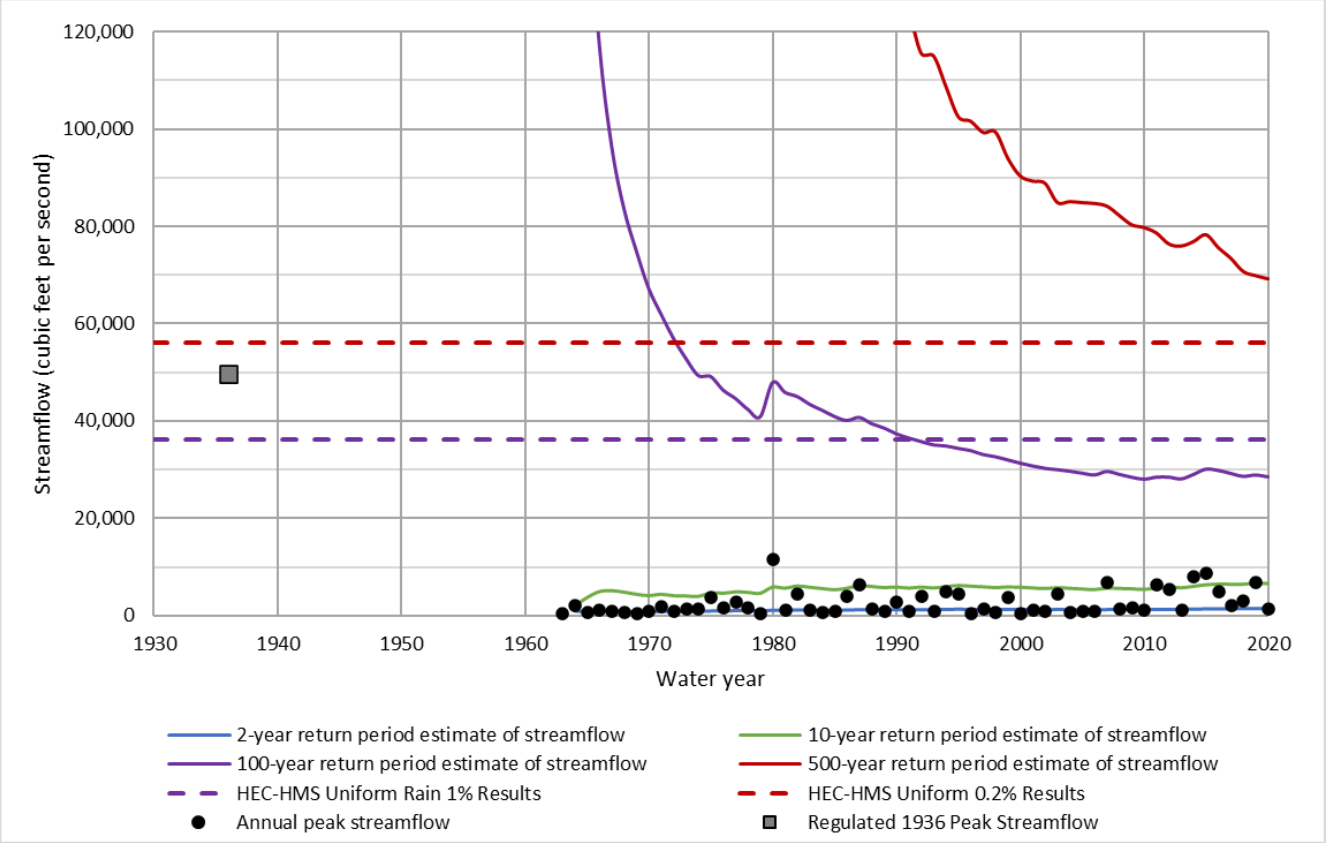

Figure 12.26b: Statistical Change Over Time Comparison for the Concho River at San Angelo, Texas

The next point of comparison is the Concho River at Paint Rock, Texas as shown in the following table and figures. This gage has a total drainage area of over 6,000 square miles, but only 1,200 square miles of that is downstream of O.C. Fisher and Twin Buttes Reservoirs.

There are no published FEMA flows that are available for this location. Figure 12.27a shows that the HEC-HMS elliptical storm results are significantly higher than any of the statistical or RiverWare results for this location. However, the statistical results with the 1930s regulated peaks came the closest to the HEC-HMS results because they included a large flood peak for the 1936 regulated flood event. Figure 12.27b is a change over time plot of the statistical analysis using the 1930s regulated peaks, and it shows that the HEC-HMS 1% AEP elliptical storm results fall near the mid-point of the range of variation in the 1% AEP (100-year) statistical estimates that have been observed over the past 40 years.

Table 12.27: Frequency Flow (cfs) Results Comparison for the Concho River at Paint Rock, TX

Annual Exceedance Probability (AEP)	Return Period (years)	Currently Effective FEMA FIS	Statistical Analysis of the Gage Record (Ch 5) (58 years)	HEC-HMS Uniform Rain Frequency Storm (Ch 6) (1200 sq mi)	HEC-HMS Elliptical Frequency Storm (Ch 7) (6088 sq mi)	Statistical Analysis of Extended RiverWare Record (Ch 8) (90 years)	Statistical Analysis with Historic 1930s Storms (Ch 10)
0.002	500		78,400	215,800	168,800	60,900	165,200
0.005	200		56,700	168,100	129,500	47,800	105,100
0.01	100		43,300	134,800	99,700	38,800	72,700
0.02	50		32,100	99,600	71,000	30,800	48,900
0.04	25		23,000	46,000	42,200	23,600	31,700
0.1	10		13,500	17,400	14,800	15,400	16,400
0.2	5		8,140	8,130	8,170	10,100	9,010
0.5	2		3,000	2,990	2,790	4,270	2,980

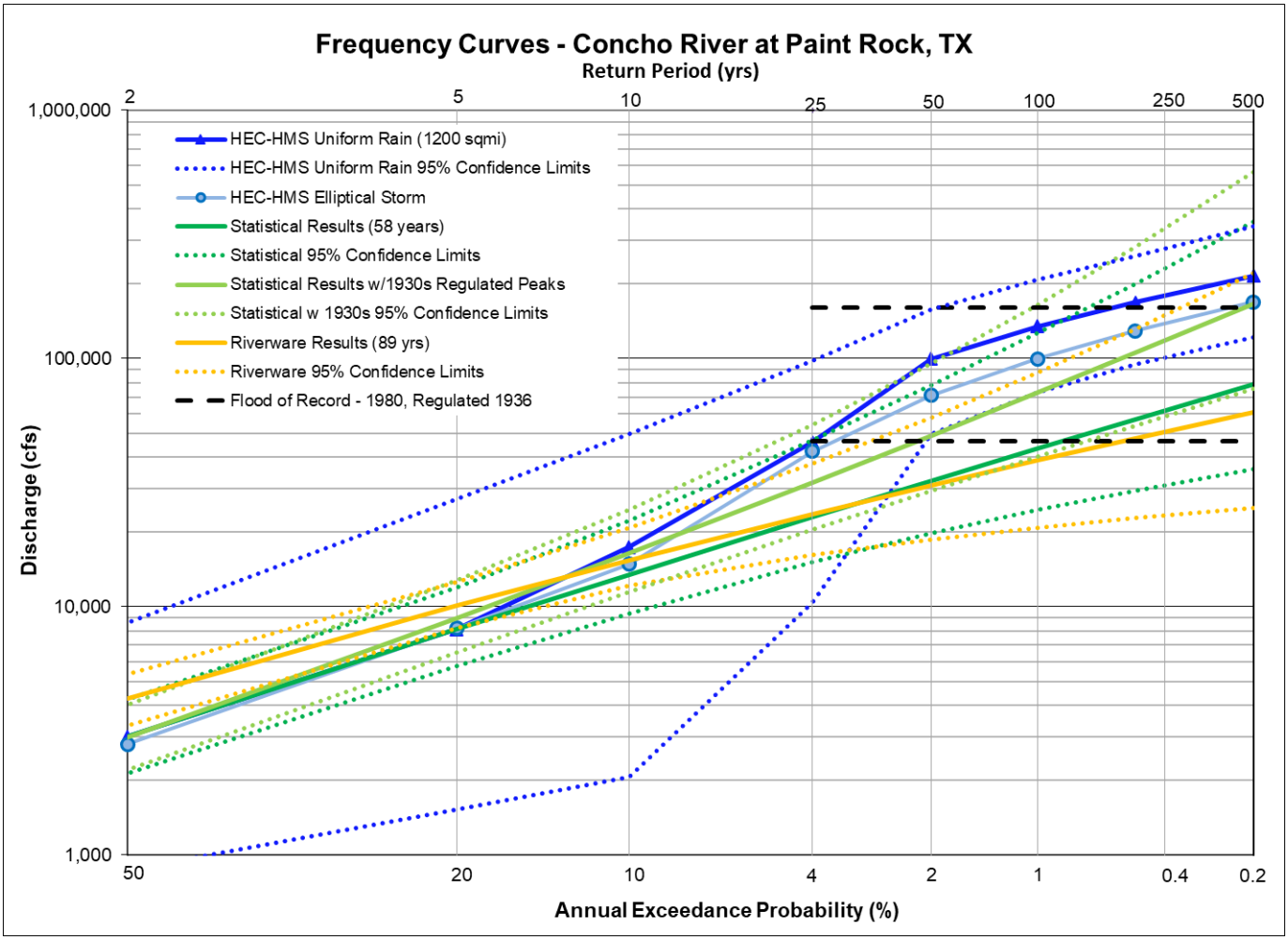

Figure 12.27a: Flow Frequency Curve Comparison for the Concho River at Paint Rock, TX

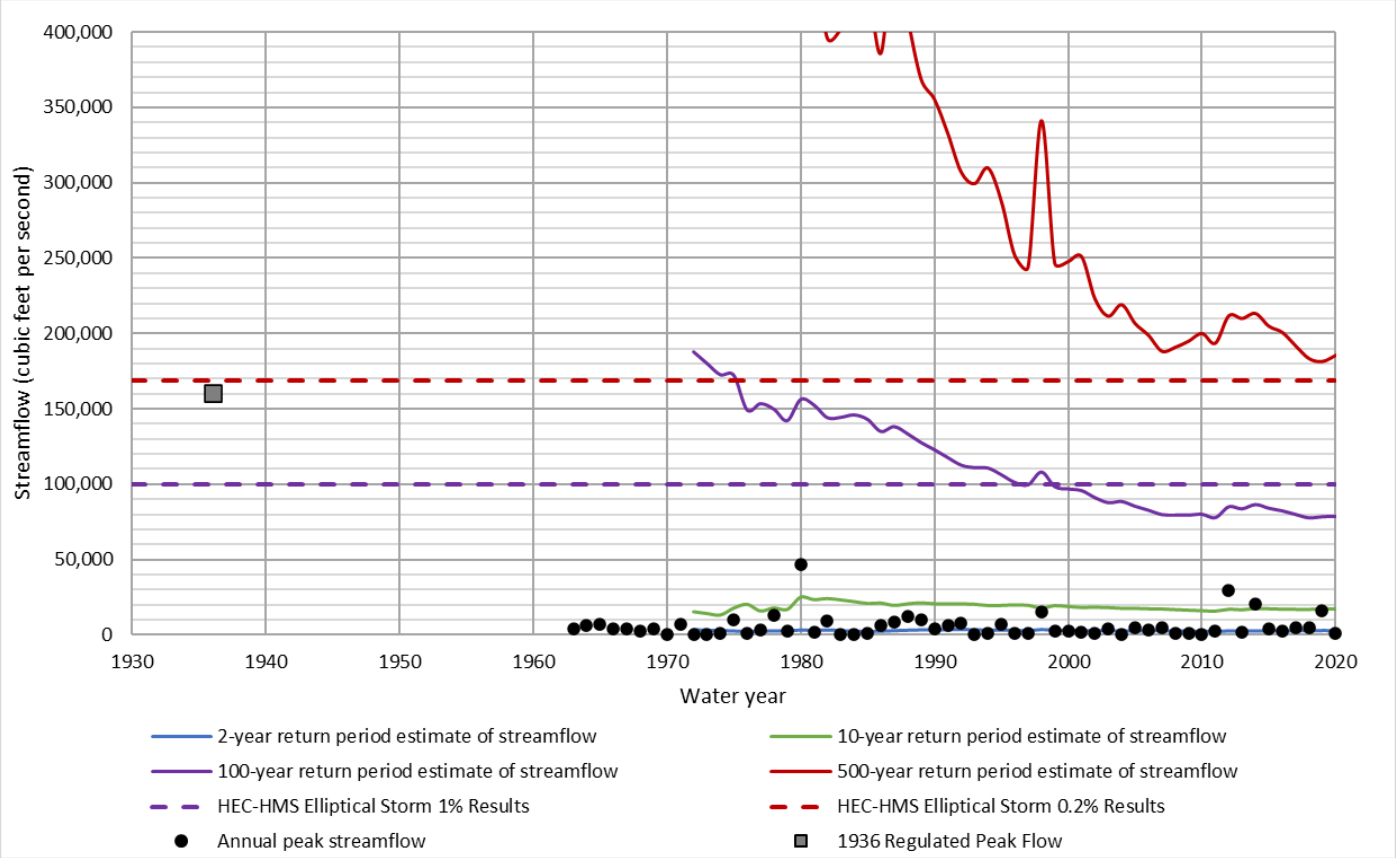

Figure 12.27b: Statistical Change Over Time Comparison for the Concho River at Paint Rock, TX

12.1.3 Pecan Bayou and San Saba Basin Gage Locations

Table 12.28: Frequency Flow (cfs) Results Comparison for Hords Creek near Coleman, TX

Annual Exceedance Probability (AEP)	Return Period (years)	Currently Effective FEMA FIS	Approx BLE Data from FEMA	Statistical Analysis of the Gage Record (Ch 5) (78 years)	HEC-HMS Uniform Rain Frequency Storm (Ch 6) (58 sq mi)	Statistical Analysis of Extended RiverWare Record (Ch 8) (89 years)	Reservoir Analysis of Hords Creek Lake (Ch 9)
0.002	500	43,300		33,100	29,900	29,200	500
0.005	200			24,900	24,000	22,000	215
0.01	100	24,990		19,500	19,600	17,400	205
0.02	50	19,150		14,900	15,100	13,300	200
0.04	25			10,900	10,900	9,840	195
0.1	10	9,000		6,660	6,530	6,090	185
0.2	5			4,100	4,020	3,820	180
0.5	2			1,530	1,520	1,500	170

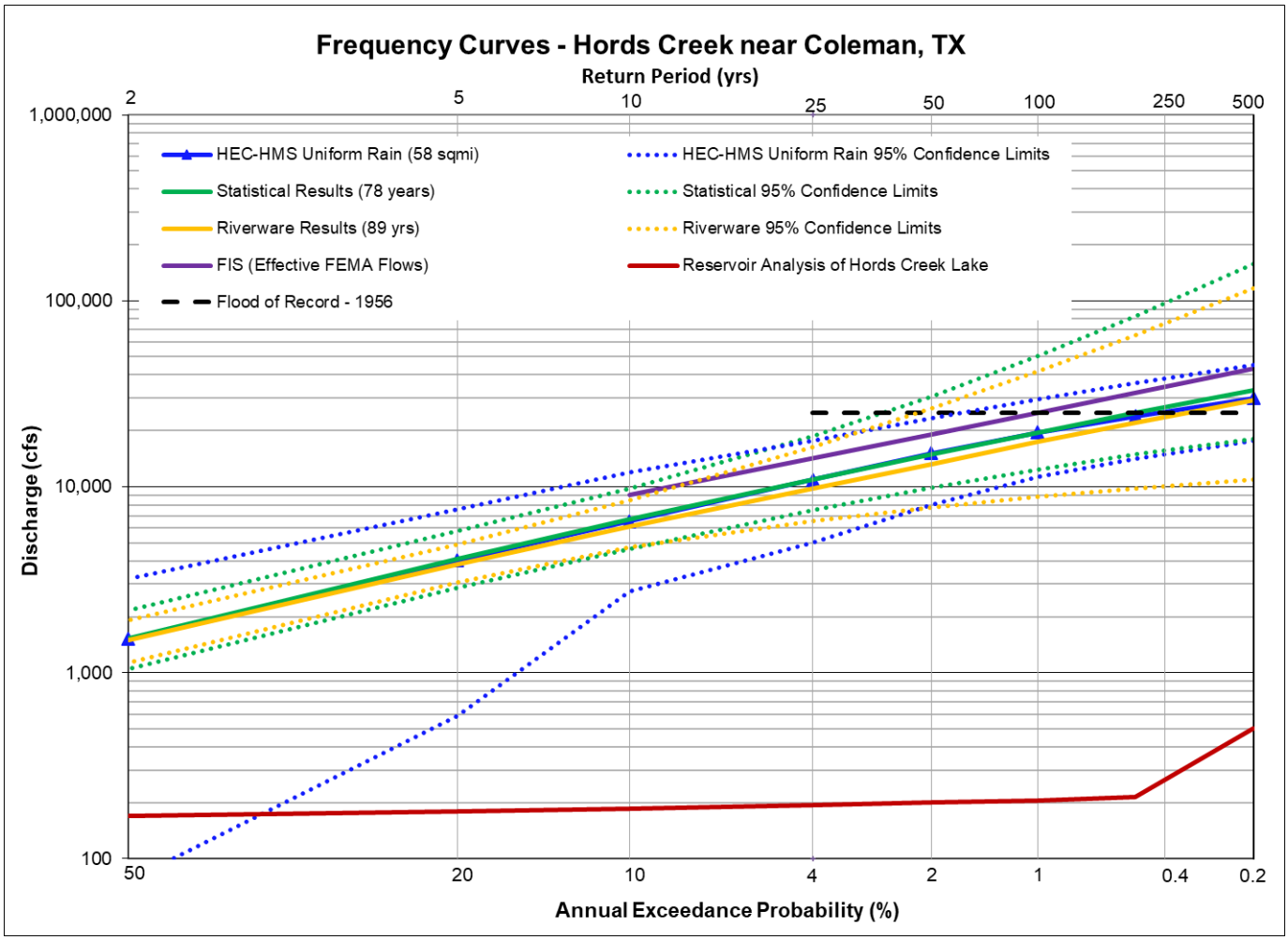

Figure 12.28: Flow Frequency Curve Comparison for Hords Creek near Coleman, TX

The first point of comparison in the Pecan Bayou watershed is Hords Creek near Coleman, Texas, as shown in the preceding table and figure. This gage has a drainage area of 107 square miles, of which 45% is controlled by Hords Creek Reservoir. Hords Creek is a flood control reservoir operated by USACE.

The effective FEMA flows for this location were based on a 1972 statistical analysis of the gage record, and they are higher than both the current statistical analysis and the HEC-HMS uniform rain results. Figure 12.28 shows that there happens to be very tight agreement between the HEC-HMS results and statistical results based on 78 years of record. The figure also shows that the results of the reservoir analysis for Hords Creek Reservoir are much lower. This means that the dominant flood risk for this location is from runoff downstream of the dam and that Hord Creek Reservoir does a good job of controlling the flows from further upstream.

The next point of comparison is Pecan Bayou at Brownwood, Texas as shown in the following table and figure. This gage has a drainage area of about 1,650 square miles, but only 100 square miles of that is downstream of Lake Brownwood.

The effective FEMA flow for this location came from a HEC-1 rainfall runoff model for the Brown County FIS. Figure 12.29 shows that the effective FEMA 1% AEP (100-yr) flow is almost identical to the HEC-HMS 1% AEP flow using the uniform rainfall method. However, the uniform method is generally not appropriate for drainage areas over 1,000 square miles. As shown in Figure 12.29, the rest of the results, including the HEC-HMS elliptical storms and the current statistical analysis, were much lower than the effective FEMA flow. Figure 12.29 also shows that there is strong agreement between the results of the HEC-HMS elliptical storms, the current statistical analysis of the gage record, the RiverWare analysis, and the reservoir analysis of Lake Brownwood.

Table 12.29: Frequency Flow (cfs) Results Comparison for Pecan Bayou at Brownwood, TX

Annual Exceedance Probability (AEP)	Return Period (years)	Currently Effective FEMA FIS	Approx BLE Data from FEMA	Statistical Analysis of the Gage Record (Ch 5) (86 years)	HEC-HMS Uniform Rain Frequency Storm (Ch 6) (1650 sqmi)	HEC-HMS Elliptical Frequency Storm (Ch 7) (1650 sqmi)	Statistical Analysis of Extended RiverWare Record (Ch 8) (89 years)	Reservoir Analysis of Brownwood Lake (Ch 9)
0.002	500			40,800	125,800	80,400	52,300	56,760
0.005	200			34,000	89,000	53,300	44,000	44,700
0.01	100	62,247		28,900	62,900	37,100	37,500	33,585
0.02	50			24,100	41,300	22,800	31,000	26,160
0.04	25			19,400	25,800	18,900	24,600	16,100
0.1	10			13,500	15,000	13,900	16,400	12,900
0.2	5			9,350	9,300	9,270	10,600	7,860
0.5	2			4,280	4,230	4,060	3,890	1,625

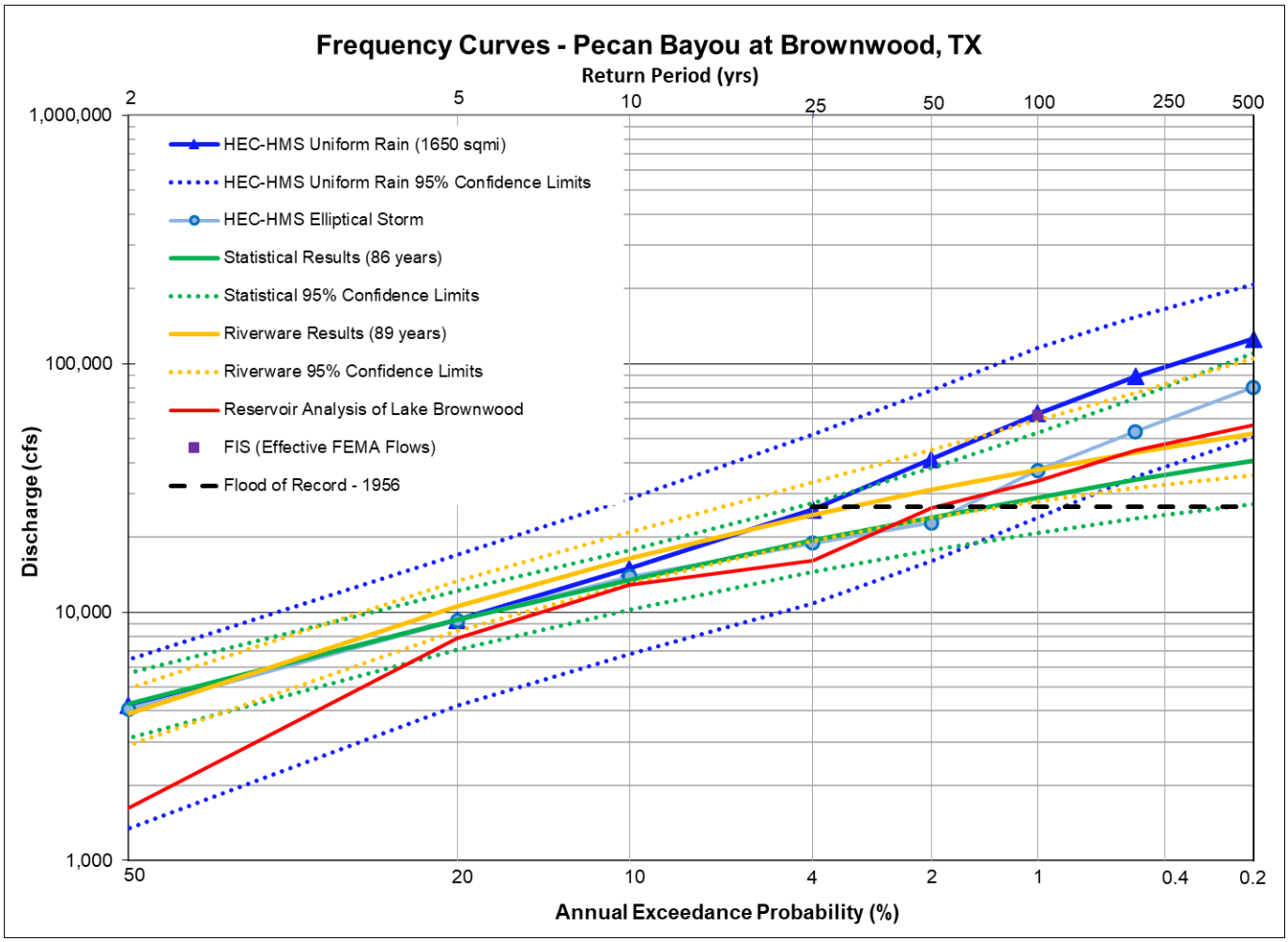

Figure 12.29: Flow Frequency Curve Comparison for Pecan Bayou at Brownwood, TX

Table 12.30: Frequency Flow (cfs) Results Comparison for Pecan Bayou near Mullin, TX

Annual Exceedance Probability (AEP)	Return Period (years)	Currently Effective FEMA FIS	Approx BLE Data from FEMA	Statistical Analysis of the Gage Record (Ch 5) (51 years)	HEC-HMS Uniform Rain Frequency Storm (Ch 6) (2070 sq mi)	HEC-HMS Elliptical Frequency Storm (Ch 7) (2070 sq mi)
0.002	500			78,500	112,900	99,900
0.005	200			57,900	87,500	76,100
0.01	100			45,200	67,700	58,100
0.02	50			34,600	46,200	38,000
0.04	25			25,800	29,900	27,200
0.1	10			16,500	18,100	17,000
0.2	5			11,000	11,000	10,900
0.5	2			5,110	5,100	4,830

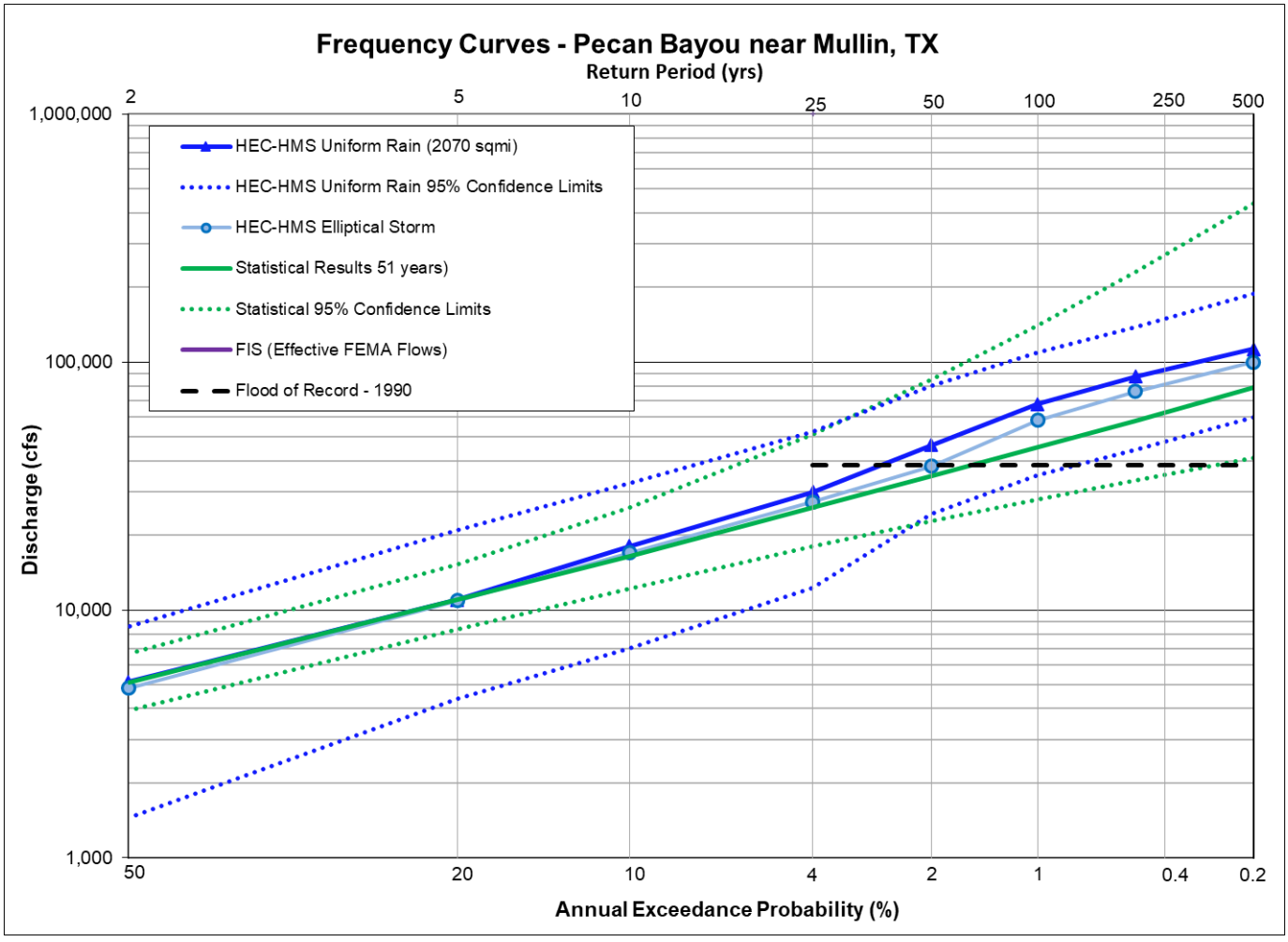

Figure 12.30a: Flow Frequency Curve Comparison for Pecan Bayou near Mullin, TX

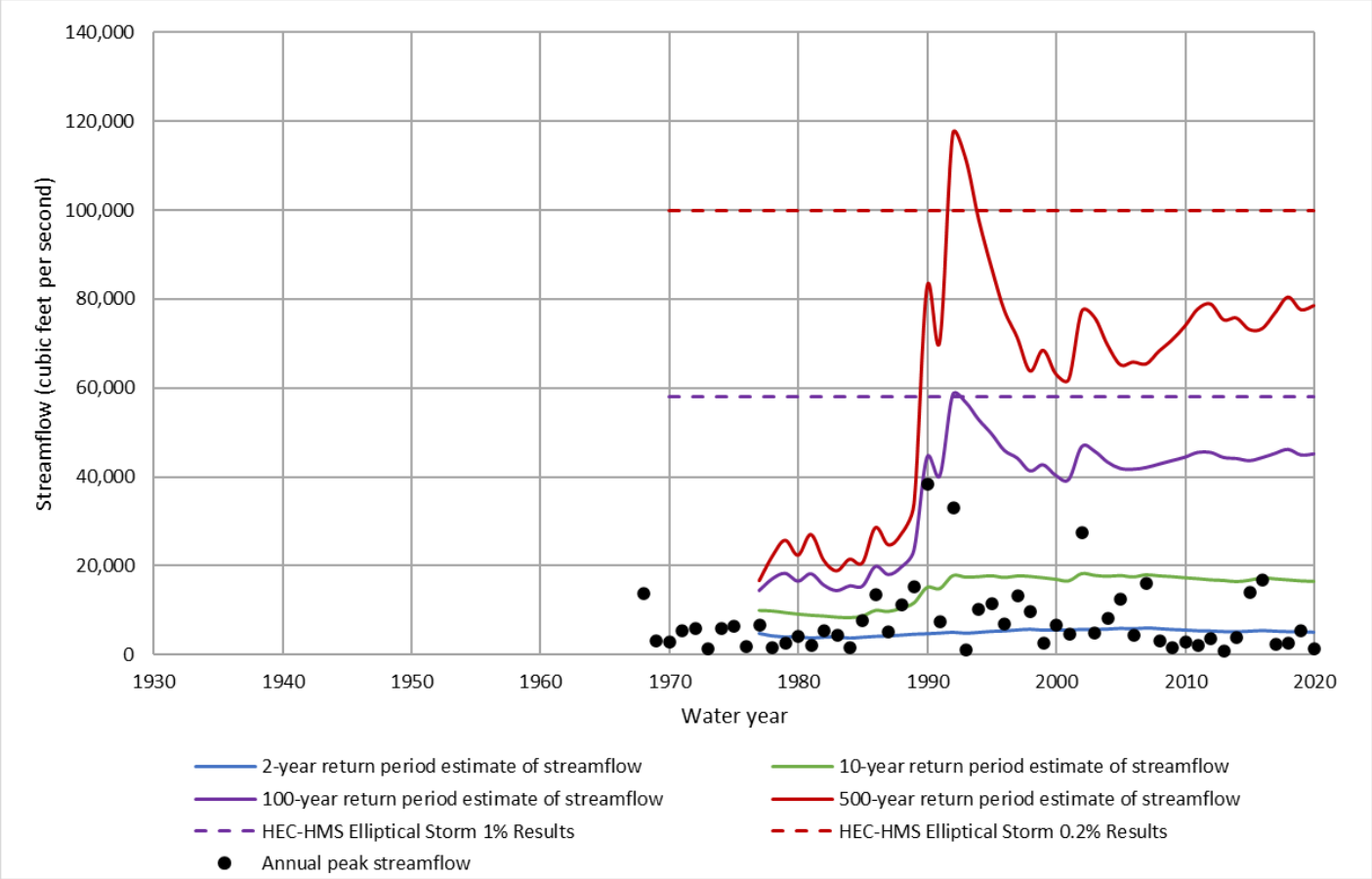

Figure 12.30b: Statistical Change Over Time Comparison for Pecan Bayou near Mullin, TX

The next point of comparison is Pecan Bayou near Mullin, Texas as shown in the preceding table and figures. This gage has a drainage area of about 2,070 square miles, and about 500 square miles of that is downstream of Lake Brownwood.

There are no published FEMA flows for this location. As shown in Figure 12.30a, the HEC-HMS elliptical storm results generally show good agreement with the current statistical results based on 51 years of record, and they are both well within one another's confidence bounds. Figure 12.30b illustrates how the results of the statistical analysis of the gage record have varied over time. This figure shows that while the 2-yr and 10-yr statistical estimates are generally stable, the 100-year and 500-year estimates are still moving up and down based on the preceding floods that have occurred. This figure also shows that the HEC-HMS results fall within that range of variation.

Table 12.31: Frequency Flow (cfs) Results Comparison for the San Saba River at Menard, TX

Annual Exceedance Probability (AEP)	Return Period (years)	Currently Effective FEMA FIS	Approx BLE Data from FEMA	Statistical Analysis of the Gage Record (Ch 5) (105 years)	Alternate Statistical Analysis of the Gage Record (Ch 5) (39 years)	HEC-HMS Uniform Rain Frequency Storm (Ch 6) (1140 sq mi)	HEC-HMS Elliptical Frequency Storm (Ch 7) (1140 sq mi)
0.002	500	318,000		222,000	255,000	328,700	260,600
0.005	200			172,000	176,000	250,800	197,600
0.01	100	177,000		136,000	126,000	198,700	156,900
0.02	50	129,000		103,000	84,200	145,900	118,600
0.04	25			72,400	51,600	85,100	72,300
0.1	10	56,000		39,000	22,000	42,200	38,900
0.2	5			19,900	8,850	17,000	20,000
0.5	2			4,200	1,130	4,140	4,140

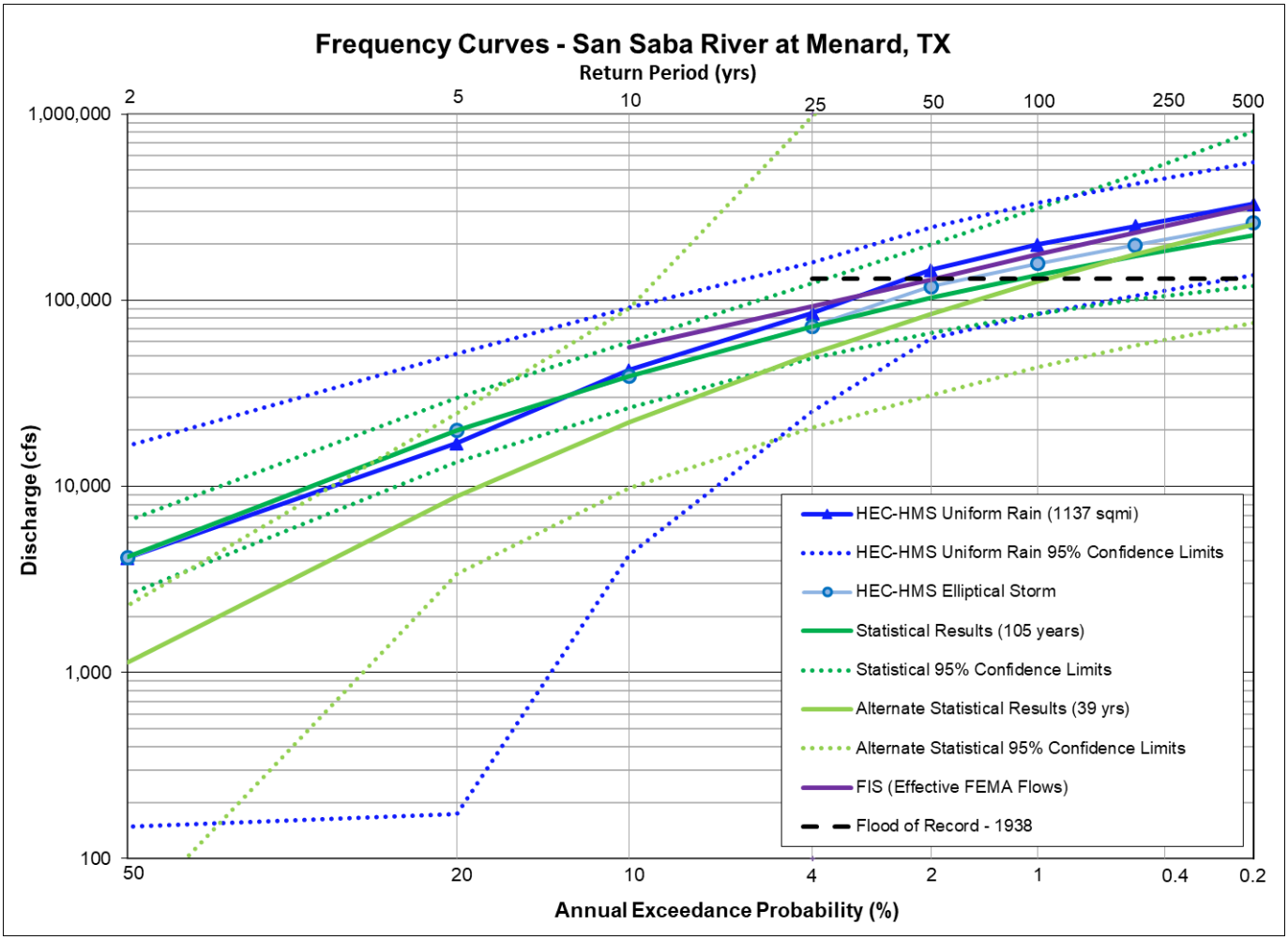

Figure 12.31a: Flow Frequency Curve Comparison for the San Saba River at Menard, TX

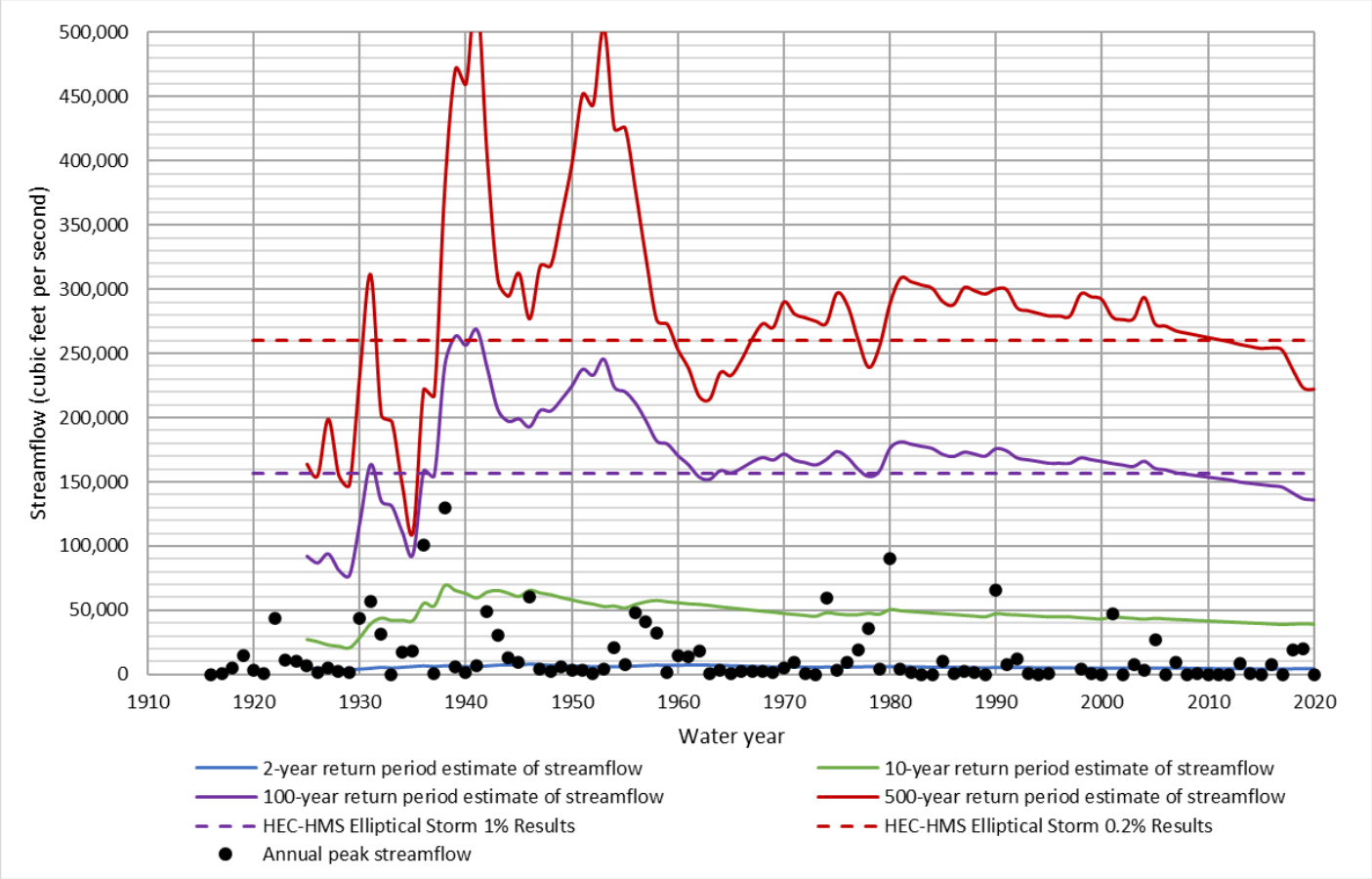

Figure 12.31b: Statistical Change Over Time Comparison for the San Saba River at Menard, TX

The first point of comparison in the San Saba watershed is the San Saba River at Menard, Texas as shown in the preceding table and figures. This gage has a drainage area of about 1,100 square miles with no significant reservoirs. This gage is also in the portion of the watershed that is experiencing declining flow trends.

The effective FEMA flows for this location came from a 1986 statistical analysis of the gage record for the Menard County FIS. Figure 12.31a shows that the additional 35 years of record in the current statistical analysis has reduced the 1% AEP (100-yr) flow estimate from 177,000 cfs in the FIS to 136,000 cfs in the current analysis. Figure 12.31a also shows that the HEC-HMS elliptical storm results generally show good agreement with the current statistical results based on 105 years of record, and they are both well within one another's confidence bounds.

Figure 12.31b illustrates how the results of the statistical analysis of the gage record have varied over time. This figure shows that even after more than 100 years of record, the 1% and 0.2% AEP (100-yr and 500-yr) statistical flow estimates are still moving up and down based on the preceding floods that have occurred. This figure also shows that the HEC-HMS elliptical results fall near the mid-point of that variation over the last 60 years. One can also see the declining flow trends illustrated in the 10-year estimate that continues to trend downward even after 100 years of record.

Table 12.32: Frequency Flow (cfs) Results Comparison for the San Saba River near Brady, TX

Annual Exceedance Probability (AEP)	Return Period (years)	Currently Effective FEMA FIS	Approx BLE Data from FEMA	Statistical Analysis of the Gage Record (Ch 5) (41 years)	Alternate Statistical Analysis of the Gage Record (Ch 5) (105 years)	HEC-HMS Uniform Rain Frequency Storm (Ch 6) (1640 sq mi)	HEC-HMS Elliptical Frequency Storm (Ch 7) (1640 sq mi)
0.002	500			256,000	262,000	420,600	290,500
0.005	200			171,000	188,000	314,700	218,200
0.01	100			121,000	141,000	243,200	175,600
0.02	50			82,400	102,000	180,700	129,000
0.04	25			53,000	70,300	87,500	78,700
0.1	10			26,100	38,300	37,900	38,300
0.2	5			13,000	20,900	15,300	17,700
0.5	2			3,170	6,030	3,200	3,600

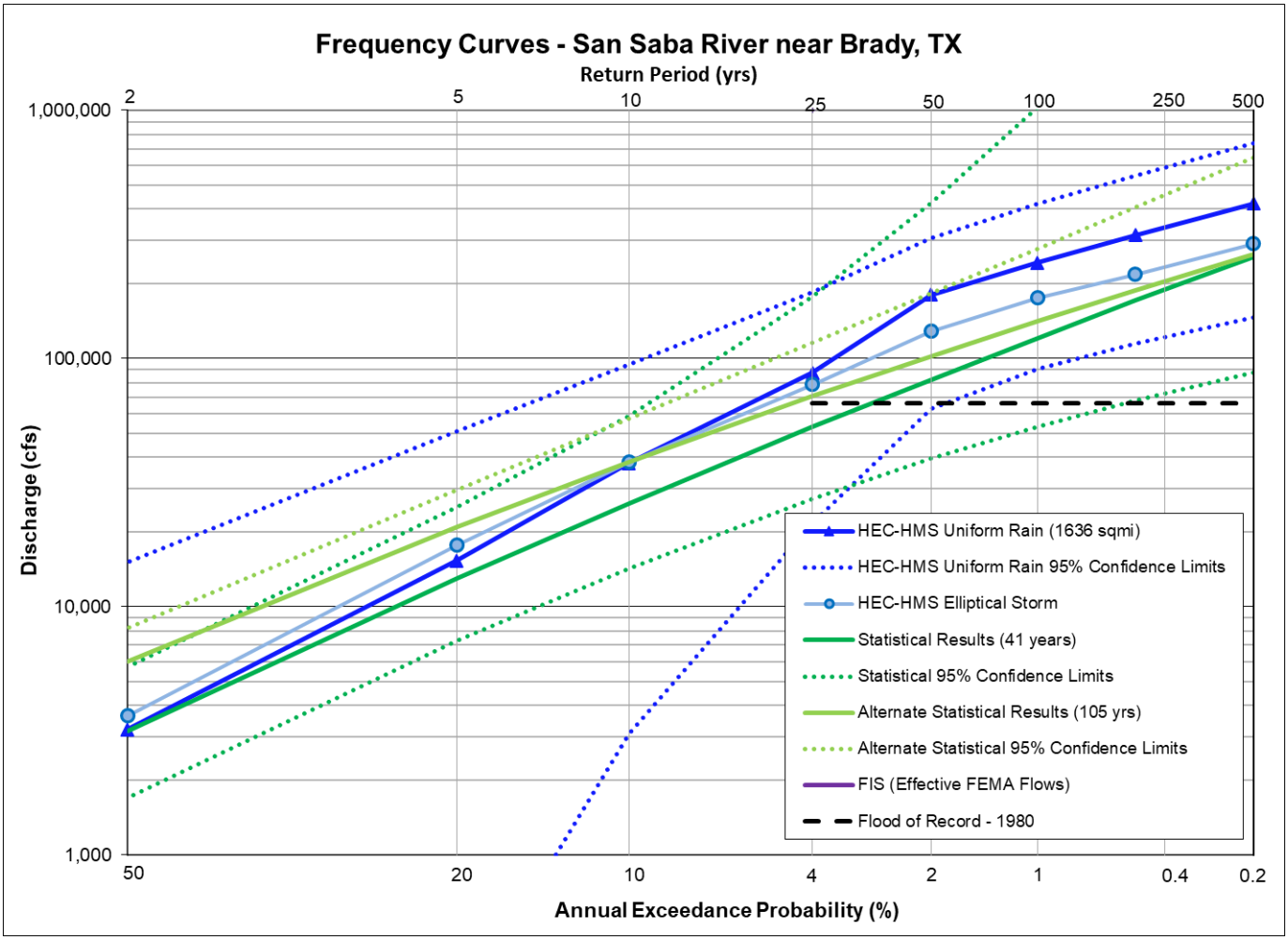

Figure 12.32: Flow Frequency Curve Comparison for the San Saba River near Brady, TX

The next point of comparison is the San Saba River near Brady, Texas as shown in the preceding table and figure. This gage has a drainage area of about 1,600 square miles with no significant reservoirs upstream. This gage is also in the portion of the watershed that is experiencing declining flow trends.

There are no published FEMA flows for this location. Figure 12.32 shows that the HEC-HMS elliptical storm results are slightly higher than the current statistical results, but they are both well within one another's confidence bounds.

The next point of comparison is Brady Creek near Brady, Texas as shown in the following table and figure. This gage has a drainage area of about 600 square miles, but Brady Creek Reservoir controls about 500 square miles of that area. This gage is also in the portion of the watershed that is experiencing declining flow trends.

The effective FEMA flows for this location were based on a 1980 SCS rainfall runoff model for the City of Brady's FIS. As shown in Figure 12.33, the effective FEMA flows are very close to the HEC-HMS and statistical results at the 1% AEP, but they are substantially lower than the other analyses at the 0.2% AEP. Figure 12.33 also shows that there is very tight agreement between the current statistical results and HEC-HMS results at this location.

Table 12.33: Frequency Flow (cfs) Results Comparison for Brady Creek at Brady, TX

Annual Exceedance Probability (AEP)	Return Period (years)	Currently Effective FEMA FIS	Approx BLE Data from FEMA	Statistical Analysis of the Gage Record (Ch 5) (58 years)	HEC-HMS Uniform Rain Frequency Storm (Ch 6) (130 sq mi)	HEC-HMS Elliptical Frequency Storm (Ch 7) (654 sq mi)
0.002	500	25,400		62,800	54,700	46,900
0.005	200			37,300	35,000	36,000
0.01	100	25,200		24,200	26,900	28,100
0.02	50	20,400		15,100	18,900	20,000
0.04	25			8,900	10,600	10,000
0.1	10	12,360		3,920	3,950	3,990
0.2	5			1,810	1,830	1,770
0.5	2			407	390	430

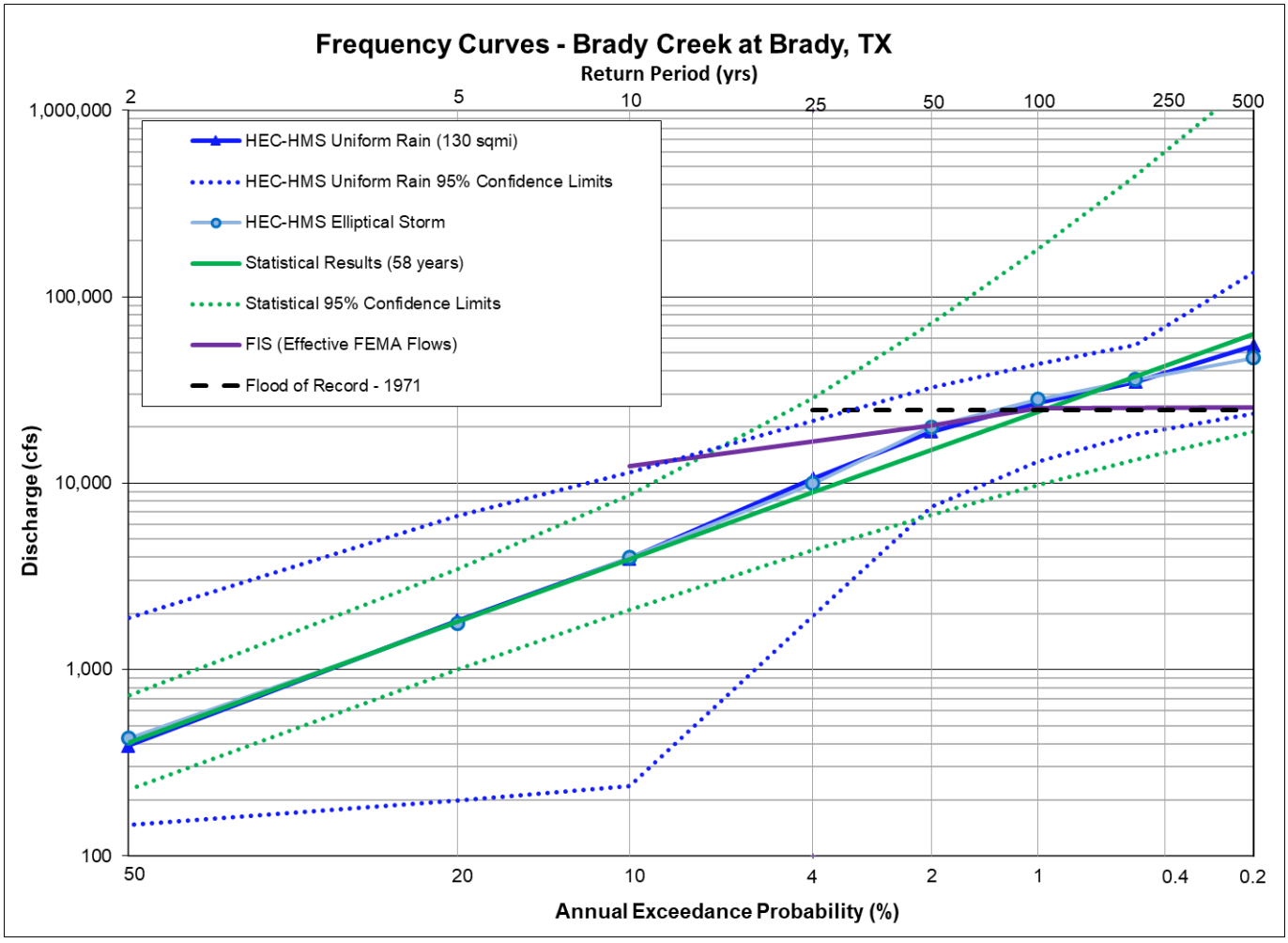

Figure 12.33: Flow Frequency Curve Comparison for Brady Creek at Brady, TX

Table 12.34: Frequency Flow (cfs) Results Comparison for the San Saba River at San Saba, TX

Annual Exceedance Probability (AEP)	Return Period (years)	Currently Effective FEMA FIS	2002 FDEP Study Elliptical Storm	Statistical Analysis of the Gage Record (Ch 5) (105 years)	Alternate Statistical Analysis of the Gage Record (Ch 5) (40 years)	HEC-HMS Uniform Rain Frequency Storm (Ch 6) (3050 sq mi)	HEC-HMS Elliptical Frequency Storm (Ch 7) (3050 sq mi)
0.002	500	340,771	372,000	285,000	190,000	602,800	374,200
0.005	200			197,000	125,000	442,000	272,200
0.01	100	151,301	183,000	145,000	88,000	336,500	205,400
0.02	50	106,071	144,000	103,000	60,100	242,300	137,800
0.04	25		101,000	70,600	39,400	102,200	93,300
0.1	10	38,878	55,300	38,700	20,400	39,500	50,000
0.2	5		25,200	21,800	11,000	14,700	26,400
0.5	2		11,500	7,050	3,370	3,330	8,760

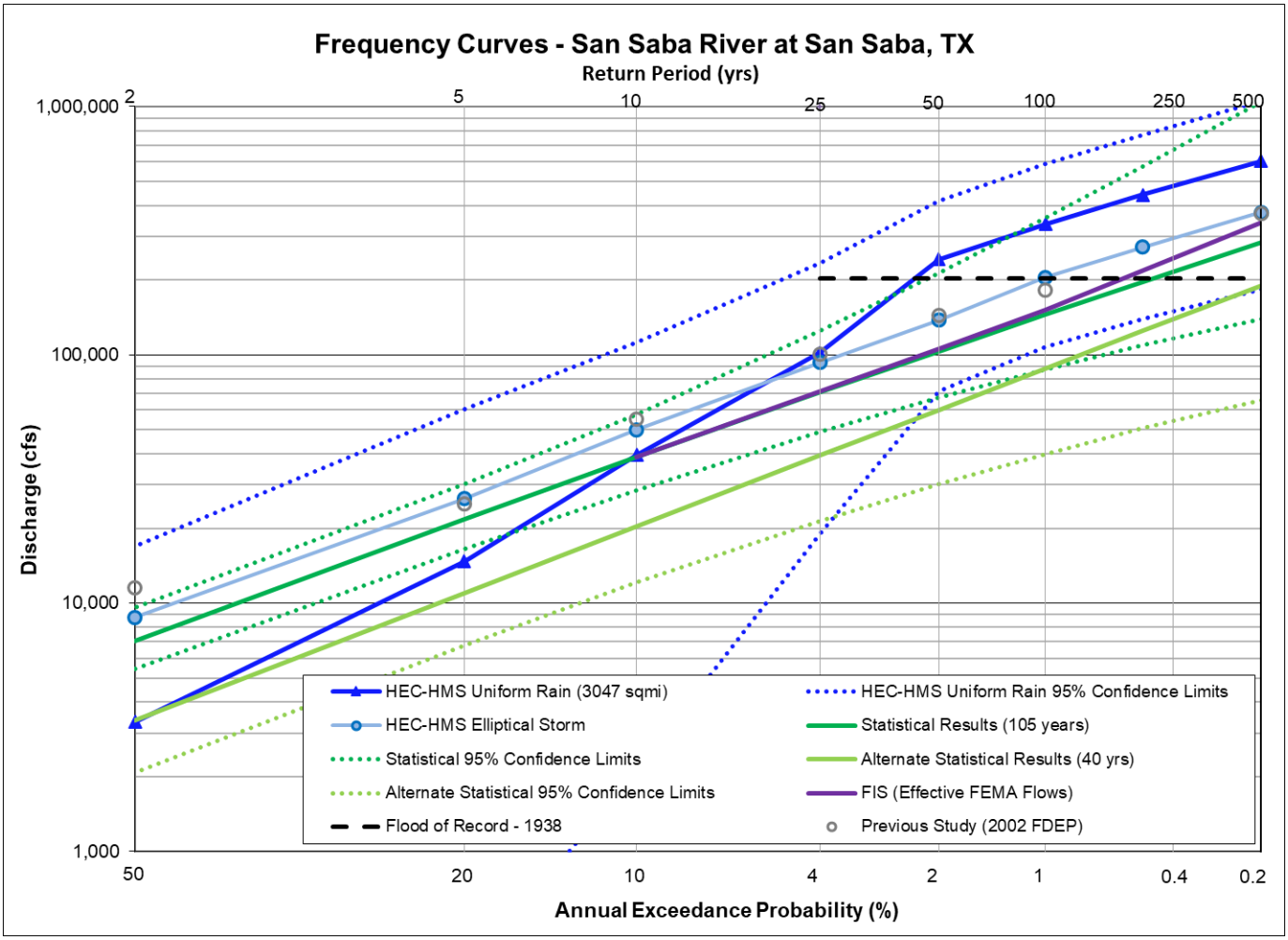

Figure 12.34a: Flow Frequency Curve Comparison for the San Saba River at San Saba, TX

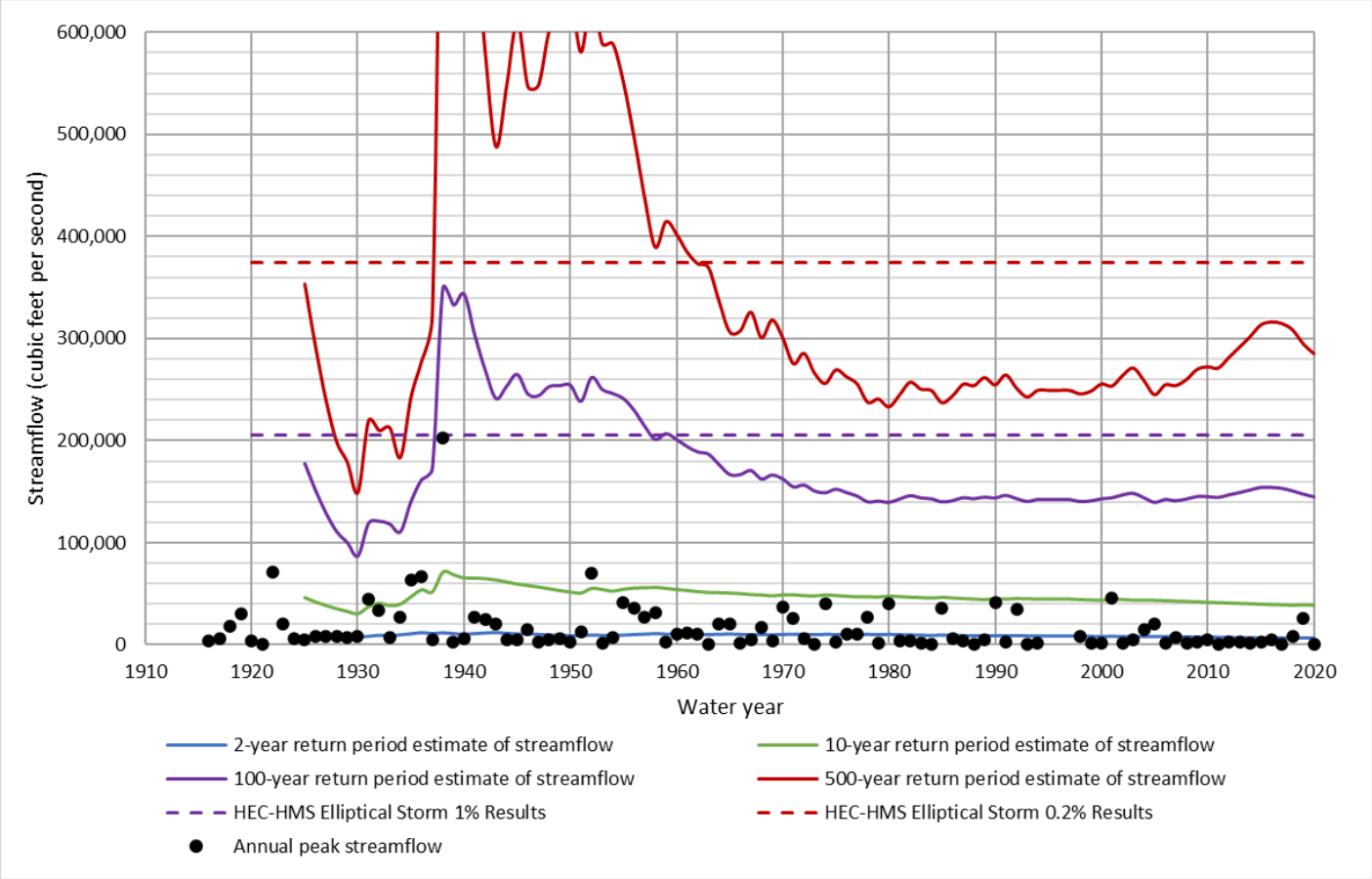

Figure 12.34b: Statistical Change Over Time Comparison for the San Saba River at San Saba, TX

The final point of comparison in the San Saba watershed is the San Saba River at San Saba, Texas as shown in the preceding table and figures. This gage has a drainage area of about 3,000 square miles. The only significant reservoir upstream is Brady Creek Reservoir, which controls about 500 of the 3,000 square miles. This gage is also in the portion of the watershed that is experiencing declining flow trends.

The effective FEMA flows for this location were based on a 1988 SCS rainfall runoff model for San Saba County's FIS. Figure 12.34a shows that the FEMA flows are lower than the HEC-HMS elliptical storm results but are very close to the results of the current statistical analysis. Published flows were also available from the 2002 Flood Damage Evaluation Project (FDEP) which were based on elliptical design storms. Figure 12.34a shows that the HEC-HMS elliptical storm results from the current study are very close to the 2002 FDEP results.

Figure 12.34b illustrates how the results of the statistical analysis of the gage record have varied over time. This figure shows that even after more than 100 years of record, the 1% and 0.2% AEP (100-yr and 500-yr) statistical flow estimates are still moving up and down based on the preceding floods that have occurred. Since no large floods have occurred in the past 50 years, the current statistical results are at a low point relative to the past estimates. However, just because a large flood hasn't occurred lately does not mean it can't occur in the future. This figure also shows that the 1% AEP HEC-HMS elliptical result is nearly identical to the observed 1938 flood of record and that the HEC-HMS elliptical results fall within the range of variation that as occurred over the past 100 years. One can also see the declining flow trends illustrated in this figure by 10-year estimate line that continues to trend downward even after 100 years of record.

12.1.4 Llano and Pedernales River Gage Locations

Table 12.35: Frequency Flow (cfs) Results Comparison for the North Llano River near Junction, TX

Annual Exceedance Probability (AEP)	Return Period (years)	Currently Effective FEMA FIS	Approx BLE Data from FEMA	Statistical Analysis of the Gage Record (Ch 5) (105 years)	HEC-HMS Uniform Rain Frequency Storm (Ch 6) (901 sq mi)	HEC-HMS Elliptical Frequency Storm (Ch 7) (901 sq mi)
0.002	500	409,000		169,000	320,300	261,400
0.005	200			146,000	252,800	201,800
0.01	100	231,000		126,000	203,500	164,400
0.02	50	170,000		104,000	155,800	126,800
0.04	25	63,400		80,900	101,900	91,800
0.1	10			49,800	55,400	50,000
0.2	5			28,200	28,200	27,700
0.5	2			6,640	6,600	6,340

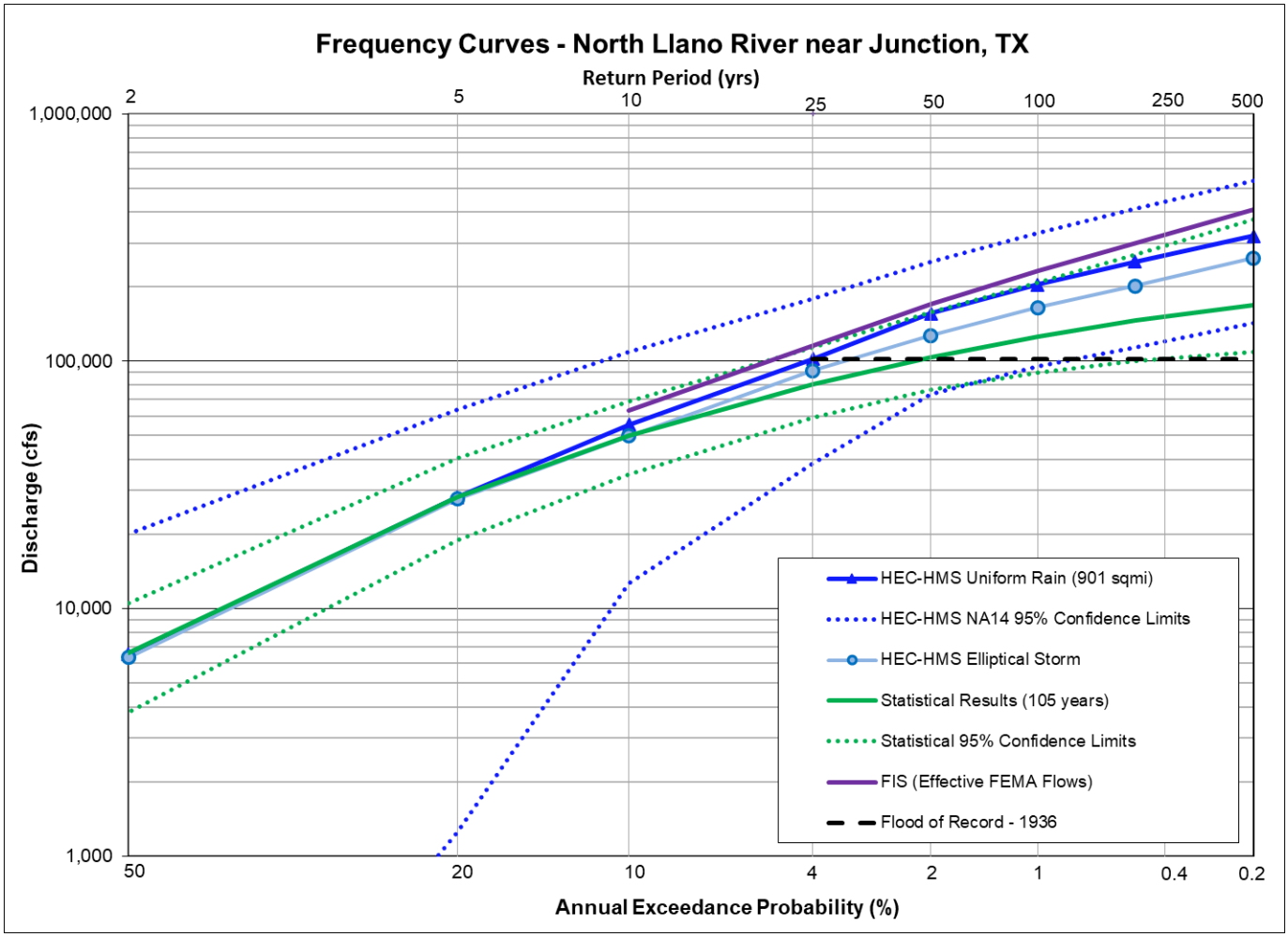

Figure 12.35: Flow Frequency Curve Comparison for the North Llano River near Junction, TX

The first point of comparison in the Llano River watershed is the North Llano River near Junction, Texas as shown in the preceding table and figures. This gage has a drainage area of about 900 square miles in the steep and flashy watersheds of the Texas Hill Country, and it has no significant reservoirs upstream. There are no trends in annual peak streamflow for this portion of the watershed.

The effective FEMA flows for this location were based on a 1978 statistical analysis of the gage record. Figure 12.35 shows that the 1% AEP (100-year) result of the current statistical analysis is almost 50% lower than the effective FEMA flow, and the main difference between these two analyses is the additional 40+ years of record that have occurred since 1978. Figure 12.35 also shows that the HEC-HMS elliptical storm results are about midway between the 1978 statistical results and the current statistical results, which is a reasonable estimate since the 1% and 0.2% AEP statistical estimates are still not yet stable, even with over 100 years of record.

The next point of comparison is the Llano River near Junction, Texas as shown in the following table and figures. This gage has a drainage area of over 1,800 square miles in the steep and flashy watersheds of the Texas Hill Country, and it has no significant reservoirs upstream. There are no trends in annual peak streamflow for this portion of the watershed.

The effective FEMA flows for this location were based on a 1978 statistical analysis of the gage record. Figure 12.36a shows that the results of the current statistical analysis are significantly lower than the effective FEMA flow, and the main difference between these two analyses is the additional 40+ years of record that have occurred since 1978. Figure 12.36a also shows that the HEC-HMS elliptical storm results are about midway between the old statistical results and the new statistical results.

Figure 12.36b is a plot of the change in the statistical results over time as new flood events have been added to the record. Although the 1% AEP statistical estimate appears to be somewhat stable over the last 20 years, this can be somewhat deceiving as it would only take one large flood to increase that estimate again. It generally takes a length of record that is 3 to 4 times the length of the return period being estimated for the results of a statistical analysis to stabilize. The 10-year statistical estimate in this plot confirms that trend, and it has been stable for the past 50+ years. Figure 12.36b also shows that the 1% AEP HEC-HMS elliptical storm estimate is well within the range over variation in the statistical estimates over the past 80 years and that it is approximately equal to the 1935 flood of record.

Table 12.36: Frequency Flow (cfs) Results Comparison for the Llano River near Junction, TX

Annual Exceedance Probability (AEP)	Return Period (years)	Currently Effective FEMA FIS	Approx BLE Data from FEMA	Statistical Analysis of the Gage Record (Ch 5) (105 years)	HEC-HMS Uniform Rain Frequency Storm (Ch 6) (1860 sq mi)	HEC-HMS Elliptical Frequency Storm (Ch 7) (1860 sq mi)
0.002	500	781,000		353,000	761,300	511,700
0.005	200			302,000	595,800	389,700
0.01	100	375,000		258,000	478,400	313,100
0.02	50	258,000		211,000	365,900	235,700
0.04	25			161,000	232,300	172,300
0.1	10	84,200		97,000	116,400	94,500
0.2	5			53,500	53,400	51,000
0.5	2			12,000	12,000	10,600

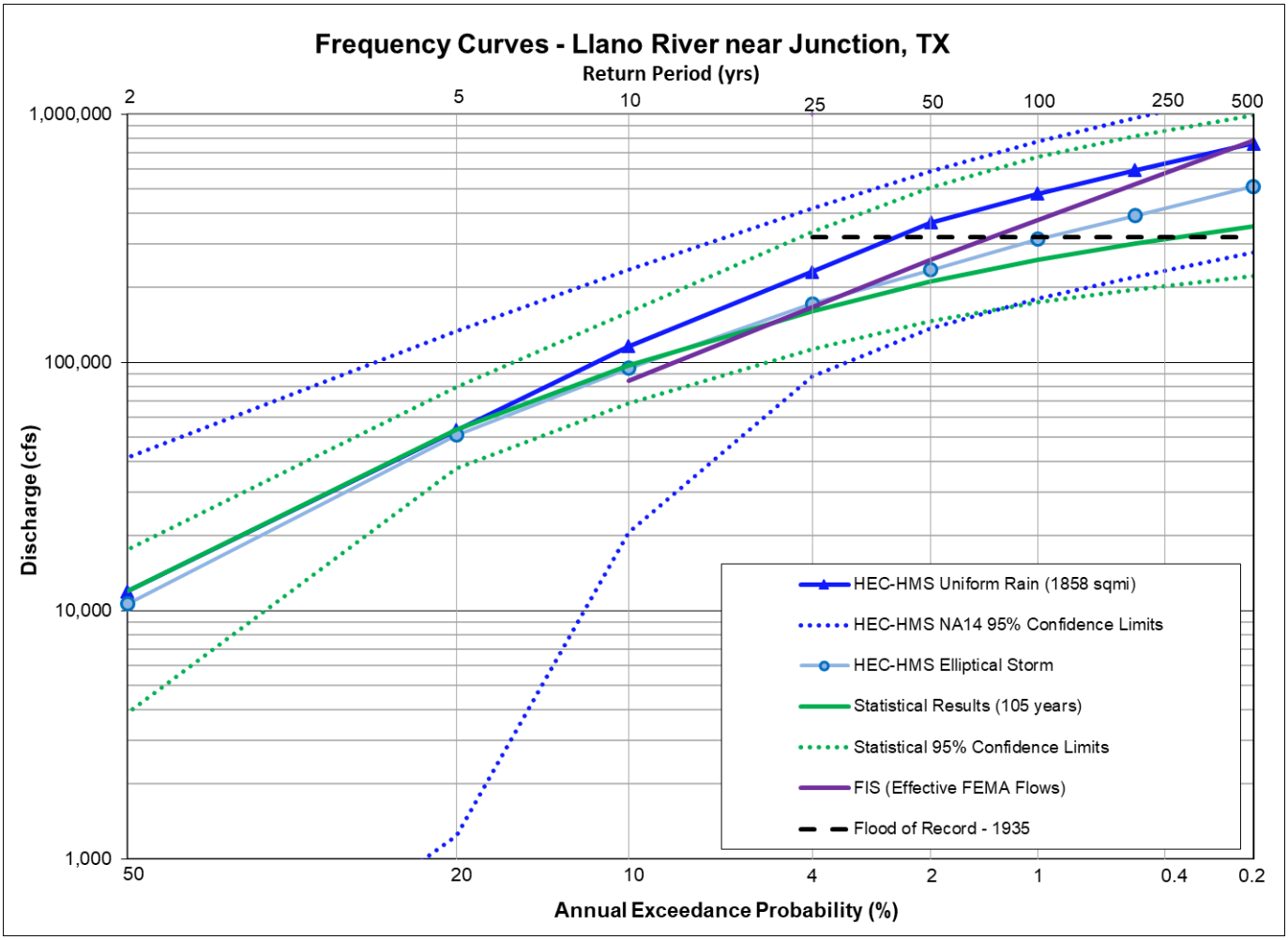

Figure 12.36a: Flow Frequency Curve Comparison for the Llano River near Junction, TX

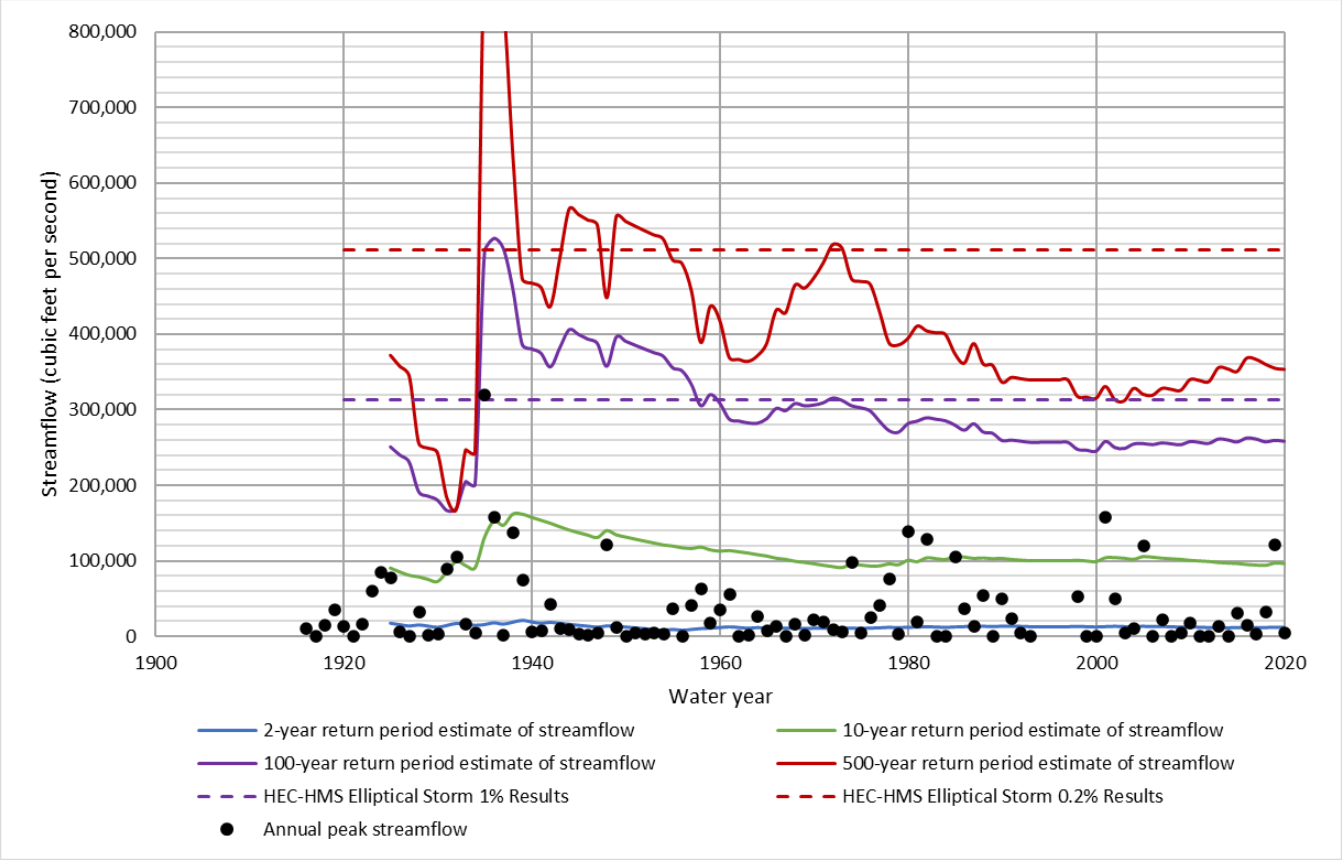

Figure 12.36b: Statistical Change Over Time Comparison for the Llano River near Junction, TX

The next point of comparison is the Llano River near Mason, Texas as shown in the following table and figure. This gage has a drainage area of over 3,200 square miles in the steep and flashy watersheds of the Texas Hill Country, and it has no significant reservoirs upstream. There are no trends in annual peak streamflow for this portion of the watershed.

There are no published FEMA flows for this location. Figure 12.37 shows that the HEC-HMS elliptical storm results are lower than the current statistical results based on 53 years of record, and the 1% AEP HEC-HMS elliptical storm is approximately equal to the RiverWare estimate of the 1935 flood. The HEC-HMS results are also more consistent with the results at the upstream and downstream gages, as shown in Figures 12.36a and 12.39a.

Table 12.37: Frequency Flow (cfs) Results Comparison for the Llano River near Mason, TX

Annual Exceedance Probability (AEP)	Return Period (years)	Currently Effective FEMA FIS	Approx BLE Data from FEMA	Statistical Analysis of the Gage Record (Ch 5) (53 years)	HEC-HMS Uniform Rain Frequency Storm (Ch 6) (3250 sq mi)	HEC-HMS Elliptical Frequency Storm (Ch 7) (3250 sq mi)	Statistical Analysis of Extended RiverWare Record (Ch 8) (89 years)
0.002	500			755,000	879,800	547,500	750,000
0.005	200			552,000	677,100	435,500	588,000
0.01	100			420,000	533,500	359,200	469,000
0.02	50			306,000	399,300	277,200	358,000
0.04	25			211,000	257,900	209,800	256,000
0.1	10			113,000	127,800	114,800	142,000
0.2	5			59,600	65,700	62,700	74,600
0.5	2			15,200	19,000	17,800	17,100

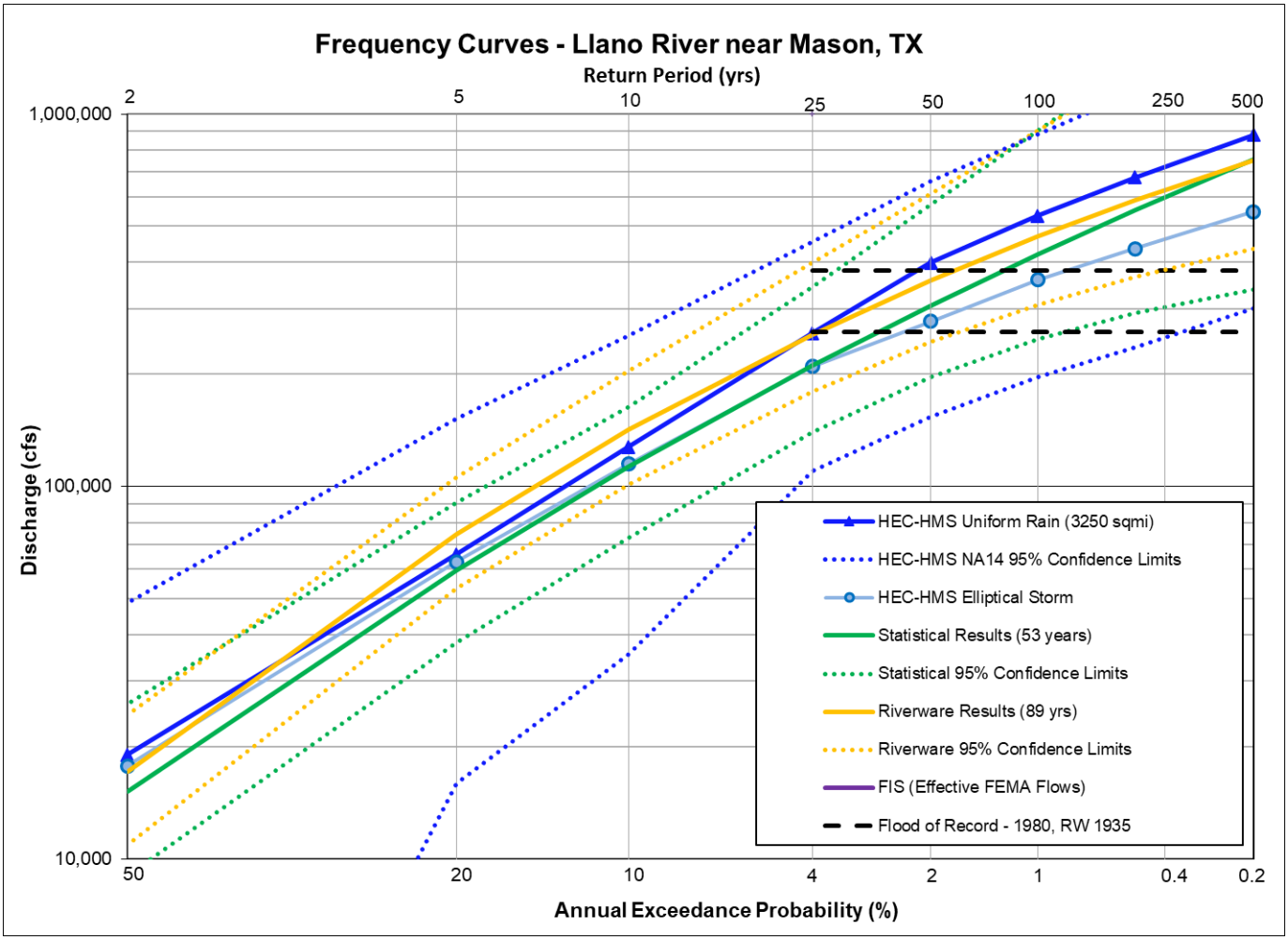

Figure 12.37: Flow Frequency Curve Comparison for the Llano River near Mason, TX

Table 12.38: Frequency Flow (cfs) Results Comparison for Beaver Creek near Mason, TX

Annual Exceedance Probability (AEP)	Return Period (years)	Currently Effective FEMA FIS	Approx BLE Data from FEMA	Statistical Analysis of the Gage Record (Ch 5) (56 years)	HEC-HMS Uniform Rain Frequency Storm (Ch 6) (215 sq mi)
0.002	500			93,500	164,500
0.005	200			76,200	131,700
0.01	100			63,200	109,200
0.02	50			50,600	87,100
0.04	25			38,600	58,700
0.1	10			24,000	30,700
0.2	5			14,500	14,500
0.5	2			4,620	4,700

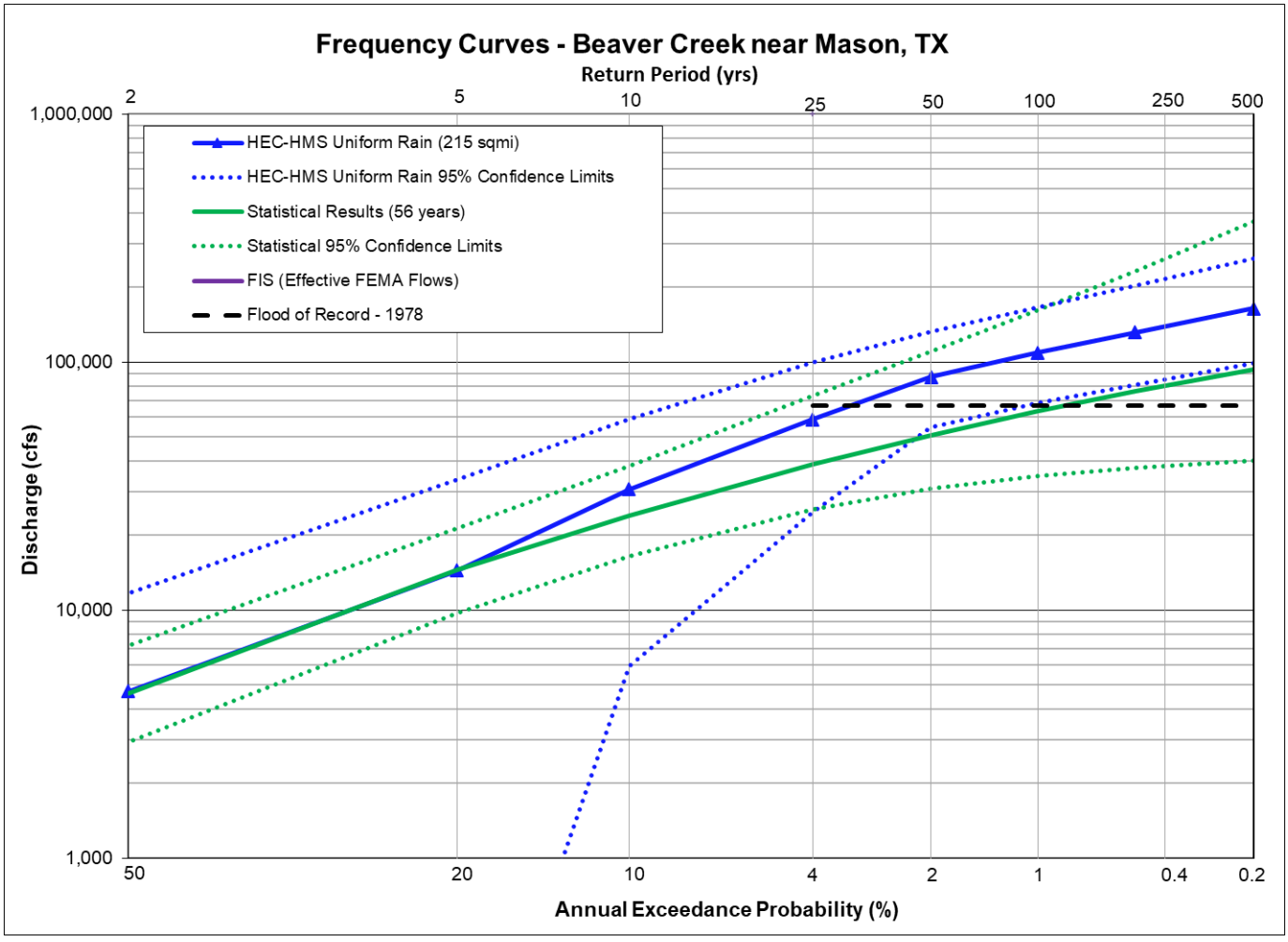

Figure 12.38: Flow Frequency Curve Comparison for Beaver Creek near Mason, TX

The next point of comparison is Beaver Creek near Mason, Texas as shown in the preceding table and figure. This gage has a drainage area of 215 square miles in the Texas Hill Country, and it has no significant reservoirs upstream. There are no trends in annual peak streamflow for this portion of the watershed.

There are no published FEMA flows for this location. Figure 12.38 shows that the HEC-HMS uniform rain results are higher than the current statistical results based on 56 years of record. However, while the HEC-HMS results are still well within the confidence bounds of the statistical analysis, the results of the current statistical analysis are actually below the lower confidence bound of NOAA Atlas 14's rainfall depths in HEC-HMS. This is an indication that the available data sample for the statistical analysis at this location did not include the type of large flood that is predicted by NOAA Atlas 14's regional analysis. Therefore, the current statistical results may be underestimating the magnitude of the 1% and 0.2% AEP (100-yr and 500-yr) events.

The next point of comparison is the Llano River at Llano, Texas as shown in the following table and figures. This gage has a drainage area of almost 4,200 square miles in the steep and flashy watersheds of the Texas Hill Country, and it has no significant reservoirs upstream. There are no trends in annual peak streamflow for this portion of the watershed.

The pending FEMA flows for this location were based on a 2012 statistical analysis of the gage record. Figure 12.39a shows that the results of the pending FEMA flows are significantly lower than the results of the current statistical analysis with the main difference between being the additional 10 years of data that have been added to the record. Figure 12.39a also shows that the HEC-HMS elliptical storm results happen to be nearly identical to the results of the current statistical analysis based on over 100 years of record.

Published frequency flows were also available from the 2002 FDEP study, and the HEC-HMS elliptical storms from the current study show strong agreement with the results of that previous study. In fact, the 1% AEP (100-yr) results from the two elliptical storm studies are within about 5% of one another other.

Figure 12.39b is a plot of the change in the statistical results over time as new flood events have been added to the record. From this plot, one can see that while the 2-year and 10-year statistical estimates have been stable for decades, the 100-yr and 500-yr estimates continue to experience significant movement, even after 80+ years of record. This makes sense as it generally takes a length of record that is 3 to 4 times the length of the return period being estimated for the results of a Bulletin 17C statistical analysis to stabilize. Figure 12.39b also shows that the 1% AEP HEC-HMS elliptical storm estimate is well within the range over variation in the statistical estimates over the past 80 years and that it happens to be approximately equal to the current 100-year statistical estimate.

Table 12.39: Frequency Flow (cfs) Results Comparison for the Llano River at Llano, TX

Annual Exceedance Probability (AEP)	Return Period (years)	Currently Effective FEMA FIS	2002 FDEP Study Elliptical Storm	Statistical Analysis of the Gage Record (Ch 5) (81 years)	HEC-HMS Uniform Rain Frequency Storm (Ch 6) (4200 sq mi)	HEC-HMS Elliptical Frequency Storm (Ch 7) (4200 sq mi)	Statistical Analysis of Extended RiverWare Record (Ch 8) (89 years)
0.002	500	585,000	555,000	725,000	1,042,900	716,900	725,000
0.005	200			545,000	792,800	541,400	551,000
0.01	100	380,000	405,000	425,000	635,100	428,100	434,000
0.02	50	298,000	334,000	321,000	482,100	317,200	331,000
0.04	25		248,000	231,000	318,100	233,300	240,000
0.1	10	140,000	147,000	134,000	158,200	127,100	142,000
0.2	5		92,200	77,800	78,300	71,700	83,300
0.5	2		30,800	24,800	21,500	20,100	27,000

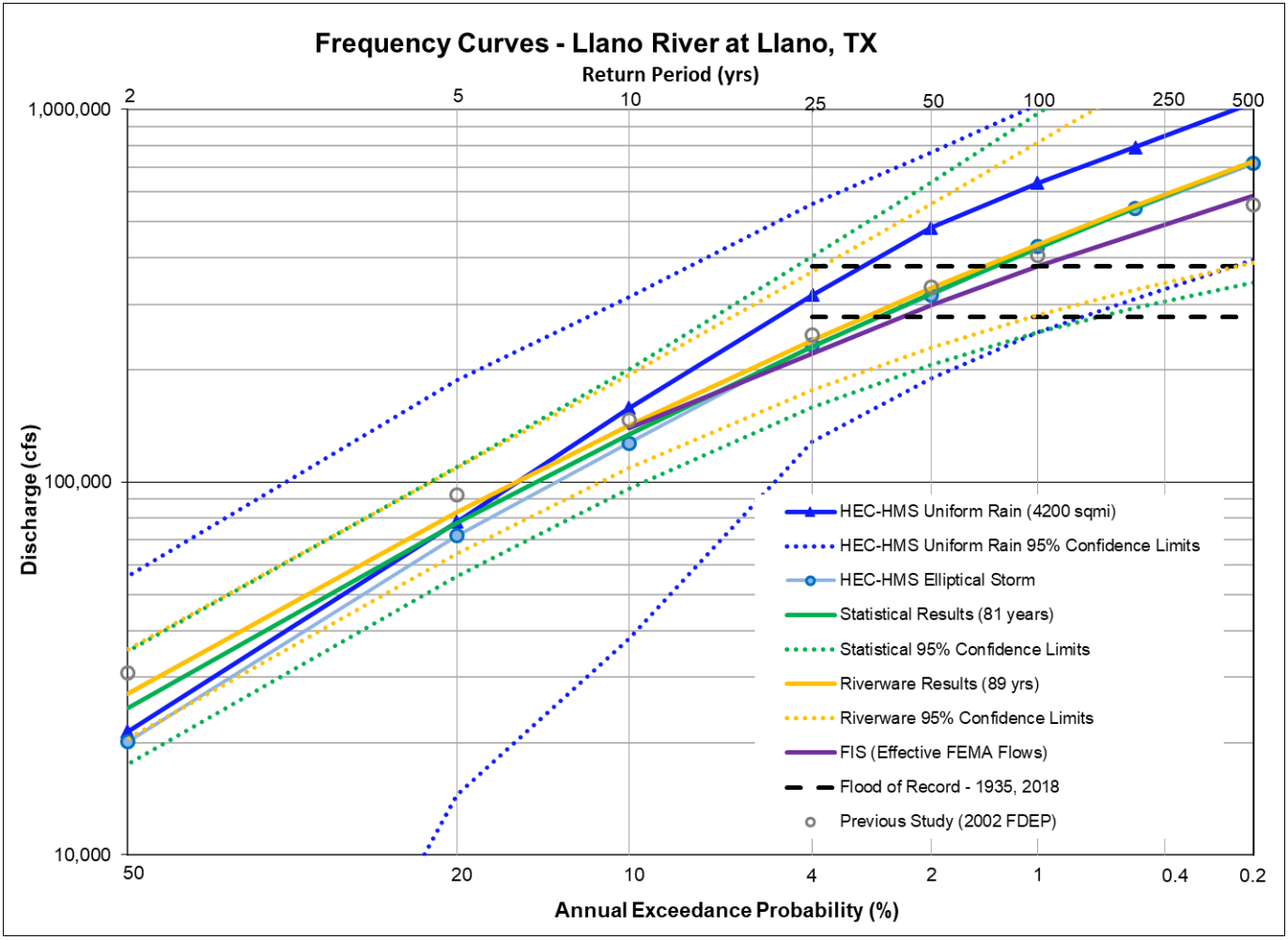

Figure 12.39a: Flow Frequency Curve Comparison for the Llano River at Llano, TX

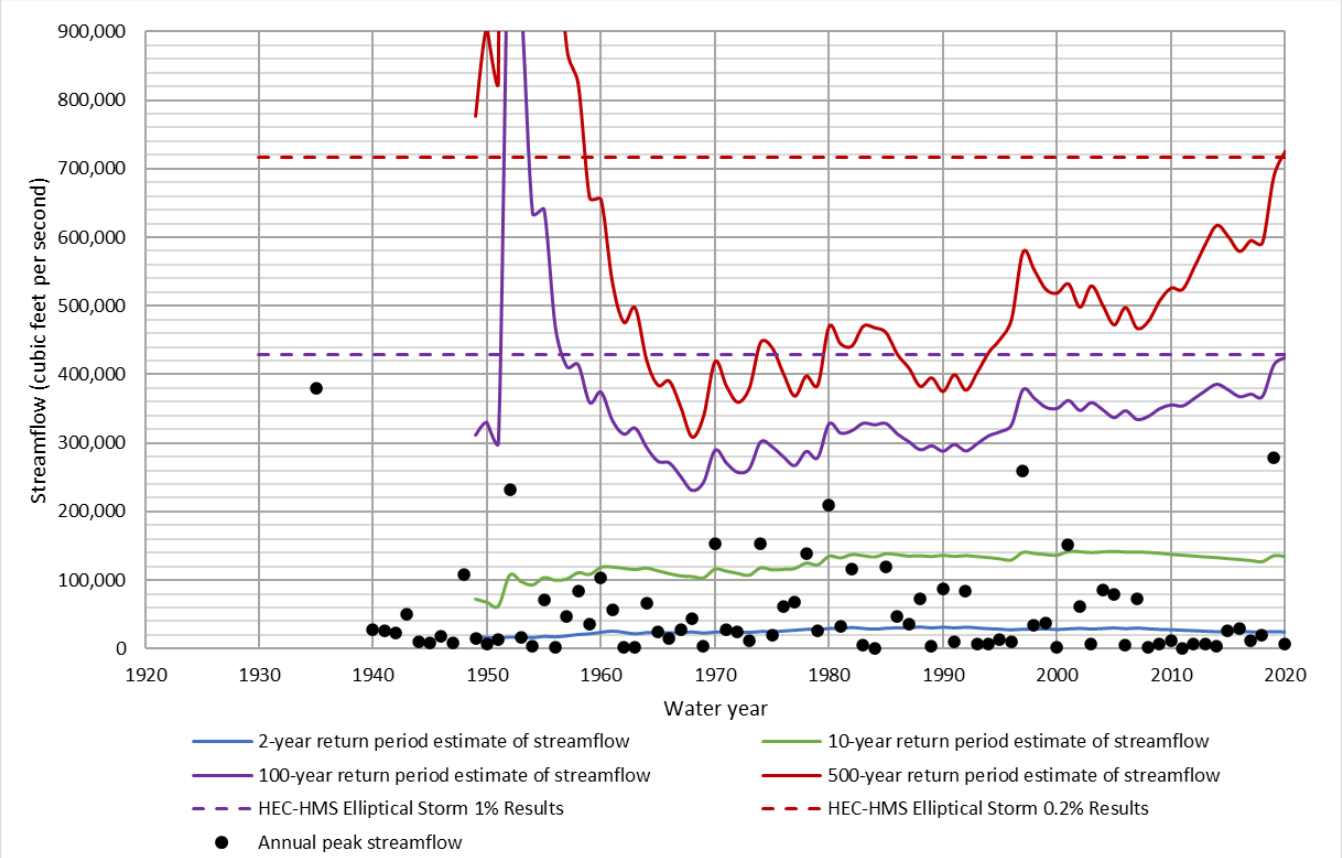

Figure 12.39b: Statistical Change Over Time Comparison for the Llano River at Llano, TX

The next point of comparison is Sandy Creek near Kingsland, Texas as shown in the following table and figure. This gage has a drainage area of 215 square miles in the Texas Hill Country, and it has no significant reservoirs upstream. There are no trends in annual peak streamflow for this portion of the watershed.

There are no detailed FEMA Flood Insurance Studies (FIS) for this location, but approximate frequency flows are available from FEMA's recently published Base Level Engineering (BLE) data, as shown in Figure 12.40. These flows were based on regional regression equations, and as Figure 12.40 shows, they are significantly higher than both the current statistical analysis and the HEC-HMS results. Figure 12.40 also shows that there is fairly close agreement between the HEC-HMS results and the current statistical analysis based on 54 years of record with the HEC-HMS results being slightly higher at the 1% AEP (100-yr) frequency. Figure 12.40 also shows that the HEC-HMS 1% AEP results are lower than the 1952 flood of record at this location.

Table 12.40: Frequency Flow (cfs) Results Comparison for the Sandy Creek near Kingsland, TX

Annual Exceedance Probability (AEP)	Return Period (years)	Currently Effective FEMA FIS	Approx BLE Data from FEMA	Statistical Analysis of the Gage Record (Ch 5) (54 years)	HEC-HMS Uniform Rain Frequency Storm (Ch 6) (346 sq mi)	HEC-HMS Elliptical Frequency Storm (Ch 7) (346 sq mi)
0.002	500		240,424	245,000	233,600	221,600
0.005	200			167,000	182,700	172,900
0.01	100		194,577	123,000	148,400	140,500
0.02	50		144,072	87,900	115,700	109,200
0.04	25		102,147	60,900	79,300	73,500
0.1	10		59,088	34,900	42,400	34,900
0.2	5			21,000	21,100	21,100
0.5	2			8,170	8,200	8,200

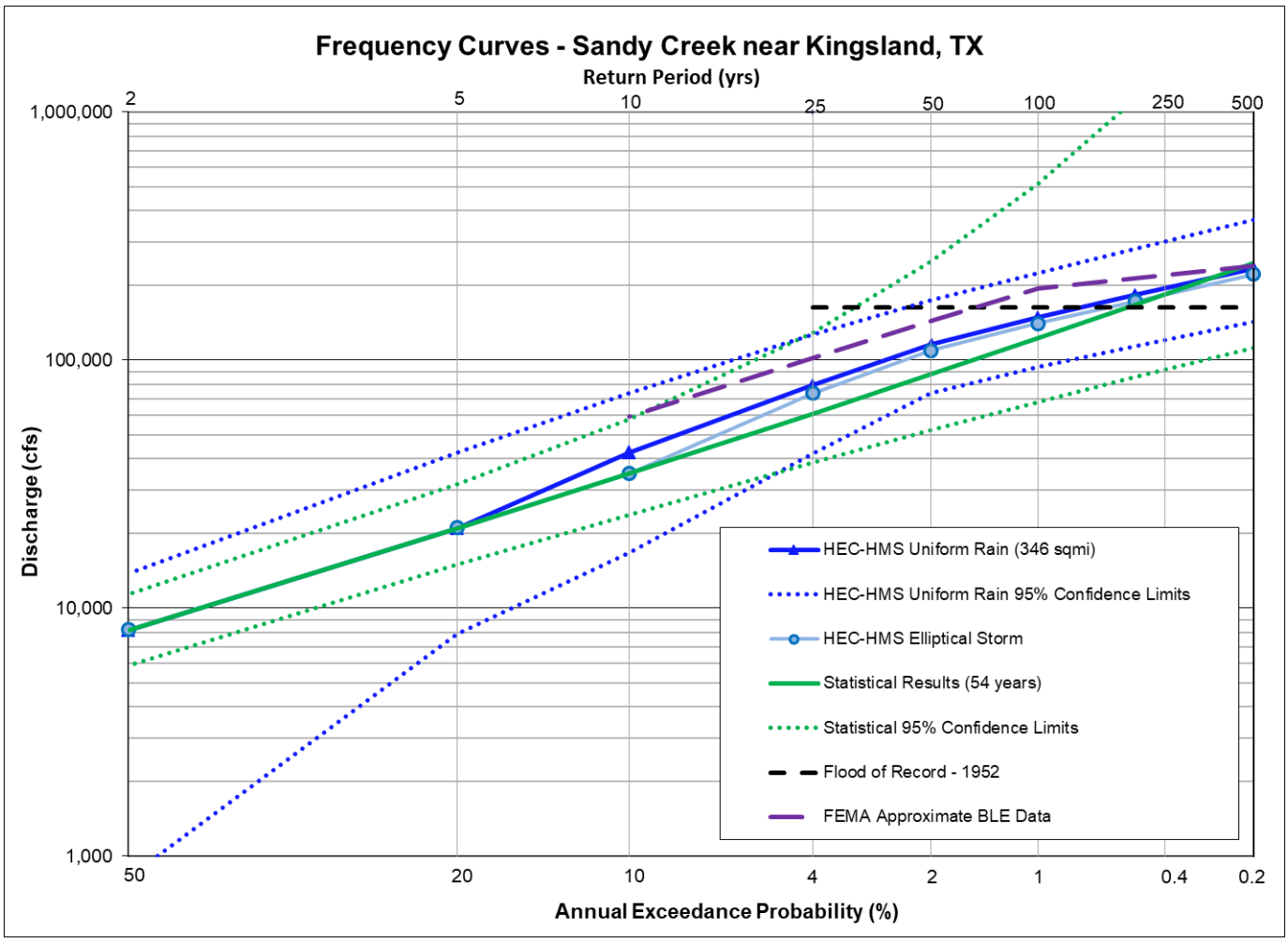

Figure 12.40: Flow Frequency Curve Comparison for the Sandy Creek near Kingsland, TX

Table 12.41: Frequency Flow (cfs) Results Comparison for the Pedernales near Fredericksburg, TX

Annual Exceedance Probability (AEP)	Return Period (years)	Currently Effective FEMA FIS	Approx BLE Data from FEMA	Statistical Analysis of the Gage Record (Ch 5) (42 years)	HEC-HMS Uniform Rain Frequency Storm (Ch 6) (370 sq mi)	HEC-HMS Elliptical Frequency Storm (Ch 7) (370 sq mi)
0.002	500		192,089	240,000	273,600	249,300
0.005	200			175,000	214,900	194,000
0.01	100		127,076	133,000	171,300	154,300
0.02	50		100,863	97,000	131,400	116,500
0.04	25		77,004	66,900	89,000	73,500
0.1	10		48,679	36,200	44,800	36,300
0.2	5			19,400	19,300	19,300
0.5	2			5,120	5,150	5,130

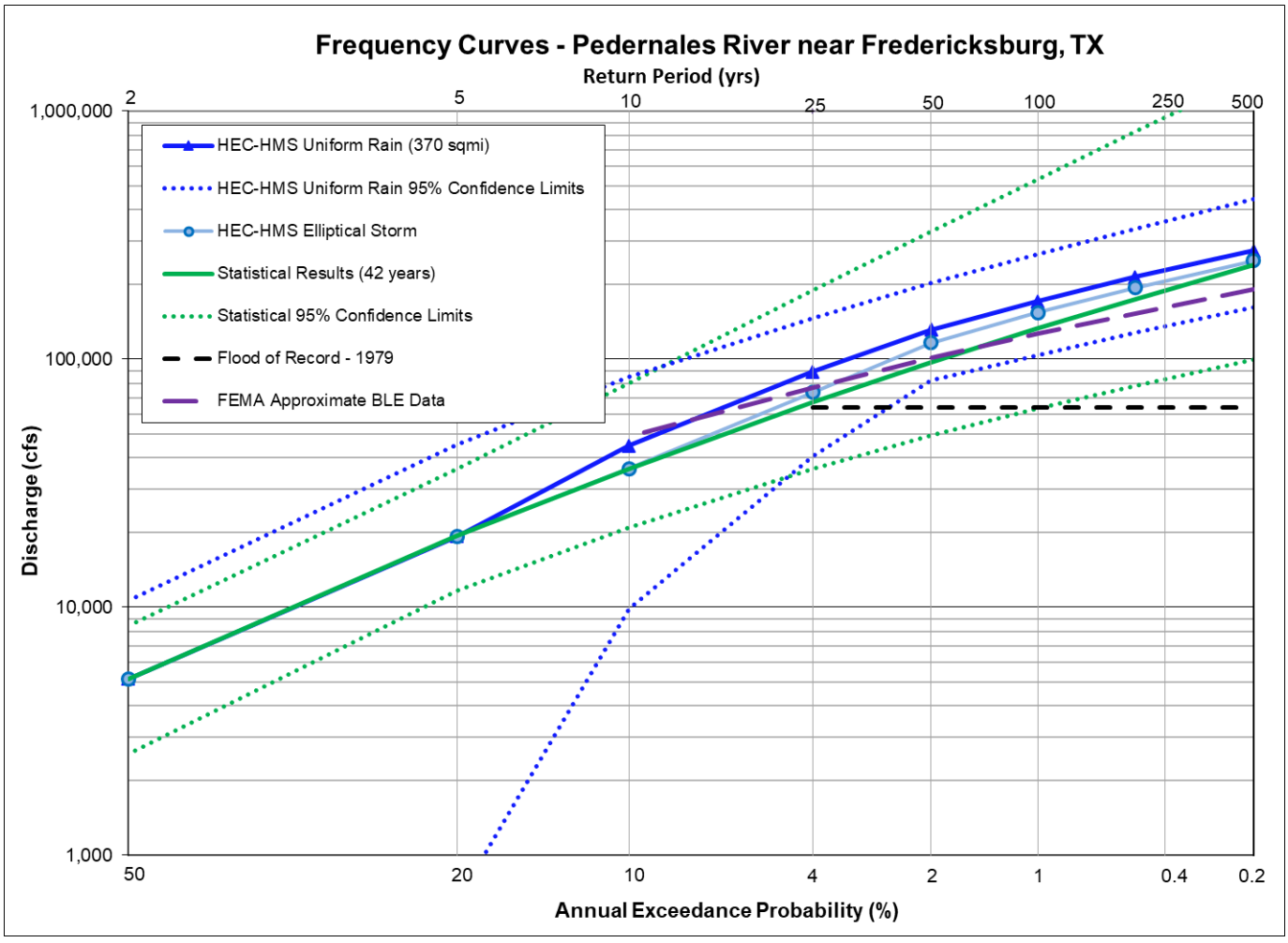

Figure 12.41: Flow Frequency Curve Comparison for the Pedernales near Fredericksburg, TX

The next point of comparison is the Pedernales River near Fredericksburg, Texas as shown in the preceding table and figure. This gage has a drainage area of about 370 square miles in the steep and flashy watersheds of the Texas Hill Country, and it has no significant reservoirs upstream. There are no trends in annual peak streamflow for this portion of the watershed.

This location has approximate frequency flows from FEMA's recently published Base Level Engineering (BLE) data, as shown in Figure 12.41. These flows were based on a recent (2020) statistical analysis of the gage record, and as would be expected, they are fairly similar to the results of the current study's statistical analysis. Figure 12.41 also shows that the HEC-HMS results are slightly higher than the statistical results for the 1% AEP (100-yr) frequency, but this gage has a fairly short period of record with only 42 years of data. Figure 12.41 also shows that the HEC-HMS and statistical results are both well within one another's confidence bounds.

The next point of comparison is the Pedernales River at LBJ Ranch near Stonewall, Texas as shown in the following table and figure. This LCRA gage has a drainage area of about 625 square miles in the steep and flashy watersheds of the Texas Hill Country, and it has no significant reservoirs upstream. There are no trends in annual peak streamflow for this portion of the watershed.

This location has both effective FEMA flows from a detailed Flood Insurance Stud (FIS) and approximate frequency flows from FEMA's recently published Base Level Engineering (BLE) data, as shown in Figure 12.42. The effective FIS flows were based on a 1997 Bulletin 17B statistical analysis of the gage record, while the BLE approximate flows were based on a more recent (2020) statistical analysis. The two purples lines on Figure 12.42 are a good illustration of how much the results of a Bulletin 17C analysis can vary just based on additional data being added to the record. Figure 12.42 also shows that the HEC-HMS elliptical storm results are about midway between the effective FIS and the BLE flows at the 1% AEP frequency. Both the HEC-HMS results and the statistical results are also well within one another's confidence bounds.

Table 12.42: Frequency Flow (cfs) Results Comparison for the Pedernales River at LBJ Ranch near Stonewall, TX

Annual Exceedance Probability (AEP)	Return Period (years)	Currently Effective FEMA FIS	Approx BLE Data from FEMA	Statistical Analysis of the Gage Record (Ch 5) (26 years)	HEC-HMS Uniform Rain Frequency Storm (Ch 6) (625 sq mi)	HEC-HMS Elliptical Frequency Storm (Ch 7) (625 sq mi)
0.002	500	436,000	221,492	268,000	400,800	340,300
0.005	200			203,000	290,600	245,700
0.01	100	247,000	148,263	159,000	221,600	185,300
0.02	50	186,000	118,397	120,000	156,100	132,400
0.04	25		91,049	85,500	101,900	79,700
0.1	10	81,100	58,291	48,200	56,600	47,300
0.2	5			26,660	29,000	26,700
0.5	2			7,250	7,180	7,250

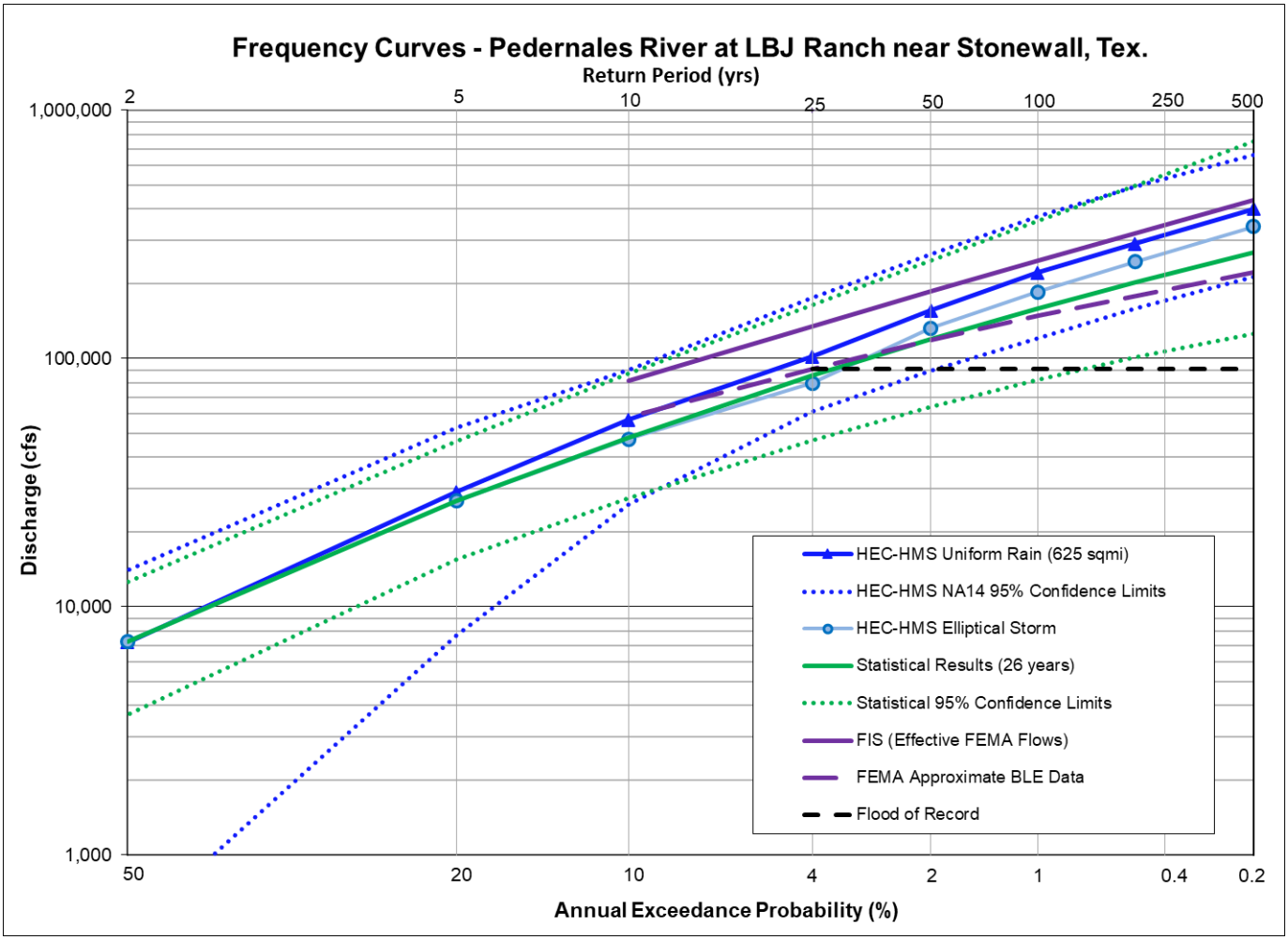

Figure 12.42: Flow Frequency Curve Comparison for the Pedernales River at LBJ Ranch near Stonewall, TX

Table 12.43: Frequency Flow (cfs) Results Comparison for the Pedernales River near Johnson City, TX

Annual Exceedance Probability (AEP)	Return Period (years)	Currently Effective FEMA FIS	Approx BLE Data from FEMA	Statistical Analysis of the Gage Record (Ch 5) (82 years)	HEC-HMS Uniform Rain Frequency Storm (Ch 6) (900 sq mi)	HEC-HMS Elliptical Frequency Storm (Ch 7) (900 sq mi)
0.002	500		258,911	479,000	455,100	374,300
0.005	200			352,000	322,200	288,800
0.01	100	269,000	173,161	272,000	244,800	231,700
0.02	50		138,214	204,000	187,800	180,200
0.04	25		106,288	147,000	136,700	140,000
0.1	10		68,116	87,600	83,100	87,500
0.2	5			53,000	50,500	52,900
0.5	2			19,500	19,500	19,500

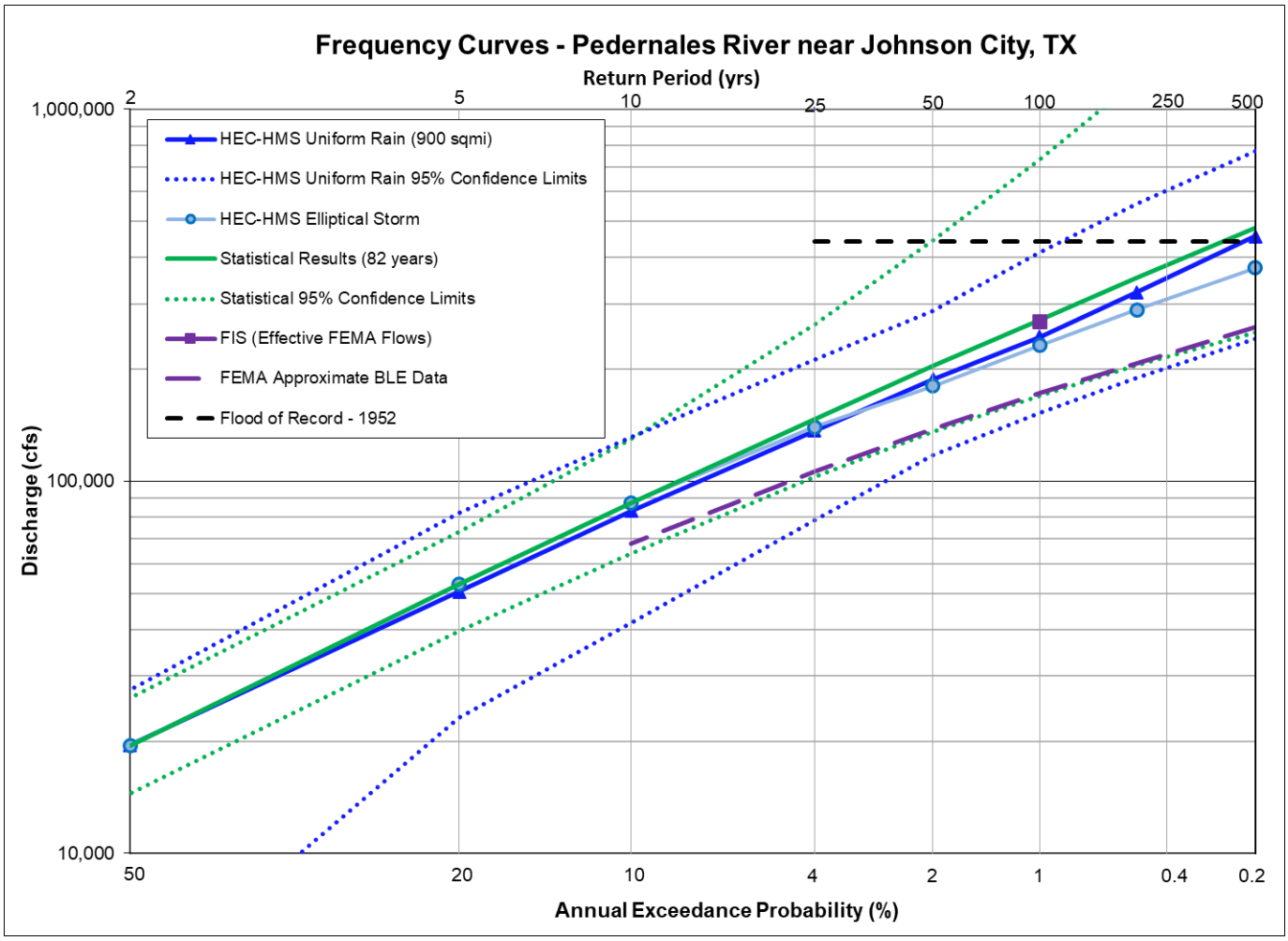

Figure 12.43a: Flow Frequency Curve Comparison for the Pedernales River near Johnson City, TX

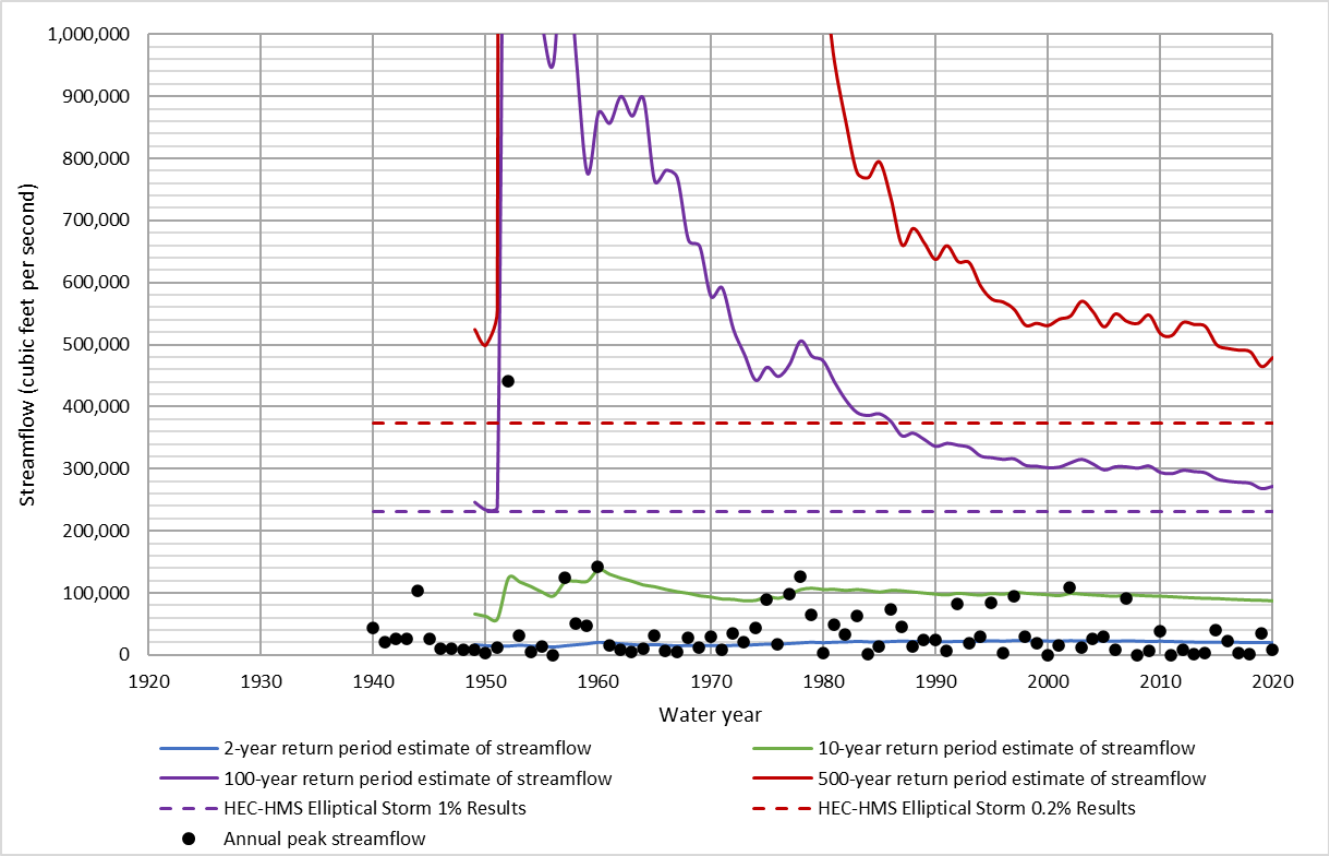

Figure 12.43b: Statistical Change Over Time Comparison for the Pedernales River near Johnson City, TX

The final point of comparison on the Pedernales is the Pedernales River near Johnson City, Texas as shown in the preceding table and figures. This USGS gage has a drainage area of about 900 square miles in the steep and flashy watersheds of the Texas Hill Country, and it has no significant reservoirs upstream. There are no trends in annual peak streamflow for this portion of the watershed.

This location has both an effective FIS FEMA flow and approximate frequency flows from FEMA's recently published Base Level Engineering (BLE) data, as shown in Figure 12.43a. The effective FIS flows were based on a 1989 USACE study of unknown methodology while the BLE approximate flows were based on regional regression equations. Figure 12.43a shows that the effective FIS flow matches the current study's statistical analysis closely, while the BLE flows are much lower and are actually near the lower confidence bounds of the current Bulletin 17C analysis. The HEC-HMS elliptical storm results, on the other hand, are just slightly lower than the current statistical analysis, and both the HEC-HMS results and the statistical results are well within one another's confidence bounds.

Figure 12.43b shows the change in the statistical results over time as new flood events have been added to the record. From this plot, one can see that while the 2-year and 10-year statistical estimates have been relatively stable for decades, the 100-yr and 500-yr estimates continue to experience significant downward movement even after 80+ years of record. In this case, the 1952 flood was a high outlier that caused the Bulletin 17B/C analyses to greatly overestimate the 1% and 0.2% AEP frequency flows for several decades, and it appears that the statistical estimates have still not returned to normal levels. Rainfall records show that the 1952 flood on the Pedernales River resulted from over 20 inches of rainfall in less than 24 hours (Breeding, 1954). According to NOAA Atlas 14, that would be approximately equivalent to a 0.1% AEP (1,000-year) storm for that area (NOAA, 2018), and indeed, the HEC-HMS elliptical storm results on Figures 12.43a and 12.43b show that the 1952 flood of record is greater than a 0.2% AEP (500-year) storm.

12.1.5 Barton and Onion Creek Gage Locations

Table 12.44: Frequency Flow (cfs) Results Comparison for Bull Creek at Loop 360 near Austin

Annual Exceedance Probability (AEP)	Return Period (years)	Currently Effective FEMA FIS	Approximate BLE Data from FEMA	Statistical Analysis of the Gage Record (Ch 5) (42 years)	HEC-HMS Uniform Rain Frequency Storm (Ch 6) (23 sq mi)
0.002	500	37,700		36,800	44,000
0.005	200			28,800	35,600
0.01	100	25,600		23,500	29,900
0.02	50	20,900		18,700	24,700
0.04	25			14,400	17,500
0.1	10	11,900		9,490	10,900
0.2	5			6,350	6,400
0.5	2			2,840	2,830

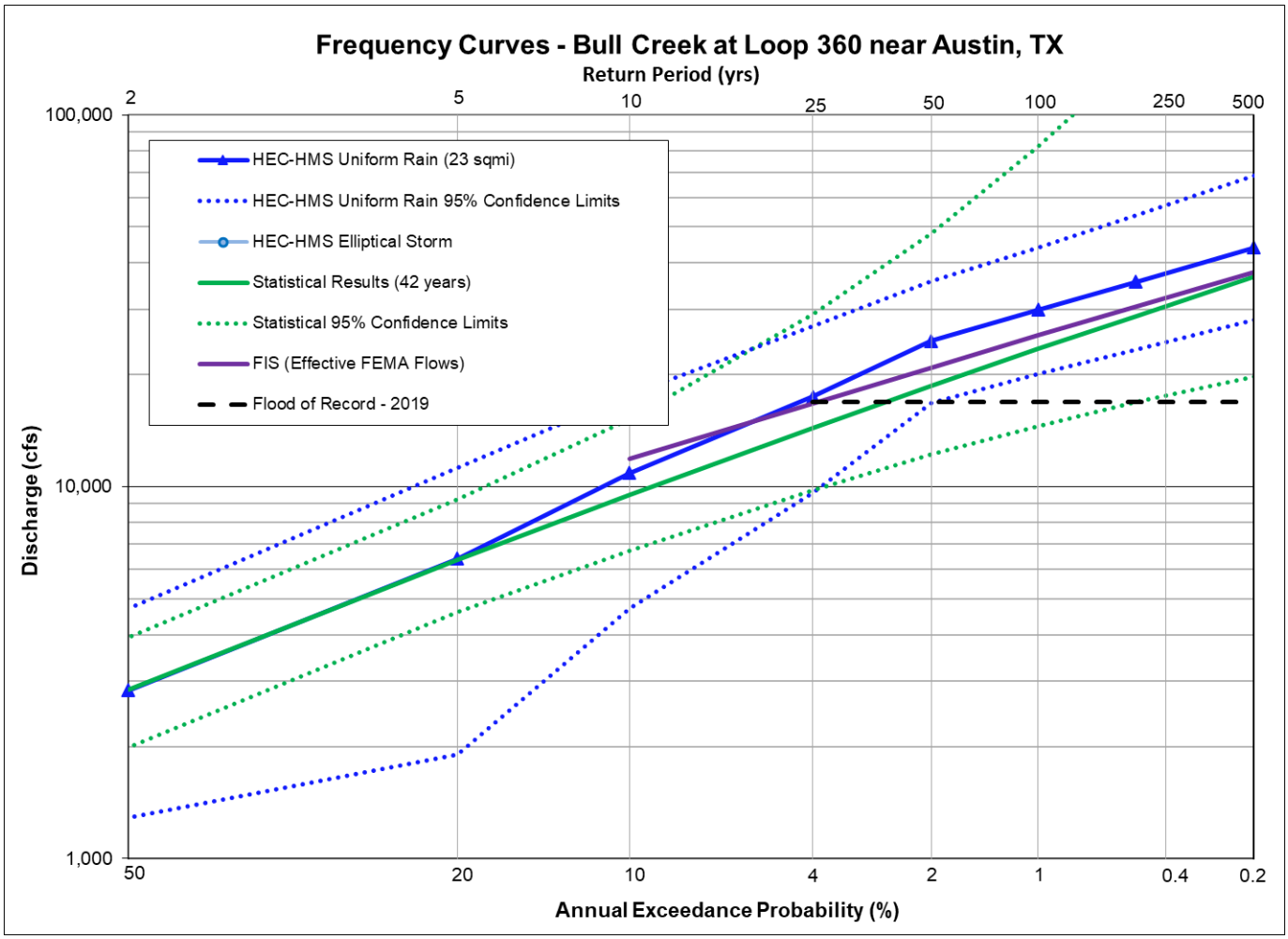

Figure 12.44: Flow Frequency Curve Comparison for Bull Creek at Loop 360 near Austin

The first point of comparison in this portion of the watershed is Bull Creek at Loop 360 near Austin, Texas as shown in the preceding table and figure. This gage has a drainage area of 23 square miles in a fairly steep watershed in the urbanized Austin area. It has no significant reservoirs upstream.

The effective FEMA frequency flows for this location were based on a 2013 HEC-HMS model for the Travis County FIS. As shown in Figure 12.44, the effective FEMA flows are slightly higher than the statistical results based on 42 years of record, but slightly lower than the calibrated HEC-HMS results of the current study. Both the HEC-HMS and statistical results are well within one another's confidence bounds.

The next point of comparison is Barton Creek near Oak Hill, Texas as shown in the following table and figure. This gage has a drainage area of about 90 square miles and is located in a fairly steep watershed in the urbanized Austin area. It has no significant reservoirs upstream.

There are no published FEMA flows for this location. As shown in Figure 12.45, the calibrated HEC-HMS results are slightly higher than the current statistical results based on 44 years of record, but both the HEC-HMS and statistical results are well within one another's confidence bounds.

Table 12.45: Frequency Flow (cfs) Results Comparison for Barton Creek near Oak Hill

Annual Exceedance Probability (AEP)	Return Period (years)	Currently Effective FEMA FIS	Approximate BLE Data from FEMA	Statistical Analysis of the Gage Record (Ch 5) (44 years)	HEC-HMS Uniform Rain Frequency Storm (Ch 6) (90 sq mi)
0.002	500			63,400	87,000
0.005	200			50,800	67,500
0.01	100			41,600	53,700
0.02	50			32,800	41,300
0.04	25			24,600	28,100
0.1	10			15,000	17,000
0.2	5			8,870	10,200
0.5	2			2,730	2,760

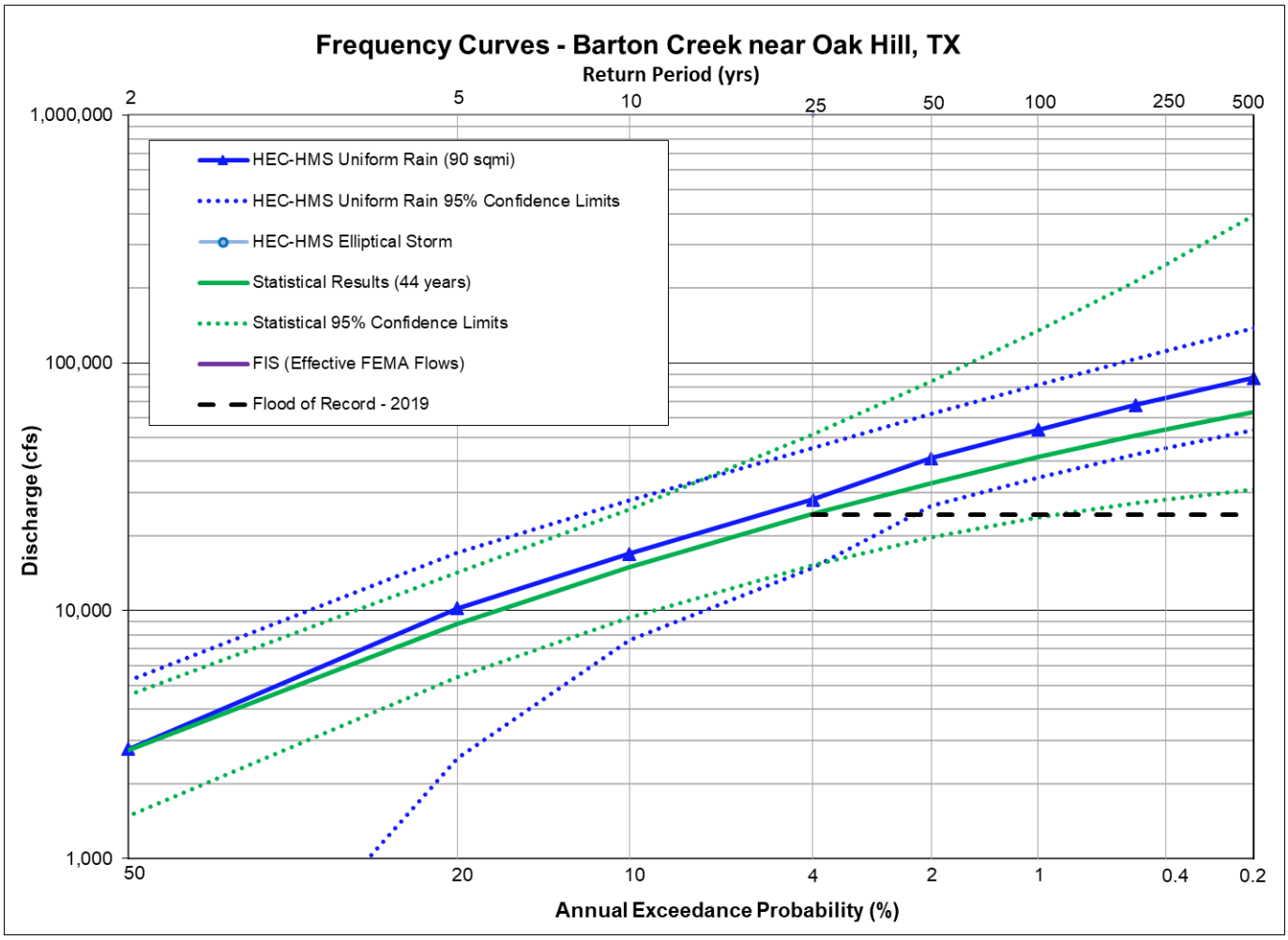

Figure 12.45: Flow Frequency Curve Comparison for Barton Creek near Oak Hill

Table 12.46: Frequency Flow (cfs) Results Comparison for Barton Creek at Lost Creek Blvd

Annual Exceedance Probability (AEP)	Return Period (years)	Currently Effective FEMA FIS	Approximate BLE Data from FEMA	Statistical Analysis of the Gage Record (Ch 5) (32 years)	HEC-HMS Uniform Rain Frequency Storm (Ch 6) (108 sq mi)
0.002	500			69,400	92,900
0.005	200			56,000	71,000
0.01	100			46,000	56,100
0.02	50			36,400	42,100
0.04	25			27,300	28,100
0.1	10			16,500	16,700
0.2	5			9,570	9,700
0.5	2			2,780	2,600

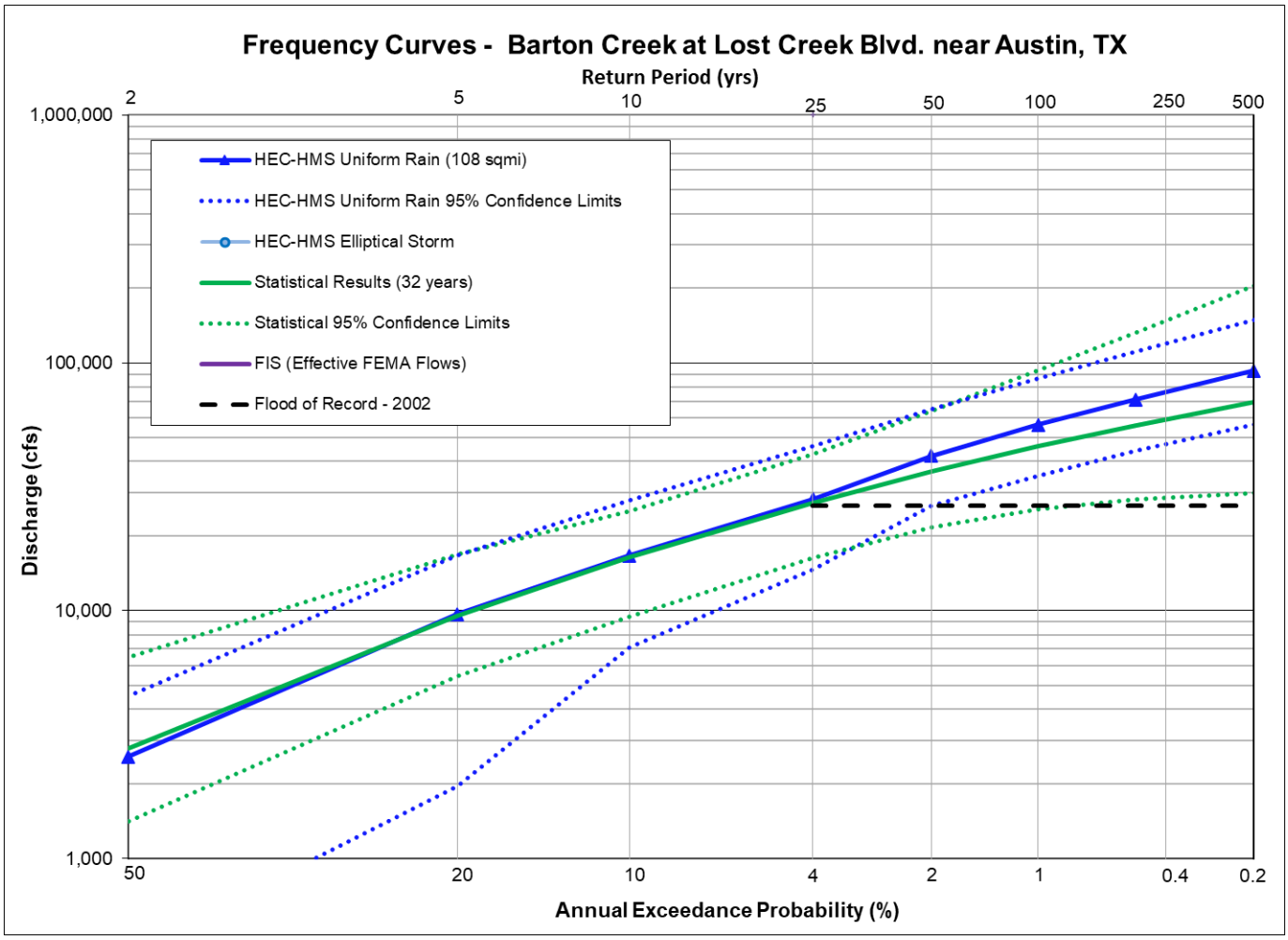

Figure 12.46: Flow Frequency Curve Comparison for Barton Creek at Lost Creek Blvd

The next point of comparison on Barton Creek is Barton Creek at Lost Creek Blvd as shown in the preceding table and figure. This gage has a drainage area of about 107 square miles and is located in a fairly steep watershed in the urbanized Austin area. There are no significant reservoirs upstream.

There are no published FEMA flows for this location. As shown in Figure 12.46, the calibrated HEC-HMS results are slightly higher than the current statistical results based on 32 years of record, but both the HEC-HMS and statistical results are well within one another's confidence bounds.

The next point of comparison is Barton Creek at Loop 360, Austin, Texas as shown in the following table and figure. This gage has a drainage area of about 116 square miles and is located in a fairly steep watershed in the urbanized Austin area. There are no significant reservoirs upstream.

There are no published FEMA flows for this location. As shown in Figure 12.47, the calibrated HEC-HMS results are very close to the current statistical results based on 45 years of record, and both the HEC-HMS and statistical results are well within one another's confidence bounds.

Table 12.47: Frequency Flow (cfs) Results Comparison for Barton Creek at Loop 360, Austin, TX

Annual Exceedance Probability (AEP)	Return Period (years)	Currently Effective FEMA FIS	Approximate BLE Data from FEMA	Statistical Analysis of the Gage Record (Ch 5) (45 years)	HEC-HMS Uniform Rain Frequency Storm (Ch 6) (117 sq mi)
0.002	500			89,400	93,600
0.005	200			67,300	71,200
0.01	100			52,500	56,100
0.02	50			39,500	41,900
0.04	25			28,500	28,000
0.1	10			16,500	16,600
0.2	5			9,540	9,600
0.5	2			2,990	3,040

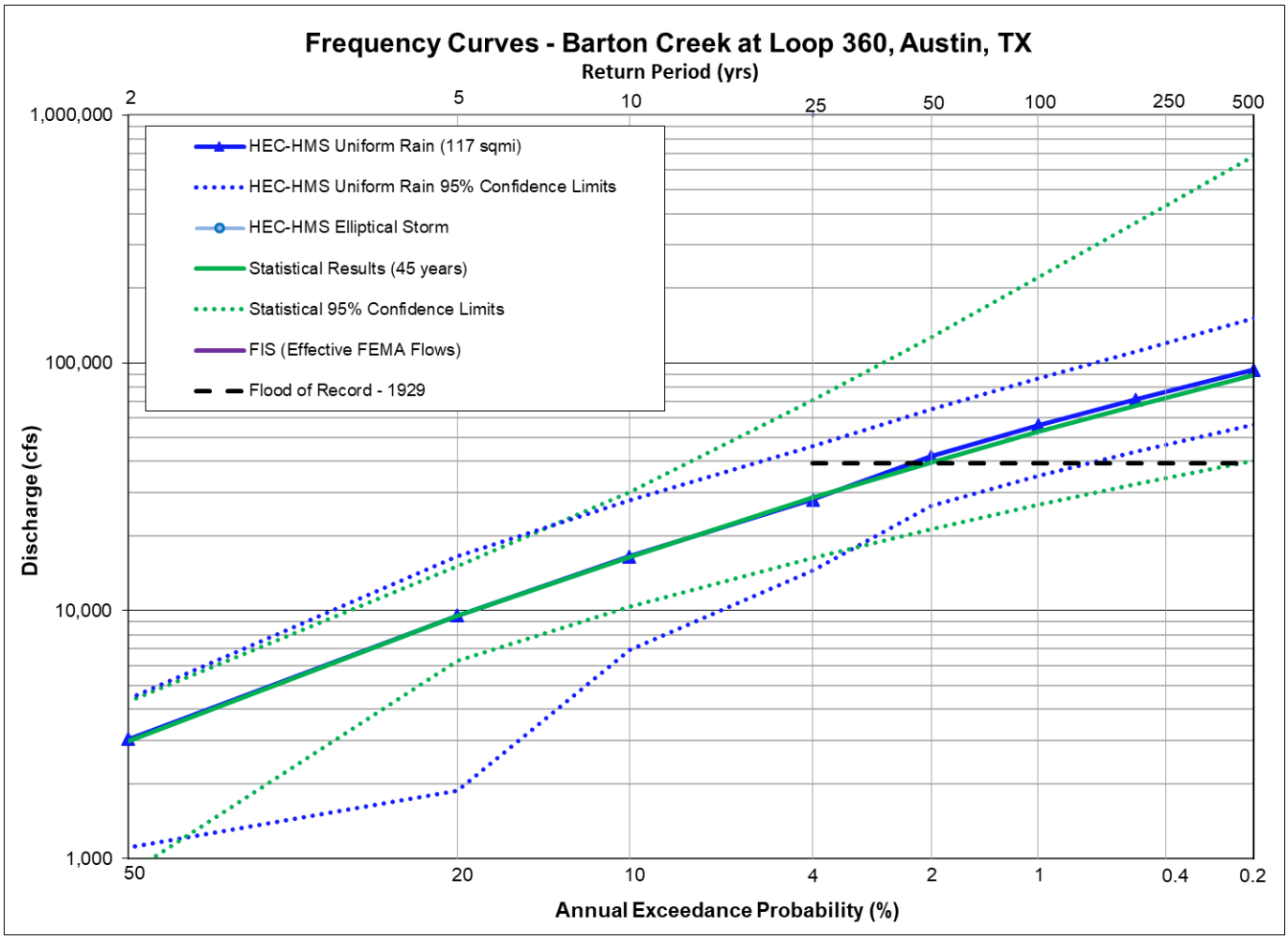

Figure 12.47: Flow Frequency Curve Comparison for Barton Creek at Loop 360, Austin, TX

Table 12.48: Frequency Flow (cfs) Results Comparison for Barton Creek abv Barton Springs

Annual Exceedance Probability (AEP)	Return Period (years)	Currently Effective FEMA FIS	Approximate BLE Data from FEMA	Statistical Analysis of the Gage Record (Ch 5) (23 years)	HEC-HMS Uniform Rain Frequency Storm (Ch 6) (120 sq mi)
0.002	500			79,600	93,800
0.005	200			58,700	71,200
0.01	100			45,200	56,000
0.02	50			33,600	41,900
0.04	25			23,900	28,000
0.1	10			13,700	16,500
0.2	5			7,820	9,500
0.5	2			2,460	3,060

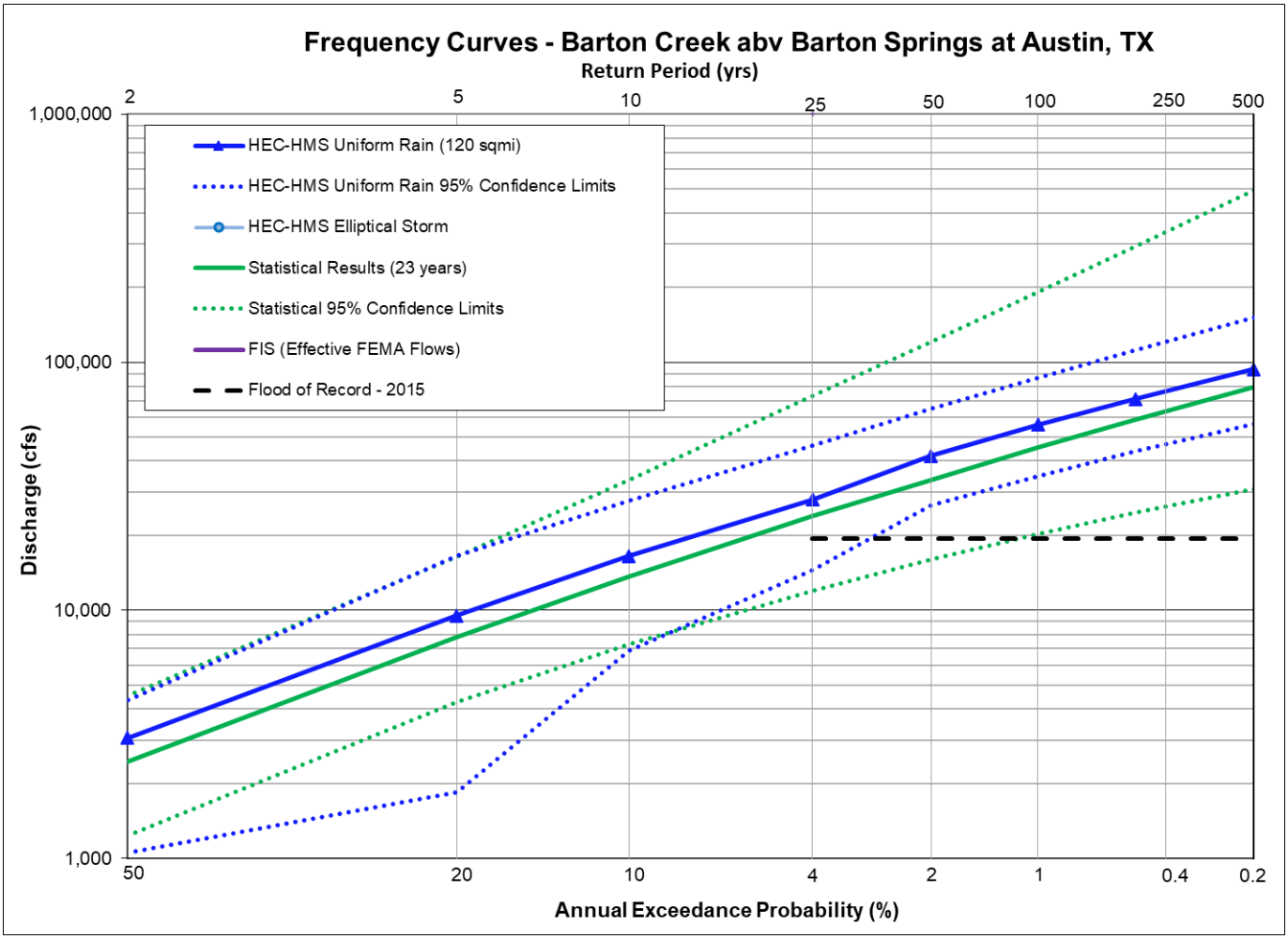

Figure 12.48: Flow Frequency Curve Comparison for Barton Creek abv Barton Springs

The next point of comparison on Barton Creek is Barton Creek above Barton Springs, as shown in the preceding table and figure. This gage has a drainage area of over 120 square miles and is located in a fairly steep watershed in the urbanized Austin area. There are no significant reservoirs upstream.

There are no published FEMA flows for this location. As shown in Figure 12.48, the calibrated HEC-HMS results are slightly higher than the current statistical results based on 23 years of record, and both the HEC-HMS and statistical results are well within one another's confidence bounds.

The next point of comparison is Walnut Creek at Webberville Rd, Austin, Texas as shown in the following table and figure. This gage has a drainage area of over 50 square miles and is in a highly urbanized watershed in the Austin area. There are no significant reservoirs upstream.

The currently effective FEMA flows for this location were based on a 2005 HEC-HMS model for the Travis County FIS. As shown in Figure 12.49a, the effective FEMA flows are very similar to the HEC-HMS results from the current study. The statistical results based on 55 years of gage record, on the other hand, are much lower than the HEC-HMS results, as shown in Figure 12.49a. In fact, the HEC-HMS results are above the upper confidence bounds of the statistical analysis. However, there is a higher degree of uncertainty associated with the larger floods in this gage's annual peak flow record.

The largest flood of record at this location is 16,400 cfs, which is quite low for an urban watershed of this size. The USGS has a note in their database about this gage that states, "Above 25 ft (≈ 10,000 cfs), water breaks out of main channel about 1/4 mile above gage and crosses FM Road 969 east of gage through a culvert and over the road." See Figure 12.49b for the location of this overflow diversion upstream of the gage site. Figure 12.49c illustrates that the magnitude of these diversions could be substantial. It compares the peak magnitude and volume of streamflow during the October 2013 flood event at the Webberville Road gage versus the upstream Dessau Rd gage that has only half the drainage area of Webberville Rd. As one can see in Figure 12.49c, the peak magnitude was cut in half from the discharge at the upstream gage. Although some streamflow is known to exit the channel at stages greater than approximately 25 feet, it could be that the rating curve for the site underestimates this diversion at higher stages. This means that the peak annual flows recorded for other large floods at Webberville Road could have been underestimated, and the Bulletin 17C analysis may not be reliable for estimating the total flow on Walnut Creek.

Table 12.49: Frequency Flow (cfs) Results Comparison for Walnut Creek at Webberville Rd, Austin, TX

Annual Exceedance Probability (AEP)	Return Period (years)	Currently Effective FEMA FIS	Approximate BLE Data from FEMA	Statistical Analysis of the Gage* Record (Ch 5) (55 years)	HEC-HMS Uniform Rain Frequency Storm (Ch 6) (52 sq mi)
0.002	500	50,810		21,700	53,600
0.005	200			19,400	42,800
0.01	100	32,440		17,700	35,400
0.02	50	26,860		15,800	28,600
0.04	25			13,800	20,400
0.1	10	17,250		11,000	13,400
0.2	5			8,760	8,800
0.5	2			5,300	5,340

* NOTE: Gage does not record flows > 10,000 cfs.

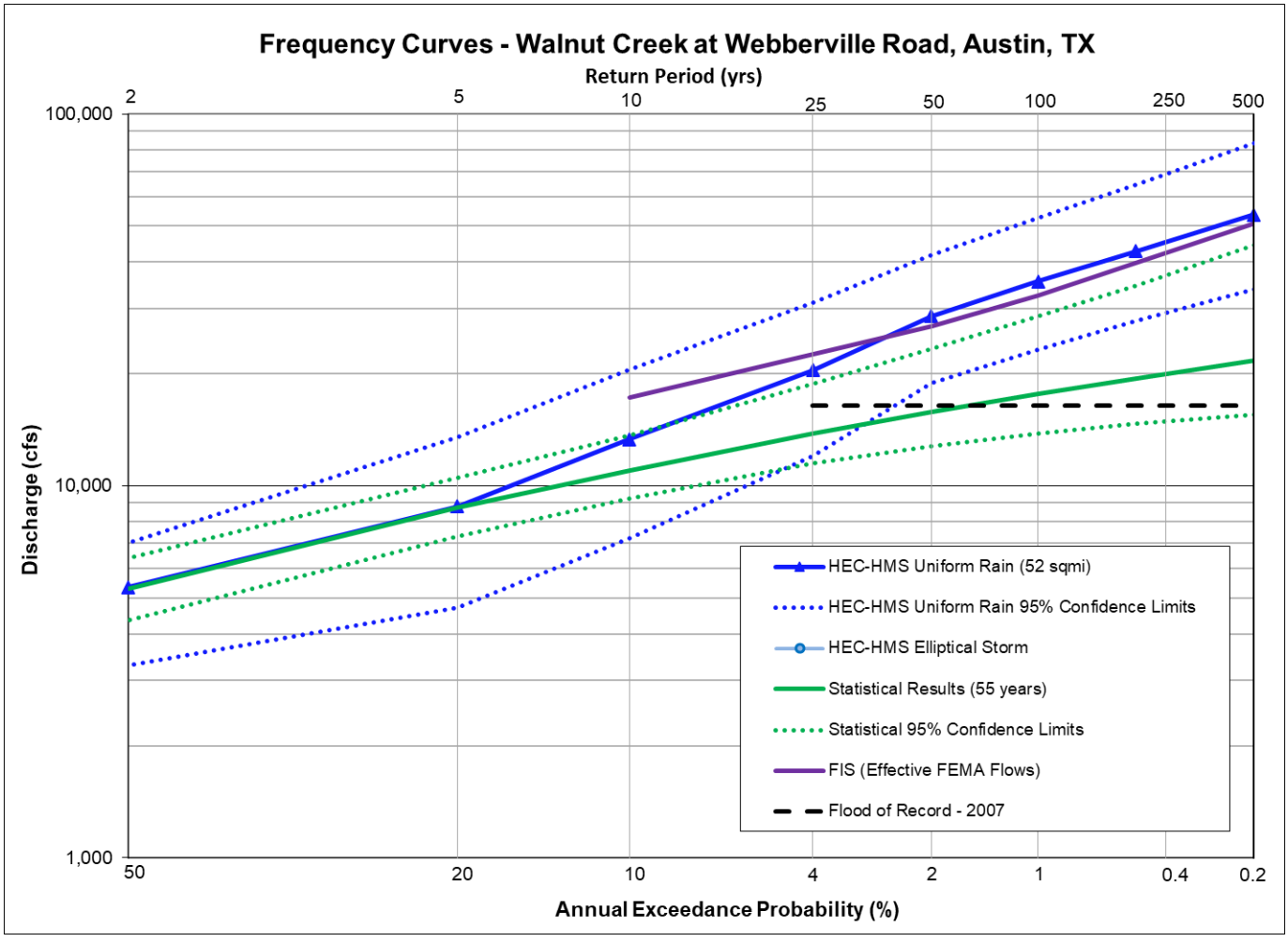

Figure 12.49a: Flow Frequency Curve Comparison for Walnut Creek at Webberville Rd, Austin, TX

Figure 12.49b: Location of the Diversion Upstream of the USGS Gage on Walnut Creek at Webberville Rd

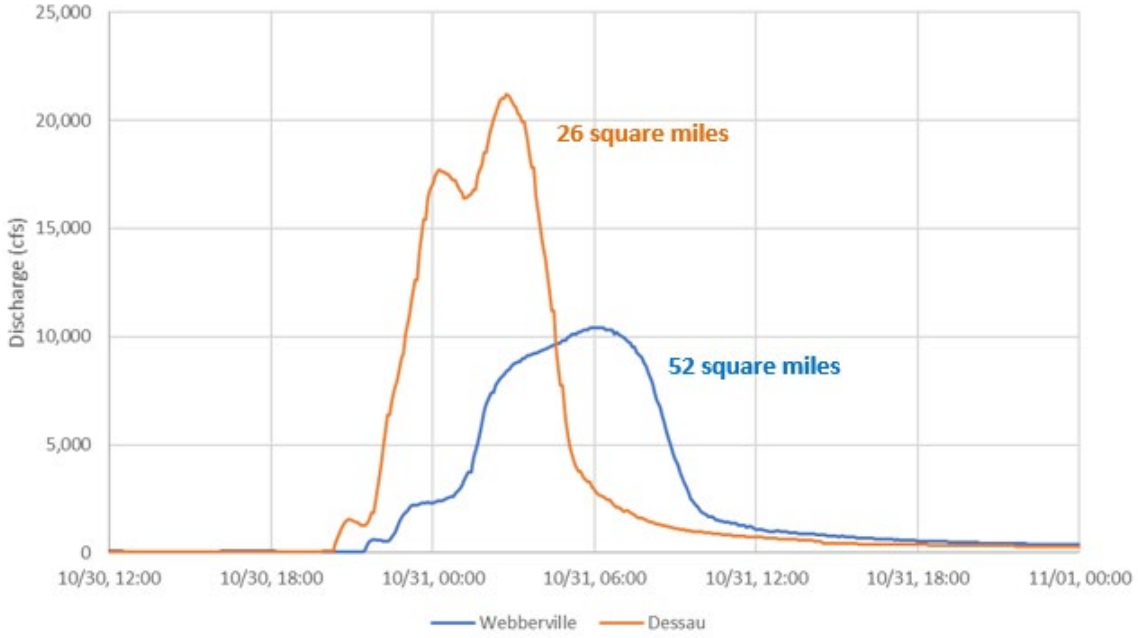

Figure 12.49c: Comparison of Oct 2013 Hydrographs at the Dessau Rd and Webberville Rd Gages

Table 12.50: Frequency Flow (cfs) Results Comparison for Onion Creek near Driftwood, TX

Annual Exceedance Probability (AEP)	Return Period (years)	Currently Effective FEMA FIS	Preliminary FEMA FIS, 2019	Statistical Analysis of the Gage Record (Ch 5) (41 years)	HEC-HMS Uniform Rain Frequency Storm (Ch 6) (124 sq mi)
0.002	500	90,740	116,220	48,600	127,500
0.005	200			39,200	98,100
0.01	100	52,540	75,420	32,500	78,300
0.02	50	40,770	57,380	26,200	59,800
0.04	25			20,400	35,800
0.1	10	18,660	19,800	13,400	18,300
0.2	5			8,810	8,880
0.5	2			3,600	3,680

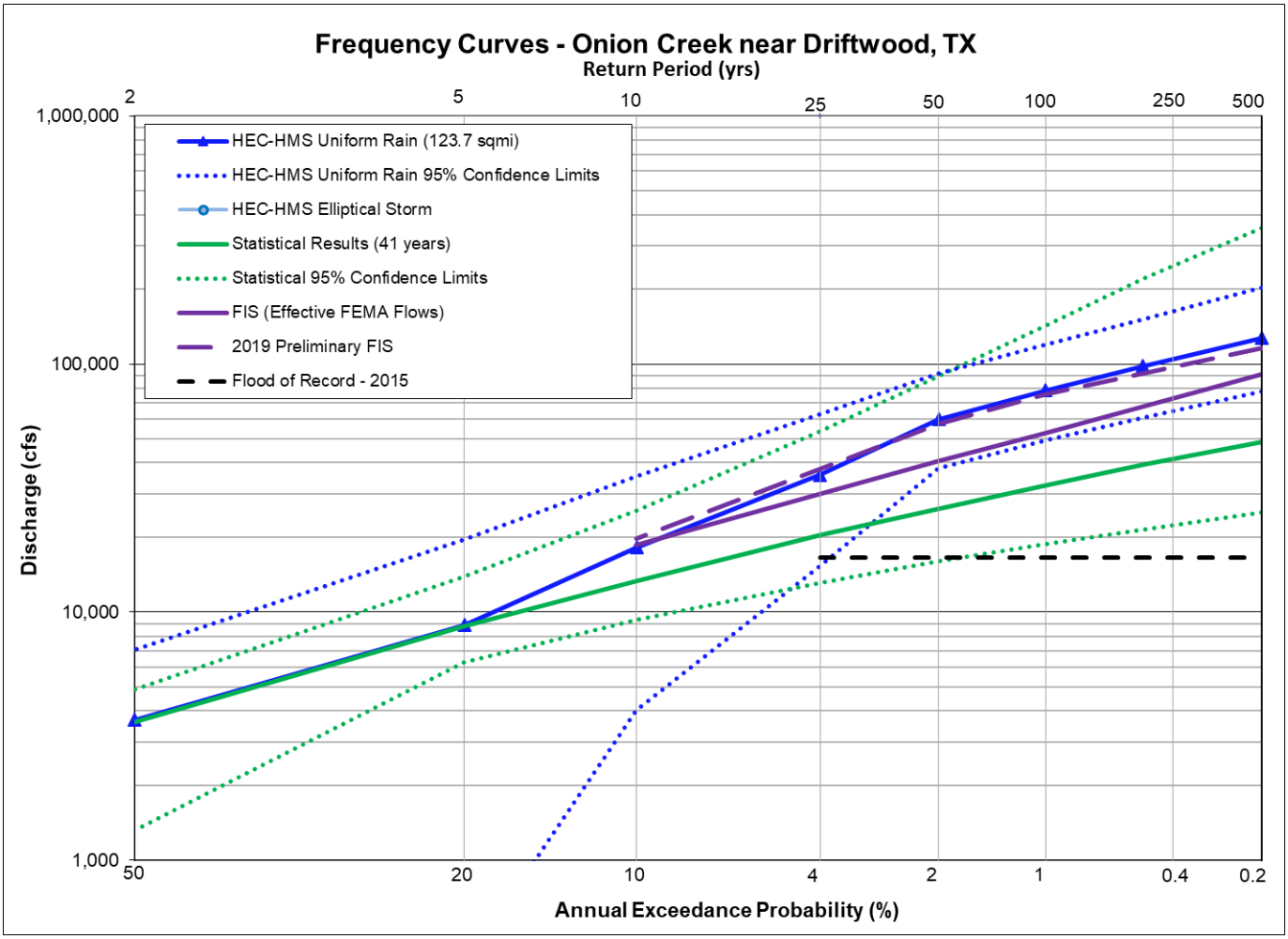

Figure 12.50: Flow Frequency Curve Comparison for Onion Creek near Driftwood, TX

The first point of comparison on Onion Creek is Onion Creek near Driftwood, Texas, as shown in the preceding table and figure. This gage has a drainage area of over 120 square miles and is fairly steep watershed in the Austin area. There are no significant reservoirs upstream.

The currently effective FEMA flows for this location were published in the 2005 Hays County FIS but were based on 1994 regional regression equations. The updated preliminary FIS, on the other hand, was based on a combination of regression equations and a 2019 statistical analysis of the gage record. As shown in Figure 12.50, the preliminary FIS frequency flows are very close to the HEC-HMS results from the current study. Figure 12.50 also shows that the results of current statistical analysis based on 42 years of gage record were much lower than both the FEMA flows and the HEC-HMS results. In fact, the current Bulletin 17C statistical results are below the confidence bounds of NOAA Atlas 14's rainfall depths. The HEC-HMS results, on the other hand, are well within the confidence bounds of the statistical analysis. This is an indication that the uncertainty is greater in the statistical analysis than it is in the HEC-HMS results.

Furthermore, the largest flood of record at this location was only 16,600 cfs, which is a lower than expected value for a watershed of this size (see the Baton Creek gages for comparison). There are only six field measurements of discharge greater than 500 cfs at this location to establish the rating curve, and all measurements are rated as poor, which represent an estimated error of 25% or greater. This is because the streamgage was originally established with the purpose of collecting rainfall and runoff data for estimating groundwater recharge and quality rather than peak streamflow. As such, the peak streamflow record and flood frequency analysis is understood to have a higher degree of error than other statistical analyses in this report. More information on the streamgage and uncertainty associated with the statistical analysis may be found in Appendix A.

The next point of comparison is Onion Creek at Buda, Texas as shown in the following table and figure. This LCRA gage has a drainage area of about 167 square miles in the Austin area. There are no significant reservoirs upstream.

The currently effective FEMA flows for this location were published in the 2005 Hays County FIS but were based on 1994 regional regression equations. The updated preliminary FIS, on the other hand, was based on a combination of regression equations and a 2019 statistical analysis of the gage record. As shown in Figure 12.51, the currently effective FEMA flows are fairly close to the current statistical results, but those results were only based on 25 years of record. The updated preliminary FIS flows are a bit higher, but the HEC-HMS results from the current study are higher still. The HEC-HMS results were the first analysis to use the NOAA Atlas 14 rainfall depths for this site. The HEC-HMS and statistical results are also well within one another's confidence bounds, as shown in Figure 12.51.

Table 12.51: Frequency Flow (cfs) Results Comparison for Onion Creek at Buda, TX

Annual Exceedance Probability (AEP)	Return Period (years)	Currently Effective FEMA FIS	Preliminary FEMA FIS, 2019	Statistical Analysis of the Gage Record (Ch 5) (25 years)	HEC-HMS Uniform Rain Frequency Storm (Ch 6) (167 sq mi)
0.002	500	108,570	124,090	117,000	156,100
0.005	200			86,900	122,900
0.01	100	62,600	80,140	67,100	97,800
0.02	50	48,480	61,100	50,000	74,200
0.04	25			35,500	50,300
0.1	10	22,070	22,300	20,300	26,100
0.2	5			11,600	11,600
0.5	2			3,600	3,670

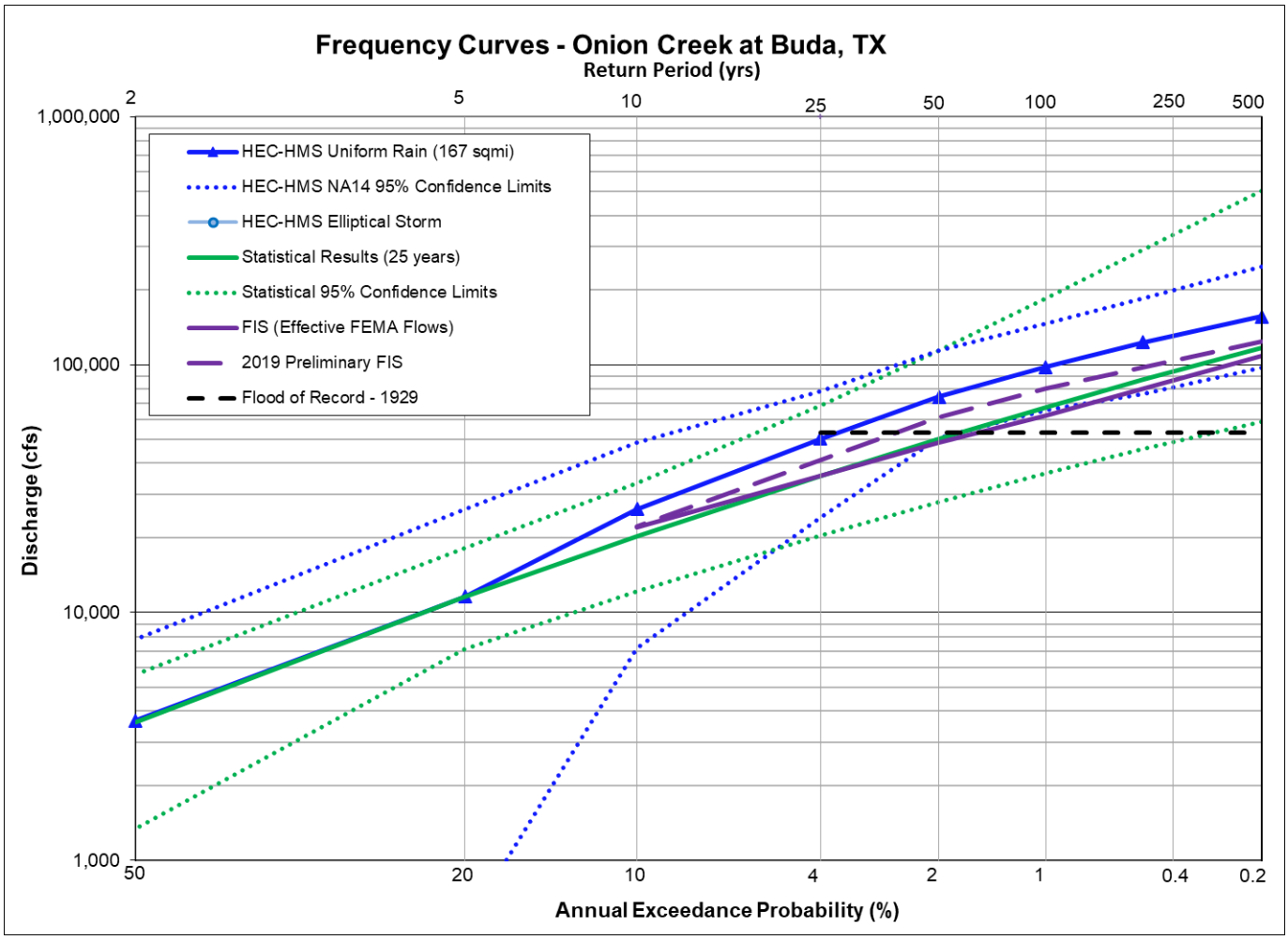

Figure 12.51: Flow Frequency Curve Comparison for Onion Creek at Buda, TX

Table 12.52: Frequency Flow (cfs) Results Comparison for Onion Creek at US Hwy 183, Austin, TX

Annual Exceedance Probability (AEP)	Return Period (years)	Currently Effective FEMA FIS	Approximate BLE Data from FEMA	Statistical Analysis of the Gage Record (Ch 5) (53 years)	HEC-HMS Uniform Rain Frequency Storm (Ch 6) (324 sq mi)	HEC-HMS Elliptical Frequency Storm (Ch 7) (324 sq mi)
0.002	500	179,800		365,000	227,800	215,300
0.005	200			247,000	179,500	170,400
0.01	100	121,900		179,000	146,400	137,800
0.02	50	95,100		125,000	116,000	109,000
0.04	25			83,000	78,000	86,500
0.1	10	34,400		43,700	41,800	52,200
0.2	5			23,700	23,600	28,500
0.5	2			7,070	6,950	6,900

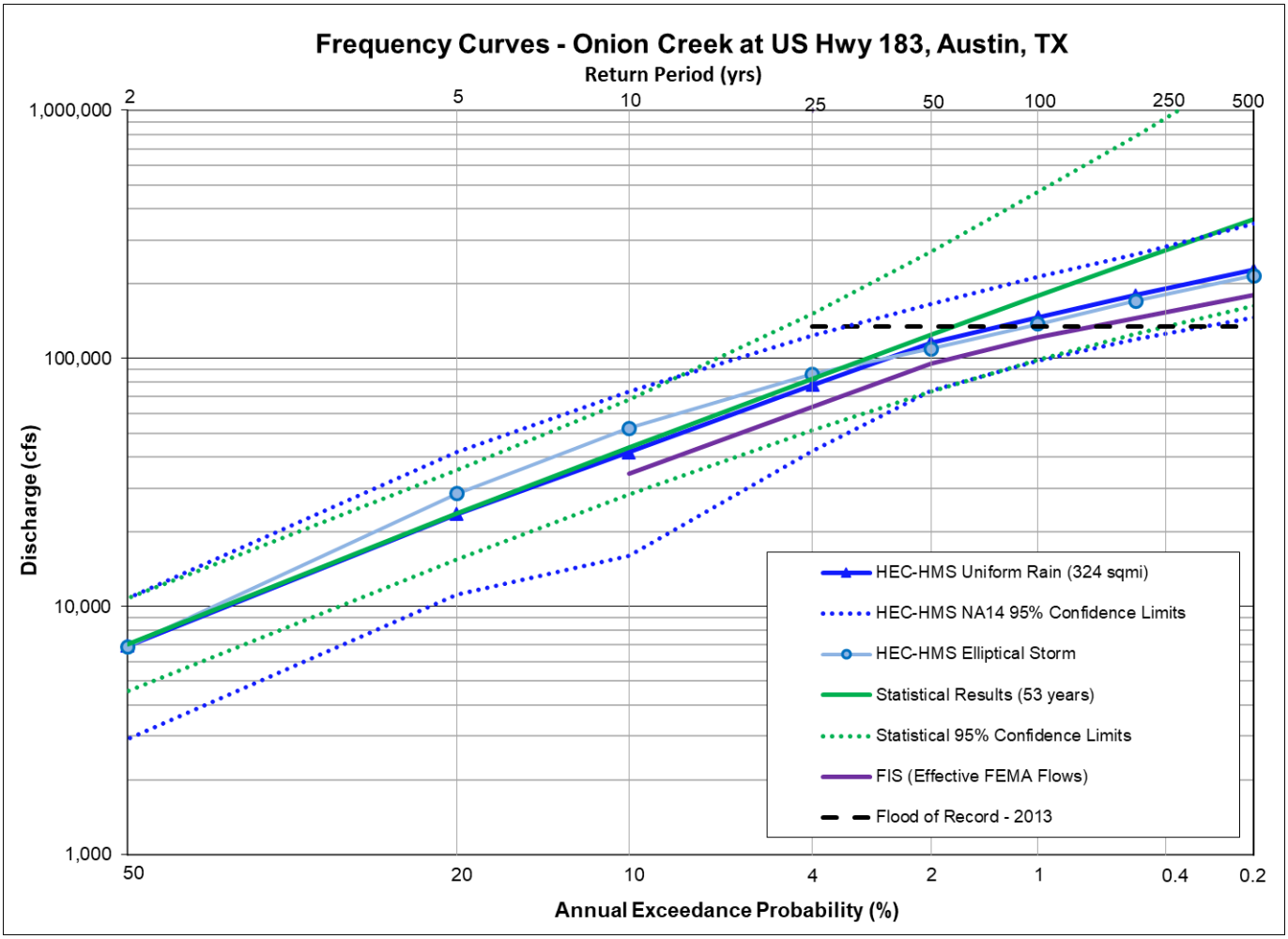

Figure 12.52a: Flow Frequency Curve Comparison for Onion Creek at US Hwy 183, Austin, TX

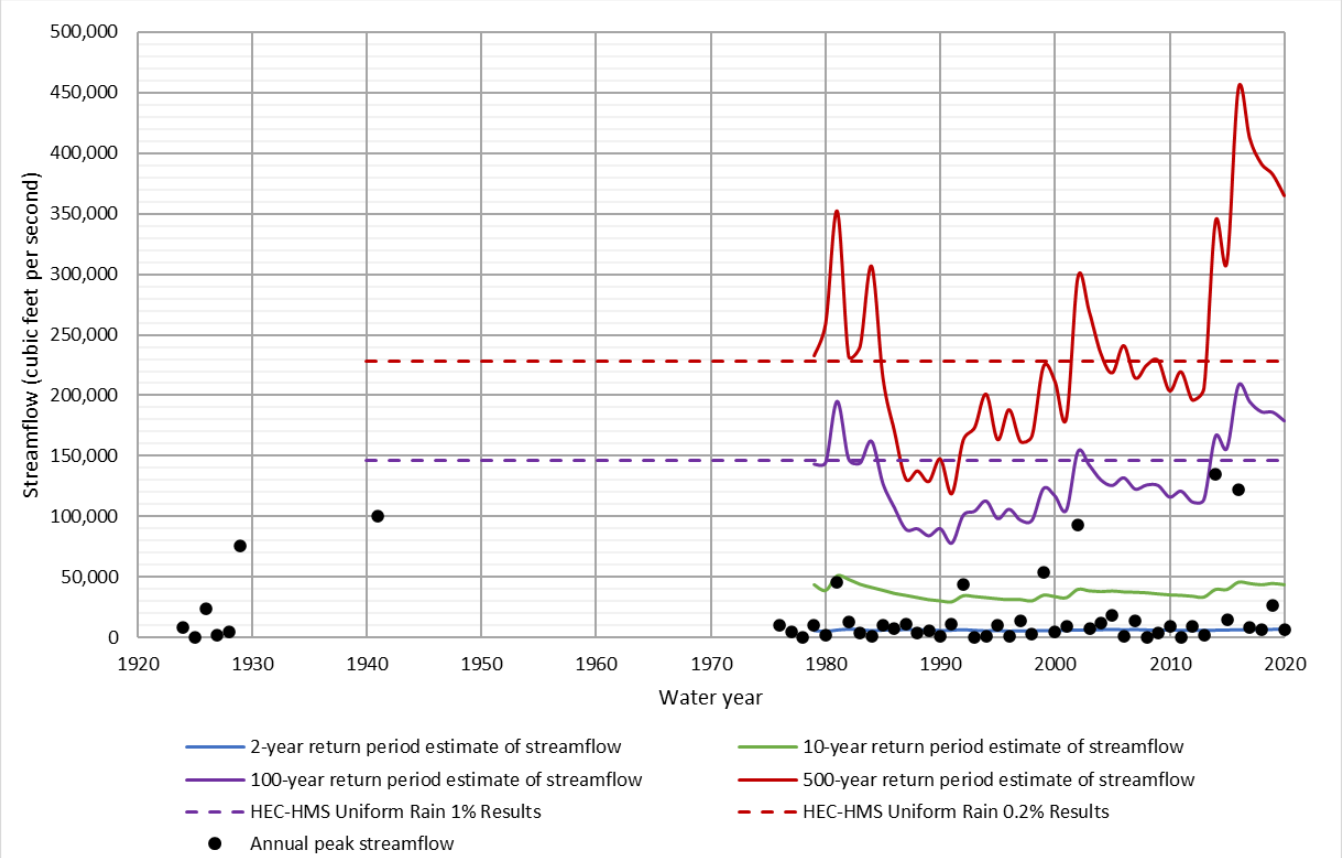

Figure 12.52b: Statistical Change Over Time Comparison for Onion Creek at US Hwy 183, Austin, TX

The final point of comparison on Onion Creek is Onion Creek at US Hwy 183 in Austin, Texas, as shown in the preceding table and figures. This USGS gage has a drainage area of over 320 square miles in the Austin area. There are no significant reservoirs upstream.

The currently effective FEMA flows for this location were published in the 2020 FIS for Travis County and were based on a 2016 HEC-HMS model and a statistical analysis of the gage record. As shown in Figure 12.52a, the currently effective FEMA flows are significantly lower than both the current statistical analysis and the HEC-HMS results from the current study. The currently effective flows did not include NOAA Atlas 14, which increased the expected rainfall depths in the Austin are considerably.

Figure 12.52a also shows that the results from the calibrated HEC-HMS model with NOAA Atlas 14 were significantly lower than the results of the statistical analysis based on 53 years of data at the 1% and 0.2% AEP frequencies. Figure 12.52b sheds some additional insight as to why that is. Figure 12.52b shows the change in the statistical results over time as new flood events have been added to the record. From this plot, one can see that 1% and 0.2% AEP (100-yr and 500-yr) statistical estimates were significantly increased after two recent large flood events in 2013 and 2015. Therefore, the statistical estimates may currently be overestimated due to the influence of those two recent large events. Figure 12.52b also shows that the HEC-HMS results for the 1% and 0.2% AEP (100-yr and 500-yr) frequencies fall near the midpoint of the statistical estimates over the last 40 years.

12.1.6 LCRA's Streamgage Locations

The following 19 streamgage locations are operated by LCRA. They are located on various smaller tributaries scattered throughout the Lower Colorado River basin, and all have less than 330 square miles in drainage area. Since these are all locations with relatively small drainage areas, elliptical frequency storms were not analyzed for any of these locations. These LCRA gages were installed in the late 1990s or early 2000s and have 20 to 25 years of gage record; therefore, a statistical change over time comparison plot is not available for any of these locations. Furthermore, the relatively short period of record for these gages greatly increases the uncertainty in the statistical analysis of the gage record. As a result, the HEC-HMS model is considered a more reliable source of flood frequency estimates for rare events like the 100-year (1% AEP) flood. However, the gage records still provide valuable estimates of smaller floods such as the 2- or 5-year (50% or 20% AEP) flood. The LCRA gage locations are presented in this section in alphabetical order.

5% and 95% Confidence Limits are included in the flood frequency curve comparison plots for both the statistical analysis and the HEC-HMS model results. In these plots, one may notice that the statistical confidence limits get wider with the rarer frequencies on the right-hand side of the graph, while the HEC-HMS confidence limits get narrower. Statistical confidence limits naturally get wider as the sample size gets smaller compared to the frequency of the event being estimated. HEC-HMS, on the other hand, shows greater uncertainty in the small, frequent events. This is because the natural variation in model parameters such as loss rates has a greater relative effect on the smaller rainfall events rather than the large ones. For example, a 2-inch variation in initial losses would have a much larger relative effect on a 4-inch, 2-year storm than it would on a 14-inch, 100-year storm. These confidence limits help illustrate why the HEC-HMS model loss rates are adjusted to better match the statistical results for the frequent events like the 2-year storm, but they are not adjusted for the rare events like the 100-yr storm.

Where available, the effective FEMA discharges from detailed Flood Insurance Studies (FIS) are included on the figures and tables. Of these 19 LCRA stream gages, effective FIS FEMA discharges were only available for three locations: Backbone Creek at Marble Falls, Comanche Creek near Mason, and Gilleland Creek near Manor. The differences between the effective FEMA FIS discharges and the current study analyses depend to a great degree on how and when those effective FIS discharges were calculated. For Backbone and Comanche Creeks, the HEC-HMS results from the current study happened to match very closely with the effective FIS discharges, which were also calculated from rainfall-runoff models. For Gilleland Creek, on the other hand, the effective FIS discharges plotted above the upper confidence bounds of both the HEC-HMS model and the statistical analysis. This is an indication that the effective FIS discharges may have been overestimated at this location.

Approximate FEMA discharges from the available published Base Level Engineering (BLE) data is also included on these figures and tables. BLE data was available for 12 of the 19 LCRA stream gages in this section. The hydrology for the currently available BLE data was based on approximate methods such as USGS regional regression equations. The regional regression equations provide a simple method to estimate frequency discharges based on physical parameters such as area and slope. However, it can be hit-or-miss as to whether those equations are a good fit for a particular watershed, and the figures in this section demonstrate that. For Buckners Creek, Cummins Creek, Little Llano River, and San Fernando Creek, the BLE discharges happened to fall very close to the results from this study's calibrated HEC-HMS model. However, for other locations, the BLE discharges seemed to significantly over or underestimate the flood risk. For Gilleland Creek, Hickory Creek, Johnson Creek, and Sandy Creek, the published BLE discharges were much higher than the calibrated HEC-HMS results and fell along the upper 5% confidence limit of the NOAA Atlas 14 rainfall depths. For Cypress and North Grape Creeks, on the other hand, the published BLE discharges were much lower than the calibrated HEC-HMS results and actually fell below the lower 95% confidence limits of NOAA Atlas 14 rainfall depths.

Table 12.53: Frequency Flow (cfs) Results Comparison for Backbone Creek at Marble Falls, TX

Annual Exceedance Probability (AEP)	Return Period (years)	Currently Effective FEMA FIS	Approximate BLE Data from FEMA	Statistical Analysis of the Gage Record (Ch 5) (23 years)	HEC-HMS Uniform Rain Frequency Storm (Ch 6) (30 sq mi)
0.002	500	39,330		85,500	44,000
0.005	200			60,700	35,300
0.01	100	28,640		44,900	29,100
0.02	50	25,390		31,700	23,700
0.04	25			21,000	19,400
0.1	10	15,670		10,500	11,100
0.2	5			5,210	5,200
0.5	2			1,140	1,100

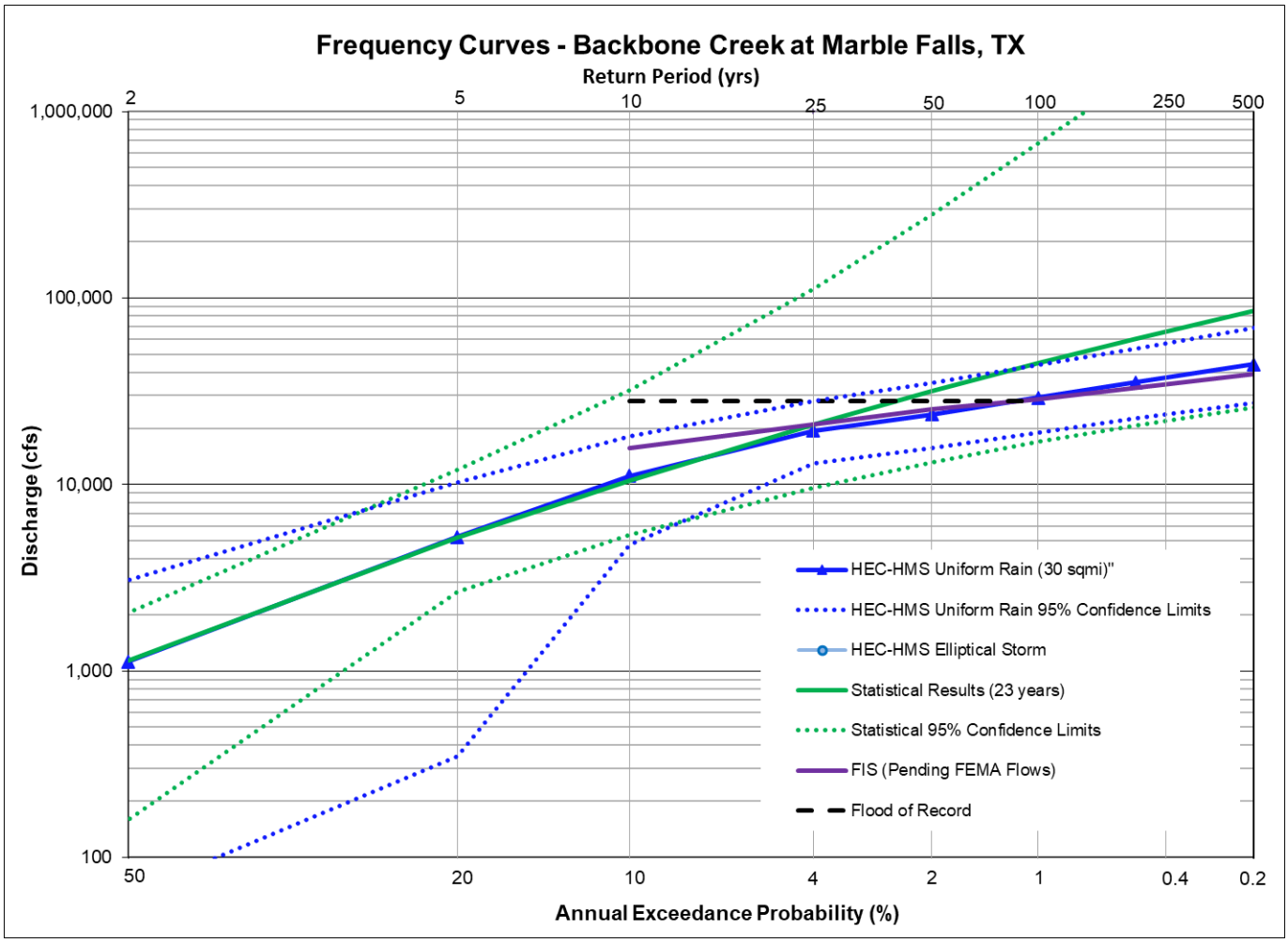

Figure 12.53: Flow Frequency Curve Comparison for Backbone Creek at Marble Falls, TX

Table 12.54: Frequency Flow (cfs) Results Comparison for Buckners Creek near Muldoon, TX

Annual Exceedance Probability (AEP)	Return Period (years)	Currently Effective FEMA FIS	Approximate BLE Data from FEMA	Statistical Analysis of the Gage Record (Ch 5) (23 years)	HEC-HMS Uniform Rain Frequency Storm (Ch 6) (92 sq mi)
0.002	500		70,907	101,000	57,000
0.005	200			72,800	44,900
0.01	100		41,320	55,100	36,900
0.02	50		31,495	40,400	28,900
0.04	25		23,152	28,300	23,100
0.1	10		14,193	15,900	15,900
0.2	5			9,050	9,200
0.5	2			2,870	3,000

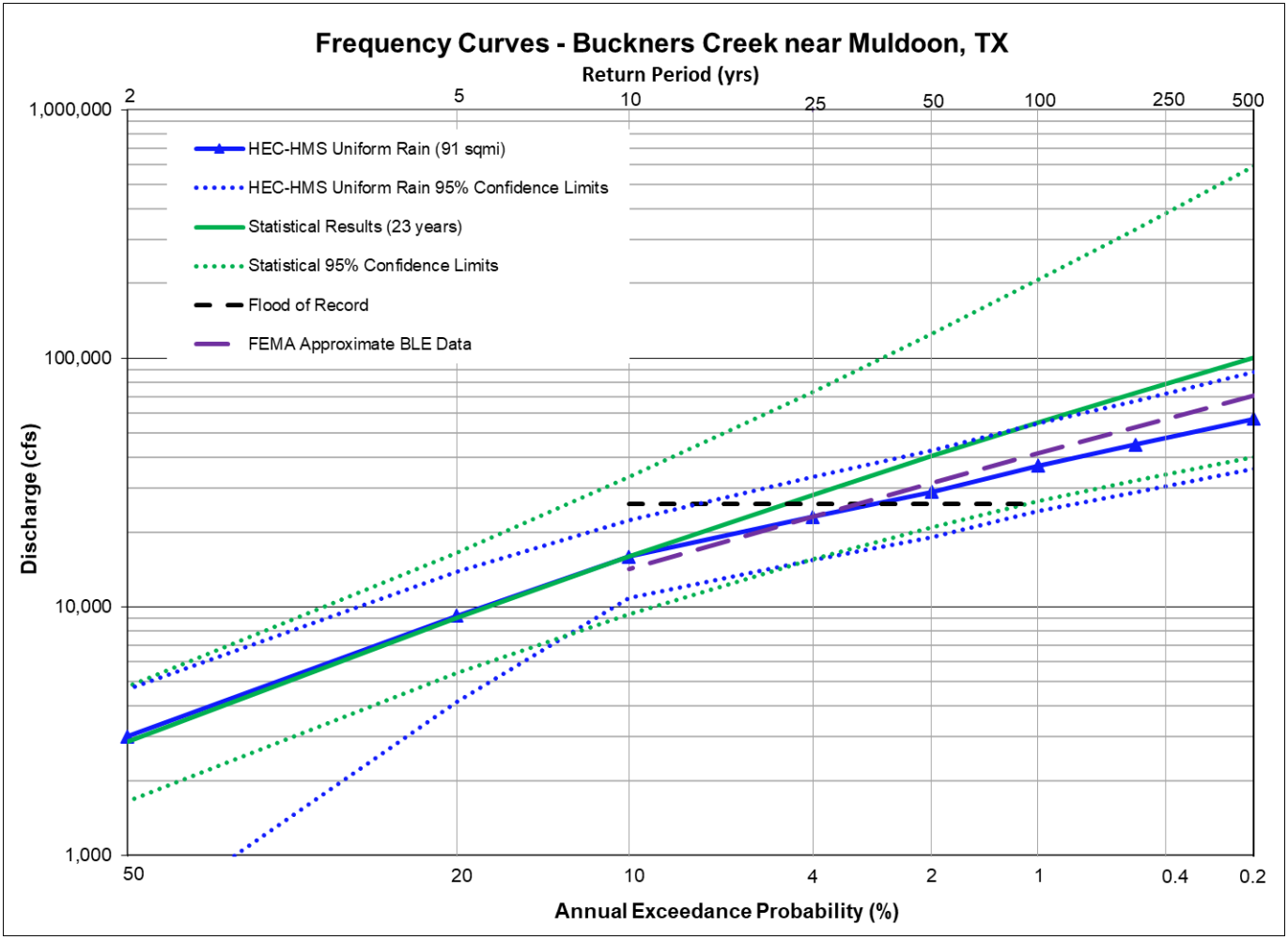

Figure 12.54: Flow Frequency Curve Comparison for Buckners Creek near Muldoon, TX

Table 12.55: Frequency Flow (cfs) Results Comparison for Cherokee Creek nr Bend, TX

Annual Exceedance Probability (AEP)	Return Period (years)	Currently Effective FEMA FIS	Approximate BLE Data from FEMA	Statistical Analysis of the Gage Record (Ch 5) (22 years)	HEC-HMS Uniform Rain Frequency Storm (Ch 6) (159 sq mi)
0.002	500			98,100	124,600
0.005	200			70,600	97,800
0.01	100			53,000	80,200
0.02	50			37,900	62,000
0.04	25			25,600	33,700
0.1	10			13,200	14,300
0.2	5			6,720	6,800
0.5	2			1,570	1,600

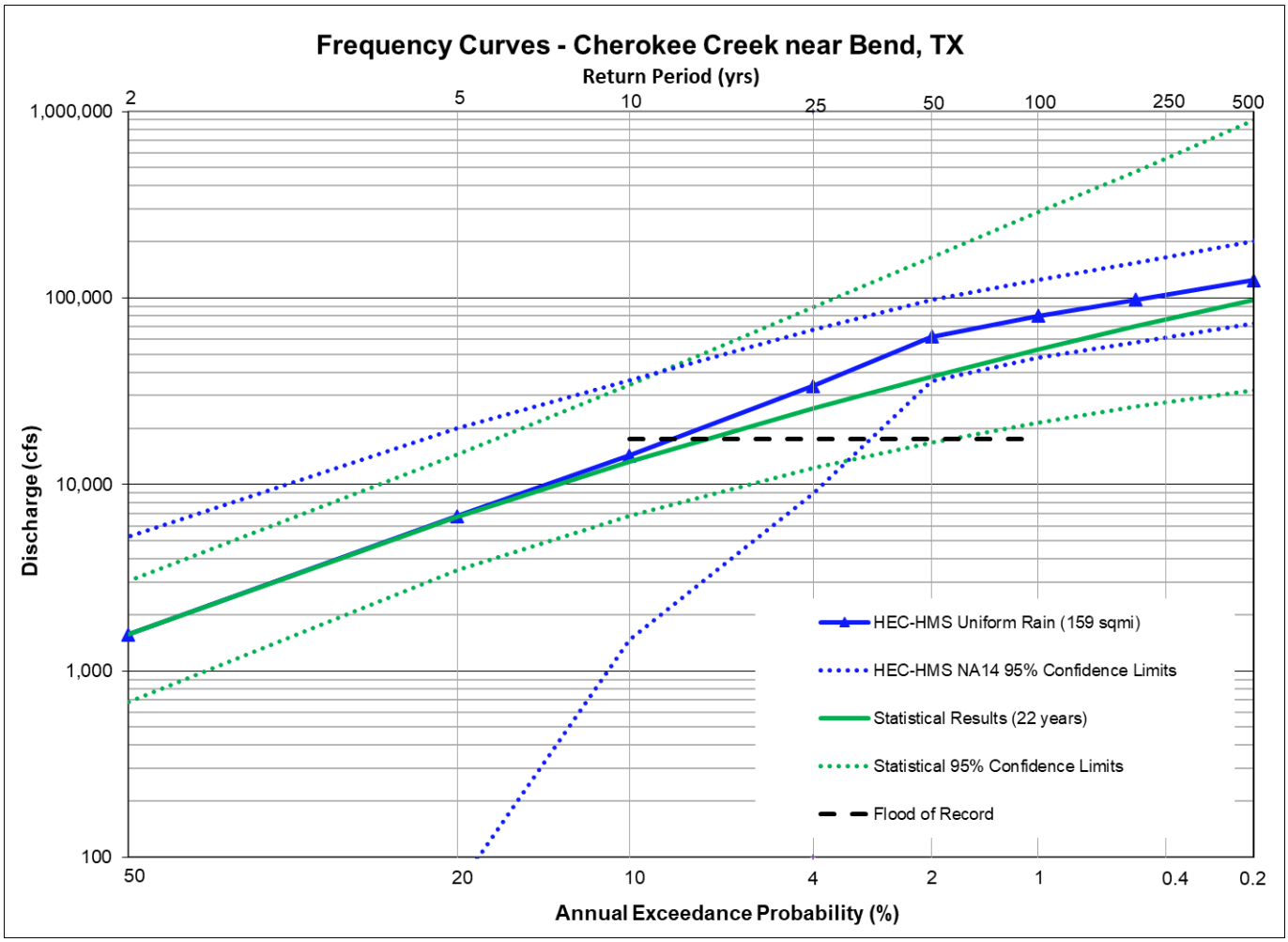

Figure 12.55: Flow Frequency Curve Comparison for Cherokee Creek nr Bend, TX

Table 12.56: Frequency Flow (cfs) Results Comparison for Comanche Creek near Mason, TX

Annual Exceedance Probability (AEP)	Return Period (years)	Currently Effective FEMA FIS	Approximate BLE Data from FEMA	Statistical Analysis of the Gage Record (Ch 5) (21 years)	HEC-HMS Uniform Rain Frequency Storm (Ch 6) (46 sq mi)
0.002	500	39,500		21,900	41,600
0.005	200			17,200	33,900
0.01	100	27,310		13,800	28,500
0.02	50	22,900		10,500	23,300
0.04	25			7,420	12,900
0.1	10	13,830		4,010	5,800
0.2	5			2,040	2,000
0.5	2			419	440

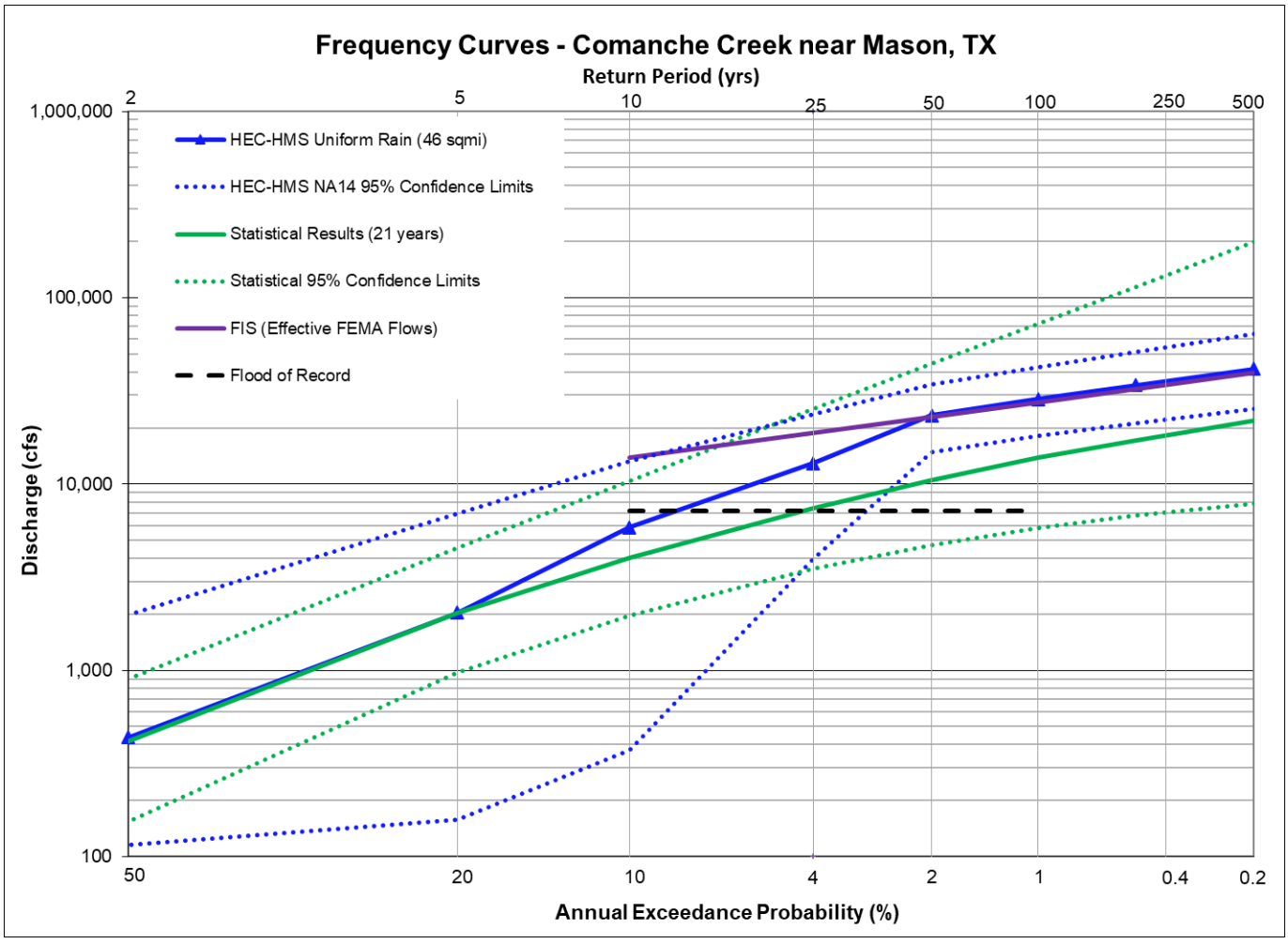

Figure 12.56: Flow Frequency Curve Comparison for Comanche Creek near Mason, TX

Table 12.57: Frequency Flow (cfs) Results Comparison for Cummins Creek near Frelsburg, TX

Annual Exceedance Probability (AEP)	Return Period (years)	Currently Effective FEMA FIS	Approximate BLE Data from FEMA	Statistical Analysis of the Gage Record (Ch 5) (24 years)	HEC-HMS Uniform Rain Frequency Storm (Ch 6) (252 sq mi)
0.002	500		113,283	167,000	132,100
0.005	200			119,000	100,800
0.01	100		66,763	89,700	78,300
0.02	50		51,151	66,300	56,700
0.04	25		37,811	47,500	42,000
0.1	10		23,432	28,600	27,800
0.2	5			17,800	18,900
0.5	2			7,380	8,200

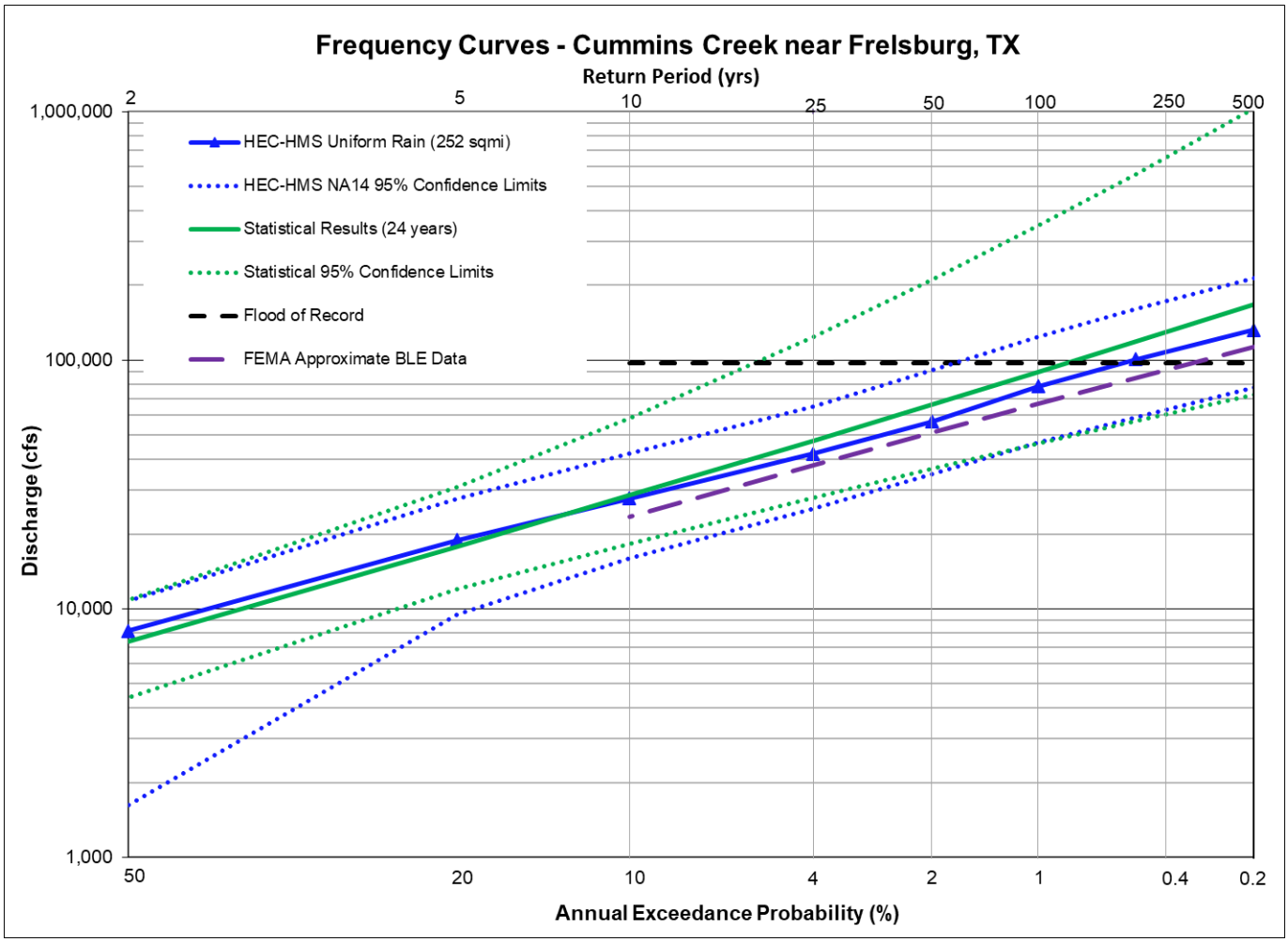

Figure 12.57: Flow Frequency Curve Comparison for Cummins Creek near Frelsburg, TX

Table 12.58: Frequency Flow (cfs) Results Comparison for Cypress Creek near Cypress Mill, TX

Annual Exceedance Probability (AEP)	Return Period (years)	Currently Effective FEMA FIS	Approximate BLE Data from FEMA	Statistical Analysis of the Gage Record (Ch 5) (20 years)	HEC-HMS Uniform Rain Frequency Storm (Ch 6) (71 sq mi)
0.002	500		58,309	144,000	115,900
0.005	200			108,000	94,000
0.01	100		33,422	84,300	80,200
0.02	50		25,353	63,300	65,900
0.04	25		18,886	45,200	45,100
0.1	10		11,988	25,800	26,400
0.2	5			14,500	14,500
0.5	2			4,280	4,300

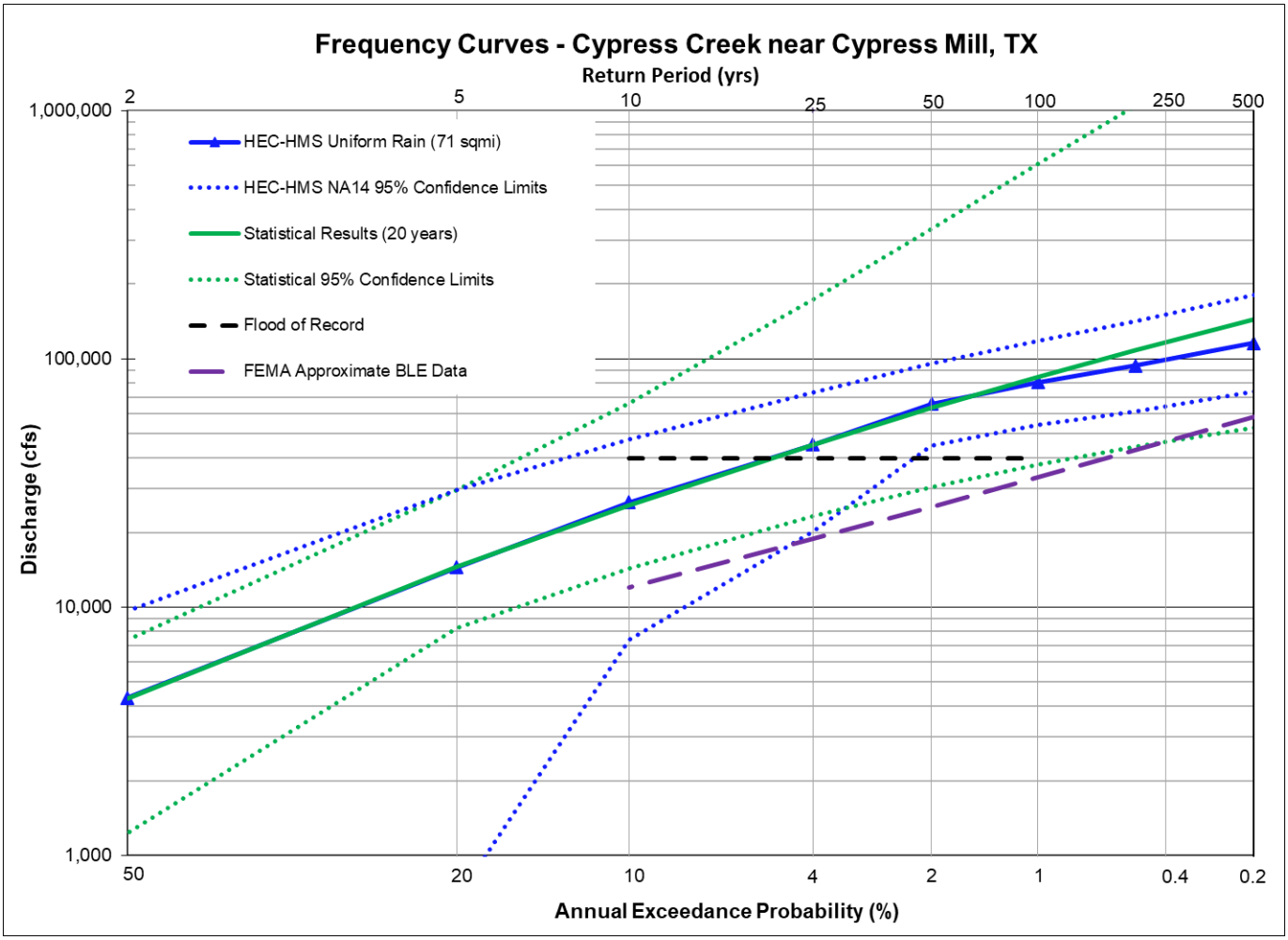

Figure 12.58: Flow Frequency Curve Comparison for Cypress Creek near Cypress Mill, TX

Table 12.59: Frequency Flow (cfs) Results Comparison for Gilleland Creek near Manor, TX

Annual Exceedance Probability (AEP)	Return Period (years)	Currently Effective FEMA FIS	Approximate BLE Data from FEMA	Statistical Analysis of the Gage Record (Ch 5) (26 years)	HEC-HMS Uniform Rain Frequency Storm (Ch 6) (41 sq mi)
0.002	500	51,100	52,977	11,600	28,800
0.005	200			10,200	22,700
0.01	100	33,600	29,564	9,120	18,800
0.02	50	27,200	22,083	7,980	14,900
0.04	25		15,938	6,800	10,100
0.1	10	15,000	9,502	5,180	6,400
0.2	5			3,900	3,900
0.5	2			2,090	2,100

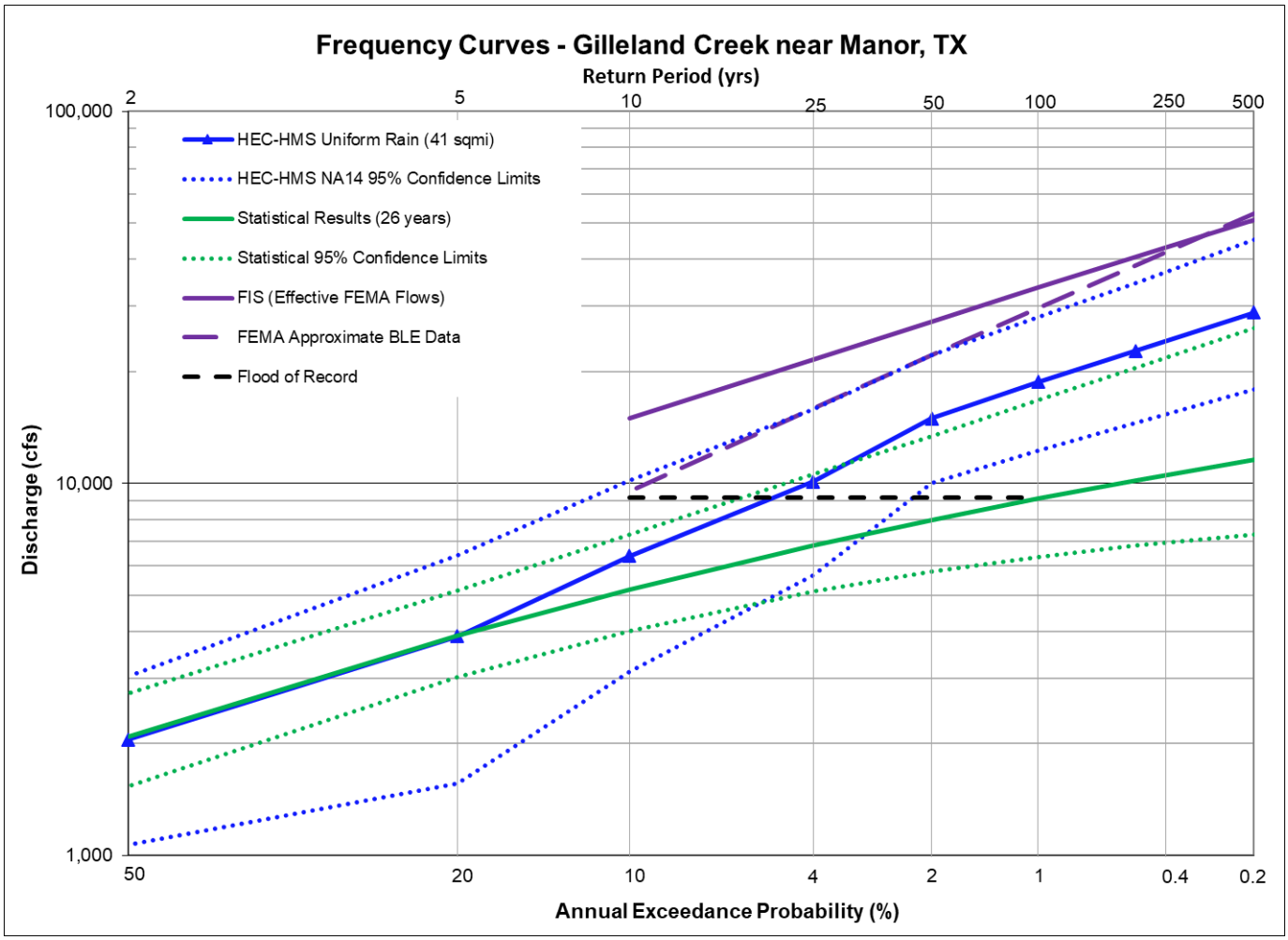

Figure 12.59: Flow Frequency Curve Comparison for Gilleland Creek near Manor, TX

Table 12.60: Frequency Flow (cfs) Results Comparison for Hamilton Creek near Marble Falls, TX

Annual Exceedance Probability (AEP)	Return Period (years)	Currently Effective FEMA FIS	Approximate BLE Data from FEMA	Statistical Analysis of the Gage Record (Ch 5) (18 years)	HEC-HMS Uniform Rain Frequency Storm (Ch 6) (78 sq mi)
0.002	500			117,000	83,500
0.005	200			82,300	66,300
0.01	100			61,000	54,800
0.02	50			43,900	44,000
0.04	25			30,200	30,200
0.1	10			16,700	17,400
0.2	5			9,430	9,500
0.5	2			3,020	3,100

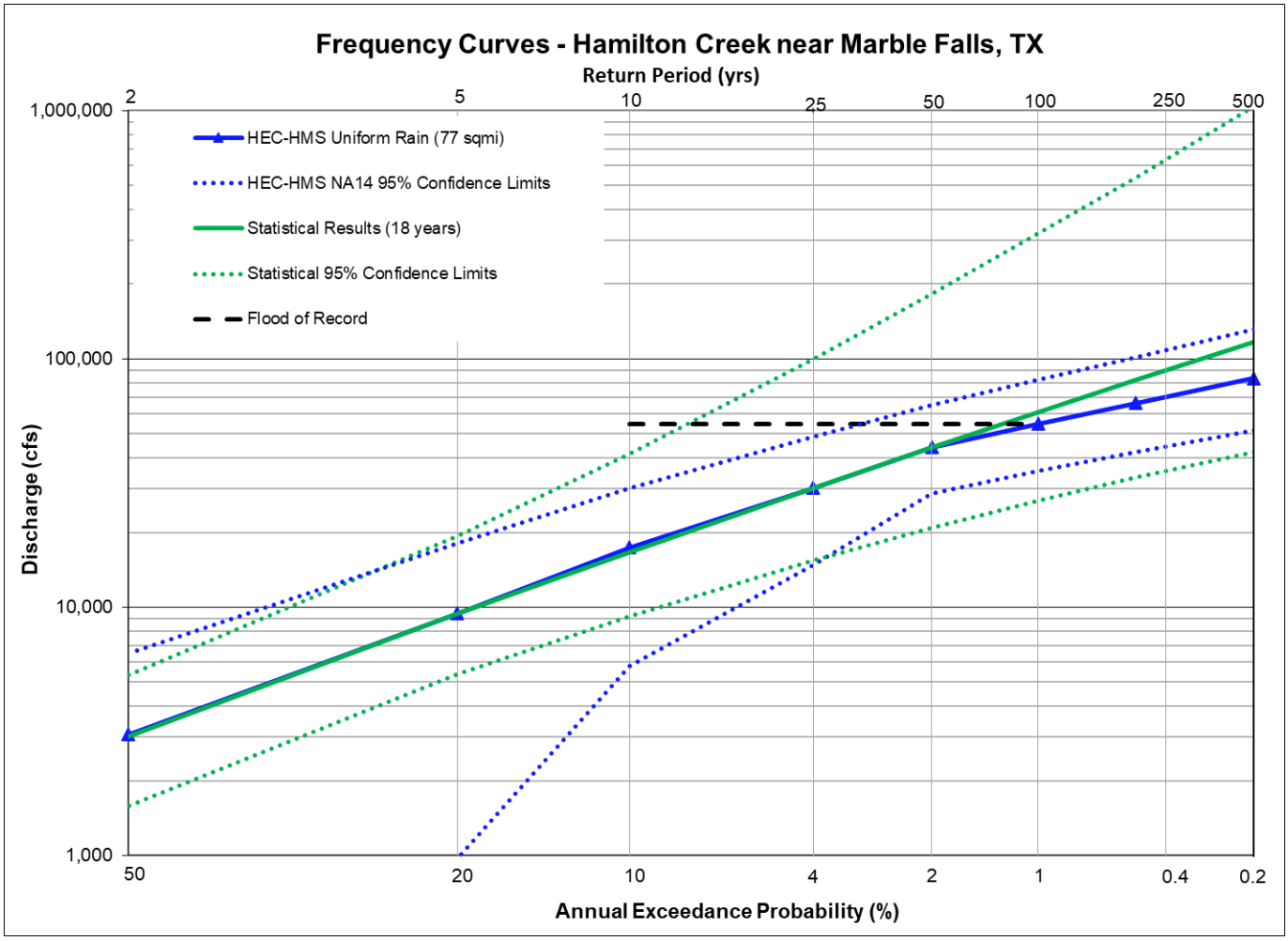

Figure 12.60: Flow Frequency Curve Comparison for Hamilton Creek near Marble Falls, TX

Table 12.61: Frequency Flow (cfs) Results Comparison for Hickory Creek near Castell, TX

Annual Exceedance Probability (AEP)	Return Period (years)	Currently Effective FEMA FIS	Approximate BLE Data from FEMA	Statistical Analysis of the Gage Record (Ch 5) (21 years)	HEC-HMS Uniform Rain Frequency Storm (Ch 6) (168 sq mi)
0.002	500		147,403	52,300	123,500
0.005	200			38,200	96,600
0.01	100		117,854	29,500	78,000
0.02	50		85,815	22,100	60,300
0.04	25		59,459	16,000	33,300
0.1	10		33,416	9,660	13,400
0.2	5			5,970	6,000
0.5	2			2,330	2,300

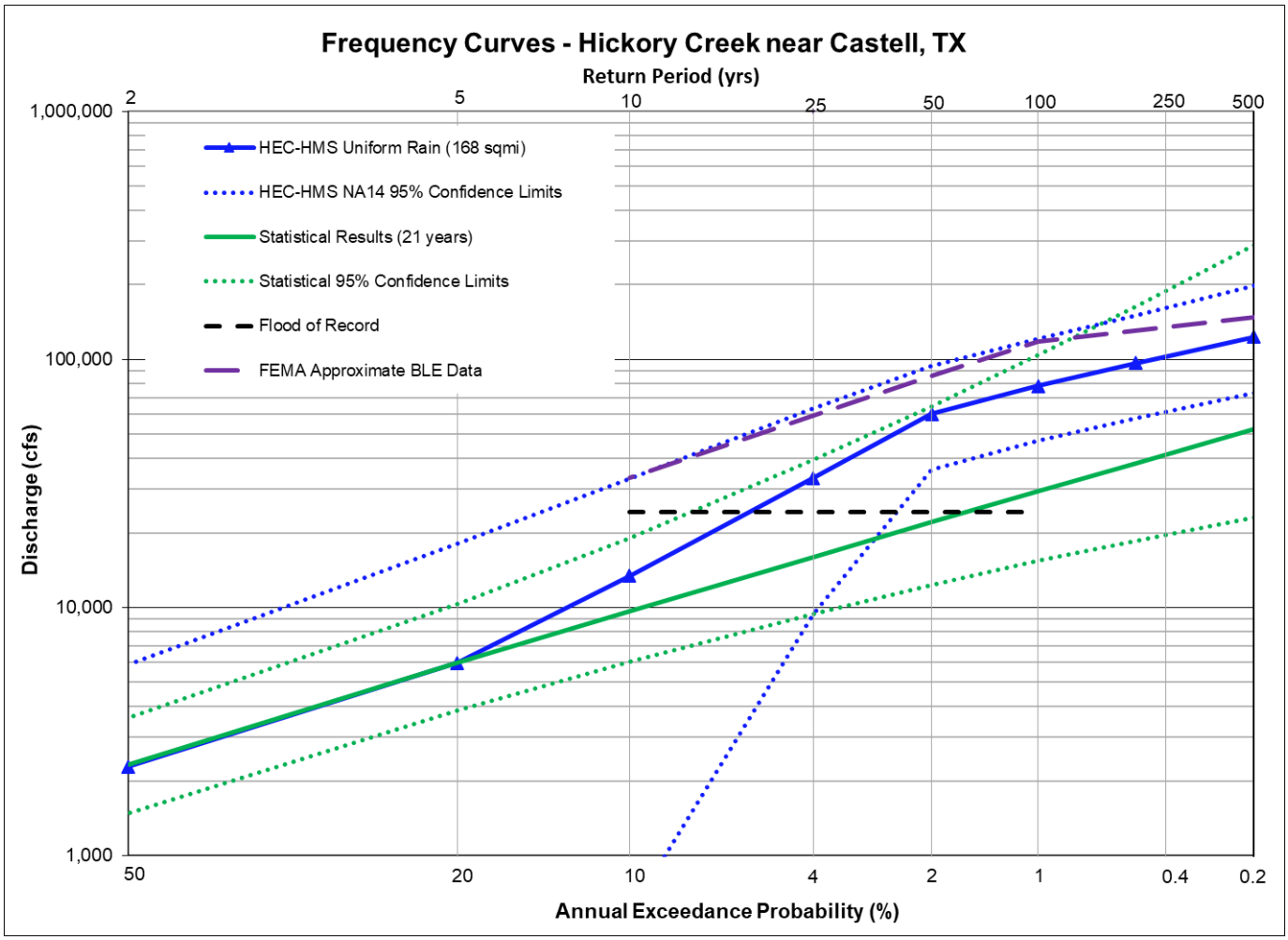

Figure 12.61: Flow Frequency Curve Comparison for Hickory Creek near Castell, TX

Table 12.62: Frequency Flow (cfs) Results Comparison for James River nr Mason, TX

Annual Exceedance Probability (AEP)	Return Period (years)	Currently Effective FEMA FIS	Approximate BLE Data from FEMA	Statistical Analysis of the Gage Record (Ch 5) (22 years)	HEC-HMS Uniform Rain Frequency Storm (Ch 6) (326 sq mi)
0.002	500			242,000	263,000
0.005	200			166,000	215,100
0.01	100			120,000	181,600
0.02	50			82,900	147,600
0.04	25			53,600	111,800
0.1	10			26,000	35,600
0.2	5			12,500	12,600
0.5	2			2,620	2,600

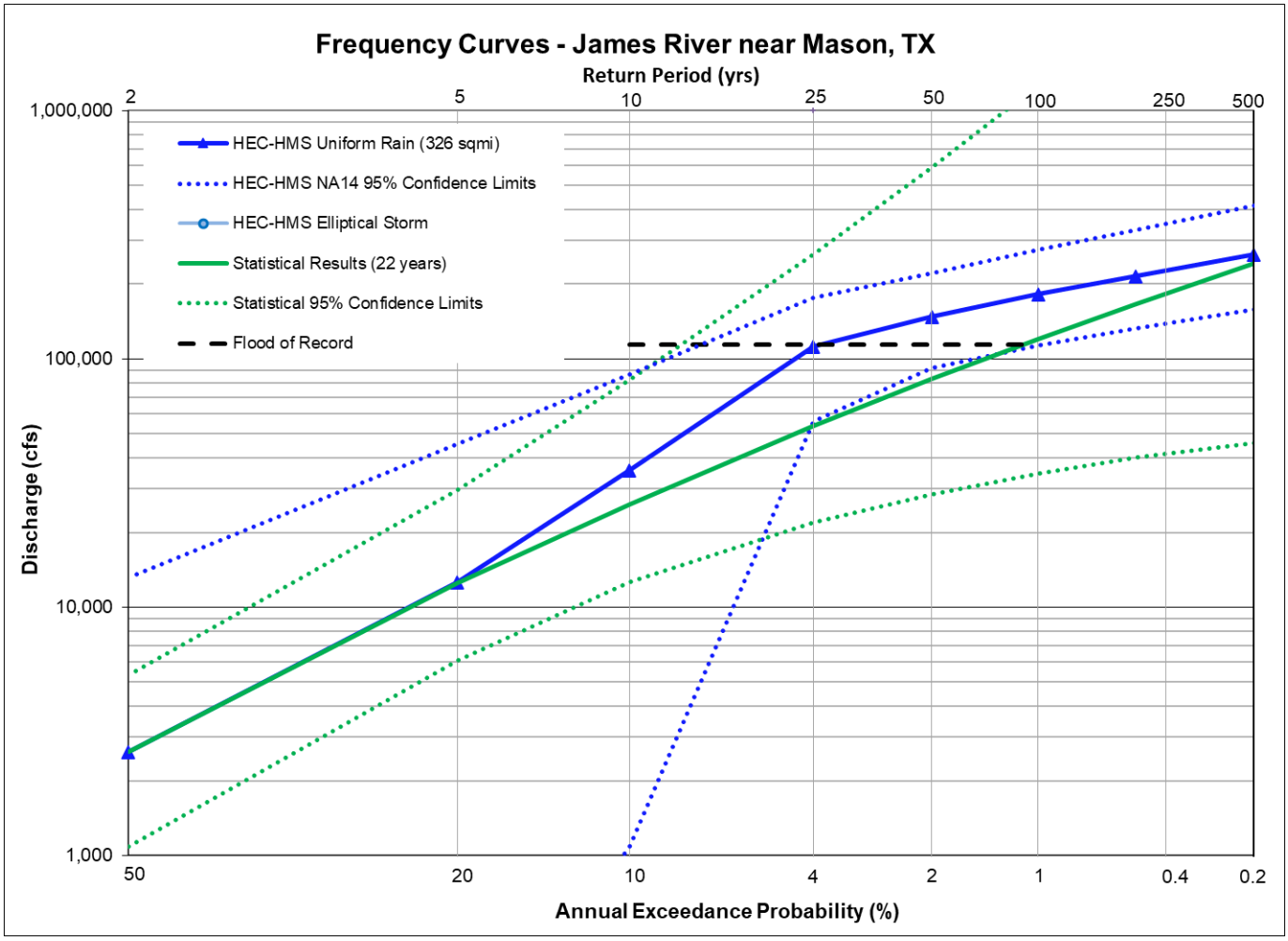

Figure 12.62: Flow Frequency Curve Comparison for James River nr Mason, TX

Table 12.63: Frequency Flow (cfs) Results Comparison for Johnson Creek near Llano, TX

Annual Exceedance Probability (AEP)	Return Period (years)	Currently Effective FEMA FIS	Approximate BLE Data from FEMA	Statistical Analysis of the Gage Record (Ch 5) (18 years)	HEC-HMS Uniform Rain Frequency Storm (Ch 6) (47 sq mi)
0.002	500		77,250	163,000	57,200
0.005	200			90,000	46,700
0.01	100		58,910	54,300	39,500
0.02	50		41,202	30,600	32,600
0.04	25		25,814	15,800	19,100
0.1	10		13,697	5,400	5,900
0.2	5			1,860	1,800
0.5	2			206	210

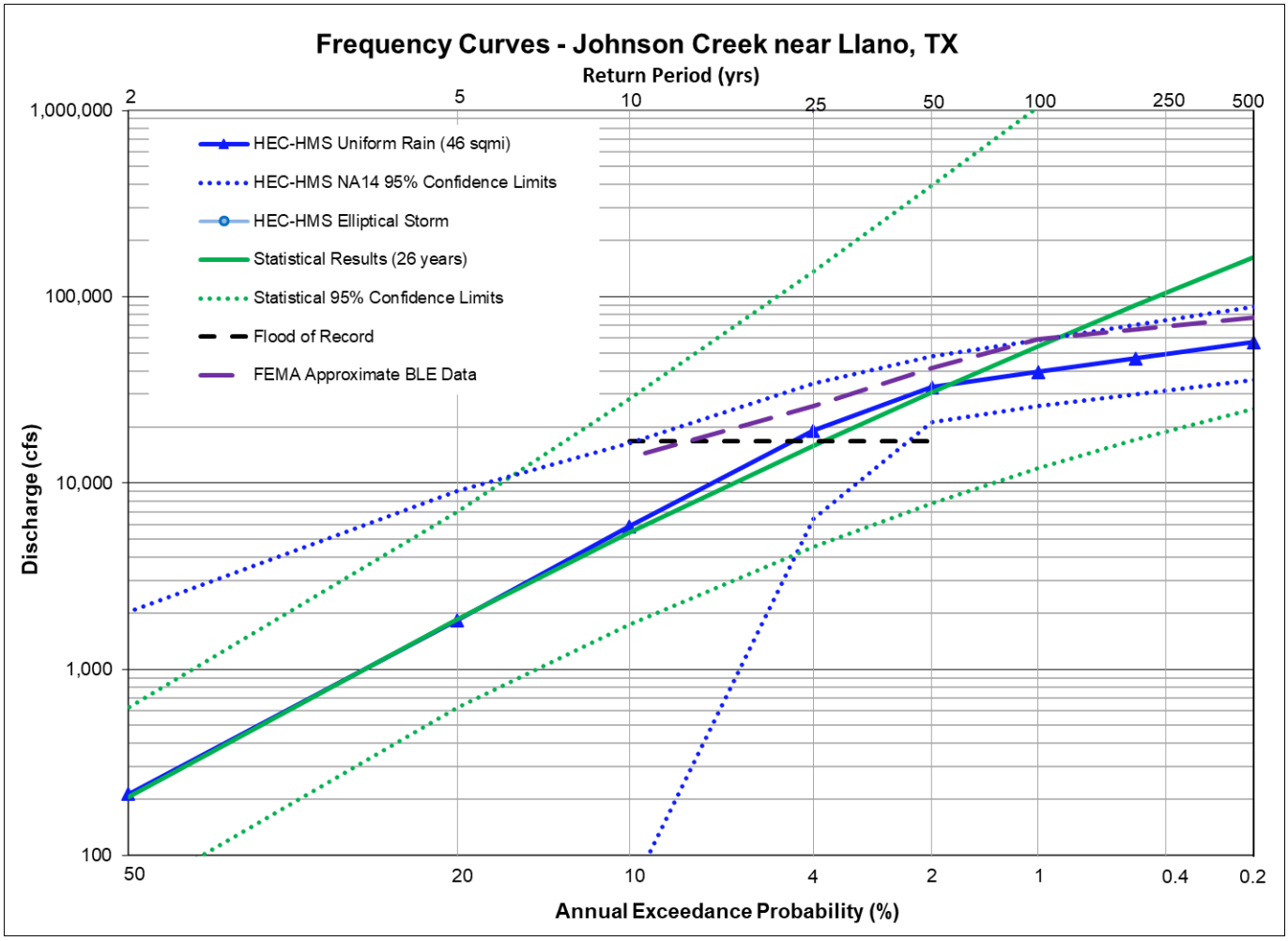

Figure 12.63: Flow Frequency Curve Comparison for Johnson Creek near Llano, TX

Table 12.64: Frequency Flow (cfs) Results Comparison for Johnson Fork near Junction, TX

Annual Exceedance Probability (AEP)	Return Period (years)	Currently Effective FEMA FIS	Approximate BLE Data from FEMA	Statistical Analysis of the Gage Record (Ch 5) (21 years)	HEC-HMS Uniform Rain Frequency Storm (Ch 6) (293 sq mi)
0.002	500			889,000	214,000
0.005	200			441,000	176,000
0.01	100			246,000	146,500
0.02	50			130,000	116,100
0.04	25			63,200	71,000
0.1	10			20,600	26,000
0.2	5			7,100	7,200
0.5	2			897	890

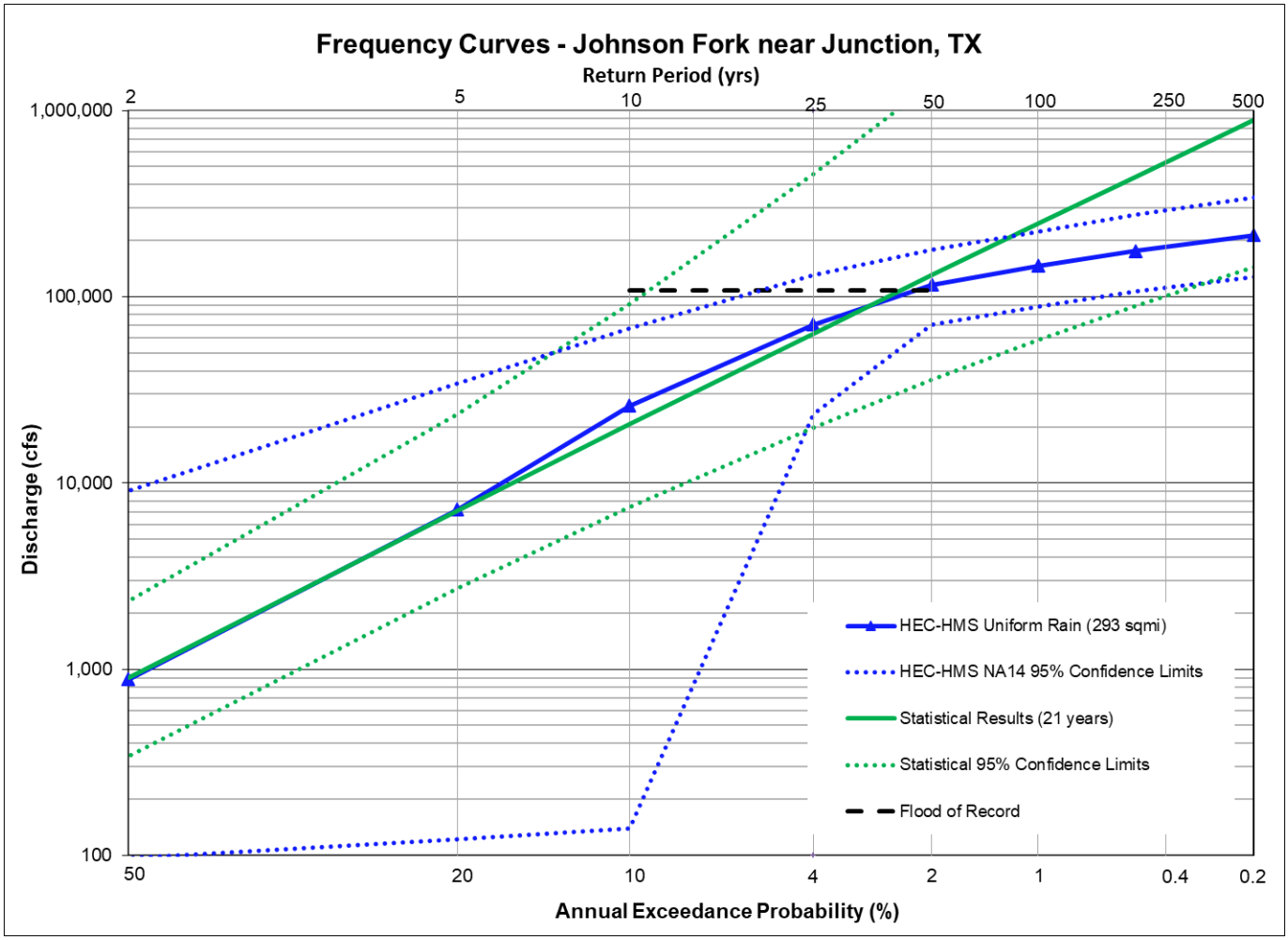

Figure 12.64: Flow Frequency Curve Comparison for Johnson Fork near Junction, TX

Table 12.65: Frequency Flow (cfs) Results Comparison for Little Llano River near Llano, TX

Annual Exceedance Probability (AEP)	Return Period (years)	Currently Effective FEMA FIS	Approximate BLE Data from FEMA	Statistical Analysis of the Gage Record (Ch 5) (21 years)	HEC-HMS Uniform Rain Frequency Storm (Ch 6) (48 sq mi)
0.002	500		63,626	69,700	67,500
0.005	200			51,800	55,300
0.01	100		48,628	39,000	47,000
0.02	50		34,071	27,300	39,100
0.04	25		21,571	17,400	22,500
0.1	10		11,454	7,590	8,100
0.2	5			2,980	2,900
0.5	2			313	310

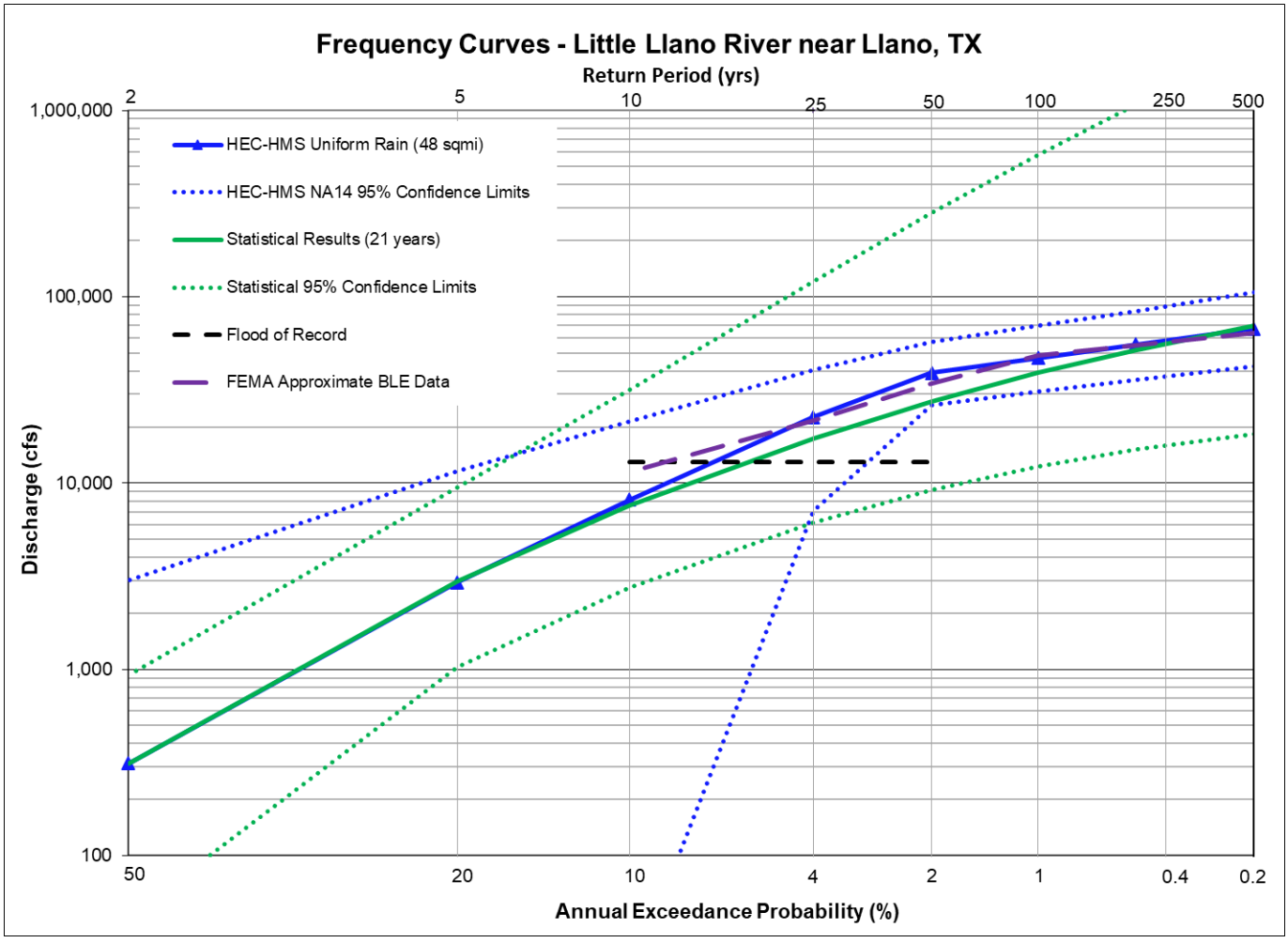

Figure 12.65: Flow Frequency Curve Comparison for Little Llano River near Llano, TX

Table 12.66: Frequency Flow (cfs) Results Comparison for North Grape Creek near Johnson City, TX

Annual Exceedance Probability (AEP)	Return Period (years)	Currently Effective FEMA FIS	Approximate BLE Data from FEMA	Statistical Analysis of the Gage Record (Ch 5) (19 years)	HEC-HMS Uniform Rain Frequency Storm (Ch 6) (89 sq mi)
0.002	500		63,595	73,300	127,600
0.005	200			56,900	103,700
0.01	100		36,713	45,600	87,700
0.02	50		27,950	35,300	72,500
0.04	25		20,888	26,100	47,200
0.1	10		13,325	15,800	24,500
0.2	5			9,500	12,800
0.5	2			3,180	3,200

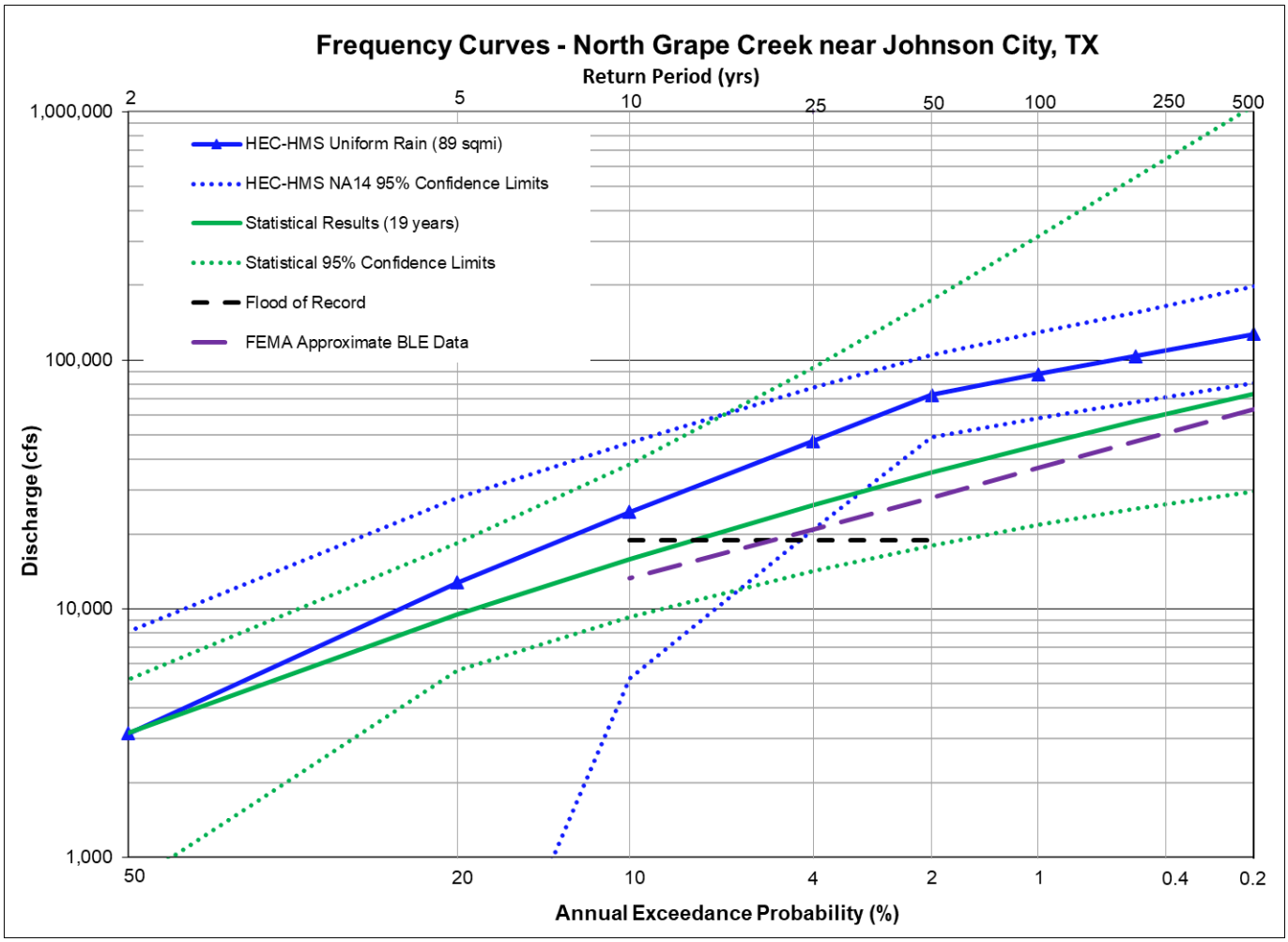

Figure 12.66: Flow Frequency Curve Comparison for North Grape Creek near Johnson City, TX

Table 12.67: Frequency Flow (cfs) Results Comparison for San Fernando Creek near Llano, TX

Annual Exceedance Probability (AEP)	Return Period (years)	Currently Effective FEMA FIS	Approximate BLE Data from FEMA	Statistical Analysis of the Gage Record (Ch 5) (22 years)	HEC-HMS Uniform Rain Frequency Storm (Ch 6) (129 sq mi)
0.002	500		98,166	188,000	106,800
0.005	200			127,000	85,400
0.01	100		77,886	90,600	70,700
0.02	50		56,537	61,100	56,500
0.04	25		38,877	38,300	38,300
0.1	10		21,614	17,600	19,300
0.2	5			7,920	7,900
0.5	2			1,430	1,400

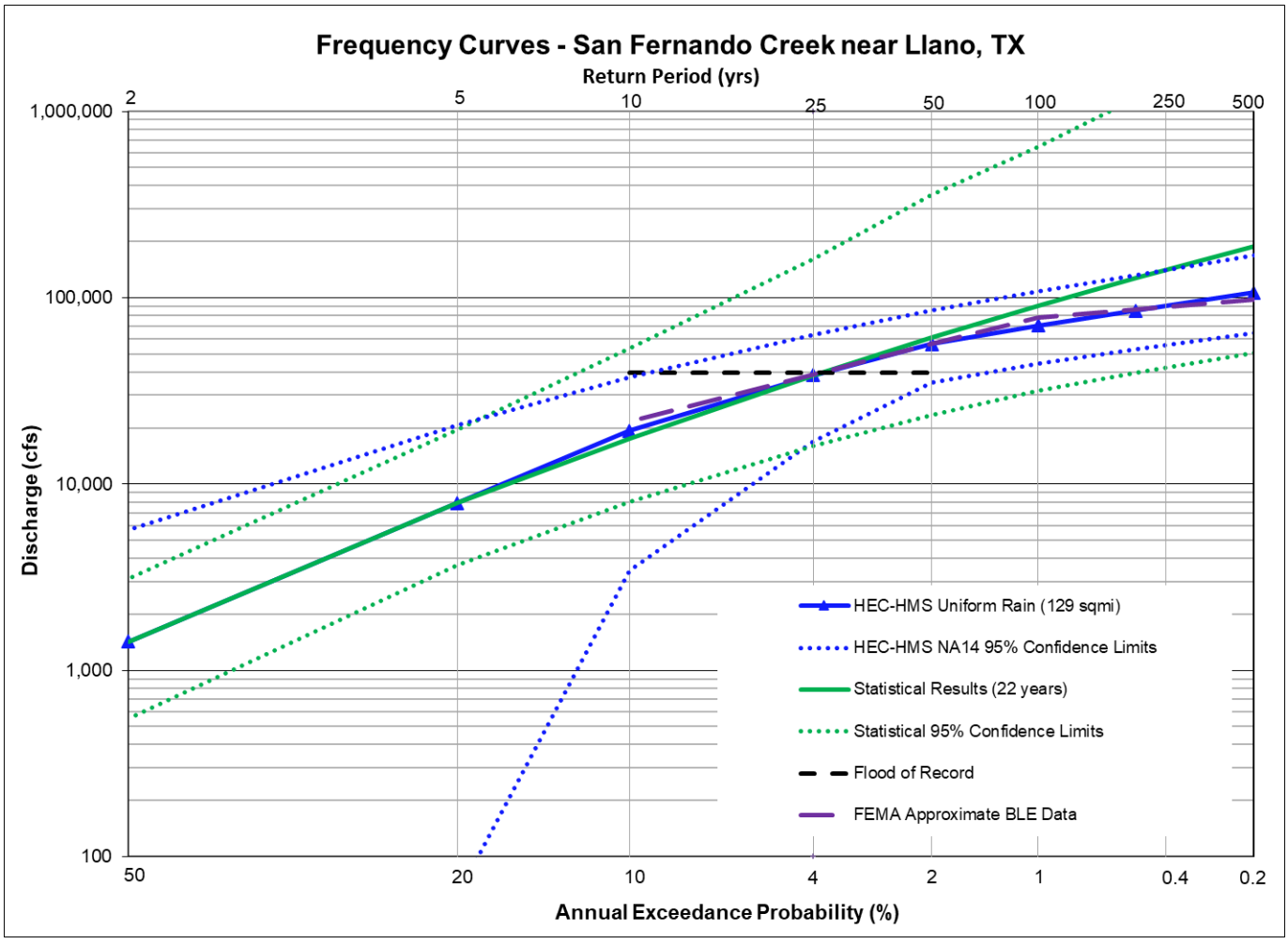

Figure 12.67: Flow Frequency Curve Comparison for San Fernando Creek near Llano, TX

Table 12.68: Frequency Flow (cfs) Results Comparison for Sandy Creek near Willow City, TX

Annual Exceedance Probability (AEP)	Return Period (years)	Currently Effective FEMA FIS	Approximate BLE Data from FEMA	Statistical Analysis of the Gage Record (Ch 5) (18 years)	HEC-HMS Uniform Rain Frequency Storm (Ch 6) (152 sq mi)
0.002	500		154,824	60,300	124,400
0.005	200			46,100	98,400
0.01	100		123,260	36,400	80,800
0.02	50		89,780	27,800	64,100
0.04	25		61,977	20,200	39,600
0.1	10		34,693	11,900	16,400
0.2	5			6,980	7,000
0.5	2			2,230	2,300

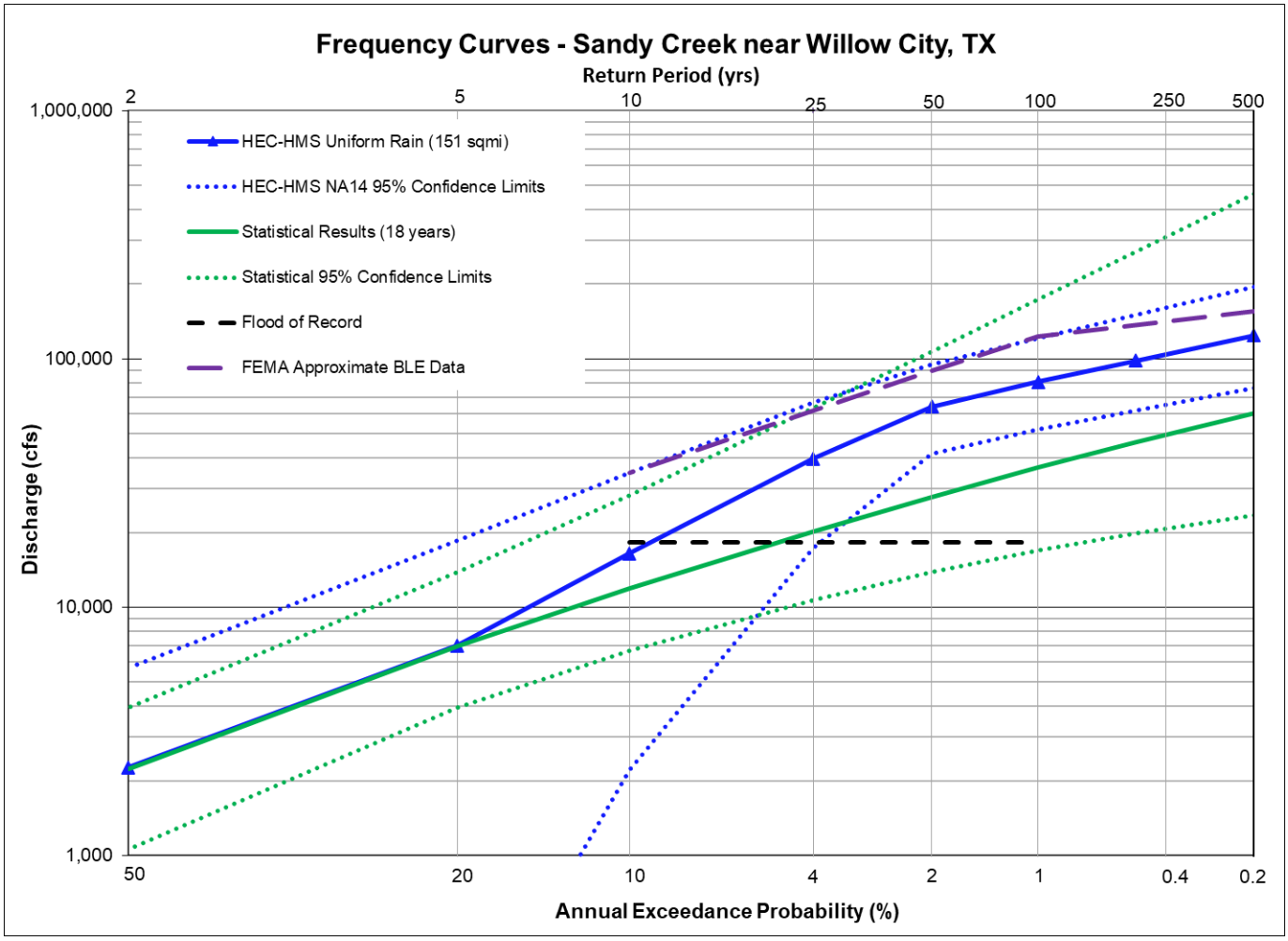

Figure 12.68: Flow Frequency Curve Comparison for Sandy Creek near Willow City, TX

Table 12.69: Frequency Flow (cfs) Results Comparison for Sandy Creek near Click. TX

Annual Exceedance Probability (AEP)	Return Period (years)	Currently Effective FEMA FIS	Approximate BLE Data from FEMA	Statistical Analysis of the Gage Record (Ch 5) (19 years)	HEC-HMS Uniform Rain Frequency Storm (Ch 6) (300 sq mi)
0.002	500		230,158	157,000	201,500
0.005	200			121,000	157,900
0.01	100		185,737	96,800	128,400
0.02	50		137,134	74,300	100,100
0.04	25		96,763	54,300	69,700
0.1	10		55,655	31,900	37,900
0.2	5			18,500	19,400
0.5	2			5,600	5,700

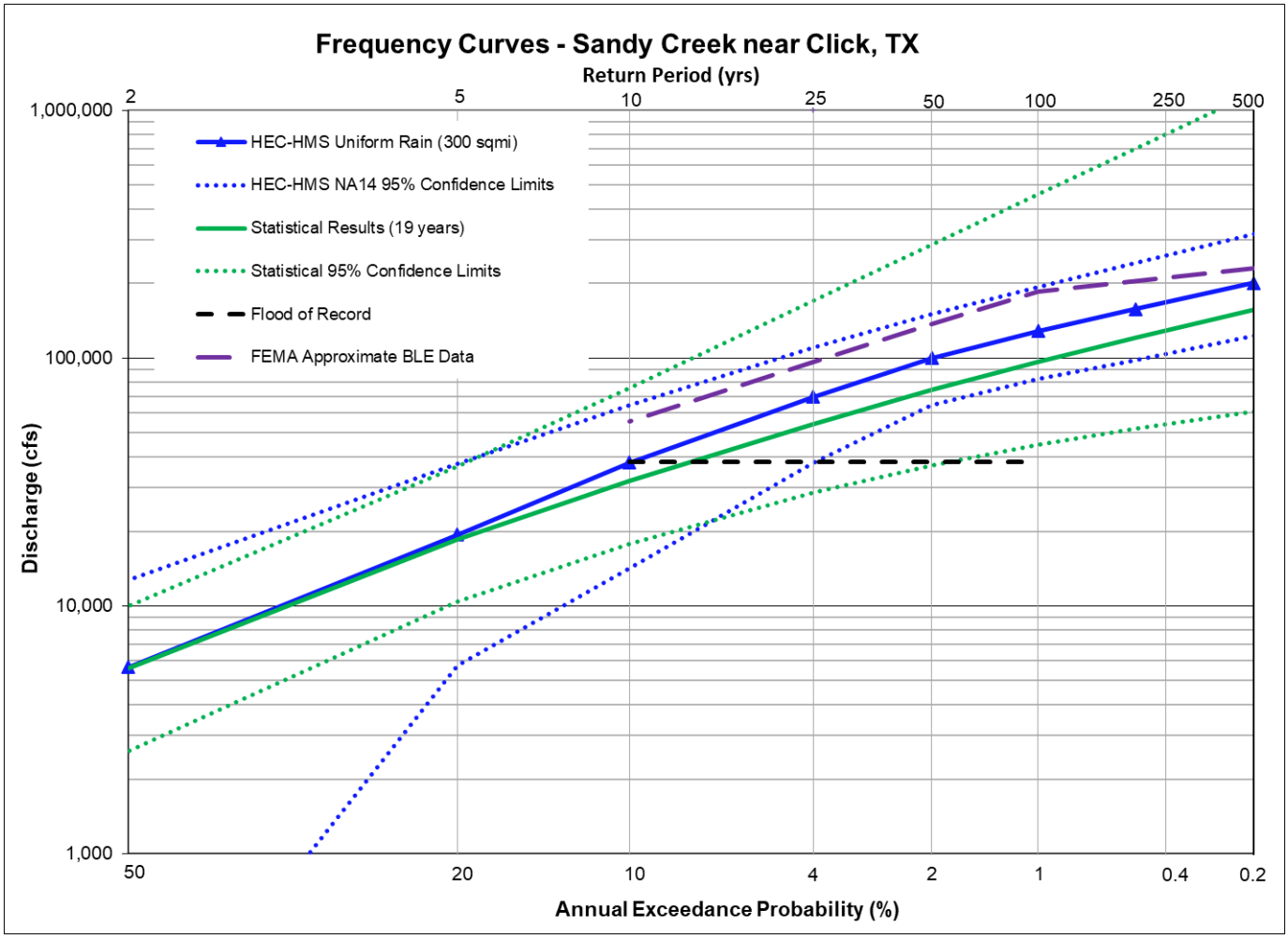

Figure 12.69: Flow Frequency Curve Comparison for Sandy Creek near Click. TX

Table 12.70: Frequency Flow (cfs) Results Comparison for Wilbarger Creek near Elgin, TX

Annual Exceedance Probability (AEP)	Return Period (years)	Currently Effective FEMA FIS	Approximate BLE Data from FEMA	Statistical Analysis of the Gage Record (Ch 5) (18 years)	HEC-HMS Uniform Rain Frequency Storm (Ch 6) (164 sq mi)
0.002	500		111,298	92,800	76,900
0.005	200			73,900	59,800
0.01	100		62,422	60,700	48,200
0.02	50		46,711	48,400	37,300
0.04	25		33,718	37,200	29,200
0.1	10		20,127	24,100	21,100
0.2	5			15,500	14,800
0.5	2			6,170	6,400

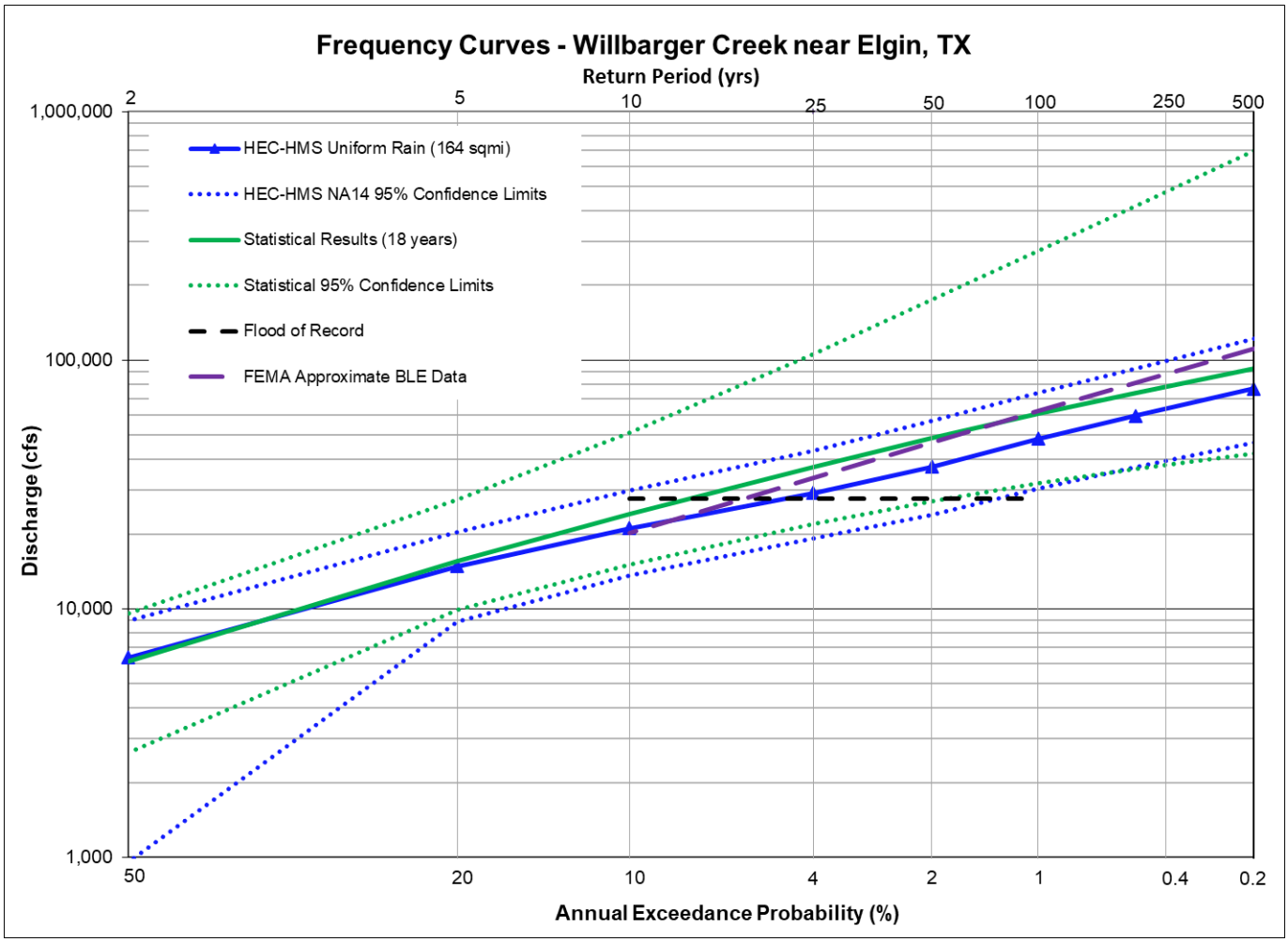

Figure 12.70: Flow Frequency Curve Comparison for Wilbarger Creek near Elgin, TX

Table 12.71: Frequency Flow (cfs) Results Comparison for Willow Creek near Mason, TX

Annual Exceedance Probability (AEP)	Return Period (years)	Currently Effective FEMA FIS	Approximate BLE Data from FEMA	Statistical Analysis of the Gage Record (Ch 5) (18 years)	HEC-HMS Uniform Rain Frequency Storm (Ch 6) (58 sq mi)
0.002	500			85,300	50,400
0.005	200			51,800	40,700
0.01	100			33,700	34,100
0.02	50			20,800	27,800
0.04	25			11,800	15,500
0.1	10			4,730	5,600
0.2	5			1,900	1,900
0.5	2			285	300

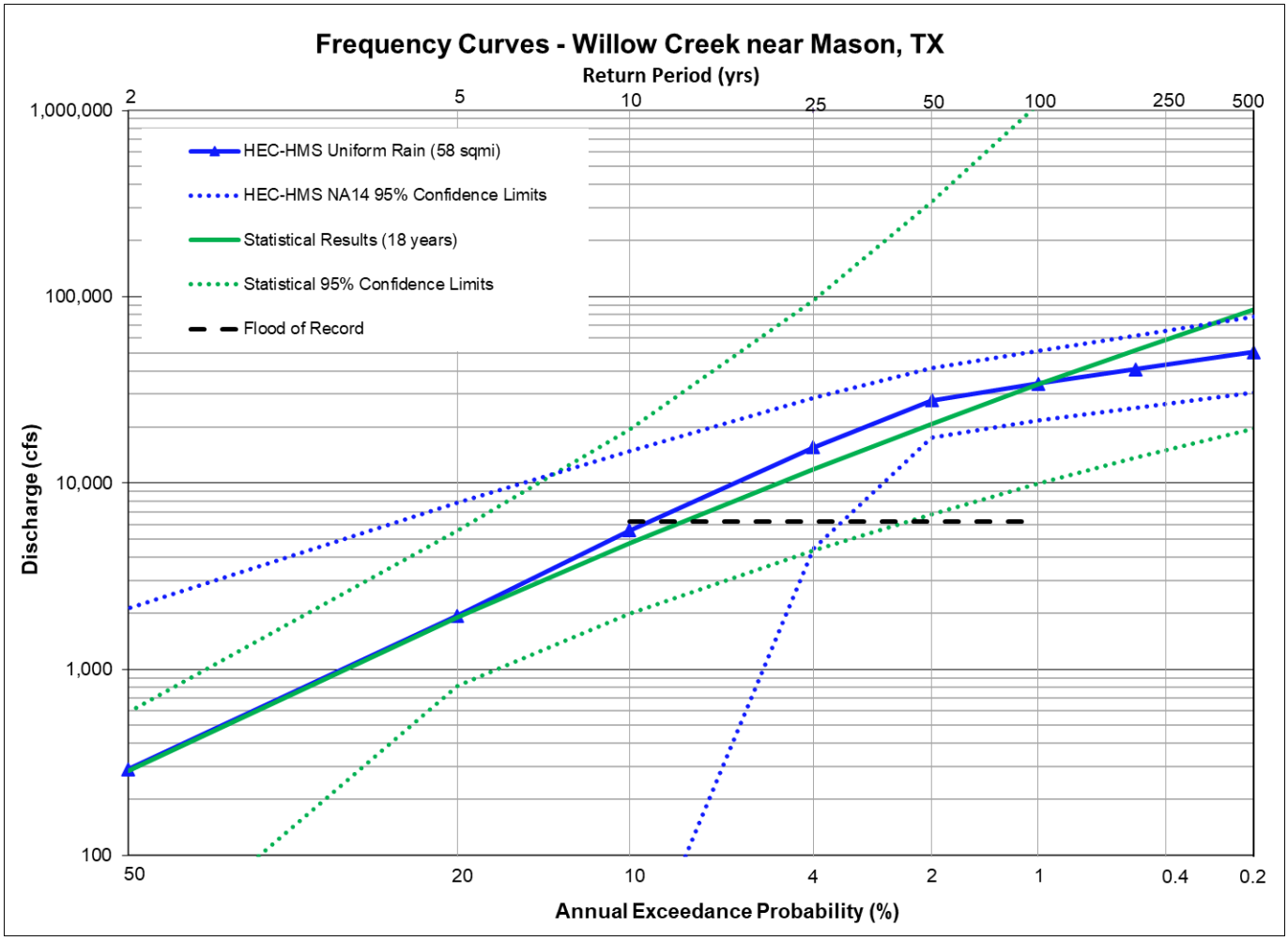

Figure 12.71: Flow Frequency Curve Comparison for Willow Creek near Mason, TX

12.2 LAKE ELEVATION COMPARISONS

The final comparisons of the reservoirs frequency pool elevation estimates are given in the tables in this section of the report. Blank cells indicate data was not available at that specific location. The figures in this section of the report include plots of the estimated pool frequency curves at each reservoir along with the previous published elevations from the effective FEMA Flood Insurance Studies (FIS), the 2002 FDEP study, and other previously published studies. Additional discussion of the results is included with the table and figure for each reservoir.

Table 12.72: Frequency Pool Elevation (ft NAVD88) Comparison for Oak Creek Reservoir

Annual Exceedance Probability (AEP)	Return Period (years)	Currently Effective FEMA FIS	Previous Studies	HEC-HMS Uniform Rain Frequency Storm	HEC-HMS Elliptical Frequency Storm	Reservoir Analysis in RMC-RFA	Operational Reference	Reference Elevation
0.002	500			2011.8			Top of Dam	2014.6
0.005	200			2010.6				
0.01	100			2009.5				
0.02	50			2008.2			Spillway Crest	2005.6
0.04	25			2005.8				
0.1	10			2003.6				
0.2	5			2002.4				
0.5	2			2001.4			Normal Pool	2000.6

Oak Creek Reservoir is a 39,000 acre-ft water supply reservoir that is operated by the City of Sweetwater. It has an uncontrolled service spillway and a drainage area of about 240 square miles. There are no published pool frequency elevations available from FEMA or others for this lake. Due to its relatively small drainage area, the only frequency analysis completed for this lake was the HEC-HMS unform rainfall method, and those results are presented in the table above. As one can see from this table, the HEC-HMS results show that the 1% AEP pool is about 9 feet above its normal pool elevation.

Table 12.73: Frequency Pool Elevation (ft NAVD88) Comparison for Ballinger Lake (Lower)

Annual Exceedance Probability (AEP)	Return Period (years)	Currently Effective FEMA FIS	Previous Studies	HEC-HMS Uniform Rain Frequency Storm	HEC-HMS Elliptical Frequency Storm	Reservoir Analysis in RMC-RFA	Operational Reference	Reference Elevation
0.002	500			1677.8			Top of Dam	1692.4
0.005	200			1676.4				
0.01	100			1675.3				
0.02	50			1674.1			Spillway Crest	1668.4
0.04	25			1672.4				
0.1	10			1670.8				
0.2	5			1670				
0.5	2			1669.3			Normal Pool	1668.4

Lake Ballinger consists of two lakes in series which are operated by the City of Ballinger for water supply. Both have simple uncontrolled spillways at their conservation pool levels. The upper dam was built in 1947. The lower dam was built in 1985. The data in the table above pertains to the reservoir formed by the lower (downstream) dam. The lower dam is located on Valley Creek, and it has a drainage area of about 230 square miles. There are no published pool frequency elevations available from FEMA or others for this lake. Due to its relatively small drainage area, the only frequency analysis completed for this lake was the HEC-HMS unform rainfall method, and those results are presented in the table below. As one can see from this table, the normal pool and the spillway crest for this lake are the same elevation, and the HEC-HMS results show that the 1% AEP pool is almost 7 feet above its normal pool elevation.

Table 12.74: Frequency Pool Elevation (ft NAVD88) Comparison for O.C. Fisher Reservoir

Annual Exceedance Probability (AEP)	Return Period (years)	Currently Effective FEMA FIS	Previous Studies	HEC-HMS Uniform Rain Frequency Storm	HEC-HMS Elliptical Frequency Storm	Reservoir Analysis in RMC-RFA	Operational Reference	Reference Elevation
0.002	500	1948.0		1940.1	1932.6	1942.6	Top of Dam	1964.0
0.005	200			1937.3	1925.9	1935.9		
0.01	100	1937.0		1930.9	1919.2	1924.0	Easement	1952.5
0.02	50	1930.0		1922.9	1910.0	1915.9	Spillway Crest	1939.0
0.04	25			1909.5	1899.1	1911.7		
0.1	10	1918.0		1899.0	1889.8	1908.5		
0.2	5			1892.6	1887.5	1904.6		
0.5	2			1887.3	1885.3	1886.9	Normal Pool	1908.5

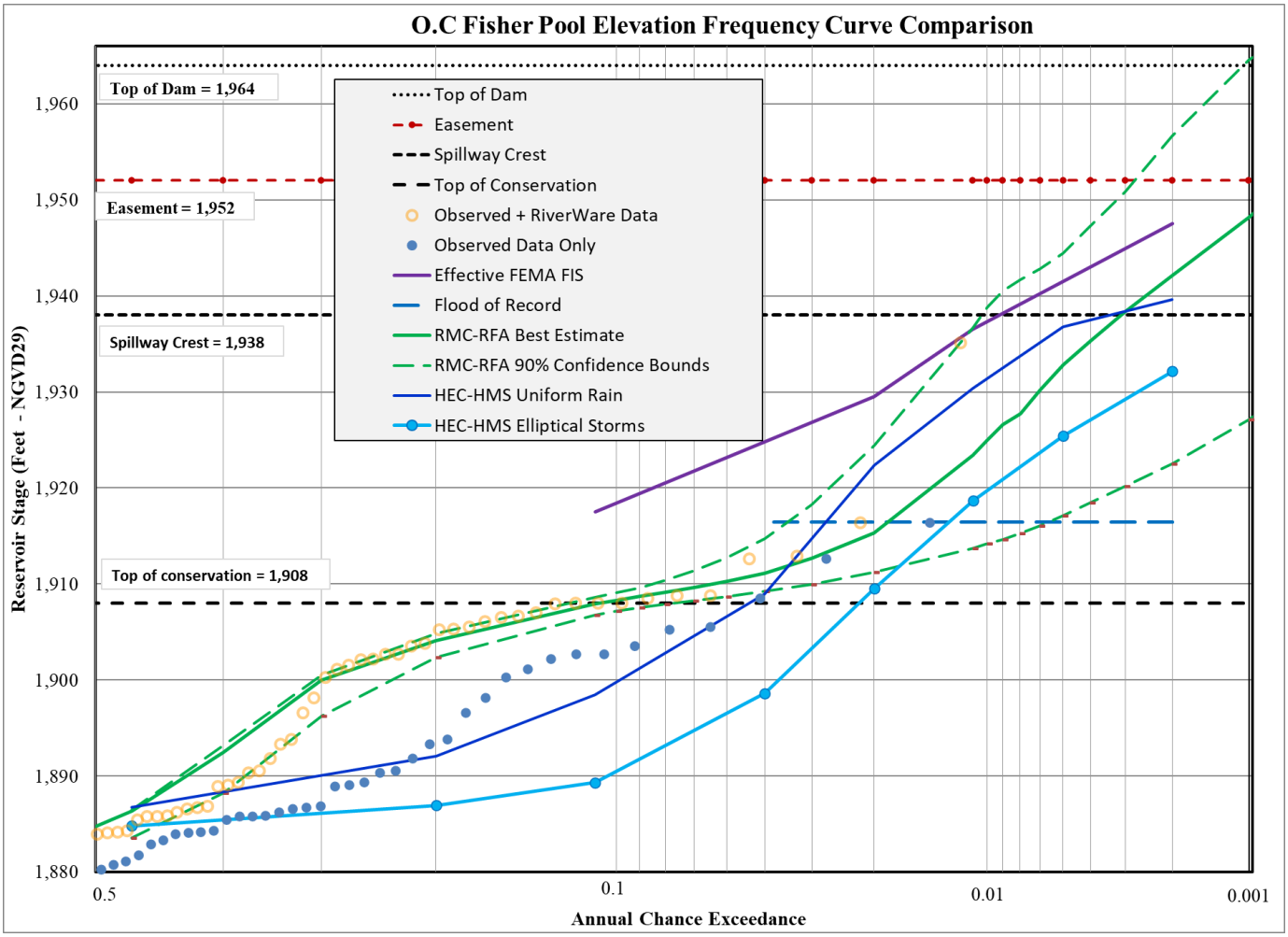

Figure 12.74: Pool Elevation Frequency Curve Comparison for O.C. Fisher Reservoir

O.C. Fisher Reservoir is a flood control reservoir that is operated by USACE. It has gated outlets as well as an uncontrolled emergency spillway. The dam is located on the North Concho River just upstream of the City of San Angelo, and it has a drainage area of about 1,460 square miles. The effective FEMA pool frequency elevations for this lake came from a 1990 SUPER statistical analysis for the Tom Green County FIS. More information on the SUPER model can be found in section 8.1.1 of this report. This reservoir is located in the portion of the watershed that is experiencing declining flow trends, and its observed pool elevation has been anywhere from 10 to 60 feet below its conservation pool for the past 50 years. In fact, this reservoir has not reached "normal pool" (or top of conservation pool) since the 1950s. The preceding table compares the new frequency pool elevation results from HEC-HMS and RMC-RFA to the previous FEMA study and the dam's operational levels. As one can see from this table, the 1% AEP pool elevations from both the HEC-HMS and RMC-RFA analysis are much lower that the effective FEMA 1% AEP (100-yr) elevation. This is most likely because the effective FEMA elevations that were calculated in 1990 did not include the most recent 30+ years of declining inflows to the dam.

Figure 12.74 compares the results of the RMC-RFA reservoir analysis, the HEC-HMS modeling, and the previous water surface elevations from the FEMA FIS. The differences in the results on this figure are primarily the result of the strong declining flow trends on the North Concho River. The FEMA FIS has the highest pool elevation estimates because it was based on the earliest part of the record. The RMC-RFA results are in the middle because they were based on the entire period of record, from the high flow period of the 1930s to the low flow period of the most recent decades. The HEC-HMS elliptical storms had the lowest pool elevation estimates because their initial pool elevations and inflows were calibrated to the most recent 30 years of record. However, the HEC-HMS results also include the NOAA Atlas 14 rainfall depths. While RMC-RFA does a good job of accounting for variable pool elevations and inflow volumes to a reservoir, it does not account for non-stationary watershed conditions such as are being observed in the North Concho watershed. Therefore, in this particular case, the HEC-HMS elliptical results are probably a better estimate of current conditions at O.C. Fisher reservoir.

Twin Buttes Reservoir is a flood control reservoir that is operated by the Bureau of Reclamation. It has gated outlets as well as an uncontrolled emergency spillway. The dam is located on the just upstream of Lake Nasworthy and the City of San Angelo. The reservoir consists of two pools across the South Concho River and Middle Concho-Spring Creek which are connected by a 3-mile-long equalizing channel. It has a drainage area of about 3,200 square miles. The effective FEMA pool frequency elevations for this lake came from a 1990 SUPER statistical analysis for the Tom Green County FIS. More information on the SUPER model can be found in section 8.1.1 of this report. This reservoir is located in the portion of the watershed that is experiencing declining flow trends, and its observed pool elevation has been well below its conservation pool for the past several decades.

As one can see from the Table and Figure below, the effective FIS elevations are fairly close to both the RMC-RFA reservoir analysis and the HEC-HMS elliptical storm results at the 1% and 0.2% AEP (100-yr and 500-yr) frequencies. There is also fairly good agreement between the RMC-RFA and HEC-HMS elliptical storm results for the 50-year through 500-year frequency events. For the more frequent events, the RMC-RFA results computed elevations that are closer to conservation pool, while the HEC-HMS results trended several feet lower. This is primarily due to the differing assumptions in the initial pool elevations. RMC-RFA does account for variable pool elevations in its initial conditions; however, it also assumes stationary watershed conditions. Since this watershed is experiencing declining flow trends, the levels of inflows and initial pool elevations that were typical in the 1950s and 1960s may no longer be typical today. The HEC-HMS modeling, on the other hand, assumed a single starting pool elevation for each frequency storm, but that initial pool elevation was selected based on typical conditions of the most recent 30 years of record. Therefore, the HEC-HMS elliptical storm results may be more representative of the current watershed conditions for the frequent events, while the RMC-RFA stochastic analysis better represents the variable conditions and inflow volumes for the rare flood events like the 1% AEP.

Table 12.75: Frequency Pool Elevation (ft NAVD88) Comparison for Twin Buttes Reservoir

Annual Exceedance Probability (AEP)	Return Period (years)	Currently Effective FEMA FIS	Previous Studies	HEC-HMS Uniform Rain Frequency Storm	HEC-HMS Elliptical Frequency Storm	Reservoir Analysis in RMC-RFA	Operational Reference	Reference Elevation
0.002	500	1970.0		1984.5	1971.5	1975.5	Top of Dam	1991.6
0.005	200			1978.0	1964.7	1968.2		
0.01	100	1960.0		1972.2	1959.3	1957.6	Easement	1985.5
0.02	50	1956.0		1965.1	1952.2	1952.1	Spillway Crest	1969.7
0.04	25			1955.1	1944.8	1947.5		
0.1	10	1947.0		1944.0	1937.5	1943.1		
0.2	5			1938.8	1934.4	1940.9		
0.5	2			1934.3	1933.5	1934.6	Normal Pool	1940.8

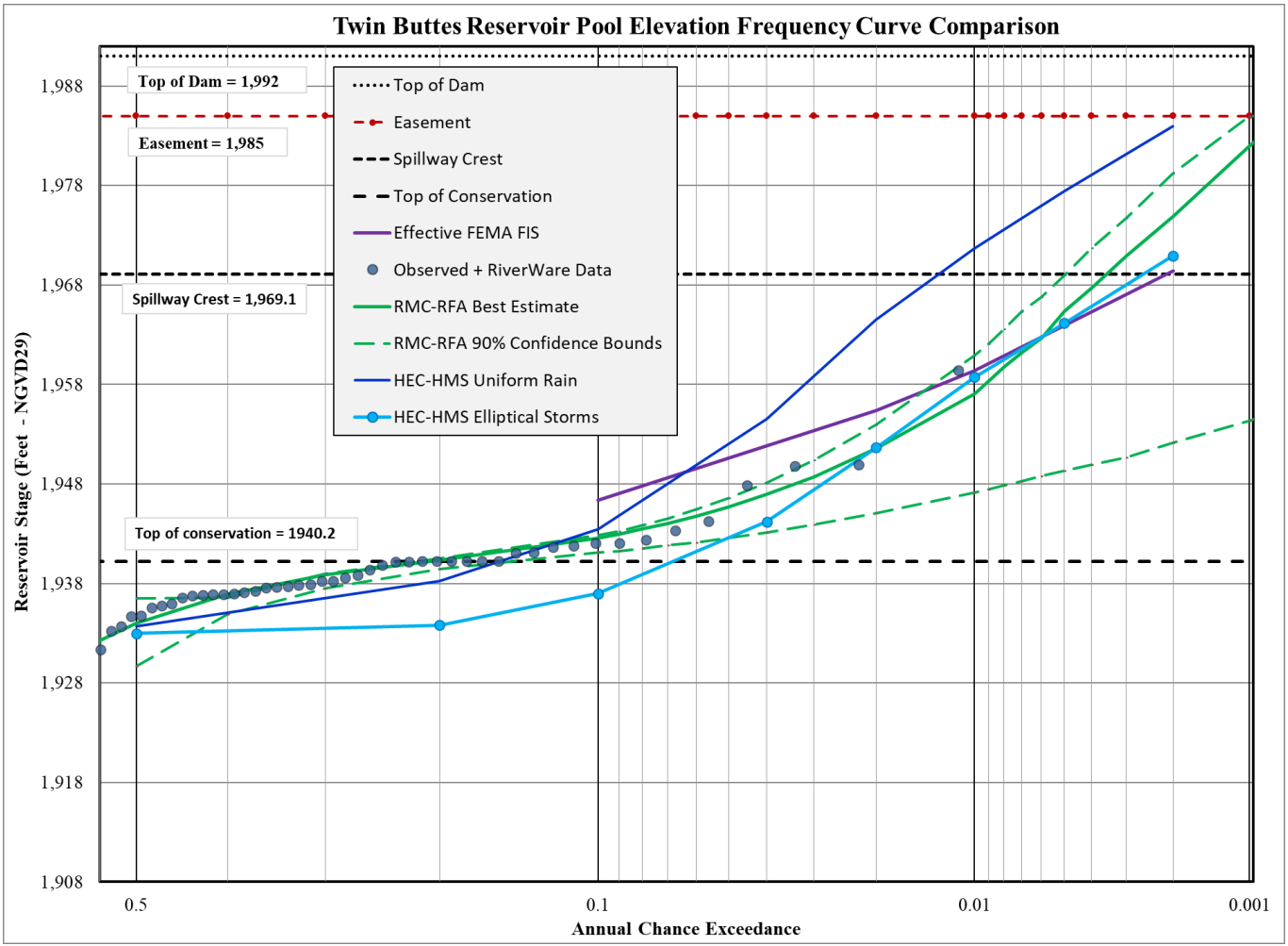

Figure 12.75: Pool Elevation Frequency Curve Comparison for Twin Buttes Reservoir

Table 12.76: Frequency Pool Elevation (ft NAVD88) Comparison for O.H. Ivie Reservoir

Annual Exceedance Probability (AEP)	Return Period (years)	Currently Effective FEMA FIS	Previous Studies	HEC-HMS Uniform Rain Frequency Storm	HEC-HMS Elliptical Frequency Storm	Reservoir Analysis in RMC-RFA	Operational Reference	Reference Elevation
0.002	500			1567.4	1560.9	1553.7	Top of Dam	1584.0
0.005	200			1564.0	1557.1	1553.2		
0.01	100			1560.1	1554.8	1553.0		
0.02	50			1556.4	1553.8	1552.8	Spillway Crest	1565.3
0.04	25			1553.3	1552.2	1552.4		
0.1	10			1552.0	1550.1	1552.3		
0.2	5			1551.4	1549.1	1552.0		
0.5	2			1549.4	1548.3	1551.0	Normal Pool	1551.8

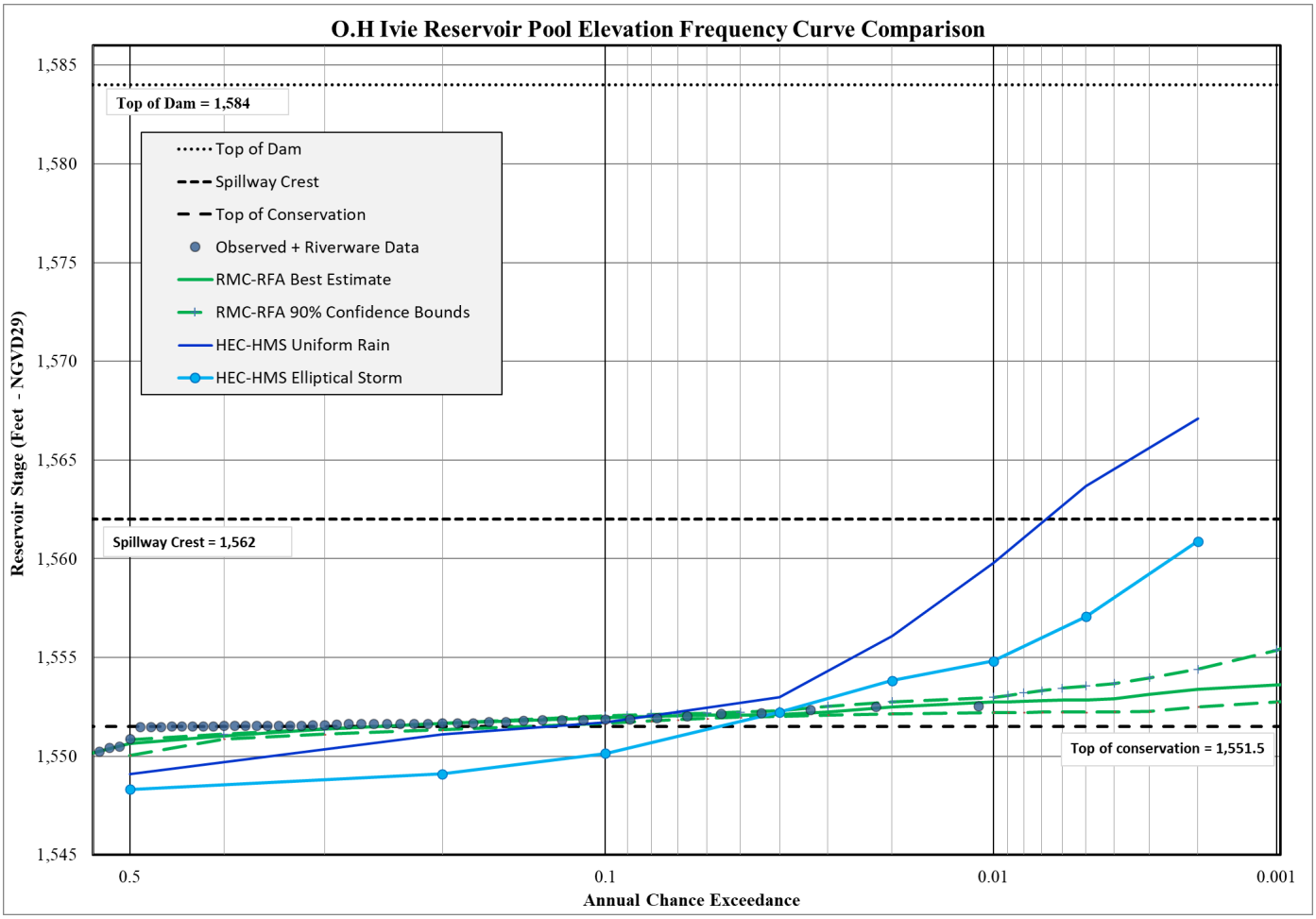

Figure 12.76: Pool Elevation Frequency Curve Comparison for O.H. Ivie Reservoir

O.H. Ivie Lake is water supply lake that is operated by the Colorado River Municipal Water District. It has a service spillway with tainter gates and an uncontrolled emergency spillway with a fuse plug. The dam is located on the Colorado River downstream of the Concho River basin, and it has an uncontrolled drainage area of approximately 3,400 square miles. The reservoir began operations in 1990, so it has a fairly short period of record, and it is also located in the portion of the watershed that is experiencing declining flow trends. There are no published frequency pool elevations from FEMA or other studies for this reservoir.

As one can see from Figure 12.76, the RMC-RFA analysis assumes an idealized reservoir operation from the RiverWare model where the pool is maintained at close to the top of conservation pool for more than 99% of the time. However, observed records show that the average elevation of the past 30 years has been about 15 feet below conservation pool. The HEC-HMS modeling assumed an initial pool elevation based on typical conditions of the most recent 30 years of record, therefore it calculated lower pool elevations for the frequency events. For the rare events, the RMC-RFA stochastic analysis used variable elevations and inflow volumes, but the statistics for those inflow volumes were based on somewhat limited observed data. The inflow volumes for the HEC-HMS elliptical storms, on the other hand, were based on a host of regional and observed data including NOAA Atlas 14 rainfall depths, area-reductions from regional observed storms, and calibrated loss rates from recent storms. Therefore, it calculated higher pool elevations for the rare events like the 1% AEP (100-yr) flood. In addition, the RMC-RFA methods were designed for estimating pool frequencies for reservoirs with substantial flood storage volumes, and they are not as reliable for reservoirs with level pool operations like O.H. Ivie. In those cases, the smaller timesteps in HEC-HMS tend to do a better job of estimating pool elevations and outflows for the rare frequency events.

Table 12.77: Frequency Pool Elevation (ft NAVD88) Comparison for Lake Coleman

Annual Exceedance Probability (AEP)	Return Period (years)	Currently Effective FEMA FIS	Previous Studies	HEC-HMS Uniform Rain Frequency Storm	HEC-HMS Elliptical Frequency Storm	Reservoir Analysis in RMC-RFA	Operational Reference	Reference Elevation
0.002	500			1734.5			Top of Dam	1740.0
0.005	200			1733.0				
0.01	100			1731.8				
0.02	50			1730.4			Spillway Crest	1726.5
0.04	25			1728.9				
0.1	10			1726.2				
0.2	5			1722.7				
0.5	2			1719.5			Normal Pool	1718.0

Lake Coleman is a water supply reservoir operated by the City of Coleman. It has a 24-inch service outlet for small releases and an uncontrolled emergency spillway. The dam is located on Jim Ned Creek in the Pecan Bayou watershed, and it has a drainage area of approximately 300 square miles. There are no published frequency pool elevations from FEMA or other studies for this reservoir. Due to its relatively small drainage area, the only frequency analysis completed for this lake was the HEC-HMS unform rainfall method, and those results are presented in the table above. As one can see from this table, the HEC-HMS results show that the reservoir is predicted to reach the spillway crest approximately every 10-25 years, and the 1% AEP pool elevation is about 6 feet above the spillway crest.

Table 12.78: Frequency Pool Elevation (ft NAVD88) Comparison for Hords Creek Reservoir

Annual Exceedance Probability (AEP)	Return Period (years)	Currently Effective FEMA FIS	2009 USACE Analysis	HEC-HMS Uniform Rain Frequency Storm	HEC-HMS Elliptical Frequency Storm	Reservoir Analysis in RMC-RFA	Operational Reference	Reference Elevation
0.002	500			1921.3		1918.4	Top of Dam	1939.0
0.005	200			1920.7		1914.9		
0.01	100		1915.4	1920.0		1910.2	Easement	1925.4
0.02	50		1912.4	1917.0		1907.4	Spillway Crest	1920.4
0.04	25			1914.2		1905.4		
0.1	10			1908.6		1902.8		
0.2	5			1905.1		1901.2		
0.5	2			1901.5		1897.1	Normal Pool	1900.4

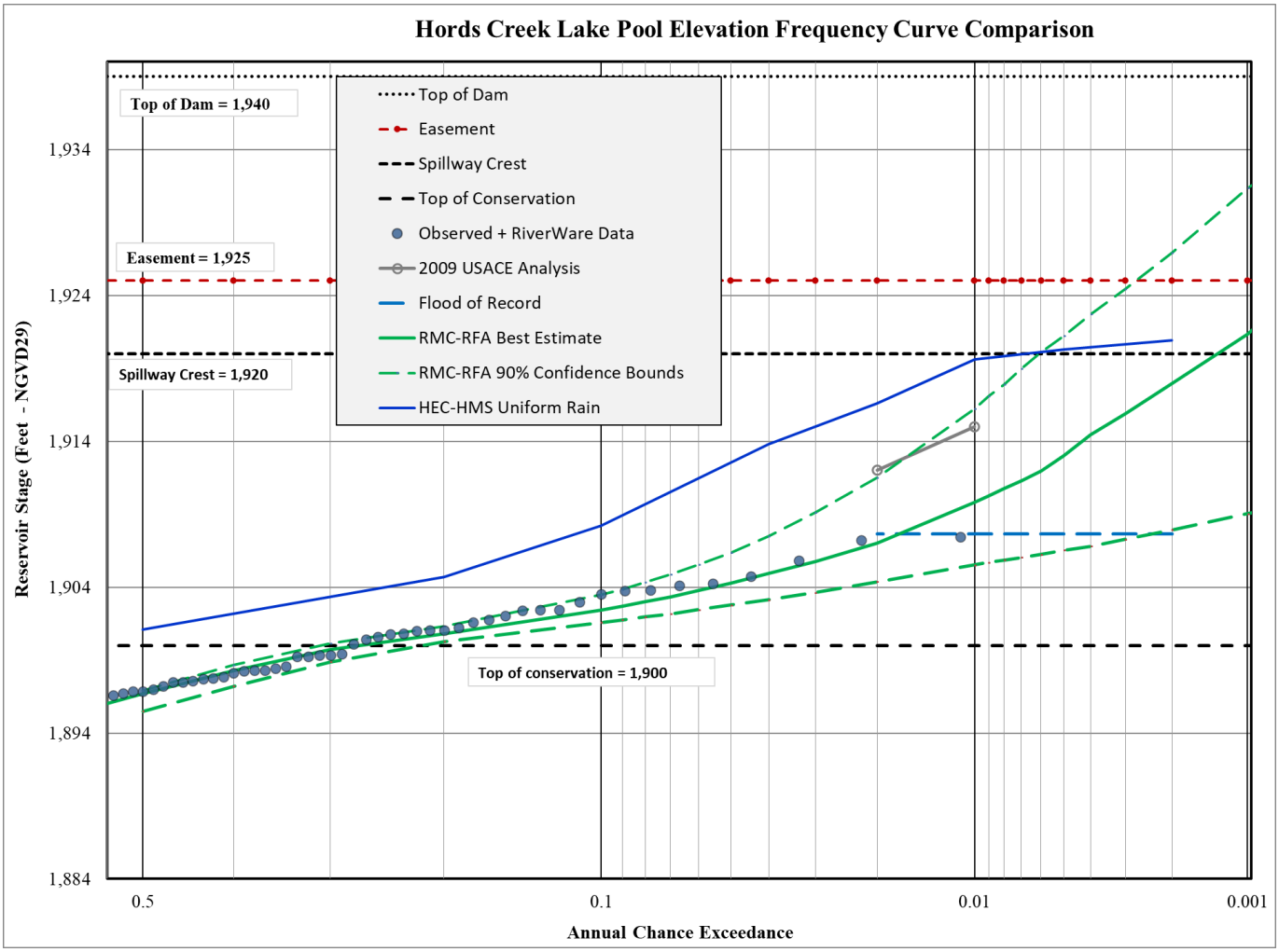

Figure 12.78: Pool Elevation Frequency Curve Comparison for Hords Creek Reservoir

Hords Creek Lake is a flood control reservoir that is operated by USACE. It has a gated outlet and an uncontrolled emergency spillway. The dam is located on Jim Ned Creek in the Pecan Bayou watershed, and it has a drainage area of approximately 49 square miles. The reservoir began operations in 1948, so it has a fairly long period of record, and it is located in the portion of the watershed that is experiencing declining flow trends. There are no published FEMA pool elevations for this reservoir, but there are frequency pool elevations from a previous 2009 reservoir analysis by USACE, as shown in the table above.

Table 12.78 shows that the results from the new RMC-RFA reservoir analysis are about 5 feet lower than the 2009 USACE analysis. This is likely due to the effects of the record drought that occurred between 2010 and 2014 which was added to the record in the most recent analysis. Since that drought, Hords Creek Reservoir has still not returned (as of 2023) to its top of conservation pool elevation. Figure 12.78 also shows that the HEC-HMS uniform rain results were several feet higher than the RMC-RFA results. This is because the RMC-RFA methodology better accounts for the variable starting pool elevations and inflow volumes that can be experienced by the reservoir during a flood event. The HEC-HMS modeling, on the other hand, assumed a single starting pool elevation that was near conservation pool for each frequency storm. In addition, since Hords Creek has such a large flood storage capacity, high pool elevations are often the result of a series of storms rather than a single storm, and the RMC-RFA analysis better accounts for these variables.

Lake Brownwood is a water supply reservoir that is operated by the Brown County Water Improvement District. It has a service spillway and an emergency spillway, both of which are not controlled by gates. The dam was constructed in 1933 and is one of the oldest dams in the basin. It is located on Pecan Bayou just upstream of the City of Brownwood, and it has a drainage area of approximately 1,500 square miles. There are no published frequency pool elevations from FEMA or other studies for this reservoir.

The Table and Figure below show the results from the HEC-HMS and RMC-RFA analyses that were completed for this study. As one can see from this figure, the RMC-RFA and HEC-HMS elliptical storm results were within one foot of one another for the 50% through 4% AEP (2-year through 25-year) events, but for the rare events like the 1% and 0.2% AEP (100-yr and 500-yr), the HEC-HMS elliptical storm results trend several feet higher than the RMC-RFA results. However, 1% AEP results from the HEC-HMS elliptical storms are very close to the flood of record from the RiverWare data. In addition, the RMC-RFA methods were designed for estimating pool frequencies for reservoirs with substantial flood storage volumes, and they are not as reliable for reservoirs with level pool operations like Lake Brownwood. In those cases, the smaller timesteps in HEC-HMS tend to do a better job of estimating pool elevations and outflows for the rare frequency events.

Table 12.79: Frequency Pool Elevation (ft NAVD88) Comparison for Lake Brownwood

Annual Exceedance Probability (AEP)	Return Period (years)	Currently Effective FEMA FIS	Previous Studies	HEC-HMS Uniform Rain Frequency Storm	HEC-HMS Elliptical Frequency Storm	Reservoir Analysis in RMC-RFA	Operational Reference	Reference Elevation
0.002	500			1447.1	1441.7	1436.1	Top of Dam	1470.0
0.005	200			1442.9	1437.9	1434.6		
0.01	100			1439.6	1435.4	1433.1		
0.02	50			1436.1	1433.3	1431.9	Spillway Crest	1425.0
0.04	25			1433.2	1431.6	1430.7		
0.1	10			1430.6	1430.3	1429.1		
0.2	5			1429.0	1428.8	1427.8		
0.5	2			1427.3	1426.9	1426.0	Normal Pool	1425.0

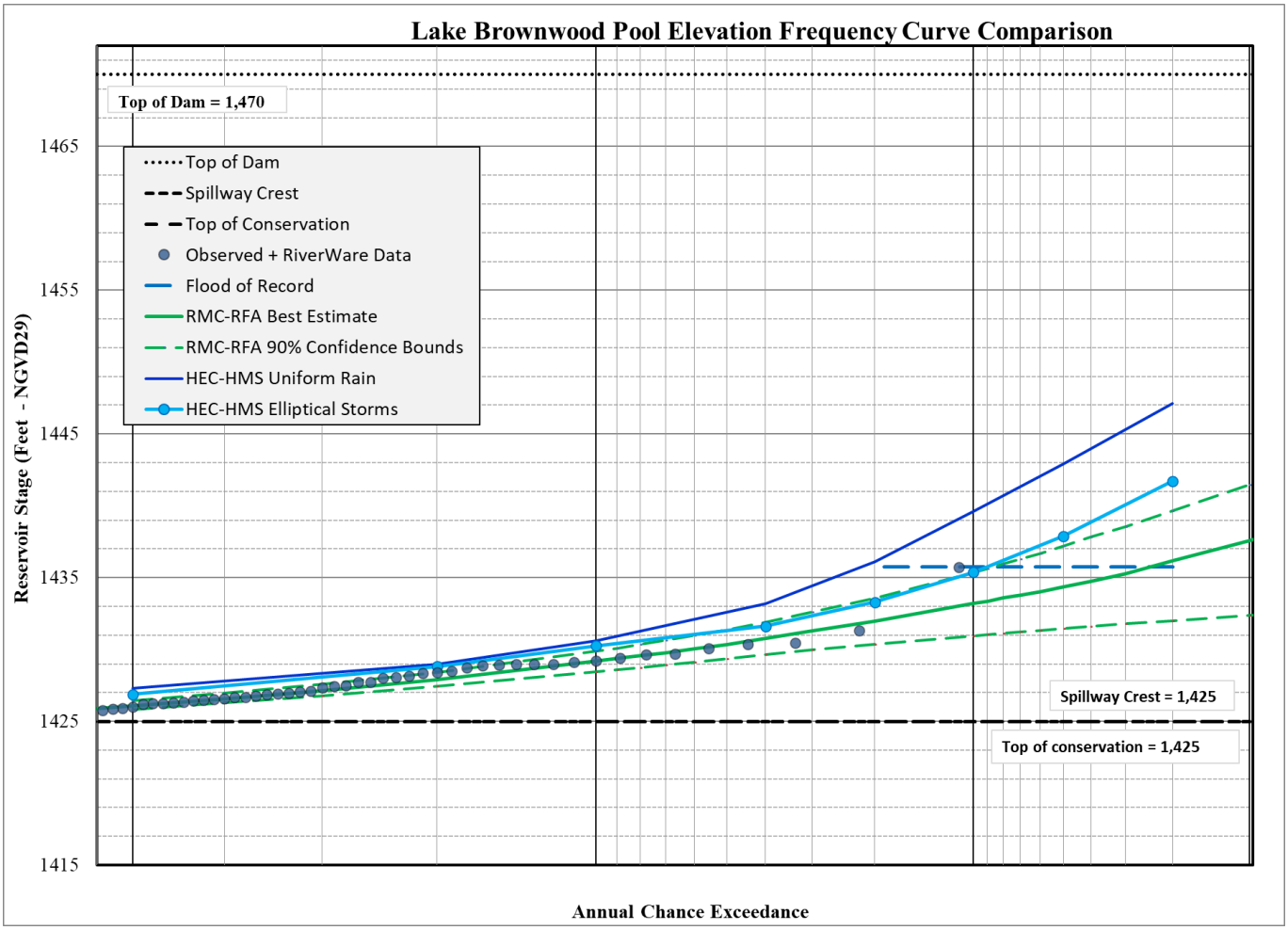

Figure 12.79: Pool Elevation Frequency Curve Comparison for Lake Brownwood

Table 12.80: Frequency Pool Elevation (ft NAVD88) Comparison for Brady Creek Reservoir

Annual Exceedance Probability (AEP)	Return Period (years)	Currently Effective FEMA FIS	Previous Studies	HEC-HMS Uniform Rain Frequency Storm	HEC-HMS Elliptical Frequency Storm	Reservoir Analysis in RMC-RFA	Operational Reference	Reference Elevation
0.002	500			1768.5	1765.9		Top of Dam	1783.2
0.005	200			1765.7	1763.1			
0.01	100			1763.2	1757.6			
0.02	50			1756.6	1752.4		Spillway Crest	1762.3
0.04	25			1752.3	1748.0			
0.1	10			1748.6	1746.4			
0.2	5			1746.7	1745.3			
0.5	2			1744.4	1744.1		Normal Pool	1743.2

Brady Creek Reservoir is a water supply reservoir operated by the City of Brady. It has a service spillway and an emergency spillway, both of which are not controlled by gates. The dam was constructed in 1963 and is located on Brady Creek in the San Saba watershed. It has a drainage area of approximately 500 square miles. There are no published frequency pool elevations from FEMA or other studies for this reservoir.

The table above shows the HEC-HMS results for Brady Creek reservoir along with its operational levels. With a drainage area of 500 square miles, both uniform rain and elliptical storms can provide reasonable results in HEC-HMS. The uniform rain method produced higher pool elevations due to a higher overall rainfall volume. According to the uniform rainfall results, the spillway crest would be exceeded once in approximately 100-years (1% AEP), while the elliptical storms do not exceed the spillway until the 0.5% AEP (200-year) event.

Lake Buchanan is the upstream dam in the Highland Lakes chain of lakes that is operated by the Lower Colorado River Authority (LCRA). It has a gated service spillway and an uncontrolled spillway. The dam was constructed in 1937, and the reservoir experienced its flood of record immediately afterwards in 1938. The dam is located on the Colorado River downstream of its confluence with the San Saba River, and it has an uncontrolled drainage area of approximately 10,700 square miles. The effective FEMA pool elevations are based on the results of the 2002 Flood Damage Evaluation Project (FDEP).

The dam has undergone a change in its operational plan as of 2023. As a result, two different analyses were completed in RMC-RFA. One was intended to match the historic operations (1990 Operational Plan), and the other is intended to match the new (2023) operational plan. The results of both of those analyses are shown in the table and figure below. More information on the differences between these two operational plans can be found in section 9.9 of this report. The HEC-HMS results also assumed that the 2023 operational plan is the best representation of current conditions. Both the HEC-HMS elliptical results and the RMC-RFA results for the 2023 Operational plan showed that the current effective FEMA 1% AEP elevation would be maintained, and they calculated slightly lower elevations than the FIS for the 0.2% AEP event.

Table 12.81: Frequency Pool Elevation (ft NAVD88) Comparison for Lake Buchanan

Annual Exceedance Probability (AEP)	Return Period (years)	Currently Effective FEMA FIS	2002 FDEP Study	HEC-HMS Uniform Rain Frequency Storm	HEC-HMS Elliptical Frequency Storm	Reservoir Analysis in RMC-RFA (1990 Operational Plan)	Reservoir Analysis in RMC-RFA (2023 Operational Plan)	Operational Reference	Reference Elevation
0.002	500	1022.7	1022.7	1025.1	1022.5	1022.3	1021.4	Top of Dam	1026.1
0.005	200			1023.3	1021.7	1022.1	1021.3		
0.01	100	1021.0	1021.0	1022.9	1021.0	1021.9	1020.9		
0.02	50	1020.5	1020.5	1022.0	1020.5	1021.7	1021.1	Spillway Crest	1020.4
0.04	25		1020.5	1020.6	1020.3	1021.5	1020.7		
0.1	10	1020.5	1020.5	1020.3	1019.9	1021.3	1020.6		
0.2	5		1020.0	1020.0	1019.7	1020.9	1020.5	Easement	1020.3
0.5	2		1020.0	1019.5	1019.4	1019.8	1019.6	Normal Pool	1020.3

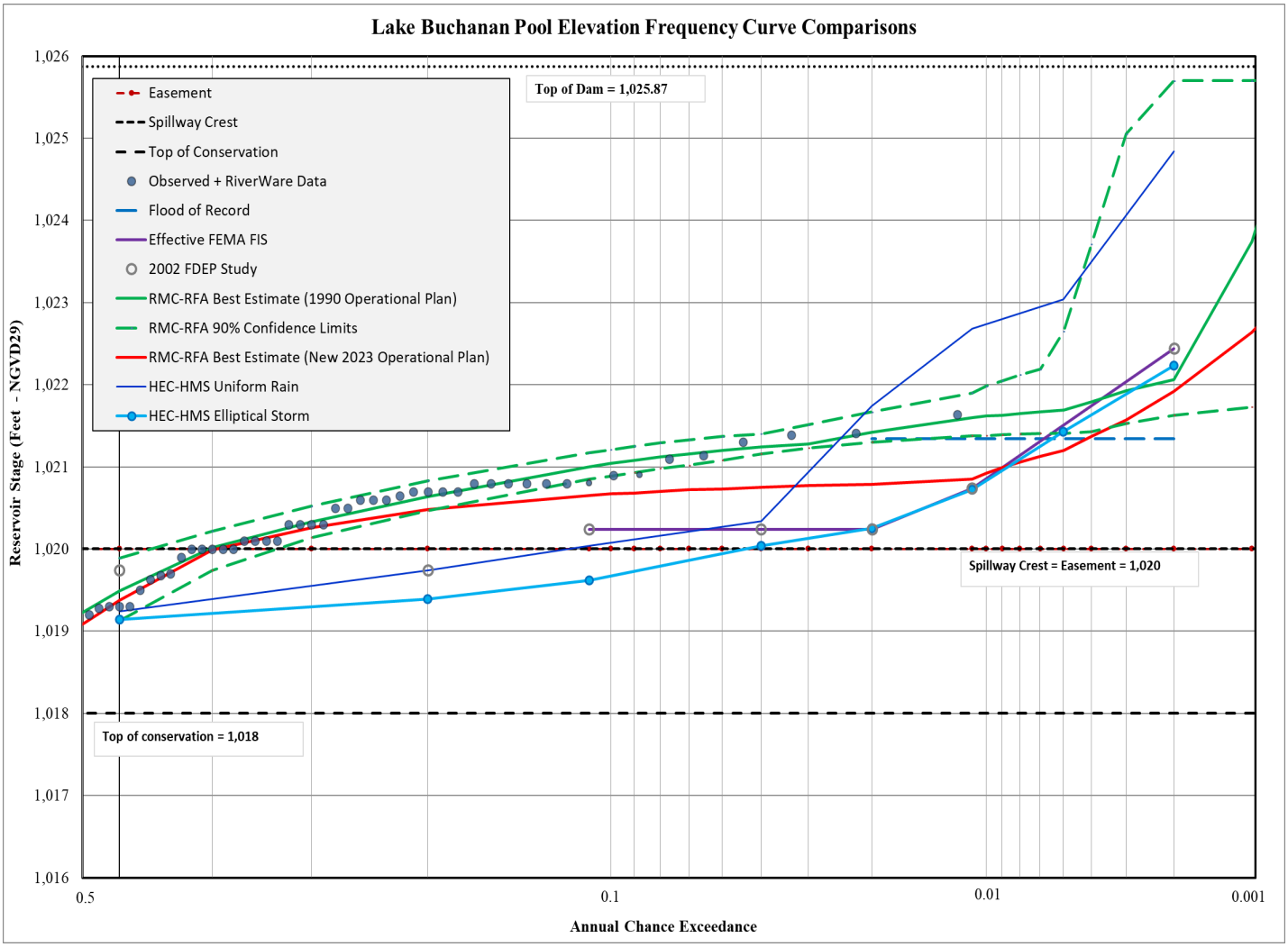

Figure 12.81: Pool Elevation Frequency Curve Comparison for Lake Buchanan

Table 12.82: Frequency Pool Elevation (ft NAVD88) Comparison for Lake LBJ

Annual Exceedance Probability (AEP)	Return Period (years)	Currently Effective FEMA FIS (Burnet County)	2002 FDEP Study	HEC-HMS Uniform Rain Frequency Storm	HEC-HMS Elliptical Frequency Storm	Reservoir Analysis in RMC-RFA	Operational Reference	Reference Elevation
0.002	500	839.5	829.2	848.3	842.2	831.0	Top of Dam	838.0
0.005	200			844.8	837.2	830.0		
0.01	100	828.1	827.9	842.2	831.0	829.3		
0.02	50	825.8	825.2	837.5	828.7	828.6	Spillway Crest	835.5
0.04	25		824.8	829.2	827.9	828.1		
0.1	10	825.4	824.8	827.7	827.1	826.6		
0.2	5		824.8	826.8	826.5	825.8	Easement	825.0
0.5	2		824.8	825.8	825.6	825.4	Normal Pool	825.0

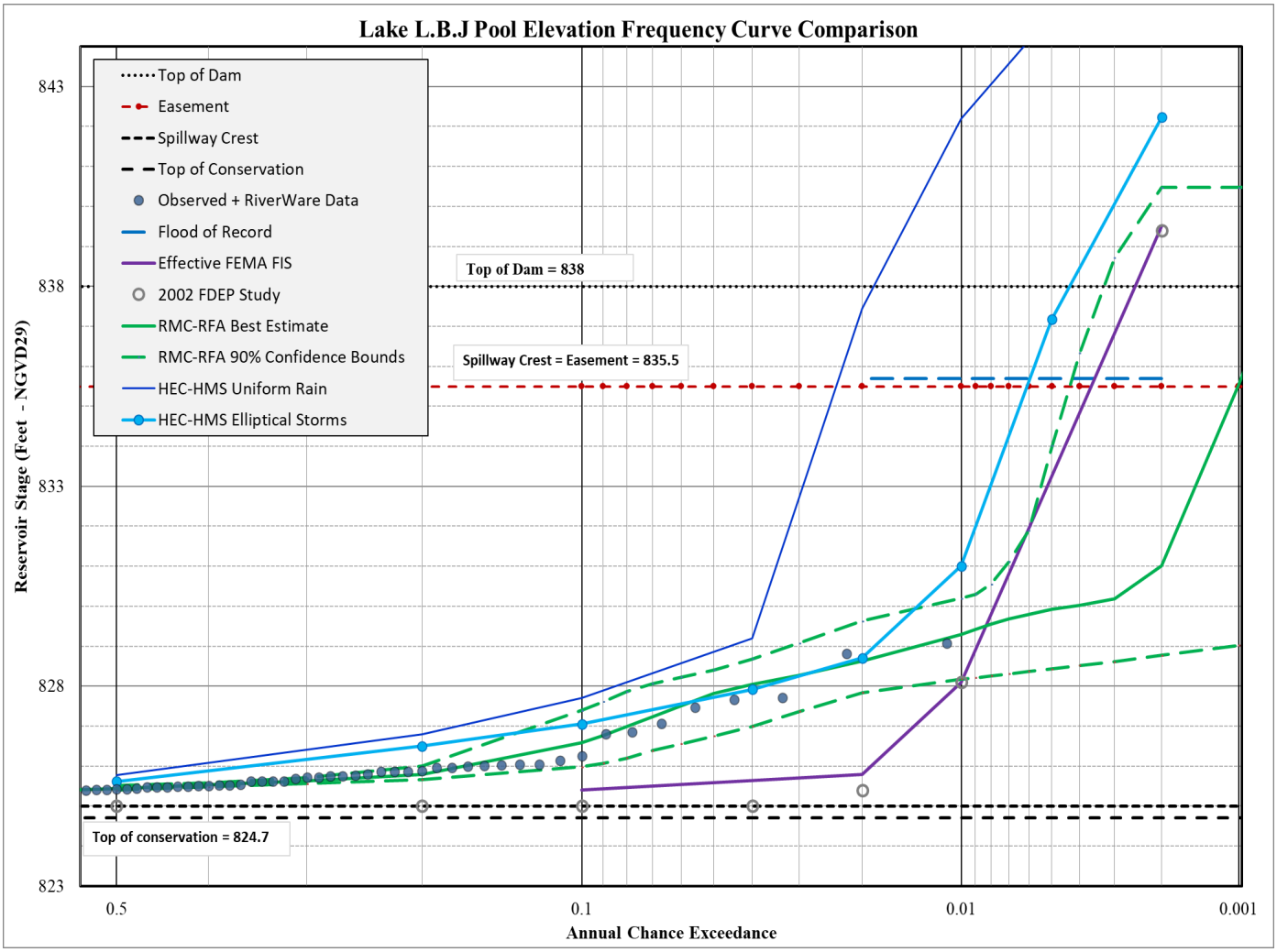

Figure 12.82: Pool Elevation Frequency Curve Comparison for Lake LBJ

Lake LBJ is the next downstream dam in the Highland Lakes chain that is operated by LCRA. The dam has ten 50' by 30' tainter gates that are operated to maintain a level pool elevation near 825 ft. The dam was constructed in 1951. The dam is located on the Colorado River downstream of its confluence with the Llano River, and it has an uncontrolled drainage area of approximately 15,700 square miles. The effective FEMA FIS pool elevations are based on the results of the 2002 Flood Damage Evaluation Project (FDEP).

The preceding table and figure show the results of the new HEC-HMS and RMC-RFA analyses alongside the previously published frequency pool elevations. As one can see from this figure, the results of both the RMC-RFA analysis and the HEC-HMS elliptical storms are significantly higher than the effective FEMA elevations up to the 1% AEP event. However, when comparing the results to the observed data points, both RMC-RFA and HEC-HMS do a much better job of following the trend in the observed data than the effective FIS elevations. Figure 12.82 also shows that the HEC-HMS elliptical storm and RMC-RFA results stay close to one another through the 2% AEP (50-yr) frequency, but then the HEC-HMS elliptical storm results trend higher than the RMC-RFA results. However, the HEC-HMS elliptical storms assign a more reasonable frequency to the 1952 flood of record, which was just above the spillway crest. It should be noted that a tenth floodgate was added to the dam in 1971, which may have reduced that 1952 flood elevation to just below the spillway crest. However, in either case, the HEC-HMS estimate of the flood of record's return period remains between 100 and 200 years, rather than the RMC-RFA results which would place the return period of that event at roughly 1,000 years.

In addition, the RMC-RFA methods were designed for estimating pool frequencies for reservoirs with substantial flood storage volumes, and they are not as reliable for reservoirs with level pool operations like Lake LBJ. In those cases, the smaller timesteps in HEC-HMS tend to do a better job of estimating pool elevations and outflows for the rare frequency events. This is especially true for Lake LBJ where the inflows for rare floods are driven by the flashy Llano River watershed.

Lake Travis is the next downstream dam in the Highland Lakes chain of lakes that is operated by LCRA. Lake Travis is a major flood control reservoir that is operated in cooperation with USACE during flood events. The dam has a gated outlet and an uncontrolled emergency spillway. Lake Travis was completed in 1940 and has provided flood protection benefits to the City of Austin ever since. It is located on the Colorado River just downstream of its confluence with the Pedernales River, and it has an uncontrolled drainage area of approximately 17,500 square miles. The effective FEMA FIS pool elevations are based on the results of the 2002 Flood Damage Evaluation Project (FDEP).

The following table and figure show the results of the new HEC-HMS and RMC-RFA analyses alongside the previously published frequency pool elevations. One can see from this figure that the results of the new RMC-RFA analysis are very close to the effective FEMA FIS elevations, especially for the 1% and 0.2% AEP events. Both of these analyses show that the spillway crest would be exceeded by a 2% AEP event. One can also see from this figure that the RMC-RFA results follow the observed data well. Lake Travis is exactly the type of reservoir that RMC-RFA was designed to analyze. This is because the RMC-RFA methodology better accounts for the variable starting pool elevations and inflow volumes that can be experienced by the reservoir during a flood event. The HEC-HMS modeling, on the other hand, assumed a single starting pool elevation at conservation pool for each frequency storm. In addition, due to the large flood storage capacity at Lake Travis, the inflow volume from a single storm is often insufficient to fill its flood pool. Therefore, high pool elevations at Lake Travis are often the result of a series of storms rather than a single storm. The RMC-RFA analysis better accounts for the varying pool elevations that result from series of storms. Figure 12.83 shows that the HEC-HMS elliptical storm results are sometimes below the lower confidence bound of the RMC-RFA results. This is further indication that it would take more than a single 2-day storm event to fill Lake Travis' massive flood pool.

Table 12.83: Frequency Pool Elevation (ft msl) Comparison for Lake Travis

Annual Exceedance Probability (AEP)	Return Period (years)	Currently Effective FEMA FIS	2002 FDEP Study	HEC-HMS Uniform Rain Frequency Storm	HEC-HMS Elliptical Frequency Storm	Reservoir Analysis in RMC-RFA	Operational Reference	Reference Elevation
0.002	500	732.5	736.4	755.9	732.0	735.2	Top of Dam	750.0
0.005	200			748.8	721.7	730.1		
0.01	100	721.8	721.8	742.6	714.8	721.7	Easement	715.0
0.02	50	716.5	716.5	736.2	709.3	716.1	Spillway Crest	714.0
0.04	25		713.5	724.3	695.7	713.3		
0.1	10	696.8	696.8	711.1	688.6	698.5		
0.2	5		690.9	695.4	685.7	690.8		
0.5	2		685.0	686.2	683.0	683.2	Normal Pool	681.0

NOTE: Elevations for Lake Travis are in "msl", which is LCRA's Hydromet Datum.
The datum conversion from msl to NAVD88 is +0.6 ft for Lake Travis.

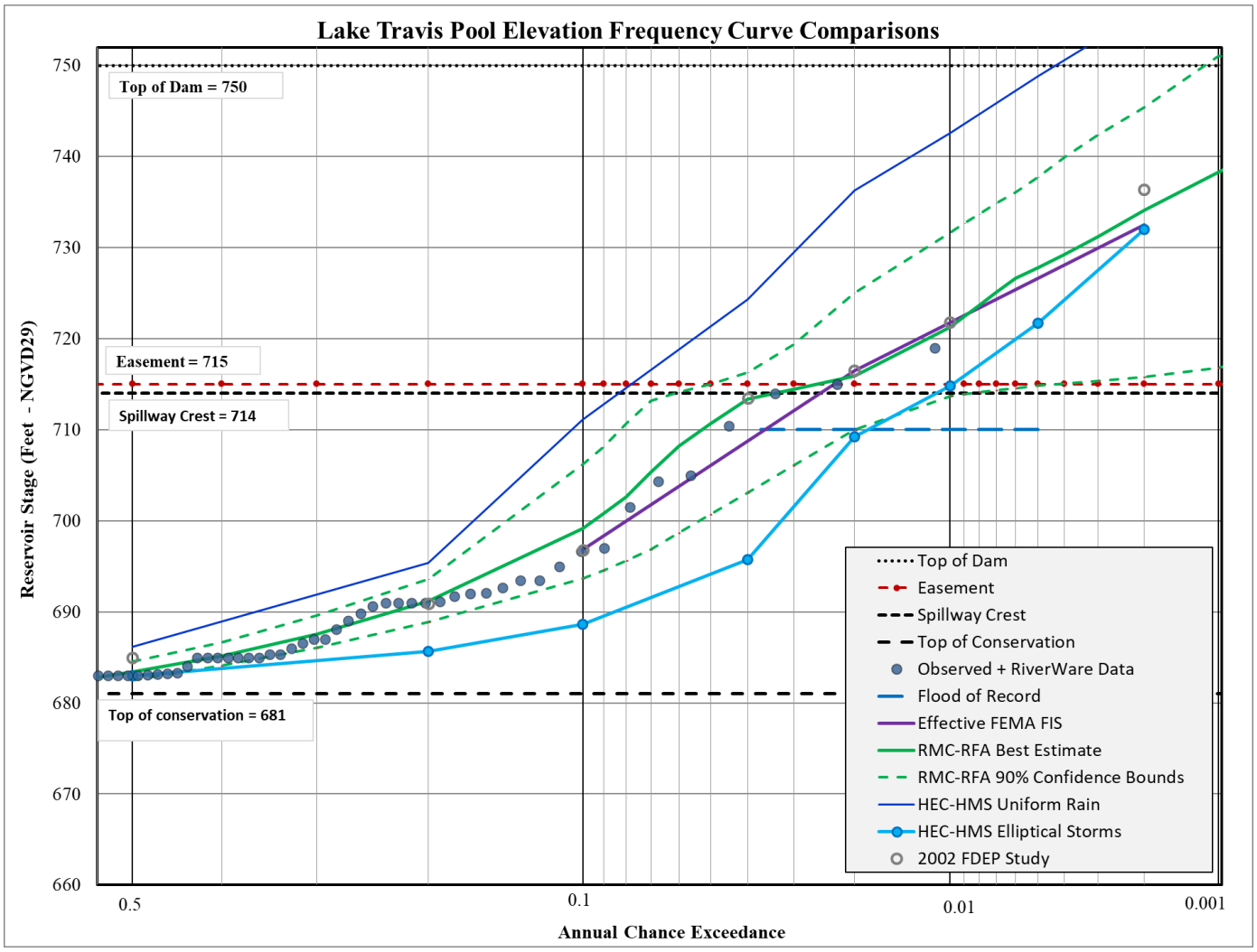

Figure 12.83: Pool Elevation Frequency Curve Comparison for Lake Travis

13 Frequency Flow Recommendations

The final recommendations for the InFRM Watershed Hydrology Assessments are formulated through a rigorous process which requires technical feedback and collaboration between all the InFRM subject matter experts. This process includes the following steps at a minimum: (1) comparing the results of the various hydrologic methods to one another, (2) performing an investigation into the reasons for any significant differences in results at each location in the watershed, (3) selecting the draft recommended methods, (4) performing internal and external technical reviews of the hydrologic analyses and the draft recommendations, and finally, (5) finalizing the study recommendations.

After completing this process for the Lower Colorado River basin, the frequency discharges that are recommended for adoption by the InFRM team were a combination of the results from the following methods: HEC-HMS NOAA Atlas 14 uniform rain frequency storms (Chapter 6), HEC-HMS NOAA Atlas 14 elliptical frequency storms (Chapter 7), the RiverWare analysis (Chapter 8) and the RMC-RFA Reservoir Analyses (Chapter 9). Detailed breakouts of the recommended peak frequency discharges and pool elevations for each location in the watershed are given in Tables 13.1 and 13.2. The USGS and LCRA gage locations whose results were examined and compared in Chapter 12 are highlighted in Table 13.1.

The statistical results from Chapters 5, 8 and 10 were used as points of comparison, especially at the frequent end of the curves, but in most cases, the InFRM team chose not to adopt the statistical flow frequency results directly. One reason for this decision was the tendency of the statistical results to change after each significant flood event, as demonstrated in the statistical change over time comparison figures included in Chapter 12. In addition, some of the basic assumptions of a Bulletin 17C statistical analysis are being violated in the upstream portion of the study area. Bulletin 17C assumes that the sample of observed floods is stationary and homogeneous, but these assumptions are not true for the portion of the watershed that is experiencing downward trends in annual peak streamflow (which is generally upstream of San Saba, Texas). For other parts of the basin that are not experiencing significant trends in annual peak streamflow, climate variability between wet and dry conditions can still result in non-representative samples in the gage record. Chapter 11 discusses examples in the Colorado River basin where one gage location has been hit heavily by large storms and another is missed almost entirely. These non-representative samples can bias the statistical frequency flow results upward or downward, depending on the storms that have occurred above that particular gage. Even the 95% confidence bounds of a Bulletin 17C statistical analysis can shift dramatically over time based on the available sample of observed floods (see Figure 12.5a for a good example).

Rainfall runoff modeling, on the other hand, is based on physical watershed characteristics, such as drainage area and stream slope, that do not tend to change as much over time. Climate variability can also be accounted for in the watershed model by using regional rainfall information from NOAA Atlas 14 and by adjusting soil loss rates to be consistent with recent observed storms and appropriate for the rarity of the event in question. Another reason for the selection of the HEC-HMS modeling discharges was the ability to directly calculate frequency discharges for locations within the Colorado River watershed that do not coincide with a stream gage.

Rainfall-runoff modeling in HEC-HMS was used to simulate the physical processes that occur in the Colorado River basin during intense storm events, including the movement of water across the land surface and through the streams and rivers. The HEC-HMS model for the Colorado River basin underwent extensive calibration to accurately simulate the response of the watershed to a range of observed flood events, including large events similar to a 1% ACE (100-yr) flood. In fact, a total of 38 recent storm events and over 400 individual calibrations were used to fine tune the HEC-HMS model; thereby bestowing a high degree of confidence in the HEC-HMS model's results.

In addition to extensive calibration, best available precipitation frequency estimates from NOAA Atlas 14 (NOAA, 2018) were used to build frequency storms within the HEC-HMS model. NOAA Atlas 14 is the most accurate, up-to-date, and comprehensive study of rainfall depths in Texas. NOAA Atlas 14 used a regional statistical approach that incorporated at least 1,000 cumulative years of daily data and 500 cumulative years of sub-daily data into each station's rainfall frequency estimate. This regional approach yielded better estimates of rare rainfall depths such as the 1% and 0.2% AEP (100-yr and 500-yr) depths than can be achieved by using data from a single location. For these reasons, the calibrated HEC-HMS watershed modeling with the NOAA Atlas 14 rainfall depths was adopted as having the most complete accounting of both the historic rainfall data and the physical processes at work in the watershed.

Between the uniform rain and the elliptical frequency storms in HEC-HMS, the uniform rain method is simpler and well suited for smaller drainage areas, while the elliptical storm method is more complex and better suited for larger drainage areas. Both this study and the previous InFRM Watershed Hydrology Assessments have confirmed that the results of the uniform rainfall method are generally reasonable up to at least 1,000 square miles (InFRM, 2019) (InFRM, 2021) (InFRM, 2022). For larger drainage areas in the Lower Colorado River basin, which sometimes exceeded 25,000 square miles, the elliptical storm results from HEC-HMS did a better job of producing reasonable runoff volumes and subsequently peak stream flows. Table 13.1 indicates the locations where the recommended results transitioned from uniform rainfall results to elliptical storm results along each stream and river. The exact locations of the transitions between uniform and elliptical storms generally occurred at locations with drainage areas between 400 and 1,000 square miles and were placed at significant confluences or reservoirs to avoid any jumps or dips in the peak flows due to a change in the rainfall method.

For the reservoirs in the Lower Colorado River basin, the recommended frequency pool elevations and releases often came from the RMC-RFA reservoir analyses from Chapter 9. The RMC-RFA reservoir analyses were performed for 10 of the largest reservoirs in the study area. The RMC-RFA analyses utilized stochastic techniques and included the most comprehensive accounting for the operations of the dam, the variability and frequency of its inflow volumes, and the range of its starting pool elevations. This type of detailed reservoir analysis lends a higher level of confidence to the resulting frequency estimates of its pool elevations. The RMC-RFA software was designed to analyze reservoirs that have a significant flood storage capacity, and it works best for those types of reservoirs (examples include Lake Travis, Twin Buttes, and Hords Creek). However, it does not always do as good of a job for reservoirs with level-pool operations and very little flood storage capacity (examples include Lake Brownwood and Lake LBJ). In those cases, the frequency storms in HEC-HMS sometimes did a better job of simulating the rapid changes in dam outflows during a large storm event. Table 13.2 records the recommended frequency pool elevations and methodology for each reservoir analyzed in this study. More discussion on the analyses for each reservoir can be found in section 12.2 of the previous report chapter.

For the reaches downstream of significant flood control dams, there are two distinct sources of flooding: (1) a large release from the dam and (2) rainfall runoff from the local drainage area downstream of the dam. The first flooding source was analyzed through the RMC-RFA reservoir analysis methods. For the second flooding source, peak flows from the local rainfall runoff were calculated in the HEC-HMS model with the NOAA Atlas 14 rainfall patterns of Chapters 6 and 7. The frequency peak flows from these two flooding sources were then compared to one another for each reach of the river, and the higher of the two peak flows were recommended for adoption. In general, the results showed that releases from the dams dominate in the reaches immediately downstream of the dam, but that the flows from the local rainfall runoff quickly become dominant as one moves further downstream.

In some cases, one may observe that the recommended frequency peak discharges decrease in the downstream direction. This is not an uncommon phenomenon for some river reaches as flood waters spread out into the floodplain and the hydrograph becomes dampened as it moves downstream. This can be due to a combination of peak attenuation due to river routing as well as the difference in timing between the peak of the main stem river versus the runoff from the local tributaries.

Table 13.1: Summary of Recommended Frequency Peak Discharges (cfs) for the Lower Colorado River Basin

Location Description	Drainage Area* (sq mi)	50% AEP 2-yr	20% AEP 5-yr	10% AEP 10-yr	4% AEP 25-yr	2% AEP 50-yr	1% AEP 100-yr	0.5% AEP 200-yr	0.2% AEP 500-yr	Hydrologic Method
Colorado River downstream of E.V. Spence Reservoir	-	2,000	2,000	7,500	11,000	20,000	22,000	23,000	25,000	Reservoir Analysis
Colorado River at Robert Lee, TX (USGS Gage 08124000)	30.9	2,000	2,000	7,500	11,000	20,000	22,000	23,000	25,000	HEC-HMS Uniform Rain / Reservoir Analysis
Colorado River below Turkey Creek	177.5	2,000	2,000	7,500	14,500	34,100	49,000	63,200	79,300	HEC-HMS Uniform Rain / Reservoir Analysis
Colorado River above Oak Creek	330.8	2,000	2,000	7,500	15,200	36,200	52,000	66,800	86,900	HEC-HMS Uniform Rain / Reservoir Analysis
Inflow to Oak Creek Reservoir	237.4	3,400	8,000	14,500	29,100	49,600	65,000	79,300	99,200	HEC-HMS Uniform Rain
Outflow from Oak Creek Reservoir	237.4	800	1,800	4,000	10,000	24,400	39,200	53,500	76,100	HEC-HMS Uniform Rain
Oak Creek above the Colorado River	337.4	700	1,700	4,100	10,200	21,300	32,600	44,500	62,200	HEC-HMS Uniform Rain
Colorado River below Oak Creek	668.2	2,000	3,000	7,900	24,500	54,300	76,900	98,300	127,000	HEC-HMS Uniform Rain / Reservoir Analysis
Colorado River above Valley Creek	844.9	2,200	5,000	9,700	24,200	52,300	74,900	98,100	130,000	HEC-HMS Uniform Rain
Valley Creek below subbasin CO_ValleyCr_S10	141.1	2,900	5,800	10,200	19,400	33,000	42,800	52,100	64,800	HEC-HMS Uniform Rain
Valley Creek above upper & lower Ballinger City Lakes	231.2	2,400	4,900	9,000	17,600	30,400	40,200	49,800	63,500	HEC-HMS Uniform Rain
Valley Creek below the lower Ballinger City Lake	231.2	1,900	4,500	8,500	16,700	29,000	38,400	48,300	61,300	HEC-HMS Uniform Rain
Colorado River near Ballinger, TX (USGS Gage 08126380)	1076.2	2,590	7,500	13,700	34,300	67,400	95,000	123,200	163,100	HEC-HMS Elliptical Storms
Colorado River above Elm Creek	1130.3	2,370	7,460	13,500	33,700	65,900	93,100	120,900	160,300	HEC-HMS Elliptical Storms
Bluff Creek below Mill Creek	107.4	2,600	6,000	9,500	15,500	21,800	31,400	40,700	52,500	HEC-HMS Uniform Rain
Elm Creek at Ballinger, TX (USGS Gage 08127000)	466.8	3,920	9,520	14,900	25,200	33,900	52,800	72,000	98,400	HEC-HMS Elliptical Storms
Colorado River below Elm Creek	1597.2	2,310	7,580	14,500	39,300	74,100	111,300	148,400	202,200	HEC-HMS Elliptical Storms
Colorado River above the Concho River	1826.2	2,220	6,920	13,400	36,800	69,400	105,300	141,000	193,300	HEC-HMS Elliptical Storms
High Lonesome Draw below subbasin CN_Mconcho_S20	404.4	140	3,080	8,800	24,700	41,600	58,200	70,900	88,500	HEC-HMS Elliptical Storms
High Lonesome Draw below subbasin CN_Mconcho_S30	496.5	170	2,810	9,100	27,000	46,200	65,300	80,300	100,900	HEC-HMS Elliptical Storms
Centralia Draw below High Lonesome Draw	745.2	200	2,140	8,400	28,800	51,200	73,700	91,600	117,200	HEC-HMS Elliptical Storms

Location Description	Drainage Area* (sq mi)	50% AEP 2-yr	20% AEP 5-yr	10% AEP 10-yr	4% AEP 25-yr	2% AEP 50-yr	1% AEP 100-yr	0.5% AEP 200-yr	0.2% AEP 500-yr	Hydrologic Method
Centralia Draw below North Creek	946.0	300	1,590	7,700	27,900	50,200	72,700	90,800	116,700	HEC-HMS Elliptical Storms
Middle Concho River below the Centrailia Draw	1349.1	1,540	6,580	15,800	39,500	64,200	90,000	112,000	143,100	HEC-HMS Elliptical Storms
Middle Concho River above Kiowa Creek	1642.5	1,770	6,680	16,500	43,900	73,200	104,100	130,600	169,700	HEC-HMS Elliptical Storms
Middle Concho River below Kiowa Creek	1731.3	1,870	6,900	16,700	45,000	75,400	107,400	135,100	175,500	HEC-HMS Elliptical Storms
Middle Concho River below Big Hollow Draw	1887.2	1,440	6,680	16,200	43,500	73,200	104,500	131,900	171,500	HEC-HMS Elliptical Storms
Middle Concho River above West Rocky Creek	2007.5	1,520	6,290	15,300	42,000	70,900	101,600	128,300	167,000	HEC-HMS Elliptical Storms
Middle Concho River below West Rocky Creek	2121.6	1,400	6,410	15,600	42,100	71,000	101,700	128,600	167,300	HEC-HMS Elliptical Storms
Middle Concho River abv Tankersley (USGS Gage 08128400)	2133.0	1,520	6,250	15,300	41,800	70,700	101,300	128,000	166,700	HEC-HMS Elliptical Storms
Spring Creek below O-Nine Draw	198.5	210	4,100	13,100	31,700	49,400	63,400	76,300	94,100	HEC-HMS Uniform Rain
Spring Creek above Tankersley, TX (USGS Gage 08129300)	427.2	330	2,800	9,000	23,000	36,700	56,000	74,700	97,400	HEC-HMS Uniform Rain
Dove Creek at Knickerbocker, TX (USGS Gage 08130500)	224.4	1,100	5,100	10,600	19,800	30,000	39,500	48,700	62,100	HEC-HMS Uniform Rain
Dove Creek above Spring Creek	251.7	930	4,500	9,300	17,400	26,400	34,800	43,200	55,600	HEC-HMS Uniform Rain
Spring Creek near San Angelo, TX (USGS Gage 08130700)	678.9	260	8,850	20,000	35,100	50,000	67,400	84,100	108,500	HEC-HMS Elliptical Storms
South Concho River below subbasin CN_Sconcho_S10	159.3	920	5,200	13,900	26,100	33,400	42,900	51,800	64,300	HEC-HMS Uniform Rain
South Concho River at Christoval, TX (USGS Gage 08128000)	415.4	800	6,460	21,200	42,300	55,700	73,300	90,300	115,300	HEC-HMS Elliptical Storms
Inflow to Twin Buttes Reservoir	3422.5	1,240	4,300	18,200	51,300	80,500	116,900	151,000	202,800	HEC-HMS Elliptical Storms
South Concho River below Twin Buttes Reservoir	3422.5	100	700	3,000	3,300	5,000	9,000	9,000	9,100	HEC-HMS Elliptical Storms / Reservoir Analysis
Pecan Creek nr San Angelo, TX (USGS Gage 08131400)	81.0	280	2,000	4,900	13,100	23,700	30,000	36,200	43,500	HEC-HMS Uniform Rain
Inflow to Lake Nasworthy	107.2	440	1,600	4,200	11,600	21,200	27,400	33,900	41,800	HEC-HMS Uniform Rain
South Concho River below Lake Nasworthy	107.2	440	1,600	4,200	11,600	21,200	27,400	33,900	41,800	HEC-HMS Uniform Rain
South Concho River above the North Concho River	139.2	1,700	2,200	4,900	12,100	21,400	27,800	34,600	43,100	HEC-HMS Uniform Rain
North Concho River abv Sterling City (USGS Gage 08133250)	201.0	610	2,300	5,200	12,100	23,500	33,100	41,300	52,600	HEC-HMS Uniform Rain
North Concho River above Lacy Creek	288.6	590	2,300	5,400	12,900	25,400	35,800	45,100	57,700	HEC-HMS Uniform Rain

Location Description	Drainage Area* (sq mi)	50% AEP 2-yr	20% AEP 5-yr	10% AEP 10-yr	4% AEP 25-yr	2% AEP 50-yr	1% AEP 100-yr	0.5% AEP 200-yr	0.2% AEP 500-yr	Hydrologic Method
Lacy Creek below Apple Creek	146.1	430	2,100	4,700	12,200	24,900	35,100	43,200	54,000	HEC-HMS Uniform Rain
Lacy Creek above the North Concho River	278.5	410	1,900	4,400	12,000	25,000	35,600	44,700	56,500	HEC-HMS Uniform Rain
North Concho River below Lacy Creek	567.1	710	4,970	10,000	24,500	40,300	58,900	76,100	97,500	HEC-HMS Elliptical Storms
North Concho River at Sterling City (USGS Gage 08133500)	586.0	870	4,740	9,700	23,600	38,900	56,900	73,700	94,500	HEC-HMS Elliptical Storms
North Concho River above Sterling Creek	609.8	340	3,970	8,600	22,000	36,700	54,200	70,700	90,900	HEC-HMS Elliptical Storms
North Concho River below Sterling Creek	808.4	570	4,520	9,300	22,900	38,300	56,600	73,800	95,000	HEC-HMS Elliptical Storms
North Concho River above Walnut Creek	1004.0	620	4,190	8,800	21,800	36,700	54,500	71,200	92,000	HEC-HMS Elliptical Storms
North Concho River below Walnut Creek	1070.3	550	4,220	8,700	21,600	36,200	53,900	70,500	91,000	HEC-HMS Elliptical Storms
North Concho River nr Carlsbad, TX (USGS Gage 08134000)	1220.7	1,800	4,770	8,300	21,100	37,900	54,900	71,300	91,800	HEC-HMS Elliptical Storms
North Concho River above Grape Creek	1250.2	2,840	6,120	9,800	22,900	39,700	57,000	73,400	93,700	HEC-HMS Elliptical Storms
North Concho River below Grape Creek	1360.1	2,620	5,830	9,600	24,000	42,900	62,100	80,400	103,100	HEC-HMS Elliptical Storms
North Concho River nr Grape Creek (USGS Gage 08134250)	1364.9	2,170	5,610	9,300	23,600	42,400	61,400	79,500	102,200	HEC-HMS Elliptical Storms
Inflow to OC Fisher Reservoir	1462.8	2,080	5,460	9,100	23,300	42,200	61,500	79,800	102,900	HEC-HMS Elliptical Storms
North Concho River below OC Fisher Reservoir	1462.8	12	196	849	2,600	2,700	2,850	3,100	3,250	Reservoir Analysis / RiverWare
North Concho River at San Angelo (former USGS 08135000)	22.1	1,500	1,900	2,700	4,800	9,700	11,800	13,700	16,200	HEC-HMS Uniform Rain
Concho River at San Angelo, TX (USGS Gage 08136000)	161.2	3,000	3,800	6,900	15,200	27,400	36,200	45,300	56,200	HEC-HMS Uniform Rain
Concho River above Crows Nest Creek	300.8	2,600	4,700	9,500	23,600	44,700	59,700	74,800	94,800	HEC-HMS Uniform Rain
Concho River above Lipan Creek	470.3	3,280	6,510	11,200	30,400	51,500	68,600	83,300	103,000	HEC-HMS Elliptical Storms
Dry Lipan Creek below Ninemile Creek	142.1	740	2,400	5,100	12,700	24,800	32,700	39,900	50,100	HEC-HMS Uniform Rain
Lipan Creek above Concho River	308.3	840	2,700	5,800	15,000	30,000	40,400	50,700	65,700	HEC-HMS Uniform Rain
Concho River below Lipan Creek	778.6	5,220	9,770	14,900	37,100	62,900	86,500	110,100	143,300	HEC-HMS Elliptical Storms
Concho River above Kickapoo Creek	895.4	4,880	9,450	14,600	37,300	62,700	87,100	111,300	145,400	HEC-HMS Elliptical Storms
Kickapoo Creek below Welch Creek	138.7	1,200	3,200	6,500	14,900	27,900	36,200	43,800	54,500	HEC-HMS Uniform Rain
Kickapoo Creek above the Concho River	300.0	1,100	3,000	5,900	13,500	25,300	33,600	41,100	51,900	HEC-HMS Uniform Rain
Concho River below Kickapoo Creek	1195.4	3,730	8,920	15,400	42,400	72,100	101,000	129,500	167,500	HEC-HMS Elliptical Storms
Concho River at Paint Rock, TX (USGS Gage 08136500)	1202.9	2,790	8,170	14,800	42,200	71,000	99,700	129,500	168,800	HEC-HMS Elliptical Storms

Location Description	Drainage Area* (sq mi)	50% AEP 2-yr	20% AEP 5-yr	10% AEP 10-yr	4% AEP 25-yr	2% AEP 50-yr	1% AEP 100-yr	0.5% AEP 200-yr	0.2% AEP 500-yr	Hydrologic Method
Concho River above the Colorado River	1393.8	3,830	8,760	15,300	43,700	72,700	101,600	130,200	171,500	HEC-HMS Elliptical Storms
Colorado River below the Concho River	3220.0	4,290	12,000	21,600	63,500	112,000	168,000	223,600	305,400	HEC-HMS Elliptical Storms
Inflow to OH Ivie Reservoir	3395.3	4,220	12,000	22,100	64,100	112,200	168,100	224,200	306,000	HEC-HMS Elliptical Storms
Colorado River below OH Ivie Reservoir	3395.3	1,500	1,500	1,500	32,700	80,300	125,900	154,700	188,300	HEC-HMS Elliptical Storms / Reservoir Analysis
Colorado River near Stacy, TX (USGS Gage 08136700)	3535.2	1,500	2,590	6,700	32,700	80,100	125,800	154,600	188,400	HEC-HMS Elliptical Storms / Reservoir Analysis
Colorado River below Panther Creek	3637.6	1,500	1,500	2,400	20,100	55,500	99,800	139,000	178,400	HEC-HMS Elliptical Storms / Reservoir Analysis
Colorado River below Salt Creek	3743.1	1,500	1,500	2,300	20,500	55,600	99,800	139,100	178,500	HEC-HMS Elliptical Storms / Reservoir Analysis
Colorado River above Bull Creek	3819.8	6,920	14,200	20,900	38,800	54,500	71,200	88,000	112,100	HEC-HMS Elliptical Storms
Colorado River below Bull Creek	3884.4	7,840	16,200	24,100	45,600	65,900	86,300	106,600	135,800	HEC-HMS Elliptical Storms
Colorado River below Elm Creek	3965.4	7,550	16,300	23,600	45,200	67,400	89,200	110,500	141,700	HEC-HMS Elliptical Storms
Colorado River above Home Creek	4104.2	7,850	17,500	24,500	45,600	70,600	95,600	120,200	157,100	HEC-HMS Elliptical Storms
Home Creek at US-283 Hwy	148.2	3,300	4,500	6,700	9,400	25,400	39,400	53,000	71,200	HEC-HMS Uniform Rain
Home Creek above Mukewater Creek	250.3	2,400	3,200	5,200	8,700	26,200	42,500	58,700	82,000	HEC-HMS Uniform Rain
Home Creek above the Colorado River	382.8	5,900	7,400	10,800	24,700	50,800	75,100	99,900	134,400	HEC-HMS Uniform Rain
Colorado River below Home Creek	4487.0	10,570	19,500	28,700	57,400	98,400	139,200	182,200	245,400	HEC-HMS Elliptical Storms
Colorado River at Winchell, TX (USGS Gage 08138000)	4535.4	9,410	18,600	27,300	56,600	98,100	140,000	183,200	249,600	HEC-HMS Elliptical Storms
Colorado River above Clear Creek	4635.4	8,770	17,500	25,100	48,700	78,700	120,600	166,400	234,700	HEC-HMS Elliptical Storms
Colorado River below Clear Creek	4758.9	12,400	20,800	26,400	50,500	79,000	122,000	169,400	242,900	HEC-HMS Elliptical Storms
Colorado River below Buffalo Creek	4940.0	15,380	22,400	24,800	48,700	74,600	107,400	156,300	218,500	HEC-HMS Elliptical Storms
Colorado River above Pecan Bayou	5045.9	14,560	22,500	25,700	47,100	68,100	97,700	138,500	198,200	HEC-HMS Elliptical Storms
Jim Ned Creek above South Fork Jim Ned Creek	150.7	2,500	9,800	14,400	21,900	30,200	39,700	48,700	61,000	HEC-HMS Uniform Rain
Inflow to Lake Coleman	302.3	1,700	7,200	12,500	25,700	42,100	63,300	84,200	112,000	HEC-HMS Uniform Rain
Jim Ned Creek below Lake Coleman	302.3	390	1,800	1,800	13,600	30,000	52,900	75,900	106,000	HEC-HMS Uniform Rain
Jim Ned Creek above Indian Creek	386.2	360	1,800	4,500	11,900	28,100	51,100	78,200	114,000	HEC-HMS Uniform Rain

Location Description	Drainage Area* (sq mi)	50% AEP 2-yr	20% AEP 5-yr	10% AEP 10-yr	4% AEP 25-yr	2% AEP 50-yr	1% AEP 100-yr	0.5% AEP 200-yr	0.2% AEP 500-yr	Hydrologic Method
Jim Ned Creek nr Coleman, TX (USGS Gage 08140860)	447.0	350	1,800	4,200	12,100	27,200	50,600	78,000	117,000	HEC-HMS Uniform Rain
Inflow to Hords Creek Reservoir	48.9	2,300	6,200	10,600	18,600	22,800	27,700	32,400	39,100	HEC-HMS Uniform Rain
Hords Creek below Hords Creek Reservoir	48.9	170	180	185	195	200	205	215	1,100	HEC-HMS Uniform Rain / Reservoir Analysis
Hords Creek near Coleman, TX (USGS Gage 08142000)	57.8	1,500	4,000	7,200	10,900	15,100	19,600	24,000	29,900	HEC-HMS Uniform Rain
Hords Creek above Jim Ned Creek	97.1	1,700	5,000	7,100	10,700	16,000	22,000	28,200	37,900	HEC-HMS Uniform Rain
Jim Ned Creek below Hords Creek	544.0	5,530	11,800	17,300	22,600	25,300	49,700	76,800	118,300	HEC-HMS Elliptical Storms
Jim Ned Creek at FM-585	632.9	8,030	16,700	24,400	30,900	33,100	52,500	73,200	102,200	HEC-HMS Elliptical Storms
Jim Ned Creek above Lake Brownwood	732.6	6,600	14,800	22,100	28,800	31,100	50,600	71,600	101,700	HEC-HMS Elliptical Storms
North Prong Pecan Bayou at SH-36	101.8	390	1,100	4,100	10,800	18,100	27,400	36,400	47,600	HEC-HMS Uniform Rain
Pecan Bayou below South Prong Pecan Bayou	189.6	2,300	3,300	5,900	17,700	30,800	48,400	65,200	86,200	HEC-HMS Uniform Rain
Pecan Bayou above Burnt Branch	309.4	7,200	12,600	16,600	22,700	35,100	55,300	76,700	109,000	HEC-HMS Uniform Rain
Pecan Bayou above Turkey Creek	451.4	5,100	11,400	16,500	25,700	40,200	61,000	86,900	123,000	HEC-HMS Uniform Rain
Pecan Bayou nr Cross Cut, TX (USGS Gage 08140700)	543.9	5,200	12,000	18,700	30,700	45,000	67,900	97,700	139,000	HEC-HMS Uniform Rain
Pecan Bayou below Red River	642.7	9,900	15,100	22,000	37,400	53,100	75,100	101,000	146,000	HEC-HMS Uniform Rain
Inflow to Lake Brownwood	1513.0	10,340	25,200	37,100	53,800	66,500	99,300	133,400	189,500	HEC-HMS Elliptical Storms
Pecan Bayou below Lake Brownwood	1513.0	4,240	9,870	14,900	20,500	25,000	39,100	54,300	82,500	HEC-HMS Elliptical Storms
Pecan Bayou at Brownwood, TX (USGS Gage 08143500)	1603.8	4,060	9,270	13,900	18,900	22,800	37,100	53,300	80,400	HEC-HMS Elliptical Storms
Pecan Bayou below Devils River	1753.0	7,200	12,400	17,900	26,500	35,200	46,700	58,100	72,800	HEC-HMS Elliptical Storms
Pecan Bayou above Blanket Creek	1826.2	5,490	10,500	15,200	22,100	28,800	37,000	44,900	55,400	HEC-HMS Elliptical Storms
Blanket Creek at US-183 Hwy	104.1	150	2,100	5,500	10,300	18,000	24,600	30,800	38,800	HEC-HMS Uniform Rain
Blanket Creek above Pecan Bayou	197.0	1,100	3,800	6,300	10,200	16,900	32,400	46,200	62,900	HEC-HMS Uniform Rain
Pecan Bayou nr Mullin, TX (USGS Gage 0813600)	2023.2	4,830	10,900	17,000	27,200	38,000	58,100	76,100	99,900	HEC-HMS Elliptical Storms
Pecan Bayou above Colorado River	2155.4	5,200	11,400	16,900	27,800	39,200	61,900	84,000	115,700	HEC-HMS Elliptical Storms
Colorado River below Pecan Bayou	7201.3	13,540	22,900	28,400	55,100	80,900	119,000	163,700	233,100	HEC-HMS Elliptical Storms
Colorado River near Goldthwaite, TX (LCRA Gage 1277)	7228.4	10,750	21,100	25,100	51,500	78,000	115,700	147,500	216,800	HEC-HMS Elliptical Storms

Location Description	Drainage Area* (sq mi)	50% AEP 2-yr	20% AEP 5-yr	10% AEP 10-yr	4% AEP 25-yr	2% AEP 50-yr	1% AEP 100-yr	0.5% AEP 200-yr	0.2% AEP 500-yr	Hydrologic Method
Colorado River above the San Saba River	7339.7	11,130	21,500	24,900	48,400	71,200	106,300	135,000	191,500	HEC-HMS Elliptical Storms
North Valley Prong below Poor Hollow	306.9	750	5,000	14,600	29,400	51,800	66,700	81,100	101,500	HEC-HMS Uniform Rain
San Saba Rv at FM 864 nr Fort McKavett, TX (USGS Gage)	622.8	800	5,500	29,300	40,300	84,300	111,900	136,500	173,300	HEC-HMS Elliptical Storms
San Saba River above Rocky Creek	721.4	990	5,920	29,300	41,100	86,900	114,800	141,600	183,600	HEC-HMS Elliptical Storms
San Saba River below Rocky Creek	831.2	1,530	6,820	29,300	43,000	91,600	122,600	151,400	197,600	HEC-HMS Elliptical Storms
San Saba River above Las Moras Creek	989.0	1,410	12,800	30,300	50,600	100,400	137,200	171,700	226,000	HEC-HMS Elliptical Storms
San Saba River at Menard, TX (USGS Gage 081445000)	1136.9	4,140	20,000	38,900	72,300	118,600	156,900	197,600	260,600	HEC-HMS Elliptical Storms
San Saba River above Elm Creek	1244.6	3,570	19,200	39,900	77,600	126,600	166,000	203,800	272,200	HEC-HMS Elliptical Storms
San Saba River below Elm Creek	1318.2	4,000	19,800	41,900	82,200	132,800	174,500	213,400	283,700	HEC-HMS Elliptical Storms
San Saba River above Calf Creek	1422.3	2,860	16,500	38,100	76,500	129,500	174,800	218,600	296,800	HEC-HMS Elliptical Storms
San Saba River below Calf Creek	1490.6	2,810	16,500	38,900	78,800	132,800	179,400	224,000	304,300	HEC-HMS Elliptical Storms
San Saba River below Rumsey Creek	1594.0	2,430	15,900	40,100	82,000	137,200	185,800	232,000	313,500	HEC-HMS Elliptical Storms
San Saba River nr Brady, TX (USGS Gage 08144600)	1636.4	3,630	17,700	38,300	78,700	129,000	175,600	218,200	290,500	HEC-HMS Elliptical Storms
Katemcy Creek below subbasin SS_KatemcyCr_S10	40.2	630	890	1,200	4,100	11,600	14,700	17,700	22,200	HEC-HMS Uniform Rain
San Saba River below Katemcy Creek	1688.6	2,370	15,900	39,800	81,700	137,800	188,200	236,300	321,200	HEC-HMS Elliptical Storms
San Saba River above Tiger Creek	1721.9	2,400	15,100	38,300	78,600	135,000	185,100	233,200	317,800	HEC-HMS Elliptical Storms
San Saba River below Tiger Creek	1804.6	2,170	15,700	39,500	80,800	139,100	191,200	240,800	328,400	HEC-HMS Elliptical Storms
San Saba River above Brady Creek	1941.6	2,030	15,300	39,700	80,800	142,100	197,200	249,900	342,400	HEC-HMS Elliptical Storms
Brady Creek at US-83 Hwy near Eden, TX	101.6	420	860	1,400	3,400	6,700	14,000	21,400	30,900	HEC-HMS Uniform Rain
Brady Creek near Melvin, TX	252.6	770	2,500	4,100	7,700	12,800	24,400	37,300	55,000	HEC-HMS Uniform Rain
Brady Creek below South Brady Creek	396.5	820	3,100	5,600	11,200	18,800	36,400	55,600	79,800	HEC-HMS Uniform Rain
Inflow to Brady Creek Reservoir	524.0	1,200	4,100	7,500	15,500	25,700	48,300	73,400	105,000	HEC-HMS Uniform Rain
Brady Creek below Brady Creek Reservoir	524.0	140	390	610	1,030	1,500	5,800	23,800	49,700	HEC-HMS Uniform Rain
Brady Creek At Brady, TX (USGS Gage 08145000)	130.3	390	1,800	3,900	10,600	18,900	26,900	35,000	54,700	HEC-HMS Uniform Rain
Brady Creek below Little Brady Creek	226.2	720	1,000	3,300	14,300	34,300	48,600	61,900	79,100	HEC-HMS Uniform Rain
Brady Creek above the San Saba River	279.3	1,000	1,200	2,900	14,300	45,100	61,700	78,000	100,000	HEC-HMS Uniform Rain

Location Description	Drainage Area* (sq mi)	50% AEP 2-yr	20% AEP 5-yr	10% AEP 10-yr	4% AEP 25-yr	2% AEP 50-yr	1% AEP 100-yr	0.5% AEP 200-yr	0.2% AEP 500-yr	Hydrologic Method
San Saba River below Brady Creek	2220.9	5,170	19,000	55,800	91,400	137,900	201,100	255,900	340,000	HEC-HMS Elliptical Storms
San Saba River above Wallace Creek	2324.2	6,410	21,800	54,400	94,100	142,000	207,900	268,800	361,900	HEC-HMS Elliptical Storms
San Saba River below Wallace Creek	2381.1	5,510	20,700	53,700	94,000	139,600	206,900	269,400	363,000	HEC-HMS Elliptical Storms
San Saba River below Richland Springs Creek	2486.6	6,520	23,400	54,400	97,300	143,400	214,200	281,600	383,800	HEC-HMS Elliptical Storms
San Saba Rv at San Saba, TX (USGS Gage 08146000)	2523.4	8,760	26,400	50,000	93,300	137,800	205,400	272,200	374,200	HEC-HMS Elliptical Storms
San Saba River above Colorado River	2626.2	3,190	13,600	37,200	78,800	137,100	208,700	279,200	390,700	HEC-HMS Elliptical Storms
Colorado River below San Saba River	9965.8	11,730	23,400	40,700	79,100	139,800	214,900	286,500	398,500	HEC-HMS Elliptical Storms
Colorado River at San Saba, TX (USGS Gage 08147000)	10002.8	11,980	25,600	43,400	87,000	144,200	223,600	299,100	413,400	HEC-HMS Elliptical Storms
Colorado River at Bend, TX (LCRA Gage 1925)	10139.1	5,070	14,700	33,900	62,700	115,500	183,600	239,100	329,600	HEC-HMS Elliptical Storms
Cherokee Creek above Buffalo Creek	69.7	2,200	7,500	12,700	23,500	36,700	45,200	54,100	67,100	HEC-HMS Uniform Rain
Cherokee Creek nr Bend, TX (LCRA Gage 1929)	158.8	1,600	6,800	14,300	33,700	62,000	80,200	97,800	125,000	HEC-HMS Uniform Rain
Cherokee Creek above the Colorado River	175.9	1,000	5,300	11,800	28,600	55,800	74,800	93,800	123,000	HEC-HMS Uniform Rain
Colorado River below Cherokee Creek	10321.4	7,990	18,700	36,500	63,500	112,900	179,600	236,000	326,700	HEC-HMS Elliptical Storms
Colorado River below Yancey Creek	10425.2	9,250	20,700	36,600	63,100	111,900	177,200	234,700	325,700	HEC-HMS Elliptical Storms
Colorado River above Fall Creek	10494.2	6,350	16,600	34,000	61,300	112,100	176,800	234,400	323,600	HEC-HMS Elliptical Storms
Colorado River below Fall Creek	10548.1	5,090	14,800	33,100	60,700	112,400	176,500	234,200	323,000	HEC-HMS Elliptical Storms
Inflow to Lake Buchanan	10694.7	11,700	26,200	37,600	62,800	110,000	163,200	221,800	307,400	HEC-HMS Elliptical Storms
Colorado River below Lake Buchanan	10694.7	8,880	19,500	31,100	59,200	108,700	152,000	217,600	307,000	HEC-HMS Elliptical Storms
Inflow to Inks Lake	10734.3	8,820	19,200	30,500	59,200	109,500	152,300	219,700	308,100	HEC-HMS Elliptical Storms
Colorado River below Inks Lake	10734.3	8,820	19,200	30,500	59,200	109,300	152,300	219,300	308,100	HEC-HMS Elliptical Storms
Colorado River above the Llano River	10769.8	8,350	18,700	30,700	58,200	108,200	152,000	218,100	307,300	HEC-HMS Elliptical Storms
South Llano River below subbasin LN_SLlano_S20	156.6	3,600	10,000	20,000	38,800	57,000	70,500	83,900	103,000	HEC-HMS Uniform Rain
South Llano River at CR-900	253.2	2,200	9,200	22,000	48,700	76,900	97,500	117,000	145,000	HEC-HMS Uniform Rain
South Llano River above Deer Creek	305.9	2,000	8,700	22,000	50,900	82,900	107,000	130,000	162,000	HEC-HMS Uniform Rain
South Llano River below Deer Creek	433.8	4,100	13,700	30,200	71,600	118,000	153,000	188,000	233,000	HEC-HMS Uniform Rain
South Llano River above Paint Creek	524.1	3,600	13,600	33,400	78,700	131,000	172,000	213,000	268,000	HEC-HMS Uniform Rain

Location Description	Drainage Area* (sq mi)	50% AEP 2-yr	20% AEP 5-yr	10% AEP 10-yr	4% AEP 25-yr	2% AEP 50-yr	1% AEP 100-yr	0.5% AEP 200-yr	0.2% AEP 500-yr	Hydrologic Method
Paint Creek below Hunger Creek	113.1	5,900	12,700	22,600	39,700	53,400	65,400	77,900	93,700	HEC-HMS Uniform Rain
Paint Creek above the South Llano River	217.7	4,700	14,400	30,700	60,000	84,100	105,000	125,000	152,000	HEC-HMS Uniform Rain
South Llano River at Telegraph (LCRA gage)	741.8	15,260	53,800	84,300	130,100	171,000	221,200	275,700	348,800	HEC-HMS Elliptical Storms
South Llano River below Chalk Creek	849.8	13,920	51,200	84,400	136,100	179,900	235,400	293,300	373,900	HEC-HMS Elliptical Storms
South Llano River at Junction, TX (USGS Gage 08149900)	878.9	12,990	49,300	82,300	134,400	178,800	233,800	292,600	374,000	HEC-HMS Elliptical Storms
South Llano River above the Llano River	932.6	13,270	49,700	81,700	135,900	180,000	236,000	295,100	379,800	HEC-HMS Elliptical Storms
North Llano River Headwaters	103.0	2,300	6,700	11,400	18,700	27,200	34,000	40,600	49,900	HEC-HMS Uniform Rain
Dry Llano River above the North Llano River	226.5	3,100	11,700	20,300	34,000	50,100	63,400	76,300	94,400	HEC-HMS Uniform Rain
North Llano River below Buffalo Draw	111.6	1,900	6,000	10,100	16,900	24,800	31,200	37,500	46,300	HEC-HMS Uniform Rain
North Llano River above Dry Llano River	166.1	1,900	7,200	13,000	22,900	34,300	43,400	52,700	65,700	HEC-HMS Uniform Rain
North Llano River below Dry Llano River	392.6	7,050	22,000	35,300	58,600	77,100	96,300	116,100	144,700	HEC-HMS Elliptical Storms
North Llano River above Maynard Creek	447.7	5,800	20,500	34,600	60,200	80,100	101,400	123,400	154,700	HEC-HMS Elliptical Storms
North Llano River below Maynard Creek	520.6	5,620	22,200	38,800	68,300	90,900	116,100	141,500	177,900	HEC-HMS Elliptical Storms
North Llano River below Copperas Creek	656.9	6,350	24,300	43,300	79,400	108,300	139,400	169,700	215,300	HEC-HMS Elliptical Storms
North Llano River near Roosevelt (LCRA Gage)	703.0	6,300	25,000	45,000	83,100	113,600	146,500	178,500	226,600	HEC-HMS Elliptical Storms
North Llano River above Bear Creek	763.9	6,190	25,800	45,700	84,300	116,100	150,600	184,000	236,600	HEC-HMS Elliptical Storms
Bear Creek below West Bear Creek	104.8	2,600	7,500	13,200	21,500	30,900	38,400	45,800	56,200	HEC-HMS Uniform Rain
Bear Creek above the North Llano River	131.7	2,800	8,600	15,700	26,000	37,600	47,100	56,300	69,500	HEC-HMS Uniform Rain
North Llano River below Bear Creek	895.6	6,190	27,600	50,200	92,200	127,300	165,300	203,200	263,100	HEC-HMS Elliptical Storms
North Llano River nr Junction, TX (USGS Gage 08148500)	901.7	6,340	27,700	50,000	91,800	126,800	164,400	201,800	261,400	HEC-HMS Elliptical Storms
North Llano River above the South Llano River	919.1	6,320	27,700	50,500	92,100	127,600	165,900	204,100	264,800	HEC-HMS Elliptical Storms
Llano River below the North and South Llano Rivers	1851.7	11,470	52,500	96,200	174,100	236,800	315,500	391,000	512,500	HEC-HMS Elliptical Storms
Llano River nr Junction, TX (USGS Gage 08150000)	1858.2	10,640	51,000	94,500	172,300	235,700	313,100	389,700	511,700	HEC-HMS Elliptical Storms
Llano River above Johnson Fork	1869.2	10,610	50,300	93,300	168,300	233,100	311,200	387,500	509,300	HEC-HMS Elliptical Storms
Johnson Fork above Allen Creek	126.3	2,500	6,600	15,800	37,000	57,600	70,700	84,500	102,100	HEC-HMS Uniform Rain

Location Description	Drainage Area* (sq mi)	50% AEP 2-yr	20% AEP 5-yr	10% AEP 10-yr	4% AEP 25-yr	2% AEP 50-yr	1% AEP 100-yr	0.5% AEP 200-yr	0.2% AEP 500-yr	Hydrologic Method
Johnson Fort below Mudge Draw	234.0	1,500	8,700	25,900	63,700	100,000	124,000	149,000	180,000	HEC-HMS Uniform Rain
Johnson Fork near Junction, TX (LCRA Gage 2313)	292.8	900	7,200	26,000	71,000	116,000	147,000	176,000	214,000	HEC-HMS Uniform Rain
Johnson Fork above the Llano River	322.1	2,100	6,200	24,300	70,700	118,000	150,000	182,000	223,000	HEC-HMS Uniform Rain
Llano River below Johnson Fork	2191.3	10,920	52,600	100,400	180,700	262,000	346,600	440,300	584,200	HEC-HMS Elliptical Storms
Llano River below Gentry Creek	2247.6	12,690	50,100	91,300	169,800	248,600	338,800	432,400	578,400	HEC-HMS Elliptical Storms
Llano River above Big Saline Creek	2392.9	8,790	51,200	97,100	175,700	247,300	332,700	423,100	565,200	HEC-HMS Elliptical Storms
Llano River below Big Saline Creek	2478.2	9,050	51,000	97,000	175,400	248,300	333,000	423,900	566,600	HEC-HMS Elliptical Storms
Llano River below Leon Creek	2609.2	8,460	50,900	97,000	175,500	246,900	332,200	422,400	564,400	HEC-HMS Elliptical Storms
Llano River above the James River	2760.3	8,010	49,300	97,000	175,100	244,600	330,100	418,800	559,500	HEC-HMS Elliptical Storms
James River below Little Devils River	244.5	3,000	11,700	30,400	88,000	114,000	140,000	165,000	202,000	HEC-HMS Uniform Rain
James River near Mason (LCRA Gage 2399)	326.3	2,600	12,600	35,600	112,000	148,000	182,000	215,000	263,000	HEC-HMS Uniform Rain
James River above Llano River	339.6	2,200	12,300	35,700	113,000	149,000	184,000	218,000	267,000	HEC-HMS Uniform Rain
Llano River below the James River	3100.0	19,570	70,600	126,600	222,600	283,100	359,000	430,400	534,500	HEC-HMS Elliptical Storms
Llano River above Comanche Creek	3175.6	13,140	58,400	111,800	207,800	267,400	345,900	420,000	529,100	HEC-HMS Elliptical Storms
Comanche Creek near Mason (LCRA Gage 2424)	46.3	400	2,000	5,800	12,900	23,300	28,500	33,900	41,600	HEC-HMS Uniform Rain
Comanche Creek above the Llano River	68.7	4,700	9,600	12,900	16,900	24,500	31,300	38,300	48,200	HEC-HMS Uniform Rain
Llano River below Comanche Creek	3244.3	17,130	66,400	122,100	217,600	283,600	364,900	441,100	554,400	HEC-HMS Elliptical Storms
Llano Rv nr Mason, TX (USGS Gage 08150700)	3250.8	17,760	62,700	114,800	209,800	277,200	359,200	435,500	547,500	HEC-HMS Elliptical Storms
Beaver Creek below Squaw Creek	166.3	5,000	13,300	27,000	50,300	72,900	90,700	109,000	135,000	HEC-HMS Uniform Rain
Beaver Ck nr Mason, TX (USGS Gage 08150800)	215.3	4,700	14,500	30,700	58,700	87,100	109,000	132,000	165,000	HEC-HMS Uniform Rain
Llano River below Beaver Creek	3470.0	17,500	73,000	133,800	246,700	327,400	428,800	524,800	663,500	HEC-HMS Elliptical Storms
Willow Creek near Mason (LCRA Gage 2443)	57.9	290	1,900	5,600	15,500	27,800	34,100	40,700	50,400	HEC-HMS Uniform Rain
Willow Creek above the Llano River	78.2	2,100	7,500	10,400	13,800	27,800	35,800	43,900	55,800	HEC-HMS Uniform Rain
Llano River below Willow Creek	3556.9	17,540	77,000	139,200	250,700	333,500	437,900	536,000	680,300	HEC-HMS Elliptical Storms
Llano River at RM-2768 at Castell, TX	3639.4	16,240	72,700	132,400	242,900	326,000	428,500	529,400	678,000	HEC-HMS Elliptical Storms
Llano River above Hickory Creek	3723.8	15,950	72,400	131,100	232,600	311,500	412,400	512,500	664,400	HEC-HMS Elliptical Storms

Location Description	Drainage Area* (sq mi)	50% AEP 2-yr	20% AEP 5-yr	10% AEP 10-yr	4% AEP 25-yr	2% AEP 50-yr	1% AEP 100-yr	0.5% AEP 200-yr	0.2% AEP 500-yr	Hydrologic Method
Hickory Creek below Marshall Creek	98.4	3,500	6,800	12,500	25,700	42,300	53,300	64,800	81,800	HEC-HMS Uniform Rain
Hickory Creek near Castell (LCRA Gage)	168.0	2,300	6,000	13,400	33,300	60,300	78,000	96,600	123,000	HEC-HMS Uniform Rain
Llano River below Hickory Creek	3891.8	17,520	78,200	139,100	243,800	327,300	435,600	542,500	705,700	HEC-HMS Elliptical Storms
Llano River above San Fernando Creek	3924.8	18,270	77,100	137,300	242,200	325,300	432,800	540,300	703,100	HEC-HMS Elliptical Storms
San Fernando Creek near Llano (LCRA Gage 2616)	128.9	1,400	7,900	19,300	38,300	56,500	70,700	85,400	107,000	HEC-HMS Uniform Rain
San Fernando Creek above the Llano River	135.5	1,000	7,400	18,600	37,300	56,000	70,500	85,600	107,000	HEC-HMS Uniform Rain
Llano River below San Fernando Creek	4060.3	18,820	71,600	129,800	235,700	319,300	429,300	540,700	712,800	HEC-HMS Elliptical Storms
Johnson Creek near Llano (LCRA Gage)	46.6	210	2,400	5,900	19,100	32,600	39,500	46,700	57,200	HEC-HMS Uniform Rain
Johnson Creek above the Llano River	52.8	560	2,400	6,100	18,300	34,400	42,400	50,300	62,000	HEC-HMS Uniform Rain
Llano River below Johnson Creek	4118.4	18,720	72,700	130,700	236,400	320,600	430,200	542,200	714,000	HEC-HMS Elliptical Storms
Llano River below Pecan Creek	4187.0	22,250	75,500	132,200	238,300	323,000	433,800	545,600	716,200	HEC-HMS Elliptical Storms
Llano River at Llano, TX (USGS Gage 08151500)	4202.0	20,110	71,700	127,100	233,300	317,200	428,100	541,400	716,900	HEC-HMS Elliptical Storms
Llano River above the Little Llano River	4279.1	17,240	73,100	130,100	235,000	317,400	425,400	534,900	705,100	HEC-HMS Elliptical Storms
Little Llano River near Llano (LCRA gage 2669)	48.2	310	2,900	8,100	22,500	39,100	47,000	55,300	67,500	HEC-HMS Uniform Rain
Little Llano River above the Llano River	52.6	140	2,400	7,200	21,400	38,400	46,800	55,500	68,100	HEC-HMS Uniform Rain
Llano River below the Little Llano River	4331.6	15,910	72,500	129,700	233,900	316,000	423,000	532,500	702,100	HEC-HMS Elliptical Storms
Llano River above Honey Creek	4410.8	14,250	62,900	110,800	203,500	290,000	395,300	503,200	670,200	HEC-HMS Elliptical Storms
Honey Creek near Kingsland (LCRA Gage 2694)	25.9	3,200	10,100	12,900	15,000	24,000	28,900	34,100	41,800	HEC-HMS Uniform Rain
Honey Creek above the Llano River	39.7	2,800	9,800	13,400	16,500	28,000	34,900	42,000	52,900	HEC-HMS Uniform Rain
Llano River below Honey Creek	4450.5	13,010	60,400	107,500	199,600	286,400	390,000	495,600	655,900	HEC-HMS Elliptical Storms
Llano River above the Colorado River	4465.4	13,650	61,100	106,700	197,400	284,400	388,000	495,200	662,200	HEC-HMS Elliptical Storms
Colorado River below the Llano River	15235.2	20,370	69,400	115,600	212,100	284,800	411,500	544,900	765,900	HEC-HMS Elliptical Storms
Colorado River above Sandy Creek	15262.7	20,070	68,600	115,300	211,500	284,200	412,000	553,800	770,800	HEC-HMS Elliptical Storms
Sandy Creek below Crabapple Creek	148.4	2,300	7,100	16,400	39,600	63,900	80,400	97,900	124,000	HEC-HMS Uniform Rain
Sandy Creek near Willow City (LCRA Gage 2851)	151.6	2,300	7,000	16,400	39,600	64,100	80,800	98,400	124,000	HEC-HMS Uniform Rain
Sandy Creek near Click (LCRA Gage 2878)	300.0	5,700	19,400	37,900	69,700	100,000	128,000	158,000	201,000	HEC-HMS Uniform Rain

Location Description	Drainage Area* (sq mi)	50% AEP 2-yr	20% AEP 5-yr	10% AEP 10-yr	4% AEP 25-yr	2% AEP 50-yr	1% AEP 100-yr	0.5% AEP 200-yr	0.2% AEP 500-yr	Hydrologic Method
Sandy Ck nr Kingsland, TX (USGS Gage 08152000)	346.2	8,200	21,100	42,400	79,300	116,000	148,000	183,000	234,000	HEC-HMS Uniform Rain
Walnut Creek near Kingsland (LCRA Gage 2897)	23.3	9,000	17,200	23,300	30,100	35,500	41,600	48,400	58,300	HEC-HMS Uniform Rain
Walnut Creek above Sandy Creek	27.4	9,800	19,500	26,800	34,700	40,700	47,800	55,600	67,300	HEC-HMS Uniform Rain
Sandy Creek below Walnut Creek	388.0	11,800	25,700	42,700	79,900	118,100	153,300	189,800	244,500	HEC-HMS Uniform Rain
Sandy Creek above the Colorado River	391.2	10,800	25,600	42,600	79,900	118,200	153,500	190,100	245,000	HEC-HMS Uniform Rain
Colorado River below Sandy Creek	15653.9	20,440	71,300	119,400	221,900	301,200	435,200	572,600	812,400	HEC-HMS Elliptical Storms
Inflow to Lake LBJ	15701.7	19,510	70,200	117,700	218,900	298,400	431,000	566,100	804,000	HEC-HMS Elliptical Storms
Colorado River below Lake LBJ	15701.7	18,270	63,400	106,600	205,300	299,300	368,800	436,100	649,700	HEC-HMS Elliptical Storms
Backbone Creek at Marble Falls (LCRA Gage 2992)	30.1	1,100	5,200	11,100	19,400	23,700	29,100	35,300	44,000	HEC-HMS Uniform Rain
Backbone Creek above the Colorado River	40.3	2,000	6,100	10,700	19,900	24,800	31,100	38,400	49,200	HEC-HMS Uniform Rain
Colorado River below Backbone Creek	15757.8	19,970	69,300	114,500	214,700	295,900	370,500	473,300	736,800	HEC-HMS Elliptical Storms
Inflow to Lake Marble Falls	15783.9	22,470	70,700	110,100	205,800	299,900	369,400	468,600	725,500	HEC-HMS Elliptical Storms
Colorado River below Lake Marble Falls	15783.9	22,470	70,700	110,100	205,900	289,400	369,400	468,600	725,500	HEC-HMS Elliptical Storms
Hamilton Creek near Marble Falls (LCRA Gage 3018)	77.5	3,100	9,500	17,400	30,200	44,000	54,800	66,300	83,500	HEC-HMS Uniform Rain
Hamilton Creek above the Colorado River	84.3	3,300	10,100	18,300	32,000	46,700	58,300	70,800	89,400	HEC-HMS Uniform Rain
Colorado River below Hamilton Creek	15874.3	22,070	71,100	113,400	212,500	296,100	371,600	484,700	747,900	HEC-HMS Elliptical Storms
Colorado River below Double Horn Creek	15929.1	22,540	69,700	109,100	206,300	289,800	370,900	480,200	738,000	HEC-HMS Elliptical Storms
Colorado River above the Pedernales River	16007.6	15,530	47,000	73,400	169,700	265,600	377,800	460,600	615,300	HEC-HMS Elliptical Storms
Pedernales River below North Creek	118.2	6,400	14,700	26,300	47,500	65,300	80,100	95,800	117,000	HEC-HMS Uniform Rain
Pedernales River below Spring Creek	212.4	5,200	17,000	34,500	67,800	98,100	124,000	150,000	185,000	HEC-HMS Uniform Rain
Pedernales River above Wolf Creek	218.1	4,900	16,600	34,000	67,100	97,300	123,000	149,000	185,000	HEC-HMS Uniform Rain
Pedernales River below Wolf Creek	257.0	4,800	16,700	35,100	71,000	105,000	135,000	165,000	206,000	HEC-HMS Uniform Rain
Pedernales River above Live Oak Creek	313.0	4,500	16,300	35,500	73,900	113,000	148,000	183,000	233,000	HEC-HMS Uniform Rain
Pedernales River below Live Oak Creek	359.3	5,200	19,300	44,100	87,200	129,000	168,000	210,000	267,000	HEC-HMS Uniform Rain
Pedernales Rv nr Fredericksburg (USGS Gage 08152900)	369.6	5,100	19,300	44,800	89,000	131,000	171,000	215,000	274,000	HEC-HMS Uniform Rain
Pedernales River above South Grape Creek	507.6	7,230	29,500	48,600	79,400	133,200	181,300	231,500	316,600	HEC-HMS Elliptical Storms

Location Description	Drainage Area* (sq mi)	50% AEP 2-yr	20% AEP 5-yr	10% AEP 10-yr	4% AEP 25-yr	2% AEP 50-yr	1% AEP 100-yr	0.5% AEP 200-yr	0.2% AEP 500-yr	Hydrologic Method
South Grape Creek near Luckenbach (LCRA Gage 3328)	27.3	4,000	10,900	17,700	25,400	30,000	35,700	41,700	50,600	HEC-HMS Uniform Rain
South Grape Creek above the Pedernales River	63.0	2,700	8,100	14,000	21,800	26,300	32,100	38,200	47,000	HEC-HMS Uniform Rain
Pedernales River below South Grape Creek	570.6	8,720	30,900	52,600	82,700	138,000	191,700	249,800	346,600	HEC-HMS Elliptical Storms
Pedernales River at LBJ Ranch near Stonewall (LCRA Gage)	625.6	7,250	26,700	47,300	79,700	132,400	185,300	245,700	340,300	HEC-HMS Elliptical Storms
Pedernales River below Williams Creek	668.2	11,490	34,100	57,300	93,600	140,400	197,600	265,200	369,400	HEC-HMS Elliptical Storms
Pedernales River above North Grape Creek	730.0	11,100	33,600	58,100	95,000	139,800	196,600	265,500	371,700	HEC-HMS Elliptical Storms
North Grape Creek near Johnson City (LCRA Gage 3369)	89.0	3,200	12,800	24,500	47,200	72,500	87,700	103,700	128,000	HEC-HMS Uniform Rain
Pedernales River below North Grape Creek	845.3	17,280	44,400	76,000	121,800	160,800	211,500	264,700	349,300	HEC-HMS Elliptical Storms
Pedernales Rv nr Johnson City, TX (USGS Gage 08153500)	900.9	19,480	52,900	87,500	140,000	180,200	231,700	288,800	374,300	HEC-HMS Elliptical Storms
Pedernales River above Miller Creek	959.5	15,530	41,900	75,000	127,000	168,800	226,200	288,800	379,300	HEC-HMS Elliptical Storms
Miller Creek near Johnson City (LCRA Gage 3491)	87.5	14,100	30,200	47,200	64,500	79,300	96,800	116,000	143,000	HEC-HMS Uniform Rain
Pedernales River below Miller Creek	1048.0	15,910	44,800	81,500	140,800	188,900	253,900	327,900	431,000	HEC-HMS Elliptical Storms
Pedernales River above Flat Creek	1080.1	14,490	41,800	77,600	136,800	185,500	252,300	326,900	432,700	HEC-HMS Elliptical Storms
Flat Creek nr Pedernales Falls State Park (LCRA Gage 3529)	30.7	8,100	16,400	23,800	31,300	38,000	45,700	54,500	67,200	HEC-HMS Uniform Rain
Flat Creek above Pedernales River	37.1	8,700	18,300	27,100	35,900	43,700	52,700	63,100	78,100	HEC-HMS Uniform Rain
Pedernales River below Flat Creek	1117.2	15,190	51,300	81,300	133,500	185,800	254,800	327,100	433,200	HEC-HMS Elliptical Storms
Pedernales River above Cypress Creek	1150.6	13,420	48,400	79,800	132,900	185,100	255,400	330,100	437,000	HEC-HMS Elliptical Storms
Cypress Creek near Cypress Mill (LCRA Gage 3558)	71.2	4,300	14,500	26,400	45,100	65,900	80,200	94,000	116,000	HEC-HMS Uniform Rain
Pedernales River below Cypress Creek	1232.3	13,810	53,700	90,500	145,800	198,400	271,700	353,400	471,900	HEC-HMS Elliptical Storms
Pedernales River above the Colorado River	1280.9	9,550	42,300	76,900	137,000	192,700	269,900	351,700	471,000	HEC-HMS Elliptical Storms
Colorado River below the Pedernales River	17288.5	13,950	54,100	106,600	217,100	356,100	521,300	678,900	850,000	HEC-HMS Elliptical Storms
Cow Creek near Lago Vista (LCRA Gage 3920)	42.7	2,400	5,200	8,400	12,600	16,100	20,900	25,300	32,100	HEC-HMS Uniform Rain
Cow Creek above the Colorado River	56.5	2,200	5,100	8,500	13,000	17,000	22,900	28,000	35,900	HEC-HMS Uniform Rain
Colorado River below Cow Creek	17353.4	13,880	54,400	108,800	220,900	361,300	530,200	685,200	862,700	HEC-HMS Elliptical Storms
Big Sandy 2 Creek near Jonestown (LCRA Gage 3953)	34.1	6,400	13,400	20,000	27,500	33,700	41,300	48,800	59,900	HEC-HMS Uniform Rain

Location Description	Drainage Area* (sq mi)	50% AEP 2-yr	20% AEP 5-yr	10% AEP 10-yr	4% AEP 25-yr	2% AEP 50-yr	1% AEP 100-yr	0.5% AEP 200-yr	0.2% AEP 500-yr	Hydrologic Method
Big Sandy 2 Creek above the Colorado River	73.5	8,900	17,500	25,300	34,500	42,100	51,400	66,600	89,600	HEC-HMS Uniform Rain
Colorado River below Big Sandy Creek 2	17505.5	14,000	54,900	108,200	228,900	375,200	556,500	729,700	908,500	HEC-HMS Elliptical Storms
Inflow to Lake Travis / Marshall Ford	17530.7	14,160	55,500	107,700	230,000	376,500	558,900	735,100	914,100	HEC-HMS Elliptical Storms
Colorado River below Marshall Ford Dam	17530.7	5,000	30,000	30,000	30,000	72,620	90,000	161,970	261,100	Reservoir Analysis
Colorado River above Bull Creek	43.7	5,000	30,000	30,000	30,000	72,620	90,000	161,970	261,100	Reservoir Analysis
Bull Ck at Loop 360 nr Austin, TX (USGS Gage 08154700)	22.7	2,800	6,400	10,900	17,500	24,700	29,900	35,600	44,000	HEC-HMS Uniform Rain
Colorado River below Bull Creek	77.0	11,900	30,000	31,300	45,400	72,620	90,000	161,970	261,100	HEC-HMS Uniform Rain / Reservoir Analysis
Inflow to Lake Austin	91.1	11,400	30,000	34,000	50,000	72,620	90,000	161,970	261,100	HEC-HMS Uniform Rain / Reservoir Analysis
Colorado River below Lake Austin	91.1	11,400	30,000	34,000	50,000	72,620	90,000	161,970	261,100	HEC-HMS Uniform Rain / Reservoir Analysis
Colorado River above Barton Creek	99.7	10,300	30,000	34,600	52,000	72,620	90,000	161,970	261,100	HEC-HMS Uniform Rain / Reservoir Analysis
Barton Ck at SH 71 nr Oak Hill, TX (USGS Gage 08155200)	89.6	2,800	10,200	17,000	28,100	41,300	53,700	67,500	87,000	HEC-HMS Uniform Rain
Barton Ck at Lost Ck Blvd nr Austin (USGS Gage 08155240)	107.9	2,600	9,700	16,700	28,100	42,100	56,100	71,000	92,900	HEC-HMS Uniform Rain
Barton Ck at Loop 360, Austin (USGS Gage 08155300)	116.9	3,000	9,600	16,600	28,000	41,900	56,100	71,200	93,600	HEC-HMS Uniform Rain
Barton Ck abv Barton Spgs at Austin (USGS Gage 08155400)	120.0	3,100	9,500	16,500	28,000	41,900	56,000	71,200	93,800	HEC-HMS Uniform Rain
Colorado River below Barton Creek	219.7	12,000	30,000	39,400	61,100	83,100	106,000	161,970	261,100	HEC-HMS Uniform Rain / Reservoir Analysis
Inflow to Lady Bird Lake	248.3	12,200	30,000	42,600	69,100	93,700	121,000	161,970	261,100	HEC-HMS Uniform Rain / Reservoir Analysis
Colorado River below Lady Bird Lake	248.3	12,200	30,000	42,600	69,100	93,700	121,000	161,970	261,100	HEC-HMS Uniform Rain / Reservoir Analysis
Colorado River at Austin, TX (USGS Gage 08158000)	250.2	11,600	30,000	41,100	65,700	88,900	115,000	161,970	261,100	HEC-HMS Uniform Rain / Reservoir Analysis
Colorado River above Walnut Creek	270.7	11,300	30,000	38,000	62,700	85,300	113,000	161,970	261,100	HEC-HMS Uniform Rain / Reservoir Analysis

Location Description	Drainage Area* (sq mi)	50% AEP 2-yr	20% AEP 5-yr	10% AEP 10-yr	4% AEP 25-yr	2% AEP 50-yr	1% AEP 100-yr	0.5% AEP 200-yr	0.2% AEP 500-yr	Hydrologic Method
Walnut Ck at Webberville Rd, Austin (USGS Gage 08158600)	51.7	5,300	8,800	13,400	20,400	28,600	35,400	42,800	53,600	HEC-HMS Uniform Rain
Walnut 1 Creek above the Colorado River	56.5	5,600	9,000	13,700	21,000	29,500	36,500	44,500	56,700	HEC-HMS Uniform Rain
Colorado River below Walnut 1 Creek	327.2	13,800	30,000	45,900	75,400	104,000	138,000	180,000	261,100	HEC-HMS Uniform Rain / Reservoir Analysis
Colorado River at Del Valle, TX (LCRA Gage)	341.2	14,000	30,000	45,500	73,900	102,000	134,000	174,000	261,100	HEC-HMS Uniform Rain / Reservoir Analysis
Colorado River above Onion Creek	347.8	13,400	30,000	42,000	71,000	98,600	131,000	169,000	261,100	HEC-HMS Uniform Rain / Reservoir Analysis
Onion Creek at RR-1826	104.6	4,800	10,400	19,800	36,900	58,700	75,100	92,600	119,000	HEC-HMS Uniform Rain
Onion Ck nr Driftwood, TX (USGS Gage 08158700)	123.7	3,700	8,900	18,300	35,800	59,800	78,300	98,100	128,000	HEC-HMS Uniform Rain
Onion Creek at Buda (LCRA Gage)	167.3	3,700	11,600	26,100	50,300	74,200	97,800	123,000	156,000	HEC-HMS Uniform Rain
Onion Ck at I-35 nr Twin Creeks Rd (USGS Gage 08158827)	234.0	5,000	17,100	34,200	65,800	99,900	121,000	153,000	194,000	HEC-HMS Uniform Rain
Onion Ck at US Hwy 183, Austin, TX (USGS Gage 08159000)	323.7	6,900	23,600	41,800	78,000	116,000	146,000	180,000	228,000	HEC-HMS Uniform Rain
Onion Creek above the Colorado River	345.0	7,700	24,500	42,500	78,400	118,000	150,000	185,000	234,000	HEC-HMS Uniform Rain
Colorado River below Onion Creek	692.9	17,600	46,700	79,100	137,600	182,000	241,100	305,800	406,200	HEC-HMS Elliptical Storms
Colorado River above Gilleland Creek	699.2	17,180	45,200	75,700	131,800	175,900	237,200	301,700	398,900	HEC-HMS Elliptical Storms
Gilleland Creek near Manor (LCRA Gage 5417)	41.4	2,100	3,900	6,400	10,100	14,900	18,800	22,700	28,800	HEC-HMS Uniform Rain
Gilleland Creek above the Colorado River	75.3	3,200	4,400	9,200	15,600	22,900	29,500	36,400	47,300	HEC-HMS Uniform Rain
Colorado River near Webberville (LCRA Gage)	774.5	19,670	48,500	79,900	137,900	183,200	249,300	316,400	417,600	HEC-HMS Elliptical Storms
Colorado River below Dry Creek	855.1	17,950	45,600	69,400	107,100	137,000	183,400	245,100	341,700	HEC-HMS Elliptical Storms
Wilbarger Creek near Elgin (LCRA Gage)	163.7	6,400	14,800	21,100	29,200	37,300	48,200	59,800	76,900	HEC-HMS Uniform Rain
Wilbarger Creek above the Colorado River	181.1	6,600	14,600	20,900	29,300	37,300	48,400	60,600	78,600	HEC-HMS Uniform Rain
Colorado River below Wilbarger Creek	1058.9	19,400	42,600	64,400	97,600	122,900	162,300	206,700	280,100	HEC-HMS Elliptical Storms
Big Sandy 1 Creek near Elgin (LCRA Gage 5473)	62.6	5,600	5,700	9,500	14,000	17,500	22,400	27,600	35,500	HEC-HMS Uniform Rain
Big Sandy 1 Creek above the Colorado River	109.6	6,500	6,600	12,200	18,800	24,100	31,600	40,300	53,100	HEC-HMS Uniform Rain
Colorado River at Sim Gideon River Plant (LCRA Gage)	1171.4	19,530	42,900	64,600	97,800	122,800	162,300	206,100	278,200	HEC-HMS Elliptical Storms

Location Description	Drainage Area* (sq mi)	50% AEP 2-yr	20% AEP 5-yr	10% AEP 10-yr	4% AEP 25-yr	2% AEP 50-yr	1% AEP 100-yr	0.5% AEP 200-yr	0.2% AEP 500-yr	Hydrologic Method
Colorado River at Bastrop, TX (USGS Gage 08159200)	1223.8	19,790	42,700	64,200	96,900	121,000	159,600	202,400	267,200	HEC-HMS Elliptical Storms
Cedar Creek below Maha Creek	95.5	600	9,800	15,600	23,300	29,400	37,500	46,300	58,300	HEC-HMS Uniform Rain
Cedar Creek near Bastrop (LCRA Gage 5521)	130.4	500	9,100	16,800	27,600	36,500	47,400	58,600	75,900	HEC-HMS Uniform Rain
Cedar Creek above Walnut Creek	142.5	500	7,500	14,600	24,600	33,300	45,600	58,400	76,100	HEC-HMS Uniform Rain
Cedar Creek below Walnut Creek	280.1	800	12,700	25,200	43,100	57,900	79,000	100,000	130,000	HEC-HMS Uniform Rain
Cedar Creek below Bastrop (LCRA Gage)	345.4	1,000	13,800	27,900	48,800	66,000	91,300	117,000	153,000	HEC-HMS Uniform Rain
Cedar Creek above the Colorado River	350.5	1,100	13,800	27,700	48,600	65,700	91,000	116,000	153,000	HEC-HMS Uniform Rain
Colorado River near Upton (LCRA Gage)	1602.9	23,350	46,800	68,600	100,400	124,600	164,100	209,000	268,300	HEC-HMS Elliptical Storms
Colorado Rv at Smithville, TX (USGS Gage 08159500)	1705.8	21,720	41,800	62,000	90,400	114,400	149,500	190,900	245,500	HEC-HMS Elliptical Storms
Colorado River below Bartons Creek	1789.8	22,060	43,900	64,300	93,500	117,400	154,600	197,200	257,600	HEC-HMS Elliptical Storms
Colorado River below Pin Oak Creek	1925.4	24,270	46,600	66,300	94,900	118,500	156,000	199,000	261,600	HEC-HMS Elliptical Storms
Colorado River below Rabbs Creek	2089.1	24,550	45,200	62,600	87,500	110,700	146,400	186,700	250,100	HEC-HMS Elliptical Storms
Colorado Rv abv La Grange, TX (USGS Gage 08160400)	2117.3	25,340	46,000	62,800	87,000	108,500	143,200	182,600	244,000	HEC-HMS Elliptical Storms
Buckners Creek near Muldoon (LCRA Gage 5608)	91.6	3,000	9,200	15,900	23,100	28,900	36,900	44,900	57,000	HEC-HMS Uniform Rain
Buckners Creek above the Colorado River	185.7	4,800	10,600	16,100	22,500	28,600	38,200	49,400	65,100	HEC-HMS Uniform Rain
Colorado River below Buckners Creek	2305.9	25,480	47,000	64,000	88,600	110,500	146,200	186,300	248,800	HEC-HMS Elliptical Storms
Colorado River below Williams Creek	2409.2	27,290	48,900	65,600	89,400	111,000	146,300	186,100	248,500	HEC-HMS Elliptical Storms
Colorado River below Bruch Creek	2491.3	26,350	47,600	62,500	84,200	105,800	140,400	179,000	241,300	HEC-HMS Elliptical Storms
Colorado River above Cummins Creek	2569.8	26,920	48,700	63,400	84,400	106,600	141,800	180,300	242,900	HEC-HMS Elliptical Storms
Cummings Creek at SH-237	80.8	3,300	9,800	14,600	20,500	26,600	34,600	42,600	53,900	HEC-HMS Uniform Rain
Cummings Creek at SH-159	176.7	6,900	13,100	19,400	29,400	41,200	57,000	73,500	96,800	HEC-HMS Uniform Rain
Cummings Creek near Frelsburg (LCRA Gage 5696)	251.9	8,200	18,900	27,800	42,000	56,700	78,300	100,800	132,100	HEC-HMS Uniform Rain
Cummins Creek above the Colorado River	315.3	6,000	19,000	31,500	49,600	67,700	92,700	119,300	155,200	HEC-HMS Uniform Rain
Colorado River at Columbus, TX (USGS Gage 08161000)	2885.1	28,700	51,000	65,700	86,400	108,400	144,800	183,800	246,200	HEC-HMS Elliptical Storms
Colorado River near Altair (LCRA Gage 6377)	2979.6	28,840	49,300	61,500	78,300	93,100	116,900	139,100	181,100	HEC-HMS Elliptical Storms

Location Description	Drainage Area* (sq mi)	50% AEP 2-yr	20% AEP 5-yr	10% AEP 10-yr	4% AEP 25-yr	2% AEP 50-yr	1% AEP 100-yr	0.5% AEP 200-yr	0.2% AEP 500-yr	Hydrologic Method
Colorado River near Garwood (LCRA Gage)	3090.4	29,040	49,900	62,100	79,000	93,700	116,200	140,300	181,400	HEC-HMS Elliptical Storms
Colorado River below Marys Branch	3153.1	29,400	49,700	61,500	78,600	93,400	116,100	140,300	181,600	HEC-HMS Elliptical Storms
Colorado River below Robb Slough	3216.2	28,690	48,700	59,100	75,800	91,400	114,500	138,900	177,100	HEC-HMS Elliptical Storms
Colorado Rv at Wharton, TX (USGS Gage 08162000)	3248.3	27,530	48,700	58,600	71,100	81,000	101,600	124,800	160,000	HEC-HMS Elliptical Storms
Colorado River near Lane City, TX (LCRA Gage 6537)	3277.9	27,670	49,000	58,800	70,900	80,200	98,900	124,400	157,700	HEC-HMS Elliptical Storms
Jones Creek at US-59 Hwy at Pierce, TX	29.3	1,200	2,800	4,400	6,200	7,700	9,700	11,700	14,500	HEC-HMS Uniform Rain
Jones Creek below East Fork Jones Creek	62.6	1,700	4,500	7,400	11,500	15,100	19,400	23,600	29,400	HEC-HMS Uniform Rain
Jones Creek above the Colorado River	83.1	2,600	5,900	9,100	14,300	19,200	25,200	30,700	38,400	HEC-HMS Uniform Rain
Colorado River below Jones Creek	3396.5	27,900	49,400	59,200	71,000	79,800	97,300	121,500	157,300	HEC-HMS Elliptical Storms
Blue Creek below East Fork Blue Creek	50.6	2,700	6,500	9,800	13,700	16,800	20,800	24,800	30,700	HEC-HMS Uniform Rain
Blue Creek above the Colorado River	80.4	4,400	10,300	15,500	22,200	27,200	33,800	40,400	50,100	HEC-HMS Uniform Rain
Colorado River below Blue Creek	3498.6	27,860	49,700	59,400	71,100	79,400	95,800	119,000	155,300	HEC-HMS Elliptical Storms
Colorado River near Bay City, TX (USGS Gage 08162500)	3529.6	25,930	49,100	59,400	71,700	79,800	95,600	117,900	154,400	HEC-HMS Elliptical Storms
Colorado River near Buckeye, TX	3556.8	27,290	49,900	59,800	71,400	79,700	95,200	116,700	153,200	HEC-HMS Elliptical Storms
Colorado River near Wadsworth, TX (USGS Gage 08162501)	3595.2	27,130	50,000	59,900	71,400	79,700	94,800	116,300	152,700	HEC-HMS Elliptical Storms
Colorado River nr Matagorda, TX (LCRA Gage)	3629.9	27,380	49,900	59,500	71,100	79,200	94,600	115,800	152,700	HEC-HMS Elliptical Storms
Colorado River at the Gulf of Mexico	3632.5	27,610	49,800	59,300	70,900	79,000	94,500	115,700	152,800	HEC-HMS Elliptical Storms

* NOTE: The Drainage Areas listed in this table include only the contributing drainage area that is located downstream of significant flood control reservoirs.

Table 13.2: Recommended Frequency Peak Pool Elevations (feet NAVD88) for Reservoirs in the Lower Colorado River Basin

Reservoir Name	Drainage Area*	50%	20%	10%	4%	2%	1%	0.50%	0.20%	Hydrologic Method
	sq mi	2-YR	5-YR	10-YR	25-YR	50-YR	100-YR	200-YR	500-YR	
E.V. Spence Reservoir	5,018	1890.46	1897.57	1898.82	1899.73	1900.35	1900.97	1902.12	1903.24	Reservoir Analysis
Oak Creek	237.4	2001.4	2002.4	2003.6	2005.8	2008.2	2009.5	2010.6	2011.8	HEC-HMS Uniform Rain
Ballinger Lake, Lower	231.2	1669.3	1670	1670.8	1672.4	1674.1	1675.3	1676.4	1677.8	HEC-HMS Uniform Rain
Twin Buttes Reservoir	3422.5	1933.53	1934.37	1937.54	1944.77	1952.11	1957.62	1968.23	1975.47	HEC-HMS Elliptical Storms / Reservoir Analysis
O.C. Fisher Reservoir	1462.8	1885.32	1887.47	1889.84	1899.12	1910.03	1919.18	1925.92	1932.64	HEC-HMS Elliptical Storms
O.H. Ivie Reservoir	3395.3	1548.32	1549.1	1550.14	1552.24	1553.83	1554.82	1557.07	1560.88	HEC-HMS Elliptical Storms
Lake Coleman	302.3	1719.5	1722.7	1726.2	1728.9	1730.4	1731.8	1733.0	1734.5	HEC-HMS Uniform Rain
Hords Creek Reservoir	48.9	1897.12	1901.21	1902.84	1905.36	1907.42	1910.22	1914.87	1921.3	Reservoir Analysis / HEC-HMS Uniform Rain
Lake Brownwood	1513.0	1426.89	1428.82	1430.25	1431.62	1433.3	1435.39	1437.88	1441.71	HEC-HMS Elliptical Storms
Brady Creek Reservoir	524.0	1744.4	1746.7	1748.6	1752.3	1756.6	1763.2	1765.7	1768.5	HEC-HMS Uniform Rain
Lake Buchanan	10694.7	1019.4	1019.65	1019.88	1020.3	1020.51	1020.98	1021.69	1022.49	HEC-HMS Elliptical Storms
Lake LBJ	15701.7	825.62	826.5	827.05	827.92	828.71	831.01	837.17	842.23	HEC-HMS Elliptical Storms
Lake Travis**	17530.7	683.16	690.76	698.48	713.28	716.06	721.69	730.11	735.23	Reservoir Analysis

* The Drainage Areas listed in this table include only the contributing drainage area that is located downstream of significant flood control reservoirs.

** Elevations for Lake Travis are in “msl”, which is LCRA’s Hydromet Datum. The datum conversion from msl to NAVD88 is +0.6 ft for Lake Travis.

14 Conclusions

This report summarizes new analyses that were completed as part of an InFRM Watershed Hydrology Assessment (WHA) to estimate the 1% annual chance (100-yr) flow, along with other frequency flows, for various stream reaches throughout the Lower Colorado River Basin in Texas. In addition to the partnered federal agencies of the InFRM team, regional stakeholders such as the Lower Colorado River Authority (LCRA), the Texas Water Development Board (TWDB), and the City of Austin also participated in the updates and review processes for this study. This study represents a significant step forward towards increasing resiliency against flood hazards across the Lower Colorado River basin.

14.1 RECOMMENDED 1% AEP (100-YEAR) FREQUENCY FLOWS

The flow frequency results that were recommended for adoption generally came from a combination of the watershed model results using NOAA Atlas 14 uniform rain, elliptical storms, and reservoir analysis techniques. Other methods, such as the statistical and RiverWare results, were used as points of comparison to fine tune the model for the frequent storms, but in general, they were not adopted directly due to their tendency to change after each significant flood event. Since the calibrated watershed model simulates the physical processes that occur during a storm event, it can produce more reliable and consistent estimations of the flow expected during a 1% annual chance (100-yr) storm. In addition, NOAA Atlas 14's regional rainfall depths for Texas shed new light on the depths and frequency of rainfall that could be expected in the Colorado River basin. Both uniform rain and elliptical shaped frequency storms were run in the watershed model. The elliptical frequency storm results were generally recommended for river reaches with large drainage areas, while the uniform rain results were recommended for the smaller drainage areas. The expected impacts of reservoir operations from the major reservoirs were also analyzed in detail for this study, and recommendations were made for the frequency dam releases and pool elevations for the reaches immediately upstream and downstream of the dams.

Figure 14.1 shows the trends in the recommended 1% AEP (100-year) peak discharges versus drainage area for all the major rivers and tributaries in the Lower Colorado study area. This figure shows that the discharges for the analyzed locations followed generally expected patterns of increasing peak flow with drainage area, with exceptions for the effects of reservoirs. For example, the four outlier dots along the bottom of the graph represent reservoir outflows from the flood control reservoirs of Hords Creek, Brady Creek, OC Fisher and Twin Buttes. The relative magnitudes of the 1% AEP (100-year) discharges of different tributaries in this graph generally make sense. For example, the Concho and Pecan Bayou watersheds in the upper, drier portion of the study area have the lowest peak discharges relative to their drainage areas, while steep, flashy rivers like the Llano and Pedernales, on the other hand, have the highest peak discharges relative to their drainage areas.

Similarly, this study found that peak discharges on the Colorado River mainstem are largely driven by its major tributaries. Upstream of the Concho River, Colorado River flows are similar to the Concho watershed. Between the Concho River and the San Saba River, Colorado River 1% AEP (100-year) flows generally stay between 100,000 and 150,000 cfs. Downstream of the San Saba River, 1% AEP flows increase to about 200,000 cfs. Downstream of the Llano River, Colorado River peak flows jump up to about 400,000 cfs and then climb to over 500,000 cfs downstream of the Pedernales River. Below Lake Travis, Colorado River 1% AEP flows (100-year) are greatly reduced to between 90,000 and 150,000 cfs upstream of Onion Creek. Just below Onion Creek, the 1% AEP flows on the Colorado River peak jump to about 250,000 cfs and then begin to decrease in the downstream direction due to floodplain storage and a lack of major tributaries between Onion Creek and the Gulf. Between Bastrop and the Gulf, 1% AEP peak flows on the Colorado River generally stay between 150,000 and 100,000 cfs and decrease in the downstream direction.

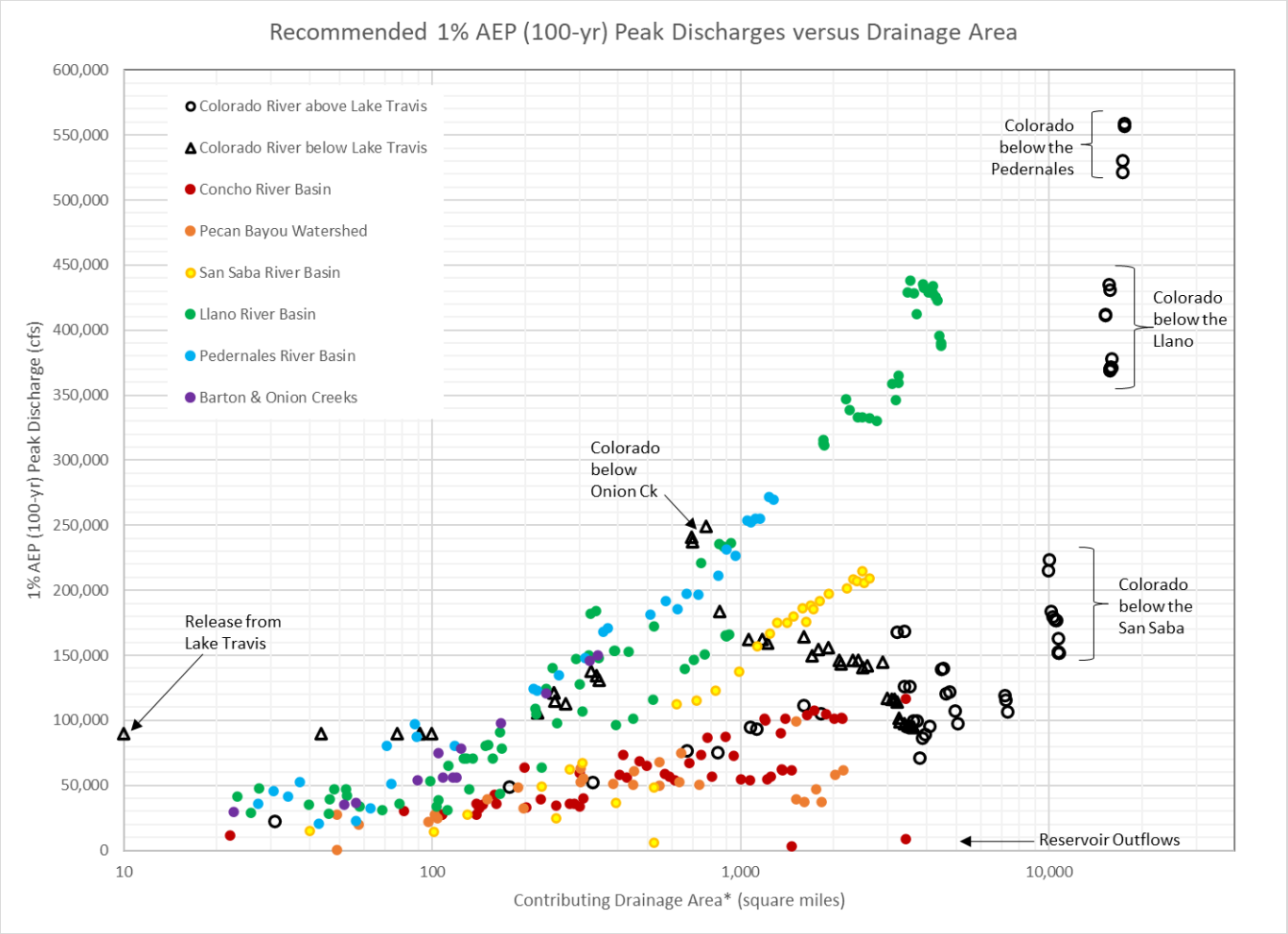

* NOTE: The Drainage Areas shown on this figure only include the contributing areas below significant flood control reservoirs.

Figure 14.1: Recommended 1% AEP (100-year) Peak Discharges versus Drainage Area

14.2 UNIQUE ASPECTS OF THE LOWER COLORADO INFRM WHA

14.2.1 Declining Flow Trends Upstream of San Saba, TX

Statistically significant downward trends in annual peak streamflow were observed in this study, particularly in the portion of the Colorado River basin that is upstream from the USGS stream gage for the Colorado River near San Saba, TX. The data indicate that a pronounced and enduring shift in basin hydrology likely occurred sometime in the 1960s followed by a slower, more gradual decline in stream flows that persists to the present time. These downward trends in streamflow were also confirmed in another study by Harwell and others (2020), which analyzed precipitation, streamflow, and potential flood storage trends in the Colorado River basin in Texas. Additionally, the Harwell study (2020) found no significant trends in annual precipitation across the Colorado River basin. However, the gages that indicated a downward trend in annual peak streamflow also showed downward trends in the ratio of streamflow volume to precipitation volume on an annual time step, which indicates a change in the way the Colorado River basin responds to precipitation events over time. Figure 14.2 gives an example of these declining streamflow trends in the annual peak streamflow data for the Colorado River near Ballinger, Texas. More information on the declining flow trends was included in Chapter 5.

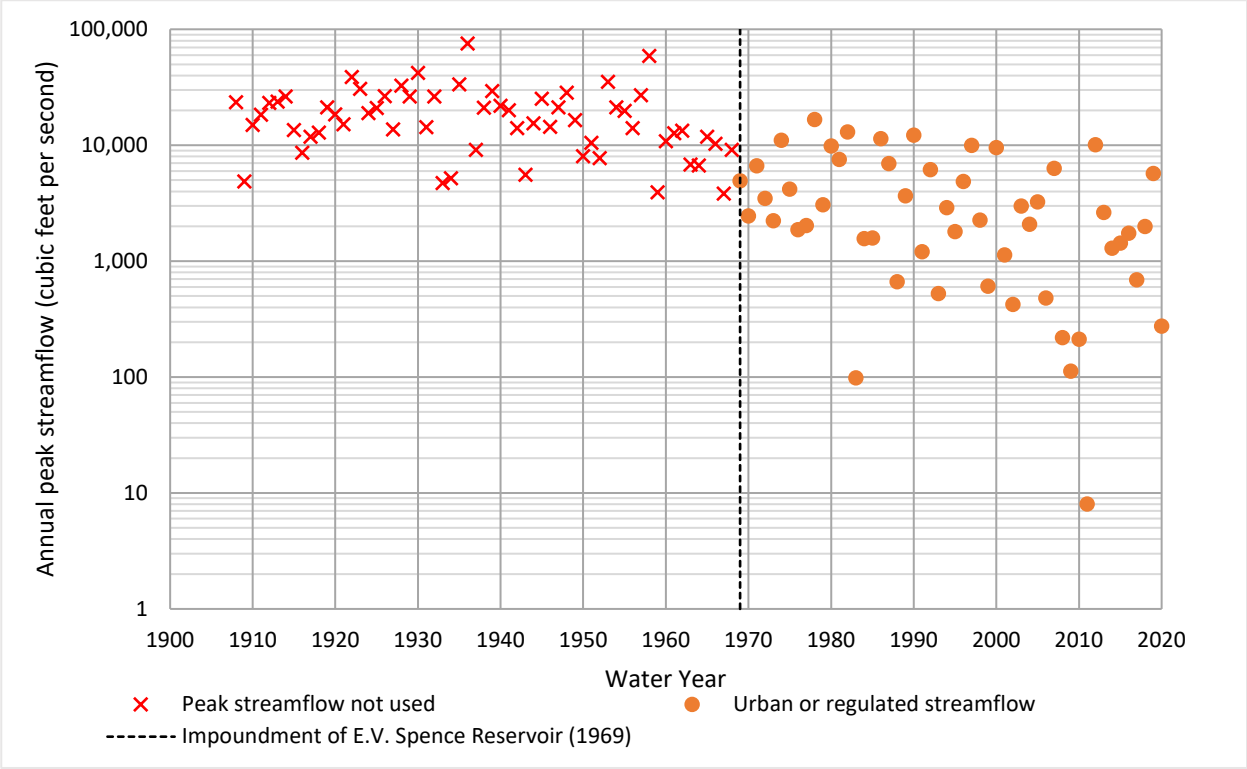

Figure 14.2: Example of Declining Streamflow Trends for the Colorado River near Ballinger, TX

It is a common practice in hydrology to test streamflow data for trends and understand how those trends may affect a flood frequency analysis. However, a problem arises when these trends are not only long-term and persistent, but also result from multiple interconnected factors. Such is the case of the Colorado River basin. The science and methodology behind untangling these intertwined causes of peak flow declines are beyond the scope of the present study and are still an ongoing area of scientific research.

However, the present study did attempt to account for the effects of these declining streamflow trends on the flood frequency analysis in a few ways. First, in the statistical analyses of the gage records, the early potion of the record prior to the 1960s change point was excluded from some of the gage analyses upstream of San Saba which had strong declining flow trends. The results of the frequency analysis based on the more recent record were then compared to the statistical results which included the entire period of record. The difference between the results of these two statistical analyses gave a better understanding of the magnitudes of the shifts in the streamflow over time. Second, in the HEC-HMS rainfall runoff modeling, a climate adjustment was made to the losses applied to the frequency storms to better align them with the observed loss rates from recent storm events for different regions of the basin. The climate adjustment allowed the model to differentiate between west Texas soils, which tend to have drier antecedent conditions, versus central and coastal Texas soils, which tend to have wetter antecedent conditions. It also ensured that the loss rates being applied to the frequency storms were an accurate representation of current conditions.

14.2.2 Historic 1930s Storms Analyses

One other unique aspect of the Lower Colorado River basin led to an additional analysis for the InFRM Watershed Hydrology Assessment (WHA). For many locations in the Lower Colorado River basin, the largest floods of record occurred in the 1930s, and since then, no other observed floods have some close to the magnitudes of flooding observed in the 1930s. In many cases, the rainfall and peak discharges from these floods were on the order of a 1% AEP (100-yr) flood or larger, which means that they are of high interest for flood studies such as this one.

However, there is a complication in that those floods occurred before most of the major reservoirs in the river basin were built.

For this study, additional analysis was performed in HEC-HMS to recreate two of those 1930s storm events with the goal of estimating what the peak flows on the rivers would have been with all of the current reservoir regulation in place. The regulated peak flows from those storm events were then added to the Bulletin 17C analysis of select stream gages as a sensitivity test of the statistical flood frequency estimates. The results of the historic 1930s storm analysis were documented in Chapter 10 and in Appendix F.

14.3 COMPARISON OF RESULTS WITH EFFECTIVE FEMA FIS FLOWS

Previously published frequency discharges from effective FEMA Flood Insurance Studies (FIS) in the Colorado River Basin were available for approximately 27% of the locations that were analyzed in this study, and the results of the current study were compared to those previously published values. Table 14.1 and Figure 14.3 compare the recommended 1% AEP (100-year) peak flows from the current study to the available effective FEMA FIS 1% AEP (100-year) peak flows at various locations across the study area.

Table 14.1: Comparison of Recommended versus Effective FEMA FIS 1% AEP (100-year) Peak Flows across the Colorado River Basin

Location Number	Location Description	Drainage Area* (sq mi)	Recommended 1% AEP (100-yr) Peak Flow (cfs)	FEMA FIS 1% AEP (100-yr) Peak Flow (cfs)	FIS Description	Last FIS Hydrology Update	% Difference from FIS
1	Colorado River near Ballinger, TX (USGS Gage 08126380)	1076.2	95,000	50,120	City of Ballinger 1990 Effective FIS	1988	90%
2	Colorado River above Elm Creek	1130.3	93,100	50,120	City of Ballinger 1990 Effective FIS	1988	86%
3	Colorado River below Elm Creek	1597.2	111,300	104,280	City of Ballinger 1990 Effective FIS	1988	7%
4	Middle Concho River abv Tankersley (USGS Gage 08128400)	2133.0	101,300	60,150	Tom Green County 2012 Effective FIS	1990	68%
5	Dove Creek at Knickerbocker, TX (USGS Gage 08130500)	224.4	39,500	64,240	Tom Green County 2012 Effective FIS	1990	-39%
6	Dove Creek above Spring Creek	251.7	34,800	63,230	Tom Green County 2012 Effective FIS	1990	-45%
7	Spring Creek near San Angelo, TX (USGS Gage 08130700)	678.9	67,400	175,000	Tom Green County 2012 Effective FIS	1990	-61%
8	South Concho River at Christoval, TX (USGS Gage 08128000)	415.4	73,300	131,750	Tom Green County 2012 Effective FIS	1990	-44%
9	Inflow to Twin Buttes Reservoir	3422.5	116,900	131,800	Tom Green County 2012 Effective FIS	1990	-11%
10	South Concho River below Twin Buttes Reservoir	3422.5	9,000	25,000	Tom Green County 2012 Effective FIS	1990	-64%
11	Pecan Creek nr San Angelo, TX (USGS Gage 08131400)	81.0	30,000	21,620	Tom Green County 2012 Effective FIS	1990	39%
12	South Concho River below Lake Nasworthy	107.2	27,400	25,000	Tom Green County 2012 Effective FIS	1990	10%
13	South Concho River above the North Concho River	139.2	27,800	24,200	Tom Green County 2012 Effective FIS	1990	15%
14	North Concho River nr Carlsbad, TX (USGS Gage 08134000)	1220.7	54,900	122,900	Tom Green County 2012 Effective FIS	1990	-55%
15	North Concho River above Grape Creek	1250.2	57,000	123,500	Tom Green County 2012 Effective FIS	1990	-54%
16	North Concho River below Grape Creek	1360.1	62,100	134,800	Tom Green County 2012 Effective FIS	1990	-54%
17	North Concho River nr Grape Creek (USGS Gage 08134250)	1364.9	61,400	134,400	Tom Green County 2012 Effective FIS	1990	-54%
18	Inflow to OC Fisher Reservoir	1462.8	61,500	141,100	Tom Green County 2012 Effective FIS	1990	-56%
19	North Concho River below OC Fisher Reservoir	1462.8	2,850	20,000	Tom Green County 2012 Effective FIS	1990	-86%
20	North Concho River at San Angelo (former USGS 08135000)	22.1	11,800	20,000	Tom Green County 2012 Effective FIS	1990	-41%
21	Concho River at San Angelo, TX (USGS Gage 08136000)	161.2	36,200	29,800	Tom Green County 2012 Effective FIS	1990	21%
22	Concho River above Crows Nest Creek	300.8	59,700	55,750	Tom Green County 2012 Effective FIS	1990	7%
23	Concho River above Lipan Creek	470.3	68,600	71,450	Tom Green County 2012 Effective FIS	1990	-4%

Location Number	Location Description	Drainage Area* (sq mi)	Recommended 1% AEP (100-yr) Peak Flow (cfs)	FEMA FIS 1% AEP (100-yr) Peak Flow (cfs)	FIS Description	Last FIS Hydrology Update	% Difference from FIS
24	Hords Creek near Coleman, TX (USGS Gage 08142000)	57.8	19,600	24,990	City of Coleman 1980 Effective FIS	1972	-22%
25	Pecan Bayou at Brownwood, TX (USGS Gage 08143500)	1603.8	37,100	62,247	Brown County 2018 Effective FIS	1979	-40%
26	San Saba Rv at FM 864 nr Fort McKavett, TX (USGS Gage)	622.8	111,900	124,000	Menard County 1987 Effective FIS	1986	-10%
27	San Saba River above Rocky Creek	721.4	114,800	124,000	Menard County 1987 Effective FIS	1986	-7%
28	San Saba River at Menard, TX (USGS Gage 081445000)	1136.9	156,900	177,000	Menard County 1987 Effective FIS	1986	-11%
29	San Saba River above Elm Creek	1244.6	166,000	177,000	Menard County 1987 Effective FIS	1986	-6%
30	San Saba River below Elm Creek	1318.2	174,500	190,000	Menard County 1987 Effective FIS	1986	-8%
31	San Saba River above Calf Creek	1422.3	174,800	190,000	Menard County 1987 Effective FIS	1986	-8%
32	Brady Creek At Brady, TX (USGS Gage 08145000)	130.3	26,900	25,200	City of Brady 1981 Effective FIS	1980	7%
33	San Saba Rv at San Saba, TX (USGS Gage 08146000)	2523.4	205,400	151,301	San Saba Co 1991 Effective FIS	1988	36%
34	Outflow from Lake Buchanan	10694.7	152,000	157,000	Llano County 2012 Effective FIS	2002	-3%
35	Inflow to Inks Lake	10734.3	152,300	157,000	Llano County 2012 Effective FIS	2002	-3%
36	Colorado River below Inks Lake	10734.3	152,300	157,000	Llano County 2012 Effective FIS	2002	-3%
37	South Llano River above the Llano River	932.6	236,000	231,000	City of Junction 1997 Effective FIS	1978	2%
38	North Llano River nr Junction, TX (USGS Gage 08148500)	901.7	164,400	231,000	City of Junction 1997 Effective FIS	1978	-29%
39	Llano River nr Junction, TX (USGS Gage 08150000)	1858.2	313,100	375,000	City of Junction 1997 Effective FIS	1978	-17%
40	Comanche Creek near Mason (LCRA Gage 2424)	46.3	28,500	27,310	City of Mason 1979 Effective FIS	1978	4%
41	Llano River above Hickory Creek	3723.8	412,400	380,000	City of Llano - Pending FIS	2012	9%
42	Llano River below Hickory Creek	3891.8	435,600	380,000	City of Llano - Pending FIS	2012	15%
43	Llano River above San Fernando Creek	3924.8	432,800	380,000	City of Llano - Pending FIS	2012	14%
44	Llano River below San Fernando Creek	4060.3	429,300	380,000	City of Llano - Pending FIS	2012	13%
45	Llano River below Johnson Creek	4118.4	430,200	380,000	City of Llano - Pending FIS	2012	13%
46	Llano River below Pecan Creek	4187.0	433,800	380,000	City of Llano - Pending FIS	2012	14%
47	Llano River at Llano, TX (USGS Gage 08151500)	4202.0	428,100	380,000	City of Llano - Pending FIS	2012	13%
48	Llano River above the Little Llano River	4279.1	425,400	380,000	City of Llano - Pending FIS	2012	12%
49	Llano River below the Little Llano River	4331.6	423,000	380,000	City of Llano - Pending FIS	2012	11%

Location Number	Location Description	Drainage Area* (sq mi)	Recommended 1% AEP (100-yr) Peak Flow (cfs)	FEMA FIS 1% AEP (100-yr) Peak Flow (cfs)	FIS Description	Last FIS Hydrology Update	% Difference from FIS
50	Llano River above Honey Creek	4410.8	395,300	380,000	City of Llano - Pending FIS	2012	4%
51	Llano River above the Colorado River	4465.4	388,000	307,143	Llano County Effective FIS	2002	26%
52	Inflow to Lake LBJ	15701.7	431,000	367,600	Llano County 2012 Effective FIS	2002	17%
53	Colorado River below Lake LBJ	15701.7	368,800	330,269	Burnet County 2019 Effective FIS	1990	12%
54	Backbone Creek at Marble Falls (LCRA Gage 2992)	30.1	29,100	28,640	Burnet County 2019 Effective FIS	2015	2%
55	Backbone Creek above the Colorado River	40.3	31,100	33,710	Burnet County 2019 Effective FIS	2015	-8%
56	Inflow to Lake Marble Falls	15783.9	369,400	365,700	Llano County 2012 Effective FIS	2002	1%
57	Colorado River below Lake Marble Falls	15783.9	369,400	365,700	Llano County 2012 Effective FIS	2002	1%
58	Colorado River below Double Horn Creek	15929.1	370,900	368,900	Burnet County 2019 Effective FIS	1990	1%
59	Pedernales River at LBJ Ranch near Stonewall (LCRA Gage)	625.6	185,300	247,000	Gillespie County 2001 Effective FIS	1997	-25%
60	Pedernales Rv nr Johnson City, TX (USGS Gage 08153500)	900.9	231,700	269,000	Blanco County 1991 Effective FIS	1979	-14%
61	Pedernales River below Cypress Creek	1232.3	271,700	330,000	Travis County 2020 Effective FIS	2018	-18%
62	Pedernales River above the Colorado River	1280.9	269,900	330,000	Travis County 2020 Effective FIS	2018	-18%
63	Big Sandy 2 Creek near Jonestown (LCRA Gage 3953)	34.1	41,300	38,000	Travis County 2020 Effective FIS	2009	9%
64	Big Sandy 2 Creek above the Colorado River	73.5	51,400	48,000	Travis County 2020 Effective FIS	2009	7%
65	Colorado River below Lake Travis	17530.7	90,000	90,000	Travis County 2020 Effective FIS	2002	0%
66	Bull Ck at Loop 360 nr Austin, TX (USGS Gage 08154700)	22.7	29,900	25,600	Travis County 2020 Effective FIS	2013	17%
67	Inflow to Lake Austin	91.1	90,000	90,100	Travis County 2020 Effective FIS	2002	0%
68	Colorado River below Lake Austin	91.1	90,000	90,100	Travis County 2020 Effective FIS	2002	0%
69	Colorado River above Barton Creek	99.7	90,000	90,100	Travis County 2020 Effective FIS	2002	0%
70	Colorado River below Barton Creek	219.7	106,000	90,100	Travis County 2020 Effective FIS	2002	18%
71	Inflow to Lady Bird Lake	248.3	121,000	90,100	Travis County 2020 Effective FIS	2002	34%

Location Number	Location Description	Drainage Area* (sq mi)	Recommended 1% AEP (100-yr) Peak Flow (cfs)	FEMA FIS 1% AEP (100-yr) Peak Flow (cfs)	FIS Description	Last FIS Hydrology Update	% Difference from FIS
72	Colorado River below Lady Bird Lake	248.3	121,000	90,100	Travis County 2020 Effective FIS	2002	34%
73	Colorado River at Austin, TX (USGS Gage 08158000)	250.2	115,000	90,100	Travis County 2020 Effective FIS	2002	28%
74	Colorado River above Walnut Creek	270.7	113,000	90,100	Travis County 2020 Effective FIS	2002	25%
75	Walnut Ck at Webberville Rd, Austin (USGS Gage 08158600)	51.7	35,400	32,440	Travis County 2020 Effective FIS	2005	9%
76	Walnut 1 Creek above the Colorado River	56.5	36,500	32,440	Travis County 2020 Effective FIS	2005	13%
77	Colorado River below Walnut 1 Creek	327.2	138,000	90,100	Travis County 2020 Effective FIS	2002	53%
78	Colorado River at Del Valle, TX (LCRA Gage)	341.2	134,000	90,100	Travis County 2020 Effective FIS	2002	49%
79	Colorado River above Onion Creek	347.8	131,000	90,100	Travis County 2020 Effective FIS	2002	45%
80	Onion Creek at RR-1826	104.6	75,100	72,960	Hays County 2019 Preliminary FIS	2018	3%
81	Onion Ck nr Driftwood, TX (USGS Gage 08158700)	123.7	78,300	75,420	Hays County 2019 Preliminary FIS	2018	4%
82	Onion Creek at Buda (LCRA Gage)	167.3	97,800	80,140	Hays County 2019 Preliminary FIS	2018	22%
83	Onion Ck at I-35 nr Twin Creeks Rd (USGS Gage 08158827)	234.0	121,000	90,200	Travis County 2020 Effective FIS	2016	34%
84	Onion Ck at US Hwy 183, Austin, TX (USGS Gage 08159000)	323.7	146,000	121,900	Travis County 2020 Effective FIS	2016	20%
85	Onion Creek above the Colorado River	345.0	150,000	122,800	Travis County 2020 Effective FIS	2016	22%
86	Colorado River below Onion Creek	692.9	241,100	90,000	Travis County 2020 Effective FIS	2002	168%
87	Colorado River above Gilleland Creek	699.2	237,200	90,000	Travis County 2020 Effective FIS	2002	164%
88	Gilleland Creek near Manor (LCRA Gage 5417)	41.4	18,800	33,600	Travis County 2020 Effective FIS	2018	-44%
89	Gilleland Creek above the Colorado River	75.3	29,500	25,700	Travis County 2020 Effective FIS	2018	15%
90	Colorado River near Webberville (LCRA Gage)	774.5	249,300	109,500	Travis County 2020 Effective FIS	2002	128%
91	Colorado River at Bastrop, TX (USGS Gage 08159200)	1223.8	159,600	142,020	Bastrop County 2016 Effective FIS	1987	12%
92	Cedar Creek below Maha Creek	95.5	37,500	28,290	Bastrop County 2016 Effective FIS	1977	33%
93	Colorado Rv at Smithville, TX (USGS Gage 08159500)	1705.8	149,500	152,200	Fayette County 2006 Effective FIS	2002	-2%

Location Number	Location Description	Drainage Area* (sq mi)	Recommended 1% AEP (100-yr) Peak Flow (cfs)	FEMA FIS 1% AEP (100-yr) Peak Flow (cfs)	FIS Description	Last FIS Hydrology Update	% Difference from FIS
94	Colorado Rv abv La Grange, TX (USGS Gage 08160400)	2117.3	143,200	152,200	Fayette County 2006 Effective FIS	2002	-6%
95	Buckners Creek above the Colorado River	185.7	38,200	50,986	Fayette County 2006 Effective FIS	2005	-25%
96	Colorado River below Bruch Creek	2491.3	140,400	125,000	Colorado County 2011 Effective FIS	2002	12%
97	Colorado River at Columbus, TX (USGS Gage 08161000)	2885.1	144,800	135,000	Colorado County 2011 Effective FIS	2002	7%
98	Colorado River near Altair (LCRA Gage 6377)	2979.6	116,900	120,700	Colorado County 2011 Effective FIS	2002	-3%
99	Colorado River below Robb Slough	3216.2	114,500	95,415	Wharton County 2017 Effective FIS	2002	20%
100	Colorado Rv at Wharton, TX (USGS Gage 08162000)	3248.3	101,600	95,415	Wharton County 2017 Effective FIS	2002	6%
101	Colorado River near Lane City, TX (LCRA Gage 6537)	3277.9	98,900	95,415	Wharton County 2017 Effective FIS	2002	4%
102	Colorado River below Jones Creek	3396.5	97,300	104,100	Matagorda County 2021 Pending FIS	2002	-7%
103	Colorado River below Blue Creek	3498.6	95,800	98,500	Matagorda County 2021 Pending FIS	2002	-3%
104	Colorado River near Bay City, TX (USGS Gage 08162500)	3529.6	95,600	99,700	Matagorda County 2021 Pending FIS	2002	-4%
105	Colorado River near Buckeye, TX	3556.8	95,200	99,200	Matagorda County 2021 Pending FIS	2002	-4%
106	Colorado River near Wadsworth, TX (USGS Gage 08162501)	3595.2	94,800	95,600	Matagorda County 2021 Pending FIS	2002	-1%
107	Colorado River nr Matagorda, TX (LCRA Gage)	3629.9	94,600	93,500	Matagorda County 2021 Pending FIS	2002	1%

* NOTE: The Drainage Areas listed in this table include only the contributing drainage area that is located downstream of significant flood control reservoirs.

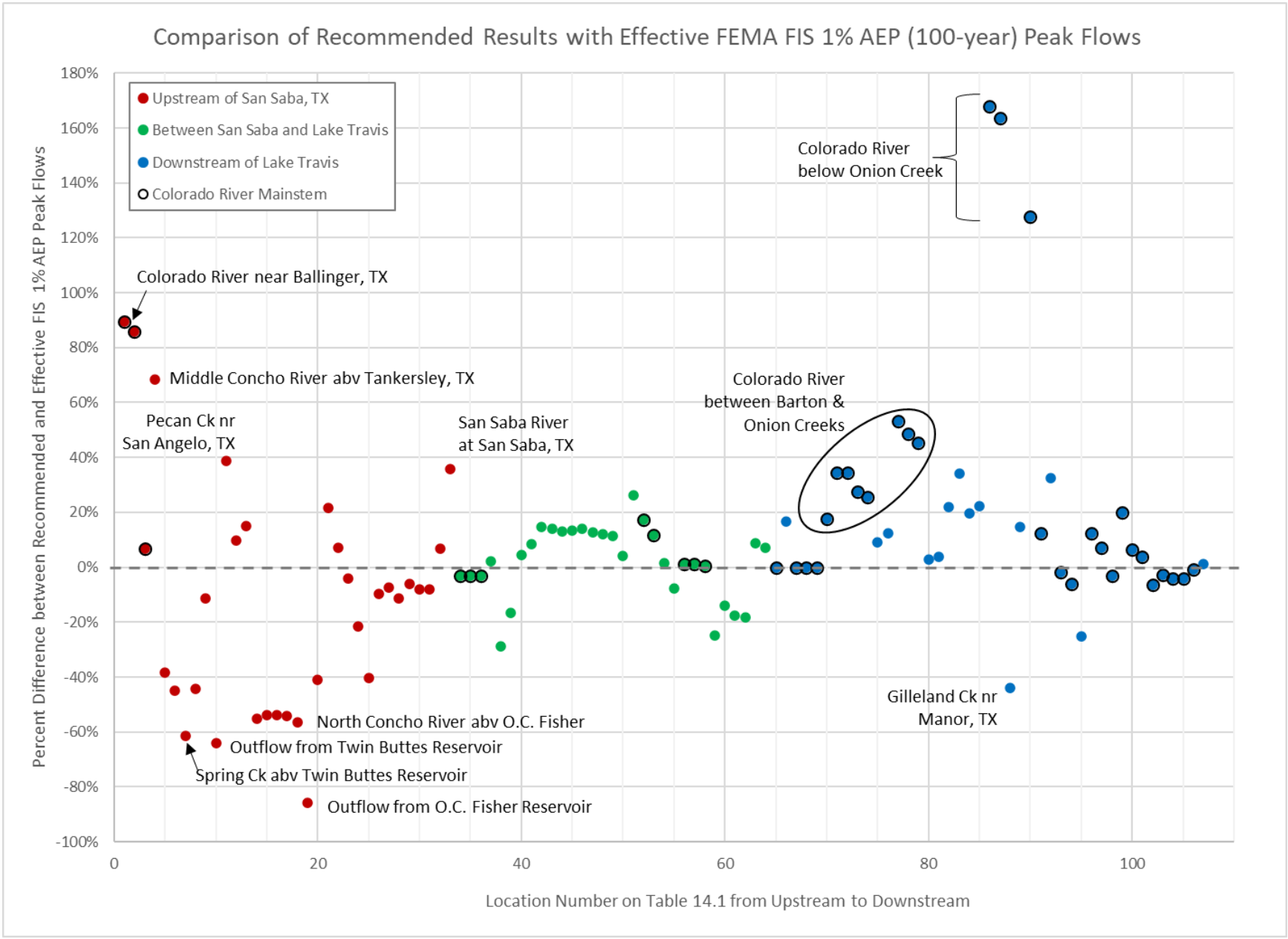

Figure 14.3: Percent Difference between the Recommended versus Effective FEMA FIS 1% AEP (100-year) Peak Flows across the Colorado River Basin

The recommended results from this study differed significantly from the effective FEMA Flood Insurance Studies (FIS) frequency flows in many locations. The new flow frequency results were higher than the previously published results in some areas, while they were lower in other areas. Figure 14.3 shows the percent difference between the recommended 1% AEP peak flows versus the previously published FEMA FIS 1% AEP peak flows. The largest percent differences were generally seen in the area upstream of San Saba, which is also the portion of the basin that is experiencing declining stream flow trends. Most of the analyzed locations upstream of San Saba showed a decrease (negative percent difference) in the recommended 1% AEP (100-yr) peak flows when compared to the effective FIS discharges. This result is consistent with the observed declining trends in streamflow. The differences in the 1% AEP (100-year) flow estimates upstream of San Saba were as high as +/- 80%, as shown in Figure 14.3. There were also some locations upstream of San Saba that showed a significant increase from the effective FIS 1% AEP (100-year) peak flow values. The locations that showed a significant increase upstream of San Saba were generally locations whose FIS hydrology had not been updated in more than 30 years, as shown in Table 14.1, and those FIS flows were often based on outdated methods and/or statistics.

For the areas of the basin between San Saba and Lake Travis, which includes the Llano and Pedernales Rivers, the percent differences from the effective FIS discharges were generally smaller. Figure 14.3 shows that most of the differences in this area of the basin were less than 20%, and the average percent difference was +/- 10%. This portion of the basin did not show any significant trends in streamflow, and some of the FIS discharges in this area came from the 2002 Flood Damage Evaluation Project (FDEP), which used similar methods to the current study. Therefore, it makes sense that the changes in flood frequency estimates were smaller in this portion of the basin.

For the portion of the basin that is downstream of Lake Travis, the percent differences in peak flow were mostly positive, indicating an increase in the 1% AEP (100-year) flow estimates, as shown on Figure 14.3. In fact, the average difference in the 1% AEP peak flow for this portion of the basin was +20%. One reason for this increase are the increased frequency rainfall depths from NOAA Atlas 14. The 100-year rainfall in Austin, Texas increased by close to 30% when compared to previous rainfall estimates (NOAA, 2018). These increases in rainfall depths led to increases in peak flow on many of the tributaries around Austin such as Barton and Onion Creeks.

For the Colorado River mainstem downstream of Lake Travis, the other contributing factor to the increases in the 1% AEP (100-year) peak flow estimates had to do with the assumption surrounding the dominant source of flooding. For most of the effective FIS, the 1% AEP peak flow on the Colorado River was assumed to originate from a large release from Lake Travis of 90,000 cfs. That assumption was carried down the Colorado River from Lake Travis, past Onion Creek, and ended just upstream of Bastrop, TX on the effective FIS. The current study also recommended 90,000 cfs as the 1% AEP peak release from Lake Travis. However, the current study's rainfall runoff modeling showed that runoff from the uncontrolled drainage area downstream of Lake Travis surpasses 90,000 cfs downstream of Barton Creek. Figure 14.3 shows that the difference in the 1% AEP flow estimate jumps from zero percent upstream of Barton Creek to between 20% and 50% between Barton and Onion Creeks. Downstream of Onion Creek, the increase in the 1% AEP (100-year) peak flow jumps to more than 100% of the effective FIS flow. This is because the effective FIS assumed that the 1% AEP peak flow on the Colorado River downstream of Onion Creek would still be the 90,000 cfs release from Lake Travis. However, the current study showed that Onion Creek alone can produce a 1% AEP (100-year) peak discharge of 150,000 cfs. When combined with the urbanized and uncontrolled drainage area between Lake Travis and Onion Creek, the recommended 1% AEP (100-year) discharges on the Colorado River below Onion Creek were found to be as much as 240,000 cfs, which represents a 167% increase over the effective FIS flow for that reach.

Of the reservoirs that were analyzed in the present study, only five had published effective FEMA FIS pool elevations. Those were Twin Buttes, O.C. Fisher, Lake Buchanan, Lake LBJ and Lake Travis. Table 14.2 and Figures 14.4 through 14.8 compare the results of the current study to the previous published 1% AEP (100-year) FEMA FIS elevations.

Table 14.2: Comparison of Recommended vs. Effective FEMA FIS 1% AEP (100-year) Reservoir Elevations (feet NAVD88)

Reservoir Name	Recommended WHA 100-year Elevation	Effective FEMA FIS 100-year Elevation	Difference (feet)
Twin Buttes Reservoir	1957.6	1960.0	-2.4
O.C. Fisher Reservoir	1919.2	1937.0	-17.9
Lake Buchanan	1021.0	1021.0	0.0
Lake LBJ	831.0	828.1	2.9
Lake Travis**	721.7	721.8	-0.1

** Elevations for Lake Travis are in "msl", which is LCRA's Hydromet Datum. The datum conversion from msl to NAVD88 is +0.6 ft for Lake Travis.

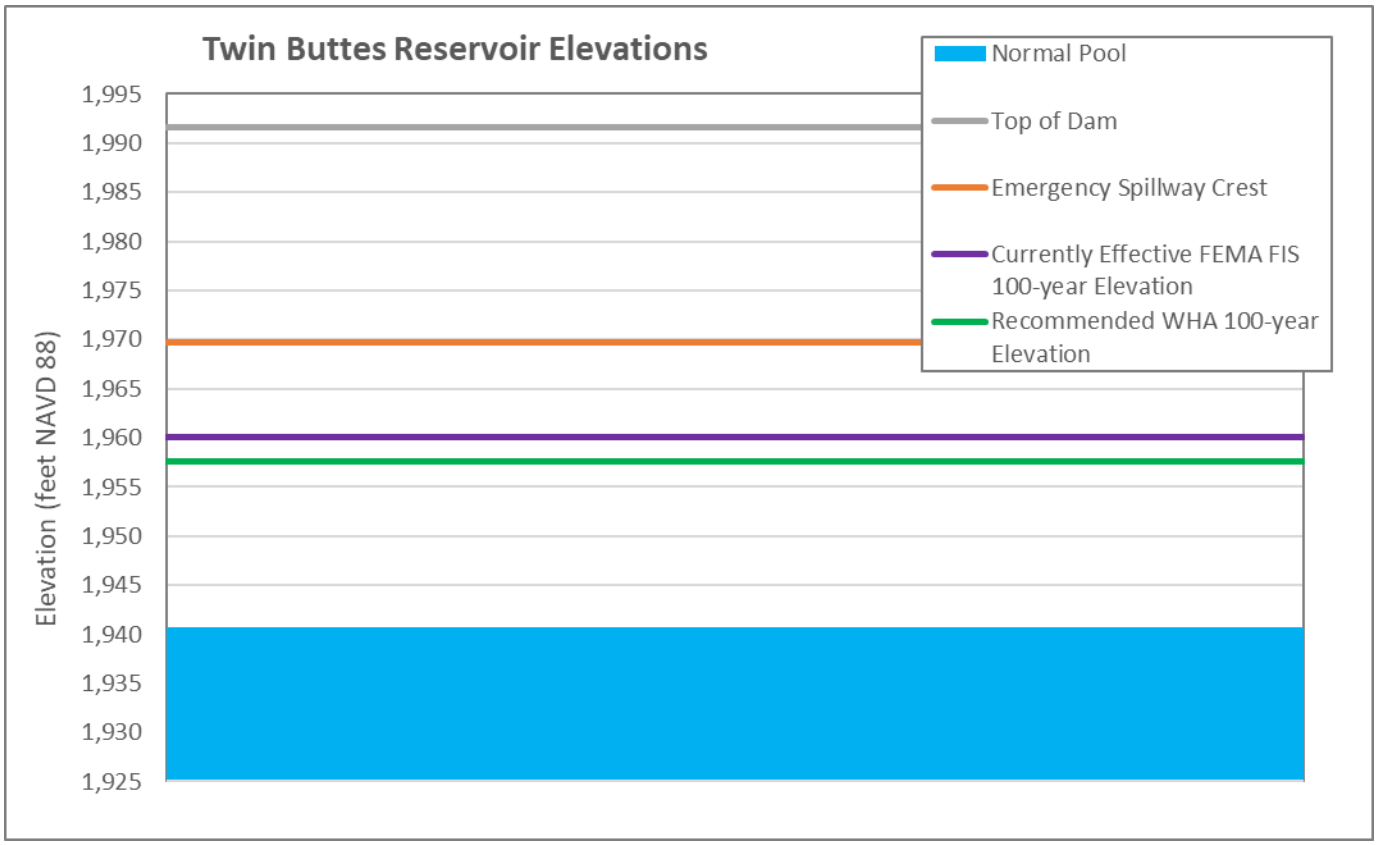

Figure 14.4: Comparison of Recommended 1% AEP (100-year) Pool Elevation Results for Twin Buttes Reservoir

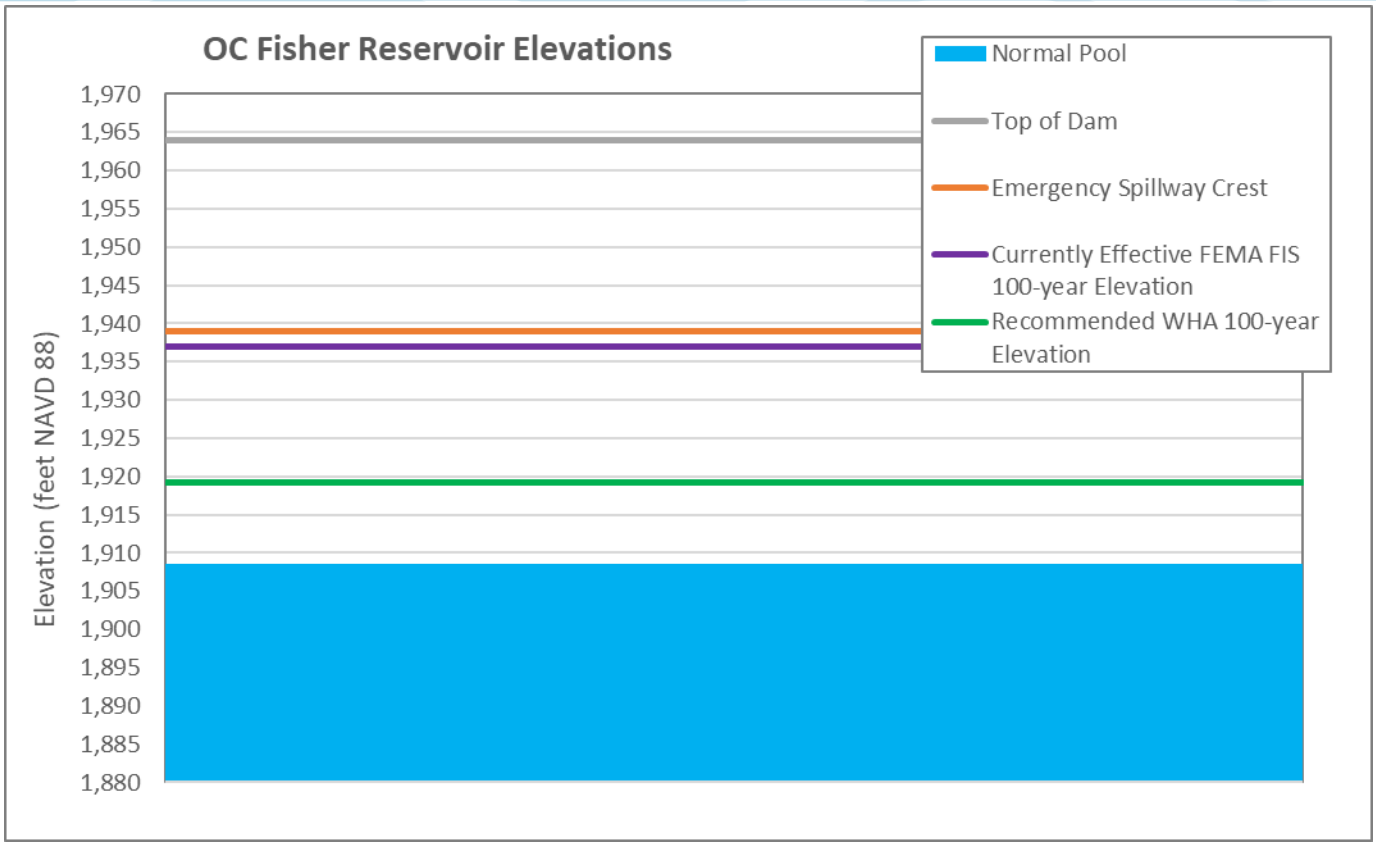

Figure 14.5: Comparison of Recommended 1% AEP (100-year) Pool Elevation Results for O.C. Fisher Reservoir

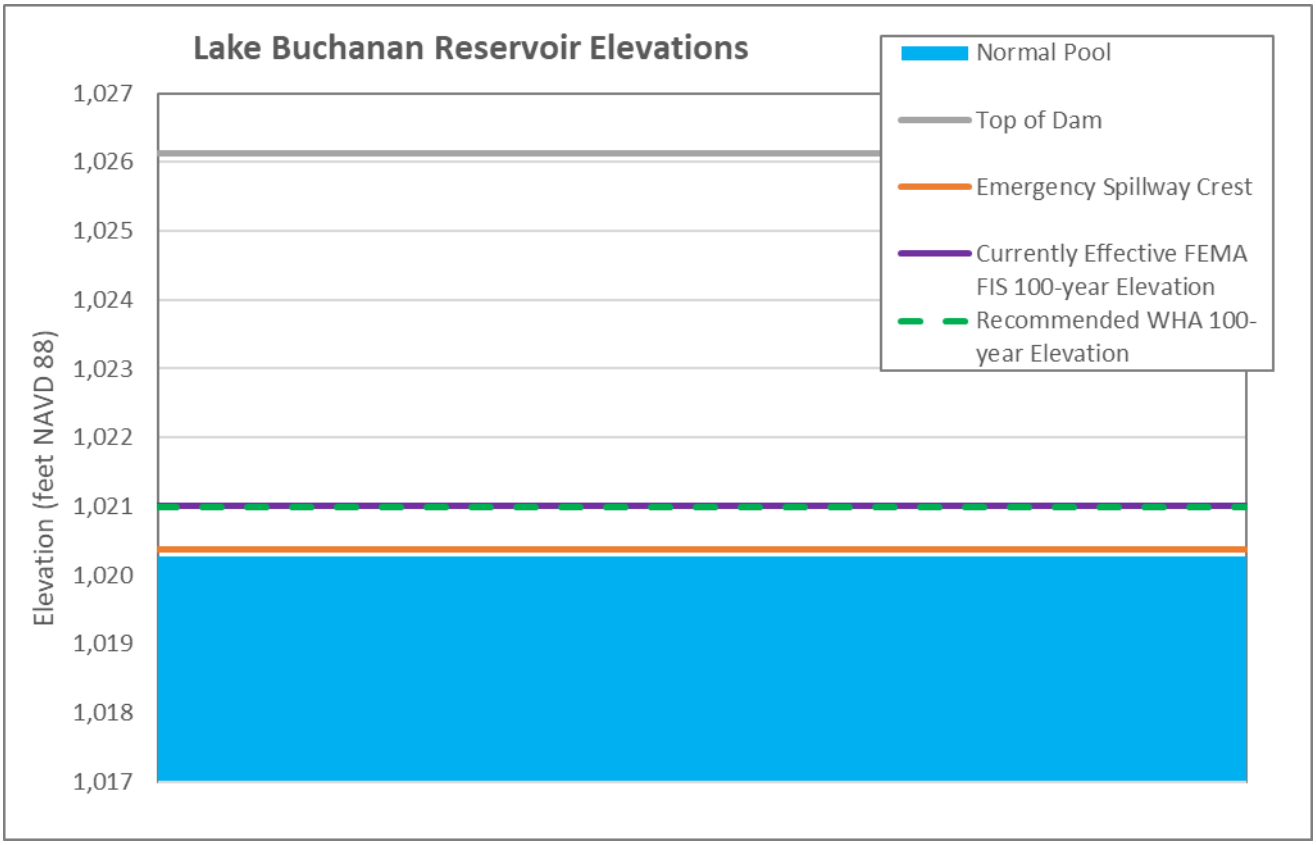

Figure 14.6: Comparison of Recommended 1% AEP (100-year) Pool Elevation Results for Lake Buchanan

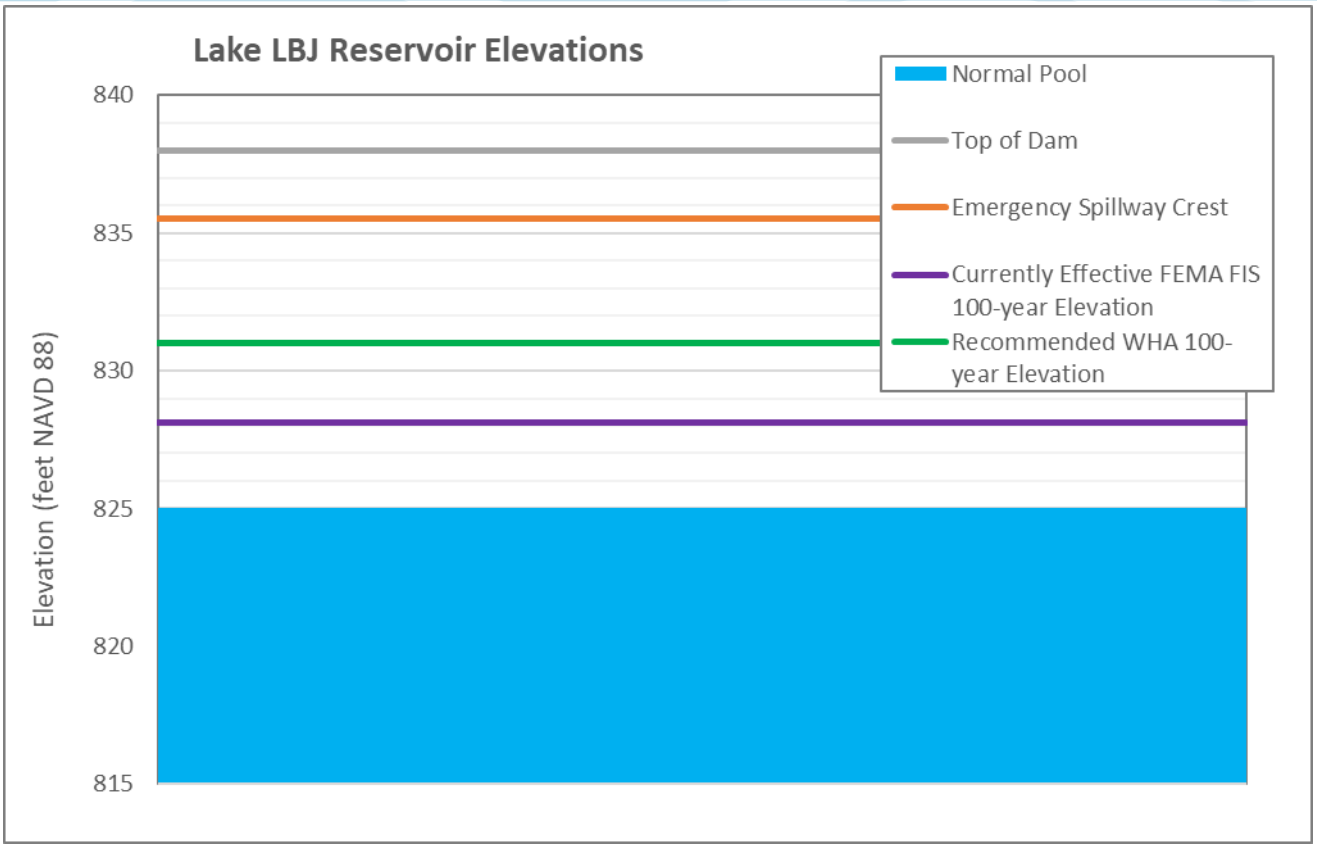

Figure 14.7: Comparison of Recommended 1% AEP (100-year) Pool Elevation Results for Lake LBJ

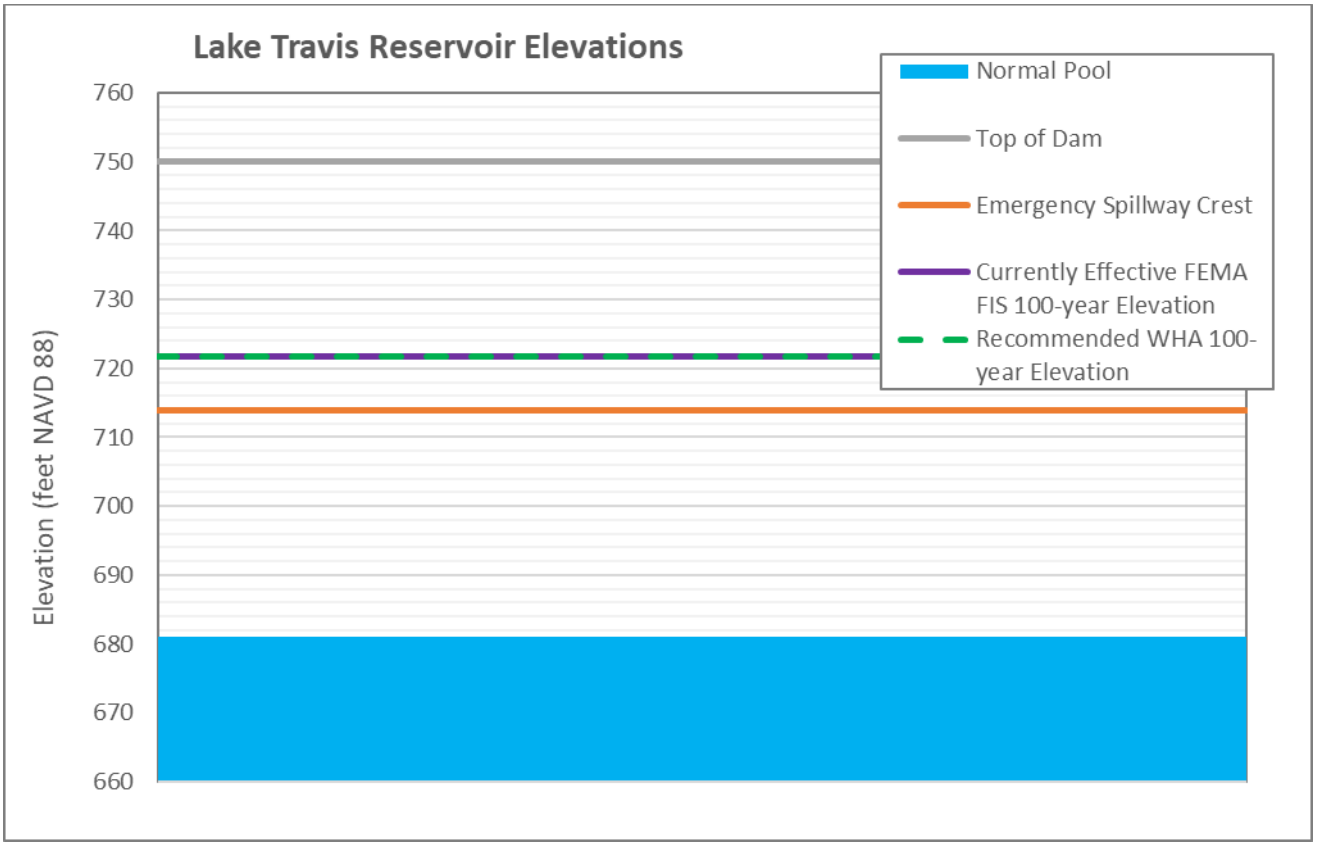

Figure 14.8: Comparison of Recommended 1% AEP (100-year) Pool Elevation Results for Lake Travis

As one can see from Figures 14.4 and 14.5, the recommended 1% AEP (100-yr) pool elevations for Twin Buttes and O.C. Fisher are significantly lower than the effective FIS elevations. This is largely due to the effects of the declining streamflow trends in that portion of the basin. The frequency pool elevations from the effective FIS were calculated based on the period of record prior to 1990; therefore, they did not include the most recent 30-year period which showed the observed pool elevations often staying 30 feet or more below "normal pool".

For Lake Buchanan and Lake Travis, the recommended 1% AEP (100-yr) pool elevations were almost identical to the effective FEMA FIS elevations. Lake Buchanan recently (2023) adopted a new operation plan, and one of the goals of that plan was to maintain the current effective FIS pool elevations and releases for the 1% and 0.2% AEP (100-yr and 500-yr) frequencies. This study analyzed the operations of Lake Buchanan with that new operational plan, and the results confirmed that the effective elevations would be maintained. For Lake Travis, there have been no significant changes to its operational plan, but the reservoir analysis that was performed for this study happened to calculate a 1% AEP (100-yr) pool elevation that was very similar to the effective FIS.

For Lake LBJ, the recommended 1% AEP (100-yr) pool elevation is almost 3-foot higher than the effective FIS. The effective FIS pool elevations came from the 2002 FDEP study. The current analysis includes an additional 20 years of record, which included a very large inflow event from the Llano River in 2018. Elevations and releases from Lake LBJ for rare floods are often driven by inflows from the flashy 4,000 square mile Llano River watershed. The HEC-HMS model in this study was calibrated to the 2018 flood event along with other flood events, and the elliptical frequency storms confirmed that a 1% AEP (100-yr) storm on the Llano River would cause higher pool elevations Lake LBJ.

14.4 COMPARISON OF RESULTS WITH BLE DATA

At the time of this publication (2023), FEMA's Base Level Engineering (BLE) data was not yet available for most of the study area. BLE data are an approximate source of flood hazard estimation, similar to FEMA's Zone A mapping. As such, the hydrology for most of the currently available BLE data is based on approximate methods. As of this writing (2023), BLE data was only available for Llano County, the Pedernales River basin, and the Lower Colorado watershed between Austin and Columbus, Texas. Table 14.2 and Figure 14.4 compare the 1% AEP (100-year) peak flows from the published BLE data to the recommend results from this study. In this figure, a positive difference indicates that the BLE data is higher than the recommended values, while a negative difference indicates that the BLE data is lower than the recommended values.

One can see in Figure 14.4 that the BLE data in Llano County generally overestimated the 1% AEP peak flows by 10% to 50% when compared to the results of this study which used more detailed methods, and at one location, the BLE data overestimated the 1% AEP peak flow by over 100%. The BLE data in Llano County used USGS regression equations, which provide a simple method to estimate frequency discharges based on physical parameters such as area and slope. However, it is often hit-or-miss as to whether the regression equations are a good fit for a particular watershed. The tributaries to the Pedernales River also used regression equations for the BLE data, and in that case, the regression equations underestimated the peak flow values by 50% to 60%.

The BLE data for the Pedernales River and the Lower Colorado River and tributaries was based on Bulletin 17C statistical analyses. As one can see from Figure 14.4, the results from Bulletin 17C are a little closer to the recommended WHA results, but there is still quite a bit of scatter in those results. The Bulletin 17C flows in the BLE data were usually within +/- 30% of the recommended results from this study, but there were a couple of locations where the differences were +60% and -40%, as shown on Figure 14.4.

Overall, there are significant differences between the hydrology used in the BLE data and the results of the present study. FEMA and the TWDB have plans to regularly update the BLE data throughout Texas on a recurring cycle. Since the results of the InFRM Watershed Hydrology Assessments (WHAs) provide a more detailed and accurate estimate of frequency flows across a given watershed, it is recommended that the hydrology of the BLE data be updated to be consistent with the results of the InFRM WHAs whenever they are available. Updating the hydrology with the WHA results will greatly increase the accuracy of the flood risk estimates in the BLE data, and the TWDB is already incorporating this recommendation into their BLE development plans.

Table 14.2: Comparison of the Published BLE versus Recommended WHA 1% AEP (100-year) Peak Flows

Location Number	Location Description	Drainage Area* (sq mi)	Recommended WHA 1% AEP (100-yr) Peak Flow (cfs)	BLE Data 1% AEP (100-yr) Peak Flow (cfs)	BLE Data Source	BLE Hydrologic Method	% Difference from Recommended
1	Hickory Creek near Castell (LCRA Gage)	168.0	78,000	117,854	Llano County, 2017	USGS Regression Equations	51%
2	San Fernando Creek near Llano (LCRA Gage 2616)	128.9	70,700	77,886	Llano County, 2017	USGS Regression Equations	10%
3	Johnson Creek near Llano (LCRA Gage)	46.6	39,500	58,910	Llano County, 2017	USGS Regression Equations	49%
4	Little Llano River near Llano (LCRA gage 2669)	48.2	47,000	48,628	Llano County, 2017	USGS Regression Equations	3%
5	Honey Creek near Kingsland (LCRA Gage 2694)	25.9	28,900	61,243	Llano County, 2017	USGS Regression Equations	112%
6	Sandy Creek near Willow City (LCRA Gage 2851)	151.6	80,800	123,260	Llano County, 2017	USGS Regression Equations	53%
7	Sandy Creek near Click (LCRA Gage 2878)	300.0	128,000	185,737	Llano County, 2017	USGS Regression Equations	45%
8	Sandy Ck nr Kingsland, TX (USGS Gage 08152000)	346.2	148,000	194,577	Llano County, 2017	USGS Regression Equations	31%
9	Walnut Creek near Kingsland (LCRA Gage 2897)	23.3	41,600	49,504	Llano County, 2017	USGS Regression Equations	19%
14	Pedernales Rv nr Fredericksburg (USGS Gage 08152900)	369.6	171,000	127,076	Pedernales, 2021	Bulletin 17C Analysis	-26%
15	South Grape Creek near Luckenbach (LCRA Gage 3328)	27.3	35,700	18,447	Pedernales, 2021	USGS Regression Equations	-48%
16	Pedernales River at LBJ Ranch near Stonewall (LCRA Gage)	625.6	185,300	148,263	Pedernales, 2021	Bulletin 17C Analysis	-20%
17	North Grape Creek near Johnson City (LCRA Gage 3369)	89.0	87,700	36,713	Pedernales, 2021	USGS Regression Equations	-58%
18	Pedernales Rv nr Johnson City, TX (USGS Gage 08153500)	900.9	231,700	173,161	Pedernales, 2021	Bulletin 17C Analysis	-25%
19	Miller Creek near Johnson City (LCRA Gage 3491)	87.5	96,800	39,058	Pedernales, 2021	USGS Regression Equations	-60%
20	Cypress Creek near Cypress Mill (LCRA Gage 3558)	71.2	80,200	33,422	Pedernales, 2021	USGS Regression Equations	-58%
25	Colorado River at Austin, TX (USGS Gage 08158000)	250.2	115,000	72,970	Lower Colorado Cummins, 2018	Bulletin 17C Analysis	-37%
26	Gilleland Creek near Manor (LCRA Gage 5417)	41.4	18,800	29,564	Lower Colorado Cummins, 2018	Bulletin 17C Analysis	57%
27	Wilbarger Creek near Elgin (LCRA Gage)	163.7	48,200	62,422	Lower Colorado Cummins, 2018	Bulletin 17C Analysis	30%
28	Colorado River at Bastrop, TX (USGS Gage 08159200)	1223.8	159,600	125,100	Lower Colorado Cummins, 2018	Bulletin 17C	-22%

Location Number	Location Description	Drainage Area* (sq mi)	Recommended WHA 1% AEP (100-yr) Peak Flow (cfs)	BLE Data 1% AEP (100-yr) Peak Flow (cfs)	BLE Data Source	BLE Hydrologic Method	% Difference from Recommended
29	Colorado Rv at Smithville, TX (USGS Gage 08159500)	1705.8	149,500	152,900	Lower Colorado Cummins, 2018	Bulletin 17C	2%
30	Colorado Rv abv La Grange, TX (USGS Gage 08160400)	2117.3	143,200	183,500	Lower Colorado Cummins, 2018	Bulletin 17C	28%
31	Buckners Creek near Muldoon (LCRA Gage 5608)	91.6	36,900	41,320	Lower Colorado Cummins, 2018	Bulletin 17C Analysis	12%
32	Cummings Creek near Frelsburg (LCRA Gage 5696)	251.9	78,300	66,763	Lower Colorado Cummins, 2018	Bulletin 17C Analysis	-15%
33	Colorado River at Columbus, TX (USGS Gage 08161000)	2885.1	144,800	139,500	Lower Colorado Cummins, 2018	Bulletin 17C	-4%

* NOTE: The Drainage Areas listed in this table include only the contributing drainage area that is located downstream of significant flood control reservoirs.

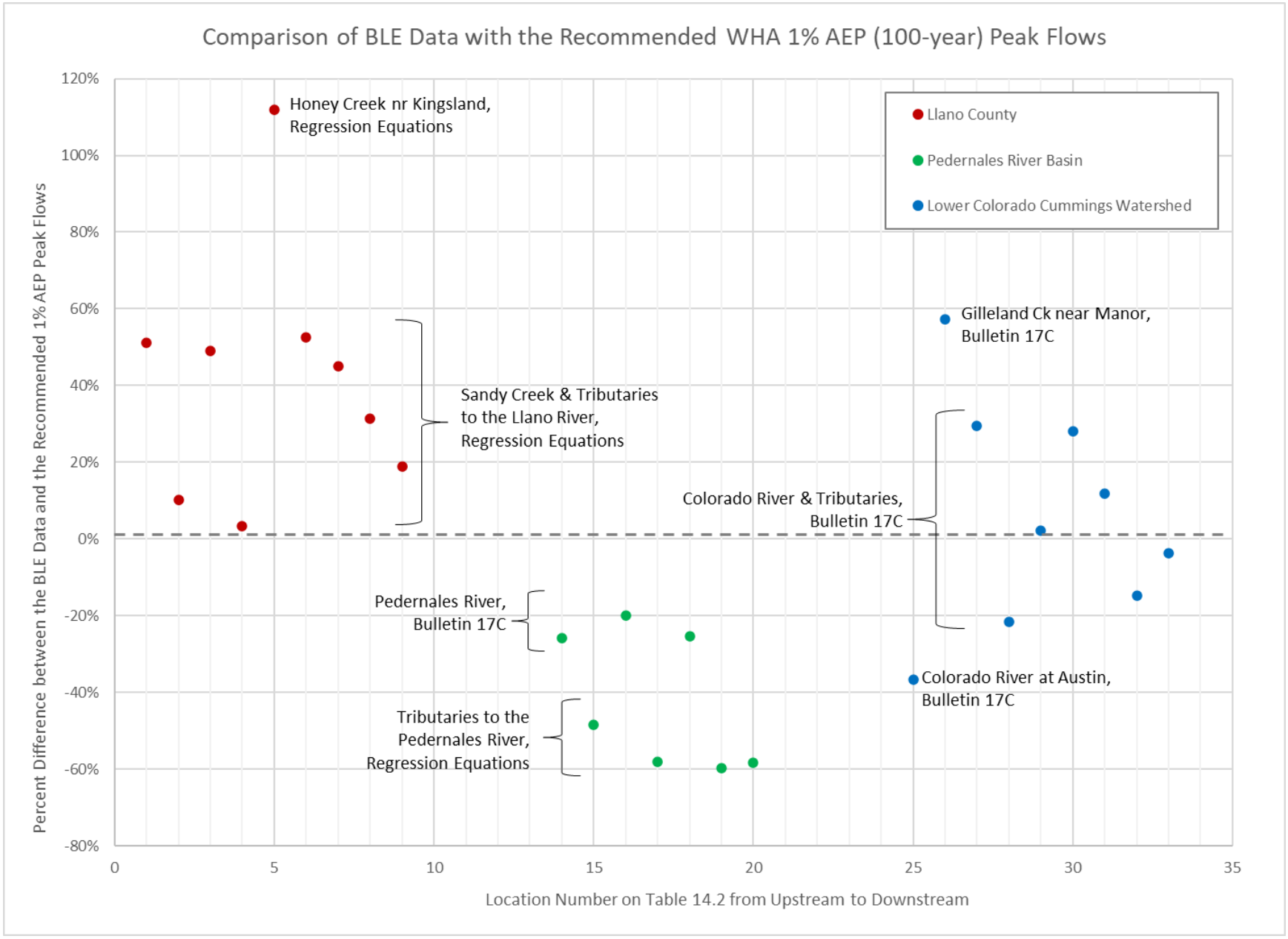

Figure 14.4: Percent Difference between the Published BLE versus the Recommended WHA 1% AEP (100-year) Peak Flows

14.5 RECOMMENDATIONS FOR IMPLEMENTATION

Over the last 10 years alone, Texas has experienced a series of major flood events that have resulted in severe losses of human life and property damages. Therefore, it is imperative that future updates to the published flood insurance rate maps for the Lower Colorado River Basin accurately reflect the known levels of flood risk in the basin. The recommended results from this study represent the best available estimate of flood risk for the larger streams in the Lower Colorado River basin, based on a range of hydrologic methods performed by an expert team of engineers and scientists from multiple federal agencies. For smaller tributaries in the Lower Colorado River basin, the recommended results from the watershed model provide a good starting point which could be further refined by adding additional subbasins and using methodologies that are consistent with this study.

As a result of the level of investment, analyses, and collaboration that went into this Watershed Hydrology Assessment, the flood risk estimates contained in this report are recommended as the basis for future NFIP studies or other federal flood risk studies within the Lower Colorado River basin. These federally developed frequency flow results form a consistent understanding of hydrology across the Colorado watershed, which is a key requirement outlined in FEMA's General Hydrologic Considerations Guidance. Furthermore, the models and data used to produce these flood risk estimates are available upon request, at no charge, to communities, local stakeholders, and architecture engineering firms. Requests for the models should be sent to the InFRM team through the InFRM website at www.InFRM.us.

While the results from this study should be considered the best available estimates of flood risk for many areas of the Colorado River basin, significant uncertainty still remains, as it does in any hydrologic study. Because of this uncertainty and because of the potential impacts that these estimates can have on life and property, the InFRM team strongly recommends and supports local communities that implement higher floodplain standards, such as additional freeboard requirements, floodplain management practices based on standards greater than the 1% annual chance flood, and/or "no valley storage loss" criteria. Higher freeboard requirements and standards greater than the 1% annual chance flood help mitigate for the uncertainty and variability in flood risk estimation, while the preservation of valley storage helps to stabilize flood elevations while allowing permitted development in the floodplain (NCTCOG, 2020).

One issue that has not been adequately addressed in the present study is the impact of future land use and future climate conditions on the hydrology of the Lower Colorado River basin. Future growth of the Austin metropolitan area is expected to drive increases in urban land use in Travis County and the surrounding areas. While there are straightforward and standard techniques that can be used to estimate the impacts of future land use on the hydrology of the Lower Colorado River basin, estimating the effects of future climate conditions on flood frequency and severity is still an area of ongoing research.

NOAA's Hydrometeorological Design Study Center (HDSC) is currently working on a national publication called NOAA Atlas 15, which will include estimates of frequency rainfall depths under future climate conditions (NOAA, 2022b). The InFRM team is currently waiting on additional guidance from NOAA Atlas 15, which is scheduled to be completed in 2026, in order to quantify the effects of future climate change on the hydrology of Texas and the Lower Colorado River basin. A quantitative assessment of future climate and future land use conditions may then be added as an addendum to this report.

15 References and Resources

15.1 REFERENCES

Asquith, W.H., *Effects of regulation on L-moments of annual peak streamflow in Texas*: U.S. Geological Survey Water-Resources Investigations Report 01–4243, 66 p., http://pubs.usgs.gov/wri/wri014243/; 2001.

Asquith, W.H., *Distributional analysis with L-moment statistics using the R environment for statistical computing*: Ph.D. dissertation, Texas Tech University, accessed on June 3, 2016 at https://ttu-ir.tdl.org/ttu-ir/handle/2346/ETD-TTU-2011-05-1319; 2011a.

Asquith, W.H., *Distributional analysis with L-moment statistics using the R environment for statistical computing*: CreateSpace, [print-on-demand], ISBN 978–146350841–8, [reprinting of Asquith (2011a), with errata]; 2011b.

Asquith, W.H., and Roussel, M.C., *Regression equations for estimation of annual peak-streamflow frequency for undeveloped watersheds in Texas using an L-moment-based, PRESS-minimized, residual-adjusted approach*: U.S. Geological Survey Scientific Investigations Report 2009–5087, 48 p., http://pubs.usgs.gov/sir/2009/5087/; 2009.

Asquith, W.H., England, J.F., and Herrmann, G.R. (contributor), 2020, *MGBT—Multiple Grubbs-Beck low-outlier test: U.S. Geological Survey software release, R package*, Reston, Va., accessed July 27, 2020, at https://doi.org/10.5066/P9CW9EF0.

Asquith, W.H. and Famiglietti, J.S. *Precipitation Areal-Reduction Factor Estimation Using an Annual-Maxima Centered Approach.* Journal of Hydrology. 2000.

Asquith, W.H., Roussel, M.C., Atlas of *Depth-Duration Frequency of Precipitation Annual Maxima for Texas*; U.S. Geological Survey Scientific Investigations Report 2004-5041; 2009.

Asquith, W.H., Roussel, M.C., and Vrabel, Joseph, *Statewide analysis of the drainage-area ratio method for 34 streamflow percentile ranges in Texas*: U.S. Geological Survey Scientific Investigation Report 2006–5286, 34 p., 1 appendix, http://pubs.usgs.gov/sir/2006/5286/; 2006.

Asquith, W.H., and Slade, R.M., 1995, Flood frequency in Texas—Calculation of peak-streamflow frequency at gaging stations: U.S. Geological Survey Fact Sheet FS-181-95, 2 p., accessed May 24, 2022, at https://doi.org/10.3133/fs18195

Asquith, W.H., and Slade, R.M., *Regional equations for estimation of peak-streamflow frequency for natural basins in Texas*: U.S. Geological Survey Water-Resources Investigations Report 96-4307, 68p., accessed September 21, 2017 at https://doi.org/10.3133/wri964307; 1997

Asquith, W.H., and Thompson, D.B., *Alternative regression equations for estimation of annual peak-streamflow frequency for undeveloped watersheds in Texas using PRESS minimization*: U.S. Geological Survey Scientific Investigations Report 2008–5084, 40 p., http://pubs.usgs.gov/sir/2008/5084/; 2008.

Asquith, W.H., Yesildirek, M.V., Landers, R.N., Cleveland, T.G., Fang, Z.N., and Zhang, J., 2021, *Technique to estimate generalized skew coefficients of annual peak streamflow for natural basins in Texas*, in Cleveland, T.G., Fang, Z.N., Zhang, J., and Landers, R.N., 2021, Develop a generalized skew update and regional study of other measures of distribution shape for Texas flood frequency analyses: Texas Department of Transportation Research Report 0-6977-1, chapter N, p. 1-19, accessed Jun. 1, 2022, at https://rosap.ntl.bts.gov/view/dot/60662.

Banner, J.L., Jackson, C.S., Yang, Z., Hayhoe, K., Woodhouse, C., Gulden, L., Jacobs, K., North, G., Leung, R., Washington, W., Jiang, X., and Casteel, R., 2010, *Climate change impacts on Texas water—A white paper assessment of the past, present, and future recommendations for action*: Texas Water Journal v. 1 no. 1, p. 1-19, accessed Mar. 16, 2021, at https://doi.org/10.21423/twj.v1i1.1043.

Barbie, D.L., Wehmeyer, L.L., and May, J.E., 2012, *Analysis of trends in selected streamflow statistics for the Concho River Basin, Texas, 1916–2009*: U.S. Geological Survey Scientific Investigations Report 2012–5193, 15 p, accessed Sep. 2, 2020, at https://doi.org/10.3133/sir20125193.

Box, T.W., 1967, Range deterioration in west Texas: The Southwestern Historical Quarterly, v. 71, no. 1, p. 37-45, accessed August 8, 2022, at https://www.jstor.org/stable/30237942.

Breeding, S.D. and Dalrymple, T. *Texas Floods of 1938 and 1939.* USGS Water Supply Paper 914. 1944.

Breeding, S.D. and Montgomery, J.H. *Floods of September 1952 in the Colorado and Guadalupe River Basins, Central Texas.* USGS Water Supply Paper 1260-A. 1954.

Cohn, T. A., Lane, W. L., and Baier, W. G. *An algorithm for computing moments-based flood quantile estimates when historical flood information is available*. Water Resources Research, 33(9):2089–2096. 1997.

Cohn, T. A., Lane, W. L., and Stedinger, J. R. *Confidence intervals for Expected Moments Algorithm flood quantile estimates.* Water Resources Research, 37(6):1695–1706. 2001.

Cohn, T.A., England, J.F., Berenbrock, C.E., Mason, R.R., Stedinger, J.R., and Lamontagne, J.R., 2013, A generalized Grubbs-Beck test statistic for detecting multiple potentially influential low outliers in flood series: Water Resources Research, v. 49, no. 8, p. 5047–5058. [Also available at https://doi.org/10.1002/wrcr.20392.]

Cohn, T.A., and Lins, H.F., 2005, *Nature's style—Naturally trendy*: Geophysical Research Letters (L23402), v. 32, no. 23, 5p., accessed June 9, 2022, at https://doi.org/10.1029/2005GL024476.

Cunderlik, J.M., and Burn, D.H., 2003, *Non-stationary pooled flood frequency analysis:* Journal of Hydrology, v. 276, no. 1–4, p. 210–233, accessed June 9, 2022, at https://doi.org/doi:10.1016/S0022-1694(03)00062-3.

Dalrymple, T., 1939. Water-Supply Paper 796-G – Major Texas Floods of 1935. U.S. Department of the Interior. https://pubs.usgs.gov/wsp/0796g/report.pdf

Dalrymple, T. 1937. Water-Supply Paper 816 – Major Texas Floods of 1936. U.S. Department of the Interior. https://pubs.usgs.gov/wsp/0816/report.pdf

Duan, Q. Y., Gupta, V. K., & Sorooshian, S. *Shuffled complex evolution approach for effective and efficient global minimization. Journal of optimization theory and applications*, 76(3), 501-521. 1993.

England, J.F., Jr.; Cohn, T.A.; Faber, B.A.; Stedinger, J.R.; Thomas, W.O., Jr.; Veilleux, A.G.; Kiang, J.E.; and Mason, R.R., Jr., 2019, *Guidelines for determining flood flow frequency—Bulletin 17C* (ver. 1.1, May 2019): U.S. Geological Survey Techniques and Methods, book 4, chap. B5, 148 p., accessed June 29, 2022, at https://doi.org/10.3133/tm4B5.

Faber, B. *Flood Frequency Analysis. "Lecture 3.4 Uncertainty in Frequency Estimates,"* Training at the USACE Hydrologic Engineering Center (HEC), May 2018.

FEMA, *Base Level Engineering (BLE) Analysis, Region 6 Neches River Watershed*. https://webapps.usgs.gov/infrm/estBFE/. August 2019.

FEMA, *Flood Insurance Study for Hardin County, TX and Incorporated Areas*, FIS Number 48199CV000A, Revised October 6, 2010.

FEMA, *Flood Insurance Study for Jefferson County, TX and Incorporated Areas*, Community Number 480385V000, Revised August 6, 2002.

FEMA, *Preliminary Flood Insurance Study for Jefferson County, TX and Incorporated Areas*, FIS Number 48245CV000A, Revised 2011.

Flynn, K.M., Kirby, W.H., and Hummel, P.R., 2006, User's Manual for Program PeakFQ Annual Flood-Frequency Analysis Using Bulletin 17B Guidelines: U.S. Geological Survey, Techniques and Methods Book 4, Chapter B4; 42 p, accessed May 26, 2022 at https://doi.org/10.3133/tm4B4.

George, P.G., Mace, R.E., and Petrossian, R., 2011, *Aquifers of Texas*: Texas Water Development Board Report 380, 172 p., accessed September 21, 2020, at http://www.twdb.texas.gov/publications/reports/numbered_reports/index.asp.

Good, P.I., and Hardin, J.W., *Common errors in statistics (and how to avoid them)*: New York, John Wiley, ISBN 0–471–46068–0, 2006.

Gumbel, E. J., 1958, *Statistics of extremes*, Columbia Univ. press, New York. 1958.

Gupta, R. D. *Hydrology and Hydraulic Systems*. Long Grove: Waveland Press. 2008.

Halff Associates, 2002. *Colorado River Flood Damage Evaluation Project (FDEP) Volume 1. Hydrology-Hydraulics Appendix.*

Hansen, E.M., L.C. Schreiner, and J.F. Miller. *Application of Probable Maximum Precipitation Estimates – United States East of the 105th Meridian*. *Hydrometeorological Report No. 52*. National Weather Service, Washington D.C. 1982.

Harwell, G.R., McDowell, J.S., Gunn, C.L., and Garrett, B.S., 2020, *Precipitation, temperature, groundwater-level elevation, streamflow, and potential flood storage trends within the Brazos, Colorado, Big Cypress, Guadalupe, Neches, Sulphur, and Trinity River Basins in Texas through 2017* (ver. 1.1, April 2020): U.S. Geological Survey Scientific Investigations Report 2019–5137, 94 p., accessed June 29, 2022, at https://doi.org/10.3133/sir20195137.

Helsel, D.R., Hirsch, R.M., Ryberg, K.R., Archfield, S.A., and Gilroy, E.J., 2020, *Statistical methods in water resources*: U.S. Geological Survey Techniques and Methods, book 4, chap. A3, 458 p., accessed June 29, 2022, https://doi.org/10.3133/tm4a3. [Supersedes USGS Techniques of Water-Resources Investigations, book 4, chap. A3, version 1.1.]

Hershfield, D.M. *Rainfall-Intensity-Duration-Frequency Curves for Selected Stations in the United States, Alaska, Hawaiian Islands, and Puerto Rico*. *Technical Paper 25*. U.S. Weather Bureau. 1955.

Hershfield, D.M. *Rainfall Intensity-Frequency Regime. Technical Paper 29, Part 1 The Ohio Valley, Part 2 Southeastern United States*. U.S. Weather Bureau. 1957, 1958.

Hershfield, D.M. *Rainfall frequency atlas of the United States for durations from 30 minutes to 24 hours and return periods from 1 to 100 years, TP 40*. National Weather Service. 1961.

Hirsh, R.M. *A Comparison of Four Streamflow Record Extension Techniques.* US Geological Survey, Water Resources Research, Vol. 18, No. 4, Pages 1081-1088, Aug 1982.

Hirsch, R.M., 2018*, Daily Streamflow Trend Analysis*: U.S. Geological Survey Water Data for the Nation Blog, accessed July 19, 2021, at https://waterdata.usgs.gov/blog/quantile-kendall/.

Hirsch, R.M., and De Cicco, L.A., 2015*, User guide to Exploration and Graphics for RivEr Trends (EGRET) and dataRetrieval—R packages for hydrologic data* (version 2.0, February 2015): U.S. Geological Survey Techniques and Methods book 4, chap. A10, 93 p., accessed June 9, 2022, at https:// doi.org/10.3133/tm4A10.

Hirsch, R.M. and Stedinger, J.R. *Plotting positions for historical floods and their positions*, Water Resources Research, Vol 23, No. 4, p. 715–727, accessed on March 30, 2018 at https://doi.org/10.1029/WR023i004p00715. 1987.

Hodgkins, G.A., Dudley, R.W., Archfield, S.A., and Renard, B., 2019, Effects of climate, regulation, and urbanization on historical flood trends in the United States: Journal of Hydrology 573(2019) p. 697-709, accessed Nov. 2, 2020, at https://doi.org/10.1016/j.jhydrol.2019.03.102.

Hoerling, M.P., Dettinger, M., Wolter, K., Lukas, J., Eischeid, J., Nemani, R., Liebmann, B., and Kunkel, K.E., 2013, Present Weather and Climate—Evolving Conditions, *in* Garfin, G., Jardine, A., Merideth, R., Black, M., and LeRoy, S., Assessments of climate change in the southwest United States, a report prepared for the National Climate Assessment by the Southwest Climate Alliance, Island Press, Washington D.C., 553 p., accessed June 23, 2022, at https://link-springer-com.usgslibrary.idm.oclc.org/book/10.5822/978-1-61091-484-0.

Hollander, M., and Wolfe, D.A., *Nonparametric statistical procedures*: John Wiley and Sons, New York, 503 p. 1973.

Interagency Advisory Committee on Water Data [IACWD], *Guidelines for determining flood flow frequency: Bulletin 17B*, Reston, Virginia, U.S. Department of the Interior, Geological Survey, accessed on May 10, 2016 at http://water.usgs.gov/osw/bulletin17b/dl_flow.pdf; 1982.

Interagency Flood Risk Management (InFRM). *Watershed Hydrology Assessment for the Guadalupe River Basin.* 2019.

Interagency Flood Risk Management (InFRM). *Watershed Hydrology Assessment for the Trinity River Basin.* 2021.

Jiang, X., and Yang, Z., 2012, *Projected changes of temperature and precipitation in Texas from downscaled global climate models*: Climate Research 53, p. 229-244, accessed Mar. 16 2021, at https://doi.org/10.3354/cr01093.

Judd, L., Asquith, W.H., and Slade, R.M., *Techniques to estimate generalized skew coefficients of annual peak streamflow for natural basins in Texas*: U.S. Geological Survey Water Resource Investigations Report 96–4117, 28 p., http://pubs.usgs.gov/wri/wri97-4117/; 1996.

Kang, B., Kim, E., Kim, J., & Moon, S. *Comparative study on spatiotemporal characteristics of fixed-area and storm-centered ARFs*. 2019.

Liu, L., Hong, Y., Hocker, J.E., Shafer, M.A., Carter, L.M., Gourley, J.J., Bednarczyk, C.N., Yong, B., and Adhikari, P., 2012, *Analyzing projected changes and trends of temperature and precipitation in the southern USA from 16 downscaled global climate trends*: Theoretical and Applied Climatology, v. 109, p. 345–360, accessed Mar. 16, 2021, at https://doi.org/10.1007/s00704-011-0567-9.

Lower Colorado River Authority [LCRA], 2022, Key elevations for Lake Travis during floods, accessed June 23, 2022, at https://www.lcra.org/water/floods/key-elevations-for-lake-travis-during-floods/.

Mallakpour, I., and Villarini, G., 2016*, A simulation study to examine the sensitivity of the Pettitt test to detect abrupt changes in mean*, Hydrological Sciences Journal, vol. 61, no. 2, p. 245-254, accessed 23 July, 2020, at https://doi.org/10.1080/02626667.2015.1008482.

McEnroe, B. and Gonzalez, P. *Storm Duration and Antecedent Moisture Conditions for Flood Discharge Estimation*. Kansas Department of Transportation. November 2003.

MetStat, 2017. Storm Precipitation Report 14-18 September 1936. Prepared for USACE Fort Worth District.

Minshall, N.E. *Predicting Storm Runoff on Small Experimental Watersheds*. Paper No. 3333, ASCE. 1962.

Moriasi, D.N., et al. *Model Evaluation Guidelines for Systematic Quantification of Accuracy in Watershed Simulations*. American Society of Agricultural and Biological Engineers. 2007.

Moriasi, D.N., et al. *Hydrologic and Water Quality Models: Performance Measures and Evaluation Criteria*. American Society of Agricultural and Biological Engineers. 2012.

Myers, Vance, *Meteorology of Hypothetical Flood Sequences in the Mississippi River Basin, HMR 35*. US Weather Bureau and Army Corps of Engineers. 1959.

Myers, Vance. *Criteria and Limitations for the Transposition of Large Storms Over Various Size Watersheds.* U.S. Weather Bureau and U.S. Department of Commerce. 1966.

Meyers, V.A., Zehr, R.M., *A Methodology for Point-to-Area Rainfall Frequency Ratios. NOAA Technical Report NWS 24.* National Weather Service. 1980.

North Central Texas Council of Governments (NCTCOG). *Corridor Certificate Manual, Trinity River Corridor*. 4th Edition. Available online at http://trinityrivercdc.com/ 2020.

Natural Resources Conservation Service (NRCS), United States Department of Agriculture (USDA). *Web Soil Survey*. Available online at https://websoilsurvey.nrcs.usda.gov/. Accessed July 2014.

National Centers for Environmental Information (NCEI), U.S. climatological divisions: National Oceanic and Atmospheric Administration, accessed on July 24, 2016 at https://www.ncdc.noaa.gov/monitoring-references/maps/images/us-climate-divisions-names.jpg; 2016a.

NCEI, Climate indices: National Oceanic and Atmospheric Administration, accessed on July 24, 2016 at http://www7.ncdc.noaa.gov/CDO/CDODivisionalSelect.jsp; 2016b.

NCEI, Historical Palmer Drought Indices: National Oceanic and Atmospheric Administration, accessed on July 24, 2016 at http://www.ncdc.noaa.gov/temp-and-precip/drought/historical-palmers.php and http://www.ncdc.noaa.gov/temp-and-precip/drought/historical-palmers/overview; 2016c.

NCEI. State Summaries 149-TX, NOAA Technical Report NESDIS 149-TX. https://statesummaries.ncics.org/chapter/tx/ 2017.

NCEI, U.S. climate divisions—History of the U.S. climate divisional dataset: National Oceanic and Atmospheric Administration, accessed on May 10, 2016 at http://www.ncdc.noaa.gov/monitoring-references/maps/us-climate-divisions.php; 2016d.

National Drought Mitigation Center; U.S. Department of Agriculture; National Oceanic and Atmospheric Administration (2019). United States Drought Monitor. University of Nebraska-Lincoln. https://data.nal.usda.gov/dataset/united-states-drought-monitor. Accessed 2023-07-25

Nielsen-Gammon, J., Holman, S., Buley, A. & Jorgensen, S. (2021a). Assessment of Historic and Future Trends of Extreme Weather in Texas, 1900-2036. Office of the Texas State Climatologist. OSC-202101. https://climatexas.tamu.edu/files/ClimateReport-1900to2036-2021Update

Nielsen-Gammon, J. & Jorgensen, S. (2021b). Climate Change Recommendations for Regional Flood Planning. Office of the Texas State Climatologist. OSC Report 2021-01.

Nelder, J. A., & Mead, R. *A simple method for function minimization.* The computer journal, 7(4), 308-313. 1965.

Nelson, T.L. *Synthetic Unit Hydrograph Relationships Trinity River Tributaries, Fort Worth-Dallas Urban Area*, 1979.

NOAA, 2020, *Climate Data Online*: Web Services Documentation, accessed Dec. 3, 2020, at https://www.ncdc.noaa.gov/cdo-web/webservices/v2#gettingStarted.

NOAA, Hydrometeorological Design Studies Center, *Precipitation Frequency Data Server (PFDS).* https://hdsc.nws.noaa.gov/hdsc/pfds/ Accessed Dec 2021.

NOAA, *NOAA Atlas 14 Precipitation Frequency Atlas of the United States: Volume 11 Version 2.0: Texas*. 2018.

NOAA, National Weather Service, Office of Water Prediction. (2022a). Analysis of Impact of Nonstationary Climate on NOAA Atlas 14 Estimates. https://hdsc.nws.noaa.gov/hdsc/files25/NA14_Assessment_report_202201v1.pdf

NOAA, National Weather Service. (2022b). Public Information Statement 22-59. Soliciting Comments on Proposed Methods to Update the National Precipitation Frequency Standard through November 15, 2022. https://www.weather.gov/media/notification/pdf2/pns22-59_atlas_15.pdf

Palmer, W., *Meteorological drought*: U.S. Department of Commerce, Weather Bureau Research Paper 45. 1965.

Pettitt, A.N., 1979, A non-parametric approach to the change-point problem: Journal of the Royal Statistical Society. Series C (Applied Statistics), v.28, no.2, p.126-135, accessed June 29, 2022, at https://www.jstor.org/stable/2346729.

PRISM Climate Group, 2018, Northwest Alliance for Computational Science and Engineering—Time series values for individual locations, accessed on July 30, 2018, at http://www.prism.oregonstate.edu/explorer/.

Rantz, S.E., and others, 1982, Measurement and computation of streamflow: U.S. Geological Survey Water Supply Paper 2175, 2 v., 631 p., accessed Sep. 2, 2020, at https://doi.org/10.3133/wsp2175.

RiverWare. *Technical Documentation Version 7.4*, *USACE-SWD Methods*, Center for Advanced Decision Support for Water and Environmental Systems (ADSWES), University of Colorado Boulder. 2019.

Rodman, P.K. *Effects of Urbanization on Various Frequency Peak Discharges*, 1977.

Ruggles, F.H. Jr., 1966*, Floods on small streams in Texas:* U.S. Geological Survey Open-File Report 66-119, 98 p., accessed June 30, 2022, at https://doi.org/10.3133/ofr66119.

Ryberg, K.R., Hodgkins, G.A., and Dudley, R.W., 2019, *Change points in annual peak streamflows—Method comparisons and historical changes points in the United States*: Journal of Hydrology, v. 583, no. 124307, 13 p., accessed July 22, 2020, at https://doi.org/10.1016/j.jhydrol.2019.124307.

Ryberg, K.R., Kolars, K.A., Kiang, J.E., and Carr, M.L., 2020, *Flood-frequency estimation for very low annual exceedance probabilities using historical, paleoflood, and regional information with consideration of*

nonstationarity: U.S. Geological Survey Scientific Investigations Report 2020–5065, 89 p., accessed June 9, 2022, at https://doi.org/10.3133/sir20205065.

Sauer, S. P., 1972, *Factors Contributing to Unusually Low Runoff During the Period 1962–68 in the Concho River Basin, Texas*: U.S. Geological Survey Water-Supply Paper 1999-L, 48 p, accessed Sep. 2, 2020, at https://doi.org/10.3133/wsp1999L.

Slade, R.M. Jr., Asquith, W.H., 1996, *Peak data for U.S. Geological Survey gaging stations, Texas network and computer program to estimate peak-streamflow frequency*: U.S. Geological Survey Open-File Report 96-148, 57p., accessed June 30, 2022, at https://doi.org/10.3133/ofr96148.

Slade, R. M., 2020, *Runoff inflow volumes to the Highland Lakes in Central Texas--Temporal trends in volumes and relations between volumes and selected climactic indices*: Texas Water Journal v. 11, no. 1, p. 32–60, accessed June 9, 2022, at https://journals.tdl.org/twj/index.php/twj/article/view/7025.

Smeins, F.E., Fuhlendorf, S.D., and Taylor, C.A., 1997, *Environmental and land use changes—A long-term perspective*: Juniper symposium, Texas A&M Research and Extension Center, accessed August 8, 2022, at https://texnat.tamu.edu/library/symposia/juniper-ecology-and-management/environmental-and-land-use-changes-a-long-term-perspective/.

State of Texas, Board of Water Engineers. *Texas Floods of April – May – June 1957*. October 1957.

Snyder, F.F. *Synthetic Unit Graphs.* Transactions. American Geophysical Union. 1938.
Texas Water Development Board (TWDB), *Chapter 4: Climate of Texas*, *Water for Texas 2012 State Water Plan*. 2012.

Texas Water Development Board [TWDB], 1997, *Lake Brownwood Hydrographic Survey Report*, accessed July 20, 2021, at http://www.twdb.texas.gov/surfacewater/surveys/completed/files/brownwood/1997-04/Brownwood1997_FinalReport.PDF.

Texas Water Development Board [TWDB], 2001, *Texas Water Development Board Report 347: Surveys of irrigation in Texas 1958, 1964, 1969, 1974, 1979, 1984, 1989, 1994, and 2000*, accessed October 5, 2020, at https://www.twdb.texas.gov/publications/reports/numbered_reports/doc/R347/Report347.asp.

Texas Water Development Board [TWDB], 2020, *Water Data for Texas*: accessed September 21, 2020, at https://www.waterdatafortexas.org/reservoirs/statewide.

Texas Water Development Board [TWDB], 2022, *Texas lakes and reservoirs—History of reservoir construction in Texas*, accessed June 13, 2022, at http://www.twdb.texas.gov/surfacewater/rivers/reservoirs/index.asp.

University of Colorado Boulder, 2020, Center of advanced Decision Support for Water and Environmental System (RiverWare), Version 8.0.1, retrieved from www.riverware.org

USACE. Engineer Manual 1110-3-1411, “Standard Project Flood Determinations.” Available from: http://www.publications.usace.army.mil/Portals/76/Publications/EngineerManuals/EM_1110-2-1411.pdf

USACE, 2003. *Final interim feasibility report and integrated environmental assessment for the Pecan Bayou Watershed, Brownwood, Texas,* accessed June 9, 2022, at https://www.swf.usace.army.mil/Portals/47/docs/ContinuingAuthoritiesProgram/Willis%20Creek/February%202003%20Final%20Feasibility%20Report%20and%20Environmental%20Assessment.pdf.

USACE, 2022, Hydrologic Engineering Center Hydrologic Modeling System (HEC-HMS): U.S. Army Corps of Engineers software version 4.10, accessed July 2022, at https://www.hec.usace.army.mil.

USACE, 2022, Hydrologic Engineering Center's Meteorological Visualization Utility Engine (HEC-MetVue) U.S. Army Corps of Engineers software version 3.1, accessed January 2022, at https://www.hec.usace.army.mil.

USACE, 2022, Hydrologic Engineering Center Statistical Software Package (HEC-SSP): U.S. Army Corps of Engineers software version 2.2, accessed Dec 2019, at https://www.hec.usace.army.mil.

USACE. *Hydrologic Hazard Curves for Success Dam*, Sacramento District, 26 p. 2017.

USACE. *Inflow Design Floods for Dam and Reservoirs*. ER 110-8-2(FR). 1991.

USACE. *National Inventory of Dams (NID)*. https://nid.sec.usace.army.mil/ords/f?p=105:1 Accessed June 2016.

USACE. *Storm rainfall in the United States, depth, area, duration data*. Revised January 2, 1962. 1945.

USACE, Fort Worth District. *Determination of Percent Sand in Watersheds.* 1986.

USACE, Fort Worth District. *SWFHYD "NUDALLAS" Documentation*, 1989.

USACE, Fort Worth District. *Mansfield (Marshall Ford) Dam and Lake Travis, Colorado River Basin, TX Water Control Manual.* Revised Sept 2013.

USACE, Fort Worth District. *Corps Water Management System (CWMS) Final Report for the Colorado River Watershed*. February 2015.

USACE, Risk Management Center (RMC). *Probable maximum flood analysis for Whittier Narrows Dam*. 2017.

USACE, 2018, *Risk Management Center Reservoir Frequency Analysis (RMC-RFA*), Version 1.1.0, obtained from RMC.

U.S. Department of Agriculture (USDA). *Urban hydrology for small watersheds*. Soil Conservation Service, Engineering Division. Technical Release 55 (TR-55). 1986.

USGCRP. (2017). Climate Science Special Report: Fourth National Climate Assessment, Volume I [Wuebbles, D.J., D.W. Fahey, K.A. Hibbard, D.J. Dokken, B.C. Stewart, and T.K. Maycock (eds.)]. U.S. Global Change Research Program, Washington, DC, USA, 470 pp., doi: 10.7930/J0J964J6.

U.S. Geological Survey (USGS), *Description of Gaging Station on Colorado River at Austin, Tex*. 1963.

U.S. Geological Survey (USGS), *PeakFQ—Flood Frequency Analysis Based on Bulletin 17B and recommendations of the Advisory Committee on Water Information (ACWI) Subcommittee on Hydrology (SOH) Hydrologic Frequency Analysis Work Group (HFAWG)*: accessed on May 7, 2016 at http://water.usgs.gov/software/PeakFQ/. 2014.

U.S. Geological Survey (USGS). *3DEP LiDAR Explorer*. Available from: https://prd-tnm.s3.amazonaws.com/LidarExplorer/index.html#/. Accessed in May of 2018. 2018.

U.S. Geological Survey, *Computation of annual exceedance probability (AEP) for characterization of observed flood peaks*: U.S. Geological Survey Office of Surface Water Technical Memorandum 2013.01 accessed on July 1, 2015 at http://water.usgs.gov/admin/memo/SW/sw13.01.pdf; 2012.

U.S. Geological Survey [USGS], *USGS Water data for the Nation: U.S. Geological Survey National Water Information System (NWIS) database*: accessed in May 18,2022, at https://doi.org/10.5066/F7P55KJN. 2022.

Veilleux, A.G., Cohn, T.A., Kathleen M. Flynn, K.M., Mason, R.R., Jr., and Hummel, P.R., *Estimating magnitude and frequency of floods using the PeakFQ 7.0 program*: U.S. Geological Survey Fact Sheet 2013–3108, 2 p., http://pubs.usgs.gov/fs/2013/3108/; 2013.

Venkataraman, K., Tummuri, S., Medina, A., Perry, J., 2016, *21st century drought outlook for major climate divisions of Texas based on CMIP5 multimodel ensemble—Implications for water resource management*: Journal of Hydrology 534(2016) p. 200-316, accessed March 16, 2021, at http://doi.org/10.1016/j.jhydrol.2016.01.001.

Wilcox, B.P., Huang, Y., and Walker, J.W., 2008, *Long-term trends in streamflow from semiarid rangelands—Uncovering drivers of change*: Global Change Biology vol 14, p. 1676-1689, accessed December 22, 2020, at https://doi.org/10.1111/j.1365-2486.2008.01578.x.

15.2 SOFTWARE

ArcGIS, Environmental Systems Research Institute, Inc., ArcMap 10.2.2: Retrieved from http://www.esri.com/.

CWMS, US Army Corps of Engineers, Corps Water Management System, CWMS 2.1, retrieved from http://www.hec.usace.army.mil.

HEC-DSSVue, US Army Corps of Engineers, HEC-DSSVue 2.0.1: Retrieved from http://www.hec.usace.army.mil.

HEC-GeoHMS, US Army Corps of Engineers, HEC-GeoHMS 10.2: Retrieved from http://www.hec.usace.army.mil

HEC-HMS, US Army Corps of Engineers, Hydrologic Engineering Center Hydrologic Modeling System, HEC-HMS 4.3: Retrieved from http://www.hec.usace.army.mil

HEC-MetVue, US Army Corps of Engineers, Hydrologic Engineering Center Meteorological Visualization Utility Engine, HEC-MetVue 3.1 (2019): Retrieved from http://www.hec.usace.army.mil

HEC-RAS, US Army Corps of Engineers, Hydrologic Engineering Center River Analysis System, HEC-RAS 5.0.7: Retrieved from http://www.hec.usace.army.mil.

HEC-SSP, US Army Corps of Engineers, Hydrologic Engineering Center Statistical Software Package, HEC-SSP 2.2: Retrieved from http://www.hec.usace.army.mil

PeakFQ, U.S. Geological Survey (USGS), Hydrologic Frequency Analysis Work Group (HFAWG). PeakFQ retrieved from http://water.usgs.gov/software/PeakFQ/

Python Software Foundation. Python Language Reference, version 2.7. Retrieved from http://www.python.org.

RiverWare, Center of Advanced Decision Support for Water and Environmental System (CADSWES), University of Boulder, RiverWare 7.4, retrieved from www.Riverware.org.

RMC-RFA, UA Army Corps of Engineers, *Risk Management Center Reservoir Frequency Analysis (RMC-RFA),* Version 1.0.0, obtained from the USACE Risk Management Center. 2017.

15.3 DATA SOURCES, GUIDANCE & PROCEDURES

Environmental Systems Research Institute, Inc. (ESRI). United States National Boundary, County Boundaries, Street Centerlines.
Available from: http://www.esri.com/software/arcgis/arcgisonline/services/map-services

Environmental Systems Research Institute, Inc. (ESRI),
http://www.esri.com/software/arcgis/arcgisonline/map_services.html

ESRI Streetmap2D Image Service - ESRI basemap data, DeLorme basemap layers, Automotive Navigation Data (AND) road data, U.S. Geological Survey (USGS) elevation data, UNEP-WCMC parks and protected areas for the world, Tele Atlas Dynamap® and Multinet® street data for North America and Europe and First American (CoreLogic) parcel data for the United States.
ESRI World Imagery Service - Imagery from NASA, icubed, U.S. Geological Survey (USGS), U.S. Department of Agriculture Farm Services Agency (USDA FSA), GeoEye, and Aerials Express.
ESRI. ArcGIS software. Application reference available from: http://www.esri.com/

Federal Emergency Management Agency (FEMA). Publication 64, "Federal Guidelines for Dam Safety, Emergency Action Planning for Dam Owners," Federal Emergency Management Agency (FEMA) U.S. Department of Homeland Security (DHS), Washington, D.C., 2004.
Available from: http://www.fema.gov/library/viewRecord.do?id=1672

Gesch, D., Oimoen, M., Greenlee, S., Nelson, C., Steuck, M., and Tyler, D. "The National Elevation Dataset: Photogrammetric Engineering and Remote Sensing," v. 68, no. 1, p. 5-11, 2002.

Texas Department of Transportation (TxDOT). 2019 Roadway Inventory. Available from:
https://www.txdot.gov/inside-txdot/division/transportation-planning/roadway-inventory.html

USACE. Engineering and Construction Bulletin 2008-10, CECW-CE, March 24, 2008.

USACE. Guideline RD-13, "Flood Emergency Plans -- Guidelines for Corps Dams," USACE Hydrologic Engineering Center, Davis, CA, June 1980.
Available from: http://www.hec.usace.army.mil/publications/pub_download.html

USACE, HEC. HEC-GeoRAS software.
Available from: http://www.hec.usace.army.mil/software/hec-ras/hec-georas_downloads.html

USACE, HEC. HEC-RAS software.
Available from: http://www.hec.usace.army.mil/software/hec-ras/hecras-download.html

USACE, HEC. "HEC-GeoRAS User's Manual," Davis, CA, September 2005.

USACE, HEC. "HEC-HMS Hydrologic Modeling System User's Manual," USACE, Davis, CA, November 2006.

USACE, HEC. "HEC-RAS River Analysis System, Hydraulic Reference Manual," Davis, CA, November 2002.

USACE, HEC. "HEC-RAS River Analysis System User's Manual," Davis, CA, November 2006.

U.S. Department of Agriculture, Farm Service Agency. National Agriculture Imagery Program Images.
Available from: http://www.fsa.usda.gov/FSA/apfoapp?area=home&subject=prog&topic=nai

U.S. Geological Survey (USGS). 3DEP LiDAR Explorer. Available from: https://prd-tnm.s3.amazonaws.com/LidarExplorer/index.html#/.

U.S. Geological Survey (USGS). National Elevation Dataset. Available from: http://ned.usgs.gov/

U.S. Geological Survey (USGS). National Hydrography Dataset. Available from: http://nhd.usgs.gov/data.html

16 Terms of Reference

Acronym	Definition
2D	two-dimensional
3DEP	three-dimensional Elevation Program
AEP	annual exceedance probability
BFE	base flood elevations
BLE	Base Level Engineering
cfs	cubic feet per second
CWMS	Corps Water Management System
DDF	Depth Duration Frequency
DEM	digital elevation model
DSS	data storage system
EM	Engineering Manual
ER	Engineering Regulation
EMA	expected moment algorithm
ERDC	Engineering Research & Development Center of USACE
FEMA	Federal Emergency Management Agency
FIS	flood insurance study
GeoHMS	Geospatial Hydrologic Model System extension
GIS	Geographic Information Systems
HEC	Hydrologic Engineering Center
HMS	Hydrologic Modeling System
IACWD	Interagency Advisory Committee on Water Data
InFRM	Interagency Flood Risk Management
LCRA	Lower Colorado River Authority
LiDAR	Light (Laser) Detection and Range
LOC	Line of organic correlation
LPIII	Log Pearson III
MMC	Modeling, Mapping, and Consequences Production Center
NA14	NOAA Atlas 14
NAD 83	North American Datum of 1983
NCDC	National Climatic Data Center
NED	National Elevation Dataset
NGVD 29	National Geodetic Vertical Datum of 1929
NHD	National Hydrography Dataset
NID	National Inventory of Dams
NLCD	National Land Cover Database
NOAA	National Oceanic and Atmospheric Administration
NRCS	Natural Resources Conservation Service
NSE	Nash Sutcliffe Efficiency
NWIS	National Water Information System
NWS	National Weather Service
PDSI	Palmer Drought Severity Index
PeakFQ	Peak Flood Frequency
PFDS	Precipitation Frequency Data Server
PMP	Probable Maximum Precipitation
QPF	Quantitative Precipitation Forecast
RAS	River Analysis System
ResSim	Reservoir System Simulation
RFA	Reservoir Frequency Analysis
RFC	River Forecast Center
RMC	Risk Management Center

Acronym	Definition
RMSE	root mean square error
RSR	observed standard deviation ratio
SCS	Soil Conservation Service
SHG	Standard Hydrologic Grid
SME	subject matter expert
SOP	Standard Operating Procedures
sq mi	square miles
SSP	Statistical Software Package
gSSURGO	Gridded Soil Survey Geographic Database
TWDB	Texas Water Development Board
TxDOT	Texas Department of Transportation
USACE	U.S. Army Corps of Engineers
USDA	U.S. Department of Agriculture
USGS	U.S. Geological Survey
WCM	Water Control Manual
WGRFC	West Gulf River Forecast Center